VOLUME 29 / NUMBER 20
OCTOBER 23, 1991
ACC. NOS. N91-28131 TO N91-29138

STAR

AN ABSTRACT JOURNAL

Scientific and Technical Aerospace Reports

PRODUCED BY THE
SCIENTIFIC AND TECHNICAL
INFORMATION
PROGRAM

NASA

NATIONAL AERONAUTICS AND SPACE ADMINISTRATION

***Scientific and Technical Aerospace Reports* (*STAR*)** is an abstract journal that provides comprehensive coverage of worldwide aerospace-related reports. It is a major product of the International Aerospace Database managed by the NASA Scientific and Technical Information (STI) Program. The coverage includes reports on aeronautics, space, and supporting disciplines. *STAR* lists current, publicly available reports entered into the NASA STI Database during the 2-week period preceding publication. A typical citation and abstract appear on page viii. They explain how to read the items that are announced in this journal.

NASA sponsors a companion journal, *International Aerospace Abstracts* (*IAA*), that lists abstracts of the open literature on aerospace subjects available worldwide. *IAA* is available through the American Institute of Aeronautics and Astronautics.

Entries found in *STAR* and *IAA* are available through NASA's online service, RECON, as the International Aerospace Database and through DIALOG as the Aerospace Database.

Information on aerospace and related subjects is gathered by the NASA STI Program through national and international agreements and exchanges and is made available to the NASA community as well as to the public in many forms through various outlets. The section on NASA STI Program Products and Services contains additional information.

US ISSN 0036-8741

Volume 29 Number 20 / OCTOBER 23, 1991

TABLE OF CONTENTS

AERONAUTICS For related information see also *Astronautics.*

01 AERONAUTICS (GENERAL) .... **N.A.**

02 AERODYNAMICS **3279**
Includes aerodynamics of bodies, combinations, wings, rotors, and control surfaces; and internal flow in ducts and turbomachinery. For related information see also *34 Fluid Mechanics and Heat Transfer.*

03 AIR TRANSPORTATION AND SAFETY **3281**
Includes passenger and cargo air transport operations; and aircraft accidents. For related information see also *16 Space Transportation* and *85 Urban Technology and Transportation.*

04 AIRCRAFT COMMUNICATIONS AND NAVIGATION **3282**
Includes digital and voice communication with aircraft; air navigation systems (satellite and ground based); and air traffic control. For related information see also *17 Space Communications, Spacecraft Communications, Command and Tracking* and *32 Communications and Radar.*

05 AIRCRAFT DESIGN, TESTING AND PERFORMANCE **3282**
Includes aircraft simulation technology. For related information see also *18 Spacecraft Design, Testing and Performance* and *39 Structural Mechanics.* For land transportation vehicles see *85 Urban Technology and Transportation.*

06 AIRCRAFT INSTRUMENTATION **3286**
Includes cockpit and cabin display devices; and flight instruments. For related information see also *19 Spacecraft Instrumentation* and *35 Instrumentation and Photography.*

07 AIRCRAFT PROPULSION AND POWER .... **N.A.**
Includes prime propulsion systems and systems components, e.g., gas turbine engines and compressors; and onboard auxiliary power plants for aircraft. For related information see also *20 Spacecraft Propulsion and Power, 28 Propellants and Fuels,* and *44 Energy Production and Conversion.*

08 AIRCRAFT STABILITY AND CONTROL **3286**
Includes aircraft handling qualities; piloting; flight controls; and autopilots. For related information see also *05 Aircraft Design, Testing and Performance.*

09 RESEARCH AND SUPPORT FACILITIES (AIR) **3286**
Includes airports, hangars and runways; aircraft repair and overhaul facilities; wind tunnels; shock tubes; and aircraft engine test stands. For related information see also *14 Ground Support Systems and Facilities (Space).*

ASTRONAUTICS For related information see also *Aeronautics.*

12 ASTRONAUTICS (GENERAL) **3288**
For extraterrestrial exploration see *91 Lunar and Planetary Exploration.*

13 ASTRODYNAMICS **3288**
Includes powered and free-flight trajectories; and orbital and launching dynamics.

14 GROUND SUPPORT SYSTEMS AND FACILITIES (SPACE) **3289**
Includes launch complexes, research and production facilities; ground support equipment, e.g., mobile transporters; and simulators. For related information see also *09 Research and Support Facilities (Air).*

15 LAUNCH VEHICLES AND SPACE VEHICLES .... **N.A.**
Includes boosters; operating problems of launch/space vehicle systems; and reusable vehicles. For related information see also *20 Spacecraft Propulsion and Power.*

16 SPACE TRANSPORTATION **3289**
Includes passenger and cargo space transportation, e.g., shuttle operations; and space rescue techniques. For related information see also *03 Air Transportation and Safety* and *18 Spacecraft Design, Testing and Performance.* For space suits see *54 Man/System Technology and Life Support.*

17 SPACE COMMUNICATIONS, SPACECRAFT COMMUNICATIONS, COMMAND AND TRACKING . **N.A.**
Includes telemetry; space communications networks; astronavigation and guidance; and radio blackout. For related information see also *04 Aircraft Communications and Navigation* and *32 Communications and Radar.*

N.A.—no abstracts were assigned to this category for this issue.

18 SPACECRAFT DESIGN, TESTING AND PERFORMANCE 3290
Includes satellites; space platforms; space stations; spacecraft systems and components such as thermal and environmental controls; and attitude controls. For life support systems see *54 Man/System Technology and Life Support.* For related information see also *05 Aircraft Design, Testing and Performance, 39 Structural Mechanics,* and *16 Space Transportation.*

19 SPACECRAFT INSTRUMENTATION .... N.A.
For related information see also *06 Aircraft Instrumentation* and *35 Instrumentation and Photography.*

20 SPACECRAFT PROPULSION AND POWER 3291
Includes main propulsion systems and components, e.g., rocket engines; and spacecraft auxiliary power sources. For related information see also *07 Aircraft Propulsion and Power, 28 Propellants and Fuels, 44 Energy Production and Conversion,* and *15 Launch Vehicles and Space Vehicles.*

CHEMISTRY AND MATERIALS

23 CHEMISTRY AND MATERIALS (GENERAL) .... N.A.

24 COMPOSITE MATERIALS 3303
Includes physical, chemical, and mechanical properties of laminates and other composite materials. For ceramic materials see *27 Nonmetallic Materials.*

25 INORGANIC AND PHYSICAL CHEMISTRY 3307
Includes chemical analysis, e.g., chromatography; combustion theory; electrochemistry; and photochemistry. For related information see also *77 Thermodynamics and Statistical Physics.*

26 METALLIC MATERIALS 3312
Includes physical, chemical, and mechanical properties of metals, e.g., corrosion; and metallurgy.

27 NONMETALLIC MATERIALS 3321
Includes physical, chemical, and mechanical properties of plastics, elastomers, lubricants, polymers, textiles, adhesives, and ceramic materials. For composite materials see *24 Composite Materials.*

28 PROPELLANTS AND FUELS 3330
Includes rocket propellants, igniters and oxidizers; their storage and handling procedures; and aircraft fuels. For related information see also *07 Aircraft Propulsion and Power, 20 Spacecraft Propulsion and Power,* and *44 Energy Production and Conversion.*

29 MATERIALS PROCESSING 3331
Includes space-based development of products and processes for commercial application. For biological materials see *55 Space Biology.*

ENGINEERING For related information see also *Physics.*

31 ENGINEERING (GENERAL) 3332
Includes vacuum technology; control engineering; display engineering; cryogenics; and fire prevention.

32 COMMUNICATIONS AND RADAR 3333
Includes radar; land and global communications; communications theory; and optical communications. For related information see also *04 Aircraft Communications and Navigation* and *17 Space Communications, Spacecraft Communications, Command and Tracking.* For search and rescue see *03 Air Transportation and Safety,* and *16 Space Transportation.*

33 ELECTRONICS AND ELECTRICAL ENGINEERING 3336
Includes test equipment and maintainability; components, e.g., tunnel diodes and transistors; microminiaturization; and integrated circuitry. For related information see also *60 Computer Operations and Hardware* and *76 Solid-State Physics.*

34 FLUID MECHANICS AND HEAT TRANSFER 3341
Includes boundary layers; hydrodynamics; fluidics; mass transfer and ablation cooling. For related information see also *02 Aerodynamics* and *77 Thermodynamics and Statistical Physics.*

35 INSTRUMENTATION AND PHOTOGRAPHY 3348
Includes remote sensors; measuring instruments and gauges; detectors; cameras and photographic supplies; and holography. For aerial photography see *43 Earth Resources and Remote Sensing.* For related information see also *06 Aircraft Instrumentation* and *19 Spacecraft Instrumentation.*

36 LASERS AND MASERS 3350
Includes parametric amplifiers. For related information see also *76 Solid-State Physics.*

37 MECHANICAL ENGINEERING **3353**
Includes auxiliary systems (nonpower); machine elements and processes; and mechanical equipment.

38 QUALITY ASSURANCE AND RELIABILITY **3357**
Includes product sampling procedures and techniques; and quality control.

39 STRUCTURAL MECHANICS **3359**
Includes structural element design and weight analysis; fatigue; and thermal stress. For applications see *05 Aircraft Design, Testing and Performance* and *18 Spacecraft Design, Testing and Performance.*

GEOSCIENCES For related information see also *Space Sciences.*

42 GEOSCIENCES (GENERAL) .... **N.A.**

43 EARTH RESOURCES AND REMOTE SENSING **3366**
Includes remote sensing of earth resources by aircraft and spacecraft; photogrammetry; and aerial photography. For instrumentation see *35 Instrumentation and Photography.*

44 ENERGY PRODUCTION AND CONVERSION **3366**
Includes specific energy conversion systems, e.g., fuel cells; global sources of energy; geophysical conversion; and windpower. For related information see also *07 Aircraft Propulsion and Power, 20 Spacecraft Propulsion and Power,* and *28 Propellants and Fuels.*

45 ENVIRONMENT POLLUTION **3369**
Includes atmospheric, noise, thermal, and water pollution.

46 GEOPHYSICS **3371**
Includes aeronomy; upper and lower atmosphere studies; ionospheric and magnetospheric physics; and geomagnetism. For space radiation see *93 Space Radiation.*

47 METEOROLOGY AND CLIMATOLOGY **3375**
Includes weather forecasting and modification.

48 OCEANOGRAPHY **3377**
Includes biological, dynamic, and physical oceanography; and marine resources. For related information see also *43 Earth Resources and Remote Sensing.*

LIFE SCIENCES

51 LIFE SCIENCES (GENERAL) **3378**

52 AEROSPACE MEDICINE **3380**
Includes physiological factors; biological effects of radiation; and effects of weightlessness on man and animals.

53 BEHAVIORAL SCIENCES **3381**
Includes psychological factors; individual and group behavior; crew training and evaluation; and psychiatric research.

54 MAN/SYSTEM TECHNOLOGY AND LIFE SUPPORT **3381**
Includes human engineering; biotechnology; and space suits and protective clothing. For related information see also *16 Space Transportation.*

55 SPACE BIOLOGY .... **N.A.**
Includes exobiology; planetary biology; and extraterrestrial life.

MATHEMATICAL AND COMPUTER SCIENCES

59 MATHEMATICAL AND COMPUTER SCIENCES (GENERAL) **3382**

60 COMPUTER OPERATIONS AND HARDWARE **3382**
Includes hardware for computer graphics, firmware, and data processing. For components see *33 Electronics and Electrical Engineering.*

61 COMPUTER PROGRAMMING AND SOFTWARE **3383**
Includes computer programs, routines, algorithms, and specific applications, e.g., CAD/CAM.

62 COMPUTER SYSTEMS **3388**
Includes computer networks and special application computer systems.

63 CYBERNETICS 3390
Includes feedback and control theory, artificial intelligence, robotics and expert systems. For related information see also *54 Man/System Technology and Life Support.*

64 NUMERICAL ANALYSIS 3391
Includes iteration, difference equations, and numerical approximation.

65 STATISTICS AND PROBABILITY .... N.A.
Includes data sampling and smoothing; Monte Carlo method; and stochastic processes.

66 SYSTEMS ANALYSIS 3394
Includes mathematical modeling; network analysis; and operations research.

67 THEORETICAL MATHEMATICS .... N.A.
Includes topology and number theory.

PHYSICS For related information see also *Engineering.*

70 PHYSICS (GENERAL) 3394
For precision time and time interval (PTTI) see *35 Instrumentation and Photography;* for geophysics, astrophysics or solar physics see *46 Geophysics, 90 Astrophysics,* or *92 Solar Physics.*

71 ACOUSTICS 3395
Includes sound generation, transmission, and attenuation. For noise pollution see *45 Environment Pollution.*

72 ATOMIC AND MOLECULAR PHYSICS 3395
Includes atomic structure, electron properties, and molecular spectra.

73 NUCLEAR AND HIGH-ENERGY PHYSICS 3404
Includes elementary and nuclear particles; and reactor theory. For space radiation see *93 Space Radiation.*

74 OPTICS 3405
Includes light phenomena and optical devices. For lasers see *36 Lasers and Masers.*

75 PLASMA PHYSICS 3406
Includes magnetohydrodynamics and plasma fusion. For ionospheric plasmas see *46 Geophysics.* For space plasmas see *90 Astrophysics.*

76 SOLID-STATE PHYSICS 3423
Includes superconductivity. For related information see also *33 Electronics and Electrical Engineering* and *36 Lasers and Masers.*

77 THERMODYNAMICS AND STATISTICAL PHYSICS 3434
Includes quantum mechanics; theoretical physics; and Bose and Fermi statistics. For related information see also *25 Inorganic and Physical Chemistry* and *34 Fluid Mechanics and Heat Transfer.*

SOCIAL SCIENCES

80 SOCIAL SCIENCES (GENERAL) 3436
Includes educational matters.

81 ADMINISTRATION AND MANAGEMENT 3436
Includes management planning and research.

82 DOCUMENTATION AND INFORMATION SCIENCE 3437
Includes information management; information storage and retrieval technology; technical writing; graphic arts; and micrography. For computer documentation see *61 Computer Programming and Software.*

83 ECONOMICS AND COST ANALYSIS .... N.A.
Includes cost effectiveness studies.

84 LAW, POLITICAL SCIENCE AND SPACE POLICY .... N.A.
Includes NASA appropriation hearings; aviation law; space law and policy; international law; international cooperation; and patent policy.

85 URBAN TECHNOLOGY AND TRANSPORTATION 3440
Includes applications of space technology to urban problems; technology transfer; technology assessment; and surface and mass transportation. For related information see *03 Air Transportation and Safety, 16 Space Transportation,* and *44 Energy Production and Conversion.*

SPACE SCIENCES For related information see also *Geosciences*.

88 SPACE SCIENCES (GENERAL) .... **N.A.**

89 ASTRONOMY **3441**
Includes radio, gamma-ray, and infrared astronomy; and astrometry.

90 ASTROPHYSICS **3442**
Includes cosmology; celestial mechanics; space plasmas; and interstellar and interplanetary gases and dust. For related information see also *75 Plasma Physics*.

91 LUNAR AND PLANETARY EXPLORATION **3446**
Includes planetology; and manned and unmanned flights. For spacecraft design or space stations see *18 Spacecraft Design, Testing and Performance*.

92 SOLAR PHYSICS **3447**
Includes solar activity, solar flares, solar radiation and sunspots. For related information see *93 Space Radiation*.

93 SPACE RADIATION **3448**
Includes cosmic radiation; and inner and outer earth's radiation belts. For biological effects of radiation see *52 Aerospace Medicine*. For theory see *73 Nuclear and High-Energy Physics*.

GENERAL

Includes aeronautical, astronautical, and space science related histories, biographies, and pertinent reports too broad for categorization; histories or broad overviews of NASA programs.

99 GENERAL **3448**

SUBJECT INDEX **I-1**

PERSONAL AUTHOR INDEX **I-67**

CORPORATE SOURCE INDEX **I-75**

CONTRACT NUMBER INDEX **I-87**

REPORT/ACCESSION NUMBER INDEX **I-91**

APPENDIX **A-1**

TYPICAL CITATION AND ABSTRACT

NASA SPONSORED

ON MICROFICHE

ACCESSION NUMBER → **N91-10047*#** Georgia Inst. of Tech., Atlanta. School of Aerospace Engineering. ← **CORPORATE SOURCE**

TITLE → **NONLINEAR FEEDBACK CONTROL FOR HIGH ALPHA FLIGHT Final Report, Jan. 1989 - Apr. 1990**

AUTHOR → Harold Stalford Apr. 1990 ← **PUBLICATION DATE** 15 p

CONTRACT OR GRANT → (Grant NAG1-959)

REPORT NUMBERS → (NASA-CR-186545; NAS 1.26;186545) Avail: NTIS HC/MF ← **AVAILABILITY SOURCE** A03 ← **PRICE CODE**

COSATI CODE → CSCL 01C

Analytical aerodynamic models are derived from a high alpha 6 DOF wind tunnel model. One detail model requires some interpolation between nonlinear functions of alpha. One analytical model requires no interpolation and as such is a completely continuous model. Flight path optimization is conducted on the basic maneuvers: half-loop, 90 degree pitch-up, and level turn. The optimal control analysis uses the derived analytical model in the equations of motion and is based on both moment and force equations. The maximum principle solution for the half-loop is poststall trajectory performing the half-loop in 13.6 seconds. The agility induced by thrust vectoring capability provided a minimum effect on reducing the maneuver time. By means of thrust vectoring control the 90 degrees pitch-up maneuver can be executed in a small place over a short time interval. The agility capability of thrust vectoring is quite beneficial for pitch-up maneuvers. The level turn results are based currently on only outer layer solutions of singular pertrubation. Poststall solutions provide high turn rates but generate higher losses of energy than that of classical sustained solutions.

Author

VOLUME 29 NUMBER 20 / OCTOBER 23, 1991

Scientific and Technical Aerospace Reports

A Semimonthly Publication of the National Aeronautics and Space Administration

01 AERONAUTICS (GENERAL)

No abstracts in this category.

02 AERODYNAMICS

Includes aerodynamics of bodies, combinations, wings, rotors, and control surfaces; and internal flow in ducts and turbomachinery.

For related information see also *34 Fluid Mechanics and Heat Transfer.*

N91-28131*# National Aeronautics and Space Administration. Langley Research Center, Hampton, VA.
A METHODOLOGY FOR USING NONLINEAR AERODYNAMICS IN AEROSERVOELASTIC ANALYSIS AND DESIGN
Walter A. Silva May 1991 15 p Previously announced as A91-32025
(NASA-TM-104087; NAS 1.15:104087) Avail: NTIS HC/MF A03 CSCL 01A

A methodology is presented for using the Volterra-Wiener theory of nonlinear systems in aeroservoelastic (ASE) analyses and design. The theory is applied to the development of nonlinear aerodynamic response models that can be defined in state-space form and are, therefore, appropriate for use in modern control theory. The theory relies on the identification of nonlinear kernels that can be used to predict the response of a nonlinear system due to an arbitrary input. A numerical kernel identification technique, based on unit impulse responses, is presented and applied to a simple bilinear, single-input single-output (SISO) system. The linear kernel (unit impulse response) and the nonlinear second-order kernel of the system are numerically-identified and compared with the exact, analytically-defined and linear and second-order kernels. This kernel identification technique is then applied to the CAP-TSD (Computational Aeroelasticity Program-Transonic Small Disturbance) code for identification of the linear and second-order kernels of a NACA64A010 rectangular wing undergoing pitch at $M = 0.5$, $M = 8.5$ (transonic), and $M = 0.93$ (transonic). Results presented demonstrate the feasibility of this approach for use with nonlinear, unsteady aerodynamic responses. Author

N91-28132*# National Aeronautics and Space Administration. Langley Research Center, Hampton, VA.
TRANSONIC SHOCK-INDUCED DYNAMICS OF A FLEXIBLE WING WITH A THICK CIRCULAR-ARC AIRFOIL
Robert M. Bennett, Bryan E. Dansberry, Moses G. Farmer, Clinton V. Eckstrom, David A. Seidel, and Jose A. Rivera, Jr. May 1991 12 p Presented at the 32d Structures, Structural Dynamics and Materials Conference, Baltimore, MD, 7-10 Apr. 1991 Previously announced as A91-32023
(NASA-TM-104088; NAS 1.15:104088; AIAA-Paper-91-1107) Avail: NTIS HC/MF A03 CSCL 01A

Transonic shock boundary layer oscillations occur on rigid models over a small range of Mach numbers on thick circular-arc airfoils. Extensive tests and analyses of this phenomena have been made in the past but essentially all of them were for rigid models. A simple flexible wing model with an 18 pct. circular arc airfoil was constructed and tested in the Langley Transonic Dynamics Tunnel to study the dynamic characteristics that a wing might have under these circumstances. In the region of shock boundary layer oscillations, buffeting of the first bending mode was obtained. This mode was well separated in frequency from the shock boundary layer oscillations. A limit cycle oscillation was also measured in a third bending like mode, involving wind vertical bending and splitter plate motion, which was in the frequency range of the shock boundary layer oscillations. Several model configurations were tested, and a few potential fixes were investigated. Author

N91-28133# Sandia National Labs., Albuquerque, NM.
AN EXPERIMENTAL INVESTIGATION OF THE EFFECT OF VORTEX GENERATORS ON THE AERODYNAMIC CHARACTERISTICS OF A NACA 0021 AIRFOIL UNDERGOING LARGE AMPLITUDE PITCH OSCILLATIONS
M. L. Rueger and G. M. Gregorek (Ohio State Univ., Columbus.) Apr. 1991 153 p
(Contract DE-AC04-76DP-00789)
(DE91-012102; SAND-90-7111) Avail: NTIS HC/MF A08

A NACA 0021 14-chord airfoil was subjected to large amplitude pitch oscillations in The Ohio State University Low Speed Wind Tunnel at a Reynolds number of 1.2 times 10(exp 6). Surface pressures were measured with an electronically scanned pressure measurement system at sampling rates up to 50 Hz. Data were acquired for the clean airfoil and for the airfoil with vortex generators located at 0.1 and 0.3 chord distances aft of the leading edge. The vortex generators increase the maximum lift coefficient and the lift curve slope for both the static and dynamic tests. The magnitude and detail of the vortex generator effects were found to depend on the amplitude and frequency of the pitch oscillations. DOE

N91-28134*# National Aeronautics and Space Administration. Ames Research Center, Moffett Field, CA.
ROTOR AND CONTROL SYSTEM LOADS ANALYSIS OF THE XV-15 WITH THE ADVANCED TECHNOLOGY BLADES
Joseph J. Totah and John F. Madden, III Apr. 1991 23 p Presented at the American Helicopter Society National Technical Specialists' Meeting on Innovations in Rotorcraft Test Technologies for the 90's, Scottsdale, AZ, Oct. 1990 Previously announced as A91-31291
(NASA-TM-102876; A-90316; NAS 1.15:102876) Avail: NTIS HC/MF A03 CSCL 01A

An analysis of the rotor and control system loads of the XV-15 with the Advanced Technology Blades (XV-15/ATB) was conducted to study the effects of modifications designed to alleviate high collective actuator loads encountered during initial flight tests. Rotor loads predictions were correlated with flight data to establish accuracies of the methodology used in the analysis. Control system loads predictions were then examined and were also correlated with flight data. The results showed a significant reduction in 3/rev collective actuator loads of the XV-15/ATB when the control system stiffness was increased and the rotor blade chord balance and tip twist were modified. Author

N91-28135*# National Aeronautics and Space Administration. Langley Research Center, Hampton, VA.

VAPORIZING PARTICLE VELOCIMETER Patent Application

Leonard M. Weinstein, inventor (to NASA) 14 Jun. 1991 14 p
(NASA-Case-LAR-14685-1; NAS 1.71:LAR-14685-1; US-Patent-Appl-SN-718313) Avail: NTIS HC/MF A03 CSCL 01A

A velocimeter measures flow characteristics of a flow traveling through a chamber in a given direction. Tracer particles are entrained in the flow and a source of radiant energy produces an output stream directed transverse to the chamber and having a sufficient intensity to vaporize the particles as they pass through the output stream. Each of the vaporized particles explodes to produce a shock wave and a hot core, and a flow visualization system tracks the motion of the hot cores and shock waves to thereby measure velocity of each tracer particle, and temperature of the flow around the tracer. NASA

N91-28136*# National Aeronautics and Space Administration. Lewis Research Center, Cleveland, OH.

EVALUATION OF A TECHNIQUE TO GENERATE ARTIFICIALLY THICKENED BOUNDARY LAYERS IN SUPERSONIC AND HYPERSONIC FLOWS

A. R. Porro, W. R. Hingst, D. O. Davis, and A. B. Blair, Jr. (National Aeronautics and Space Administration. Langley Research Center, Hampton, VA.) Washington Aug. 1991 28 p
(NASA-TP-3142; E-5660; NAS 1.60:3142) Avail: NTIS HC/MF A03 CSCL 01A

The feasibility of using a contoured honeycomb model to generate a thick boundary layer in high-speed, compressible flow was investigated. The contour of the honeycomb was tailored to selectively remove momentum in a minimum of streamwise distance to create an artificially thickened turbulent boundary layer. Three wind tunnel experiments were conducted to verify the concept. Results indicate that this technique is a viable concept, especially for high-speed inlet testing applications. In addition, the compactness of the honeycomb boundary layer simulator allows relatively easy integration into existing wind tunnel model hardware. Author

N91-28137*# National Aeronautics and Space Administration. Langley Research Center, Hampton, VA.

EXPERIMENTAL FLUTTER BOUNDARIES WITH UNSTEADY PRESSURE DISTRIBUTIONS FOR THE NACA 0012 BENCHMARK MODEL

Jose A. Rivera, Jr., Bryan E. Dansberry, Moses G. Farmer, Clinton V. Eckstrom, David A. Seidel, and Robert M. Bennett Jul. 1991 9 p Presented at the 32nd Structures, Structural Dynamics, and Materials Conference, Baltimore, MD, 8-10 Apr. 1991; cosponsored by AIAA, ASME, ASCE, AHS, and ASC Previously announced in IAA as A91-31900
(NASA-TM-104072; NAS 1.15:104072) Avail: NTIS HC/MF A02 CSCL 01A

The Structural Dynamics Div. at NASA-Langley has started a wind tunnel activity referred to as the Benchmark Models Program. The objective is to acquire test data that will be useful for developing and evaluating aeroelastic type Computational Fluid Dynamics codes currently in use or under development. The progress is described which was achieved in testing the first model in the Benchmark Models Program. Experimental flutter boundaries are presented for a rigid semispan model (NACA 0012 airfoil section) mounted on a flexible mount system. Also, steady and unsteady pressure measurements taken at the flutter condition are presented. The pressure data were acquired over the entire model chord located at the 60 pct. span station. Author

N91-28138*# Vigyan Research Associates, Inc., Hampton, VA.

A STUDY OF RESIDUAL INTERFERENCE EFFECTS IN ADAPTIVE WALL TESTING OF A 7-INCH CHORD CAST-10-2/DOA 2 AIRFOIL MODEL

A. V. Murthy Washington Aug. 1991 62 p
(Contract NAS1-18585)
(NASA-CR-4390; NAS 1.26:4390) Avail: NTIS HC/MF A04 CSCL 01A

The residual interferences present in the testing of a CAST10-2/DOA2 airfoil model in the Langley 0.3 m Transonic Cryogenic Tunnel (0.3 m TCT) is examined. The 7.1 inch chord airfoil model was tested in the 0.3 m TCT adaptive wall test section with a nominal 13 inch square cross section. The test data obtained on the same model during different tunnel entries showed different levels of residual interference. The present study shows that for valid comparison of the test data from adaptive wall tunnels, it is necessary to account for residual interferences, in particular the blockage correction to the Mach number. Author

N91-28139 Tel-Aviv Univ. (Israel). Dept. of Fluid Mechanics and Heat Transfer.

AN ACTIVE DELAY OF SEPARATION ON TWO-DIMENSIONAL AIRFOILS M.S. Thesis

Doron Neuburger Apr. 1989 117 p In HEBREW; ENGLISH summary
(ITN-91-85142) Copyright Avail: Tel-Aviv Univ., Exact Sciences Library, Ramat Aviv 69978, Israel

Experiments were performed on delaying the onset of stall on airfoils at high angles of attack. Small, 2-D, periodic perturbations were induced on the upper surface of the airfoil, at the point of natural boundary layer separation. Amplification of these perturbations by the shear layer between the separated boundary layer and the free air stream increases the mixing between the fluid in the neighborhood of the airfoil and the free stream. Thus, fluid with high kinetic energy is brought closer to the airfoil surface, resulting in improved performance. The experiments were performed on a NACA-0015 airfoil with a stubby trailing edge and on a Wortmann FX63-137 airfoil. A subsonic wind tunnel was used, with free stream velocities of 10, 15 and 20 m/sec, corresponding to Reynolds numbers of 200,000, 300,000 and 400,000. Measurements of pressure distributions along the airfoil chord enabled the lift and pitching moment coefficients to be calculated. The total drag coefficient was calculated from the measured velocity distribution of the wake. Implementation of the control method increased the stall angle, enabling the maximum lift coefficient to be achieved with reduced drag. The governing factors were found to be the Reynolds number and the frequency and intensity of the perturbation. An optimal flap vibration frequency was found for all free stream velocities, and a linear relationship was found between the maximum lift coefficient and the angle of stall, when the optimum vibration frequency was applied. The improvement in lift coefficient increased with increasing free stream velocity and flap vibration amplitude. ISA

N91-28140 North Carolina State Univ., Raleigh.

AN ABBREVIATED REYNOLDS STRESS TURBULENCE MODEL FOR AIRFOIL FLOWS Ph.D. Thesis

Richard Lee Gaffney, Jr. 1990 164 p
Avail: Univ. Microfilms Order No. DA9112157

An abbreviated Reynolds stress turbulence model is presented for solving turbulent flow over airfoils. The model consists of two partial differential equations, one for the Reynolds shear stress and the other for the turbulent kinetic energy. The normal stresses and the dissipation rate of turbulent kinetic energy are computed from algebraic relationships having the correct asymptotic near wall behavior. This allows the model to be integrated all the way to the wall without the use of wall functions. Results for a flat plate at zero angle of attack, a NACA 0012 airfoil, and a RAE 2822 airfoil are presented. Flat plate results are compared to the law of the wall and the experimental data of Klebanoff. Airfoil results are compared favorably with the pressure distributions found experimentally and from the eddy viscosity model. The predicted skin friction is found to be too high over the front portion of the airfoil but then relaxes down to give good agreement with experimental values. The behavior of the skin friction is attributed to an inadequate representation of the normal stresses.
Dissert. Abstr.

N91-28141 Illinois Univ., Urbana-Champaign.
ANALYSIS OF PASSIVE AND ACTIVE DISCRETE-DISTRIBUTED LINEAR DYNAMICAL SYSTEMS USING GREEN'S FUNCTION METHODS Ph.D. Thesis
Donald Michael McFarland 1990 156 p
Avail: Univ. Microfilms Order No. DA9114342

A detailed, rigorous analysis of the dynamics of a large class of linear passive discrete-distributed mechanical systems was performed, unifying and extending previous results in the field. A distributed parameter system, represented by the Green's function of its governing differential equation, and a multiplicity of arbitrarily located lumped parameter systems are coupled at discrete points and the resulting combined system is considered as a whole. Modal analysis is used extensively, and the discrete-continuous nature of the operators and eigenfunctions is explicitly addressed. Dissert. Abstr.

N91-28142# New York Univ., New York. Inst. of Mathematical Sciences.
A COMPARISON OF THE POTENTIAL AND THE EULER FORMULATIONS OF THE EQUATIONS OF MOTION FOR TRANSONIC FLOW
K. McGrattan May 1991 100 p
(Contract DE-FG02-88ER-25053)
(DE91-014731; DOE/ER-25053/4) Avail: NTIS HC/MF A05

This report discusses the following topics: models of transonic flow; the BGKM computer code; wave drag and the entropy inequality; supercritical airfoil computations; and vortex dynamics. DOE

N91-28143*# National Aeronautics and Space Administration. Langley Research Center, Hampton, VA.
LONGITUDINAL AERODYNAMIC CHARACTERISTICS OF A SUBSONIC, ENERGY-EFFICIENT TRANSPORT CONFIGURATION IN THE NATIONAL TRANSONIC FACILITY
Peter F. Jacobs and Blair B. Gloss Aug. 1989 70 p
(NASA-TP-2922; L-16569; NAS 1.60:2922) Avail: NTIS HC/MF A04 CSCL 01A

The Reynolds number, aeroelasticity, boundary layer transition, and nonadiabatic wall temperature effects, and data repeatability was determined in the National Transonic Facility (NTF) for a subsonic, energy efficient transport model. The model was tested over a Mach number range of 0.50 to 0.86 and a Reynolds number range of 1.9 million to approximately 23.0 million (based on mean geometric chord). The majority of the data was taken using cryogenic nitrogen (data at 1.9 million Reynolds number was taken in air). Force and moment, wing pressure, and wing thermocouple data are presented. The data indicate that increasing Reynolds number resulted in greater effective camber of the supercritical wing and horizontal tail, resulting in greater lift and pitching moment coefficients at nearly all angles of attack for $M = 0.82$. As Reynolds number was increased, untrimmed L/D increased, the angle of attack for maximum L/D decreased, drag creep was reduced significantly, and drag divergence Mach number increased slightly. Data repeatability for both modes of operation of the NTF (air and cryogenic nitrogen) was generally very good, and nonadiabatic wall effects were estimated to be small. Transition-free and transition-fixed configurations had significantly different force and moment data at $M = 0.82$ for low Reynolds number, and very small differences were noted at high Reynolds numbers. Author

N91-28144 Washington Univ., Saint Louis, MO.
A CHEMICALLY REACTING, TURBULENT STRATIFIED INTERFACE Ph.D. Thesis
Shenqyang Steven Shy 1990 128 p
Avail: Univ. Microfilms Order No. DA9109827

The stability of stratocumulus clouds with evaporative cooling effects is explored in lab simulations. Two distinct classes of mixing processes can occur across a stratified interface. Linear mixing occurs when the density of the mixed parcels is linearly intermediate between that of the constituents. Nonlinear mixing is mixing induced buoyancy reversal, with a mixture density as a nonlinear function of composition, in which mixtures can become more dense than even the underlying fluid. Three experiments under different forcing conditions in water tanks are carried out to study the instabilities and entrainment mechanisms across stratified interfaces. A simple model of the interface has three requirements for buoyancy reversal instability: the mixed fluid must be sufficiently dense; the vortices must complete a rotation; and they must be above the mixing transition if the fluids are liquids. This implies certain limits on the buoyancy reversal parameter and the Richardson, Reynolds, and Schmidt numbers. Dissert. Abstr.

N91-28145 Pennsylvania State Univ., University Park.
STUDIES OF THE TWO-PHASE PLUME JET AND WALL EROSION IN A VERTICAL LAUNCHING SYSTEM Ph.D. Thesis
Yeu-Pin Yeh 1990 242 p
Avail: Univ. Microfilms Order No. DA9117764

The vertical launching system (VLS) produces a two-phase exhaust plume due to the metalized solid propellant employed in rocket motors. The gas management of the exhaust plume in the present VLS mainly comprises key issues: plume jet inducing the erosion of ablative materials used as thermal protection plates in the VLS, strong pressure waves travelling in the system, undesirable high rate of pressurization in the plenum chamber and central uptake duct in the VLS. A series of subscale VLS tests were conducted to simulate the plume exhaust processes in the actual VLS. In the theoretical study, a comprehensive model was developed to describe the process of the plume impinging upon the ablative sample to produce a surface erosion. The behavior of exhaust plume is simulated by a turbulent circular jet impinging upon the sample under different aspect ratios and inlet turbulence conditions. Dissert. Abstr.

03 AIR TRANSPORTATION AND SAFETY

Includes passenger and cargo air transport operations; and aircraft accidents.

For related information see also *16 Space Transportation* and *85 Urban Technology and Transportation.*

N91-28146# Arizona State Univ., Tempe. Dept. of Mechanical and Aerospace Engineering.
COMPUTER SIMULATION OF AN AIRCRAFT SEAT AND OCCUPANT(S) IN A CRASH ENVIRONMENT: PROGRAM SOM-LA/SOM-TA USER MANUAL Final Report, Jul. 1989 - Feb. 1990
David H. Laananen May 1991 229 p
(Contract DTFA03-89-A-00004)
(CR-R-90026; DOT/FAA/CT-90/4) Avail: NTIS HC/MF A11

A three-dimensional mathematical model of a seat, occupant(s), and restraint system was developed for use in aircraft crashworthiness analysis. Programs SOM-LA (Seat/Occupant Model - Light Aircraft) and SOM-TA (Seat/Occupant Model - Transport Aircraft) combine a lumped parameter model of aircraft occupants with a finite element model of the seat structure. The intent of these programs is to aid in evaluation of the performance of aircraft seat and restraint systems in crash environments. Four different cases are described, and the listing of input data is presented for each. Author

N91-28147# Argonne National Lab., IL.
ASSESSING THE RISK OF TRANSPORTING HAZARDOUS MATERALS BY AIRCRAFT: A CASE STUDY
M. J. Davis and L. A. Haroun 1991 10 p Presented at the 84th Annual Meeting and Exhibition of the Air and Waste Management Association (AWMA), Vancouver, British Columbia, 16-21 Jun. 1991
(Contract W-31-109-eng-38)
(DE91-014016; ANL/CP-71294; CONF-910659) Avail: NTIS HC/MF A02

The risk assessment discussed involves the transport of polychlorinated biphenyls (PCBs) by aircraft. It resulted from the need to transport a large quantity of PCBs and PCB-contaminated equipment from Canada to the United States following closure of various radar stations in the CADIN-Pinetree line. As part of the planning process conducted prior to shipping the material, an assessment of the upper bounds of potential risks associated with the operation was carried out. The results apply to air shipments of the material to the United States. The major concern associated with the transport of these materials by aircraft involved the potential for release of PCBs and trichlorobenzene (TCB), which was also present in some of the fluids being transported. Therefore, the focus of the assessment was on accidents that could potentially result in the release of these toxic compounds and their by-products to the environment. The approach used is based on conservative assumptions that allow placing an upper bound on the risks associated with a severe accident. DOE

04 AIRCRAFT COMMUNICATIONS AND NAVIGATION

Includes digital and voice communication with aircraft; air navigation systems (satellite and ground based); and air traffic control.

For related information see also *17 Space Communications, Spacecraft Communications, Command and Tracking* and *Communications and Radar.*

N91-28148# Lawrence Livermore National Lab., CA.
WFOV STAR TRACKER CAMERA
I. T. Lewis, A. G. Ledebuhr, T. S. Axelrod, J. F. Kordas, and R. F. Hills Apr. 1991 13 p Presented at the SPIE International Symposium on Optical Engineering and Photonics in Aerospace Sensing, Orlando, 1-5 Apr. 1991
(Contract W-7405-eng-48)
(DE91-012776; UCRL-JC-105345; CONF-910450-11) Avail: NTIS HC/MF A03

A prototype wide-field-of-view (WFOV) star tracker camera has been fabricated and tested for use in spacecraft navigation. The most unique feature of this device is its 28 degree by 44 degree field of view (FOV) which views a large enough sector of the sky to ensure the existence of at least 5 stars of m(sub v) = 4.5 or brighter in all viewing directions. The wide field of view (WFOV) requirement and the need to maximize both collection aperture (F/1.28) and spectral input band (0.4 to 1.1 microns) to meet the light gathering needs for the dimmest star have dictated the use of a novel concentric optical design, which employs a fiber optic faceplate field flattener. The main advantage of the WFOV configuration is the smaller star map required for position processing, which results in less processing power and faster matching. Additionally, a size and mass benefit is seen with a larger FOV/smaller effective focal length (efl) sensor. Prototype hardware versions have included both image intensified and un-intensified CCD cameras. Integration times of less than or equal to 50 msec have been demonstrated with both the intensified and un-intensified versions. DOE

N91-28149 Nottingham Univ. (England).
KINEMATIC GPS SURVEYING Ph.D. Thesis
Philip John Summerfield 1990 262 p
Avail: Univ. Microfilms Order No. BRD-91986

From the time of its initial development, the Global Positioning System (GPS) has demonstrated its ability to routinely determine relative baseline vectors to the order of one to two parts per million in the baseline length. The analytical procedures involved require carrier phase observations to be recorded for substantial periods of time. Typically, for baseline lengths ranging from 50 to 500 kilometers, the interval may range from 60 minutes to in excess of 4 hours before an acceptable solution is obtained. These time intervals are clearly prohibitive for everyday survey applications where hundreds of much shorter baselines, typically 20 to 2000 meters, are involved. At present, conventional, terrestrial surveying techniques are probably as accurate and certainly are more economical, both in terms of time and cost. Using alternative observational and computational techniques, it is possible to determine the three dimensional vector between two GPS receivers in a greatly reduced time interval. The second receiver is capable of moving between points of unknown coordinates along a traverse. The kinematic trials undertaken in the course of this research demonstrate that millimetric accuracies are achievable over baseline lengths up to 200 meters. More importantly, the required time interval has been reduced to a minimum of just one observational epoch of 5 seconds. Described here are the hardware requirements, field procedures and software considerations which will help Kinematic GPS Surveying to replace conventional surveying techniques even in real-time applications.
Dissert. Abstr.

05 AIRCRAFT DESIGN, TESTING AND PERFORMANCE

Includes aircraft simulation technology.

For related information see also *18 Spacecraft Design, Testing and Performance* and *39 Structural Mechanics.*For land transportation vehicles see *85 Urban Technology and Transportation.*

N91-28150# Advisory Group for Aerospace Research and Development, Neuilly-Sur-Seine (France). Structures and Materials Panel.
LANDING GEAR DESIGN LOADS
1990 283 p In FRENCH and ENGLISH Meeting held in Povoa de Varzim, Portugal, 8-12 Oct. 1990
(AGARD-CP-484; ISBN-92-835-0611-1) Copyright Avail: NTIS HC/MF A13; Non-NATO Nationals requests available only from AGARD/Scientific Publications Executive

Papers presented to a Specialists Meeting organized by the Structures and Materials Panel are reported. The meeting provided a forum for the exchange of experiences between the NATA nations with the aim of advancing landing gear design criteria and methods of landing gear analysis. The meeting reviewed existing design practices and specifications, considered the various methods for load measurement and data analysis, and formulated guidelines for future design procedures. For individual titles, see N91-28151 through N91-28166.

N91-28151# National Defence Headquarters, Ottawa (Ontario). Directorate Aerospace Support Engineering.
FAILURE ANALYSIS CASE HISTORIES OF CANADIAN FORCES AIRCRAFT LANDING GEAR COMPONENTS
P. Beaudet and M. Roth (Department of National Defence, Ottawa, Ontario) *In* AGARD, Landing Gear Design Loads 1990, 24 p (For primary document see N91-28150 20-05)
Copyright Avail: NTIS HC/MF A13; Non-NATO Nationals requests available only from AGARD/Scientific Publications Executive

Despite the extensive landing gear design analyses and tests carried out by the designers and manufacturers, and the large number of trouble-free landings accumulated by the users, the Canadian Forces, as well as others, have experienced a range of problems or failures with landing gear components. Different data banks were surveyed and over 200 cases histories on more than 20 aircraft types were reviewed in order to assess trends in failure mechanisms and their causes. Fatigue and corrosion were found to be the main mechanisms. Fatigue occurred mainly in steel components while corrosion occurred mainly with aluminum alloy components and wheels. Very few overload failures were noted. Different failure causes were identified. Design deficiencies and manufacturing defects led mainly to fatigue failures while poor material selection and improper field series of preventive measures was either recommended or re-emphasized. While fatigue can best be addressed by improving the quality of manufacturing and by better characterizing in-service and manufacturing stress, much work remains to be done on the time-dependent degradation processes. Their synergism with fatigue and corrosion has often been neglected in both the design and testing stages as well as in the maintenance domain. Author

N91-28152# Aeronautical Systems Div., Wright-Patterson AFB, OH.

APPLICATION OF THE AIR FORCE GUIDE SPECIFICATION 87221A TO GROUND LOADS

Dan Sheets and Robert Gerami *In* AGARD, Landing Gear Design Loads 1990 6 p (For primary document see N91-28150 20-05)

Copyright Avail: NTIS HC/MF A13; Non-NATO Nationals requests available only from AGARD/Scientific Publications Executive

The U.S. Air Force has eliminated the use of rigid and mandatory structural design specifications. In their place a new approach has been instituted that requires that every system structural specification be rationally tailored to the actual anticipated aircraft usage. The Air Force Guide Specification (AFGS-87221A) produces total system performance requirements as opposed to the old approach of meeting selected, isolated criteria. This new approach entails the conversion of operational requirements into the associated and anticipated loading environments. Examples of how this new design approach is applied are given. Author

N91-28153# Messerschmitt-Boelkow-Blohm G.m.b.H., Munich (Germany, F.R.).

DEVELOPMENT OF UNDERCARRIAGE DESIGN LOADS

G. Kempf and G. H. Haines (DowtyAerospace Gloucester, England) *In* AGARD, Landing Gear Design Loads 1990 12 p (For primary document see N91-28150 20-05)

Copyright Avail: NTIS HC/MF A13; Non-NATO Nationals requests available only from AGARD/Scientific Publications Executive

During the different phases of development from feasibility studies to the final design, the landing gear designer applies increasingly refined methods of analysis to derive the loads to which the system is designed. Future design procedures should reflect such a staged approach leading to designs which are fully optimized with the aid of rational methods of analysis to meet the complete range of aircraft operating conditions. Here, the design process is described. Comparisons are made of design load cases obtained using current landing gear requirements and those derived by rational analysis. These comparisons are made for the critical phases of landing touchdown, derotation onto the nosegear, landing roll out, repaired runway operation, etc. The application of the rational method of analysis to determining aircraft operating envelopes under asymmetric landing conditions is also discussed. Finally areas of work are identified which need addressing further, in order that a staged approach can be adopted completely in the future military landing gear design procedures. Author

N91-28154# Wright Research Development Center, Wright-Patterson AFB, OH.

RECENT DEVELOPMENTS IN THE AREA OF AIRCRAFT ROUGH FIELD PERFORMANCE

David Morris and Tony Gerardi *In* AGARD, Landing Gear Design Loads 1990 10 p (For primary document see N91-28150 20-05)

Copyright Avail: NTIS HC/MF A13; Non-NATO Nationals requests available only from AGARD/Scientific Publications Executive

Under project Have Bounce (HB), the USAF successfully determined the level of surface roughness that could be tolerated by most aircraft in the inventory. The runway roughness capability of each aircraft was determined by developing a sophisticated computer model of each aircraft. In most cases these computer models were validated with aircraft tests on rapidly repaired runways. This multimillion dollar effort has resulted in the definition of surface roughness criteria (repair criteria) for each aircraft. The knowledge gained as a result of all the testing and computer modeling has led to a much more thorough understanding of the complex interaction between the flexible structure, landing gear, and rough pavement. Discussed here is the development, laboratory qualification testing, and taxi testing of an improved F-15 rough field landing gear which provides a significant improvement in rough field and sink rate performance over the existing F-15 landing gear. This landing gear design utilizes passive, internal strut modification to achieve this performance without any effect on reliability and maintainability. Also discussed are the advantages of an automated Personal Computer (PC) based process for selecting the minimum operating strip (MOS) and for determining the minimum level of runway repair required. As backup to this automated approach, a novel technique for quantifying the ability of a given aircraft to traverse rough surfaces is also discussed. This method assigns a Vulnerability Index (VI) to each aircraft. The VI is a reflection of the aircraft's ability to absorb the energy that is transmitted from the pavement to the struts and the airframe. This method will give the base commander a tool for making good intuitive decisions in the event that the automated process cannot be used. It can also be used as a validation technique for the automated method. Author

N91-28155# British Aerospace Public Ltd. Co., Kingston-upon-Thames (England). Aerodynamics Dept.

THE SPECIAL REQUIREMENTS OF A VSTOL AIRCRAFT

D. C. Thorby, J. Johnson, A. B. K. Auld, H. T. Newman, and M. J. Brooker *In* AGARD, Landing Gear Design Loads 1990 24 p (For primary document see N91-28150 20-05)

Copyright Avail: NTIS HC/MF A13; Non-NATO Nationals requests available only from AGARD/Scientific Publications Executive

The special landing gear requirements of the Harrier family of aircraft are described. Only topics peculiar to the Vertical and Short Take Off and Landing (VSTOL) aspects of this aircraft are addressed. Of the four possible modes of take-off, ramp-assisted (the ski jump) presents unique landing gear problems. This is described, covering the design of ramp profiles and the procedures used to establish service operating limits for the landing gear, including the effects of ship motion. The particular problems associated with vertical landing are discussed. This mode of landing can produce landing gear side loads potentially much higher than are normally possible in a conventional landing with forward speed. Clearance procedures using a multivariate approach are described. The Harrier has also been cleared for operation on unprepared rough fields. The Monte Carlo method, applied to the results of numerical modeling using computer-generated surfaces, is described. Other topics discussed are runway directional stability, and the load and directional stability implications of converting to radial tires. Author

N91-28156# Messerschmitt-Boelkow-Blohm G.m.b.H., Munich (Germany, F.R.). Military Airplane Div.

CONSIDERATIONS ON OPTIMALITY OF LANDING GEAR ARRANGEMENT AND DESIGN

A. J. Krauss *In* AGARD, Landing Gear Design Loads 1990 11 p (For primary document see N91-28150 20-05)

Copyright Avail: NTIS HC/MF A13; Non-NATO Nationals requests available only from AGARD/Scientific Publications Executive

Much effort has been spent and is still being spent on development and improvement of optimization procedures and computer codes. The formal task of optimization is to quantify that set of design variables which both satisfies a set of constraints and yields the absolute maximum or minimum of an objective function. One of the intrinsic problems of optimization is that the objective must be expressed as a numerical quantity, which often leads to conversion problems (in which way can one convert a quality into a nonnegative real number?). An other even more serious problem is that formal optimization requires that the dependence of the objective on the design variables must be analytically defined. In relation to these problems it appears of secondary importance that in most cases the optimization process will stop at the local optimum which is closest to the starting design, albeit there might exist better optimum solutions across the surrounding ridges of the objective function. Before formal (automatic) optimization methods are called in, the design must therefore be developed to a starting point in reasonable vicinity to the real optimum. A retractable landing gear is complex, requires a lot of internal space on the airplane, features a variety of doors, spoils the cleanliness of the structure by large cutouts and local introduction of large loads, and adds weight. Unquestionably the landing gear impairs flight performance proper of an airplane. However, operational benefit from a landing gear apparently is big enough to outweigh said disadvantages. It appears that the

primary objective of airplane design is operational usefulness. Now, having accepted the landing gear as a basically useful subsystem, the aircraft designer should proceed by integrating the landing gear into overall functional optimization of the system. Based on a functionally sound general arrangement of the landing gear, specialists for aircraft-integrating the landing gear loads evaluation teamed with landing gear design specialists should provide for optimum detail characteristics fulfilling a variety of design criteria.
Author

N91-28157# Aeronautical Research Inst. of Sweden, Bromma. Structures Dept.

LONG TIME MEASUREMENTS OF LANDING GEAR LOADS ON SAAB SF-340 COMMUTER AIRCRAFT

A. I. Gustavsson, A. F. Blom, and L. Helmersson (Saab-Scania, Linkoping, Sweden) *In* AGARD, Landing Gear Design Loads 1990 16 p Sponsored in part by the Swedish Board for Technical Development; the Swedish Civil Aviation Admin.; and SAAB-SCANIA AB (For primary document see N91-28150 20-05)

Copyright Avail: NTIS HC/MF A13; Non-NATO Nationals requests available only from AGARD/Scientific Publications Executive

Strain gauge measurements of forces acting on the nose gear and main gears of the commuter aircraft SAAB SF-340 are discussed. During initial flight tests, forces in the longitudinal, transversal and vertical directions were measured for various maneuvers such as take-off, landing, taxiing and towing. The investigation revealed high transversal loads at the main gears at touch-down. The nose gear is most severely strained when steering during taxiing run and when the aircraft is towed connected to a tractor with a tow-bar. The results from such initial measurements formed the basis for a subsequent investigation with on line data acquisition of landing gear loads on a commuter aircraft in service at Swedair AB. The data acquisition system and the data analysis methods are described in some detail. The data acquisition was continuously carried out during nearly six months, and included various parameters such as different aircraft weight and static landing gear loads. Results from these measurements are presented as cumulative exceedances of longitudinal, transversal and vertical loads obtained from the rain-flow count analysis performed on-line during the measurements. Author

N91-28158# Deutsche Airbus G.m.b.H., Bremen (Germany, F.R.).

OPERATIONAL LOADS ON LANDING GEAR

V. Ladda and H. Struck *In* AGARD, Landing Gear Design Loads 1990 16 p (For primary document see N91-28150 20-05)

Copyright Avail: NTIS HC/MF A13; Non-NATO Nationals requests available only from AGARD/Scientific Publications Executive

Prior statistics of airworthiness authorities indicate that landing gear (safe life design) often fail during scheduled aircraft service. Therefore investigations have been carried out during the last two decades in Germany with the aim of determining operational loads acting on the landing gear during service and defining the load cases which have to be taken into consideration for fatigue investigations related to landing gear and airframe. Statistics about failures on landing gear for civil and military aircraft and relevant load cases as well as information about essential fatigue requirements are presented. Some results of different landing gear load measurements are compared and discussed. These results, presented in form of cumulative frequency distributions for the taxiing and landing impact load cases, originate from the following measurements: Airbus A320; Airbus A310; Airbus A300; VFW 614; F-104 G. The impact of towing and push back operations on the nose landing gear using conventional and advanced towing methods is discussed. The primary results of the landing gear loads measurements are accentuated. Examples for the disposition of landing gear fatigue tests are considered, and essential future actions concerning load monitoring activities including hard- and overweight landing detection are reviewed. Author

N91-28159# Wright Research Development Center, Wright-Patterson AFB, OH.

LANDING GEAR IMPROVEMENTS FOR TRANSPORT AIRCRAFT

J. Greer McClain and B. M. Crenshaw (Lockheed Aeronautical Systems Co., Marietta, GA.) *In* AGARD, Landing Gear Design Loads 1990 17 p (For primary document see N91-28150 20-05)

Copyright Avail: NTIS HC/MF A13; Non-NATO Nationals requests available only from AGARD/Scientific Publications Executive

Discussed here are development, testing, and analysis of retrofit nose and main landing gears designed for improvement in C-130 transport aircraft rough field capabilities, concentrating primarily upon analytical model prediction aspects which might be applicable to other gear designs. Two levels of improvement are examined, with the second level resulting in a new longer stroke strut designed to retract into existing stowage volume. All improved gears are qualified by laboratory drop tests and also are compared with test results. Model improvements are developed where necessary, with particular attention to representing strut friction, predicting strut rebound damping, and modeling transition from isothermal toward adiabatic conditions in the strut inflation gas. Rough field capability estimates for the C-130 equipped with these gears are made. Recommendations for further analytical model improvements are included. Author

N91-28160# Messier-Hispano-Bugatti S.A., Montrouge (France).

NUMERICAL SIMULATION OF THE DYNAMIC BEHAVIOR OF LANDING GEARS [SIMULATION NUMERIQUE DU COMPORTEMENT DYNAMIQUE DES ATTERRISSEURS]

Jean Luc Engerand *In* AGARD, Landing Gear Design Loads 1990 28 p In FRENCH; ENGLISH summary (For primary document see N91-28150 20-05)

Copyright Avail: NTIS HC/MF A13; Non-NATO Nationals requests available only from AGARD/Scientific Publications Executive

The aim here is to describe the Messier-Bugatti analysis and numerical simulation system used for solving landing gear dynamics problems. The system is designed around a finite elements software package for the analysis of mechanisms and flexible bodies. The following examples of applications are examined: simulation of landing, simulation of taxiing on rough fields or repaired runways, simulation of extension and retracting, simulation of catapulting, and analysis of shimmy stability. Author

N91-28161# Dassault (E. M.) Co., Saint Cloud (France).

CALCULATION OF INTERACTIONS BETWEEN AIR AND GROUND OF LANDING

Yves Martin-Siegfried *In* AGARD, Landing Gear Design Loads 1990 23 p In FRENCH; ENGLISH summary (For primary document see N91-28150 20-05)

Copyright Avail: NTIS HC/MF A13; Non-NATO Nationals requests available only from AGARD/Scientific Publications Executive

The author presents the present state-of-the-art for the calculation of the ground dynamic response of the aircraft. The analysis tool described here forms a special branch of the CATINA-ELFINI system, the general purpose program for computer aided design (CAD) and structural analysis of DASSAULT. The system handles a large set of problems for ground dynamic response: landing impact, rough runway rolling and take off, catapulting and landing on carrier, etc. In these calculations, the structure is represented by a finite element model of the whole aircraft coupled with models of landing gears, aerodynamics, and other special systems (e.g., catapult). The time integration is performed via implicit finite differences scheme. The method handles nonlinearities with three levels of condensation: one time before integration; at each time step linearization of smooth nonlinearities (e.g., large rotations) and condensation of the problem for only nonlinearizable D.O.F. (as lamination); and resolution at each time step of these few hard nonlinear equations by a special B.F.G.S. method. The author presents some significant types of simulation stemming from analyses of Mirage III, Super-Etendard, Mirage 2000 and Rafale. Author

N91-28162# Fokker B.V., Schipol-Oost (Netherlands).

THE USE OF MONTE CARLO SIMULATION IN DETERMINING LANDING GEAR LOADS DURING LANDING

R. vanderValk *In* AGARD, Landing Gear Design Loads 1990 12 p (For primary document see N91-28150 20-05)
Copyright Avail: NTIS HC/MF A13; Non-NATO Nationals requests available only from AGARD/Scientific Publications Executive

It is perceived by the airworthiness authorities that certification of automatic landing systems can only be done by applying statistical methods. However, if these particular statistical requirements are satisfied, there is no guarantee for the aircraft manufacturer that local limit and ultimate loads (stresses), developed during landing, occur at acceptable risk levels. Here, another approach is proposed, which is based on direct calculation of local loads by means of Monte Carlo simulation. In this context, the concept of load cases is superfluous (apart from preliminary design). Limited and ultimate loads are obtained by reading probability of exceedance distributions at desired risk levels. Maxima and minima are used for calculation of limit and ultimate loads. The whole time histories are used for the calculation of fatigue loads. Author

N91-28163# Politecnico di Milano (Italy). Dipt. di Ingegneria Aerospaziale.

DESIGN LANDING LOADS EVALUATION BY DYNAMIC SIMULATION OF FLEXIBLE AIRCRAFT

G. L. Ghiringhelli and M. Boschetto (Aeronautica Macchi S.p.A., Varese, Italy) *In* AGARD, Landing Gear Design Loads 1990 12 p (For primary document see N91-28150 20-05)
Copyright Avail: NTIS HC/MF A13; Non-NATO Nationals requests available only from AGARD/Scientific Publications Executive

Some significant applications of the integrated system GRAALL (Ground Roll Air And Landing Loads) to the analytical prediction of aircraft landing loads carried out at Aermacchi are presented. The capabilities of the system, able to treat both rigid and flexible models, make it a tool that can be profitably used during different phases of the design process. The results reported here describe the whole development of an actual design application; comparisons between analytical and experimental data are also provided. Author

N91-28164*# National Aeronautics and Space Administration. Langley Research Center, Hampton, VA.

F-106B AIRPLANE ACTIVE CONTROL LANDING GEAR DROP TEST PERFORMANCE

William E. Howell, John R. McCehee, Robert H. Daugherty, and William A. Vogler *In* AGARD, Landing Gear Design Loads 1990 8 p (For primary document see N91-28150 20-05)
Copyright Avail: NTIS HC/MF A13; Non-NATO Nationals requests available only from AGARD/Scientific Publications Executive CSCL 01C

Aircraft dynamic loads and vibrations resulting from landing impact and from runway and taxiway unevenness are recognized as significant factors in causing fatigue damage, dynamic stress on the airframe, crew and passenger discomfort, and reduction of the pilot's ability to control the aircraft during ground operations. One potential method for improving operational characteristics of aircraft on the ground is the application of active-control technology to the landing gears to reduce ground loads applied to the airframe. An experimental investigation was conducted on series-hydraulic active control nose gear. The experiments involved testing the gear in both passive and active control modes. Results of this investigation show that a series-hydraulic active-control gear is feasible and that such a gear is effective in reducing the loads transmitted by the gear to the airframe during ground operations. Author

N91-28165# BMW-A.G., Munich (Germany, F. R.). Structural Dynamics and Acoustics.

ACTIVELY DAMPED LANDING GEAR SYSTEM

Raymond Freymann *In* AGARD, Landing Gear Design Loads 1990 18 p (For primary document see N91-28150 20-05)
Copyright Avail: NTIS HC/MF A13; Non-NATO Nationals requests available only from AGARD/Scientific Publications Executive

An active control undercarriage for the alleviation of aircraft landing gear and structural loads during operation on rough runway surfaces is described. For quantitative determination of the improvements obtained with an active control undercarriage compared with conventional landing gear systems, aircraft taxiing is realistically simulated by means of a laboratory test set-up especially designed for this kind of testing. Author

N91-28166# SAC Technology Ltd., Walton-on-Thames (England).

ASSESSMENT OF THE APPLICATION OF THE WORKING GROUP 22 STANDARD BUMP CONCEPT TO A CURRENT MILITARY AIRCRAFT

E. F. Wild, B. R. Morris, and A. E. Dudman (British Aerospace Public Ltd. Co., Bristol, England) *In* AGARD, Landing Gear Design Loads 1990 19 p (For primary document see N91-28150 20-05)
Copyright Avail: NTIS HC/MF A13; Non-NATO Nationals requests available only from AGARD/Scientific Publications Executive

The application of standardized runway repair obstacles (SRO) for design purposes and post-design capability determinations was a basic outcome of SMP Working Group 22 deliberations. The WG 22 standardized shapes have been the basics of clearance work for a current military aircraft. To verify the adequacy of the SRO profile for this work the response to real repair profiles, obtained from practice repairs, has been related to the response to the SRO. Some comments on the SRO as a representation of real repairs and on some undesirable features of real repair profiles are presented. Author

N91-28167# Lawrence Livermore National Lab., CA.

EFFECTIVENESS OF TILTROTOR SUPPORT TO GROUND COMBAT

A. S. Warshawsky, D. U. Olness, J. E. Pimper, M. J. Uzelac, and J. Wilson Jan. 1991 144 p
(Contract W-7405-eng-48)
(DE91-013603; UCRL-ID-106416) Avail: NTIS HC/MF A07

The Janus combat simulation was used to compare the relative effectiveness of three aircraft fleets to reinforce a ground combat operation. The relative capabilities of these fleets were compared in terms of the outcome of the reinforced combat operation instead of simply tabulating tonnage delivered. The tactical scenario stressed time-sensitive mobility requirements and the requirement to negotiate a mid-intensity air defense threat. A fleet composed of V-22 tiltrotors and CH-53E helicopters was shown to be more effective than one composed of CH-60(S) and CH-53E helicopters. DOE

N91-28168*# Sikorsky Aircraft, Stratford, CT.

TECHNOLOGY NEEDS FOR HIGH SPEED ROTORCRAFT (2)

Mark W. Scott Aug. 1991 253 p
(Contract NAS2-13058)
(NASA-CR-177590; A-91215; NAS 1.26:177590) Avail: NTIS HC/MF A12 CSCL 01C

An analytical study was conducted to identify rotorcraft concepts best capable of combining a cruise speed of 350 to 450 knots with helicopter-like low speed attributes, and to define the technology advancements needed to make them viable by the year 2000. A systematic approach was used to compare the relative attributes and mission gross weights for a wide range of concepts, resulting in a downselect to the most promising concept/mission pairs. For transport missions, tilt-wing and variable diameter tilt-rotor (VDTR) concepts were found to be superior. For a military scout/attack role, the VDTR was best, although a shrouded rotor concept could provide a highly agile, low observable alternative if its weight empty fraction could be reduced. A design speed of 375 to 425 knots was found to be the maximum desirable for transport missions, with higher speed producing rapidly diminishing benefits in productivity. The key technologies that require advancement to make the tilt-wing and VDTR concepts viable are in the areas of wing and proprotor aerodynamics, efficient structural design, flight controls, refinement of the geared flap pitch control system, expansion of the speed/descent envelope, and the structural and aerodynamic tradeoffs of wing thickness and forward sweep. For the shrouded rotor, weight reduction is essential, particularly with respect to the mechanism for covering the rotor in cruise. Author

N91-28169 Ohio State Univ., Columbus.
QUESTIONS: ASSESSING THE STRUCTURE OF KNOWLEDGE AND THE USE OF INFORMATION IN DESIGN PROBLEM-SOLVING Ph.D. Thesis
James Richard McCracken 1990 288 p
Avail: Univ. Microfilms Order No. DA9111763

The exploratory, descriptive study of crew system design was conducted to develop basic information for development of an information support system for crew system design. Sampling methods used were interviews, investigator participation as a design group member, observation of design team integration meetings, and diaries kept by designers. Dissert. Abstr.

06 AIRCRAFT INSTRUMENTATION

Includes cockpit and cabin display devices; and flight instruments.

For related information see also *19 Spacecraft Instrumentation* and *35 Instrumentation and Photography.*

N91-28170# EG and G Energy Measurements, Inc., Las Vegas, NV.
THE IN-FLIGHT CALIBRATION OF A HELICOPTER-MOUNTED DAEDALUS MULTISPECTRAL SCANNER
L. K. Balick, C. J. Golanics, J. E. Shines, S. F. Biggar, and P. N. Slater (Arizona Univ., Tucson.) 1991 10 p Presented at the SPIE International Symposium on Optical Engineering and Photonics in Aerospace Sensing, Orlando, 1-5 Apr. 1991
(Contract DE-AC08-88NV-10617)
(DE91-013054; EGG-10617-1127; CONF-910450-12) Avail: NTIS HC/MF A02

A convenient way that was used to calibrate, in-flight, a helicopter mounted Daedalus multispectral scanner is described. It used four large canvas panels laid out in a square with a Spectralon panel as a reference. A calibrated Barnes modular multispectral radiometer, carried on a 2.2 m boom was rotated around a 2.5 m high tripod at the center of the square. The radiometer sampled the four large panels and the Spectralon panel once every two minutes. Atmospheric spectral transmittance measurements were made using a filter radiometer on an autotracking mount during the morning of the flight. The reflectance and optical depth data were used in an atmospheric radiative transfer code to predict the spectral radiances at the scanner. The calibration was completed by comparing the image digital counts to the predicted spectral radiances. DOE

07 AIRCRAFT PROPULSION AND POWER

Includes prime propulsion systems and systems components, e.g., gas turbine engines and compressors; and onboard auxilliary power plants for aircraft.

For related information see also *20 Spacecraft Propulsion and Power, 28 Propellants and Fuels,* and *44 Energy Production and Conversion.*

No abstracts in this category.

08 AIRCRAFT STABILITY AND CONTROL

Includes aircraft handling qualities; piloting; flight controls; and autopilots.

For related information see also *05 Aircraft Design, Testing and Performance.*

N91-28171 Illinois Univ., Urbana-Champaign.
ROBUST BIFURCATION BEHAVIOR IN THE PRESENCE OF EXTERNAL RANDOM EXCITATION Ph.D. Thesis
Gerard Siew Bing Leng 1990 186 p
Avail: Univ. Microfilms Order No. DA9114312

The effects of random external excitation on systems with marginally stable/unstable (critical) modes undergoing a soft loss of stability is examined within the context of bifurcation theory. Physically the problem is motivated by the flight dynamics of aircraft at large angles of attack and sideslip in a turbulent atmosphere. A qualitative criterion for robust bifurcation behavior is suggested. It is also found that the bifurcation behavior of systems with one critical mode is robust in the sense that the deterministic characteristics carry over to the steady state probability density function for the system in the presence of random external excitation. For systems with two critical modes, the bifurcation behavior is robust under special conditions on the relative degree of mode interaction and excitation intensities. Dissert. Abstr.

N91-28172 Princeton Univ., NJ.
STOCHASTIC ROBUSTNESS OF LINEAR MULTIVARIABLE CONTROL SYSTEMS: TOWARDS COMPREHENSIVE ROBUSTNESS ANALYSIS Ph.D. Thesis
Laura Ryan Ray 1991 287 p
Avail: Univ. Microfilms Order No. DA9112953

Stochastic robustness, a simple numerical procedure for estimating the stability and performance effects of parameter uncertainty in multivariable linear, time-invariant control systems, is introduced. Based on Monte Carlo evaluation of the system's closed-loop eigenvalues given parameter statistics, this analysis approach introduces the probability of instability as a scalar stability robustness measure. The related stochastic root locus, a portrayal of the root probability density, provides insight into modal variation characteristics of the closed-loop system. Dissert. Abstr.

09 RESEARCH AND SUPPORT FACILITIES (AIR)

Includes airports, hangars and runways; aircraft repair and overhaul facilities; wind tunnels; shock tubes; and aircraft engine test stands.

For related information see also *14 Ground Support Systems and Facilities (Space).*

N91-28173# Los Alamos National Lab., NM.
AIR COMBAT ENVIRONMENT TEST AND EVALUATION FACILITY AND THE DEVELOPMENT OF THE OFFENSIVE SENSORS LABORATORY
K. Lee, K. Hannon, and D. Macone (Naval Air Test Center, Patuxent River, MD.) Apr. 1991 13 p Presented at the 4th Joint Service Test Technology Symposium (TTS), Laurel, 8-11 Apr. 1991
(Contract W-7405-eng-36)
(DE91-011398; LA-UR-91-1117; CONF-9104232-1) Avail: NTIS HC/MF A03

Recent combat experience has brought to light a critical need to assess the mission effectiveness of Naval aviation weapons systems and vehicles against a myriad of new threats. Flight testing is the primary source of data on the effectiveness of our aircraft and weapons, but flight testing is costly and limited to only a few of the most crucial questions. Flight testing is also inherently a public event; it can be observed with impunity. Hence, flight testing is patently unsatisfactory for dealing with many issues related to national security interests. Senior decision-makers in the DoD require objective, quantitative assessments of the effectiveness of our weapons and people against literally thousands of possible combinations of threat and contingency planning conditions. A revolutionary approach is needed to obtain the requisite data. The Naval Air Test Center (NATC) has begun to develop an innovative system, known as the Air Combat Environment Test and Evaluation Facility (ACETEF), to meet this need. ACETEF is a fully integrated ground test facility that will use state-of-the-art simulation and stimulation techniques to provide test scenarios, which will reproduce the conditions of actual combat. This is being accomplished by integration of existing laboratories and development of new laboratories such as the Communications, Navigation and Identification (CNI) Laboratory and the Offensive Sensors Laboratory (OSL). This paper will describe ACETEF and the OSL development effort. DOE

N91-28174# Los Alamos National Lab., NM.
GENERATING STRONG SHOCK WAVES WITH A SUPERSONIC PERISTALTIC PUMP
R. Menikoff and K. S. Lackner 1991 5 p Presented at the 1991 American Physical Society (APS) Conference on Shock Compression of Condensed Matter, Williamsburg, 17-20 Jul. 1991
(Contract W-7405-eng-36)
(DE91-013228; LA-UR-91-1614; CONF-9107105-8) Avail: NTIS HC/MF A01

An axially phased implosion of a cylindrical tube with a phase velocity exceeding the sound speed of the fill material acts as a peristaltic pump which drives a shock wave along the axis. The region behind the onset of the phased implosion forms a converging-diverging nozzle. When appropriately designed the flow approaches a steady state in which the shock is planar and propagates near the nozzle entrance. The steady-state flow and the approach toward it have been derived in a one-dimensional model. The steady-state nozzle flow is well characterized: uniform across the channel, simple, and predictable in the axial direction. The flow in the converging section is very stable and not affected by the flow in the diverging section. These properties form the basis of an alternative shock tube design which is not limited in pressure by material strength of the tube wall. Experiments with a simple design have corroborated the theoretical predictions. A super-shock tube, in which the phased implosion is driven by high explosives, can reach extremely high pressures and energy densities. With a well characterized drive system, measurements of the steady-state shape of the nozzle can be used to determine the equation of state along an isentrope behind the axial shock. DOE

N91-28175*# National Aeronautics and Space Administration. Langley Research Center, Hampton, VA.
IMPROVED METHOD AND APPARATUS FOR MACH NUMBER CHANGE IN WIND TUNNEL Patent Application
Richard L. Puster, inventor (to NASA) 26 Jun. 1991 15 p
(NASA-Case-LAR-13548-1; NAS 1.71:LAR-13548-1; US-Patent-Appl-SN-721039) Avail: NTIS HC/MF A03 CSCL 14B

A description of an insert in a wind tunnel nozzle is presented. The insert has a variable sized passageway that helps create two pressure regions which, in turn, create a diffusion shock wave system and a compression wave system with each system having a plurality of waves. The diffusion shock wave system compresses a flow while the compression wave system turns the flow and is attenuated by the flow itself. NASA

N91-28176# Federal Aviation Administration, Atlantic City, NJ.
RUNWAY VISUAL RANGE (RVR) OPERATIONAL TEST AND EVALUATION (OT AND E)/INTEGRATION TEST PLAN
Joseph Goslin, Frances A. Mackuse, Bruce E. Ware, and Alanna Randazzo Aug. 1991 44 p
(DOT/FAA/CT-TN91/4) Avail: NTIS HC/MF A03

The Runway Visual Range (RVR) System consists of a group of sensors with associated software/firmwave, displays, and data distribution links. The data provided by this array of sensors provides runway visual range at various points of a precision approach runway. These RVR products are automatically processed and distributed to air traffic controllers. The data is then presented to the pilot by the controller in a numerical format equating to the number of feet forward along the runway that a pilot may be expected to see. Author

N91-28177# Los Alamos National Lab., NM.
COMPARISONS BETWEEN FAST SHOCK TUBE CALCULATIONS AND TESTS
J. F. Kerrisk and J. K. Meier 1991 5 p Presented at the 1991 American Physical Society (APS) Conference on Shock Compression of Condensed Matter, Williamsburg, 17-20 Jul. 1991
(Contract W-7405-eng-36)
(DE91-013496; LA-UR-91-1527; CONF-9107105-20) Avail: NTIS HC/MF A01

Tests were done to diagnose various aspects of the behavior of the shocked foam in the core of the fast shock tube. Calculations and test results of shock behavior in the foam are in good agreement. However, calculations with different foam equations of state differ in some details. Precursor shocks at the foam/high explosive interface were observed in some tests; a modified assembly procedure eliminated this problem. Calculations of shape and velocity of plates in direct contact with the foam are in relatively good agreement. Expansion of shocked foam down a barrel is complicated by perturbations from the barrel inlet and from deformed regions of the barrel. DOE

N91-28178# Sandia National Labs., Albuquerque, NM.
SANDIA'S NEW HYPERVELOCITY LAUNCHER (HVL)
L. C. Chhabildas, L. M. Barker, J. R. Asay, T. G. Trucano, and G. I. Kerley May 1991 28 p
(Contract DE-AC04-76DP-00789)
(DE91-014335; SAND-91-0657) Avail: NTIS HC/MF A03

A systematic study is described which addresses the technical issues associated with launching flier-plates intact to hypervelocities. First, very high pressures are needed to launch the flier plates to hypervelocities, and second this high pressure loading must be uniform and nearly shockless. To achieve both these criteria, a graded-density material referred to as a pillow is used to impact a flier plate. When this graded-density material is used to impact a flier plate at high velocities on a two-stage light-gas gun, nearly shockless megabar pressure pulses are introduced into the flier plate. Since the loading on the flier plate is shockless, melting of the flier plate is prevented. This technique has been used to launch a 2-mm thick titanium alloy (Ti-6Al-4V) plate to a velocity of 8.1 km/s, and a 1-mm thick aluminum alloy (6061-T6) plate to a velocity of 10.4 km/s. A method is described by which the flier plate velocities could be further augmented to velocities approaching 14 km/s. DOE

N91-28179# Los Alamos National Lab., NM.
HYPERVELOCITY PLATE ACCELERATION
S. P. Marsh and T. H. Tan 1991 8 p Presented at the 1991 American Physical Society (APS) Conference on Shock Compression of Condensed Matter, Williamsburg, 17-20 Jul. 1991
(Contract W-7405-eng-36)
(DE91-014738; LA-UR-91-2001; CONF-9107105-43) Avail: NTIS HC/MF A02

Shock tubes have been used to accelerate 1.5-mm-thick stainless steel plates to high velocity while retaining their integrity. The fast shock tubes are 5.1-cm-diameter, 15.2-cm-long cylinders of PBX-9501 explosive containing a 1.1-cm-diameter cylindrical core of low-density polystyrene foam. The plates have been placed directly in contact with one face of the explosive system. Plane-wave detonation was initiated on the opposite face. A Mach disk was formed in the imploding styrofoam core, which provided the impulse required to accelerate the metal plate to high velocity. Parametric studies were made on this system to find the effect of varying plate metal, plate thickness, foam properties, and addition of a barrel. A maximum plate velocity of 9.0 km/s has been observed. DOE

12 ASTRONAUTICS (GENERAL)

For extraterrestrial exploration see *91 Lunar and Planetary Exploration.*

N91-28180*# National Aeronautics and Space Administration, Washington, DC.
REPORT OF THE ADVISORY COMMITTEE ON THE FUTURE OF THE US SPACE PROGRAM
17 Dec. 1990 66 p Sponsored by NASA, Washington
(NASA-TM-105030; NAS 1.15:105030; PB91-181529) Avail: NTIS HC/MF A04 CSCL 22A

Th topics discussed include the following: (1) NASA space programs; (2) historical aspects; (3) space transportation; (4) space exploration; (5) program management; (6) resources; and (7) recommendations. Author

N91-28181# Army War Coll., Carlisle Barracks, PA.
SPACE SYSTEMS REQUIREMENTS: THE NAVY APPROACH Study Project
Gary D. Hagen 5 Apr. 1991 76 p
(AD-A236490) Avail: NTIS HC/MF A05 CSCL 22/1

Each of the armed services has a unique approach and bureaucracy for identifying systems requirements and applications of space systems to its operational forces. The historical and existing institutional structure of the naval space organization, some of the uses of space systems by operational units, and the naval processes for identification of future systems requirements are reviewed. Observations are made that the Navy experienced great success early on in the use of space. After a period of seeming malaise, the Navy's space program began a renaissance in the 1980s which is still in progress. A review of selected portions of the history of the U.S. space efforts in general, the naval space program in particular, and the military challenge of Soviet space achievements is presented. Portions of current institutional structuring of naval space organization are the result of policy decisions made 30 years ago. Suggestions are offered toward potential enhancement of the Navy space requirements process in the increasingly joint environment. GRA

N91-28182*# National Academy of Sciences - National Research Council, Washington, DC.
THE 1990 UPDATE TO STRATEGY FOR EXPLORATION OF THE INNER PLANETS
Larry W. Esposito, Robert O. Pepin, Andrew F. Cheng, Bruce M. Jakosky, Jonathan I. Lunine, Lucy-Ann McFadden, Christopher P. McKay, William B. McKinnon, Duane O. Muhleman, and Philip Nicholson (Cornell Univ., Ithaca, NY.) et al 1990 53 p
(Contract NASw-4102)
(NASA-CR-188728; NAS 1.26:188728) Avail: NTIS HC/MF A04 CSCL 22A

The Committee on Planetary and Lunar Exploration (COMPLEX) has undertaken to review and revise the 1978 report Strategy for Exploration of the Inner Planets, 1977-1987. The committee has found the 1978 report to be generally still pertinent. COMPLEX therefore issues its new report in the form of an update. The committee reaffirms the basic objectives for exploration of the planets: to determine the present state of the planets and their satellites, to understand the processes active now and at the origin of the solar system, and to understand planetary evolution, including appearance of life and its relation to the chemical history of the solar system. Author

N91-28237*# Martin Marietta Aerospace, Denver, CO. Dept. of Astronautics.
HUMANS TO MARS IN 1999
Robert Zubrin and David Baker *In* NASA, Washington, Space Transportation Propulsion Technology Symposium. Volume 3: Panel Session Summaries and Presentations May 1991 p 881-891 (For primary document see N91-28235 20-20)
Avail: NTIS HC/MF A99 CSCL 22A

N91-28253*# General Dynamics Corp., San Diego, CA.
THE SPACE EXPLORATION INITIATIVE. OPERATIONAL EFFICIENCY PANEL SPACE-BASING TECHNOLOGY REQUIREMENTS
Luis R. Pena *In* NASA, Washington, Space Transporation Propulsion Technology Symposium. Volume 3: Panel Session Summaries and Presentations May 1991 p 1051-1062 (For primary document see N91-28235 20-20)
Avail: NTIS HC/MF A99 CSCL 22A

N91-28258*# University of Central Florida, Orlando. Dept. of Mechanical Engineering.
DETERMINING CRITERIA FOR SINGLE STAGE TO ORBIT
Douglas G. Thorpe *In* NASA, Washington, Space Transporation Propulsion Technology Symposium. Volume 3: Panel Session Summaries and Presentations May 1991 p 1187-1201 (For primary document see N91-28235 20-20)
Avail: NTIS HC/MF A99 CSCL 22A

N91-28265*# General Dynamics Corp., San Diego, CA. Space Systems Div.
CULTURAL CHANGES IN AEROSPACE
Bill Strobl *In* NASA, Washington, Space Transportation Propulsion Technology Symposium. Volume 3: Panel Session Summaries and Presentations May 1991 p 1285-1290 (For primary document see N91-28235 20-20)
Avail: NTIS HC/MF A99 CSCL 22A

13 ASTRODYNAMICS

Includes powered and free-flight trajectories; and orbital and launching dynamics.

N91-28183 Nottingham Univ. (England).
PRECISE ORBIT DETERMINATION FOR GPS SATELLITES Ph.D. Thesis
Stephen Whalley 1990 256 p
Avail: Univ. Microfilms Order No. BRD-91989

The NAVSTAR Global Positioning System (GPS) has been under development by the U.S. Department of Defense since 1973. Although GPS was developed for precise instantaneous position and velocity determination, it can be used for high position relative positioning, with numerous applications for both surveyors and geodesists. The high resolution of the satellite's carrier phase has enabled relative positioning accuracies of the order of one part per million to be routinely obtained from only one or two hours of data. These accuracies are obtained using the broadcast ephemeris, which is the orbit data that is broadcast in the satellite's radio transmission. However, the broadcast ephemeris is estimated to be in error by up to 25 meters, and this error is one of the principle limitations for precise relative positioning with GPS. An alternative to the broadcast ephemeris is to determine the satellite orbits using the carrier phase measurements obtained from a network of GPS tracking stations. Described here are the algorithms and processing techniques used for the determination of GPS satellite orbits using double differenced carrier phase measurements. The data from these different GPS campaigns have been analyzed, which demonstrate a GPS orbital accuracy of between two and four meters, giving baseline accuracies of the order of one or two parts in ten million. Dissert. Abstr.

14 GROUND SUPPORT SYSTEMS AND FACILITIES (SPACE)

Includes launch complexes, research and production facilities; ground support equipment, e.g., mobile transporters; and simulators.

For related information see also *09 Research and Support Facilities (Air).*

N91-28184*# National Aeronautics and Space Administration. Langley Research Center, Hampton, VA.
SUSPENSION DEVICE FOR LOW-FREQUENCY STRUCTURES Patent Application
Meng-Sang Chew, inventor (to NASA) (Old Dominion Univ., Norfolk, VA.), Jer-Nan Juang, inventor (to NASA), and Li-Farn Yang, inventor (to NASA) 28 Mar. 1991 19 p
(NASA-Case-LAR-14272-1-CU; NAS 1.71:LAR-14272-1-CU; US-Patent-Appl-SN-678553) Avail: NTIS HC/MF A03 CSCL 14B

A suspension device is provided for simulating the free-free boundary conditions of space for a low frequency structure. A support cable is connected at one end to the test structure and is vertically guided by a guiding ring. The other end of the cable is connected to a cam having an outer circumference which supports the cable. A drive axle passes through the cam center of rotation and is rotatably journalled in a suitable manner to a rigid structure. Two torsion springs are provided about the drive axle. One end of each spring is connected to a respective face of the cam and the other end is connected to the fixed support. The cam is shaped and the torsion springs selected such that Wr(sub (t)) = T(sub s(t)), wherein W is the weight of the test structure; r(sub (t)) is the instantaneous moment arm defined as the perpendicular distance from the rotational center of the cam to the cable at time t, and T(sub s(t)) is the total spring torque exerted by the two springs on the cam at time t. The test structure is accordingly vertically suspended by the cable and the instantaneous moment arm compensates for any increased spring torque arising from a vertical displacement of the test structure to simulate space conditions. NASA

N91-28185 Pennsylvania State Univ., University Park.
A THEORETICAL AND EXPERIMENTAL STUDY OF THE INTERIOR BALLISTIC PROCESSES OF AN ELECTROTHERMAL GUN Ph.D. Thesis
Jun-Lon Chen 1990 225 p
Avail: Univ. Microfilms Order No. DA9117664

Both theoretical and experimental studies of the interior ballistic processes of an electrothermal (ET) gun are addressed. In the theoretical model, a gun system is divided into four different regions: (1) the Taylor cavity region created by the plasma jet and gaseous combustion products; (2) the continuous working fluid (i.e., liquid propellant region); (3) the dispersed droplet region; and (4) the projectile and barrel. The control volumes for these four different regions are first specified; then first principles of physics are applied to derive the governing equations for each region. A modified SIMPLE algorithm, which is suitable for highly compressible flow, is applied to solve the governing equations. Dissert. Abstr.

15 LAUNCH VEHICLES AND SPACE VEHICLES

Includes boosters; operating problems of launch/space vehicle systems; and reusable vehicles.

For related information see also *20 Spacecraft Propulsion and Power.*

N91-28267*# Vitro Corp., Washington, DC.
LAUNCH OPERATIONS MANPOWER YESTERDAY, TODAY AND TOMORROW
George Ojalehto *In* NASA, Washington, Space Transportation Propulsion Technology Symposium. Volume 3: Panel Session Summaries and Presentations May 1991 p 1303-1312 (For primary document see N91-28235 20-20)
Avail: NTIS HC/MF A99 CSCL 22D

16 SPACE TRANSPORTATION

Includes passenger and cargo space transportation, e.g., shuttle operations; and space rescue techniques.

For related information see also *03 Air Transportation and Safety* and *18 Spacecraft Design, Testing and Performance.* For space suits see *54 Man/System Technology and Life Support.*

N91-28186*# National Aeronautics and Space Administration. Lyndon B. Johnson Space Center, Houston, TX.
THERMALLY ACTIVATED RETAINER MEANS Patent Application
Margaret E. Grimaldi, inventor (to NASA) and Leslie S. Hertz, inventor (to NASA) 15 Jul. 1991 15 p
(NASA-Case-MSC-21793-1; NAS 1.71:MSC-21793-1; US-Patent-Appl-SN-731829) Avail: NTIS HC/MF A03 CSCL 22B

A retainer member suitable for retaining a gap filler placed in gaps between adjacent tile members is presented. One edge of the retainer member may be attached to the gap filler and another edge may be provided with a plurality of tab members which in an intermediate position do not interfere with placement or removal of the gap filler between tile members. The retainer member may be fabricated from a shape memory alloy which when heated to a specified memory temperature will thermally activate the tab members to predetermined memory positions engaging the tile members to retain the gap filler in the gap. This invention has particular application to the thermal tiles on space vehicles such as the Space Shuttle Orbiter. NASA

N91-28187# Edgerton, Germeshausen and Grier, Inc., Idaho Falls, ID.
HEAT RESISTANT MATERIALS AND THEIR FEASIBILITY ISSUES FOR A SPACE NUCLEAR TRANSPORTATION SYSTEM
C. S. Olsen 1991 10 p Presented at the 1st International Conference on Heat-Resistant Materials, Lake Geneva, 22-26 Sep. 1991
(Contract DE-AC07-76ID-01570)
(DE91-014071; EGG-M-90485; CONF-910909-5) Avail: NTIS HC/MF A02

A number of nuclear propulsion concepts based on solid-core nuclear propulsion are being evaluated for a nuclear propulsion transportation system to support the Space Exploration Initiative (SEI) involving the reestablishment of a manned lunar base and the subsequent exploration of Mars. These systems will require high-temperature materials to meet the operating conditions with appropriate reliability and safety built into these systems through the selection and testing of appropriate materials. The application of materials for nuclear thermal propulsion (NTP) and nuclear electric propulsion (NEP) systems and the feasibility issues identified for their use will be discussed. Some mechanical property measurements have been obtained, and compatibility tests were conducted to help identify feasibility issues. DOE

N91-28254*# Martin Marietta Aerospace, Denver, CO.
SPACE TRANSFER VEHICLES AND SPACE BASING
Joe Kelley *In* NASA, Washington, Space Transporation Propulsion Technology Symposium. Volume 3: Panel Session Summaries and Presentations May 1991 p 1063-1106 (For primary document see N91-28235 20-20)
Avail: NTIS HC/MF A99 CSCL 22B

N91-28263*# National Aeronautics and Space Administration, Washington, DC.
LESSONS LEARNED AND THEIR APPLICATION TO PROGRAM DEVELOPMENT AND CULTURAL ISSUES

Gilbert L. Roth *In its* Space Transportation Propulsion Technology Symposium. Volume 3: Panel Session Summaries and Presentations May 1991 p 1261-1276 (For primary document see N91-28235 20-20)
Avail: NTIS HC/MF A99 CSCL 22B

N91-28264*# Lockheed Space Operations Co., Washington, DC.
SPACE SHUTTLE REQUIREMENTS/CONFIGURATION EVOLUTION
E. P. Andrews *In* NASA, Washington, Space Transportation Propulsion Technology Symposium, Volume 3: Panel Session Summaries and Presentations May 1991 p 1277-1284 (For primary document see N91-28235 20-20)
Avail: NTIS HC/MF A99 CSCL 22B

17 SPACE COMM., SPACECRAFT COMM., COMMAND & TRACKING

Includes telemetry; space communications networks; astronavigation and guidance; and radio blackout.

For related information see also *04 Aircraft Communications and Navigation* and *32 Communications and Radar.*

No abstracts in this category.

18 SPACECRAFT DESIGN, TESTING AND PERFORMANCE

Includes satellites; space platforms; space stations; spacecraft systems and components such as thermal and environmental controls; and attitude controls.

For life support systems see *54 Man/System Technology and Life Support.* For related information see also *05 Aircraft Design, Testing and Performance, 39 Structural Mechanics,* and *16 Space Transportation.*

N91-28188# Oak Ridge National Lab., TN.
PERTURBED ENVIRONMENT ASSESSMENTS FOR SPACE VEHICLES
C. M. Haaland Jun. 1991 29 p
(Contract DE-AC05-84OR-21400)
(DE91-012630; ORNL/TM-11722) Avail: NTIS HC/MF A03

Three topics are discussed which are relevant to the technical assessment of the adequacy of environmental and response function analyses for space vehicles. First, a matrix is presented which summarizes exoatmospheric environmental modifiers and subsequent vehicular responses. Second, the early-time beta spectrum from a pulsed reactor experiment is compared with a beta spectrum which has been used for exoatmospheric analyses, showing that the average energy of the latter is significantly lower. Third, x ray transport results are compared between ATR5 and XPRT5 for the high endoatmospheric regime (80 to 200 kilofeet altitude). Results are within less than 3 pct. for altitudes of 150 kft and above, where the buildup factors are low, but differences up to 43 pct. occur at lower altitudes. Possible reasons for these discrepancies are discussed. DOE

N91-28189*# National Aeronautics and Space Administration. Marshall Space Flight Center, Huntsville, AL.
APPLICATIONS OF LOW LIFT TO DRAG RATIO AEROBRAKES USING ANGLE OF ATTACK VARIATION FOR CONTROL
J. A. Mulqueen Jun. 1991 99 p
(NASA-TM-103544; NAS 1.15:103544) Avail: NTIS HC/MF A05 CSCL 22B

Several applications of low lift to drag ratio aerobrakes are investigated which use angle of attack variation for control. The applications are: return from geosynchronous or lunar orbit to low Earth orbit; and planetary aerocapture at Earth and Mars. A number of aerobrake design considerations are reviewed. It was found that the flow impingement behind the aerobrake and the aerodynamic heating loads are the primary factors that control the sizing of an aerobrake. The heating loads and other loads, such as maximum acceleration, are determined by the vehicle ballistic coefficient, the atmosphere entry conditions, and the trajectory design. Several formulations for defining an optimum trajectory are reviewed, and the various performance indices that can be used are evaluated. The 'nearly grazing' optimal trajectory was found to provide the best compromise between the often conflicting goals of minimizing the vehicle propulsive requirements and minimizing vehicle loads. The relationship between vehicle and trajectory design is investigated further using the results of numerical simulations of trajectories for each aerobrake application. The data show the sensitivity of the trajectories to several vehicle parameters and atmospheric density variations. The results of the trajectory analysis show that low lift to drag ratio aerobrakes, which use angle of attack variation for control, can potentially be used for a wide range of aerobrake applications. Author

N91-28190 Alabama Univ., Huntsville.
DISCRETE POSYNOMIAL PROGRAMMING WITH APPLICATIONS TO SPACECRAFT PROTECTIVE STRUCTURES DESIGN OPTIMIZATION Ph.D. Thesis
Robert Alan Mog 1990 168 p
Avail: Univ. Microfilms Order No. DA9113971

The development of a discrete optimization technique for posynomial programs results in global nonlinear optimization under duality. The dual-to-primal variable transformation is eased under what is defined as posyserparable conditions. Additionally, partial invariance approaches may be successfully used under these conditions to reduce dual program degree of difficulty. Primal approaches using penalty function techniques supported by search methods result in less derivation and sufficiently fast convergence, but no guarantee of global optimality and little analytic information. Both dual and primal techniques have excellent application to discrete protective structures design optimization problems employing hypervelocity impact predictors. Dissert. Abstr.

N91-28191* National Aeronautics and Space Administration, Washington, DC.
LARGE SPACE STRUCTURES AND SYSTEMS IN THE SPACE STATION ERA: A BIBLIOGRAPHY WITH INDEXES
John J. Ferrainolo, comp. and George F. Lawrence, comp. May 1991 329 p
(NASA-SP-7085(02); NAS 1.21:7085(02)) Avail: NTIS HC A15 CSCL 22B

Bibliographies and abstracts are listed for 1219 reports, articles, and other documents introduced into the NASA scientific and technical information system between July 1, 1990 and December 31, 1990. The purpose is to provide helpful information to the researcher, manager, and designer in technology development and mission design according to system, interactive analysis and design, structural and thermal analysis and design, structural concepts and control systems, electronics, advanced materials, assembly concepts, propulsion, and solar power satellite systems. Author

19 SPACECRAFT INSTRUMENTATION

For related information see also *06 Aircraft Instrumentation* and *35 Instrumentation and Photography.*

No abstracts in this category.

20 SPACECRAFT PROPULSION AND POWER

Includes main propulsion systems and components, e.g., rocket engines; and spacecraft auxilliary power sources.

For related information see also *07 Aircraft Propulsion and Power, 28 Propellants and Fuels, 44 Energy Production and Conversion,* and *15 Launch Vehicles and Space Vehicles.*

N91-28192*# Thiokol Corp., Brigham City, UT. Space Operations.

FOLLOW-ON CABLE COUPLING LIGHTNING TEST, VOLUME 1 Final Test Report

Richard Danforth 31 Oct. 1990 43 p
(Contract NAS8-30490)
(NASA-CR-184123; NAS 1.26:184123; TWR-60187-Vol-1; Publ-91230) Avail: NTIS HC/MF A03 CSCL 21H

A redesigned solid rocket motor test article was subjected to simulated lightning strikes. This test was performed to evaluate the effects of lightning strike to the redesigned motor and Space Transportation System. The purpose of the test was to evaluate the performance of systems tunnel design changes when subjected to the lightning discharges. The goal of the design changes was to reduce lightning induced coupling to cables within the systems tunnel. The test article was subjected to several different amounts and kinds of discharges. Changes in coupling levels detected during the tests are recorded. The dominant mode of coupling appears to be caused by the diffusion of the magnetic fields through the system tunnel covers. The results from bond strap integrity testing showed that 16 of 18 bond straps survived. Design change evaluations showed that coupling reduction ranged from 0 to 36 decibels for each type of cable. The type of cable has less effect on coupling than does strike location and strike levels. Recommendations for design changes are made. Author

N91-28193*# National Aeronautics and Space Administration, Washington, DC.

SPACE TRANSPORTATION PROPULSION TECHNOLOGY SYMPOSIUM. VOLUME 2: SYMPOSIUM PROCEEDINGS

May 1991 693 p Symposium held in State College, PA, 25-29 Jun. 1990
(NASA-CP-3112-Vol-2; NAS 1.55:3112-Vol-2) Avail: NTIS HC/MF A99 CSCL 21H

The Space Transportation Propulsion Symposium was held to provide a forum for communication within the propulsion technology developer and user communities. Emphasis was placed on propulsion requirements and initiatives to support current, next generation, and future space transportation systems, with the primary objectives of discerning whether proposed designs truly meet future transportation needs and identifying possible technology gaps, overlaps, and other programmatic deficiencies. Key space transportation propulsion issues were addressed through four panels with government, industry, and academia membership. The panels focused on systems engineering and integration; development, manufacturing and certification; operational efficiency; and program development and cultural issues. For individual titles, see N91-28194 through N91-28234.

N91-28194*# National Aeronautics and Space Administration. Marshall Space Flight Center, Huntsville, AL.

THE SPACE EXPLORATION INITIATIVE

Pete Priest *In* NASA, Washington, Space Transportation Propulsion Technology Symposium. Volume 2: Symposium Proceedings May 1991 p 5-38 (For primary document see N91-28193 20-20)
Avail: NTIS HC/MF A99 CSCL 21H

A number of view graph charts are presented which outline the presentation. Outlined are reasons for going to Mars, why it is necessary to go to the Moon first, and the presidential decision on the space exploration initiative. Other representative charts are entitled: Lunar transportation system requirement drivers; Mars transportation system requirement drivers; National space policy goals; Exploration hardware needed; Mars mission profile; Science on the Moon and Mars; and Two independent reviews. E.R.

N91-28195*# National Aeronautics and Space Administration, Washington, DC.

NASA'S ADVANCED SPACE TRANSPORTATION SYSTEM LAUNCH VEHICLES

Darrell R. Branscome *In its* Space Transportation Propulsion Technology Symposium. Volume 2: Symposium Proceedings May 1991 p 39-6 (For primary document see N91-28193 20-20)
Avail: NTIS HC/MF A99 CSCL 21H

Some insight is provided into the advanced transportation planning and systems that will evolve to support long term mission requirements. The general requirements include: launch and lift capacity to low earth orbit (LEO); space based transfer systems for orbital operations between LEO and geosynchronous equatorial orbit (GEO), the Moon, and Mars; and Transfer vehicle systems for long duration deep space probes. These mission requirements are incorporated in the NASA Civil Needs Data Base. To accomplish these mission goals, adequate lift capacity to LEO must be available: to support science and application missions; to provide for construction of the Space Station Freedom; and to support resupply of personnel and supplies for its operations. Growth in lift capacity must be time phased to support an expanding mission model that includes Freedom Station, the Mission to Planet Earth, and an expanded robotic planetary program. The near term increase in cargo lift capacity associated with development of the Shuttle-C is addressed. The joint DOD/NASA Advanced Launch System studies are focused on a longer term new cargo capability that will significantly reduce costs of placing payloads in space. Author

N91-28196*# Aerospace Industries Association of America, Inc., Washington, DC.

MAINTAINING TECHNICAL EXCELLENCE REQUIRES A NATIONAL PLAN

T. F. Davidson *In* NASA, Washington, Space Transportation Propulsion Technology Symposium. Volume 2: Symposium Proceedings May 1991 p 69-84 (For primary document see N91-28193 20-20)
Avail: NTIS HC/MF A99 CSCL 21H

To meet the challenge of technical excellence, AIA established a rocket propulsion committee to develop the National Rocket Propulsion Strategic Plan. Developing such a plan required a broad spectrum of experience and disciplines. The Strategic Plan team needed the participation of industry, government, and academia. The plan provides, if followed, a means for the U.S. to maintain technical excellence and world leadership in rocket propulsion. To implement the National Rocket Propulsion Strategic Plan is to invest in the social, economic, and technological futures of America. The plan lays the basis for upgrading existing propulsion systems and a firm base for future full scale development, production, and operation of rocket propulsion systems for space, defense, and commercial applications. Author

N91-28197*# National Aeronautics and Space Administration. John F. Kennedy Space Center, Cocoa Beach, FL.

A WHITE PAPER: OPERATIONAL EFFICIENCY. NEW APPROACHES TO FUTURE PROPULSION SYSTEMS

Russel Rhodes and George Wong (Rockwell International Corp., Canoga Park, CA.) *In* NASA, Washington, Space Transportation Propulsion Technology Symposium. Volume 2: Symposium Proceedings May 1991 p 85-106 (For primary document see N91-28193 20-20)
Avail: NTIS HC/MF A99 CSCL 21H

Advanced launch systems for the next generation of space transportation systems (1995 to 2010) must deliver large payloads (125,000 to 500,000 lbs) to low earth orbit (LEO) at one tenth of today's cost, or 300 to 400 \$/lb of payload. This cost represents an order of magnitude reduction from the Titan unmanned vehicle cost of delivering payload to orbit. To achieve this sizable reduction, the operations cost as well as the engine cost must both be lower than current engine system. The Advanced Launch System (ALS) is studying advanced engine designs, such as the Space Transportation Main Engine (STME), which has achieved notable reduction in cost. The results are presented of a current study wherein another level of cost reduction can be achieved by designing the propulsion module utilizing these advanced engines for enhanced operations efficiency and reduced operations cost. Author

N91-28198*# Rockwell International Corp., Canoga Park, CA.
OPERATIONALLY EFFICIENT PROPULSION SYSTEM STUDY (OEPPS)
G. S. Wong, G. S. Waldrop, R. J. Byrd, and J. M. Ziese *In* NASA, Washington, Space Transportation Propulsion Technology Symposium. Volume 2: Symposium Proceedings May 1991 p 107-126 (For primary document see N91-28193 20-20)
(Contract NAS10-11568)
Avail: NTIS HC/MF A99 CSCL 21H

A description is presented, through view graphs, of the problems encountered in today's launch vehicles and how these problems have adversely affected the ability to achieve serviceability, reliability, and operability. The need is emphasized to recognize and understand the operations problems and the effort that must be made to avoid them in future designs. Technology areas that will enhance operations requirements are also presented. Author

N91-28199*# Rockwell International Corp., Canoga Park, CA. COMSTAC Technology and Innovation Working Group.
EXPENDABLE LAUNCH VEHICLE PROPULSION
Paul N. Fuller *In* NASA, Washington, Space Transportation Propulsion Technology Symposium. Volume 2: Symposium Proceedings May 1991 p 127-148 (For primary document see N91-28193 20-20)
Avail: NTIS HC/MF A99 CSCL 21H

The current status is reviewed of the U.S. Expendable Launch Vehicle (ELV) fleet, the international competition, and the propulsion technology of both domestic and foreign ELVs. The ELV propulsion technology areas where research, development, and demonstration are most needed are identified. These propulsion technology recommendations are based on the work performed by the Commercial Space Transportation Advisory Committee (COMSTAC), an industry panel established by the Dept. of Transportation. Author

N91-28200*# National Aeronautics and Space Administration, Washington, DC.
SPACE SHUTTLE PROPULSION SYSTEMS
Russell Bardos *In its* Space Transportation Propulsion Technology Symposium. Volume 2: Symposium Proceedings May 1991 p 149-166 (For primary document see N91-28193 20-20)
Avail: NTIS HC/MF A99 CSCL 21H

This is a presentation of view graphs. The design parameters are given for the redesigned solid rocket motor (RSRM), the Advanced Solid Rocket Motor (ASRM), Space Shuttle Main Engine (SSME), Solid Rocket Booster (SRB) separation motor, Orbit Maneuvering System (OMS), and the Reaction Control System (RCS) primary and Vernier thrusters. Space shuttle propulsion issues are outlined along with ASA program definition, ASA program selection methodology, its priorities, candidates, and categories. E.R.

N91-28201*# National Aeronautics and Space Administration, Washington, DC.
CURRENT SYSTEMS: UPPER STAGES
Charles R. Gunn *In its* Space Transportation Propulsion Technology Symposium. Volume 2: Symposium Proceedings May 1991 p 167-173 (For primary document see N91-28193 20-20)
Avail: NTIS HC/MF A99 CSCL 21H

The United States orbital transfer vehicles are presented: PAM-D (Payload Assist Module); PAM-D2; IUS (Inertial Upper Stage); and TOS (Transfer Orbit Stage). This presentation is represented by viewgraphs. B.G.

N91-28202*# Pratt and Whitney Aircraft, West Palm Beach, FL. Space Propulsion and Systems.
CRYOGENIC UPPER STAGE PROPULSION: RL10 AND DERIVATIVE ENGINES
James R. Brown *In* NASA, Washington, Space Transportation Propulsion Technology Symposium. Volume 2: Symposium Proceedings May 1991 p 174-195 (For primary document see N91-28193 20-20)
Avail: NTIS HC/MF A99 CSCL 21H

The capabilities and characteristics of the RL10 rocket engine are examined. The engine model history is presented. The RL10 derivatives are also outlined. The presentation is represented by viewgraphs. B.G.

N91-28203*# Jet Propulsion Lab., California Inst. of Tech., Pasadena. Propulsion and Chemical Systems Section.
SATELLITE/SPACECRAFT PROPULSION
Mack W. Dowdy *In* NASA, Washington, Space Transportation Propulsion Technology Symposium. Volume 2: Symposium Proceedings May 1991 p 197-223 (For primary document see N91-28193 20-20)
Avail: NTIS HC/MF A99 CSCL 21H

Propulsion system performance has high leverage for many future missions because of large propellant mass requirements. Relatively small performance improvements can translate into large increases in payload and science return. Contamination control becomes more important as science instruments become more sensitive. This places more emphasis on exhaust plume contamination control. The need for reliable operation and long life places increased importance on health monitoring and control of spacecraft propulsion systems. The need for accurate spacecraft pointing and control increases the need for small impulse-bit thrusters. This presentation is represented by viewgraphs. Author

N91-28204*# National Aeronautics and Space Administration. Lyndon B. Johnson Space Center, Houston, TX.
SHUTTLE DERIVED MANNED TRANSPORTATION SYSTEMS
Wayne L. Ordway *In* NASA, Washington, Space Transportation Propulsion Technology Symposium. Volume 2: Symposium Proceedings May 1991 p 225-245 (For primary document see N91-28193 20-20)
Avail: NTIS HC/MF A99 CSCL 21H

Shuttle derivatives have been under study by the National Aeronautics and Space Administration (NASA) for a number of years. With Space Station Freedom and the Lunar/Mars Initiative established as national objectives, the demand for access to earth orbit is accelerating. These objectives have resulted in efforts to address additional launch requirements that must be met as the turn of the century approaches. Among the top level requirements are increased safety, higher reliability, lower cost, and the need for heavy lift launch capability. To satisfy these requirements, some of the largest technology demands will be placed upon the propulsion systems. Shuttle derived manned concepts are presented and the associated propulsion issues which arise from the top level requirements are discussed. These concepts are presented in terms of an overall architecture which can be achieved with modest up-front development. Author

N91-28205*# National Aeronautics and Space Administration. Marshall Space Flight Center, Huntsville, AL.
NEXT GENERATION EARTH-TO-ORBIT SPACE TRANSPORTATION SYSTEMS: UNMANNED VEHICLES AND LIQUID/HYBRID BOOSTERS
Uwe Hueter *In* NASA, Washington, Space Transportation Propulsion Technology Symposium. Volume 2: Symposium Proceedings May 1991 p 247-270 (For primary document see N91-28193 20-20)
Avail: NTIS HC/MF A99 CSCL 21H

The United States civil space effort when viewed from a launch vehicle perspective tends to categorize into pre-Shuttle and Shuttle eras. The pre-Shuttle era consisted of expendable launch vehicles where a broad set of capabilities were matured in a range of vehicles, followed by a clear reluctance to build on and utilize those systems. The Shuttle era marked the beginning of the U.S. venture into reusable space launch vehicles and the consolidation of launch systems used to this one vehicle. This led to a tremendous capability, but utilized men on a few missions where it was not essential and compromised launch capability resiliency in the long term. Launch vehicle failures, between the period of Aug. 1985 and May 1986, of the Titan 34D, Shuttle Challenger, and the Delta vehicles resulted in a reassessment of U.S. launch vehicle capability. The reassessment resulted in President Reagan issuing a new National Space Policy in 1988 calling for more coordination between Federal agencies, broadening the launch capabilities and preparing for manned flight beyond the Earth into the solar system. As a result, the Department of Defense (DoD) and NASA are jointly assessing the requirements and needs for this nations's future transportation system. Reliability/safety, balanced fleet, and resiliency are the cornerstone to the future. An insight is provided into the current thinking in establishing future unmanned earth-to-orbit (ETO) space transportation needs and capabilities. A background of previous launch capabilities, future needs, current and proposed near term systems, and system considerations to assure future mission need will be met, are presented. The focus is on propulsion options associated with unmanned cargo vehicles and liquid booster required to assure future mission needs will be met. Author

N91-28206*# National Aeronautics and Space Administration. Marshall Space Flight Center, Huntsville, AL.

SOLID ROCKET PROPULSION

Ronald L. Nichols and C. Clinton *In* NASA, Washington, Space Transportation Propulsion Technology Symposium. Volume 2: Symposium Proceedings May 1991 p 271-278 (For primary document see N91-28193 20-20)

Avail: NTIS HC/MF A99 CSCL 21H

The solid rocket motor failure database; current programs; and shortfalls of solid rocket propulsion are examined. This presentation is represented by viewgraphs. Author

N91-28207*# Thiokol Corp., Brigham City, UT.

NEXT GENERATION SOLID BOOSTERS

R. K. Lund *In* NASA, Washington, Space Transportation Propulsion Technology Symposium. Volume 2: Symposium Proceedings May 1991 p 279-286 (For primary document see N91-28193 20-20)

Avail: NTIS HC/MF A99 CSCL 21H

Space transportation solid rocket motor systems; Shuttle derived heavy lift launch vehicles; advanced launch system (ALS) derived heavy lift launch vehicles; large launch solid booster vehicles are outlined. Performance capabilities and concept objectives are presented. Small launch vehicle concepts; enabling technologies; reusable flyback booster system; and high-performance solid motors for space are briefly described. This presentation is represented by viewgraphs. B.G.

N91-28208*# National Aeronautics and Space Administration. Marshall Space Flight Center, Huntsville, AL.

ADVANCED LAUNCH SYSTEM

Jan C. Monk *In* NASA, Washington, Space Transportation Propulsion Technology Symposium. Volume 2: Symposium Proceedings May 1991 p 287-299 (For primary document see N91-28193 20-20)

Avail: NTIS HC/MF A99 CSCL 21H

The Advanced Launch System (ALS) is presented. The costs, reliability, capabilities, infrastructure are briefly described. Quality approach, failure modes, structural design, technology benefits, and key facilities are outlined. This presentation is represented by viewgraphs. B.G.

N91-28209*# Air Force Avionics Lab., Wright-Patterson AFB, OH.

SPACE SYSTEMS PROPULSION TECHNOLOGY

Dale Hite *In* NASA, Washington, Space Transportation Propulsion Technology Symposium. Volume 2: Symposium Proceedings May 1991 p 301-309 (For primary document see N91-28193 20-20)

Avail: NTIS HC/MF A99 CSCL 21H

The following topics are presented in viewgraph form: (1) space systems propulsion technology vision; (2) orbit transfer and maneuvering propulsion; (3) modular/storable orbit transfer/ maneuvering propulsion; (4) cryogenic orbital transfer vehicle (OTV) propulsion; (5) advanced propulsion; (6) high energy density matter; (7) nuclear propulsion; (8) space launch propulsion; (9) advanced launch development program technologies at the Astronautics Laboratory (AL); and (10) AL support to the National Aerospace Plane (NASP). K.S.

N91-28210*# National Aeronautics and Space Administration, Washington, DC.

NEXT GENERATION: UNMANNED LAUNCH VEHICLES AND UPPER STAGES: THE NEEDS

Charles R. Gunn *In its* Space Transportation Propulsion Technology Symposium. Volume 2: Symposium Proceedings May 1991 p 311-325 (For primary document see N91-28193 20-20)

Avail: NTIS HC/MF A99 CSCL 21H

The focus is on common vehicle elements, higher mission success, and lower transportation cost with respect to the common needs of the Department of Defense, NASA, and U.S. Industry. The following are presented in viewgraph form: (1) perspectives on mission costs and failures; (2) the recurring costs of the Delta 7925, Atlas/Centar, Titan 3, and Titan 4; (3) U.S. launches from 1957-1987 of Vanguard, Jupiter, Thor/Delta, Juno, Atlas, Scout, Redstone, Saturn, Titan, and the Space Transportation System; and (4) subsystem sources of failure. The following topics are also briefly presented: (1) engine costs; (2) a summary of flight experience; (3) recommendations for next generation space transportation; (4) low cost engine demonstration; and (5) the next generation commercial expendable launch vehicle (ELV) needs estimate. K.S.

N91-28211*# National Aeronautics and Space Administration. Marshall Space Flight Center, Huntsville, AL.

NEXT GENERATION: IN-SPACE TRANSPORTATION SYSTEM(S)

Fredrick Huffaker, Jerry Redus, and David L. Kelley *In* NASA, Washington, Space Transportation Propulsion Technology Symposium. Volume 2: Symposium Proceedings May 1991 p 327-352 (For primary document see N91-28193 20-20)

Avail: NTIS HC/MF A99 CSCL 21H

The development of the next generation In-Space Transportation System presents a unique challenge to the design of a propulsion system for the Space Exploration Initiative (SEI). Never before have the requirements for long-life, multiple mission use, space basing, high reliability, man-rating, and minimum maintenance come together with performance in one system that must protect the lives of space travelers, support the mission logistics needs, and do so at an acceptable cost. The challenge that is presented is to quantify the bounds of these requirements. The issue is one of degree. The length of acceptable life in space, the time it takes for reuse to pay off, and the degree to which space basing is practical (full, partial, or expended) are the issues that determine the reusable bounds of a design and include dependability, contingency capabilities, resiliency, and minimum dependence on a maintenance node in preparation for and during a mission. Missions to planet earth, other non-NASA missions, and planetary missions will provide important but less demanding requirements for the transportation systems of the future. The mission proposed for the SEI require a family of transportation vehicles to meet the requirements for establishing a permanent human presence on the Moon and eventually on Mars. Specialized vehicles are needed to accomplish the different phases of each mission. These large scale missions require assembly in space and will provide the greatest usage of the planned integrated transportation system. The current approach to defining the In-Space Transportation System for the SEI Moon missions with later Mars mission applications is presented. Several system development options, propulsion concepts, current/proposed activities are reviewed, and key propulsion design criteria, issues, and technology challenges for the next generation In-Space Transportation System(s) are outlined. Author

N91-28212*# National Aeronautics and Space Administration. Lewis Research Center, Cleveland, OH.
ADVANCED CRYO PROPULSION SYSTEMS
William K. Tabata *In* NASA, Washington, Space Transportation Propulsion Technology Symposium. Volume 2: Symposium Proceedings May 1991 p 353-364 (For primary document see N91-28193 20-20)
Avail: NTIS HC/MF A99 CSCL 21H

The following topics are presented in viewgraph form: (1) advanced space engine (ASE) chronology; (2) an ASE description; (3) a single expander; (4) a dual expander; (5) split expander; (6) launch vehicle start; (7) space start; (8) chemical transfer propulsion; and (9) an advanced expander test bed. K.S.

N91-28213*# National Aeronautics and Space Administration. Langley Research Center, Hampton, VA.
PROPULSION STUDIES FOR ADVANCED MANNED LAUNCH SYSTEMS
D. Freeman *In* NASA, Washington, Space Transportation Propulsion Technology Symposium. Volume 2: Symposium Proceedings May 1991 p 365-381 (For primary document see N91-28193 20-20)
Avail: NTIS HC/MF A99 CSCL 21H

The topics covered include the following: (1) the next manned space transportation system; (2) development of a new hydrogen booster engine (like the Space Transportation Booster Engine); (3) development of a new hydrogen engine (like the Space Transportation Main Engine); and (4) an increase in oxidizer to fuel ratio from the current Space Shuttle Main Engine level. This document is presented in viewgraph form. K.S.

N91-28214*# National Aeronautics and Space Administration, Washington, DC.
NATIONAL AERO-SPACE PLANE (NASP) PROGRAM
Ming H. Tank *In its* Space Transportation Propulsion Technology Symposium. Volume 2: Symposium Proceedings May 1991 p 383-407 (For primary document see N91-28193 20-20)
Avail: NTIS HC/MF A99 CSCL 21H

A program to develop the technology for reusable airbreathing hypersonic/transatmospheric vehicles is addressed. Information on the following topics is presented in viewgraph form: (1) the National Aerospace Plane (NASP) program schedule; (2) the NASP program organization; (3) competitive strategy; (4) propulsion options; (5) wind tunnel data available for NASP; (6) ground track of envelope expansion; and (7) altitude vs. Mach number. A NASP/Space Shuttle comparison, NASP configuration matrix, and the propulsion concept of a high speed scramjet are also briefly addressed. K.S.

N91-28215*# National Aeronautics and Space Administration. Lewis Research Center, Cleveland, OH.
FUTURISTIC SYSTEMS: SOLAR AND NUCLEAR ELECTRIC PROPULSION
Dave Byers *In* NASA, Washington, Space Transportation Propulsion Technology Symposium. Volume 2: Symposium Proceedings May 1991 p 409-429 (For primary document see N91-28193 20-20)
Avail: NTIS HC/MF A99 CSCL 21H

The following topics are addressed: (1) in-space propulsion impacts; (2) electric propulsion; (3) mission impacts of electric propulsion; and (4) summaries of electric propulsion status and solar and nuclear propulsion. K.S.

N91-28216*# National Aeronautics and Space Administration, Washington, DC.
NUCLEAR THERMAL PROPULSION
Gary L. Bennett *In its* Space Transportation Propulsion Technology Symposium. Volume 2: Symposium Proceedings May 1991 p 431-449 (For primary document see N91-28193 20-20)
Avail: NTIS HC/MF A99 CSCL 21H

This document is presented in viewgraph form, and the topics covered include the following: (1) the direct fission-thermal propulsion process; (2) mission applications of direct fission-thermal propulsion; (3) nuclear engines for rocket vehicles; (4) manned mars landers; and (5) particle bed reactor design. K.S.

N91-28217*# National Aeronautics and Space Administration, Washington, DC.
SPACE FUSION ENERGY CONVERSION USING A FIELD REVERSED CONFIGURATION REACTOR: A NEW TECHNICAL APPROACH FOR SPACE PROPULSION AND POWER
Norman R. Schulze, George H. Miley, and John F. Santarius (Wisconsin Univ., Madison.) *In its* Space Transportation Propulsion Technology Symposium. Volume 2: Symposium Proceedings May 1991 p 451-499 (For primary document see N91-28193 20-20)
Avail: NTIS HC/MF A99 CSCL 21H

The fusion energy conversion design approach, the Field' Reversed Configuration (FRC) - when burning deuterium and helium-3, offers a new method and concept for space transportation with high energy demanding programs, like the Manned Mars Mission and planetary science outpost missions require. FRC's will increase safety, reduce costs, and enable new missions by providing a high specific power propulsion system from a high performance fusion engine system that can be optimally designed. By using spacecraft powered by FRC's the space program can fulfill High Energy Space Missions (HESM) in a manner not otherwise possible. FRC's can potentially enable the attainment of high payload mass fractions while doing so within shorter flight times. Author

N91-28218*# Jet Propulsion Lab., California Inst. of Tech., Pasadena. Propulsion Systems Section.
ADVANCED PROPULSION CONCEPTS
Robert H. Frisbee *In* NASA, Washington, Space Transportation Propulsion Technology Symposium. Volume 2: Symposium Proceedings May 1991 p 501-521 (For primary document see N91-28193 20-20)
Avail: NTIS HC/MF A99 CSCL 21H

A variety of Advanced Propulsion Concepts (APC) is discussed. The focus is on those concepts that are sufficiently near-term that they could be developed for the Space Exploration Initiative. High-power (multi-megawatt) electric propulsion, solar sails, tethers, and extraterrestrial resource utilization concepts are discussed. A summary of these concepts and some general conclusions on their technology development needs are presented. Author

N91-28219*# Pennsylvania State Univ., University Park.
A REVIEW OF LIQUID ROCKET PROPULSION PROGRAMS IN JAPAN
Charles L. Merkle *In* NASA, Washington, Space Transportation Propulsion Technology Symposium. Volume 2: Symposium Proceedings May 1991 p 523-547 (For primary document see N91-28193 20-20)
Avail: NTIS HC/MF A99 CSCL 21H

An assessment of Japan's current capabilities in the areas of space and transatmospheric propulsion is presented. The primary focus is upon Japan's programs in liquid rocket propulsion and in space plane and related transatmospheric areas. Brief reference is also made to their solid rocket programs, as well as to their supersonic air breathing propulsion efforts that are just getting underway. Author

N91-28220*# Rockwell International Corp., Canoga Park, CA. Rocketdyne Advanced Programs.
SPACE TRANSPORTATION PROPULSION USSR LAUNCHER TECHNOLOGY, 1990
In NASA, Washington, Space Transportation Propulsion Technology Symposium. Volume 2: Symposium Proceedings May

1991 p 549-580 (For primary document see N91-28193 20-20)
Avail: NTIS HC/MF A99 CSCL 21H

Space transportation propulsion U.S.S.R. launcher technology is discussed. The following subject areas are covered: Energia background (launch vehicle summary, Soviet launcher family) and Energia propulsion characteristics (booster propulsion, core propulsion, and growth capability). Author

N91-28221*# Orbital Technologies Corp., Madison, WI.
OVERVIEW OF EUROPEAN AND OTHER NON-US/USSR/JAPAN LAUNCH VEHICLE AND PROPULSION TECHNOLOGY PROGRAMS
Eric E. Rice *In* NASA, Washington, Space Transportation Propulsion Technology Symposium. Volume 2: Symposium Proceedings May 1991 p 581-615 (For primary document see N91-28193 20-20)
Avail: NTIS HC/MF A99 CSCL 21H

The following subject areas are covered: majority of propulsion technology development work is directly related to the ESA's Ariane 5 program and heavily involves SEP (Societe Europeenne de Propulsion) in all areas; Hermes; advanced work on magnetic bearings for turbomachinery; electric propulsion using Cs and Xe propellants done by SEP in France, MBB ERNO in West Germany, and by Culham Lab in UK; successfully tested fired H/O composite nozzle exit cone on 3rd stage of Ariane; turbine blades made of composites to allow increase in gas temperature and improvement in efficiency; combined cycle (turboramjet-rocket) engine analysis work done by Hyperspace; and ESA advanced program studies. Author

N91-28222*# Pennsylvania State Univ., University Park. Dept. of Mechanical Engineering.
AN OVERVIEW OF THE PENN STATE PROPULSION ENGINEERING RESEARCH CENTER
Charles L. Merkle *In* NASA, Washington, Space Transportation Propulsion Technology Symposium. Volume 2: Symposium Proceedings May 1991 p 629-635 (For primary document see N91-28193 20-20)
Avail: NTIS HC/MF A99 CSCL 21H

An overview of the Penn State Propulsion Engineering Research Center is presented. The following subject areas are covered: research objectives and long term perspective of the Center; current status and operational philosophy; and brief description of Center projects (combustion, fluid mechanics and heat transfer, materials compatibility, turbomachinery, and advanced propulsion concepts). Author

N91-28223*# Pennsylvania State Univ., University Park. Dept. of Mechanical Engineering.
CRYOGENIC COMBUSTION LABORATORY
R. J. Santoro and Kenneth K. Kuo *In* NASA, Washington, Space Transportation Propulsion Technology Symposium. Volume 2: Symposium Proceedings May 1991 p 637-644 (For primary document see N91-28193 20-20)
Avail: NTIS HC/MF A99 CSCL 21H

The objective is to establish a major experimental laboratory for studying fundamental processes such as mixing and combustion under liquid rocket engine conditions. The capability of this laboratory will include operation using a variety of fuel and oxidizer systems including liquid oxygen and liquid hydrocarbons. In addition to providing the proper facilities for supplying and controlling these fuels and oxidizers, a specific effort is being made to provide a state-of-the-art diagnostic capability for combustion measurements. In particular, optical and laser-based techniques are being emphasized for measurements of species, velocities, and spray characteristics. Author

N91-28224*# Pennsylvania State Univ., University Park. Dept. of Mechanical Engineering.
IGNITION AND COMBUSTION OF METALLIZED PROPELLANTS c25
Stephen R. Turns *In* NASA, Washington, Space Transportation Propulsion Technology Symposium. Volume 2: Symposium Proceedings May 1991 p 645-653 (For primary document see N91-28193 20-20)
Avail: NTIS HC/MF A99 CSCL 21B

The overall objective is the development of a fundamental understanding of the ignition and combustion of aluminum-based slurry (or gel) propellant droplets using a combination of experiment and analysis. Specific objectives are the following: (1) The development and application of a burner/spray rig and single particle optical diagnosis to study the detailed ignition and combustion behavior of small droplets; (2) Understanding the role of surfactants and gellants (or other additives) in promoting or inhibiting secondary atomization of propellant droplets; and (3) The extension of previously developed analytical models and the development of new models to address the phenomena associated with microexplosions (secondary atomization). Author

N91-28225*# Pennsylvania State Univ., University Park. Dept. of Mechanical Engineering.
LIQUID-PROPELLANT DROPLET VAPORIZATION AND COMBUSTION IN HIGH PRESSURE ENVIRONMENTS c25
Vigor Yang *In* NASA, Washington, Space Transportation Propulsion Technology Symposium. Volume 2: Symposium Proceedings May 1991 p 655-662 (For primary document see N91-28193 20-20)
Avail: NTIS HC/MF A99 CSCL 21B

In order to correct the deficiencies of existing models for high-pressure droplet vaporization and combustion, a fundamental investigation into this matter is essential. The objective of this research are: (1) to acquire basic understanding of physical and chemical mechanisms involved in the vaporization and combustion of isolated liquid-propellant droplets in both stagnant and forced-convective environments; (2) to establish droplet vaporization and combustion correlations for the study of liquid-propellant spray combustion and two-phase flowfields in rocket motors; and (3) to investigate the dynamic responses of multicomponent droplet vaporization and combustion to ambient flow oscillations. Author

N91-28226*# Pennsylvania State Univ., University Park. Dept. of Mechanical Engineering.
SPRAY COMBUSTION UNDER OSCILLATORY PRESSURE CONDITIONS c25
H. R. Jacobs and R. J. Santoro *In* NASA, Washington, Space Transportation Propulsion Technology Symposium. Volume 2: Symposium Proceedings May 1991 p 663-674 (For primary document see N91-28193 20-20)
Avail: NTIS HC/MF A99 CSCL 21B

The performance and stability of liquid rocket engines is often argued to be significantly impacted by atomization and droplet vaporization processes. In particular, combustion instability phenomena may result from the interactions between the oscillating pressure field present in the rocket combustor and the fuel and oxidizer injection process. Few studies have been conducted to examine the effects of oscillating pressure fields on spray formation and its evolution under rocket engine conditions. The pressure study is intended to address the need for such studies. In particular, two potentially important phenomena are addressed in the present effort. The first involves the enhancement of the atomization process for a liquid jet subjected to an oscillating pressure field of known frequency and amplitude. The objective of this part of the study is to examine the coupling between the pressure field and or the resulting periodically perturbed velocity field on the breakup of the liquid jet. In particular, transverse mode oscillations are of interest since such modes are considered of primary importance in combustion instability phenomena. The second aspect of the project involves the effects of an oscillating pressure on droplet coagulation and secondary atomization. The objective of this study is to examine the conditions under which phenomena following the atomization process are affected by perturbations to the pressure or velocity fields. Both coagulation and represent a coupling mechanism between the pressure field and the energy release process in rocket combustors. It is precisely this coupling which drives combustion instability phenomena. Consequently, the present effort is intended to provide the fundamental insights needed to evaluate these processes as important mechanisms in liquid rocket instability phenomena. Author

N91-28227*# Pennsylvania State Univ., University Park. NASA Center for Space Propulsion Engineering.
LIQUID JET BREAKUP AND ATOMIZATION IN ROCKET CHAMBERS UNDER DENSE SPRAY CONDITIONS
Kenneth K. Kuo, Fan-Bill Cheung, Roger D. Woodward, and Kenneth N. Garner *In* NASA, Washington, Space Transportation Propulsion Technology Symposium. Volume 2: Symposium Proceedings May 1991 p 675-681 (For primary document see N91-28193 20-20)
Avail: NTIS HC/MF A99 CSCL 21H

Two advanced diagnostic techniques were established and employed in this project. The first technique involves the use of a real-time x ray radiography system along with a high-speed CCD Xybion camera and an advanced digital image processor to investigate the breakup processes of the liquid core. The focus of this part of the project is to determine the inner structure of the liquid jet and via thin sheets of laser light, with the scatters light being photographed by a Xybion electronic camera synchronized to the laser pulse. This technique, which is capable of recording the breakup event occurring within 25 nano-seconds, enables us to freeze the motions of the jet and liquid droplets. The focus of this part of the project is to determine the outer structure of the liquid jet and to discover the configuration of the surface waves, the spray pattern, and the droplet size distribution in the non-dilute region. Results obtained by these two advanced diagnostic techniques will provide the much needed database for model development and accurate prediction of engine performance. The present work also represents a breakthrough in the area of advanced diagnostics of dense sprays. Author

N91-28228*# Pennsylvania State Univ., University Park. Dept. of Mechanical Engineering.
DROPLET-TURBULENCE INTERACTIONS IN SUBCRITICAL AND SUPERCRITICAL EVAPORATING SPRAYS
Domenic A. Santavicca, Edward Coy, Stuart Greenfield, and Young-Hoon Song *In* NASA, Washington, Space Transportation Propulsion Technology Symposium. Volume 2: Symposium Proceedings May 1991 p 683-689 (For primary document see N91-28193 20-20)
Avail: NTIS HC/MF A99 CSCL 21H

The objective of this research is to obtain an improved understanding of droplet turbulence interactions in vaporizing liquid sprays under conditions typical of those encountered in liquid fueled rocket engines. The interaction between liquid droplets and the surrounding turbulent gas flow affects droplet dispersion, droplet collisions, droplet vaporization and gas-phase, fuel-oxidant mixing, and therefore has a significant effect on the engine's combustion characteristics. An example of this is the role which droplet-turbulence interactions are believed to play in combustion instabilities. Despite their importance, droplet-turbulence interactions and their effect on liquid fueled rocket engine performance are not well understood. This is particularly true under supercritical conditions, where many conventional concepts, such as surface tension, no longer apply. Our limited understanding of droplet-turbulence interactions, under both subcritical conditions, represents a major limitation in our ability to design improved liquid previously unavailable information and valuable new insights which will directly impact the design of future liquid fueled rocket engines, as well as, allow for the development of significantly improved spray combustion models, making such models useful design tools. Author

N91-28229*# Pennsylvania State Univ., University Park. Dept. of Engineering Science and Mechanics.
COMPOSITE MATERIAL SYSTEMS FOR HYDROGEN MANAGEMENT c24
R. N. Pangborn and R. A. Queeney *In* NASA, Washington, Space Transportation Propulsion Technology Symposium. Volume 2: Symposium Proceedings May 1991 p 691-697 (For primary document see N91-28193 20-20)
Avail: NTIS HC/MF A99 CSCL 11D

The task of managing hydrogen entry into elevated temperature structural materials employed in turbomachinery is a critical engineering area for propulsion systems employing hydrogen or decomposable hydrocarbons as fuel. Extant structural materials, such as the Inconel series, are embrittled by the ingress of hydrogen in service, leading to a loss of endurance and general deterioration of load-bearing dependability. Although the development of hydrogen-insensitive material systems is an obvious engineering option, to date insensitive systems cannot meet the time-temperature-loading service extremes encountered. A short-term approach that is both feasible and technologically sound is the development and employment of hydrogen barrier coatings. The present project is concerned with developing, analyzing, and physically testing laminate composite hydrogen barrier systems, employing Inconel 718 as the structural material to be protected. Barrier systems will include all metallic, metallic-to-ceramic, and, eventually, metallic/ceramic composites as the lamellae. Since space propulsion implies repetitive engine firings without earth-based inspection and repair, coating durability will be closely examined, and testing regimes will include repetitive thermal cycling to simulate damage accumulation. The target accomplishments include: generation of actual hydrogen permeation data for metallic, ceramic-metallic, and hybrid metallic/ceramic composition barrier systems, practically none of which is currently extant; definition of physical damage modes imported to barrier systems due to thermal cycling, both transient temperature profiles and steady-state thermal mismatch stress states being examined as sources of damage; and computational models that incorporate general laminate schemes as described above, including manufacturing realities such as porosity, and whatever defects are introduced through service and characterized during the experimental programs. Author

N91-28230*# Pennsylvania State Univ., University Park. Dept. of Mechanical Engineering.
ROBUST AND REAL-TIME CONTROL OF MAGNETIC BEARINGS FOR SPACE ENGINES c37
Alok Sinha, Kon-Well Wang, K. Mease, and S. Lewis *In* NASA, Washington, Space Transportation Propulsion Technology Symposium. Volume 2: Symposium Proceedings May 1991 p 699-707 (For primary document see N91-28193 20-20)
Avail: NTIS HC/MF A99 CSCL 13K

Currently, NASA Lewis Research Center is developing magnetic bearings for Space Shuttle Main Engine (SSME) turbopumps. The control algorithms which have been used are based on either the proportional-intergral-derivative control (PID) approach or the linear quadratic (LQ) state space approach. These approaches lead to an acceptable performance only when the system model is accurately known, which is seldom true in practice. For example, the rotor eccentricity, which is a major source of vibration at high speeds, cannot be predicted accurately. Furthermore, the dynamics of a rotor shaft, which must be treated as a flexible system to model the elastic rotor shaft, is infinite dimensional in theory and the controller can only be developed on the basis of a finite number of modes. Therefore, the development of the control system is further complicated by the possibility of closed loop system instability because of residual or uncontrolled modes, the so called spillover problem. Consequently, novel control algorithms for magnetic bearings are being developed to be robust to inevitable parametric uncertainties, external disturbances, spillover phenomenon and noise. Also, as pointed out earlier, magnetic bearings must exhibit good performance at a speed over 30,000 rpm. This implies that the sampling period available for the design of a digital control system has to be of the order of 0.5 milli-seconds. Therefore, feedback coefficients and other required controller parameters have to be computed off-line so that the on-line computational burden is extremely small. The development of the robust and real-time control algorithms is based on the sliding mode control theory. In this method, a dynamic system is made to move along a manifold of sliding hyperplanes to the origin of the state space. The number of sliding hyperplanes equals that of actuators. The sliding mode controller has two parts; linear state feedback and nonlinear terms. The nonlinear terms guarantee that the systems would reach the intersection of all sliding hyperplanes and remain on it when bounds on the errors in the system parameters and external disturbances are known. The linear part of the control drives the system to the origin of state space. Another important feature is that the controller parameter can be computed off-line. Consequently, on-line computational burden is small. Author

N91-28231*# Pennsylvania State Univ., University Park. Dept. of Mechanical Engineering.

ANALYSIS OF FOIL BEARINGS FOR HIGH SPEED OPERATION IN CRYOGENIC APPLICATIONS **c37**

Marc Carpino *In* NASA, Washington, Space Transportation Propulsion Technology Symposium. Volume 2: Symposium Proceedings May 1991 p 709-715 (For primary document see N91-28193 20-20)

Avail: NTIS HC/MF A99 CSCL 13K

The general objective of this project is to develop analysis tools which are required for the design of foil bearings to be used in cryogenic applications. During the second year of this project, a general analysis approach and code for journal bearings operating under steady state conditions will be completed. This will be followed by the initiation of an investigation into transient behavior of foil bearings to determine their performance in rotor systems. Foil bearings have been proposed as an alternative to rolling element bearings for use in cryogenic turbopumps in liquid propellant rocket engines. This type of bearing offers several advantages over rolling element bearings since they would use the cryogenic pump fluid for a lubricant and have structural flexibility. These bearings have the potential of high reliability and long life. The bearing surface is constructed of a 'foil' which resists deflection by a combination of bending, membrane, and elastic foundation effects. The relative motion between the rotating shaft and the foil causes pressure in the fluid film to develop. This pressure deflects the the foil surface away from the shaft. Once a full fluid film is established between the foil and the rotor shaft, contact no longer takes place and there is no subsequent wear of the surfaces. The flexible foil structure of the bearing allows it to compensate for minor tolerance and manufacturing defects. This same flexibility also has a significant effect on the dynamic performance of the rotor-bearing system. Author

N91-28232*# Pennsylvania State Univ., University Park. Dept. of Mechanical Engineering.

A STUDY OF METHODS TO INVESTIGATE NOZZLE BOUNDARY LAYER TRANSITION **c34**

Laura L. Pauley *In* NASA, Washington, Space Transportation Propulsion Technology Symposium. Volume 2: Symposium Proceedings May 1991 p 717-724 (For primary document see N91-28193 20-20)

Avail: NTIS HC/MF A99 CSCL 20D

To further investigate nozzle flow, numerical computations are employed. The computations produce complete flow velocity and temperature fields within the nozzle. As a check, these results can be compared with experimental data at the wall. Once an accurate numerical scheme has been validated, it can be used as a design tool to predict the performance of other nozzle designs without the cost of experimental testing. Typically, the numerical analysis assumes either a laminar boundary layer or a fully turbulent boundary layer which is steady and two-dimensional. Boundary layer transition is not considered. Computing both the completely laminar boundary layer and the completely turbulent boundary layer conditions gives the minimum and maximum wall heat flux possible for a specified geometry. When the experimental heat flux measurements lie between these two values, the nature of the boundary layer is unknown. The boundary layer may have transitioned from laminar to turbulent; three-dimensional structures may be present in the boundary layer, or the inlet flow conditions may not be correctly specified in the computation. Author

N91-28233*# Pennsylvania State Univ., University Park. Dept. of Aerospace Engineering.

OPTICAL DIAGNOSTIC INVESTIGATION OF LOW REYNOLDS NUMBER NOZZLE FLOWS **c34**

Michael M. Micci *In* NASA, Washington, Space Transportation Propulsion Technology Symposium. Volume 2: Symposium Proceedings May 1991 p 725-732 (For primary document see N91-28193 20-20)

Avail: NTIS HC/MF A99 CSCL 20D

The objectives are to obtain temperature, density and velocity profile measurements in the expansion region of low Reynolds number nozzles through the use of optical diagnostics. An LIF system will be used to probe the expansion of a microwave-heated expansion in the Center vacuum facility The experimental measurements made in this program will be compared to numerical predictions obtained by Drs. Charles Merkle and Lyle Long. Author

N91-28234*# Pennsylvania State Univ., University Park. Dept. of Mechanical Engineering.

CFD APPLICATIONS IN CHEMICAL PROPULSION ENGINES

Charles L. Merkle *In* NASA, Washington, Space Transportation Propulsion Technology Symposium. Volume 2: Symposium Proceedings May 1991 p 733-742 (For primary document see N91-28193 20-20)

Avail: NTIS HC/MF A99 CSCL 21H

The present research is aimed at developing analytical procedures for predicting the performance and stability characteristics of chemical propulsion engines. Specific emphasis is being placed on understanding the physical and chemical processes in the small engines that are used for applications such as spacecraft attitude control and drag make-up. The small thrust sizes of these engines lead to low nozzle Reynolds numbers with thick boundary layers which may even meet at the nozzle centerline. For this reason, the classical high Reynolds number procedures that are commonly used in the industry are inaccurate and of questionable utility for design. A complete analysis capability for the combined viscous and inviscid regions as well as for the subsonic, transonic, and supersonic portions of the flowfield is necessary to estimate performance levels and to enable tradeoff studies during design procedures. Author

N91-28235*# National Aeronautics and Space Administration, Washington, DC.

SPACE TRANSPORTATION PROPULSION TECHNOLOGY SYMPOSIUM. VOLUME 3: PANEL SESSION SUMMARIES AND PRESENTATIONS

May 1991 620 p Symposium held in State College, PA, 25-29 Jun. 1990

(NASA-CP-3112-Vol-3; NAS 1.55:3112-Vol-3) Avail: NTIS HC/MF A99 CSCL 21H

The Space Transportation Propulsion Technology Symposium was held at the Pennsylvania State University on June 25 to 29, 1990. Emphasis was placed on propulsion requirements and initiatives to support current, next generation, and future space transportation systems, with the primary objectives of discerning whether proposed designs truly meet future transportation needs and identifying possible technology gaps, overlaps and other programmatic deficiencies. Key space transportation propulsion issues are addressed through four panels with government, industry, and academia membership. The panel focused on systems engineering and integration; development, manufacturing, and certification; operational efficiency; program development; and cultural issues. For individual titles, see N91-28236 through N91-28272.

N91-28236*# National Aeronautics and Space Administration. Lyndon B. Johnson Space Center, Houston, TX.

HEAVY-LIFT LAUNCH VEHICLE PROPULSION CONSIDERATIONS

Wayne L. Ordway *In* NASA, Washington, Space Transportation Propulsion Technology Symposium. Volume 3: Panel Session

Summaries and Presentations May 1991 p 871-880 (For primary document see N91-28235 20-20)
Avail: NTIS HC/MF A99 CSCL 21H

Information on heavy-lift launch vehicle (HLLV) propulsion is given in viewgraph form. The objective was to investigate Earth to orbit options which minimize on-orbit operations and impacts to Space Station Freedom, have a reasonable capability to support Mars missions, and minimize mass in low Earth orbit. Potential synergism with the Space Transportation System is considered. Launch vehicle sizing results, HLLV thrust requirements, and propulsion system reliability are covered. Author

N91-28237*# Martin Marietta Aerospace, Denver, CO. Dept. of Astronautics.
HUMANS TO MARS IN 1999 **c12**
Robert Zubrin and David Baker *In* NASA, Washington, Space Transportation Propulsion Technology Symposium. Volume 3: Panel Session Summaries and Presentations May 1991 p 881-891 (For primary document see N91-28235 20-20)
Avail: NTIS HC/MF A99 CSCL 22A

A set of vehicle designs and a mission architecture that was developed to send humans to Mars in the 1990's are discussed. Launching, landing, a 500 day stay on Mars, and a return to Earth are discussed. The plan is not merely a one shot expedition, but puts into place immediately an economical method of Earth-Mars transportation, real surface exploratory mobility, and significant base capabilities that can rapidly evolve into a mostly self-sufficient Mars colony. Since the plans call for the use of a combination of off the shelf technology and new technology that can be easily developed, the authors argue that there is no reason to postpone the exploration of Mars until several decades after a lunar base build-up. Author

N91-28238*# National Aeronautics and Space Administration. Lewis Research Center, Cleveland, OH.
PROBABILISTIC STRUCTURAL ANALYSIS METHODS FOR SPACE TRANSPORTATION PROPULSION SYSTEMS **c39**
C. C. Chamis, N. Moore, C. Anis, J. Newell, V. Nagpal, and S. Singhal (Sverdrup Technology, Inc., Brook Park, OH.) *In* NASA, Washington, Space Transportation Propulsion Technology Symposium. Volume 3: Panel Session Summaries and Presentations May 1991 p 895-914 (For primary document see N91-28235 20-20)
Avail: NTIS HC/MF A99 CSCL 20K

Information on probabilistic structural analysis methods for space propulsion systems is given in viewgraph form. Information is given on deterministic certification methods, probability of failure, component response analysis, stress responses for 2nd stage turbine blades, Space Shuttle Main Engine (SSME) structural durability, and program plans. . Author

N91-28239*# National Aeronautics and Space Administration. Lyndon B. Johnson Space Center, Houston, TX.
TECHNOLOGY TRANSFER METHODOLOGY **c85**
Rich Labotz, Don Connell, and Ken Kroll (Pratt and Whitney Aircraft, West Palm Beach, FL.) *In* NASA, Washington, Space Transportation Propulsion Technology Symposium. Volume 3: Panel Session Summaries and Presentations May 1991 p 915-921 (For primary document see N91-28235 20-20)
Avail: NTIS HC/MF A99 CSCL 05A

Information on technology transfer methodology is given in viewgraph form. Information is given on new systems development, the developer's perspective, barriers to providing a home for technology, and incentives for using new technologies. Author

N91-28240*# Aerojet-General Corp., Sacramento, CA. Propulsion Div.
TECHNOLOGY TRANSFER METHODOLOGY **c85**
Rich LaBotz *In* NASA, Washington, Space Transportation Propulsion Technology Symposium. Volume 3: Panel Session Summaries and Presentations May 1991 p 923-929 (For primary document see N91-28235 20-20)
Avail: NTIS HC/MF A99 CSCL 05A

Information on technology transfer methodology is given in viewgraph form. Topics covered include problems in economics, technology drivers, inhibitors to using improved technology in development, technology application opportunities, and co-sponsorship of technology. Author

N91-28241*# Lockheed Engineering and Sciences Co., Las Cruces, NM.
NATIONAL TEST BED CONCEPT
Roger Meyer and Melvin McIlwain (Aerojet Solid Propulsion Co., Sacramento, CA.) *In* NASA, Washington, Space Transportation Propulsion Technology Symposium. Volume 3: Panel Session Summaries and Presentations May 1991 p 931-935 (For primary document see N91-28235 20-20)
Avail: NTIS HC/MF A99 CSCL 21H

Information on the National Test Bed concept is given in outline form. Program objectives include the development of a national test bed for propulsion system testing, the efficient utilization of NASA's limited funding for future propulsion system development and sustained flight support, ensuring that adequate test facilities are available within NASA to support future propulsion systems, and the development and maintenance within NASA and the private sector of the technical skills and expertise for future propulsion system development. Proposed actions and programs as well as major milestones are outlined. Author

N91-28242*# TRW Space Technology Labs., Redondo Beach, CA.
HISTORICAL PROBLEM AREAS LESSONS LEARNED
Bob Sackheim and Dale A. Fester (Martin Marietta Aerospace, Denver, CO.) *In* NASA, Washington, Space Transportation Propulsion Technology Symposium. Volume 3: Panel Session Summaries and Presentations May 1991 p 937-946 (For primary document see N91-28235 20-20)
Avail: NTIS HC/MF A99 CSCL 21H

Historical problem areas in space transportation propulsion technology are identified in viewgraph form. Problem areas discussed include materials compatibility, contamination, pneumatic/feed system flow instabilities, instabilities in rocket engine combustion and fuel sloshing, exhaust plume interference, composite rocket nozzle failure, and freeze/thaw damage. Author

N91-28243*# Martin Marietta Aerospace, Denver, CO. Astronautics Group.
HISTORICAL PROBLEM AREAS: LESSONS LEARNED FOR EXPENDABLE AND REUSABLE VEHICLE PROPULSION SYSTEMS
Dale A. Fester *In* NASA, Washington, Space Transportation Propulsion Technology Symposium. Volume 3: Panel Session Summaries and Presentations May 1991 p 947-951 (For primary document see N91-28235 20-20)
Avail: NTIS HC/MF A99 CSCL 21H

The following subject areas are covered: expendable launch vehicle lessons learned, upper stage/transfer vehicle lessons learned, shuttle systems - reuse, and reusable system issues and lessons learned. Author

N91-28244*# National Aeronautics and Space Administration. Lyndon B. Johnson Space Center, Houston, TX.
MANUFACTURING PROCESSES
Jay Bennet, David Brower, Stan Levine, Ray Walker, and John Wooten (Rockwell International Corp., Canoga Park, CA.) *In* NASA, Washington, Space Transportation Propulsion Technology Symposium. Volume 3: Panel Session Summaries and Presentations May 1991 p 953-959 (For primary document see N91-28235 20-20)
Avail: NTIS HC/MF A99 CSCL 21H

The following issues are covered: process development frequently lags behind material development, high fabrication costs, flex joints (bellows) - a continuing program, SRM fabrication-induced defects, and in-space assembly will require simplified design. Author

N91-28245*# National Aeronautics and Space Administration. Marshall Space Flight Center, Huntsville, AL.
MATERIALS SUB-PANEL
Bil Bhat, Brad Cowles, Bob Dreshfield, and Bob Jewett (Rockwell International Corp., Canoga Park, CA.) *In* NASA, Washington, Space Transportation Propulsion Technology Symposium. Volume 3: Panel Session Summaries and Presentations May 1991 p 961-963 (For primary document see N91-28235 20-20)
Avail: NTIS HC/MF A99 CSCL 21H

The following subject areas are covered: general issues (unique operating/storage environments, adapt existing materials/develop rocket materials, long lead time for new materials, high cost, integration of materials development and manufacturing technology, and availability of materials data); technical issues (materials characterization for operating and storage environments, advanced materials development, availability and dissemination of materials properties, advanced materials tests facilities, fire hazards, and propellants); major objectives (materials characterization, advanced materials development, and materials data base development/maintenance); and candidate programs (materials characterization, advanced materials development, and aerospace materials data base). Author

N91-28246*# National Aeronautics and Space Administration. Lewis Research Center, Cleveland, OH.
OVERALL GOALS
George Baaklini, Joseph S. Heyman, Eric Madaras, Charles Salkowski, Bert Weston, and Ken Woodis (National Aeronautics and Space Administration. Marshall Space Flight Center, Huntsville, AL.) *In* NASA, Washington, Space Transportation Propulsion Technology Symposium. Volume 3: Panel Session Summaries and Presentations May 1991 p 965-971 (For primary document see N91-28235 20-20)
Avail: NTIS HC/MF A99 CSCL 21H

Space transportation propulsion systems symposium is discussed. The following subject areas are covered: overall goals; main issues; materials characterization; reduction of manufacturing defects; standards and certification; advanced NDE techniques; designing for inspectability; candidate programs/milestones; and NDE technology potentials. Author

N91-28247*# National Aeronautics and Space Administration. Lewis Research Center, Cleveland, OH.
CONCURRENT ENGINEERING
C. C. Chamis, L. Leger, D. Hunter, C. Jones, R. Sprague, L. Berke, J. Newell, and S. Singhal (Sverdrup Technology, Inc., Brook Park, OH.) *In* NASA, Washington, Space Transportation Propulsion Technology Symposium. Volume 3: Panel Session Summaries and Presentations May 1991 p 973-988 (For primary document see N91-28235 20-20)
Avail: NTIS HC/MF A99 CSCL 21H

The following subject areas are covered: issues (liquid rocket propulsion - current development approach, current certification process, and costs of engineering changes); state of the art (DICE information management system, key government participants, project development strategy, quality management, and numerical propulsion system simulation); needs identified; and proposed program. Author

N91-28248*# National Aeronautics and Space Administration. John C. Stennis Space Center, Bay Saint Louis, MS.
LIFE CYCLE COST BASED PROGRAM DECISIONS
James S. Dick *In* NASA, Washington, Space Transportation Propulsion Technology Symposium. Volume 3: Panel Session Summaries and Presentations May 1991 p 989-1023 (For primary document see N91-28235 20-20)
Avail: NTIS HC/MF A99 CSCL 21H

The following subject areas are covered: background (space propulsion facility assessment team final report); changes (Advanced Launch System, National Aerospace Plane, and space exploration initiative); life cycle cost analysis rationale; and recommendation to panel. Author

N91-28249*# National Aeronautics and Space Administration. John C. Stennis Space Center, Bay Saint Louis, MS.
INFUSION OF INSTRUMENTATION TECHNOLOGY (ENGINE PLUME DIAGNOSTICS) INTO OPERATIONAL TEST PROGRAMS
E. G. Woods *In* NASA, Washington, Space Transportation Propulsion Technology Symposium. Volume 3: Panel Session Summaries and Presentations May 1991 p 1025-1030 (For primary document see N91-28235 20-20)
Avail: NTIS HC/MF A99 CSCL 21H

The following subject areas are covered: hierarchy of civil space technology program; evolution of technology development; technology validation process; potential impacts; impacts of technology infusion into flight certifications; potential solutions; examples of current technology infusion into flight certification; OAET-CSTI health monitoring and controls; and challenges for future space vehicle propulsion systems. Author

N91-28250*# National Aeronautics and Space Administration. Marshall Space Flight Center, Huntsville, AL.
LIQUID ROCKET ENGINE FLIGHT CERTIFICATION
Steve Richards *In* NASA, Washington, Space Transportation Propulsion Technology Symposium. Volume 3: Panel Session Summaries and Presentations May 1991 p 1031-1038 (For primary document see N91-28235 20-20)
Avail: NTIS HC/MF A99 CSCL 21H

The following subject areas are covered: current rocket engine certification process; certification issues; engine characteristics; engine design and mission requirements; structural design criteria; structural design factors of safety; component/subsystem testing; system level development tests; certification/qualification tests; observations; and proposed actions/programs. Author

N91-28251*# Rockwell International Corp., Huntsville, AL. Space Transportation Systems Div.
TEST VS. SIMULATION
Charles C. Wood *In* NASA, Washington, Space Transportation Propulsion Technology Symposium. Volume 3: Panel Session Summaries and Presentations May 1991 p 1039-1045 (For primary document see N91-28235 20-20)
Avail: NTIS HC/MF A99 CSCL 21H

The following topics are presented in tabular form: (1) simulation capability assessments (no propulsion system test); (2) advanced vehicle simulation capability assessment; (3) systems tests identified events; (4) main propulsion test article (MPTA) testing evaluation; (5) Saturn 5, 1B, and 1 testing evaluation. Special vehicle simulation issues that are propulsion related are briefly addressed. K.S.

N91-28252*# National Aeronautics and Space Administration, Washington, DC.
DEVELOPMENT PROGRAM ENHANCEMENT SUGGESTIONS (PROPULSION RELATED)
In its Space Transportation Propulsion Technology Symposium. Volume 3: Panel Session Summaries and Presentations May 1991 p 1047 (For primary document see N91-28235 20-20)
Avail: NTIS HC/MF A99 CSCL 21H

The following topics are briefly addressed in this one page document: (1) potential instrumentation difficulties; (2) hazardous fluid leakage; (3) propellant loading procedures and operations; (4) pressurization systems; and (5) propellant mass uncertainty. K.S.

N91-28253*# General Dynamics Corp., San Diego, CA.
THE SPACE EXPLORATION INITIATIVE. OPERATIONAL EFFICIENCY PANEL SPACE-BASING TECHNOLOGY REQUIREMENTS **c12**
Luis R. Pena *In* NASA, Washington, Space Transporation Propulsion Technology Symposium. Volume 3: Panel Session Summaries and Presentations May 1991 p 1051-1062 (For primary document see N91-28235 20-20)
Avail: NTIS HC/MF A99 CSCL 22A

The topics covered include the following: (1) space basing technology requirements sources; (2) orbit transfer vehicle (OTV) processing heritage; (3) ground processing progression to space processing; (4) technology requirements for space based OTV servicing and maintenance; (5) design and development schedule for OTV's and OTV accommodations/ support hardware; (6) cryogenic technology test program development; (7) cryogenic propellant transfer, storage, and reliquefaction management summary; (8) propellant transfer technology analysis and ground testing; (8) OTV propellant storage depot development critical scaling relationships; (9) flight experiment options; (10) OTV maintenance; (11) automated fault detection/ isolation and system checkout summary; (12) engine replacement; (13) alternative docking operation; (14) OTV/payload integration; and (15) technology criticality and capability assessment. This document is presented in viewgraph form. K.S.

N91-28254*# Martin Marietta Aerospace, Denver, CO.
SPACE TRANSFER VEHICLES AND SPACE BASING **c16**
Joe Kelley *In* NASA, Washington, Space Transporation Propulsion Technology Symposium. Volume 3: Panel Session Summaries and Presentations May 1991 p 1063-1106 (For primary document see N91-28235 20-20)
Avail: NTIS HC/MF A99 CSCL 22B

The topics covered include the following: (1) space basing agenda; (2) mission scenario 4E-5B, crew and Lunar Excursion Vehicle (LEV) delivery; (3) final concept candidate, crew concept 4E-2B; (4) space transfer vehicle (STV) concept 4E-5B; (5) configuration summary for crew concept 4E-5B; (6) configuration definition for crew concept 4E-5B; (7) low earth orbit node assembly and checkout operations; (8) criteria for operation objectives; (9) LTV and STV main engines; (10) Space Station Freedom impacts; (11) aerobrakes; and (12) on orbit operations. This document is presented in viewgraph form. K.S.

N91-28255*# Boeing Aerospace Co., Seattle, WA.
STV ENGINE DESIGN CONSIDERATIONS **c29**
In NASA, Washington, Space Transporation Propulsion Technology Symposium. Volume 3: Panel Session Summaries and Presentations May 1991 p 1107-1125 (For primary document see N91-28235 20-20)
Avail: NTIS HC/MF A99 CSCL 21H

The topics covered include the following: (1) engine design criteria and issues; (2) design requirements for man rating; (3) test requirements for man rating; (4) design requirements for space basing; (5) engine operation requirements; (6) health monitoring; (7) lunar transfer vehicle (LTV) feed system; (8) lunar excursion vehicle (LEV) propellant system; (9) area ratio gimbal angle limits; (10) reaction control system; and (11) engine configuration and characteristics. This document is presented in viewgraph form. K.S.

N91-28256*# Aerojet-General Corp., Sacramento, CA.
THE PROPULSION SYSTEM IS THE KEY TO AIRLINE-LIKE OPERATION OF ETO VEHICLES
Charles J. OBrien *In* NASA, Washington, Space Transporation Propulsion Technology Symposium. Volume 3: Panel Session Summaries and Presentations May 1991 p 1127-1133 (For primary document see N91-28235 20-20)
Avail: NTIS HC/MF A99 CSCL 21H

The topics covered include the following: (1) Advanced Launch System (ALS); (2) life cycle cost/lb payload; (3) current operational cost; (4) major cost driver; (5) fully automated operations; (6) technology impacts on vehicle dry mass efficiency; (7) single stage to orbit (SSTO) approach; and (8) efficient SSTO propulsion system operations. K.S.

N91-28257*# University of Central Florida, Orlando. Dept. of Mechanical Engineering.
SPACE SHUTTLE WITH COMMON FUEL TANK FOR LIQUID ROCKET BOOSTER AND MAIN ENGINES (SUPERTANKER SPACE SHUTTLE)
Douglas G. Thorpe *In* NASA, Washington, Space Transporation Propulsion Technology Symposium. Volume 3: Panel Session Summaries and Presentations May 1991 p 1135-1185 (For primary document see N91-28235 20-20)
Avail: NTIS HC/MF A99 CSCL 21H

An operation and schedule enhancement is shown that replaces the four-body cluster (Space Shuttle Orbiter (SSO), external tank, and two solid rocket boosters) with a simpler two-body cluster (SSO and liquid rocket booster/external tank). At staging velocity, the booster unit (liquid-fueled booster engines and vehicle support structure) is jettisoned while the remaining SSO and supertank continues on to orbit. The simpler two-bodied cluster reduces the processing and stack time until SSO mate from 57 days (for the solid rocket booster) to 20 days (for the liquid rocket booster). The areas in which liquid booster systems are superior to solid rocket boosters are discussed. Alternative and future generation vehicles are reviewed to reveal greater performance and operations enhancements with more modifications to the current methods of propulsion design philosophy, e.g., combined cycle engines, and concentric propellant tanks. Author

N91-28258*# University of Central Florida, Orlando. Dept. of Mechanical Engineering.
DETERMINING CRITERIA FOR SINGLE STAGE TO ORBIT **c12**
Douglas G. Thorpe *In* NASA, Washington, Space Transporation Propulsion Technology Symposium. Volume 3: Panel Session Summaries and Presentations May 1991 p 1187-1201 (For primary document see N91-28235 20-20)
Avail: NTIS HC/MF A99 CSCL 22A

The criteria for single stage to orbit (SSTO) vehicles are determined. The Saturn 5 launch vehicle and Space Shuttle are examined to validate the assumptions and results. This velocity is then used to determine if the selected vehicle can achieve orbit and calculate its payload capacity. The Saturn 5 launch vehicle with the following stages is examined: (1) second stage (S2) with Space Shuttle Main Engines (SSME); (2) second stage (S2) with J2 engines; (3) third stage (S4B) with SSME; and (4) third stage (S4B) with J2 engines. The Space Shuttle with the following configurations is examined: (1) external tank with SSME; (2) external tank with J2 engines; and (3) Atlas rocket booster (current configuration). Author

N91-28259*# National Aeronautics and Space Administration. John C. Stennis Space Center, Bay Saint Louis, MS.
JOHN C. STENNIS SPACE CENTER ROLES AND MISSIONS
Don J. Chenevert *In* NASA, Washington, Space Transportation Propulsion Technology Symposium. Volume 3: Panel Session Summaries and Presentations May 1991 p 1203-1230 (For primary document see N91-28235 20-20)
Avail: NTIS HC/MF A99 CSCL 21H

Space transportation propulsion systems; diagnostics testbed facility characteristics; engine plume diagnostics; and thermal infrared imaging technology development are outlined. This presentation is represented by viewgraphs. B.G.

N91-28260*# National Aeronautics and Space Administration, Washington, DC.
EFFECTIVITY OF ATMOSPHERIC ELECTRICITY ON LAUNCH AVAILABILITY **c47**
John A. Ernst *In its* Space Transportation Propulsion Technology Symposium. Volume 3: Panel Session Summaries and Presentations May 1991 p 1231-1241 (For primary document see N91-28235 20-20)
Avail: NTIS HC/MF A99 CSCL 04B

Thunderstorm days at KSC; percentage of frequency of thunderstorms (1957-1989); effect of lightning advisory on ground operations; Shuttle launch history; Shuttle launch weather history; applied meteorology unit; and goals/operational benefits. This presentation is represented by viewgraphs. B.G.

N91-28261*# Rockwell International Corp., Huntsville, AL.
PROPULSION SYSTEM GROUND TESTING
Charles C. Wood *In* NASA, Washington, Space Transportation Propulsion Technology Symposium. Volume 3: Panel Session

Summaries and Presentations May 1991 p 1243-1254 (For primary document see N91-28235 20-20)
Avail: NTIS HC/MF A99 CSCL 21H

The objective is to provide management visibility relative to the roles of simulation and propulsion system testing for future development programs through assessment of current propulsion related simulation capabilities and review of contributions from propulsion system test programs. The presentation is represented by viewgraphs. Author

N91-28262*# General Dynamics Corp., San Diego, CA. Space Systems Div.
PROPULSION TECHNOLOGIES FOR NEAR TERM
Gopal Mehta *In* NASA, Washington, Space Transportation Propulsion Technology Symposium. Volume 3: Panel Session Summaries and Presentations May 1991 p 1255-1258 (For primary document see N91-28235 20-20)
Avail: NTIS HC/MF A99 CSCL 21H

Propulsion system requirements and considerations; cost effective approach; booster recovery module; and commercial vehicles - evolutionary approach are outlined. This presentation is represented by viewgraphs. B.G.

N91-28263*# National Aeronautics and Space Administration, Washington, DC.
LESSONS LEARNED AND THEIR APPLICATION TO PROGRAM DEVELOPMENT AND CULTURAL ISSUES c16
Gilbert L. Roth *In its* Space Transportation Propulsion Technology Symposium. Volume 3: Panel Session Summaries and Presentations May 1991 p 1261-1276 (For primary document see N91-28235 20-20)
Avail: NTIS HC/MF A99 CSCL 22B

The knowledge used today is contained in an untold number of technical and managerial handbooks. This knowledge is derived from the known strengths and weaknesses experienced during the execution of programs and projects that are being used today. The purpose is to stir up thought, not on specific experiences, but on implementation of lessons learned from these experiences. B.G.

N91-28264*# Lockheed Space Operations Co., Washington, DC.
SPACE SHUTTLE REQUIREMENTS/CONFIGURATION EVOLUTION c16
E. P. Andrews *In* NASA, Washington, Space Transportation Propulsion Technology Symposium, Volume 3: Panel Session Summaries and Presentations May 1991 p 1277-1284 (For primary document see N91-28235 20-20)
Avail: NTIS HC/MF A99 CSCL 22B

Space Shuttle chronology; Space Shuttle comparison; Cost comparison; Performance; Program ground rules; Sizing criteria; Crew/passenger provisions; Space Shuttle Main Engine (SSME) characteristics; Space Shuttle program milestones; and Space Shuttle requirements are outlined. This presentation is represented by viewgraphs. B.G.

N91-28265*# General Dynamics Corp., San Diego, CA. Space Systems Div.
CULTURAL CHANGES IN AEROSPACE c12
Bill Strobl *In* NASA, Washington, Space Transportation Propulsion Technology Symposium. Volume 3: Panel Session Summaries and Presentations May 1991 p 1285-1290 (For primary document see N91-28235 20-20)
Avail: NTIS HC/MF A99 CSCL 22A

Cultural changes; people and jobs; examples of cultural changes required; advanced launch system (ALS) philosophy; ALS operability capabilities; and ALS operability in design are outlined. This presentation is represented by viewgraphs. B.G.

N91-28266*# Pratt and Whitney Aircraft, West Palm Beach, FL.
BUSINESS NOT AS USUAL
In NASA, Washington, Space Transportation Propulsion Technology Symposium. Volume 3: Panel Session Summaries and Presentations May 1991 p 1291-1301 Prepared in cooperation with Rockwell International Corp.; and Aerojet-General Corp. (For primary document see N91-28235 20-20)
Avail: NTIS HC/MF A99 CSCL 21H

Typical design simplification ideas which reduce costs; combustion chamber design simplification; combustion chambers; castings vs. machined and welded forgings; automated inspection; and life cycle costs are outlined. This presentation is represented by viewgraphs. B.G.

N91-28267*# Vitro Corp., Washington, DC.
LAUNCH OPERATIONS MANPOWER YESTERDAY, TODAY AND TOMORROW c15
George Ojalehto *In* NASA, Washington, Space Transportation Propulsion Technology Symposium. Volume 3: Panel Session Summaries and Presentations May 1991 p 1303-1312 (For primary document see N91-28235 20-20)
Avail: NTIS HC/MF A99 CSCL 22D

The manpower to accomplish spacecraft launch operations was analyzed. It seems that the ratio of personnel to launches was much higher in the beginning of the space program than in later years. The analysis was performed to see why the operational efficiency was better then than now and how that efficiency can be reattained. E.R.

N91-28268*# National Aeronautics and Space Administration, Washington, DC.
MAJOR SYSTEM ACQUISITIONS PROCESS (A-109) c81
C. Saric *In its* Space Transportation Propulsion Technology Symposium. Volume 3: Panel Session Summaries and Presentations May 1991 p 1313-1323 (For primary document see N91-28235 20-20)
Avail: NTIS HC/MF A99 CSCL 05A

The Major System examined is a combination of elements (hardware, software, facilities, and services) that function together to produce capabilities required to fulfill a mission need. The system acquisition process is a sequence of activities beginning with documentation of mission need and ending with introduction of major system into operational use or otherwise successful achievement of program objectives. It is concluded that the A-109 process makes sense and provides a systematic, integrated management approach along with appropriate management level involvement and innovative and 'best ideas' from private sector in satisfying mission needs. Author

N91-28269*# National Aeronautics and Space Administration. Marshall Space Flight Center, Huntsville, AL.
THE CASE FOR TEAMING ON THE ALS-STME PROGRAM c81
S. F. Morea *In* NASA, Washington, Space Transportation Propulsion Technology Symposium. Volume 3: Panel Session Summaries and Presentations May 1991 p 1325-1335 (For primary document see N91-28235 20-20)
Avail: NTIS HC/MF A99 CSCL 05A

The analysis concludes that the nation needs to proceed with a new LOX/LH2 rocket engine program now. It is also concluded that open competition now will have deleterious impacts on the competitive viability of the liquid rocket engine industry. Teaming, however, provides a way to solve todays concerns while enhancing the option for open competition in the future. Author

N91-28270*# National Aeronautics and Space Administration, Washington, DC.
SPACE SHUTTLE MAIN ENGINE: CERTIFICATION FOR MANNED SPACE FLIGHT
Ronald G. Weesner *In its* Space Transportation Propulsion Technology Symposium. Volume 3: Panel Session Summaries and Presentations May 1991 p 1337-1345 (For primary document see N91-28235 20-20)
Avail: NTIS HC/MF A99 CSCL 21H

SSME requirements were identified in NASA approved documents. Design verification specifications (DVS) are used to define requirements and method of verification. Detailed and complete plans provide for verification of each requirement by lab tests, component tests, and engine tests. These tests are planned to expose problems early. The culmination of the development process is engine certification. The certification consists of two certification cycles on each of two engines. The certification cycle is made up of 10 tests and 5000 seconds. Author

N91-28271*# National Aeronautics and Space Administration. Marshall Space Flight Center, Huntsville, AL.
SPACE TRANSPORTATION MAIN ENGINE RELIABILITY AND SAFETY
Jan C. Monk *In* NASA, Washington, Space Transportation Propulsion Technology Symposium. Volume 3: Panel Session Summaries and Presentations May 1991 p 1347-1357 (For primary document see N91-28235 20-20)
Avail: NTIS HC/MF A99 CSCL 21H

Viewgraphs are used to illustrate the reliability engineering and aerospace safety of the Space Transportation Main Engine (STME). A technology developed is called Total Quality Management (TQM). The goal is to develop a robust design. Reducing process variability produces a product with improved reliability and safety. Some engine system design characteristics are identified which improves reliability. E.R.

N91-28272*# Thiokol Corp., Brigham City, UT. Space Operations.
POSSIBLE FUNDING STRATEGIES c83
T. F. Davidson *In* NASA, Washington, Space Transportation Propulsion Technology Symposium. Volume 3: Panel Session Summaries and Presentations May 1991 p 1359-1362 (For primary document see N91-28235 20-20)
Avail: NTIS HC/MF A99 CSCL 05C

Funding strategies are examined for the AIA rocket propulsion strategic plan. Either the government, industry, or universities can fund the project alone, or it was concluded, it works best if is a combination of these sources. E.R.

N91-28273# Naval Postgraduate School, Monterey, CA.
IMPACT OF ION PROPULSION ON PERFORMANCE, DESIGN, TESTING, AND OPERATION OF A GEOSYNCHRONOUS SPACECRAFT M.S. Thesis
Spotrizano D. Lugtu Jun. 1990 175 p
(AD-A237028) Avail: NTIS HC/MF A08 CSCL 21/3

The implementation issues of an ion propulsion subsystem (IPS) on a geosynchronous communications satellite are presented. As an example, Ultra High Frequency (UHF) Follow-On class satellite is selected for this study. The issues include: (1) impact of integration of IPS with other subsystems, such as the electrical power subsystem to take care of the heavy demand of power requirements and location of the subsystem with least impact on attitude control and plume impingement on solar arrays, (2) environmental consideration-particulate contamination electrostatic discharge (ESD), and electromagnetic interference (EMI), and finally risks and benefits. Ion propulsion offers significant advantages over chemical propulsion due to its high specific impulse and the advent of xenon thruster technology, multikilowatt spacecraft, and nickel-hydrogen (Ni-H2) batteries with demonstrated high cycle life have combined to make the ion thruster attractive for North-South Station Keeping (NSSK). GRA

N91-28274# Sandia National Labs., Albuquerque, NM.
ATTITUDE CONTROL OF A SPINNING ROCKET VIA THRUST VECTORING
J. E. White 19 Dec. 1990 36 p Presented at the American Institute of Aeronautics and Astronautics (AIAA) Guidance, Navigation and Control Conference, New Orleans, 12-14 Aug. 1991
(Contract DE-AC04-76DP-00789)
(DE91-006267; SAND-90-3230C; CONF-910847-1) Avail: NTIS HC/MF A03

Two controllers are developed to provide attitude control of a spinning rocket that has a thrust vectoring capability. The first controller has a 'single-input single output' design that ignores the gyroscopic coupling between the control channels. The second controller has a multi-input multi-output structure that is specifically intended to account for the gyroscopic coupling effects. A performance comparison between the two approaches is conducted for a range of roll rates. Each controller is tested for the ability to track step commands, and for the amount of coupling impurity. Both controllers are developed via a linear quadratic regulator synthesis procedure, which is motivated by the multi-input multi-output nature of the second controller. Time responses and a singular value analysis are used to evaluate controller performance. The development and comparison is described of two controllers that are designed to provide attitude control of a spinning rocket that is equipped with thrust vector control. DOE

N91-28275# Lawrence Livermore National Lab., CA.
SPACE PROPULSION BY FUSION IN A MAGNETIC DIPOLE
E. Teller, A. J. Glass, T. K. Fowler, A. Hasegawa, and John F. Santarius (Wisconsin Univ., Madison.) 12 Apr. 1991 48 p Presented at the 1st International A.D. Sakharov Conference on Physics, Moscow (USSR), 27-31 May 1991
(Contract W-7405-eng-48)
(DE91-012033; UCRL-JC-106807; CONF-9105177-1) Avail: NTIS HC/MF A03

A conceptual design is discussed for a fusion rocket propulsion system based on the magnetic dipole configuration. The dipole is found to have features well suited to space applications. Example parameters are presented for a system producing a specific power of 1 kW/kg, capable of interplanetary flights to Mars in 90 days and to Jupiter in a year, and of extra-solar-system flights to 1000 astronomical units (the Tau mission) in 20 years. This is about 10 times better specific power toward 10 kW/kg are discussed, as in an approach to implementing the concept through proof-testing on the moon. DOE

N91-28276# Pacific Northwest Lab., Richland, WA.
SPGD: A CENTRAL POWER SYSTEM FOR SPACE
R. D. Widrig 1991 5 p Presented at the SEE/AIAA Meeting: Power From Space, Paris, France, 1-13 Apr. 1991
(Contract DE-AC06-76RL-01830)
(DE91-012610; PNL-SA-18750; CONF-910456-1) Avail: NTIS HC/MF A01

The Space Power Generation and Distribution (SPGD) concept for providing power to any satellite in earth orbit via power beaming is described. Other applications such as providing power for terrestrial or space exploration purposes are identified. An assessment of SPGD versus conventional space power is summarized concluding SPGD appears extremely attractive for the space future. DOE

N91-28277*# National Aeronautics and Space Administration. Lewis Research Center, Cleveland, OH.
SEI POWER SOURCE ALTERNATIVES FOR ROVERS AND OTHER MULTI-kWe DISTRIBUTED SURFACE APPLICATIONS
David J. Bents, L. L. Kohout, Barbara I. McKissock, C. D. Rodriguez, C. A. Withrow, A. Colozza, James C. Hanlon, and Paul C. Schmitz (Sverdrup Technology, Inc., Brook Park, OH.) 1991 13 p Presented at the European Space Power Conference, Florence, Italy, 2-5 Sep. 1991; sponsored by ESA
(Contract NAS3-25266)
(NASA-TM-104360; E-6155; NAS 1.15:104360) Avail: NTIS HC/MF A03 CSCL 10B

To support the Space Exploration Initiative (SEI), a study was performed to investigate power system alternatives for the rover vehicles and servicers that were subsequently generated for each of these rovers and servicers, candidate power sources incorporating various power generation and energy storage technologies were identified. The technologies were those believed most appropriate to the SEI missions, and included solar, electrochemical, and isotope systems. The candidates were characterized with respect to system mass, deployed area, and volume. For each of the missions a preliminary selection was made. Results of this study depict the available power sources in

light of mission requirements as they are currently defined.
Author

N91-28278*# National Aeronautics and Space Administration. Lewis Research Center, Cleveland, OH.
COMPARISON OF DYNAMIC ISOTOPE POWER SYSTEMS FOR DISTRIBUTED PLANET SURFACE APPLICATIONS
David J. Bents, Barbara I. McKissock, James C. Hanlon, Paul C. Schmitz (Sverdrup Technology, Inc., Brook Park, OH.), Carlos D. Rodriguez, and Colleen A. Withrow Washington Aug. 1991 14 p
(NASA-TM-4303; E-5905; NAS 1.15:4303) Avail: NTIS HC/MF A03 CSCL 10B

Dynamic isotope power system (DIPS) alternatives were investigated and characterized for the surface mission elements associated with a lunar base and subsequent manned Mars expedition. System designs based on two convertor types were studied. These systems were characterized parametrically and compared over the steady-state electrical output power range 0.2 to 20 kWe. Three methods of thermally integrating the heat source and the Stirling heater head were considered, depending on unit size. Figures of merit were derived from the characterizations and compared over the parametric range. Design impacts of mission environmental factors are discussed and quantitatively assessed.
Author

N91-28279# Edgerton, Germeshausen and Grier, Inc., Idaho Falls, ID.
SMALL EX-CORE HEAT PIPE THERMIONIC REACTOR CONCEPT (SEHPTR)
M. G. Jacox, R. G. Bennett, L. B. Lundberg, B. G. Miller, and R. L. Drexler 1991 6 p Presented at the 26th Intersociety Energy Conversion Engineering (IECE) Conference, Boston, 3-9 Aug. 1991
(Contract DE-AC07-76ID-01570)
(DE91-014073; EGG-M-91251; CONF-910801-6) Avail: NTIS HC/MF A02

The Idaho National Engineering Laboratory (INEL) has developed an innovative space nuclear power concept with unique features and significant advantages for both Defense and Civilian space missions. The Small Ex-core Heat Pipe Thermionic Reactor (SEHPTR) concept was developed in response to Air Force needs for space nuclear power in the range of 10 to 40 kilowatts. This paper describes the SEHPTR concept and discusses the key technical issues and advantages of such a system. DOE

23 CHEMISTRY AND MATERIALS (GENERAL)

No abstracts in this category.

24 COMPOSITE MATERIALS

Includes physical, chemical, and mechanical properties of laminates and other composite materials.

For ceramic materials see *27 Nonmetallic Materials.*

N91-28280# Southwest Research Inst., San Antonio, TX.
FRACTURE MICROMECHANICS OF INTERMETALLIC AND CERAMIC MATRIX CONTINUOUS FIBER COMPOSITES Technical Report, 29 Apr. 1990 - 29 Apr. 1991
D. L. Davidson May 1991 45 p
(Contract N00014-85-C-0206)
(AD-A236638; SwRI-06-8602/6) Avail: NTIS HC/MF A03 CSCL 11/4

Micromechanics parameters for fatigue cracks growing perpendicular to fibers were measured through small port holes in the matrix made by electropolishing, were used to determine fiber stresses, which ranged from 1.1 to 4 GPa. Crack opening displacements at maximum load and residual crack opening displacements (at minimum load) were measured. Matrix was removed along the crack flanks after completion of the tests to reveal the extent and nature of fiber damage. Analyses were made of these parameters, and it was found possible to link the extent of fiber debonding to residual COD and the shear stress for debonding, estimated at 245 MPa, to COD. Measured experimental parameters were used to compute crack growth rates using a wall known fracture mechanics model for fiber bridging tailored to these experiments. The potential for microstructural manipulation to yield further increases in fatigue crack growth resistance for the metals and alloys currently being used in gas turbine construction is small. Studies of fatigue crack growth through aluminum, titanium and superalloys show that there are many similarities in the mechanisms of crack growth and the crack tip micromechanics for these materials. Conversely, composite materials reinforced with continuous strong fibers offer the promise of drastic increases in fatigue crack growth resistance. GRA

N91-28281# California Univ., Berkeley. Lawrence Berkeley Lab.
ALUMINA-SILICON CARBIDE COMPOSITES FROM COATED POWDERS Ph.D. Thesis
T. D. Mitchell, Jr. Dec. 1990 59 p
(Contract DE-AC03-76SF-00098)
(DE91-012357; LBL-30474) Avail: NTIS HC/MF A04

Previous technology for alumina coating of silicon carbide whiskers was applied to silicon carbide platelets. Process parameters were developed to ensure successful coating of platelets and to produce composites of varying final platelet volume fractions. Coated whisker composites were hot pressed to near full density or pressureless sintered to closed porosity despite high whisker loading. In some cases, pressureless sintering resulted in near full density with high (30 volume percent) whisker loading. Coated platelet composites were hot pressed to near full density and pressureless sintered to closed porosity with high loading (35 volume percent). Mechanical properties of these composites were evaluated, including fracture toughness and bend strength. DOE

N91-28282# Edgerton, Germeshausen and Grier, Inc., Idaho Falls, ID.
A REVIEW OF SILICON CARBIDE/METAL INTERACTIONS WITH RELEVANCE TO SILICON CARBIDE JOINING
B. H. Rabin Apr. 1991 19 p
(Contract DE-AC07-76ID-01570)
(DE91-012768; EGG-MS-9633) Avail: NTIS HC/MF A03

The current understanding of elevated temperature interactions between metals and silicon carbide ceramics is reviewed. For each of the metals examined, details available in the literature regarding wetting, reaction mechanisms, kinetics, and product phases are described, and these observations are discussed on the basis of phase equilibria considerations. The implications of these findings with respect to joining silicon carbide ceramics for elevated temperature applications are discussed. DOE

N91-28283# Oak Ridge National Lab., TN.
TECHNOLOGIES AVAILABLE FROM MARTIN MARIETTA ENERGY SYSTEMS, INC.
1991 29 p
(Contract DE-AC05-84OR-21400)
(DE91-013027; ORNL/M-1312) Avail: NTIS HC/MF A03

This document summarizes some of the specific technologies available from Oak Ridge National Laboratory (ORNL) and the other Oak Ridge plants managed and operated by Martin Marietta Energy Systems, Inc. (Energy Systems) for the Department of Energy (DOE). From the beginning, we have concentrated our efforts on those areas of technology development for which we have become known as a center of excellence. Our most notable area of success is in advanced materials. From superalloys to ceramics to electronic materials, Oak Ridge is internationally

recognized as a leader in advanced materials. Other areas where we have unique technical expertise include: analytical instruments, waste management, intelligent systems, and chemical processing.
DOE

N91-28284# Lawrence Livermore National Lab., CA.

THE APPLICATION OF X RAY TOMOGRAPHIC MICROSCOPY TO CHEMICAL VAPOR INFILTRATION PROCESSING OF CERAMIC MATRIX COMPOSITES

J. H. Kinney, M. C. Nichols, S. R. Stock, T. L. Starr, and C. A. Lundgren (Du Pont de Nemours, E. I. and Co., Wilmington, DE) Apr. 1991 7 p Presented at the 2nd American Society for Nondestructive Testing (ASNT) on Industrial Computed Tomography Conference, San Diego, 20-24 May 1991
(Contract W-7405-eng-48)
(DE91-011871; UCRL-JC-107069; CONF-9105166-3) Avail: NTIS HC/MF A02

Before ceramic composite materials can be used in critical structures it will be necessary to reduce the amount of porosity which remains after processing. Complete densification of chemical vapor infiltrated (CVI) composites has yet to be attained due to the enclosure of pores by growth of the matrix on surrounding fibers. If the residual porosity cannot be significantly reduced during processing, much of the anticipated fracture toughness of Ceramic Matrix Composites (CMC's) may be lost. Clearly, a noninvasive technique is required for making dynamic observations of matrix growth during CVI processing. Though there are many NDE techniques which might be applied to pore characterization, all of them have drawbacks when imaging complex, overlapping microstructures. For example, techniques such as fluorescent penetrant and infrared inspection reveal only surface flaws and cannot be applied universally to all classes of materials. X-ray tomographic microscopy (XTM) is a high resolution, noninvasive technique which is ideally suited for imaging materials microstructures in three-dimensions. The XTM allows imaging of microporosity between individual filaments in the fiber bundles, measurement of channel porosity between individual cloth layers, and characterization of the interconnectivity of the large through-ply holes that remain after processing. This paper reports the results of an XTM study on unreacted fiber preforms and fully dense CMC's with the express purpose of demonstrating that XTM has the spatial resolution and the contrast sensitivity to measure the important microstructural features in these materials. DOE

N91-28285# Lawrence Livermore National Lab., CA.

MULTIAXIAL FAILURE CHARACTERIZATION OF COMPOSITES

S. E. Groves, R. J. Sanchez, and W. W. Feng Feb. 1991 19 p Presented at the 8th International Conference on Composite Materials, Honolulu, 15-19 Jul. 1991 Revised
(Contract W-7405-eng-48)
(DE91-011925; UCRL-JC-105244-Rev-1; CONF-910731-2-Rev-1) Avail: NTIS HC/MF A03

The primary objective was to develop a multiaxial testing capability for continuous fiber composites using the axial/torsion/internal pressurization of tubes. This capability enables one to generate the 2-D (in-plane) failure surface for these materials. The multiaxial test specimen consists of a 5.08 cm (2.0 in.) diameter composite tube with 15 degrees cast epoxy end cones for gripping. The unique advancement with this new technique is the simple, but very efficient, gripping mechanism that provides a very smooth transition in load from the grip into the specimen. This has eliminated grip related stress risers in the composite tube. Consequently, most of the failures occur in the gage section of the tube. This system is coupled into a biaxial MTS servo hydraulic test machine capable of simultaneously applying axial load, torque, and internal pressure, providing one complete control of the axial, transverse, and shear stresses that develop in the wall of the composite tube. The failure results are presented which were obtained to date for various laminate configurations of Toray 1000/DER332-T403 filament wound carbon/epoxy tubes along with T300/F263 prepreg carbon/epoxy tubes. The goal of the efforts is to develop a more fully characterized 3-D failure criterion for these materials. This model will then be incorporated into a large 3-D orthotropic finite element model for structural analysis as well as a specialized 3-D orthotropic finite element model capable of detailed sub-ply level analysis on sub-structural components. DOE

N91-28286# Lawrence Livermore National Lab., CA.

ON THE FINITE-STRAIN-INVARIANT FAILURE CRITERION FOR COMPOSITES

W. W. Feng and S. E. Groves Feb. 1991 9 p Presented at the 8th International Conference on Composite Materials, Honolulu, 15-19 Jul. 1991
(Contract W-7405-eng-48)
(DE91-011924; UCRL-JC-106555; CONF-910731-3) Avail: NTIS HC/MF A02

The finite-strain-invariant failure criterion developed by Feng is being evaluated with the experimental data for a boron/epoxy, symmetrically balanced, angle-ply laminate. The results indicate that the failure-criterion prediction agrees with the experimental data and that the failure criterion also predicts the matrix-dominated or fiber-dominated modes of failure. Two special isotropic cases in infinitesimal strain theory are obtained. The failure criteria for these special cases preserve the mathematical forms of both the generalized Von Mises yield criterion and the Von Mises yield criterion in plasticity. DOE

N91-28287# Michigan State Univ., East Lansing. Dept. of Metallurgy, Mechanics and Material Science.

SOFTENING MECHANISMS AND MICROSTRUCTURAL INSTABILITIES DURING HIGH TEMPERATURE, LOW CYCLE FATIGUE OF Ni, Ni3Al, AND THEIR METAL MATRIX COMPOSITES

D. S. Grummon and G. Gottstein 30 Sep. 1990 12 p
(Contract DE-FG02-85ER-45205)
(DE91-012714; DOE/ER-45205/6) Avail: NTIS HC/MF A03

Progress is discussed in the following areas: modification of reinforcements for aluminide matrix composites, dynamic recrystallization and microstructure development, computer modelling of microstructural stability, texture development during dynamic recrystallization, and creep in Ni3Al. DOE

N91-28288# Los Alamos National Lab., NM.

ZrO2 REINFORCED-MoSi2 MATRIX COMPOSITES

J. J. Petrovic, R. E. Honnell, T. E. Mitchell, R. K. Wade, and K. J. McClellan (Case Western Reserve Univ., Cleveland, OH.) 1991 16 p Presented at the 15th Annual Conference on Composites and Advanced Ceramics, Cocoa Beach, 13-16 Jan. 1991
(Contract W-7405-eng-36)
(DE91-013074; LA-UR-91-1642; CONF-910162-7) Avail: NTIS HC/MF A03

ZrO2 particle-MoSi2 matrix composites were fabricated by wet processing/hot pressing, using high quality unstabilized, partially stabilized, and fully stabilized ZrO2 powders. Composite room temperature indentation fracture toughness increased with increasing volume fraction of ZrO2 reinforcement. Unstabilized ZrO2 produced the highest composite fracture toughness, 7.8 MPa m(sup (1/2)) as compared to 2.6 MPa m(sup (1/2)) for pure MoSi2. Unstabilized ZrO2 composites exhibited matrix microcracking, and the spontaneous tetragonal-to-monoclinic ZrO2 phase transformation induced significant plastic deformation in the MoSi2 matrix. Partially stabilized ZrO2 produced a lesser extent of composite fracture toughening, possibly as a result of an inhomogeneous ZrO2 particle distribution and presence of a glassy phase. DOE

N91-28289*# National Aeronautics and Space Administration. Lewis Research Center, Cleveland, OH.

APPARATUS FOR INTERCALATING LARGE QUANTITIES OF FIBROUS STRUCTURES Patent Application

James R. Gaier, inventor (to NASA) 24 Jul. 1991 13 p
(NASA-Case-LEW-15077-2; NAS 1.71:LEW-15077-2; US-Patent-Appl-SN-735548) Avail: NTIS HC/MF A03 CSCL 11D

Apparatus for intercalating large quantities of fibrous structures uses a rotatable reaction chamber containing a liquid phase intercalate. The intercalate liquid phase is controlled by appropriately heating, cooling or pressurizing the reaction. Rotation of the chamber containing the fiber sample ensures total submergence if the fiber during intercalation. Intercalated graphite fibers having metal-like resistivities are produced and are conceivably useful as electrical conductors. NASA

N91-28290*# National Aeronautics and Space Administration. Langley Research Center, Hampton, VA.

PROCESS FOR APPLICATION OF POWDER PARTICLES TO FILAMENTARY MATERIALS Patent Application

Robert M. Baucom, inventor (to NASA), John J. Snoha, inventor (to NASA), and Joseph M. Marchello, inventor (to NASA) (Old Dominion Univ., Norfolk, VA.) 16 May 1990 20 p
(NASA-Case-LAR-14231-1-CU; NAS 1.71:LAR-14231-1-CU; US-Patent-Appl-SN-524109) Avail: NTIS HC/MF A03 CSCL 11D

This invention is a process for the uniform application of polymer powder particles to a filamentary material in a continuous manner to form a uniform composite prepreg material. A tow of the filamentary material is fed under carefully controlled tension into a spreading unit, where it is spread pneumatically into an even band. The spread filamentary tow is then coated with polymer particles from a fluidized bed, after which the coated filamentary tow is fused before take-up on a package for subsequent utilization. This process produces a composite prepreg uniformly without imposing severe stress on the filamentary material, and without requiring long, high temperature residence times for the polymer. NASA

N91-28291# Ames Lab., IA.

STRENGTH AND ELECTRICAL CONDUCTIVITY OF DEFORMATION PROCESSED Cu-15 v/o Fe METAL COMPOSITES PRODUCED BY POWDER METALLURGY/TECHNIQUES Ph.D. Thesis

G. A. Jerman 30 May 1991 156 p
(Contract W-7405-eng-82)
(DE91-013658; IS-T-1560) Avail: NTIS HC/MF A08

Copper based deformation processed metal matrix composites have been recently developed which exhibit high strengths with high electrical conductivities. The high strengthening is achieved through the establishment of second phase fibers in a Cu matrix. The most suitable second phase materials are BCC metals such as Nb, Cr, V, Ta, and Fe. The most economically attractive combination is the Cu-Fe system. Previous attempts at processing Cu-Fe composites have been hampered by the presence of Fe dissolved in the Cu matrix. Because of the large detriment dissolved Fe poses to the conductivity of the Cu matrix, cast processing the undeformed composites has led to low overall conductivity. To overcome this obstacle, powder metallurgy techniques have been adopted to consolidate blended elemental Cu and Fe powders. By controlling the time and temperature of the consolidation process, a Cu-15 v/o Fe metal matrix composite has been developed which matches the strength and conductivity properties of a similar cast Cu-15 v/o Nb alloy. The highest achievable strength was 1462 MPa with an attendant conductivity of 59 percent IACS. DOE

N91-28292*# Virginia Polytechnic Inst. and State Univ., Blacksburg. Dept. of Engineering Science and Materials.

DAMAGE DEVELOPMENT UNDER COMPRESSION-COMPRESSION FATIGUE LOADING IN A STITCHED UNIWOVEN GRAPHITE/EPOXY COMPOSITE MATERIAL Interim Report No. 86

Nancy E. Vandermey, Don H. Morris, and John E. Masters Jul. 1991 126 p
(Grant NAG1-343)
(NASA-CR-188693; NAS 1.26:188693; CCMS-91-16; VPI-E-91-14) Avail: NTIS HC/MF A07 CSCL 11D

Damage initiation and growth under compression-compression fatigue loading were investigated for a stitched uniweave material system with an underlying AS4/3501-6 quasi-isotropic layup. Performance of unnotched specimens having stitch rows at either 0 degree or 90 degrees to the loading direction was compared. Special attention was given to the effects of stitching related manufacturing defects. Damage evaluation techniques included edge replication, stiffness monitoring, x-ray radiography, residual compressive strength, and laminate sectioning. It was found that the manufacturing defect of inclined stitches had the greatest adverse effect on material performance. Zero degree and 90 degree specimen performances were generally the same. While the stitches were the source of damage initiation, they also slowed damage propagation both along the length and across the width and affected through-the-thickness damage growth. A pinched layer zone formed by the stitches particularly affected damage initiation and growth. The compressive failure mode was transverse shear for all specimens, both in static compression and fatigue cycling effects. Author

N91-28293*# National Aeronautics and Space Administration. Langley Research Center, Hampton, VA.

LOCAL DELAMINATION IN LAMINATES WITH ANGLE PLY MATRIX CRACKS. PART 1: TENSION TESTS AND STRESS ANALYSIS

T. Kevin OBrien and S. J. Hooper (Wichita State Univ., KS.) Jun. 1991 33 p Presented at the 4th ASTM Conference on Composite Materials: Fatigue and Fracture, Indianapolis, IN, 6-7 May 1991 Prepared in cooperation with Army Aviation Systems Command, Hampton, VA
(NASA-TM-104055; NAS 1.15:104055; AVSCOM-TR-91-B-010-Pt-1) Avail: NTIS HC/MF A03 CSCL 11D

Quasi-static tension tests were conducted on AS4/3501-6 graphite epoxy laminates. Dye penetrant enhanced x-radiography was used to document the onset of matrix cracking and the onset of local delaminations at the intersection of the matrix cracks and the free edge. Edge micrographs taken after the onset of damage were used to verify the location of the matrix cracks and local delamination through the laminate thickness. A quasi-3D finite element analysis was conducted to calculate the stresses responsible for matrix cracking in the off-axis plies. Laminated plate theory indicated that the transverse normal stresses were compressive. However, the finite element analysis yielded tensile transverse normal stresses near the free edge. Matrix cracks formed in the off-axis plies near the free edge where in-plane transverse stresses were tensile and had their greatest magnitude. The influence of the matrix crack on interlaminar stresses is also discussed. Author

N91-28294 Case Western Reserve Univ., Cleveland, OH.

PROCESSING, COMPATIBILITY AND OXIDATION OF DIBORIDE-REINFORCED OXIDE MATRIX COMPOSITES FOR ULTRAHIGH-TEMPERATURE APPLICATIONS Ph.D. Thesis

Ahmed Abada 1990 254 p
Avail: Univ. Microfilms Order No. DA9035265

Promising results for the development of a ceramic/ceramic composite to be used for structural applications in the ultra high temperature range (1650 to 1850 C) were obtained for alumina reinforced with titanium or zirconium diboride coated with molybdenum disilicide. Calculations of the compatibility and stability of oxide matrices with the diborides in vacuum showed positive energies of formation, indicating suitability of reinforcement of alumina under vacuum conditions. Stability and chemical compatibility of the particulate and ternary composites in their as hot pressed states and following their vacuum and air oxidation treatment were characterized. Dissert. Abstr.

N91-28295 Washington Univ., Seattle.

THE EFFECT OF DUCTILE INNERLAYERS ON THE MECHANICAL PERFORMANCE OF FIBER-REINFORCED COMPOSITE MATERIALS Ph.D. Thesis

Meng-Bor Hsu 1990 162 p
Avail: Univ. Microfilms Order No. DA9114714

The effects of ductile innerlayers on the mechanical behavior

of unidirectional fiber reinforced composites were studied. Two fiber systems were used as the reinforcement; a monofilament system and a roving system. The ductile innerlayer materials were applied on fiber surfaces using coating equipment that was first designed for monofilament coating. For composites reinforced by rovings, problems such as nonuniform fiber distribution and resin starvation in spaces between closely packed filaments arise from the coating process. Even with these problems, improvement in transverse tensile strength, longitudinal compressive strength, flexural fatigue resistance, and fatigue endurance limit were achieved. For monofilament systems, properties such as flexural strength, interlaminar shear strength, and transverse tensile strength are improved by the application of ductile innerlayers. Three mechanisms were shown to be responsible for the improvements: by acting as a spacer and preventing fiber-fiber contact; local ductility is provided near the fiber-matrix interface and lowering stress concentrations; and healing surface flaws in large diameter fiber systems, thus increasing fiber strength.
Dissert. Abstr.

N91-28296 Northwestern Univ., Evanston, IL.
INVESTIGATION OF THERMOMECHANICAL BEHAVIOR OF METAL MATRIX COMPOSITES Ph.D. Thesis
Dimitrios Karalekas 1990 231 p
Avail: Univ. Microfilms Order No. DA9114571

A combined experimental/analytical study was conducted of the mechanical and thermal properties of a SiC/6061-Al filamentary composite. Longitudinal and transverse tensile stress-strain curves were obtained up to failure of the unidirectional composite for temperatures up to 288 C. The longitudinal and transverse thermal deformation was also measured as a function of temperature up to 482 C. A two-material composite cylinder model (CCM) was considered for the study of the mechanical and thermal behavior of the composite at different temperatures. An elastoplastic analysis of the model was performed in which the fabric was taken to be linear elastic and the matrix elastoplastic with work hardening. The complete three dimensional stress distribution in the composite was determined. Dissert. Abstr.

N91-28297 Northwestern Univ., Evanston, IL.
TRIBOLOGY OF ALUMINUM-BASED METAL MATRIX COMPOSITES: FUNDAMENTAL STUDY OF WEAR BEHAVIOR AS INFLUENCED BY MICROSTRUCTURE Ph.D. Thesis
Yi-Ming Pan 1990 176 p
Avail: Univ. Microfilms Order No. DA9114612

Rolling and sliding wear experiments were conducted on selected aluminum-based metal matrix composites against hard iron base counterfaces. Wear morphology and surface chemistry in these composites after tribo-contact were characterized using a variety of analytical techniques to increase understanding of wear mechanisms. Different wear behavior for rolling and sliding wear, which have different temporal contact stress state, was investigated considering the phases, their interface and microstructure, and the role of heat treatment. Dissert. Abstr.

N91-28298 Ohio State Univ., Columbus.
JOINING OF ALUMINUM-BASED PARTICULATE-REINFORCED METAL-MATRIX COMPOSITES Ph.D. Thesis
Sudhakar Kolli 1990 287 p
Avail: Univ. Microfilms Order No. DA9111734

Some 25 Vol pct. SiCp/6061 Al metal matrix composite (MMC) material were joined by the transient liquid phase diffusion bonding process using a Gleeble 1500 system. In order to understand the effects of the bonding thermomechanical cycle on the mechanical and metallurgical properties of the base material, thermal and thermomechanical simulation studies were performed with a regular heat treatment furnace and the Gleeble system. Thermal simulation conditions included temperatures ranging from 500 to 590 C and times from 5 to 9 minutes. Thermo-mechanical simulation conditions ranged temperatures from 540 to 580 C, times from 5 to 60 minutes, and pressures from 350 to 900 psi, with resulting deformation at the interface from 1.8 to 11.9 pct. Degradation in base material mechanical properties with time, temperature, and loading was observed. The simulated bond structures were characterized with optical and scanning electron microscopy and bonding temperatures and times selected. Dissert. Abstr.

N91-28299 Virginia Polytechnic Inst. and State Univ., Blacksburg.
AN ANALYSIS OF INTERLAMINAR STRESSES IN UNSYMMETRICALLY LAMINATED PLATES Ph.D. Thesis
Donald Scott Norwood 1990 354 p
Avail: Univ. Microfilms Order No. DA9116674

The results of a numerical study in interlaminar stresses within unsymmetrically laminated plates are presented. The study focused on the linear thermoelastic response of thin square laminated composite plates subjected to extensional, compressive, or thermal loading. Symmetric and unsymmetric 0/90, +45/-45, and 0/+45 laminate stacking sequences are examined to determine the effects of mismatch between adjacent layers in Poisson's ratio, coefficient of mutual influence, and coefficients of thermal expansion. For laminates subjected to external loading, the mismatch in material properties between adjacent layers causes interlaminar stresses to arise near the free edges. For the laminates and loading conditions considered, the results show that the out-of-plane deflections of unsymmetric laminates reduce interlaminar shear stresses. Dissert. Abstr.

N91-28300 Brunel Univ., Uxbridge (England).
THE INFLUENCE OF DEFECTS ON THE MECHANICAL PROPERTIES OF SHORT FIBRE REINFORNCED THERMOPLASTICS Ph.D. Thesis
Ali Zadhoush 1989 294 p
Avail: Univ. Microfilms Order No. BRDX92240

The objective was to understand the role of defects in determining the mechanical properties of short fiber reinforced thermoplastic parts produced by the injection molding process and to understand methods for suppressing defects by their elimination or by management of reinforcing fiber orientations. The following types of microstructural inhomogeneities were purposely introduced into injection moldings: (1) particulate impurities; (2) micro-voids; (3) micro-cracks; and (4) different geometries of preferred orientation of fibers. The study materials were based on carbon fiber and glass fiber reinforced thermoplastics. Macro- and micro-radiography and sectioning combined with scanning electron microscopy were the main techniques used for mechanical and microstructural characterization. Dissert. Abstr.

N91-28301 Drexel Univ., Philadelphia, PA.
DAMAGE PROGRESSION DURING STATIC AND FATIGUE LOADING IN METAL MATRIX COMPOSITES, VOLUMES 1-3 Ph.D. Thesis
John G. Bakuckas, Jr. 1991 812 p
Avail: Univ. Microfilms Order No. DA9119028

The objective is to gain a rational understanding of the damage initiation and progression in a variety of metal matrix composites (MMC) during both static and fatigue loading. An extensive two prong investigation involving experimental and analytical phases was undertaken in order to characterize damage progression in center notched MMC. Experimentally, the crack tip damage growth was studied utilizing several techniques including optical observations, use of the laser interferometric displacement gauge, acoustic emission, and fractography. The effects of heat treatment, constituents, and laminate configuration are addressed. In the analytical phase, the mechanics which govern the onset of damage formation in center cracked unidirectional MMC monolayers are predicted. A unique analytical technique to numerically simulate the subsequent damage progression is presented which manifests the individual microfailure mechanisms and their interaction in the evolution of the failure process ahead of an existing crack. Numerical simulations of the failure process was performed in several center-cracked unidirectional monolayered composites. The numerical simulations are correlated with experimental results in terms of the observed failure process, the notched strength, and load-COD data. Excellent agreement between the optical observations and the numerical simulation of the failure process

was obtained. The numerical simulations captured the salient features observed in the sequential failure process. When correlated with the experimental results, the numerical simulations provided a better insight into the failure process in MMC. The appropriate selection of constituent components in the development of damage tolerant MMC for a particular application can be achieved by using this numerical technique.
Dissert. Abstr.

N91-28302 Drexel Univ., Philadelphia, PA.
FINITE ELEMENT MODELING OF 2-D DELAMINATION GROWTH IN LAMINATED COMPOSITES Ph.D. Thesis
Chung Keun Gim 1990 282 p
Avail: Univ. Microfilms Order No. DA9115905

A plate finite element analysis procedure was developed to study the growth behavior of two-dimensional delamination in laminated composite plates. The finite element procedure is based on the laminated plate theory which includes the effect of transverse shear deformation and in-plane loading. The classical fracture mechanics criterion of strain energy release rate is used to study the delamination growth. A special multiple-point constraint algorithm which ensures the compatibility and equilibrium conditions at the crack front is incorporated in the finite element formulation. To compute the energy release rate, a virtual crack closure formulation is followed. Dissert. Abstr.

N91-28303 Virginia Polytechnic Inst. and State Univ., Blacksburg.
HIGH-RESOLUTION INTERFEROMETRIC MEASUREMENTS OF RESIDUAL STRAINS IN COMPOSITES Ph.D. Thesis
Joosik Lee 1990 121 p
Avail: Univ. Microfilms Order No. DA9116634

As composites are more widely accepted as structural materials, residual stresses in them become a more serious issue. In order to measure residual strains more effectively, a new method of measuring them is required. Moire interferometry combined with the cut-and-sectioning method was developed for effective measurement of residual strains in fiber-reinforced composites. Also, in order to determine residual strains on a within-the-ply basis, a new high resolution data reduction procedure was developed. Dissert. Abstr.

N91-28229*# Pennsylvania State Univ., University Park. Dept. of Engineering Science and Mechanics.
COMPOSITE MATERIAL SYSTEMS FOR HYDROGEN MANAGEMENT
R. N. Pangborn and R. A. Queeney *In* NASA, Washington, Space Transportation Propulsion Technology Symposium. Volume 2: Symposium Proceedings May 1991 p 691-697 (For primary document see N91-28193 20-20)
Avail: NTIS HC/MF A99 CSCL 11D

25 INORGANIC AND PHYSICAL CHEMISTRY

Includes chemical analysis, e.g., chromatography; combustion theory; electrochemistry; and photochemistry.

For related information see also *77 Thermodynamics and Statistical Physics..*

N91-28304# California Inst. of Tech., Pasadena. Dept. of Chemistry.
APPLICATIONS OF SCANNING TUNNELING MICROSCOPY TO ELECTROCHEMISTRY
Nathan S. Lewis 31 May 1991 11 p
(Contract N00014-88-K-0482)
(AD-A237021) Avail: NTIS HC/MF A03 CSCL 09/1

The focus of research in the last year has been STM (Scanning Tunneling Microscopy) studies of electrode solution interfaces. STM, and its derivatives (e.g., AFM, Atomic Force Microscopy) are the only surface analytic methods capable of yielding real-space, atomic resolution, electronic and structural maps of immersed electrode surfaces. To achieve this goal, in the previous contract period we have developed STM tip preparation methodologies that enable atomic resolution imaging of electrode surfaces in solutions containing high (0.1 M) concentrations of electron donar and acceptor species. These techniques have significantly extended the applicability of STM to electrochemical investigations. Recent STM investigations of electrochemical systems surface under varied media. GRA

N91-28305# Lawrence Livermore National Lab., CA.
CHEMISTRY AND MATERIALS SCIENCE RESEARCH REPORT
Mar. 1991 122 p
(Contract W-7405-eng-48)
(DE91-011507; UCID-20622-90-2) Avail: NTIS HC/MF A06

The research reported here in summary form was conducted during the second half of FY90 under the auspices of Weapons-Supporting Research (WSR) and Institutional Research and Development (IR and D). The results reported here are for work in progress; as such, they may be preliminary, fragmentary, or incomplete. Areas covered are as follows: Synchrotron-Radiation-Based Materials Science; Fundamental Aspects of Metal Processing; Energetic Materials; Tritium; High-Transition-Temperature Superconductivity; Plutonium; Interfaces, Adhesion, and Bonding; Photocatalysis on Doped Aerogel; Structural Transformation and Precursor Phenomena in Advanced Materials: Theory and Experiments; Laser-Induced Chemistry; Molecular Plasmas; Chemistry of Defects; The Use of Short Pulses with Energetic Materials; NMR Investigations of Crosslinking in Melamine Formaldehyde Aerogels; Surface Magnetism in Ultrathin Films of Fe/Cu(001); Damage Initiation and Accumulation during Fatigue in Metal-Matrix Composites; Reactivity of the V=O Bond; The Structure-Property Link in Subnanometer Materials; and Thermodynamic and Mechanical Properties of Al-Li alloys. DOE

N91-28306# Lawrence Livermore National Lab., CA.
PROTON ENERGY LOSS (PEL) MATERIAL CHARACTERIZATION
D. L. Weirup, C. M. Logan, A. E. Pontau, A. J. Antolak, and D. H. Morse (Sandia National Labs., Livermore, CA.) 1991 9 p Presented at the 2nd American Society for Nondestructive Testing (ASNT) on Industrial Computed Tomography Conference, San Diego, 20-24 May 1991
(Contracts W-7405-eng-48; DE-AC04-76DP-00789)
(DE91-011545; UCRL-JC-104112; CONF-9105166-4) Avail: NTIS HC/MF A02

Proton Energy Loss (PEL), has proven to be a valuable method of material characterization. Unlike x-ray methods which are sensitive almost exclusively to the high Z elements of a material, PEL provides information on all elements. With the current system we are capable of gathering a 2-D mapping of areal density or a tomographic slice through a material. Multiple slices can be combined to form a full three-dimensional rendered image of the object. We have used the PEL system to characterize materials and to study machining and assembly techniques. DOE

N91-28307# Lawrence Livermore National Lab., CA.
CONTINUUM X RAY GAUGING OF MULTIPLE-ELEMENT MATERIALS
D. L. Lewis, C. M. Logan, and M. R. Gabel (Minnesota Mining and Mfg. Co., Saint Paul.) Feb. 1991 5 p Presented at the American Society for Nondestructive Testing Spring Conference, Oakland, 18-22 Mar. 1991
(Contract W-7405-eng-48)
(DE91-011923; UCRL-JC-104111; CONF-910399-3) Avail: NTIS HC/MF A01

We have developed a system for elemental quantification of materials with known constituents. It utilizes an x ray tube to generate a photon spectrum and an energy-dispersive detector to measure the photon transmission of a material at selected energies. The abundance of each element is than iteratively extracted using characteristic attenuation coefficients and the material bulk density and thickness. DOE

N91-28308# California Univ., Berkeley. Lawrence Berkeley Lab.
SOME NEW APPROACHES TO SEMICLASSICAL AND QUANTUM TRANSITION STATE THEORY
W. H. Miller Oct. 1990 15 p Presented at the 8th European Conference on Dynamics of Molecular Collisions, Bernkastel-Kues, Fed. Republic of Germany, 10-14 Sep. 1990
(Contract DE-AC03-76SF-00098)
(DE91-012345; LBL-29938; CONF-9009383-1) Avail: NTIS HC/MF A03

Semiclassical and quantum mechanical transition state theory is reviewed and two new approaches are described. One is the general implementation of a semiclassical rate expression that involves the 'good' action-angle variables associated with the saddle point (i.e., transition state) of a potential energy surface. The other is an evaluation of a formally exact quantum expression for the rate in terms of Siegert eigenvalues associated with the transition state. Siegert eigenvalues are usually associated with scattering resonances, so their identification with the saddle point of a potential surface, and the expression for the reaction rate in terms of them, is quite an unexpected and novel development. DOE

N91-28309# Oak Ridge National Lab., TN.
CHEMICAL CHARACTERIZATION OF MICROPARTICLES BY LASER ABLATION IN AN ION TRAP MASS SPECTROMETER
J. M. Dale, W. B. Whitten, and J. M. Ramsey 1991 3 p Presented at the American Society for Mass Spectrometry (ASMS) Meeting, Nashville, 19-24 May 1991
(Contract DE-AC05-84OR-21400)
(DE91-012513; CONF-9105181-6) Avail: NTIS HC/MF A01

A new technique is being developed for the chemical characterization of microparticles based upon the use of electrodynamic traps. The electrodynamic trap has achieved widespread use in the mass spectrometry community in the form of the ion trap mass spectrometer or quadrupole ion trap. Small macroscopic particles can be confined or leviated within the electrode structure of a three-dimensional quadrupole electrodynamic trap in the same way as fundamental charges or molecular ions by using a combination of ac and dc potentials. The concept is to use the same electrode structure to perform both microparticle levitation and ion trapping/mass analysis. The microparticle will first be trapped and spatially stabilized within the trap for characterization by optical probes, i.e., absorption, fluorescence, or Raman spectroscopy. After the particle has been optically characterized, it is further characterized using mass spectrometry. Ions are generated from the particle surface using laser ablation or desorption. The characteristics of the applied voltages are changed to trap the ions formed by the laser with the ions subsequently mass analyzed. The work described focuses on the ability to perform laser desorption experiments on microparticles contained within the ion trap. Laser desorption has previously been demonstrated in ion trap devices by applying the sample to a probe which is inserted so as to place the sample at the surface of the ring electrode. The technique requires the placement of a microparticle in the center of the trap. The initial experiments have been performed on falling microparticles rather than levitated particles to eliminate voltage switching requirements when changing from particle to ion trapping modes. DOE

N91-28310# Oak Ridge National Lab., TN.
ANALYSIS OF METALS IN SOLUTION USING ELECTROSPRAY IONIZATION MASS SPECTROMETRY
G. J. VanBerkel, S. A. McLuckey, and G. L. Glish 1991 3 p Presented at the American Society for Mass Spectrometry (ASMS) Meeting, Nashville, 19-24 May 1991
(Contract DE-AC05-84OR-21400)
(DE91-012522; CONF-9105181-1) Avail: NTIS HC/MF A01

Electrospray ionization-mass spectrometry (ES-MS) has gained most of its recent attention because of the ability to produce multiply charged ions from very large biomolecules making them amenable to analysis by most modern mass spectrometers. However, ES-MS is equally well suited for compounds of low or moderate molecular weight that are difficult to volatilize intact by others methods. Moreover, the early work of Fenn and co-workers (1,2) and recent reports by Kebarle and co-workers (3,4) attest to the applicability of ES-MS to the study of the gas-phase chemistry of multiply solvated or coordinated metal ions. The utility of ES-MS for the analysis of metals in solution derives in part from the facility with which the metal ions are solvated by or form complexes with the ES solvent or other reagents added to the solvent. Solvation and complexation can be a hindrance, however, in the analytical application of ES-MS to the analysis of metals in solution, especially solutions of metals in water. The data presented here demonstrate that many of the problems in the ES-MS analysis of metals can be overcome by complexing the metals with crown ethers and/or extracting the metals from water into an organic phase using crown ethers. DOE

N91-28311# Oak Ridge National Lab., TN.
EXPERIMENTAL STUDIES OF THE VOLATILITY OF AMMONIUM CHLORIDE
D. A. Palmer and J. M. Simonson 1991 18 p Presented at the International Conference on Cycle Chemistry in Fossil Plants, Baltimore, 4-6 Jun. 1991
(Contract DE-AC05-84OR-21400)
(DE91-012526; CONF-9106189-1) Avail: NTIS HC/MF A03

A platinum-lined autoclave is being used to investigate the partitioning of ammonia and chloride between the vapor and liquid phases of aqueous ammonium chloride. The apparatus is designed to allow the sampling of both phases via inert tubing (platinum and PEEK tubing and valves) over a temperature range of approximately 150 to 350 C. Initial experiments have been carried out at 150 C using acidic ammonium chloride solutions with varying molalities and acidities and a range of vapor sampling rates to ensure equilibrium had been established. Relatively high molalities of NH4Cl were used to provide sufficient solute partitioning to the vapor phase to allow precise determination of the vapor-phase composition by ion chromatography. The ammonium concentration in the vapor phase in excess of that calculated for ammonia volatility provides a direct measure of the maximum volatility of ammonium chloride at that temperature. The calculation of the expected ammonia and hydrochloric acid volatilities is based on a knowledge of the activity coefficients of the ionic species in solution as well as the equilibrium constants for the liquid-vapor partitioning. Activity coefficients of all the ionic solutes and the volatility of HCl were measured in this laboratory; the thermodynamics of the volatility of ammonia are described in previously published works. The results at 150 C are used to demonstrate how maximum ammonium chloride concentrations in the vapor phase can be calculated, including the proportion of total vapor-phase chloride due to NH4Cl and HCl partitioning, for solution compositions relevant to power generating cycles. It should be emphasized that this study is still in progress and that temperatures corresponding to those in power-generating plants will be investigated. DOE

N91-28312# Stanford Univ., CA.
ULTRA-LOW TEMPERATURE PROPERTIES OF AMORPHOUS SOLIDS
1991 5 p
(Contract DE-FG03-90ER-45435)
(DE91-012782; DOE/ER-45435/T1) Avail: NTIS HC/MF A01

Substantial progress was made in making the new top-loading demagnetization cryostat fully operational. In addition, preliminary studies were made of a number of dielectric glasses, and have proceeded with plans to fabricate samples by sputter deposition of SiO2. Further, a helium liquifier was ordered which will substantially lower the costs of running the cryostat, and begun screening perspective graduate students to bring the complement of students on this grant up to a total of three. DOE

N91-28313# Lawrence Livermore National Lab., CA.
EQUATION-OF-STATE FROM SIO2 AEROGEL HUGONIOT DATA
R. Grover, F. Ree, and N. C. Holmes May 1991 15 p Presented at the 1991 American Physical Society (APS) Conference on Shock

Compression of Condensed Matter, Willamsburg, 17-20 Jul. 1991
(Contract W-7405-eng-48)
(DE91-011480; UCRL-JC-10639; CONF-9107105-3) Avail: NTIS HC/MF A03

The significance of the new aerogel data for the equation of state of SiO2 is discussed. On this basis the use of SiO2 aerogels as a standard witness material for Hugoniot release wave measurements is advocated. We compare the Hugoniot data of Holmes on aerogel samples of density 0.128 gm/cc with a multiphase EOS for quartz developed by F. Ree some 15 years ago. His tabular EOS includes compositional changes arising from both chemical and ionization equilibrium, and is found to be in excellent agreement with the Hugoniot data and its extension to higher pressures. The roles of phase and compositional changes along the aerogel Hugoniot and the close agreement with the measured linear shock velocity relation are discussed. In this connection, a useful simple Grueneisen EOS model for quartz with an energy dependent gamma is derived from the linear velocity relation and is supported by the Ree EOS. DOE

N91-28314# Sandia National Labs., Albuquerque, NM.
SOL-GEL KINETICS BY NMR
R. A. Assink and B. D. Kay 1991 6 p Presented at the Symposium on Preceramic and Inorganic/Organic Hybrid Materials, New York, 25-30 Aug. 1991
(Contract DE-AC04-76DP-00789)
(DE91-011500; SAND-91-0695C; CONF-910888-1) Avail: NTIS HC/MF A02

The chemical synthesis of advanced ceramic and glass materials by the sol-gel process has become an area of increasing activity in the field of material science. The sol-gel process provides a means to prepare homogeneous, high purity materials with tailored chemical and physical properties. This paper surveyed the nuclear magnetic resonance (NMR) studies of silicon-based sol-gel kinetics. A review of the various models which have been used to analyze the chemical kinetics of various sol-gel systems was presented. The utility of NMR spectroscopy was demonstrated in investigating the influence that various reaction conditions have on the reaction pathways by which sol-gel derived materials are synthesized. By observing in a direct fashion the chemical pathway of the sol-gel, it is often possible to relate the final properties of the material to the formulation and reaction conditions of the sol-gel. The study of reaction kinetics by NMR is expected to play an increasingly important role in understanding sol-gel processing and material properties. DOE

N91-28315# California Univ., Berkeley. Lawrence Berkeley Lab.
ENERGY DISSIPATION IN CHEMICAL REACTIONS ON ULTRAFAST TIMESCALES
D. J. Russell, M. E. Paige, and C. B. Harris Oct. 1990 20 p Presented at the Conference on Rate Processes in Dissipative Systems: 50 Years After Kramers, Tufting, Fed. Republic of Germany, Sep. 1990
(Contract DE-AC03-76SF-00098)
(DE91-012342; LBL-29735; CONF-9009382-1) Avail: NTIS HC/MF A03

A series of picosecond experiments and computer simulations is presented that test collisional and hydrodynamic models for vibrational relaxation in liquids. The relationships between isolated binary collision models (IBC) and stochastic dynamics is presented. The appropriateness of IBC theory in describing vibrational relaxation in liquids is also discussed. DOE

N91-28316# National Inst. of Standards and Technology, Boulder, CO. Thermophysics Div.
INTEGRATED THEORETICAL AND EXPERIMENTAL STUDY OF THE THERMOPHYSICAL PROPERTIES OF FLUID MIXTURES
J. F. Ely Nov. 1990 14 p
(Contract DE-AI05-89ER-13992)
(DE91-012660; DOE/ER-13992/T1) Avail: NTIS HC/MF A03

In this report we highlight the progress made during the period February 1990 through February 1991. The objective of this research is twofold: (1) Development of predictive and correlative procedures for the thermophysical properties of complex fluids and fluid mixtures; and (2) Furthering our basic understanding of fluid behavior with advances in microscopic theory, computer simulation and selected experimentation. Substantial progress has been made in both of these areas. DOE

N91-28317# Pacific Northwest Lab., Richland, WA.
ELECTROCHEMICAL PROCESSES AT SOLID ELECTRODE-ELECTROLYTE-GAS INTERFACES
G. E. Youngblood, W. J Weber, and J. L. Bates May 1991 11 p Presented at the 5th Annual Conference on Fossil Energy Materials, Oak Ridge, 13-16 May 1991
(Contract DE-AC06-76RL-01830)
(DE91-012922; PNL-SA-19298; CONF-9105184-3) Avail: NTIS HC/MF A03

Electrochemical reactions at solid electrolyte-electrode-gas interfaces are being investigated with ac impedance and dc polarization techniques using an unbonded interface cell (UIC). The UIC approach eliminates influence of sample size and interface morphology resulting from electrode-electrolyte fabrication. The electrochemical reactions of oxygen with solid electrode (La(sub 1-x)Sr(sub x)MnO3 or Pt) and solid electrolyte (0.08Y(sub 2)O3 0.92ZrO2 interfaces are described. DOE

N91-28318# Brookhaven National Lab., Upton, NY.
THE SOLUBILITY AND DISSOCIATION KINETICS OF HYDROXYMETHYL HYDROPEROXIDE IN AQUEOUS SOLUTION
Xianliang Zhou and Yin-Nan Lee Apr. 1991 11 p Presented at the 5th International Conference on Precipitation Scavenging and Atmosphere Surface Exchange Process, Richland, 15-19 Jul. 1991
(Contract DE-AC02-76CH-00016)
(DE91-013336; BNL-45331; CONF-9107104-4) Avail: NTIS HC/MF A03

The Henry's Law solubility of hydroxymethyl hydroperoxide (HMP) and its equilibrium and reaction kinetics in aqueous solution were studied. The equilibrium constants of H2O2 + CH2O = HMP(1) and HMP + CH2O = BHMP(2) are K(sub 1) = 2.35 x 10(exp -2) e(exp 2610/T) M(exp -1) and K(sub 2) = 1.04 x 10(exp -3) e(exp 2779/T) M(exp -1), respectively. Both the forward and reverse rates of reaction (1) were base catalyzed between pH 5 and 8. The temperatures dependences of these two rate constants at pH 7.07 between 5 and 35 C are k(sub 1) = 6.0 x 10(exp 13) e(exp -9450/T) M(exp -1) s(exp -1) and k(sub -1) = 1.0 x 10(exp 15) e(exp -11800/T) s(exp -1). The Henry's Law constant of HMP was determined to be 4.1 x 10(exp 5) and 6.5 x 10(exp 5) M atm(exp -1) at 22.0 and 10.0 C, respectively. Exhibiting a large solubility, HMP is expected to be efficiently scavenged by hydrometeors. Because of its rapid decomposition at neutral pH, aqueous HMP is expected to be stable only at pH less than or equal to 5.5. DOE

N91-28319# Sandia National Labs., Albuquerque, NM.
SEMICONDUCTOR BRIDGE (SCB) RESEARCH AND DEVELOPMENT
R. W. Bickes, Jr. and C. B. McCampbell (SCB Technologies, Inc., Albuquerque, NM.) 1991 18 p Presented at the High Tech Seminar on Blasting Technology: Instrumentation and Explosives Applications, San Diego, 1-7 Jun. 1991
(Contract DE-AC04-76DP-00789)
(DE91-011493; SAND-91-0310C; CONF-9106183-1) Avail: NTIS HC/MF A03

Sandia National Laboratories has developed a semiconductor bridge (SCB) igniter for the ignition of a variety of explosive materials. When subjected to a low-energy current pulse, the bridge bursts into a plasma causing rapid ignition of the explosive material pressed against the bridge. Despite the low energies required for ignition, SCB components have proven to be explosively safe, meeting both no-fire and electrostatic discharge (ESD) safety requirements. In fact, SCB no-fire current levels are as much as

80 percent of the all-fire current levels. Heat transfer from the SCB into the explosive is a convective process involving the transport of the plasma into the powder bed; this efficient process produces ignition in a few microseconds for primary explosive powders and a few tens of microseconds for pyrotechnic or secondary explosive materials. Consequently, the scatter in firing times for SCB devices is correspondingly small. In addition, SCB operation is essentially independent of powder type and powder variations over a large range of temperature conditions. On-chip circuitry can be incorporated to protect SCB devices from severe radio frequency (RF) and ESD environments. Finally, since SCB devices are processed using standard semiconductor fabrication techniques, sophisticated circuitry can be added to the chip. Such circuitry can include timing delays, logic and/or computer control to allow the devices to be controlled and fired at the precise times determined by the field engineer. Such smart SCB devices can be produced cost effectively to meet the needs of blasting engineers for applications requiring minimal ground shock and/or efficient rubblization. DOE

N91-28320# Stanford Univ., CA. Dept. of Chemistry.

THERMODYNAMICS AND EFFICIENCY IN COMBUSTION AND ENGINES

J. Ross 1991 20 p
(Contract DE-FG03-86ER-13479)
(DE91-012781; DOE/ER-13479/T1) Avail: NTIS HC/MF A03

The project objective is the formulation of thermodynamics for systems far from equilibrium with emphasis on efficiency of combustion reactions in power production. The concept of increases in efficiency by means of external periodic perturbations was demonstrated both theoretically and experimentally. Research is being carried out on systems with many degrees of freedom and experiments are suggested on the optimization of efficiency in the combustion of methane at high temperatures and the combustion of acetaldehyde at cool flame temperatures. DOE

N91-28321*# National Aeronautics and Space Administration. Langley Research Center, Hampton, VA.

ACOUSTOPHORESIS METHOD AND APPARATUS Patent Application

Joseph S. Heyman, inventor (to NASA) 17 Dec. 1990 15 p
(NASA-Case-LAR-13388-1; NAS 1.71:LAR-13388-1; US-Patent-Appl-SN-628062) Avail: NTIS HC/MF A03 CSCL 07D

A method and apparatus are provided for acoustophoresis, i.e., the separation of species via acoustic waves. An ultrasonic transducer applies an acoustic wave to one end of a sample container containing at least two species having different acoustic absorptions. The wave has a frequency tuned to or harmonized with the point of resonance of the species to be separated. This wave caused the species to be driven to an opposite end of the sample container for removal. A second ultrasonic transducer may be provided to apply a second, oppositely directed acoustic wave to prevent undesired streaming. In addition, a radio frequency tuned to the mechanical resonance and coupled with a magnetic field can serve to identify a species in a medium comprising species with similar absorption coefficients, whereby an acoustic wave having a frequency corresponding to this gyrational rate can then be applied to sweep the identified species to one end of the container for removal. NASA

N91-28322 Stanford Univ., CA.

HIGH-RESOLUTION MEASUREMENTS OF THE THERMAL CONDUCTIVITY AND BOUNDARY RESISTANCE OF HELIUM-4 NEAR THE LAMBDA POINT Ph.D. Thesis

Qiang Li 1991 124 p
Avail: Univ. Microfilms Order No. DA9115808

High resolution measurements of the thermal conductivity of bulk helium and the thermal boundary resistance between helium and copper in the region from 10(exp -7) to 10(exp -3) K above the lambda transition are described, using thermometry with a resolution better than 10(exp -9) K. In this region both properties are predicted to exhibit singular behavior as the transition is approached. The thermal conductivity of bulk helium was separated from boundary resistance by subtraction of data from runs with cell spacings ranging from 0.073 to 0.012 cm. By extrapolating the data to zero spacing, the first measurements of the boundary resistance above the lambda transition were obtained. The results are compared with recent calculations using renormalization group analysis. When the effect of gravity is taken into account, the thermal conductivity data agrees with the renormalization group analysis. When the effect of gravity is taken into account, the thermal conductivity data agrees with the renormalization group analysis to within a few percent over the whole range measured. However, the boundary resistance data yields an exponent three times smaller than that predicted. Two completely independent data sets were obtained, and the results were consistent. Dissert. Abstr.

N91-28323# California Univ., Davis. Dept. of Chemistry.

STUDIES RELEVANT TO THE CATALYTIC ACTIVATION OF CARBON MONOXIDE

P. C. Ford 11 May 1990 16 p
(Contract DE-FG03-85ER-13317)
(DE91-012661; DOE/ER-13317/T1) Avail: NTIS HC/MF A03

Mechanistic studies were made of the nucleophilic activation of carbon monoxide such as homogeneous catalysis of the water gas shift and key steps in the relevant catalytic cycles. In addition, new investigations of related processes involved in the catalytic activation of carbon monoxide and other C(1) compounds were initiated. These include the application of fast reaction techniques to prepare and to investigate quantitatively reactive organometallic intermediates relevant to the activation of hydrocarbons toward carbonylation and other functionalizations. DOE

N91-28324# Los Alamos National Lab., NM.

DIRECT MONTE CARLO SIMULATION OF CHEMICAL EQUILIBRIUM COMPOSITION OF MOLECULAR FLUID MIXTURES UNDER SHOCK CONDITIONS

M. S. Shaw 1991 10 p Presented at the 1991 American Physical Society (APS) Conference on Shock Compression of Condensed Matter, Williamsburg, 17-20 Jul. 1991
(Contract W-7405-eng-36)
(DE91-013075; LA-UR-91-1638; CONF-9107105-7) Avail: NTIS HC/MF A02

A new Monte Carlo simulation method is implemented which holds the number and kind of atoms constant rather than the number and kind of molecules for a molecular fluid mixture. Chemical reactions are allowed as a correlated move of atoms such as an interchange of atoms between molecules. Equilibrium chemical composition is determined as an average over the simulation along with equation of state quantities. Results are presented for N2 + O2 (equilibrium) 2NO at 30 GPa and 3000 K. The equilibrium composition is shown to be sensitive to the potentials between unlike species. DOE

N91-28325# Los Alamos National Lab., NM.

VIBRATIONAL SPECTROSCOPY OF SHOCK-COMPRESSED LIQUID CO

D. S. Moore, S. C. Schmidt, M. S. Shaw, and J. D. Johnson 1991 10 p Presented at the 1991 American Physical Society (APS) Conference on Shock Compression of Condensed Matter, Williamsburg, 17-20 Jul. 1991
(Contract W-7405-eng-36)
(DE91-013204; LA-UR-91-1666; CONF-9107105-9) Avail: NTIS HC/MF A02

Single-pulse, multiplex, coherent anti-Stokes Raman spectroscopy (CARS) was used to observe the vibrational spectra of liquid CO shock compressed to several pressures and temperatures up to 9.9 GPa and 2010 K. The experimental spectra were compared to synthetic spectra calculated using a semiclassical model for CARS intensities and estimated vibrational frequencies, peak Raman susceptibilities, and Raman line widths. A comparison of these data with results in the isoelectronic and materially very similar N2 show a significant difference in vibrational frequency shift with pressure. DOE

N91-28326# Lawrence Livermore National Lab., CA.
LINKED GAS CHROMATOGRAPH-THERMAL ENERGY ANALYZER/ION TRAP MASS SPECTROMETER
A. Alcaraz, W. H. Martin, and B. D. Andresen May 1991 4 p
Presented at the American Society for Mass Spectrometry (ASMS) Meeting, Nashville, 19-24 May 1991
(Contract W-7405-eng-48)
(DE91-013585; UCRL-JC-107081; CONF-9105181-15) Avail: NTIS HC/MF A01

The capability of comparing a nitrogen chromatogram generated from a gas chromatograph (GC, Varian model 3400) linked to a thermal energy analyzer (TEA, Thermedics Inc. Model 610) with a total ion chromatogram (from a Finnigan-MAT Ion Trap Mass Spectrometer, ITMS) has provided a new means to screen and identifying trace levels of nitrogen-containing compounds in complex mixtures. Prior to the work described here, it has not been possible to simultaneously acquire TEA and MS data. What was needed was a viable GC-TEA/ITMS interface to combine the capabilities of both instruments. DOE

N91-28327# Louisville Univ., KY. Dept. of Chemical Engineering.
MECHANISM OF HYDRODENITROGENATION. PART 5: X RAY DIFFRACTION OF MOLYBDENUM CATALYSTS
R. Miranda 1990 13 p
(Contract DE-FG22-89PC-89771)
(DE91-013853; DOE/PC-89771/5-Pt-5) Avail: NTIS HC/MF A03

Efficient nitrogen removal from heterocyclic aromatics in liquid fuels calls for the development of catalysts with better HDN activity than is available with the traditional HDS catalysts. In this project it is proposed that the selectivity of the HDN reaction can be affected by an alteration of the catalyst acidity since it is possible that an acidic Hofmann-like deamination pathway is operative in parallel with the hydrogenolysis of saturated C--N--C bonds. To understand better the role of acidic sites in the presence of hydrogenation and hydrogenolysis sites, molybdena was supported on a series of acidic aluminas, and the resulting new acidity and molybdic phases were characterized. X-ray diffraction was utilized to determine the nature of the supported phases of Mo over silica, alumina and silica-aluminas. After impregnation and calcination, the oxidic molybdena formed dispersed species (probably of the dioxo type) over gamma-alumina, and dispersed agglomerates of MoO3 over silica. However, on silica-alumina, molybdate was found to interact so strongly with the aluminum cations that it formed Al2 MoO4 sub 3, possibly by corrosive chemisorption during impregnation, or by Al diffusion into molybdena during calcination. After a treatment of education of reduction with hydrogen at 500 C, highly dispersed Mo species are formed. These species are x-ray amorphous. Having been derived from different precursors, those species have different reducibility and acidity for different support compositions. DOE

N91-28328# Lehigh Univ., Bethlehem, PA.
ANALYTICAL ELECTRON MICROSCOPY OF CATALYST PREPARATIONS
C. E. Lyman May 1991 8 p
(Contract DE-FG02-86ER-45269)
(DE91-014126; DOE/ER-45269/2) Avail: NTIS HC/MF A02

Following the discovery last period of methods to control the distribution of two metals in a catalyst support, we decided to make a change of direction in this program. It was felt that testing of the catalysts should be in the next major effort. Thus, the current graduate student on the program, Rollin Lakis, is now building a catalyst testing facility which allows sampling for electron microscopy. Testing should begin next month. An important method for stabilization of alkali metals on catalyst surfaces during specimen preparation for electron microscopy has been discovered. By coating the catalyst surface with a thin layer of chromium, metals such as Na, K, and Cs have been immobilized for useful analytical measurements. This achievement has been a major goal of this program from its inception. Further work in this area will show the significant advantages of this discovery to the petroleum and chemical industries. DOE

N91-28329# SRI International Corp., Menlo Park, CA.
COMBUSTION RESEARCH PROGRAM: FLAME STUDIES, LASER DIAGNOSTICS, AND CHEMICAL KINETICS
1991 19 p
(Contract DE-FG03-86ER-13571)
(DE91-014824; DOE/ER-13571/1) Avail: NTIS HC/MF A03

Progress is reported on combustion research. Topics include: flame studies and diagnostics; quenching of diatomic hydrides; quenching of NH2 radicals at room temperature; ammonia photolysis in a jet; collisional quenching of NH in high rotational levels; laser-induced fluorescence detection of vinyl radicals; reaction of hydroxyl radicals with ethylene; reaction of methyl radicals with oxygen; heat of formation of alkyl free radicals; and transition state theory-based rate constant estimations. DOE

N91-28330 Duke Univ., Durham, NC.
THERMAL CONDUCTIVITY OF SOLID HYDROGEN AT LOW TEMPERATURE Ph.D. Thesis
Xiaoyu Li 1990 181 p
Avail: Univ. Microfilms Order No. DA9113431

The results of a study on the properties of solid hydrogen at very low temperatures by means of thermal conductivity, continuous wave (CW) nuclear magnetic resonance (NMR), and specific heat measurements are presented. The experiment consists of two major parts: the study of quantum diffusion in low ortho concentration solids, and the study of the orientational order-disorder phase transition in high ortho concentration solids. The effect of quantum diffusion on the thermal conductivity and the NMR signal of isolated ortho hydrogen molecules were measured on a solid sample with ortho concentration ranging from 4 to 0.5 percent, in the temperature range 0.1 K less than T less than 2.0 K. Thermal conductivity in the orientational ordered phase was measured, and was found to have very large values. The pure ortho hydrogen solid may have a thermal conductivity comparable with that of a pure para hydrogen solid. The observed thermal conductivities at constant concentration were found to fall into two distinguishable branches. The CW NMR spectra and the specific heat of the solid were measured simultaneously with the thermal conductivity. The width of the order-disorder phase transition was also studied and discussed. Dissert. Abstr.

N91-28331# Wisconsin Univ., Madison. Dept. of Chemical Engineering.
THERMODYNAMIC AND KINETIC ASPECTS OF SURFACE ACIDITY
J. A. Dumesic 1991 31 p
(Contract DE-FG02-84ER-13183)
(DE91-014039; DOE/ER-13183/5) Avail: NTIS HC/MF A03

A continuing goal of our research for the Department of Energy has been to develop methods to characterize catalyst acidity and to understand the chemical and structural properties that control the number, type and strength of catalytic acid sites. During the past year we have employed microcalorimetry, thermogravimetry and nuclear magnetic resonance to study the acidity of various zeolite catalysts. Our microcalorimetric studies have involved the adsorption of micro-mol quantities of probe materials (e.g., pyridine) onto catalysts and measurement of the heats evolved. Such measurements over a range of coverages yield the acid strength distribution. We have employed thermogravimetry to monitor the weight change of catalysts upon the adsorption of the probe molecule to determine the number of acid sites and the corresponding adsorption isotherms. Finally, nuclear magnetic resonance is a technique which has a number of applications to the study of acidic catalysts. Various NMR nuclei, Al-27, Si-29, and H-1 in particular, are routinely used to probe various catalyst features. In this report we describe the use of deuterium NMR as a probe of catalyst acidity. Our studies of catalyst acidity have concentrated in two areas. The first area of investigation involves the acidic properties of pure zeolites, specifically H-mordenite, H-ZSM-5, and H-Y. A second area of concentration is on a series of H-Y zeolites in a clay matrix, dealuminated by steaming. These catalysts are similar to those used industrially for catalytic cracking. DOE

N91-28332# Rochester Univ., NY.
TRANSITION METAL ACTIVATION AND FUNCTIONALIZATION OF CARBON-HYDROGEN BONDS
W. D. Jones Jun. 1991 33 p
(Contract DE-FG02-86ER-13569)
(DE91-014261; DOE/ER-13569/6) Avail: NTIS HC/MF A03

This project is directed towards the continued investigation of the fundamental thermodynamic and kinetic factors that influence carbon-hydrogen bond activation at homogeneous transition metal centers. The project is also directed towards the conversion of hydrocarbons into functionalized products of potential use to the chemical industry. In the past two years, advances have been made in both understanding the interactions of hydrocarbons with metals and in the functionalization of hydrocarbons. Major advances that have been made include: (1) We have found that RhCl(PR3)2(CNR) complexes can catalyze the insertion of isonitriles into the C-H bonds of arenes upon photolysis. (2) We have also examined reactions of a series of arenes with (C5Me5)Rh(PMe3)PhH and begun to map out the kinetic and thermodynamic preferences for arene coordination. (3) We have begun to examine the reactions of rhodium isonitrile pyrazolylborates for alkane and arene C-H bond activation. A new, labile, carbodiimide precursor has been developed for these studies. (4) We have completed studies of the reactions of (C5Me5)Rh(PMe3)H2 with D2 and PMe3 that indicate that both eta(sup 5) yields eta(sup 3) ring slippage and metal to ring hydride migration occur more facilely than thermal reductive elimination of H2. (5) We have examined the reactions of heterocycles with (C5Me5)Rh(PMe3)PhH and found that pyrrole and furan undergo C-H or N-H activation. Thiophene, however, undergoes C-S bond oxidative addition, and the mechanism of activation has been shown to proceed through sulfur coordination prior to C-S insertion. DOE

N91-28333# Wayne State Univ., Detroit, MI. Dept. of Chemistry.
REACTIVE CHARACTERIZATION AS A PROBE OF THE NATURE OF CATALYTIC SITES
A. Brenner 11 Jun. 1991 17 p
(Contract DE-FG02-88ER-13879)
(DE91-014536; DOE/ER-13879/3) Avail: NTIS HC/MF A03

This research program is primarily concerned with achieving a better understanding of the nature of active sites on heterogeneous catalysts. It is extremely rare that the identity of an active site is known for a heterogeneous catalyst. At a simpler level, it is often impossible to meaningfully compare the activities of different types of catalysts and this impedes achieving a unified understanding of catalytic action. Active sites often caught for only a very small fraction of the surface of a catalyst. The classical method of selective poisoning yields an upper limit to the number of active sites, but there is no lower bound. Spectroscopic techniques typically assay the dominant surface species without regard to what is the active component. This research program has developed novel methods to gain information on the nature of active sites. It was a general objective of this program to provide for the first time a meaningful tabulation of activities for the H2-D2 exchange reaction and the comparison of activities for different types of catalysts. Most of the effort in this project has been directed to the following areas. (1) Develop a new technique to measure the number of active sites on a catalyst. (2) Determine the activity for H2-D2 exchange for a variety of transition metals and metal oxides and develop methods to meaningfully compare the activities. (3) Develop the concept of reactive characterization to see if it can be used to assess the morphology of catalysts containing very small metal ensembles and to differentiate between local and global active sites. DOE

N91-28224*# Pennsylvania State Univ., University Park. Dept. of Mechanical Engineering.
IGNITION AND COMBUSTION OF METALLIZED PROPELLANTS
Stephen R. Turns *In* NASA, Washington, Space Transportation Propulsion Technology Symposium. Volume 2: Symposium Proceedings May 1991 p 645-653 (For primary document see N91-28193 20-20)
Avail: NTIS HC/MF A99 CSCL 21B

N91-28225*# Pennsylvania State Univ., University Park. Dept. of Mechanical Engineering.
LIQUID-PROPELLANT DROPLET VAPORIZATION AND COMBUSTION IN HIGH PRESSURE ENVIRONMENTS
Vigor Yang *In* NASA, Washington, Space Transportation Propulsion Technology Symposium. Volume 2: Symposium Proceedings May 1991 p 655-662 (For primary document see N91-28193 20-20)
Avail: NTIS HC/MF A99 CSCL 21B

N91-28226*# Pennsylvania State Univ., University Park. Dept. of Mechanical Engineering.
SPRAY COMBUSTION UNDER OSCILLATORY PRESSURE CONDITIONS
H. R. Jacobs and R. J. Santoro *In* NASA, Washington, Space Transportation Propulsion Technology Symposium. Volume 2: Symposium Proceedings May 1991 p 663-674 (For primary document see N91-28193 20-20)
Avail: NTIS HC/MF A99 CSCL 21B

26 METALLIC MATERIALS

Includes physical, chemical, and mechanical properties of metals, e.g., corrosion; and metallurgy.

N91-28334*# Martin Marietta Labs., Baltimore, MD.
MICROSTRUCTURE-PROPERTY RELATIONSHIPS IN Al-Cu-Li-Ag-Mg WELDALITE (TM) ALLOYS, PART 2 Final Report, 1 Oct. 1988 - 1 Oct. 1990
T. J. Langan and J. R. Pickens Washington NASA May 1991 99 p
(Contract NAS1-18531)
(NASA-CR-4364; NAS 1.26:4364; MML-TR-90-27C-Pt-2) Avail: NTIS HC/MF A05 CSCL 11F

The microstructure and mechanical properties of the ultrahigh strength Al-Cu-Li-Ag-Mg alloy, Weldalite (tm) 049, were studied. Specifically, the microstructural features along with tensile strength, weldability, Young's modulus and fracture toughness were studied for Weldalite (tm) 049 type alloys with Li contents ranging from 1.3 to 1.9 wt. pct. The tensile properties of Weldalite 049 and Weldalite 049 reinforced with TiB2 particles fabricated using the XD (tm) process were also evaluated at cryogenic, room, and elevated temperatures. In addition, an experimental alloy, similar in composition to Weldalite 049 but without the Ag+Mg, was fabricated. The microstructure of this alloy was compared with that of Weldalite 049 in the T6 condition to assess the effect of Ag+Mg on nucleation of strengthening phases in the absence of cold work. For individual titles, see N91-28335 through N91-28340.

N91-28335*# Martin Marietta Labs., Baltimore, MD.
IDENTIFICATION OF STRENGTHENING PHASES IN Al-Cu-Li ALLOY WELDALITE (TM) 049
In its Microstructure-Property Relationships in Al-Cu-Li-Ag-Mg Weldalite (tm) Alloys, Part 2 May 1991 p 16-3 (For primary document see N91-28334 20-26)
(Contract NAS1-18531)
Avail: NTIS HC/MF A05 CSCL 11F

Microstructure property relationships were determined for a family of ultrahigh strength weldable Al-Cu-Li based alloys referred to as Weldalite (tm) alloys. The highest strength variant of this family, Weldalite 049, has a high Cu/Li wt pct. ratio with a nominal composition of Al-6.3Cu-1.3Li-0.4Ag-0.4Mg-0.14Zr. Increasing the alloy's lithium content above 1.3 wt pct. resulted in a decrease in both yield and ultimate tensile strength. Strength was shown to be strongly dependent on lithium content, with a maximum in strength occurring in the range of about 1.1 to 1.4 wt pct. lithium. The strengthening phases present in Weldalite 049 (1.3Li) and an Al-6.3Cu-1.9Li-0.4Mg-0.14Zr alloy were identified using transmission electron microscopy (TEM). Author

N91-28336*# Martin Marietta Labs., Baltimore, MD.

THE INFLUENCE OF Ag+Mg ADDITIONS ON THE NUCLEATION OF STRENGTHENING PRECIPITATES IN A NON-COLD-WORKED Al-Cu-Li ALLOY

In its Microstructure-Property Relationships in Al-Cu-Li-Ag-Mg Weldalite (tm) Alloys, Part 2 May 1991 p 34-4 (For primary document see N91-28334 20-26)
(Contract NAS1-18531)
Avail: NTIS HC/MF A05 CSCL 11F

Aluminum-copper-lithium alloys generally require cold work to attain their highest strengths in artificially aged tempers. These alloys are usually strengthened by a combination of the metastable delta prime (Al3Li) and theta prime (Al2Cu) phases and the equilibrium T sub 1 (Al2CuLi) phase, and where the T sub 1 phase is a more potent strengthener than the delta prime. Various investigators have shown that the high strengths obtained after artificial aging associated with cold work result from the heterogeneous precipitation of T sub 1 on matrix dislocations. The objective here is to elucidate the mechanism by which the Ag+Mg additions stimulate the precipitation of T sub 1 type precipitates without cold work. To accomplish this, the microstructure of an Al-6.3Cu-1.3Li-0.14Zr model alloy was evaluated in a T6 type temper with and without the Ag+Mg addition. Author

N91-28337*# Martin Marietta Labs., Baltimore, MD.

THE EFFECT OF TiB2 REINFORCEMENT ON THE MECHANICAL PROPERTIES OF AN Al-Cu-Li ALLOY-BASED METAL-MATRIX COMPOSITE

In its Microstructure-Property Relationships in Al-Cu-Li-Ag-Mg Weldalite (tm) Alloys, Part 2 May 1991 p 50-6 (For primary document see N91-28334 20-26)
(Contract NAS1-18531)
Avail: NTIS HC/MF A05 CSCL 11F

The addition of ceramic particles to aluminum based alloys can substantially improve mechanical properties, especially Young's modulus and room and elevated temperature strengths. However, these improvements typically occur at the expense of tensile ductility. The mechanical properties are evaluated to a metal matrix composite (MMC) consisting of an ultrahigh strength aluminum lithium alloy, Weldalite (tm) 049, reinforced with TiB2 particles produced by an in situ precipitation technique called the XD (tm) process. The results are compared to the behavior of a nonreinforced Weldalite 049 variant. It is shown that both 049 and 049-TiB2 show very attractive warm temperature properties e.g., 625 MPa yield strength at 150 C after 100 h at temperature. Weldalite 049 reinforced with a nominal 4 v pct. TiB2 shows an approx. 8 pct. increase in modulus and a good combination of strength (529 MPa UTS) and ductility (6.5 pct.) in the T3 temper. And the high ductility of Weldalite 049 in the naturally aged and underaged tempers makes the alloy a good, high strength matrix for ceramic reinforcement. Author

N91-28338*# Martin Marietta Labs., Baltimore, MD.

WELDABILITY OF WELDALITE (TM) 049 WITH AND WITHOUT TiB2 REINFORCEMENT

In its Microstructure-Property Relationships in Al-Cu-Li-Ag-Mg Weldalite (tm) Alloys, Part 2 May 1991 p 69-7 (For primary document see N91-28334 20-26)
Avail: NTIS HC/MF A05 CSCL 11F

The effects are assessed of TiB2 reinforcement and parent alloy Li content on the weldability of Weldalite (tm) 049 type alloys. Welding trials were performed using either AC or DC polarity gas tungsten arc (GTA) welding according to described procedures. The welding was performed under conditions of high restraint on 5 cm (2 in) wide x 25.4 cm (10 in) long plates machined from the 0.952 cm (0.375 in) extruded bar parallel to the extrusion direction. A 37.5 deg bevel was machined on the center edge of the extruded bar. Cut rod filler wire was machined from three alloys, and one commercially available 2319 filler wire was also used. The preliminary assessment of the weldability revealed no propensity for hot cracking under conditions of high restraint. This result is significant, because hot cracking has been reported for all other leading aluminum lithium alloys welded with certain conventional filler alloys. The strengths for Weldalite parent welded with parent filler obtained were higher than those for alloys used in launch systems, such as 2219 and 2014 welded with 2319 and 4043 fillers, respectively. Even higher values were obtained by variable polarity plasma arc welding (e.g., 54 ksi (372 MPa) mean tensile strength). Author

N91-28339*# Martin Marietta Labs., Baltimore, MD.

EFFECT OF Li LEVEL, ARTIFICIAL AGING, AND TiB2 REINFORCEMENT ON THE FRACTURE TOUGHNESS OF WELDALITE (TM) 049-TYPE ALLOYS

In its Microstructure-Property Relationships in Al-Cu-Li-Ag-Mg Weldalite (tm) Alloys, Part 2 May 1991 p 80-8 (For primary document see N91-28334 20-26)
Avail: NTIS HC/MF A05 CSCL 11F

Plane strain fracture toughness (K sub IC) was evaluated for Weldalite (tm) 049 with and without TiB2 reinforcement. For the nonreinforced variant, changes in toughness were measured for various aging conditions and lithium levels. Toughness testing was carried out on fatigue precracked compact tension (CT) specimens at 24 C, as per ASTM standard E-399. Toughness was measured as a function of aging time at 160 C for the two Weldalite 049(1.3) heats. The composition of these heats differed only in that 0.03 wt pct. Ti was added to one as an additional grain refiner. Both heats showed a decrease in toughness with increasing aging time, although toughness values for one were significantly higher than for the other. This greater toughness may be due to a subtle change in the grain size resulting for the presence of Ti or, alternatively, to differences in texture or substructure formed during extrusion. Author

N91-28340*# Martin Marietta Labs., Baltimore, MD.

EFFECT OF Li LEVEL, ARTIFICIAL AGING, AND TiB2 REINFORCEMENT ON THE MODULUS OF WELDALITE (TM) 049

In its Microstructure-Property Relationships in Al-Cu-Li-Ag-Mg Weldalite (tm) Alloys, Part 2 May 1991 p 86-9 (For primary document see N91-28334 20-26)
Avail: NTIS HC/MF A05 CSCL 11F

The dynamic Young's Modulus (E) was determined for (1) alloys 049(1.3)(heat 072), (2) 049(1.9), and (3) 049(1.3) TiB2 in the T3 temper and after aging at 160 C were made on a single 0.953 cm (0.375 in) cube to reduce scatter from microstructural inhomogeneities. Both shear and transverse wave velocities were measured for the L, LT, and ST directions by a pulse echo technique. These velocities were then used to calculate modulus. The change is shown in E with aging time at 160 C (320 F) for the three alloys. It is clear from the plots that aging has a minor, but measurable, influence on the E of alloys 049(1.3) and 049(1.9): E decreases by -2.5 pct. for 2 and 3 during the initial stages of artificial aging. This decrease in E generally follows the strength reversion. On further aging beyond the reversion well, E increases and then decreases again as the alloy overage. The slightly higher modulus in the T8 than in the T3 temper is consistent with the presence of the high modulus T sub 1 phase in the T8 temper. A similar change in E was observed on aging for the TiB2 reinforced variant that also follows the aging curve. Author

N91-28341*# National Aeronautics and Space Administration. Marshall Space Flight Center, Huntsville, AL.

THE EFFECT OF STRESS ON HYDROGEN UPTAKE AND DESORPTION BY A-286

Merlin D. Danford May 1991 19 p
(NASA-TM-103537; NAS 1.15:103537) Avail: NTIS HC/MF A03
CSCL 11F

The uptake and desorption of hydrogen by A-286 as a function of stress was studied using electrochemical methods. It was found that the apparent surface hydrogen concentration, the mean hydrogen concentration, and the hydrogen distribution uniformity all increased up to a stress level 50 percent of yield and decreased thereafter. The value of the hydrogen diffusion coefficient was relatively unaffected by stress while the percent of trapped hydrogen appeared to decrease with increasing stress. Author

N91-28342# Joint Publications Research Service, Arlington, VA.
JPRS REPORT: SCIENCE AND TECHNOLOGY. USSR: MATERIALS SCIENCE
10 Apr. 1991 32 p Transl. into ENGLISH from various Russian articles
(JPRS-UMS-91-003) Avail: NTIS HC/MF A03

This is a compilation of translated articles from Russian publications. The subject areas are as follows: Analysis, Testing; Corrosion; Nonferrous Metals, Alloys; Brazes, Solders; Nonmetallic Materials; Treatments; and Welding, Brazing, Soldering. Some representative titles are as follows: Development of new methods for ultrasonic testing of composite materials based on use of radar signals; The effect of chromium on the corrosion behavior of rapidly solidified Fe-Si alloys; Friction conditions in pressing high strength titanium alloys and selection of vitreous lubricants; An image analyzer for ceramics research; Thermoplastic treatment with cyclic phase recrystallization in the manufacturing processes of thick steel plates; and Cyclical crack resistance of high strength steel welded joints. E.R.

N91-28343# Naval Air Development Center, Warminster, PA. Air Vehicle and Crew Systems Technology Dept.
RAPID SOLIDIFICATION PROCESSING OF Al3Ti AND Al3Ti PLUS COPPER Progress Report, Oct. 1989 - Oct. 1990
William F. Frazier, John Benci, Joseph Zanter, and Harry Tyndall
1 Dec. 1990 41 p
(NADC Proj. RS-3-4-A50)
(AD-A236600; NADC-91002-60) Avail: NTIS HC/MF A03
CSCL 07/2

The development of advanced airframes and propulsion systems has generated significant research and development activity in the area of light weight, high temperature intermetallic alloys, e.g., alpha-two and gamma titanium aluminides. However, Al3Ti, an intermetallic which has a low density (3.35 g/cu cm) and a high melting point (1350 C) has received little scientific scrutiny, principally because of its intrinsically low ductility. X ray diffraction, and optical and electron microscopy were used to interrogate the microstructure of Al3Ti and Al3Ti plus copper in their as-cast and melt spun conditions. Rapid solidification enhanced chemical uniformity and the addition of copper transformed the structure of Al3Ti from tetragonal DO22 into cubic Li2, a structure with a higher crystallographic symmetry. GRA

N91-28344# Oak Ridge National Lab., TN.
APPLICATION OF ELECTRON ENERGY LOSS SPECTROSCOPY TO MICROANALYSIS OF IRRADIATED STAINLESS STEELS
E. A. Kenik, J. Bentley, and N. D. Evans (Oak Ridge Associated Universities, Inc., TN.) 1991 3 p Presented at the 49th Electron Microscopy Society of America (EMSA) Annual Meeting, San Jose, 4-9 Aug. 1991
(Contracts DE-AC05-84OR-21400; DE-AC05-76OR-00033)
(DE91-009913; CONF-910870-2) Avail: NTIS HC/MF A01

Energy dispersive x ray spectroscopy (EDXS) has limited application to microanalysis of radioactive materials because of degraded detector performance and the intrinsic spectrum associated with the radioactive decay. Electron energy loss spectroscopy (EELS) is not affected by specimen radioactivity and also offers the possibility of improved spatial resolution. Measurements of radiation-induced segregation (RIS) in irradiated stainless steels have been made by both techniques. Analytical electron microscopy was performed at 100 kV in a Philips EM400T/FEG, equipped with an EDAX 9100/70 EDXS system and a Gatan 666 parallel detection EELS (PEELS). Microanalysis was performed in the STEM mode (less than 2-nm-diam probe with greater than 0.5 nA) with the same acquisition time (50 s) used for both techniques. DOE

N91-28345# California Univ., Berkeley. Lawrence Berkeley Lab. Center for Advanced Materials.
TENSILE DEFORMATION OF Al-Cu-Li-Zr ALLOY 2090-T8E41 AT 298 AND 77 K
D. Yao, D. Chu, and J. W. Morris, Jr. Mar. 1991 9 p Presented at the Annual Meeting and Exhibition of the Minerals, Metals and Materials Society (TMS), New Orleans, 17-21 Feb. 1991
(Contract DE-AC03-76SF-00098)
(DE91-011885; LBL-30421; CONF-910202-16) Avail: NTIS HC/MF A02

The deformation behavior of a 12.7 mm (0.5 in.) 2090-T8E41 (Vintage I) plate material in tension is studied at 298 and 77 K. An increase in the roughness of slip relief patterns is observed on polished surfaces of deformed tensile specimens tested at 77 K. The increased roughness at the lower temperature is believed to be induced by a microstructural factor that resists the transmission of slip from grain to grain and results in reduced slip continuity across grain boundaries. The reduced slip continuity is believed to encourage greater deformation homogeneity at the lower test temperature and, subsequently, results in an improved work hardening capacity. A microstructural relation between the increased slip discontinuity and the improvement in the work hardening characteristic and subsequent mechanical properties at low temperatures is proposed. DOE

N91-28346# Sandia National Labs., Albuquerque, NM.
EFFECTS OF SAMPLE SIZE AND LOADING RATE ON THE TRANSITION BEHAVIOR OF A DCI ALLOY
R. Salzbrenner and T. B. Crenshaw 1991 30 p Presented at the 23rd National Symposium on Fracture Mechanics, College Station, 18-20 Jun. 1991
(Contract DE-AC04-76DP-00789)
(DE91-012015; SAND-91-1020C; CONF-910624-2) Avail: NTIS HC/MF A03

The measurement and understanding of the fracture toughness of ductile cast irons (DCI) are critical to the analysis of nuclear transportation casks made from these alloys. Cask containment must be assured for all loading events from normal handling to accidents during which high loads can be delivered at elevated rates. Cask walls are commonly in the range of 20 to 50 cm thick (or greater) in order to provide requisite nuclear shielding, and this requires that associated mechanical constraint effects must be considered. At elevated temperatures (i.e., in the vicinity of ambient) DCI behaves in an elastic-plastic manner, even for large section sizes (B greater than 20 cm) and moderately high loading rates. However, as the temperature is lowered or the loading rate is increased, ferritic DCI alloys exhibit a relatively sharp transition to linear elastic behavior, with a significant decrease in the fracture toughness. The fracture toughness of a DCI alloy has been measured using linear elastic and elastic-plastic experimental techniques. Measurements have been made as a function of temperature, loading rate and section size. The loading rates span the range which a cask could experience during normal transport and handling, as well as accident events. DOE

N91-28347# Ames Lab., IA.
INTERPRETING SOLIDIFICATION PHENOMENA AND MICROSTRUCTURAL EVOLUTION IN METALS THROUGH THE USE OF TRANSPARENT MODEL ALLOY SYSTEMS
R. N. Grugel (Vanderbilt Univ., Nashville, TN.) and R. Trivedi 1991 34 p Presented at the Metallography: 75 Years Later, Atlantic City, 8-10 May 1991
(Contract W-7405-eng-82)
(DE91-012629; IS-M-667; CONF-9105189-1) Avail: NTIS HC/MF A03

It is well established that the material properties of alloys are directly related to the scale and distribution of their microstructural constituents. The advances and applications of metallographic techniques for the examination of solidified microstructures have proven invaluable in ascertaining these structure-property relationships. Unfortunately, many aspects of microstructural evolution can only be inferred from a post-solidification examination. The use of transparent compounds which freeze in a manner analogous to metals circumvents this problem by allowing direct and continual observation of solidification events during both transient and steady state growth. The role is discussed of these compounds in promoting understanding of solidification phenomena. Examples of dendritic, eutectic, and monotectic microstructural development, pertinent to theory and practice, are presented and compared with their metal counterparts. DOE

N91-28348# Oak Ridge National Lab., TN.
IRRADIATION CREEP BY CLIMB-ENABLED GLIDE DRIVEN BY TRANSIENT POINT DEFECT PROCESSES
L. K. Mansur 1991 10 p Presented at the International Conference on Physics of Irradiation Effects in Metals, Siofok (Hungary), 20-24 May 1991
(Contract DE-AC05-84OR-21400)
(DE91-012950; CONF-9105130-1) Avail: NTIS HC/MF A02

Irradiation creep takes place over a wide temperature range by processes fundamentally different from thermal creep. In recent work, it has been shown that transients and spatial inhomogeneities in point defect fluxes are important in driving irradiation creep. Earlier theoretical work had centered on the contributions of quasi-stationary and uniform point defect concentrations to creep. In the present paper, mechanisms that depend in an essential way on these inconstancies are emphasized. Creep by climb-enabled glide driven by startup-induced, glide-induced, and cascade-induced mechanisms are explored. Calculated results are presented and compared with experimental data. DOE

N91-28349# Oak Ridge National Lab., TN.
COMPARISONS OF IRRADIATION-INDUCED SHIFTS IN FRACTURE TOUGHNESS, CRACK ARREST TOUGHNESS, AND CHARPY IMPACT ENERGY IN HIGH-COPPER WELDS
W. R. Corwin, R. K. Nanstad, and S. K. Iskander 1991 7 p Presented at the 11th International Conference on Structural Mechanics in Reactor Technology, Tokyo (Japan), 18-23 Aug. 1991
(Contract DE-AC05-84OR-21400)
(DE91-008881; CONF-910817-3) Avail: NTIS HC/MF A02

The Heavy-Section Steel Irradiation (HSSI) Program is examining relative shifts and changes in shape of fracture and crack-arrest toughness versus temperature behavior for two high-copper welds. Fracture toughness 100-MPa sq. root of m temperature shifts are greater than Charpy 41-J shifts for both welds. Mean curve fits to the fracture toughness data provide mixed results regarding curve shape changes, but curves constructed as lower boundaries indicate lower slopes. Preliminary crack-arrest toughness results indicate that shifts of lower-bound curves are approximately the same as CVN 41-J shifts with no shape changes. DOE

N91-28350# Oak Ridge National Lab., TN.
THE RATE (TIME)-DEPENDENCE MECHANICAL BEHAVIOR OF MODIFIED 9Cr-1Mo. PART 2: ISOTHERMAL MODELING AT 538 C
P. S. Majors, E. Krempl (Rensselaer Polytechnic Inst., Troy, NY.), and M. B. Ruggles 1991 8 p Presented at the 11th International Conference on Structural Mechanics in Reactor Technology, Tokyo (Japan), 18-23 Aug. 1991
(Contracts DE-AC05-84OR-21400; DE-FG02-86ER-13566)
(DE91-011100; CONF-910817-13-Pt-2) Avail: NTIS HC/MF A02

The viscoplasticity theory based on overstress (VBO) has been modified to produce effects of recovery of state. The ability to model recovery as well as rate dependence is demonstrated by the simulation of two experiments which were conducted on modified 9Cr--1Mo steel at 538 C. Experimental and numerical results compare reasonably well. DOE

N91-28351# Lawrence Livermore National Lab., CA.
CROSS-SECTIONAL TEM SPECIMEN PREPARATION OF FREE-STANDING METAL MULTI-LAYERED FILMS
M. Wall Mar. 1991 6 p Presented at the 25th Annual Microbeam Analysis Society Meeting, San Jose, 4-9 Aug. 1991
(Contract W-7405-eng-48)
(DE91-011117; UCRL-JC-106766; CONF-910872-2) Avail: NTIS HC/MF A02

The cross-sectional preparation of free-standing metal multilayered films will be discussed. Production of large flat transparent regions in cross-sectional TEM specimens is usually quite difficult. This difficulty arises from the fact that these types of specimens are usually a composite of dissimilar ion and chemical etching rate materials. With a unique combination of electroplating, lapping, dimpling, and ion milling it will be shown that it is possible to produce large thin areas from specimens of dissimilar materials. DOE

N91-28352# Oak Ridge National Lab., TN.
HIGH-TEMPERATURE SOLUTION ANNEALING AS AN IASCC MITIGATION TECHNIQUE
A. J. Jacobs, C. M. Shepherd, G. E. C. Bell, and G. P. Wozadlo (General Electric Co., Pleasanton, CA.) 1991 26 p Presented at the 5th International Symposium on Environmental Degradation on Materials in Nuclear Power Systems, Water Reactors, Monterey, 25-29 Aug. 1991
(Contract DE-AC05-84OR-21400)
(DE91-012220; CONF-910808-1) Avail: NTIS HC/MF A03

Pre-irradiation solution annealing treatments for limited times in the temperature range from 1204 to 1316 C were shown to be effective in eliminating irradiation assisted stress corrosion cracking (IASCC) in type 304 stainless steel (SS), which had been irradiated to fluences between 2.58 and 3.08 x 10(exp 21) n/sq cm (E greater than 1 MeV). Varying resistance to IASCC as a function of heat treatment parameters was demonstrated in constant extension rate tensile (CERT) tests performed in boiling water reactor (BWR) simulated water. Measures of IASCC susceptibility used in the CERT tests (percent IGSCC, percent elongation, and maximum stress) could not be correlated with data obtained from HNO3/Cr(+6) corrosion tests, or from Auger and analytical electron microscopy (AEM) analyses of grain boundary composition. Corrosion test data, however, could be correlated with the Auger and AEM results. The absence of a correlation between IASCC susceptibility and the grain boundary contents of Si, P, and S suggests that other impurities that are known to segregate and undergo nuclear transmutations, such as N and B, may play an important role in the IASCC mechanism. Tensile test data showed that the high temperature solution annealed (HTSA) material had undergone less radiation strengthening than mill annealed (MA) material. Elongations of approximately 10 percent were measured in the HTSA material compared to 2 percent in the MA material. DOE

N91-28353# Ames Lab., IA.
EXAFS STUDIES OF ELASTIC STRAIN IN DILUTE BINARY ALLOYS Ph.D. Thesis
A. Parakka 14 May 1991 89 p
(Contract W-7405-eng-82)
(DE91-012678; IS-T-1562) Avail: NTIS HC/MF A05

The study of bimetallic alloys is of great interest because of their wide use in industry catalysts. Catalytic properties of material are very much dictated by their surface properties. Surface segregation-the phenomenon where the surface concentration of one of the species differs from that in the bulk-in such bimetallic alloys is then of great importance since surface properties are greatly affected by the surface composition. Several theories have been forwarded to predict which component of the alloy is expected to segregate to the surface in such binary alloys. In this report, the EXAFS analysis of a nickel-platinum alloy system is discussed. Data Acquisition, data analysis, results, and a discussion are topics presented in this report. DOE

N91-28354# Pacific Northwest Lab., Richland, WA.
EFFECTS OF RESIDUAL STRESSES ON THE FRACTURE TOUGHNESS OF ZIRCALOY-2 TUBES
H. P. Mohamadian, A. R. Mirshams (Southern Univ., Baton Rouge, LA.), and M. E. Cunningham May 1991 19 p Presented at the Conference on the Practical Applications of Residual Stress Technology, Indianapolis, 15-17 May 1991
(Contract DE-AC06-76RL-01830)
(DE91-012736; PNL-SA-18689; CONF-910591-2) Avail: NTIS HC/MF A03

Data applicable to evaluating the fracture toughness of Zircaloy-2 pressure tubes were evaluated according to the criteria in ASTM Standards E399 and E813. It was found that the data did not meet the criteria specified in the standards, thus making it necessary to account for residual stress in determining the fracture toughness of the tubes. Therefore, residual stress in pressure tube specimens was experimentally determined to allow the incorporation of residual stresses in the calculation of fracture toughness. Sections of as fabricated 82.5 mm OD Zircaloy-2 tubes in the 30 percent cold worked condition were used in testing. Electrochemical Machining (ECM) was used to remove material from the interior of the tube, while measuring the resulting change in strain on the exterior of the tube with delta rosette strain gages. Utilization of this technique to reduce the cross sectional area of a tube without introducing additional stresses offers an accurate procedure for obtaining data to calculate the residual stress distribution. Assuming elastic anisotropy, the stress equations developed by Voyiadjis, Kiousis, and Hartley were used to determine the residual tangential, radial, and longitudinal stresses as a function of wall thickness. Additionally, these equations allow the determination of the shear stress and subsequently the principal stress profiles. It was found that the measured residual stress level was high enough that it must be accounted for when determining the fracture toughness of the subject Zircaloy-2 tubes. DOE

N91-28355# Oak Ridge K-25 Site, TN. UEO Enrichment Technical Operations Div.
THE EFFECT OF FLUORIDE GASES ON CYLINDER VALVE CORROSION
J. F. Preston and C. P. Hammett Mar. 1991 50 p
(Contract DE-AC05-84OT-21400)
(DE91-012745; K/ETO-56) Avail: NTIS HC/MF A03

In October 1988, it was first learned that a uranium hexafluoride cylinder valve on an El Dorado cylinder was found to be severely corroded at Paducah. Aluminum bronze CDA alloy 636, a copper-based alloy with 3 to 4 percent aluminum and 0.7 to 1.3 percent silicon, is specified for uranium hexafluoride cylinder valves. A section of a typical unused valve was provided for exposure studies in the Trace Gas Studies Facility (TGSF), manufactured according to the schematic in Figure 2. While the capabilities of the TGSF have evolved over time, its principle mission is to measure the permeability of nine-inch barrier samples in inert and production gas environments. The external lines and other components are wrapped with high temperature fiber glass heat tapes to prevent metal halides from depositing in the lines. The cylinder valve corrosion studies were performed in a sample cylinder attached to the external manifold. These studies have indicated that exposure of cylinder valve samples to AsF(sub 5), HF, or UF(sub 6), alone, or UF(sub 6) in combination with AsF(sub 5) or HF over periods of 8 days at 66 C did not result in observable surface corrosion. However, binary mixtures of HF + 20 percent AsF(sub 5) at 60 C and ternary mixtures of UF(sub 6) + 20 percent HF + 20 percent AsF(sub 5) at 66 C began to show changes in surface morphology after only a day of exposure. It was also determined that sample exposure to the ternary gas mixture at 25 C did not result in observable corrosion over an 8-day period. DOE

N91-28356# Edgerton, Germeshausen and Grier, Inc., Idaho Falls, ID.
MECHANISMS OF BACTERIAL METALS REMOVAL FROM SOLIDS
A. E. Torma and P. A. Pryfogle 1990 8 p Presented at the Workshop on Biological Remediation of Contaminated Sediments With Special Emphasis on the Great Lakes, Manitowoc, 17-19 Jul. 1990
(Contract DE-AC07-76ID-01570)
(DE91-012808; EGG-M-90290; CONF-9007211-1) Avail: NTIS HC/MF A02

The Great Lakes area sediments are contaminated with varying amounts of heavy metals and polychlorinated organic matter. With respect to the bioremediation of metallic contents of these sediments, it was shown that a number of microorganisms exist which can effectively solubilize heavy metals. The basic reaction mechanisms of bioleaching processes were discussed and the effects of semiconductor character of the sulfide substrate explained. A special emphasis was made to comment on INEL's bioremediation capability. DOE

N91-28357# Marquette Univ., Milwaukee, WI. Dept. of Chemistry.
RESONANCE RAMAN AND PHOTOPHYSICAL STUDIES OF TRANSITION METAL COMPLEXES IN SOLUTION AND ENTRAPPED IN ZEOLITES
J. R. Kincaid 29 Mar. 1991 5 p
(Contract DE-FG02-86ER-13619)
(DE91-013010; DOE/ER-13619/5) Avail: NTIS HC/MF A01

This program is subdivided into two major categories: the study of complexes of Ru(II) in fluid solution and the investigation of the effects of incorporation of such complexes into organized assemblies. At first, clear evidence is presented for the somewhat unexpected observation of quite specific localization of excited state electron density on a rather small fragment of the coordinated asymmetric bidentate ligand. Thus far, two examples of this behavior were documented and the results will soon be submitted for publication. Next, continuing efforts are described of efforts to develop effective methods for selective preparation of heteroleptic complexes within the supercages of Y-type zeolite. Also described are Resonance Raman studies of Ru(bipyrazine)3(2+) in solutions of varying concentrations of H2SO4; from 0 to 96 pct. DOE

N91-28358# Oak Ridge National Lab., TN.
AQUEOUS CORROSION CHARACTERISTICS AND CORROSION-RELATED CRACKING SUSCEPTIBILITIES OF Fe3Al-TYPE IRON ALUMINIDES
R. A. Buchanan and J. G. Kim (Tennessee Univ., Knoxville.) Apr. 1991 40 p
(Contract DE-AC05-84OR-21400)
(DE91-013028; ORNL/Sub-88-07685/01) Avail: NTIS HC/MF A03

In certain fossil energy applications, iron aluminides may be subjected to ambient temperature aqueous corrosion conditions. The aqueous corrosion characteristics and the cracking tendencies under aqueous-corrosion conditions were studied. Electrochemical, immersion and electrochemical-mechanical evaluation techniques were employed. For a range of iron-aluminide compositions, cyclic anodic polarization tests were conducted in a number of electrolytes to provide information on anodic dissolution characteristics including tendencies for either active uniform corrosion, localized corrosion, or passivation. Average corrosion penetration rates were determined by application of Tafel methods or the polarization resistance method in combination with Faraday's law. Immersion test methods were employed to verify corrosion behavior as determined by electrochemical methods and to evaluate localized corrosion initiation times. U-bend corrosion tests were conducted at open circuit corrosion potentials and at potentiostatically controlled anodic and cathodic potentials to investigate the cracking tendencies of selected iron aluminides and to provide information on the cracking mechanism. And finally, slow strain rate corrosion tests were conducted at open circuit and potentiostatically controlled cathodic potentials to study the ductility response as related to cracking tendencies and the mechanism responsible. DOE

N91-28359# Oak Ridge National Lab., TN.

PROPERTIES OF LARGE HEATS OF Fe3Al-BASED ALLOYS

V. K. Sikka, C. G. McKamey, C. R. Howell, and R. H. Baldwin Mar. 1991 39 p
(Contract DE-AC05-84OR-21400)
(DE91-013268; ORNL/TM-11796) Avail: NTIS HC/MF A03

The scaleup of three Fe3Al-based alloys at several commercial vendors is described. The scaleup processes examined the effect of crucible materials (MgO versus Al2O3), melting practice, vacuum induction melting, vacuum arc remelting, electroslag remelting, and processing under commercial conditions. Each alloy is designed for a specific use: sulfidation resistance, room temperature ductility, and high temperature strength. One of the alloys was also scaled up through powder production by nitrogen gas atomization. The scaled-up heats varied in size from 50 to 250 kg (100 to 500 lb). The ingot sizes varied from 38 to 203 mm (1 1/2 to 8 in.) diam. The scaleup processes occurred at Ametek Specialty Metal Products Division; Haynes International, Inc.; Carpenter Technology Corporation; Special Metals Corporation; and Precision Rolled Products, Inc. The processing of 102 mm diam (4 in.) ingots at the Oak Ridge National Laboratory into plate and sheet is described in detail. Tensile and creep data on a large powder metallurgy and cast-and-worked alloys are presented. Recommendations are made for future work on the heats scaled up in this study. DOE

N91-28360# Oak Ridge National Lab., TN.

EROSION STUDIES ON A Fe3Al-BASED IRON ALUMINIDE AND 1100 Al

M. Rao and J. Keiser 1991 12 p Presented at the 5th Annual Conference on Fossil Energy Materials, Oak Ridge, 13-16 May 1991
(Contract DE-AC05-84OR-21400)
(DE91-012529; CONF-9105184-2) Avail: NTIS HC/MF A03

Samples of a Fe3Al-based iron aluminide alloy were eroded using nominally spherical steel shot. Two distinct erosion mechanisms were observed: extrusion of platelets resulting from spherical particle impacts and cutting of the target by angular particles either present in the initial erodent or formed on impact by fracture of the shot. The overall erosion resistance of the alloy was judged to be relatively good and may be improved by increasing the alloy's ductility. Measurements using a mechanical properties microprobe (MPM) showed that significant work hardening occurred due to erosion, but the hardness dropped off near the surface, apparently due to thermal effects. In contrast no sub-surface softening was observed in samples of 1100 Al which were also eroded by steel shot. In order to model the impact process, single 343 micron WC spheres were shot at the two alloys at velocities between 20 and 900 m/s. Compared to the iron aluminide, the craters on 1100 Al show better developed lips and features indicative of sustained plastic deformation. Both alloys showed thermally induced subsurface softening at high velocities. At lower velocities, only the iron aluminide showed clear thermal effects. Results of the single particle and multiple particle impact tests are reconciled in terms of deformation behavior and thermal effects. DOE

N91-28361# Argonne National Lab., IL.

EVALUATION OF AGING OF CAST STAINLESS STEEL COMPONENTS

H. M. Chung Feb. 1991 17 p Presented at the American Society of Mechanical Engineers (ASME) Pressure Vessels and Piping Conference, San Diego, 23-27 Jun. 1991
(Contract W-31-109-eng-38)
(DE91-014013; ANL/CP-70872; CONF-910602-45) Avail: NTIS HC/MF A03

Cast stainless steel is used extensively in nuclear reactors for primary-pressure-boundary components such as primary coolant pipes, elbows, valves, pumps, and safe ends. These components are, however, susceptible to thermal aging embrittlement in light water reactors because of the segregation of Cr atoms from Fe and Ni by spinodal decomposition in ferrite and the precipitation of Cr-rich carbides on ferrite/austenite boundaries. A recent advance in understanding the aging kinetics is presented. Aging kinetics are strongly influenced by the synergistic effects of other metallurgical reactions that occur in parallel with spinodal decomposition, i.e., clustering of Ni, Mo, and Si solute atoms and the nucleation and growth of G-phase precipitates in the ferrite phase. A number of methods are outlined for estimating aging embrittlement under end-of-life of life-extension conditions, depending on several factors such as degree of permissible conservatism, availability of component archive material, and methods of estimating and verifying the activation energy of aging. DOE

N91-28362# Edgerton, Germeshausen and Grier, Inc., Idaho Falls, ID.

SUBSTRUCTURE AND ELECTRICAL RESISTIVITY ANALYSES OF PURE TUNGSTEN SHEET

C. L. Trybus, C. H. Sellers, and R. A. Anderl 1991 5 p Presented at the Annual Meeting and Exhibition of the Minerals, Metals and Materials Society (TMS), New Orleans, 17-21 Feb. 1991
(Contract DE-AC07-76ID-01570)
(DE91-014098; EGG-M-90504; CONF-910202-18) Avail: NTIS HC/MF A01

The substructure of pure tungsten sheet (0.025 mm thick) is examined and quantified by transmission electron microscopy (TEM). Dislocation populations and arrangements are evaluated for as-worked and various annealed conditions of the tungsten sheet. The worked (rolled) tungsten substructure was nonhomogeneous, consisting of areas of very high and low dislocation densities. These results are correlated to resistivity measurements of the tungsten sheet following thermal cycling to 1200 C to determine the substructural changes as a function of temperature. The comparison between the two characterization techniques is used to examine the relationship between structural and electronic properties in tungsten. DOE

N91-28363*# National Aeronautics and Space Administration. Goddard Space Flight Center, Greenbelt, MD.

HIGH TEMPERATURE SOLDER DEVICE FOR FLAT CABLES Patent Application

Carl L. Haehner, inventor (to NASA) 20 Jun. 1991 16 p
(NASA-Case-GSC-13344-1; NAS 1.71:GSC-13344-1; US-Patent-Appl-SN-718046) Avail: NTIS HC/MF A03 CSCL 11F

A high temperature solder device for flat cables includes a microwelder, an anvil which acts as a heat sink and supports a flexible flat ribbon cable that is to be connected to a multiple pin connector. The microwelder is made from a modified commercially available resistance welding machine such as the Split Tip Electrode microwelder by Weltek, which consists of two separate electrode halves with a removable dielectric spacer in between. The microwelder is not used to weld the items together, but to provide a controlled compressive force on, and energy pulse to, a solder preform placed between a pin of the connector and a conductor of the flexible flat ribbon cable. When the microwelder is operated, an electric pulse will flow down on electrode, through the solder preform and back up the other electrode. This pulse of electrical energy will cause the solder preform to heat up amd melt, joining the pin and conductor. NASA

N91-28364# Pacific Northwest Lab., Richland, WA.

ADVANCEMENTS IN ULTRATHINNING SECTION TECHNIQUES FOR THE CHARACTERIZATION OF BRITTLE MATERIALS

N. T. Saenz May 1991 22 p Presented at the Metallography: 75 Years Later, Atlantic City, 8-10 May 1991
(Contract DE-AC06-76RL-01830)
(DE91-012930; PNL-SA-18472; CONF-9105189-2) Avail: NTIS HC/MF A03

The use of ultrathin sections, on the order of 1/6 to 1/10 the thickness of conventional 30 microns thin sections, constitutes a significant advancement in the characterization of brittle materials. At a time when greater emphasis is being placed on optimum resolution and interfacial characterization of brittle materials, this approach makes possible a whole new order of optical access to microstructural detail. With the evolution of improved mounting media and polishing equipment, ultrathinning section techniques have also improved to produce sections that reduce preparation time and operator dependence. Preparation methods and examples of materials examination using this ultrathinning technique are discussed. DOE

N91-28365# Lawrence Livermore National Lab., CA.
SHOCK-INDUCED OPTICAL EMISSION IN Al2O3 AT 200 GPa: IMPLICATIONS FOR SHOCK TEMPERATURE MEASUREMENTS IN METALS
C. S. Yoo, N. C. Holmes, and E. F. See May 1991 6 p
Presented at the 1991 American Physical Society (APS) Conference on Shock Compression of Condensed Matter, Williamsburg, 17-20 Jul. 1991
(Contract W-7405-eng-48)
(DE91-013584; UCRL-JC-106341; CONF-9107105-24) Avail: NTIS HC/MF A02

A knowledge of the optical property of window materials at shock pressures above 100 GPa is crucial for determining shock temperatures in metals. We have examined the optical properties of Al2O3 at 200 to 300 GPa pressures using a time-resolved optical method. Strong emission is observed from the shocked Al2O3. Wavelength- and time-dependence of the emission will be presented. A new electro-optical technique facilitating time-resolved optical measurements at a 2-stage light gas gun will be described. DOE

N91-28366# Los Alamos National Lab., NM.
THE PRESSURE-INDUCED MOTT TRANSITION IN TRANSITION-METAL IODIDES
M. P. Pasternak, R. D. Taylor, and R. Jeanloz (California Univ., Berkeley.) 1991 24 p Presented at the 5th Joint Magnetism and Magnetic Materials (MMM/INTERMAG) Conference, Pittsburgh, 18-21 Jun. 1991
(Contract W-7405-eng-36)
(DE91-013671; LA-UR-91-1538; CONF-910608-4) Avail: NTIS HC/MF A03

Many of the Transition Metal (TM) compounds, because of exchange and correlation interactions within the narrow and poorly overlapping d-bands, become antiferromagnetic insulators, the Mott Insulators (MI). The properties of the MI and their gradual transition into the non-correlated metallic state (the Mott Transition) are of crucial importance for the elucidation of HTS materials features in particular and to magnetism in general. The transition of the MI into a metal can be achieved either by doping or by high pressure. To yield the definitive data on the Mott transition high pressure work on well characterized materials should be sought. The present studies provide for the first time extensive information on the Mott-Hubbard gap closure induced by high pressure. High pressure studies using Diamond Anvil Cells were conducted in several (TM)I2 compounds. They all have layered structures and other antiferromagnetically at ambient pressure. I-129 Moessbauer Spectroscopy (MS) was used to study the properties of the (TM)(2+) sublattice magnetization as a function of pressure and temperature, and X-ray diffraction was used to look for possible crystallographic transitions and to obtain the equation of state. Results show that the high pressure transition at P(sub c) from a magnetic to a non-magnetic state is not accompanied by crystallographic changes. Previous studies with NiI2 have confirmed the presence of a metallic state at P greater than P(sub c). Inherent to the pressure behavior of the magnetic state is the gradual increase of T(sub N) in all cases and a slight increase in the TM(2+) moments with pressure increase. The collapse of the magnetic state is abrupt for some cases (NiI2) and gradual for others (CoI2), indicative of different band-overlap mechanisms. DOE

N91-28367# Oak Ridge National Lab., TN.
WELDABILITY OF IRON ALUMINIDES
T. Zacharia and S. A. David 1991 9 p Presented at the 5th Annual Conference on Fossil Energy Materials, Oak Ridge, 13-16 May 1991
(Contract DE-AC05-84OR-21400)
(DE91-013730; CONF-9105184-6) Avail: NTIS HC/MF A02

Improvements in the ductility of iron aluminide alloys, achieved through control of composition and microstructure, has led to growing interest in using these materials for structural applications. Weldability is a key issue in the utilization of these alloys for structural components. This paper describes the welding and welding behavior of an Fe3Al alloy (FA-129) containing niobium and carbon. Weldability of this alloy has been found to be a strong function of composition, welding process and processing conditions. Crack free welds were made on both sheet and plate material using the electron beam (EB) welding process. Gas tungsten arc (GTA) welds, on the other hand, exhibited a tendency for delayed cold cracking. However, the study clearly demonstrated that successful welds can be made using matching filler metal and proper choice of processing conditions. DOE

N91-28368# Nebraska Univ., Lincoln. Dept. of Physics.
MAGNETIC STUDIES OF IRON-RARE-EARTH-METALLOID ALLOYS
1991 8 p
(Contract DE-FG02-86ER-45262)
(DE91-013856; DOE/ER-45262/4) Avail: NTIS HC/MF A02

This research is focused on studying new phases and microstructures of rare-earth and transition-metal alloys and compounds. In particular we investigate several classes of materials which are expected to have high magnetizations and coercivities, which are necessary conditions for high performance permanent magnet and related applications. Hard and semi-hard magnetic materials form the basis of much of the electric power and information storage industries and the discovery of new and less expensive materials with outstanding properties is of great interest. Our work is centered on two general types of problems. One is the growth and control of the microstructure of thin films with specified magnetic anisotropies. Particular attention is paid to nanoscale variations in atomic order in multilayered samples to achieve the desired properties. The second type of problem involves fundamental electronic structure and its relation to the magnetic properties of new Fe-and Co-rich phases containing rare earths. These studies involve a variety of experimental measurements and theoretical calculations. DOE

N91-28369# Oregon State Univ., Corvallis. Dept. of Physics.
THEORETICAL STUDIES OF ZIRCONIA AND RELATED MATERIALS
H. J. F. Jansen 1991 7 p
(Contract DE-FG06-88ER-45352)
(DE91-013906; DOE/ER-45352/3) Avail: NTIS HC/MF A02

The starting point for all our investigations of phase transitions in zirconia are total energy electronic structure calculation. In the last two years we have performed many computer calculations pertaining to cubic, tetragonal, and monoclinic zirconia. The results of this work provide us with an excellent data base needed to construct effective potentials between the different atoms in zirconia. These potentials are necessary ingredients for our molecular dynamics simulations, which we perform to incorporate the effects of a non-zero temperature. The molecular dynamics calculations will provide us with the information concerning the phase transitions in zirconia. In addition, we are investigating Slater-Koster type interpolations of the band structure of zirconia. This is a second way of interpolating the total energy data of zirconia. DOE

N91-28370# Brookhaven National Lab., Upton, NY.
BRITTLE BEHAVIOR OF SSC YOKES
M. L. Rehak and J. R. Turner (Superconducting Super Collider Lab., Dallas, TX.) 1991 8 p Presented at the 3rd Annual International Industrial Symposium on the Super Collider (IISSC), Atlanta, 13-15 Mar. 1991
(Contract DE-AC02-76CH-00016)
(DE91-014031; BNL-45541; CONF-910340-42) Avail: NTIS HC/MF A02

In liquid helium at 4 K ultra-low carbon steel is known to be brittle. Fracture toughness and ultimate strength measured by the National Institute of Standards and Technology (NIST) are used here to examine the brittle behavior of the SSC yokes. The fracture toughness K(sub Ic) of the material is used to estimate the maximum allowable length of pre-existing cracks. Tensile properties of the steel at 4 K are compared with maximum tensile stresses obtained from the ANSYS finite element analysis of the DSX201 cross-section. DOE

N91-28371# Oak Ridge National Lab., TN.

APFIM CHARACTERIZATION OF THE SPINODAL DECOMPOSITION IN DUPLEX STAINLESS STEELS

J. E. Brown, G. D. W. Smith, P. H. Pumphrey (National Power Technology and Environmental Centre, Leatherhead, England), and M. K. Miller 1991 8 p Presented at the 5th International Symposium on Environmental Degradation on Materials in Nuclear Power Systems - Water Reactors, Monterey, 25-29 Aug. 1991
(Contract DE-AC05-84OR-21400)
(DE91-014256; CONF-910808-3) Avail: NTIS HC/MF A02

An atom probe field ion microscope characterization of two CF3 steels with 15 and 25 volume percent ferrite aged at 400 C for up to 10,000 h and service materials from the Shippingport main and check valves aged for approximately 13 years at approximately 280 C has been performed. In all these materials, the ferrite phase was found to have decomposed into an ultrafine scale two phase microstructure consisting of an iron-rich alpha phase and a chromium-enriched alpha' phase. The scale of the decomposition in the Shippingport materials was much finer that than found in the CF3 material subjected to accelerated aging at 400 C. DOE

N91-28372# Pennsylvania Univ., Philadelphia. Dept. of Materials Science and Engineering.

ATOMISTIC STUDIES OF GRAIN BOUNDARIES IN ALLOYS AND COMPOUNDS

V. Vitek 1991 7 p
(Contract DE-FG02-87ER-45295)
(DE91-014516; DOE/ER-45295/T1) Avail: NTIS HC/MF A02

In this research project we investigate theoretically, by computer modeling, the atomic structure of grain boundaries in binary alloys. The goal is to elucidate which structural, chemical and possibly electronic features distinguish alloys from pure metals and are responsible for remarkably different fracture properties of alloys and pure metals. In the case of disordered alloys we concentrate on the model system Cu-Bi and investigate the following three problems: (1) Segregation behavior; (2) Development of faceting and associated two-dimensional structural phase transitions; and (3) The structure of Sigma = 3 facets which have developed as a result of segregation and are at the same time observed by the high resolution electron microscopy (HREM). In the case of ordered alloys we explore grain boundaries in Ni3Al and Cu3Au. The aim is to study the relationship between the ordering tendency, which is quantitatively very different in these two alloys, and grain boundary structure and properties. In both cases we shall investigate the boundary properties which relate to the mechanical behavior using the recently developed concept of depicting the grain boundary as a heterogeneous continuum composed of particles, identified with Voronoi polyhedra associated with individual atoms, which possess different elastic properties. DOE

N91-28373*# National Aeronautics and Space Administration. Langley Research Center, Hampton, VA.

TEST OF SUPERPLASTICALLY FORMED CORRUGATED ALUMINUM COMPRESSION SPECIMENS WITH BEADED WEBS

Randall C. Davis, Dick M. Royster, Thomas T. Bales, William F. James (Lockheed Engineering and Sciences Co., Hampton, VA.), and Joseph M. Shinn, Jr. Jun. 1991 33 p
(NASA-TM-104119; NAS 1.15:104119) Avail: NTIS HC/MF A03 CSCL 11F

Corrugated wall sections provide a highly efficient structure for carrying compressive loads in aircraft and spacecraft fuselages. The superplastic forming (SPF) process offers a means to produce complex shells and panels with corrugated wall shapes. A study was made to investigate the feasibility of superplastically forming 7475-T6 aluminum sheet into a corrugated wall configuration and to demonstrate the structural integrity of the construction by testing. The corrugated configuration selected has beaded web segments separating curved-cap segments. Eight test specimens were fabricated. Two specimens were simply a single sheet of aluminum superplastically formed to a beaded-web, curved-cap corrugation configuration. Six specimens were single-sheet corrugations modified by adhesive bonding additional sheet material to selectively reinforce the curved-cap portion of the corrugation. The specimens were tested to failure by crippling in end compression at room temperature. Author

N91-28374 Illinois Univ., Urbana-Champaign.

HYDROGEN EMBRITTLEMENT OF SELECTED NICKEL AND IRON BASE SUPERALLOYS Ph.D. Thesis

Peter David Hicks 1990 248 p
Avail: Univ. Microfilms Order No. DA9114264

Two nickel base superalloys (IN718 and IN625) and one iron base superalloy (A286) were chosen as candidates for hydrogen embrittlement (HE). The HE susceptibility of these alloys, in both annealed (ann) and aged conditions to: a mild gaseous hydrogen (H) environment, dynamic H charging, and H precharging, was evaluated in constant extension rate tests (CERT) and subcritical crack growth (SCG) studies. CERT testing showed that all three alloys were not embrittled in a 101 kPa H2 gas environment, but that they all showed a tendency for brittle cracking under severe dynamic cathodic charging (up to 500 A/sq m). SCG tests showed a typical three stage SCG behavior for IN718 (aged) and IN625 (ann) for intermediate hydrogen concentrations. For all alloys, the threshold stress intensity decreases. Hydrogen enhanced localization of plasticity and void pressurization due to H are used to explain the observed HE of these alloys. The effect of H on the stacking fault energy, dislocation dynamics, trapping sites, microstructure, and cracking ahead of the main crack front are discussed. Dissert. Abstr.

N91-28375 Ohio State Univ., Columbus.

LASER SURFACE MODIFICATION TO IMPEDE HYDROGEN INGRESS INTO STEEL Ph.D. Thesis

Murali Manohar 1990 214 p
Avail: Univ. Microfilms Order No. DA9111755

One of the serious limitations of high strength steels is their susceptibility to hydrogen induced fracture. Experiments conducted to examine the effect of laser surface alloying with the nobel metals Pt, Pd, and Au were carried out using the CO2 laser. The hydrogen absorption behavior was studied using the electrochemical permeation test and the susceptibility to hydrogen induced fracture was assessed using the slow strain rate tension test. In addition, attempts were made to characterize the surface using optical and electron metallography, microhardness testing, and Auger electron spectroscopy. The results obtained showed that laser surface melting was effective in improving the resistance to hydrogen induced fracture and that this improvement resulted from reduced absorption of hydrogen at the surface. Laser surface alloying with Pt, Pd, and Au resulted in even greater reduction in hydrogen absorption. Reverse specimen experiments showed that this effect of laser surface modification was an electrochemical one and that the modified surface did not act as a barrier. Each noble metal behaved differently and the observed reduction in hydrogen absorption appeared to be unrelated to changes in the microstructure or the hardness of the modified surface.
Dissert. Abstr.

N91-28376# Los Alamos National Lab., NM.

SYNTHESIS OF METASTABLE ALUMINUM-BASED INTERMETALLICS BY MECHANICAL ALLOYING

R. B. Schwarz, S. Srinivasan, and P. B. Desch 1991 18 p Presented at the International Symposium on Mechanical Alloying, Kyoto, Japan, 7-10 May 1991

(Contract W-7405-eng-36)
(DE91-013651; LA-UR-91-1490; CONF-9105182-2) Avail: NTIS HC/MF A03

Mechanical alloying (MA) has been used to prepare fine grained powders of Al 25 at. pct. X (X = Ti, Zr, Hf) having the metastable cubic L1 sub 2 structure. Hexane (C6H14) is added to the milling media to avoid the agglomeration of the aluminum powder. Carbon from the decomposition of the hexane incorporates into the powder to form a fine dispersion of carbides. These carbides are beneficial because they limit grain growth during consolidation and add strength to the alloy. The mechanically alloyed powders were consolidated using conventional hot pressing and nonconventional dynamic pressing. Hot pressing was used to consolidate mechanically alloyed L1 sub 2-Al3Ti powder in the presence of excess of Al. The compact has the DO22 structure. Its room temperature compressive strength is 1.2 GPa (exceeding that of cast Al3Ti by a factor of 10). At 400 C, the compressive strength decreases to 1 GPa. The ductility, which is negligible at room temperature, increases to 6 pct. at 400 C. Dynamic pressing was used to consolidate L1 sub 2-Al5CuZr2 powder. The compact, having the L1 sub 2 structure, has fine grains (44 nm) and a fine dispersion of ZrC precipitates (7 nm). Its hardness is in the range of 1030 kg/sq mm. Current efforts are to investigate ternary alloys based on fine grained trialuminides which include a ductile second phase. DOE

N91-28377# Argonne National Lab., IL.
TEMPERATURE DEPENDENCE OF THE ELASTIC BEHAVIOR OF STRUCTURALLY DISORDERED METALLIC SUPERLATTICES
J. A. Jaszczak and D. Wolf May 1991 7 p Presented at the Spring Meeting of the Materials Research Society (MRS), Anaheim, 29 Apr. - 3 May 1991
(Contract W-31-109-eng-38)
(DE91-014007; ANL/CP-73338; CONF-910406-19) Avail: NTIS HC/MF A02

The structure and elastic properties of superlattices composed of high-angle twist grain boundaries on (100) planes of copper are investigated as a function of both the modulation wavelength and temperature via molecular dynamics simulations. Comparison is made with zero temperature results, where a stiffening of the Young's modulus normal to the interfaces and a softening of the modulus for shear parallel to the interfaces has previously been observed. The differences between the effects of homogeneous (temperature induced) and inhomogeneous (interface induced) structural disorder on the elastic properties is explored. DOE

N91-28378# Oak Ridge National Lab., TN.
CORROSION OF REFRACTORY METALS IN LIQUID METAL AND GASEOUS ENVIRONMENTS
J. R. DiStefano 1991 17 p Presented at the 1st International Conference on Heat-Resistant Materials, Lake Geneva, 22-26 Sep. 1991
(Contract DE-AC05-84OR-21400)
(DE91-009555; CONF-910909-1-Draft) Avail: NTIS HC/MF A03

In general, refractory metals and alloys are very compatible with liquid or boiling alkali metals. However, corrosion resistance of niobium and tantalum requires maintaining low oxygen in the system. When the refractory metal contains a strong oxide former (Zr, Hf), additional oxygen in the solid metal can be tolerated if it is tied up as a stable oxide (ZrO2, HfO2). In sodium or potassium systems, oxygen in either the liquid metal or refractory metal can contribute to reduced corrosion resistance. The mechanical properties of refractory metals are very sensitive to interstitial elements such as oxygen, nitrogen, hydrogen, and carbon. Oxidation in air or other oxidizing environments is rapid above 300 to 400 C, and some type of protection must be provided (vacuum, inert gas, coating) if refractory metals are to be used at high temperatures. Oxidation of niobium and tantalum alloys is more complex than for molybdenum and tungsten due to the formation of different oxide phases that exhibit differing degrees of protectiveness. At low to intermediate temperatures niobium and tantalum also react with hydrogen environments, and embrittlement has been reported both from hydride formation as well as from solid solution effects. At high temperatures niobium and tantalum react with nitrogen or carbon to form very stable compounds while the nitrides and carbides of molybdenum and tungsten are considerably less stable. DOE

N91-28379# Sandia National Labs., Albuquerque, NM.
MICROSTRUCTURAL CHARACTERIZATION OF SOLDERS AND BRAZES FOR ADVANCED PACKAGING TECHNOLOGY
A. D. Romig, Jr., D. R. Frear, P. F. Hlava, F. M. Hosking, J. J. Stephens, and P. T. Vianco 1991 38 p Presented at the 49th Electron Microscopy Society of America (EMSA) Annual Meeting and the 25th Annual Microbeam Analysis Society Meeting, San Jose, CA, 4-9 Aug. 1991
(Contract DE-AC04-76DP-00789)
(DE91-011503; SAND-91-0698C; CONF-910870-13; CONF-910872-5) Avail: NTIS HC/MF A03

Historically, the electronics industry has always attempted to increase the speed of electronic components and decrease the size of electronic assemblies by developing and manufacturing smaller and faster basic level components (e.g., integrated circuits). However, it is now becoming apparent that the next significant advancement in electronic assembly size and speed may come not as a result of smaller and faster devices, but rather as a consequence of smaller and more closely spaced packages. This increased packaging density will occur at early levels of assembly as industry moves towards multichip modules. It will also occur at later packaging steps as industry continues to expand the use of surface mount technology (SMT) and mixed mounting technology (through hole attachment as well as SMT on one circuit board). Furthermore, there will be an increased propensity to use higher packaging density on printed wiring boards (PWB) and to place more PWB's in a given volume at yet the next level of packaging. One class of materials on which this advanced packaging technology will place severe new demands will be the alloys used to join assemblies and subassemblies (e.g., solders and brazes). These materials will be taxed both from the perspective of enhanced manufacturability as well as greater in-service robustness. Selected cases are used to illustrate how advanced microstructural characterization techniques can be used to improve packaging technology. The specific case studies discussed are: (1) Microstructural Characterization of Solders; (2) Microstructural Characterization of Solder Joint Embrittlement of Leaded, Surface Mount Transistors; (3) Microstructural Characterization of Metal/Ceramic Brazes in Electronic Applications; and (4) Microstructural Characterization of Direct Brazing of Graphite to Copper. DOE

N91-28380# Edgerton, Germeshausen and Grier, Inc., Idaho Falls, ID.
EFFECTS OF VARIOUS PARAMETERS ON THE FATIGUE LIFE OF ALLOY 718
G. E. Korth 1991 40 p Presented at the Special Emphasis Symposium on Superalloys 718, 625, and Various Derivatives, Pittsburgh, 23-26 Jun. 1991
(Contract DE-AC07-76ID-01570)
(DE91-014100; EGG-M-90292; CONF-910614-4) Avail: NTIS HC/MF A03

A data bank from over 700 tests on several heats of Alloy 718 with various test parameters is used to show the effects of temperature, strain rate, hold time, grain size, mean stress, surface roughness, and thermal aging on fatigue life. Both strain controlled and stress controlled tests were conducted providing data from 10(exp 2) to 10(exp 9) cycles to failure. Empirical curve fitting of the data was performed using a multiple regression analysis performance. DOE

N91-28381# Oak Ridge National Lab., TN.
ALLOY DEVELOPMENT OF Fe3Al FOR IMPROVED CREEP RUPTURE PROPERTIES
C. G. McKamey and P. J. Maziasz 1991 11 p Presented at the 5th Annual Conference on Fossil Energy Materials, Oak Ridge,

13-16 May 1991
(Contract DE-AC05-84OR-21400)
(DE91-014541; CONF-9105184-7) Avail: NTIS HC/MF A03

Our efforts to develop Fe3Al-based iron aluminides for fossil energy structural applications continue. Using alloy development and thermomechanical processing techniques, alloys with room temperature tensile ductilities of 10 to 20 percent and yield strengths of 500 MPa at temperatures to 600 C have been produced. Preliminary creep rupture studies have shown that Fe3Al, which has very poor creep resistance, can be strengthened significantly by alloy additions, particularly by small additions of Mo, Nb, and Zr. The reason for this improvement in creep life with alloying additions is under study and may be the result of a combination of factors, including grain boundary strengthening, resistance to dynamic recrystallization during stressing, precipitation strengthening, and changes in dislocation formation and mobility. Preliminary transmission electron microscopy analysis indicates that Fe3Al fails along weak grain boundaries and/or sub-grain boundaries formed by dislocation pileups. Additions of niobium affects the dislocation structure and produces precipitates which strengthen high-angle boundaries and pin dislocations; together, these factors appear to reduce dislocation sub grain boundary formation. These results indicate that controlling the composition and the microstructure through macro- and microalloying and/or thermomechanical processing can further improve the creep-rupture life and reduce the minimum creep rate. DOE

N91-28382# Oak Ridge National Lab., TN.
PROCESSING AND FABRICATION OF Fe3Al-BASED ALLOYS
V. K. Sikka 1991 7 p Presented at the 1st International Conference on Heat-Resistant Materials, Lake Geneva, 22-26 Sep. 1991
(Contract DE-AC05-84OR-21400)
(DE91-014546; CONF-910909-7) Avail: NTIS HC/MF A02

The Fe3AL-based iron-aluminide alloys offer excellent oxidation and sulfidation resistance. The commercial applications of these alloys require additional information about their processing and fabrication. This paper presents information regarding alloy compositions, melting, and fabrication. The melting described is of experimental heats and scale-up heats at several vendors. Data about the recovery of alloying elements and the impurity pick-up during various melting processes are presented. Details are presented of a study conducted at Special Metals Corporation on the melting of heats in two different crucible materials and by three different processes. Brief descriptions are also given about forms from these ingots. DOE

N91-28383# Delaware Univ., Newark. Dept. of Physics and Astronomy.
FUNDAMENTAL MAGNETIC STUDIES OF IRON-RARE-EARTH-METALLOID ALLOYS
G. C. Hadjipanayis 19 Feb. 1991 7 p
(Contract DE-FG02-90ER-45413)
(DE91-014816; DOE/ER-45413/1) Avail: NTIS HC/MF A02

This project is focussed on the study of magnetic and structural properties of new phases and special microstructures that have potential for relatively high coercivity. Hard and semihard magnets find wide applications in industry including electric power and information storage devices. The discovery of new and less expensive materials with better properties is of great interest. Our efforts are focused in the following three areas: (1) the search of Fe-rich new phases and compounds with high magnetization, anisotropy and Curie temperature that can be used for permanent magnet development; (2) the use of rapid solidification techniques (melt-spinning) to prepare these phases into fine grain microstructures that can lead to high coercivities; and (3) the relationships of hard magnetic properties to microstructures and magnetic domain structure determined by transmission electron microscopy. DOE

27 NONMETALLIC MATERIALS

Includes physical, chemical, and mechanical properties of plastics, elastomers, lubricants, polymers, textiles, adhesives, and ceramic materials.

For composite materials see *24 Composite Materials.*

N91-28384*# Florida Univ., Gainesville. Dept. of Materials Science and Engineering.
ION BEAM SPUTTERED COATINGS OF BIOGLASS M.S. Thesis Final Report
Larry L. Hench, J. Wilson, and Patricia Henrietta A Ruzakowski 1 Mar. 1982 227 p
(Grant NsG-3273)
Copyright Avail: NTIS HC/MF A11 CSCL 11C

The ion beam sputtering technique available at the NASA-Lewis was used to apply coatings of bioglass to ceramic, metallic, and polymeric substrates. Experiments in vivo and in vitro described investigate these coatings. Some degree of substrate masking was obtained in all samples although stability and reactivity equivalent to bulk bioglass was not observed in all coated samples. Some degree of stability was seen in all coated samples that were reacted in vitro. Both metallic and ceramic substrates coated in this manner failed to show significantly improved coatings over those obtained with existing techniques. Implantation of the coated ceramic substrate samples in bone gave no definite bonding as seen with bulk glass; however, partial and patchy bonding was seen. Polymeric substrates in these studies showed promise of success. The coatings applied were sufficient to mask the underlying reactive test surface and tissue adhesion of collagen to bioglass was seen. Hydrophilic, hydrophobic, charged, and uncharged polymeric surfaces were successfully coated. Author

N91-28385# Lowell Univ., MA. Dept. of Chemistry.
PHOTOCROSS-LINKED SECOND ORDER NONLINEAR OPTICAL POLYMERS Technical Report No. 13, 1 Jun. 1990 - 31 May 1991
Y. M. Chen, B. K. Mandal, J. Y. Lee, P. Miller, and J. Kumar 3 May 1991 8 p
(Contract N00014-90-J-1148)
(AD-A235855; Rept-1148-13) Avail: NTIS HC/MF A02 CSCL 07/6

A method is reported to obtain stable second order nonlinear optical (NLO) properties in polymeric thin films. Photocross-linking between the NLO active molecules and a photoreactive polymer is achieved by ultraviolet irradiation subsequent to poling. The thin film exhibits a nonlinear coefficient d33 of 16.5 pm/V at a doping level of 20 percent by weight of NLO active molecules and possesses quite stable second order nonlinear optical properties. GRA

N91-28386# Lowell Univ., MA. Dept. of Chemistry.
NEW PHOTOCROSSLINKABLE POLYMERS FOR SECOND ORDER NONLINEAR OPTICAL PROCESSES Technical Report No. 20, 1 Jun. 1990 - 31 May 1991
B. K. Mandal, R. J. Jeng, J. Kumar, and S. Tripathy 3 May 1991 15 p
(Contract N00014-90-J-1148)
(AD-A235856) Avail: NTIS HC/MF A03 CSCL 07/6

Polymeric systems have been established as useful materials for second order nonlinear optical (NLO) processes, viz. frequency doubling, linear electro-optic effect, frequency mixing and parametric oscillation. Crosslinked systems are reported to exhibit stable second order properties. The system can be poled and photocrosslinked in the poled state to yield a material with stable optical nonlinearity. This approach is based on the inter- and intramolecular photocrosslinking reactions of a photoreactive functionalized polymer. Since the second order susceptibility is directly proportional to the concentration of the nonlinear species and the temporal stability is dependent on the mobility of the nonlinear species in the polymer matrix, large and stable second order NLO properties are expected from these photocrosslinked polymers. In this communication, the synthesis and detailed characterization of this class of polymer are reported. GRA

N91-28387# Rutgers - The State Univ., Piscataway, NJ. Coll. of Engineering.
AN EXTENSION OF A KINETIC THEORY OF POLYMER CRYSTALLIZATION THROUGH THE EXCLUSION OF NEGATIVE BARRIERS
Louis Petrone, Jerry I. Scheinbeim, and Brian A. Newman May 1991 51 p
(Contract N00014-88-K-0122)
(AD-A236999; TR-22) Avail: NTIS HC/MF A04 CSCL 07/6

The simplest version of the Lauritzen-Hoffman (LH) model of polymer crystallization which applies to infinitely long model polymer molecules crystallizing on an existing substrate of infinite width, is re-examined. The mathematical expressions for the model free energy barriers are observed to take on negative values at high supercooling. Since such negative barriers appear to be physically unrealizable for the crystallization process, the LH model is extended by imposing a mathematical constraint on the expressions for the barriers, to forbid them from ever being negative. GRA

N91-28388# Rutgers - The State Univ., Piscataway, NJ. Coll. of Engineering.
EFFECT OF TCP DOPING ON THE REMNANT POLARIZATION IN UNIAXIALLY ORIENTED POLY(VINYLIDENE FLUORIDE) FILMS
Y. Takase, Jerry I. Scheinbeim, and Brian A. Newman May 1991 31 p
(Contract N00014-88-K-0122)
(AD-A237001; TR-16) Avail: NTIS HC/MF A03 CSCL 09/1

Uniaxially stretched films of poly (vinylidene fluoride) were doped (1 wt. percent) with plasticizer, tricrecyl phosphate (TCP). This slight doping with TCP was found to enhance the amount of remnant polarization in the region of low poling fields and high poling fields. The pyroelectric coefficient has shown that the doping enhances a quite stable (up to about 140 C) remnant polarization after high field poling. GRA

N91-28389# Rutgers - The State Univ., Piscataway, NJ. Dept. of Mechanics and Materials Science.
EFFECT OF WATER CONTENT ON THE PIEZOELECTRIC PROPERTIES OF NYLON 11 AND NYLON 7
Brian A. Newman, K. G. Kim, and Jerry I. Scheinbeim May 1991 22 p
(Contract N00014-88-K-0122)
(AD-A237013) Avail: NTIS HC/MF A03 CSCL 20/5

Studies of the piezoelectric properties of odd numbered nylons such as Nylon 11 and Nylon 7 are important, not only in their own right, but because they provide a way to examine the generality of concepts put forward to explain the piezoelectric and pyroelectric properties of poly(vinylidene fluoride) films. Over the past several years, a series of studies of Nylon 11 and Nylon 7 have been carried out. In a recent study appropriate sample preparation and poling techniques were described, which gave rise to mechanically unoriented but polarized films of Nylon 11 with values of the piezoelectric strain coefficient, d31, as high as 7.1 pc/n. GRA

N91-28390# Oak Ridge National Lab., TN.
NITROGEN AND BORON-CONTAINING POLYMERS AS PRECURSORS OF CERAMIC MATERIALS
L. Maya 1991 4 p Presented at the 202nd National Meeting of the American Chemical Society (ACS), New York, 25-30 Aug. 1991
(Contract DE-AC05-84OR-21400)
(DE91-008890; CONF-910812-1) Avail: NTIS HC/MF A01

The hydroboration was discussed of polybutdiene, along with the preparation of polymeric cyanoborane by passing hydrogen chloride through a suspension of sodium cyanotrihydroborate in dry ether, and the pyrolysis of melamine, dicyandiamide, 1,2,4 triazole, diamino maleonitrite, polymerized HCN, dicyano imideazole, tetracyanoethylene, and hexaaza triphenylenehexa carbonitrile. The physical and chemical characterization of the products is reported. DOE

N91-28391# Massachusetts Inst. of Tech., Cambridge. Dept. of Materials Science and Engineering.
RADIATION DISORDER AND APERIODICITY IN IRRADIATED CERAMICS
L. W. Hobbs 1991 3 p
(Contract DE-FG02-89ER-45396)
(DE91-010257; DOE/ER-45396/2) Avail: NTIS HC/MF A01

Three lines of research have been pursued over the 18-month period since program funding began on 22 June 1989. These are: (1) providing computer graphic representation of the physical models of tetrahedral network glass structure that Dr. Carol Marians had developed during a previous DOE-funded program, to assign coordinates to the tetrahedron vertices, and to minimize the energies of these configurations in order to provide a relaxed set of coordinates which could be compared to diffraction data; (2) establishing an ion implantation facility at MIT in order to initiate ion implantation into pyrophosphates in order to investigate radiation-induced disorder of partial network structures; and (3) exploring information about amorphization and glass network structure that can be adducted from energy-filtered electron diffraction patterns of silica polymorphs rendered progressively metamict by electron irradiation. DOE

N91-28392# California Univ., Santa Barbara.
POLYMERS AT SURFACES
P. Pincus 1991 7 p
(Contract DE-FG03-87ER-45288)
(DE91-011000; DOE/ER-45288/T1) Avail: NTIS HC/MF A02

In part one, published papers, papers accepted for publication, and those submitted or under preparation are listed. In part two, the author discusses future investigations. The areas covered are polyelectrolytes, brush dynamics, and mixed copolymer membranes. At the end, personnel working on the research are listed. DOE

N91-28393# Sandia National Labs., Albuquerque, NM.
MECHANICAL MODELING OF STRESS GENERATION DURING CURE OF ENCAPSULATING RESINS
R. R. Lagasse, R. S. Chambers, T. R. Guess, D. J. Plazek, and C. Bero (Pittsburgh Univ., PA.) 1991 11 p Presented at the Spring Meeting of the Materials Research Society (MRS), Anaheim, 29 Apr. - 3 May 1991
(Contract DE-AC04-76DP-00789)
(DE91-011496; SAND-90-3033C; CONF-910406-4) Avail: NTIS HC/MF A03

We have developed a numerical model for calculating stresses generated during cure of shrinking encapsulating resins. Mechanical modeling of polymer encapsulated electronic devices usually focuses on stress generated during cooling after cure. The stress developed during cure, due to shrinkage of the encapsulant, is normally neglected. That assumption is valid if both the shear and bulk moduli of the encapsulant at the cure temperature are negligible with respect to the moduli at lower temperatures. Our measurements on a model epoxy encapsulant show that the shear modulus during cure, varying from 0 to 6 MPa, is at least 100 times smaller than that at ambient temperature. In contrast, the bulk modulus at the cure temperature is only 2.5 times smaller. Since the bulk modulus during cure cannot be neglected, significant stress can be produced if volume shrinkage is constrained by a stiff mold or embedded elements. In fact, mechanical failure of encapsulating materials during cure has been evident in some of our experiments. Using measurements of shear and bulk moduli plus volume shrinkage as inputs to a finite element model, we have successfully predicted the shrinkage strains and stresses developed during cure of a model epoxy resin inside a cylindrical tube. Consideration of cure shrinkage stress has led to a process modification that appears to reduce mechanical failures in a real encapsulated device. DOE

N91-28394# Lawrence Livermore National Lab., CA.
PERSPECTIVE ON PLATING FOR PRECISION FINISHING
J. W. Dini Apr. 1991 29 p Presented at the American Society for Precision Engineering (ASPE) Conference, Tucson,

15-18 Apr. 1991
(Contract W-7405-eng-48)
(DE91-011927; UCRL-JC-106852; CONF-9104206-3) Avail: NTIS HC/MF A03

This paper is intended as an overview on platings for precision finishing operations. After a brief review of the two processes (polishing and precision machining) by which a coating on a part can be converted to a precision surface, the coatings which work successfully in these applications will be discussed. Then adhesion and stress aspects of deposits will be covered. Electroless nickel, which is a particularly attractive coating for precision finishing applications, will be discussed in some detail, from its early years as the Kanigen process to the present. Since microstructural changes in deposits are important for precision parts, this aspect will be covered for electroless nickel, copper and silver deposits. Lastly, some words will be directed at potential future electrodeposited coatings including nickel-phosphorus alloys, and various silver alloys. DOE

N91-28395# Sandia National Labs., Albuquerque, NM.

AEROGEL COMPOSITES FOR RADIOLUMINESCENT LIGHT/POWER SOURCES

C. S. Askley, S. T. Reed, C. J. Brinker, R. J. Walko, R. E. Ellefson, and J. T. Gill (EG and G Mound Applied Technologies, Miamisburg, OH.) 1991 11 p Presented at the 5th International Conference on Ultrastructure Processing of Ceramics, Glasses, Composites and Advanced Optical Materials, Orlando, 17-21 Feb. 1991
(Contracts DE-AC04-76DP-00789; DE-AC04-88DP-43495)
(DE91-012012; SAND-90-2634C; CONF-910291-3) Avail: NTIS HC/MF A03

Aerogels are attractive matrices for phosphor particles for radioluminescent light and power applications. Unique aerogel properties such as transparency, high surface area and pore volume, low density, and tailorable surface chemistry provide advantages that allow much higher tritium loading than is currently available using existing technology. Additional research and development is needed to further improve the performance of the aerogel/phosphor volumetric lights and power sources. These materials are promising candidates to provide the high light output required for new RL light application as well as for long-term, low-level power source. DOE

N91-28396# California Univ., Davis. Dept. of Mechanical Engineering.

RADIATION DAMAGE OF CERAMICS BY ELECTRON MICROSCOPY

D. G. Howitt 1991 5 p
(Contract DE-FG03-86ER-45279)
(DE91-012186; DOE/ER-45279/3) Avail: NTIS HC/MF A01

Investigations are being conducted into the mechanisms of radiation damage that occur in dielectric and semiconducting materials under electron irradiation. The aim of this work is to quantify the different effects as well as to provide improved methods for the analysis of these materials by electron microscopy. The research has clearly shown that processes other than direct displacement and radiolysis contribute to material decomposition and that diffusion induced by charge imbalance, vacancy assisted displacement and surface reactions can play a major role. DOE

N91-28397# Oak Ridge National Lab., TN.

CHARACTERIZATION OF SILICON NITRIDE SYNTHESIZED BY MICROWAVE HEATING

J. O. Kiggans, C. R. Hubbard, R. R. Steele, H. D. Kimrey, C. E. Holcombe, and T. N. Tiegs 1991 8 p Presented at the 93rd Annual Meeting and Exposition of the American Ceramic Society (ACerS), Cincinnati, 28 Apr. - 2 May 1991
(Contract DE-AC05-84OR-21400)
(DE91-012219; CONF-910430-3) Avail: NTIS HC/MF A02

Recently, a new procedure was developed for the nitridation of high purity silicon via microwave heating. Silicon samples were processed to various stages of nitridation utilizing microwave heating and then analyzed by x-ray diffraction and by scanning electron microscopy. These data were compared to that obtained from samples nitrided by conventional heating methods. DOE

N91-28398# Wisconsin Univ., Madison.

ORDERED CERAMIC MEMBRANES

M. A. Anderson, W. A. Zeltner, and C. G. Hill, Jr. 1991 24 p
(Contract DE-AS07-86ID-12626)
(DE91-012248; DOE/ID-12626/T2) Avail: NTIS HC/MF A03

Ceramic membranes have been formed from colloidal sols coated on porous clay supports. These supported membranes have been characterized in terms of their permeabilities and permselectivities to various aqueous test solutions. The pore structures of these membranes have been characterized by preparing unsupported membranes of the corresponding material and performing N2 adsorption-desorption studies on these membranes. To date, membranes have been prepared from a variety of oxides, including TiO2, SiO2, ZrO2, and Al2O3, as well as Zr-, V-, and Mo-doped TiO2. In many of these membranes pore diameters are less than 2 nm, while in others the pore diameters are between 3 and 5 nm. Procedures for fabricating porous clay supports with reproducible permeabilities for pure water are also discussed. DOE

N91-28399# California Univ., Berkeley. Lawrence Berkeley Lab.

A STUDY OF THE INFLUENCE OF TEMPERATURE GRADIENTS ON DENSIFICATION OF GLASS POWDER COMPACTS Ph.D. Thesis

R. B. Clinque 12 Dec. 1990 45 p
(Contract DE-AC03-76SF-00098)
(DE91-012337; LBL-29994) Avail: NTIS HC/MF A03

In the present study, we are concerned with the influence of temperature gradients on densification during the early stages of sintering in glass powder compacts. Glass was chosen primarily because it is of interest to determine if gradients can enhance densification, not only by diffusion in crystalline particles, but also by viscous flow. A second reason for using glass was that glasses clearly have the isotropic surface energies assumed in sintering models. The assumption that surface energies are isotropic is not always valid for crystalline ceramics and that assumption has been shown to lead to predictions for grain growth which are in conflict with observations. Furthermore, grain boundary free energies, which are often neglected in sintering models, are absent when glass is sintered. DOE

N91-28400# Pacific Northwest Lab., Richland, WA.

THE AVIAN EGGSHELL AS A MODEL OF BIOMINERALIZATION

J. L. Arias, M. S. Fernandez, V. J. Laraia, J. Janicki, A. H. Heuer, and A. I. Caplan (Case Western Reserve Univ., Cleveland, OH.) Nov. 1990 9 p Presented at the Fall Meeting of the Materials Research Society (MRS), Boston, 24 Nov. - 1 Dec. 1990
(Contract DE-AC06-76RL-01830)
(DE91-012608; PNL-SA-18812; CONF-901105-124) Avail: NTIS HC/MF A02

The avian eggshell is one of the most rapidly mineralizing biological systems known. By understanding the key components and steps in this process, it is hoped that relevant information is provided for fabrication of ceramic composites. The calcification of the eggshell occurs in three main steps: (1) fabrication of an organic matrix; (2) nucleation of an inorganic phase on the organic matrix; and (3) space filling growth of the calcite phase. The different layers of an eggshell can be separately isolated and studied. In this preliminary communication, the organization of the shell matrix and membranes and their association with the crystal phase, the immunohistochemical occurrence and distribution of types I and X collagen, and of different proteoglycans are reviewed. Also the preliminary findings of the remineralization of the intact or modified eggshell are presented. These experiments allow us to identify the essential steps in forming a natural composite ceramic. DOE

N91-28401# United Technologies Corp., East Hartford, CT.
INVESTIGATION OF LASER DIAGNOSTICS OF PACVD PROCESSES FOR DEPOSITING HARD FACE COATINGS
W. C. Roman 1 May 1991 7 p
(Contract DE-FG02-86ER-13560)
(DE91-012642; DOE/ER-13560/5) Avail: NTIS HC/MF A02

The objective is to improve the understanding of the mechanisms which govern the nonequilibrium reactive plasma of the mechanisms which govern the atomistic or molecular deposition of hard face coatings for erosion resistant applications. The goal is to provide a predictive capability that is severely lacking in the present science base of PACVD processing for depositing hard face coatings. Advanced laser diagnostics was used to probe the plasma for improving process control. DOE

N91-28402# Sandia National Labs., Albuquerque, NM.
SUBGAP ABSORPTION IN CONJUGATED POLYMERS
M. Sinclair, C. H. Seager, D. McBranch, A. J. Heeger, and G. L. Baker 1991 6 p Presented at the Spring Meeting of the Materials Research Society (MRS), Anaheim, 29 Apr. - 3 May 1991
(Contract DE-AC04-76DP-00789)
(DE91-012655; SAND-90-3023C; CONF-910406-10) Avail: NTIS HC/MF A02

Along with X(exp (3)), the magnitude of the optical absorption in the transparent window below the principal absorption edge is an important parameter which will ultimately determine the utility of conjugated polymers in active integrated optical devices. With an absorptance sensitivity of less than 10(exp -5), Photothermal Deflection Spectroscopy (PDS) is ideal for determining the absorption coefficients of thin films of transparent materials. PDS was used to measure the optical absorption spectra of the conjugated polymers poly-1,4-phenylene vinylene (and derivitives) and polydiacetylene-4BCMU in the spectral region from 0.55 to 3 eV. The spectra show that the shape of the absorption edge varies considerably from polymer to polymer, with polydiacetylene-4BCMU having the steepest absorption edge. The minimum absorption coefficients measured varied somewhat with sample age and quality, but were typically in the range 1 to 10/cm. In the region below 1 eV, overtones of C-H stretching modes were observed, indicating that further improvements in transparency in this spectral region might be achieved via deuteration or fluorination. DOE

N91-28403*# National Inst. of Standards and Technology, Gaithersburg, MD.
CHEMISTRY OF ELECTRONIC CERAMIC MATERIALS. PROCEEDINGS OF THE INTERNATIONAL CONFERENCE ON THE CHEMISTRY OF ELECTRONIC CERAMIC MATERIALS Final Report
P. K. Davies and R. S. Roth Jan. 1991 535 p Conference held in Jackson, WY, 17-22 Aug. 1990 Prepared in cooperation with Pennsylvania Univ., Philadelphia Sponsored in part by NASA, Navy, and Idaho National Engineering Lab., Idaho Falls
(NASA-CR-188688; NAS 1.26:188688; PB91-178822; NIST/SP-804) Avail: NTIS HC/MF A23 CSCL 11C

The conference was held at Jackson Hole, Wyoming from August 17 to 22, 1990, and in an attempt to maximize the development of this rapidly moving, multidisciplinary field, this conference brought together major national and international researchers to bridge the gap between those primarily interested in the pure chemistry of inorganic solids and those interested in the physical and electronic properties of ceramics. With the many major discoveries that have occurred over the last decade, one of the goals of this meeting was to evaluate the current understanding of the chemistry of electronic ceramic materials, and to assess the state of a field that has become one of the most important areas of advanced materials research. The topics covered include: crystal chemistry; dielectric ceramics; low temperature synthesis and characterization; solid state synthesis and characterization; surface chemistry; superconductors; theory and modeling. GRA

N91-28404# National Inst. of Standards and Technology, Gaithersburg, MD.
US ASSESSMENT OF THE NEW DIAMOND TECHNOLOGY IN JAPAN Final Report
A. Feldman and L. H. Schwartz Jan. 1991 100 p
(PB91-167395; NIST/SP-807) Avail: NTIS HC/MF A05 CSCL 11C

The purpose is to assess the level of scientific activity, areas of intended commercialization, progress in commercialization, the role of the Japanese Government in assisting industry to exploit the new diamond technology, and the relative positions of Japan and the U.S. in all aspects of synthesized diamond technology. Japanese efforts were chosen for assessment because Japan is the apparent world leader in the drive for commercialization of the technology. The principle focus is on diamond produced by chemical vapor deposition, with a peripheral investigation of cubic boron nitride and diamond-like carbon. Based on the assessment, a set of conclusions and recommendations is presented. The assessment is based on site visits in Japan between 28 May to Jun. 5 1990. GRA

N91-28405# Oak Ridge National Lab., TN.
IN-SITU REM IMAGING OF SURFACE PROCESSES ON CERAMIC BULK CRYSTALS FROM 300 TO 1670 K IN A CONVENTIONAL TEM
Z. L. Wang (Tennessee Univ., Knoxville.) and J. Bentley 1991 2 p Presented at the 49th Electron Microscopy Society of America (EMSA) Annual Meeting San Jose, 4-9 Aug. 1991
(Contract DE-AC05-84OR-21400)
(DE91-009923; CONF-910870-4) Avail: NTIS HC/MF A01

Studying the behavior of surfaces at high temperatures is of great importance for understanding the properties of ceramics and associated surface-gas reactions. Atomic processes occurring on bulk crystal surfaces at high temperatures can be recorded by reflection electron microscopy (REM) in a conventional transmission electron microscope (TEM) with relatively high resolution, because REM is especially sensitive to atomic-height steps. DOE

N91-28406# Tennessee Univ., Knoxville. Dept. of Materials Science and Engineering.
MECHANICAL PROPERTIES OF DIAMOND AND DIAMOND-LIKE FILMS
C. J. McHargue 1991 8 p Presented at the 1991 Applied Diamond Conference, Alburn, 20-22 Aug. 1991
(Contract DE-AC05-84OR-21400)
(DE91-011373; CONF-910854-2) Avail: NTIS HC/MF A02

A discussion of the factors influencing hardness and elastic modulus measurements of thin films and hard materials is given with emphasis on DLC and diamond. Hardness values ranging from 5 to 15 GPa and elastic (Young's) modulus of 40 to 130 GPa were found for DLC films deposited by a variety of techniques. Both hardness and modulus values for CVD diamond films were similar to those measured on the (100) plane of a natural Type 2a diamond. DOE

N91-28407# Ames Lab., IA.
ENERGY DISPERSIVE X RAY DIFFRACTION STUDY OF GLASSY Bi2Sr2CaCu2O(x) FILAMENTS PRODUCED BY GAS-JET FIBERIZATION Ph.D. Thesis
J. P. Hammonds 2 May 1991 55 p
(Contract W-7405-eng-82)
(DE91-012021; IS-T-1527) Avail: NTIS HC/MF A04

Energy dispersive x ray diffraction was used to study the local order of samples of Bi2Sr2CaCu2O(x) samples produced by gas jet fiberization. This material assumes a structure which is superconducting above 90 K if annealed above 820 C. These same samples form an intermediate phase, which resembles the crystal structure of the Bi2Sr2CuO(x) superconductor if annealed between 450 and 600 C. The purpose of this study was to investigate the development of this intermediate phase and the local order of the glassy material from the as blown fibers. The measured density function for the samples annealed in this intermediate temperature range are in good agreement with distributions calculated from known crystal structures for these materials. The glassy sample, on the other hand, showed differences that were not completely explained by the present work, but opened paths for further study. DOE

N91-28408# Lawrence Livermore National Lab., CA.
MELAMINE-FORMALDEHYDE AEROGELS
C. T. Alviso and R. W. Pekala Apr. 1991 12 p Presented at the 202nd National Meeting of the American chemical Society (ACS), New York, 25-30 Aug. 1991
(Contract W-7405-eng-48)
(DE91-012084; UCRL-JC-104674; CONF-910812-3) Avail: NTIS HC/MF A03

The ability to tailor the structure and properties of aerogels at the nanometer scale opens up exciting possibilities for these unique, low density materials. Traditional inorganic aerogels have been formed from the hydrolysis and condensation of metal alkoxides (e.g., tetramethoxy silane). Previously, we reported the synthesis of organic aerogels based upon the aqueous, polycondensation of resorcinol with formaldehyde. Although these aerogels exhibit minimal light scattering, their dark red color limits their use in certain optical applications. In this paper, we discuss the synthesis and characterization of melamine-formaldehyde aerogels -- a new type of organic aerogel that is both colorless and transparent. DOE

N91-28409# Texas Univ., Austin.
MODEL CATALYTIC OXIDATION STUDIES USING SUPPORTED MONOMETALLIC AND HETEROBIMETALLIC OXIDES
J. G. Ekerdt 30 Apr. 1991 6 p
(Contract DE-FG05-86ER-13604)
(DE91-012144; DOE/ER-13604/16) Avail: NTIS HC/MF A02

This research program is directed toward developing a fundamental understanding of how catalyst composition, redox ability, and structure control the catalytic properties of metal oxides. Oxide systems that permit examination of the role of metal oxide cations separately and in pairwise combinations are being developed. Organometallic complexes containing C(sub 3)-allyl, cyclopentadienyl, or carbonyl ligands are exchanged with the hydroxide ligands of silica, alumina, titania, zirconia and magnesia supports. The exchange technique is used to achieve high metal oxide loadings without the formation of supported crystallites over silica. The organometallic route may also lead to oxygen-bridged cations and/or cation pairs over the supports prior to full oxidation. The anchored complex is subsequently oxidized to generate a supported oxide. DOE

N91-28410# Argonne National Lab., IL.
DEVELOPMENT OF NONDESTRUCTIVE EVALUATION METHODS AND PREDICTION OF EFFECTS OF FLAWS ON THE FRACTURE BEHAVIOR OF STRUCTURAL CERAMICS
W. A. Ellingson, J. P. Singh, N. Gopalsami, S. L. Dieckman, A. S. Wagh, C. Y. Chu, and T. Luethi 1991 18 p Presented at the 5th Annual Conference on Fossil Energy Materials, Oak Ridge, 13-16 May 1991
(Contract W-31-109-eng-38)
(DE91-012471; ANL/CP-73152; CONF-9105184-1) Avail: NTIS HC/MF A03

To establish predictive performance (i.e., fracture behavior) of structural ceramic composites by nondestructive evaluation methods, nondestructive evaluation (NDE) methods were developed which are suitable for characterizing and sizing flaws and material variations, and flaws and material variation related to mechanical properties were studied. Critical flaws and mechanical properties in whisker reinforced composites are found to be affected by the amount and mode of packing of whiskers in the matrix. Analysis of the flaw population and the resulting mechanical properties are evaluated in both green (cold pressed) and dense (hot pressed) Si3N4 whisker reinforced Si3N4 matrix composites. Detection of whisker concentrations are being measured by X ray computed tomography and nuclear magnetic resonance imaging. DOE

N91-28411# Sandia National Labs., Albuquerque, NM.
RESPONSE OF THE POLYMERS KEL-F, POLYSULFONE, HIGH DENSITY POLYETHYLENE AND POLYMETHYLMETHACRYLATE TO SHOCK LOADING AND RELEASE FROM 0.3 TO 2.4 GPa
M. U. Anderson 1991 5 p Presented at the 7th American Physical Society (APS) Topical Conference on Shock Compression of Condensed Matter, Williamsburg, 17-20 Jun. 1991
(Contract DE-AC04-76DP-00789)
(DE91-012867; SAND-91-0054C; CONF-910654-2) Avail: NTIS HC/MF A01

The Bauer PVDF stress-rate gauge has been used to study the response of the cited polymers from measurements at the impact surface and 'in-situ' at sample thicknesses of 1.5 and 3 mm. The PVDF stress-rate dependent piezoelectric output combined with appropriate signal recording techniques allow accurate recording over the broad range of stress rates encountered during shock compression of polymers. Strong viscous response effects are observed. The release velocity is found to increase strongly with pressure, and the release-rate history is recorded with PVDF as a continuous function of pressure. DOE

N91-28412# Pacific Northwest Lab., Richland, WA.
ULTRA-FINE POWDERS USING GLYCINE-NITRATE COMBUSTION SYNTHESIS
L. A. Chick, L. R. Pederson, J. L. Bates, and G. D. Maupin May 1991 11 p Presented at the 5th Annual Conference on Fossil Energy Materials, Oak Ridge, 13-16 May 1991
(Contract DE-AC06-76RL-01830)
(DE91-012926; PNL-SA-19249; CONF-9105184-4) Avail: NTIS HC/MF A03

Fabrication of advanced, multifunctional materials frequently requires the synthesis of complex, ultrafine powders comprised of a single phase containing several elements (multicomponent) or of several phases that are intimately mixed on a microscale (composite). A new combustion synthesis method, the glycine/nitrate process (GNP), is particularly useful for synthesizing ultrafine, multicomponent oxide powders. Examples discussed include La(Sr)CrO3 and La(Sr)FeO3 perovskites and a composite of three phases, NiO, NiFe2O4, and Cu metal. The GNP consists of two basic steps. First, metal nitrates and a low molecular weight amino acid are dissolved in water. Second, the solution is boiled until it thickens. This viscous liquid ignites and undergoes self-sustaining combustion, producing an ash composed of the oxide product. Most refractory oxides that are composed of a combination of metals having stable nitrates should be possible to synthesize using GNP. DOE

N91-28413# Oak Ridge National Lab., TN.
DRYING OF GELCAST CERAMICS
O. O. Omatete, R. A. Strehlow, and C. A. Walls 1991 13 p Presented at the 93rd Annual Meeting and Exposition of the American Ceramic Society (ACerS), Cincinnati, 28 Apr. - 2 May 1991
(Contract DE-AC05-84OR-21400)
(DE91-012955; CONF-910430-9) Avail: NTIS HC/MF A03

Plates (8.9 x 90.2 x 228.6 mm) of silicon nitride, sialon, and alumina made by gelcasting, a generic near-net-shape forming process, were dried in a controlled humidity chamber. No constant rate period was found in drying the gelcast plates. A linear shrinkage of 3 to 4 pct. was observed, the shrinkage stopping after only about 20 pct. of the total moisture had been lost. Dried parts, free of warpage and cracking, were obtained in reasonable times by controlling the humidity and temperature. DOE

N91-28414# Los Alamos National Lab., NM.
INVESTIGATION OF INTERLAYER MATERIALS FOR THE MICROWAVE JOINING OF SiC
R. Silberglitt, D. Palaith, W. M. Black, H. S. Saadaldin (George Mason Univ., Fairfax, VA.), J. D. Katz, and R. D. Blake 1991 9 p Presented at the 93rd Annual Meeting and Exposition of the American Ceramic Society (ACerS), Cincinnati, 28 Apr. - 2 May 1991

(Contract W-7405-eng-36)
(DE91-013311; LA-UR-91-1560; CONF-910430-11) Avail: NTIS HC/MF A02

Microwave joining of ceramics has the potential for increased speed and convenience. Joints have been made in alumina, mullite, and silicon nitride with flexure strength approaching, and in some cases exceeding, that of the as-received material in a fraction of the time that is customarily required with conventional techniques. This paper describes the initial results of investigations aimed at applying microwave joining to SiC and other carbide ceramics. DOE

N91-28415# Los Alamos National Lab., NM.
MICROWAVE ENHANCED DIFFUSION?
J. D. Katz, R. D. Blake, and V. M. Kenkre (New Mexico Univ., Albuquerque.) 1991 14 p Presented at the 93rd Annual Meeting and Exposition of the American Ceramic Society (ACerS), Cincinnati, 28 Apr. - 2 May 1991
(Contract W-7405-eng-36)
(DE91-013312; LA-UR-91-1559; CONF-910430-10) Avail: NTIS HC/MF A03

The observation of more rapid reaction and/or sintering during microwave processing of ceramics has lead to speculation that microwave processing results in enhanced diffusion. The loss mechanisms by which microwaves interact with a crystal lattice have been reviewed. These mechanisms were evaluated with regard to the atomic theory of diffusion. The potential for these loss mechanisms to influence atomic diffusion, and thus produce enhancement will be discussed. Existing evidence, both direct and indirect, regarding microwave enhanced diffusion has been reviewed and will be discussed along with recent experimental data. DOE

N91-28416# International Centre for Theoretical Physics, Trieste (Italy).
RESONANT METHOD FOR THE MEASUREMENT OF THE GLASS TRANSITION TEMPERATURE AT HIGH FREQUENCIES
F. Povolo, A. J. Marzocca, and S. N. Goyanes (Buenos Aires Univ., Argentina) Aug. 1990 13 p
(DE91-618684; IC-90/233) Avail: NTIS HC/MF A03

A resonant method for the accurate determination of the glass transition temperature in polymers is presented. A composite oscillator driven by a piezoelectric crystal, in longitudinal oscillations and at a frequency of the order of 50 k Hz, is employed. The changes in the storage modulus of the specimen with temperature can be obtained from the changes in the resonant frequency of the composite. Finally, some data obtained in a specimen of vulcanized rubber are discussed in detail. DOE

N91-28417# Sandia National Labs., Albuquerque, NM.
FERROELECTRIC FATIGUE IN MODIFIED BULK LEAD ZIRCONATE TITANATE CERAMICS
W. Y. Pan, C. F. Yue (New Mexico Inst. of Mining and Technology, Socorro.), and B. A. Tuttle 1991 13 p Presented at the 93rd Annual Meeting and Exposition of the American Ceramic Society (ACerS), Cincinnati, 28 Apr. - 2 May 1991
(Contract DE-AC04-76DP-00789)
(DE91-012647; SAND-91-0951C; CONF-910430-4) Avail: NTIS HC/MF A03

Ferroelectric fatigue behavior was studied of modified bulk lead zirconate titanate (PZT) ceramics. For fatigued PZT ceramics, the experiments have shown that virgin, unfatigued ferroelectric properties are measured when the direction of the applied field is changed by 90 degs with respect to the direction of the fatigue field. Further, it was shown that the fatigue effects for these polycrystalline ceramics are not confined to regions near the electrode-ceramic interface. The fatigued state is characterized by an increase in unit cell volume and an increase in unit cell anisotropy, with respect to the virgin state. Preferred orientation of the polar axes in directions perpendicular and parallel to the applied field direction were detected for fatigued ceramics. The observed fatigue phenomena was described using a model that couples the applied electric field, ionic defects, the spontaneous polarization, and the ferroelastic behavior of these PZT ceramics. DOE

N91-28418*# National Aeronautics and Space Administration. Lewis Research Center, Cleveland, OH.
ELEVATED-TEMPERATURE FRACTURE RESISTANCES (K(SUB IC), R-CURVES, GAMMA SUB (OMEGA OF)) OF MONOLITHIC AND COMPOSITE CERAMICS USING CHEVRON-NOTCHED, BEND TESTS
Asish Ghosh, M. G. Jenkins, M. K. Ferber, J. Peussa (Federation of Finnish Metal, Engineering, and Electronic Technology Industries, Helsinki.), and Jonathan A. Salem 1991 2 p Presented at the International Conference Fracture Mechanics of Ceramics, Nagoya (Japan), 15-17 Jul. 1991
(Contract DE-AC05-84OR-21400)
(NASA-TM-105090; NAS 1.15:105090; DE91-012961; CONF-9107113-1) Avail: NTIS HC/MF A01 CSCL 11C

The quasi-static fracture behaviors of monolithic ceramics (SiC, Si3N4, MgAl2O4), self-reinforced monoliths (acicular grained Si3N4, acicular grained mullite), and ceramic matrix composites (SiC whisker/Al2O3 matrix, TiB2 particulate/SiC matrix, SiC fiber/CVI SiC matrix, Al2O3 fiber/CVI SiC matrix) were measured over the temperature range of 20 to 1400 C. The chevron notched, bend bar test geometry was essential for characterizing the elevated temperature fracture resistances of this wide range of quasi-brittle materials during stable crack growth. Fractography revealed the differences in the fracture behavior of the different materials at the various temperatures. The fracture resistances of the self-reinforced monoliths were comparable to those of the composites and the fracture mechanisms were found to be similar at room temperature. However at elevated temperatures the differences of the fracture behavior became apparent where the superior fracture resistance of the self-reinforced monoliths were attributed to the minor amounts of glassy, intergranular phases which were often more abundant in the composites and affected the fracture behavior when softened by elevated temperatures. DOE

N91-28419# Los Alamos National Lab., NM.
RELIABLE MODELING OF COMPLEX BEHAVIOR
U. F. Kocks 1991 15 p Presented at the Annual Meeting and Exhibition of the Minerals, Metals and Materials Society (TMS), New Orleans, 17-21 Feb. 1991
(Contract W-7405-eng-36)
(DE91-013385; LA-UR-91-1892; CONF-910202-17) Avail: NTIS HC/MF A03

The status of modeling for large-strain plasticity is assessed, and this overview is used to emphasize some general points concerning modeling in Materials Science. While a physical foundation is essential in order to achieve generality and some measure of confidence in extrapolations, phenomenological constraint is equally crucial to achieve reliability and predictive value in descriptions of the macroscopic behavior despite the enormous complexity of the underlying physics. Many details that may be of interest in modeling the physical foundation lose importance in the integration to an overall materials response, which depends on few parameters and is quite reproducible. From this point of view, the current understanding of large-strain plasticity is adequate in many respects. However, some problems are highlighted in which more quantitative modeling results would impact the reliability and generality of macroscopic properties descriptions, and which seem amenable to treatment with current techniques and resources. DOE

N91-28420# Los Alamos National Lab., NM.
SHOCK INITIATION OF PENTAERYTHRITOL TETRANITRATE CRYSTALS: STERIC EFFECTS DUE TO PLASTIC FLOW
J. J. Dick, E. Garcia, and D. C. Shaw 1991 5 p Presented at the 1991 American Physical Society (APS) Conference on Shock Compression of Condensed Matter, Williamsburg, 17-20 Jul. 1991
(Contract W-7405-eng-36)

(DE91-013389; LA-UR-91-1730; CONF-9107105-13) Avail: NTIS HC/MF A01

Complete results are presented of the analysis of steric hindrance due to edge dislocation motion in the different crystal slip systems associated with different crystal orientations relative to the shock wave in pentaerythritol tetranitrate (PETN). A systematic search was done for close intermolecular atom-atom approaches during the shear displacement associated with motion of an edge dislocation. A graphical display of results is given. The number and severity of close approaches or contacts correlates well with the measured shock initiation sensitivity of groups of zone axes (100), (101), (001), and (110) orientations of PETN single crystals. This forms the basis of a new model of shock initiation of detonation in homogeneous solids. DOE

N91-28421# Tennessee Univ., Knoxville. Dept. of Chemistry.

ANALYSIS OF THE SURFACE HETEROGENEITY OF DIFFERENT SAMPLES OF ALUMINUM OXIDE CERAMIC POWDERS

J. Roles, G. Guiochon, and K. McNerney (Coors Porcelain Co., Golden, CO.) 1991 39 p
(Contracts DE-FG05-88ER-13859; DE-FG05-86ER-13487)
(DE91-013527; DOE/ER-13859/11) Avail: NTIS HC/MF A03

The homogeneity of the surface of the particles of powders can be characterized by determining the adsorption energy distribution for different probe compounds selected for exhibiting different types of interaction energy with the chemical group which can be found on the surface. We describe the results obtained by performing this investigation on a number of different alumina samples. Significant differences between the adsorption energy distributions of high quality alumina powders for ceramics have been found for 1-chlorobutane. The same samples had identical adsorption energy distributions for diethylether. The differences observed for the adsorption energy distribution of 1-chlorobutane, a weak acid, are correlated with significant differences between the process performance of the samples. Performance degrade with increasing fractional surface coverage of a high energy mode of the distribution. DOE

N91-28422# Lawrence Livermore National Lab., CA.

EXPERIMENTS AND CALCULATIONS OF JET PENETRATION IN GLASS

B. Moran, L. A. Glenn, and A. Kusubov May 1991 12 p
Presented at the Combat Vehicle Survivability Symposium, Gaithersburg, 14-17 Apr. 1991
(Contract W-7405-eng-48)
(DE91-013567; UCRL-JC-107276; CONF-9104264-1) Avail: NTIS HC/MF A03

We have performed a number of experiments with 1.5-in precision shaped charges to measure the penetration as a function of time in various targets and to evaluate our glass-fracture model. Target materials used were 6061-T6 aluminum, 4340 steel, Pyrex glass, and a glass-aluminum composite target. Time-resolved measurements indicate two distinct phases of jet penetration in glass: an initial hydrodynamic phase, and a second phase characterized by a slower penetration velocity. Our calculations show that at an early time, a crater is formed around the jet and only the tip of the undisturbed jet interacts with the glass. At a later time, the glass has collapsed on the jet and penetration is caused by a disturbed and fragmented jet. We measured the degradation of the jet after penetrating a glass layer and found that a composite glass-aluminum target stops the jet in roughly the same thickness as does steel. DOE

N91-28423*# National Aeronautics and Space Administration. Lewis Research Center, Cleveland, OH.

PRETREATMENT OF LUBRICATED SURFACES WITH SPUTTERED CADMIUM OXIDE Patent Application

Robert L. Fusaro, inventor (to NASA) 24 Jun. 1991 12 p
(NASA-Case-LEW-14474-1; NAS 1.71:LEW-14474-1; US-Patent-Appl-SN-720133) Avail: NTIS HC/MF A03 CSCL 11C

Cadmium oxide is used with a dry solid lubricant on a surface to improve wear resistance. The surface topography is first altered by photochemical etching to a predetermined pattern. The cadmium oxide is then sputtered onto the altered surface to form an intermediate layer to more tightly hold the dry lubricant, such as graphite. NASA

N91-28424*# National Aeronautics and Space Administration. Langley Research Center, Hampton, VA.

PROCESS FOR BONDING ELASTOMERS TO METAL Patent Application

George E. Dickerson, inventor (to NASA) and Henry L. Kelley, inventor (to NASA) 26 Jun. 1991 13 p
(NASA-Case-LAR-13645-1; NAS 1.71:LAR-13645-1; US-Patent-Appl-SN-721038) Avail: NTIS HC/MF A03 CSCL 11C

A process for bonding elastomeric material to a metal part includes coating a heat curable adhesive on the surfaces of the metal part to be bonded. The metal part is placed in a mold, a bottom plate and an upper transfer pot of a transfer molding machine is preheated to a predetermined cure temperature. A predetermined quantity of uncured elastomeric material is loaded into the transfer pot. The mold containing the adhesive coated metal part is clamped to the bottom plate, and almost contemporaneously, the uncured elastomeric material is pressed into the mold while maintaining heat and pressure in the mold for a time sufficient to vulcanize and thereby cure the elastomeric material simultaneously with the adhesive, whereby contacting surfaces of the metal part are strongly bonded to the vulcanized elastomeric material. NASA

N91-28425*# National Aeronautics and Space Administration. Langley Research Center, Hampton, VA.

POLYIMIDES PREPARED FROM 3,5-DIAMINO BENZO TRIFLUORIDE Patent Application

Margaret K. Gerber, inventor (to NASA), J. Richard Pratt, inventor (to NASA) (PRC Kentron, Inc., Hampton, VA.), Terry L. St. Clair, inventor (to NASA), and Anne K. St. Clair, inventor (to NASA) 31 Oct. 1989 13 p
(NASA-Case-LAR-14206-1; NAS 1.71:LAR-14206-1; US-Patent-Appl-SN-429574) Avail: NTIS HC/MF A03 CSCL 11C

High performance, thermooxidatively stable polyimides are prepared by reacting aromatic diamines with pendant trifluoromethyl groups and dianhydriges in an amide solvent to form a poly(amic acid), followed by cyclizing the poly(amic acid) to form the corresponding polyimide. NASA

N91-28426 Council for National Academic Awards (England).

RELATIONSHIPS BETWEEN POLYMER-ADDITIVE MOLECULAR STRUCTURE AND INTUMESCENT FLAME RETARDANT BEHAVIOR Ph.D. Thesis

Edwyn Christopher Mo Anderton 1990 274 p
Avail: Univ. Microfilms Order No. BRDX92294

Studies of the relationship between the molecular structure of a range of organophosphorus based polymer additives and their ability to confer intumescent flame retardant properties on the resulting polymers are described. The development of intumescent flame retardants is discussed along with the principles of flame retardancy in general. Much of the work centered around the chemistry or a key starting material, pentaerythritol phosphate (PEPA). Various derivatives of PEPA were synthesized, most containing reactive functional groups which facilitated future development of the compound. The derivatives containing no reactive groups were investigated for their intumescent behavior in their own right. Derivatives of PEPA containing an acidic functionality were utilized in the production of intumescent salt systems using cations with a high nitrogen content in the form of s-triazines. The most promising was trimethyl olmelamine salt of a bis-PEPA derivative of phosphoric acid. Metal salts of acidic PEPA derivatives were also investigated. Derivatives of PEPA containing a carbon-carbon double bond were investigated for their potential to polymerize and form more stable additives. Only one such polymer was successfully synthesized, the being poly(PEPA methacrylate). Despite being non-intumescent, this polymer has potential as a flame retardant additive. The monomer was found to compolymerize with methyl methacrylate to form a polymer of high thermal stability. When investigating the relationship between the molecular structure of the compounds developed and their intumescent behavior, it was observed that only compounds containing an ionizable hydrogen atom exhibited intumescent decomposition on pyrolysis. Dissert. Abstr.

N91-28427# Sandia National Labs., Albuquerque, NM.
MEASUREMENTS OF PHOTO-INDUCED CHANGES IN CONJUGATED POLYMERS
C. H. Seager, M. B. Sinclair, D. McBranch, A. J. Heeger, and G. L. Baker (Bell Communications Research, Inc., Red Bank, NJ.) 1991 15 p Presented at the Spring Meeting of the Materials Research Society (MRS), Anaheim, 29 Apr. - 3 May 1991
(Contract DE-AC04-76DP-00789)
(DE91-013262; SAND-91-1000C; CONF-910406-14) Avail: NTIS HC/MF A03

We have used the highly sensitive technique of Photothermal Deflection Spectroscopy (PDS) to measure changes in the infrared absorption spectra of MEHPPV, P3HT and Polydiacetylene-4BCMU induced by pumping these polymers with light above the (pi)--(pi)* transition energy. In contrast to previous chopped light transmission measurements of these effects, the PDS technique can directly measure the buildup or decay of the absorption coefficient, (alpha), on the time scale of seconds to days. In the case of MEHPPV we observe that the time scale of seconds to days. In the case of MEHPPV we observe that above-gap light causes the appearance of a broad infrared peak in (alpha), which continues to grow-in hours after the pump light is first applied. For this polymer the general shape of the absorption spectra in the unpumped state mimics the photo-induced changes, suggesting that remnant photo-induced states determine the maximum transparency observed under normal experimental conditions. For P3HT and to a lesser extent, MEHPPV, we also observe irreversible photo-induced absorption components which we tentatively identify with photo-induced oxidation of the polymer matrix. DOE

N91-28428# Tennessee Univ., Knoxville. Dept. of Chemistry.
VALIDITY OF THE MODEL USED TO RELATE THE ENERGY DISTRIBUTION AND THE ADSORPTION ISOTHERM
J. Roles and G. Guiochon 1991 17 p
(Contract DE-FG05-88ER-13859)
(DE91-013528; DOE/ER-13859/12) Avail: NTIS HC/MF A03

We discuss here the problems associated with the derivation of the energy distribution of diethylether on the surface of the fine, solid particles used as raw material for the preparation of alumina ceramics. Adsorption isotherms can be used to understand various aspects of the interactions of the adsorbate molecules with themselves or with the surface of the adsorbent. Currently, we are using the adsorption isotherms of various selected probes to investigate the degree of heterogeneity of a solid surface. The adsorption energy distribution of a probe compound on a surface can be calculated by solving a Fredholm integral equation. DOE

N91-28429# Midwest Research Inst., Golden, CO.
NOVEL WAYS OF DEPOSITING ZnTe FILMS BY A SOLUTION GROWTH TECHNIQUE
R. W. Birkmire (Delaware Univ., Newark.) Jun. 1991 28 p
(Contract DE-AC02-83CH-10093)
(DE91-002189; SERI/TP-210-4319) Avail: NTIS HC/MF A03

Cu-doped ZnTe films, less than 1000 A, were reproducibly deposited for the first time by an electrochemical method. A CdTe/CdS/ITO/glass substrate is externally short circuited to a zinc counter electrode in an aqueous bath consisting of ZnCl2 and TeO2 to complete an electrochemical cell. Control of both pH and TeO2 concentration was necessary to deposit single phase ZnTe films. A copper complex was added to the bath to control the ZnTe conductivity and dope the films p-type. CdTe/CdS solar cells using the ZnTe:Cu as the primary contact to the CdTe have achieved efficiencies of approximately 9 percent. DOE

N91-28430# California Univ., Santa Barbara.
POLYMERS AT SURFACES
P. Pincus 1991 7 p
(Contract DE-FG03-87ER-45288)
(DE91-013642; DOE/ER-45288/T2) Avail: NTIS HC/MF A02

Three areas of polymer research are discussed. In the first area, polyelectrolytes, the properties of polyelectrolytes were actively considered at the solid-liquid interface with emphasis on aspects relating to colloid stabilization. In particular, the case of polyelectrolytes end grafted to a dielectric surface was treated and determined the cornal structure and the disjoining pressure that results when two opposing surfaces approach one another. The second area, brush dynamics, boundary lubrication and, more generally, problems associated with sliding friction, often involve surface protection with polymeric films. In order to understand energy dissipation mechanisms as well as the physical chemistry of the lubrication process, the dynamical properties were studied of polymers which are attached to solid surfaces. The last area is mixed copolymer membranes. The possibility is now being explored of extending these concepts to the case of copolymer lamellar phases and copolymer solutions. The goal is to determine the conditions required to fabricate microemulsions and vesicular phases where the small surfactant amphiphiles are replaced by block copolymers. DOE

N91-28431# Pacific Northwest Lab., Richland, WA.
COMPUTER MODELING OF CERAMIC MELTERS TO ASSESS IMPACTS OF PROCESS AND DESIGN VARIABLES ON PERFORMANCE
L. L. Eyler, M. L. Elliott, D. L. Lessor, and P. S. Lowery May 1991 20 p Presented at the 5th International Symposium on Ceramics in Nuclear and Hazardous Waste Management, Cincinnati, 29 Apr. - 3 May 1991
(Contract DE-AC06-76RL-01830)
(DE91-013668; PNL-SA-19418; CONF-9104261-4) Avail: NTIS HC/MF A03

Results of numerical modeling of the melt pool of high level liquid waste vitrification melters which demonstrate impact of design variables are presented. They are in support of programs to evaluate melter operation characteristics and performance. Included are investigations into power skewing and alternating current electric field phase angle in a dual electrode pair reference design. Power skewing, the ratio of upper-to-lower electrode pair power, can lead to stratification which may enhance heating of the cold cap regions, but may also enhance development of a sludge layer. Phase angle between alternating current fields affects joule heat and temperature fields. In a three-electrode, sloped-bottom advanced design, bimodal convective stability is investigated to assess impact of perturbations. Electrode cooling and asymmetries of the cold cap and exterior boundaries can affect melt convective pattern which in turn may impact mixing uniformity, cold cap heat transfer, and development of sludge layers. DOE

N91-28432# Pacific Northwest Lab., Richland, WA.
BEHAVIOR OF RuO2 IN A GLASS MELT
P. R. Hrma and W. T. Cobb May 1991 6 p Presented at the 5th International Symposium on Ceramics in Nuclear and Hazardous Waste Management, Cincinnati, 29 Apr. - 3 May 1991
(Contract DE-AC06-76RL-01830)
(DE91-013717; PNL-SA-19544; CONF-9104261-5) Avail: NTIS HC/MF A02

Samples of a borosilicate glass melt containing 0.27 wt pct of RuO2 particles, approx. 1 micron in diameter, were subjected to heat treatments at 1050 C in alumina and metallic crucibles and investigated by optical microscopy. The results indicate that RuO2 particles agglomerate before sedimentation. Agglomerations appear to be produced in the melt meniscus and the thin film of melt above the meniscus, where high velocity gradients bring the RuO2 particles into contact. DOE

N91-28433# Clark-Atlanta Univ., GA. Dept. of Chemistry.

SEMI-EMPIRICAL CALCULATIONS ON MODEL SYSTEMS FOR ORGANOSILYLDIAMINE PRECERAMIC POLYMERS

Y. H. Mariam, K. Feng, and P. Abrahams Dec. 1990 9 p
Presented at the 199th National Meeting of the American Chemical Society (ACS), Boston, 22-27 Apr. 1990
(Contract DE-FG05-87ER-45306)
(DE91-013721; DOE/ER-45306/4; CONF-900402-14) Avail: NTIS HC/MF A02

Polymerization pathways are not very well understood in oligomeric/polymeric systems containing Si and N. Because of the interest in these systems as precursors to ceramic materials, understanding of the polymerization mechanisms is important in order to control pathways of chain growth, termination and branching. Such mechanistic studies, in turn, can lead to improved synthetic methodologies by, for example, improving yield, increasing molecular weight, and shortening reaction times. Mechanistic studies are however very challenging to tackle by experiment alone. Work was initiated utilizing molecular orbital approaches primarily to model reactions between dichlorosilanes and ethylenediamine. The interest in these reactions stems from the observation that these monomers provide polymers/oligomers which can serve as precursors to Si-N-C(-O) ceramics. The initial studies reported here, involved comparison of geometries of model systems, the assessment of Si-N bonding interactions, and the participation of d orbitals on Si in these interactions, etc. DOE

N91-28434# Sandia National Labs., Albuquerque, NM.

ADHESION BETWEEN CVD DIAMOND FILMS AND TUNGSTEN

M. Alam, D. E. Peebles, and D. R. Tallant 1991 21 p Presented at the 179th Meeting of the Electrochemical Society, Washington, 5-10 May 1991
(Contract DE-AC04-76DP-00789)
(DE91-013757; SAND-90-2961C; CONF-910552-11) Avail: NTIS HC/MF A03

Adhesion between diamond films synthesized by a chemical vapor deposition (CVD) method and tungsten has been investigated by a scratch and pull testing method. Diamond films have been deposited at temperatures from 1173 to 1323 K with a growth rate ranging from 0.2 to 0.45 micrond per hour. The films are highly crystalline and are dominated by (100) faces at low temperatures, changing to (111) at higher temperatures. Grain size and residual stress in the films increases with increasing deposition temperature. X-ray diffraction shows the expected diamond diffraction peaks plus peaks attributed to WC and W(2)C. Raman spectroscopy shows a sharp diamond band for all of the films, with a small broad peak, attributed to amorphous carbon. There is no distinct correlation between diamond/amorphous carbon intensity with deposition temperature. Scratch adhesion testing shows the expected failure mode for brittle coatings, but can not be quantified because of severe degradation of the diamond stylus tip. Sebastion pull testing shows that the failure mode of the films correlates with deposition temperature, but specific adhesion strength values do not. Efforts are continuing to correlate adhesion strength with deposition and structural parameters of the diamond films. DOE

N91-28435# Argonne National Lab., IL.

CREEP AND DIFFUSION IN NONSTOICHIOMETRIC OXIDES

A. Dominiques-Rodriguez, J. Castaing (Seville Univ., Spain), K. C. Goretta, and J. L. Routbort Apr. 1991 13 p Presented at the 93rd Annual Meeting and Exposition of the American Ceramic Society (ACerS), Cincinnati, 28 Apr. - 2 May 1991
(Contract W-31-109-eng-38)
(DE91-013766; ANL/CP-71926; CONF-910430-13) Avail: NTIS HC/MF A03

The relation between high-temperature creep and diffusion has been extensively investigated. In elemental solids, the relationship is based on comparisons of activation energies for creep and self- diffusion. In binary oxides, the chemical potential of oxygen provides an additional and powerful tool for comparisons which has been used by several workers. Carefully interpreted creep data can elucidate diffusion mechanisms in oxides. This paper will review the well-known simple oxides CoO and NiO and show the validity of the comparison in the more complex oxides MnO, FeO, and YBa2Cu3O(x). DOE

N91-28436# Los Alamos National Lab., NM.

SESAME EQUATION OF STATE NUMBER 7740: POLYCARBONATE

J. C. Boettger Jun. 1991 6 p
(Contract W-7405-eng-48)
(DE91-013970; LA-12120-MS) Avail: NTIS HC/MF A02

An equation of state (EOS) for polycarbonate (a widely used polymer) has been generated with the computer code GRIZZLY and will be added to the SESAME library as material number 7740. Although a number of the input parameter used in the calculations are based on rough estimates. Material number 7740 provides a good match to experimental Hugoniot data and should be reliable on or near the principal Hugoniot. DOE

N91-28437# Edgerton, Germeshausen and Grier, Inc., Idaho Falls, ID.

RECENT ASME CODE SECTION 11 DEVELOPMENTS FOR SURFACE EXAMINATION THROUGH COATINGS

J. F. Cook 1991 2 p Presented at the American Society of Mechanical Engineers (ASME) Pressure Vessels and Piping Conference, San Diego, 23-27 Jun. 1991
(Contract DE-AC07-76ID-01570)
(DE91-014069; EGG-M-91085; CONF-910602-46) Avail: NTIS HC/MF A01

Code Case N-458, Magnetic Particle Examination of Coated Materials, and Code Case N-485, Eddy Current Examination of Coated Ferritic Surfaces as an Alternative to Surface Examination, were approved in 1990 for Section 11, Division 1 of the ASME Boiler and Pressure Vessel Code. Activity that led to these cases, research results on which the requirements in these cases were based, and future ASME Code plans related to surface examination through coatings are discussed. DOE

N91-28438# Oak Ridge National Lab., TN.

COCRYSTALLIZATION IN BLENDS OF POLY(BUTYLENE TEREPHTHALATE) AND POLY(ESTER-ETHER) SEGMENTED BLOCK COPOLYMERS

K. P. Gallagher, Xuifang Zhang, J. P. Runt, Gia Huynh-ba (Du Pont de Nemours, E. I. and Co., Wilmington, DE), and J. S. Lin 1991 6 p Presented at the 202nd National Meeting of the American Chemical Society (ACS), New York, 25-30 Aug. 1991
(Contract DE-AC05-84OR-21400)
(DE91-012224; CONF-910812-4) Avail: NTIS HC/MF A02

Only a few cases of cocrystallization (i.e., crystallization of two different polymers into the same crystalline lamellae) have been reported in the literature and, of these, all of the blended polymers are very similar in chemical structure. In addition, there is an indication that some of these blends only cocrystallize upon rapid crystallization. Blends of poly(butylene terephthalate) (PBT) and poly(ester-ether) segmented block copolymers (PEE) seem to be excellent candidates to exhibit cocrystallization for a number of reasons. First, it is well known that only the hard segments in PEE crystallize and they are identical in chemical structure to PBT. Second, pure PBT and PEE crystallize into the same unit cell and have identical lattice parameters. These two conditions that arise from the blocky nature of the copolymer make it possible, in principle, for both polymers to crystallize into the same lamellae. However, if PBT and PEE are separated into two phases in the melt, it is difficult to imagine cocrystallization occurring since both polymers could not be located at the crystallization growth front at the same time. Therefore, another necessary condition for cocrystallization is at least partial melt miscibility. Optical microscopy and small angle light scattering experiments were conducted on this blend, but no separate crystallization of the component polymers could be detected. This was taken as evidence that cocrystallization is likely in this blend. DOE

N91-28439# Sandia National Labs., Albuquerque, NM.

SHOCK-WAVE PROPERTIES OF HIGH-STRENGTH CERAMICS

D. Grady 1991 4 p Presented at the 1991 American Physical Society (APS) Conference on Shock Compression of Condensed Matter, Williamsburg, 17-20 Jul. 1991
(Contract DE-AC04-76DP-00789)
(DE91-014105; SAND-91-0039C; CONF-9107105-30) Avail: NTIS HC/MF A01

The shock and release response of a suite of high-strength ceramics has been investigated with controlled planar impact methods and velocity interferometry diagnostics. The study provides Hugoniot, yield and post-yield compressive strength, phase transformation and tensile spall material properties data for these ceramics. DOE

N91-28440# Boston Univ., MA. Dept. of Chemistry.
PHOTOINDUCED ELECTRON TRANSFER IN ORDERED POLYMERS
G. Jones, II 20 Oct. 1990 20 p
(Contract DE-FG02-88ER-13905)
(DE91-014512; DOE/ER-13905/2) Avail: NTIS HC/MF A03

Photochemical studies on organic polymers or biopolymers (particularly synthetic peptides) that have been modified by covalent attachment (or other means of binding) of organic chromophores and electron transfer agents are described. Specific projects involve peptide conjugates bearing electroactive residues such as tryptophan and specifically labeled at the N- or C-terminus of peptide chains; the electrostatic binding of organic dyes to poly-electrolytes (polyacrylates) for which the formation of dimeric aggregates of bound dye that display unusual photophysical and electron transfer properties is important; a study of the binding of dyes and electron transfer agents to the protein mimic, polyvinyl-2-pyrrolidinone (PVP), in hydrophobic domains that depend on specific H-bond interaction; and completion of an earlier study having to do with the triplet state properties of charge-transfer (CT) complexes of a high potential quinone and various electron donors. DOE

28 PROPELLANTS AND FUELS

Includes rocket propellants, igniters, and oxidizers; their storage and handling procedures; and aircraft fuels.

For related information see also *07 Aircraft Propulsion and Power, 20 Spacecraft Propulsion and Power,* and *44 Energy Production and Conversion.*

N91-28441# Pacific Northwest Lab., Richland, WA.
DEVELOPMENT OF BIOMASS AS AN ALTERNATIVE FUEL FOR GAS TURBINES
J. T. Hamrick (Aerospace Research Corp., Roanoke, VA.) Apr. 1991 145 p
(Contract DE-AC06-76RL-01830)
(DE91-012129; PNL-7673) Avail: NTIS HC/MF A07

A program to develop biomass as an alternative fuel for gas turbines was started at Aerospace Research Corporation in 1980. The research culminated in construction and installation of a power generation system using an Allison T-56 gas turbine at Red Boiling Springs, Tennessee. The system has been successfully operated with delivery of power to the Tennessee Valley Authority (TVA). Emissions from the system meet or exceed EPA requirements. No erosion of the turbine has been detected in over 760 hours of operation, 106 of which were on line generating power for the TVA. It was necessary to limit the turbine inlet temperature to 1450 F to control the rate of ash deposition on the turbine blades and stators and facilitate periodic cleaning of these components. Results of tests by researchers at Battelle Memorial Institute -- Columbus Division, give promise that deposits on the turbine blades, which must be periodically removed with milled walnut hulls, can be eliminated with addition of lime to the fuel. Operational problems, which are centered primarily around the feed system and engine configuration, have been adequately identified and can be corrected in an upgraded design. The system is now ready for development of a commercial version. The US Department of Energy (DOE) provided support only for the evaluation of wood as an alternative fuel for gas turbines. However, the system appears to have high potential for integration into a hybrid system for the production of ethanol from sorghum or sugar cane. DOE

N91-28442# Sandia National Labs., Albuquerque, NM.
INVESTIGATION OF THE DEFLAGRATION-TO-DETONATION (DDT) PROCESS: THE ROLE OF IGNITION AND EXPLOSIVE PROPERTIES IN DDT
A. J. Grimley, J. G. Harlan, and J. W. Fronabarger (Crane Unidynamics, Phoenix, AZ.) 1991 20 p Presented at the 16th International Pyrotechnic Seminar, Jonkoping (Sweden), 24-28 Jun. 1991
(Contract DE-AC04-76DP-00789)
(DE91-011956; SAND-91-0067C; CONF-9106187-1) Avail: NTIS HC/MF A03

A study is being conducted into the importance of a variety of parameters on the 'deflagration to detonation transition' (DDT) phenomenon. In this series two different inorganic igniter materials with very different gas production and propagation properties were used. The DDT explosive column utilizes either of two organic explosives with different physical and chemical characteristics (including chemical structure), in a variety of pressing densities and particle sizes. The methodology of the test series also allows the evaluation of the relative importance of several parameters such as the density, burn rate and crystal morphology of the explosive, the gas production rate of the deflagration and the gas permeability of the explosive column. DOE

N91-28443# Los Alamos National Lab., NM.
SHOCK COMPRESSION OF DUPONT DETASHEET AT LOW STRESS
B. W. Asay, J. B. Ramsay, M. U. Anderson, and R. A. Graham (Sandia National Labs., Albuquerque, NM.) 1991 5 p Presented at the 1991 American Physical Society (APS) Conference on Shock Compression of Condensed Matter, Williamsburg, 17-20 Jul. 1991
(Contracts W-7405-eng-36; DE-AC04-76DP-00789)
(DE91-013229; LA-UR-91-1612; CONF-9107105-14) Avail: NTIS HC/MF A01

Detasheet is a DuPont-manufactured sheet explosive (rho sub 0 = 1. 48 g/cu cm) that consists of 63 percent PETN and 8 percent nitrocellulose with various plasticizers and binders as the remainder. It is used extensively in metal forming and other industrial applications, as well as in military applications. Its shock and initiation response are only incompletely understood. This paper presents the first full nonreactive Hugoniot data for Detasheet. To obtain the data, the piezoelectric polymer stress-rate gauge, polyvinylidine fluoride (PVDF), was used to measure the input and transmitted stress wave profiles and the transit times through the samples. Because of the response sensitivity of the PVDF gauge and the flexible nature of Detasheet, special procedures were developed to achieve intimate contact with the gauges and samples while preserving a known sample thickness. The viscoplastic and initiation behavior of Detasheet were clearly observed by means of the PVDF gauges. DOE

N91-28444*# National Aeronautics and Space Administration. Langley Research Center, Hampton, VA.
IMPROVING THE PERFORMANCE OF BLASTING CAPS Patent Application
Laurence J. Bement, inventor (to NASA), Ronnie B. Perry, inventor (to NASA), and Morry L. Schimmel, inventor (to NASA) (Schimmel Co., Saint Louis, MO.) 5 Apr. 1991 10 p
(NASA-Case-LAR-13832-1; NAS 1.71:LAR-13832-1; US-Patent-Appl-SN-682151) Avail: NTIS HC/MF A02 CSCL 19A

Common blasting caps are made from an aluminum shell in the form of a tube which is closed at both ends. One end, which is called the output end, terminates in a principal side or face, and contains a detonating agent which communicates with a means for igniting the detonating agent. The improvement of the present invention is a flat, steel foil bonded to the face in a position which is aligned perpendicularly to the longitudinal axis of the tube. NASA

N91-28445# Fluor Daniel, Inc., Irvine, CA.
PACIFIC NORTHWEST HYDROGEN FEASIBILITY STUDY
Mar. 1991 59 p
(Contract DE-AM79-86BP-63056)
(DE91-013427; DOE/BP-63056/3) Avail: NTIS HC/MF A04

The use of hydrogen as fuel to produce electric power or as a substitute for gasoline in automotive engines has aroused considerable interest at various times over the past century. The primary reason for hydrogen's appeal is that its combustion produces no environmentally noxious species. In contrast to fossil fuels, only water vapor is produced when hydrogen is burned in a power plant or automobile. A second major advantage to hydrogen is the prospect of an almost inexhaustible supply source in water. Water can be broken down to yield hydrogen through a process called electrolysis. Although this process is well known and thoroughly understood, the electrolysis step itself requires electric power input. It is the cost of the electricity for this separation that has inhibited the widespread use of this approach to date. For a utility company, hydrogen has another application. Because hydrogen can be produced during times of off-peak demand, stored, and then used as a power source during times of peak demand, the utility company can use hydrogen as a means of load smoothing across a daily or seasonal demand cycle. The specific objective of the study described in this report was to assess the potential role of hydrogen, for the present and in the near term (the next 20 years), for the Pacific Northwest area of the United States. DOE

N91-28446 Iowa Univ., Iowa City.
ANALYSIS OF SHOCK PROPAGATION AND SHOCK-INITIATED REACTION IN GRANULAR ENERGETIC MATERIALS Ph.D. Thesis
Long-Jeng Chen 1990 241 p
Avail: Univ. Microfilms Order No. DA9112405

Propagation of weak shock waves through granular, energetic materials can, in some instances, result in localized heating and initiation of reaction. A model is developed that is capable of predicting shock induced reaction in granular materials. The governing equations of reactive solid/gas flow are formulated, and an appropriate solution technique is used to integrate the system of equations. In order to model the shock initiation process for these aggregate, reactive materials, a reliable simulation of shock propagation prior to initiation is essential. A finite-difference numerical scheme for two-phase flow (solid, gas) is used to model the behavior of weakly shocked granular material. Dissert. Abstr.

N91-28447# Lawrence Livermore National Lab., CA.
MECHANISMS OF EBW HE INITIATION
A. M. Frank 15 May 1991 8 p Presented at the 1991 American Physical Society (APS) Conference on Shock Compression of Condensed Matter, Williamsburg, 17-20 Jul. 1991
(Contract W-7405-eng-48)
(DE91-013565; UCRL-JC-105647; CONF-9107105-22) Avail: NTIS HC/MF A02

Exploding bridgewire (EBW) initiation of high explosives (HE) has been used for many years without a clear understanding of the mechanisms involved. Evidence indicates that the shock pressures produced by the EBW may be insufficient for direct initiation and that the electric field about the wire at the time of burst ionizes the surface of the HE. We hypothesize that the ionization pre-sensitizes the HE so that a weak shock can then initiate a detonation wave. DOE

N91-28448# Los Alamos National Lab., NM.
THE DEFLAGRATION-TO-DETONATION TRANSITION IN GRANULAR HMX
J. M. McAfee, B. Asay, A. W. Campbell, and J. B. Ramsay 1991 66 p Presented at the Research Center for Energetic Materials (RCEM) Open Seminar on Safety and Hazards Evaluation, Socorro, 9 Apr. 1991
(Contract W-7405-eng-36)
(DE91-014591; LA-UR-91-2103; CONF-9104269-1-Vugraphs)
Avail: NTIS HC/MF A04

The transition from deflagration to detonation in porous beds of explosive and propellant has received considerable attention both experimentally and theoretically. In many cases, the use of a hot-gas-producing igniter complicates the interpretation and subsequent modeling of experiments because considerable effort is required to account for the effect of the igniter gases on the granular bed. Hot-wire ignition is less intrusive; however, the ignition front is not planar. Thus the early events in these experiments cannot be approximated as one-dimensional. We have studied the deflagration-to-detonation behavior of granular HMX confined in steel tubes with x-radiography, light emission, stress gauges, and various pin techniques. Simplification and consistency of results were obtained by igniting the HMX with a piston (initially at rest and in contact with the HMX) driven into the bed. A gasless igniter is used to start the burning of the piston propellant (low-density HMX) providing the piston with a smooth initial motion. Analysis of the data gives a detailed picture of the DDT process under these conditions. The qualitative and quantitative experimental results show the transition from the burning to detonation is discontinuous. The results are discussed in terms of a descriptive model. DOE

N91-28449*# National Aeronautics and Space Administration. Lewis Research Center, Cleveland, OH.
SLUSH HYDROGEN PROPELLANT PRODUCTION, TRANSFER, AND EXPULSION STUDIES AT THE NASA K-SITE FACILITY
Terry L. Hardy and Margaret V. Whalen 1991 11 p Presented at the Conference on Advanced Space Exploration Initiative Technologies, Cleveland, OH, 4-6 Sep. 1991; cosponsored by AIAA and OAI
(NASA-TM-105191; E-6493; NAS 1.15:105191; AIAA-91-3550)
Avail: NTIS HC/MF A03 CSCL 21I

Slush hydrogen is currently being considered as a fuel for the National AeroSpace Plane (NASP) because it offers the potential for decreased vehicle size and weight. However, no large scale data was available on the production, transfer, and tank pressure control characteristics required to use the fuel for the NASP. Therefore, experiments were conducted at NASA-Lewis K-Site Facility to improve the slush hydrogen data base. Slush hydrogen was produced using the evaporative cooling, or freeze-thaw, technique in batches for approx. 800 gallons. This slush hydrogen was pressure transferred to a 5 ft diameter spherical test tank following production, and flow characteristics were measured during this transfer process. The slush hydrogen in the test tank was pressurized and expelled using a pressurized expulsion technique to obtain information on tank pressure control for the NASP. Results from the production, transfer, pressurization, and pressurized expulsion tests are described. Author

29 MATERIALS PROCESSING

Includes space-based development of products and processes for commercial applications.
For biological materials see *55 Space Biology.*

N91-28450# California Univ., Berkeley. Lawrence Berkeley Lab.
ON ACCURATE DETERMINATION OF CONTACT ANGLE
P. Concus (Stanford Univ., CA.) and R. Finn May 1991 11 p Presented at the International Union of Theoretical and Applied Mechanics (IUTAM) Symposium on Microgravity Fluid Mechanics, Bremen, Fed. Republic of Germany, 2-6 Sep. 1991
(Contract DE-AC03-76SF-00098)
(DE91-013849; LBL-30497; CONF-9109167-1) Avail: NTIS HC/MF A03

Methods are proposed that exploit a microgravity environment to obtain highly accurate measurement of contact angle. These methods, which are based on our earlier mathematical results, do not require detailed measurement of a liquid free-surface, as they incorporate discontinuous or nearly-discontinuous behavior of the liquid bulk in certain container geometries. Physical testing is planned in the forthcoming IML-2 space flight and in related preparatory ground-based experiments. DOE

N91-28255*# Boeing Aerospace Co., Seattle, WA.
STV ENGINE DESIGN CONSIDERATIONS
In NASA, Washington, Space Transporation Propulsion Technology Symposium. Volume 3: Panel Session Summaries and Presentations May 1991 p 1107-1125 (For primary document see N91-28235 20-20)
Avail: NTIS HC/MF A99 CSCL 21H

31 ENGINEERING (GENERAL)

Includes vacuum technology; control engineering; display engineering; cryogenics; and fire prevention.

N91-28451# Sandia National Labs., Albuquerque, NM.
FLUXLESS SOLDERING OF Ni-Au PLATED KOVAR WITH A LASER
F. M. Hosking and D. M. Keicher 1991 10 p Presented at the Spring Meeting of the Materials Research Society (MRS), Anaheim, 29 Apr. - 3 May 1991
(Contract DE-AC04-76DP-00789)
(DE91-013261; SAND-90-3007C; CONF-910406-13) Avail: NTIS HC/MF A02

Typical soldering processes use reactive fluxes to promote wetting. Most flux residues left after soldering must be removed with halogenated or CFC solvents. Recent legislation has mandated the reduction or elimination of the use of these solvents. There has consequently been a significant effort to develop alternative, environmentally conscious manufacturing technologies that will satisfy this objective. We are currently characterizing and developing a fluxless laser soldering process that will hermetically join Ni-Au electroplated Kovar lids and base plates. A test matrix was designed to investigate the effects of laser heating, joint design, and base/filler metal interactions on achieving fluxless soldering with a 100 watt CW Nd:YAG laser. Two solder alloys, 80In-15Pb-5Ag and 63SN-37Pb (wt. percentage) were used. Satisfactory solder joints were produced with both solder alloys, although the SnPb alloy gave relatively better wetting. Wetting generally increased with increasing laser power, decreasing beam spot size, and decreasing travel speed. The effects of the laser and processing parameters on fluxless soldering will be discussed. DOE

N91-28452# EG and G Rocky Flats, Inc., Golden, CO.
CHANGES WITH MATERIAL PROPERTIES OF ACOUSTIC EMISSION PRODUCED DURING SINGLE POINT MACHINING
C. R. Heiple, S. H. Carpenter, and D. L. Armentrout 1990 16 p Presented at the 10th International Acoustic Emission Symposium, Sendai (Japan), 22-25 Oct. 1990
(Contract DE-AC34-90DP-62349)
(DE91-011913; RFP-4413; CONF-9010364-1) Avail: NTIS HC/MF A03

Acoustic emission was monitored during single point, continuous machining of 4340 steel and Ti-6Al-4V as a function of heat treatment. Acoustic emission produced during tensile and compressive deformation of these alloys has been previously characterized as a function of heat treatment. Heat treatments which increase the strength of 4340 steel increase the amount of acoustic emission produced during deformation, while heat treatments which increase the strength of Ti-6Al-4V decrease the amount of acoustic emission produced during deformation. If chip deformation were the primary source of acoustic emission during single point machining, then opposite trends in the level of acoustic emission produced during machining as a function of material strength would be expected for these two alloys. Trends in rms acoustic emission level with increasing strength were similar for both alloys, demonstrating that chip deformation is not a major source of acoustic emission in single point machining. The data suggest that sliding friction between the nose and/or flank of the tool and the newly machined surface is the primary source of acoustic emission. DOE

N91-28453# EG and G Rocky Flats, Inc., Golden, CO.
ORIGIN OF ACOUSTIC EMISSION PRODUCED DURING SINGLE POINT MACHINING
C. R. Heiple, S. H. Carpenter, and D. L. Armentrout 1991 24 p Presented at the International Cost on Acoustic Emission in Manufacturing, Berkeley, 12-14 Jun. 1991
(Contract DE-AC34-90DP-62349)
(DE91-011915; RFP-4447; CONF-9106184-1) Avail: NTIS HC/MF A03

Acoustic emission was monitored during single point, continuous machining of 4340 steel and Ti-6Al-4V as a function of heat treatment. Acoustic emission produced during tensile and compressive deformation of these alloys has been previously characterized as a function of heat treatment. Heat treatments which increase the strength of 4340 steel increase the amount of acoustic emission produced during deformation, while heat treatments which increase the strength of Ti-6Al-4V decrease the amount of acoustic emission produced during deformation. If chip deformation were the primary source of acoustic emission during single point machining, then opposite trends in the level of acoustic emission produced during machining as a function of material strength would be expected for these two alloys. Trends in rms acoustic emission level with increasing strength were similar for both alloys, demonstrating that chip deformation is not a major source of acoustic emission in single point machining. Acoustic emission has also been monitored as a function of machining parameters on 6061-T6 aluminum, 304 stainless steel, 17-4PH stainless steel, lead, and teflon. The data suggest that sliding friction between the nose and/or flank of the tool and the newly machined surface is the primary source of acoustic emission. Changes in acoustic emission with tool wear were strongly material dependent. DOE

N91-28454*# National Aeronautics and Space Administration. Langley Research Center, Hampton, VA.
FLUSH MOUNTING OF THIN FILM SENSORS Patent Application
Thomas C. Moore, Sr., inventor (to NASA) 6 May 1991 10 p
(NASA-Case-LAR-14446-1; NAS 1.71:LAR-14446-1; US-Patent-Appl-SN-699288) Avail: NTIS HC/MF A02 CSCL 13H

Flush mounting of a sensor on a surface is provided by first forming a recessed area on the surface. Next an adhesive bonding mixture is introduced into the recessed area. The adhesive bonding mixture is chosen to provide thermal expansion matching with the surface surrounding the recessed area. A strip of high performance polymeric tape is provided, with the sensor attached to the underside thereof, and the tape is positioned over the recessed area so that it acts as a carrier of the sensor. A shim having flexibility so that it will conform to the surface surrounding the recessed area is placed over the tape, and a vacuum pad is placed over the shim. The area above the surface is then evacuated while holding the sensor flush with the surface during curing of the adhesive bonding mixture. After such curing, the pad, shim, and tape are removed from the sensor, electrical connections for the sensor are provided, after which the remaining space in the recessed area is filled with a polymeric foam. NASA

N91-28455*# National Aeronautics and Space Administration. Langley Research Center, Hampton, VA.
METHOD AND APPARATUS FOR CLEANING RUBBER DEPOSITS FROM AIRPORT RUNWAYS AND ROADWAYS Patent Application
Sandy M. Stubbs, inventor (to NASA) 3 Apr. 1991 11 p
(NASA-Case-LAR-14483-1; NAS 1.71:LAR-14483-1; US-Patent-Appl-SN-682153) Avail: NTIS HC/MF A03 CSCL 13H

A method and apparatus for cleaning rubber deposits from surfaces such as airport runways and roadways is disclosed. The apparatus includes a large vehicle that has the capacity to be loaded so as to effectively add weight to rubber cleaning tires of the vehicle. In addition, the vehicle has a water tank and sprinkler system so that the surface may be wetted down in front of the tires as the vehicle proceeds across the surface. The cleaning tires of the apparatus are aligned so that they are at a yaw angle to the direction of travel, and the cleaning tire assembly is attached to the underside of the trailer of the vehicle and positioned between a forward and rear water tank. In addition, this tire assembly is equipped with a means of loading the tires onto the contaminated surface. The method comprises driving such a vehicle at low speeds down the surface as the road is being wet in front of the cleaning tires. The effect of the angled tires is to create a scrubbing action that not only heats the rubber deposits by friction but also causes it to be removed from the surface. The rubber that does not stick to the cleaning tires is then removed from the surface by sweeping. NASA

N91-28456# Los Alamos National Lab., NM.
SUPERCRITICAL FLUIDS CLEANING
S. Butner, D. Hjeresen, L. Silva, D. Spall, and R. Stephenson 1991 8 p Presented at the Aerospace Hazardous Waste Minimization Conference, Seattle, 20-26 Jun. 1991
(Contract W-7405-eng-36)
(DE91-013374; LA-UR-91-1801; CONF-9106193-1) Avail: NTIS HC/MF A02

This paper discusses a proposed multi-party research and development program which seeks to develop supercritical fluid cleaning (SFC) technology as an alternative to existing solvent cleaning applications. While SCF extraction technology has been in commercial use for several years, the use of these fluids as cleaning agents poses several new technical challenges. Problems inherent in the commercialization of SCF technology include: the cleaning efficacy and compatibility of supercritical working fluids with the parts to be cleaned must be assessed for a variety of materials and components; process parameters and equipment design have been optimized for extractive applications and must be reconsidered for application to cleaning; and co-solvents and entrainers must be identified to facilitate the removal of polar inorganic and organic contaminants, which are often not well solvated in supercritical systems. The proposed research and development program would address these issues and lead to the development and commercialization of viable SCF-based technology for precision cleaning applications. This paper provides the technical background, program scope, and delineates the responsibilities of each principal participant in the program. DOE

N91-28457# Los Alamos National Lab., NM.
A GEOMETRY BASED METHOD OF INTEGRATED ENGINEERING DESIGN, ANALYSIS, AND OPTIMIZATION
R. M. Dolin and R. J. Bernhard (Purdue Univ., West Lafayette, IN.) 1991 25 p Presented at the 13th Biennial American Society of Mechanical Engineers (ASME) Mechanical Vibration and Noise Conference, Miami, 22-25 Sep. 1991
(Contract W-7405-eng-36)
(DE91-008588; LA-UR-91-533; CONF-910957-1) Avail: NTIS HC/MF A03

A data structure is presented for integrating geometric modeling with analysis and optimization. The data structure is integer based; using a hierarchical integer-pointer scheme to define and manipulate geometry. The integer nature of the data structure leads to fast and accurate operations. Engineers interact with the data structure at shape level. Variables of shapes are constrained and related to each other so that a reduced set of design variables result. These design variables are used to pose both analysis and optimization problems. The design variables represent natural variables of a design (e.g., lengths, radii, etc). Heuristics are used to simplify the integrated modeling, analysis, and optimization procedures. The resulting engineering environment concurrently poses analysis and optimization problems during model generation, leading to an integrated geometry based method of analysis and optimization. An example problem is given. DOE

32 COMMUNICATIONS AND RADAR

Includes radar; land and global communications; communications theory; and optical communications.

For related information see also *04 Aircraft Communications and Navigation* and *17 Space Communications, Spacecraft Communications, Command and Tracking.* For search and rescue see *03 Air Transportation and Safety,* and *16 Space Transportation.*

N91-28458# Dartmouth Coll., Hanover, NH. School of Engineering.
TROPOSPHERIC SCATTER PROPAGATION AT 5 AND 16 GHz: RESULTS FOR A 161 km PATH Final Technical Report, Jun. 1988 - Jun. 1989
Robert K. Crane Oct. 1990 46 p
(Contract F30602-88-D-0027)
(AD-A237012; RADC-TR-90-259) Avail: NTIS HC/MF A03 CSCL 25/5

Simultaneous transmission loss measurements were made at Ku-band (16 GHz) and C-band (5 GHz) on a 161 km tropospheric scatter link between Prospect Hill in Waltham, MA and Mt. Tug in Enfield, NH. The experiment was conducted to demonstrate the feasibility of using the higher frequency for scatter communication. Between April and September, 1987, two-frequency observations were obtained during a variety of weather conditions. Clear weather measurements were made to generate transmission loss estimates for comparison with tropospheric scatter model predictions. Observations during times with precipitation were made to assess the anticipated problems of an excess of transmission loss due to attenuation by rain at the higher frequency and an increase in delay spread due to scattering by rain. GRA

N91-28459# Naval Postgraduate School, Monterey, CA.
DESIGN OF AN INTERACTIVE SATELLITE COMMUNICATIONS SYSTEM ANALYSIS PROGRAM M.S. Thesis
Charles C. Howard Jun. 1990 76 p
(AD-A237030) Avail: NTIS HC/MF A05 CSCL 25/5

The design of an interactive satellite communications system analysis program is addressed. The program provides the capability to analyze/design a system comprised of two earth terminals and one or two geosynchronous satellites. The principal goal is to simplify the analysis/design process via a graphically oriented, menu-driven computer program. The program leads the user methodically through the process and provides feedback that enables the user to visualize the elements of the system and their role relative to the other system components. Hypertext concepts are employed in an object-oriented programming environment to achieve the graphics orientation. The success of the program validates the use of innovative software tools to design programs that can enhance user understanding and increase productivity. GRA

N91-28460# Rome Air Development Center, Griffiss AFB, NY.
PROCEEDINGS OF THE 1990 ANTENNA APPLICATIONS SYMPOSIUM, VOLUME 1 Interim Report
Paul Mayes Apr. 1991 302 p Symposium held 26-28 Sep. 1990
(AD-A237056; RL-TR-91-156-Vol-1) Avail: NTIS HC/MF A14 CSCL 09/1

The Proceedings of the 1990 Antenna Applications Symposium is a collection of state-of-the-art papers relating to phased array antennas, multibeam antennas, satellite antennas, microstrip antennas, reflector antennas, HF, VHF, UHF and various other antennas. GRA

N91-28461# Rome Air Development Center, Griffiss AFB, NY.
PROCEEDINGS OF THE 1990 ANTENNA APPLICATIONS SYMPOSIUM, VOLUME 2 Interim Report
Paul Mayes Apr. 1991 284 p Symposium held 26-28 Sep. 1990
(AD-A237057; RL-TR-91-156-Vol-2) Avail: NTIS HC/MF A13 CSCL 09/1

Papers are presented which relate to phased array antennas,

multibeam antennas, satellite antennas, microstrip antennas, reflector antennas, HF, VHF, UHF and various other antennas.
GRA

N91-28462# Lawrence Livermore National Lab., CA.
LOCALIZED WAVES IN COMPLEX ENVIRONMENTS
R. W. Ziolkowski, I. M. Besieris, and A. M. Shaarawi (Cairo Univ., Egypt) Jun. 1990 12 p Presented at the International Conference on Directions in Electromagnetic Wave Modeling, New York City, 22-24 Oct. 1990
(Contract W-7405-eng-48)
(DE91-011934; UCRL-JC-104164; CONF-9010232-3) Avail: NTIS HC/MF A03

Localized scalar and electromagnetic wave solutions in a variety of complex environments will be reviewed. Like their free-space counterparts, these acoustic and electromagnetic localized wave (LW) solutions can be optimized so that they are localized near the direction of propagation and their original amplitude is recovered out to extremely large distances from their initial location. Pulses with these very desirable localized transmission characteristics may have a number of potential applications in the areas of directed energy transmission, secure communications, and remote sensing.
DOE

N91-28463# Oak Ridge National Lab., TN.
AN ASSESSMENT OF THE LIFETIME OF FARADAY SHIELD ELEMENTS
J. B. O. Caughman, II, D. N. Ruzic (Illinois Univ., Urbana.), D. J. Hoffman, R. A. Langley, M. B. Lewis, and P. M. Ryan 1990 6 p Presented at the 13th IEEE Symposium on Fusion Energy, Knoxville, TN, 3-6 Sep. 1990
(Contract DE-AC05-84OR-21400)
(DE91-012228; CONF-9009381-1) Avail: NTIS HC/MF A02

The interaction of plasma with RF fields from an ion cyclotron range of frequencies (ICRF) antenna has been studied to estimate the amount of Faraday shield erosion expected in normal ICRF heating operation. Plasma parameters and ion energies have been measured in the near field of an antenna and used in a model to estimate the erosion rate of the Faraday shield surface. Experiments were conducted on the RF Test Facility, a magnetic mirror device at Oak Ridge National Laboratory, using a single-strap resonant loop antenna with a two-tier Faraday shield. The outer tier, facing the plasma, was layered with graphite tiles. The antenna was operated at currents and voltages within 50 percent of those expected in tokamaks. The time-varying floating potential was measured with a capacitively coupled probe, and the time-averaged floating potential, electron temperature, and electron density were measured with a Langmuir probe. Ion energies were measured with a gridded energy analyzer located below the antenna, and samples of silicon were placed on the Faraday shield surface to estimate the incident ion energy. The capacitive probe measurements show that the RF floating potential follows the magnetic field pattern of the antenna, indicating that the electromagnetic fields are responsible for the potential formation. Plasma parameters and ion energies have been correlated with the antenna current and used in a computational model of the plasma sheath to predict the amount of erosion expected from the Faraday shield elements exposed to plasma. Predictions of light ion sputtering of candidate Faraday shield materials are presented.
DOE

N91-28464# Los Alamos National Lab., NM.
RECOVERY OF SATURATED VIDEO SIGNALS FROM VIDICONS BY DYNAMIC CATHODE BIASING
G. J. Yates May 1991 25 p
(Contract W-7405-eng-36)
(DE91-012402; LA-12091-MS) Avail: NTIS HC/MF A03

Vidicons used for imaging of pulsed or transient light sources must instantaneously record gray scale images on photoconductive targets. Typical targets, which store photocharge proportional to the varying light intensity in the optical image, have larger positive charge storage capacity than the negative charge available from the electron beam used for neutralizing the target during read-out. Therefore, the target has much higher dynamic range, typically 3 to 5 times larger than the beam. The result is that several scans of the target are required to obtain all the charge from a fully charged target. For applications where only one scan of the target is permissible, this can result in reading the target data in saturated form, with the loss of gray scale information. However, with dynamic rebiasing of the vidicon cathode, the data can be recovered unsaturated. This technique is extremely powerful because it allows instantaneous adjustment after the target has been exposed to light pulses but before the target is read out. In effect, a real time gain or sensitivity control function is implemented by the technique. Alternatively, the technique can be viewed as a means to dynamically select strategic portions of the vidicon transfer curve for immediate read-out, which otherwise would either be saturated if read out immediate read-out, which otherwise would either be saturated if read out immediately or would require several read-outs. Although only transient imaging applications (usually with single field read-out) are addressed, the technique should find application in conventional continuous read-write TV cameras. The principle of operation, associated circuitry, and examples of image retrieval are presented.
DOE

N91-28465# Advisory Group for Aerospace Research and Development, Neuilly-Sur-Seine (France). Avionics Panel Working Group 13.
CONSIDERATIONS FOR NATO SATELLITE COMMUNICATIONS IN THE POST 2000 ERA
A. Nejat Ince, ed. (Marmara Research Inst., Gebze, Turkey) Jun. 1991 322 p
(AGARD-AG-330; ISBN-92-835-0622-7) Copyright Avail: NTIS HC/MF A14; Non-NATO Nationals requests available only from AGARD/Scientific Publications Executive

A substantial amount of information, some of it original, is presented on almost every aspect of satellite communications (systems architecture, design, devices, techniques, and technologies for space, ground and system control segments) which, it is hoped, will be found useful by a wide range of readers including military and political decision makers, planners, and the R and D community.
Author

N91-28466 Colorado Univ., Boulder.
MEASUREMENT OF THE MICROWAVE PROPAGATION DELAY INDUCED BY ATMOSPHERIC WATER VAPOR Ph.D. Thesis
Steven Jay Walter 1990 265 p
Avail: Univ. Microfilms Order No. DA9117091

The Slant Path Atmospheric Refraction Calibrator (SPARC) was developed to measure the water vapor induced propagation delay experienced by radio signal traversing an atmospheric path. SPARC is a refractometer which compares the propagation time of an optical signal with that of a microwave signal. Since the refractivity of dry air is similar for both the microwave and optical signals, the difference in arrival times between the two signals is a sensitive measure of the microwave refractivity due to the presence of water vapor. SPARC is capable of measuring the difference in the optical and microwave arrival time with an accuracy of about ten picoseconds.
Dissert. Abstr.

N91-28467# Lawrence Livermore National Lab., CA.
ELECTROSTATIC DISCHARGE EFFECTS ON EBW DETONATORS
R. S. Lee and R. E. Lee Apr. 1991 17 p Presented at the 16th International Pyrotechnic Seminar, Jonkoping (Sweden), 24-28 Jun. 1991
(Contract W-7405-eng-48)
(DE91-013250; UCRL-JC-105644; CONF-9106187-2) Avail: NTIS HC/MF A03

With appropriate circuit resistance and inductance and sufficient stored energy, discharging a charged human body or component through an exploding bridgewire (EBW) detonator may cause the detonator to function or may damage the detonator. We have studied the effects of electrostatic discharge (ESD) on a number of exploding bridgewire detonators which were subjected to discharges which passed directly through the bridgewires (pin-to-pin), as well as discharges which passed from the bridge to the metal case of the detonator (pin-to-case). We have performed calculations to determine the values of inductance and resistance for which burst and melt may occur for given ESD sources, using a phenomenological model of bridgewire burst in a computer code called FIRESET. Bridge melt was computed using the same computer code, but using experimental values of bridge resistivity and specific heat up to melt. DOE

N91-28468 Tel-Aviv Univ. (Israel).

MUTUAL INTERFERENCE BETWEEN MANY SIMILAR RADARS OPERATING IN PHYSICAL PROXIMITY Ph.D. Thesis

Moshe Levin Oct. 1989 298 p In HEBREW; ENGLISH summary

(ITN-91-85139) Copyright Avail: Tel-Aviv Univ., Exact Sciences Library, Ramat Aviv 69978, Israel

A modification to the radar coherent pulse train signal was developed, which enables the signal reflected from a target to be extracted from the mutual interference among neighboring transmitters. This signal enables interference to be suppressed, under specific delays, regardless of the interference signal strength. A further advantage of this signal is its relatively simple processing by an I and Q sampler and DFT processor. Without additional processing a single interfering impulse can mask the target. A random delay was introduced between pulses and scans, to create statistical independence and random distribution of the interfering impulses in each scan. The probability of interference from a neighboring system was calculated as a function of the random delay and the interfering impulse phase. The impulses were suppressed by adding a median filter before the DFT processor. This was a nonlinear filter, capable of suppressing several strong impulses, the number of which depends on the filter length, which is the total number of pulses on which it operates. This number can be increased by representing the complex number in the I and Q sampler by magnitude and phase. For a high signal to noise ratio, a median filter in the magnitude channel alone suffices to remove interference; when this is not enough, an additional filter, based on a median filter can be used in the phase channel. The latter filter is activated only when interference is detected in the magnitude channel. A computer simulation, of the operation of neighboring car collision avoidance systems, verified the theoretical results and showed that the proposed signal processing can enable such radar systems to operate with high detection probability and low interference probability. ISA

N91-28469 Tel-Aviv Univ. (Israel). Dept. of Electronic Communication, Control and Computer Systems.

FLUCTUATIONS IN NEAR-SURFACE BACKSCATTERING TO A DESCENDING CW RADAR M.S. Thesis

Ben-Tsiyon Klibansky May 1989 200 p In HEBREW; ENGLISH summary

(ITN-91-85140) Copyright Avail: Tel-Aviv Univ., Exact Sciences Library, Ramat Aviv 69978, Israel

The operation of a radar-activated proximity fuse in an artillery shell or mortar bomb depends on the Doppler modification of the echo as the projectile approaches the surface. Explosion at the correct height depends on the return signal amplitude, which strongly depends on the surface characteristics. Periodic modulations have been detected in the backscattering amplitude, as the projectile falls. Earth backscatter models were constructed as a basis for designing a fuse with improved distance measurement accuracy. For mortar bombs, most of the land models fit the data recorded, indicating that the sum of the returns from many scatterers creates the observed oscillation pattern. The return amplitude builds up very rapidly as the fuse approaches the earth. For flat trajectory projectiles, there is high frequency modulation of the return, which is attributed to the relatively high horizontal velocity component. Several models were found to fit the recorded surface backscatter data. The relationship between the return signal spectrum and the elevation angle suggests a possibility for improving the design and performance of the fuse electronic processor. ISA

N91-28470 Tel-Aviv Univ. (Israel). Dept. of Electrical Engineering and Electronics.

PERFORMANCE EVALUATION OF PARTIAL RESPONSE CONTINUOUS PHASE MODULATION: DISCRIMINATOR DETECTION M.S. Thesis

Eyal Trachtman Sep. 1989 164 p

(ITN-91-85145) Copyright Avail: Tel-Aviv Univ., Exact Sciences Library, Ramat Aviv 69978, Israel

The principles of continuous phase modulation (CPM) are reviewed and signalling schemes based on it are discussed. The discriminator detector is widely used to detect CPM signals on band limited channels; it is a non-coherent detector which is widely used in mobile communication applications in which fading makes coherent detection difficult; it is suitable for frequency hopping systems. The detector's inferior response to that of a coherent detector can be compensated by suitable design. The performance is compared of various receivers which use the discriminator detector, using an especially written computer simulation. Receiver schemes considered included: Full response signal with integrate and dump filter; Integrate and dump filter with differential symbol detection; zero forcing linear equalization with symbol detection; Decision feedback equalization (DFE); Maximum likelihood sequence estimation; and Tomlinson filter configuration. The Tomlinson filter configuration, which has not previously been used in a CPM communication system, was compared with the other systems with respect to performance and complexity. For all CPM and detection schemes there are optimum values of h, the modulation index and there is no benefit in increasing the value of h and, therefore the bandwidth, beyond this value. Results are presented for various signal schemes, which indicate that detectability performance can be improved and bandwidth reduced by using a partial response CPM. There is a tradeoff between detectability performance and bandwidth, as a function of the baseband pulse duration. It was found that quaternary signal schemes gave better detectability performance than binary schemes, for the same bit-rates. The simulation results indicated that the Tomlinson-DFE configuration was effective for the partial response M-ary CPM channel with discriminator detection; spectral efficiency was not seriously degraded by precoding using the Tomlinson filter, and there was no degradation of spectral efficiency. ISA

N91-28471 Tel-Aviv Univ. (Israel). Dept. of Electronic Systems.

WIDEBAND ADAPTIVE HF MODEM M.S. Thesis

Doron Rainish Jun. 1989 191 p In HEBREW; ENGLISH summary

(ITN-91-85147) Copyright Avail: Tel-Aviv Univ., Exact Sciences Library, Ramat Aviv 69978, Israel

Difficulties inherent in the usually used systems of high frequency (HF) radio communication are discussed: Restricted bandwidth, information rates limited to about 2,400 bits/sec., and vulnerability to interference. A new HF signalling technique was investigated, especially effective on wide bandwidths. It splits the available power into narrow, independent sub-bands, so avoiding the effects of coherence bandwidth. Also, it distributes the power optimally in the noncontinuous, narrowband, interference free gaps, by using a signalling type optimally chosen for the specific channel. A wide, noncontinuous, interference free bandwidth is used, by means of coding gain, to provide a high rate, reliable communication channel. The interference profile is reported to the transmitter by the receiver, during link establishment and, if necessary, during the transmission, together with channel parameters such as multipath spread and Doppler spread. The optimizing criterion is the maximum number of error free bits of information per watt; the generalized cutoff rate was used as an estimate of the error free bit rate. Thus, the system adapts itself to the system parameters, such as modulation type and rate, code rate and number of sub-bands, which yield the maximum cutoff rate for a given power. Performance evaluation showed that efficient high rate information transfer is possible, using wideband HF links, and that implementation is not too complex to be feasible. ISA

N91-28472 Alabama Univ., Birmingham.
GRAVITATIONAL INFLUENCE OF A STATIC RING-LIKE DISTRIBUTION OF MASS ON ELECTROMAGNETIC WAVES
Ph.D. Thesis
Joseph Obi Otu 1990 55 p
Avail: Univ. Microfilms Order No. DA9114889

The influence of the gravitational field due to a static, axially symmetric, ring-like mass distribution on electromagnetic waves is studied. An exact metric equivalent to the general Weyl metric is obtained by solving the Einstein vacuum field equations in oblate spheroidal coordinates. The vacuum field solutions are free from singularities in all regions of space in the whole range of oblate coordinates. In a static field the source structure can be represented through a multipole expansion in a suitable coordinate system. Oblate coordinates are thus used to derive the relativistically invariant multipole moments of the ring mass. Maxwell's equations in curved space-time are used to derive a wave equation valid in flat space-time but with the curvature effects shown up as a medium with an effective index of refraction. Wave propagation is studied numerically and analytically for waves along the symmetry axis. It is concluded, as verified by the numerical and analytical solutions, that the wave amplitude does not change for waves traveling along the symmetry axis. Dissert. Abstr.

N91-28473# Sandia National Labs., Albuquerque, NM.
PERFORMANCE OF A POLARIZATION ISOLATION ENHANCEMENT METHOD IN THE PRESENCE OF ERRORS
B. C. Brock 1991 21 p Presented at the 1991 Institute of Electrical and Electronics Engineers (IEEE) AP-S Symposium, Ontario (Canada), 24-28 Jun. 1991
(Contract DE-AC04-76DP-00789)
(DE91-013571; SAND-90-3172C; CONF-9106118-3) Avail: NTIS HC/MF A03

A radar measurement system designed to obtain complete backscattering polarization matrix data requires an antenna with feed structures which excite two orthogonal polarizations (or two) orthogonally polarized antennas for quasi-backscatter measurement). Unfortunately, due to construction tolerances and the laws of electromagnetics, there will be coupling between the polarization excitation ports. The result is that the actual polarizations produced are really not orthogonal. However, it is possible to characterize the coupling in such a way that it can be cancelled to a degree through a calibration procedure. Such a procedure has been independently developed at the Sandia National Laboratories Antenna Development Division for a linearly polarized system. The primary focus of this paper is to examine the effect which measurement error will exert on the successful application of that method. DOE

N91-28474# Los Alamos National Lab., NM.
DESIGN OF A MULTIVARIABLE RF CONTROL SYSTEM USING GAIN-SHAPING IN THE FREQUENCY DOMAIN
C. D. Ziomek, S. P. Jachim, and E. F. Natter 1991 4 p Presented at the 1991 Institute of Electrical and Electronics Engineers (IEEE) Particle Accelerator Conference (PAC), San Francisco, 6-9 May 1991
(Contract W-7405-eng-36)
(DE91-013859; LA-UR-91-1483; CONF-910505-222) Avail: NTIS HC/MF A01

Due to the time-varying nature of the radio-frequency (RF) accelerator, RF field amplitude and phase parameters must be precisely controlled in order to confine and accelerate the charged particle beam. Typically, a feedback control system regulates the RF field, rejects noise and disturbances, and maintains operational stability over changes in the electrical structure of the accelerator. This paper describes a multivariable control system that compensates the electrical structure of the accelerator by using gain-shaping in the frequency domain. The amplitude and phase quantities have been resolved into in-phase and quadrature (I and Q) variables. These orthogonal variables have simple mathematical relationships, and can be analyzed using linear transfer function matrices. The transfer matrix theory has been applied to the design of the multivariable control system that regulates the RF field in-phase and quadrature components. Frequency-domain controllers compensate these two signals to provide desired frequency response characteristics. A control predistorter performs an inverse coupling function, so that the I and Q components are effectively decoupled by the accelerator. Furthermore, computer interface circuitry allows the adaptive optimization of the mathematical transfer functions of the compensators. DOE

N91-28475# Sandia National Labs., Albuquerque, NM.
BOREHOLE RADAR EVALUATION PROGRAM: ANTENNA DESIGNS FOR OPTIMAL DIRECTIONALITY
J. G. Castle and H. E. Morris May 1991 41 p
(Contract DE-AC04-76DP-00789)
(DE91-014322; SAND-90-1050) Avail: NTIS HC/MF A03

The thrust of this progress report deals with the significant advances we have made in the past few months toward optimal radiating efficiency and optimal directionality from antenna arrays that fit inside a 5.5 in.-OD tool. The reasons spawning this development effort on antennas are the many uses for underground radar systems that can be built around such high-performance antennas. Targets of interest include large man-made voids, natural voids in strata, fractures zones in hard rock, edges and internal faults in salts domes and glaciers, etc. Recent progress includes observation of the radiation patterns of several dipole arrays which we designed to fit within a 5.5-inch OD borehole tool and to radiate efficiently at wavelengths in the band from 0.4 meter to 2 meters with optimal directionality. Front-to-back ratios of 15 dB are consistently observed in the horizontal plane of these arrays. These antennas are observed to radiate with high efficiencies, less than 1 dB loss, into air at 1.3 meter wavelength. DOE

N91-28476# California Univ., Berkeley. Lawrence Berkeley Lab.
HIGH ORDER CALCULATION OF THE MULTIPOLE CONTENT OF THREE DIMENSIONAL ELECTROSTATIC GEOMETRIES
M. Berz, W. M. Fawley, and K. Hahn Apr. 1991 4 p Presented at the 1991 Institute of Electrical and Electronics Engineers (IEEE) Particle Accelerator Conference (PAC), San Francisco, 6-9 May 1991
(Contract DE-AC03-76SF-00098)
(DE91-014707; LBL-30322-Rev; CONF-910505-323-Rev; HIFAN-499) Avail: NTIS HC/MF A01

We present an accurate and simple method of 3-D multipole decomposition of the field of arbitrary electrode geometries. The induced charge on the surface is obtained by inverting the capacity matrix. The multipole moment decomposition of the resulting potential is readily accomplished using Differential Algebra methodology. The method is applied to the focussing lattice geometry of the MBE-4 accelerator at LBL. Multipole terms of up to the order 5 are computed, and a numerical accuracy of less than 1 percent is obtained. The effective quadrupole and dodecapole field strength are in good agreement with previous results. DOE

33 ELECTRONICS AND ELECTRICAL ENGINEERING

Includes test equipment and maintainability; components, e.g., tunnel diodes and transistors; microminiaturization; and integrated circuitry.

For related information see also *60 Computer Operations and Hardware* and *76 Solid-State Physics.*

N91-28477# North Carolina Univ., Chapel Hill. Dept. of Computer Science.
BUILDING MICROELECTRONIC SYSTEMS IN A UNIVERSITY ENVIRONMENT
John Poulton 1990 14 p
(Contract N00014-86-K-0680)
(AD-A236629) Avail: NTIS HC/MF A03 CSCL 09/1

A technical and social experiment to build a laboratory that designs' and fabricates microelectronic systems in support of research in computer architecture is described. This experiment has been fairly successful by several measures: A number of systems were built and demonstrated, some of significant size and complexity, spanning a fairly wide range of approaches and applications. The lab's original premis was validated, demonstrating economics of scale by sharing a system building facility over multiple projects. Most importantly, experimental systems were fielded on a long term, maintainable basis. The Microelectronic Systems Laboratory (MSL) may serve as a useful model for others who want to develop system-building capability in a university setting. GRA

N91-28478# Cornell Univ., Ithaca, NY. School of Applied and Engineering Physics.

ULTRA-HIGH FREQUENCY SUPERCONDUCTIVE DEVICES Final Report, Oct. 1986 - Mar. 1990

Robert A. Buhrman May 1991 25 p
(Contract F19628-86-K-0034)
(AD-A236795; RL-TR-91-55) Avail: NTIS HC/MF A03 CSCL 09/1

Advanced superconducting tunnel junctions were developed for application in superconducting local oscillators and superconducting mixers operating in the Terahertz (0.2 to 2.0 THz) frequency regime. The research was focused on the development of stable, all refractory, high critical current density, small area tunnel junctions based on NbN superconducting thin films. A successful process for fabrication of approx. 1 sq. micron NbN-MgO-NbN Josephson tunnel junctions was developed with the junctions having critical current densities equal to or greater than 10.000 A/sq. cm. Such junctions were found to be very rugged and reliable. In experiments in which such junctions were coupled capacitively to a nearby, on-chip, Josephson junction detector, the NbN junctions were found to be effective voltage tunable oscillators from 300 GHz to above 1.4 Thz. Direct measurement of the response of the detector junction indicated that the oscillator voltage was typically 1.5 mV in amplitude. This indicated that the Terahertz oscillator power was of the order of 0.5 micro-W, of which, due to impedance mismatch, 0.01 micro W was typically coupled into the detector junction. This power is quite adequate for local oscillator applications in Terahertz mixer applications that might employ a superconducting SIS detector. GRA

N91-28479# Oregon Univ., Eugene. Dept. of Chemistry.

A COMPARATIVE SECOND HARMONIC STUDY OF Cu(111) IN UHV AND IN SOLUTION Technical Report No. 4, Sep. 1990 - Jun. 1991

R. Bradley, A. Friedrich, E. L. Wong, and G. L. Richmond 17 May 1991 11 p
(Contract N00014-89-J-1261)
(AD-A237023) Avail: NTIS HC/MF A03 CSCL 09/1

Important new information is provided about the surface properties of a copper single crystal electrode as examined by surface optical second harmonic (SH) generation. The unique aspect of the work is that SH response from the Cu(111) electrode surface was examined and compared with identical studies performed on this surface in ultra-high vacuum. The results provide compelling evidence for the existence of surface oxides even under conditions where one might expect the electrode surface to be oxide free. GRA

N91-28480# Midwest Research Inst., Golden, CO.

RESEARCH ON STABLE, HIGH-EFFICIENCY AMORPHOUS SILICON MULTIJUNCTION MODULES

A. Catalano, R. Arya, M. Bennett, B. Fieselmann, Y. Li, J. Morris, J. Newton, R. Podlesny, S. Wiedeman, and L. Yang (Solarex Corp., Newtown, PA.) Apr. 1991 70 p
(Contract DE-AC02-83CH-10093)
(DE91-002138; SERI/TP-214-4271) Avail: NTIS HC/MF A04

Progress on the development of solar cell modules is discussed. Topics include the preparation and performance of semiconductor junctions. Research work in non-semiconductor materials is presented, and the design and testing of triple stacked solar cells is presented, too. DOE

N91-28481# Oak Ridge National Lab., TN.

AUTOMATED VERIFICATION OF SYSTEM CONFIGURATION

W. H. Andrews, Jr., S. P. Baker, and A. V. Blalock 1991 10 p
Presented at the 1991 Joint Instrument Society of America/Electric Power Research Institute (ISA/EPRI) Controls and Automation Conference, St. Petersburg, 3-5 Jun. 1991
(Contract DE-AC05-84OR-21400)
(DE91-012520; CONF-9106188-1) Avail: NTIS HC/MF A02

Errors in field wiring can result in significant correction costs (if the errors are discovered prior to use), in erroneous or unusable data (if the errors are not discovered in time), or in serious accidents (if the errors corrupt critical data). Detailed field wiring checkout rework are tedious and expensive, but they are essential steps in the quality assurance process for large, complex instrumentation and control systems. A recent Oak Ridge National Laboratory (ORNL) development, the CONFiguration IDEnification System (CONFIDES) automates verification of field wiring. In CONFIDES, an identifier module is installed on or integrated into each component (e.g., sensor, actuator, cable, distribution panel) to be verified. Interrogator modules, controlled by a personal computer (PC), are installed at the connections of the field wiring to the inputs of the data acquisition and control system (DACS). Interrogator modules poll the components connected to each channel of the DACS and can determine the path taken by each channel's signal to or from the end device for that channel. The system will provide not only the identification (ID) code for the cables and patch panels in the path to a particular sensor or actuator but for individual cable conductor IDs as well. One version of the system uses existing signal wires for communications between CONFIDES modules. Another, more powerful version requires a single dedicated conductor in each cable. Both version can operate with or without instrument power applied and neither interferes with the normal operation of the DACS. Identifier modules can provide a variety of information including status and calibration data. DOE

N91-28482# National Inst. of Standards and Technology, Boulder, CO. Electromagnetic Fields Div.

TRANSMISSION/REFLECTION AND SHORT-CIRCUIT LINE PERMITTIVITY MEASUREMENTS

J. Baker-Jarvis Jul. 1990 156 p
(PB91-171959; NIST/TN-1341) Avail: NTIS HC/MF A08; also available SOD HC $8.50 as 003-003-03058-9 CSCL 09C

The transmission/reflection and short circuit line methods for measuring complex permittivity are examined. Equations for permittivity are developed from first principles. Robust algorithms that eliminate the ill-behaved nature of the commonly used transmission/reflection method at frequencies corresponding to integral multiples of one-half wavelength in the sample are presented. An uncertainty analysis is presented which yields estimates of the errors incurred due to the uncertainty in scattering parameters, length measurement and reference plane position. The indications from the derived equations are presented. In addition, equations for determining complex permittivity independent of reference plane position and sample length are derived. Equations that are derived for permittivity determination using the short circuit line, allow for the positioning of the sample arbitrarily in the sample holder. GRA

N91-28483# Sandia National Labs., Albuquerque, NM.

PREPARATION OF IONIC MEMBRANES FOR ZINC/BROMINE STORAGE BATTERIES

R. A. Assink and C. Arnold, Jr. 1991 5 p Presented at the 26th Intersociety Energy Conversion Engineering (IECE) Conference, Boston, 3-9 Aug. 1991
(Contract DE-AC04-76DP-00789)
(DE91-012008; SAND-90-3186C; CONF-910801-1) Avail: NTIS HC/MF A01

Zinc/bromine flow batteries are being developed for vehicular and utility load leveling applications. During charge, an aqueous zinc bromide salt is electrolyzed to zinc metal and molecular bromine. During discharge, the zinc and bromine react to again form the zinc bromide salt. One serious disadvantage of the microporous separators presently used in the zinc/bromine battery is that modest amounts of bromine and negatively charged bromine moieties permeate through these materials and react with the zinc anode. This results in partial self-discharge of the battery and low coulombic efficiencies. Our approach to this problem is to impregnate the microporous separators with a soluble cationic polyelectrolyte. In laboratory screening tests a sulfonated polysulfone resin and fully fluorinated sulfonic acid polymer substantially reduced bromine permeation with only modest increases in the area resistance. DOE

N91-28484# Oak Ridge National Lab., TN.
MONOLITHIC FRONT END ELECTRONICS FOR SILICON CALORIMETERS
G. T. Alley, M. L. Bauer, C. L. Britton, Jr., R. A. Todd, A. L. Wintenberg, and E. J. Kennedy (Tennessee Univ., Knoxville.) May 1991 15 p Presented at the International Symposium on Electronic Instrumentation in Physics, Dubna, USSR, 14 May 1991
(Contract DE-AC05-84OR-21400)
(DE91-012063; CONF-9105174-1) Avail: NTIS HC/MF A03

This paper describes preamplifiers designed specifically to address the requirements of silicon calorimetry for the Superconductivity Super Collider (SSC). Some considerations are described for the design of a silicon-based sampling calorimetry detector for the SSC. For optimal performance, the front-end electronics must be matched to the detector characteristics and have the speed required by the high SSC interaction rates. The relation between the signal-to-noise ratio of the calorimeter electronics and the charge collection time, the preamplifier power dissipation, detector capacitance and leakage, charge gain, and signal shaping and sampling was studied. The electrostatic transformer connection was analyzed and found to be unusable for a tightly arranged calorimeter because of stray capacitance effects. Some results of radiation effects on selected junction field-effect transistors, MOS field-effect transistors, and bipolar junction transistors are presented. The evaluations include dc parameters, as well as capacitive variations and noise evaluations. The tests are made at the low current and voltage levels (in particular, at currents (le) 1 mA) that are essential for the low-power regimes required by SSC circuitry. Detailed noise data are presented both before and after 5-Mrad (gamma) total-dose exposure. SPICE radiation models for three high-frequency bipolar processes are compared for a typical charge-sensitive preamplifier. Eight different preamplifiers designed for detector capacitances ranging from 20 pF to 500 pF and operating temperatures from 25 C to -20 C are discussed. The different topologies and their features are discussed in addition to the design methodologies employed. The results for noise, power consumption, speed, and radiation damage effects as well as data for post-damage annealing are presented for VTC process preamplifiers. Simulations for the VHF process circuits are presented. DOE

N91-28485# Sandia National Labs., Albuquerque, NM.
EXPLORATORY BATTERY TECHNOLOGY DEVELOPMENT REPORT FOR FY90
N. J. Magnani, P. C. Butler, A. A. Akhil, J. W. Braithwaite, J. M. Freese, and S. E. Lott Apr. 1991 116 p
(Contract DE-AC04-76DP-00789)
(DE91-012131; SAND-91-0672) Avail: NTIS HC/MF A06

Sandia National Laboratories, Albuquerque, manages the Utility Battery Exploratory Technology Development Program, which is sponsored by the U.S. Department of Energy's Office of Energy Management. In this capacity, Sandia is responsible for the engineering analyses and development of advanced rechargeable batteries for stationary energy storage applications. This report details the technical achievements realized during fiscal year 1990. DOE

N91-28486# Los Alamos National Lab., NM.
A HIGH POWER KLYSTRODE WITH POTENTIAL FOR SPACE APPLICATION
D. W. Reid, D. H. Preist, and M. B. Shrader (Varian Associates, San Carlos, CA.) 1991 5 p Presented at the 1991 Institute of Electrical and Electronics Engineers (IEEE) Particle Accelerator Conference (PAC), San Francisco, 6-9 May 1991
(Contract W-7405-eng-36)
(DE91-013046; LA-UR-91-1461; CONF-910505-150) Avail: NTIS HC/MF A01

A 500 kW peak power, 50 kW average, 425 MHz Klystrode was designed and built. The high power Klystrode design evolved from earlier work on the new line of UHF TV Klystrodes. The 500 kW program was undertaken to determine experimentally if a Klystrode would be a viable device in space applications at this power level at 425 MHz. Testing has proceeded in three phases. The initial testing was done in a beam simulation device to determine the characteristics of the gridded gun. The second phase consisted of low duty cycle, full voltage, and current RF testing. The third phase involved full duty cycle and long pulses (11 ms). DOE

N91-28487# Sandia National Labs., Albuquerque, NM.
DURABILITY OF POLYMERIC MATERIALS USED IN ZINC/BROMINE FLOW BATTERIES
C. Arnold, Jr. 1991 20 p Presented at the 26th Intersociety Energy Conversion Engineering (IECE) Conference, Boston, 3-9 Aug. 1991
(Contract DE-AC04-76DP-00789)
(DE91-012864; SAND-91-1096C; CONF-910801-2) Avail: NTIS HC/MF A03

The lifetimes of zinc/bromine flow batteries may be limited by the durability of components which are fabricated from thermoplastic materials and exposed to the bromine-containing electrolyte. Examples of such components are flowframes and carbon-filled plastic electrodes. In early versions of the zinc/bromine battery, flowframes and electrodes were made from polypropylene and copolymers of propylene and ethylene. In later versions of the zinc/bromine battery, polyvinyl chloride (PVC) was used as the material to fabricate flowframes and polyethylene was used as the material used to fabricate both flowframes and electrodes. We found that carbon-plastic electrodes made from polypropylene or polypropylene rich copolymers were swelled and chemically attacked by the bromine-containing electrolytes. As a result, warpage occurred and the battery failed. On the basis of accelerated aging studies we estimated the lifetimes of the electrode and its polypropylene based component to be 96 and 10 months, respectively. The enhanced stability of the electrode was attributed to the presence of carbon which is known to be an antioxidant for thermoxidation. In accelerated exposure tests, bromine-containing electrolytes were also found to attack and leach out the additives used in PVC flowframes. PVC itself was only slightly degraded by the electrolyte. A commercial fluorocarbon, Tefzel, which contains no additives, was determined to be stable in bromine-containing electrolytes and is recommended as a replacement for PVC. Currently, aging studies on carbon-filled polyethylene electrodes are in progress. DOE

N91-28488# Los Alamos National Lab., NM.
MODELING OF A 1700-MHz CLUSTER CAVITY OF PLANAR TRIODES
D. E. Rees and C. Friedrichs, Jr. 1991 4 p Presented at the 1991 Institute of Electrical and Electronics Engineers (IEEE) Particle Accelerator Conference (PAC), San Francisco, 6-9 May 1991
(Contract W-7405-eng-36)
(DE91-013049; LA-UR-91-1458; CONF-910505-149) Avail: NTIS HC/MF A01

In this paper we present the modeling and design of a 1700-MHz cluster-cavity vacuum tube amplifier. We used a three-dimensional, finite-difference code (MAFIA) to characterize the modes that the resonant structure of the amplifier will support. We describe the characteristics of the tube, including performance predictions. DOE

N91-28489# Lawrence Livermore National Lab., CA.
A CHOPPER DRIVEN 11.4-GHz TRAVELING-WAVE RF GENERATOR
G. Westenskow, J. Boyd, T. Houck, D. Rogers, R. Ryne, J. Haimson, and B. Mecklenburg (Haimson Research Corp., Palo Alto, CA.) May 1991 5 p Presented at the 1991 Institute of Electrical and Electronics Engineers (IEEE) Particle Accelerator Conference (PAC), San Francisco, 6-9 May 1991
(Contract W-7405-eng-48)
(DE91-013568; UCRL-JC-105585; CONF-910505-178) Avail: NTIS HC/MF A01

A high power 11.4 GHz RF generator was tested which consists of a 5.7 GHz chopping system and two 11.4 GHz traveling wave output structures. The device was designed to generate about 500 MW of pulsed RF power at 11.4 GHz when driven by a 1-kA, 3 MeV induction beam. Problems with beam breakup in the output structures have limited the width of the RF output pulse for currents above 600 Amps. Short RF pulses were produced up to 420 MW. Modifications are being made to decrease the growth of the beam-breakup fields in the output structures and will use the chopping section to study various extraction structures and to study reacceleration of a bunched beam by induction cells. DOE

N91-28490*# National Aeronautics and Space Administration. Langley Research Center, Hampton, VA.
METHOD OF PREFORMING AND ASSEMBLING SUPERCONDUCTING CIRCUIT ELEMENTS Patent Application
Gene H. Haertling, inventor (to NASA) (Clemson Univ., SC.) and John D. Buckley, inventor (to NASA) 6 Mar. 1991 17 p
(NASA-Case-LAR-14395-1-CU; NAS 1.71:LAR-14395-1-CU; US-Patent-Appl-SN-666536) Avail: NTIS HC/MF A03 CSCL 09A

The invention is a method of preforming and pretesting rigid and discrete superconductor circuit elements to optimize the superconductivity development of the preformed circuit element prior to its assembly, and encapsulation on a substrate and final environmental testing of the assembled ceramic superconductive elements. NASA

N91-28491# Edgerton, Germeshausen and Grier, Inc., Idaho Falls, ID.
LABORATORY TESTING OF THE DUAL TRACTION BATTERY GC12V100
J. E. Hardin Jan. 1991 30 p
(Contract DE-AC07-76ID-01570)
(DE91-012743; EGG-EP-9296) Avail: NTIS HC/MF A03

Testing performed on two groups of Johnson Controls GC12V100 batteries connected in a series parallel arrangement is described. The Soleq Corporation proposed the concept of two or more parallel strings of batteries for powering an electric van and has in fact implemented it in one or more vehicles. The concept of parallel batteries has as its objectives (1) the ability to use 12 volt modules while maintaining a reduced current draw for each parallel string of modules, and (2) increased reliability. The expectation of increased reliability is based on the presumption that one battery string could provide a limp home capability for an Electric Vehicle (EV) if the other string failed during vehicle operation. This concept has not been widely used in prior EV designs, and certain problems were anticipated in the use of a single battery charger to charge parallel strings of batteries. A relatively simple test series was planned to evaluate the feasibility of this approach. DOE

N91-28492# Los Alamos National Lab., NM.
FIELDS AND TRAJECTORIES IN THE MAGNICON
P. J. Tallerico and D. E. Rees 1991 4 p Presented at the 1991 Institute of Electrical and Electronics Engineers (IEEE) Particle Accelerator Conference (PAC), San Francisco, 6-9 May 1991
(Contract W-7405-eng-36)
(DE91-013070; LA-UR-91-1444; CONF-910505-159) Avail: NTIS HC/MF A01

The magnicon is a new type of deflection modulated microwave amplifier that has great potential for high power, high efficiency microwave generation. The magnicon has two (trademark)110 cavities, each with fields rotating at microwave frequencies. The first cavity deflection modulates an electron beam into an expanding spiral path, and the second extracts kinetic energy from the modulated beam. Static magnetic fields employed in the second cavity produce cyclotron motion at frequencies employed in the second cavity produce cyclotron motion at frequencies that are multiples of the microwave frequency. The results of calculations performed on this beam-wave system, with a first-order numerical model, provide guidance for magnicon experimental designs. Field calculations were also done with the 3-D electromagnetic field simulation code, MAFIA. The field and trajectory calculations demonstrate that very high output power and dc-to-rf conversion efficiencies are possible with the magnicon. DOE

N91-28493# Oak Ridge National Lab., TN.
DESORPTION OF Al, Au, Ag USING SURFACE PLASMON EXCITATION
E. T. Arakawa, I. Lee, and T. A. Callcott 1991 5 p Presented at the HASRD Workshop on Laser Ablation: Mechanisms and Application, Oak Ridge, 8-10 Apr. 1991
(Contract DE-AC05-84OR-21400)
(DE91-013726; CONF-9104192-9) Avail: NTIS HC/MF A01

A promising method of photodesorption is described which greatly amplifies electric field strength in the surface region through the excitation of surface plasmons. Data is presented on the yield of desorbed Al, Au, and Ag atoms as a function of incident angle in the attenuated total reflection (ATR) geometry. Data is also presented on the kinetic energy distribution of the desorbed atoms. Finally, the mechanism responsible for the desorption is discussed briefly. DOE

N91-28494# Brookhaven National Lab., Upton, NY.
THYRISTOR CONVERTER SIMULATION AND ANALYSIS
S. Y. Zhang 1991 3 p Presented at the 1991 Institute of Electrical and Electronics Engineers (IEEE) Particle Accelerator Conference (PAC), San Francisco, 6-9 May 1991
(Contract DE-AC02-76CH-00016)
(DE91-013802; BNL-45435; CONF-910505-245) Avail: NTIS HC/MF A01

In this paper we present a simulation on thyristor converters. The simulation features nonlinearity, non-uniform firing, and the commutations. Several applications such as a current regulation, a converter frequency characteristics analysis, and a power line disturbance analysis will be presented. DOE

N91-28495# Brookhaven National Lab., Upton, NY.
PERTURBATION TREATMENT OF THE LONGITUDINAL COUPLING IMPEDANCE OF A TOROIDAL BEAM TUBE
H. Hahn and S. Tepikian 1991 4 p Presented at the 1991 Institute of Electrical and Electronics Engineers (IEEE) Particle Accelerator Conference (PAC), San Francisco, 6-9 May 1991
(Contract DE-AC02-76CH-00016)
(DE91-013884; BNL-45513; CONF-910505-238) Avail: NTIS HC/MF A01

A simple analytical expression for the longitudinal coupling impedance of a toroidal beam tube below the resonance region has been derived by expanding the electromagnetic fields of the toroidal beam tube in a power series in curvature and substituting directly into Maxwell's equations. The resulting expression consists of the impedance of the straight beam pipe plus correction terms due to the curvature. It has been verified that this result gives excellent agreement to the exact solution below the first resonance. DOE

N91-28496# Sandia National Labs., Albuquerque, NM.
FEASIBILITY STUDY OF A 200 AMPERE BATTERY
A. R. Baldwin Jun. 1991 55 p
(Contract DE-AC04-76DP-00789)
(DE91-014673; SAND-90-2112) Avail: NTIS HC/MF A04

The results of a Sandia National Laboratories program to design and develop a high-current thermal battery for the Hypersonic Weapons Technology Program are presented. The feasibility of a

200 A, 150 s, 12 Vdc primary battery was demonstrated under ambient conditions. New header feedthrough design concepts were used, and new internal current collectors and internal power leads were considered. The Li(Si)/LiBr-LiCl-LiF/FeS2 electrochemical system has shown exceptional performance at the high-current operation conditions. A high-rate Zinc/Silver Oxide secondary cell was also evaluated, and the results are presented in this report. These cells exhibited excellent high-rate discharge performance. DOE

N91-28497# Fermi National Accelerator Lab., Batavia, IL.
A 10,000 A 1000 Vdc SOLID STATE DUMP SWITCH
A. Visser May 1991 7 p Presented at the 4th European Conference on Power Electronics and Applications, Florence, Italy, 3-6 Sep. 1991
(Contract DE-AC02-76CH-03000)
(DE91-014141; FNAL/C-91/114; CONF-910936-1) Avail: NTIS HC/MF A02

The superconducting magnet test program at Fermilab requires a switch, called a dump switch, rated 10,000 A, 1000 Vdc, which must be able to continuously carry rated current. A dump resistor rated 2 MJoules, is connected in parallel with the switch contacts and dissipates the stored energy from a magnet when the switch opens. The required switch opening time is 250 microsec maximum after detection of a fault or a trip command. A successful switch can be constructed from six parallel inverter type Silicon Controlled Rectifiers (SCR's) which each carry their share of the load current. These run SCR's are mounted at watercooled heatsinks and are commutated off from stored energy in capacitors. Each parallel SCR is connected in series with a 1 m(Omega) watercooled resistor to assure dc current sharing and turn on. A description of the control and construction of the switch is presented. DOE

N91-28498# California Univ., Berkeley. Lawrence Berkeley Lab.
FIXTURE EFFICIENCY PROGRAM
M. J. Siminovitch, F. M. Rubinstein, and M. Packer Apr. 1991 15 p Presented at the Association of Energy Engineers Conference, Anaheim, 22-26 Apr. 1991
(Contract DE-AC03-76SF-00098)
(DE91-014470; LBL-30646; CONF-9104272-1) Avail: NTIS HC/MF A03

This paper describes the research program involved with the development of energy efficient fluorescent fixtures. The program effort is directed at improving the efficiency of both compact and T12 fluorescent fixtures by the development of advanced thermal management systems. Most enclosed compact and T12 fluorescent fixtures produce elevated lamp wall temperatures that result in reduced light output and efficiency of the lamp ballast system. Fixture efficiencies for these types of enclosed fixtures typically range between 50 and 70 percent. Approximately half of the efficiency losses are due to thermal affects and half due to optical factors. This indicates that substantial conservation potential exists by enhancing the thermal performance of fluorescent fixtures. The ongoing program is directed at developing enhanced fixture geometries that mitigate these thermal losses, and at working with the fixture industry to transfer these thermal management systems to the marketplace. DOE

N91-28499# Los Alamos National Lab., NM.
PROCYON EXPERIMENTS UTILIZING FOIL-FUSE OPENING SWITCHES
D. G. Rickel, I. R. Lindemuth, R. E. Reinovsky, J. H. Brownell, J. H. Goforth, A. E. Greene, H. W. Kruse, H. Oona, J. V. Parker, and P. J. Turchi 1991 5 p Presented at the 8th IEEE Pulsed Power Conference, San Diego, 17-19 Jun. 1991
(Contract W-7405-eng-36)
(DE91-014605; LA-UR-91-2049; CONF-910640-18) Avail: NTIS HC/MF A01

The Los Alamos National Laboratory has applied the explosive magnetic flux compression generator (FCG) technology to the high-energy foil-implosion project, Trailmaster, to reach energy levels unattainable by other methods under current budget constraints. A required component for FCG systems is a power-conditioning stage that matches the slow risetime of the energy source with the fast-risetime requirements of the foil-implosion load. Currently, the Trailmaster concept is based on a two-step process of combining an intermediate power compression stage with a plasma flow switch (PFS) that will deliver energy to an imploding foil on the order of 100 ns. The intermediate power compression stage, which is the main emphasis of this report, consists of an energy storage inductor loaded by the FCG (the energy source) and an associated opening and closing switch. In our Procyon testing series, a subtask of the Trailmaster project, we have explored two approaches for opening and closing switches. One uses an explosive opening switch (EFF) and a detonator-initiated closing switch, the topic of another paper at this conference, and a resistive fuse opening switch, a surface tracking closing switch (STS), the subject of this presentation. This latter concept was successfully tested last summer with a complete plasma flow switch assembly, but the dynamic implosion foil was replaced by a rigid passive inductive load. We present data on the performance of the fuse opening switch, the surface tracking closing switch, and the plasma flow switch. DOE

N91-28500# Sandia National Labs., Albuquerque, NM.
SOME HIGH VOLTAGE DC BREAKDOWN PROPERTIES OF THICK FILM CIRCUITS ON ALUMINA
G. L. Dybwad and S. E. Garrett Jun. 1991 31 p
(Contract DE-AC04-76DP-00789)
(DE91-014675; SAND-90-2092) Avail: NTIS HC/MF A03

This report describes high voltage dc breakdown tests on various PtAu and Au thick film hybrid microcircuits on alumina (Al_2O_3). Samples were prepared with current thick film design and manufacturing rules. The purpose was to determine the voltage margins between current design rules and typical applied voltages on real circuits. We also analyzed what happened during a breakdown event. We used a versatile computer-controlled test set to obtain breakdown data. This showed that design conductors 10 mil wide with equal design spaces on alumina and coated with a fired protective glaze (DuPont 9137) had the highest breakdown values (2700 Vdc). Bare design circuits and Au conductor crossover features had a lower breakdown value (1400 to 1600 Vdc). Both these values are well above logic circuit applied voltages (less than or equal to 50v). This may account for the excellent field performance obtained to date. Ambient humidity changes to 43 percent R.H. and voltage rise rates between 3 and 2300 V/sec had little influence on breakdown values (less than or equal to 200 Vdc). Voltage breakdown values were little influenced by our two geometries: point-to-line samples which simulated corners and long parallel line samples. Breakdown behaved like a spark in air rather than an arc. Breakdown in glaze went through it to air rather than along the glaze/alumina interface. The spark was found to be similar to lightning in that it consisted of a string of current pulses lasting a total of 1 to 2 seconds. Spark locations were from surface asperities or defects near but not at the point of minimum optically measured separation. Hence, we found that circuits made using current design rules for hybrid microcircuit manufacture are adequate or conservative as regards safe margins against logic voltage dc breakdown to the extent studied here. DOE

N91-28501# Sandia National Labs., Albuquerque, NM.
THE SUPERCONDUCTING FLUX FLOW TRANSISTOR: MODELS AND APPLICATIONS
J. S. Martens, V. M. Hietala, T. E. Zipperian, D. S. Ginley, and C. P. Tigges 1991 6 p Presented at the 1991 Superconducting Quantum Interference Devices (IC SQUID) Meeting, Berlin, Fed. Republic of Germany, 18-21 Jun. 1991
(Contract DE-AC04-76DP-00789)
(DE91-014702; SAND-91-1272C; CONF-9106224-1) Avail: NTIS HC/MF A02

The superconducting flux flow transistor (SFFT) is a single film, active device generally made from high temperature superconducting (HTS) materials. The device is based on the magnetic control of flux motion, has gain and can operate to over

40 GHz with 3 micron feature size. Existing models are reviewed along with the latest equivalent circuit values derived from S-parameter measurements. Noise performance is compared to that predicted by a relatively simple flux noise model and recent amplifier performance is discussed. DOE

N91-28923# National Inst. for Fusion Science, Nagoya (Japan).
NONLINEAR COMPUTER ANALYSIS OF BACKWARD WAVE OSCILLATOR
T. Watanabe, K. Ogura, M. M. Ali, M. Itakura, and K. Minami (Niigata Univ., Japan) *In its* Proceedings of the Second International Toki Conference on Plasma Physics and Controlled Nuclear Fusion. Nonlinear Phenomena in Fusion Plasmas: Theory and Computer Simulation Apr. 1991 p 148-153 (For primary document see N91-28881 20-75)
Avail: NTIS HC/MF A11

N91-28924# Tsukuba Univ. (Japan). Plasma Research Center.
MODE CONVERSION OF ALFVEN WAVES INDUCED BY QUADRUPOLE MAGNETIC FIELD MODULATION
H. Hojo, M. Inutake, M. Ichimura, and S. Miyoshi *In* National Inst. for Fusion Science, Proceedings of the Second International Toki Conference on Plasma Physics and Controlled Nuclear Fusion. Nonlinear Phenomena in Fusion Plasmas: Theory and Computer Simulation Apr. 1991 p 154-157 Sponsored in part by Ministry of Education, Science and Culture (For primary document see N91-28881 20-75)
Avail: NTIS HC/MF A11

N91-28925# Tohoku Univ., Sendai (Japan). Dept. of Electrical Engineering.
NUMERICAL SIMULATION OF POTENTIAL-DRIVEN ION CYCLOTRON OSCILLATION
S. Ishiguro, K. Nakagawa, and N. Sato *In* National Inst. for Fusion Science, Proceedings of the Second International Toki Conference on Plasma Physics and Controlled Nuclear Fusion. Nonlinear Phenomena in Fusion Plasmas: Theory and Computer Simulation Apr. 1991 p 158-161 (For primary document see N91-28881 20-75)
Avail: NTIS HC/MF A11

N91-28926# Kyushu Univ., Fukuoka (Japan). Dept. of Physics.
DYNAMICS OF INTERFACES WITH INTERNAL STRUCTURES
Toshihiro Kawakatsu and Kyozi Kawasaki *In* National Inst. for Fusion Science, Proceedings of the Second International Toki Conference on Plasma Physics and Controlled Nuclear Fusion. Nonlinear Phenomena in Fusion Plasmas: Theory and Computer Simulation Apr. 1991 p 162-163 (For primary document see N91-28881 20-75)
Avail: NTIS HC/MF A11

N91-28927# National Inst. for Fusion Science, Nagoya (Japan).
NONLINEAR EQUATIONS FOR WEAKLY UNSTABLE MODES
N. Nakajima *In its* Proceedings of the Second International Toki Conference on Plasma Physics and Controlled Nuclear Fusion. Nonlinear Phenomena in Fusion Plasmas: Theory and Computer Simulation Apr. 1991 p 164-167 (For primary document see N91-28881 20-75)
Avail: NTIS HC/MF A11

N91-28928# Tokyo Inst. of Tech. (Japan). Dept. of Applied Physics.
HOLE DYNAMICS OF ONE-DIMENSIONAL PLASMA Abstract Only
K. Kitahara, N Ishibashi,, and K. Tanno *In* National Inst. for Fusion Science, Proceedings of the Second International Toki Conference on Plasma Physics and Controlled Nuclear Fusion. Nonlinear Phenomena in Fusion Plasmas: Theory and Computer Simulation Apr. 1991 p 168 (For primary document see N91-28881 20-75)
Avail: NTIS HC/MF A11

34 FLUID MECHANICS AND HEAT TRANSFER

Includes boundary layers; hydrodynamics; fluidics; mass transfer; and ablation cooling.

For related information see also *02 Aerodynamics* and *77 Thermodynamics and Statistical Physics.*

N91-28502*# Colorado Univ., Boulder. Dept. of Aerospace Engineering Sciences.
NUMERICAL SIMULATION OF PARTICLE-WAVE INTERACTION IN BOUNDARY LAYERS Final Report
S. Biringen and G. Danabasoglu [1990] 16 p
(Grant NAG1-798)
(NASA-CR-187312; NAS 1.26:187312) Avail: NTIS HC/MF A03 CSCL 20D

The effects of wall injection and particle motion on the spatial stability of two-dimensional plane channel flow are investigated. For this purpose, an accurate Navier-Stokes solver to simulate the space-time evolution of disturbances in three-dimensional flows has been developed. The code is operational on the NASA Langley CRAY2 and can be ported to any other supercomputer. The code has been tested extensively in tracking the spatial evolution of two-dimensional disturbances in plane channel flow and provided excellent agreement with the linear theory including at the inflow/outflow boundaries. Preliminary calculations have been performed to investigate the effects of stationary and moving sources of vortical disturbances simulating a particle traveling in the flow field. Results suggest that even at very low amplitudes, vortical disturbances act as amplifiers on the Tollmien-Schlichting waves promoting rapid instability. It is also found that slow moving particles are more dangerous than both stationary and fast moving particles for the same disturbance levels. Author

N91-28503*# MCAT Inst., San Jose, CA.
ALGORITHM AND CODE DEVELOPMENT FOR UNSTEADY THREE-DIMENSIONAL NAVIER-STOKES EQUATIONS Annual Report, 1 Apr. 1989 - 30 Mar. 1991
Shigeru Obayashi Jun. 1991 130 p
(Contract NCC2-605)
(NASA-CR-188039; NAS 1.26:188039; MCAT-91-005) Avail: NTIS HC/MF A07 CSCL 20D

A streamwise upwind algorithm for solving the unsteady 3-D Navier-Stokes equations was extended to handle the moving grid system. It is noted that the finite volume concept is essential to extend the algorithm. The resulting algorithm is conservative for any motion of the coordinate system. Two extensions to an implicit method were considered and the implicit extension that makes the algorithm computationally efficient is implemented into Ames's aeroelasticity code, ENSAERO. The new flow solver has been validated through the solution of test problems. Test cases include three-dimensional problems with fixed and moving grids. The first test case shown is an unsteady viscous flow over an F-5 wing, while the second test considers the motion of the leading edge vortex as well as the motion of the shock wave for a clipped delta wing. The resulting algorithm has been implemented into ENSAERO. The upwind version leads to higher accuracy in both steady and unsteady computations than the previously used central-difference method does, while the increase in the computational time is small. Author

N91-28504# Royal Aerospace Establishment, Farnborough (England).
THE APPLICATION OF PARTICLE IMAGE VELOCIMETRY (PIV) IN A SHORT DURATION TRANSONIC ANNULAR TURBINE CASCADE
S. P. Harasgama, P. J. Bryanston-Cross, C. E. Towers, and S. T. Hopwood Mar. 1991 12 p
(AD-A236639; RAE-TM-P-1203; DRIC-BR-301039) Avail: NTIS HC/MF A03 CSCL 20/4

A series of experiments was performed to demonstrate the application of Particle Image Velocimetry to turbomachinery flows.

The tests were performed at transonic speeds on a fully annular engine size turbine nozzle guide vane. The vane cascade was installed in a short duration Isentropic Light Piston Cascade (ILPC) test facility operating with high inlet turbulence levels. The technique was shown to map the whole flow field with a resolution of 0.5 mm. The quality of the results obtained are not greatly affected by local turbulence rates. The accuracy of the measurements is put at around 4 pct. of absolute velocity and is limited by the quality of the image on the film plane. The velocities derived from the PIV images were compared with predictions from a 3-D viscous numerical calculation. It is shown that the experimental and predicted results are in good agreement. It is considered that this technique has considerable potential in application to turbomachinery flow field diagnostics. GRA

N91-28505# Sandia National Labs., Albuquerque, NM.

A NUMERICAL APPROACH FOR MODELLING CAVITATING FLOWS

M. S. Ingber (New Mexico Univ., Albuquerque.) and C. E. Hailey 1991 15 p Presented at the 1st International Conference on Computational Modeling of Free and Moving Boundary Problems, Southampton, England, 2-4 Aug. 1991
(Contract DE-AC04-76DP-00789)
(DE91-009178; SAND-90-2418C; CONF-910863-1) Avail: NTIS HC/MF A03

The flow about a submerged partially or supercavitating axisymmetric body is considered both at zero and non-zero angle of attack. The direct boundary element method is used to solve for the potential flow field and to determine the cavity shape. This is accomplished by performing a Newton-Raphson iteration in which the cavity shape is perturbed in an effort to satisfy the nonlinear dynamic boundary condition along the surface of the cavity. For problems with non-zero angle of attack, the flow field is 3-D and the cavity is not symmetric. In these cases, the convergence of the Newton-Raphson iteration is sensitive to the initial estimate of the cavity shape. Methods of generating these initial estimates are discussed which have been successful in leading to convergent solutions. Also efficient methods of parameterizing the cavity are developed to reduce the computational effort. DOE

N91-28506# Lawrence Livermore National Lab., CA.

ATMOSPHERIC PROPAGATION OF HIGH-EXPLOSIVE BLAST WAVES

S. W. Kang and J. C. Kleiber, Jr. 2 Apr. 1991 41 p
(Contract W-7405-eng-48)
(DE91-012550; UCRL-LR-106630) Avail: NTIS HC/MF A03

A procedure was developed for calculating the maximum high explosive weight limit for use at Lawrence Livermore National Laboratory (LLNL) Site 300 based on the analysis of the blast-wave propagation behavior in the atmosphere. Both analytical and experimental efforts were involved, including a literature search, evaluation of other data, measurements of local weather conditions, and implementation of relevant computational programs. Major results of the present effort are: (1) Comparison of the LLNL data with other data reveals discrepancies, suggesting that local effects, such as weather conditions in the downrange regions, may play a role in affecting the wave-propagation behavior. Measurements of the local weather conditions indeed show that they differ from those at Site 300. (2) Analyses of other, newer models and data resulted in the implementation of relevant computer codes, such as the BLASTO code, to be used at Site 300. (3) A new procedure for predicting the weight limit at Site 300 was recommended. This new procedure consists of: (1) Site 300 and local valley weather measurements; (2) the LAP code; and (3) the BLASTO code. The LAP code is a modified SIPS code and computes the acoustic ray trajectories, including the focus (caustic) locations, under varying local weather conditions. The BLASTO code calculates the peak overpressure vs distance relationship for a given charge weight and weather condition. Both the LAP code and the BLASTO code were implemented and are operational at Site 300. Future plans include conducting selective tests to verify the validity of the predictive procedure recommended for Site 300. DOE

N91-28507# National Inst. of Standards and Technology, Gaithersburg, MD.

BOUSSINESQ ALGORITHM FOR ENCLOSED BOUYANT CONVECTION IN TWO DIMENSIONS

R. G. Rehm, H. C. Tang, H. R. Baum, J. S. Sims, and D. M. Corley Mar. 1991 40 p
(PB91-178848; NISTIR-4540) Avail: NTIS HC/MF A03 CSCL 20D

Approximate equations for a Boussinesq model with viscous dissipation and thermal conduction describing buoyant convection driven by a heat source in a rectangular enclosure are derived. The finite difference algorithm for computing transient solutions in two dimensions to these equations is presented. The algorithm allows the enclosure fluid to be stratified in a direction parallel to the enclosure walls initially, or for gravity to have an arbitrary direction relative to the enclosure (but with no initial stratification). Computational results of transient, two-dimensional buoyant convection for very high resolution are presented. The hydrodynamics is directly based on the time-dependent Navier-Strokes equations; the model or other empirical parameters are introduced. There is no inflow or outflow at boundaries; this assumption, although rather restrictive, allows the mathematical problem to be properly formulated so that no other empiricism is introduced by specification of the algorithmic boundary conditions. A finite-difference scheme second-order in space and first-order in time is used to integrate the evolution equations, and an elliptic solver is used to solve the pressure equation. GRA

N91-28508# Clarkson Univ., Potsdam, NY. Fluid Mechanics, Heat and Mass Transfer Lab.

EXPERIMENTAL INVESTIGATION OF PRESSURE DROP AND HEAT TRANSFER FOR AIR FLOW THROUGH ENHANCED TUBES

N. T. Obot and E. B. Esen May 1991 41 p
(Contract DE-FG02-89CE-90029)
(DE91-012151; DOE/CE-90029/5) Avail: NTIS HC/MF A03

An experimental investigation of the pressure drop and heat transfer characteristics for a smooth tube and various enhanced tubes was made. The working fluid for the experiments was air. The Reynolds number (Re) was varied between 200 and 50000 to provide data for the laminar, transition and turbulent flow regimes. Nine enhanced tubes were tested. For the spirally fluted tubes, it is established that the friction factor and Nusselt number in laminar, transitional and turbulent flow are generally higher than the smooth tube values. Using the corresponding states relations given in a previous report, it is established that the reduced heat transfer data for the spirally fluted tubes are coincident with those for the smooth tube. The validity of the frictional law of corresponding states and the existence of a definite connection between transition and the heat transfer enhancement were verified experimentally. For the three Hitachi Cable enhanced tubes, the results indicate that the behavior with respect to friction or heat transfer is about the same as that for the smooth tube in laminar flow and the transition region. There is hardly any improvement in heat transfer up to a Reynolds number of about 10000 and only very moderate increases occur at higher Reynolds numbers. In turbulent flow, the friction factor is slightly higher than the smooth tube value. The three Wieland enhanced tubes are characterized by transition Reynolds numbers that are considerably greater than those for the Hitachi tubes, the spirally fluted tubes or the value for the present smooth tube. Consequently, the friction factor and Nusselt number are generally lower than the smooth tube values within the transition region, with higher values than the smooth tube data in turbulent flow. DOE

N91-28509# Clarkson Univ., Potsdam, NY. Fluid Mechanics, Heat and Mass Transfer Lab.

PRESSURE DROP AND HEAT TRANSFER FOR SPIRALLY FLUTED TUBES INCLUDING VALIDATION OF THE ROLE OF TRANSITION

N. T. Obot, E. B. Esen, K. H. Snell, and T. J. Rabas (Argonne National Lab., IL.) 1991 8 p Presented at the ASME/AIChE/ANS National Heat Transfer Conference,

Minneapolis, 26-31 Jul. 1991
(Contract DE-FG02-89CE-90029)
(DE91-012242; CONF-910739-14) Avail: NTIS HC/MF A02

An experimental investigation was carried out to determine the pressure drop and heat transfer characteristics for spirally fluted tubes in laminar, transitional and turbulent flow of air. It is established that, in the laminar, transitional and turbulent regimes, the friction factor for the spirally fluted tube is generally higher than that for a smooth tube. The values for the critical Reynolds number at the onset of transition to turbulent flow are lower, while the corresponding critical friction factors are higher, than those for a smooth tube. Consistent with the expected effect of transition on heat transfer, the experimentally determined Nusselt numbers are generally higher than the smooth tube values. The results indicate that there is a definite connection between transition and the heat transfer enhancement. DOE

N91-28510# Edgerton, Germeshausen and Grier, Inc., Idaho Falls, ID.

GAS EVOLUTION FROM SPHERES

G. R. Longhurst Apr. 1991 17 p
(Contract DE-AC07-76ID-01570)
(DE91-012807; EGG-FSP-9634) Avail: NTIS HC/MF A03

Gas evolution from spherical solids or liquids where no convective processes are active is analyzed. Three problem classes are considered: (1) constant concentration boundary, (2) Henry's law (first order) boundary, and (3) Sieverts' law (second order) boundary. General expressions are derived for dimensionless times and transport parameters appropriate to each of the classes considered. However, in the second order case, the non-linearities of the problem require the presence of explicit dimensional variables in the solution. Sample problems are solved to illustrate the method. DOE

N91-28511# Notre Dame Univ., IN. Dept. of Chemical Engineering.

STUDY OF INTERFACIAL BEHAVIOR IN COCURRENT GAS-LIQUID FLOWS

M. J. McCready Apr. 1991 24 p
(Contract DE-FG02-88ER-13913)
(DE91-013008; DOE/ER-13913/3) Avail: NTIS HC/MF A03

As we had discussed previously, understanding of macroscopic phenomena in gas-liquid flows will not be achieved until the many microscopic events have been characterized. Because we believe that some significant progress has been made at identifying the causes of specific events (e.g., why a solitary or roll waves forms, how side bands and subharmonics arise) we have begun to address the question of spatial evolution of disturbances. A correlation between the amplitude and time period of individual waves is identified from measurements of interface tracings at certain flow conditions close to neutral stability. This suggests, in agreement with weakly nonlinear theories, that a family of steady states can simultaneously exist. From tracings taken at two closely spaced locations in the flow direction, estimates of the rate at which wave forms evolve are made. These distances, which may be greater than 20 cm, (greater than 10 wavelengths) provide further support for the idea that individual waves may either reach a steady state or oscillate around one. A suggested avenue of research is to first get better measurements which determine the rate of evolution of finite amplitude waves, then to examine the mechanism which is determining the distribution of steady states. A re-examination of the linear stability problem for cocurrent gas-liquid flows is described in which the solution to both the temporally and spatially growing waves is done. It is found that close to neutral stability, temporal growth rates can be converted to spatial growth rates with the group velocity. The utility of the complete solution over approximate analytical solutions is demonstrated. DOE

N91-28512# Oak Ridge National Lab., TN.

MODELS FOR HEAT TRANSPORT THROUGH ASSEMBLIES OF UNIFORM-DIAMETER HOLLOW SPHERES

D. W. Yarbrough, D. L. McElroy, and F. J. Weaver Apr. 1991 139 p
(Contract DE-AC05-84OR-21400)
(DE91-012998; ORNL/TM-11397) Avail: NTIS HC/MF A07

Uniform-diameter thin-wall hollow ceramic spheres are being developed as a thermal insulating material. The radial heat flow across test beds of the hollow spheres has been measured as a function of interstitial gas pressure and temperature for specimens with either nitrogen or helium as the interstitial gas. This report covers the development of equations used to model the heat flow process. The primary modes of heat transfer in this case are conduction and radiation. Convection transport is a minor but apparently not a negligible part of the overall transport. Three models have been used to describe 17 experimental data sets obtained for combinations of sphere sizes, sphere material, and interstitial gas type and pressure. In each case, the experimental data have been used to determine parameters appearing in the models. In general, the experimental thermal conductivity data for a given bed of spheres can be described to better than 10 percent over the pressure range investigated. One of the models which includes a pressure explicit function describes the data to set better than 5 percent. FORTRAN programs have been written to expedite use of the models to describe the data. These programs can be easily modified to produce thermal conductivity predictions for untested combinations of, for example, sphere size, interstitial gas type and pressure, and solid conductivity. The programs have been included in this report. DOE

N91-28513# Los Alamos National Lab., NM.

MOVING FINITE ELEMENTS: A CONTINUOUSLY ADAPTIVE METHOD FOR COMPUTATIONAL FLUID DYNAMICS

A. H. Glasser, K. Miller, and N. Carlson (California Univ., Berkeley.) 1991 6 p Presented at the Power Supercomputer Users Meeting, Gaithersburg, 21-22 May 1991
(Contract W-7405-eng-36)
(DE91-013391; LA-UR-91-1716; CONF-9105202-3) Avail: NTIS HC/MF A02

Moving Finite Elements (MFE), a recently developed method for computational fluid dynamics, promises major advances in the ability of computers to model the complex behavior of liquids, gases, and plasmas. Applications of computational fluid dynamics occur in a wide range of scientifically and technologically important fields. Examples include meteorology, oceanography, global climate modeling, magnetic and inertial fusion energy research, semiconductor fabrication, biophysics, automobile and aircraft design, industrial fluid processing, chemical engineering, and combustion research. The improvements made possible by the new method could thus have substantial economic impact. This paper describes the mathematical formulation and illustrates its use. DOE

N91-28514# Pittsburgh Energy Technology Center, PA.

A REVIEW OF THEORIES FOR FLOWING GRANULAR MATERIALS WITH APPLICATIONS TO FLUIDIZED BEDS AND SOLIDS TRANSPORT

M. Massoudi and E. J. Boyle (Morgantown Technology Center, WV.) May 1991 133 p
(DE91-013111; DOE/PETC-TR/91/8) Avail: NTIS HC/MF A07

The development is described of the theories for flowing granular materials. A historical perspective on the importance and everyday use of granular materials in engineering applications is given, and various examples of what is meant by granular material are presented. For future use and convenience, we introduce some basic definitions and fundamental concepts used in granular media are introduced. Various standard continuum theories are introduced which are implemented for specific use of granular materials for different flow conditions. The turbulence modelling of solids transport is examined by first extending the standard continuum theories to the theories of micropolar materials. The works are reviewed of investigators who postulate modelling granular materials as nonNewtonian fluids. At this stage of the historical development of these theories, it had become evident that the fluctuating velocity of individual particles plays an important role in the formulation of the stress tensors. A review is given of kinetic theory of gases as applied to flowing granular materials. The existing constitutive equations are reviewed for the solid phase in solid-gas flows, and discusses the importance and relevance of modelling the solid phase as granular material. A discussion regarding what is usually referred to as solids pressure is presented. DOE

N91-28515# Sandia National Labs., Albuquerque, NM.

ZEPHYR3D: A FINITE DIFFERENCE COMPUTER PROGRAM FOR THREE-DIMENSIONAL, TRANSIENT INCOMPRESSIBLE FLOW PROBLEMS

J. A. Schutt May 1991 104 p
(Contract DE-AC04-76DP-00789)
(DE91-014331; SAND-91-0350) Avail: NTIS HC/MF A06

This report describes the finite difference computer code ZEPHYR3D, which is designed to solve three-dimensional, transient incompressible flow problems. ZEPHYR3D includes an energy equation that allows coupled thermal/fluid problems to be solved with the limits of the Boussinesq approximation. It also includes an implementation of the Smagorinsky subgrid scale turbulence model, which allows ZEPHYR3D to perform large eddy simulation of turbulent flows. This report includes the mathematical and numerical basis for ZEPHYR3D, a user's guide, and several example/benchmark problems. These problems include flow over a backward-facing step, free convection in an enclosure, and the collapse of a mixed region in a stratified environment. DOE

N91-28516 Tel-Aviv Univ. (Israel). Dept. of Fluid Mechanics and Heat Transfer.

NUMERICAL SOLUTION OF A MOVING BOUNDARY PROBLEM AS A MODEL SOLUTION FOR A SOLAR PIPE M.S. Thesis

Yaacov Keizman Mar. 1989 169 p In HEBREW; ENGLISH summary
(ITN-91-85143) Copyright Avail: Tel-Aviv Univ., Exact Sciences Library, Ramat Aviv 69978, Israel

This research focuses on the numerical solution of a moving boundary problem as a model solution for a solar heat pipe. Herein the term solar pipe refers to a pipe which consists of two concentric tubes. A phase change material (P.C.M.) is contained in the space between the two tubes. It melts while being heated, thus storing energy in the form of latent heat. This energy is emitted when the material is cooled and solidified. The energy absorption takes place at the external perimeter of the pipe, and its release occurs at the inner perimeter, by means of forced liquid convection. The solar pipe has several advantages over conventional solar systems which are briefly detailed. A solution is presented for a set of equations which represent conductive heat transfer with a moving boundary. The solution is aimed at calculating several parameters relating to the operation of a solar pipe: The temperature distribution in the pipe cross section, the velocity of the interface and the temperature distribution in the convected liquid at the inner perimeter. On the basis of the set of differential equations, a numerical model based on a finite difference scheme was developed. The finite difference scheme is solved by a computer program, which performs a simulation of the melting and solidification of the P.C.M. The results of the numerical model are compared with an approximate analytical solution, showing good agreement. The significance of the proposed numerical model lies in some possible applications: (1) Reduction of the costs of solar energy systems; (2) the solution of similar problems in other engineering fields, where the Stefan numbers are small. Author (ISA)

N91-28517 Texas Univ., Austin.

EXPERIMENTAL STUDY OF GROWTH RATE ENHANCEMENT AND STRUCTURE OF COMPRESSIBLE TURBULENT FREE SHEAR LAYERS Ph.D. Thesis

Yiowha Richard Shau 1990 307 p
Avail: Univ. Microfilms Order No. DA9105659

An experimental investigation was made in a Mach 5 blow-down tunnel of the effects of initial conditions on the growth rate of a high Reynolds number, compressible, turbulent shear layer which is bounded by Mach 5 and 3 air streams. Main pitot pressure profiles were used to determine the growth rate of the shear layers. Also, experiments were conducted to determine if two-point fluctuating pitot pressure measurements can be used to detect and quantify the large-scale structure in the supersonic shear layer. The effects of the initial conditions on the dynamics of the large-scale structures were investigated. Dissert. Abstr.

N91-28518 Ohio State Univ., Columbus.

RECEPTIVITY OF A LAMINAR BOUNDARY LAYER TO THE INTERACTION OF A THREE-DIMENSIONAL ROUGHNESS ELEMENT WITH TIME-HARMONIC FREE-STREAM DISTURBANCES Ph.D. Thesis

Mehran Tadjfar 1990 229 p
Avail: Univ. Microfilms Order No. DA9111804

Receptivity of a laminar boundary layer due to the interaction of time-harmonic free-stream disturbances with a three dimensional roughness element is studied. The three dimensional nonlinear triple-deck equations are solved numerically to provide the basic steady-state motion. It is shown that the governing equations for the unsteady motion are the unsteady linearized three dimensional triple-deck equations. These equations can only be solved numerically. Dissert. Abstr.

N91-28519 Alabama Univ., Huntsville.

NUMERICAL ANALYSES OF AERO-OPTICAL FLOWS: AN APPLICATION OF PARALLEL ALGORITHM ON HIGH-PERFORMANCE PERSONAL COMPUTER (PC) BASE MULTITRANSPUTER SYSTEM Ph.D. Thesis

Stephen C. Chan 1990 178 p
Avail: Univ. Microfilms Order No. DA9113966

Numerical analyses of compressible viscous flow using a personal computer (PC) with a single transputer and a multi-transputer system are presented. Basic features of the aero-optical flows is investigated by using the multidimensional upwind flux difference splitting (UFDS) implicit algorithm to solve the full compressible Navier-Stokes equations. The algorithm is validated and is in good agreement with experimental data. Results confirm that this algorithm has the capability to solve a wide range of fluid problems. Predictions generated by the code replicate the same flow field features for the complex flow phenomenon which aero-optical interactions will encounter. A parallel algorithm of the present computational fluid dynamics (CFD) code is implemented for a PC-based transputer system. A single transputer version and a four-transputer version of transputer CFD code are developed. The singe transputer CFD version is used to compare the significance of turnaround time and machine roundoff errors with four different computers. Comparisons of four transputer CFD results and a single transputer CFD results are also presented. Solutions generated by the transputer do not show any significant roundoff errors. The performance of multiprocessing is below expectations due to a large overhead of synchronization and communication between processors. However, this performance can be improved significantly by some hardware and software modifications. As a whole, the transputer system demonstrates that it is feasible and more economical for CFD computations. Dissert. Abstr.

N91-28520 California Inst. of Tech., Pasadena.

STUDY OF SPHERICAL COUETTE FLOW VIA 3-D SPECTRAL SIMULATIONS: LARGE AND NARROW-GAP FLOWS AND THEIR TRANSITIONS Ph.D. Thesis

Guy Dumas 1991 231 p
Avail: Univ. Microfilms Order No. DA9113597

Incompressible, viscous flows in the spherical gap between a rotating inner-sphere and a stationary outer-shell, Spherical Couette Flows (SCF), are studied via direct numerical simulations. The investigation covers both small-gap and large-gap geometries, and is concerned primarily with the first occurrence of transition in those flows. Strong emphasis is put on the physical understanding of the basic flows and their transition mechanisms. Dissert. Abstr.

N91-28521 North Carolina State Univ., Raleigh.
DIRECT CONTACT HEAT TRANSFER TO A DISPERSAL DROPLET WITH CHANGE OF PHASE Ph.D. Thesis
Nagwa Mahmoud Elshaik 1990 167 p
Avail: Univ. Microfilms Order No. DA9112155

Direct contact, three-phase heat transfer in which latent heat from a dispersed, volatile liquid is transferred to a nonvolatile, immiscible liquid is important to many industrial processes. Here, two modes of evaporation are identified depending on the temperature difference between the dispersed and continuous phase. If the temperature difference is high, the mode is likely to be film boiling in which a droplet is supported in a bubble by a vapor film which flows out from beneath the droplet. The heat transfer responsible for the change in phase takes place across the film. The other mode of evaporation is nucleate boiling in which a thin liquid layer exists at the bottom of the bubble and there is a direct contact heat exchange between the continuous phase and the liquid layer. Analytic models for both film boiling and nucleate boiling were developed. Dissert. Abstr.

N91-28522 Tennessee Univ., Knoxville.
TRANSIENT TWO-PHASE FLOW OF CRYOGENIC FLUID IN A VERTICAL TRANSFER LINE DURING THE COOLDOWN PROCESS Ph.D. Thesis
Ali Hedayatpour 1990 158 p
Avail: Univ. Microfilms Order No. DA9112853

The analytical and numerical modeling for prediction of the thermofluid parameters of the cool down process of a vertical tube carrying cryogenic liquid are presented. Formulation of the problem is based on the flow patterns observed in the experimental studies. In this model, the flow field consists of four distinct regions of fully liquid, inverted annular film boiling, dispersed flow film boiling, and fully vapor. For the fully liquid and fully vapor regions, the 1-D two-fluid model conservation equations are applied. In addition, a 1-D energy equation is formulated to determine the tube wall history. The numerical approximations are based on the finite difference technique. Calculation for inverted annular flow are based on a semi-implicit model while computations for the wall, fully liquid, and dispersed flow regions are performed explicitly. Comparison of calculated results with experimental data for water and liquid nitrogen are presented. Author

N91-28523 Johns Hopkins Univ., Baltimore, MD.
AN EXPERIMENTAL INVESTIGATION OF A COMPLIANT SURFACE BENEATH A TURBULENT BOUNDARY LAYER Ph.D. Thesis
David Earl Hess 1991 201 p
Avail: Univ. Microfilms Order No. DA9113679

The interaction between a passive compliant surface and a turbulent boundary layer was studied using a 0.6 m diameter water tunnel. The key idea was the simultaneous determination of surface displacement and turbulence structure. A standard turbulent boundary layer over a flat plate was identified by measuring the first four moments of the streamwise velocity component. Then, two compliant surfaces, consisting of different mixtures of silicone elastomer and silicone oil, were studied by replacing a rigid insert in the flat plate. Varying the amount and viscosity of the oil in the mix allowed one to alter the response of the surface at a variety of Reynolds numbers of interest; in each case, a stable pattern of small amplitude displacements representing the footprints of individual flow structures was obtained. A localized averaging technique (VITA) was used to study any changes in the bursting process that might occur in the presence of a compliant surface. The results indicate that positive pressure pulses which are known to accompany bursting events in the buffer layer produced associated negative displacements in the compliant material beneath. Dissert. Abstr.

N91-28524 Miami Univ., Coral Gables, FL.
EXPERIMENTAL AND THEORETICAL INVESTIGATION OF UNSTEADY FORCED CONVECTION IN DUCTS Ph.D. Thesis
Weigong Li 1990 275 p
Avail: Univ. Microfilms Order No. DA9114806

An experimental apparatus was designed, built, and used to study transient forced convection in a duct for sinusoidal variation of heat input at the inlet, covering both laminar and turbulent flow. The experimental study covered a wide range of Reynolds numbers and the frequencies of heat input in the thermal entrance region. The temperature variation along the rectangular duct in response to the timewise variation of inlet temperature was recorded and the amplitudes at various locations along the rectangular duct are presented in graphical form. Some of the experimental study was repeated for the thermal entrance region. The effects of the thermal boundary conditions on the amplitude along the length of the duct were studied for various values of the Reynolds number and inlet frequency. A general boundary condition of the fifth kind that accounts for both external convection and wall thermal capacitance effects is considered, and an analytical solution is obtained through extending the generalized integral transform technique. The theoretical dimensionless temperature amplitudes along the duct for both laminar and turbulent flow were compared with experimental findings to provide validation of the mathematical model used. Dissert. Abstr.

N91-28525 Illinois Univ., Urbana-Champaign.
AN EXPERIMENTAL STUDY OF THE EFFECT OF SMALL PARTICLES ON THE FLUID TURBULENCE IN FULLY DEVELOPED FLOW OF AIR IN A HORIZONTAL PIPE Ph.D. Thesis
Lucia M. Liljegren 1990 217 p
Avail: Univ. Microfilms Order No. DA9114317

Measurements of the mean and fluctuating velocities of both the solid and gas phases in a dilute suspension flowing through a 5 in diameter horizontal pipe are presented. Velocity measurements for both phases were obtained using Laser Doppler Velocimetry; signal discrimination was accomplished through application of the Phase Doppler principle. Measurements were performed in air containing spherical glass beads with a volume-mean diameter of approx. 45 microns and flowing with a mean centerline velocity between 17 and 24 m/s. The glass particles were able to respond to the most energetic turbulent disturbances in the fluid. The measured particle velocity intensities in pipe flow were found to exceed the levels predicted on the basis of theoretical analyses and experimental measurements of the particle velocity characteristics in grid turbulence. Dissert. Abstr.

N91-28526 Toledo Univ., OH.
SOLUTION TO QUASI-AXISYMMETRIC INTERNAL COMPRESSIBLE FLOWS USING THE STREAM TUBE APPROACH Ph.D. Thesis
Marwan Zabdawi 1990 246 p
Avail: Univ. Microfilms Order No. DA9112760

A computer code was written to solve for the axisymmetric viscous/inviscid internal compressible flows with variable fluid properties in variable area ducts. Only laminar subsonic or supersonic flows were considered throughout the ducts. Grid resolution was obtained by slicing and refining the flow into cores (stream tubes), which were simulated simultaneously with the numerical solution. The method of influence coefficients was used to develop the nonlinear differential equations for the Mach profile, and the two dimensionality of the pressure field was accounted for by coupling the cores through the use of curvature of the stream tubes. The coupling of the individual cores generated a tri-diagonal matrix at each step and was solved for in an iterative manner by the Thomas algorithm until the core diameters had converged. Both adiabatic and diabatic flows were considered, and a quadratic fit was used for the velocity profile at each step. A fourth-order Runge-Kutta integration technique modified by Gill's constants, was used to solve for the flow parameters.
Dissert. Abstr.

N91-28527# California Univ., Berkeley. Lawrence Berkeley Lab.
A MATHEMATICAL MODEL FOR TWO-PHASE WATER, AIR, AND HEAT FLOW AROUND A LINEAR HEAT SOURCE EMPLACED IN A PERMEABLE MEDIUM

C. Doughty and K. Pruess Mar. 1991 11 p Presented at the ASME/AIChE/ANS National Heat Transfer Conference, Minneapolis, 26-31 Jul. 1991
(Contract DE-AC03-76SF-00098)
(DE91-014614; LBL-30050; CONF-910739-18) Avail: NTIS HC/MF A03

A semianalytical solution for transient two-phase water, air, and heat flow in a uniform porous medium surrounding a constant-strength linear heat source has been developed, using a similarity variable (eta)=r/(radical)t (r is radial distance, t is time). Although the similarity transformation requires a simplified radial geometry, all the physical mechanisms involved in two-phase fluid and heat flow may be taken into account in a rigorous way. The solution includes nonlinear thermophysical fluid and material properties, such as relative permeability and capillary pressure variations with saturation, and density and viscosity variations with temperature and pressure. The resulting governing equations form a set of coupled nonlinear ODEs, necessitating numerical integration. The solution has been applied to a partially saturated porous medium initially at a temperature well below the saturation temperature, which is the setting for the potential nuclear waste repository site at Yucca Mountain, Nevada. The resulting heat and fluid flows provide a stringent test of many of the capabilities of numerical simulation models, making the similarity solution a useful tool for model verification. Comparisons to date have shown excellent agreement between the TOUGH2 simulator and the similarity solution for a variety of conditions. DOE

N91-28528# Los Alamos National Lab., NM.
SHOCK AND RESHOCK OF AN UNSTABLE FLUID INTERFACE
R. F. Benjamin 1991 9 p Presented at the Workshop on Physics of Compressible, Turbulent Mixing, Royaumont (France), 17-19 Jun. 1991
(Contract W-7405-eng-36)
(DE91-014737; LA-UR-91-2003; CONF-9106222-2) Avail: NTIS HC/MF A02

Difficulties with experimental studies of the Richtmyer-Meshkov Instability are examined. We consider optical systems for explosively driven experiments with liquids, and the problems of the interfacial membrane and diffusion in experiments with gases. We show how the membrane induces deviation from impulsive loading of the unstable interface. Also, we summarize recent analyses of our experiments with a perturbed interface between gases, and show how accelerative instabilities can affect an equation-of-state experiment. DOE

N91-28529 Essex Univ., Colchester (England).
NUMERICAL SOLUTION OF A FREE-BOUNDARY VISCOUS FLOW Ph.D. Thesis
Peter Bamidele Shola 1990 126 p
Avail: Univ. Microfilms Order No. BRD-92378

A slow steady 2-D viscous liquid in a trough, set up by the sliding of the horizontal base of its container, with a constant speed in its own plane is considered. Numerical solutions for the shape of the surface of the liquid in the container, as well as descriptions of the flow in the interior of the liquid were obtained for small values of the capillary number, and for a range of values of the other physical parameters which determines the flow. The numerical procedure that was followed is based on the vorticity-stream function iterative approach; the normal stress equations being used to predict the liquid surface. The whole iterative procedure is carried out in a fixed rectangular domain of a plane into which the physical plane is transformed. A critical discussion of the numerical methods employed, and some interpretive remarks concerning the nature of solutions are presented. Dissert. Abstr.

N91-28530 Michigan Univ., Ann Arbor.
USE OF A ROTATED RIEMANN SOLVER FOR THE TWO-DIMENSIONAL EULER EQUATIONS Ph.D. Thesis
David William Levy 1990 159 p
Avail: Univ. Microfilms Order No. DA9116236

A scheme for the 2-D Euler equations that uses flow parameters to determine the direction for upwind differencing is described. This approach exploits the multi-dimensional nature of the equations and reduces the grid dependence of conventional schemes. Several angles are tested as the dominant upwind direction, including the local flow, pressure gradient, and velocity magnitude gradient angles. Roe's approximate Riemann solver is used to calculate fluxes in the upwind direction, as well as for the flux component normal to the upwinding direction. The approach is first tested for 2-D scalar convection, where data used to calculate cell face fluxes are interpolated to lie along characteristic lines. The scheme is shown to have accuracy comparable to a high order MUSCL scheme. A method is also implemented to preserve monotonicity. Solutions of the Euler equations are calculated for a variety of test cases, including channel flows and flows about airfoils. Dissert. Abstr.

N91-28531 Pennsylvania State Univ., University Park.
EXPERIMENTS ON THE INSTABILITIES IN SWIRLING AND NON-SWIRLING FREE JETS Ph.D. Thesis
Jayanta Panda 1990 191 p
Avail: Univ. Microfilms Order No. DA9117730

Instabilities present in a free swirling jet in Reynolds number range from 20,000 to 60,000 and swirl number of 0.45 were studied using smoke visualization and hot wire measurements. A nonswirling jet of Reynolds number 60,000 produced from the same facility was also studied for validation of the experimental procedures and direct comparison with the swirling jet. Time-mean velocity components and turbulence intensity were surveyed using a single hot wire (nonswirling jet) and a V wire (swirling jet) probe. To enhance the understanding of these instabilities, axisymmetric and helical waves were excited in the Strouhal number range 0.75 to 1.5 (swirling jet) and 0.9 to 3.75 (nonswirling jet) by acoustic excitation. Dissert. Abstr.

N91-28532 Michigan State Univ., East Lansing.
THE NUMERICAL SOLUTION OF CONFINED LAMINAR FLOW PAST A MOVING BOUNDARY Ph.D. Thesis
Bashar Sulaiman AbdulNour 1990 213 p
Avail: Univ. Microfilms Order No. DA9117786

The solution of the time-dependent, viscous, incompressible, 2-D, confined flow past a moving boundary is considered. The problem is modeled as a laminar flow in the entry region of a rectangular channel with uniform inlet velocity upstream and a fully-developed parabolic profile downstream. A numerical solution is obtained from the continuity and Navier-Stokes equations and the appropriate boundary conditions. It provides an exact solution over the entire domain, in the sense that it utilizes all terms in the describing equations. The vorticity-stream function formulation is selected for the treatment of the problem. After discretizing the nondimensional governing equations in finite difference form, the Alternating Direction Implicit Method is used to solve the vorticity equation while the iterative Successive Over Relaxation Method is used to solve the stream function equation. The vorticity wall condition is derived by expanding in a Taylor series. This second order scheme maintains the diagonal dominance of the system of equations at high Reynolds number, thereby expanding the domain of convergence. The vorticity, stream function, and velocity components are calculated at each grid point for Reynolds numbers ranging between 10 and 5000. The plane channel flow is investigated first, and this steady flow solution is obtained as the asymptotic solution for a large portion of the unsteady flow. The results of this investigation are presented. Dissert. Abstr.

N91-28533 Cincinnati Univ., OH.
A CRITICAL ANALYSIS OF ANISOTROPIC K-EPSILON MODELING AND ITS APPLICATION TO TURBULENCE-DRIVEN SECONDARY FLOWS Ph.D. Thesis
Peeush Kumar Bishnoi 1990 218 p
Avail: Univ. Microfilms Order No. DA9108604

The nonlinear k-epsilon model of turbulence was analyzed for incompressible internal turbulent flow. The main objective was to evaluate the nonlinear k-epsilon model of Speziale and compare it with the existing two equation nonlinear models. Particular attention was given to the modeling of turbulent flow characteristics near the wall. An extensive survey of the existing low-Reynolds number k-epsilon models was performed, leading to the selection of an appropriate model. Computations were also performed with the 'law-of-the-wall approach' for the wall region. For the fully developed flow considered in a 2-D channel and a square duct, the complete equations were solved in Cartesian-coordinate formulation. Since the main objectives is to evaluate the model, the governing equations for developing turbulent flow in a 2-D channel were simplified. The resulting equations are essentially the modified boundary layer equations that include the streamwise gradients of the normal Reynolds stresses. The governing differential equations were solved using a second-order accurate finite-difference scheme. The discretization of the equations was performed in a transformed computational plane where the grid distribution is uniform. A cubic spline approximation was used to represent the third-order derivative of velocity in the governing equations for developing flow in channel. A finite-difference approximation for these terms was found to be unstable. The tri-diagonal coefficient matrix of the set of discretized equations for the channel flows was inverted using the Thomas algorithm. Correspondingly, a strong implicit procedure was used for the solution of the discretized equations representing the fully developed flow in a straight square duct. The computed results for the three flows examined were compared with a variety of available data, and the results are presented. Dissert. Abstr.

N91-28534 Arizona State Univ., Tempe.
NEAR-WALL MODELLING OF COMPLEX TURBULENT FLOWS Ph.D. Thesis
Yong-Gen Lai 1990 276 p
Avail: Univ. Microfilms Order No. DA9116759

A systematic way to examine the characteristics of near-wall turbulence is presented and a second-order closure is formulated based on near-wall analysis. The proposed model has the properties that the modelled terms satisfy the exact near-wall behavior while a high-Reynolds-number model is recovered far away from the wall. The proposed model is first validated against fully-developed turbulent channel and pipe flow with and without heat transfer in a wide range of Reynolds numbers. The model is then applied to calculate complex turbulent flows such as 2-D curved channel flow and a 3-D curved-pipe flow. Dissert. Abstr.

N91-28535 State Univ. of New York at Buffalo, Amherst.
THE COMPUTATION OF COMPLEX, TWO-DIMENSIONAL TURBULENT FLOWS USING REYNOLDS STRESS CLOSURE Ph.D. Thesis
William Charles Lasher 1990 181 p
Avail: Univ. Microfilms Order No. DA9115114

A framework for computing complex, two dimensional turbulent flows is presented. The turbulence closure problem is defined. Commonly used Reynolds stress closures are reviewed, and strengths and weaknesses of the models are discussed. The finite volume technique, commonly used for these types of calculations, is reviewed, and alternative formulations are discussed. Techniques necessary to ensure numerical stability are discussed. The calculation of turbulent flow over a backward facing step is reviewed. A dilemma in the context of Reynolds averaging is also discussed. Dissert. Abstr.

N91-28536 Council for National Academic Awards (England).
PREDICTION OF THE FLOW AND HEAT TRANSFER BETWEEN A ROTATING AND A STATIONARY CONE Ph.D. Thesis
Nicholas Edward May 1990 370 p
Avail: Univ. Microfilms Order No. BRDX92318

The development of a theoretical method for predicting the turbulent flow and heat transfer in the cavity between a rotating and a stationary cone is discussed. The developed method is the integral method, which reduces the governing partial differential equations to ordinary differential equations. A number of solution methods for these equations are described, and the optimum in terms of speed and accuracy is indicated. A computer program which solves the full Reynolds-averaged Navier-Stokes and energy equations in steady and axisymmetric form, using a finite difference method is modified for use in the conical geometry. Dissert. Abstr.

N91-28537 Washington State Univ., Pullman.
A STUDY ON PARTICLE DISPERSION IN TWO-DIMENSIONAL MIXING LAYER FLOWS Ph.D. Thesis
Feng Wen 1990 140 p
Avail: Univ. Microfilms Order No. DA9116591

The study of solid particle dispersion in mixing layer flows is undertaken to improve the understanding of technological processes and natural phenomena. Mixing layer flows are characterized by large scale vortical structures which grow and interact in time. The particle dispersion model, which is based on the ratio of the particle aerodynamic response time to the large scale structure time scale, is investigated experimentally and numerically. Dissert. Abstr.

N91-28538*# National Aeronautics and Space Administration. Lewis Research Center, Cleveland, OH.
CRYOGENIC TRANSFER OPTIONS FOR EXPLORATION MISSIONS
David J. Chato 1991 12 p Presented at the Conference on Advanced Space Exploration Initiative Technologies, Cleveland, OH, 4-6 Sep. 1991; cosponsored by AIAA and OAI
(NASA-TM-105197; E-6499; NAS 1.15:105197; AIAA-91-3541)
Avail: NTIS HC/MF A03 CSCL 20D

The literature of in-space cryogenic transfer is reviewed in order to propose transportation concepts to support the Space Exploration Initiative (SEI). Forty-nine references are listed and key findings are synopsized. An assessment of the current maturity of cryogenic transfer system technology is made. Although the settled transfer technique is the most mature technology, the No-Vent Fill technology is maturing rapidly. Future options for development of cryogenic transfer technology are also discussed. Author

N91-28232*# Pennsylvania State Univ., University Park. Dept. of Mechanical Engineering.
A STUDY OF METHODS TO INVESTIGATE NOZZLE BOUNDARY LAYER TRANSITION
Laura L. Pauley *In* NASA, Washington, Space Transportation Propulsion Technology Symposium. Volume 2: Symposium Proceedings May 1991 p 717-724 (For primary document see N91-28193 20-20)
Avail: NTIS HC/MF A99 CSCL 20D

N91-28233*# Pennsylvania State Univ., University Park. Dept. of Aerospace Engineering.
OPTICAL DIAGNOSTIC INVESTIGATION OF LOW REYNOLDS NUMBER NOZZLE FLOWS
Michael M. Micci *In* NASA, Washington, Space Transportation Propulsion Technology Symposium. Volume 2: Symposium Proceedings May 1991 p 725-732 (For primary document see N91-28193 20-20)
Avail: NTIS HC/MF A99 CSCL 20D

N91-28890# Korea Advanced Inst. of Science and Technology, Chongryang (Republic of Korea).
ION TEMPERATURE GRADIENT TURBULENCE AND COHERENT STRUCTURES Abstract Only
D. I. Choi, B. G. Hong, F. Romanelli, and M. Ottaviani (Associazione EURATOM-CNEN Sulla Fusione, Frascati, Italy) *In* National Inst. for Fusion Science, Proceedings of the Second International Toki Conference on Plasma Physics and Controlled Nuclear Fusion. Nonlinear Phenomena in Fusion Plasmas: Theory and Computer Simulation Apr. 1991 p 30 (For primary document see N91-28881 20-75)
Avail: NTIS HC/MF A11

N91-28942# Duesseldorf Univ. (Germany, F.R.).
FORMATION AND DYNAMICS OF SOLITARY WAVES AND VORTICES IN DRIVEN AND DAMPED SYSTEMS

K. H. Spatschek, P. Heiermann, E. W. Laedke, V. Naulin, and H. Pietsch *In* National Inst. for Fusion Science, Proceedings of the Second International Toki Conference on Plasma Physics and Controlled Nuclear Fusion. Nonlinear Phenomena in Fusion Plasmas: Theory and Computer Simulation Apr. 1991 p 212-215 (For primary document see N91-28881 20-75)
Avail: NTIS HC/MF A11

35 INSTRUMENTATION AND PHOTOGRAPHY

Includes remote sensors; measuring instruments and gages; detectors; cameras and photographic supplies; and holography.

For aerial photography see *43 Earth Resources and Remote Sensing*. For related information see also *06 Aircraft Instrumentation*, and *19 Spacecraft Instrumentation*.

N91-28539*# Wisconsin Univ., Madison. Dept. of Electrical and Computer Engineering.
SYSTEM AND COMPONENT DESIGN AND TEST OF A 10 HP, 18,000 RPM AC DYNAMOMETER UTILIZING A HIGH FREQUENCY AC VOLTAGE LINK, PART 1 Final Report
Thomas A. Lipo and Irfan Alan Jun. 1991 227 p
(Grant NAG3-940)
(NASA-CR-188442; NAS 1.26:188442) Avail: NTIS HC/MF A11 CSCL 14B

Hard and soft switching test results conducted with one of the samples of first generation MOS-controlled thyristor (MCTs) and similar test results with several different samples of second generation MCT's are reported. A simple chopper circuit is used to investigate the basic switching characteristics of MCT under hard switching and various types of resonant circuits are used to determine soft switching characteristics of MCT under both zero voltage and zero current switching. Next, operation principles of a pulse density modulated converter (PDMC) for three phase (3F) to 3F two-step power conversion via parallel resonant high frequency (HF) AC link are reviewed. The details for the selection of power switches and other power components required for the construction of the power circuit for the second generation 3F to 3F converter system are discussed. The problems encountered in the first generation system are considered. Design and performance of the first generation 3F to 3F power converter system and field oriented induction moter drive based upon a 3 kVA, 20 kHz parallel resonant HF AC link are described. Low harmonic current at the input and output, unity power factor operation of input, and bidirectional flow capability of the system are shown via both computer and experimental results. The work completed on the construction and testing of the second generation converter and field oriented induction motor drive based upon specifications for a 10 hp squirrel cage dynamometer and a 20 kHz parallel resonant HF AC link is discussed. The induction machine is designed to deliver 10 hp or 7.46 kW when operated as an AC-dynamo with power fed back to the source through the converter. Results presented reveal that the proposed power level requires additional energy storage elements to overcome difficulties with a peak link voltage variation problem that limits reaching to the desired power level. The power level test of the second generation converter after the addition of extra energy storage elements to the HF link are described. The importance of the source voltage level to achieve a better current regulation for the source side PDMC is also briefly discussed. The power levels achieved in the motoring mode of operation show that the proposed power levels achieved in the generating mode of operation can also be easily achieved provided that no mechanical speed limitation were present to drive the induction machine at the proposed power level. Author

N91-28540# University Coll. of North Wales, Bangor. School of Mathematics and Computer Science.
MODIFICATION AND EVALUATION OF ELASTOMER TEST MACHINE (ETM) Final Report, 23 Sep. 1988 - 23 Sep. 1990
D. K. Das-Gupta Jan. 1991 32 p
(Contract DAJA45-88-C-0038)
(AD-A236143; R/D-6101-MS-01) Avail: NTIS HC/MF A03 CSCL 14/2

The Elastomer Test Machine (ETM) which was constructed in May 1988 has been modified to include synchronization of the linear table with the Ram Action of the press, a new linear Model 2, measurement of the horizontal force of the sample and a sip ring system for the measurement and control of temperature. The Elastomer samples can now be tested at different temperatures (greater than 140 C) in the stationary impact mode, in two linear abrasion mode and in a rotational mode (and combinations thereof). Temporal qualitative data on load and displacement can be recorded which may provide a qualitative analysis of the elastomer degradation process. A comprehensive set of test data were obtained with the ETM using all the modes for 57 different elastomer samples, provided by the US Army (51 samples) and the US Navy (6 samples). The ETM tests provide a performance analysis of any track pad elastomer material and may predict a projected service life. GRA

N91-28541# Tennessee Univ., Tullahoma. Space Inst.
A PC BASED FREQUENCY DOMAIN LV PROCESSOR
T. C. Layne, T. V. Giel, Jr., and R. L. Clippard 1991 17 p
Presented at the 4th International Conference on Laser Anemometry, Cleveland, 5-9 Aug. 1991
(Contract DE-AC02-79ET-10815)
(DE91-009056; DOE/ET-10815/157; CONF-910861-1) Avail: NTIS HC/MF A03

A PC based laser Doppler velocimeter (LV) data system was developed. The data system uses frequency domain processing for multiple component LV individual signal realization. The system is based on a standard add in board for IBM PC's which has a transient digitizer and programmable digital signal processor (DSP) on board. Custom software written for both the general purpose DSP and the PC is described. The DSP is programmed to implement the frequency domain LV signal processor and the PC is programmed to provide a user interface and data archiving capability. The resulting data system is a low cost alternative to dedicated commercial velocimeter signal processors. Furthermore, the general purpose utility of the PC is still available when LV signal acquisition and processing is not active. Typical optical signal data processing is presented to illustrate data system performance. DOE

N91-28542# Lawrence Livermore National Lab., CA.
X RAY FIDUCIAL FOILS
C. Alford, F. Serduke, D. Makowiecki, A. Jankowski, and M. Wall 13 Mar. 1991 21 p Presented at the International Conference on Metallurgical Coatings and Thin Films (ICMCTF), Waldorf, 22-26 Apr. 1991
(Contract W-7405-eng-48)
(DE91-011193; UCRL-JC-105704; CONF-9104231-2) Avail: NTIS HC/MF A03

An x-ray spectrum from a laser fusion experiment was passed through an Al, Si, Y multilayer foil. The position of the absorption edges of the Al, Si, and Y was used to calibrate the x-ray energy spectrum recorded on photographic film. The foil consisted of 4000 A of Al, 6000 A of Si, and 4000 A of Y sputter deposited on a 1.5 microns thick Mylar film. It was necessary to layer the structure in order to achieve the required mechanical strength and dimensional stability. The results include analysis of the x-ray energy spectrum and microstructural characterization of the foil using x-ray diffraction and transmission electron microscopy. DOE

N91-28543# Sandia National Labs., Albuquerque, NM.
AN EVALUATION OF MONOCHROME SOLID-STATE VIDEO CAMERAS
D. A. Greenwoll Apr. 1991 99 p
(Contract DE-AC04-76DP-00789)
(DE91-012368; SAND-90-2533) Avail: NTIS HC/MF A05

The parameters used to select and evaluate monochrome (black and white) solid-state imager closed circuit television cameras used in perimeter video assessment systems are discussed. Ten current-production makes and models of cameras were evaluated for sensitivity, resolution, and image quality. Comparisons in these parameters were made to thermionic image-tube cameras. DOE

N91-28544# Sandia National Labs., Albuquerque, NM.

A CONTROLLED DISPERSION PARALLEL WAVELENGTH X RAY SPECTROMETER FOR ELECTRON MICROSCOPY

C. E. Fiori, S. A. Wight (National Inst. of Standards and Technology, Gaithersburg, MD.), and A. D. Romig, Jr. 1991 4 p Presented at the 25th Annual Microbeam Analysis Society Meeting, San Jose, 4-9 Aug. 1991

(Contract DE-AC04-76DP-00789)

(DE91-012011; SAND-91-1056C; CONF-910872-4) Avail: NTIS HC/MF A01

A new technique is described for the detection of x rays in electron column instruments used in microanalysis. In electron column instruments, the point source of x rays is produced by the interaction of a focused electron beam with the sample. Neither of the conventional methods, wavelength dispersive (WDS) nor energy dispersive (EDS) based spectrometry, is optimized for low Z element quantitative analysis. In WDS applications, where the analyte elements are Be through P, chemical effects complicate the x ray measurement process. Peak positions and shapes are altered, sometimes very strongly, by the electron configurations of the analyte atoms and neighboring atoms. In these cases, the ideal spectrometer would profile the peak and some small amount of continuum on either side of the peak such that an accurate peak area could be calculated. Present WDS spectrometers are serial in nature and cannot directly measure peak areas, often causing errors in the determination of light element concentrations. Bastin and co-workers have developed an elegant method to provide accurate area determinations, using the serial spectrometer, by a three point procedure. The parallel wavelength dispersive spectrometer (PWDS) proposed here is ideally suited for those applications. DOE

N91-28545# Los Alamos National Lab., NM.

A MICROWAVE INTERFEROMETER TO MEASURE PARTICLE AND SHOCK VELOCITIES SIMULTANEOUSLY

G. G. Luther, L. Vesser, and B. Warthen (EG and G Energy Measurements, Inc., Los Alamos, NM.) 1991 10 p Presented at the 1991 American Physical Society (APS) Conference on Shock Compression of Condensed Matter, Williamsburg, 17-20 Jul. 1991

(Contract W-7405-eng-36)

(DE91-013077; LA-UR-91-1636; CONF-9107105-15) Avail: NTIS HC/MF A02

A microwave interferometric technique has been developed which measures the particle velocity, the shock velocity and gives information as to the index of refraction of the shocked material. The system has been tested at X-band from 40 to 300 kBAR. Experiments are underway to extend the frequency into the K-band and the pressure range to 600 kBAR. The apparatus will be described and data presented. DOE

N91-28546*# National Aeronautics and Space Administration. Langley Research Center, Hampton, VA.

PRESSURE TRANSDUCER AND SYSTEM FOR CRYOGENIC ENVIRONMENTS Patent Application

John J. Chapman, inventor (to NASA) 23 Apr. 1991 31 p

(NASA-Case-LAR-14579-1; NAS 1.71:LAR-14579-1; US-Patent-Appl-SN-690198) Avail: NTIS HC/MF A03 CSCL 14B

A silicon pressure die is bonded to a borosilicate substrate above the pneumatic port. A Wheatstone bridge circuit is formed on the silicon pressure die and has bridge elements of silicon doped with boron to a deposit density level of approximately 1 x 10(exp 19)-10(exp 21) boron/cu cm. A current source is provided to excite the Wheatstone bridge circuit. In addition, a temperature sensor is provided to provide temperature readings. An array may be formed of the resulting pressure transducers. This unique solution of materials permits operation of a pressure transducer in cryogenic environments. NASA

N91-28547 Stanford Univ., CA.

PHONON-MEDIATED DETECTION OF ELEMENTARY PARTICLES USING SILICON CRYSTAL ACOUSTIC DETECTORS Ph.D. Thesis

Betty Aileen Young 1991 148 p

Avail: Univ. Microfilms Order No. DA9115868

A research group at Stanford is developing Silicon Crystal Acoustic Detectors (SiCADs) which operate at cryogenic temperatures and sense phonons generated when an incident particle scatters off a nucleus or electron in the crystalline Si wafer substrate. In the present design photon sensors consist of a thin film labyrinth pattern of superconducting titanium, which is dc current biased at a temperature just below its superconducting to normal transition (approx. 430 mK). The motivation for developing SiCADs includes their many direct applications to neutrino physics, particle astrophysics, and solid state physics. Dissert. Abstr.

N91-28548# California Univ., Berkeley. Lawrence Berkeley Lab.

ADVANCING CONVENTIONAL HIGH-RESOLUTION ELECTRON MICROSCOPY

R. Gronsky Mar. 1991 5 p Presented at the 49th Electron Microscopy Society of America (EMSA) Annual Meeting, San Jose, 4-9 Aug. 1991

(Contract DE-AC03-76SF-00098)

(DE91-013773; LBL-30549; CONF-910870-15) Avail: NTIS HC/MF A01

Due to the exceptional performance of most modern commercial transmission electron microscopes, the achievement of phase-contrast imaging resolution in the sub-2 A range is today a routine exercise, provided the samples are compliant. Nonetheless, there remains room for improvement, and the purpose of this manuscript is to highlight procedures that might be employed by the practicing microscopist for advancing conventional high resolution electron microscopy. DOE

N91-28549# EG and G Energy Measurements, Inc., Las Vegas, NV.

MEASURING NEUTRON FLUENCES AND GAMMA/X RAY FLUXES WITH CCD CAMERAS

G. J. Yates, G. W. Smith (Atomic Weapons Research Establishment, Aldermaston, England), P. Zagarino, and M. C. Thomas 1991 37 p Presented at the IEEE Annual International Nuclear and Space Radiation Effects Conference, San Diego, 15-19 Jul. 1991

(Contract DE-AC08-88NV-10617)

(DE91-014119; EGG-10617-2095; CONF-910751-9) Avail: NTIS HC/MF A03

Volume and area measurements of transient radiation-induced pixel charge in English Electric Valve (EEV) Frame Transfer (FT) charge coupled devices (CCDs) from irradiation with pulsed neutrons (14 MeV) and Bremsstrahlung photons (16-MeV endpoint) are utilized to calibrate the devices as radiometric imaging sensors capable of distinguishing between the two types of ionizing radiation. Measurements indicate approximately 0.5 V/rad responsivity with greater than or equal to 1 rad required for saturation from photon irradiation. Neutron-generated localized charge centers or 'peaks' binned by area and amplitude as functions of fluence in the 10(exp 5) to 10(exp 7) n/sq cm range indicate smearing over approximately 1 to 10 percent of CCD array with charge per pixel ranging between noise and saturation levels. DOE

N91-28550# Oak Ridge National Lab., TN.

THIN FILM HYDROGEN SENSOR

R. J. Lauf and B. S. Hoffheins 1991 9 p Presented at the Hydrogen Leak Detection Interchange Meeting, Houston, 4-5 Jun. 1991

(Contract DE-AC05-84OR-21400)

(DE91-014197; CONF-9106214-1) Avail: NTIS HC/MF A02

A miniature, solid state hydrogen sensor intended for use wherever one needs to selectively detect the presence of gaseous hydrogen was designed, constructed, and tested. A notable feature of this sensor is that it is insensitive to the presence or absence of air inert gases, etc. The design is inherently simple, rugged, and stable, and can be manufactured by standard techniques. The concept of operation relies on the fact that when palladium metal is exposed to hydrogen gas it rapidly comes to equilibrium by absorbing hydrogen. Most hydrogen partial pressures of interest (10(exp -3) to 1 psia) will be in equilibrium with the palladium/hydrogen solid solution (alpha-phase). The electrical resistivity of the solid solution will depend on its hydrogen concentration. A the same time, palladium will not be adversely affected by other species such as oxygen and water. DOE

36 LASERS AND MASERS

Includes parametric amplifiers.
For related information see also *76 Solid-State Physics.*

N91-28551# Lawrence Livermore National Lab., CA.
MODAL STUDY OF REFRACTIVE EFFECTS ON X RAY LASER COHERENCE
P. Amendt, R. A. London, and M. Strauss (Israel Atomic Energy Commission, Beersheba.) Apr. 1991 7 p Presented at the Conference on Short-Wavelength Coherent Radiation: Generation and Application, Monterey, 4-10 Apr. 1991
(Contract W-7405-eng-48)
(DE91-012083; UCRL-JC-105736; CONF-9104164-3) Avail: NTIS HC/MF A02

The role of smoothly varying transverse gain and refraction profiles on x-ray laser intensity and coherence is analyzed by modally expanding the electric field within the paraxial approximation. Comparison with a square transverse profile reveals that smooth-edged profiles lead to: (1) a greatly reduced number of guided modes, (2) the continued cancellation of local intensity from a loosely guided mode by resonant free modes, (3) and the absence of extraneous (or anomalous) free mode resonances. These generic spectral properties ,should enable a considerable simplification in analyzing and optimizing the coherence properties of laboratory soft x-ray lasers. DOE

N91-28552# Stanford Linear Accelerator Center, CA.
SIMULATION OF A STORAGE RING FREE ELECTRON LASER WITH A MAPPING ALGORITHM FOR DISTRIBUTION FUNCTIONS
V. Ziemann May 1991 3 p Presented at the 1991 Institute of Electrical and Electronics Engineers (IEEE) Particle Accelerator Conference (PAC), San Francisco, 6-9 May 1991
(Contract DE-AC03-76SF-00515)
(DE91-012387; SU-SLAC-PUB-5478; CONF-910505-71) Avail: NTIS HC/MF A01

A model for the simulation of the time dependent behavior and the analysis of the equilibrium of the coupled system of storage ring and Free Electron Laser (FEL) is presented. The analysis comprises both amplifier and oscillator FEL. Bunch lengthening and energy widening due to wake forces are taken into account in a self-consistent way. The method is based on a mapping algorithm for means and correlations of the electron distribution function, pioneered by K. Hirata. The evolution of the laser field in the oscillator FEL is described by supermodes. The model is used to simulate an FEL in a small 500 MeV storage ring with 100 m circumference. Typical values for the output power, spatial, and spectral characteristics of the emitted radiation are presented. DOE

N91-28553# Sandia National Labs., Albuquerque, NM.
DIFFRACTION PATTERNS PRODUCED BY PERIODIC AND TURBULENT FLOWING GASES INCLUDING APPLICATIONS OF PHOTOREFRACTIVE TEMPORAL FILTERING
A. Corvo May 1991 55 p
(Contract DE-AC04-76DP-00789)
(DE91-012636; SAND-91-0121) Avail: NTIS HC/MF A04

The diffraction patterns produced by passing a laser beam through two different types of flowing gases are calculated. The first type of flow consists of periodic lines of gas flowing transverse to the beam's propagation. The second flow is turbulent. The measurable parameters in the diffraction patterns are derived and related to the gas temperature, pressure, velocity, and (in the case of the turbulent flow) to the flow's structure constant. A discussion on using the photorefractive effect to study turbulent flows is also given. In the latter case a method that relates the flow's structure constant to the decay time of the photorefractive crystal is given. DOE

N91-28554# Oak Ridge National Lab., TN.
LASER EJECTION OF Ag(SUP +) IONS FROM A ROUGHENED SILVER SURFACE: ROLE OF THE SURFACE PLASMON
M. J. Shea (Vanderbilt Univ., Nashville, TN.) and R. N. Compton 1991 5 p Presented at the HASRD Workshop on Laser Ablation: Mechanisms and Application, Oak Ridge, 8-10 Apr. 1991
(Contract DE-AC05-84OR-21400)
(DE91-012945; CONF-9104192-5) Avail: NTIS HC/MF A01

Laser irradiation of metal surfaces with sufficiently intense light gives to laser produced plasmas. Previously, plasmas from the metals Mg, Bi, Pd, Al, Cu, and Au were studied. The laser plasma occurred with a sudden threshold in laser power. Laser irradiation yielded thermal ions at laser powers less than the plasma thershold, a full plasmas occurred upon reaching the plasma threshold. A detailed study of laser plasma production for palladium loaded with hydrogen (deuterium) has been published. The mass-resolved ion kinetic energy distributions are determined in order to study the physics of laser ablation. The kinetic energy distributions (KEDs) of silver ions exhibit a marked departure from the KEDs of other laser produced plasmas. In addition to the thermal ions, a second peak at 3.6 eV (FWHM = 2 eV) appeared for laser energies below the onset of plasma formation. DOE

N91-28555# Oak Ridge National Lab., TN.
EVAPORATION AS A DIAGNOSTIC TEST FOR HYDRODYNAMIC COOLING OF LASER-ABLATED CLUSTERS
C. E. Klots 1991 3 p Presented at the HASRD Workshop on Laser Ablation: Mechanisms and Application, Oak Ridge, 8-10 Apr. 1991
(Contract DE-AC05-84OR-21400)
(DE91-013416; CONF-9104192-8) Avail: NTIS HC/MF A01

The properties of materials laser-ablated from a surface are of considerable interest. The interrogation of these properties inevitably occurs at a point some distance from the surface. One might then ask what processes have occurred in the intervening path length. Immediately, for example, one wonders whether the material was released as such from the surface or was formed as a result of collisions at a distant point. Similarly, one might ask if an observed temperature of the materials is characteristic of the ablation process of of subsequent events. We will indicate here how measurements of metastable evaporation rates can provide clues which are pertinent to these questions. DOE

N91-28556# Los Alamos National Lab., NM.
X RAY GENERATION BY HIGH IRRADIANCE EXAWATT/SQ CM SUBPICOSECOND LASERS
G. A. Kyrala, R. D. Fulton, D. E. Casperson, E. K. Wahlin, L. A. Jones, G. T. Schappert, J. A. Cobble, and A. J. Taylor 1991 17 p Presented at the Conference on Short-Wavelength Coherent Radiation: Generation and Application, Monterey, 4-10 Apr. 1991
(Contract W-7405-eng-36)
(DE91-013497; LA-UR-91-1526; CONF-9104164-5) Avail: NTIS HC/MF A03

We have studied the interaction of 290-fsec, 308-nm laser pulses with aluminum targets at irradiances exceeding 5 times 10(exp 18) W/sq cm (5 EW/sq cm). The x-ray spectrum shows a hot electron component with a characteristic temperature of 30 keV, and a low temperature component of 1 keV. Imaging of the x-rays shows an emission region of few micrometers for the hot component and a larger region for the 1 keV emission. The X-ray spectrum is dominated by the hydrogen and helium like lines from aluminum, with the brightest lines radiating 0.6 percent of the incident laser light energy. The spectral luminosity of the L(sub alpha) line was measured to be 3 times 10(exp 14) W/sq cm/eV/sr. DOE

N91-28557*# National Aeronautics and Space Administration. Goddard Space Flight Center, Greenbelt, MD.

EDGE TECHNIQUE FOR MEASUREMENT OF LASER FREQUENCY SHIFTS INCLUDING THE DOPPLER SHIFT Patent Application

Larry Korb, inventor (to NASA) 20 May 1991 39 p
(NASA-Case-GSC-13343-1; NAS 1.71:GSC-13343-1; US-Patent-Appl-SN-702529) Avail: NTIS HC/MF A03 CSCL 20E

A method is disclosed for determining the frequency shift in a laser system by transmitting an outgoing laser beam. An incoming laser beam having a frequency shift is received. A first signal is acquired by transmitting a portion of the incoming laser beam to an energy monitor detector. A second signal is acquired by transmitting a portion of the incoming laser beam through an edge filter to an edge detector, which derives a first normalized signal which is proportional to the transmission of the edge filter at the frequency of the incoming laser beam. A second normalized signal is acquired which is proportional to the transmission of the edge filter at the frequency of the outgoing laser beam. The frequency shift is determined by processing the first and second normalized signals. NASA

N91-28558# Los Alamos National Lab., NM.

TIME-RESOLVED EMITTANCE MEASUREMENTS OF AN EXCIMER-LASER-DRIVEN METAL PHOTOCATHODE

T. Kauppila, R. Carlson, D. Moir, and R. Ridlon 1991 4 p
Presented at the 1991 Institute of Electrical and Electronics Engineers (IEEE) Particle Accelerator Conference (PAC), San Francisco, 6-9 May 1991
(Contract W-7405-eng-36)
(DE91-013066; LA-UR-91-1451; CONF-910505-154) Avail: NTIS HC/MF A01

The velvet cathode material of a 4-MeV, electron beam injector was replaced with a metal cathode and driven by an ArF excimer laser. Time resolved measurements of photo electron current and effective cathode temperature were made. A streak camera and B-dot (magnetic field) probes were the primary diagnostics for the experiment. The streak camera determined effective cathode temperature in a single spatial dimension. Time integrated photography was used to observe plasma formation in the cathode region. The results will be used to ascertain the feasibility of long pulse (75 ns) beam generation for injection into a linear induction accelerator. DOE

N91-28559# Lawrence Livermore National Lab., CA.

IRRADIANCE COMPENSATION CONTROL FOR HIGH-ENERGY LASER PROPAGATION. PART 1: THEORY AND FOURIER CONTROL MODEL PROPAGATION RESULTS

J. R. Morris, D. Gavel, and T. J. Karr 18 Apr. 1991 23 p
(Contract W-7405-eng-48)
(DE91-013130; UCRL-ID-107112-Pt-1) Avail: NTIS HC/MF A03

Irradiance compensation is a method of reducing the effect of small-scale perturbation growth on ground-to-space propagation of high power laser beams. A technique is described for irradiance compensation that uses a pair of continuous faceplate discrete actuator mirrors to approximate ideal bandlimited compensation. No mirror technology beyond that already developed for phase compensation is needed. One mirror imposes a phase on the high power beam which is converted into the desired irradiance profile by propagation. The other mirror removes the phase generated by the first mirror and by propagation. The equations are described that give the required phase at the first mirror in terms of the irradiance to be created by propagation to the second mirror. Simulations are described of this technique with the ORACLE thermal blooming code. After the irradiance compensation the resulting beam is return-wave phase compensated for the phase distortion in the atmosphere, and it is propagated through the atmosphere. Both the irradiance and the phase compensation were modeled using Fourier filters to describe the discrete mirrors. Results of the simulations are almost the same as for ideal irradiance compensation, i.e., propagation remains stable at power levels 2 to 3 times higher than that for phase compensation alone. This indicates that the next step in evaluating the utility of irradiance compensation is worthwhile. The control model for this next step is described in Part 2. DOE

N91-28560# Lawrence Livermore National Lab., CA.

RING-LASER SOLITONS: A MULTIPASS APPROACH

R. J. Hawkins and Y. Yamamoto (Nippon Telegraph and Telephone Public Corp., Tokyo, Japan) 27 Nov. 1990 7 p Presented at the CLEO 1991: Conference on Lasers and Electro-Optics, Baltimore, 12-17 May 1991
(Contract W-7405-eng-48)
(DE91-013242; UCRL-JC-105481; CONF-910595-11) Avail: NTIS HC/MF A02

We show that higher-order solitons are possible in ring lasers by deriving a modified nonlinear Schroedinger equation based on the discrete-element structure of the ring laser and discuss the implications of this derivation for soliton propagation in these lasers. DOE

N91-28561# Lawrence Livermore National Lab., CA.

HIGH-PEAK POWER-Nd:GLASS LASER FACILITIES FOR END USERS

J. T. Hunt 18 Jan. 1991 28 p Presented at the OE/LASE 1991: 4th Society of Photo-Optical Instrumentation Engineers (SPIE) International Symposium, Los Angeles, 20-25 Jan. 1991
(Contract W-7405-eng-48)
(DE91-013246; UCRL-JC-105998; CONF-910123-32) Avail: NTIS HC/MF A03

The emphasis in developing the inertial confinement fusion (ICF) systems has been on increasing the power and energy of the laser. In particular, at Lawrence Livermore National Laboratory (LLNL), the power and energy per beamline has increased approximately tenfold for each new generation of laser with a concomitant decrease in cost achieved. The decrease in cost was with both technology development and economy of scale. However, up until now, we have not looked back and asked the question: How does one make the present and earlier generation Nd:Glass lasers smaller, less complex, simple to operate, and more affordable? In this context, our goal is to produce a set of laser system designs from which could be constructed an affordable laser with beam powers ranging from one to ten terawatts and beam energies between 10 and 1000 joules. The design of these systems would be flexible enough that frequency converters could be added to provide target irradiation wavelength capability from one micron down to the ultraviolet. Similarly, the capability to add a reasonable range of temporal pulse shapes and the capability to compress the temporal pulse could be accommodated in these designs. A secondary goal is to keep development costs to a minimum by using only modest extrapolations of today's technologies. DOE

N91-28562# Sandia National Labs., Albuquerque, NM.

STUDIES OF LASER-DRIVEN FLYER ACCELERATION USING OPTICAL FIBER COUPLING

W. M. Trott 1991 17 p Presented at the 1991 American Physical Society (APS) Conference on Shock Compression of Condensed Matter, Williamsburg, 17-20 Jul. 1991
(Contract DE-AC04-76DP-00789)
(DE91-013503; SAND-91-0148C; CONF-9107105-19) Avail: NTIS HC/MF A03

An optically recording velocity interferometer system has been used to measure acceleration histories and maximum velocities for laser-driven aluminum foil targets launched from the output face of optical fibers. Peak flyer velocities have been determined as a function of various parameters, including driving laser fluence, laser pulse duration and target thickness. The results at high fluences are consistent with a nearly constant efficiency of coupling optical energy into flyer kinetic energy and a small ablated mass fraction; however, the coupling efficiency falls off rapidly at fluences less than 15 J-cm(exp -2). Measurement of the time delay between laser pulse arrival at the target and the onset of flyer motion have also been performed. Significant delays are observed at low fluences, arising from the increased time required for plasma formation at the fiber/foil interface under these conditions. DOE

N91-28563# Los Alamos National Lab., NM.
E-BEAM ACCELERATOR CAVITY DEVELOPMENT FOR THE GROUND-BASED FREE ELECTRON LASER
N. K. Bultman and G. Spalek 1991 5 p Presented at the 1991 Institute of Electrical and Electronics Engineers (IEEE) Particle Accelerator Conference (PAC), San Francisco, 6-9 May 1991
(Contract W-7405-eng-36)
(DE91-013760; LA-UR-91-1495; CONF-910505-227) Avail: NTIS HC/MF A01

Los Alamos National Laboratory is designing and developing four prototype accelerator cavities for high power testing on the Modular Component Technology Development (MCTD) test stand at Boeing. These cavities provide the basis for the e-beam accelerator hardware that will be used in the Ground Based Free Electron Laser (GBFEL) to be sited at the White Sands Missile Range (WSMR) in New Mexico. DOE

N91-28564# Los Alamos National Lab., NM.
H(-) BEAM CHARACTERIZATION USING LASER-INDUCED NEUTRALIZATION
V. W. Yuan, R. Garcia, K. F. Johnson, K. Saadatmand, O. R. Sander, D. Sandoval, and M. Shinas 1991 4 p Presented at the 1991 Institute of Electrical and Electronics Engineers (IEEE) Particle Accelerator Conference (PAC), San Francisco, 6-9 May 1991
(Contract W-7405-eng-36)
(DE91-013501; LA-UR-91-1522; CONF-910505-172) Avail: NTIS HC/MF A01

The laser-induced neutralization techniques (LINDA) are important as a noninterceptive diagnostic for quantitatively measuring beam emittance values. It is also valuable for its capability to characterize, both quantitatively and qualitatively, the performance and match of linac components. We present LINDA experimental results that show how the output beam of a radio-frequency quadrupole (RFQ) and drift-tube linac (DTL) combination changes with the variation of RFQ-DTL relative phase and of DTL cavity power. We also present results showing the effect of a longitudinal buncher on beam emissions. DOE

N91-28565# Los Alamos National Lab., NM.
PERFORMANCE OF THE PHOTOINJECTOR ACCELERATOR FOR THE LOS ALAMOS FREE-ELECTRON LASER
P. G. OShea, S. C. Bender, B. E. Carlsten, J. W. Early, D. W. Feldman, R. B. Feldman, W. J. D. Johnson, A. H. Lumpkin, R. L. Sheffield, and R. W. Springer et al 1991 4 p Presented at the 1991 Institute of Electrical and Electronics Engineers (IEEE) Particle Accelerator Conference (PAC), San Francisco, 6-9 May 1991
(Contract W-7405-eng-36)
(DE91-013682; LA-UR-91-1535; CONF-910505-186) Avail: NTIS HC/MF A01

The Los Alamos free-electron laser (FEL) facility has been greatly modified by the replacement of the thermionic electron gun and bunchers with a 1300 MHz RF photoinjector. Two more accelerator tanks were added to increase the beam energy to 40 MeV. Preliminary studies at 15 MeV demonstrated excellent beam quality with a normalized emittance of 40 (pi) mm-mrad. The beam quality is now sufficient to allow harmonic lasing in the visible. At present FEL experiments are beginning at a wavelength near 3 microns. The performance of the photoinjector accelerator is examined. DOE

N91-28566# Los Alamos National Lab., NM.
SHORT WAVELENGTH FELS
R. L. Sheffield 1991 6 p Presented at the 1991 Institute of Electrical and Electronics Engineers (IEEE) Particle Accelerator Conference (PAC), San Francisco, 6-9 May 1991
(Contract W-7405-eng-36)
(DE91-013759; LA-UR-91-1500; CONF-910505-230) Avail: NTIS HC/MF A02

The generation of coherent ultraviolet and shorter wavelength light is presently limited to synchrotron sources. The recent progress in the development of brighter electron beams enables the use of much lower energy electron RF linacs to reach short-wavelengths than previously considered possible. This paper will summarize the present results obtained with synchrotron sources, review proposed short-wavelength free electron laser (FEL) designs and then present a new design which is capable of over an order of magnitude higher power to the extreme ultraviolet. DOE

N91-28567# Sandia National Labs., Albuquerque, NM.
NUMERICAL AND ANALYTICAL ANALYSIS OF THIN LASER-DRIVEN FLYER PLATES
A. V. Farnsworth, Jr. and R. J. Lawrence 1991 5 p Presented at the 1991 American Physical Society (APS) Conference on Shock Compression of Condensed Matter, Williamsburg, 17-20 Jul. 1991
(Contract DE-AC04-76DP-00789)
(DE91-013748; SAND-91-0197C; CONF-9107105-28) Avail: NTIS HC/MF A01

When a short high-intensity laser pulse is transmitted through a small diameter optical fiber onto a thin metallic foil placed on the fiber end, the inner surface of the foil is explosively vaporized and the bulk of the flyer material is driven off at high velocities. Experiments have been performed, in which the foil velocity has been monitored with time, for a variety of energies, pulse lengths, and fiber diameters. We have compared the data with results of both analytical and computational investigations. The two-dimensional radiation hydrodynamics code, LASNEX, has been used to provide detailed predictions of the acceleration histories, taking into account the reflection, deposition, and re-radiation processes in the driving plasma. Careful comparison with data has increased our understanding of the governing processes. The late-time velocity of the flyer has been studied using a simple model employing global conservation of mass, momentum and energy in conjunction with the well-known Gurney theory for explosively driven flyer plates. Together, these techniques have allowed quite complete understanding of the phenomena, and it has been possible to match most of the features seen in the expanding body of experimental data. DOE

N91-28568# Lawrence Livermore National Lab., CA.
REDUCTION OF ENERGY SWEEP OF THE ETA-2 BEAM
W. E. Nexsen, S. L. Allen, F. W. Chambers, R. A. Jong, A. C. Paul, S. E. Sampayan, and W. C. Turner May 1991 5 p Presented at the 1991 Institute of Electrical and Electronics Engineers (IEEE) Particle Accelerator Conference (PAC), San Francisco, 6-9 May 1991
(Contract W-7405-eng-48)
(DE91-013824; UCRL-JC-105557; CONF-910505-235) Avail: NTIS HC/MF A01

The ETA-2 electron beam will be used to drive a high power microwave frequency FEL for plasma heating experiments. For maximum FEL output power the beam energy at the entrance to the wiggler should be within +/- 1 percent of the wiggler resonance value. In initial operations the ETA-2 beam energy stayed within this range for a maximum time of less than 13 ns. Much of the energy variation was due to the design of the pulsed power feeds to the accelerator induction cells. A new multicable pulsed power feed design was tested in a shortened version of ETA-2 where it extended the time during which the beam energy stayed within the +/- 1 percent limits to greater than 40 ns. These design changes are now being incorporated into the full accelerator. DOE

N91-28569# Brookhaven National Lab., Upton, NY.
BEAM EMITTANCE AND THE EFFECTS OF THE RF, SPACE CHARGE AND WAKE FIELDS: APPLICATION TO THE ATF PHOTOELECTRON BEAM
Z. Parsa 1991 3 p Presented at the 1991 Institute of

Electrical and Electronics Engineers (IEEE) Particle Accelerator Conference (PAC), San Francisco, 6-9 May 1991
(Contract DE-AC02-76CH-00016)
(DE91-014789; BNL-46191; CONF-910505-329) Avail: NTIS HC/MF A01

Laser driven photoelectron guns are of interest for use in new methods of accelerations, future development of Linear Colliders, and new experiments such as Free Electron Laser (FEL) and Inverse Free Electron Laser (IFEL) experiments. Such guns are potential source of low emittance-high current and short bunch length electron beams, where the emitted electrons are accelerated quickly to a relativistic energy by a strong rf, electric field in the cavity. We present a brief overview of the beam dynamic studies, e.g., emittance for the Brookhaven National Laboratory (BNL) ATF high brightness photocathode radio frequency gun (now in operation), and show the effects of the rf, Space Charge, and Wake fields on the photoelectrons. DOE

N91-28570# Oak Ridge National Lab., TN.
LASER RANGE CAMERA CALIBRATION
K. Storjohann and E. Saltzen Jul. 1991 17 p
(Contract DE-AC05-84OR-21400)
(DE91-014939; ORNL/TM-11723) Avail: NTIS HC/MF A03

This paper describes an imaging model that was derived for use with a laser range camera (LRC) developed by the Advanced Intelligent Machines Division of Odetics. However, this model could be applied to any comparable imaging system. Both the derivation of the model and the determination of the LRC's intrinsic parameters are explained. For the purpose of evaluating the LRC's external orientation (extrinsic parameters), a transformation of the LRC's imaging model into a standard camera's (SC) pinhole model is derived. By virtue of this transformation, the evaluation of the LRC's external orientation can be found by applying any SC calibration technique. Experimental results prove the accuracy of the derived camera model as well as the proposed calibration procedure. DOE

N91-28571# Lawrence Livermore National Lab., CA.
PLATINUM SOLUBILITY IN PHOSPHATE LASER GLASS
Y. T. Hayden, J. H. Campbell, S. A. Payne, and G. D. Wilke 12 Jun. 1991 16 p Presented at the 93rd Annual Meeting and Exposition of the American Ceramic Society (ACerS), Cincinnati, 28 Apr. - 2 May 1991
(Contract W-7405-eng-48)
(DE91-015123; UCRL-JC-105475; CONF-910430-15) Avail: NTIS HC/MF A03

Microscopic platinum inclusions (approximately 10 to 20 microns), that originate from the melt containers, have been a major cause of optical damage in phosphate laser glasses. One way to eliminate such inclusions is to dissolve them in the glass matrix. The relative solubility of platinum in three commercial phosphate laser glasses is reported. The results show that the lowest Al2O3-containing phosphate glass has the highest Pt solubility. Moreover, the Pt solubility decreases linearly with increasing, Al2O3 content. Activation energies for Pt dissolution are found to be nearly equivalent for the three glasses. Laser-excited fluorescence of the Pt-ion is reported. DOE

N91-28572 Stanford Univ., CA.
NUMERICAL INVESTIGATION OF THE THRUST EFFICIENCY OF A LASER-PROPELLED VEHICLE Ph.D. Thesis
James Randolph Mulroy 1991 172 p
Avail: Univ. Microfilms Order No. DA9115826

The flow situation for a thruster propelled by ablated gas which is energized by a laser pulse is numerically simulated. The flow is axisymmetric and nonsteady, and is assumed to be inviscid due to its high Reynolds number. The high pressure expansion of the laser heated gas generated thrust as it pushes against the vehicle. Gas expansion lateral to the thrust vector causes performance to decrease. The vehicle geometry and the laser pulse characteristics determine the degree to which the flow is one dimensional. As the thruster's parameters are varied, its impulse is calculated and compared to the limiting impulse of a one-dimensional system, and thus the thrust efficiency is computed. Dissert. Abstr.

N91-28914# Osaka Univ., Suita (Japan). Inst. of Laser Engineering.
TURBULENT MIXING DUE TO RAYLEIGH-TAYLOR INSTABILITY IN LASER DRIVEN IMPLOSION
H. Takabe and A. Yamamoto *In* National Inst. for Fusion Science, Proceedings of the Second International Toki Conference on Plasma Physics and Controlled Nuclear Fusion. Nonlinear Phenomena in Fusion Plasmas: Theory and Computer Simulation Apr. 1991 p 115-118 (For primary document see N91-28881 20-75)
Avail: NTIS HC/MF A11

37 MECHANICAL ENGINEERING

Includes auxiliary systems (nonpower); machine elements and processes; and mechanical equipment.

N91-28573# Department of Energy, Washington, DC. Office of the Deputy Assistant Secretary for Transportation Technologies.
ELECTRIC AND HYBRID VEHICLES PROGRAM
Apr. 1991 32 p
(DE91-013113; DOE/CE-0305P) Avail: NTIS HC/MF A03

The Electric and Hybrid Vehicles Program FY 1990 continued to emphasize battery, fuel cell, and propulsion systems development up to the level of the testing and evaluation of proof-of-concept vehicles in the laboratory and in fleet operations. Progress made in developing electric and hybrid vehicle technologies is described beginning with highlights of recent accomplishments in FY 1990. Detailed descriptions of the program activities during FY 1990 is given on battery, fuel cell, propulsion system developments, and the testing and evaluation of new technology in fleet site operations and laboratories. In accordance with the reporting requirements of the Act, the Annual Report contains a status report on incentives and use of foreign components and concludes with a List of Publications resulting from the DOE program. DOE

N91-28574# Oak Ridge National Lab., TN.
DYNAMIC COUPLING EFFECTS IN MODELING AND CONTROL OF HARD CONTACT MOTION OF A MANIPULATOR
M. A. Unseren 1991 23 p Presented at the 3rd IEEE International Conference on Systems Engineering: Concurrent Engineering, Dayton, 1-3 Aug. 1991
(Contract DE-AC05-84OR-21400)
(DE91-010393; CONF-910871-1) Avail: NTIS HC/MF A03

In the previous work on the hard contact motion of a single manipulator, only the kinematic coupling effects were taken into account. In this paper the dynamic coupling effects are considered in the modeling and control of an N-joint, serial link manipulator turning a crank mechanism. By dynamically distributing the load, i.e., the crank, the generalized contact forces are decomposed into internal stress and motion components. A rigid body model is developed for the entire closed-chain system. It is shown here that a subset of the internal stress contact forces may be explicitly controlled while simultaneously and independently controlling the position of the system. DOE

N91-28575# Idaho National Engineering Lab., Idaho Falls.
ADVANCING ELECTRIC VEHICLE TECHNOLOGY
1991 13 p
(Contract DE-AC07-76ID-01570)
(DE91-013004; INEL/MISC-91055; BP-625) Avail: NTIS HC/MF A03

Since its inception in 1984, the INEL Electric and Hybrid Vehicle Program has encompassed a spectrum of interrelated engineering activities for electric vehicle technology. The principal categories, described herein, are: laboratory testing of materials components, and subsystems; field testing of operational configurations; design evaluation of candidate components and systems; technology overview; data analysis and trending; technical assessments; and mathematical modeling/computer simulation of operating conditions and equipment response; project management/coordination of both INEL activities and U.S. Department of Energy-sponsored industrial activities; and cooperative technology development and transfer with industry and academia. Current program activities are directed toward the evaluation of electric vehicles, battery and powertrain system and subsystem technology, and battery system design and integration through comprehensive laboratory and field testing. DOE

N91-28576# Carnegie-Mellon Univ., Pittsburgh, PA. Robotics Inst.

A METHODOLOGY TO DETERMINE THE DYNAMIC CONFIGURATION OF A RECONFIGURABLE MANIPULATOR

A. Krishnan (Illinois Univ., Urbana.) and P. K. Khosla 1990 8 p
Presented at the 1st International Symposium on Measurement and Control in Robotics, Houston, 20-22 Jun. 1990
(Contract DE-FG02-89ER-14042)
(DE91-010732; DOE/ER-14042/1; CONF-9006333-1) Avail: NTIS HC/MF A02

Typical tasks involved in the factory shop-floor range from simple pick and place operations to complex systems used for seam welding and assembly. In order to improve the quality and through-put of a product, specialized robots are used whose configurations are appropriate for the particulate task. The Reconfigurable Modular Manipulator System (RMMS) consists of modular links and joints which can be assembled into many manipulator configurations. This capability allows the RMMS to be rapidly reconfigured in order to custom tailor it to specific tasks. In this paper we discuss the issues of determining manipulator configuration from task requirements. We first show that task requirements can be broadly classified into kinematic and dynamic requirements. We then use dynamic requirements, in particular, the bound on the joint velocities and accelerations to select appropriate joint modules. We present our algorithm to select joint modules using bounds on joint velocities and accelerations. We use these bounds and the knowledge of previous module selections to calculate the maximum joint torques required. The algorithm ensures that the selected joint modules will have sufficient torque ratings. DOE

N91-28577# Argonne National Lab., IL.

BOUNDARY LUBRICATION OF CERAMIC MATERIALS BY SOFT METALLIC COATING AND SYNTHETIC OIL

O. O. Ajayi, A. Erdemir, J.-H. Hsieh, R. A. Erck, and F. A. Nichols May 1991 18 p Presented at the 4th International Symposium on Ceramic Materials and Components for Engines, Goeteborg (Sweden), 10-12 Jun. 1991
(Contract W-31-109-eng-38)
(DE91-014017; ANL/CP-72362; CONF-910617-2) Avail: NTIS HC/MF A03

Boundary lubrication of metallic materials often relies on surface reaction-generated films. This approach is intrinsically more difficult for ceramic materials because of their relatively lower chemical reactivity. The viability is studied of boundary lubrication of ceramics by the use of a thin soft metallic film as a boundary film. Lubrication of Si3N4 and ZrO2 ceramics with coatings of Ag or Au prepared by Ion Beam Assisted Deposition (IBAD) and a synthetic oil was investigated. Through this method, the friction coefficient during sliding contact of ceramics was reduced (as low as 0.05) to the level that is obtained in most boundary lubricated situations. Furthermore, wear was virtually eliminated. The method was found to be effective from room temperature up to 250 C. DOE

N91-28578*# National Aeronautics and Space Administration. Goddard Space Flight Center, Greenbelt, MD.

IMPROVED SUPERCONDUCTING BEARINGS Patent Application

Yury Flom, inventor (to NASA) and James D. Royston, inventor (to NASA) 17 Apr. 1991 24 p
(NASA-Case-GSC-13346-1; NAS 1.71:GSC-13346-1; US-Patent-Appl-SN-691609) Avail: NTIS HC/MF A03 CSCL 13I

An improved superconducting bearing is presented. Rotor is confined within two superconducting circular bearing structures, each of which has a number of embedded heating elements, and will levitate rotor which has embedded magnets in its end. Heating elements are connected to a feedback control unit, as are rotor position sensors. The temperature profiles of each circular bearing structure is then adjusted according to the information on rotor position provided to control unit by position sensors. Novelty is believed to reside in providing a superconducting circular bearing structure allowing for a control of the levitating forces. NASA

N91-28579*# National Aeronautics and Space Administration. Goddard Space Flight Center, Greenbelt, MD.

ROLLER LOCKING BRAKE Patent Application

John M. Vranish, inventor (to NASA) 28 Mar. 1991 17 p
(NASA-Case-GSC-13376-1; NAS 1.71:GSC-13376-1; US-Patent-Appl-SN-677008) Avail: NTIS HC/MF A03 CSCL 13I

A roller locking brake structure includes a roller locking/lifting ring, a housing, a set of conical locking rollers, a striker ring, and a drive disc. The roller locking/lifting ring includes respective V-shaped locking cam surface segments for each locking roller which is in the form of a truncated cone and provides a force and torque reaction surface for forces and torques generated in the braking process as well as providing a channel for a magnetic coil and flux return path of a magnetic circuit used to release a conical roller when the brake is off. The locking conical rollers couple the ring to the rim surfaces of the drive disc which provides another cam surface. The striker ring is located adjacent the rollers and is pulled down against the small end of the rollers by an electromagnetic coil when energized to decouple the locking rollers from the drive disc and thus cease the braking action. NASA

N91-28580*# National Aeronautics and Space Administration. Langley Research Center, Hampton, VA.

NONCIRCULAR ROLLING JOINTS FOR VIBRATIONAL REDUCTION IN SLEWING MANEUVERS Patent Application

Meng-Sang Chew, inventor (to NASA) (Old Dominion Univ., Norfolk, VA.), Jer-Nan Juang, inventor (to NASA), and Li-Farn Yang, inventor (to NASA) 28 Mar. 1991 22 p
(NASA-Case-LAR-14515-1-CU; NAS 1.71:LAR-14515-1-CU; US-Patent-Appl-SN-678551) Avail: NTIS HC/MF A03 CSCL 13K

A rolling joint is provided for obtaining slewing maneuvers for various apparatus including space structures, space vehicles, robotic manipulators and simulators. Two noncircular cylinders, namely a drive and a driven cylinder, are provided in driving contact with one another. This contact is maintained by two pairs of generally S-shaped bands, each pair forming a generally 8-shaped coupling tightly about the circumferential periphery of the noncircular drive and driven cylinders. A stationarily fixed arm extends between and is rotably journalled with a drive axle and a spindle axle respectively extending through selected rotational points of the drive cylinder and of the driven cylinder. The noncircular cylinders are profiled to obtain the desired varying gear ratio. The novelty of the present invention resides in using specifically profiled noncircular cylinders to obtain a desired varying gear ratio. NASA

N91-28581*# National Aeronautics and Space Administration. Goddard Space Flight Center, Greenbelt, MD.

SPLINE-LOCKING PAYLOAD FASTENER Patent Application

John M. Vranish, inventor (to NASA) 5 Jun. 1991 17 p
(NASA-Case-GSC-13378-1; NAS 1.71:GSC-13378-1; US-Patent-Appl-SN-710633) Avail: NTIS HC/MF A03 CSCL 13K

The invention consists of a locking spline payload fastener comprised of a spring-loaded male spline nut located at the tip of a threaded male positioning member that is affixed to a body being fastened. A complimentary female type spline fitting adapted to engage the spline nut is located at the lower end of a female conical receiving member which is affixed to a receiving body to which the payload body is being fastened. During a fastening guidance and mating procedure, the male nut and female spline fitting are aligned in a soft docking phase which is followed by a forward movement of the spline nut against and into the female spline fitting. This is then followed by a rotation of the male spline nut into a locking arrangement with the female spline fitting. To release the fastener, the process is reversed. Novelty is believed to reside in the concept of a self aligning spline system including a threaded male spline nut which upon engaging a female spline fitting, travels up a driven threaded shank to effect a locking operation. NASA

N91-28582*# National Aeronautics and Space Administration. Goddard Space Flight Center, Greenbelt, MD.

COUPLING DEVICE WITH IMPROVED THERMAL INTERFACE Patent Application

M. Bruce Milam, inventor (to NASA) 13 Jun. 1991 23 p
(NASA-Case-GSC-13251-1; NAS 1.71:GSC-13251-1; US-Patent-Appl-SN-714814) Avail: NTIS HC/MF A03 CSCL 13K

The primary object of the present invention is to provide a simple, reliable, and lightweight coupling that will also have an efficient thermal interface. A further object of the invention is to provide a coupling that is capable of blind mate with little or no insertion forces. Another object of the invention is to provide a coupling that acts as a thermal regulator to maintain a constant temperature on one side of the coupling. A still further object of the invention is to increase the available surface area of a coupling thus providing a larger area for the conduction of heat across the thermal interface. Another object of the invention is to provide a fluidic coupling that has no fluid passing across the interface, thus reducing the likelihood of leaks and contamination. The foregoing objects are achieved by utilizing, as in the prior art, a hot area (at an elevated temperature as compared to a cold area) with a need to remove excess heat from the hot area to a cold area. In this device, the thermal interface will occur not on a planar horizontal surface, but along a non-planar vertical surface, which will reduce the reaction forces and increase the thermal conductivity of the device. One non-planar surface is a surface on a cold pin extending from the cold area and the other non-planar surface is a surface on a hot pin extending from the hot area. The cold pin is fixed and does not move while the hot pin is a flexible member and its movement towards the cold pin will bring the two non-planar surfaces together forming the thermal interface. The actuating member for my device is a shape-memory actuation wire which is attached through an aperture to the hot pin and through another aperture to an actuation wire retainer. By properly programming the actuation wire, heat from the hot area will cause the actuation wire to bend the hot wire heat from the hot area will cause the actuation wire to bend the hot pin towards the cold pin forming the coupling and desired thermal interface. The shape-memory actuation wire is made of a shape-memory-effect alloy such as Nitinol. NASA

N91-28583 Tel-Aviv Univ. (Israel). Dept. of Solid Mechanics Materials and Structures.

PLANNING OF MINIMUM-TIME TRAJECTORIES FOR ROBOTIC ARMS M.S. Thesis

Vladimir Netzer Nov. 1989 147 p In HEBREW; ENGLISH summary
(ITN-91-85141) Copyright Avail: Tel-Aviv Univ., Exact Sciences Library, Ramat Aviv 69978, Israel

In many industrial applications that incorporate robotic manipulators, the time required to accomplish a task is an important design factor. Reducing the operation time is a main goal when planning such a task, and that can be achieved if the robot actuators are operated at their maximum capacity. During the last decade substantial effort was invested to find an optimal solution for the minimum time trajectory of a robot arm moving along a specified path and considering actuator constraints. A method is proposed for planning a minimum time trajectory of a manipulator moving along a predefined path with a specified velocity profile. Also, a near optimal algorithm is proposed that provides the minimum traversal time of the manipulator when only the path is specified, without considering the shape of the velocity profile. Both algorithms take into account the full nonlinear dynamics of the manipulator and the actuator constraints. Applying a nonlinear optimization technique, the time optimal trajectory is computed. The implemented solutions assume a specific shape of the velocity profile and thus they avoid the numeric integration of the equations of motion. The proposed method can be used as a design tool for an optimal trajectory of a robotic arm. Author (ISA)

N91-28584 Illinois Univ., Urbana-Champaign.

ROBUST LOW-ORDER CONTROL OF FLEXIBLE JOINT MANIPULATORS Ph.D. Thesis

Joaquin Astorga 1990 124 p
Avail: Univ. Microfilms Order No. DA9114166

The application of novel linear time invariant techniques to the design of low-order controllers for flexible joint manipulators. The nonlinear manipulator model is linearized via the perturbation method about an unstable operating point. Some nonlinear terms are treated as an external disturbance, and parametric uncertainty is represented as the structured uncertainty of the nominal plant. The H infinity-norm approach is then utilized to design a robust state feedback controller to stabilize the linear system and to give a specified bound on the disturbance rejection of the closed-loop system with enough robustness margin as to stabilize the actual nonlinear model. The nominal linear system with the state feedback controller determines the reference dynamics to be retained by the low-order controller based on the projective controls approach. The residual dynamics of the closed-loop system are selected under a suitable criterion to enhance disturbance rejection. The nonlinear model of the manipulator is also treated as a nonlinear system with structured uncertainty and sufficient conditions are determined for stability and disturbance rejection using linear state feedback and full-order controllers. Examples are given in the case of the one-link and two-link manipulators. The decentralized control option is also studied. The design of the controllers is based on a linear decoupled model obtained from the linearized model. The methodology here follows the same two phases of design used in the centralized case. Adaptive mechanisms are illustrated to improve the robust performance of the low-order decentralized control. Dissert. Abstr.

N91-28585 Texas Univ., Arlington.

ANALYSIS AND MODELING OF EARLY VISION TASKS FOR ROBOT STEREO VISION Ph.D. Thesis

Charles E. Coldwell, Jr. 1990 130 p
Avail: Univ. Microfilms Order No. DA9111902

In the past, research into the problems of robot or machine stereo vision has concentrated on the processing of image data acquired from commercially available sensors, rather than the sensor systems themselves. The present work seeks a different approach: the performance requirements of the stereo correspondence task, implemented by correlation, are used to constrain the design of the sensor system hardware and software. The result is an economical yet robust system for generation of a 1-1/2 D range sketch, using single line sensors, and a comprehensive model of a stereo vision system. The model is then evaluated using both a simulation, and a test bed system which implements many of the features described in the modeling and analysis. Dissert. Abstr.

N91-28586 Oregon State Univ., Corvallis.

KINEMATIC ANALYSIS OF LEGGED SYSTEM LOCOMOTION ON SMOOTH HORIZONTAL SURFACES Ph.D. Thesis

Yoon Su Baek 1990 151 p
Avail: Univ. Microfilms Order No. DA9113879

A model of legged locomotion is presented in which position and velocity of body are directly controlled by positions and velocities of the feet. One central relationship between foot acceleration, leg stroke, and body velocity is developed. Procedures for determining all parameters of a step sequence including periods

of constant body velocity (steady state) and constant linear acceleration of body (transient state) are presented. When analyzing walking, designing a walking machine, or designing a stepping sequence for an existing walking machine, it is important to understand constraints placed on body motion by motion of a single leg. Two dimensionless numbers which describe foot velocity profile are developed. Two dimensionless numbers which describe foot velocity profile are developed. Two additional dimensionless numbers result from constraint of leg workspace by foot acceleration and body velocity during steady state. These numbers provide useful relationships for design procedures. Defining a walking sequence requires transformation of objectives from global to body coordinates and continuously accounting for the relationship between these two systems. The technique that is described does this when body acceleration is non-zero as well as when body velocity is constant. Relationship between body and global coordinates is tracked for one leg pair using two diagrams: (1) position of feet relative to body versus time; and (2) distances moved by feet and body in the global frame. A closed form inverse kinematic solution and an algorithm to find workspace for a general three-revolute manipulator are presented.
Dissert. Abstr.

N91-28587 Michigan State Univ., East Lansing.
NUMERICAL SIMULATION OF THE AIR AND FUEL MIXING PROCESS IN FUEL-INJECTED ENGINES USING DISCRETE VORTEX DYNAMICS Ph.D. Thesis
Asuquo Bassey Ebiana 1990 314 p
Avail: Univ. Microfilms Order No. DA9111586

Here, the initial vorticity distribution inside a cylinder is approximated by discrete fluid vortices, each of quasi-Gaussian shaped distribution. The initialization scheme makes use of prescribed velocity data and an imaging system for the vortices found by modifying the circle theorem of Milne-Thomson. Fuel injection is simulated using a discrete jet model analogous to Ashurst's scheme. At each step, a grid-insensitive Vortex-In-Cell (VIC) solution technique is used to approximate the velocity field inside the cylinder. Subgrid accuracy is achieved through quadratic spline interpolation using Couet's numerical filter. Each vortex is advanced every time step using Heun's second order accurate time integration scheme. Predictions of the numerical studies show excellent agreement with theoretical results obtained using the method of images. Dissert. Abstr.

N91-28588 Iowa Univ., Iowa City.
RECURSIVE LINEARIZATION OF MULTIBODY DYNAMICS AND APPLICATION TO CONTROL DESIGN Ph.D. Thesis
Tsung-Chieh Lin 1990 186 p
Avail: Univ. Microfilms Order No. DA9112449

The nonlinear equations of motion in multi-body dynamics pose a difficult problem in linear control design. One solution is to have the nonlinear model linearized. Intuitively, the simplest linear model would be an extraction from a nonlinear model by omitting nonlinear effects such as Coriolis force, centrifugal force, and other forces interacting between bodies. The linearization developed in this research starts with nonlinear equations of motion written in the Newton-Euler form, which are easy to construct. Then, they are transformed into joint coordinate representation in two steps: Cartesian variables into state variables, and state variables into joint variables. At each transformation the kinematic relations are replaced with their linearized relations. A new computational method for linearization is obtained by applying a series of first-order analytical approximations to the recursive kinematic relationships. The method has proved to be computationally more efficient. In addition, a parallel algorithm for the linearization is also discussed. Dissert. Abstr.

N91-28589 Pennsylvania Univ., Philadelphia.
MECHANICAL DESIGN OPTIMIZATION OF ROBOT MANIPULATOR PERFORMANCE Ph.D. Thesis
Nathan Thatcher Ulrich 1990 123 p
Avail: Univ. Microfilms Order No. DA9112634

Mechanical design techniques for improving the performance of robot manipulators are discussed. The research is especially concerned with the behavior of robots in unstructured environments. In such a setting, the total system mass, the energy efficiency and the ability of a manipulator arm to interact positively with its surroundings is also important. Included here are three methods of overcoming performance limitations. A method of passive and energy-conservative mechanical gravity compensation is developed which can be applied to a wide range of manipulator geometries, two examples of which are presented. Experimental verification of compensation performance for one and two link implementations is reported, which shows the method to be accurate to well within one percent, and to be stable under a wide range of dynamic and static loading conditions. A method is presented for modifying the transmission characteristics of a robot manipulator to improve the predictability of actuator response. This is accomplished by optimizing the transmitted inertia matrix relating actuator inputs to joint outputs. Included is an application of this technique to a two-joint planar manipulator. Dissert. Abstr.

N91-28590 North Carolina State Univ., Raleigh.
THERMAL AND NON-NEWTONIAN EFFECTS IN ELASTOHYDRODYNAMIC LUBRICATION OF ROLLING-SLIDING CONTACTS Ph.D. Thesis
Moosa Zand 1990 132 p
Avail: Univ. Microfilms Order No. DA9112203

A numerical solution to the elastohydrodynamic lubrication of rolling-sliding contacts including both the thermal and non-Newtonian effects has been obtained using the central finite difference technique. The computational scheme requires the simultaneous solution of the non-Newtonian Reynolds, the elasticity, the load, the viscosity, and the energy equations. The non-Newtonian behavior of the lubricant is approximated by the Ree-Eyring model. The results include the lubricant pressure profile, film thickness, and 2-D temperature distribution along the rolling direction, and the traction force on the surface of the rollers at various high loads and slip ratios. Results show that film thickness is almost parallel in the contact region with a constriction occuring after the maximum of the pressure spike. The minimum film thickness is directly proportional to the slip and the load.
Dissert. Abstr.

N91-28591# Pacific Northwest Lab., Richland, WA.
ROBOTIC MANNEQUIN TECHNOLOGY FOR ENHANCED PRODUCT TESTING
B. A. Fecht and D. W. Bennett Jun. 1991 7 p Presented at the 4th International Symposium on the Performance of Protective Clothing, Montreal, Quebec, 18-20 Jun. 1991
(Contract DE-AC06-76RL-01830)
(DE91-013787; PNL-SA-19455; CONF-9106202-1) Avail: NTIS HC/MF A02

Engineers at Pacific Northwest Laboratory (PNL) have developed several articulated robotic mannequin systems which closely simulate human anthropometric shape, complex motion and physiological function. These systems provide highly reproducible and realistic tests which aid in the evaluation of high performance clothing, consumer products, and human comfort.
DOE

N91-28592# Argonne National Lab., IL.
SEALANT RESEARCH FOR SOFC
I. Bloom and M. Krumpelt 1991 4 p Presented at the Morgantown Energy Technology Center (METC) Contractors Review Meeting, Morgantown, 5-6 Jan. 1991
(Contract W-31-109-eng-38)
(DE91-014012; ANL/CP-73132; CONF-9101102-1) Avail: NTIS HC/MF A01

The objective of the sealant work is to develop materials that can form gas-tight seals in a solid oxide fuel cell (SOFC). These materials must be chemically and thermally stable at 1000 C in H2, O2, and water vapor and must be compatible with the fuel cell components. The key to the development of suitable sealing materials is the matching of chemical and thermal properties of the materials involved. Reactive glasses were evaluated. DOE

N91-28593# Los Alamos National Lab., NM.
SPHERE LAPPING
P. R. Hannah and D. D. Stewart Jun. 1991 73 p
(Contract W-7405-eng-36)
(DE91-014287; LA-12024-MS) Avail: NTIS HC/MF A04

This report contains a distillation of the sphere lapping work carried out at the Los Alamos National Laboratory over a period of years. It is not a general guide to the lapping of precision spheres, but is rather a document best understood by a technician sitting before the equipment at the laboratory. The information is presented from the point of view of practitioners who, over time, have gained some knowledge that is valuable to share. The report provides a step-by-step procedure, which if followed, should yield a dimensionally accurate, round, and smooth sphere. Information has also been included on the lapping of a variety of different materials as well as numerous processing techniques and tips. Information about the physics of the lapping process will not be found in this book, as there are many excellent texts available that thoroughly cover the subject. DOE

N91-28594# Oak Ridge National Lab., TN.
WELDING OF DUCTILE INTERMETALLIC ALLOYS
S. A. David and T. Zacharia 1991 13 p Presented at the 1st International Conference on Heat-Resistant Materials, Lake Geneva, 22-26 Sep. 1991
(Contract DE-AC05-84OR-21400)
(DE91-009553; CONF-910909-2) Avail: NTIS HC/MF A03

Ordered intermetallic alloys are a unique class of material that have potential for structural applications at elevated temperatures. The welding and weldability of these alloys is described. Weldability of these alloys was found to be a strong function of alloy composition, welding process and process parameters. Phase transformations associated with the weld thermal cycle play a critical role in determining their weldability. Defect-free welds were produced in several of these alloys by careful selection of welding processes and welding parameters. DOE

N91-28595# Edgerton, Germeshausen and Grier, Inc., Idaho Falls, ID.
A LASER BASED TECHNIQUE FOR PARTICLE SIZING TO STUDY TWO PHASE EXPANSION IN TURBINES
D. Y. Goswami, S. Hingorani (Auburn Univ., AL.), and G. Mines 1991 9 p Presented at the International Solar Energy Conference, Reno, 17-22 Mar. 1991
(Contract DE-AC07-76ID-01570)
(DE91-014172; EGG-M-91136; CONF-910379-1) Avail: NTIS HC/MF A02

Efficiency of binary power cycles can be improved by expanding the hydrocarbon working fluids through two phase region in a turbine and exiting at saturated or superheated condition. This improvement can be achieved if there is no condensation during the expansion or if there is condensation, the droplet size is extremely small. In order to verify this, a particle sizing technique is needed for extremely small particles in flow. A laser based technique is developed by which it is possible to detect particles as small as 10 angstroms in size. The basis of the technique is that particles of size less than one third of the wavelength of the incident radiation will scatter according of Rayleigh scattering theory. According to this theory, the intensity of the scattered light will be the same in the forward as well as in the backward directions. Therefore, measurement of the scattered intensity at two or three different angles will confirm the presence of Rayleigh scattering. The size of the particles can, then, be calculated from the measured scattered intensity according to the Rayleigh scattering equation. DOE

N91-28596# Maryland Univ., College Park.
THE CREATION OF MULTI-DEGREE-OF-FREEDOM MECHANISMS FOR ROBOTIC APPLICATIONS
Lung-Wen Tsai Jun. 1991 5 p
(Contract DE-FG05-88ER-13977)
(DE91-014359; DOE/ER-13977/4) Avail: NTIS HC/MF A01

This research is concerned with one of the most difficult stages of mechanical design, namely the conceptual synthesis of mechanisms. The main objective of this research is to develop systematic methodologies for the creation of multi-DOF (Degree-Of-Freedom) mechanisms for robotic applications. However, the analysis and control of such mechanisms have also been studied. Four major areas of interest have been studied: (1) redundant-drive backlash-free manipulators, (2) dynamic analysis and synthesis of geared robotic mechanisms, (3) tendon-driven manipulators, and (4) bevel-gear-type robotic wrist mechanisms. DOE

N91-28597 Carnegie-Mellon Univ., Pittsburgh, PA.
STOCHASTIC PLANS FOR ROBOTIC MANIPULATION Ph.D. Thesis
Kenneth Yigael Goldberg 1990 144 p
Avail: Univ. Microfilms Order No. DA9117508

Geometric uncertainty is unavoidable when programming robots for physical applications. Researchers propose a stochastic framework for manipulation planning where plans are ranked on the basis of expected cost. That is, the researchers express the desirability of states and actions with a cost function and describe uncertainty with probability distributions. They illustrate the approach with a new design for a programmable parts feeder, a mechanism that orients two dimensional parts using a sequence of open-loop mechanical motions. They present a planning algorithm that accepts an n sided polygonal part as input and, in time, O(n exp 2), generates a stochastically optimal plan for orienting the part. Dissert. Abstr.

N91-28598 Illinois Univ., Chicago.
SELECTED TOPICS IN MECHANISMS AND ROBOTICS: SINGULARITIES, INVERSE KINEMATICS, AND COLLISION DETECTION Ph.D. Thesis
Jonathan Charles Kieffer 1990 312 p
Avail: Univ. Microfilms Order No. DA9115012

Two problems are addressed: (1) inverse kinematics for spatial linkage and manipulators with prescribed untimed spatial end-effector trajectories, and (2) swept volume determination and interference detection for moving 3-dimensional solids. Dissert. Abstr.

N91-28230*# Pennsylvania State Univ., University Park. Dept. of Mechanical Engineering.
ROBUST AND REAL-TIME CONTROL OF MAGNETIC BEARINGS FOR SPACE ENGINES
Alok Sinha, Kon-Well Wang, K. Mease, and S. Lewis *In* NASA, Washington, Space Transportation Propulsion Technology Symposium. Volume 2: Symposium Proceedings May 1991 p 699-707 (For primary document see N91-28193 20-20)
Avail: NTIS HC/MF A99 CSCL 13K

N91-28231*# Pennsylvania State Univ., University Park. Dept. of Mechanical Engineering.
ANALYSIS OF FOIL BEARINGS FOR HIGH SPEED OPERATION IN CRYOGENIC APPLICATIONS
Marc Carpino *In* NASA, Washington, Space Transportation Propulsion Technology Symposium. Volume 2: Symposium Proceedings May 1991 p 709-715 (For primary document see N91-28193 20-20)
Avail: NTIS HC/MF A99 CSCL 13K

38 QUALITY ASSURANCE AND RELIABILITY

Includes product sampling procedures and techniques; and quality control.

N91-28599# Lawrence Livermore National Lab., CA.
X RAY TOMOGRAPHIC MICROSCOPY (XTM)
J. Celeste Oct. 1990 7 p Presented at the 2nd American Society for Nondestructive Testing (ASNT) on Industrial Computed Tomography Conference, San Diego, 20-24 May 1991

(Contract W-7405-eng-48)
(DE91-011930; UCRL-JC-105138; CONF-9105166-5) Avail: NTIS HC/MF A02

X ray tomographic microscopy (XTM) is a high resolution, three dimensional computed tomography (CT) system with a spatial resolution better that 0.005 mm. With this resolution it is now possible to image the microstructure of materials in millimeter-size samples. XTM differs from conventional optical and electron-beam microscopy in that the sample need not be harmed prior to characterization. There is no requirement for flat optical surfaces or thin sections. Materials are examined in their unaltered state. The three-dimensional imaging capability makes XTM ideally suited for materials research. In XTM, the x ray attenuation coefficient at any location in a material is determined from a finite set of x ray attenuation measurements (projection data) taken at different angles. The projection data is the transmitted x ray intensity reaching a position-sensitive detector after passing through the sample. The data for reach angular view is stored and the three-dimensional image is generated by tomographic reconstruction techniques. The attenuation coefficient is directly related to material chemistry and density. High spatial resolution is required to provide microstructure information in the region of interest. DOE

N91-28600# Pacific Northwest Lab., Richland, WA.

NONDESTRUCTIVE TESTING STANDARDS AND THE ASME CODE

J. C. Spanner Apr. 1991 37 p Presented at the ASTM Symposium on Nondestructive Testing Standards, Gaithersburg, 8-11 Apr. 1991
(Contract DE-AC06-76RL-01830)
(DE91-012643; PNL-SA-18369; CONF-9104111-2) Avail: NTIS HC/MF A03

Nondestructive testing (NDT) requirements and standards are an important part of the ASME Boiler and Pressure Vessel Code. The evolution of these requirements and standards is reviewed in the context of the unique technical and legal stature of the ASME Code. The coherent and consistent manner by which the ASME Code rules are organized is described, and the interrelationship between the various ASME Code sections, the piping codes, and the ASTM Standards is discussed. Significant changes occurred in ASME Sections 5 and 11 during the 1980s, and these are highlighted along with projections and comments regarding future trends and changes in these important documents. DOE

N91-28601# Oak Ridge National Lab., TN.

X RAY MICROIMAGING OF ELEMENTAL COMPOSITION AND MICROSTRUCTURE FOR MATERIALS SCIENCE

G. E. Ice and C. J. Sparks 1991 2 p Presented at the Workshop on Application of Synchrotron Radiation To Chemical Engineering Science, Argonne, 22-23 Apr. 1991
(Contract DE-AC05-84OR-21400)
(DE91-012052; CONF-9104201-1) Avail: NTIS HC/MF A01

X rays have many advantages over electrons and other charged particles for the microcharacterization of materials. X rays are more efficient in photoejecting inner shell electrons which results in characteristic x ray fluorescence. X rays also produce less Bremsstrahlung which yields far higher signal-to-background than obtained with electrons. Minimum detectable limits (MDL) for X ray excited fluorescence can be a few parts per billion; 10(exp -3) to 10(exp -5) less than for electron excitation. The third generation synchrotron radiation sources such as the Advanced Photon Source will for the first time provide x ray sources as brilliant as the most advanced electron probes. It will therefore soon be possible to develop a submicron x ray probe with unprecedented low levels of detection in diffraction, EXAFS, Auger, Photoelectron and fluorescence spectroscopies for structural and chemical characterization. Some applications to materials science are shown. DOE

N91-28602# Lawrence Livermore National Lab., CA.

MODEL-BASED COMPUTED TOMOGRAPHY FOR NONDESTRUCTIVE EVALUATION Ph.D. Thesis

S. G. Azevedo Mar. 1991 221 p
(Contract W-7405-eng-48)
(DE91-013462; UCRL-LR-106884) Avail: NTIS HC/MF A10

X-ray Computer Tomography (CT) has become a routine medical diagnostic for cross-sectional imaging of the body. Yet, even with over two decades of experience in the medical field, CT technology is not routinely used in industrial settings for nondestructive evaluation (NDE). The sparsity of industrial CT systems is due not only to large initial capital costs, but also to several problems of a physical nature and a mathematical nature. In this research, we have taken a fresh look at the industrial CT imaging problem and present several major contributions to the field. Explicit relationships of the underlying mathematics, along with new properties, are summarized. Conventional methods of image reconstruction are then developed, and their strengths and limitations are established for practical industrial CT. New methods for geometry estimation from unreconstructed projection data are developed that are effective for both experimental and simulated data. A major study of image reconstruction from incomplete measurements, a common problem plaguing industrial CT, is presented. First, previously proposed techniques are studied in the context of NDE, then a class of reconstruction methods -- the domain-iterative algorithms, some of which are new -- is developed under a common framework and shown to have an infinite number of hybrid methods. Implementation of domain-iterative methods is limited by computer requirements and by alignment accuracy between the data and models. New techniques for addressing these problems are presented. A fast, parallel technique for computing Radon transform and backprojection operations is described. Software simulations of this technique are tested, while a hardware implementation is on-going in a separate project. Future research areas in industrial CT are summarized. DOE

N91-28603# California Univ., Berkeley. Lawrence Berkeley Lab.

IMPROVING FATIGUE LIFE IN NEAR-EUTECTIC Sn Pb SOLDERS Ph.D. Thesis

T. S. E. Summers May 1991 147 p
(Contract DE-AC03-76SF-00098)
(DE91-013844; LBL-30605) Avail: NTIS HC/MF A07

Due to technical advances in packaging technology, solder joint thermal shear fatigue failures pose reliability concerns and limit current packaging designs in the electronics industry. Past work has shown that thermal fatigue failures, as well as isothermal fatigue and creep failures, in the commonly used near-eutectic Sn-Pb solders are preceded by the formation of a band of coarsened material. Examination of crept and fatigued eutectic solder joints shows that shear deformation concentrates along relatively soft heterogeneities, the eutectic grain and colony boundaries, in the as-cast microstructure which happen to line up into long straight bands parallel to the applied shear strain. Improvement of the fatigue properties requires an elimination or, at least, a reduction in the length of these long straight boundaries. Several methods of doing that are proposed. These methods basically fall into two groups: one involving homogenization of the as-cast microstructure aimed at eliminating these heterogeneities and the other involved with breaking up the as-cast microstructure in such a way that long straight boundaries do not form parallel to the direction of shear. To study the effect of homogenization of the microstructure, room temperature aging of solder joints was studied. Softening was found to occur over a period of about 40 to 50 weeks levelling off at about 70 to 75 percent of the initial strength (31 MPa). The effect of breaking up the as-cast microstructure was studied by comparing various off-eutectic alloys. The alloys studied consisted of Pb with 40 and 50 wt. percent Sn in addition to the near-eutectic 63Sn-37Pb alloy. In addition, the Pb-rich 20Sn-80Pb and 5Sn-95Pb alloys were studied in fatigue at 75 C. DOE

N91-28604 Colorado State Univ., Fort Collins.

SIGNATURE ANALYSIS TECHNIQUE FOR DIAGNOSING FAILURES IN MECHANICAL SYSTEMS Ph.D. Thesis

Moses O. J. Eze 1990 123 p
Avail: Univ. Microfilms Order No. DA9117174

The use of acoustic data to determine when and why a machine is malfunctioning is investigated. The use of manufacturing tool that supplements the human ear's ability to detect mechanical problem in a complex mechanical device. The research focuses on the detection of mechanical malfunctions through the employment of sound signals emitted from the failing device. The detection system uses a previously developed data base of analyzed signals to characterize new and unknown signals. The signal parameters and characteristics generated through the analysis are used as input to the computerized signal data base to search for a matching signal or the closest signal if one exists. A technique for dealing with situations for which no match exists in the data base is also examined. Dissert. Abstr.

N91-28605*# National Aeronautics and Space Administration. Lewis Research Center, Cleveland, OH.
NONDESTRUCTIVE EVALUATION TOOLS AND EXPERIMENTAL STUDIES FOR MONITORING THE HEALTH OF SPACE PROPULSION SYSTEMS
Edward R. Generazio 1991 44 p Presented at the Conference on Advanced Space Exploration Initiative Technologies, Cleveland, OH, 4-6 Sep. 1991; cosponsored by AIAA and OAI
(NASA-TM-105164; E-6453; NAS 1.15:105164; AIAA-91-3433)
Avail: NTIS HC/MF A03 CSCL 14D

An overview is given of background and information on space propulsion systems on both the programmatic and technical levels. Feasibility experimental studies indicate that nondestructive evaluation tools such as ultrasonic, eddy current and x-ray may be successfully used to monitor the life limiting failure mechanisms of space propulsion systems. Encouraging results were obtained for monitoring the life limiting failure mechanisms for three space propulsion systems; the degradation of tungsten arcjet and magnetoplasmadynamic electrodes; presence and thickness of spallable electrically conducting molybdenum films in ion thrusters; and the degradation of the catalyst in hydrazine thrusters. Author

39 STRUCTURAL MECHANICS

Includes structural element design and weight analysis; fatigue; and thermal stress.

For applications see *05 Aircraft Design, Testing and Performance* and *18 Spacecraft Design, Testing and Performance.*

N91-28606# Brookhaven National Lab., Upton, NY.
PREDICTION OF HIGH LEVEL VIBRATION TEST RESULTS BY USE OF AVAILABLE INELASTIC ANALYSIS TECHNIQUES
C. H. Hofmayer, Y. J. Park, and J. F. Costello (Nuclear Regulatory Commission, Washington, DC.) 1991 7 p Presented at the 11th International Conference on Structural Mechanics in Reactor Technology, Tokyo (Japan), 18-23 Aug. 1991
(Contract DE-AC02-76CH-00016)
(DE91-009437; BNL-NUREG-45835; CONF-910817-6) Avail: NTIS HC/MF A02

As part of a cooperative study between the United States and Japan, the U.S. Nuclear Regulatory Commission and the Ministry of International Trade and Industry of Japan agreed to perform a test program that would subject a large scale piping model to significant plastic strains under excitation conditions much greater than the design condition for nuclear power plants. The objective was to compare the results of the tests with state-of-the-art analyses. Comparisons were done at different excitation levels from elastic to elastic-plastic to levels where cracking was induced in the test model. The program was called the High Level Vibration Test (HLVT). The HLVT was performed on the seismic table at the Tadotsu Engineering Laboratory of Nuclear Power Engineering Test Center in Japan. The test model was constructed by modifying the 1/2.5 scale model of one loop of a PWR primary coolant system which was previously tested by NUPEC as part of their seismic proving test program. A comparison of various analysis techniques with test results shows a higher prediction error in the detailed strain values than in the overall response values. This prediction error is magnified as the plasticity in the test model increases. There is no significant difference in the peak responses between the simplified and the detailed analyses. A comparison between various detailed finite element model runs indicates that the material properties and plasticity modeling have a significant impact on the plastic strain responses under dynamic loading reversals. DOE

N91-28607# Oak Ridge National Lab., TN.
APPLICATIONS OF A 2-D MOVING FINITE ELEMENT FORMULATION TO ELASTIC/VISCOPLASTIC DYNAMIC FRACTURE ANALYSIS
J. C. Thesken (Royal Inst. of Tech., Stockholm, Sweden), B. R. Bass, and J. S. Parrott 1991 7 p Presented at the 11th International Conference on Structural Mechanics in Reactor Technology, Tokyo (Japan), 18-23 Aug. 1991
(Contract DE-AC05-84OR-21400)
(DE91-009930; CONF-910817-10) Avail: NTIS HC/MF A02

Current efforts to resolve the near crack tip fields in elastic/viscoplastic materials using finite element methods have failed to achieve a finite non-zero energy flow to the crack tip. Motivated by these difficulties, a moving element formulation incorporating a variable order singular element to enhance the local crack tip description is presented. The moving mesh zone is embedded in a finite global mesh to provide a functional tool for the analysis of dynamic crack growth experiments. The necessary elasto-dynamic formulations have been previously implemented in a transient finite element program DYNCRACK and checked against known analytical solutions. These results have encouraged an attempt to include Perzyna's elastic-viscoplastic model in the formulation. However, the introduction of non-linear history dependent material behavior into a moving element scheme requires a method to interpolate related field quantities to new Gauss point positions for each time step. The following summary of numerical procedures outlines the approach taken to develop a transient elastic/viscoplastic moving finite element formulation. Results for a standard test problem are then compared to those obtained using the nodal relaxation technique. Further development of the code is discussed with respect to applications to dynamic fracture experiments. DOE

N91-28608# Johns Hopkins Univ., Baltimore, MD. Dept. of Materials Science and Engineering.
CRITICAL ISSUES IN DE-ALLOYING AND TRANSCRYSTALLINE STRESS-CORROSION CRACKING
K. Sieradzki and J. W. Wagner Mar. 1991 7 p
(Contract DE-FG02-90ER-45421)
(DE91-010190; DOE/ER-45421/1) Avail: NTIS HC/MF A02

This report details the past (June 1990 to February 1991) research activities and second year research plans on the program, Critical Issues in De-alloying and Transcrystalline Stress-Corrosion Cracking which was funded in July 1990 by the Office of Basic Energy Sciences of The United States Department of Energy. The three major components of the program relate to: (1) kinetic aspects of the selective dissolution in alloys and the coarsening of de-alloyed layers; (2) measurements of crack dynamics during film induced cleavage processes; and (3) mechanical properties of the intrinsic de-alloyed layers responsible for film-induced cleavage events. Progress in each of these areas is discussed. DOE

N91-28609# Argonne National Lab., IL.
PLASTIC ANALYSIS OF A CIRCULAR ROD SUBJECTED TO SINUSOIDAL THERMAL CYCLING
M. J. Lee, L. K. Chang, and E. E. Feldman 1991 18 p Presented at the American Society of Mechanical Engineers (ASME) Pressure Vessels and Piping Conference, San Diego, 23-27 Jun. 1991
(Contract W-31-109-eng-38)
(DE91-011845; ANL/CP-72538; CONF-910602-34) Avail: NTIS HC/MF A03

This paper presents a finite element analysis of the elasto-plastic behavior of a circular rod subjected to sinusoidal thermal cycling. Differences between elastic and plastic behaviors are compared. The impact of Biot number and cyclic frequency on the stress and strain field are discussed. the strain range index is devised to evaluate the potential structural damage on the rod surface, and a simple engineering approach is proposed to predict total strain range for fatigue damage evaluation. DOE

N91-28610# Fermi National Accelerator Lab., Batavia, IL.
DESIGN AND ANALYSIS OF THE 50 mm COLLIDER DIPOLE VACUUM VESSEL
T. Heger, D. Arnold, and T. Nicol Mar. 1991 13 p Presented at the 3rd Annual International Industrial Symposium on the Super Collider (IISSC), Atlanta, 13-15 Mar. 1991
(Contract DE-AC02-76CH-03000)
(DE91-012490; FNAL-TM-1727; CONF-910340-13) Avail: NTIS HC/MF A03

In this study, a finite element model is used to predict the vacuum vessel's response to loads resulting from its own self-weight and shipping and handling. Structural members of the cold mass support system must behave elastically during assembly and transport of the magnets so that alignment with respect to an external reference is reproducible. Included are the deflection and stress analyses of the vacuum vessel for the SSC 50 mm collider dipole cryostats. In addition, material selection and stress relieving techniques are discussed. Several methods of local structural reinforcement were analyzed prior to the selection of the current design. The results from these analyses are given for comparison. DOE

N91-28611# Oak Ridge National Lab., TN.
INFLUENCE OF CRACK DEPTH ON THE FRACTURE TOUGHNESS OF REACTOR PRESSURE VESSEL STEEL
T. J. Theiss and J. W. Bryson 1991 39 p Presented at the American Society for Testing Materials (ASTM) Symposium on Constraint Effects in Fracture, Indianapolis, 8 May 1991
(Contract DE-AC05-84OR-21400)
(DE91-012537; CONF-9105188-1) Avail: NTIS HC/MF A03

The Heavy Section Steel Technology Program (HSST) at Oak Ridge National Laboratory (ORNL) is investigating the influence of flaw depth on the fracture toughness of reactor pressure vessel (RPV) steel. Recently, it has been shown that, in notched beam testing, shallow cracks tend to exhibit an elevated toughness as a result of a loss of constraint at the crack tip. The loss of constraint takes place when interaction occurs between the elastic-plastic crack-tip stress field and the specimen surface nearest the crack tip. An increased shallow-crack fracture toughness is of interest to the nuclear industry because probabilistic fracture-mechanics evaluations show that shallow flaws play a dominant role in the probability of vessel failure during postulated pressurized-thermal-shock (PTS) events. Tests have been performed on beam specimens loaded in 3-point bending using unirradiated reactor pressure vessel material (A533 B). Testing has been conducted using specimens with a constant beam depth (W = 94 mm) and within the lower transition region of the toughness curve for A533 B. Test results indicate a significantly higher fracture toughness associated with the shallow flaw specimens compared to the fracture toughness determined using deep-crack (a/W = 0.5) specimens. Test data also show little influence of thickness on the fracture toughness for the current test temperature (-60 C). DOE

N91-28612# Sandia National Labs., Livermore, CA.
THE SNL, LIVERMORE, HOPKINSON BAR APPARATUS FOR COMPRESSIVE MATERIALS TESTING AT HIGH STRAIN-RATES
W. A. Kawahara, S. L. Brndon, and J. J. Totten May 1991 21 p
(Contract DE-AC04-76DR-00789)
(DE91-013132; SAND-91-8215) Avail: NTIS HC/MF A03

The Hopkinson bar is a stress-wave apparatus for measuring the dynamic stress-strain curve of materials in the 1,000/sec strain-rate regime. This report presents a brief heuristic review of one-dimensional elastic wave and Hopkinson bar relations, followed by a description of SNL, Livermore's prototype system and sample test data. DOE

N91-28613# Los Alamos National Lab., NM.
MESA: A 3-D EULERIAN HYDROCODE FOR PENETRATION MECHANICS STUDIES
D. A. Mandell, K. S. Holian, and R. Henninger 1991 8 p Presented at the 1991 American Physical Society (APS) Conference on Shock Compression of Condensed Matter, Williamsburg, 17-20 Jul. 1991
(Contract W-7405-eng-36)
(DE91-013308; LA-UR-91-1587; CONF-9107105-10) Avail: NTIS HC/MF A02

We describe an explicit, finite-difference hydrocode, MESA, and compare calculations to metal and ceramic plate impacts with spall and to Taylor cylinder tests. The MESA code was developed with support from DARPA, the Army, and the Marine Corps for use in armor/anti-armor problems primarily, but the code has been used for a number of other applications. MESA includes 2-D and 3-D Eulerian hydrodynamics, a number of material strength and fracture models, and a programmed burn high explosives model. DOE

N91-28614# Oak Ridge National Lab., TN.
ASSESSMENT OF DUCTILE FRACTURE METHODOLOGY BASED ON APPLICATIONS TO LARGE-SCALE EXPERIMENTS
B. R. Bass, C. E. Pugh, J. Keeney-Walker, H. Schulz, and J. Sievers (Gesellschaft fuer Reaktorsicherheit, Cologne, Germany, F.R.) 1991 13 p Presented at the 11th International Conference on Structural Mechanics in Reactor Technology, Tokyo (Japan), 18-23 Aug. 1991
(Contract DE-AC05-84OR-21400)
(DE91-009920; CONF-910817-11) Avail: NTIS HC/MF A03

A summary of the present status of the Project for Fracture Analysis of Large-Scale International Reference Experiment (FALSIRE) is given. Fracture assessments compiled from Project FALSIRE for five pressurized thermal shock experiments are compared. Some observations are made concerning predictive capabilities of the fracture methodologies used in these assessments. DOE

N91-28615# Oak Ridge National Lab., TN.
THE RATE (TIME)-DEPENDENT MECHANICAL BEHAVIOR OF MODIFIED 9Cr-1Mo STEEL. PART 1: EXPERIMENTS AT 538 C
M. B. Ruggles, S. Cheng, and E. Krempl (Rensselaer Polytechnic Inst., Troy, NY.) 1991 8 p Presented at the 11th International Conference on Structural Mechanics in Reactor Technology, Tokyo (Japan), 18-23 Aug. 1991
(Contract DE-AC05-84OR-21400)
(DE91-011097; CONF-910817-12-Pt-1) Avail: NTIS HC/MF A02

An experimental technique for measuring internal back stress was proposed by Mitra and McLean in 1966. Later stress and strain transient dip tests were introduced. Recently dip tests have attracted the interest of researchers in the area of constitutive equations. The purpose of this effort is to investigate the internal stress behavior for modified 9Cr-1Mo steel at 538 C. Test results may be used to further improve unified viscoplastic models of the overstress type, where thorough understanding of the back stress behavior is important. The present paper also reports on uniaxial monotonic tests at strain rates ranging from 5.0 x 10(exp -3) to 1.0 x 10(exp -7) s(exp -1) with relaxation tests which were performed to determine short term mechanical behavior and influence of the recovery of state. DOE

N91-28616# Sandia National Labs., Albuquerque, NM.
MONITORING STRUCTURAL RESPONSE IN PRESSURIZED ENVIRONMENTS. PART 1: INSTRUMENTATION TECHNIQUES
D. P. Roach and L. R. Dorrell 1991 18 p Presented at the American Society of Mechanical Engineers (ASME) Pressure Vessels and Piping Conference, San Diego, 23-27 Jun. 1991
(Contract DE-AC04-76DP-00789)

(DE91-012654; SAND-90-2690C; CONF-910602-42) Avail: NTIS HC/MF A03

There are various methods which can be used to monitor the structural response of pressure vessels, submerged pipelines, deep sea vehicles, submarines and offshore structures. Numerous experimental techniques have been developed at Sandia National Laboratories in order to measure the strain, displacement and acceleration of a structural member. These techniques have been successfully implemented in adverse environments of 2500 PSI and 300 F. This paper discusses the performance of various instrumentation schemes, the environmental protection of these diagnostics under pressure, and the means by which data are extracted from a closed pressure system. In a separate paper - Part 2: Applications - specific hydrostatic and dynamic pressure tests are used to demonstrate how these techniques are employed, the problems encountered, and the importance of the data obtained. It has been shown that the effect of fluid pressure on a strain gage response is linear and, therefore, actual strain can be calculated from the indicated strain. One particular compensation technique, which simultaneously eliminates the effects of temperature and pressure, is described here. DOE

N91-28617# Los Alamos National Lab., NM.

DYNAMIC PLASTICITY IN TRANSITION FROM THERMAL ACTIVATION TO VISCOUS DRAG

J. N. Johnson and D. L. Tonks 1991 9 p Presented at the 1991 American Physical Society (APS) Conference on Shock Compression of Condensed Matter, Williamsburg, 17-20 Jul. 1991
(Contract W-7405-eng-36)
(DE91-013031; LA-UR-91-1648; CONF-9107105-6) Avail: NTIS HC/MF A02

For low-to-intermediate rates of mechanical loading, plastic deformation, is controlled by thermal activation or mechanical penetration of dislocations through barriers. These barriers can be solute atoms, impurities, or, in the case of very pure materials, other dislocations. At some point between intermediate strain rates (10 -- 10(exp 4)/s) and the higher strain rates (10(exp 5) to 10(exp 7)/s) associated with weak shock compression, the plastic deformation process makes a transition from being dominated by stress-assisted thermal activation to being controlled by the time it takes a mobile dislocation to get from one barrier to the next; this latter time depends on the effective stress and viscous drag force provided by the perfect lattice. Some of the models that describe this process are reviewed, along with various hardening mechanisms. Distinction is made between simple rate-dependent models (in which in shear stress depends on the current plastic strain rate and plastic strain) and path-dependent models (in which the shear stress depends on the current plastic strain rate and all past history through one, or more, internal state variables). A way in which shock wave data can be used to extend intermediate strain rate models into the viscous drag regime is described. DOE

N91-28618# Los Alamos National Lab., NM.

OVERDRIVEN SHOCKS IN SOLIDS AND LIQUIDS

D. C. Wallace 1991 5 p Presented at the 1991 American Physical Society (APS) Conference on Shock Compression of Condensed Matter, Williamsburg, 17-20 Jul. 1991
(Contract W-7405-eng-36)
(DE91-013370; LA-UR-91-1820; CONF-9107105-12) Avail: NTIS HC/MF A01

The structure of overdriven shocks in solids and liquids is analyzed in terms of the underlying physical concepts, without resorting to formal mathematics. Two dissipative processes are required for the existence of a steady-wave shock, namely plastic flow in a solid, or viscous flow in a liquid, and heat transport in either a solid or liquid. The first requirement is the analog of Rayleigh's theorem for gases, and the second requirement extends Rayleigh's findings. For metals, the shock analysis yields approximate plastic flow data at strain rates approaching 10(exp 12) per s. The shock risetime in solid or liquid metals is predicted to decrease to around a picosecond, as the shock strength increases through the overdriven threshold. DOE

N91-28619# Oak Ridge National Lab., TN.

NEAR CRACK TIP TRANSVERSE STRAIN EFFECTS ESTIMATED WITH A LARGE STRAIN HOLLOW CYLINDER ANALOGY

J. G. Merkle 1991 34 p Presented at the 23rd National Symposium on Fracture Mechanics, College Station, 18-20 Jun. 1991
(Contract DE-AC05-84OR-21400)
(DE91-012072; CONF-910624-1) Avail: NTIS HC/MF A03

In order to study effects of constraint on fracture toughness, it is important to select the right location within the crack-tip field for investigation. In 1950 Hill postulated that close to a circular notch tip the principal stress directions would be radial and circumferential, so that the plastic slip lines (maximum shear stress trajectories) would be logarithmic spirals. The resulting equation for stress normal to the notch symmetry plane, neglecting strain hardening, was identical to that for the circumferential stress near the bore of an ideally plastic thick-walled hollow cylinder under external radial tension, because the relevant geometries are identical. In 1969, Rice and Johnson developed a near crack-tip, plane strain, large-strain rigid-plastic analysis considering strain hardening and assuming an infinitely sharp initial crack tip. Shortly afterwards, Merkle, following Hill's suggestion, proposed an approximate analysis of the stresses and strains ahead of a blunted crack tip on the plane of symmetry, based on a circular blunted crack tip. The analysis amounted to a hollow cylinder analogy, including the effects of strain hardening. The original hollow cylinder analogy was based on small strain theory, and the calculated strain distributions did not agree well with the Rice and Johnson results very near the blunted crack tip. Therefore, the hollow cylinder analogy equations have been rederived, based on large strain theory, and the agreement with the Rice and Johnson results and other more recent numerical results is good. Calculations illustrate the effects of transverse strain on the principal stresses very close to a blunting crack tip and show that, theoretically, a singularity still exists at the tip of a blunting crack. DOE

N91-28620# Los Alamos National Lab., NM.

THE DATASHOP: A DATABASE OF WEAK-SHOCK CONSTITUTIVE DATA

D. L. Tonks May 1991 135 p
(Contract W-7405-eng-36)
(DE91-013349; LA-12068-MS) Avail: NTIS HC/MF A07

Experimental velocity profiles for weak shock waves of a variety of metals are analyzed to determine the plastic strain, plastic strain rate, and deviatoric stress through the shock front. (A weak shock wave is one that is not yet overdriven, i.e., it has an elastic precursor.) A steady-wave weak shock analysis is used for most of the data. In some cases a numerical characteristics-code calculation is used to correct for reflections created when the steady wave passes through a sample-window interface or reflects from a free surface. (The effects of a sample-window interface are minor for windows closely matched in impedance to the sample.) The data are collected here in the form of the DataShoP database: Data (from) Sho(ckwave) P(rofiles). The data are presented in the form of both figures and tables. The tables are available on request on a floppy disk. The collection of data here is a repository of basic material high-strain-rate information for the modeler or theorist. Wave propagation calculations and other such analysis have already been performed leaving the user free to concentrate on questions of basic material behavior. DOE

N91-28621# Los Alamos National Lab., NM.

A STUDY OF THE IMPACT OF REACTION RATES ON EQUATION OF STATE

P. K. Tang 1991 5 p Presented at the 1991 American Physical Society (APS) Conference on Shock Compression of Condensed Matter, Williamsburg, 17-20 Jul. 1991
(Contract W-7405-eng-36)
(DE91-013375; LA-UR-91-1789; CONF-9107105-16) Avail: NTIS HC/MF A01

We present experimental evidence on high explosives pushing metal plates that shows the tendency of the equation of state behaving more energetically in the low-pressure region. We believe the deficiency in predicting low- and also high-pressure performance has a theoretical origin, and it is related to reaction rate. The reaction process with a slow stage generates a higher effective Chapman-Jouguet pressure. The development of an equation of state based on this information, using the classical detonation theory but without the consideration of the slow component in reaction, would produce a more energetic condition in the low-pressure region and a less powerful one in high pressure. We demonstrate how a polytropic gas equation of state is constructed, and the properties it possesses are mentioned. Finally, we show how the effective Chapman-Jouguet condition comes about and define the property of a pseudo Hugoniot associated with it. DOE

N91-28622*# National Aeronautics and Space Administration. Lewis Research Center, Cleveland, OH.
VISCOPLASTIC ANALYSIS OF AN EXPERIMENTAL CYLINDRICAL THRUST CHAMBER LINER
Vinod K. Arya and Steven M. Arnold Jun. 1991 22 p Submitted for publication LIMITED REPRODUCIBILITY: More than 20% of this document may be affected by color photographs Original contains color illustrations
(NASA-TM-103287; E-5746; NAS 1.15:103287) Avail: NTIS HC/MF A03; 10 functional color pages CSCL 20K

A viscoplastic stress-strain analysis of an experimental cylindrical thrust chamber is presented. A viscoelastic constitutive model incorporating a single internal state variable that represents kinematic hardening was employed to investigate whether such a viscoplastic model could predict the experimentally observed behavior of the thrust chamber. Two types of loading cycles were considered: a short cycle of 3.5 sec. duration that corresponded to the experiments, and an extended loading cycle of 485.1 sec. duration that is typical of the Space Shuttle Main Engine (SSME) operating cycle. The analysis qualitatively replicated the deformation behavior of the component as observed in experiments designed to simulate SSME operating conditions. The analysis also showed that the mode and location in the component may depend on the loading cycle. The results indicate that using viscoplastic models for structural analysis can lead to a more realistic life assessment of thrust chambers. Author

N91-28623# Oak Ridge National Lab., TN.
CRACK INITIATION UNDER GENERALIZED PLANE STRAIN CONDITIONS
D. K. M. Shum and J. G. Merkle 1991 35 p Presented at the 23rd National Symposium on Fracture Mechanics, College Station, 18-20 Jun. 1991
(Contract DE-AC05-84OR-21400)
(DE91-013410; CONF-910624-3) Avail: NTIS HC/MF A03

A method for estimating the decrease in crack-initiation toughness, from a reference plane strain value, due to positive straining along the crack front of a circumferential flaw in a reactor pressure vessel is presented in this study. This method relates crack initiation under generalized plane strain conditions with material failure at points within a distance of a few crack-tip-opening displacements ahead of a crack front, and involves the formulation of a micromechanical crack-initiation model. While this study is intended to address concerns regarding the effects of positive out-of-plane straining on ductile crack initiation, the approach adopted in this work can be extended in a straightforward fashion to examine conditions of macroscopic cleavage crack initiation. Provided single-parameter dominance of near-tip fields exists in the flawed structure, results from this study could be used to examine the appropriateness of applying plane strain fracture toughness to the evaluation of circumferential flaws, in particular to those in ring-forged vessels which have no longitudinal welds. In addition, results from this study could also be applied toward the analysis of the effects of thermal streaming on the fracture resistance of circumferentially oriented flaws in a pressure vessel. DOE

N91-28624# Los Alamos National Lab., NM.
RESIDUAL STRESS MEASUREMENT USING THE PULSED NEUTRON SOURCE AT LANSCE
M. A. M. Bourke, J. A. Goldstone, and T. M. Holden (Atomic Energy of Canada Ltd., Chalk River, Ontario) 1991 14 p Presented at the North Atlantic Treaty Organization (NATO) Advanced Research Workshop on Measurement of Residual Stress and Applied Stress Using Neutron Diffraction, Oxford, England, 18-22 Mar. 1991
(Contract W-7405-eng-36)
(DE91-013494; LA-UR-91-1530; CONF-9103130-2) Avail: NTIS HC/MF A03

The presence of residual stress in engineering components can effect their mechanical properties and structural integrity. Neutron diffraction is the only measuring technique which can make spatially resolved nondestructive strain measurements in the interior of components. By recording the change in the crystalline interplanar spacing, elastic strains can be measured for individual lattice reflections. Using a pulsed neutron source, all the lattice reflections are recorded in each measurement which allows anisotropic effects to be studied. Measurements made at the Manuel Lujan Jr Neutron Scattering Centre (LANSCE) demonstrate the potential for stress measurements on a pulsed source and indicate the advantages and disadvantages over measurements made on a reactor. DOE

N91-28625# Los Alamos National Lab., NM.
STRESS FIELDS GENERATED BY KINETIC ENERGY PROJECTILE INTERACTION WITH CERAMIC TARGETS
M. W. Burkett and D. A. Rabern 1991 5 p Presented at the 1991 American Physical Society (APS) Conference on Shock Compression of Condensed Matter, Williamsburg, 17-20 Jul. 1991
(Contract W-7405-eng-36)
(DE91-013687; LA-UR-91-1693; CONF-9107105-23) Avail: NTIS HC/MF A01

Two-dimensional axisymmetric calculations were performed with the Eulerian hydrocode MESA2D and the Lagrangian structural analysis code PRONTO2D. The calculated stress distributions were compared shortly after impact and found to be similar in magnitude and profile. For certain geometric configurations, the interaction of the kinetic energy penetrators with the ceramic targets produce high compressive principal stresses as well as, significant tensile principal stresses ahead of the projectile/ceramic interface. The principal tensile stresses fracture the ceramic ahead of the penetrator. The crack trajectories measured from a recovered ceramic target were compared with crack trajectory estimates based upon MESA2D principal stress states within the tile. The fracture process degrades the ceramic and allows the projectile to penetrate a fractured ceramic media. DOE

N91-28626*# Analytical Services and Materials, Inc., Hampton, VA.
INTERLAMINAR FRACTURE CHARACTERIZATION: A CURRENT REVIEW
Roderick H. Martin Jul. 1991 50 p Prepared for presentation at the 2nd Japan International SAMPE Symposium, Tokyo, Japan, 11-14 Dec. 1991
(Contract NAS1-18599)
(NASA-CR-187573; NAS 1.26:187573) Avail: NTIS HC/MF A03 CSCL 20K

Interlaminar fracture characterization has been investigated for several years. Only now is it well enough understood for standardization organizations to attempt to write standard test methods. A review of the current philosophies in characterizing interlaminar fracture is presented. First, the mode 1, double cantilever beam test (DCB) for measuring G(sub 1c) and the end notched flexure (ENF) test for measuring G(sub 2c) are discussed. These tests have undergone the most extensive research throughout the years and are furthest towards standardization. In addition, the mode 2, end loaded split (ELS) specimen is discussed. Mixed mode fracture is also discussed and the recently developed mixed mode bending (MMB) test is detailed. Then, tests for evaluating mode 3 fracture toughness, including the split cantilever beam (SCB), are reviewed. Finally, the work done on interlaminar fracture characterization in fatigue is reviewed. Author

N91-28627*# National Aeronautics and Space Administration. Lewis Research Center, Cleveland, OH.

ASTROP2 USERS MANUAL: A PROGRAM FOR AEROELASTIC STABILITY ANALYSIS OF PROPFANS

G. V. Narayanan (Sverdrup Technology, Inc., Brook Park, OH.) and K. R. V. Kaza Washington Aug. 1991 75 p
(Contract NAS3-25266)
(NASA-TM-4304; E-5768; NAS 1.15:4304) Avail: NTIS HC/MF A04 CSCL 20K

A user's manual is presented for the aeroelastic stability and response of propulsion systems computer program called ASTROP2. The ASTROP2 code preforms aeroelastic stability analysis of rotating propfan blades. This analysis uses a two-dimensional, unsteady cascade aerodynamics model and a three-dimensional, normal-mode structural model. Analytical stability results from this code are compared with published experimental results of a rotating composite advanced turboprop model and of nonrotating metallic wing model. Author

N91-28628# Lawrence Livermore National Lab., CA.

SHOCK COMPRESSION OF LOW-DENSITY MICROCELLULAR MATERIALS

N. C. Holmes and E. F. See May 1991 6 p Presented at the 1991 American Physical Society (APS) Conference on Shock Compression of Condensed Matter, Williamsburg, 17-20 Jul. 1991
(Contract W-7405-eng-48)
(DE91-013586; UCRL-JC-106338; CONF-9107105-25) Avail: NTIS HC/MF A02

We describe a precise new technique for shock velocity measurements in low-density microcellular materials (LDMM). This optical method uses an image-converter streak camera to record shock arrivals across stepped samples, using the emission of a thin metallic layer as an indicator. Real-time calibration of the sweep allows absolute accuracy of better than 0,5 percent at the 95 percent confidence level. The analysis of the data is described. We have applied this method to study the shock compression of a silica aerogel LDMM with an initial density of 0.128 g/cm(exp 3). Further applications of this method, and applications to problems of current interest are briefly discussed. DOE

N91-28629# Argonne National Lab., IL.

CALCULATION OF PRESSURE DISTRIBUTION IN VACUUM SYSTEMS USING A COMMERCIAL FINITE ELEMENT PROGRAM

J. Howell, B. Wehrle, and H. Jostlein (Fermi National Accelerator Lab., Batavia, IL.) 1991 4 p Presented at the 1991 Institute of Electrical and Electronics Engineers (IEEE) Particle Accelerator Conference (PAC), San Francisco, 6-9 May 1991
(Contract W-31-109-eng-38)
(DE91-013611; ANL/CP-73246; CONF-910505-191) Avail: NTIS HC/MF A01

The finite element method has proven to be a very useful tool for calculating pressure distributions in complex vacuum systems. A number of finite element programs have been developed for this specific task. For those who do not have access to one of these specialized programs and do not wish to develop their own program, another option is available. Any commercial finite element program with heat transfer analysis capabilities can be used to calculate pressure distributions. The approach uses an analogy between thermal conduction and gas conduction with the quantity temperature substituted for pressure. The thermal analogies for pumps, gas loads and tube conductances are described in detail. The method is illustrated for an example vacuum system. A listing of the ANSYS data input file for this example is included. DOE

N91-28630# Pacific Northwest Lab., Richland, WA.

ANALYSIS OF BRITTLE INTERGRANULAR CRACK PROPAGATION DURING STRESS CORROSION CRACKING

R. H. Jones Apr. 1991 9 p Presented at the Spring Meeting of the Materials Research Society (MRS), Anaheim, 29 Apr. - 3 May 1991
(Contract DE-AC06-76RL-01830)
(DE91-013666; PNL-SA-18938; CONF-910406-21) Avail: NTIS HC/MF A02

Crack growth rates during intergranular stress corrosion, in materials such as Fe in Ca(NO3)2 at +750 mV (SEC), appear to exceed rates which can occur by dissolution and ion transport within the crack. Brittle crack jumps induced by a corrosion or stress corrosion process, and which magnify the dissolution supported crack velocity by a factor of up to 10(exp 3), could explain this behavior. Hydrogen can induce these very fast crack growth rates, but these rates were obtained at electrochemical potentials where H reduction is not thermodynamically possible. Other possible mechanisms for this accelerated crack growth include: (1) intergranular corrosion altered tearing modulus; (2) grain boundary dealloying; or (3) adsorption induced brittle fracture. Examination of each of these mechanisms suggests that intergranular corrosion could reduce the tearing modulus through changes in the crack shape. However, crack opening analysis clearly shows that the crack tip is shielded from the applied stress intensity and that an embrittlement process which reduces the interface toughness is need for brittle intergranular crack jumps to occur. Further research is in progress to identify the source of this embrittlement. DOE

N91-28631# Sandia National Labs., Albuquerque, NM.

NON-STEADY WAVE PROFILES AND THE FOURTH-POWER LAW

J. Swegle 1991 4 p Presented at the 1991 American Physical Society (APS) Conference on Shock Compression of Condensed Matter, Williamsburg, 17-20 Jul. 1991
(Contract DE-AC04-76DP-00789)
(DE91-013576; SAND-91-0060C; CONF-9107105-27) Avail: NTIS HC/MF A01

The strain rate in steady shock waves is proportional to the fourth power of shock amplitude for a wide variety of materials over a broad range of strain rates. A model based on this observation gives good agreement not only with steady-wave profiles but also with data on non-steady waves in aluminum. In apparent contrast, data on vanadium and uranium at low strain rates indicates a departure from the fourth power law if the wave profiles are assumed to be steady. However, when predicted profiles are produced by allowing the waves to propagate and evolve over the actual experimental sample thickness, the fourth power model gives excellent agreement with the wave profile data even though the wave profiles in the calculations have not yet reached steady state. The implication is that the experimental data do not represent steady waves, and the model is predicting the correct evolution of non-steady waves in vanadium and uranium. DOE

N91-28632# Los Alamos National Lab., NM.

NEUTRON DIFFRACTION DETERMINATION OF THE RESIDUAL STRESS REDISTRIBUTION IN CRACKED AUTOFRETTAGED TUBING

M. A. M. Bourke, H. J. McGillivray, G. A. Webster, and P. J. Webster (Salford Univ., England) 1991 13 p Presented at the North Atlantic Treaty Organization (NATO) Advanced Research Workshop on Measurement of Residual Stress and Applied Stress Using Neutron Diffraction, Oxford, England, 18-22 Mar. 1991
(Contract W-7405-eng-36)
(DE91-013688; LA-UR-91-1687; CONF-9103130-3) Avail: NTIS HC/MF A03

Neutron diffraction has been used to measure the residual stress distributions in uncracked and fatigue cracked rings taken from a high strength, low alloy steel autofrettage tube with a bore diameter of 60 mm and a wall thickness of 32 mm. Stresses were determined to a precision of +/- 10 MPa. Three crack sizes were examined. No appreciable stress redistribution was observed until the crack was grown into a region which originally contained tensile residual hoop stress. When this occurred an increase in residual hoop tension was observed ahead of the crack tip.

Qualitative agreement was achieved between the measured hoop stress distribution and values predicted using a boundary element method. DOE

N91-28633# Los Alamos National Lab., NM.

A NEW MODEL OF RATE DEPENDENT ELASTIC-PLASTIC FLOW

J. E. Hammerberg, D. L. Preston, and D. C. Wallace 1991 5 p Presented at the 1991 American Physical Society (APS) Conference on Shock Compression of Condensed Matter, Williamsburg, 17-20 Jul. 1991
(Contract W-7405-eng-36)
(DE91-014600; LA-UR-91-2058; CONF-9107105-37) Avail: NTIS HC/MF A01

We present the results of 2D lagrangian hydrodynamic simulations of cylinder impact experiments using a recently developed model for rate-dependent elastic-plastic flow. This model, which takes advantage of empirical scaling relations in terms of melting temperature and shear modulus, is consistent with the very high strain-rate behavior deduced from overdriven shock data, and is in good agreement with the temperature and density dependence of the flow stress where known. Calculations for uranium and copper are discussed. DOE

N91-28634# Los Alamos National Lab., NM.

BAUSCHINGER EFFECT DURING SHOCK LOADING

G. T. Gray, III, R. S. Hixson, and C. E. Morris 1991 12 p Presented at the 1991 American Physical Society (APS) Conference on Shock Compression of Condensed Matter, Williamsburg, 17-20 Jul. 1991
(Contract W-7405-eng-36)
(DE91-014606; LA-UR-91-2041; CONF-9107105-32) Avail: NTIS HC/MF A03

Parallel shock recovery and wave profile experiments have been performed that exhibit a Bauschinger effect in Si-bronze shocked to 10 GPa. The unloading wave profile in Si-bronze exhibited a quasi-elastic release that had greater departure from the ideal elastic-plastic response than the pure copper samples. The reload mechanical response of Si-bronze that was preshocked to 10 GPa exhibited less hardening than the annealed material to an equivalent strain while the reverse hardening effect was true for copper. The importance of a microstructurally-controlled Bauschinger component to defect storage during the shock process is discussed in light of shock recovery, wave profile, and deformation substructure results. DOE

N91-28635# Los Alamos National Lab., NM.

SHEAR STRESS PREDICTION IN SHOCK LOADED COPPER

P. S. Follansbee 1991 5 p Presented at the 1991 American Physical Society (APS) Conference on Shock Compression of Condensed Matter, Williamsburg, 17-20 Jul. 1991
(Contract W-7405-eng-36)
(DE91-014740; LA-UR-91-1994; CONF-9107105-34) Avail: NTIS HC/MF A01

The stress-strain behavior during the shock rise of a 30 and 54 kbar shock in copper is modeled using a plastic constitutive model that includes rate and temperature dependent hardening and accounts for the transition from thermally activated to viscous drag controlled deformation at high strain rates. A slight modification to the treatment of the mobile dislocation density within the model from that originally proposed leads to better agreement with the shock data than achieved previously. The results indicate that the deformation mechanism during the shock rise is a drag mechanism. DOE

N91-28636# Los Alamos National Lab., NM.

QUANTUM MECHANICAL EFFECTS ON THE SHOCK HUGONIOT

B. I. Bennett and D. A. Liberman (Lawrence Livermore National Lab., CA.) 1991 9 p Presented at the 1991 American Physical Society (APS) Conference on Shock Compression of Condensed Matter, Williamsburg, 17-20 Jul. 1991
(Contract W-7405-eng-36)
(DE91-014750; LA-UR-91-1964; CONF-9107105-40) Avail: NTIS HC/MF A02

Calculations of the locus of shock Hugoniot states of aluminum, using two equations of state that either omit or include a quantum mechanical treatment for the material's electronic excitations, will be presented. The difference between the loci will be analyzed in the context of a comparison between an ab initio quantum mechanical model and a semiclassical treatment of the electronic states. The theoretical results are compared with high pressure (4 to 300 Mbars) data. DOE

N91-28637# Los Alamos National Lab., NM.

EQUATION OF STATE AND CRUSHING DYNAMICS OF LOW-DENSITY SILICA AEROGELS

R. Rabie and J. J. Dick 1991 5 p Presented at the 1991 American Physical Society (APS) Conference on Shock Compression of Condensed Matter, Williamsburg, 17-20 Jul. 1991
(Contract W-7405-eng-36)
(DE91-014766; LA-UR-91-1944; CONF-9107105-46) Avail: NTIS HC/MF A01

Shock compression of low-density silica aerogels reveals a rate process associated with the crushing dynamics of the aerogel structure. Embedded magnetic impulse velocity gauge (MIV) experiments have been accomplished on density 0.3 and 0.12 g/cc materials. The crushing rate has been determined for the low pressure (approximately 0.1 to 0.2 GPa) regime, and equation of state (EOS) data have been required. The crushing rate increases with applied pressure in this low pressure region. DOE

N91-28638 Georgia Inst. of Tech., Atlanta.

STABILITY OF CYLINDRICAL LAMINATES BY HIGHER ORDER SHEAR DEFORMABLE THEORIES Ph.D. Thesis

John S. Anastasiadis 1990 304 p
Avail: Univ. Microfilms Order No. DA9115370

A higher order theory is developed, which includes initial geometric imperfections and transverse shear effects, for a laminated cylindrical configuration, under the actions of lateral pressure, axial compression, and torsion. The terms which must be eliminated to reduce the set to lower order theories are clearly identified. Then, specialization to the geometry case of a symmetric laminated shell free of initial geometric imperfections, is made for lateral pressure and axial compression. This geometry provides a membrane prebuckling state; bifurcational buckling from this state to a buckled state is possible. The perturbation technique is applied to produce the buckling equations and the related boundary conditions. Galerkin's procedure is applied to some special cases in order to solve the eigenboundary value problem. A parametric study is performed for all shell parameters. The special cases considered are first order shear deformation theory, higher order shear deformation theory, first order shear deformation theory with the use of a shear correction factor, and classical theory. Results are generated for two geometry cases, the infinitely long cylinder, and the finite length cylinder. The parametric study establishes the effect of length to radius ratio, thickness to radius ratio, lamina stacking, and the theory used for the prediction of critical loads. Dissert. Abstr.

N91-28639 Illinois Inst. of Tech., Chicago.

FLUTTER OF LAMINATED RECTANGULAR PLATES INCLUDING FINITE DEFLECTION AND SHEAR DEFORMATION Ph.D. Thesis

Jongsik Woo 1990 219 p
Avail: Univ. Microfilms Order No. DA9117598

Linear and nonlinear flutter of thin and moderately thick composite plates are investigated. For arbitrarily laminated thin rectangular plates the nonlinear large deflection theory of von Karman is used and the so-called first order shear deformation theory is used for the analysis of moderately thick composite plates. Linear static piston theory is used for aerodynamic pressure. The governing equations of motion and boundary conditions are derived based on the Hamilton's variational principle. Full-mode displacement function with the aid of the Galerkin's approximation is employed for more accurate analyses. Dissert. Abstr.

N91-28640 Virginia Polytechnic Inst. and State Univ., Blacksburg.
THE SOLUTION OF VARIABLE-GEOMETRY TRUSS PROBLEMS USING NEW HOMOTOPY CONTINUATION METHODS Ph.D. Thesis
Veeraraghavan Arun 1990 145 p
Avail: Univ. Microfilms Order No. DA9116621

Basic Variable-Geometry Truss (VGT) Theory is described, and criteria used in the determination of valid VGT unit cells is presented. The VGT's have been widely recognized as adaptive or collapsing structures for space and military applications. Four of the VGT unit cells, tetrahedral, octahedral, decahedral, and dodecahedral, are discussed in detail. The typical modeling and formulation procedure for developing the kinematic equations associated with the forward kinematic problem of each type of cell is described. A new and efficient technique for solving the forward kinematics problem of VGT's is also presented. All VGT problems lead to systems of eqautions. Commonly, such systems are solved by an iterative numerical method, usually a Newton method or a variant. For such methods to yield a solution, a starting point sufficiently close to the actual solution must be supplied. For systems of the size of those encountered in VGT problems, this is a formidable task. On the other hand, recently developed methods in homotopy continuation for polynomials are not only global, but also exhaustive. Homotopies are a traditional part of topology and have only recently begun to be used for practical numerical computation. Polynomial continuation is used to track the solutions of the systems of equations describing the kinematics of VGT's. Dissert. Abstr.

N91-28641 Lowell Univ., MA.
A STUDY OF THE BUCKLING AND VIBRATION BEHAVIOR OF AN INITIALLY STRESSED THICK PLATE BY GALERKIN'S METHOD Ph.D. Thesis
Shou Rei Chang 1990 85 p
Avail: Univ. Microfilms Order No. DA9112373

The effects of initial, in-plane compressive (tensile) plus bending stress on the vibratory behavior of thick rectangular plates with one pair of opposite sides clamped and the other pair simply supported are investigated. Since an exact solution for this problem cannot be found for the specified boundary conditions for an initially stressed plate, Galerkin's method is used for the purpose of finding an approximate solution to the differential equations of the motion. The results of this research contribute toward a basic understanding of the vibration of initially stressed thick rectangular plates and the relationship between static buckling behavior, and the vibrational behavior. Results are presented for various bending stresses and aspect ratios. Dissert. Abstr.

N91-28642 California Univ., Los Angeles.
EXPLICIT MODELS FOR PROPORTIONAL DAMPING IN TIMOSHENKO BEAMS Ph.D. Thesis
Jung-Wei Cheng 1991 113 p
Avail: Univ. Microfilms Order No. DA9115433

Explicit representations of proportional damping operators in Timoshenko beams and an asymptotically proportional damping operator for the beam torsion are presented. The proportional damping operators are square roots of the stiffness operators. They are calculated using the Balakrishnan formula of the square root operator. An asymptotically proportional damping operator for the beam torsion of a cantilevered beam with tip mass is obtained by simplifying its corresponding square root operator. It contains the finite Hilbert transform and a non-local term at the boundary to preserve the nonnegative definiteness. Dissert. Abstr.

N91-28643*# Wayne State Univ., Detroit, MI. Dept. of Mathematics.
ACTIVE CONTROL OF PANEL VIBRATIONS INDUCED BY BOUNDARY-LAYER FLOW Annual Report, 10 Aug. 1990 - 9 Aug. 1991
Pao-Liu Chow 24 Aug. 1991 13 p
(Grant NAG1-1175)
(NASA-CR-188733; NAS 1.26:188733) Avail: NTIS HC/MF A03 CSCL 20K

Some problems in active control of panel vibration excited by a boundary layer flow over a flat plate are studied. In the first phase of the study, the optimal control problem of vibrating elastic panel induced by a fluid dynamical loading was studied. For a simply supported rectangular plate, the vibration control problem can be analyzed by a modal analysis. The control objective is to minimize the total cost functional, which is the sum of a vibrational energy and the control cost. By means of the modal expansion, the dynamical equation for the plate and the cost functional are reduced to a system of ordinary differential equations and the cost functions for the modes. For the linear elastic plate, the modes become uncoupled. The control of each modal amplitude reduces to the so-called linear regulator problem in control theory. Such problems can then be solved by the method of adjoint state. The optimality system of equations was solved numerically by a shooting method. The results are summarized. Author

N91-28644*# Applied Research Associates, Inc., Raleigh, NC.
PROBABILISTIC STRUCTURAL MECHANICS RESEARCH FOR PARALLEL PROCESSING COMPUTERS Final Report
Robert H. Sues, Heh-Chyun Chen, Lawrence A. Twisdale, and William R. Martin (Michigan Univ., Ann Arbor.) Aug. 1991 74 p
(Contract NAS3-25824)
(NASA-CR-187162; NAS 1.26:187162; ARA-5589) Avail: NTIS HC/MF A04 CSCL 20K

Aerospace structures and spacecraft are a complex assemblage of structural components that are subjected to a variety of complex, cyclic, and transient loading conditions. Significant modeling uncertainties are present in these structures, in addition to the inherent randomness of material properties and loads. To properly account for these uncertainties in evaluating and assessing the reliability of these components and structures, probabilistic structural mechanics (PSM) procedures must be used. Much research has focused on basic theory development and the development of approximate analytic solution methods in random vibrations and structural reliability. Practical application of PSM methods was hampered by their computationally intense nature. Solution of PSM problems requires repeated analyses of structures that are often large, and exhibit nonlinear and/or dynamic response behavior. These methods are all inherently parallel and ideally suited to implementation on parallel processing computers. New hardware architectures and innovative control software and solution methodologies are needed to make solution of large scale PSM problems practical. Author

N91-28238*# National Aeronautics and Space Administration. Lewis Research Center, Cleveland, OH.
PROBABILISTIC STRUCTURAL ANALYSIS METHODS FOR SPACE TRANSPORTATION PROPULSION SYSTEMS
C. C. Chamis, N. Moore, C. Anis, J. Newell, V. Nagpal, and S. Singhal (Sverdrup Technology, Inc., Brook Park, OH.) *In* NASA, Washington, Space Transportation Propulsion Technology Symposium. Volume 3: Panel Session Summaries and Presentations May 1991 p 895-914 (For primary document see N91-28235 20-20)
Avail: NTIS HC/MF A99 CSCL 20K

42 GEOSCIENCES (GENERAL)

No abstracts in this category.

43 EARTH RESOURCES AND REMOTE SENSING

Includes remote sensing of earth resources by aircraft and spacecraft; photogrammetry; and aerial photography.

For instrumentation see *35 Instrumentation and Photography.*

N91-28645# Geological Survey, Denver, CO.
CLOSE-RANGE GEOPHOTOGRAMMETRIC MAPPING OF TRENCH WALLS USING MULTI-MODEL STEREO RESTITUTION SOFTWARE
J. A. Coe, E. M. Taylor, and S. P. Schilling 1991 14 p Presented at the 1991 ACSM/ASPRS (American Society for Photogrammetry and Remote Sensing) Annual Conference, Baltimore, 25-29 Mar. 1991
(Contract DE-AI08-78ET-44802)
(DE91-013105; CONF-9103172-2) Avail: NTIS HC/MF A03

Methods for mapping geologic features exposed on trench walls have advanced from conventional gridding and sketch mapping to precise close-range photogrammetric mapping. In our study, two strips of small-format (60 x 60) stereo pairs, each containing 42 photos and covering approximately 60 m of nearly vertical trench wall (2 to 4 m high), were contact printed onto eight 205 x 255-mm transparent film sheets. Each strip was oriented in a Kern DSR15 analytical plotter using the bundle adjustment module of Multi-Model Stereo Restitution Software (MMSRS). We experimented with several systematic-control-point configurations to evaluate orientation accuracies as a function of the number and position of control points. We recommend establishing control-point columns (each containing 2 to 3 points) in every 5th photo to achieve the 7-mm Root Mean Square Error (RMSE) accuracy required by our trench-mapping project. DOE

N91-28646 Ohio State Univ., Columbus.
ANALYTICAL CALIBRATION OF THE AIRBORNE PHOTOGRAMMETRIC SYSTEM USING A PRIORI KNOWLEDGE OF THE EXPOSURE STATION OBTAINED FROM KINEMATIC GLOBAL POSITIONING SYSTEM TECHNIQUES Ph.D. Thesis
Lewis A. Lapine 1990 363 p
Avail: Univ. Microfilms Order No. DA9111738

In the future, the position of the camera exposure station will be determined by very accurate navigation systems, such as NAVSTAR Global Positioning System (GPS). Kinematic GPS techniques provide the means to accurately position the airborne system over a dense set of signalized geodetic control points so that the entire airborne system can be calibrated in the environment in which it normally operates. In this research the calibration technique is instrumented, obvious sources of systematic error are analyzed, and the technique is demonstrated by calibrating an airborne system. The lens system, as well as aircraft induced systematic errors were modelled and verified. The airborne calibration improved the overall performance of the system. Dissert. Abstr.

N91-28647 Louisiana State Univ., Baton Rouge.
A NEW APPROACH TO ANALYZING HIGH-RESOLUTION AERIAL PHOTOGRAPHS OF URBAN AREAS Ph.D. Thesis
Timothy Dwayne Phillips 1990 217 p
Avail: Univ. Microfilms Order No. DA9112263

A new approach is proposed for analyzing high resolution aerial photographs of urban areas. A high level analysis approach is considered. A unique use of three basic ideas is introduced: (1) the use of context, expectations, selective attention, and the perceptual cycle; (2) analyzing the image through a hierarchy of increasingly specific labels; and (3) the interplay between the segmentation and interpretation processes. These are developed in a computer vision system for analyzing aerial photographs. The system comprises: (1) a control mechanism; (2) a knowledge base; (3) a belief maintenance system; and (4) an image processing interface. Dissert. Abstr.

44 ENERGY PRODUCTION AND CONVERSION

Includes specific energy conversion systems, e.g., fuel cells; global sources of energy; geophysical conversion; and windpower.

For related information see also *07 Aircraft Propulsion and Power, 20 Spacecraft Propulsion and Power,* and *28 Propellants and Fuels.*

N91-28648*# Rockwell International Corp., Canoga Park, CA. Rocketdyne Div.
ISSUES CONCERNING CENTRALIZED VERSUS DECENTRALIZED POWER DEPLOYMENT Final Report
Kenneth J. Metcalf, Richard B. Harty, and James F. Robin Mar. 1991 114 p
(Contract NAS3-25808)
(NASA-CR-187121; NAS 1.26:187121) Avail: NTIS HC/MF A06 CSCL 10B

The results of a study of proposed lunar base architectures to identify issues concerning centralized and decentralized power system deployment options are presented. The power system consists of the energy producing system (power plant), the power conditioning components used to convert the generated power into the form desired for transmission, the transmission lines that conduct this power from the power sources to the loads, and the primary power conditioning hardware located at the user end. Three power system architectures, centralized, hybrid, and decentralized, were evaluated during the course of this study. Candidate power sources were characterized with respect to mass and radiator area. Two electrical models were created for each architecture to identify the preferred method of power transmission, dc or ac. Each model allowed the transmission voltage level to be varied at assess the impact on power system mass. The ac power system models also permitted the transmission line configurations and placements to determine the best conductor construction and installation location. Key parameters used to evaluate each configuration were power source and power conditioning component efficiencies, masses, and radiator areas; transmission line masses and operating temperatures; and total system mass. Author

N91-28649# Akron Univ., OH. Dept. of Chemistry.
DYNAMICS OF CHARGE-TRANSFER EXCITED STATES RELEVANT TO PHOTOCHEMICAL ENERGY CONVERSION
E. C. Lim 1991 5 p
(Contract DE-FG02-89ER-14024)
(DE91-012669; DOE/ER-14024/1) Avail: NTIS HC/MF A01

Photoinduced Charge Transfer (CT) processes in a series of N-R-N systems, where N stands for naphthalene and R is -CH-, -O-, etc., were studied in solvents of different polarity. In N-CH2-N and N-O-N, time resolved emission spectra show that initial naphthalene-like monomer band undergoes gradual shift and broadening to yield a structured emission at longer wavelength, as the delay after the laser excitation is increased. Further delay leads to mostly structureless band at still longer wavelength, which resembles the bicimer emission in polar solvents. Formation of the precursor state, and hence the CT state, is shown to involve rotation of one electronically excited moiety with respect to the other to form a twisted structure. Studies of the kinetics of these systems under varying experimental conditions show that the twisted intramolecular CT state can be formed on nanosecond time scales by one-photon excitation of one of the chromophores into a singlet state or on microsecond time scales by two-photon excitations of both chromophores into the lowest triplet state. The fluorescence excitation and dispersed fluorescence spectra of the van der Waals complexes of fluorene with durene, 1,2,4,5-tetrafluorobenzene, and 1,2,4,5-tetrachlorobenzene were studied in supersonic jets. The fluorene tetrachlorobenzene system, unlike the others, exhibits exciplex formation upon excitation of fluorene to its lowest excited singlet state (S sub 1). The stability of the fluorene tetrachlorobenzene exciplex state is attributed to the small electronic gap between S sub 1 fluorene and S sub 1 tetrachlorobenzene, which increases exciton resonance between the component molecules. DOE

N91-28650# Midwest Research Inst., Golden, CO.
POLYCRYSTALLINE THIN FILM PHOTOVOLTAIC TECHNOLOGY
H. S. Ullal, K. Zweibel, R. L. Mitchell, and R. Noufi Mar. 1991 8 p Presented at the World Congress of the International Solar Energy Society, Denver, 19-23 Aug. 1991
(Contract DE-AC02-83CH-10093)
(DE91-002136; SERI/TP-211-4212; CONF-910802-1) Avail: NTIS HC/MF A02

Low-cost, high-efficiency thin-film modules are an exciting photovoltaic technology option for generating cost-effective electricity in 1995 and beyond. The significant technical progress made in the following thin films is reviewed: copper indium diselenide, cadmium telluride, and polycrystalline thin silicon films. Also, the recent US DOE/SERI initiative to commercialize these emerging technologies is discussed. DOE

N91-28651# Sandia National Labs., Albuquerque, NM.
UNITED STATES DEPARTMENT OF ENERGY SOLAR RECEIVER TECHNOLOGY DEVELOPMENT
P. C. Klimas, R. B. Diver, and J. M. Chavez 1990 17 p Presented at the 5th International Symposium on Solar High-Temperature Technologies, Davos, Switzerland, 27-31 Aug. 1990
(Contract DE-AC04-76DP-00789)
(DE91-012653; SAND-90-0934C; CONF-9008139-4) Avail: NTIS HC/MF A03

The United States Department of Energy (DOE), through Sandia National Laboratories, has been conducting a Solar Thermal Receiver Technology Development Program, which maintains a balance between analytical modeling, bench and small scale testing, and experimentation conducted at scales representative of commercially-sized equipment. Central receiver activities emphasize molten salt-based systems on large scales and volumetric devices in the modeling and small scale testing. These receivers are expected to be utilized in solar power plants rated between 100 and 200 MW. Distributed receiver research focuses on liquid metal refluxing devices. These are intended to mate parabolic dish concentrators with Stirling cycle engines in the 5 to 25 kW(sub e) power range. The effort in the area of volumetric receivers is less intensive and highly cooperative in nature. A ceramic foam absorber of Sandia design was successfully tested on the 200 kW(sub t) test bed at Plataforma Solar during 1989. Material integrity during the approximately 90-test series was excellent. Significant progress has been made with parabolic dish concentrator-mounted receivers using liquid metals (sodium or a potassium/sodium mixture) as heat transport media. Sandia has successfully solar-tested a pool boiling reflux receiver sized to power a 25 kW Stirling engine. Boiling stability and transient operation were both excellent. This document describes these activities in detail and will outline plans for future development. DOE

N91-28652# Westinghouse Electric Corp., Pittsburgh, PA. Science and Technology Center.
DEVELOPMENT OF A CURRENT COLLECTION LOSS MANAGEMENT SYSTEM FOR SDI HOMOPOLAR POWER SUPPLIES
D. W. Brown 3 Apr. 1991 113 p
(Contract DE-AC03-86SF-16518)
(DE91-012779; DOE/SF-16518/T1) Avail: NTIS HC/MF A06

High speed, high power density current collection systems have been identified as an enabling technology required to construct homopolar power supplies to meet SDI missions. This work is part of a three-year effort directed towards the analysis, experimental verification, and prototype construction of a current collection system designed to operate continuously at 2 kA/sq cm, at a rubbing speed of 200 m/s, and with acceptable losses in a space environment. To date, no system has achieved these conditions simultaneously. This is the final report covering the three year period of performance on DOE contract AC03-86SF-16518. Major areas covered include design, construction and operation of a cryogenically cooled brush test rig, design and construction of a high speed brush test rig, optimization study for homopolar machines, loss analysis of the current collection system, and an application study which defines the air-core homopolar construction necessary to achieve the goal of 80 kW/kg generator power density. DOE

N91-28653# Sandia National Labs., Albuquerque, NM.
SECOND-GENERATION CENTRAL RECEIVER TECHNOLOGY COMPARISON
P. C. Klimas and M. Becker 1990 11 p Presented at the 5th International Symposium on Solar High-Temperature Technologies, Davos, Switzerland, 27-31 Aug. 1990
(Contract DE-AC04-76DP-00789)
(DE91-012865; SAND-90-0947C; CONF-9008139-5) Avail: NTIS HC/MF A03

Fifteen years of solar thermal technology development have produced a considerable amount of knowledge relating to the production of electricity from central receiver power plants. This body of knowledge is under examination by researchers from the United States and the Federal Republic of Germany for the purpose of defining the next generation central receiver electricity producers. This second generation power plant is expected to represent a significant step towards commercialization of these systems. During the course of the study, specific activities needed to realize this next-step technology are being defined. The study is an international team effort. Under the International Energy Agency Small Solar Power Systems project, researchers from DLR, Interatom, Sandia National Laboratories, and Bechtel have designed a study in which technologies relating to existing systems are quantified, logical next-step systems are characterized, and future potential advances are identified. The receiver concepts under investigation are: salt-in-tube, volumetric, and direct absorption. Two plant performance levels are examined, 30 and 100 MW(sub e). Each concept is applied with common capacity factors, solar multiples, and types and sizes of heliostats at each performance level. Availability and uncertainty analyses are also performed. Annual energy production figures are calculated using the SOLERGY computer code. Capital and Operation and Maintenance cost methodologies are mutually agreed upon in order that levelized energy cost calculations will be consistent for each power plant. During the course of this effort, further potential advances in central receiver technology have continued to become apparent. These possible areas for improvement will be described. An additional comparison is being made between central receivers and trough-based systems. DOE

N91-28654# Pacific Northwest Lab., Richland, WA.
APPLICATIONS AND CHALLENGES FOR THERMAL ENERGY STORAGE
L. D. Kannberg and J. T. Tomlinson (Oak Ridge National Lab., TN.) Apr. 1991 23 p Presented at the 5th International Conference on Thermal Energy Storage (TES), The Hague, Netherlands, 13-16 May 1991
(Contract DE-AC06-76RL-01830)
(DE91-012873; PNL-SA-19359; CONF-910568-2) Avail: NTIS HC/MF A03

New thermal energy storage (TES) technologies are being developed and applied as society strives to relieve increasing energy and environmental stresses. Applications for these new technologies range from residential and district heating and cooling using waste and solar energy, to high-temperature energy storage for power production and industrial processes. In the last two decades there has been great interest and development of heat storage systems, primarily for residential and commercial buildings. While development has continued, the rate of advancement has slowed with current technology considered adequate for electrically charged heat storage furnaces. Use of chill storage for building diurnal cooling has received substantial development. DOE

N91-28655# Oak Ridge National Lab., TN.
MAKING ENERGY EFFICIENCY HAPPEN
E. Hirst 1991 18 p Presented at the Technologies for a Greenhouse Constrained Society Conference, Oak Ridge, 11-13 Jun. 1991
(Contract DE-AC05-84OR-21400)
(DE91-013057; CONF-9106195-1) Avail: NTIS HC/MF A03

Improving energy efficiency is the least expensive and most effective way to address simultaneously several national issues. Improving efficiency saves money for consumers, increases economic productivity and international competitiveness, enhances national security by lowering oil imports, and reduces the adverse environmental effects of energy production. This paper discusses some of the many opportunities to improve efficiency, emphasizing the roles of government and utilities. DOE

N91-28656# Midwest Research Inst., Golden, CO.
SOLTECH 91: PROCEEDINGS, VOLUME 2
W. Traugott, ed., R. Hewett, ed., and D. Menicucci, ed. Apr. 1991 317 p Conference held in Burlingame, 26-29 Mar. 1991 Prepared in cooperation with Sandia National Labs., Albuquerque, NM
(Contract DE-AC02-83CH-10093)
(DE91-013767; SERI/CP-250-4254-Vol-2; CONF-9103109-Vol-2) Avail: NTIS HC/MF A14

This document is a limited Proceedings, documenting the presentations given at the symposia conducted by the U.S. Department of Energy's (DOE) Solar Industrial Program and Solar Thermal Electric program at SOLTECH91. The SOLTECH91 national solar energy conference was held at Burlingame, California during the period March 26 to 29, 1991. The Solar Energy Research Institute manages the Solar Industrial Program; Sandia National Laboratories (Albuquerque) manages the Solar Thermal Electric Program. The symposia sessions were as follows: solar industrial program and thermal electric program overviews; current and near-term solar industrial applications; solar detoxification of organics in water; and solar thermal electric systems. For each presentation given in these symposia, these Proceedings provide a one- to two-page abstract and copies of the viewgraphs and/or 35 mm slides utilized by the speaker. Some speakers provided additional materials in the interest of completeness. The materials presented in this document were not subjected to a peer review process. Individual papers have been cataloged separately. DOE

N91-28657# International Fuel Cells Corp., South Windsor, CT.
ADVANCED WATER-COOLED PHOSPHORIC ACID FUEL CELL DEVELOPMENT
Jul. 1990 35 p
(Contract DE-AC21-88MC-24221)
(DE90-009700; DOE/MC-24221/2881) Avail: NTIS HC/MF A03

The Advanced Water Cooled Phosphoric Acid Fuel Cell Development program is being conducted by International Fuel Cells Corporation (IFC) to improve the performance and minimize the cost of water cooled, electric utility phosphoric acid fuel cell stacks. The program adapts the existing on-site Configuration B cell design to electric utility operating conditions and introduces additional new design features. Task 1 consists of the conceptual design of a full- scale electric utility cell stack that meets program objectives. Tasks 2 and 3 develop the materials and processes required to fabricate the components that meet the program objective. The design of the small area and two 10-sq. ft. short stacks is conducted in Task 4. The conceptual design also is updated to incorporate the results of material and process developments, as well as results of stack tests conducted in Task 6. Fabrication and assembly of the short stacks are conducted in Task 5 and subsequent tests are conducted in Task 6. The Contractor expects to enter into a contract with The Electric Power Research Institute (EPRI) to assemble and endurance test the second 10-sq. ft. short stack. This report describes the cell design and development effort that is being conducted to demonstrate by subscale stack test, the technical achievements made toward the above program objectives. DOE

N91-28658# Midwest Research Inst., Golden, CO.
SOLTECH 91: PROCEEDINGS, VOLUME 1
W. Traugott, ed., R. Hewett, ed., and D. Menicucci, ed. Apr. 1991 312 p Conference helh in Burlinghame, 26-29 Mar. 1991 Prepared in cooperation with Sandia National Labs., Albuquerque, NM
(Contract DE-AC02-83CH-10093)
(DE91-002163; SERI/CP-250-4254-Vol-1; CONF-9103109-Vol-1) Avail: NTIS HC/MF A14

This document is a limited Proceedings, documenting the presentations given at the symposia conducted by the U.S. Department of Energy's (DOE) Solar Industrial Program and Solar Thermal Electric Program at SOLTECH91. The SOLTECH91 national solar energy conference was held in Burlingame, California during the period March 26 to 29, 1991. The Solar Energy Research Institute manages the Solar Industrial Program; Sandia National Laboratories (Albuquerque) manages the Solar Thermal Electric Program. The symposia sessions were as follows: (1) Solar Industrial Program and Solar Thermal Electric Program Overviews; (2) Current and Near-Term Solar Industrial Applications; Solar Detoxification of Organics in Water; and Solar Thermal Electric Systems. For each presentation given in these symposia, these Proceedings provide a one- to two-page abstract and copies of the viewgraphs and/or 35 mm slides utilized by the speaker. Some speakers provided additional materials in the interest of completeness. The materials presented in this document were not subjected to a peer review process. Individual papers have been cataloged separately. DOE

N91-28659# International Fuel Cells Corp., South Windsor, CT.
ADVANCED WATER-COOLED PHOSPHORIC ACID FUEL CELL DEVELOPMENT
1990 30 p
(Contract DE-AC21-88MC-24221)
(DE91-012243; DOE/MC-24221/T19; FCR-11137) Avail: NTIS HC/MF A03

The Advanced Water Cooled Phosphoric Acid Fuel Cell Development program is being conducted by International Fuel Cells Corporation (IFC) to improve the performance and minimize the cost of water cooled, electric utility phosphoric acid fuel cell stacks. The program adapts the existing on-site Configuration B cell design to electric utility operating conditions and introduces additional new design features. Task 1 consists of the conceptual design of a full- scale electric utility cell stack that meets program objectives. Tasks 2 and 3 develop the materials and processes required to fabricate the components that meet the program objective. The design of the small area and two 10 sq ft short stack is conducted in Task 4. The conceptual design also is updated to incorporate the results of material and process developments, as well as results of stack tests conducted in Task 6. Fabrication and assembly of the short stacks are conducted in Task 5 and subsequent tests are conducted in Task 6. The Contractor expects to enter into a contract with The Electric Power Research Institute (EPRI) to assemble and endurance test the second 10 sq ft short stack. This report describes the cell design and development effort that is being conducted to demonstrate by subscale stack test, the technical achievements made toward the above program objectives. DOE

N91-28660# Brookhaven National Lab., Upton, NY.
GEOTHERMAL MATERIALS DEVELOPMENT
L. E. Kukacka Feb. 1991 13 p
(Contract DE-AC02-76CH-00016)
(DE91-013972; BNL-45998) Avail: NTIS HC/MF A03

Advances in the development of new materials, the commercial availabilities of which are essential for the attainment of Hydrothermal Category Level 1 and 2 Objectives, continue to be made in the Geothermal Materials Development Project. Many successes have already accrued and the results transferred to industry. In FY 1990, the R and D efforts were focused on reducing well drilling and completion costs and on mitigating corrosion in well casing. Activities on lost circulation control materials, CO2 resistant lightweight cements, and thermally conductive corrosion and scale-resistant protective liner systems have reached the final development stages, and cost-shared field tests are planned for the FY 1991 to 1992 time frame. Technology transfer efforts on high temperature elastomers for use in drilling tools are continuing under Geothermal Drilling Organization (GDO) sponsorship. DOE

N91-28661# Los Alamos National Lab., NM.
RECENT ACHIEVEMENTS IN POLYMER ELECTROLYTE FUEL CELL (PEFC) RESEARCH AT LOS ALAMOS NATIONAL LABORATORY
M. S. Wilson, T. E. Springer, T. A. Zawodzinski, and S. Gottesfeld 1991 20 p Presented at the 26th Intersociety Energy Conversion Engineering (IECE) Conference, Boston, 3-9 Aug. 1991
(Contract W-7405-eng-36)
(DE91-013683; LA-UR-91-1708; CONF-910801-5) Avail: NTIS HC/MF A03

Recent research work on the polymer electrolyte fuel cell is described. The main topics are: (1) a new approach to the fabrication of Pt/C catalyst layers of high performance employing loadings as low as 0.1 mgPt/sq cm; (2) measurements and modelling of membrane water transport and water management in the PEFC; and (3) carbon monoxide poisoning of anode electrocatalysts in the PEFC -- the problem and possible solutions. DOE

N91-28662# Sandia National Labs., Albuquerque, NM.
ONE-SUN SILICON SOLAR CELL RESEARCH
M. A. Green, J. Zhao, A. Wang, A. W. Blakers, A. M. Milne, X. Dai, C. M. Chong, S. R. Wenham, F. Zhang, and F. Yun et al Mar. 1991 68 p Prepared in cooperation with New South Wales Univ., Kensington, Australia
(Contract DE-AC04-76DP-00789)
(DE91-014329; SAND-90-7037) Avail: NTIS HC/MF A04

This report describes research for the period September 1988 to February 1990 directed at improving the performance of crystalline and polycrystalline silicon solar cells. Key results include the demonstration of 24.2 percent energy conversion efficiency for 4-sq cm crystalline cells fabricated using the development of the Passivated Emitter Cell processing sequence, the demonstration of energy conversion efficiency up to 22.4 percent for large-area, low-cost silicon concentrator cells fabricated using the laser grooved cell processing sequence, the demonstration of efficiencies up to 17.8 percent on 4-sq cm polycrystalline silicon substrates, and the demonstration of efficiencies of up to 16.7 percent on 10 sq cm polycrystalline substrates using a combined laser textured and grooved cell processing sequence. DOE

N91-28663# Midwest Research Inst., Golden, CO.
FIFTEENTH DOE SOLAR PHOTOCHEMISTRY RESEARCH CONFERENCE
1991 165 p Conference held in Snowmass, CO, 2-6 Jun. 1991
(Contract DE-AC02-83CH-10093)
(DE91-002165; SERI/CP-236-4396; CONF-9106213-Absts)
Avail: NTIS HC/MF A08

This is a compilation of abstracts from the conference. A large variety of topics pertinent to solar energy conversion are covered, including photoinduced electron transfer, photochemical energy conversion, and photosynthetic energy conversion. DOE

N91-28664# Pacific Northwest Lab., Richland, WA.
ALTERNATIVE MATERIALS FOR SOLID OXIDE FUEL CELLS: CHROMITE INTERCONNECTIONS
J. L. Bates and L. A. Chick Jun. 1991 11 p Presented at the Fuel Cell Contractors Meeting, Morgantown, 6 May - 6 Jun. 1991
(Contract DE-AC06-76RL-01830)
(DE91-014447; PNL-SA-19561; CONF-9105223-1) Avail: NTIS HC/MF A03

This research and development is directed to modification of state-of-art and to development of analogous and alterative materials such as solid oxide fuel cell electrodes and interconnections, and consists of three tasks: electrical and thermal properties of state-of-the-art and alternative interconnection materials as functions of composition, structure, synthesis and processing methods; materials synthesis and processing methods to produce state-of-the-art and alternative interconnection chromite and manganite materials that can be sintered in air below 1550 C without the use of additives; and electrochemical behavior of material interfaces to understand the kinetics and electro-chemical and chemical processes. This report discusses R&D directed toward understanding the factors that affect air sinterability, sintering mechanisms and the thermal expansion of La(1-x)Sr(x)CrO3 and Y(1-x)Ca(x)CrO3. DOE

45 ENVIRONMENT POLLUTION

Includes atmospheric, noise, thermal, and water pollution.

N91-28665# Computer Sciences Corp., Research Triangle Park, NC.
REGIONAL OXIDANT MODEL USER'S GUIDE. PART 1: THE ROM PREPROCESSORS Final Report, Aug. 1989 - Jan. 1991
L. Milich, L. Bender, T. Boehm, O. Bullock, and J. Novak Jan. 1991 356 p
(Contract EPA-68-01-7365)
(PB91-171926; EPA/600/8-90/083A; PB91-171918) Avail: NTIS HC/MF A16; also avail. in set of 3 reports HC/MF E99, as PB91-171918 CSCL 13B

The Regional Oxidant Model (ROM) determines hourly concentrations and fates of ozone and 34 other chemical species over a scale of 1000 km x 1000 km for ozone episodes of up to one month's duration. The model structure, based on phenomenological concepts, consists of 3 1/2 layers. The surfaces separating the layers respond to variations in space and time in the meteorological phenomena simulated in each layer. The model simulates many physical and chemical processes that affect the motion and distribution of chemical concentrations; among these are: horizontal transport, photochemistry, nighttime wind shear and nocturnal jet; cumulus cloud effects and mesoscale vertical motion; terrain and mesoscale eddy effects; subgrid scale chemistry processes, natural sources of hydrocarbons, NOx and stratospheric ozone; and dry deposition. The ROM is a complex model that requires users to have expertise in photochemical grid modeling. Meteorologists, engineers, and computer scientists familiar with this type of modeling will find the User's Guide relevant and helpful for running the ROM. GRA

N91-28666# Computer Sciences Corp., Research Triangle Park, NC.
REGIONAL OXIDANT MODEL USER'S GUIDE. PART 2: THE ROM PROCESSOR NETWORK Final Report, Aug. 1989 - Jan. 1991
L. Milich, L. Bender, T. Boehm, O. Bullock, and J. Novak Jan. 1991 443 p
(Contract EPA-68-01-7365)
(PB91-171934; EPA/600/8-90/083B; PB91-171918) Avail: NTIS HC/MF A19; also avail. in set of 3 reports HC/MF E99, as PB91-171918 CSCL 13B

The input/output support for the Regional Oxidant Model (ROM) processor network is described. The processor network, the regional dependencies, and the VAX/Virtual Memory System (VAX/VMS) implementation of domain changes in the Regional Oxidant Model's processor network and analysis programs are discussed. Author

N91-28667 North Carolina Univ., Chapel Hill.
THE USE OF SCIENCE IN THE MANAGEMENT OF HAZARDOUS AIR POLLUTANTS Ph.D. Thesis
Karen Marie Martin 1990 325 p
Avail: Univ. Microfilms Order No. DA9115650

A long-term comparative analysis revealed that the use of science has changed significantly over the 20 year history of the Environmental Protection Agency's (EPA's) program to develop national emission standards for hazardous air pollutants. Early

regulatory decisions to list a substance as hazardous were found to be strongly dependent upon qualitative inferences about the likelihood that the substance was, in fact, hazardous to human health, based on human epidemiological and animal toxicological studies. By the 1980's, however, listing decisions were seemingly based exclusively on a single quantitative measure of human cancer risk. Distilling all health-effects science down to a single number was seen to overwhelm the decision making process with massive amounts of highly uncertain information and theoretically unsubstantiated analyses. To the extent that regulatory decisions were then made at all, no relationship was observed between the strength of the scientific evidence and the associated listing decisions. The science that was analyzed included each of the carcinogenicity studies considered by the EPA in nearly all of its 34 hazardous air pollutant assessments. Qualitative inferences and quantitative potency and risk estimates derived from these studies were also considered. The central analysis focused on identifying patterns, or the lack of patterns, between various elements of these scientific inputs and the associated regulatory decisions. The framework for this analysis took into account both legislative constraints regarding the use of science and EPA's evolving policies. The central analysis was extended by considering the influence that nonscientific factors may have had on the use of science. The politics of outside science advisory committees was seen to extend the committees' influence well beyond science policy and assessments within EPA. Such committees, together with the courts and national politics, have had significant influence on regulatory policies as well. This research found that the resulting policy changes have greatly limited the number of substances listed as hazardous air pollutants, and significantly delayed regulatory decision making, even to the point of impasse.
Dissert. Abstr.

N91-28668 California Inst. of Tech., Pasadena.
INORGANIC COMPONENTS OF ATMOSPHERIC AEROSOLS Ph.D. Thesis
Anthony Stein Wexler 1991 190 p
Avail: Univ. Microfilms Order No. DA9113624

The inorganic components comprise 15-50 percent of the mass of atmospheric aerosols. For about the past 10 years, the mass of these components was predicted assuming thermodynamic equilibrium between the volatile aerosol-phase inorganic species NH4NO3 and NH4Cl and their gas-phase counterparts, NH3, HNO3, and HCl. This assumption is examined and it is proven that: (1) the time scales for equilibrium between the gas and aerosol phases are often too long for equilibrium to hold; and (2) even when equilibrium holds, transport considerations often govern the size distribution of these aerosol components. The temperature dependence of the diliquescence point is derived, and it is proven that in multicomponent solutions the deliquescence point is lower than for corresponding single component solutions. These theories of the transport, thermodynamic, and deliquescent properties of atmospheric aerosols are integrated into an aerosol inorganics model (AIM). The predictions of AIM are compared to fundamental thermodynamic measurements and to the predictions of other aerosol equilibrium models. In the summer and fall of 1987, the California Air Resources Board conducted the Southern California Air Quality Study (SCAQS), during which atmospheric aerosols were measured in Los Angeles. The size and composition of the aerosols were measured. When the measured ammonium and nitrate size distributions are compared, it was found that different size aerosol particles are not in mutual equilibrium. Although the SCAQS data do not indicate an overall transport-limited departure from equilibrium, they do support the hypothesis that transport considerations are essential to predicting the size distribution of the volatile inorganic species. Dissert. Abstr.

N91-28669# Pacific Northwest Lab., Richland, WA.
ENVIRONMENTAL TRADEOFFS ASSOCIATED WITH VARIOUS ENERGY PATHS: A TOTAL ENERGY CYCLE ANALYSIS APPROACH
M. Placet and K. K. Humphreys May 1991 16 p Presented at the Minerals Management Service Information Transfer Meeting, Santa Barbara, 30 May 1991
(Contract DE-AC06-76RL-01830)
(DE91-013662; PNL-SA-19619; CONF-9105206-1) Avail: NTIS HC/MF A03

Energy supply and demand decisions have traditionally been driven primarily by cost factors, but as public awareness of environmental issues has increased, environmental assessments are becoming an important part of the selection process. A principal question is: What are the environmental tradeoffs associated with various energy pathways. In order to carry out an equitable comparison of alternative energy pathways, characterizations must be made not only the primary 'energy production' and 'end use' stages of an energy pathway, but the full process of providing an energy service. This can be accomplished using a 'total energy cycle analysis' approach. This approach considers all stages of an energy cycle including raw material extraction, material transportation, raw material transformation to a refined energy form, energy storage and distribution, and end use. In recognition of the increasing need for comprehensive analysis in the decision making process, a methodology that established the principles and assumptions to be used in total energy cycle analyses is being developed. DOE

N91-28670# Argonne National Lab., IL.
HIGH-THROUGHPUT LIQUID-ABSORPTION AIR AND AEROSOL SAMPLER
S. Zaromb, J. Alcaraz, D. Lawson, K. C. Picel (University of Northern Iowa, Cedar Falls.), and C. S. Woo 1991 7 p Presented at the International Air and Waste Management (AWMA) Symposium on Measurement of Toxic and Related Air Pollutants, Durham, 7-10 May 1991
(Contract W-31-109-eng-38)
(DE91-013762; ANL/CP-71950; CONF-910555-1) Avail: NTIS HC/MF A02

A high-throughput liquid-absorption preconcentrator (HTLAP) has been developed for rapid and/or ultrasensitive detection and analysis of trace air contaminants. Its advantages result from (1) a high air-sampling rate (approximately 1 m(exp 3)/min), (2) an appreciable analyte collection efficiency (30 to 60 percent) for both vapors and aerosols, and (3) a small volume of liquid absorbent (collected at a rate of 0.1 to 2 mL/min), all of which features combine to reduce the LDL (lower detection limit) of available analytical instrumentation by a factor of greater than 1000 and/or to permit faster sampling and far more rapid on-site air monitoring than were previously practicable. LDLs of (approximately)1:10(exp 13) by volume of alkaloids have been achieved with liquid chromatography and electrochemical detection. The HTLAP is directly adaptable to most liquid-phase analyzers. The small rate of liquid collection is also compatible with available interfaces to mass spectrometers. Moreover, the HTLAP permits detection and quantitation of compounds that cannot be readily analyzed by conventional preconcentration and gas chromatography, e.g., polar or highly reactive analytes, such as primary aromatic amines or hydrazines. High selectivity and/or stabilization of labile of reactive analytes, or entrapment of volatile analytes, may be effected through a proper choice of liquid absorbent. DOE

N91-28671# Pacific Northwest Lab., Richland, WA.
MODELING MOLECULAR PROCESSES IN THE ENVIRONMENT
T. H. Dunning, S. S. Xantheas, A. C. Hess, D. F. Feller, R. A. Kendall, and R. L. Ornstein May 1991 11 p Presented at the Power Supercomputer Users Meeting, Gaithersburg, 21-22 May 1991
(Contract DE-AC06-76RL-01830)
(DE91-013790; PNL-SA-19582; CONF-9105202-4) Avail: NTIS HC/MF A03

The U.S. Department of Energy is committed to a 30-year plan for environmental restoration at all of its sites. To meet these commitments DOE has organized an ambitious Research, Development, Demonstration, Testing and Evaluation program. Basic research lays the foundation for each step in the RDDT and E program, providing new knowledge and techniques for site characterization, needs assessment, innovative remediation technology, and post-remediation evaluation and monitoring. Theoretical and computational molecular science will play a critical role in developing molecular-level descriptions of the complex systems found in the environment. Theory provides the conceptual framework for the analysis and interpretation of experimental data. Modeling and simulation provides quantitative information which may be expensive, difficult or impossible to obtain in the laboratory. Further, theory, modeling and simulation provides insights into the fundamental factors governing molecular structure and dynamics which cannot be obtained from experiment alone. Continuing advances in theoretical concepts and methodology when combined with the ongoing nearly exponential growth in computer processing speeds hold great promise for modeling the fundamental molecular processes involved in contaminant transport and transformation in the environment. DOE

N91-28672# Lawrence Livermore National Lab., CA.
TREE: A MODEL OF THE EFFECTS OF ACID PRECIPITATION AND AIR POLLUTANTS ON THE GROWTH OF TREES
J. R. Kercher, S. Cowles, and P. Anderson Jul. 1990 80 p
(Contract W-7405-eng-48)
(DE91-014131; UCRL-21290) Avail: NTIS HC/MF A05

Understanding and assessing the effects of acid precipitation and other associated air pollutants, such as ozone, on forests is a primary focus of the Forest Response Program (FRP) of the National Acid Precipitation Assessment Program (NAPAP). The capability to predict or assess the effects of acid precipitation would be enhanced with the development of realistic tree models that incorporate the effects of pollutants. The objective of models would be to predict the dry-matter yield of the various plant components (e.g., root, stem, fruit, and foliage) and simulate their development in time as a function of environmental variables (e.g., temperature, light, and precipitation) and pollutant levels. In simulation models, the state variables must be specified. This means that those plant parts or attributes are necessary to determine the plants's dynamics must be decided. In addition, those systems processes which determine the relationships between the state variables must also be decided. When realistic tree models are spoken of, those models include enough biological detail to account for the observed phenomena of pollutant effects on tree physiology and yield. Furthermore, for such simulation models the appropriate time scale must be decided over which the detailed processes may be regarded as either slowly varying or in equilibrium. Hence, the stated objective and the goal of realism impose constraints on the decisions made regarding input, outputs, state variables, processes, and times scales. DOE

N91-28673# Atmospheric and Environmental Research, Inc., Cambridge, MA.
NATURAL AND ANTHROPOGENIC CLIMATE CHANGE
W. J. Gutowski, S. A. Clough, G. Molnar, M. Iacono, and W. C. Wang (State Univ. of New York, Albany.) 1 Mar. 1991 13 p
(Contract DE-FG02-86ER-60485)
(DE91-014734; DOE/ER-60485/T2) Avail: NTIS HC/MF A03

This report covers work on grant DE-FG02-86ER-60485 and consists of two parts: (1) progress for the period 9/1/90 to 3/1/91, and (2) the plan for the remaining period 3/1/91 to 8/31/91. The project includes two tasks: atmospheric radiation and improvement of climate models to evaluate the climatic effects of radiation changes. We have been performing this work in cooperation with our project subcontractor, Atmospheric Sciences Research Center, State University of New York/Albany (Prof. W. C. Wang, principal investigator). DOE

N91-28674# Oak Ridge National Lab., TN.
ANALYSIS OF SOUTHEASTERN CANADA LAKE-WATER CHEMISTRY DATA IN RELATION TO ACIDIC DEPOSITION
R. J. Olson, R. B. Cook, B. M. Ross-Todd, and J. J. Beauchamp May 1990 89 p
(Contract DE-AC05-84OR-21400)
(DE91-014957; ORNL/TM-11576; ESD-Publ-3509) Avail: NTIS HC/MF A05

Lake-water chemistry data were obtained for lakes in southeastern Canada to study relationships between atmospheric deposition and acid-base chemistry as part of the National Acid Precipitation Assessment Program State of Science and Technology reports. Quality assurance checks were made to ensure that the data used were of sufficient quality and were comparable to data from the United States. Ninety-eight percent of the 8506 sampled lakes had pH, ANC, and SO4(2-) data and were used in our analyses. Of these, we created a subset of 4017 lakes having data for more variable (Ca(2+), Mg(2+), Na(+), K(+), DOC, and conductivity) to analyze potential sources of lake-water acidity. The objectives of this work were to determine the geographical extent and number of potentially affected systems and to infer causes of acidification based on ion ratios. DOE

N91-28675# Argonne National Lab., IL. Environmental Assessment and Information Sciences Div.
WORK PLAN FOR THE PRELIMINARY SITE INVESTIGATION FOR MCMURDO STATION, ROSS ISLAND, ANTARCTICA
J. E. Stefano, T. L. Patton, L. D. McGinnis, C. A. Bebrich, D. A. Knudson, and K. C. Picel May 1991 63 p
(Contract W-31-109-eng-38)
(DE91-015100; ANL/EAIS/TM-48) Avail: NTIS HC/MF A04

This document presents the final work plan for the preliminary site investigation to be conducted at McMurdo Station, Ross Island, Antarctica. A draft version of this report was presented to the National Science Foundation (NSF) in January 1991. This work plan includes a brief site description and background, a discussion of the environmental setting, a sampling and analytical program for data collection, and a brief description of sampling and data management procedures. A description of the geologic and geophysical investigation to be conducted is also included. DOE

46 GEOPHYSICS

Includes aeronomy; upper and lower atmosphere studies; ionospheric and magnetospheric physics; and geomagnetism.

For space radiation see *93 Space Radiation.*

N91-28676 Technische Univ., Delft (Netherlands).
COMMON REFLECTION POINT STACKING: A MACRO MODEL DRIVEN APPROACH TO DIP MOVEOUT Ph.D. Thesis
Adriaan vanderSchoot 1989 197 p
(ISBN-90-9003020-4; ETN-90-97221) Copyright Avail: Delft Geophysical B.V., P.O. Box 148, 2600 AC Delft, Netherlands

Dip Moveout (DMO) is a valuable tool in processing schemes. A depth-oriented approach to DMO, called Common Reflection Point (CRP) stacking is presented. The CRP operator design is based on a macro model of the subsurface, in which ray tracing is performed. Lateral as well as vertical velocity variations are allowed. To obtain an exact (with respect to travel times) CRP operator for the inhomogeneous media, offset ray tracing for all offsets are needed. The multi-offset ray tracing is approximated by efficient zero-offset ray tracing, in combination with a simple mathematical relation. The CRP scheme is compared with conventional DMO schemes. Attention is paid to the evaluation of CRP stacking and prestack migration on synthetic and real data. The theory presented is developed for two dimensional media and, indications of how the CRP concept can be extended to three dimensional media are given. ESA

N91-28677# California Univ., Berkeley. Lawrence Berkeley Lab.
A GRAVITY MODEL FOR THE COSO GEOTHERMAL AREA, CALIFORNIA
M. A. Feighner and N. E. Goldstein Aug. 1990 8 p Presented at the Annual Meeting of the Geothermal Resources Council and International Symposium on Geothermal Energy, Kailua Kona, 20-24 Aug. 1990
(Contract DE-AC03-76SF-00098)

(DE91-011874; LBL-28878; CONF-900823-13) Avail: NTIS HC/MF A02

Two- and three-dimensional gravity modeling was done using gridded Bouguer gravity data covering a 45 x 45 km region over the Coso geothermal area in an effort to identify features related to the heat source and to seek possible evidence for an underlying magma chamber. Isostatic and terrain corrected Bouguer gravity data for about 1300 gravity stations were obtained from the U.S. Geological Survey. After the data were checked, the gravity values were gridded at 1 km centers for the area of interest centered on the Coso volcanic field. Most of the gravity variations can be explained by two lithologic units: (1) low density wedges of Quarternary alluvium with interbedded thin basalts (2.4 g/cu cm) filling the Rose Valley and Coso Basin/Indian Wells Valley, and (2) low density cover of Tertiary volcanic rocks and intercalated Coso Formation (2.49 g/cu cm). A 3-D iterative approach was used to find the thicknesses of both units. The gravity anomaly remaining after effects from Units 1 and 2 are removed is a broad north-south-trending low whose major peak lies 5 km north of Sugarloaf Mountain, the largest of the less than 0.3 m.y. old rhyolite domes in the Coso Range. Most of this residual anomaly can be accounted for by a deep, low-density (2.47 g/cu cm) prismatic body extending from 8 to about 30 km below the surface. While some of this anomaly might be associated with fractured Sierran granitic rocks, its close correlation to a low-velocity zone with comparable geometry suggests that the residual anomaly is probably caused a large zone of partial melt underlying the rhyolite domes of the Coso Range. DOE

N91-28678 Texas Univ., Austin.
SEISMIC TRAVELTIME INVERSION IN THREE-DIMENSIONAL HETEROGENEOUS MEDIA Ph.D. Thesis
Christopher Jude Finn 1990 284 p
Avail: Univ. Microfilms Order No. DA9116854

The measured traveltimes of specular reflection events are inverted to obtain a low spatial frequency, three dimensional model of the reflector geometry, and the compressional wave propagation speed. B-spline functions are used to describe the shapes of the interfaces and the lateral variations in velocity. The inversion is performed by optimizing a maximum likelihood criterion using a Newton based iteration. Model updates are obtained by iterative forward modeling and solution of the linearized equation set derived from the maximum likelihood criterion. In the forward problem, the ray tracing equations are solved as a two point boundary value problem with appropriate internal boundary conditions at velocity discontinuities. Analytic expressions for the Frechet derivatives necessary to obtain the model updates are given. Dissert. Abstr.

N91-28679 California Univ., Los Angeles.
HIGH-TEMPERATURE ELASTICITY AND EARTH'S UPPER MANTLE Ph.D. Thesis
Donald George Isaak 1991 239 p
Avail: Univ. Microfilms Order No. DA9117374

The elastic properties of minerals are important constraints on modeling the chemistry of Earth's interior and in determining the olivine content of the upper mantle. Current efforts focus on requiring the olivine content of an assemblage to produce wave velocities which match the velocity discontinuities observed seismically at 400-km depth due to changes in elasticity and density associated with an alpha- to beta-olivine phase change. However since the elasticity of beta-olivine is not known for conditions at 400-km depth, it must be estimated, resulting in present models of the upper mantle with 40 to 70 percent olivine. Dissert. Abstr.

N91-28680 Colorado State Univ., Fort Collins.
REGIONAL-SCALE FLOW IN COMPLEX TERRAIN: AN OBSERVATIONAL AND NUMERICAL INVESTIGATION Ph.D. Thesis
James E. Bossert 1990 270 p
Avail: Univ. Microfilms Order No. DA9117164

An observational program was conducted to investigate thermally-driven flows in complex terrain on meso-beta and meso-alpha scales (100 to 500 km). Data were collected from exposed mountaintop locations. Numerical simulations were performed to provide further insight into the physical mechanisms forcing the observed regional-scale circulation system. As a result of the observations and numerical experiments, four phases of the thermally forced diurnal circulation system across the Colorado mountain barrier were identified. These consist of a daytime mountain boundary layer development phase, a late afternoon transitional phase, an evening propagating density current phase, and a late night adjustment phase. Author

N91-28681 Clemson Univ., SC.
OBSERVATIONS AND THEORETICAL STUDIES OF TIDES AND NORMAL MODES IN THE LOWER THERMOSPHERE Ph.D. Thesis
M. Amanda Clark 1990 148 p
Avail: Univ. Microfilms Order No. DA9115057

While the dynamics of neutral winds in the thermosphere are fairly well understood for altitudes above 200 km, the wind systems in the lower thermosphere and upper mesosphere (corresponding to the ionospheric D and E regions), are complex and difficult to measure. The motion of the neutral atmosphere for these altitude regions is investigated. A computational model is used to investigate the problem of the dynamics in the high latitude thermospheres. The results are also presented of an experiment in which three days of observations of neutral winds between 70 and 120 km in altitude were made. Measurements of the plasma drift velocities were made using incoherent scatter radar, and neutral winds were then calculated by using the ion velocity equation and collision frequencies calculated from the model. Author

N91-28682 Utah Univ., Salt Lake City.
HEAT FLOW DATA AND THERMAL STATE OF THE CONTINENTAL LITHOSPHERE Ph.D. Thesis
Uk Han 1991 200 p
Avail: Univ. Microfilms Order No. DA9115209

Terrestrial heat flow data from the continents were compiled and analyzed to infer the thermal state and characteristics of continental lithosphere. New heat flow determinations, published from 1974 to 1990, were compiled, catalogued, analyzed, and added to the World Heat Flow Data Collection. The heat flow data include 2869 new determinations reported in 130 separate publications. Dissert. Abstr.

N91-28683 Illinois Univ., Urbana-Champaign.
MULTIPLE FREQUENCY ATMOSPHERIC RADAR TECHNIQUES Ph.D. Thesis
Gary Richard Stitt 1990 161 p
Avail: Univ. Microfilms Order No. DA9114424

The use of multiple frequency coding to improve the vertical resolution of pulsed-Doppler very high frequency atmospheric radars, especially with regards to the two-frequency techniques known as frequency domain interferometry (FDI), is presented. This technique consists of transmitting alternate pulses on two distinct carrier frequencies. The two resulting time series are used to evaluate the normalized cross-correlation function, whose magnitude and phase are related to the thickness and position of a scattering layer. These same time series are also used to evaluate cross-spectra, which yield magnitude and phase values for each Doppler frequency component of the return signal. Dissert. Abstr.

N91-28684 Washington Univ., Seattle.
STUDIES IN CLOUD PHYSICS: ELECTRIFICATION, GLACIATION, AND TURBULENCE Ph.D. Thesis
Bradley Aaron Baker 1990 97 p
Avail: Univ. Microfilms Order No. DA9109781

Several microphysical phenomena important in clouds are examined. First, a simple working hypothesis is formulated which can account for lab results from experiments on charge transfer between colliding ice hydrometeors. A clue is provided to the physical mechanism responsible for thunderstorm electrification. Next, some current hypothesized explanations for large ice concentrations at relatively high temperatures in clouds are examined. The first among these involve phoretic forces. Diffusiophoresis and thermophoresis are phenomena by which particles are transported, through a gas in which concentration and/or temperature gradients exists, as if they were caught in a fluid flow or subjected to a force. The roles of diffusiophoresis and thermophoresis in enhancing the collection of ice contact nuclei and thus the formation of ice in clouds are examined. The hypothesis is analyzed that the high ice crystal concentrations, observed in clouds, originate in regions of cloud with supersaturations considerably higher than those achieved in apparatus used to measure ice nucleus concentrations. Turbulent entrainment and mixing were studied in cumulus clouds via cloud microphysics data and statistical analysis. Dissert. Abstr.

N91-28685 Tennessee Univ., Knoxville.
MODELING TWO-POINT SPATIAL TURBULENCE SPECTRA FOR ANALYSIS OF GUST VARIATIONS OVER AEROSPACE VEHICLES Ph.D. Thesis
Joseph Elbert Durham, Jr. 1990 80 p
Avail: Univ. Microfilms Order No. DA9112850

Analytical models for two point spatial spectra of atmospheric turbulence are developed. Models based on both the von Karman and Dryden correlation are presented. A two point autocorrelation, defined as the correlation between like components of velocity measured at two spatially separated positions, is Fourier transformed to give the spectrum. The bias and aliasing errors associated with fast Fourier transform techniques for two point spatial correlations are described. A comparison is given of the spectrum computed by the fast Fourier transform of the digitized analytical correlation, with closed form solutions. The results show that the two point spatial spectrum is extremely sensitive to bias errors. Filters for smoothing the data to minimize the bias error are studied and an optimum filter is proposed. Dissert. Abstr.

N91-28686 Oregon State Univ., Corvallis.
MODELLING AND ANALYSIS OF GEOPHYSICAL TURBULENCE: USE OF OPTIMAL TRANSFORMS AND BASIS SETS Ph.D. Thesis
Nimal Kumar Ketagoda Gamage 1990 148 p
Avail: Univ. Microfilms Order No. DA9113890

The use of efficient basis functions to model and represent flows with internal sharp velocity gradients, such as shocks or eddy microfronts, are studied. This is achieved by analyzing artificial data, observed atmospheric turbulence data, and by the use of a Burgers' equation based spectral model. The concept of an efficient decomposition of a function into a basis set is presented and alternative analysis methods are studied. The development of a spectral model using a generalized basis for the Burgers' equation is presented and simulations are performed using a modified Walsh basis and compared with the Fourier (trigometric) basis and finite difference techniques. The wavelet transform is shown to be superior to the Fourier transform or the windowed Fourier transform in terms of defining the predominant scales in time series of turbulent shear flows and in zooming in on local coherent structures associated with sharp edges. The Haar function is used as a wavelet to detect ubiquitous zones of concentrated shear in turbulent flows sometimes referred to as microfronts. The location and organization of these shear zones suggest that they may be edges of large scale eddies. Dissert. Abstr.

N91-28687 Arizona Univ., Tucson.
GRAVITY WAVE PROPAGATION IN A FRONTAL ENVIRONMENT Ph.D. Thesis
Jerry Lee Steffens 1990 156 p
Avail: Univ. Microfilms Order No. DA9111971

Results obtained by Gall, Williams, and Clark in a series of numerical frontogenesis experiments are further explored. In the course of the simulations, gravity waves were produced which grew in intensity as the fronts (one at each of the two horizontal planes bounding the model domain) increased in strength. Waves formed ahead (upwind) of and directly above the surface front, but not behind it, which suggests a connection with the banded cloud patterns often seen ahead of cold fronts. The question of the asymmetrical distribution of waves relative to the surface front was studied using the method of ray tracing. The frontal fields which served as the mean state were obtained from the anelastic model developed by Clark. The first attempts to analyze the waves underneath the surface front using linear theory produced a surprising result: If waves impinge upon a horizontal surface at a certain angle a reflected wave of infinite amplitude is produced. It is suggested that this may be a mechanism responsible for the buildup of energy beneath the front (rather than multiple reflections between the front and the ground). Dissert. Abstr.

N91-28688 Princeton Univ., NJ.
ATMOSPHERIC RESPONSES TO LOWER TROPOSPHERIC FORCING IN A MULTILAYER ISENTROPIC MODEL Ph.D. Thesis
Xin Tao 1991 270 p
Avail: Univ. Microfilms Order No. DA9112302

A multi-layer isentropic model is developed and employed to study the importance of Rossby waves in maintaining the atmospheric general circulation. The first series of experiments was aimed at studying Rossby wave propagation and breaking in the troposphere and in the atmosphere. The linear response when the forcing amplitude is small is studied in detail. The transition to nonlinear behavior as the forcing amplitude increases is investigated. The greatest mean flow modification first occurs near the critical layer in low latitudes. The over-reflection of wave activity from the critical layer has very important effects on the breakdown of the polar vortex. The results also demonstrate that Rossby waves can penetrate to higher altitude as the forcing amplitude increases. The importance of diabatic heating is investigated in a numerical experiment. The potential vorticity budget is studied. The possibility of vacillation in the stratosphere as a response to steady tropospheric forcing is discussed. It was found that it is very hard to break up the polar vortex with steady forcing of realistic amplitude in the time scale of a season. Stratospheric vacillation may be generated by a lateral critical line in a much longer time scale. An analytical analysis in a beta-plane channel model was performed to understand the relationship between vertical propagation of Rossby waves and the destruction of the PV gradient. Dissert. Abstr.

N91-28689 Arizona Univ., Tucson.
RADIATIVE TRANSFER MODEL FOR A SPHERICAL ATMOSPHERE Ph.D. Thesis
Kurtis John Thome 1990 107 p
Avail: Univ. Microfilms Order No. DA9111974

A new model for computing radiative transfer in a spherically symmetric atmosphere was developed which uses a Gauss-Sidel iteration similar to Herman (1963). To account for inhomogeneities in the horizontal intensity field, the current work introduces a conical boundary on which solutions are found. This boundary is used in an interpolation scheme to obtain the intensity at the center of the cone. The model includes absorption and aerosols, but neglects polarization and refraction. Checks of the model were performed. Results for a high sun and small optical depth compared to flat atmosphere results were consistent with geometric arguments. From the results of tests, the model was concluded to be accurate to 3 percent, and in most earth-atmosphere situations accurate to 1 percent. This accuracy is on the order of, or better than, previous techniques, and more computationally efficient than Monte Carlo simulations. The current model is more versatile and accurate than techniques that strive for computational efficiency. The model was used to examine the atmospheric limb problem. Results from this work indicate that ozone and atmospheric dust layers may be detected from limb measurements. Dissert. Abstr.

N91-28690 Illinois Univ., Urbana-Champaign.
LIDAR STUDIES OF SPORADIC SODIUM LAYERS, GRAVITY WAVES AND DENSITY SPECTRA IN THE MESOPAUSE AND STRATOPAUSE REGIONS AT URBANA AND ARECIBO Ph.D. Thesis
Timothy Jon Beatty 1990 151 p
Avail: Univ. Microfilms Order No. DA9114174

The high spatial and temporal resolution of the University of Illinois at Urbana-Champaign (UIUC) CEDAR lidar and new processing techniques have significantly improved the study of vertical and temporal structures of the middle atmosphere. First, what are believed to be the first observations of meteor ablation trails with a lidar are presented. Next, the simultaneous observations of sporadic E layer by the Arecibo 430 MHz incoherent scatter radar and a sporadic Na layer by the UIUC CEDAR Na lidar are presented. The high correlation between the altitude and abundance variation of the two layers is discussed. Finally, the results of thirty nights of lidar observations during the months of Jan., Mar., and Apr. 1989 at the Arecibo Observatory are presented. The CEDAR lidar was operated as a Rayleigh and Na lidar and was one of several optical and radar instruments participating in the AIDA Act 1989 campaign. The characteristics of the monochromatic gravity waves, gravity wave spectra, and rms density perturbations observed simultaneously in the stratopause and mesopause regions above Arecibo are described. Similarities in and differences between the wave characteristics in the two regions are discussed, and the results are compared with previous radar and lidar observations obtained at other sites.

Dissert. Abstr.

N91-28691 California Univ., Los Angeles.

AN UPPER OCEAN MODEL FOR THE CLIMATIC ASPECTS OF AIR-SEA INTERACTION Ph.D. Thesis

Mehmet Karaca 1990 172 p

Avail: Univ. Microfilms Order No. DA9115160

A model of the dynamics of the upper ocean buoyancy field is discussed in view of the air-sea interaction and its coupling to the large-scale velocity field. The model is particularly designed for the implementation of a simple and yet sufficiently realistic form of the mixed-layer dynamics into current ocean circulation models. Ocean mixed-layer dynamics is considered in the framework of a self-similar buoyancy profile governed by the Kraus-Turner budgets. The global validity of the profile is suggested by an inspection of observed oceanic data. Since the Kraus-Turner concepts rest on the budgets of buoyancy and potential energy, the incorporation of mixed-layer dynamics into a transport scheme has to invoke two transport equations. The transport determines the buoyancy distribution for given surface forcing and large-scale velocities. Relative geostrophic velocities are calculated for the midlatitude Pacific with buoyancy profiles obtained from observations. The velocity field is obtained by combining relative geostrophic velocities with observed surface velocities. In the spirit of large-scale geostrophic models of the ocean circulation, the velocities are incorporated into the transport equations. It is possible to calculate the advective buoyancy fluxes at a given location directly. A one dimensional mixed-layer model is integrated using climatological and anomalous heat and momentum fluxes produced by the UCLA Atmospheric General Circulation Model (AGCM).

Dissert. Abstr.

N91-28692 State Univ. of New York, Albany.

DEVELOPMENT AND APPLICATION OF NEW MODELING TECHNIQUES FOR MESOSCALE ATMOSPHERIC CHEMISTRY Ph.D. Thesis

Jonathan Edward Pleim 1990 233 p

Avail: Univ. Microfilms Order No. DA9112317

Modeling techniques were developed to improve the capabilities of the Regional Acid Deposition Model (RADM). Grid resolution was increased both horizontally, through the development of a nested grid version of RADM, and vertically by increasing the number of vertical layers from 6 to 15. In addition, a new algorithm for subgrid vertical transport in the convective boundary layer (CBL) structure. The resulting refined model is then used in conjunction with vertically resolved aircraft measurements to investigate the relationships between vertical chemical distributions and the dynamical and thermodynamical structure of the lower troposphere. Finally, both observed and modeled data are used to examine the interactions between chemical processes and dynamical processes, such as vertical mixing, plume dilution, and advection. A nested grid version of RADM, using a 1/3 horizontal grid cell size or 80/3 = 26.7 km, was developed so that increased resolution can be applied to critical areas while retaining influence of larger scale phenomena. Comparisons to the fourth experiment of the Oxidant and Scavenging Characteristics of April Rains (OSCAR 4) and to the high density sampling net network are discussed. An algorithm for subgrid vertical transport of trace chemical material in the convective boundary layer was developed. The model, named the Asymmetrical Convective Model (ACM) is a simple nonlocal closure model designed to simulate the asymmetrical nature of upward and downward transport in the CBL. Test results of the ACM and analysis of nested and aircraft data are presented. Examination of the interactions between various chemical and physical processes are also presented.

Dissert. Abstr.

N91-28693 Sheffield Univ. (England).

MAGNETOSPHERIC VLF LINE RADIATION Ph.D. Thesis

Keith Howard Yearby 1982 211 p

Avail: Univ. Microfilms Order No. BRDX92388

Magnetospheric very low frequency (VLF) line radiation (MLR) is a broad band VLF emission (typically 1 kHz wide centered on 3 kHz) which has line structure in its spectrum. The events studied were received during 1977-80 at Halley, Antarctica and also in the geomagnetically conjugate region (Newfoundland). The occurrence of Halley MLR events as a function of local time and geomagnetic activity and the differences in MLR activity between Halley and Siple, Antarctica are discussed. An MLR event received on 26 Jun. 1978 may be the result of magnetospheric amplification of VLF radiation of harmonics from electrical power lines (PLHR) in the conjugate region; the radiated power required was estimated to be 50 mW. Most Halley MLR events do not have any direct relation with PLHR although in several of the generation mechanisms discussed PLHR may have an indirect role. A series of measurements of the electromagnetic field near to several power transmission lines in Newfoundland were made to determine the magnitude of the unbalanced harmonic currents and the skin depth in the ground, which in turn were used to estimate the strength of PLHR entering the magnetosphere. The largest radiated power determined for a single line was 500 nW in the range 2.7 to 3.7 kHz although much larger powers may be radiated from the more industrialized regions further west. A description of the VLF receiver and some improvements made to it are given followed by a review of spectrum analysis techniques and a description of some methods used for the work on PLHR and MLR.

Dissert. Abstr.

N91-28694 Lancaster Univ. (England).

RADIO ABSORPTION IN THE ANTARCTIC IONOSPHERE: SOME OBSERVATIONS IN THE REGION OF THE MIDLATITUDE TROUGH Ph.D. Thesis

William Guy Howarth 1988 315 p

Avail: Univ. Microfilms Order No. BRDX92235

A study of the Antarctic ionosphere close to the boundary between the corotating middle latitude region and the convecting high latitude region was undertaken, and current knowledge of each region is reviewed. The analyses were carried out via the use of data derived from two radio wave experimental systems: an array of four riometers and a digital ionospheric sounder (advanced ionospheric sounder). A correlative study of ionospheric absorption measurements using the digital ionospheric sounder and the riometers showed that a thorough survey of critical frequencies must be undertaken if absorption values produced from the advanced ionospheric sounder data are to be compared with those produced from the riometer array. A particular type of event was identified, involving the midlatitude ionopheric electron density trough. The occurrence of precipitation and magnetic field events of a characteristic form are shown to be related to the position of the poleward edge of the midlatitude trough, indicating a relationship between the poleward edge and the hard particle precipitation boundary. Magnetic field and cosmic noise pulsations were studied using a cross-spectral analysis approach. Results from the analysis of two individual events suggest that the magnetic pulsations observed in each event originate from different regions of the ionosphere-magnetosphere system.

Dissert. Abstr.

47 METEOROLOGY AND CLIMATOLOGY

Includes weather forecasting and modification.

N91-28695# World Meteorological Organization, Geneva (Switzerland). World Climate Data Program.
REPORT OF MEETING OF CLICOM EXPERTS
1989 60 p Meeting held in Paris, France, 11-15 Sep. 1989
(WCDP-9; WMO/TD-342) Avail: NTIS MF A04; print copy available at WMO, Geneva, Switzerland

The meeting consisted of a review of the current status of the CLICOM project, including installation and implementations. A forum was provided for discussion of the successes and problems of CLICOM in order to resolve problems. The CLICOM systems plans and training was categorized. Plans were also made for future development of CLICOM. Author

N91-28696# Army Armament Research, Development and Engineering Center, Picatinny Arsenal, NJ.
METEOROLOGICAL INSTRUMENTATION SUPPORT FOR AN ADVERSE WEATHER TEST FACILITY
Michael J. Burke May 1991 23 p
(AD-A236605; ARFSD-TR-91006) Avail: NTIS HC/MF A03
CSCL 04/2

The various basic meteorological instruments to be utilized in support of an all weather performance reliability testing facility for smart munition's millimeter wave/infrared sensors are defined. The instrumentations discussed will measure the following environment conditions: wind direction and speed, temperature, barometric pressure, humidity, rain rate, and solar radiance. GRA

N91-28697# State Univ. of New York, Albany. Atmospheric Sciences Research Center.
DATA USERS GUIDE TO THE MOUNTAIN CLOUD CHEMISTRY PROJECT
V. A. Mohnen Mar. 1991 69 p
(PB91-168484; EPA/600/8-91/009) Avail: NTIS HC/MF A04
CSCL 04B

Atmospheric pollution is deposited on the forests of the eastern United States in a variety of forms. Concern has been raised that the exposure to and deposition of these atmospheric pollutants may play a role in the decline of these forests. The Mountain Cloud Chemistry Project (MCCP), sponsored by the U.S. Environmental Protection Agency (EPA) and the National Acid Precipitation Assessment Program (NAPAP), has studied the exposure and deposition of atmospheric constituents to these forests. Research scientists and technicians of the MCCP have measured the concentrations of atmospheric pollutants at six remote monitoring stations for four growing seasons (1986-89). Measurements of ozone, sulfur dioxide, oxides of nitrogen, hydrogen peroxide, cloud and rain water ions, meteorological parameters, and other parameters of interest were collected at sites in Howland, ME; Mt. Moosilauke, NH; Whiteface Mt., NY; Shenandoah Park, VA; and Mt. Mitchell, NC. The report served to document the type and amount of data collected for the MCCP during the four warm seasons between 1986 and 1989. Details are presented on the locations of the six research/monitoring sites, the types of measurements made, the periods of record, the quality of the data, and the availability of the data. GRA

N91-28698# International Centre for Theoretical Physics, Trieste (Italy).
RESULTS OF AGRICLIMATOLOGICAL STUDIES USING MULTIPLE SATELLITE SENSORS LIKE NOAA AVHRR; GMS IR; AND LANDSAT MSS AND TM
A. M. Choudhury Aug. 1990 5 p
(DE91-618773; IC-90/238) Avail: NTIS HC/MF A01

Bangladesh Space Research and Remote Sensing Organization (SPARRSO) routinely receives NOAA and GMS imagery and uses them in agrometeorological monitoring, it also uses LANDSAT MSS and TM data for this purpose. Analysis of multiple satellite sensor data shows advantages for high resolution sensors. However, in the ease of crop monitoring, a good correlation has been obtained between results obtained with NOAA AVHRR and LANDSAT MSS for vegetation index. Crop estimation has been made using all kinds of sensors and it has been found that higher resolution data always give more accurate results. DOE

N91-28699 Utah Univ., Salt Lake City.
PREDICTION OF FORECAST SKILL WITH A QUASI-GEOSTROPHIC MODEL Ph.D. Thesis
Timothy Wayne Barker 1991 153 p
Avail: Univ. Microfilms Order No. DA9117779

Numerical weather prediction models exhibit striking variations in the skill of their forecasts. Some studies have claimed that these variations are related to systematic phenomena and could be predicted a priori. Some of these methods for making a prediction of forecast skill are tested here with a large number of extended-range forecasts that are distributed evenly through a long climatology. A perfect model approach is used so that systematic model forecast errors are eliminated. The model used is a simple, quasi-geostropic, 2-level, T21 truncation model. The computational efficiency of this model allows a large number of extended range forecasts to be made. Forcings for the model are calculated from observations, and help the model to produce a fairly realistic climatology. The prediction of forecast skills is considered for time-averaged forecasts, a variety of spatial domains, and various spectral waves. Spread of ensemble forecasts provides some predictive information about the skill of the ensemble mean forecast. There is some positive correlation between ensemble spread and ensemble forecast error for days 20 to 40, when forecasts usually have no skill. With this model, some correlation between initial flow pattern and forecast skill is found at extended ranges, almost at the same level as the correlation between forecast flow pattern and forecast skill for forecasts beyond just a few days. Persistence of the forecasts or the verifying analysis shows little ability to predict forecast skill above what could be found for totally random forecasts. The size of the initial or forecast errors correlates well only with the size of the errors a few days later in the forecast. Medium and extended range forecasts that are skillful are more likely to be the result of a return of skill behavior rather than a continuously small error growth rate. Dissert. Abstr.

N91-28700# Lawrence Livermore National Lab., CA.
ARAC: A COMPUTER-BASED EMERGENCY-RESPONSE DOSE-ASSESSMENT SERVICE WITH GLOBAL APPLICATION POTENTIAL
T. J. Sullivan May 1991 18 p Presented at the 10th International System Safety Society (SSS) Conference, Dallas, 18-22 Jul. 1991
(Contract W-7405-eng-48)
(DE91-013248; UCRL-JC-107201; CONF-9107114-1) Avail: NTIS HC/MF A03

Over the past 17 years, the Lawrence Livermore National Laboratory's Atmospheric Release Advisory Capability (ARAC) has developed and evolved a computer-based, real-time, radiological-dose-assessment service for the United States Departments of Energy and Defense. This service is built on the integrated components of real-time computer-acquired meteorological data, extensive computer databases, numerical atmospheric-dispersion models, graphical displays, and operational assessment-staff expertise. The focus of ARAC is the off-site problem where regional meteorology and topography are dominant influences on transport and dispersion. Through application to numerous radiological accidents/releases on scales from small accidental ventings to the Chernobyl reactor disaster, ARAC has developed methods to provide emergency dose assessments from the local to the hemisphere scale. DOE

N91-28701 Illinois Univ., Urbana-Champaign.
LOW-LEVEL CURVATURE SHEAR AND SUPERCELL THUNDERSTORM BEHAVIOR Ph.D. Thesis
Harold Edward Brooks 1990 239 p
Avail: Univ. Microfilms Order No. DA9114183

Tornadoes pose threats to lives and property, and accurately issuing warnings of their occurrence represents a challenge to meteorologists. One tool that will become increasingly important in responding to this challenge is Doppler radar which is used to detect rotation over several kilometers within thunderstorms in a region known as the mesocyclone. Preliminary studies indicate the use of Doppler radar to issue tornado warnings based on mid-level mesocyclones yields a 50 pct. false alarm rate, indicating that only half of storms with strong mid-level rotation have strong low level rotation. The link between mid-level and low level rotation is examined using a numerical storm model. A case study with different amounts of curvature shear is presented, followed by a series of simulations using idealized wind profiles in which the storm relative curvature shear is varied. All of the simulated storms produce strong mid-level rotation. A set of simulations with strong storm relative low level environmental curvature shear produce flows resembling those observed in low levels of tornadic thunderstorms by Doppler radar. Rectilinear shear (straight line hodograph) cases produce no organized rotation at low levels. This result implies that information about the environmental winds in the vicinity of thunderstorms can be used to improve the tornado warning process. Dissert. Abstr.

N91-28702 Alabama Univ., Huntsville.
PREDICTING THUNDERSTORM EVOLUTION USING GROUND-BASED LIGHTNING DETECTION NETWORKS Ph.D. Thesis
Steven Jay Goodman 1990 209 p
Avail: Univ. Microfilms Order No. DA9113968

Lightning measurements acquired by a ground based network of magnetic direction finders are used to diagnose and predict the existence, temporal evolution, and decay of thunderstorms over a wide range of space and time scales extending over four orders of magnitude. The nonlinear growth and decay of thunderstorms and their accompanying cloud-to-ground lightning activity is described by the three parameter logistic growth model. The growth rate is shown to be a function of the storm size and duration, and the limiting value of the total lightning activity is related to the available energy in the environment. A new technique is described for removing systematic bearing errors from direction finder data where radar echoes are used to constrain site error correction and optimization (best point estimate) algorithms. A nearest neighbor pattern recognition algorithm is used to cluster the discrete lightning discharges into storm cells and the advantages and limitations of different clustering strategies for storm identification and tracking are examined. Dissert. Abstr.

N91-28703 Florida State Univ., Tallahassee.
INITIALIZATION OF CLOUD AND RADIATION IN THE FLORIDA STATE UNIVERSITY GLOBAL SPECTRAL MODEL Ph.D. Thesis
Allan Meredith Weiner 1990 259 p
Avail: Univ. Microfilms Order No. DA9113957

Satellite observed outgoing longwave radiation (OLR) is used to initialize the clouds and radiation of the Florida State University Global Spectral Model. A one-parameter method and two different six-parameter methods of initialization are formulated. The one-parameter method is shown to be the most efficient and to produce the best results. The effects of the cloud and radiation initialization on a five day forecast are presented. The initialization procedure produces a better forecast of OLR than the control experiment by such a large extent that the five day forecast of the initialization experiment has approximately the same verification score as the initial data of the control experiment. The cloud forecasts (high, middle, and low) of the initialization experiment prominently show the cloud signatures of the monsoon, the Pacific and Atlantic Ocean intertropical convergence zones (ITCZ's), and the African rainbelt, but the cloud signatures of the control experiment are weak or nonexistent. The moist static stability budgets show that the initialization procedure had a large impact on the forecast after five days of integration by producing a monsoon and typhoon that were stronger and better defined. Additionally, radiative destabilization forcing budgets of the initialization experiment were an order of magnitude greater than the control experiment for the Atlantic Ocean ITCZ. The effect of initialization on precipitation forecasts was also investigated. It was found that the model precipitation decreases after initialization. This is attributed to the model formulation of precipitation, and a new formulation is suggested for further investigation. Dissert. Abstr.

N91-28704 Florida State Univ., Tallahassee.
ON THE INITIATION OF SURFACE CYCLONES BY UPPER TROPOSPHERIC DISTURBANCES Ph.D. Thesis
Jeffrey Stuart Whitaker 1990 121 p
Avail: Univ. Microfilms Order No. DA9113958

It is hypothesized that surface cyclogenesis in the Northern Hemisphere storm track regions can be described by the structural modification of baroclinic wave packets traversing a zonally varying flow field. This hypothesis is tested using a linear, quasi-geostrophic model with zonal variation in the basic state and the Ekman layer.The basic state consists of a region of strong low-level baroclinicity and weak Ekman dissipation, flanked by regions of weak low-level baroclinicity, strong Ekman dissipation, and enhanced low-level stability. Model calculations show that an isolated disturbance upstream of the mid-channel baroclinic zone evolves rapidly into a wave packet with maximum amplitude at the surface within a few days of entering the mid-channel baroclinic zone. The growth rate of an individual surface disturbance can exceed the growth rates of both the most unstable eigenmode of the zonally varying basic state and the most unstable eigenmode of a zonally homogeneous basic state characteristic of the mid-channel baroclinic zone. The surface cyclogenesis is due to the constructive interference between the several most unstable eigenmodes of the zonally varying basic state. The addition of a simple parameterization of latent heat release in the mid-channel baroclinic zone does not significantly alter the initiation of surface cyclones, but results in cyclones of smaller scale which undergo a longer period of rapid development. Dissert. Abstr.

N91-28705 Illinois Univ., Urbana-Champaign.
A NUMERICAL SIMULATION OF A TORNADO-SCALE VORTEX IN A THREE-DIMENSIONAL CLOUD MODEL Ph.D. Thesis
Louis John Wicker 1990 273 p
Avail: Univ. Microfilms Order No. DA9114463

The process of tornadogenesis is examined within the context of a fully 3-D cloud model. Very high horizontal and vertical resolution is used to capture a developing tornado-scale vortex during the simulation of a strongly rotating supercell storm simulated within the 3 Apr. 1964 environment from Witchita Falls, Texas. To better represent the influence of surface friction on the vortex flow, a simple surface layer parameterization of the vertical fluxes of horizontal momentum is added to the model. Results from the simulation show that a tornado-scale vortex forms along the western edge of the mesocyclone, intensifies and rotates cyclonically around the center of the mesocyclone over a several minute period. The inclusion of the surface layer parameterization increases the low-level velocity convergence. Surface vertical vorticity is greater than 0.43/sec for thirty seconds and greater than 0.3/sec for several minutes. During tornadogenesis, pressures at the surface fall 3-4 mb in thirty seconds and a pressure gradient develops of over 7 mb from the outer edge of the tornado to the center. A vortex tube extends from the surface to over 2.5 km aloft and tilts to the northwest. Analyses show that tornadogenesis occurs when the vertical velocity gradients along the western side of the mesocyclone increase and that the principle mechanism for intensifying the vertical vorticity is convergence. Analyses also show that the development of the occlusion updraft along the western edge of the mesocyclone is related to advection of warm air southwestward over the gust front and the lowering of pressure aloft within the mesocyclone core. Dissert. Abstr.

N91-28706 Georgia Inst. of Tech., Atlanta.
A CLOUD FRACTION AND RADIATIVE TRANSFER MODEL Ph.D. Thesis
Gang Luo 1990 159 p
Avail: Univ. Microfilms Order No. DA9115387

The development and evaluation of a cloud fraction model for short wave radiative transfer calculations are described. The model considers four effects: (1) a new version of cloudy line-of-sight probability of a random overlap broken cloud field was formulated; (2) the difference between the beam transmittance of a broken cloud field and that of an overcast cloud layer is characterized; (3) a parameterization was made to describe the anisotropy of the upward and downward irradiance off a cloud side; and (4) a set of equations were established to evaluate down-welling irradiance at the ground surface and up-welling irradiance at the top of the atmosphere, with consideration of the cloud-cloud interaction term. The modeling of cloudy line-of-sight probabilities for cylindrical and ellipsoidal clouds is compared with a 3-D Monte Carlo simulation for a random-overlap, broken cloud field and the observational data from the Georgia Tech Solar Energy Meteorological Research and Training Sites (SEMRTS). The model also calculates the radiative transfer in a cylindrical cloud field to compare against the results of other reseachers. The results of these comparisons are discussed. Dissert. Abstr.

N91-28260*# National Aeronautics and Space Administration, Washington, DC.
EFFECTIVITY OF ATMOSPHERIC ELECTRICITY ON LAUNCH AVAILABILITY
John A. Ernst *In its* Space Transportation Propulsion Technology Symposium. Volume 3: Panel Session Summaries and Presentations May 1991 p 1231-1241 (For primary document see N91-28235 20-20)
Avail: NTIS HC/MF A99 CSCL 04B

48 OCEANOGRAPHY

Includes biological, dynamic, and physical oceanography; and marine resources.

For related information see also *43 Earth Resources and Remote Sensing.*

N91-28707# Coastal Engineering Research Center, Vicksburg, MS.
ALASKA WAVE DATA INDEX Final Report
David D. McGehee and Lynn D. Leslie Apr. 1991 154 p
Sponsored by Corps of Engineers
(AD-A236635; CERC-91-1) Avail: NTIS HC/MF A08 CSCL 08/3

The Alaska coastline extends over 40,000 miles and is constantly impacted by waves that vary widely with time and position. The ability to monitor and ultimately predict these wave conditions is of vital concern to coastal communities, offshore industries, and State and Federal agencies. An index of available wave data was compiled to aid in planning future data collection efforts. The index is presented in tables providing information on the location, schedule, and type of data collected and a point of contact for additional inquiry. All gaged sites are plotted on a series of maps by index number. Coastal areas covered included the Beaufort Sea, Bering Sea, Chukchi Sea, and Gulf of Alaska. GRA

N91-28708 Nottingham Univ. (England).
THE DETERMINATION OF MEAN SEA LEVEL USING GPS Ph.D. Thesis
Guy Ashbourne Basker 1990 286 p
Avail: Univ. Microfilms Order No. BRD-91976

There are many examples worldwide where an anomaly between geodetic and oceanographic methods of leveling has lead to an apparent slope in mean sea level. The single common factor to the apparent sea slopes in Australia, Brazil, Great Britain, Japan, and the United States is that they occur on a north-south rather than an east-west basis. Extensive investigations into these various sea slope anomalies have failed to determine which of the two methods of leveling is in error. There has been much discussion concerning the British sea slope in a variety of ways, and has produced consistent and similar results for the slope of the mean sea surface or mean sea level. However, these results disagree significantly with those obtained from either the Second or Third Geodetic Levelings of Great Britain. The development of the Global Positioning System (GPS) has heralded a revolution in both navigation and geodetic techniques. The aim of the research project is to use GPS to measure ellipsoidal height differences between various tide gauges, to combine these with a high precision geoid, and hence to independently determine the slope of mean sea level. A number of GPS observation campaigns were undertaken. A pilot project was observed in May 1987, and this was followed by a major observation campaign in May 1988. Further observations were made in Jul. 1989 and Jan. 1990. Both the various methods of leveling and the GPS are reviewed. The fieldwork and associated data processing are described, and the results are presented. Dissert. Abstr.

N91-28709 Hawaii Univ., Honolulu.
NORMAL MODE DECOMPOSITION OF SMALL-SCALE OCEANIC MOTIONS Ph.D. Thesis
Ren-Chieh Lien 1990 140 p
Avail: Univ. Microfilms Order No. DA9118044

Small-scale oceanic motions are expected to contain both gravity waves and vortical motion. The vortical motion carries the perturbation potential velocity of the system. Using eigenvectors of the linear equation of motion, the gravity mode and the vortical mode are defined. The vortical mode carries the linear perturbation potential vorticity and is horizontally nondivergent, whereas the gravity mode does not carry the linear perturbation potential velocity. In an unforced, inviscid, linearized system, the gravity mode reduces to free linear gravity waves and the vortical mode to a steady geostrophic flow. Dissert. Abstr.

N91-28710 Oregon State Univ., Corvallis.
A STUDY OF EL NINO/SOUTHERN OSCILLATION: NUMERICAL EXPERIMENTS AND DATA ANALYSIS Ph.D. Thesis
Joong Bae Ahn 1990 197 p
Avail: Univ. Microfilms Order No. DA9113877

For the purpose of investigating the fundamental nature of the interannual oscillation observed in the tropical Pacific in conjunction with El Nino/Southern Oscillation (ENSO), the Comprehensive Ocean Atmosphere Data Set was analyzed. Based upon this analysis, an intermediate tropical atmosphere-ocean coupled model was developed. For reason of their particular importance to atmosphere-ocean interactions, moisture processes such as condensation-convergence, evaporation-sea surface temperature, and evaporation-wind feedbacks were given special emphasis in both the data analysis and modeling processes. Dissert. Abstr.

N91-28711 Wisconsin Univ., Madison.
INTERACTIONS BETWEEN THE NORTH PACIFIC OCEAN AND THE NORTHERN HEMISPHERE ATMOSPHERE DURING EL NINO Ph.D. Thesis
Michael Adam Alexander 1990 167 p
Avail: Univ. Microfilms Order No. DA9108699

Model simulations are used to examine sea surface temperature (SST) anomalies in the North Pacific during the fall and winter of El Nino episodes and the extent to which these anomalies influence the atmospheric circulation. A mixed layer ocean model of the North Pacific is forced by Community Climate Model (CCM) fields containing the El Nino signal (prescribed warm SSTs in the tropical Pacific). The ocean model generally reproduces the features of the observed midlatitude SST anomaly pattern: warm water in the northeast Pacific and an elliptically shaped cold pool in the central Pacific. In these regions, a large fraction of the temperature anomalies are significant as indicated by the t-statistic. The model SST anomalies are primarily caused by changes in the sensible and latent heat flux and to a lesser extent the longwave radiation flux. Dissert. Abstr.

51 LIFE SCIENCES (GENERAL)

N91-28712# Lawrence Livermore National Lab., CA.
THE USE OF AMS TO THE BIOMEDICAL SCIENCES
J. S. Vogel Apr. 1991 17 p Presented at the Environment Canada Workshop on Canadian Requirements for The Center for Accelerator Mass Spectrometry (AMS), Burlington, Ontario (Canada), 15-16 Apr. 1991
(Contract W-7405-eng-48)
(DE91-012037; UCRL-JC-107116; CONF-9104245-1) Avail: NTIS HC/MF A03

The Center for Accelerator Mass Spectroscopy (AMS) began making AMS measurements in 1989. Biomedical experiments were originally limited by sample preparation techniques, but we expect the number of biomedical samples to increase five-fold. While many of the detailed techniques for making biomedical measurements resemble those used in other fields, biological tracer experiments differ substantially from the observational approaches of earth science investigators. The role of xenobiotius in initiating mutations in cells is of particular interest. One measure of the damage caused to the genetic material is obtained by counting the number of adducts formed by a chemical agent at a given dose. AMS allows direct measurement of the number of adducts through stoichiometric quantification of the C-14 label attached to the DNA after exposure to a labelled carcinogen. Other isotopes of interest include tritium, Cl-36, Se-79, Ca-41, Al-26, and I-129. Our experiments with low dose environmental carcinogens reflect the protocols which will become a common part of biomedical AMS. In biomedical experiments, the researcher defines the carbon to be analyzed through dissection and/or chemical purification; thus the sample is merely combusted and graphitized at the AMS facility. However, since biomedical samples can have a C-14 range of five orders of magnitude, preparation of graphite required construction of a special manifold to prevent cross-contamination. Additionally, a strain of C-14-depleted C57BL/6 mice is being developed to further reduce background in biomedical experiments. AMS has a bright and diverse future in radioisotope tracing. Such work requires a dedicated amalgamation of AMS scientists and biomedical researchers who will redesign experimental protocols to maximize the AMS technique and minimize the danger of catastrophic contamination. DOE

N91-28713# Purdue Univ., West Lafayette, IN. Dept. of Biological Sciences.
REGULATION OF PHOTOSYNTHETIC MEMBRANE COMPONENTS IN CYANOBACTERIA
L. A. Sherman 1991 11 p
(Contract DE-FG02-89ER-14028)
(DE91-012713; DOE/ER-14028/2) Avail: NTIS HC/MF A03

The major objectives are to analyze gene regulation under different environmental conditions and to determine the role of the psbO protein (MSP, the manganese stabilizing protein, the 33 kDa protein) in O2-evolution. These objectives are studied in the transformable cyanobacteria Synechococcus sp. PCC7942 and Synechocystis sp. PCC6803, respectively. A deletion strain (Delta psbO) was used in Synechocystis that completely lacks the gene or the gene product, and which can grow photosynthetically at about 2/3 the normal rate. This deletion strain was used to construct site directed mutations at specific, externally located, charged residues. In particular, residues and domains that enable MSP to interact with the PSII reaction center components were analyzed. The gene which codes for the novel chlorophyll protein complex which is synthesized during iron deficiency was identified and cloned. The apoprotein, isiA, has an amino acid sequence very similar to that of the gene product of psbC (CP43) except for the lack of most of the large lumenal loop E. It was found that an insertion mutant in isiA can grow normally in regular iron sufficient medium and in partially iron deficient cultures. A putative candidate for irpR was identified, the iron regulated DNA binding protein that is used to control gene expression based on iron concentrations. DOE

N91-28714# Los Alamos National Lab., NM.
SPONTANEOUS EMERGENCE OF A METABOLISM
R. J. Bagley and J. D. Farmer (Los Alamos National Lab., NM.) 1990 51 p Presented at the Artificial Life Conference, Santa Fe, Feb. 1990
(Contract W-7405-eng-36)
(DE91-013684; LA-UR-91-1707; CONF-9002163-2) Avail: NTIS HC/MF A04

Networks of catalyzed reactions with nonlinear feedback have been proposed to play an important role in the origin of life. We investigate this possibility in a polymer chemistry with catalyzed cleavage and condensation reactions. We study the properties of a well-stirred reactor driven away from equilibrium by the flow of mass. Under appropriate non-equilibrium conditions, the nonlinear feedback of the reaction network focuses the material of the system into a few specific polymer species. The network of catalytic reactions digests the material of its environment, incorporating it into its own form. We call the result an autocatalytic metabolism. Under some variations it persists almost unchanged, while in other cases it dies. We argue that the dynamical stability of autocatalytic metabolisms gives them regenerative properties that allow them to repair themselves and to propagate through time. DOE

N91-28715# Pacific Northwest Lab., Richland, WA.
MICROBEAM STUDIES OF THE SENSITIVITY OF STRUCTURES WITHIN LIVING CELLS
L. A. Braby May 1991 32 p Presented at the Scanning Microscopy Meeting, Bethesda, 3-9 May 1991
(Contract DE-AC06-76RL-01830)
(DE91-012927; PNL-SA-19443; CONF-9105197-1) Avail: NTIS HC/MF A03

Determining the biological effects of low doses of high LET radiation is complicated by the stochastic nature of charged-particle interactions. Populations of cells exposed to very low doses contain a few cells which have been hit by a charged particle, while the majority of the cells receive no radiation damage. At somewhat higher doses, a few cells receive two or more events. We have developed a special irradiation facility at PNL to control the actual number of charged-particle tracks that pass through cell nuclei. This approach can be used to investigate the effects of the interaction between irradiated and unirradiated cells in an organized system, as well as to study the effects of spatial and temporal distribution of radiation damage within single cells. We expect that this approach will lead to a better understanding of the mechanisms of high LET radiation effects. DOE

N91-28716# Columbia Univ., New York, NY. Center for Radiological Research.
RADIATION PHYSICS, BIOPHYSICS, AND RADIATION BIOLOGY
E. J. Hall and M. Zaider May 1991 100 p
(Contract DE-FG02-88ER-60631)
(DE91-012883; DOE/ER-60631/7) Avail: NTIS HC/MF A05

Research is a blend of physics, chemistry, and biology, involving research at the basic level with the admixture of a small proportion of pragmatic or applied research in support of radiation protection and/or radiotherapy. Current research topics include: oncogenic transformation assays, mutation studies involving interactions between radiation and environmental contaminants, isolation, characterization and sequencing of a human repair gene, characterization of a dominant transforming gene found in C3H 10T1/2 cells, characterize ab initio the interaction of DNA and radiation, refine estimates of the radiation quality factor Q, a new mechanistic model of oncogenesis showing the role of long term low dose medium LET radiation, and time dependent modeling of radiation induced chromosome damage and subsequent repair or misrepair. DOE

N91-28717# California Inst. of Biological Research, La Jolla.
NOVEL METHODS FOR PHYSICAL MAPPING OF THE HUMAN GENOME APPLIED TO THE LONG ARM OF CHROMOSOME 5
M. McClelland Jan. 1991 17 p

(Contract DE-FG03-89ER-60913)
(DE91-012894; DOE/ER-60913/T1) Avail: NTIS HC/MF A03

The objective was to develop novel methods for mapping of the human genome. The techniques to assessed were: (1) three methods for the production of unique sequence clones from the region of interest; (2) novel methods for the production and separation of multi-megabase DNA fragments; (3) methods for the production of physical linking clones that contain rare restriction sites; (4) application of these methods and available resources to map the region of interest. Rare-cleavage tools were developoed based on restriction enzymes and methylases. The effect of methylation on enzymes used for genome mapping was studied. Characterization was made of two new isoschizomers. A reliable way to produce partial digests of DNA in agarose was developd and applied to the human genome. And a method was applied to double the apparent specificity of rare-cutter endonucleases. DOE

N91-28718# Oak Ridge National Lab., TN.

PHOTOBIOTECHNOLOGY: ALGAL HYDROGEN PRODUCTION AND PHOTOCONDUCTIVITY OF METALIZED CHLOROPLASTS

E. Greenbaum 1991 7 p Presented at the International Symposium on New Biomaterials and Global Ecology, Tokyo (Japan), 25-27 Jun. 1991
(Contract DE-AC05-84OR-21400)
(DE91-013232; CONF-9106192-1) Avail: NTIS HC/MF A02

Sustained hydrogen photoevolution from Chlamydomonas reinhardtii and C. Moewusii was measured under an anoxic, CO2 containing atmosphere. It has been discovered that light intensity and temperature influence the partitioning of reductant between the hydrogen photoevolution pathway and the Calvin cycle. Under low incident light intensity (1-3 W m(sup minus 2)) or low temperature (approx. 0 C), the flow of photosynthetic reductant to the Calvin cycle was reduced, and reductant was partitioned to the hydrogen pathway as evidenced by sustained H2 photoevolution. Under saturating light (25 W m(sup minus 2)) and moderate temperature 20 plus minus 5 C, the Calvin cycle became the absolute sink for reductant with the exception of a burst of H2 occurring at light on. A novel photobiophysical phenomenon was observed in isolated spinach chloroplasts that were metalized by precipitating colloidal platinum onto the surface of the thylakoid membranes. A two-point irradiation and detection system was constructed in which a continuous beam helium-neon laser (lambda) = 632.8 nm) was used to irradiate the platinized chloroplasts at varying perpendicular distances from a single linear platinum electrode in pressure contact with the platinized chloroplasts. No external voltage bias was applied to the system. The key objective of the experiments reported in this report was to measure the relative photoconductivity of the chloroplast-metal composite matrix. DOE

N91-28719# Oak Ridge National Lab., TN.

BIOMARKER-BASED BIOMONITORING FOR EVALUATING HEALTH AND ECOLOGICAL EFFECTS ON ENVIRONMENTAL CONTAMINATION

J. F. McCarthy, L. R. Shugart, and B. D. Jimenez 1991 43 p Presented at the Hazardous Waste Site Investigations: Toward Better Decisions, Gatlinburg, 21-24 May 1990
(Contract DE-AC05-84OR-21400)
(DE91-013729; CONF-900556-2) Avail: NTIS HC/MF A03

A research approach is described for assessing the biological and ecological significance of contaminants present in the environment. The approach uses wild animals and introduced caged animals near hazardous waste sites as (1) sentinels of bioavailable contaminants, (2) predictors of adverse ecological effects, and (3) surrogates to estimate the potential exposure and risks to humans living near these sites. Evidence of exposure in animals on the site provides a temporally-integrated' measure of bioavailable contaminant levels and is therefore much more relevant to the potential risk to humans than is the analytically measurable concentration of contaminants in the soil, water, or air. The research approach utilizes biomarkers (biochemical, molecular and cellular indicators of exposure) and measures of body burden of persistent compounds (such as polychlorinated biphenyls; PCBs) in wild animals captured on a hazardous waste disposal site and in adjacent uncontaminated reference areas to identify and quantify the potential for exposure to bioavailable contaminants. Unexposed animals confined at sites confirm the potential for environmental exposure. Relationships between biomarker response and adverse ecological effects are determined from measures of animal health and population structure. The potential risk to humans is extrapolated from the animal exposure data using pharmacodynamic models. DOE

N91-28720# California Univ., Berkeley. Lawrence Berkeley Lab.

CHROMOSOMAL CHANGES IN CULTURED HUMAN EPITHELIAL CELLS TRANSFORMED BY LOW- AND HIGH-LET RADIATION

Tracy Chui-Hsu Yang, L. M Craise, J. C. Prioleau, M. R. Stampfer, and J. S. Rhim Nov. 1990 13 p Presented at the COSPAR Plenary Conference, The Hague, Netherlands, 25 Jun. - 6 Jul. 1990
(Contract DE-AC03-76SF-00098)
(DE91-013772; LBL-30024; CONF-9006220-9) Avail: NTIS HC/MF A03

For a better assessment of radiation risk in space, an understanding of the responses of human cells, especially the epithelial cells, to low- and high-LET radiation is essential. In our laboratory, we have successfully developed techniques to study the neoplastic transformation of two human epithelial cell systems by ionizing radiation. These cell systems are human mammary epithelial cells (H184B5) and human epidermal keratinocytes (HEK). Both cell lines are immortal, anchorage dependent for growth, and nontumorigenic in athymic nude nice. Neoplastic transformation was achieved by irradiation cells successively. Our results showed that radiogenic cell transformation is a multistep process and that a single exposure of ionizing radiation can cause only one step of transformation. It requires, therefore, multihits to make human epithelial cells fully tumorigenic. Using a simple karyotyping method, we did chromosome analysis with cells cloned at various stages of transformation. We found no consistent large terminal deletion of chromosomes in radiation-induced transformants. Some changes of total number of chromosomes, however, were observed in the transformed cells. These transformants provide an unique opportunity for further genetic studies at a molecular level. DOE

N91-28721# California Univ., Berkeley. Lawrence Berkeley Lab.

GENETIC CHANGES IN MAMMALIAN CELLS TRANSFORMED BY HELIUM CELLS

M. Durante, G. Grossi (Naples Univ., Italy), T. C. Yang, and R. Roots Nov. 1990 12 p Presented at the COSPAR Plenary Conference, The Hague, Netherlands, 25 Jun. - 6 Jul. 1990
(Contract DE-AC03-76SF-00098)
(DE91-013778; LBL-30025; CONF-9006220-10) Avail: NTIS HC/MF A03

Midterm Syrian Hamster embryo (SHE) cells were employed to study high LET-radiation induced tumorigenesis. Normal SHE cells (secondary passage) were irradiated with accelerated helium ions at an incident energy of 22 MeV/u (9 to 10 keV/micron). Transformed clones were isolated after growth in soft agar of cells obtained from the foci of the initial monolayer plated postirradiation. To study the progression process of malignant transformation, the transformed clones were followed by monolayer subculturing for prolonged periods of time. Subsequently, neoplasia tests in nude mice were done. In this work, however, we have focused on karyotypic changes in the banding patterns of the chromosomes during the early part of the progressive process of cell transformation for helium ion-induced transformed cells. DOE

N91-28722# California Univ., Berkeley. Lawrence Berkeley Lab.

PROTEIN-DIRECTED MODULATION OF HIGH-LET HYPERTHERMIC RADIOSENSITIZATION Ph.D. Thesis

P. Chang Apr. 1991 100 p
(Contract DE-AC03-76SF-00098)
(DE91-013783; LBL-30680) Avail: NTIS HC/MF A05

The importance of protein synthesis (PS) in development of thermotolerance was studied in CHO-SC1 cells and its mutant CHO-tsH1. SC1 cells show classic biphasic survival curves after continuous heating (greater than 41 C); tsH1 cells do not. tsH1 cells do show thermotolerance similar to SC1 cells when incubated at 35 C, but survival at the nonpermissive temperature 40 C was greatly reduced in the absence of PS. We believe PS is not required for the initial onset of thermotolerance, but is required for sustaining it. The combined effects of heat and high-LET radiation were studied. SC1 cells show different survival curves depending on the order of treatment; tsH1 cells have the same response in either case. Increased radiosensitivity in SC1 cells depends on PS following irradiation and is LET-dependent. These results suggest that high-LET radiation induced cellular damage can be potentiated with heat-induced PS during post-irradiation heat treatment. DOE

N91-28723# Arizona State Univ., Tempe.
ANTENNA ORGANIZATION IN GREEN PHOTOSYNTHETIC BACTERIA
R. E. Blankenship 1990 23 p
(Contract DE-FG02-85ER-13388)
(DE91-014814; DOE/ER-13388/5) Avail: NTIS HC/MF A03

Chlorosomes are bag-like structures attached to the cytoplasmic side of the inner cell membrane, and transfer energy into the membrane where long-term energy storage is carried out by the photochemical reaction center. Evidence is now overwhelming that the chlorosome represents a very different type of antenna from that found in any other system yet studied. The idea that the pigments in chlorosomes are organized into molecular aggregates by direct pigment-pigment interactions has now gained essentially universal acceptance among the workers in the field of photosynthesis, largely due to the work from our laboratory. The challenge is now to understand at a molecular level how the pigment oligomers are packaged into the chlorosome and how they function to make an efficient antenna system. The role of proteins in the chlorosome is now very unclear, and some workers believe they play essentially no role. Several lines of current and planned experiments are directed at understanding these questions. A major conceptual breakthrough was the discovery of a previously unrecognized control system that serves to regulate the flux of energy through the system in response to the redox potential of the cell. Each of these areas is described. DOE

N91-28724# Alabama Univ., University. Dept. of Chemistry.
MAGNETIC RESONANCE AND OPTICAL SPECTROSCOPIC STUDIES OF CAROTENOIDS
L. D. Kispert May 1991 14 p
(Contract DE-FG05-86ER-13465)
(DE91-014361; DOE/ER-13465/6) Avail: NTIS HC/MF A03

The role was studied of a host lattice in the formation of radicals and excited singlet and triplet states that are relevant to photosynthesis. Particular emphasis is being placed on determining what is special about carotenoids that natural photosynthetic systems require them as antennae as well as for protection. The host matrix is manipulated so as to understand the carotenoid function (protection, quenching, energy transfer and antenna) and the structure of carotenoid cations. To characterize their properties, EPR, ENDOR, optical, molecular orbital and electrochemical studies were performed of carotenoids and carotenoid cations produced chemically, electrochemically, radiolytically (x ray irradiated freon matrices) and photolytically (solution photolysis by excimer radiation) as a function of the host matrix. DOE

N91-28725# Los Alamos National Lab., NM.
PLANT GROWTH IS INFLUENCED BY GLUTAMINE SYNTHETASE-CATALYZED NITROGEN METABOLISM
P. J. Langston-Unkefer 11 Jun. 1991 20 p Presented at the DOE Workshop on Marker-Aided Selection, Gatlinburg, 13-14 Jun. 1991
(Contract W-7405-eng-36)
(DE91-014592; LA-UR-91-2100; CONF-9106225-1) Avail: NTIS HC/MF A03

Ammonia assimilation has been implicated as participating in regulation of nitrogen fixation in free-living bacteria. In fact, these simple organisms utilize an integrated regulation of carbon and nitrogen metabolism; we expect to observe an integration of nitrogen and carbon fixation in plants; how could these complex systems grow efficiently and compete in the ecosystem without coordinating these two crucial activities? We have been investigating the role of ammonia assimilation regulating the complex symbiotic nitrogen fixation of legumes. Just as is observed in the simple bacterial systems, perturbation of ammonia assimilation in legumes results in increased overall nitrogen fixation. The perturbed plants have increased growth and total nitrogen fixation capability. Because we have targeted the first enyzme in ammonia assimilation, glutamine synthetase, this provides a marker that could be used to assist selection or screening for increased biomass yield. DOE

52 AEROSPACE MEDICINE

Includes physiological factors; biological effects of radiation; and effects of weightlessness on man and animals.

N91-28726*# National Aeronautics and Space Administration. Goddard Space Flight Center, Greenbelt, MD.
DIRECTION DISCRIMINATING HEARING AID Patent Application
M. Jhabvala, inventor (to NASA) and H. C. Lin, inventor (to NASA) (Maryland Univ., College Park.) 9 Jun. 1989 22 p
(NASA-Case-GSC-13027-1; NAS 1.71:GSC-13027-1; US-Patent-Appl-SN-363807) Avail: NTIS HC/MF A03 CSCL 06L

It is an object of this invention to provide an improvement in hearing aids. It is another object of this invention to provide a hearing aid which is directionally sensitive. It is a further object of this invention to provide an improvement in hearing aids which are able to detect not only the direction from which the sound originates, but also to provide a visual indication of both the direction and intensity of the sounds. It is still another object of this invention to provide a directional hearing aid comprised of integrated circuits in order to minimize size and power dissipation. The foregoing and other objects of the invention are achieved by a multi-channel hearing aid device which is able to signal to the wearer in a binaural or a quadraphonic configuration whether sound is coming from the left or right, front or back, or both. For each channel, which operate in pairs, the sound is picked up by a respective microphone amplified and rectified into a DC voltage. The DC voltage is next fed to a three bit analog to digital converter comprised of seven parallel comparators and eight by three encoder. The three bit binary codes from the encoder are coupled into a logic circuit where the three bit binary codes are decoded to seven output levels which are used to drive an indicator which provides a visual indication of the sound level received. The three bit binary codes for each pair of channels are also fed into a digital comparator. The output of the two channels is such that if, for example, the signal coming from the right is louder than that coming from the left, the outputs of the logic unit of the right channel will be enabled and the corresponding indicator activated, indicating the direction of the sound source. Also an indication of the loudness is provided for that channel. The preferred embodiment only gives an indication for the stronger channel because it is deemed that a multiple channel indication, with relative volumes being indicated, would lead to confusion. NASA

N91-28727*# National Aeronautics and Space Administration. Goddard Space Flight Center, Greenbelt, MD.
DEVICE FOR REMOVING FOREIGN OBJECTS FROM ANATOMIC ORGANS Patent Application
Earl D. Angulo, inventor (to NASA) 19 Mar. 1991 18 p

(NASA-Case-GSC-13306-1; NAS 1.71:GSC-13306-1; US-Patent-Appl-SN-674828) Avail: NTIS HC/MF A03 CSCL 06K

A device is disclosed for removing foreign objects from anatomic organs such as the ear canal or throat. It has a housing shaped like a flashlight, an electrical power source such as a battery or AC power from a wall socket, and a tip extending from the housing. The tip has at least one wire loop made from a shape-memory-effect alloy such as Nitinol switchably connected to the electrical power source such that when electric current flows through the wire loop the wire loop heats up and returns to a previously programmed shape such as a curet or tweezers so as to facilitate removal of the foreign object. NASA

N91-28728# Michigan Univ., Ann Arbor. School of Medicine.
NEW TECHNIQUES FOR POSITRON EMISSION TOMOGRAPHY IN THE STUDY OF HUMAN NEUROLOGICAL DISORDERS
D. E. Kuhl 1991 7 p
(Contract DE-FG02-87ER-60561)
(DE91-013855; DOE/ER-60561/5) Avail: NTIS HC/MF A02

We continue our focus to develop more cost effective and efficient means for producing new functionally specific tracers and more simple, less expensive, means for acquiring and interpreting quantitative data. These improved processes are required for the future growth of positron emission tomography (PET) and for the transfer of this technology to clinical use. Our approach concentrates on two separate yet related areas, radiosynthesis and data analysis. The program is divided into four subprojects, the first pair related to radiosynthesis, and the second pair related to data analysis. Progress during the past project year has been excellent in both accomplishment and publication record. DOE

N91-28729* National Aeronautics and Space Administration, Washington, DC.
AEROSPACE MEDICINE AND BIOLOGY: A CONTINUING BIBLIOGRAPHY WITH INDEXES (SUPPLEMENT 352)
Aug. 1991 61 p
(NASA-SP-7011(352); NAS 1.21:7011(352)) Avail: NTIS HC A04; NTIS standing order as PB89-912300, $10.50 domestic, $21.00 foreign CSCL 06E

This bibliography lists 147 reports, articles and other documents introduced into the NASA Scientific and Technical Information System during July 1991. Subject coverage includes: aerospace medicine and psychology, life support systems and controlled environments, safety equipment, exobiology and extraterrestrial life, and flight crew behavior and performance. Author

53 BEHAVIORAL SCIENCES

Includes psychological factors; individual and group behavior; crew training and evaluation; and psychiatric research.

N91-28730*# National Aeronautics and Space Administration. Lyndon B. Johnson Space Center, Houston, TX.
AN ACCELERATED TRAINING METHOD FOR BACK PROPAGATION NETWORKS Patent Application
Robert O. Shelton, inventor (to NASA) 17 Jun. 1991 42 p
(NASA-Case-MSC-21625-1; NAS 1.71:MSC-21625-1; US-Patent-Appl-SN-716182) Avail: NTIS HC/MF A03 CSCL 05I

The principal objective is to provide a training procedure for a feed forward, back propagation neural network which greatly accelerates the training process. A set of orthogonal singular vectors are determined from the input matrix such that the standard deviations of the projections of the input vectors along these singular vectors, as a set, are substantially maximized, thus providing an optimal means of presenting the input data. Novelty exists in the method of extracting from the set of input data, a set of features which can serve to represent the input data in a simplified manner, thus greatly reducing the time/expense to training the system. NASA

54 MAN/SYSTEM TECHNOLOGY AND LIFE SUPPORT

Includes human engineering; biotechnology; and space suits and protective clothing.

For related information see also *16 Space Transportation.*

N91-28731# Navy Clothing and Textile Research Facility, Natick, MA.
THE CHEMICAL RESISTANCE OF PROTECTIVE HANDWEAR AVAILABLE THROUGH THE NAVY'S SUPPLY SYSTEM Final Report, Oct. 1989 - Sep. 1990
Andra Kirsteins Apr. 1991 30 p
(AD-A235874; NCTRF-184) Avail: NTIS HC/MF A03 CSCL 06/12

The Navy Clothing and Textile Research Facility (NCTRF) evaluated seven types of chemical protective gloves, available through the Navy's supply system, for their chemical resistance against a selected list of 10 hazardous chemicals found aboard ship. The purpose of this study was to generate information that could be used in the development of a material for multi-purpose hazardous-chemical protective handwear. Such a glove would eliminate the need for a variety of gloves in the supply system that are procured for a specific use. It should be noted that these gloves were not tested for their intended uses, since this was not the scope of the study. The study revealed that none of the current gloves protects against all of the tested chemicals. Results from this study further justify the need for the development of a multi-purpose hazardous-chemical protective glove material. GRA

N91-28732# Edgerton, Germeshausen and Grier, Inc., Idaho Falls, ID.
USING HSYS IN THE ANALYSIS OF HUMAN-SYSTEM INTERACTIONS: EXAMPLES FROM THE OFFSHORE PETROLEUM INDUSTRY
J. L. Harbour and S. G. Hill 1990 5 p Presented at the Human Factors Society Conference, Orlando, 8-12 Oct. 1990
(Contract DE-AC07-76ID-01570)
(DE91-013218; EGG-M-90269; CONF-9010155-5) Avail: NTIS HC/MF A01

In an attempt to better understand the interactional relationship between humans and operational systems, HSYS was developed. The HSYS methodology provides a systematic process for analyzing Human-SYStem interactions in complex operational settings. HSYS focuses on system interactions from the human's perspective and is built around a linear model of human performance, termed the Input-Action model. According to the model, all human actions involve, to varying degrees, five sequential steps: Input Detection, Input Understanding, Action Selection, Action Planning, and Action Execution. Based on the Input-Action model, a series of flowcharts, supported by detailed topical modules, have been developed to analyze each of the five main components in depth. During initial validation efforts, the HSYS methodology was used to analyze 28 accidents which occurred in the offshore petroleum industry from 1980 to 1989. Although numerous factors contributed to the various accident sequences examined, one frequently identified problem was a lack of situational awareness by crew members either immediately preceding the accident or during the actual accident sequence itself. A major contributor to this lack of awareness was inadequate input detection, caused by either inadequate input recognition, inadequate input discrimination, or inadequate attention. In most instances, the root causes for these inabilities were associated with inadequate sensor/display arrays and/or poor human-machine interface design and engineering. DOE

N91-28733 Tel-Aviv Univ. (Israel). Dept. of Interdisciplinary Studies.
HUMAN BODY PROTECTION IN A DYNAMIC ENVIRONMENT. CUSHIONING MECHANICS M.S. Thesis
Israel Zanger Jul. 1989 101 p In HEBREW; ENGLISH

summary
(ITN-91-85149) Copyright Avail: Tel-Aviv Univ., Exact Sciences Library, Ramat Aviv 69978, Israel

The principles of cushioning mechanics were defined and the transfer of vibration to a sitting human body in a dynamic environment was analyzed. The vibration damping properties of potential cushioning materials were classified. A mathematical approximation was established, which relates the damping efficiency of cushioning materials to the contact pressure. Several cushioning mechanics principles were formulated: An optimal domain for each material contact pressure; quasi-uniformity of contact pressure distribution; directional damping properties; and optimal damping of wide-spectrum vibration. Attention to these principles can lead to the design of cushions with optimal damping efficiencies. A test stand was assembled on which a series of transducers measured the acceleration transmitted through a cushioned chair into a sitting human body. The measured filtering efficiencies agreed well with predictions made according to the above principles. The principles were used to develop a methodology for the design of protective dynamic cushions, which can be applied to protection of instruments and delicate structures as well as to human protection. The methodology was applied to the design of cushions for a helicopter seat and for a combat vehicle seat; both proved superior to the articles in current use.
ISA

55 SPACE BIOLOGY

Includes exobiology; planetary biology; and extraterrestrial life.

No abstracts in this category.

59 MATHEMATICAL AND COMPUTER SCIENCES (GENERAL)

N91-28734# Argonne National Lab., IL.
RESEARCH IN MATHEMATICS AND COMPUTER SCIENCE AT ARGONNE, SEPTEMBER 1989-FEBRUARY 1991
G. W. Pieper Mar. 1991 69 p
(Contract W-31-109-eng-38)
(DE91-012989; ANL-91/16) Avail: NTIS HC/MF A04

The research activities in the Mathematics and Computer Science Division are reviewed. A brief look is given at the MCS staff and the research facilities and then the diverse research projects carried out in the division are discussed. Projects funded by non-DOE sources are also discussed, and new technology transfer activities are described. Further information on staff, visitors, workshops, and seminars is found in the appendixes.
DOE

60 COMPUTER OPERATIONS AND HARDWARE

Includes hardware for computer graphics, firmware, and data processing.

For components see *33 Electronics and Electrical Engineering.*

N91-28735 Technische Univ., Delft (Netherlands).
HIGH-SPEED AND HIGH-RESOLUTION ANALOG-TO-DIGITAL AND DIGITAL-TO-ANALOG CONVERTERS Ph.D. Thesis
Rudy Johan vandePlassche 1989 220 p
(ETN-90-97265) Copyright Avail: Philips Research Labs., P.O. Box 80.000, 5600 JA Eindhoven, Netherlands

Analog-to-digital and digital-to-analog converters are important building blocks connecting the analog world of transducers with the digital world of computing, signal processing and data acquisition systems. The converter as part of a system is described. The converter specifications are discussed. Measurement set-ups and measurement methods are introduced to verify the performance given. High speed A/D (analog/digital) converters using a folding and interpolation scheme are described. A theoretical treatment of the signal dependent delay of zero crossings of limiting amplifiers is given. Seven high resolution A/D and D/A converters are discussed. Sample-and-hold amplifiers are described. Nine reference current sources based on the bandgap principle of silicon are examined.
ESA

N91-28736 Technische Univ., Delft (Netherlands). Dept. of Electrical Engineering.
MEASURING AND MODELLING DISK I/O SUBSYSTEMS Ph.D. Thesis
Gilles Eliza Houtekamer 1989 257 p
(ISBN-90-6275-567-4; ETN-90-97266) Copyright Avail: Gilbert Houtekamer, Koninklijke Bibliotheek, The Hague, Netherlands

The main objectives of this project were to provide more insight into I/O (input/output) workload parameters, to design a tool that could be used to measure workload parameters, to build a model describing current subsystem implantation, and to evaluate possible future implementations. New controller schemes are proposed. Many aspects of I/O susbsystem analysis were covered: the low-level workload analysis; the rotary position sensing and pending models for non-cached configurations; the discussion of existing and newly proposed improved configurations; and the discussion of operating system control mechanisms for paging and swapping.
ESA

N91-28737# California Univ., Berkeley. Lawrence Berkeley Lab.
THE ROLE OF THE UNIX(TM) CENTRAL COMPUTING FACILITY IN A MULTI-PURPOSE NATIONAL LABORATORY
C. A. Eades Mar. 1991 13 p Presented at the Conference on Computing in High Energy Physics, Tsukuba, Japan, 11-15 Mar. 1991
(Contract DE-AC03-76SF-00098)
(DE91-012361; LBL-30411; CONF-910373-11) Avail: NTIS HC/MF A03

In the last ten years, a significant change has been seen in the role of the central computing facility. This has been brought about by the new technology and the evolving needs of the research community. The current efforts are discussed of the central computing facility's UNIX Group at Lawrence Berkeley Laboratory to address these changes in technology and the needs of its research groups. There are three general areas of discussion. In the first, management, the costs are discussed of system management in a distributed computing environment; current computing issues, including the impact of workstation technology on the laboratory infrastructure, the advantages and disadvantages of diskless workstations in the laboratory environment as well as the need for high reliability file services it implies. In the second, mass storage, the need for and an implementation of mass storage service to the laboratory community is discussed. Issues are also discussed such as network access and integration strategies. In the third, other types of service provided by the central facility are also discussed, including common software export via high availability Network File Services servers, distributed high quality output devices and the role of the central facility in providing computer security.
DOE

N91-28738# Oak Ridge National Lab., TN.
PERFORMANCE OF THE INTEL iPSC/860 AND NCUBE 6400 HYPERCUBES
T. H. Dunigan Apr. 1991 26 p
(Contract DE-AC05-84OR-21400)
(DE91-012370; ORNL/TM-11790) Avail: NTIS HC/MF A03

The performance of the Intel iPSC/860 hypercube and the Ncube 6400 hypercube are compared with earlier hypercubes from

Intel and Ncube. Computation and communication performance for a number of low-level benchmarks are presented for the Intel iPSC/1, iPSC/2, and iPSC/860 and for the Ncube 3200 and 6400. File I/O performance of the iPSC/860 and Ncube 6400 are compared. DOE

N91-28739 Utah Univ., Salt Lake City.
MICROCOMPUTERS: AN EXPLORATORY STUDY OF THEIR AVAILABILITY AND USE IN THE RESEARCH PROCESS AND THEIR CONTRIBUTION TO RESEARCHER PRODUCTIVITY Ph.D. Thesis
John Charles Bernhardt 1990 233 p
Avail: Univ. Microfilms Order No. DA9112745

The primary purpose was to determine what relationship existed between the reported average percentage of research hours involving microcomputer use during the years 1987 to 1989 and 10 measures of researcher productivity. The measures of researcher productivity used included: (1) total number of research achievements; (2) total number of academic journal publications; (3) total number of top-tier journal publications; (4) total number of meetings presentations; and (5) total number of proceedings publications during the 3-year period as well as counterpart variables adjusted for average weekly hours of research effort. Dissert. Abstr.

N91-28740 Illinois Univ., Urbana-Champaign.
PARALLEL INPUT/OUTPUT ARCHITECTURES FOR MULTIPROCESSORS Ph.D. Thesis
Narasimha Reddy Laks Annapareddy 1990 170 p
Avail: Univ. Microfilms Order No. DA9114162

Several aspects of solving the input/output (I/O) problem are examined. The increasing processor speeds and the emerging multiprocessor machines have improved the processing power of a system at a tremendous pace. This has not been followed by corresponding improvements in other parts of the system, mainly the I/O subsystem. This could lead to a huge imbalance in the system and, if not corrected, the gains made in the processing power will be of little use as the problem solving speed will be determined by the slower I/O operations. A number of issues in solving the I/O problem are addressed. The effects of I/O on problem solution are studied by tracing a number of applications on a multiprocessor. This study is aimed at gaining an understanding of how I/O accesses can be more efficiently done and how I/O systems need to be organized to effectively address the I/O problem. Another aim is to explore compiler techniques to reduce the I/O problem. Since the I/O device speeds are not improving dramatically, the I/O power can only be significantly improved through parallel organizations. An extensive evaluation of these parallel organizations is presented. Different parallel I/O (disk) organizations are evaluated in different workloads. A methodology for interfacing I/O processors with a multiprocessor system is presented. This methodology is shown to have a number of advantages over the previous approaches. When data are distributed on multiple disks, fault tolerance becomes a problem. A technique is presented for achieving fault tolerance in a multiple disk system. A number of compiler techniques are also proposed to reduce the I/O problem by suitable transformation of programs. A number of open problems in this area are highlighted. Dissert. Abstr.

61 COMPUTER PROGRAMMING AND SOFTWARE

Includes computer programs, routines, alogorithms, and specific applications, e.g., CAD/CAM.

N91-28741# Oak Ridge National Lab., TN.
THE apGA: AN ADAPTIVE PARALLEL GENETIC ALGORITHM
G. E. Liepins and S. Baluja (Virginia Univ., Charlottesville.) 1991 9 p Presented at the 4th International Conference on Genetic Algorithms, San Diego, Jul. 1991
(Contract DE-AC05-84OR-21400)
(DE91-009559; CONF-910784-2) Avail: NTIS HC/MF A02

We develop a parallel variant of the standard generational genetic algorithm (apGA) that combines aggressive search with perpetual novelty, yet is able to preserve enough genetic structure to optimally solve variably scaled, non-uniform block deceptive and hierarchical deceptive problems. The apGA combines elitism, adaptive mutation, adaptive exponential scaling, and temporal memory. We present empirical results for six classes of problems, including the DeJong test suite. Although we have not investigated hybrids, we note that apGA could be incorporated into other recent GA variants such as GENITOR, CHC, and the recombination stage of mGA. DOE

N91-28742# Carnegie-Mellon Univ., Pittsburgh, PA. Software Engineering Inst.
SUPPORT MATERIALS FOR FORMAL SPECIFICATION OF SOFTWARE Final Report
Alfs Berztiss Oct. 1987 83 p Prepared in cooperation with Pittsburgh Univ.
(Contract F19628-90-C-0003)
(AD-A236121; CMU/SEI-SM-8-1-0) Avail: NTIS HC/MF A05 CSCL 12/5

Topics addressed include: Examples of Predicative Specifications; The SF (Set-Function) Methodology; SF Specification: Boat Hire; SF Specification: A Library System; SF Specification: An Elevator Controller; The Specification Process; and Formal Specification Courses. GRA

N91-28743# Carnegie-Mellon Univ., Pittsburgh, PA. Software Engineering Inst.
THE SOFTWARE TECHNICAL REVIEW PROCESS Final Report
James S. Collofello Jun. 1988 20 p Prepared in cooperation with Arizona State Univ., Tempe
(Contract F19628-90-C-0003)
(AD-A236139; SEI-CM-3-1-5) Avail: NTIS HC/MF A03 CSCL 12/5

This module consists of a comprehensive examination of the technical review process in the software development and maintenance life cycle. Formal review methodologies are analyzed in detail from the perspective of the review participants, project management and software quality assurance. Sample review agendas are also presented for common types of reviews. The objective of the module is to provide the student with the information necessary to plan and execute highly efficient and cost effective technical reviews. GRA

N91-28744# Carnegie-Mellon Univ., Pittsburgh, PA. Software Engineering Inst.
SOFTWARE METRICS Final Report
Everald E. Mills Dec. 1988 45 p Prepared in cooperation with Seattle Univ., WA
(Contract F19628-90-C-0003)
(AD-A236140; SEI-CM-12-1-1) Avail: NTIS HC/MF A03 CSCL 12/5

Effective management of any process requires quantification, measurement, and modeling. Software metrics provide a quantitative basis for the development and validation of models of the software development process. Metrics can be used to improve software productivity and quality. This module introduces the most commonly used software metrics and reviews their use in constructing models of the software development process. Although current metrics and models are certainly inadequate, a number of organizations are achieving promising results through their use. Results should improve further as additional experience with various metrics and models is gained. GRA

N91-28745# Rome Air Development Center, Griffiss AFB, NY.
A SURVEY OF RELIABILITY, MAINTAINABILITY, SUPPORTABILITY, AND TESTABILITY SOFTWARE TOOLS Report, Aug. 1990 - Jan. 1991

Joseph A. Caroli Apr. 1991 113 p
(AD-A236148; RL-TR-91-87) Avail: NTIS HC/MF A06 CSCL 12/5

This report contains over 300 summaries of Reliability, Maintainability, Supportability, and Testability (R/M/S/T) software tools. Information is provided relative to tool name, description, operating environment and point of contact. The computer program summaries are unbiased and not based on actual evaluations of the products. The intent is to provide a complete (as possible) listing of all software that exists to help design for R/M/S/T. GRA

N91-28746# North Carolina Univ., Chapel Hill. Dept. of Computer Science.

PROTOTYPING PARALLEL AND DISTRIBUTED PROGRAMS IN PROTEUS

Peter H. Mills, Lars S. Nyland, Jan F. Prins, John H. Reif, and Robert A. Wagner Oct. 1990 18 p
(Contract N00014-90-K-0004)
(AD-A236597; TR90-041) Avail: NTIS HC/MF A03 CSCL 12/5

Prototyping is an important technique in software development for early exploration and validation of requirements. When prototyping concurrent behavior, a wide spectrum of models used to construct parallel programs must be embraced, reflecting a variety of underlying system architectures. Proteus, a language, suitable for prototyping parallel and distributed programs is presented. Proteus starts with the high-level set-theoretic notations of SETL and REFINE. It is extended to this base with the barrier-merge parallel construct, which partitions the variables used for communication in its shared memory model into shared and private sets. Each parallel process receives an independent copy of the private variables. These private copies are independently updated, and may be merged into the global state at specifiable barrier synchronization points: at these points a portion of the merged state may be reflected back into each private state. A layered language structure is envisioned which will express the various programming models, such as communicating sequential processes and data-level parallelism, in terms of this common foundation. A common foundation also facilitates the prototyping of heterogeneous systems whose concurrent parts are programmed following different models. GRA

N91-28747*# Illinois Univ., Urbana. Coordinated Science Lab.

COMPILE-TIME ESTIMATION OF COMMUNICATION COSTS IN MULTICOMPUTERS

Manish Gupta and Prithviraj Banerjee 22 May 1991 24 p
(Contract NAG1-613; N00014-91-J-1096; NSF MIP-86-57563)
(NASA-CR-188675; NAS 1.26:188675; AD-A236601; UILU-ENG-91-2226; CRHC-91-16) Avail: NTIS HC/MF A03 CSCL 09/2

An important problem facing numerous research projects on parallelizing compilers for distributed memory machines is that of automatically determining a suitable data partitioning scheme for a program. Any strategy for automatic data partitioning needs a mechanism for estimating the performance of a program under a given partitioning scheme, the most crucial part of which involves determining the communication costs incurred by the program. A methodology is described for estimating the communication costs at compile-time as functions of the numbers of processors over which various arrays are distributed. A strategy is described along with its theoretical basis, for making program transformations that expose opportunities for combining of messages, leading to considerable savings in the communication costs. For certain loops with regular dependences, the compiler can detect the possibility of pipelining, and thus estimate communication costs more accurately than it could otherwise. These results are of great significance to any parallelization system supporting numeric applications on multicomputers. In particular, they lay down a framework for effective synthesis of communication on multicomputers from sequential program references. GRA

N91-28748# Carnegie-Mellon Univ., Pittsburgh, PA. Software Engineering Inst.

A DESIGN SPACE AND DESIGN RULES FOR USER INTERFACE SOFTWARE ARCHITECTURE Final Report

Thomas G. Lane Nov. 1990 64 p
(Contract F19628-90-C-0003)
(AD-A237049; CMU/SEI-90-TR-22; ESD-TR-90-223) Avail: NTIS HC/MF A04 CSCL 12/5

The architecture of a user interface software system can be described in terms of a fairly small number of key functional and structural choices. This report presents a design space that identifies these key choices and classifies the alternatives available for each choice. The design space is a useful framework for organizing and applying design knowledge. The report presents a set of design rules expressed in the terms of the design space. These rules can help a software designer to make good structural choices based on the functional requirements for a user interface system. Extension of this work might eventually provide automated assistance for structural design. GRA

N91-28749# Pacific Northwest Lab., Richland, WA.

CHOOSING PROCESSOR ARRAY CONFIGURATION BY PERFORMANCE MODELING FOR A HIGHLY PARALLEL LINEAR ALGEBRA ALGORITHM

R. J. Littlefield and K. J. Maschhoff Apr. 1991 17 p Presented at the 6th Distributed Memory Computing Conference, Portland, 28 Apr. - 2 May 1991
(Contract DE-AC06-76RL-01830)
(DE91-012486; PNL-SA-18917; CONF-9104158-2) Avail: NTIS HC/MF A03

Many linear algebra algorithms utilize an array of processors across which matrices are distributed. Given a particular matrix size and a maximum number of processors, what configuration of processors, i.e., what size and shape array, will execute the fastest is examined. The answer to this question depends on tradeoffs between load balancing, communication startup and transfer costs, and computational overhead. In this paper we analyze in detail one algorithm: the blocked factored Jacobi method for solving dense eigensystems. A performance model is developed to predict execution time as a function of the processor array and matrix sizes, plus the basic computation and communication speeds of the underlying computer system. In experiments on a large hypercube (up to 512 processors), this model has been found to be highly accurate (mean error (approximately) 2 percent) over a wide range of matrix sizes (10 x 10 through 200 x 200) and processor counts (1 to 512). The model reveals, and direct experiment confirms, that the tradeoffs mentioned above can be surprisingly complex and counterintuitive. Decision procedures are proposed based directly on the performance model to choose configurations for fastest execution. The model-based decision procedures are compared to a heuristic strategy and shown to be significantly better. DOE

N91-28750# Edgerton, Germeshausen and Grier, Inc., Idaho Falls, ID.

SOFTWARE DEVELOPMENT EXPERIENCES WITH A DISTRIBUTED DATABASE IN A LARGE, DISTRIBUTED COMPUTER SYSTEM

B. J. Groeneveld, L. A. Dean, and J. A. Goetsch Apr. 1991 21 p Presented at the Database Colloquium '91, San Diego, 24-26 Jun. 1991
(Contract DE-AC07-76ID-01570)
(DE91-012818; EGG-M-91023; CONF-9106191-2) Avail: NTIS HC/MF A03

This paper discusses experience obtained in developing software that uses a distributed database management system in a large, heterogeneous, multihost-computer environment. The environment is under development at the Idaho National Engineering Laboratory for the United States Air Force's Tactical Air Command. Emphasis is on implementation issues surrounding usage of Oracle Corporation's Relational Database Management System (RDBMS). However, many items are applicable to other RDBMSs as well. The reader is first given an overview of the project and environment in which the experience was gained. The paper then discusses individual experiences and their related design and implementation consequences. Finally, the paper closes with a discussion of future project directions regarding the database. DOE

N91-28751# Oak Ridge National Lab., TN.

BAYESIAN DESIGN AND ANALYSIS OF COMPUTER EXPERIMENTS: USE OF DERIVATIVES IN SURFACE PREDICTION

M. D. Morris, T. J. Mitchell, and D. Ylvisaker (California Univ., Los Angeles.) Jun. 1991 26 p
(Contract DE-AC05-84OR-21400)
(DE91-013147; ORNL/TM-11699) Avail: NTIS HC/MF A03

The work of Currin et al. and others in developing fast predictive approximations of computer models is extended for the case in which derivatives of the output variable of interest with respect to input variables are available. In addition to describing the calculations required for the Bayesian analysis, the issue of experimental design is also discussed, and an algorithm is described for constructing maximun distance designs. An example is given based on a demonstration model of eight inputs and one output, in which predictions based on a maximun design, a Latin hypercube design, and two compromise designs are evaluated and compared. DOE

N91-28752# Office of Technology Assessment, Washington, DC.

SEEKING SOLUTIONS: HIGH-PERFORMANCE COMPUTING FOR SCIENCE

Apr. 1991 47 p
(PB91-169763; OTA-BP-TCT-77) Avail: NTIS HC/MF A03; also available SOD HC $2.25 as 052-003-01227-8 CSCL 09B

Information technology is a critical element for science and engineering. The U.S. is building a nationwide computer communication infrastructure to provide high-speed data services to the R and D community, but the mere installation of hardware is not enough. Whether or not very fast data communication networks and high performance computers deliver their promise benefits depends on the institutions, processes, and policies that are established to design and manage the new system. High performance computing is examined as part of the infrastructure proposed in the Office of Science and Technology Policy (OSTP) initiative. GRA

N91-28753# Oak Ridge National Lab., TN.

SEARCHING FOR CONSENSUS PATTERNS ON A HYPERCUBE

X. Guan, R. C. Mann, R. Mural, and E. Uberbacher 1991 5 p Presented at the 6th Distributed Memory Computing Conference, Portland, 28 Apr. - 2 May 1991
(Contract DE-AC05-84OR-21400)
(DE91-013233; CONF-9104158-3) Avail: NTIS HC/MF A01

In DNA sequence analysis, consensus patterns (those that are not precisely conserved in location or with the same sequence of letters) are frequently sought among a number of sequences to find important biological features. Sequential algorithms for finding consensus patterns are time-consuming due to the nature of the inexact occurrences of the patterns. Here we show that consensus pattern search can be done efficiently on the hypercube. We describe our implementation of two algorithms to find consensus patterns on an Intel iPSC/860 Hypercube and various techniques to speed up the computation. DOE

N91-28754# Virginia Univ., Charlottesville. Dept. of Computer Science.

EMBEDDING ADAMS IN FORTRAN

G. C. Watson 1991 55 p
(Contract DE-FG05-88ER-25063)
(DE91-014346; DOE/ER-25063/T10) Avail: NTIS HC/MF A04

ADAMS is a database language which can be embedded in a number of conventional programming languages such as C, FORTRAN and Pascal. A prototype preprocessor was developed which allows the embedding of ADAMS statements in the FORTRAN programming language. Reasons are discussed for designing ADAMS to support multiple host languages, and why FORTRAN was the language chosen for the prototype preprocessor. Details concerning the conversion of the existing ADAMS preprocessor to the prototype are discussed in some detail. In addition, research issues concerning heterogeneous language constructs and data representation are discussed. DOE

N91-28755# Oak Ridge National Lab., TN.

SOLVING COMPUTATIONAL GRAND CHALLENGES USING A NETWORK OF HETEROGENEOUS SUPERCOMPUTERS

A. Beguelin, J. Dongarra, A. Geist, R. Manchek, and V. Sunderam (Emory Univ., Atlanta, GA.) 1991 7 p Presented at the 5th Society for Industrial and Applied Mathematics (SIAM) Conference, Houston, 22-25 Mar. 1991
(Contract DE-AC05-84OR-21400)
(DE91-013725; CONF-910326-5) Avail: NTIS HC/MF A02

This paper describes simple experiments connecting a Cray XMP, an Intel iPSC/860, and a Thinking Machines CM2 together over a high speed network to form a much larger virtual computer. It also describes our experience with running a Computational Grand Challenge on a Cray XMP and an iPSC/860 combination. The purpose of the experiments is to demonstrate the power and flexibility of the PVM (Parallel Virtual Machine) system to allow programmers to exploit a diverse collection of the most powerful computers available to solve Grand Challenge problems. DOE

N91-28756# Sandia National Labs., Albuquerque, NM.

LOAD-BALANCING AND PERFORMANCE OF A GRIDLESS PARTICLE SIMULATION ON MIMD, SIMD, AND VECTOR SUPERCOMPUTERS

S. Plimpton, I. Shokair, J. Wagner, and J. Jortner 1991 6 p Presented at the 5th Society for Industrial and Applied Mathematics (SIAM) Conference, Houston, Apr. 1991
(Contract DE-AC04-76DP-00789)
(DE91-013758; SAND-90-2671C; CONF-9104265-1) Avail: NTIS HC/MF A02

Our charged particle simulation models a relativistic electron beam for which the field solution is local and thus requires no grid. We have implemented the simulation on a CRAY and on two parallel machines, a nCUBE 2 and Connection Machine. We present implementation details and contrast the approaches necessary for the three architectures. On the parallel machines a dynamic load-balancing problem arises because the beam grows uniformly in one dimension from a few hundred to hundreds of thousands of particles as the simulation progresses. We discuss a folded Gray-code mapping of the processors to the length scale of the simulation that expands (or shrinks) as the beam changes length so as to minimize inter-processor communication. This improves the efficiency of the nCUBE version of the simulation which runs at 10x the speed of the vectorized CRAY version. DOE

N91-28757# Virginia Univ., Charlottesville. School of Engineering and Applied Science.

AN INTRODUCTION TO THE ADAMS INTERFACE LANGUAGE, PART 1

J. L. Pfaltz, J. C. French, and A. Grimshaw 17 Apr. 1991 36 p
(Contract DE-FG05-88ER-25063)
(DE91-014344; DOE/ER-25063/T8-Pt-1; IPC-TR-91-06-Pt-1)
Avail: NTIS HC/MF A03

ADAMS provides an interface between host application programs and a space of persistent data items, or a database. The interface consists of ways to describe a user's space of persistent data items, sometimes called a data description language, or DDL, together with mechanisms to access those items, which is sometimes called a data manipulation language, or DML, or a query language. In this part we concentrate only on the descriptive power of ADAMS. What kinds of databases can be represented in ADAMS. In Part 2, we will focus on the manipulative and query power of ADAMS. Every database implementation is eventually grounded in a number of primitive concepts which are fundamental to understanding the system. ADAMS is based on six primitive concepts: attribute, codomain, element, map, sequence, and set, which we regard as fundamental to all database implementation. We show that ADAMS has at least the same descriptive power as the more traditional database models, such as the relational model, the semantic model, and the object-oriented model by showing all such database configurations can be expressed in terms of these primitives. DOE

N91-28758# Argonne National Lab., IL.
AN ITERATIVE SUBSTRUCTURING ALGORITHM FOR PROBLEMS IN THREE DIMENSIONS
B. F. Smith 1991 7 p Presented at the 5th Conference on Domain Decomposition Methods for Partial Differential Equations, Norfolk, 6-8 May 1991
(Contract W-31-109-eng-38)
(DE91-014388; ANL/CP-73224; CONF-9105217-1) Avail: NTIS HC/MF A02

In domain decomposition algorithms with more than a few subdomains, there is a crucial need for a mechanism to provide for global communication of information at each step of the iterative process. The convergence rate will decay rapidly with an increasing number of subdomains if communication is only between neighboring subdomains. For iterative substructuring algorithms (those domain decomposition algorithms that use nonoverlapping subdomains), the method that provides for good global communication in two dimensions does not work well for problems in three dimensions. An alternative approach for providing global communication is presented that works well in three dimensions. Sample theoretical and numerical results are presented. DOE

N91-28759# California Univ., Berkeley. Lawrence Berkeley Lab.
COMPUTING MINIMAL SURFACES VIA LEVEL SET CURVATURE FLOW Ph.D. Thesis
D. L. Chopp May 1991 66 p
(Contract DE-AC03-76SF-00098)
(DE91-014709; LBL-30685) Avail: NTIS HC/MF A04

Given a finite union (Gamma) of fixed closed curves in R(sup 3), there is an associated problem of finding a surface with mean curvature zero which has (Gamma) as its boundary. In this paper, a new approach to numerically solving this minimal surface problem is introduced. The surface is represented as a level set of a global function (Phi): R(sup 3) yields R. The surface evolves according to mean curvature flow until a steady state solution is achieved. A new system of interpolatory boundary conditions are used to maintain the connection between the moving surface and the fixed boundary contour. DOE

N91-28760 Tel-Aviv Univ. (Israel). Dept. of Electronics Communications Control and Computer Systems.
EFFICIENT SOFT DECISION DECODING OF REED-MULLER CODES AND RELATED NON-LINEAR GENERALIZATIONS M.S. Thesis
Shmuel Aran Oct. 1989 229 p In HEBREW; ENGLISH summary
(ITN-91-85146) Copyright Avail: Tel-Aviv Univ., Exact Sciences Library, Ramat Aviv 69978, Israel

Effective coding algorithms were developed for Reed-Muller (R-M) codes and their nonlinear generalizations, to reduce the complexity of soft decision coding. The aim was to recognize the optimal subcode which could be decoded using the Wagner rule, while effectively preparing values for all its cosets. The criteria for choosing a code are discussed and a measuring technique for comparing the performance of the suggested algorithms is selected. The algorithm selected was developed by Forney, using trellis diagrams based on a squaring construction method. Reed-Muller codes were built and decoded using squaring constructions. First order R-M codes had a decoding algorithm which used the Hadamard transformation and the Green machine. A soft decision algorithm was developed for decoding 2nd order R-M codes. The decoding of higher order R-M codes is discussed and a generalization applicable to all R-M codes is developed. Efficient decoding of nonlinear generalizations of 1st order R-M codes was found to be possible, because each nonlinear code comprises a collection of cosets of the 1st order R-M code. The codes discussed include Nordstrom-Robinson, Kerdock and Delsarte-Goethals codes. The operational and conceptual analyses of results are presented, to perform optimal soft decision decoding, with high coding gain and minimal use of computation resources. ISA

N91-28761 Pennsylvania Univ., Philadelphia.
A LOGIC MODEL FOR MODEL MANAGEMENT: AN EMBEDDED LANGUAGES APPROACH Ph.D. Thesis
Hemant Kumar Bhargava 1990 177 p
Avail: Univ. Microfilms Order No. DA9112534

The executable modeling language (EML) is extended. It is argued that existing modeling systems lack adequate means for representing, and usefully extracting, much information about models and modeling elements other than that required to just solve models. It aims to provide a formal, general means to represent and usefully extract such information, by developing the embedded languages technique and applying it to model management. In the embedded languages technique (as applied to model management), an EML, which partially formalizes the target language that is used to represent, describe, and reason about models, is embedded within a formal embedding language for model management. The technique creates dual interpretation for the symbols and expressions in the embedded language through rules of formation, such that terms and formulas in the embedded language can be treated as terms in the embedding language. This strategy enables the embedded language to: (1) represent rigorously, flexibly, and with generality, a rich variety of qualitative knowledge about models that could normally not be stated in the modeling language itself; (2) use this knowledge in defining inferences that are useful in the modeling process; (3) represent rules of formation for expressions in the modeling language, and use them to examine validity of model declarations; and (4) embed and integrate multiple languages. This technique was applied to develop a prototype modeling system, now in use at the U.S. Coast Guard, for the rapid development, documentation, and use of a wide class of models. Dissert. Abstr.

N91-28762# Argonne National Lab., IL.
A MULTILINGUAL PARALLELIZATION OF THE ICOSAHEDRAL-HEXAGONAL GRID SYSTEM FOR INTEGRATION ON THE SPHERE
S. J. Hammond (Maine Univ., Orono.) 1991 7 p Presented at the 5th National Conference on Undergraduate Research, Pasadena, 21-23 Mar. 1991
(Contract W-31-109-eng-38)
(DE91-013615; ANL/CP-73154; CONF-9103136-6) Avail: NTIS HC/MF A02

The objective was to use these multilingual programming techniques to parallelize an existing Fortran program. This program is an implementation of the shallow water equations using the icosahedral hexagonal grid system to integrate over a sphere. An objective was to test the usefulness of multilingual techniques, to evaluate the new language PCN (Program Composition Notation), and to investigate the parallel execution characteristics of the icosahedral-hexagonal algorithm. Two features of PCN make it a useful language for parallelization. The first of these is single assignment variables. Communication and synchronization between processes is represented by reading and writing to these variables. This feature simplifies the specification of complex protocols, reducing them to variable creation and assignment. Second, PCN decouples process mapping from concurrent execution. Mapping is specified annotations to procedure calls, which indicate the processor on which execution of the procedure is to take place. Variables passed into the procedure then become message streams to that processor. DOE

N91-28763# California Univ., Berkeley. Lawrence Berkeley Lab.
VISUALIZATION USING A DATA FLOW-BASED PARADIGM

W. Bethel, N. Johnston, and H. Holmes Mar. 1991 6 p
Presented at the Conference on Computing in High Energy Physics, Tsukuba, Japan, 11-15 Mar. 1991
(Contract DE-AC03-76SF-00098)
(DE91-013851; LBL-30412; CONF-910373-13) Avail: NTIS HC/MF A02

A new computer data analysis and display technology has become available to the scientific community. This technology is the result of the conjunction of recent advances in computer graphics (in surface lighting and shading, object oriented three dimensional hierarchical geometry structures, and volume data rendering techniques); window systems (the wide acceptance of the X window system); user interfaces (the visual programming paradigm); software engineering techniques (the data flow based visualization concept); and affordable, high performance graphics workstations that support this software. At Lawrence Berkeley Laboratory, we have made extensive use of Stardent Computer's Application Visualization System, a prime example of such a visualization tool, on data from a wide cross-section of scientific disciplines, including Particle Physics, Earth Sciences, Mathematics, Research Medicine and the Human Genome Center. DOE

N91-28764# Edgerton, Germeshausen and Grier, Inc., Idaho Falls, ID. National Low-Level Waste Management Program.

GUIDELINES FOR ACQUISITION, INSTALLATION, AND TESTING OF PERFORMANCE ASSESSMENT SOFTWARE

R. R. Seitz, S. D. Matthews, and K. M. Kostelnik Sep. 1990 82 p
(Contract DE-AC07-76ID-01570)
(DE91-013910; DOE/LLW-102; MISC-90087) Avail: NTIS HC/MF A05

This document presents general guidelines and quality assurance recommendations for acquired performance assessment software to be used for activities in support of low-level radioactive waste disposal facilities. Recommendations are presented for establishing a computer directory structure, configuration control, and software testing analyses. The appendices contain examples of the directory structure and file management system as implemented at the Idaho National Engineering Laboratory (INEL) for the UNSAT-H, Version 2.0 code. Results of the various software analysis performed on UNSAT-H are also presented. DOE

N91-28765# Argonne National Lab., IL.

AUTOMATED REASONING CONTRIBUTES TO MATHEMATICS AND LOGIC

L. Wos, S. Winker, W. McCune, R. Overbeek, E. Lusk, R. Stevens, and R. Butler (University of North Florida, Jacksonville.) 1990 15 p Presented at the Computer Aided Deduction Conference (CADE), Kaiserslautern, Fed. Republic of Germany, 23-27 Jul. 1990
(Contract W-31-109-eng-38)
(DE91-014005; ANL/CP-72570; CONF-900765-2) Avail: NTIS HC/MF A03

Some results are presented of the research focusing on the use of our newest automated reasoning program OTTER to prove theorems from Robbins algebra, equivalential calculus, implicational calculus, combinatory logic, and finite semigroups. Included among the results are answers to open questions and new shorter and less complex proofs to know theorems. To obtain these results, the usual paradigm was relied upon, which heavily emphasizes the role of demodulation, subsumption, set of support, weighting, paramodulation, hyperresolution, and UR resolution. It is believed that all of these components are essential, even though little light is shed on the relative importance of each, the coupling of the various components, and the metarules for making the most effective choices. Indeed, without these components, a program will too often offer inadequate control over the redundancy and irrelevancy of deduced information. Experimental evidence is included to support the position, examples producing success when the paradigm is employed, and examples producing failure when it is not. In addition to providing evidence that automated reasoning has made contributions to both mathematics and logic, the theorems discussed also serve nicely as challenge problems for testing the merits of a new idea or a new program and provide interesting examples for comparing different paradigms. DOE

N91-28766# Oak Ridge National Lab., TN.

SCIENTIFIC DATA VISUALIZATION

R. J. Toedte and B. S. Wallace 18 Apr. 1991 9 p Presented at the 1991 Oak Ridge American Society for Metals (ASM) International Educational Symposium, Oak Ridge, 18 Apr. 1991
(Contract DE-AC05-84OR-21400)
(DE91-014216; CONF-9104267-1) Avail: NTIS HC/MF A02

The Computing and Telecommunication Division's (C and TD) Graphics Development Section (GDS) established a Visualization Laboratory at the Oak Ridge National Laboratory (ORNL) in FY90 to support the Office of Laboratory Computing's (OLC) Strategic Plan. The Strategic Plan's goal of making ORNL one of the nation's top scientific computing laboratories will require the integration of scientific visualization into ORNL's everyday scientific research. The Visualization Laboratory serves as a catalyst for bringing computing into scientific research as a tool for understanding scientific results and for presenting scientific results. The Visualization Lab promotes the use of scientific visualization to C and TD customers by producing demo video tapes, technical brochures, giving technical presentations, providing customer consultation in the area of hardware/software evaluation and procurement, and the production of graphic images from scientific data. This report contains lists of the hardware and software. DOE

N91-28767# Sandia National Labs., Albuquerque, NM.

GENERAL IMPLEMENTATION OF THIN-SLOT ALGORITHMS INTO THE FINITE-DIFFERENCE TIME-DOMAIN CODE, TSAR, BASED ON A SLOT DATA FILE

D. J. Riley and C. D. Turner Jun. 1991 74 p
(Contract DE-AC04-76DP-00789)
(DE91-014336; SAND-91-1061) Avail: NTIS HC/MF A04

Two methods for modeling arbitrary narrow apertures in finite difference time-domain (FDTD) codes are presented in this paper. The first technique is based on the hybrid thin-slot algorithm (HTSA) which models the aperture physics using an integral equation approach. This method can model slots that are narrow both in width and depth with regard to the FDTD spatial cell, but is restricted to planar apertures. The second method is based on a contour technique that directly modifies the FDTD equations local to the aperture. The contour method is geometrically more flexible than the HTSA, but the depth of the aperture is restricted to the actual FDTD mesh. A technique to incorporate both narrow-aperture algorithms into the FDTD code, TSAR, based on a slot data file is presented. Results for a variety of complex aperture contours are provided, and limitations of the algorithms are discussed. DOE

N91-28768# California Univ., Berkeley. Lawrence Berkeley Lab.

ELASTIC TRACKING VERSUS NEURAL NETWORK TRACKING FOR VERY HIGH MULTIPLICITY PROBLEMS

M. Harlander and M. Gyulassy Apr. 1991 11 p Presented at the Austrian Artificial Intelligence Conference, Vienna (Austria), 24-27 Sep. 1991
(Contract DE-AC03-76SF-00098)
(DE91-011825; LBL-30512; CONF-9109135-1) Avail: NTIS HC/MF A03

A new Elastic Tracking (ET) algorithm is proposed for finding tracks in very high multiplicity and noisy environments. It is based on a dynamical reinterpretation and generalization of the Radon transform and is related to elastic net algorithms for geometrical optimization. ET performs an adaptive nonlinear fit to noisy data with a variable number of tracks. Its numerics is more efficient than that of the traditional Radon or Hough transform method because it avoids binning of phase space and the costly search for valid minima. Spurious local minima are avoided in ET by introducing a time dependent effective potential. The method is shown to be very robust to noise and measurement error and extends tracking capabilities to much higher track densities than possible via local road finding or even the novel Denby-Peterson neural network tracking algorithms. DOE

N91-28769 California Univ., Los Angeles.
ORDER REDUCTION AND SYNTHESIS OF TRANSFER FUNCTION MODELS Ph.D. Thesis
John T. Spanos 1990 137 p
Avail: Univ. Microfilms Order No. DA9115291

Methods and algorithms for the approximation of high order transfer function models are developed. Specifically, input, single-output (SISO) transfer functions; and (2) synthesis of SISO transfer functions from frequency response data. In connection with the model order reduction problem, the transfer function is parameterized as a ratio of two polynomials and the numerator and denominator coefficients which minimize the integral of the magnitude-squared of the frequency response error are sought. Based on gradient information, two iterative algorithms are developed which search for a minimum of this nonlinear least squares criterion. Frequency dependent weightings are also introduced into the formulation allowing freedom in shaping the approximation error over the frequency domain. In connection with the transfer function synthesis problem, iterative algorithms for minimizing two criteria are proposed: (1) the weighted sum of the magnitude squared of the frequency response errors; and (2) the magnitude of the maximum error. For the minimization of the nonlinear least squares criterion, gradient and Hessian information are employed to develop a quadratically convergent algorithm of the Newton type. For the minimization of the minimax criterion, an iterative algorithm is proposed which computes the coefficients of the unknown transfer function by solving a sequence of nonlinear frequency weighted least squares problems where the weights are updated recursively. The proposed model reduction and synthesis algorithms are demonstrated with many numerical examples. Dissert. Abstr.

62 COMPUTER SYSTEMS

Includes computer networks and special application computer systems.

N91-28770# North Carolina Univ., Chapel Hill. Dept. of Computer Science.
PROVIDING COMMON ACCESS MECHANISMS FOR DISSIMILAR NETWORK INTERCONNECTION NODES M.S. Thesis
John Menges Feb. 1991 105 p
(Contract N00014-86-K-0680)
(AD-A236630; TR91-013) Avail: NTIS HC/MF A06 CSCL 12/7

Over the past several years, thousands of Local Area Networks (LANs) around the world have been interconnected to form huge computer networks. These interconnections between LANs have been made using a variety of different classes of Interconnection Nodes (INs) made by many different vendors. Management of these essentially similar INs has been more difficult than necessary because of the dissimilar methods required to manage the various IN types. The design and implementation is described of access mechanisms that make it possible to manage the similar aspects of the various IN types in a common manner, without sacrificing the type-specific functions of the various proprietary management systems. GRA

N91-28771# North Carolina Univ., Chapel Hill. Dept. of Computer Science.
TAXONOMY AND ALGORITHMS FOR VOLUME RENDERING ON MULTICOMPUTERS
Ulrich Neumann 1990 18 p
(Contract N00014-86-K-0680)
(AD-A236632) Avail: NTIS HC/MF A03 CSCL 12/6

The design space of parallel volume rendering algorithms is large and relatively uncharted. No adequate framework currently exists for classifying approaches so that distinctions between them are clearly understood based on the categories they fall into. An analytical decomposition is presented of volume rendering tasks that yields a taxonomy of volume rendering algorithms for distributed memory multicomputers. In addition to the primary categories, secondary attributes are introduced to build a hierarchical classification system. Representative algorithms in each category are described and analyzed, giving insight into a whole range of approaches; some as yet untried. GRA

N91-28772# Lawrence Livermore National Lab., CA.
THE CACHE GROUP SCHEME FOR HARDWARE-CONTROLLED CACHE COHERENCE AND THE GENERAL NEED FOR HARDWARE COHERENCE CONTROL IN LARGE-SCALE MULTIPROCESSORS Ph.D. Thesis
J. E. Hoag Mar. 1991 79 p
(Contract W-7405-eng-48)
(DE91-012106; UCRL-LR-106975) Avail: NTIS HC/MF A05

A scheme that employs cache grouping and incomplete directory state in order to reduce the cost of maintaining directory state is introduced. This thesis discusses the cache grouping scheme, describes the protocols necessary for its implementation, and gives the results of detailed simulations of the scheme using various application codes. The effects of changing cache group size and using sophisticated multicast and combination features in the interconnect are explored. It is discovered that the cache grouping scheme can equal the performance of full-directory schemes, while costing much less. The system is relatively insensitive to cache group size. Advanced multicast and combination features in the network work best when used together, and have especially beneficial effects for codes that exhibit a high rate of one-to-many invalidates. The simulation of a machine employing the cache grouping scheme indicates significant performance gains over an identical machine without a shared data cache. We also discuss the time and coding required to coax efficiency out of codes run on large scale parallel machines without hardware coherent cache mechanisms. DOE

N91-28773# Ames Lab., IA.
TOWARD A BETTER PARALLEL PERFORMANCE METRIC
Xian-He Sun and J. L. Gustafson Jan. 1991 24 p
(Contract W-7405-eng-82)
(DE91-012627; IS-5053) Avail: NTIS HC/MF A03

Due to programming difficulty, parallel algorithms are commonly compared with different levels of programming effort. They are also compared on different architectures. The fairness of parallel performance metrics is studied. Theoretical and experimental results show that the most commonly used performance metric, parallel speedup, is unfair, in that it favors slow processors and poorly coded programs. Two new performance metrics are introduced. The first one, sizeup, provides a fair performance measurement. The second one is a generalization of speedup: the generalized speedup. The relation between sizeup, speedup, and generalized speedup are studied. A real application was implemented on an nCUBE 2 multicomputer. The experimental results match the analytical results closely. DOE

N91-28774# Lawrence Livermore National Lab., CA.
SPLIT-JOIN AND MESSAGE PASSING PROGRAMMING MODELS ON THE BBN TC2000
E. D. Brooks, III, B. C. Gorda, K. H. Warren, and T. S. Welcome Jan. 1991 9 p Presented at the 20th International Conference on Parallel Processing, St. Charles, 12-16 Aug. 1991
(Contract W-7405-eng-48)
(DE91-008067; UCRL-JC-106181; CONF-910858-1) Avail: NTIS HC/MF A02

The BBN TC2000 is a scalable general purpose parallel architecture capable of efficiently supporting both shared memory and message passing programming paradigms. We describe the TC2000 machine architecture and the programming models which we have implemented on it. The parallel programming models are implemented in a portable manner and will be useful on the scalable shared memory machines we expect to see in the future. DOE

N91-28775# Sandia National Labs., Albuquerque, NM.
AN INTERDISCIPLINARY APPROACH TO MASSIVELY PARALLEL COMPUTATION
S. S. Dosanjh and W. J. Camp 1991 6 p Presented at the Supercomputing USA/Pacific '91, Santa Clara, 19-21 Jun. 1991
(Contract DE-AC04-76DP-00789)
(DE91-012652; SAND-91-1143C; CONF-9106179-2) Avail: NTIS HC/MF A02

The MPCRL is comprised of an interdisciplinary team of physical and chemical scientists, engineers, mathematicians and computer scientists. We are developing a computing infrastructure for massively parallel machines and we are applying this rapidly evolving technology to problems ranging from quantum chemistry to SDI tracking and correlating. This paper summarizes some of the work being conducted in mathematics, computer science and applications. DOE

N91-28776*# National Aeronautics and Space Administration. Lewis Research Center, Cleveland, OH.
DESCRIPTION OF REAL-TIME Ada SOFTWARE IMPLEMENTATION OF A POWER SYSTEM MONITOR FOR THE SPACE STATION FREEDOM PMAD DC TESTBED
Kimberly Ludwig (Sverdrup Technology, Inc., Brook Park, OH.), Michael Mackin, and Theodore Wright 1991 8 p Presented at the 26th Intersociety Energy Conversion Engineering Conference, Boston, MA, 4-9 Aug. 1991; cosponsored by ANS, SAE, ACS, AIAA, ASME, IEEE, and AIChE
(NASA-TM-105157; E-6444; NAS 1.15:105157) Avail: NTIS HC/MF A02 CSCL 09B

The Ada language software development to perform the electrical system monitoring functions for the NASA Lewis Research Center's Power Management and Distribution (PMAD) DC testbed is described. The results of the effort to implement this monitor are presented. The PMAD DC testbed is a reduced-scale prototype of the electrical power system to be used in the Space Station Freedom. The power is controlled by smart switches known as power control components (or switchgear). The power control components are currently coordinated by five Compaq 382/20e computers connected through an 802.4 local area network. One of these computers is designated as the control node with the other four acting as subsidiary controllers. The subsidiary controllers are connected to the power control components with a Mil-Std-1553 network. An operator interface is supplied by adding a sixth computer. The power system monitor algorithm is comprised of several functions including: periodic data acquisition, data smoothing, system performance analysis, and status reporting. Data is collected from the switchgear sensors every 100 milliseconds, then passed through a 2 Hz digital filter. System performance analysis includes power interruption and overcurrent detection. The reporting mechanism notifies an operator of any abnormalities in the system. Once per second, the system monitor provides data to the control node for further processing, such as state estimation. The system monitor required a hardware time interrupt to activate the data acquisition function. The execution time of the code was optimized using an assembly language routine. The routine allows direct vectoring of the processor to Ada language procedures that perform periodic control activities. A summary of the advantages and side effects of this technique are discussed. Author

N91-28777*# Boeing Military Airplane Development, Seattle, WA.
TOWARD A FORMAL VERIFICATION OF A FLOATING-POINT COPROCESSOR AND ITS COMPOSITION WITH A CENTRAL PROCESSING UNIT Final Report
Jing Pan, Karl N. Levitt (California Univ., Davis.), and Gerald C. Cohen 5 Aug. 1991 110 p
(Contract NAS1-18586)
(NASA-CR-187547; NAS 1.26:187547) Avail: NTIS HC/MF A06 CSCL 09B

Discussed here is work to formally specify and verify a floating point coprocessor based on the MC68881. The HOL verification system developed at Cambridge University was used. The coprocessor consists of two independent units: the bus interface unit used to communicate with the cpu and the arithmetic processing unit used to perform the actual calculation. Reasoning about the interaction and synchronization among processes using higher order logic is demonstrated. Author

N91-28778# Sandia National Labs., Albuquerque, NM.
REQUIREMENTS FOR A NETWORK STORAGE SERVICE
S. M. Kelly and R. A. Haynes 1991 11 p Presented at the NSSDC Conference on Mass Storage Systems and Technologies for Space and Earth Science Applications Greenbelt, 23-25 Jul. 1991
(Contract DE-AC04-76DP-00789)
(DE91-014106; SAND-91-1290C; CONF-9107131-1) Avail: NTIS HC/MF A03

Sandia National Laboratories provides a high performance classified computer network as a core capability in support of its mission of nuclear weapons design and engineering, physical sciences research, and energy research and development. The network, locally known as the Internal Secure Network (ISN), was designed in 1989 and comprises multiple distributed local area networks (LANs) residing in Albuquerque, New Mexico and Livermore, California. The TCP/IP protocol suite is used for inter-node communications. Scientific workstations and mid-range computers, running UNIX-based operating systems, compose most LANs. The current file server on the supercomputer LAN is an implementation of the Common File System developed by Los Alamos National Laboratory. Subsequent to the design of the ISN, Sandia reviewed its mass storage requirements and choose to enter into a competitive procurement to replace the existing file server with one more adaptable to a UNIX/TCP/IP environments. The requirements study for the network was the starting point for the requirements study for the new file server. The file server is called the Network Storage Service (NSS) and its requirements are described in this paper. The next section gives an application or functional description of the NSS. The final section adds performance, capacity, and access constraints to the requirements. DOE

N91-28779# Virginia Univ., Charlottesville. Inst. for Parallel Computation.
PERFORMANCE MEASUREMENT OF A PARALLEL INPUT/OUTPUT SYSTEM FOR THE INTEL IPSC/2 HYPERCUBE
J. C. French, T. W. Pratt, and M. Das 30 Jan. 1991 14 p Presented at the 1991 Association for Computing Machines (ACM) Sigmetrics Conference on Measurement and Modeling of Computer Systems, Charlottesville, May 1991
(Contract DE-FG05-88ER-25063)
(DE91-014219; IPC-TR-91-002; CONF-9105215-1) Avail: NTIS HC/MF A03

The Intel Concurrent File System (CFS) for the iPSC/2 hypercube is one of the first production file systems to utilize the declustering of large files across numbers of disks to improve I/O performance. The CFS also makes use of dedicated I/O nodes operating asynchronously, which provide file caching and prefetching. Processing of I/O requests is distributed between the computer node that initiates the request and the I/O nodes that service the request. The effects of the various design decisions in the Intel CFS are difficult to determine without measurements of an actual system. We present performance measurements of the CFS for a hypercube with 32 compute nodes and four I/W nodes (four disks). Measurement of read/write rates for one compute node to one I/O node, one compute node to multiple I/O nodes, and multiple compute nodes to multiple I/O nodes form the basis for the study. Additional measurements show the effects of different buffer sizes, caching, prefetching, and file preallocation on system performance. DOE

N91-28780# Oak Ridge National Lab., TN.
NETWORK BASED CONCURRENT COMPUTING ON THE PVM SYSTEM
G. A. Geist and V. S. Sunderam (Emory Univ., Atlanta, GA.) Jun.

1991 25 p
(Contract DE-AC05-84OR-21400)
(DE91-014961; ORNL/TM-11760) Avail: NTIS HC/MF A03

Concurrent computing environments based on loosely coupled networks have proven effective as resources for multiprocessing. Experiences with and enhancements to PVM (Parallel Virtual Machine) are described in this paper. PVM is a software package that allows the utilization of a heterogeneous network of parallel and serial computers as a single computational resource. This report also describes an interactive graphical interface to PVM, and porting and performance results from production applications. DOE

N91-28781# Lawrence Livermore National Lab., CA.
THE PCP/PFP PROGRAMMING MODELS ON THE BBN TC2000
E. D. Brooks, III, B. C. Gorda, and K. H. Warren Mar. 1991 9 p Presented at the 1st Inernational Conference of the Austrian Center for Parallel Computation, Salzburg (Austria), 30 Sep. - 2 Oct. 1991
(Contract W-7405-eng-48)
(DE91-011537; UCRL-JC-107019; CONF-9109137-1) Avail: NTIS HC/MF A02

The PCP/PFP programming models which are used on the BBN TC2000 are described. The parallel programming models are implemented in a portable manner and will be useful on the scalable shared memory machines expected in the future. The TC2000 machine architecture is then described which is a scalable general purpose parallel architecture capable of efficiently supporting both shared memory and message passing programming paradigms. A PCP implementation of the Gauss elimination algorithm which exploits the large local memories on the TC2000 is briefly described. DOE

N91-28782# Virginia Univ., Charlottesville.
CONCURRENT ACCESS TO O-TREES Ph.D. Thesis
L. D. Loyd May 1991 89 p
(Contract DE-FG05-88ER-25063)
(DE91-014348; DOE/ER-25063/T12) Avail: NTIS HC/MF A05

With the advent of parallel computing, issues of concurrent access to, and manipulation of, database index structures have become increasingly vital. In this thesis, we introduce a highly optimistic method for concurrent access to indices that involves no locking for searching, insertion, splitting, or simple deletion and minimal locking for merging. The method uses node version numbers to control the writing of nodes and depends heavily upon retry techniques. The index structure used is the O-tree, developed by Ratko Orlandic. We perform an analysis of the algorithm and the number of messages required to perform insertions using the locking algorithm of Lehman and Yao and the optimistic approach we present. The analysis shows a marked decrease in message traffic using our retry techniques for a reasonable number of processes inserting entries into the same tree. DOE

63 CYBERNETICS

Includes feedback and control theory, artificial intelligence, robotics and expert systems.

For related information see also *54 Man/System Technology and Life Support.*

N91-28783# Oak Ridge National Lab., TN.
CONTROL OF AUTONOMOUS MOBILE ROBOTS USING CUSTOM-DESIGNED QUALITATIVE REASONING VLSI CHIPS AND BOARDS
F. G. Pin and R. S. Pattay 1991 9 p Presented at the 9th Symposium on Energy Engineering Sciences, Argonne, 14-15 May 1991
(Contract DE-AC05-84OR-21400)
(DE91-012527; CONF-9105116-2) Avail: NTIS HC/MF A02

Two types of computer boards including custom-designed VLSI chips have been developed to provide a qualitative reasoning capability for the real-time control of autonomous mobile robots. The design and operation of these boards are described and an example of application of qualitative reasoning for the autonomous navigation of a mobile robot in a-priori unknown environments is presented. Results concerning consistency and modularity in the development of qualitative reasoning schemes as well as the general applicability of these techniques to robotic control domains are also discussed. DOE

N91-28784# Oak Ridge National Lab., TN.
PROPOSAL FOR CONTINUED BASIC RESEARCH IN INTELLIGENT MACHINES AT THE CENTER FOR ENGINEERING SYSTEMS ADVANCED RESEARCH: FISCAL YEARS 1992-1996
R. C. Mann, M. Beckerman, K. Fujimura, J. P. Jones, E. M. Oblow, F. G. Pin, and M. A. Unseren May 1991 120 p
(Contract DE-AC05-84OR-21400)
(DE91-012997; ORNL/TM-11810; CESAR-91/07) Avail: NTIS HC/MF A06

This proposal describes the context and technical direction during the next five years for the DOE/ER/BES-sponsored basic research program in intelligent machines at the Center for Engineering Systems Advanced Research (CESAR) at the Oak Ridge National Laboratory (ORNL). Research will address issues related to autonomous systems in unstructured dynamic work environments. Specifically, the work will focus on multiple cooperating robotic systems, combined mobility and manipulation, intelligent sensor systems, machine learning, and embedded high performance computing. Focus for proof-of-principle experiments demonstrating innovative development will be delivered from a number of application areas related to DOE missions. DOE

N91-28785*# National Aeronautics and Space Administration. Goddard Space Flight Center, Greenbelt, MD.
DRIVEN SHIELDING CAPACITIVE PROXIMITY SENSOR Patent Application
John M. Vranish, inventor (to NASA) and Robert L. McConnell, inventor (to NASA) 6 Jun. 1991 12 p
(NASA-Case-GSC-13377-1; NAS 1.71:GSC-13377-1; US-Patent-Appl-SN-710845) Avail: NTIS HC/MF A03 CSCL 09B

A capacitive proximity sensing element, backed by a reflector driven at the same voltage as and in phase with the sensor, is used to reflect the field lines away from a grounded robot arm towards an intruding object, thus dramatically increasing the senors's range and sensitivity. NASA

N91-28786# Pennsylvania State Univ., University Park.
A RECONFIGURABLE STRATEGY FOR DISTRIBUTED DIGITAL PROCESS CONTROL
H. E. Garcia, A. Ray, and Robert M. Edwards 1990 6 p Presented at the 6th Yale Workshop on Adaptive and Learning Systems, New Haven, 15-17 Aug. 1990
(Contract DE-FG07-89ER-12889)
(DE91-013740; CONF-9008209-1) Avail: NTIS HC/MF A02

A reconfigurable control scheme is proposed which, unlike a preprogrammed one, uses stochastic automata to learn the current operating status of the environment (i.e., the plant, controller, and communication network) by dynamically monitoring the system performance and then switching to the appropriate controller on the basis of these observations. The potential applicability of this reconfigurable control scheme to electric power plants is being investigated. The plant under consideration is the Experimental Breeder Reactor (EBR-II) at the Argonne National Laboratory site in Idaho. The distributed control system is emulated on a ring network where the individual subsystems are hosted as follows: (1) the reconfigurable control modules are located in one of the network modules called Multifunction Controller; (2) the learning modules are resident in a VAX 11/785 mainframe computer; and (3) a detailed model of the plant under control is executed in the same mainframe. This configuration is a true representation of the network-based control system in the sense that it operates in real time and is capable of interacting with the actual plant. DOE

64 NUMERICAL ANALYSIS

Includes iteration, difference equations, and numerical approximation.

N91-28787*# Illinois Univ., Chicago. Dept. of Mathematics, Statistics and Computer Science.
THE SYMBOLIC COMPUTATION AND AUTOMATIC ANALYSIS OF TRAJECTORIES Semiannual Status Report, 1 Jul. - 31 Dec. 1990
Robert Grossman Apr. 1991 55 p
(Grant NAG2-513)
(NASA-CR-188159; NAS 1.26:188159) Avail: NTIS HC/MF A04 CSCL 12A

Research was generally done on computation of trajectories of dynamical systems, especially control systems. Algorithms were further developed for rewriting expressions involving differential operators. The differential operators involved arise in the local analysis of nonlinear control systems. An initial design was completed of the system architecture for software to analyze nonlinear control systems using data base computing. For individual titles, see N91-28788 through N91-28790.

N91-28788*# Illinois Univ., Chicago. Dept. of Mathematics, Statistics, and Computer Science.
USING TREES TO COMPUTE APPROXIMATE SOLUTIONS TO ORDINARY DIFFERENTIAL EQUATIONS EXACTLY
Robert Grossman *In its* The Symbolic Computation and Automatic Analysis of Trajectories Apr. 1991 25 p (For primary document see N91-28787 20-64)
(LAC90-R24) Avail: NTIS HC/MF A04 CSCL 12A

Some recent work is reviewed which relates families of trees to symbolic algorithms for the exact computation of series which approximate solutions of ordinary differential equations. It turns out that the vector space whose basis is the set of finite, rooted trees carries a natural multiplication related to the composition of differential operators, making the space of trees an algebra. This algebraic structure can be exploited to yield a variety of algorithms for manipulating vector fields and the series and algebras they generate. Author

N91-28789*# Arizona State Univ., Tempe.
COMPUTATIONS INVOLVING DIFFERENTIAL OPERATORS AND THEIR ACTIONS ON FUNCTIONS
Peter E. Crouch, Robert Grossman, and Richard Larson (Illinois Univ., Chicago.) *In* Illinois Univ., The Symbolic Computation and Automatic Analysis of Trajectories Apr. 1991 12 p Submitted for publication (For primary document see N91-28787 20-64)
(Grants NSF INT-89-14643; NSF DMS-89-04740)
Avail: NTIS HC/MF A04 CSCL 12A

The algorithms derived by Grossmann and Larson (1989) are further developed for rewriting expressions involving differential operators. The differential operators involved arise in the local analysis of nonlinear dynamical systems. These algorithms are extended in two different directions: the algorithms are generalized so that they apply to differential operators on groups and the data structures and algorithms are developed to compute symbolically the action of differential operators on functions. Both of these generalizations are needed for applications. Author

N91-28790*# Illinois Univ., Chicago. Dept. of Mathematics, Statistics, and Computer Science.
BIALGEBRA DEFORMATIONS AND ALGEBRAS OF TREES
Robert Grossman and David Radford *In its* The Symbolic Computation and Automatic Analysis of Trajectories Apr. 1991 6 p Submitted for publication (For primary document see N91-28787 20-64)
(Grant NSF DMS-89-04740)
Avail: NTIS HC/MF A04 CSCL 12A

Let A denote a bialgebra over a field k and let A sub t = A((t)) denote the ring of formal power series with coefficients in A. Assume that A is also isomorphic to a free, associative algebra over k. A simple construction is given which makes A sub t a bialgebra deformation of A. In typical applications, A sub t is neither commutative nor cocommutative. In the terminology of Drinfeld, (1987), A sub t is a quantum group. This construction yields quantum groups associated with families of trees. Author

N91-28791# Naval Postgraduate School, Monterey, CA.
MULTIDIMENSIONAL SPECTRAL ESTIMATION USING ITERATIVE METHODS M.S. Thesis
Roderick C. Wester Jun. 1990 42 p
(AD-A237025) Avail: NTIS HC/MF A03 CSCL 12/3

The topic of multi-dimensional autoregressive (AR) spectral estimation is examined. An iterative algorithm for the solution of toeplitz block-toeplitz matrix equations is presented. This leads to a fast solution of the two dimensional normal equation compared with direct inversion of the autocorrelation matrix. The covariance method is used to estimate the autocorrelation function. Because the resulting matrix is not toeplitz block-toeplitz, a modified iterative algorithm is presented. Quarter-plane and nonsymmetric half-plane support are used, as well as combined quadrant averaging. Results of computer simulation show that in some cases a single iteration is sufficient to produce an acceptable spectral estimate. Because the AR parameters are estimated from previous values, this suggests the possibility to estimate spectral densities of slowly varying random processes. GRA

N91-28792# Stanford Linear Accelerator Center, CA.
A 2D FIELD SOLVER FOR PERIODIC STRUCTURES WITH SPECIAL CORNER ELEMENTS
E. Nelson May 1991 4 p Presented at the 1991 Institute of Electrical and Electronics Engineers (IEEE) Particle Accelerator Conference (PAC), San Francisco, 6-9 May 1991
(Contract DE-AC03-76SF-00515)
(DE91-012323; SU-SLAC-PUB-5532; CONF-910505-80) Avail: NTIS HC/MF A01

A 2d finite element field solver has been written which allows quasi-periodic boundary conditions, making it ideal for calculating traveling waves in periodic structures. Special elements are used at corners for improved accuracy. Comparisons with URMEL, URMEL-T, SUPERFISH and analytic solutions are made, showing that this code yields better eigenvalues than the URMELs despite the use of a coarser mesh. DOE

N91-28793# Argonne National Lab., IL. High Energy Physics Div.
QUANTIZED PLANES AND MULTIPARAMETER DEFORMATIONS OF HEISENBERG AND GL(N) ALGEBRAS
D. B. Fairlie (Durham Univ., England) and C. Zachos 1991 12 p Presented at the Miami North Atlantic Treaty Organization (NATO) ARW Conference on Quantum Field Theory, Statistical Mechanics, Quantum Groups and Topology, Coral Gables, 11 Jan. 1991
(Contract W-31-109-eng-38)
(DE91-012481; ANL-HEP-CP-91-28; DTP-91/19; CONF-9101101-1) Avail: NTIS HC/MF A03

The work is summarized on explicitly deforming classical oscillators to multiparameter quantum oscillators which do not commute with each other. These anyonic oscillators lead to the construction of a consistent quantum algebra GL(sub q)(N) with (N -1) (N -2)/2 independent parameters, some of whose features and applications are discussed. DOE

N91-28794# Superconducting Super Collider Lab., Dallas, TX.
ZLIB: A NUMERICAL LIBRARY FOR DIFFERENTIAL ALGEBRA (A USER'S GUIDE FOR VERSION 1.0)
Yiton Yan and Chiung-Ying Yan Dec. 1990 37 p
(Contract DE-AC02-89ER-40486)
(DE91-012552; SSCL-300) Avail: NTIS HC/MF A03

Given an efficient numerical method and a supercomputer, differential algebra can be a powerful tool for the study of accelerator physics. ZLIB, which has a style similar to the numerical library IMSL, was developed to offer efficient numerical routines on supercomputers for differential algebra. ZLIB uses dynamic memory and is both vectorized and parallelized (multi-tasked) besides being scalarly optimized. These are two sub-libraries in ZLIB, TPALIB and ZPLIB, with unique data structures for flexibility. The TPALIB is more flexible in dealing with a different number of variables, and therefore is more suitable for use in extracting maps. The ZPLIB is more flexible in dealing with a different number of orders, and therefore is more suitable for use in analyzing a map. Use of ZLIB in a scalar computer is also recommended. DOE

N91-28795# Edgerton, Germeshausen and Grier, Inc., Idaho Falls, ID.

A PARALLEL ALGORITHM FOR SOLVING LINEAR EQUATIONS ARISING FROM ONE-DIMENSIONAL NETWORK PROBLEMS

G. L. Mesina Jan. 1991 11 p Presented at the International Topical Meeting on Advances in Mathematics, Computation and Reactor Physics, Pittsburgh, 28 Apr. - 2 May 1991
(Contract DE-AC07-76ID-01570)
(DE91-012815; EGG-M-90383; CONF-910414-36) Avail: NTIS HC/MF A03

One-dimensional (1-D) network problems, such as those arising from 1- D fluid simulations and electrical circuitry, produce systems of sparse linear equations which are nearly tridiagonal and contain a few non-zero entries outside the tridiagonal. Most direct solution techniques for such problems either do not take advantage of the special structure of the matrix or do not fully utilize parallel computer architectures. A new parallel direct linear equation solution algorithm is described, called TRBR, which is especially designed to take advantage of this structure on MIMD shared memory machines. The new method belongs to a family of methods which split the coefficient matrix into the sum of a tridiagonal matrix T and a matrix comprised of the remaining coefficients R. Efficient tridiagonal methods are used to algebraically simplify the linear system. A smaller auxiliary subsystem is created and solved and its solution is used to calculate the solution of the original system. The newly devised BR method solves the subsystem. The serial and parallel operation counts are given for the new method and related earlier methods. TRBR is shown to have the smallest operation count in this class of direct methods. Numerical results are given. Although the algorithm is designed for 1-D networks, it was applied successfully to 3-D problems as well. DOE

N91-28796# Stanford Linear Accelerator Center, CA.

SYMPLECTIC FULL-TURN MAPS IN A FOURIER REPRESENTATION

J. S. Berg (Stanford Univ., CA.) and R. L. Warnock May 1991 3 p Presented at the 1991 Institute of Electrical and Electronics Engineers (IEEE) Particle Accelerator Conference (PAC), San Francisco, 6-9 May 1991
(Contract DE-AC03-76SF-00515)
(DE91-012912; SU-SLAC-PUB-5458; CONF-910505-94) Avail: NTIS HC/MF A01

We have developed a method that uses an arbitrary symplectic tracking code to generate an exactly symplectic full-turn or multi-turn map. The map is obtained from a generating function, which is a finite Fourier series in the final angle coordinates. The Fourier coefficients are represented as a B-spline series in the initial action coordinates. We achieve fast iteration of this implicitly defined map, and good accuracy. As a first application, we treat a simplified model of arcs of the superconducting super collider (SSC). DOE

N91-28797# Oak Ridge National Lab., TN.

PARALLELIZING ACROSS TIME WHEN SOLVING TIME-DEPENDENT PARTIAL DIFFERENTIAL EQUATIONS

P. H. Worley 1991 8 p Presented at the 5th Society for Industrial and Applied Mathematics (SIAM) Conference, Houston, 22-25 Mar. 1991
(Contract DE-AC05-84OR-21400)
(DE91-012948; CONF-910326-4) Avail: NTIS HC/MF A02

The standard numerical algorithms for solving time-dependent partial differential equations (PDE's) are inherently sequential in the time direction. This paper describes algorithms for the time-accurate solution of certain classes of linear hyperbolic and parabolic PDE's that can be parallelized in both time and space and have serial complexities that are proportional to the serial complexities of the best known algorithms. The algorithms for parabolic PDE's are variants of the waveform relaxation multigrid method (WFMG) of Lubich and Ostermann where the scalar ordinary differential equations (ODE's) that make up the kernel of WFMG are solved using a cyclic reduction type algorithm. The algorithms for hyperbolic PDE's use the cyclic reduction algorithm to solve ODE's along characteristics. DOE

N91-28798# Stanford Linear Accelerator Center, CA.

REFINEMENT OF THE HAMILTON-JACOBI SOLUTION USING A SECOND CANONICAL TRANSFORMATION

W. E. Gabella (Colorado Univ., Boulder.), R. D. Ruth, and R. L. Warnock May 1991 4 p Presented at the 1991 Institute of Electrical and Electronics Engineers (IEEE) Particle Accelerator Conference (PAC), San Francisco, 6-9 May 1991
(Contracts DE-AC03-76SF-00515; DE-FG02-86ER-40302)
(DE91-012965; SU-SLAC-PUB-5565; CONF-910505-104) Avail: NTIS HC/MF A01

Two canonical transformations are implemented to find approximate invariant surface for a nonlinear, time-periodic Hamiltonian. The first transformation is found from the non-perturbative, iterative solution of the Hamilton-Jacobi equation. The residual angle dependence remaining after performing the transformation is mostly eliminated by a second, perturbative transformation. This refinement can improve the accuracy, or the speed, of the invariant surface calculation. The motion of a single particle in one transverse dimension is studied in a storage ring example where strong sextupole magnets are the source of nonlinearity. The refined transformation to action-angle variables, and the corresponding invariant surface, can attain accuracy similar to that of a good non-perturbative transformation in half the computation time. DOE

N91-28799# Los Alamos National Lab., NM.

A NEW WAKE-POTENTIAL CALCULATION METHOD USING ORTHOGONAL POLYNOMIALS

Tai-Sen F. Wang and B. Zotter (European Organization for Nuclear Research, Geneva, Switzerland) 1991 4 p Presented at the 1991 Institute of Electrical and Electronics Engineers (IEEE) Particle Accelerator Conference (PAC), San Francisco, 6-9 May 1991
(Contract W-7405-eng-36)
(DE91-013045; LA-UR-91-1462; CONF-910505-107) Avail: NTIS HC/MF A01

A method is presented for calculating the wake potential of a bunched beam of arbitrary charge distribution, directly from the wake potential of a shorter bunch, by using orthogonal polynomial expansions. Combined with the table-look-up technique, this method leads to an effective computation scheme for repetitive evaluation of wake potentials of different charge distributions under the same boundary conditions. DOE

N91-28800# EG and G Mound Applied Technologies, Miamisburg, OH.

OPERATIONAL INTERPOLATION OF DATA IN TRIANGULAR ARRAY

G. L. Silver 13 May 1991 36 p
(Contract DE-AC04-88DP-43495)
(DE91-012987; MLM-3689) Avail: NTIS HC/MF A03

New equations are derived for the operational interpolation of four data in triangular array. The equations are alternatives to similar equations derived by the finite element method, but are often better predictors and sometimes yield more than one interpolating surface. A method is derived for representing four data in rectangular array by an equation containing sines and cosines or hyperbolic sines and cosines. DOE

N91-28801# International Centre for Theoretical Physics, Trieste (Italy).

TOWARDS THE EXACT NATURE OF A CERTAIN ERROR TERM

S. D. Adhikari Aug. 1990 10 p
(DE91-617574; IC-90/244) Avail: NTIS HC/MF A02

The average behavior of the arithmetic function (delta sub k), defined by: delta sub k n = max d epsilon N : d n,(d,k)=1), where k is a positive integer, has been investigated by several authors. Clearly it is enough to consider square-free k's. The earlier estimate is improved upon where lim sup (sub X yields infinity) E sub k (x)/x, where E sub k (x) is the error term. DOE

N91-28802# International Centre for Theoretical Physics, Trieste (Italy).

STABILITY THEORY OF CRITICAL CASES AND THE BIFURCATION POINTS OF THE STATIONARY SOLUTIONS OF THE LORENZ MODEL

A. A. Bakasov and B. B. Govorkov, Jr. (Joint Inst. for Nuclear Research, Moscow, USSR) Aug. 1990 23 p
(DE91-617575; IC-90/247) Avail: NTIS HC/MF A03

The critical case in stability theory is the case when it is impossible to study the stability of solutions over the linear part of ordinary differential equations. This situation is usual at the bifurcation points. There exists a powerful and constructive approach to investigate the stability: the theory of critical cases created by Lyapunov. The famous Lorenz model is used in this article as an illustration of the power of the method (new results). DOE

N91-28803# International Centre for Theoretical Physics, Trieste (Italy).

SPIN 4 AND 7/2 EXTENDED CONFORMAL ALGEBRA

De-Hai Zhang and Chao-Shang Huang (Academia Sinica, Beijing, China) Jul. 1990 8 p
(DE91-617609; IC-90/211) Avail: NTIS HC/MF A02

A new extended conformal algebra with the additional generators of spin 4 and 7/2 fields is given. The basic four point correlation functions and all structure constants are calculated. Entering of the spin 4 field into the expansion of the two spin 7/2 field operator product make this algebra to have an arbitrary value of the central charge. DOE

N91-28804# International Centre for Theoretical Physics, Trieste (Italy).

A CLUSTER APPROXIMATION FOR THE TRANSFER-MATRIX METHOD

A. Surda Aug. 1990 25 p
(DE91-617790; IC-90/253) Avail: NTIS HC/MF A03

A cluster approximation for the transfer-method is formulated. The calculation of the partition function of lattice models is transformed to a nonlinear mapping problem. The method yields the free energy, correlation functions, and the phase diagrams for a large class of lattice models. The high accuracy of the method is exemplified by the calculation of the critical temperature of the Ising model. DOE

N91-28805# Sandia National Labs., Albuquerque, NM.

EZEKIEL GRAPHS

G. J. Simmons 1991 13 p Presented at the 22nd Southeastern Conference on Combinatorics, Graph Theory and Computing, Baton Rouge, 11-15 Feb. 1991
(Contract DE-AC04-76DP-00789)
(DE91-012656; SAND-91-0217C; CONF-9102117-1) Avail: NTIS HC/MF A03

In spite of the old adage that no finite sequence of symbols is random, there are many instances in which it is desirable to quantify how random a finite sequence is. Pseudorandom number generators and cryptographic key generators typically expand a short, randomly chosen, seed sequence into a much longer sequence which should appear random to anyone ignorant of the seed. Unique initiating signals chosen to minimize the likelihood of an accidental initiation of an important action should be random to lessen the chance of their natural occurrence, etc. Consequently, numerous tests for the randomness of finite sequences have been proposed. John Milnor argued that if a binary sequence is random then the fraction of 1's, r sub 1, should be very nearly 1/2 in it and in all of what he called its derivatives. Since every sequence has a unique derivative this defines a natural family of digraphs, G sub n, on 2 sup n vertices in which vertices are labeled with n-bit binary sequences and an edge is directed from the vertex labeled with the sequence A to the vertex labeled with the sequence B if B is the derivative of A. Each component of G sub n is eventually cyclic. A special case is examined in which the sequences in a cycle are all cyclic shifts of a single sequence, hence the name of Ezekiel graphs. Surprising, there are Ezekiel graphs for which r sub 1 is as close to 1/2 as is numerically possible, i.e., that satisfy Milnor's test for randomness as closely as it can be satisfied, even though the sequence of sequences are about as far from random as is conceivable. The existence and properties of Ezekiel sequences are investigated from an algebraic standpoint. DOE

N91-28806*# Institute for Computer Applications in Science and Engineering, Hampton, VA.

MAPPING IMPLICIT SPECTRAL METHODS TO DISTRIBUTED MEMORY ARCHITECTURES Final Report

Andrea L. Overman (National Aeronautics and Space Administration. Langley Research Center, Hampton, VA.) and John VanRosendale Jun. 1991 10 p Submitted for publication
(Contract NAS1-18605)
(NASA-CR-187592; NAS 1.26:187592; ICASE-91-52) Avail: NTIS HC/MF A02 CSCL 12A

Spectral methods were proven invaluable in numerical simulation of PDEs (Partial Differential Equations), but the frequent global communication required raises a fundamental barrier to their use on highly parallel architectures. To explore this issue, a 3-D implicit spectral method was implemented on an Intel hypercube. Utilization of about 50 percent was achieved on a 32 node iPSC/860 hypercube, for a 64 x 64 x 64 Fourier-spectral grid; finer grids yield higher utilizations. Chebyshev-spectral grids are more problematic, since plane-relaxation based multigrid is required. However, by using a semicoarsening multigrid algorithm, and by relaxing all multigrid levels concurrently, relatively high utilizations were also achieved in this harder case. Author

N91-28807# California Univ., Berkeley. Lawrence Berkeley Lab.

INVARIANT METRICS FOR HAMILTONIAN SYSTEMS

G. Rangarajan, A. J. Dragt, and F. Neri (Los Alamos National Lab., NM.) May 1991 4 p Presented at the 1991 Institute of Electrical and Electronics Engineers (IEEE) Particle Accelerator Conference (PAC), San Francisco, 6-9 May 1991
(Contract DE-AC03-76SF-00098)
(DE91-014236; LBL-30705; CONF-910505-295) Avail: NTIS HC/MF A01

In this paper, invariant metrics are constructed for Hamiltonian systems. These metrics give rise to norms on the space of homogeneous polynomials of phase-space variables. For an accelerator lattice described by a Hamiltonian, these norms characterize the nonlinear content of the lattice. Therefore, the performance of the lattice can be improved by minimizing the norm as a function of parameters describing the beam-line elements in the lattice. A four-fold increase in the dynamic aperture of a model FODO cell is obtained using this procedure. DOE

N91-28808 Texas Univ., Austin.

REGULARIZATION OF THE LAGRANGE PLANETARY EQUATIONS FOR NUMERICAL USE Ph.D. Thesis

Daniel Edward Snow 1990 135 p
Avail: Univ. Microfilms Order No. DA9116981

A system of equations was developed which, for a certain dynamic system with a specific range of initial conditions, can be numerically integrated faster and more accurately than the cartesian state vector for the body of interest. It is shown that by using regularization in combination with Lagrange's Planetary Equations,

this goal can be accomplished. The analytic tools needed to regularize Lagrange's Planetary Equations are first developed with the realization that the equations will be numerically integrated. Two dynamical models (the Circular Restricted Three Body Problem and the Oblate Central Body Problem) are then studied for a satellite in an orbit with both high inclination and eccentricity. It is shown that both in dynamical models, the numerical integration of the newly developed equations is both faster and more accurate than integrations of the cartesian state of the satellite.
Dissert. Abstr.

N91-28931# Nagoya Univ. (Japan). Dept. of Physics.
POINT VORTEX DESCRIPTION OF A MODON SOLUTION
Chihiro Matsuoka and Kazuhiro Nozaki *In* National Inst. for Fusion Science, Proceedings of the Second International Toki Conference on Plasma Physics and Controlled Nuclear Fusion. Nonlinear Phenomena in Fusion Plasmas: Theory and Computer Simulation Apr. 1991 p 174-176 (For primary document see N91-28881 20-75)
Avail: NTIS HC/MF A11

65 STATISTICS AND PROBABILITY

Includes data sampling and smoothing; Monte Carlo method; and stochastic processes.

N91-28940# Princeton Univ., NJ. Plasma Physics Lab.
STATISTICAL MECHANICS USING SYMBOLIC DYNAMICS
Roscoe B. White and Alexander B. Rechester (Massachusetts Inst. of Tech., Cambridge.) *In* National Inst. for Fusion Science, Proceedings of the Second International Toki Conference on Plasma Physics and Controlled Nuclear Fusion. Nonlinear Phenomena in Fusion Plasmas: Theory and Computer Simulation Apr. 1991 p 204-207 (For primary document see N91-28881 20-75)
(Contract DE-AC02-76CH-03073)
Avail: NTIS HC/MF A11

66 SYSTEMS ANALYSIS

Includes mathematical modeling; network analysis; and operations research.

N91-28809# Los Alamos National Lab., NM.
DEFENDING THE DEFENDERS: BRILLIANT PEBBLE DEFENSE AGAINST POP-UP NEUTRAL PARTICLE BEAM SUPPRESSION ATTACKS
G. H. Canavan May 1991 12 p
(Contract W-7405-eng-36)
(DE91-012521; LA-11822-MS) Avail: NTIS HC/MF A03

Pop-up neutral particle beams (NPBs) can suppress brilliant pebbles. For attrition attacks, modest shielding should suffice, although the pebbles' survivability could be degraded. NPBs are difficult to negate once operational; it appears necessary to destroy them during ascent. Doing so effectively would require the prompt destruction of all heavy launches from missile launch areas.
DOE

N91-28810# Los Alamos National Lab., NM.
INTERCEPTOR COMBINATIONS FOR THEATER DEFENSE
G. H. Canavan May 1991 13 p
(Contract W-7405-eng-36)
(DE91-012990; LA-12069-MS) Avail: NTIS HC/MF A03

Simple models bound costs for ground- and space-based (GBI and SBI) theater defenses. GBIs are preferred for simultaneous attacks within a few theaters; SBIs are for drawn-out attacks within or between several theaters. For missiles of a given range, there is a relatively sharp transition from one type of interceptor to the other.
DOE

67 THEORETICAL MATHEMATICS

Includes topology and number theory.

No abstracts in this category.

70 PHYSICS (GENERAL)

For precision time and time interval (PTTI) see *35 Instrumentation and Photography;* for geophysics, astrophysics or solar physics see *46 Geophysics, 90 Astrophysics,* or *92 Solar Physics.*

N91-28811# Joint Publications Research Service, Arlington, VA.
JPRS REPORT: SCIENCE AND TECHNOLOGY. USSR: PHYSICS AND MATHEMATICS
14 Dec. 1990 40 p Transl. into ENGLISH from various Russian articles
(JPRS-UPM-90-006) Avail: NTIS HC/MF A03

This is a compilation of translated articles from Russian publications. The subject areas are as follows: Acoustics; Fluid Dynamics; Lasers; Nuclear Physics; Optics, Spectroscopy; Plasma Physics; Superconductivity; and Differential Equations. Some representative titles are: Shock wave pattern in transient glow discharge plasmas with ultraviolet basing; Spontaneous loss of scale invariance in fractal turbulence; Effect of heating on efficiency of excimer pumped pulsed dye lasers; Effect of carbon recrystallization in high pressure chamber on structure of synthesized diamond polycrystals; Efficiency of polarized phase conjugation in optical fiber crystal system; Charged particle acceleration by strong langmuir waves in nonuniform plasma flows; Model of self induced fluctuation superconductivity; and Spaces of linear differential equations and flag manifolds. E.R.

N91-28812# State Univ. of New York, Buffalo. Dept. of Chemistry.
EXACT SOLUTION OF A QUANTUM FORCED TIME-DEPENDENT HARMONIC OSCILLATOR
Kyu H. Yeon, Thomas F. George, and Chung I. Um Jun. 1991 21 p
(Contract N00014-90-J-1193)
(AD-A236633; UBUFFALO/DC/91/TR-51) Avail: NTIS HC/MF A03 CSCL 20/10

The Schrodinger equation is used to exactly evaluate the propagator, wave function, energy expectation values, uncertainty values and coherent state for a harmonic oscillator with a time dependent frequency and an external driving time dependent force. These quantities represent the solution of the classical equation of motion for the time dependent harmonic oscillator. GRA

N91-28813# European Organization for Nuclear Research, Geneva (Switzerland).
MIND OVER MATTER: THE INTELLECTUAL CONTENT OF EXPERIMENTAL PHYSICS
V. L. Telegdi (California Inst. of Tech., Pasadena.) 2 Nov. 1990 20 p
(DE91-617571; CERN-90-09) Avail: NTIS HC/MF A03

The author presents a new way of teaching experimental physics using Selenyi's experiment on dipole radiation, Michelson's optical demonstration of the earth rotation, the direct measurement of the helicity of the electron neutrino by Goldhaber, grodzins, and Sunyar and the determination of the helicity of the muonic neutrino by Grenas et al. DOE

N91-28814# Oak Ridge National Lab., TN.
LIGHT WEIGHT, HIGH FIELD, STABLE, SUPERCONDUCTING MAGNETS FOR ADVANCED TRANSPORTATION SYSTEMS
M. S. Lubell, L. Dresner, W. J. Kenney, J. W. Lue, J. N. Luton, and S. W. Schwenterly 1991 8 p Presented at the Technological Issues of Superconducting Maglev Transportation, Upton, 23-24

May 1991
(Contract DE-AC05-84OR-21400)
(DE91-013667; CONF-9105133-1) Avail: NTIS HC/MF A02

Although the Guideway may be the most expensive component of a MAGLEV system, the importance of a suitable magnet system should not be underestimated. The reliability of operation of MAGLEV depends on the superconducting magnets performing to their specifications in a reliable manner (i.e., without training or quenching). Besides reliability the magnets should produce high field, be sufficiently stable to withstand reasonable perturbations, be light weight, be protected in the event of a quench, and be economical (although performance should outweigh cost). We propose to develop superconducting magnets that have these features. Our magnet designs are based on internally cooled, cable-in-conduit superconductor with Polymer Matrix Composites (PMC) as the structural reinforcement. Although the initial work is with metallic superconductors such as NbTi, the processes being developed will be applicable to the High Temperature Ceramic Superconductors when they become suitable for magnet applications. DOE

N91-28815# Argonne National Lab., IL.
EFFECT OF GUIDEWAY DISCONTINUITIES ON MAGNETIC LEVITATION AND DRAG FORCES
T. D. Rossing, R. Korte (University of Northern Illinois, De Kalb.), and J. R. Hull 1991 13 p Presented at the 5th Joint Magnetism and Magnetic Materials (MMM/INTERMAG) Conference, Pittsburgh, 18-21 Jun. 1991
(Contract W-31-109-eng-38)
(DE91-014011; ANL/CP-71981; CONF-910608-5) Avail: NTIS HC/MF A03

Transients in the lift and drag forces on a NdFeB permanent magnet were observed as the magnet passed over various discontinuities in a rotating aluminum disk at velocities of 4 to 25 m/s. For full cuts in the disk, the amplitude of the lift and drag transients and the waveform of the drag transient depend on the width, and the amplitudes are much larger than for partial cuts. The use of a backing plate to join two cut segments is ineffective. DOE

71 ACOUSTICS

Includes sound generation, transmission and attenuation. For noise pollution see *45 Environmental Pollution.*

N91-28816# Pennsylvania State Univ., University Park. Applied Research Lab.
SOUND PROPAGATION IN THE ATMOSPHERE: ANALYSIS OF SIGNAL AMPLITUDE AND PHASE TEMPORAL AND SPATIAL VARIATIONS
S. R. Solomon and D. W. Thomson Jun. 1991 208 p
(Contract N00014-86-K-0688)
(AD-A237034; PSU/ARL-TR-91-007) Avail: NTIS HC/MF A10 CSCL 20/1

Temporal and spatial variations of the signal amplitude and phase were studied by use of a well developed atmospheric sound propagation prediction model. Modifications were made to this ray tracing model to incorporate the calculation of phase. Full documentation on the original and its modifications were provided. Two case studies were performed using actual meteorological data as input. The first study was representative of long distance (25 km) sound propagation in a mountainous region. The second was representative of sound propagation over much shorter distances (600 m) in a forest environment. The results of both signal amplitude and phase were displayed in a statistical format. This format was an aid to analyzing and explaining the temporal and spatial variabilities. GRA

N91-28817 Southampton Univ. (England).
A RECIPROCITY TECHNIQUE FOR THE CHARACTERISATION OF SOUND TRANSMISSION INTO AIRCRAFT FUSELAGES
Ph.D. Thesis
James Meredith Mason 1990 163 p
Avail: Univ. Microfilms Order No. BRDX92098

Experimental determination of the sound insulation of propfan aircraft fuselage structures is problematic. The use of full scale flight tests to study and optimize sidewall design is expensive, while the use of simplified excitation tests is questionable, due to the complicated nature of propeller sound fields and their interaction with the fuselage. The development and evaluation is described of a new experimental reciprocity technique for calibrating a fuselage as a transmitter of pressure acting on the external surface to the interior: it is based upon the use of a transducer which measures the volume velocity of the vibrating fuselage surface. The data generated may be combined with any impinging sound field to obtain a prediction of cabin sound pressure level. Interior noise predictions are obtained for plane wave excitation and a representation of propeller sound field excitation. The important features relating to correct representation of the excitation field and the fuselage structure are isolated, within the scope of the models evaluated. Also, a statistical perturbation technique is described which shows confidence in the predictions. Dissert. Abstr.

N91-28818 California Univ., Los Angeles.
QUADRUPOLE PHENOMENA OF NOISE FROM A SUBSONIC JET IMPINGING ON A LARGE, RIGID, AND FLATE PLATE
Ph.D. Thesis
Jianping Shen 1990 151 p
Avail: Univ. Microfilms Order No. DA9115281

The aerodynamic sound generated by a subsonic jet impinging on a large, rigid, and flat plate were studied. Cross correlation techniques were used to discriminate against unwanted noise. Correlation between the signals from the surface transducers on the plate and from the far field microphone were measured at different jet speeds, nozzle sizes, nozzle-to-plate distances and impinging angles. For each case, the microphone was placed at different locations around the jet, so that the directivity pattern was obtained. Those obtained by using correlation were compared with the patterns by using the microphone alone. The comparison showed that the correlation approach resulted in obviously quadrupole-like directivity patterns, while the overall microphone measurements revealed little information on directivity of the acoustic field. The correlation was also measured between hot-wire and far field microphone, and similar directivity patterns were obtained. Based on the experimental results, an exploratory physical model based on the coherent structure of turbulent flow was proposed to explain the mechanism of the quadrupole radiation caused by a turbulent source. Dissert. Abstr.

N91-28819 Purdue Univ., West Lafayette, IN.
REAL-TIME ADAPTIVE ACTIVE CONTROL OF SOUND FIELDS
Ph.D. Thesis
George Richard Batta 1990 189 p
Avail: Univ. Microfilms Order No. DA9116353

A general strategy is developed for the attenuation of sound in 3-D acoustic fields. This strategy includes a classification scheme for active noise control problems based on characterizations of the noise source, the acoustic field, the desired attenuation, and the control system. This classification scheme provides a framework for the analysis of active noise control problems. Both adaptive and non-adaptive active noise control algorithms are developed based on minimum variance feedback control theory. Dissert. Abstr.

72 ATOMIC AND MOLECULAR PHYSICS

Includes atomic structure, electron properties, and molecular spectra.

N91-28820# State Univ. of New York, Buffalo. Dept. of Chemistry.
PHASE-CONJUGATED FLUORESCENCE

Henk F. Arnoldus and Thomas F. George Jan. 1991 56 p
(Contract N00014-90-J-1193; NSF CHE-90-16789)
(AD-A231114; UBUFFALO/DC/91/TR-40) Avail: NTIS HC/MF A04 CSCL 20/5

Fluorescent emission by an atom near a phase conjugator (PC) based on four-wave mixing is studied from first principles. The Maxwell Heisenberg equations are solved for the radiation field, and with an asymptotic expansion an expression is derived for the field in the far zone. The total emitted power which can be measured by a detector in this region is evaluated, and it is found that this power acquires three distinct contributions. First, there are photons which are emitted by the atom directly towards the detector, and without any interaction with the medium. Second, there are photons that first travel towards the surface of the PC, and they have a certain probability of being reflected in the specular direction and towards the detector. The third kind of radiation consists of phase-conjugated photons, which are emitted independently of the previous ones. It is shown that the first two processes are a result of simple atomic spontaneous decay, but that the emission of a phase-conjugated fluorescent photon involves a three-photon process. The latter process has a probability proportional to the population of the atomic ground state. It is pointed out that an atom in its ground state polarizes the nonlinear medium of the PC, which subsequently can emit spontaneously two photons. An absorption-emission-absorption process by the atom then produces a fluorescent photon, together with a spontaneous excitation of the atom. GRA

N91-28821# Cornell Univ., Ithaca, NY. Dept. of Chemistry.
EVIDENCE OF VIBRATIONAL MODE-COUPLING IN 2-FLUORETHANOL VIA HIGH RESOLUTION INFRARED SPECTROSCOPY IN A MOLECULAR BEAM
Christopher L. Brummel, Steven W. Mork, and Laura A. Philips 29 May 1991 8 p
(Contract N00014-90-J-1971)
(AD-A236132; TR-1) Avail: NTIS HC/MF A02 CSCL 20/5

The rotationally resolved high resolution spectrum of 2-fluoroethanol in a molecular beam has been measured in an effort to determine the extent of mode-selective vibrational coupling. The high resolution spectrum of an asymmetric CH stretch clearly demonstrates that mode-coupling is present in 2-fluoroethanol. The extent of mode-coupling is significantly less than would be predicted based on previous work on molecules of a similar size and density of states. The small amount of mode-coupling in the CH stretch is consistent with the slow photoisomerization rate of 2-fluoroethanol upon excitation of the CH stretch, and is evidence that supports mode-selective vibrational coupling in the isomerization reaction of 2-fluoroethanol. GRA

N91-28822# Cornell Univ., Ithaca, NY. Dept. of Chemistry.
HIGH RESOLUTION INFRARED SPECTROSCOPY OF 2-FLUORETHANOL IN A MOLECULAR BEAM
Christopher L. Brummel, Steven W. Mork, and Laura A. Philips 29 May 1991 52 p
(Contract N00014-90-J-1971)
(AD-A236149; TR-2) Avail: NTIS HC/MF A04 CSCL 20/5

The high resolution infrared spectrum of 2-fluoroethanol (2FE) in a molecular beam was obtained in the region of 2990-2977/cm. This spectral region contains the asymmetric CH stretch of the fluorinated carbon. Excitation of the CH stretch has previously been observed to photochemically isomerize 2FE from the Gg' to the Tt conformation. The high resolution spectrum of this transition provides the information necessary to quantitatively evaluate the amount of vibrational mode-coupling between the asymmetric CH stretch and the torsional reactive coordinate. Minimal amounts of vibrational mode-coupling was observed in the spectrum which is consistent with the slow photoisomerization rate. The correlation of the amount of mode coupling and the isomerization rate supports the conclusion that mode selective vibrational coupling plays an important role in the photochemical dynamics. It is further suggested that the strong intramolecular attractive interactions limit the magnitude of the vibrational mode coupling. GRA

N91-28823# North Carolina Univ., Chapel Hill. Dept. of Computer Science.
THE 1992 - 1997 RENEWAL PROPOSAL INTERACTIVE GRAPHICS FOR MOLECULAR STUDIES Annual Progress Report No. 17
Frederick P. Brooks, Jr. and William V. Wright 24 Jan. 1991 37 p
(Contract N00014-86-K-0680)
(AD-A236598; TR91-020) Avail: NTIS HC/MF A03 CSCL 06/5

The UNC Resource develops forefront molecular graphics techniques and harnesses them into prototype research tools designed for biochemists studying macromolecules. The end objective is understanding the structure and function of proteins and nucleic acids, crucial to understanding disease and to designing drugs. The Resource is the only molecular graphics group composed chiefly of computer scientists, not chemists. As such, special capabilities and facilities are inherent. Close collaboration is experienced with biochemists and bridges are built between the disciplines. A trailblazer molecular graphics facility is maintained along with a top-performance hardware-software configuration, continually advancing the state of the art and testing the trailblazer against real users. Visiting chemists from everywhere are welcomed and they are helped in the use of the facility. Radical new molecular graphics ideas are generated into the prototype stage. Winning ideas are spun off to the thriving commercial industry or into autonomous research projects. Although commercial products cannot be developed and supported, each prototype is tested on users who come here; then it is distributed to interested users, it is documented, installed, bugs are fixed, and telephone support is provided. GRA

N91-28824# Lawrence Livermore National Lab., CA.
ENHANCING ATOM DENSITIES IN SOLID HYDROGEN BY ISOTOPIC SUBSTITUTION
G. W. Collins, P. C. Souers, E. R. Mapoles, and F. Magnotta 2 Apr. 1991 8 p Presented at the Air Force High Energy Density Materials Contractors Conference, Albuquerque, 24-27 Feb. 1991
(Contract W-7405-eng-48)
(DE91-011189; UCRL-JC-106508; CONF-9102109-2) Avail: NTIS HC/MF A02

Atomic hydrogen inside solid H2 increases the energy density by 200 MegaJoules/cu m, for each percent mole fraction stored. How many atoms can be stored in solid hydrogen? To answer this, we need to know: (1) how to produce and trap hydrogen atoms in solid hydrogen, (2) how to keep the atoms from recombining into the ground molecular state, and (3) how to measure the atom density in solid hydrogen. Each of these topics will be addressed in this paper. Hydrogen atoms can be trapped in solid hydrogen by co-condensing atoms and molecules, external irradiation of solid H2, or introducing a radioactive impurity inside the hydrogen lattice. Tritium, a heavy isotope of hydrogen, is easily condensed as a radioactive isotopic impurity in solid H2. Although tritium will probably not be used in future rockets, it provides a way of applying a large, homogeneous dose to solid hydrogen. In all of the data presented here, the atoms are produced by the decay of tritium and thus knowing how many atoms are produced from the tritium decay in the solid phase is important. DOE

N91-28825# Lawrence Livermore National Lab., CA.
SCANNING TRANSMISSION ION MICROSCOPY (STIM): A NEW TECHNIQUE FOR DENSITY MAPPING OF MICROSTRUCTURES
S. R. Sutton, M. Cholewa, G. Bench, A. Saint, G. J. F. Legge, D. Weirup, and G. J. Flynn Feb. 1991 4 p Presented at the Lunar and Planetary Science Conference, Houston, 18-22 Mar. 1991
(Contract W-7405-eng-48)
(DE91-011917; UCRL-JC-106553; CONF-9103134-4) Avail: NTIS HC/MF A01

The density of a cosmic dust particle is an important parameter in calculating the orbital evolution timescale and temperature profile on atmospheric deceleration. Sutton and Flynn inferred the densities of 12 stony micrometeorites from the stratospheric dust collection using synchrotron x-ray fluorescence. This method used irons mass determinations to infer the particle mass and optical microscope measurements to determine volumes. These results coupled with density measurements by others suggest that stony micrometeorite densities fall into two distinct density groups, with mean values of 0.6 and 1.9 g/cu cm. Such a bimodal distribution has dramatic implications for natural segregation of dust by gravitational resonances and interpretation of degree of heating in terms of proportions of asteroidal and cometary populations. The synchrotron-inferred densities have estimated uncertainties of +/-25 percent due largely to the difficulty in determining the volumes of these irregular objects. We are presently exploring the value of Scanning Transmission Ion Microscope (STIM) for directly mapping the density distribution in individual stratospheric particles and other micrometer-sized objects. In this approach, the energy loss experienced by protons as they traverse the specimen is used to produce 3-dimensional microtomographic images of the internal structure of objects. One of the key advantages of this technique is the ability to focus this charged particle beam to below 100 nm and thereby attain extremely high resolution tomographic images. DOE

N91-28826# Sandia National Labs., Albuquerque, NM.
PROGRESS IN LIGHT ION FUSION
D. L. Cook 1991 6 p Presented at the 1991 Institute of Electrical and Electronics Engineers (IEEE) Particle Accelerator Conference (PAC), San Francisco, 6-9 May 1991
(Contract DE-AC04-76DP-00789)
(DE91-012019; SAND-91-0102C; CONF-910505-56) Avail: NTIS HC/MF A02

Advances in ion beam theory, diagnostics, and experiments in the past two years have enabled efficient generation of intense proton beams on PBFA II, and focusing of the beam power to 5.4 TW/sq cm averaged over the surface of a 6-mm-diameter target. Improvements in the ion diode magnetic field uniformity and strength produced a proton beam with good azimuthal symmetry. The beam characteristics were diagnosed using conical targets in concert with inner-shell excitation x-ray cameras and ion pinhole cameras. Asymmetry was measured to be less than 15 percent, a level adequate for beginning ion deposition experiments. Initial studies of the beam/target interaction have begun with focused proton beams. Planar, conical, and cylindrical targets have been used in the experiments. These tests have provided information on ion beam power density, uniformity, and energy deposition. Substantial improvements in power density beyond the present level require a more magnetically stiff ion beam and lower ion divergence. Future applications of pulsed power based particle accelerators have been explored through conceptual studies. A conceptual design of a Laboratory Microfusion Facility driven by light ion beams has incorporated line induction voltage adding, transit-time ion bunching, pulse shaping, and long-distance transport. The Light Ion Beam Reactor Assessment (LIBRA) design effort has shown that a light ion driven energy producer can offer competitive electricity costs. DOE

N91-28827# Lawrence Livermore National Lab., CA.
SDI: STATISTICAL DYNAMIC INTERACTIONS
M. Blann, M. G. Mustafa, G. Peilert, H. Stoecker, and W. Greiner (Johann-Wolfgang-Goethe-Univ., Frankfurt am Main, Germany, F.R.) 1 Apr. 1991 10 p Presented at the 7th Adriatic International Conference on Nuclear Physics, Brioni (Yugoslavia), 27 May - 1 Jun. 1991
(Contract W-7405-eng-48)
(DE91-012034; UCRL-JC-106927; CONF-9105144-2) Avail: NTIS HC/MF A02

We focus on the combined statistical and dynamical aspects of heavy ion induced reactions. The overall picture is illustrated by considering the reaction Ar-36 + U-238 at a projectile energy of 35 MeV/nucleon. We illustrate the time dependent bound excitation energy due to the fusion/relaxation dynamics as calculated with the Boltzmann master equation. An estimate of the mass, charge and excitation of an equilibrated nucleus surviving the fast (dynamic) fusion-relaxation process is used as input into an evaporation calculation which includes 20 heavy fragment exit channels. The distribution of excitations between residue and clusters is explicitly calculated, as is the further deexcitation of clusters to bound nuclei. These results are compared with the exclusive cluster multiplicity measurements of Kim et al., and are found to give excellent agreement. We also consider an equilibrated residue system at 25 percent lower initial excitation, which gives an unsatisfactory exclusive multiplicity distribution. This illustrates that exclusive fragment multiplicity may provide a thermometer for system excitation. This analysis of data involves successive binary decay with no compressional effects nor phase transitions. Several examples of primary versus final (stable) cluster decay probabilities for an A = 100 nucleus at excitations of 100 to 800 MeV are presented. From these results a large change in multifragmentation patterns may be understood as a simple phase space consequence, invoking neither phase transitions, nor equation of state information. These results are used to illustrate physical quantities which are ambiguous to deduce from experimental fragment measurements. DOE

N91-28828# Stanford Linear Accelerator Center, CA.
HEAVY-QUARK PHYSICS IN QUANTUM CHROMODYNAMICS
S. J. Brodsky Apr. 1991 32 p Presented at the 6th Lake Louise Winter Institute (LLWI-6): Topical Workshop on Particle Physics - The Factory Era, Lake Louise (Canada), 17-22 Feb. 1991
(Contract DE-AC03-76SF-00515)
(DE91-012113; SU-SLAC-PUB-5529; CONF-910229-3) Avail: NTIS HC/MF A03

Heavy quarks can expose new symmetries and novel phenomena in QCD not apparent in ordinary hadronic systems. In these lectures I discuss the use of effective-Lagrangian and light-cone Fock methods to analyze exclusive heavy hadron decays such as (Upsilon) (yields) p(bar p) and B (yields) (pi)(pi), and also to derive effective Schroedinger and Dirac equations for heavy quark systems. Two contributions to the heavy quark structure functions of the proton and other light hadrons are identified: an extrinsic contribution associated with leading twist QCD evolution of the gluon distribution, and a higher twist intrinsic contribution due to the hardness of high-mass fluctuations of multi-gluon correlations in hadronic wavefunctions. A non-perturbative calculation of the heavy quark distribution of a meson in QCD in one space and one time is presented. The intrinsic higher twist contributions to the pion and proton structure functions can dominate the hadronic production of heavy quark systems at large longitudinal momentum fraction x(sub F) and give anomalous contributions to the quark structure functions of ordinary hadrons at large x(sub bj). I also discuss a number of ways in which heavy quark production in nuclear targets can test fundamental QCD phenomena and provide constraints on hadronic wavefunctions. The topics include color transparency, finite formation time, and predictions for charm production at threshold, including nuclear-bound quarkonium. I also discuss a number of QCD mechanisms for the suppression of J/(psi) and (Upsilon) production in nuclear collisions, including gluon shadowing, the peripheral excitation of intrinsic heavy quark components at large x(sub F), and the coalescence of heavy quarks with co-moving spectators at low x(sub F). DOE

N91-28829# Oak Ridge National Lab., TN.
MULTILEVEL RESONANCE ANALYSIS OF Co-59 NEUTRON TRANSMISSION MEASUREMENTS
G. deSaussure, N. M. Larson, J. A Harvey, and N. W. Hill May 1991 39 p
(Contract DE-AC05-84OR-21400)
(DE91-012135; ORNL/TM-11762) Avail: NTIS HC/MF A03

High-resolution neutron transmission measurements through several thicknesses of Co-59 were performed in 1986 at the Oak Ridge Electron Linear Accelerator (ORELA) in conjunction with the ENDF/B-VI evaluation of Co-59 done at Argonne National Laboratory. These measurements have much better energy resolution than previously published transmission measurements.

The results of one of the measurements were used in the ENDF/B-VI evaluation of the total cross section above 100 keV, but the data were not used below 100 keV, where the ENDF/B-VI cross sections are represented by resolved resonance parameters based on compilation. The ENDF/B-VI resolved resonance parameters were used to compute the transmission for the sample thicknesses used in the ORELA measurements, and large discrepancies were observed between these computations and the results of the measurements. Consequently, all six ORELA transmission measurements were analyzed, in the neutron energy range from 200 eV to 100 keV, using the multilevel R-matrix computer code SAMMY which utilizes Bayes' theorem for the fitting process. The spin J of most resonances and the orbital angular momentum (ell) for the smaller resonances cannot be determined from the data and were assigned somewhat arbitrarily so as to make the s-wave level density proportional to 2J + 1 and to satisfy the Dyson-Metha (Delta)(sub 3) statistics. Calculations with the resonance parameters obtained in the analysis reproduce well the results of the ORELA transmission measurements which were done at 80 m and 200 m with sample thicknesses varying from 0.005 to 0.3 atoms/barn. The transmission measurements are not very sensitive to the values of the resonance capture widths; therefore, the capture widths obtained in this analysis have large uncertainties. DOE

N91-28830# Tri-Univ. Meson Facility, Vancouver (British Columbia).

HIGH INTENSITY NEUTRINO BEAMS AT KAON

D. Frekers Mar. 1991 8 p
(DE91-012147; TRI-PP-91-3) Avail: NTIS HC/MF A02

A possible neutrino physics program at a KAON neutrino facility is discussed and an unconventional design for a high resolution neutrino detector based entirely on scintillating fibers is presented. DOE

N91-28831# Middle Tennessee State Univ., Murfreesboro.

NUCLEAR STRUCTURE STUDIES VIA NEUTRON INTERACTIONS

R. F. Carlton Mar. 1991 25 p
(Contract DE-FG05-86ER-40293)
(DE91-012165; DOE/ER-40293/5) Avail: NTIS HC/MF A03

Research preformed consisted of: (1) publication of an experimental paper for the n + Ar-40 high resolution total cross section and submission of a theoretical paper dealing with the prediction of the average parameters deduced from the the data; (2) preliminary R-matrix analysis of the neutron total cross section data for the n + Pb-208 systems, up to an energy of 1.7 MeV; (3) completed the analysis of neutron total cross section of data for n + Fe-54 up to energy of 500 keV, with j(exp pi) values confirmed, in most cases, by differential scattering data; (4) analysis of total cross section data for the n + Sr-88 system up to an energy of 175 keV; and (5) development of a graphical interface for the code RFUNC, used to calculate the differential scattering cross sections, for comparison with measurements. DOE

N91-28832# Oak Ridge National Lab., TN.

X RAY MICROIMAGING OF ELEMENTAL COMPOSITION AND MICROSTRUCTURE FOR MATERIALS SCIENCE

G. E. Ice and C. J. Sparks 1991 33 p Presented at the Applications of Photon-In Photon-Out Spectroscopy With Third-Generation Synchrotron Radiation Sources Meeting, Washington, 25 Apr. 1991
(Contract DE-AC05-84OR-21400)
(DE91-012221; CONF-9104248-1) Avail: NTIS HC/MF A03

X rays have many advantages over electrons and other charged particles for the microcharacterization of materials. X rays are more efficient in photoejecting inner shell electrons which results in characteristic x ray fluorescence. X rays also produce less Bremsstrahlung which yields far higher signal-to-background than is obtained with electrons. Minimum detectable limits (MDL) for x ray excited fluorescence can be a few parts per billion; 10(exp -3) to 10(exp -5) less than for electron excitation. The third generation synchrotron radiation sources such as the Advanced Photon Source will for the first time provide x ray sources as brilliant as the most advanced electron probes. It will therefore soon be possible to develop a submicron x ray probe with unprecedented low levels of detection in diffraction, EXAFS, Auger, Photoelectron and fluorescence spectroscopies for structural and chemical characterization. Some applications to materials science are shown. DOE

N91-28833# Texas Univ., Austin. Dept. of Chemistry.

ELECTRON TRANSFER REACTIONS IN MICROPOROUS SOLIDS

T. E. Mallouk May 1991 4 p
(Contract DE-FG05-87ER-13789)
(DE91-012299; DOE/ER-13789/4) Avail: NTIS HC/MF A01

We are studying the synthesis of light-induced electron transfer reactions which occur within microporous materials. Some highlights of our progress in the last year are in the fields of (1) electron transfer reactions of donor/acceptor molecules at the zeolite/solution interface; (2) photochemistry of zeolite/TiO2 composites; and (3) photochemistry of layered oxide semiconductors. DOE

N91-28834# Stanford Linear Accelerator Center, CA.

SIMULATIONS ON PAIR CREATION FROM BEAM-BEAM INTERACTION IN LINEAR COLLIDERS

P. Chen, T. Tauchi, and K. Yokoya (National Lab. for High Energy Physics, Oho, Japan) May 1991 4 p Presented at the 1991 Institute of Electrical and Electronics Engineers (IEEE) Particle Accelerator Conference (PAC), San Francisco, 6-9 May 1991
(Contract DE-AC03-76SF-00515)
(DE91-012315; SU-SLAC-PUB-5557; CONF-910505-88) Avail: NTIS HC/MF A01

It has been recognized that e(sup +)e(sup minus) pair creation during the collision of intense beams in linear colliders will cause potential background problems for high energy experiments. Detailed knowledge of the angular-momentum spectrum of these low energy pairs is essential to the design of the interaction region. In this paper, we modify the computer code ABEL (Analysis of Beam-beam Effects in Linear colliders) to include the pair creation processes, using the equivalent photon approximation. Special care has been taken on the non-local nature of the virtual photon exchanges. The simulation results are then compared with known analytic formulas, and applied to the next generation colliders such as JLC. DOE

N91-28835# Oak Ridge National Lab., TN.

FIXED-WAVELENGTH R2PI/TANDEM MASS SPECTROMETRY FOR MIXTURE ANALYSIS IN THE QUADRUPOLE ION TRAP

D. E. Goeringer, G. L. Glish, and S. A. McLuckey 1991 3 p Presented at the American Society for Mass Spectrometry (ASMS) Meeting, Nashville, 19-24 May 1991
(Contract DE-AC05-84OR-21400)
(DE91-012506; CONF-9105181-2) Avail: NTIS HC/MF A01

Many aromatic molecules have strong absorption bands in the UV which are rather broad at room temperature; the ionization potentials for many such polyatomics are also often less than 9 eV. Therefore, they can be ionized with high efficiency by resonance enhanced two-photon ionization (R2PI) using the frequency-quadrupled output of the Nd:YAG laser at 266 nm (4.7 eV). Because the degree of fragmentation accompanying R2PI is a function of laser power, mass spectrometric analysis of such fragments also can often improve the specificity of the overall analysis. However, in the case of organic mixture analysis, the complexity of R2PI/fragmentation mass spectra may compromise compound identification tandem mass spectrometry (MS/MS) can also enhance the specificity of analysis over that provided by a single stage of mass spectrometry. Although R2PI/fragmentation and MS/MS can yield complementary data, situations may often occur in which the spectra reveal no unique structural information. Nevertheless, the combination of R2PI and MS/MS can still provide an advantage over the use of R2PI alone. DOE

N91-28836# Oak Ridge National Lab., TN.

SPONTANEOUS CLUSTER DECOMPOSITION IN A QUADRUPOLE ION TRAP

K. G. Asano, S. A. McLuckey, G. L. Glish, and J. E. Bartmess (Tennessee Univ., Knoxville.) 1991 3 p Presented at the American Society for Mass Spectrometry (ASMS) Meeting, Nashville, 19-24 May 1991
(Contract DE-AC05-84OR-21400)
(DE91-012519; CONF-9105181-4-Extd-Abst) Avail: NTIS HC/MF A01

Cluster ions normally found in high pressure ion sources are not usually observed under chemical ionization conditions in the quadrupole ion trap. This is mainly due to the lower pressures in the ion trap which affect third body stabilization. But, even for cluster ions injected from an external source, decomposition is observed. By injecting cluster ions of known stability and measuring the decomposition rate as a function of pressure and time, we can determine what affects various parameters have on the internal ion temperatures in the quadrupole ion trap. The desolvation experiments were carried out by injecting ions formed via electrospray into the quadrupole ion trap. The atmospheric sampling glow discharge ionization (ASGDI) source served as the interface between atmosphere and the vacuum chamber. Protonated water clusters were formed by spraying distilled water at a flow rate of 1 microL/min and protonated methanol clusters were formed by spraying HPLC grade methanol at 1 microL/min. Since fragmentation of ions upon injection into an ion trap has been observed in the lab as well as others, there was a need to determine if ions are excited during injection. Therefore, the cluster ion mass spectra from the ion trap was compared to the cluster ion mass spectra from a quadrupole mass filter using the same interface and electrospray conditions. The results showed that, under the ion injection conditions used in this study for both the water and methanol clusters, significant internal excitation did not occur during injection. The clusters, therefore, acquired the necessary energy for dissociation after they were trapped. DOE

N91-28837# Oak Ridge National Lab., TN.

SCINTILLATION DETECTOR EFFICIENCIES FOR NEUTRONS IN THE ENERGY REGION ABOVE 20 MeV

J. K. Dickens 1991 12 p Presented at the Specialists' Meeting on Neutron Cross Section Standards for the Energy Region Above 20 MeV, Uppsala, Sweden, 21-23 May 1991
(Contract DE-AC05-84OR-21400)
(DE91-012544; CONF-9105190-1) Avail: NTIS HC/MF A03

The computer program SCINFUL (for SCINtillator FUL1 response) is a program designed to provide a calculated complete pulse-height response anticipated for neutrons being detected by either an NE-213 (liquid) scintillator or an NE-110 (solid) scintillator in the shape of a right circular cylinder. The point neutron source may be placed at any location with respect to the detector, even inside of it. The neutron source may be monoenergetic, or Maxwellian distributed, or distributed between chosen lower and upper bounds. The calculational method uses Monte Carlo techniques, and it is relativistically correct. Extensive comparisons with a variety of experimental data were made. There is generally overall good agreement (less than 10 pct. differences) of results for SCINFUL calculations with measured integral detector efficiencies for the design incident neutron energy range of 0.1 to 80 MeV. Calculations of differential detector responses, i.e., yield versus response pulse height, are generally within about 5 pct. on the average for incident neutron energies between 16 and 50 MeV and for the upper 70 pct. of the response pulse height. For incident neutron energies between 50 and 80 MeV, the calculated shape of the response agrees with measurements, but the calculations tend to underpredict the absolute values of the measured responses. Extension of the program to compute responses for incident neutron energies greater than 80 MeV will require new experimental data on neutron interactions with carbon. DOE

N91-28838# California State Univ., Northridge. Dept. of Physics and Astronomy.

THEORETICAL RESEARCH IN INTERMEDIATE-ENERGY NUCLEAR PHYSICS

R. Seki 1991 10 p
(Contract DE-FG03-87ER-40347)
(DE91-012720; DOE/ER-40347/T1) Avail: NTIS HC/MF A02

The following six problems are discussed: (1) final state interactions in (electron, electron-proton) at high momentum transfer; (2) a numerical calculation of skyrmion-antiskyrmion annihilation; (3) pion-nucleus interactions above 0.5 GeV/c; (4) pionic atom anomaly; (5) baryon interactions in Skyrme model; and (6) large N(sub c) quantum hydrodynamics. The problems deal with various topics in intermediate energy nuclear physics. DOE

N91-28839# Akron Univ., OH. Dept. of Chemistry.

MOLECULAR EIGENSTATE SPECTROSCOPY: APPLICATION TO THE INTRAMOLECULAR DYNAMICS OF SOME POLYATOMIC MOLECULES IN THE 3000 TO 7000 cm(EXP -1) REGION

D. S. Perry May 1991 8 p
(Contract DE-FG02-90ER-14151)
(DE91-013154; DOE/ER-14151/1) Avail: NTIS HC/MF A02

This project uses high resolution infrared spectroscopy to probe the mechanism of intramolecular vibrational redistribution (IVR) in isolated polyatomic molecules. We have found only vibrationally anharmonic coupling in the C-H stretch region of 1-butyne but rotationally mediated coupling is evident in similar spectra of ethanol. The keyhole model of IVR was developed to account for the similarities and differences between these molecules. The concepts of the model are being implemented numerically in random matrix calculations. A second F-center laser has been purchased and is now being set up to develop an infrared double resonance technique which can be applied to this problem. DOE

N91-28840# Oak Ridge National Lab., TN.

CORRECTING CHANNELING AND DIFFRACTION EFFECTS IN QUANTITATIVE REELS SURFACE MICROANALYSIS

Z. L. Wang and J. Bentley (Tennessee Univ., Knoxville.) 1991 2 p Presented at the 49th Electron Microscopy Society of America (EMSA) Annual Meeting, San Jose, 4-9 Aug. 1991
(Contract DE-AC05-84OR-21400)
(DE91-009924; CONF-910870-3) Avail: NTIS HC/MF A01

Channeling conditions or resonance conditions have to be satisfied in order to enhance image contrast in reflection electron microscopy (REM) and the signal-to-background ratio in reflection electron energy-loss spectroscopy (REELS). The introduction of the channeling and diffraction effects can complicate surface microanalysis. In REELS, the elastic Bragg reflections and core-shell inelastic scattering may not be independent events; thus, it is necessary to measure their combined effects experimentally. A practical method is described. DOE

N91-28841# Sandia National Labs., Albuquerque, NM.

X RAY SPATIAL RESOLUTION AT INTERMEDIATE VOLTAGES: AN ASSESSMENT BY MASSIVELY PARALLEL MONTE CARLO ELECTRON TRAJECTORY SIMULATION

A. D. Romig, Jr., J. R. Michael, and J. I. Goldstein 1991 24 p Presented at the 25th Annual Microbeam Analysis Society Meeting, San Jose, CA, 4-9 Aug. 1991
(Contract DE-AC04-76DP-00789)
(DE91-012018; SAND-90-0740C; CONF-910870-14; CONF-910872-6) Avail: NTIS HC/MF A03

The best approach to the characterization of spatial resolution under various conditions is through the use of massively parallel Monte Carlo electron trajectory simulation. The spatial resolution is systematically studied in multiphase materials at intermediate voltages as a function of beam size, specimen thickness and electron beam energy by massively parallel Monte Carlo electron trajectory simulation. To provide a baseline for comparison, electron scattering in single phase homogeneous specimens was also examined. Electron scattering in single phase specimens and the fundamental definition of spatial resolution is discussed in more detail in the paper by Williams, et. al. DOE

N91-28842# British Columbia Univ., Vancouver. TRIUMF Facility.
MEASUREMENTS OF ANGULAR DISTRIBUTIONS OF ABSOLUTE CROSS SECTIONS AND ANALYZING POWERS OF THE REACTION BAR-P P YIELDS D(PI+) BETWEEN 1.3 AND 2.4 GeV
J. Yonnet, M. Boivin, A. Boudard, G. Bruge, P. Couvert, M. Garcon, C. Kerboul, B. Mayer, and R. Abegg Dec. 1990 4 p Presented at the 7th International Conference on Polarization Phenomena in Nuclear Physics, Paris, France, 9-13 Jul. 1990
(DE91-012638; TRI-PP-90-88; LNS/Ph-90-21; CONF-900726-6)
Avail: NTIS HC/MF A01

We have measured angular distributions of absolute cross sections, analyzing powers and the spin transfer parameters K(sub nn) of the reaction bar-p p yields d(pi+) at 6 incident proton energies between 1.3 and 2.4 GeV. In a first phase the data were analyzed to obtain angular distributions of absolute cross sections and analyzing powers A(sub yo). Distributions of A(sub yo) where the Mandelstam parameters t or u are equal to zero or the angle theta(sub pi)(c.m.) equals 90 deg as a function of square root of s confirm the resonance like behavior suggested by an earlier experiment. For the first time deviations from a smooth behavior are also found in the square root of s distribution (at t = 0) of the absolute cross section. DOE

N91-28843# Ames Lab., IA.
NUCLEAR MAGNETIC RESONANCE STUDIES OF ATOMIC MOTION IN LITHIUM CHLOROBORATE AND LITHIUM THIOSILICATE GLASSY FAST IONIC CONDUCTORS Ph.D. Thesis
M. Trunnell 14 May 1991 81 p
(Contract W-7405-eng-82)
(DE91-012677; IS-T-1525) Avail: NTIS HC/MF A05

The NMR spectra and T(sub 1) measurements on both the stationary B-11 in the lithium chloroborate glass and on the mobile Li-7 in both the lithium chloroborate and lithium thiosilicate glasses have yielded much useful information about the static and dynamic properties of these two glassy fast ionic conductors. The B-11 spectra for the B2O3 + 0.7Li2O + XLiCl glasses indicates that the boron nuclei sit in two different sites. The narrow central line is due to the B-11 nuclei that are in the BO4 sites where there is no EFG and therefore no electric quadrupole effects and no splitting of the line. The broader pattern consisting of the two side peaks is a result of the B-11 nuclei that sit in the BO3 sites. In these sites, the magnitude of the EFG tenser is large and second order splitting of the central transition is seen. These side peaks are smaller since they are due to essentially the same number of boron nuclei but the pattern is spread over a much larger range of frequencies. If a baseline for these spectra could be determined, the ratio of BO3 to BO4 could then be found. Nuclear spin lattice relaxation measurements of the B-11 nuclei show no dependence on the measuring frequency. Because of this, the theory proposed by Rubinstein and Resing which uses an adaptation of the Van Kronendonk theory and uses a two phonon Raman process for the relaxation is favored. Spin lattice relaxation measurements of the Li-7 nuclei do show the frequency dependence that one expects from the nuclei that are free to diffuse through the glass matrix. DOE

N91-28844# California Univ., Berkeley. Lawrence Berkeley Lab.
THE ADVANCED LIGHT SOURCE: A NEW TOOL FOR RESEARCH IN ATOMIC AND MOLECULAR PHYSICS
F. Schlachter and A. Robinson Apr. 1991 23 p Presented at the 3rd US/Mexico Atomic and Molecular Physics Workshop, Mexico City, Mexico, 13-16 Mar. 1991
(Contract DE-AC03-76SF-00098)
(DE91-012860; LBL-30582; CONF-9103146-3) Avail: NTIS HC/MF A03

The Advanced Light Source at the Lawrence Berkeley Laboratory will be the world's brightest synchrotron radiation source in the extreme ultraviolet and soft x-ray regions of the spectrum when it begins operation in 1993. It will be available as a national user facility to researchers in a broad range of disciplines, including materials science, atomic and molecular physics, chemistry, biology, imaging, and technology. The high brightness of the ALS will be particularly well suited to high-resolution studies of tenuous targets, such as excited atoms, ions, and clusters. DOE

N91-28845# Arizona Univ., Tucson. Dept. of Physics.
DYNAMICAL BEHAVIOR OF EXCITED HADRONIC MATTER
P. Carruthers and I. Sarcevic Jan. 1991 10 p
(Contract DE-FG02-88ER-40456)
(DE91-013024; DOE/ER-40456/8) Avail: NTIS HC/MF A02

Hadronic multiplicity moments referred to phase space rapidity bins of variable size give important information on the underlying correlations in the multiparticle production mechanisms for hadronic and nuclear collisions. Ordinary factorial moments given by integrals of density correlations contain background contributions that can be removed by expanding in cumulants. This expansion has a simple exact form even in the absence of rapidity translation invariance when the bin averages are done locally. These idenities were used to extract second through fifth order correlation from various reactions. The behavior of the second bin-averaged factorial moment is and must be in agreement with the identity relating it to the empirical two particle correlation function. Higher order moments were successfully explained by the linked pair approximation that expresses higher cumulant correlations as products of the two particle correlation function. Remarkably, the undetermined coefficients in this approach turn out to closely approximate those needed to give the negative binomial distribution, the latter successfully describing hadron counts in rapidity bins of arbitrary size. At collider energy, higher order cumulant correlations can be extracted, which agree well with the linked pair approximation that was introduced last year. Quantitative analysis of theses and other data show saturation of the moments for small bin size rather than scaling intermittent behavior. DOE

N91-28846# Sandia National Labs., Albuquerque, NM.
MOLECULAR DYNAMICS SIMULATIONS OF BULK DISPLACEMENT THRESHOLD ENERGIES IN Si
L. A. Miller, D. K. Brice, S. T. Picraux, and A. K. Prinja (New Mexico Univ., Albuquerque.) 1991 4 p Presented at the International Energy Agency (IEA) Workshop on the Use of Molecular Dynamics in Modeling Radiation Effects and Other Non-Equilibrium Phenomena, La Jolla, 6-8 May 1991
(Contract DE-AC04-76DP-00789)
(DE91-011957; SAND-91-0999C; CONF-9105172-1) Avail: NTIS HC/MF A01

The energetics of bulk and surface displacement defects in silicon and the effect of low energy ion bombardment on Si(100) surfaces were studied. The phase of work discussed was the characterization of the anisotropic bulk displacement threshold energy. The results of the calculations for the bulk displacement threshold energies for the different directions are 11.4 eV, 18.3 eV, 10.1 eV, and 12.5 eV for directions group or zone axes (111), (0.7041 0.7041 0.0915), (100), and (0.9397 0.2418 0.2418), respectively. These values were determined to 0.1 eV by the molecular dynamics calculations. These bulk displacement threshold energies were used to determine the average bulk displacement threshold energy about the group of zone axes (111) and (100) for angles of 30 and 20 deg, respectively, using the theoretical model outlines above. This resulted in an average bulk displacement energy through the open face of 14.8 eV in the group of zone axes (111) and 11.1 eV in the group of zone axes (100). These values are estimated to be accurate to approximately 15 percent. DOE

N91-28847# Oak Ridge National Lab., TN.
DEVELOPMENT OF NANOVOLT-RESOLUTION X RAY DIFFRACTION USING RESONANT NUCLEAR SCATTERING
B. C. Larson, J. Z. Tischler, G. E. Ice, and P. Zschack May

1991 10 p Presented at the 4th Users Meeting for the Advanced Photon Source, Argonne, 7-8 May 1991
(Contract DE-AC05-84OR-21400)
(DE91-012217; CONF-9105180-1) Avail: NTIS HC/MF A02

The aspects needed for performing nanovolt-resolution scattering spectroscopy using resonant nuclear monochromators are available, and resonant beams with sufficient fluxes for selected experiments can be obtained using wiggler beam lines. However, the availability of undulators on high energy synchrotrons will be critical to full development of this technique. DOE

N91-28848# Ohio State Univ., Columbus. Research Foundation.
STRONGLY INTERACTING FERMION SYSTEMS
J. W. Wilkins 1991 14 p
(Contract DE-FG02-88ER-45347)
(DE91-012284; DOE/ER-45347/31) Avail: NTIS HC/MF A03

Research has been concentrated primarily in three areas: aspects of high temperature superconductor systems, electronic structure, and other strongly interacting systems. In high-temperature superconductors the three major developments were: (1) a mean-field treatment of the very popular t-J model that provided the first uniform exhibition of four different possible ground states, whose diversity poses serious challenges for more exact approaches; (2) a variational wavefunction was constructed for the t(sup i)-J model (a cousin of the t-J model) which has lower ground state energies than more exotic proposed grounds states with broken time-reversal symmetry, thus diluting the interest of the high-energy theorists in high-temperature superconductivity; and (3) the de Haas-van Alphen oscillations of the so-called marginal Fermi liquid have been computed for the first time. In the electronic structure program we note first, the work of John Mintmire, on polymer systems, especially chiral polymers such as polyethylene. Second, the most striking features of a calculation of the linear polarizability of rare-gas atoms are that good agreement for the frequency-dependent polarization is achieved by adjusting the gap between the occupied and unoccupied states to get the correct static polarizability, and that adding a few basis functions to the basis set already optimized for the total energy improves the convergence of the polarizability by three orders of magnitude. We review the understanding of the recently observed Shapiro steps in Josephson junction arrays which was achieved by uniting the dynamics of the two subsystems -- the flux lattice and the junction array -- to provide a global explanation which has a topological interpretation, thus suggesting wider applicability. DOE

N91-28849# Los Alamos National Lab., NM.
ANTIPROTON-INDUCED ELASTIC AND INELASTIC SCATTERING AT INTERMEDIATE ENERGIES
W. H. Ma and D. D. Strottman 1991 4 p Presented at the 4th Conference on the Intersections Between Particle and Nuclear Physics, Tucson, 23-29 May 1991
(Contract W-7405-eng-36)
(DE91-013068; LA-UR-91-1448; CONF-9105106-3) Avail: NTIS HC/MF A01

With the construction and subsequent operation of LEAR, beams of low-energy antiproton with previously unobtainable intensity and quality were possible. Elastic and inelastic scattering experiments were performed on several nuclei in both the p- and sd-shell as well as targets of heavier mass. In the very near future experiments with antiproton having momentum of up to 2 Gev/c will be possible. It is the purpose of this brief article to report results of initial calculations of (anti p)-nucleus scattering for energies that span this new energy region and for which the elementary (anti p)N amplitudes are known. DOE

N91-28850# Oak Ridge National Lab., TN.
KINETIC ENERGY DISTRIBUTIONS OF IONS AFTER SURFACE COLLISIONS Abstract Only
R. T. Short, P. J. Todd, and C. C. Grimm 1991 2 p Presented at the American Society for Mass Spectrometry (ASMS) Meeting, Nashville, 19-24 May 1991
(Contract DE-AC05-84OR-21400)
(DE91-013412; CONF-9105181-11-Extd-Abst) Avail: NTIS HC/MF A01

As a part of the development of an organic ion microprobe, to be used for imaging of particular organic compounds in biological tissue, various methods of quadrupole-based tandem mass spectroscopy (MS/MS) have been investigated. High transmission efficiency is essential for the success of the organic ion microprobe, due to expected low analyte concentrations in biological tissue and the potential for sample damage from prolonged exposure to the primary ion beam. MS/MS is necessary for organic ion imaging because of the complex nature of the biological matrices. The goal of these studies of was to optimize the efficiency of daughter ion production and transmission by first determining daughter ion properties and then designing ion optics based on those properties. The properties of main interest are daughter ion kinetic energy and angular distribution. DOE

N91-28851# Oak Ridge National Lab., TN.
REFLECTION-ASYMMETRIC SHAPES IN ATOMIC NUCLEI
W. Nazarewicz 1991 21 p Presented at the Nuclear Shapes and Nuclear Structure At Low Excitation Energies, Cargese (France), 3-7 Jun. 1991
(Contract DE-AC05-84OR-21400)
(DE91-013414; CONF-9106196-1) Avail: NTIS HC/MF A03

Can atomic nuclei be unstable with respect to deformations that break intrinsic parity? On the theoretical side calculations indicate the existence of stable octupole deformations. There is also vast supporting experimental evidence for the presence of very collective low-energy dipole and octupole modes. In this contribution, recent advances in the physics of nuclear reflection-asymmetric shapes are discussed in terms of underlying shell effects. Particular attention is given to the recently predicted octupole excitations at superdeformed shapes. DOE

N91-28852# Oak Ridge National Lab., TN.
DESORPTION OF LARGE ORGANIC MOLECULES BY LASER-INDUCED PLASMON EXCITATION
I. Lee, T. A. Callcott (Tennessee Univ., Knoxville.), and E. T. Arakawa 1991 4 p Presented at the HASRD Workshop on Laser Ablation: Mechanisms and Application, Oak Ridge, 8-10 Apr. 1991
(Contract DE-AC05-84OR-21400)
(DE91-013415; CONF-9104192-7) Avail: NTIS HC/MF A01

Ejection of large organic molecules from surfaces by laser-induced electronic-excited desorption has attracted considerable interest in recent years. In addition to the importance of this effect for fundamental investigations of the ejection process, this desorption technique has been applied to the study of large, fragile molecules by mass spectrometry. In this paper, we present a new method to induce electronic excitation on the metal surface for the desorption of large organic molecules. DOE

N91-28853# Oak Ridge National Lab., TN. Joint Inst. for Heavy Ion Research.
SHELL MODEL CALCULATIONS AT SUPERDEFORMED SHAPES
W. Nazarewicz, J. Dobaczewski, and P. VanIsacker (Daresbury Nuclear Physics Lab., England) 1991 23 p Presented at the Workshop on Future Directions in Nuclear Physics With 4(pi) Gamma Detection Systems of the New Generation, Strasbourg (France), 4-16 Mar. 1991
(Contract DE-FG05-87ER-40361)
(DE91-012954; CONF-9103176-1) Avail: NTIS HC/MF A03

Spectroscopy of superdeformed nuclear states opens up an exciting possibility to probe new properties of the nuclear mean field. In particular, the unusually deformed atomic nucleus can serve as a microscopic laboratory of quantum mechanical symmetries of a 3-D harmonic oscillator. The classifications and coupling schemes characteristic of weakly deformed systems are expected to be modified in the superdeformed world. The superdeformed symmetries lead to new quantum numbers and new effective interactions that can be employed in microscopic calculations. New classification schemes can be directly related to certain geometrical properties of the nuclear shape. DOE

N91-28854# Brookhaven National Lab., Upton, NY.
THE EFFECT OF STRONG COULOMB CORRELATIONS ON ELECTRON-PHONON INTERACTIONS IN THE COPPER OXIDES: IMPLICATIONS FOR TRANSPORT
J. H. Kim, K. Levin, R. Wentzcovitch, and A. Auerbach (Boston Univ., MA.) 1990 17 p Presented at the Symposium on the Manifestations of the Electron-Phonon Interaction in Copper Oxides (CuO) and Related Superconductors, Oaxtepec (Mexico), 11-14 Dec. 1990
(Contract DE-AC02-76CH-00016)
(DE91-013333; BNL-46112; CONF-901291-2) Avail: NTIS HC/MF A03

The effects of strong Coulomb correlations on the electron-phonon interactions in the high temperature superconductors are investigated. Very strong Coulomb correlations, which are essential for creating the insulating state at half filling, lead to a suppression of charge fluctuations as the insulator is approached. This thereby significantly reduces the electron-phonon coupling. We present a self-consistent frozen phonon scheme which is based on a Coulomb renormalized band structure of the copper-oxygen plane as a method for calculating these effects and their influence on transport properties. The microscopic spectral function has a two-peak structure, each peak of which can be associated with primarily copper-like and oxygen-like motion. A high density of these low frequency copper-dominated modes is important, for it leads to a linear resistivity extending down to temperatures of the order of 50K. A Drude fit to low frequency ac conductivity measurements yields a decrease in the plasma frequency as the insulator is approached, as well as a relatively concentration x independent scattering time (tau). The magnitude of the latter provides an upper bound on the electron-phonon coupling constant, which is found to be rather weak in accord with our calculations. The behavior of the calculated plasma frequency is also consistent with experiment and its x dependence is associated with an increase in the effective mass, due to incipient localization, as the insulator is approached. On the other hand, the calculated x independence of the electron-phonon contribution to the resistivity is not compatible with the increase observed in the total resistivity slope as the insulator is approached. This suggests that the phonon background accounts for a significant fraction of the measured resistivity slope at high x, but this contribution is not sufficient to explain the behavior at smaller x. DOE

N91-28855# Los Alamos National Lab., NM.
OPTICAL ANALOGS OF MODEL ATOMS IN FIELDS
P. W. Milonni 2 May 1991 9 p Presented at the North Atlantic Treaty Organization (NATO) Advanced Research Workshop on Coherence in the Interaction of Radiation With Atoms, Ontario, 3-11 May 1991
(Contract W-7405-eng-36)
(DE91-013392; LA-UR-91-1714; CONF-9105204-1) Avail: NTIS HC/MF A02

The equivalence of the paraxial wave equation to a time-dependent Schroedinger equation is exploited to construct optical analogs of model atoms in monochromatic fields. The approximation of geometrical optics provides the analog of the corresponding classical mechanics. Optical analogs of Rabi oscillations, photoionization, stabilization, and the Kramers-Hennenberger transformation are discussed. One possibility for experimental realization of such optical analogs is proposed. These analogs may be useful for studies of quantum chaos when the ray trajectories are chaotic. DOE

N91-28856# Stanford Linear Accelerator Center, CA.
LIGHT-CONE QUANTIZATION OF QUANTUM CHROMODYNAMICS
S. J. Brodsky and H. C. Pauli (Max-Planck-Inst. fuer Kernphysik, Heidelberg, Germany, F.R.) Jun. 1991 45 p Presented at the 30th Schladming Winter School in Particle Physics on Field Theory, Schladming (Austria), Mar. 1991
(Contract DE-AC03-76SF-00515)
(DE91-013991; SU-SLAC-PUB-5558; CONF-9103180-1) Avail: NTIS HC/MF A03

We discuss the light-cone quantization of gauge theories from two perspectives: as a calculational tool for representing hadrons as QCD bound-states of relativistic quarks and gluons, and also as a novel method for simulating quantum field theory on a computer. The light-cone Fock state expansion of wavefunctions at fixed light cone time provides a precise definition of the parton model and a general calculus for hadronic matrix elements. We present several new applications of light-cone Fock methods, including calculations of exclusive weak decays of heavy hadrons, and intrinsic heavy-quark contributions to structure functions. A general nonperturbative method for numerically solving quantum field theories, discretized light-cone quantization, is outlined and applied to several gauge theories, including QCD in one space and one time dimension, and quantum electrodynamics in physical space-time at large coupling strength. The DLCQ method is invariant under the large class of light-cone Lorentz transformations, and it can be formulated such at ultraviolet regularization is independent of the momentum space discretization. Both the bound-state spectrum and the corresponding relativistic light-cone wavefunctions can be obtained by matrix diagonalization and related techniques. We also discuss the construction of the light-cone Fock basis, the structure of the light-cone vacuum, and outline the renormalization techniques required for solving gauge theories within the light-cone Hamiltonian formalism. DOE

N91-28857# Brown Univ., Providence, RI.
INTERACTIONS OF MOLECULES WITH SURFACES
E. F. Greene Apr. 1991 7 p
(Contract DE-FG02-85ER-13441)
(DE91-014498; DOE/ER-13441/T1; COO-4974-13) Avail: NTIS HC/MF A02

The work supported has been concerned with three aspects of the dynamics of the interactions of molecules with surfaces. These are: the ionization of atoms and molecules at surfaces studies over a range of surface temperatures and kinetic energies of the molecules; the diffraction of He atoms from surfaces undergoing phase transitions at elevated temperatures; and the efficiency with which molecules transfer energy to surfaces studied by measuring the temperature rises produced at the surfaces. DOE

N91-28858*# Fermi National Accelerator Lab., Batavia, IL.
STATISTICAL MECHANICS OF SOFT-BOSON PHASE TRANSITIONS
Arun K. Gupta, Christopher T. Hill, Richard Holman, and Edward W. Kolb (Chicago Univ., IL.) 26 Jun. 1991 45 p
(Contract NAGw-1340; NAGw-1321; DE-AC02-76ER-03066; NSF AST-88-22595)
(NASA-CR-188697; NAS 1.26:188697; FNAL-Pub-91/167-T/A; CMU-HEP91-08) Avail: NTIS HC/MF A03 CSCL 20H

The existence of structure on large (100 Mpc) scales, and limits to anisotropies in the cosmic microwave background radiation (CMBR), have imperiled models of structure formation based solely upon the standard cold dark matter scenario. Novel scenarios, which may be compatible with large scale structure and small CMBR anisotropies, invoke nonlinear fluctuations in the density appearing after recombination, accomplished via the use of late time phase transitions involving ultralow mass scalar bosons. Herein, the statistical mechanics are studied of such phase transitions in several models involving naturally ultralow mass pseudo-Nambu-Goldstone bosons (pNGB's). These models can exhibit several interesting effects at high temperature, which is believed to be the most general possibilities for pNGB's. Author

N91-28859# Argonne National Lab., IL.
MODE SELECTIVITY IN CLUSTER-MOLECULE INTERACTIONS: NI13 + D2
J. Jellinek and Z. B. Guevenc 1991 13 p Presented at the

24th Jerusalem Symposium on Quantum Chemistry, Mode-Selective Chemistry, Jerusalem (Israel), 20-24 May 1991
(Contract W-31-109-eng-38)
(DE91-013352; ANL/CP-73275; CONF-9105200-1) Avail: NTIS HC/MF A03

Results of a detailed quasiclassical simulation study of the Ni sub 13 + D sub 2 collision system are presented. The dissociative adsorption of the molecule as well as its scattering from the cluster are analyzed as functions of the initial rovibrational molecular state collision energy, and structure of the cluster. Mode-specific features of the reactive and nonreactive channels of the cluster-molecule interaction are displayed and discussed. Evidence for resonances and for a strong cluster structure-reactivity correlation is presented. DOE

N91-28860# Argonne National Lab., IL.
THE SOUDAN 2 HONEYCOMB CALORIMETER
C. Garcia-Garcia Dec. 1990 15 p Presented at the International Conference on Calorimetry in High Energy Physics, Batavia, 29 Oct. 1990
(Contract W-31-109-eng-38)
(DE91-013404; ANL-HEP-CP-90-124; CONF-9010283-7) Avail: NTIS HC/MF A03

Soudan 2 is an 1100-ton honeycomb tracking calorimeter which is being constructed to search for nucleon decay. The detector consists of finely segmented iron instrumented with long drift tubes, and records three spatial coordinates and dE/dx for every gas crossing. Excellent event reconstruction capability, particle identification and muon sign and direction determination give superior rejection of the neutrino background to nucleon decay in many modes. The first 620 tons of Soudan 2 are now in steady operation, with completion planned for 1992. Detector performance has been studied using cosmic ray tracks and a charged test beam calibration. Results on detector performance and detector response are described. DOE

N91-28861# Los Alamos National Lab., NM.
NEW TECHNIQUES IN NEUTRON DATA MEASUREMENTS ABOVE 30 MeV
P. W. Lisowski and R. C. Haight 1991 6 p Presented at the International Conference on Nuclear Data for Science and Technology, Juelich, Fed. Republic of Germany, 13-17 May 1991
(Contract W-7405-eng-36)
(DE91-013690; LA-UR-91-1684; CONF-910503-21) Avail: NTIS HC/MF A02

Recent developments in experimental facilities have enabled new techniques for measurements of neutron interactions above 30 MeV. Foremost is the development of both monoenergetic and continuous neutron sources using accelerators in the medium energy region between 100 and 800 MeV. Measurements of the reaction products have been advanced by the continuous improvement in detector systems, electronics and computers. Corresponding developments in particle transport codes and in the theory of nuclear reactions at these energies have allowed more precise design of neutron sources, experimental shielding and detector response. As a result of these improvements, many new measurements are possible and the data base in this energy range is expanding quickly. DOE

N91-28862# California Univ., Berkeley. Lawrence Berkeley Lab.
MEASUREMENTS OF IONIZATION CROSS-SECTION FOR ELECTRON ENERGY-LOSS MICROANALYSIS UNDER WELL DEFINED SCATTERING CONDITIONS
K. M. Krishnan and C. J. Echer Apr. 1991 9 p Presented at the 49th Electron Microscopy Society of America (EMSA) Annual Meeting, San Jose, 4-9 Aug. 1991
(Contract DE-AC03-76SF-00098)
(DE91-013745; LBL-30618; CONF-910870-16) Avail: NTIS HC/MF A02

Partial cross-sections required for electron energy-loss microanalysis have been measured for a series of high purity single crystal standards. For each sample four different scattering geometries were used. The experimental data were compared with theoretical calculations using both standard hydrogenic model and parametrized Hartree-Slater cross-sections. Best agreement between theory and experiment were observed for experiments performed in diffraction mode (image coupling) with the probe convergence angle (0.84 mrad) much smaller than the spectrometer collection angle (6.84 mrad). In addition, specimen thicknesses from the region of microanalysis were measured by convergent beam electron diffraction. Absolute cross-sections based on these measurements are also currently being determined. DOE

N91-28863# University of Western Michigan, Kalamazoo.
CORRELATED CHARGE-CHANGING ION-ATOM COLLISIONS
J. A. Tanis and E. M. Bernstein Apr. 1991 4 p
(Contract DE-FG02-87ER-13778)
(DE91-013640; DOE/ER-13778/4) Avail: NTIS HC/MF A01

Experimental studies were made of fundamental atomic interactions in collisions of charged projectiles with neutral targets or electrons, with a particular emphasis on two-electron interactions and electron correlation effects. Processes involving excitation, ionization, and charge transfer are investigated, for the most part, using coincidence techniques in which projectile charge-changing events are associated with x ray emission, target recoil ions, or electron emission. New measurements were conducted using accelerators at the Lawrence Berkeley Laboratory (LBL), the Indiana University Cyclotron Facility (IUCF), and Western Michigan University (WMU). Brief summaries of work completed and work in progress are given. DOE

N91-28864# Wayne State Univ., Detroit, MI.
PHOTOINDUCED CHARGE AND ENERGY TRANSFER PROCESSES IN MOLECULAR AGGREGATES
J. F. Endicott 31 May 1991 30 p
(Contract DE-FG02-88ER-13944)
(DE91-014383; DOE/ER-13944/4) Avail: NTIS HC/MF A03

The major goals of this research project are to probe fundamental aspects (such as electronic and vibrational coupling) of center-to-center energy and electron transfer in complexes containing two or more metal centers. Pursuit of these goals has involved us in a wide range of studies which span the synthesis and characterization of mono-, di-, and tri-metallic complexes, the modular construction of instrumental systems and a range of photophysical studies. Various aspects of the photoinduced transfer of charge or migration of energy between donor and acceptor transition metal complexes are described. DOE

N91-28865# Argonne National Lab., IL.
PHOTODISINTEGRATION OF THE DEUTERON AT MEDIUM AND HIGH ENERGIES
T. S. H. Lee 1991 7 p Presented at the 5th Workshop on Perspectives in Nuclear Physics At Intermediate Energies, Trieste, Italy, 6-10 May 1991
(Contract W-31-109-eng-38)
(DE91-014458; ANL/CP-73422; CONF-9105222-1) Avail: NTIS HC/MF A02

We report the results from a unitary pi NN calculation of gamma d yields np reaction up to the (Delta)-excitation energy region, and the preliminary results from a light-front calculation at high energies. DOE

N91-28866# Brookhaven National Lab., Upton, NY.
CHAOS IN THE LOWEST LANDAU LEVEL
V. J. Emery 1991 12 p Presented at the Physical Phenomena At High Magnetic Fields, Tallahassee, 15-18 May 1991
(Contract DE-AC02-76CH-00016)
(DE91-014800; BNL-46293; CONF-9105151-7) Avail: NTIS HC/MF A03

The problem of a few electrons in the lowest Landau level is discussed. Low-lying states of the three-and four-electron problems are constructed. In the classical limit, the three-body problem is integrable but there is numerical evidence of chaotic motion in the four-body problem. Consequences of classical chaos for the statistics of energy levels are described and the possibility of carrying out relevant experiments in semiconductor heterostructures is discussed. DOE

N91-28920# Hiroshima Univ. (Japan). Faculty of Science.
NONADIABATIC BEHAVIOR OF THE MAGNETIC MOMENT OF A CHARGED PARTICLE IN A DIPOLE MAGNETIC FIELD
S. Murakami, Tetsuya Sato, and A. Hasegawa (Bell Telephone Labs., Inc., Murray Hill, NJ.) *In* National Inst. for Fusion Science, Proceedings of the Second International Toki Conference on Plasma Physics and Controlled Nuclear Fusion. Nonlinear Phenomena in Fusion Plasmas: Theory and Computer Simulation Apr. 1991 p 139-142 (For primary document see N91-28881 20-75)
Avail: NTIS HC/MF A11

73 NUCLEAR AND HIGH-ENERGY PHYSICS

Includes elementary and nuclear particles; and reactor theory.

For space radiation see *93 Space Radiation*.

N91-28867# Fermi National Accelerator Lab., Batavia, IL.
MICROWAVE INSTABILITY AT TRANSITION: STABILITY DIAGRAM APPROACH
S. A. Bogacz May 1991 4 p Presented at the 1991 Institute of Electrical and Electronics Engineers (IEEE) Particle Accelerator Conference (PAC), San Francisco, 6-9 May 1991
(Contract DE-AC02-76CH-03000)
(DE91-013202; FNAL/C-91/119; CONF-910505-122) Avail: NTIS HC/MF A01

A simple model of a beam at transition driven by a storage ring impedance is formulated in the framework of the nonlinear Vlasov equation. This yields a set of coupled equations of motion describing time evolution of a single coherent mode and the overall equilibrium density distribution function. At transition, contour integration in the dispersion relation can be carried out analytically and a simple closed formula for the coherent frequency is obtained. From the resulting stability diagram, further conclusions about the growth time of the microwave instability and the longitudinal emittance blowup at transition are derived. DOE

N91-28868# Argonne National Lab., IL.
HIGH ENERGY PHYSICS DIVISION SEMIANNUAL REPORT OF RESEARCH ACTIVITIES, JULY 1, 1990--DECEMBER 31, 1990
E. Berger, ed., P. Moonier, ed., E. May, ed., and J. Norem, ed. Feb. 1991 103 p
(Contract W-31-109-eng-38)
(DE91-012339; ANL-HEP-TR-91-05) Avail: NTIS HC/MF A06

A report is presented of research and development activities conducted in the High Energy Physics Division. Analyses of data from experiments performed by members of the Division are summarized, and the status of experiments taking data and of those being prepared is reviewed. Descriptions are included of research on theoretical and phenomenological topics in particle physics. Progress reports are provided on accelerator research and development, detector research and development, and experimental facilities research. Lists are presented of publications, of colloquia and conference talks, and of significant external community activities of members of the Division. DOE

N91-28869# Stanford Linear Accelerator Center, CA.
SLC POLARIZED BEAM SOURCE ELECTRON OPTICS DESIGN
K. R. Eppley, T. L. Lavine, R. A. Early, W. B. Herrmannsfeldt, R. H. Miller, D. C. Schultz, C. M. Spencer, and A. D. Yeremian May 1991 3 p Presented at the 1991 Institute of Electrical and Electronics Engineers (IEEE) Particle Accelerator Conference (PAC), San Francisco, 6-9 May 1991
(Contract DE-AC03-76SF-00515)
(DE91-012911; SU-SLAC-PUB-5453; CONF-910505-95) Avail: NTIS HC/MF A01

This paper describes the design of the beam-line from the polarized electron gun to the linac injector in the Stanford Linear Collider (SLC). The polarized electron source is a GaAs photocathode, requiring 10(exp -11)Torr-range pressure for adequate quantum efficiency and longevity. The photocathode is illuminated by 3-nsec-long laser pulses. The quality of the optics for the 160-kV beam is crucial since electron-stimulated gas desorption from beam loss in excess of 0.1 percent of the 20-nC pulses may poison the photocathode. Our design for the transport line consists of a differential pumping region isolated by a pair of valves. Focusing is provided by a pair of Helmholtz coils and by several iron-encased solenoidal lenses. Our optics design is based on beam transport simulations using 2(1/2)-D particle-in-cell codes to model the gun and to solve the fully-relativistic time-dependent equations of motion in three dimensions for electrons in the presence of azimuthally symmetric electromagnetic fields. DOE

N91-28870# Brookhaven National Lab., Upton, NY.
BEAM CURRENT MONITORING IN THE AGS BOOSTER AND ITS TRANSFER LINES
R. L. Witkover, E. Zitvogel, and V. Castillo 1991 6 p Presented at the 1991 Institute of Electrical and Electronics Engineers (IEEE) Particle Accelerator Conference (PAC), San Francisco, 6-9 May 1991
(Contract DE-AC02-76CH-00016)
(DE91-013328; BNL-45387; CONF-910505-137) Avail: NTIS HC/MF A02

The new AGS Booster is designed to accelerate low intensity polarized protons and heavy ions, and high intensity protons. The wide range of beam parameters and the vacuum, thermal and radiation environment, presented challenges in the instrumentation design. This paper describes the problems and solutions for the beam current monitors in the Booster and its transport lines. Where available, results of the initial operation will be presented. DOE

N91-28871# Los Alamos National Lab., NM.
BEAM STRUCTURE AND TRANSVERSE EMITTANCE STUDIES OF HIGH-ENERGY ION BEAMS
K. Saadatmand, K. F. Johnson, and J. D. Schneider 1991 4 p Presented at the 1991 Institute of Electrical and Electronics Engineers (IEEE) Particle Accelerator Conference (PAC), San Francisco, 6-9 May 1991
(Contract W-7405-eng-36)
(DE91-013499; LA-UR-91-1524; CONF-910505-174) Avail: NTIS HC/MF A01

A visual diagnostic technique was developed to monitor and study ion beam structure shape and size along a transport line. In this technique, a commercially available fluorescent screen is utilized in conjunction with a video camera. This visual representation of the beam structure is digitized and enhanced through use of false color coding and displayed on a TV monitor for on-line viewing. Digitized information is stored for further off-line processing (e.g., extraction of beam profiles). An optional wire grid placed upstream of the fluor screen adds the capability of transverse emittance (or angular spread) measurement to this technique. This diagnostic allows real time observation of the beam response to parameter changes (e.g., evolution of the beam structure, shifts in the beam intensity at various spatial locations within the beam perimeter, and shifts in the beam center and position). DOE

N91-28872# State Univ. of New York, Stony Brook. Dept. of Physics.
RESEARCH IN THEORETICAL NUCLEAR PHYSICS
Jun. 1991 127 p
(Contract DE-FG02-88ER-40388)
(DE91-013644; DOE/ER-40388/71) Avail: NTIS HC/MF A07

Abstracts or ongoing projects are presented in the following areas: strong interaction physics; relativistic heavy ion physics; nuclear structure and nuclear many-body theory; and nuclear astrophysics. DOE

N91-28873# Oregon State Univ., Corvallis.
THEORETICAL STUDIES IN NUCLEAR PHYSICS
R. H. Landau and V. A. Madsen 1991 18 p
(Contract DE-FG06-86ER-40283)
(DE91-013909; DOE/ER-40283/10) Avail: NTIS HC/MF A03

This report discusses research in nuclear theory in the following areas: Isospin effects and charge exchange; inelastic and charge exchange scattering; momentum space proton scattering; pion scattering from nuclei; and antiproton studies. DOE

N91-28874# Brookhaven National Lab., Upton, NY.
SPACE CHARGE AND WAKE FIELD ANALYSIS FOR A HIGH BRIGHTNESS ELECTRON SOURCE
Z. Parsa 1991 15 p Presented at the Spring Meeting of the American Physical Society (APS), Washington, 15-18 Apr. 1991
(Contract DE-AC02-76CH-00016)
(DE91-014788; BNL-46271; CONF-910427-3) Avail: NTIS HC/MF A03

We present a brief overview of the formalism used, and some simulation results for transverse and longitudinal motion of a bunch of particles moving through a cavity (e.g., the Brookhaven National Laboratory high brightness photocathode gun), including effects of the accelerating field, space charge forces (e.g., arising from the interaction of the cavity surface and the self field of the bunch). DOE

N91-28905# Nagoya Univ. (Japan). Plasma Science Center.
RAPID ACCELERATION OF PROTONS IN A NONLINEAR MAGNETOSONIC WAVE AND THEIR ENERGY SPECTRUM
Y. Ohsawa and Y. Terashima *In* National Inst. for Fusion Science, Proceedings of the Second International Toki Conference on Plasma Physics and Controlled Nuclear Fusion. Nonlinear Phenomena in Fusion Plasmas: Theory and Computer Simulation Apr. 1991 p 83-86 (For primary document see N91-28881 20-75)
Avail: NTIS HC/MF A11

74 OPTICS

Includes light phenomena; and optical devices.
For lasers see *36 Lasers and Masers.*

N91-28875# Virginia Polytechnic Inst. and State Univ., Blacksburg.
RESEARCH AND DEVELOPMENT ENTITLED SMART STRUCTURES FOR FOSSIL ENERGY APPLICATIONS
R. O. Claus Dec. 1990 116 p
(Contract DE-AC21-89MC-25159)
(DE91-002064; DOE/MC-25159/2984) Avail: NTIS HC/MF A06

Two different fiber optic sensors were considered for use in ceramic cross flow filters. The intensity-based sensor was tested with a great degree of success. Even with a computerized data acquisition system, the intensity based sensor was unable to achieve the resolution of the Fabry-Perot sensor. Another drawback of the intensity sensor is the hysteresis behavior observed over cyclic variation of temperature. It was determined that Fabry-Perot fiber optic sensors can be used to measure thermal strains in ceramic cross flow filters with accuracies of 0.1 micron/m. The single ended approach of the reflective Fabry-Perot sensors is well suited for high thermal strain measurements; the results obtained show that the output of the fiber sensor tracks the temperature changes exactly as expected and shows no noticeable time lag between the measurand and the output signal. Sapphire fibers were manufactured with silica claddings and their spectral attenuation was measured. An intensity based sensor using sapphire fibers was fabricated and its performance calibrated. The success of the Fabry-Perot sensor has proved that such fiber optic sensors are well suited for smart structures in fossil energy applications. DOE

N91-28876# Lawrence Livermore National Lab., CA.
SIMULATION OF PLANAR INTEGRATED PHOTONICS DEVICES WITH THE LLNL TIME-DOMAIN FINITE-DIFFERENCE CODE SUITE
R. McLeod, R. J. Hawkins, and J. S. Kallman Apr. 1991 6 p Presented at the Optical Society of America (OSA) Integrated Photonic Research/Gradient Index Optic System (IPR/GIOS) Workshop, Monterey, 7-11 Apr. 1991
(Contract W-7405-eng-48)
(DE91-011929; UCRL-JC-106863; CONF-9104244-1) Avail: NTIS HC/MF A02

Interest has recently grown in applying microwave modeling techniques to optical circuit modeling. One of the simplest, yet most powerful, microwave simulation techniques is the finite-difference time-domain algorithm (FDTD). In this technique, the differential form of the time-domain Maxwell's equations are discretized and all derivatives are approximated as differences. Minor algebraic manipulations on the resulting equations produces a set of update equations that produce fields at a given time step from fields at the previous time step. The FDTD algorithm, then, is quite simple. Source fields are launched into the discrete grid by some means. The FDTD equations advance these fields in time. At the boundaries of the grid, special update equations called radiation conditions are applied that approximate a continuing, infinite space. Because virtually no assumptions are made in the development of the FDTD method, the algorithm is able to represent a wide-range of physical effects. Waves can propagate in any direction, multiple reflections within structures can cause resonances, multiple modes of various polarizations can be launched, each of which may generate within the device an infinite spectrum of bound and radiation modes. The ability to model these types of general physical effects is what makes the FDTD method interesting to the field of optics. In this paper, we discuss the application of the finite-difference time-domain technique to integrated optics. Animations will be shown of the simulations of a TE coupler, TM grating, and a TE integrated detector. DOE

N91-28877# Lawrence Livermore National Lab., CA.
REFLECTION MASK TECHNOLOGY FOR SOFT X RAY PROJECTION LITHOGRAPHY
A. M. Hawryluk, N. M. Ceglio, D. W. Pillion, D. P. Gaines, R. Browning, and R. Pease Apr. 1991 8 p Presented at the Soft-X-Ray Projection Lithography Topical Meeting, Monterey, 10-12 Apr. 1991
(Contract W-7405-eng-48)
(DE91-012561; UCRL-JC-107118; CONF-9104203-2) Avail: NTIS HC/MF A02

Soft X ray Projection Lithography (SXPL) may be used to fabricate high resolution structures for future integrated circuits. This technique uses a reflection mask which is a substrate coated with an x ray multilayer mirror and patterned with a thin (approx. 50 nm) layer of x ray absorber. Mask patterning processes must not degrade the reflectivity of the x ray mirror and mask repair techniques must be developed. The technical challenges of conventional reflecting optical imaging system designs are severe and mask technology can have a significant impact on this issue. Specifically, innovative mask designs can reduce the complexity of the optical system by decreasing the number of mirrors and replacing aspheric optical surfaces with spherical surfaces. A technique was developed called Encoded Mask Lithography, with which was designed an optical system which uses only two (spherical) imaging mirrors and has less than 100 nm spatial resolution, negligible distortion and greater than 30 mm diameter field of view. DOE

N91-28878 Tel-Aviv Univ. (Israel). Dept. of Electron Devices and Materials and Electromagnetic Radiation.
COLOR EFFECTS IN OPTICAL SYSTEMS M.S. Thesis
Moshe Peretz Oct. 1989 97 p In HEBREW; ENGLISH summary
(ITN-91-85150) Copyright Avail: Tel-Aviv Univ., Exact Sciences Library, Ramat Aviv 69978, Israel

In modern optical systems there are different combinations and divisions of optical channels. These are obtained through beam splitters and combiners. The optical elements are usually coated with optically thin films. When the element operates in the transmitting mode the film is dielectric; when it operates in the reflecting mode the film is either metallic or dielectric. The spectral response (transmission or reflection) of a thin film stack depends on the design of the stack (thickness, refractive index, and order of the layers) as well as the angle of incidence. The spectral behavior gives the possibility of creating various types of optical filters for different purposes, such as: anti-reflection coatings; long and short wave pass filters; dielectric mirrors; bandpass filters; combiners, dividers, polarizers, etc. In the great majority of cases the thin films are completely transparent, so that no energy is absorbed. Hence, the reflection is the complement of the transmission. This fact is used in the construction of dichroic beam splitters for primary color separation in, for example, color television cameras. This causes a different intensity distribution spectrum in the image, compared with that in the object. This effect was studied and a computer program was written in which the inputs are the optical system, the light sources and the coatings. The output is the image color, in the image plane, relative to the object color.

Author (ISA)

N91-28879# Maryland Univ., Baltimore. Dept. of Electrical Engineering.

PULSE PROPAGATION IN INHOMOGENEOUS OPTICAL FIBERS

C. R. Menyuk 13 Jun. 1991 7 p
(Contract DE-FG05-89ER-14090)
(DE91-014356; DOE/ER-14090/2) Avail: NTIS HC/MF A02

This year, like last, we have participated in several of the most exciting advances in photonics technology. The investment that we have made in developing codes to study solid state devices has reached fruition with several publications submitted or in progress. Our work on solid state device simulations has focused on two problems, both of which have been posed to us by our experimental collaborators at University of Maryland, Baltimore County. The first is to determine the influence which geometric effects have on propagation in GaAs/AlGaAs ridge waveguides with a quantum well layer. During the past year, our work on optical fiber switching has been extraordinarily fruitful, leading to six joint publications with scientists at AT and T Bell Laboratories and numerous conference presentations. Our work on randomly birefringence in optical communication fibers has borne significant fruit this year. Dr. Wai and his collaborators have written two papers which describe the evolution of solitons in optical fibers.

DOE

N91-28880 Stanford Univ., CA.

LASER SPECKLE VELOCIMETRY WITH PHOTOREFRACTIVE RECORDING AND ANAMORPHIC OPTICAL PROCESSING Ph.D. Thesis

Steven H. Collicott 1991 145 p
Avail: Univ. Microfilms Order No. DA9115755

Laser speckle velocimetry is an optical method used to measure instantaneous 2-D fluid velocity fields. Similarly, 2-D displacement or strain fields of solid bodies may be measured without contact. Original applications or real time optical recording materials, anamorphic optical processors, and novel imaging techniques demonstrate improved capabilities of laser speckle velocimetry. Real time recording and optical processing of double-exposure speckle patterns in photorefractive crystals (Bi12SiO20 and Bi12GeO20) are described. Polarization filtering in the optical processor is shown to increase the signal to noise ratio and permit detection of smaller signals. An original application of anamorphic optics dramatically reduces the time required for measurement of displacement fields recorded as double-exposure speckle patterns. Analysis of the fringe contrast in the output plane of the processor describes the operating range. Based on Fourier optics and the statistics of speckle patterns, this analysis also illustrates the tradeoff between spatial resolution and operating range. This permits design of an anamorphic optical processor which is two orders of magnitude faster than the standard axisymmetric optical processor for measuring 2-D displacements in double-exposure speckle patterns. Data from experiments confirm the predictions of fringe contrast and processing time. Application of oblique imaging systems to speckle velocimetry measurements of a fluid flow is described. Resulting improvements are an increase of the area of the velocity field which may be studied, a decrease in required laser energy, or tradeoffs between the two. Velocity profiles in a circular jet measured with a combination of oblique imaging and anamorphic optical processing are presented.

Dissert. Abstr.

75 PLASMA PHYSICS

Includes magnetohydrodynamics and plasma fusion.

For ionospheric plasmas see *46 Geophysics.* For space plasmas see *90 Astrophysics.*

N91-28881# National Inst. for Fusion Science, Nagoya (Japan).

PROCEEDINGS OF THE SECOND INTERNATIONAL TOKI CONFERENCE ON PLASMA PHYSICS AND CONTROLLED NUCLEAR FUSION. NONLINEAR PHENOMENA IN FUSION PLASMAS: THEORY AND COMPUTER SIMULATION

Apr. 1991 243 p Conference held in Toki City, Japan, 27-30 Nov. 1990
(NIFS-Proc-6; ISSN-0915-6348) Avail: NTIS HC/MF A11

Papers from the conference are presented, and the topics covered include the following: magnetohydrodynamic (MHD) relaxation, plasma control, tokamak devices, toroidal plasmas, magnetic field reconnection, plasma turbulence, MHD stability, mathematical models, plasma dynamics, transport properties, helical plasmas, laser plasmas, space plasmas, computerized simulation, plasma drift, and chaos and solitary waves For individual titles, see N91-28882 through N91-28943.

N91-28882# Massachusetts Inst. of Tech., Cambridge. Dept. of Physics.

NONLINEAR PHENOMENA AND PROCESSES IN HIGH ENERGY PLASMAS

B. Coppi *In* National Inst. for Fusion Science, Proceedings of the Second International Toki Conference on Plasma Physics and Controlled Nuclear Fusion. Nonlinear Phenomena in Fusion Plasmas: Theory and Computer Simulation Apr. 1991 p 3-7 Sponsored in part by DOE (For primary document see N91-28881 20-75)
Avail: NTIS HC/MF A11

Both in space physics and in the field of high energy laboratory plasmas, where fusion burn conditions can be achieved, a large class of observed phenomena required the understanding of the nonlinear processes that underlie them. Nonlinear plasma physics has had a rather humble but clearly formulated beginning: experiments on plasma waves and their nonlinear interactions have, in fact, confirmed the theories that had been developed on mode couplings, nonlinear Landau damping, etc. The phenomena that are presently confronted are considerably more complex but their importance is such that tentative and rudimentary theoretical descriptions have to be given of them. While accepting the fact that the analytical tools that were generated are not adequate for the task, that the explanations should be based on clear concepts and start from complete and correct linearized theories. In order to be specific on some of the issues involved, two rather general areas are considered: magnetic reconnection in collisionless plasmas, and transport processes in magnetically confined plasmas.

Author

N91-28883# National Inst. for Fusion Science, Nagoya (Japan).

SELF-ORGANIZING PROCESSES IN MAGNETICALLY CONFINED PLASMA

Tetsuya Sato, R. Horiuchi, K. Watanabe, T. Hayashi, and K. Kusano (Hiroshima Univ., Japan) *In its* Proceedings of the Second International Toki Conference on Plasma Physics and Controlled Nuclear Fusion. Nonlinear Phenomena in Fusion Plasmas: Theory

and Computer Simulation Apr. 1991 p 8-11 (For primary document see N91-28881 20-75)
Avail: NTIS HC/MF A11

Three snapshots of a self-organizing magnetohydrodynamic plasma are examined. A simple ordered structure (a helical structure in this case) is created from a once disordered structure (middle panel) when the entropy produced during the process is swept out from the system. The magnetohydrodynamic self-organization is governed by the nonlinearly driven reconnection whereby the magnetic helicity is conserved but the magnetic energy is stepwise decreased. The time evolutions of the average wavenumber of the magnetic energy and the magnetic helicity are examined. The case of a tokamak is discussed. Author

N91-28884# Columbia Univ., New York, NY. Dept. of Applied Physics.
CURRENT SHEET FORMATION AND RAPID RECONNECTION IN THE SOLAR CORONA Abstract Only
A. Bhattacharjee and Xiaogang Wang *In* National Inst. for Fusion Science, Proceedings of the Second International Toki Conference on Plasma Physics and Controlled Nuclear Fusion. Nonlinear Phenomena in Fusion Plasmas: Theory and Computer Simulation Apr. 1991 p 12 (For primary document see N91-28881 20-75)
Avail: NTIS HC/MF A11

It is shown that a current sheet is formed in Parker's model of the solar corona (Parker 1972) from the requirement that magnetic helicity is conserved in the presence of a very small but finite plasma resistivity. The presence of dissipation permits slippage of field-lines with respect to the plasma, and makes Van Ballegooijen's theorem (1985) inapplicable. Thus, a current sheet can be formed in the presence of smooth photospheric flows. The structure of the current sheet encompasses a thin strip spanning two Y-points. It is shown that the rapid reconnection involved in the formation of the current sheet justifies the use of helicity conservation. Implications for coronal heating and numerical simulations of the corona are discussed. Author

N91-28885# Kyoto Univ. (Japan). Research Inst. for Mathematical Sciences.
LOG-STABLE DISTRIBUTION OF ENERGY DISSIPATION IN TURBULENCE
Shigeo Kida *In* National Inst. for Fusion Science, Proceedings of the Second International Toki Conference on Plasma Physics and Controlled Nuclear Fusion. Nonlinear Phenomena in Fusion Plasmas: Theory and Computer Simulation Apr. 1991 p 13-16 (For primary document see N91-28881 20-75)
Avail: NTIS HC/MF A11

The statistical properties of small-scale motion of turbulence, especially the low-order moments such as the energy spectrum function, are well described by the Kolmogorov prediction. Since the intermittent property of velocity field had been recognized experimentally, lots of intermittency theories have been proposed by incorporating the intermittent structure of flow field, especially of the fluctuations of the energy dissipation rate field. They describe the intermittency effects qualitatively, but the quantitative agreement is still controversial. Here, a new intermittency theory is proposed and the results are compared with experiments. Author

N91-28886# Max-Planck-Inst. fuer Plasmaphysik, Garching (Germany, F.R.).
STATISTICAL PROPERTIES OF TWO-DIMENSIONAL MAGNETOHYDRODYNAMIC TURBULENCE Abstract Only
D. Biskamp and H. Welter *In* National Inst. for Fusion Science, Proceedings of the Second International Toki Conference on Plasma Physics and Controlled Nuclear Fusion. Nonlinear Phenomena in Fusion Plasmas: Theory and Computer Simulation Apr. 1991 p 17 (For primary document see N91-28881 20-75)
Avail: NTIS HC/MF A11

A brief introduction to the basic properties of magnetohydrodynamic (MHD) turbulence is presented. The statistical properties as obtained by evaluating a number of numerical turbulence simulation computations are discussed. The probability distributions (PD) of various dynamical quantities are presented, and in order to discuss intermittency, the beta-model developed for hydrodynamic turbulence is adapted to MHD. A comparison of simulation results of energy spectra with the beta-model predictions is made and results are presented. Author

N91-28887# Tokyo Univ. (Japan). Inst. of Industrial Science.
TURBULENT DYNAMO AND SUBGRID-SCALE MODELING OF MHD TURBULENCE
Akira Yoshizawa *In* National Inst. for Fusion Science, Proceedings of the Second International Toki Conference on Plasma Physics and Controlled Nuclear Fusion. Nonlinear Phenomena in Fusion Plasmas: Theory and Computer Simulation Apr. 1991 p 18-21 (For primary document see N91-28881 20-75)
Avail: NTIS HC/MF A11

A bulk turbulent dynamo model is presented for understanding of the effects of magnetohydrodynamic (MHD) fluctuations. This model can explain some interesting properties of the steady state of MHD turbulence that are related to reverse field pinch (RFP) and Earth's magnetic fields. A subgrid-scale model is also derived as a numerical approach for investigating the intermittent properties in these phenomena that are beyond the reach of the bulk dynamo model. Author

N91-28888# Wisconsin Univ., Madison.
HYBRID FLUID/KINETIC DESCRIPTIONS OF TOKAMAK PLASMAS
J. D. Callen, Z. Chang, J. B. Hollenberg, and J. P. Wang *In* National Inst. for Fusion Science, Proceedings of the Second International Toki Conference on Plasma Physics and Controlled Nuclear Fusion. Nonlinear Phenomena in Fusion Plasmas: Theory and Computer Simulation Apr. 1991 p 22-25 (For primary document see N91-28881 20-75)
(Contract DE-FG02-86ER-53218)
Avail: NTIS HC/MF A11

Collisional fluid moment descriptions have provided many useful theoretical models of the macroscopic behavior, microscopic fluidlike instabilities, and equilibrium transport properties of tokamak plasmas. However, the usual fluid moment descriptions neglect many important kinetic effects: magnetic particle trapping, Landau damping, finite Larmor radius (FLR) effects, etc.. At the other extreme, the simplest collisionless kinetic treatments of plasma instabilities often do not include many important semicollisional and nonlinear fluid effects. In order to bridge this gap and to provide a comprehensive nonlinear theory of tokamak plasmas that includes both types of effects, an exact Chapman-Enskog like approach was developed for determining the small kinetic distortions of species distribution functions that are needed to calculate the fluid moment closure relations. Author

N91-28889# Princeton Univ., NJ. Plasma Physics Lab.
THE THEORY OF TURBULENCE AND ANOMALOUS TRANSPORT IN PLASMAS: PAST, PRESENT, AND FUTURE
John A. Krommes *In* National Inst. for Fusion Science, Proceedings of the Second International Toki Conference on Plasma Physics and Controlled Nuclear Fusion. Nonlinear Phenomena in Fusion Plasmas: Theory and Computer Simulation Apr. 1991 p 26-29 (For primary document see N91-28881 20-75)
(Contract DE-AC02-76CH-03073)
Avail: NTIS HC/MF A11

The purpose is to briefly review the theory of plasma turbulence, describe some recent developments, and comment on future directions. Brief comments on resonance broadening theory (RBT), clump theory (CT), and direct interaction approximation (DIA) are made. State of the art research on realizable Markovian statistical closures are described, and the theory of rigorous bounds is introduced. Author

N91-28890# Korea Advanced Inst. of Science and Technology, Chongryang (Republic of Korea).

ION TEMPERATURE GRADIENT TURBULENCE AND COHERENT STRUCTURES Abstract Only c34

D. I. Choi, B. G. Hong, F. Romanelli, and M. Ottaviani (Associazione EURATOM-CNEN Sulla Fusione, Frascati, Italy) *In* National Inst. for Fusion Science, Proceedings of the Second International Toki Conference on Plasma Physics and Controlled Nuclear Fusion. Nonlinear Phenomena in Fusion Plasmas: Theory and Computer Simulation Apr. 1991 p 30 (For primary document see N91-28881 20-75)

Avail: NTIS HC/MF A11

To study the anomalous transport associated with the ion temperature gradient driven mode, the effect of magnetic shear on the coherent structure of the toroidal ion temperature gradient driven mode (eta(sub i)) turbulence is investigated. Recent 2-D numerical simulations of the eta(sub i) mode show that long-lived, large scale coherent structures exist and considerably affect the level of magnitude of the anomalous transport. A significant reduction of the turbulent heat flux with respect to the quasilinear estimate and positive dependence on dissipations are observed. Whether or not the nonlinear equations admit a coherent solution in the presence of the magnetic shear is addressed. The stationary solutions of the nonlinear equations describing the dynamics of eta(sub i) mode are investigated and found to be a dipolar vortex in the shearless case. This is a simple generalization of the dipolar vortex solution of the Hasegawa-Mima equation. In the presence of the magnetic shear, a modified dipolar vortex solution was found through perturbation theory. The circular boundary of shearless modon solution becomes an ellipse and the number of free parameters reduce to one. This solution is self consistent as far as the radius of the vortex is small compared with the position of the ion sound turning points. The vortex dynamics are as important as the turbulence represented by the wave components in the study of the anomalous transport. Author

N91-28891# Princeton Univ., NJ. Plasma Physics Lab.

THREE-DIMENSIONAL PARTICLE SIMULATION OF TRAPPED ELECTRON INSTABILITIES IN TOKAMAKS Abstract Only

C. Z. Cheng and H. Okuda *In* National Inst. for Fusion Science, Proceedings of the Second International Toki Conference on Plasma Physics and Controlled Nuclear Fusion. Nonlinear Phenomena in Fusion Plasmas: Theory and Computer Simulation Apr. 1991 p 31 (For primary document see N91-28881 20-75)

Avail: NTIS HC/MF A11

Anomalous plasma transport due to dissipative trapped electron instabilities in toroidal geometry is studied by means of three-dimensional particle simulations. The electron dynamic is approximated with a guiding center drift-kinetic description, and the full ion dynamic is retained. The electron-ion pitch angle scattering is simulated by a Monte Carlo collisional model. The collision frequency is chosen such that the bulk of the plasma is in the banana and the plateau regimes corresponding to high temperature tokamak experiments. Initially, the particles have Maxwellian velocity distributions with density and temperature nonuniformities. Within an electron-ion collision time, the electrons establish a neoclassical distribution, and a bootstrap current is formed which is consistent with the neoclassical theory. In the linear stage of the dissipative trapped electron instabilities, the growth rates and the radial and poloidal ballooning structures observed in the simulation agree well with linear theory. In the nonlinear stage of the dissipative trapped electron instabilities, the poloidal ballooning effect is reduced because of the generation of strong plasma turbulence due to E x B nonlinearity. The resultant wavenumber and frequency spectra resemble the experimental observations. Particle and temperature diffusion, which is relatively small in the linear stage of the dissipative trapped electron instabilities, is enhanced rapidly in the nonlinear stage leading to the stabilization of the system. The observed particle diffusion agrees well with the gyro-reduced Bohm diffusion. Author

N91-28892# Kyoto Univ. (Japan). Plasma Physics Lab.

EDGE ANOMALOUS TRANSPORT IN HELIOTRON/TORSATRON

M. Wakatani, K. Watanabe, H. Sugama, and Masatoshi Yagi (Japan Atomic Energy Research Inst., Naka.) *In* National Inst. for Fusion Science, Proceedings of the Second International Toki Conference on Plasma Physics and Controlled Nuclear Fusion. Nonlinear Phenomena in Fusion Plasmas: Theory and Computer Simulation Apr. 1991 p 32-36 (For primary document see N91-28881 20-75)

Avail: NTIS HC/MF A11

Resistive interchange instabilities (or g modes) destabilized by the pressure gradient in the unfavorable magnetic curvature region are studied to explain the edge anomalous transport which increases in the radial direction. First, a reduced resistive magnetohydrodynamic (MHD) model is applied to derive the transport coefficient. By extending this model, several new effects are investigated for comparison with the Heliotron E experiment: (1) radical electric field effect on the g modes; (2) coupling between the g mode and the resistive drift wave; and (3) coupling between the g mode and the eta(sub i) mode. Author

N91-28893# Max-Planck-Inst. fuer Plasmaphysik, Garching (Germany, F.R.).

OPTIMIZATION, NON-LOCAL MHD-MODE, AND ALPHA-PARTICLE CONFINEMENT BEHAVIOR OF HELIAS EQUILIBRIA

W. Lotz, Jurgen Nuehrenberg, and C. Schwab *In* National Inst. for Fusion Science, Proceedings of the Second International Toki Conference on Plasma Physics and Controlled Nuclear Fusion. Nonlinear Phenomena in Fusion Plasmas: Theory and Computer Simulation Apr. 1991 p 37-40 (For primary document see N91-28881 20-75)

Avail: NTIS HC/MF A11

Stellarators need optimization because classical physics issues seriously limit their viability as fusion devices. Such issues are their magnetic surfaces, their magnetohydrodynamic (MHD) and neoclassical properties, and their realization by coils. An example for stellarator optimization potential are quasi-helically symmetric toroidal magnetic fields which show that the magnetic geometry of a stellarator can be decoupled from its real space geometry. Thus, stellarator optimization does not only mean an improvement of some given basic concept but primarily the selection of basic physics properties. Stellarator optimization naturally divides into a set of general guidelines and a set of specific physics objectives. The plasma behavior in the confinement region can be optimized by noting that the geometry of the confinement boundary within the last closed flux surface completely determines the properties of the confinement region. Thus, boundary value problems may be solved during optimization, the parameters of the boundary being the optimization variables. Boundary value problems are the basic steps of the optimization procedure employed here, which allows large steps to be taken in the stellarator configurational space. The boundary representation used for Helias equilibria appears to provide a suitable configuration space. The objectives of the optimization and its result as well as aspects of the MHD stability and the collisionless alpha-particle confinement behavior of the optimized configuration are described. Author

N91-28894# National Inst. for Fusion Science, Nagoya (Japan).

EQUILIBRIUM BETA LIMIT OF HELICAL SYSTEMS

T. Hayashi, A. Takei, N. Ohyabu, and Tetsuya Sato *In its* Proceedings of the Second International Toki Conference on Plasma Physics and Controlled Nuclear Fusion. Nonlinear Phenomena in Fusion Plasmas: Theory and Computer Simulation Apr. 1991 p 41-44 (For primary document see N91-28881 20-75)

Avail: NTIS HC/MF A11

The equilibrium beta limit, which is defined by the breaking of magnetic surfaces due to the finite beta effect, is investigated for two types of helical systems. The results indicate that the breaking often imposes severer limitation on beta than the Shafranov shift. However, if controllable parameters can be properly chosen, such as the vertical field B sub upsilon, a high beta equilibrium can be obtained, such as antibeta is greater than or = 5 percent. Furthermore, a simple method is proposed, by which the breaking can be actively suppressed and fairly high beta equilibria with clearly nested magnetic surfaces can be realized. Author

N91-28895# Columbia Univ., New York, NY. Dept. of Applied Physics.
SUPPRESSION AND CONTROL OF MAGNETIC ISLANDS IN TOROIDAL PLASMAS
C. C. Hegna, A. Bhattacharjee, Y. Nakamura, and M. Wakatani (Kyoto Univ., Japan) *In* National Inst. for Fusion Science, Proceedings of the Second International Toki Conference on Plasma Physics and Controlled Nuclear Fusion. Nonlinear Phenomena in Fusion Plasmas: Theory and Computer Simulation Apr. 1991 p 45-52 (For primary document see N91-28881 20-75)
(Contract DE-FG02-86ER-53222)
Avail: NTIS HC/MF A11

Some theoretical developments on the formation and dynamics of magnetic islands in toroidal plasmas are reported. It is shown that an energetic ion population can have a significant effect on the nonlinear stability of a single-helicity tearing mode. A dynamical equation for the magnetic island width is derived from kinetic theory. It is shown that island growth can be suppressed in tokamak plasmas by injecting an energetic ion beam with a density profile which peaks just outside the rational surface. This technique can be used for suppressing major disruptions caused by the nonlinear growth of m=2, n=1 islands in a tokamak. The formation of magnetic islands as a result of plasma pressure in 3-D equilibria is also studied. The width of the equilibrium island is shown to depend on the resistive interchange properties of the plasma. This analytical theory is applied to the Heliotron-E configuration. Equilibrium beta limits due to the criterion of island overlap are investigated. It is suggested that experimental observations of internal disruptions on Heliotron-E can be interpreted as a loss of equilibrium due to island overlap. Energetic ions can also be used to reduce the size of equilibrium islands in a stellarator due to vacuum field errors. Author

N91-28896# Pohang Inst. of Science and Technology (Republic of Korea). Dept. of Physics.
THEORETICAL STUDIES OF NONLINEAR SHEATH DYNAMICS
Jae Koo Lee and Sang June Hahn *In* National Inst. for Fusion Science, Proceedings of the Second International Toki Conference on Plasma Physics and Controlled Nuclear Fusion. Nonlinear Phenomena in Fusion Plasmas: Theory and Computer Simulation Apr. 1991 p 53-56 (For primary document see N91-28881 20-75)
Avail: NTIS HC/MF A11

Kinetic particle simulation of the system consisting of plasma, sheath, material, and an external driving circuit is carried out. The nonlinear sheath dynamics on the plasma ion implantation is studied in a series of simple simulations. Other similar applications include the dc and RF glow discharges for electronic material processing such as etching or doping. The unsteady acceleration and the polarity-dependent behaviors in the pulsed plasma accelerator are also studied in view of transient sheath dynamics. Author

N91-28897# Osaka Univ., Suita (Japan). Inst. of Laser Engineering.
HYDRODYNAMIC INSTABILITIES IN LASER DRIVEN IMPLOSION
K. Mima, S. Kato, A. Nishiguchi, and H. Takabe *In* National Inst. for Fusion Science, Proceedings of the Second International Toki Conference on Plasma Physics and Controlled Nuclear Fusion. Nonlinear Phenomena in Fusion Plasmas: Theory and Computer Simulation Apr. 1991 p 57-60 (For primary document see N91-28881 20-75)
Avail: NTIS HC/MF A11

Recently, high density plasmas with a density higher than 600 times solid density have been produced by laser implosion. This compressed density agrees reasonably well with 1-D simulation. However, the neutron yield is less than 10(exp -2) to 10(exp -3) times 1-D simulation result for the high density compression. The results indicate that the outside surface of the compressed plasma is stable, but the internal hot dense plasma surface is not stable. The instabilities driven by the internal temperature and pressure gradients are discussed. By using the quasi linear approximation, the saturation level was estimated of the fluctuations to determine the convective heat flux. The self-consistent temperature profile is then found to evaluate the reduction of neutron yield. Author

N91-28898# Maryland Univ., College Park. Dept. of Physics.
SOLITONS AND CHAOS IN LASER-PLASMA INTERACTION Abstract Only
C. S. Liu, W. Shyu, P. N. Guzdar, H. H. Chen, and Y. C. Lee *In* National Inst. for Fusion Science, Proceedings of the Second International Toki Conference on Plasma Physics and Controlled Nuclear Fusion. Nonlinear Phenomena in Fusion Plasmas: Theory and Computer Simulation Apr. 1991 p 61 (For primary document see N91-28881 20-75)
Avail: NTIS HC/MF A11

Transitions from soliton to chaos in laser irradiated inhomogeneous plasmas are studied for Resonance absorption and Raman backscattering. To model resonance absorption, both driven nonlinear Schroedinger equation and Zakharov equations with in homogeneity term added were solved to show that the final states of steady state of modified Airy function; periodic solutions-representing regular soliton emission; and chaos through period doubling, 2nd frequency appearance (breather emission) and breaking of two-frequency torus through the generation of broad bands of harmonic at n(omega)sub 1 + N(omega)sub 2. Conditions for these transitions were obtained. In Raman scattering, it was found that coupled scattered light soliton and Langmuir soliton adequately describe the saturation at low laser intensity just above the inhomogeneity threshold. At higher laser intensity, transient, intermittent turbulence results. At a critical laser intensity, the interval for the turbulent transient became infinite-transition to chaos by Crisis from a stable attractor to chaotic attractor much like a phase transition. Thus these numerical solutions of nonlinear partial differential equations give two interesting routes to turbulence. Space-time turbulence is also discussed. Author

N91-28899# Osaka Univ., Suita (Japan). Inst. of Laser Engineering.
NONLINEAR EVOLUTION OF 2D AND 3D RAYLEIGH-TAYLOR INSTABILITY AT STAGNATION PHASE IN LASER IMPLOSION
Katsunobu Nishihara and Hitoshi Sakagami (Institute for Superconducting Research, Tokyo, Japan) *In* National Inst. for Fusion Science, Proceedings of the Second International Toki Conference on Plasma Physics and Controlled Nuclear Fusion. Nonlinear Phenomena in Fusion Plasmas: Theory and Computer Simulation Apr. 1991 p 62-65 (For primary document see N91-28881 20-75)
Avail: NTIS HC/MF A11

Two and three dimensional Rayleigh-Taylor instabilities of the fuel-pusher contact surface in a cylindrically or spherically stagnating system are investigated using of 2-D and 3-D fluid codes, IMPACT-2D and 3-D. Geometrical difference of the free-fall speeds following the saturation of the exponential growth is studied for planer, cylindrical and spherical geometries. Nonlinear made coupling of unstable surface waves is also investigated for a 2-D planer geometry. Author

N91-28900# Ecole Polytechnique, Palaiseau (France). Centre de Physique Theorique.
MODELS OF COLLISIONAL TRANSPORT ACROSS A MAGNETIC FIELD WITH DESTROYED SURFACES
G. Laval *In* National Inst. for Fusion Science, Proceedings of the Second International Toki Conference on Plasma Physics and Controlled Nuclear Fusion. Nonlinear Phenomena in Fusion Plasmas: Theory and Computer Simulation Apr. 1991 p 66-69 (For primary document see N91-28881 20-75)
Avail: NTIS HC/MF A11

Diffusion and heat transport of a collisional plasma across a confinement magnetic field with destroyed surfaces is studied. Only the case where, at the lowest order, the particles diffuse along the field lines is considered, i.e., assume that the mean free path is shorter than the field lines length. It is well known that, in such conditions, theories starting from linearized particle motions do not provide the right answer. Another method is tried by using exactly soluble simple models in which the full non-linearized motion is kept. In the first part, the field and collision models are introduced. These models are not self-consistent and electric fields are entirely neglected. The diffusion coefficient is obtained from a variational form from which convergent approximate solutions can be obtained. In the second part, self-consistent electric fields are introduced and their effect on the transport is estimated. Author

N91-28901# United Kingdom Atomic Energy Authority, Culham (England).
ISSUES IN DIRECT NUMERICAL SIMULATION OF PLASMA TURBULENCE AND TRANSPORT
A. Thyagaraja, W. Arter, and F. A. Haas *In* National Inst. for Fusion Science, Proceedings of the Second International Toki Conference on Plasma Physics and Controlled Nuclear Fusion. Nonlinear Phenomena in Fusion Plasmas: Theory and Computer Simulation Apr. 1991 p 70-73 (For primary document see N91-28881 20-75)
Avail: NTIS HC/MF A11

The problem of direct numerical simulation of plasma turbulence in magnetic confinement systems such as a tokamak is important in gaining a theoretical understanding of anomalous transport of particles, energy, momentum and impurities in such systems. Two approaches to this question are being developed. The design philosophy and the basic numerical problems encountered and solved in the construction of a two-fluid, 3-D, electro-magnetic, finite difference, time evolution code, CUTIE, are outlined. The importance of qualitative consistency, time-reversal, conservation properties, phase mixing, and boundary conditions are illustrated in the context of both passive and active electrostatic turbulence. A separate study was undertaken to aid in the understanding of drift wave turbulence in tokamak plasmas. In this connection a 3-D, time-dependant, electrostatic drift wave code called DRIFT was written. This has features which take account of toroidicity, non-adiabaticity and magnetic shear. The resulting code is very flexible, and was used to solve the Hasegawa-Mima equation efficiently in 2-D. Results from time-dependant, 3-D calculation run on a Cray-2 are presented. The aim is to obtain a proper physical understanding of plasma turbulence in typical tokamak conditions by calculating the power spectra of the turbulent fluctuations and their transport consequences. It is believed that this can only be achieved by a step-by-step approach to the numerics, making sure that the calculated effects represent genuine physics and are not mere artifacts of the numerical simulation. Author

N91-28902# Saskatchewan Univ., Saskatoon. Dept. of Physics.
ANOMALOUS TRANSPORT DUE TO THE SKIN SIZE ELECTROMAGNETIC DRIFT MODE IN TOKAMAKS
Akira Hirose *In* National Inst. for Fusion Science, Proceedings of the Second International Toki Conference on Plasma Physics and Controlled Nuclear Fusion. Nonlinear Phenomena in Fusion Plasmas: Theory and Computer Simulation Apr. 1991 p 74-77 Sponsored by Natural Sciences and Engineering Research Council (For primary document see N91-28881 20-75)
Avail: NTIS HC/MF A11

It is shown that a low Beta (below the magnetohydrodynamic limit) tokamak discharge is unstable against skin size electromagnetic drift mode with a maximum growth rate of the order of the ion acoustic transit frequency. The proposed anomalous electron thermal diffusivity satisfactorily recovers the Chi sub e profiles in three different types of JET discharges and in Tokamak Fusion Test Reactors ohmic discharges. Author

N91-28903# Tokyo Univ. (Japan). Faculty of Science.
MAGNETOHYDRODYNAMICAL FORMATION OF ASTROPHYSICAL JETS FROM GRAVITATIONALLY COLLAPSING OBJECTS Abstract Only c90
Yutaka Uchida *In* National Inst. for Fusion Science, Proceedings of the Second International Toki Conference on Plasma Physics and Controlled Nuclear Fusion. Nonlinear Phenomena in Fusion Plasmas: Theory and Computer Simulation Apr. 1991 p 78 Prepared in cooperation with National Inst. for Fusion Science, Nagoya, Japan (For primary document see N91-28881 20-75)
Avail: NTIS HC/MF A11

It is known that there are jet-like phenomena in a wide variety of astronomical hierarchies, ranging from substellar to galactic, with scales of 10(exp 9) cm in the case of stellar spicule jets, 10(ext 19) cm in the case of star-formation bipolar jets, and 10(exp 23) cm in the case of radio jets and lobes from active galactic nuclei and quasars. These are usually seen to be related with large scale magnetic field in a characteristic way. The case is examined of the bipolar jets in the star formation as an example, and demonstrate that a magnetohydrodynamic mechanism proposed by the present author by noting that the central active objects are gravitationally collapsing objects which brought a part of the large scale magnetic flux with their mass. The central object consisted of the accreting disk with angular momentum rotating around the forming star at the center twists up that part of the magnetic field through the differential rotation in the disk. The model predicts that the jets will be spinning inherent to the magnetic stress involved. This dynamically sweeping pinch character causing spinning jets makes a good contrast with the models proposed thus far: based on the wind from the central object having a negligibly small angular momentum, the jets in the previous models will not show any spinning. Therefore, recent detection of the spinning velocity field in some of the bipolar flows gave a strong support to our magnetic model. The model extended to the case of large scale radio jets and emanated from the central object of active galactic nuclei and quasars. Author

N91-28904# National Inst. for Fusion Science, Nagoya (Japan).
COMPUTER SIMULATION OF SOLAR WIND-MAGNETOSPHERE INTERACTION c92
K. Watanabe, Tetsuya Sato, A. Kageyama, and A. Usadi (Hiroshima Univ., Japan) *In its* Proceedings of the Second International Toki Conference on Plasma Physics and Controlled Nuclear Fusion. Nonlinear Phenomena in Fusion Plasmas: Theory and Computer Simulation Apr. 1991 p 79-82 (For primary document see N91-28881 20-75)
Avail: NTIS HC/MF A11

A 3-D high accuracy magnetohydrodynamic (MHD) simulation code was developed, in which the 4th order Runge-Kutta-Gill method and the direct finite difference method were adopted. A global 3-D MHD simulation of the magnetosphere involving the distant tail (to 100 R sub E) was performed using the new simulation code. Initially, the geomagnetic field is given as the superposition of a dipole field placed at the center of the earth and its mirror image dipole outside the solar boundary. As the solar wind flows from the solar boundary into the simulation box, the initial dipole field is deformed to the magnetosphere configuration, forming the bow shock, magnetopause, polar cusp, plasma sheet, etc. within 1.5 hours. The features of the formed magnetosphere is shown, where the magnetic field lines and solar wind streamlines are drawn for the meridian cross section. Author

N91-28905# Nagoya Univ. (Japan). Plasma Science Center.
RAPID ACCELERATION OF PROTONS IN A NONLINEAR MAGNETOSONIC WAVE AND THEIR ENERGY SPECTRUM c73
Y. Ohsawa and Y. Terashima *In* National Inst. for Fusion Science, Proceedings of the Second International Toki Conference on Plasma Physics and Controlled Nuclear Fusion. Nonlinear Phenomena in Fusion Plasmas: Theory and Computer Simulation Apr. 1991 p 83-86 (For primary document see N91-28881 20-75)
Avail: NTIS HC/MF A11

The prompt proton acceleration to relativistic energies in a large-amplitude magnetosonic wave which can take place in a rather strong magnetic field such that the electron cyclotron frequency is greater than the electron plasma frequency is described. The acceleration time is of the order of the ion cyclotron period. A fully electromagnetic, relativistic particle stimulation shows that the differential energy spectrum of those accelerated protons can be very hard; it can have a truncated power-law form with the spectral index about unity. Using these energy spectra of protons, the energy spectra of gamma rays from the decay of neutral pions are calculated. These results indicate that this mechanism can explain the rapid proton acceleration in solar flares. Author

N91-28906# Gunma Univ., Maebashi (Japan). Dept. of Electronic Engineering.

EFFECT OF PRESSURE ON MODE TRANSITION POINT OF PARTIALLY RELAXED STATES WITH PERIPHERAL LOSS

Yoshiomi Kondoh *In* National Inst. for Fusion Science, Proceedings of the Second International Toki Conference on Plasma Physics and Controlled Nuclear Fusion. Nonlinear Phenomena in Fusion Plasmas: Theory and Computer Simulation Apr. 1991 p 87-90 (For primary document see N91-28881 20-75)
Avail: NTIS HC/MF A11

The well-known beta = 0 Bessel function model configuration was used it to explain the relaxation and the production of the reversed field pinch configuration. The mode transition point from the cylindrical state to the mixed helical one was studied with the use of analytical solutions giving maximum magnetic energy and with the use of an eigenvalue analysis. Author

N91-28907# Waseda Univ., Tokyo (Japan). Dept. of Applied Physics.

RELAXED STATE AND ENTROPY PRODUCTION

T. Kato and T. Furusawa *In* National Inst. for Fusion Science, Proceedings of the Second International Toki Conference on Plasma Physics and Controlled Nuclear Fusion. Nonlinear Phenomena in Fusion Plasmas: Theory and Computer Simulation Apr. 1991 p 91-94 (For primary document see N91-28881 20-75)
Avail: NTIS HC/MF A11

To understand the relaxed states in RFP (Reverse Field Pinch), the thermodynamics of irreversible processes was introduced. Instead of the magnetic energy, the entropy production in the plasma was used. The state if the minimum entropy production subject to the invariant K(sub 0) is determined after the variational calculus with respect to the vector potential A. Author

N91-28908# Hiroshima Univ. (Japan). Faculty of Science.

SIMULATION STUDY OF MHD RELAXATION AND RECONNECTION PROCESSES

Kanya Kusano, Kaito Kunimoto, Mami Kumano, Teruo Tamano, and Tetsuya Sato (National Inst. for Fusion Science, Nagoya, Japan) *In* National Inst. for Fusion Science, Proceedings of the Second International Toki Conference on Plasma Physics and Controlled Nuclear Fusion. Nonlinear Phenomena in Fusion Plasmas: Theory and Computer Simulation Apr. 1991 p 95-97 (For primary document see N91-28881 20-75)
Avail: NTIS HC/MF A11

Several nonlinear processes in fusion plasmas were studied through the use of 3D MHD simulations. In particular, the following subject areas were covered: (1) dynamo and self-sustainment in reverse field pinch; (2) sawtooth activity in tokamak; and (3) the heating and the acceleration in magnetic reconnection process. Author

N91-28909# Gifu Univ. (Japan). Dept. of Electronics and Computer Engineering.

FINITE BETA EQUILIBRIUM FOR A PRESSURE CONFIGURATION

Shinsaku Kajita *In* National Inst. for Fusion Science, Proceedings of the Second International Toki Conference on Plasma Physics and Controlled Nuclear Fusion. Nonlinear Phenomena in Fusion Plasmas: Theory and Computer Simulation Apr. 1991 p 98-101 (For primary document see N91-28881 20-75)
Avail: NTIS HC/MF A11

The equilibrium on the toroidal plasma with a configuration of parabolically increasing pressure is investigated. The critical pressure, affection of uniform transverse field and flux surfaces are investigated and compared to the linearly increasing one. Author

N91-28910# Fukui Univ. (Japan).

APPLICATION OF MATHEMATICA TO ENERGY PRINCIPLE

T. Yamagishi *In* National Inst. for Fusion Science, Proceedings of the Second International Toki Conference on Plasma Physics and Controlled Nuclear Fusion. Nonlinear Phenomena in Fusion Plasmas: Theory and Computer Simulation Apr. 1991 p 102-105 (For primary document see N91-28881 20-75)
Avail: NTIS HC/MF A11

Magnetohydrodynamic equilibrium and stability analysis need laborious analytical works particularly in nonlinear problems and in non-symmetric systems. Most of such analytical works are substitutions of equations, performing the dot and cross products, elimination of variables, differentiations and integrations, which may be carried out by computer. Applications of Mathematica are presented to the derivation of nonlinear perturbations and evaluation of the plasma energy. The following topics are included: formal theory, energy principle, and nonlinear theory. Author

N91-28911# Tokyo Univ. (Japan). Dept. of Nuclear Engineering.

DIRECT ION HEATING IN MHD RELAXATION Abstract Only

Z. Yoshida *In* National Inst. for Fusion Science, Proceedings of the Second International Toki Conference on Plasma Physics and Controlled Nuclear Fusion. Nonlinear Phenomena in Fusion Plasmas: Theory and Computer Simulation Apr. 1991 p 106 (For primary document see N91-28881 20-75)
Avail: NTIS HC/MF A11

Dissipative power depositions through MHD relaxation into electrons and ions have been studied using classical resistivity and viscosity coefficients. In the reconnection process, perturbation currents (electron flow) and perturbation vortices (ion flow) are dissipated by resistivity and viscosity, respectively. An excess of electromagnetic energy is released through the MHD relaxation process. It is shown that the energy dissipation in the MHD relaxation process is dominated by the ion viscosity. Author

N91-28912# Nagoya Univ., Toyokawa (Japan). Solar-Terrestrial Environment Lab.

HELICAL FIELD EFFECT IN SOLAR/STELLAR WIND c92

Haruichi Washimi *In* National Inst. for Fusion Science, Proceedings of the Second International Toki Conference on Plasma Physics and Controlled Nuclear Fusion. Nonlinear Phenomena in Fusion Plasmas: Theory and Computer Simulation Apr. 1991 p 107-110 (For primary document see N91-28881 20-75)
Avail: NTIS HC/MF A11

Structure of the solar/stellar wind plasma and the helical magnetic field are studies by means of MHD simulation in an axisymmetrical system. It is shown that, when the stellar rotation is much faster than the solar rotation, the magnetic pressure force works and the interplanetary current is pinched along the rotation axis and the equatorial plane. Author

N91-28913# Aichi Univ. of Education (Japan). Dept. of Earth Sciences.

SELF-SIMILAR EVOLUTION OF NONLINEAR MAGNETIC BUOYANCY INSTABILITY

K. Shibata, T. Tajima, and R. Matsumoto (Chiba Univ., Japan) *In* National Inst. for Fusion Science, Proceedings of the Second International Toki Conference on Plasma Physics and Controlled Nuclear Fusion. Nonlinear Phenomena in Fusion Plasmas: Theory and Computer Simulation Apr. 1991 p 111-114 (For primary

document see N91-28881 20-75)
Avail: NTIS HC/MF A11

A new type of self-similar solution of ideal magnetohydrodynamics in the nonlinear stage of undular mode of magnetic buoyancy instability (Parker instability or ballooning instability) is found through MHD simulation and theory. The solution has the characteristics of nonlinear instability in Lagrangian coordinates; the fluid velocity and the Alfven speed on each magnetic loop increases exponentially with time, because the loop is evacuated by the field aligned motion of matter due to gravitational acceleration. Author

N91-28914# Osaka Univ., Suita (Japan). Inst. of Laser Engineering.
TURBULENT MIXING DUE TO RAYLEIGH-TAYLOR INSTABILITY IN LASER DRIVEN IMPLOSION **c36**
H. Takabe and A. Yamamoto *In* National Inst. for Fusion Science, Proceedings of the Second International Toki Conference on Plasma Physics and Controlled Nuclear Fusion. Nonlinear Phenomena in Fusion Plasmas: Theory and Computer Simulation Apr. 1991 p 115-118 (For primary document see N91-28881 20-75)
Avail: NTIS HC/MF A11

A simple, nonlinear diffusion model is proposed to describe the turbulent mixing generated in the laser driven implosion through the Rayleigh-Taylor instability. The model is applied to simulate the recent high density implosion experiment done at Osaka. It is demonstrated that the introduction of mixing model into the implosion code can well reproduce the experimental results as for neutron yields and maximum (pho)R. Author

N91-28915# Japan Atomic Energy Research Inst., Tokyo.
ELECTROSTATIC PARTICLE SIMULATIONS OF DENSITY AND TEMPERATURE DRIVEN MODES IN A TOROIDAL PLASMA
M. J. LeBrun, G. Furnish, and T. Tajima (Texas Univ., Austin.) *In* National Inst. for Fusion Science, Proceedings of the Second International Toki Conference on Plasma Physics and Controlled Nuclear Fusion. Nonlinear Phenomena in Fusion Plasmas: Theory and Computer Simulation Apr. 1991 p 119-122 (For primary document see N91-28881 20-75)
Avail: NTIS HC/MF A11

Simulation runs of the toroid plasma in the presence of density and temperature profiles were performed with the toroidal particle code. These calculations are fully self-consistent (electrostatic) and nonlinear, using drift dynamics electrons and full dynamics ions in a toroidal metric. Results are presented from runs using kinetic electrons, which show strong (marginally stable or unstable) modes. Author

N91-28916# Yamaguchi Univ. (Japan).
INTERNAL KINK MODE SIMULATION BY 3-D GYROKINETIC CODE
H. Naitou, O. Fukumasa, R. D. Sydora, and W. W. Lee (Princeton Univ., NJ.) *In* National Inst. for Fusion Science, Proceedings of the Second International Toki Conference on Plasma Physics and Controlled Nuclear Fusion. Nonlinear Phenomena in Fusion Plasmas: Theory and Computer Simulation Apr. 1991 p 123-126 (For primary document see N91-28881 20-75)
Avail: NTIS HC/MF A11

Three-dimensional ideal MHD simulations with kinetic modifications are possible by the use of the 3-D gyrokinetic particle code which follows a self-consistent and energy conserving set of nonlinear gyrokinetic equations. Nonlinear evolution of internal kink modes in a straight tokamak were simulated by this code. The used model is a rectangular tokamak being periodic in the z-direction and surrounded by a perfectly conducting wall. Author

N91-28917# National Inst. for Fusion Science, Nagoya (Japan).
PARTICLE SIMULATION ON THE TILT STABILIZATION OF THE FRC PLASMA
Ritoku Horiuchi and Tetsuya Sato *In its* Proceedings of the Second International Toki Conference on Plasma Physics and Controlled Nuclear Fusion. Nonlinear Phenomena in Fusion Plasmas: Theory and Computer Simulation Apr. 1991 p 127-130 (For primary document see N91-28881 20-75)
Avail: NTIS HC/MF A11

Ion kinetic stabilization of the FRC (Field Reversed Configuration) tilt disruption is investigated by means of 3-D particle simulation. The growth rate of the tilting instability decreases as the parameter bar-s decreases and the instability is completely suppressed when bar-s approximately 1, where bar-s measures the number of ion gyroradii between the magnetic separatrix line and the field-null line. It is found that this kinetic stabilization is attributed to the characteristics of the meandering ions which execute an oscillatory motion with a large amplitude around the field-null point and carry most of the ion toroidal current. Author

N91-28918# National Inst. for Fusion Science, Nagoya (Japan).
THE 3-D ELECTROMAGNETIC MACROSCALE PARTICLE SIMULATION OF INHOMOGENEOUS, MAGNETIZED PLASMAS
Motohiko Tanaka *In its* Proceedings of the Second International Toki Conference on Plasma Physics and Controlled Nuclear Fusion. Nonlinear Phenomena in Fusion Plasmas: Theory and Computer Simulation Apr. 1991 p 131-134 (For primary document see N91-28881 20-75)
Avail: NTIS HC/MF A11

An electromagnetic 'kinetic-MHD' simulation technique - Macroscale Particle Code (MPC) - was developed. The macroscale particle code is essentially an implicit particle code. The characteristics of the MACROS code are summarized. The MACROS code properly treats low frequency electromagnetic and electrostatic waves and structures. Hence Landau and cyclotron resonances are retained on top of the particle orbit effects. Moreover, the code is numerically stable in nonlinear regimes and energy conservation is acceptably good. These characteristics make this code suitable for the study of large-scale kinetic plasma problems. Author

N91-28919# Hiroshima Univ. (Japan). Faculty of Science.
STUDY OF KINK INSTABILITY AND CURRENT RELAXATION BY THREE DIMENSIONAL MACROSCALE PARTICLE SIMULATION
H. Takamaru, Motohiko Tanaka, and Tetsuya Sato (National Inst. for Fusion Science, Nagoya, Japan) *In* National Inst. for Fusion Science, Proceedings of the Second International Toki Conference on Plasma Physics and Controlled Nuclear Fusion. Nonlinear Phenomena in Fusion Plasmas: Theory and Computer Simulation Apr. 1991 p 135-138 (For primary document see N91-28881 20-75)
Avail: NTIS HC/MF A11

Using the macroscale particle simulation code (MACROS code), the authors were able to study nonlinear particle transport on the magnetohydrodynamics (MHD) (large time and space) scales. The authors apply a semi-implicit version of the MACROS code to problems with a change in the magnetic field structure. They first study qualitatively and quantitatively a pure MHD phenomenon, an ideal kink instability (m/n equals 1/1). A simple tokamak system with no toroidal effect is used to simulate the time evolution of the instability starting from a typical initial configuration. They observe an occurrence of the kink instability whose growth rate gamma MACROS given by the MACROS code takes a value up to, but not greater than twice the linear-analytical value of gamma linear. Secondly, they study a current relaxation process from an initial non-equilibrium to a force-free like equilibrium configuration. They find that kinetic effects may contribute to the relaxation process of the magnetic field current system. Author

N91-28920# Hiroshima Univ. (Japan). Faculty of Science.
NONADIABATIC BEHAVIOR OF THE MAGNETIC MOMENT OF A CHARGED PARTICLE IN A DIPOLE MAGNETIC FIELD **c72**
S. Murakami, Tetsuya Sato, and A. Hasegawa (Bell Telephone Labs., Inc., Murray Hill, NJ.) *In* National Inst. for Fusion Science, Proceedings of the Second International Toki Conference on Plasma Physics and Controlled Nuclear Fusion. Nonlinear Phenomena in Fusion Plasmas: Theory and Computer Simulation

Apr. 1991 p 139-142 (For primary document see N91-28881 20-75)
Avail: NTIS HC/MF A11

Non-adiabatic behavior of the magnetic moment of a charged particle in a dipole magnetic field is studied both numerically and analytically in the presence of a low frequency electrostatic wave with azimuthal component. The authors obtained numerically two characteristic conditions for the breakdown of mu; one is independent of the wave frequency, and the other forms a spike-like structure in the wave frequency-particle energy space. They showed analytically that the former is caused by the direct interaction between the particle and the electrostatic wave during the gyromotion and that the latter is caused by two kinds of resonances, i.e., the bounce-E x B drift resonance and the wave-drift resonance. The unstable conditions obtained by theoretical consideration showed good agreements with those of numerical results. Author

N91-28921# Japan Atomic Energy Research Inst., Ibaraki.
NUMERICAL STUDY OF ION TEMPERATURE GRADIENT MODES IN A TOKAMAK Abstract Only
Masatoshi Yagi and Masafumi Azumi *In* National Inst. for Fusion Science, Proceedings of the Second International Toki Conference on Plasma Physics and Controlled Nuclear Fusion. Nonlinear Phenomena in Fusion Plasmas: Theory and Computer Simulation Apr. 1991 p 143 (For primary document see N91-28881 20-75)
Avail: NTIS HC/MF A11

Understanding of anomalous transport processes in a tokamak is the key issue for improving the energy confinement and realizing a fusion reactor. From this point of view, the microturbulence caused by ion temperature gradient modes (eta sub i) has been extensively studied as a possible candidate for degrading the ion energy confinement. Some recent experimental results, however, show that the energy confinement time does not differ from the standard one even when eta(sub i) becomes much greater than the threshold value; that is, the eta(sub i) mode is linearly unstable. These results suggest that, when we employ the quasilinear expression of ion thermal flux as q sub i equals (e theta/T sub i)(2)F(n sub e,T sub i, ...)(eta sub i-eta sub i=(crit))(1/2), the numerical factors such as the saturation level and the value of function F may change, depending on the change of plasma parameters. The authors are now studying the three different regimes of eta(sub i) modes, based on the fluid model by Horton. The first regime is the normal density profile case (positive eta sub i modes), which is related with the standard L-mode confinement. The second regime is the flat density profile case (weak density gradient eta sub i modes), which is related with the H-mode confinement. The third regime is the flat density profile case (negative eta sub i modes), which is considered to be related with phenomena observed in H-mode discharges in D-III-D. By the kinetic theory based on the weak turbulent approximation, Harm and his coworkers found that the saturation level of the negative eta sub i mode does not show the strong dependence on the eta sub i parameter. The authors are now checking their results in the framework of the fluid model. The authors also discuss the relationship between the result of nonlinear fluid simulations and the tokamak transport analysis. Author

N91-28922# National Inst. for Fusion Science, Nagoya (Japan).
NONLINEAR BEHAVIOR AND TRANSPORT PROPERTY OF MULTIPLE-HELICITY RESISTIVE INTERCHANGE MODES NEAR MARGINALLY STABLE STATES
H. Sugama *In its* Proceedings of the Second International Toki Conference on Plasma Physics and Controlled Nuclear Fusion. Nonlinear Phenomena in Fusion Plasmas: Theory and Computer Simulation Apr. 1991 p 144-147 (For primary document see N91-28881 20-75)
Avail: NTIS HC/MF A11

Reduced magnetohydrodynamic (MHD) model equations are presented which describe resistive interchange modes. Since low beta plasma in the peripheral region is being considered, an electrostatic approximation is used in the equations. Also, the primary concern of this representation is with the transport of the stationary state in which the time variation of the magnetic field vanishes along with that of the other physical variables. Model equations are obtained in non-dimensional variables and the electrostatic potential and pressure fluctuation are expanded into Fourier series. Author

N91-28923# National Inst. for Fusion Science, Nagoya (Japan).
NONLINEAR COMPUTER ANALYSIS OF BACKWARD WAVE OSCILLATOR c33
T. Watanabe, K. Ogura, M. M. Ali, M. Itakura, and K. Minami (Niigata Univ., Japan) *In its* Proceedings of the Second International Toki Conference on Plasma Physics and Controlled Nuclear Fusion. Nonlinear Phenomena in Fusion Plasmas: Theory and Computer Simulation Apr. 1991 p 148-153 (For primary document see N91-28881 20-75)
Avail: NTIS HC/MF A11

A new treatment for nonlinear analysis for a backward wave oscillator is developed. A new scheme, Higher order Implicit Difference Method (HIDM), used to solve partial differential equations, is applied to study the propagation of electromagnetic waves in a corrugated wave guide and their coupling with relativistic electron beam. The computational results are compared with the linear dispersion relation and good agreement is obtained. Author

N91-28924# Tsukuba Univ. (Japan). Plasma Research Center.
MODE CONVERSION OF ALFVEN WAVES INDUCED BY QUADRUPOLE MAGNETIC FIELD MODULATION c33
H. Hojo, M. Inutake, M. Ichimura, and S. Miyoshi *In* National Inst. for Fusion Science, Proceedings of the Second International Toki Conference on Plasma Physics and Controlled Nuclear Fusion. Nonlinear Phenomena in Fusion Plasmas: Theory and Computer Simulation Apr. 1991 p 154-157 Sponsored in part by Ministry of Education, Science and Culture (For primary document see N91-28881 20-75)
Avail: NTIS HC/MF A11

A new type of the mode conversion of Alfven waves in the ion cyclotron range of frequency (ICRF) is presented, which is induced by the spatial modulation of a quadrupole magnetic filed. It is shown that the physical mechanism is analogous to a resonant parametric mode coupling; the coupling coefficient depends on the ellipticity of the cross section of flux surface and vanishes when the magnetic field is axisymmetric. Mode conversion of waves in a plasma is an important elementary process of plasma heating by waves. Recently a large number of theoretical studies on mode conversion have been done in the ion cyclotron range of frequency (ICRF) and in the electron cyclotron resonance heating (ECRH). Here, researchers present a new type of the mode conversion of Alfven waves in ICRF. They show here that one Alfven mode can convert to another Alfven mode due to the spatial modulation of a quadrupole magnetic field. They obtain coupled mode equations between two Alfven waves via the spatial quadrupole field modulation. If we suppose the quadrupole magnetic field modulation as a virtual mode, we can see that the conversion process is analogous to a resonant parametric mode coupling among two Alfven and the virtual modes. The solutions of the coupled mode equations show that the efficient mode conversion takes place when a resonant condition with respect to an axial wavenumber among these modes is satisfied. The authors study the mode conversion of Alfven waves propagating in a quadrupole magnetic field geometry. The basic equation to be analyzed, a Maxwell's wave equation, is given. Author

N91-28925# Tohoku Univ., Sendai (Japan). Dept. of Electrical Engineering.
NUMERICAL SIMULATION OF POTENTIAL-DRIVEN ION CYCLOTRON OSCILLATION c33
S. Ishiguro, K. Nakagawa, and N. Sato *In* National Inst. for Fusion Science, Proceedings of the Second International Toki Conference on Plasma Physics and Controlled Nuclear Fusion. Nonlinear Phenomena in Fusion Plasmas: Theory and Computer

Simulation Apr. 1991 p 158-161 (For primary document see N91-28881 20-75)
Avail: NTIS HC/MF A11

Using a two-dimensional electrostatic particle simulation code, the authors study the ion cyclotron oscillation driven by applying a positive potential to a small electrode in a magnetized plasma. It is confirmed that a direct plasma response to a two-dimensional potential structure is essential. Author

N91-28926# Kyushu Univ., Fukuoka (Japan). Dept. of Physics.
DYNAMICS OF INTERFACES WITH INTERNAL STRUCTURES **c33**
Toshihiro Kawakatsu and Kyozi Kawasaki *In* National Inst. for Fusion Science, Proceedings of the Second International Toki Conference on Plasma Physics and Controlled Nuclear Fusion. Nonlinear Phenomena in Fusion Plasmas: Theory and Computer Simulation Apr. 1991 p 162-163 (For primary document see N91-28881 20-75)
Avail: NTIS HC/MF A11

The authors develop computer simulation methods dealing with dynamical models for interfaces (or discontinuity) having internal structures, where for instance, other particles are attracted to the discontinuities. The model presented proves to be convenient for the study of the dynamics of systems containing surfactant particles. The authors show that the surfactant particles have an important role in phase separation processes. Such a feature should be utilized in controlling the phase separation processes in immiscible fluids. Author

N91-28927# National Inst. for Fusion Science, Nagoya (Japan).
NONLINEAR EQUATIONS FOR WEAKLY UNSTABLE MODES **c33**
N. Nakajima *In its* Proceedings of the Second International Toki Conference on Plasma Physics and Controlled Nuclear Fusion. Nonlinear Phenomena in Fusion Plasmas: Theory and Computer Simulation Apr. 1991 p 164-167 (For primary document see N91-28881 20-75)
Avail: NTIS HC/MF A11

For some interesting nonlinear systems, the eigenvalue in the linearized system is degenerate, i.e., there are a number eigenfunctions for a single eigenvalue. For a nondegenerate case, two types of nonlinear equation are derived by applying the perturbation theory to weakly unstable models near the marginally stable states together with the multiple-time-scale expansion. This method is extended to degenerate cases. Author

N91-28928# Tokyo Inst. of Tech. (Japan). Dept. of Applied Physics.
HOLE DYNAMICS OF ONE-DIMENSIONAL PLASMA Abstract Only **c33**
K. Kitahara, N Ishibashi,, and K. Tanno *In* National Inst. for Fusion Science, Proceedings of the Second International Toki Conference on Plasma Physics and Controlled Nuclear Fusion. Nonlinear Phenomena in Fusion Plasmas: Theory and Computer Simulation Apr. 1991 p 168 (For primary document see N91-28881 20-75)
Avail: NTIS HC/MF A11

Although steady state solutions of the Vlasov equation are known as BGK solutions, the stability of these solutions is not fully investigated. So, the authors performed an exact particle simulation in order to see the dynamics of holes in phase space. Dawson's model of electron sheets in the uniform positive background is transformed into an 2N-dimensional discrete-time mapping, which can be treated numerically exactly. The formation and persistence of a big hole from two-stream instability is analyzed. Author

N91-28929# Chubu Univ., Kasugai (Japan). Dept. of Engineering.
SHOCK AND SOLITON STRUCTURES INDUCED BY POLOIDAL FLOW IN TOKAMAKS Abstract Only
T. Taniuti, K. Watanabe, Y. Ishii, and M. Wakatani (Kyoto Univ., Japan) *In* National Inst. for Fusion Science, Proceedings of the Second International Toki Conference on Plasma Physics and Controlled Nuclear Fusion. Nonlinear Phenomena in Fusion Plasmas: Theory and Computer Simulation Apr. 1991 p 169 (For primary document see N91-28881 20-75)
Avail: NTIS HC/MF A11

When poloidal flow velocity, Up, becomes close to epsilon C sub s in tokamaks, fluid motion inside the flux surface is governed by a forced KdV equation in the small dissipation limit, where epsilon is an inverse aspect ratio and C sub s is a sound velocity. This implies that a stationary soliton structure appears at the inside region of toroidal plasma or theta is approx. pi, where theta is a poloidal angle. In the limit of large dissipation a forced Burgers equation is more appropriate. This case corresponds to an appearance of shock structure. When an averaged poloidal flow velocity is very close to epsilon C sub s, a shock may be seen in the outer region of toroidal plasma or theta is approx. 0. With the increase of the absolute vakue of (Up-epsilon C sub s) the shock position moves from theta is approx. 0 to theta is approx. pi. Recent tokamak experiments show the existence of poloidal flow with Up is approx. epsilon C sub s in the transition phase from L mode to H mode. Implications of the results in the experiment are discussed. Author

N91-28930# Tokyo Univ. (Japan). Dept. of Applied Physics.
SOLITON PHENOMENA IN ELECTRON BEAM PLASMA
Tetsu Yajima *In* National Inst. for Fusion Science, Proceedings of the Second International Toki Conference on Plasma Physics and Controlled Nuclear Fusion. Nonlinear Phenomena in Fusion Plasmas: Theory and Computer Simulation Apr. 1991 p 170-173 (For primary document see N91-28881 20-75)
Avail: NTIS HC/MF A11

As a model equation for an electron beam plasma system, the unstable nonlinear Schrodinger (UNS) equation, iq sub x plus q sub tt plus 2/q/(2)q equals 0, is proposed. Recent works on this equation are reported. The UNS equation is a canonical equation which describes nonlinear modulations of wave amplitude in unstable media. In the electron beam plasma system, near the critical wave number, the wave amplitude obeys the UNS equation. Results derived by investigating this equation show that solitons can be caused in the system. In addition, the role of solitons in unstable media is clarified. Author

N91-28931# Nagoya Univ. (Japan). Dept. of Physics.
POINT VORTEX DESCRIPTION OF A MODON SOLUTION **c64**
Chihiro Matsuoka and Kazuhiro Nozaki *In* National Inst. for Fusion Science, Proceedings of the Second International Toki Conference on Plasma Physics and Controlled Nuclear Fusion. Nonlinear Phenomena in Fusion Plasmas: Theory and Computer Simulation Apr. 1991 p 174-176 (For primary document see N91-28881 20-75)
Avail: NTIS HC/MF A11

Using the point vortex approximation, an exact solution corresponding to a modon solution in the Hasegawa-Mima equation is obtained. The stability of this solution is discussed. Author

N91-28932# National Inst. for Fusion Science, Nagoya (Japan).
STRUCTURES OF MAGNETIC FIELD LINES IN THE HELICAL TORUS
T. Hatori and T. Watanabe *In its* Proceedings of the Second International Toki Conference on Plasma Physics and Controlled Nuclear Fusion. Nonlinear Phenomena in Fusion Plasmas: Theory and Computer Simulation Apr. 1991 p 177-179 (For primary document see N91-28881 20-75)
Avail: NTIS HC/MF A11

The equation of a magnetic field line can be written in the form of a Hamiltonian equation. An explicit form for the Hamiltonian applicable to the first order of rho/R is obtained, where Rho and R are minor and major radii. Author

N91-28933# National Inst. for Fusion Science, Nagoya (Japan).
REGULAR MOTION AND SYMMETRY IN THE RELATIVISTIC STANDARD MAP
Y. Nomura, Yoshi H. Ichikawa, and W. Horton (Texas Univ.,

Austin.) *In its* Proceedings of the Second International Toki Conference on Plasma Physics and Controlled Nuclear Fusion. Nonlinear Phenomena in Fusion Plasmas: Theory and Computer Simulation Apr. 1991 p 180-183 (For primary document see N91-28881 20-75)
Avail: NTIS HC/MF A11

In nonlinear dynamical systems, area-preserving maps were investigated extensively as a useful method for characterizing the non-integrable Hamiltonian systems. Especially, the nonrelativistic acceleration of charged particles by an infinite sequence of constant amplitude longitudinal waves with equally spaced phase velocities is represented by the standard map. This map exhibits regular and chaotic motion and was studied in various fields of physics. The central problem of the standard map is a transport process under the coexistence of regular motion and chaos. Recently, Chernikov et al., introduced the relativistic generalization of the standard map. The chaotic motion is restricted to the vicinity of the fixed points and the breakup of the last KAM torus occurs at higher wave amplitude than that for the standard map. The purpose is to clarify the relativistic effects on the nonlinear motion of particles by varying the wave phase velocity in a wide range and to discuss properties of the regular motion by constructing the families of symmetry lines. Author

N91-28934# Nagoya Univ. (Japan). Dept. of Physics.
DIFFUSION AND RELAXATION IN HAMILTONIAN CHAOS
Tetsuro Konishi *In* National Inst. for Fusion Science, Proceedings of the Second International Toki Conference on Plasma Physics and Controlled Nuclear Fusion. Nonlinear Phenomena in Fusion Plasmas: Theory and Computer Simulation Apr. 1991 p 184-186 (For primary document see N91-28881 20-75)
Avail: NTIS HC/MF A11

Chaos in Hamiltonian systems have great importance in fundamental physics as a basis of classical statistical mechanics, as well as in application to plasma physics and solid state physics. Some results are introduced on the properties of global diffusion for Hamiltonian systems with many degrees of freedom, through numerical studies on coupled map lattices. Many important facts were revealed for the chaos in area preserving mappings. The phase space of area preserved mapping is filled with self-similar structure of islands and cantori, which are related to dynamical properties such as anomalous diffusion and flicker noise. Such delicate structures are expected to smear out when the number of degrees of freedom increases. The main topic is whether making the system size large enhances the chaos and diffusion. The models are (1) standard map and (2) symplectic version of the coupled map lattices. The anomalous diffusion is observed both for area preserving mappings and for systems with many degrees of freedom, reflecting the self similar structures of phase spaces. In both cases, however, they are transients appearing only for a finite time. Crossover from anomalous to normal diffusion has its origin in array-like arrangement of equivalent hierarchies of island chains in phase space, and are common to low dimensional and high dimensional systems. Author

N91-28935# Joint European Torus Project, Abingdon (England).
NON-LINEAR BEHAVIOUR IN TOKAMAKS
J. A. Wesson *In* National Inst. for Fusion Science, Proceedings of the Second International Toki Conference on Plasma Physics and Controlled Nuclear Fusion. Nonlinear Phenomena in Fusion Plasmas: Theory and Computer Simulation Apr. 1991 p 187-193 (For primary document see N91-28881 20-75)
Avail: NTIS HC/MF A11

From the many nonlinear processes occurring in tokamaks, three quite different phenomena were chosen. Firstly presented is the problem of fast instabilities which are quite subtle and require some new thinking. Secondly, disruptions are presented which are found to be rather complex. Finally, an analysis of the Kadomtsev reconnection models is presented which leads to doubts about the applicability of the resistive Ohm's law and suggests that the effect of electron inertia would be predominant. Author

N91-28936# Japan Atomic Energy Research Inst., Ibaraki.
FLUCTUATION SPECTRUM OF ION TEMPERATURE GRADIENT DRIVEN MODES IN SHEARED MAGNETIC FIELDS
Takashi Tuda, Masatoshi Yagi, and Masafumi Azumi *In* National Inst. for Fusion Science, Proceedings of the Second International Toki Conference on Plasma Physics and Controlled Nuclear Fusion. Nonlinear Phenomena in Fusion Plasmas: Theory and Computer Simulation Apr. 1991 p 194-197 (For primary document see N91-28881 20-75)
Avail: NTIS HC/MF A11

The electrostatic fluctuation due to the ion temperature gradient driven model is considered to cause the anomalous ion heat transport in L-mode discharges of a tokamak. Because of importance of this mode on the present day tokamak, the linear properties and the nonlinear saturation mechanism of the mode were studied. However, understanding on the saturation mechanism, the estimated fluctuation level and also the spectrum shape is not still satisfactory and the resulting expressions for the heat transport do now always agree with experimental results in the wide range of discharge parameters until now. For these reasons, several kinds of fluid simulation models were developed, which include the toroidal effect, neoclassical effects, and the impurity ion response, in order to investigate the ion temperature gradient driven mode in various situations and to analyze the experimental fluctuation measurements. Author

N91-28937# Chalmers Univ. of Technology, Goeteborg (Sweden). Inst. for Electromagnetic Field Theory and Plasma Physics.
EQUILIBRIA AND DYNAMICS OF TEMPERATURE IN A FUSION REACTOR PLASMA
Hans Wilhelmsson *In* National Inst. for Fusion Science, Proceedings of the Second International Toki Conference on Plasma Physics and Controlled Nuclear Fusion. Nonlinear Phenomena in Fusion Plasmas: Theory and Computer Simulation Apr. 1991 p 198-201 (For primary document see N91-28881 20-75)
Avail: NTIS HC/MF A11

Reaction-diffusion equations were studied by means of a new technique, the central expansion, which simultaneously accounts for the process of diffusion and the effects of sources, losses (represented by different powers of the temperature) as well as the effects of the boundaries. Various possibilities are discussed using new results from the central expansion analysis for describing the dynamics of complicated realistic systems. The procedure of how these results can be obtained by means of the central expansion is described in detail. It may be useful in this connection to consider the accompanying scheme of analysis. The starting point in the process of analysis is to construct a certain form of expansion, which for radially symmetric (or spatially symmetric one-dimensional) profiles contains terms of increasing powers of the spatial variable squared, where the terms have time-dependent coefficients. The expansion can be expressed as a product of the central value (amplitude) A(t) and a series in powers of chi squared. By proper account of the flux conditions at the boundary the effects of the boundary can be included directly in the form of the expansion. The next step is to introduce the expansion into the original reaction-diffusion equation, and to carry out the differentiations in space and time and the expansions of the powers in the source and loss terms. Matching separately the terms which do not depend on chi squared as well as the chi squared terms and the chi(exp 4) terms one obtains as a result of the three coupled nonlinear first order differential equations in time for the time-dependent variables, as indicated in the scheme of analysis. Author

N91-28938# Institute for Plasma Research, Gandhingar (India).
MODEL FOR MARFE-DETACHED PLASMA TRANSITION IN TOKAMAKS Abstract Only
P. K. Kaw, S. Deshpande, K. Avinash, and S. Rath *In* National Inst. for Fusion Science, Proceedings of the Second International Toki Conference on Plasma Physics and Controlled Nuclear Fusion. Nonlinear Phenomena in Fusion Plasmas: Theory and Computer

Simulation Apr. 1991 p 202 (For primary document see N91-28881 20-75)
Avail: NTIS HC/MF A11

The nonlinear saturated state of the radiative thermal-condensation instability responsible for the phenomenon of marfes observed in the tokamak edge plasmas was investigated. In essence, the problem is one of studying two-dimensional thermal equilibria in the Tokamak edge where perpendicular and parallel heat conduction balances the radiated power and heat flux to the limiter. In certain reasonable limits, the relevant nonlinear Poisson's equation can be solved exactly and the solution displays many features of the observed marfe-detached plasma transition. Numerical results which take realistic temperature dependences for thermal conductivity coefficients and generally accepted coronal radiation model are also presented. Author

N91-28939# Princeton Univ., NJ. Plasma Physics Lab.

PROPAGATION OF DRIFT WAVES IN TOROIDAL PLASMA SYSTEMS Abstract Only

S. Yoshikawa and C. Z. Cheng *In* National Inst. for Fusion Science, Proceedings of the Second International Toki Conference on Plasma Physics and Controlled Nuclear Fusion. Nonlinear Phenomena in Fusion Plasmas: Theory and Computer Simulation Apr. 1991 p 203 (For primary document see N91-28881 20-75)
Avail: NTIS HC/MF A11

Drift wave patterns in toroidal plasmas are studied. The dispersion relation was simplified to retain both the shear and the toroidal coupling effects. Since the dispersion relation does not depend on the toroidal angle, phi, the dispersion is solved in the two-dimensional space made up with minor radius and poloidal angle. The dispersion relation can be reduced into second-order, partial differential equations of a hyperbolic type. The one-dimensional convective mode analysis, which was originated in the 1960s, was extended into the two-dimensional analysis. Depending on the strength of the magnetic shear, one can obtain either the convective or the localized solutions. The results show that the plasma is expected to be unstable for large azimuthal mode number and that the plasma instability tends to be more stabilized for large mass ions. Author

N91-28940# Princeton Univ., NJ. Plasma Physics Lab.

STATISTICAL MECHANICS USING SYMBOLIC DYNAMICS **c65**

Roscoe B. White and Alexander B. Rechester (Massachusetts Inst. of Tech., Cambridge.) *In* National Inst. for Fusion Science, Proceedings of the Second International Toki Conference on Plasma Physics and Controlled Nuclear Fusion. Nonlinear Phenomena in Fusion Plasmas: Theory and Computer Simulation Apr. 1991 p 204-207 (For primary document see N91-28881 20-75)
(Contract DE-AC02-76CH-03073)
Avail: NTIS HC/MF A11

Symbolic dynamics provides a means of partitioning phase space so that information concerning the particle orbits is embedded in the partitioning. Consider a sequence of numbers x(sub 0), x(sub 1), x(sub 2)...given by the dynamics, which is called an orbit, the subscript referring to time. Define a sequence of integers s(sub 0), s(sub 1), s(sub 2)...associated with this orbit. If there is a unique correspondence between the symbol sequence and the orbit as the length of the orbit becomes infinite, then the set of such allowed sequences entirely describes the dynamics. Many examples of symbolic dynamics are known, the simplest being that associated with the logistic map, which exhibits the period doubling route to chaos. The map is used as an example, but the methods are similar also for two dimensional maps such as the Henon map and the Chirikov-Taylor map, which were also investigated. Author

N91-28941# California Univ., Berkeley. Dept. of Electrical Engineering and Computer Science.

DIFFUSION THROUGH STOCHASTIC WEBS IN TWO AND MORE DIMENSIONS

Allan J. Lichtenberg *In* National Inst. for Fusion Science, Proceedings of the Second International Toki Conference on Plasma Physics and Controlled Nuclear Fusion. Nonlinear Phenomena in Fusion Plasmas: Theory and Computer Simulation Apr. 1991 p 208-211 (For primary document see N91-28881 20-75)
(Contract N00014-84-K-0367; NSF ECS-85-17364)
Avail: NTIS HC/MF A11

Hamiltonian systems of couples oscillators or their related area preserving mappings will have a connected web of stochasticity in the action space if the system has three or more degrees of freedom. This intrinsic property of higher dimensional systems is known as the Arnold web and the diffusion through the web is called Arnold diffusion. A connected web of stochasticity can also be obtained in two degrees of freedom from a mapping derived from a linear oscillator that is perturbed by a periodic force which is harmonically related to the linear oscillator. However, the phase space topology and the diffusion are quite different in the two degree of freedom system than in the higher degree system. The topology and diffusion rate through a stochastic web in two degrees of freedom is quite different from the Arnold diffusion in higher degrees of freedom. Nevertheless, the ergodic assumption of the uniformity of an equilibrium stochastic phase space of a Hamiltonian system can be applied to both systems to relate local to global diffusion. The results of the three degree coupled standard maps can be extended to higher degree coupled mappings. Strong coupling can also be investigated numerically, but the results lose their straightforward interpretation from the three resonance model. B.G.

N91-28942# Duesseldorf Univ. (Germany, F.R.).

FORMATION AND DYNAMICS OF SOLITARY WAVES AND VORTICES IN DRIVEN AND DAMPED SYSTEMS **c34**

K. H. Spatschek, P. Heiermann, E. W. Laedke, V. Naulin, and H. Pietsch *In* National Inst. for Fusion Science, Proceedings of the Second International Toki Conference on Plasma Physics and Controlled Nuclear Fusion. Nonlinear Phenomena in Fusion Plasmas: Theory and Computer Simulation Apr. 1991 p 212-215 (For primary document see N91-28881 20-75)
Avail: NTIS HC/MF A11

In the first (introductory) part, near-integral model equations which allow spatially coherent solutions with temporal chaos are reviewed. In the second (main) part, this contribution focuses on nonlinear drift waves. The adequate model equations in simple (density and temperature) inhomogeneous situations are presented. Without driving and damping, the stability of spatially coherent structures are summarized. Also structural perturbations are included. The self-organization hypothesis is tested for two different situations. The formation of large-scale-structures on the one hand and of zonal flow on the other hand are discussed. In both cases, numerical simulations as well as analytical predictions are presented. Author

N91-28943# National Inst. for Fusion Science, Nagoya (Japan).

SOLITONS AND CHAOS IN PLASMA

Yoshi H. Ichikawa *In its* Proceedings of the Second International Toki Conference on Plasma Physics and Controlled Nuclear Fusion. Nonlinear Phenomena in Fusion Plasmas: Theory and Computer Simulation Apr. 1991 p 216 (For primary document see N91-28881 20-75)
Avail: NTIS HC/MF A11

Plasma exhibits a full variety of nonlinear phenomena. Active research in nonlinear plasma physics contributed to explore the concepts of soliton and chaos. Structure of the soliton equations and the dynamics of low dimensional Hamiltonian systems are discussed to emphasize the universality of these concepts in the wide branch of science and engineering. Author

N91-28944# Lawrence Livermore National Lab., CA.

PLASMA TRANSPORT IN A NEW CATHODIC ARC ION SOURCE, THEORY AND EXPERIMENT

D. B. Boercher, S. Falabella, and D. M. Sanders Mar. 1991 12 p Presented at the International Conference on Metallurgical

Coatings and Thin Films, San Diego, 22-26 Apr. 1991
(Contract W-7405-eng-48)
(DE91-011511; UCRL-JC-106567; CONF-9104187-3) Avail: NTIS HC/MF A03

The ever increasing demand for coatings of higher and higher quality requires the development of new methods for producing them. One of the promising new avenues involves the use of arc-produced plasmas. The principal advantage for such methods is that the plasma ions can be controlled through the use of applied electromagnetic fields, so that the energy with which the coating material arrives at the substrate can be regulated. The primary disadvantage is ridding the plasma beam of the macroparticles which are produced simultaneously with the beam. One approach to overcoming this difficulty is to pass the plasma through a magnetic filter. The large mass of the macroparticles prevents them from bending in the filter, while the plasma is directed to the substrate. The authors have developed a new macroparticle-filtered metal ion source, based on the cathodic arc, which makes use of steered arc control technology. The ion currents and electrical potentials in this source were measured at various locations and used to assess a simple computer model. The implications of this assessment for future arc source design is discussed. DOE

N91-28945# Maryland Univ., College Park.
PARTICLE CONFINEMENT AND FUELING EFFECTS ON THE MARYLAND SPHEROMAK Ph.D. Thesis
A. B. Filuk 1991 146 p
(Contract DE-FG05-86ER-53241)
(DE91-012396; DOE/ER-53241/T1) Avail: NTIS HC/MF A07

The spheromak plasma confinement concept provides the opportunity to study the evolution of a nearly force-free magnetic field configuration. The plasma currents and magnetic fields are produced self-consistently, making this type of device attractive as a possible fusion reactor. At present, spheromaks are observed to have poorer particle and magnetic confinement than expected from simple theory. The purpose of this study is to examine the role of plasma density in the decay of spheromaks produced in the Maryland Spheromak experiment. Density measurements are made with an interferometer and Langmuir probe, and results are correlated with those of other plasma diagnostics to understand the sources of plasma, the spheromak formation effects on the density, and the magnitude of particle loss during the spheromak decay. A power and particle balance computer model is constructed and applied to the spheromaks studied in order to assess the impact of high density and particle loss rate on the spheromak decay. The observations and model indicate that the decay of the spheromaks is at present dominated by impurity radiation loss. The model also predicts that high density and short particle confinement time play a critical role in the spheromak power balance when the impurity levels are reduced. DOE

N91-28946# Oak Ridge National Lab., TN.
CONFINEMENT PROJECTIONS FOR THE BURNING PLASMA EXPERIMENT (BPX)
R. J. Goldston, G. Bateman, S. M. Kaye, F. W. Perkins, N. Pomphrey, D. P. Stotler, M. C. Zarnstorff (Princeton Univ., NJ.), W. A. Houlberg, G. H. Neilson, and M. Porkolab 1991 5 p
Presented at the 1991 European Physical Society Meeting, Berlin, Fed. Republic of Germany, 3-7 Jun. 1991
(Contract DE-AC05-84OR-21400)
(DE91-012516; CONF-9106178-2) Avail: NTIS HC/MF A01

The mission of the Burning Plasma Experiment (BPX, formerly CIT) is to study the physics of self-heated fusion plasmas (Q = 5 to ignition), and to demonstrate the production of substantial amounts of fusion power (P(sub fus) = 100 to 500 MW). Confinement projections for BPX have been made on the basis of (1) dimensional extrapolation, (2) theory-based modeling calibrated to experiment, and (3) statistical scaling from the available empirical data base. The results of all three approaches, discussed roughly coincide. The third approach is presently viewed, statistical scaling, as the most reliable means for projecting the confinement performance of BPX, and especially for assessing the uncertainty in the projection. DOE

N91-28947# Oak Ridge National Lab., TN.
CHARACTERISTICS OF EDGE PLASMA TURBULENCE ON THE ATF TORSATRON
T. Uckan, C. Hidalgo, J. D. Bell, J. H. Harris, J. L. Dunlap, J. B. Wilgen, C. P. Ritz, T. L. Rhodes, and A. J. Wootton (Texas Univ., Austin.) Mar. 1991 20 p
(Contract DE-AC05-84OR-21400)
(DE91-012981; ORNL/TM-11623) Avail: NTIS HC/MF A03

Measurements of electrostatic fluctuations on the edge of the Advanced Toroidal Facility (ATF) torsatron are used to study the role of the edge turbulence in the particle transport in this current-free magnetic configuration. Spatial profiles of the plasma electron density n(sub e), temperature T(sub e), and fluctuations in density tilde n(sub e) and in the plasma floating potential tilde phi(sub f) are measured at the edge in electron cyclotron heated plasmas using a Langmuir probe array. At the last closed flux surface (LCFS), r/a approximately = 1, T(sub e) approximately = 20 to 40 eV, and n(sub e) approximately = 10(exp 12)/cc for a line-averaged electron density bar n(sub e) = (3 to 6) x 10(sup 12)/cc. The relative fluctuation levels decrease as the probe is moved into the core plasma. For T(sub e) greater than 10 eV, tilde n(sub e)/n(sub e) approximately = 5 percent, and (e(tilde phi) sub f)/T(sub e) approximately = 2(tilde n) sub e /n(sub e) at r/a = 0.95. The measured fluctuations spectra are broadband (40 t0 300 kHz) with bar k rho (sub s) approximately = 0.05 to 0.1, where (bar k) is the average wave number of the fluctuations and rho(sub s) is the ion Larmor radius at the sound speed. Near the LCFS, the density fluctuations can be approximated by tilde n(sub e)/n(sub e) approximately = 0.4/(bar k)L(sub n), where L(sub n) is the gradient scale length of n(sub e). The propagation direction of the fluctuations reverses to the electron diamagnetic direction at r/a less than 1. The phase velocity of the fluctuations and the electron drift velocity are comparable. The particles flux estimated from the fluctuations is consistent with fluxes obtained from the particle balance using the H(sub alpha) spectroscopic measurements. Many of the features seen in the ATF edge fluctuations resemble those of ohmically heated plasmas in the Texas Experimental Tokamak. DOE

N91-28948# Lawrence Livermore National Lab., CA.
MICROWAVE-GENERATED PLASMA THRUSTER
E. B. Hooper 11 May 1991 12 p
(Contract W-7405-eng-48)
(DE91-013131; UCRL-ID-107211) Avail: NTIS HC/MF A03

A concept for high power density and efficiency plasma thruster based on electron cyclotron resonance heating (ECRH) is described. Initial estimates are made of the parameters, leading to a conceptual design. An effort for detail physics design and proof-of-principal tests is also proposed. DOE

N91-28949# Wisconsin Univ., Madison. Center for Plasma Theory and Computation.
FLUID/KINETIC HYBRID MOMENT DESCRIPTION OF PLASMAS VIA A CHAPMAN-ENSKOG-LIKE APPROACH
J. P. Wang and J. D. Callen May 1991 35 p Revised
(Contract DE-FG02-86ER-53218)
(DE91-013346; UW-CPTC-90-8-Rev) Avail: NTIS HC/MF A03

A combined fluid and kinetic description of magnetically confined plasmas is developed via a Chapman-Enskog-like procedure. This approach uses the density, energy, momentum, and heat flow conservation equations, and the kinetic equation to recast the plasma kinetic equation with a full Fokker-Planck collision operator into an equation for F, the departure of the distribution function from a dynamic Maxwellian. A density, momentum, and energy conserving collision operator model is adopted in deriving the final form of the recast kinetic equation. Both general and drift-kinetic forms of the kinetic equation for F are presented. Closure of the fluid moment equations through calculation of the anisotropic stress tensor and anisotropic heat stress tensor using the kinetic solution for F is discussed. DOE

N91-28950# Maryland Univ., College Park.
MEASUREMENT OF MAGNETIC PROPERTIES OF CONFINED COMPACT TOROID PLASMA (SPHEROMAK) Ph.D. Thesis
Fu-Kwun Hwang 1991 140 p
(Contract DE-FG05-86ER-53241)
(DE91-012397; DOE/ER-53241/T2) Avail: NTIS HC/MF A07

The theoretical aspect of the spheromak is described. The MS machine hardware will be explored along with the formation scheme and diagnostic systems. The magnetic pickup probes, their calibration procedures and the data analysis methods is discussed. Observations from the probe measurements and magnetic properties of the MS spheromak are considered. The axisymmetric Grad-Shafranov equilibrium code calculations are presented and compared with the measurements. Magnetic helicity and its correlation with the experimental observations is described. DOE

N91-28951# Edgerton, Germeshausen and Grier, Inc., Idaho Falls, ID.
EVIDENCES OF TRAPPING IN TUNGSTEN AND IMPLICATIONS FOR PLASMA-FACING COMPONENTS
G. R. Longhurst, R. A. Anderl, and D. F. Holland 1990 7 p Presented at the 9th Topical Meeting on Technology of Fusion Energy, Oak Brook, 7-11 Oct. 1990
(Contract DE-AC07-76ID-01570)
(DE91-012734; EGG-M-90238; CONF-901007-68) Avail: NTIS HC/MF A02

Trapping effects that include significant delays in permeation saturation, abrupt changes in permeation rate associated with temperature changes, and larger than expected inventories of hydrogen isotopes in the material, were seen in implantation-driven permeation experiments using 25- and 50-micron thick tungsten foils at temperatures of 638 to 825 K. Computer models that simulate permeation transients reproduce the steady-state permeation and reemission behavior of these experiments with expected values of material parameters. However, the transient time characteristics were not successfully simulated without the assumption of traps of substantial trap energy and concentration. An analytical model based on the assumptions of thermodynamic equilibrium between trapped hydrogen atoms and a comparatively low mobile atom concentration successfully accounts for the observed behavior. Using steady-state and transient permeation data from experiments at different temperatures, the effective trap binding energy may be inferred. We analyze a tungsten coated divertor plate design representative of those proposed for ITER and ARIES and consider the implications for tritium permeation and retention if the same trapping we observed was present in that tungsten. Inventory increases of several orders of magnitude may result. DOE

N91-28952# Lawrence Livermore National Lab., CA.
IMPLICATIONS OF TAE MODES FOR THE DESIGN OF ITER
T. K. Fowler and D. Finkenthal (California Univ., Berkeley.) 20 May 1991 23 p
(Contract W-7405-eng-48)
(DE91-013128; UCRL-ID-107222) Avail: NTIS HC/MF A03

A simple mixing-length estimate of diffusion of alphas particles by toroidicity-induced shear Alfven eigenmodes (TAE) is used, in zero and one-dimensional models, to evaluate the importance of diffusion of meeting ignition requirements for ITER and other next-generation burning plasma experiments. It is found that, depending on a number of assumptions, diffusion could reduce that effectiveness of alpha heating in the core as much as an order of magnitude. However, the effect would be less if only alphas resonant with the Alfven waves diffuse. Also, in the Appendix it is argued that the mixing length diffusion formula, though qualitatively reasonable, may be an over estimate. DOE

N91-28953# Wisconsin Univ., Madison. Center for Plasma Theory and Computation.
FLUIDLIKE STUDIES OF THE PRESHEATH AND SHEATH REGIONS OF A PLASMA
B. J. Lee and J. D. Callen May 1991 45 p
(Contract DE-FG02-86ER-53218)
(DE91-013345; UW-CPTC-91-5) Avail: NTIS HC/MF A03

We investigate the fundamental problem of an unmagnetized, moderate collisionality (i.e., within a collision mean free path of the wall plasma flowing into a perfectly absorbing wall) including the parallel viscosity and heat flux effects. Both the collisional presheath and the collisionless sheath regions are modelled by fluidlike moment equations that are derived from kinetic theory. The electron distribution function is obtained from the solution of a Pastukhov type problem (collisional diffusion over a potential barrier) instead of from a simple Boltzmann relation. A boundary layer analysis is applied for determining the ion distribution function in the velocity space region corresponding to no net return flux from the wall. This analysis procedure provides a continuous solution over the entire region of interest. The ion viscous force deduced from this distribution function, which is a cutoff Maxwellian relaxed by collisions, is comparable to the electric field force everywhere and removes the singularity between the presheath and the sheath regions in the ion momentum equation. One of the results obtained is that the total ion heat flux is bigger than the total electron heat flux at the wall because of the thermal conduction effects. DOE

N91-28954# Lawrence Livermore National Lab., CA.
CHAMBER PROPAGATION
B. Langdon 16 Jan. 1991 8 p Presented at the International Symposium on Heavy Ion Inertial Fusion, Monterey, 3-6 Dec. 1990
(Contract W-7405-eng-48)
(DE91-012797; UCRL-JC-105806; CONF-901219-16) Avail: NTIS HC/MF A02

Propagation of a heavy ion beam to the target appears possible under conditions thought to be realizable by several reactor designs. Beam quality at the lens is believed to provide adequate intensity at the target - but the beam must pass through chamber debris and its self fields along the way. This paper reviews present consensus on propagation modes and presents recent results on the effects of photoionization of the beam ions by thermal x-rays from the heated target. Ballistic propagation through very low densities is a conservative mode. The more-speculative self-pinched mode, at 1 to 10 Torr, offers reactor advantages and is being re-examined by others. DOE

N91-28955# Lawrence Livermore National Lab., CA.
LARGE GROWTH RAYLEIGH-TAYLOR EXPERIMENTS ON NOVA
B. A. Remington, S. W. Haan, S. G. Glendinning, J. D. Kilkenny, D. H. Munro, and R. J. Wallace 22 Jan. 1991 19 p Presented at the International Conference on Research Trends in Inertial Confinement Fusion, La Jolla, 4-6 Feb. 1991
(Contract W-7405-eng-48)
(DE91-012885; UCRL-JC-106271; CONF-910247-2) Avail: NTIS HC/MF A03

Large growth Rayleigh-Taylor (RT) experiments have been conducted by pulse-shaped radiative acceleration of fluorosilicone foils with 50 micron wavelength initial surface perturbations. Foils with very small amplitude initial perturbations grow exponentially for much longer, and show growth factors of up to 60. From comparisons with 2-dimensional computer simulations, we estimate that the growth rate is approximately 60 percent of classical, the reduction attributed to ablative and gradient scale length stabilization. DOE

N91-28956# California Univ., Davis.
MEASUREMENTS OF THE ION ACOUSTIC DECAY INSTABILITY AND THE RESULTANT ENHANCED LASER ABSORPTION AND ENHANCED BREMSSTRAHLUNG IN LASER-PLASMA INTERACTION EXPERIMENTS
K. Mizuno, J. S. DeGroot, and J. H. Rogers 1 Jun. 1991 17 p
(Contract DE-FG03-89SF-18014)
(DE91-014250; DOE/SF-18014/T1) Avail: NTIS HC/MF A03

The impact was studied of the Ion Acoustic Decay Instability on Laser Fusion. It is shown that the Ion Acoustic Decay Instability

(IADI) is potentially important in laser fusion. The IADI threshold is reduced to the homogeneous collisional plasma values in a large scale plasma. The threshold was as low as I lambda sub L squared = 5 x 10(exp 12) W/sq cm - sq m. The estimate shows that the electron plasma wave excited by the IADI can significantly heat the hot electrons. It was also shown that Bremsstrahlung radiation due to electron scattering with ion acoustic turbulence is typically small. DOE

N91-28957# Department of Energy, Washington, DC. Assistant Secretary for Environment, Safety, and Health.

TIGER TEAM ASSESSMENT OF THE PRINCETON PLASMA PHYSICS LABORATORY

Mar. 1991 562 p
(DE91-014395; DOE/EH-0165) Avail: NTIS HC/MF A24

The Tiger Team Assessment of the Princeton Plasma Physics Laboratory (PPPL) was conducted. Activities of the Tiger Team Assessment resulted in identification of compliance findings or concerns and noteworthy practices and an analysis as to the root causes for noncompliance. The PPPL Tiger Team Assessment is one component of a larger, comprehensive DOE Tiger Team Assessment program for DOE facilities that will eventually encompass over 100 of the Department's operating facilities. The objective of the initiative is to provide the Secretary with information on the compliance status of DOE facilities with regard to ES and H requirements; root causes for noncompliances; adequacy of DOE and contractor ES and H management programs; response actions to address the identified problems areas; and DOE wide ES and H compliance trends and root causes. DOE

N91-28958# Lawrence Livermore National Lab., CA.

HYDRODYNAMIC EVOLUTION OF PICOSECOND LASER-PLASMAS

O. L. Landen, B. T. Vu (California Univ., Davis.), D. G. Stearns, and W. E. Alley 18 Jan. 1991 13 p Presented at the OE/LASE 1991: 4th Society of Photo-Optical Instrumentation Engineers (SPIE) International Symposium, Los Angeles, 20-25 Jan. 1991
(Contract W-7405-eng-48)
(DE91-013245; UCRL-JC-105997; CONF-910123-33) Avail: NTIS HC/MF A03

The density profile evolution of picosecond laser-plasmas has been inferred from the angular dependence of the specular reflectivity of a probe picosecond pulse. Time-resolved density profiles, critical density scale-lengths as short as 3 nm and values for the plasma collisionality are presented for a gold target irradiated by a 580 nm, 0.8 ps FWHM laser pulse with a peak intensity of up to 2 x 10(exp 13) W cm(exp -2). The results are best fitted at early times (less than 10 ps) by the self-similar isothermal exponential density profile and a critical density collision frequency of 0.3(omega), in good agreement with 1-D hydrodynamic simulations. DOE

N91-28959# Oak Ridge National Lab., TN.

SPECTROSCOPIC AND ION PROBE CHARACTERIZATION OF LASER PRODUCED PLASMAS USED FOR THIN FILM GROWTH

D. B. Geohegan May 1991 11 p Presented at the HASRD Workshop on Laser Ablation: Mechanisms and Application, Oak Ridge, 8-10 Apr. 1991
(Contract DE-AC05-84OR-21400)
(DE91-013425; CONF-9104192-6) Avail: NTIS HC/MF A03

Laser ablation for in situ film growth of 1:2:3 superconductors requires high laser energy densities and results in a dense, multicomponent laser plasma which expands into high background pressures (approximately 100 mTorr) of oxygen. The physics of the transport process in the film growth regime involves a variety of high-density collisional phenomena which one attempts to avoid in near-threshold ablation studies: laser-plasma heating and acceleration, thermalization, attenuation and reactive scattering of the plume by background gas collisions, and shock formation. Three in situ techniques are employed and reviewed to characterize these effects: optical emission spectroscopy for viewing the excited states of atoms and molecules resulting from plasma kinetics; optical absorption spectroscopy for viewing the non-emitting ground states of atoms, ions, molecules; and fast ion probes for viewing the flux of positive ions in the plasma. In this paper, spatially- and temporally-resolved optical absorption and emission spectroscopy and fast ion probes are applied to study the formation and acceleration of the laser plasma formed by KrF laser irradiation of Y1Ba2Cu3O(x) in vacuum and the propagation of the plume through background gases of oxygen and argon at pressures and laser energies typically used for thin film growth. DOE

N91-28960# Lawrence Livermore National Lab., CA.

INERTIAL CONFINEMENT FUSION

T. P. Bernat, ed. 1990 48 p
(Contract W-7405-eng-48)
(DE91-013479; UCRL-LR-105821-91-1) Avail: NTIS HC/MF A03

Papers on the following topics are presented: a nondestructive method for measuring the fill pressure and permeability of fuel-filled plastic shells; an improved method for making polystyrene microspheres; indirect-drive Rayleigh-Taylor experiments using shape laser pulses; intensity scaling of stimulated raman forward scattering; beam propagation across the target chamber in heavy-ion fusion; preparations and properties of brominated polymer coatings; and beam-smoothing capability on the Nova laser. DOE

N91-28961# Wisconsin Univ., Madison.

NONLINEAR REVERSED FIELD PINCH DYNAMICS WITH NONIDEAL BOUNDARIES

Y. L. Ho and S. C. Prager Mar. 1991 63 p
(Contract DE-FG02-85ER-53212)
(DE91-013638; DOE/ER-53212/172) Avail: NTIS HC/MF A04

The nonlinear behavior of the reversed field pinch bounded by a resistive shell or a distant conducting wall is investigated with a three-dimensional magnetohydrodynamic code. Nonlinear interaction between modes enhances fluctuation levels as the conducting wall is removed. The enhanced fluctuation induced v x b electric field, which produces the dynamo effect, suppresses toroidal current, and enhances surface helicity dissipation. Thus, loop voltage must increase to sustain the current and maintain helicity balance. DOE

N91-28962# Lawrence Livermore National Lab., CA.

EVALUATION OF CHARGED-PARTICLE REACTIONS FOR FUSION APPLICATIONS

R. M. White, D. A. Resler, and S. I. Warshaw 1991 8 p Presented at the International Conference on Nuclear Data for Science and Technology, Juelich, Fed. Republic of Germany, 13-17 May 1991
(Contract W-7405-eng-48)
(DE91-014135; UCRL-JC-107158; CONF-910503-24) Avail: NTIS HC/MF A02

New evaluations of the total reaction cross sections for H-2(d,n)He-3, H-2(d,p)H-3, H-3(t,2n)He-4, H-3(d,n)He-4, and He-3(d,p)He-4 have been completed. These evaluations are based on all known published data from 1946 to 1990 and include over 1150 measured data points from 67 references. The purpose of this work is to provide a consistent and well-documented set of cross sections for use in calculations relating to fusion energy research. A new thermonuclear data file, TDF, and a library of FORTRAN subprograms to read the file have been developed. Calculated from the new evaluations, the TDF file contains information on the Maxwellian-averaged reaction rates as a function of reaction and plasma temperature and the Maxwellian-averaged average energy of the interacting particles and reaction products. Routines are included that provide thermally-broadened spectral information for the secondary reaction products. DOE

N91-28963# Texas Univ., Austin. Inst. for Fusion Studies.

STABILITY OF ANNULAR EQUILIBRIUM OF ENERGETIC LARGE ORBIT ION BEAM

H. V. Wong, H. L. Berk, R. V. Lovelace, and N. Rostoker Mar.

1991 43 p
(Contract DE-FG05-80ET-53088)
(DE91-014365; DOE/ET-53088/484; IFSR-484) Avail: NTIS HC/MF A03

We study analytically the low frequency stability of a long thin annular layer of energetic ions in a background plasma with finite axial and zero azimuthal magnetic field. We find that although the equilibrium is susceptible to the kink instability low mode number perturbations can be stabilized in the limit of N(sub b)/N(sub i) = 0 when the current layers with respect to the placement of conducting walls. DOE

N91-28964# Texas Univ., Austin. Inst. for Fusion Studies.

TRANSPORT PROFILES INDUCED BY RADIALLY LOCALIZED MODES IN TOKAMAK

A. D. Beklemishev (Gosudarstvennyi Komitet po Ispolzovaniyu Atomnoi Energii, Moscow, USSR) and W. Horton Apr. 1991 20 p
(Contract DE-FG05-80ET-53088)
(DE91-014366; DOE/ET-53088/494; IFSR-494) Avail: NTIS HC/MF A03

We describe a new approach to the calculation of turbulent transport coefficients for radially localized modes. The theory takes into account the nonuniformity of the distribution of rational (resonant) magnetic surfaces in minor radius. This distribution function is proportional to the density of available states of excitation. The resulting density of state correction qualitatively changes the radial profile of the transport coefficients, as compared to the usual local diffusivity formulae. The correction factor calculated for the eta(sub i)-mode transport allows a much better agreement of chi(sub i) with the experimental data than previously achieved. DOE

N91-28965# Texas Univ., Austin. Inst. for Fusion Studies.

EXACT SOLUTIONS FOR A SYSTEM OF NONLINEAR PLASMA FLUID EQUATIONS

M. G. Prahovic, R. D. Hazeltine, and P. J. Morrison Apr. 1991 25 p
(Contract DE-FG05-80ET-53088)
(DE91-014367; DOE/ET-53088/495; IFSR-495) Avail: NTIS HC/MF A03

A method is presented for constructing exact solutions to a system of nonlinear plasma fluid equations that combines the physics of reduced magnetohydrodynamics and the electrostatic drift-wave description of the Charney-Hasegawa-Mima equation. The system has nonlinearities that take the form of Poisson brackets involving the fluid field variables. The method relies on modifying a class of simple equilibrium solutions, but no approximations are made. A distinguishing feature is that the original nonlinear problem is reduced to the solution of two linear partial differential equations, one fourth-order and the other first-order. The first-order equation has Hamiltonian characteristics and is easily integrated, supplying information about the general structure of solutions. DOE

N91-28966# Lawrence Livermore National Lab., CA.

THE CASCADE INERTIAL CONFINEMENT FUSION REACTOR CONCEPT

J. H. Pitts, ed. comp., W. J. Hogan, ed. comp., M. T. Tobin, ed. comp., R. F. Bourque, ed. comp., and W. R. Meier, ed. comp. (Schafer, W. J. Associates, Inc., Pleasanton, CA) 23 Dec. 1990 86 p
(Contract W-7405-eng-48)
(DE91-013852; UCRL-LR-104546) Avail: NTIS HC/MF A05

The Cascade reactor concept has the potential of converting inertial confinement fusion (ICF) energy into electrical power safely, efficiently, and with low activation. Its flexibility permits a number of options for materials, blankets, fuel-pellet designs and drivers. This report documents a theoretical and experimental study culminating in a reference Cascade conceptual design that produces 890 MW of electrical power with a net plant efficiency of 47 percent if a heavy-ion driver if used. The reactor is double-cone shaped and rotates at 50 rpm. A ceramic-granule blanket flows through the reactor held against the reactor wall by the rotation. The blanket serves several functions: it absorbs energy from fusion reactions that occur at 5 Hz in the center of the reactor, thereby protecting the reactor wall and extending its lifetime to that of power plant; it acts as a heat-exchange medium to transfer fusion energy to high-pressure helium gas used in power conversion; and it produces tritium to replace that burned in the fusion process. Cascade's illumination geometry is restricted, so that good energy coupling to presently-envisioned fuel pellets is practical only with heavy-ion drivers. Laser drivers would require the use of fuel pellets with advanced design features. We discuss the reactor concept, heat exchanger, balance of plant, other systems that would be necessary for a full-scale production of electrical power, and experiments that prove the feasibility of a flowing granular blanket. A cost study predicts that Cascade, using a heavy-ion driver, could produce electricity for between 5.5 and 6.8 cents/kWh-comparable to the cost of power using modular high-temperature gas-cooled reactors, pressurized-water reactors, or coal-fired power plants. Finally, we include an annotated bibliography of the over 50 reports which have been written about Cascade. DOE

N91-28967# Washington Univ., Seattle. Aerospace and Energetics Research Program.

FORMATION AND SUSTAINMENT OF A VERY LOW ASPECT RATION TOKAMAK USING COAXIAL HELICITY INJECTION (THE HELICITY INJECTED TORUS (HIT) EXPERIMENT)

T. R. Jarboe and B. A. Nelson 1991 36 p
(Contract DE-FG06-90ER-54095)
(DE91-013948; DOE/ER-54095/1; UWAERP-28) Avail: NTIS HC/MF A03

In this paper we will detail the progress of the Helicity Injected Tokamak experiment construction, including the following components: vacuum vessel and pumping system; helicity source and power supply; toroidal field coil and power supply; bias coil and power supply; data acquisition system; diagnostic set; and collaboration with General Atomics. DOE

N91-28968# Argonne National Lab., IL.

SIMULATION OF COMBUSTION PROCESSES IN AN MHD SECOND STAGE COMBUSTOR

S. A. Lottes and S. L. Chang 1991 12 p Presented at the 29th Symposium on Engineering Aspects of Magnetohydrodynamics, New Orleans, 18-20 Jun. 1991
(Contract W-31-109-eng-38)
(DE91-014014; ANL/CP-72369; CONF-9106106-1) Avail: NTIS HC/MF A03

Computer simulation is used to aid in the design of a magnetohydrodynamic (MHD) second stage combustor. A 2-D steady state computer model, based on mass, momentum, and energy conservation laws for multiple gas species, is used to simulate the hydrodynamics and combustion in a second stage combustor in which opposed jets of oxidizer are injected into a confined cross stream of hot gas/fuel mixture entering from the first stage. The model computes variable distributions (temperature, pressure, velocity, and species concentrations, etc.) in the combustor and predicts reacting flow heat release, mixing patterns, and combustion efficiency. The modeling aids in understanding the complex processes occurring within the combustor and helps in identification of optimum design parameters and operating conditions for the combustor to improve combustor operation and enhance downstream MHD generator performance. Results of the study indicate: (1) co-flow oxidizer jet injection (angle less than 90 degs) yields relatively poor mixing and combustion performance; (2) counter flow injection (angle greater than 90 degs) yields much better mixing and combustion performance, with an optimum injection angle in the range of 120 to 140 degs; (3) the optimum injection angle intervals for combustion efficiency and uniformity of exit temperature profile are the same; and (4) the non-reacting flow optimum injection angle interval for jet/main flow mixing is a relatively good predictor of reacting flow combustor performance in terms of combustion efficiency and uniformity of combustor exit temperature profile. DOE

N91-28969# Oak Ridge National Lab., TN.
PLASMA TURBULENCE CALCULATIONS ON SUPERCOMPUTERS
B. A. Carreras, L. A. Charlton, N. Dominguez, J. B. Drake, L. Garcia, J. N. Leboeuf, D. K. Lee, V. E. Lynch, K. Sidikman, and D. A. Spong 1991 6 p Presented at the Power Supercomputer Users Meeting, Gaithersburg, 21-22 May 1991
(Contract DE-AC05-84OR-21400)
(DE91-014210; CONF-9105202-5) Avail: NTIS HC/MF A02

The use of supercomputers to calculate the fluctuation in plasma parameters in magnetic confinement devices is discussed. DOE

N91-28970# Science Applications International Corp., San Diego, CA.
REVERSED-FIELD PINCH DYNAMICS AND TRANSPORT STUDIES
D. D. Schnack 18 Jun. 1991 161 p
(Contract DE-AC03-83ER-53150)
(DE91-014317; SAIC-91/1136/APPAT-143) Avail: NTIS HC/MF A08

This report discusses the following topics: fluctuation suppression via DC-helicity injection in a reversed-field pinch; nonlinear dynamics of field maintenance and quasi-periodic relaxation in reversed-field pinches; statistical mechanics of a three field model for electromagnetic turbulence; magnetohydrodynamic theory of the reversed-field pinch dynamo; simulation of the thin shell and secondary shell HBTX1C experiments; thermally driven edge magnetic turbulence; and theory of shear suppression of edge turbulence by externally driven radio frequency waves. DOE

N91-28971# Texas Univ., Austin. Fusion Research Center.
A PORTABLE AND INDEPENDENT EDGE FLUCTUATION DIAGNOSTIC
H. Y. W. Tsui, C. P. Ritz, and A. J. Wootton 1991 7 p
(Contract DE-FG05-89ER-53295)
(DE91-014357; DOE/ER-53295/2) Avail: NTIS HC/MF A02

The measurements of fluctuations and its associated transport with Langmuir probes have provided essential experimental information for some understanding of the turbulent transport. While such measurements have been conducted in the edge region of several tokamaks, only limited effort has been devoted to link and to consolidate these results: such effort can provide information for a more global understanding of the transport process. The purpose of this project is to provide a portable diagnostic facility to measure the edge turbulence on different devices, a signal processing package to analyze the data in a systematic manner, and a database to consolidate the experimental results. The end product which provides a collection of information for the comparisons with the theoretical models may lead to a more global understanding of the transport process. A compact self contained portable system has been designed and developed to diagnose the edge plasma of devices with a wide range of sizes and configurations. The system is capable of measuring both the mean and the fluctuation quantities of density, temperature, and potential from a standardized Langmuir probe array using a fast reciprocating probe drive. The system can also be used for other fluctuation diagnostics, such as magnetic probes, if necessary. The data acquisition and analysis is performed on a Macintosh 2fx which provides a user-friendly environment. The results obtained by the signal processing routines are stored in a tabloid format to allow comparative studies. The database is a core part of the portable signal analysis system. It allows a fast display of shot data versus each other, as well as comparison between different devices. DOE

N91-28972# Texas Univ., Austin. Inst. for Fusion Studies.
NONLINEAR DYNAMICS OF THE RELATIVISTIC STANDARD MAP
Y. Nomura, Yoshi H. Ichikawa, and W. Horton Apr. 1991 40 p
(Contract DE-FG05-80ET-53088)
(DE91-014368; DOE/ET-53088/496; IFSR-496) Avail: NTIS HC/MF A03

Heating and acceleration of charged particles by RF fields have been extensively investigated by the standard map. The question arises as to how the relativistic effects change the nonlinear dynamical behavior described by the classical standard map. The relativistic standard map is a two parameter (K, beta = omega/kc) family of dynamical systems reducing to the standard map when beta yields 0. For beta not equal to 0, the relativistic mass increase suppresses the onset of stochasticity. It is shown that the speed of light limits the rate of advance of the phase in the relativistic standard map and introduces KAM surfaces persisting in the high momentum region. An intricate structure of mixing in the higher order periodic orbits and chaotic orbits is analyzed using the symmetry properties of the relativistic standard map. The interchange of the stability of the periodic orbits in the relativistic standard map is also observed and is explained by the local linear stability of the orbits. DOE

N91-28973# General Atomic Co., San Diego, CA.
INFLUENCE OF FAST WAVES ON THE COLLECTIVE SCATTERING OF MICROWAVES IN FUSION PLASMAS
S. C. Chiu Jun. 1991 10 p Presented at the International Atomic Energy Agency (IAEA) Technical Committee Meeting on Alpha Particles in Fusion, Aspenas (Sweden), 10-14 Jun. 1991
(Contract DE-AC03-89ER-53277)
(DE91-014759; GA-A-20539; CONF-9106209-2) Avail: NTIS HC/MF A02

Microwave scattering by the fluctuations of fusion plasmas is one of the most promising (alpha)-diagnostic techniques. Previous investigations have concentrated on the fluctuations near the slow wave branch in the lower hybrid range of frequencies. The small signal and the lack of sensitivity to the contribution of (alpha)-particles to the total cross-section near the slow branch severely limits the effectiveness of this technique. In this paper, we report results of investigations of scattering by fluctuations in the lower hybrid range of frequencies near the fast branch. Surprisingly, when both fast and slow branches exist, the scattering amplitudes are comparable. More important, the (alpha)-contribution is larger for the fast branch and the fast branch has a larger parameter space where it exists. Specifically, the slow branch exists only above the lower hybrid frequency, while the fast branch can exist at all frequencies up to the electron cyclotron range of frequencies. We find numerically that the scattering amplitudes near the fast branch below the lower hybrid frequency are several orders of magnitude larger than those near the slow branch above that frequency where it can exist. This may make microwave scattering by fast waves a more attractive (alpha)-diagnostic technique. DOE

N91-28974# Texas Univ., Austin. Inst. for Fusion Studies.
STEADY-STATE DYNAMO AND CURRENT DRIVE IN A NONUNIFORM BOUNDED PLASMA
R. R. Mett and J. B. Taylor Mar. 1991 20 p
(Contract DE-FG05-80ET-53088)
(DE91-014865; DOE/ET-53088/490; IFSR-490) Avail: NTIS HC/MF A03

Current drive due to helicity injection and dynamo effect are examined in an inhomogeneous bounded plasma. Averaged over a magnetic surface, there is in general no dynamo effect independent of resistivity -- contrary to the results found previously for an unbounded plasma. The dynamo field is calculated explicitly for an incompressible visco-resistive fluid in the plane-slab model. In accord with our general conclusion, outside the Alfven resonant layer it is proportional to the resistivity. Within the resonant layer there is a contribution which is enhanced, relative to its value outside the layer, by a factor omega a(sup 2)/(eta) + nu, where omega is the wave frequency, a the plasma radius, eta the magnetic diffusivity, and nu the kinematic viscosity. However, this contribution vanishes when integrated across the layer. The average field in the layer is enhanced by factor omega a sup 2/eta + nu (sup 2/3) and is proportional to the shear in the magnetic field and the cube root of the gradient of the Alfven speed. These results are interpreted in terms of helicity balance, and reconciled with the infinite medium calculations. DOE

N91-28975# Los Alamos National Lab., NM.

PROGRESS IN THE DEVELOPMENT OF A NUMERICAL TOKAMAK

J. U. Brackbill 1991 7 p Presented at the Power Supercomputer Users Meeting, Gaithersburg, 21-22 May 1991

(Contract W-7405-eng-36)

(DE91-013386; LA-UR-91-1840; CONF-9105202-1) Avail: NTIS HC/MF A02

The progress is discussed in the following areas: numerical tokamak; plasma simulation on magnetohydrodynamic time scales; and plasma simulation in real geometries. DOE

N91-28976# California Univ., Los Angeles.

CONTINUING STUDIES OF THE PLASMA BEAT WAVE ACCELERATOR

C. Joshi 1990 91 p

(Contract DE-AS03-83ER-40120)

(DE91-013641; DOE/ER-40120/T2) Avail: NTIS HC/MF A05

A proposal is presented for the Plasma Beat Wave Accelerator program (PBWA). A summary is made of up to date progress. It is noted that although the program is for historical reasons called the Plasma Beat Wave Accelerator Program, the group is active in all areas of applications of lasers and plasmas in future high energy accelerators. These are as follows: heat gradient plasma structures; excited by plasma beat wave technique; laser wake field technique; and plasma wake field technique. Development of a photoinjector-driven, 20 MeV linac; and theoretical studies of the plasma lens and use of plasmas at the final focus. DOE

N91-28977# Colorado Univ., Boulder.

REVERSED FIELD PINCH EXPERIMENTS

S. Roberston May 1991 10 p

(Contract DE-FG02-87ER-53244)

(DE91-013643; DOE/ER-53244/17) Avail: NTIS HC/MF A02

The Reversatron RFP is usually operated with toroidal field windings which are a continuous helix of 144 turns. These windings produce a poloidal current which is uniform around the torus. The distribution of current is fixed by the geometry so that the applied field has only an $m = 0$, $n = 0$ component. The windings cannot act to stabilize an $m = 0$ mode with absolute value of n greater than 0 or any $m = 1$ mode because these modes will excite no current in the windings. It has recently been suggested that parallel connected field coils might act as a shell by forcing the flux within each winding to be the same. Coils connected in parallel must have the same voltage at their terminals and thus must enclose the same volt-seconds or flux. Data from ZT-40 show that the discharges are more quiescent when parallel or series-parallel connected windings are used. DOE

N91-28978# New York Univ., New York. Magneto-Fluid Dynamics Div.

PLASMA PROPERTIES

H. Weitzner Jun. 1991 51 p

(Contract DE-FG02-86ER-53223)

(DE91-013933; DOE/ER-53223/159) Avail: NTIS HC/MF A04

The Magneto-Fluid Dynamics Division continues to study a broad range of problems originating in plasma physics. Its principal focus is fusion plasma physics, and most particularly topics of particular significance for the world magnetic fusion program. During the calendar year 1990 we explored a wide range of topics including RF-induced transport as a plasma control mechanism, edge plasma modelling, further statistical analysis of L and H mode tokamak plasmas, antenna design, simulation of the edge of a tokamak plasma and the L-H transition, interpretation of the CCT experimental results at UCLA, turbulent transport, studies in chaos, the validity of moment approximations to kinetic equations and improved neoclassical modelling. In more basic studies we examined the statistical mechanisms of Coulomb systems and applied plasma ballooning mode theory to conventional fluids in order to obtain novel fluid dynamics stability results. In space plasma physics we examined the problem of reconnection, the effect of Alfven waves in space environments, and correct formulation of boundary conditions of the Earth for waves in the ionosphere. DOE

N91-28979# California Univ., Berkeley. Lawrence Berkeley Lab.

PLASMA IMMERSION SURFACE MODIFICATION WITH METAL ION PLASMA

I. G. Brown, K. M. Yu, and X. Godechot Apr. 1991 7 p Presented at the Spring Meeting of the Materials Research Society (MRS), Anaheim, 29 Apr. - 3 May 1991 Prepared in cooperation with Societe Anonyme d'Etudes et Realisations Nucleaires, Limeil-Brevannes

(Contract DE-AC03-76SF-00098)

(DE91-014233; LBL-29914; CONF-910406-22) Avail: NTIS HC/MF A02

We describe here a novel technique for surface modification in which metal plasma is employed and by which various blends of plasma deposition and ion implantation can be obtained. The new technique is a variation of the plasma immersion technique described by Conrad and co-workers. When a substrate is immersed in a metal plasma, the plasma that condenses on the substrate remains there as a film, and when the substrate is then implanted, qualitatively different processes can follow, including conventional high energy ion implantation, recoil implantation, ion beam mixing, ion beam assisted deposition, and metallic thin film and multilayer fabrication with or without species mixing. Multiple metal plasma guns can be used with different metal ion species, films can be bonded to the substrate through ion beam mixing at the interface, and multilayer structures can be tailored with graded or abrupt interfaces. We have fabricated several different kinds of modified surface layers in this way. DOE

N91-28980# Maryland Univ., College Park. Lab. for Plasma Research.

MARYLAND CONTROLLED FUSION RESEARCH PROGRAM

T. M. Antonsen, Jr., J. F. Drake, J. M. Finn, P. N. Guzdar, A. B. Hassam, C. S. Liu, E. Ott, R. Kleva, and F. Waelbroeck 1991 16 p

(Contract DE-FG05-86ER-53221)

(DE91-014358; DOE/ER-53221/6) Avail: NTIS HC/MF A03

In recent years, members of the Maryland Plasma Theory Group have made significant contributions to the national fusion theory program, and, in many cases, these theoretical developments helped to interpret experimental results and to design new experimental programs. In this paper, we summarize the technical progress in three major area: (1) L/H transition in tokamaks; (2) anomalous transport in tokamaks; (3) sawteeth and (4) magnetic reconnection in compact tori and RFP's. DOE

N91-28981# Maryland Univ., College Park. Lab. for Plasma Research.

JOINT PROPOSAL FOR US/USSR ON NONLINEAR DYNAMICS AND PLASMA TRANSPORT

T. M. Antonsen, Jr., J. F. Drake, J. M. Finn, P. N. Guzdar, A. B. Hassam, and R. Z. Sagdeev 1991 11 p

(Contract DE-FG05-89ER-53301)

(DE91-014360; DOE/ER-53301/3) Avail: NTIS HC/MF A03

Some areas of discussion are as follows: convection driven flow in plasma and fluids; particle transport and rotation damping by sound wave propagation along stochastic magnetic field lines; acceleration of charge article in a magnetic field by electromagnetic and electrostatic waves, lagrangian particle transport in time dependent 2-D flows; fast dynamo; 3-D flows with stagnation points and vortices; edge localized modes in Tokamaks; and code development for nonlinear analysis and visualization. DOE

N91-28982# Texas Univ., Austin. Inst. for Fusion Studies.

STABILITY OF DRIFT-WAVE MODONS IN THE PRESENCE OF TEMPERATURE GRADIENTS

D. Jovanovic (Belgrade Univ., Yugoslavia) and W. Horton May 1991 18 p

(Contract DE-FG05-80ET-53088)

(DE91-014364; DOE/ET-53088/480-Rev; IFSR-480-Rev) Avail: NTIS HC/MF A03

In the homogeneous Hasegawa-Mima equation the dipole vortex or modon solution is well known to be robustly stable from both analytic and numerical studies. In the inhomogeneous plasma where nabla T sub epsilon not = 0 the corresponding vortex has an external structure extending into the high temperature region. Lyapunov stability method is used to determine the stability properties of these extended vortex structures. Negative value of the Lyapunov functional, as a measure of the instability, is shown to be bounded by (R/L sub tau) squared where R is the radius of the core of vortex and L sub tau is scale length of the temperature gradient. DOE

N91-28983# Los Alamos National Lab., NM.

PERFORMANCE OF THE 10-kV, 5-MA PULSED-POWER SYSTEM FOR THE FRX-C COMPRESSION EXPERIMENT

D. J. Rej and W. J. Waganaar 1991 5 p Presented at the 8th IEEE Pulsed Power Conference, San Diego, 17-19 Jun. 1991

(Contract W-7405-eng-36)

(DE91-014745; LA-UR-91-1980; CONF-910640-16) Avail: NTIS HC/MF A01

Performance data are presented for the 10-kV, 5-MA, 1.5-MJ pulsed-power system developed for the Los Alamos magnetic fusion facility FRX-C. This system energizes a low-inductance magnet for the high-power, compression heating of compact toroid plasmas. An ignitron-switched, 20-mF, 10-kV, 4-MA capacitor bank is discharged to produce the main compression field, while an inductively-isolated, 10-mF, 10-kV, 1-MA bank generates an initial magnetic field to accept the translated plasma. To date, the complete system has successfully operated for two years and approximately 2000 high-power discharges. Component performance during typical and fault-mode operation is reviewed. DOE

N91-28984# Lawrence Livermore National Lab., CA. Massively Paralled Computing Initiative.

ON THE USE OF PARTICLE-IN-CELL METHODS FOR THE STUDY OF MAGNETICALLY-CONFINED FUSION PLASMAS

R. J. Procassini 12 Jun. 1991 13 p Prepared in cooperation with California Univ., Berkeley

(Contracts W-7405-eng-48; DE-FG03-86ER-53220)

(DE91-015093; UCRL-ID-107220) Avail: NTIS HC/MF A03

The applicability of electrostatic particle-in-cell (PIC) methods for the simulation of magnetically-confined fusion plasmas is investigated. The aspects of the PIC methodology which allow one to accurately model the representative charge separations found in hot fusion plasmas with far fewer simulation particles are discussed. The number of simulation particles required to resolve the collective effects of interest (such as the ambipolar potential) above the statistical fluctuations is also analyzed. DOE

76 SOLID-STATE PHYSICS

Includes superconductivity.

For related information, see also *33 Electronics and Electrical Engineering* and *36 Lasers and Masers.*

N91-28985# North Carolina Univ., Chapel Hill. Dept. of Chemistry.

A SPECTROSCOPIC DIFFERENTIAL REFLECTOMETRY STUDY OF (100), (110), (111), (311), AND (511) SILICON SURFACES Interim Technical Report

S. Chongsawangvirod and E. A. Irene 6 Dec. 1990 27 p

(Contract N00014-89-J-1178)

(AD-A231022; TR-32) Avail: NTIS HC/MF A03 CSCL 20/2

Spectroscopic Differential Reflectometry, SDR, has been applied to study differences in silicon surfaces with different crystallographic orientations and with very thin films. The SDR technique measures the normalized difference in reflectance of two adjacent samples in the spectral range of 250 to 800 nm near normal incidence. This study demonstrates the surface sensitivity of the SDR technique to the Si crystal orientations, and to the presence of thin oxide films on the Si substrate. The observed orientation dependent spectral features are interpreted in terms of the current understanding of the silicon orientation dependent oxidation kinetics. GRA

N91-28986# General Electric Co., Schenectady, NY. Corporate Research and Development Div.

DEVELOPMENT OF ELEMENTS OF A HIGH T(SUB c) SUPERCONDUCTING CABLE Report, 1 Jan. - 31 Mar. 1991

Kenneth W. Lay 31 Mar. 1991 7 p

(Contract N00014-88-C-0681)

(AD-A236151) Avail: NTIS HC/MF A02 CSCL 20/3

The redirected program is aimed at the development of long lengths of silver-clad BSCCO. BSCCO-2223 is the material of choice with 20 K as the operating temperature goal. Such a tape conductor ultimately could be used in a coil for a magnet, motor, or generator. The program is designed to tackle several key problems with parallel tasks. A large variety of BSCCO powders will be prepared. Silver tubes packed with superconductor powder will be cold deformed to form tape conductors. Alternate methods of making silver-encapsulated superconducting tape will be explored. Variations in the powders and processing parameters will be used to optimize the tape Jc. It has been convincingly demonstrated that the highest Jc tapes are prepared from powder which is not fully reacted to BSCCO-2223. The superiority of pressing over rolling for the final deformation of the tapes has been proven and tentatively explained. Equipment is now available to measure currents up to 240 A at 20 K in fields as high as 9 T. A low Jc degradation of bent tapes will allow coiled lengths to be processed. GRA

N91-28987# Cornell Univ., Ithaca, NY. Dept. of Chemistry.

THE STRUCTURE OF Ta3N5 AT 16K BY TIME-OF-FLIGHT NEUTRON DIFFRACTION

Nathaniel Brese, Michael OKeeffe, Paul Rauch, and Francis DiSalvo 30 May 1991 20 p

(Contract N00014-91-J-1269)

(AD-A236596; TR-10) Avail: NTIS HC/MF A03 CSCL 20/5

Several authors have mapped out the phase diagram of the Ta-N system. Gamma Ta2N crystallizes with close packed metal atoms; the nitrogen atoms fill the octahedral sites. Epsilon-TaN has the B35 structure-type which consists of very densely packed metal atoms; nitrogen atoms fill deformed octahedral holes. Ta4N5 and Ta5N6 can be prepared as thin films and have been analyzed by electron diffraction (Terao, 1971). At elevated temperatures, delta-TaNx forms with the rocksalt structure. Thin films are reported with the hexagonal WC structure. GRA

N91-28988# Michigan Technological Univ., Houghton.

FUNDAMENTAL THEORY OF CRYSTAL DECOMPOSITION Final Report No. 2, 1 Jan. 1989 - 31 Mar. 1991

A. B. Kunz May 1991 769 p

(Contract N00014-89-J-1601)

(AD-A236637) Avail: NTIS HC/MF A99 CSCL 07/4

Lattice defects in or on crystalline materials, determine many technologically important properties. Reliable computerized simulation of such defects are of potential value, and may be expected to contribute to a fundamental understanding of the physical processes that determine the structure and properties of these materials. In the case of point defects, it is attractive to use quantum mechanics to describe the region of the crystal in proximity to the defect, perhaps embedding this region in an external potential determined by some auxiliary principle. The hope here is that the structural response of the lattice to the point defect may then be described by some method which is simpler than the quantum mechanical method used to describe the point defect itself. In the present case, the development is begun for the case of non-metals. In many studies performed prior to the present for such systems, the use of a classical shell model, based upon point charges, and masses, interacting by simple parameterized potentials has been successful in correlating perfect lattice equilibrium data with the ground state properties of defects in these systems. Therefore, the study was begun by choosing to think of the embedding lattice in terms of the classical shell model. It was found that it is possible to retain the functional form of the shell model, but determine all needed parameters from the quantum mechanical calculation, and to augment this functional form with appropriate angular potentials as well. GRA

N91-28989# State Univ. of New York, Buffalo. Dept. of Chemistry.
INDIUM COMPOUNDS WHICH CONTAIN TWO DIFFERENT ORGANIC SUBSTITUENTS. CRYSTAL STRUCTURE OF (In(CH2CMe3) (CH2SiMe3)Cl)2, AN INTERESTING CASE OF PARTIAL LIGAND DISORDER IN THE SOLID STATE
O. T. Beachely, Jr., John D. Maloney, Melvyn R. Churchill, and Charles H. Lake 31 May 1991 31 p
(Contract N00014-90-J-1530)
(AD-A236730; TR-29) Avail: NTIS HC/MF A03 CSCL 20/2

Three new indium compounds which contain two different organic substituents, In(CH2CMe3)(CH2SiMe3)Cl, In(CH2CMe3)(C6H5)Cl, and (Me3CCH2)(Me3SiCH2)InPEt2 were prepared, purified and characterized. All compounds were characterized by partial elemental analysis (C, H and P as appropriate), cryoscopic molecular weight studies in benzene solution as well as NMR and IR spectroscopic studies. All compounds exist as dimeric molecules in solution. NMR spectral data were consistent with the presence of mixtures of cis and trans isomers in solution. GRA

N91-28990# Los Alamos National Lab., NM.
QUANTITATIVE MODELING OF THE POINT DEFECT STRUCTURES OF Fe-DOPED MgO AND MgSiO3 PEROVSKITE
L. M. Hirsch and T. J. Shankland 1991 9 p Presented at the Symposium on Point Defects and Related Properties of Ceramics, Cincinnati, 29 Apr. - 2 May 1991
(Contract W-7405-eng-36)
(DE91-011405; LA-UR-91-1286; CONF-9104236-1) Avail: NTIS HC/MF A02

Many physical and chemical processes in ceramics, such as diffusion, electrical conduction, and solid-state deformation, involve the motion of point defects. Because point defect concentrations in crystals are governed by the laws of thermodynamics, they can be quantitatively determined. In this paper we review recent progress on quantitative point defect concentration modeling in ceramics and minerals. Specific models for MgO and MgSiO3 perovskite that contain Fe as a dominant impurity are discussed. Both materials are believed to be abundant in the Earth's lower mantle and strongly control its properties. For MgO, the model indicates that electrical conduction involves Fe(3+) on Mg sites (Fe(sub Mg)), electrons, and magnesium vacancies. The threshold concentration of Fe in MgO above which other defects are affected strongly depends on oxygen fugacity and temperature. For MgSiO3 perovskite, the strong influence of temperature, pressure, and oxygen activity on defect populations is shown and its importance relative to incongruous experimental results is discussed. DOE

N91-28991# Los Alamos National Lab., NM.
GROWTH OF HIGH T(SUB c) SUPERCONDUCTING THIN FILMS FOR MICROWAVE APPLICATIONS
X. D. Wu, S. R. Foltyn, R. E. Muenchausen, R. C. Dye, D. W. Cooke, A. D. Rollett, A. R. Garcia, N. S. Nogar, A. Pique, and R. Edwards (Neccera, Inc., New Brunswick, NJ.) 1991 8 p Presented at the Superconductivity Applications for Infrared and Microwave Devices 2 Conference, Orlando, 1-5 Apr. 1991
(Contract W-7405-eng-36)
(DE91-011436; LA-UR-91-1329; CONF-9104234-3) Avail: NTIS HC/MF A02

High-(Tc) superconducting thin films of YBa2Cu3O(7-delta) (YBCO) were deposited on sapphire substrates with buffer layers of yitria-stabilized zirconia and cerium oxide by using pulsed laser deposition (PLD) technique. The epitaxial relationship between the substrate and buffer layers as well as the buffer layer and the superconducting film was established. Furthermore, using the same thin film technique, YBCO superconducting thin films were deposited on both sides of substrates of up to 5 cm in diameter. The superconducting properties of the films on both the sapphire with buffer layers and large-area substrates were comparable to the ones of the best YBCO films. DOE

N91-28992# California Univ., Berkeley. Lawrence Berkeley Lab.
SUPERCONDUCTING BOLOMETERS: HIGH-T(SUB c) AND LOW-T(SUB c)
P. L. Richards Apr. 1991 8 p Presented at the Superconductivity Applications for Infrared and Microwave Devices 2 Conference, Orlando, 1-5 Apr. 1991
(Contract DE-AC03-76SF-00098)
(DE91-011830; LBL-30573; CONF-9104234-1) Avail: NTIS HC/MF A02

A description is given of recent work at Berkeley on superconducting detectors and mixers for infrared and millimeter wavelengths. The first report is a review article which summarizes the status of development of superconducting components for infrared and millimeter wave receivers. Next, a report is given on measurements and theoretical modeling of the absorptivity (surface resistance) of high quality epitaxial films of the high-(Tc) superconductor YBCO from 750 GHz to 21 THz. The next report describes measurements of the thermal boundary resistance between YBCO films and various substrates. This resistance is much larger than expected from the acoustic impedance mismatch model and gives a thermal time constant in the nanosecond range for typical YBCO films. Then, there are reports on the design and experimental performance of two different types of high-(Tc) bolometric detectors. One is a conventional bolometer with a gold-black absorber. The other is an antenna coupled microbolometer. The properties of a low-(Tc) microbolometer are also described. The last reports describe accurate measurements and also theoretical modeling of an SIS quasiparticle waveguide mixer for W-band which uses very high quality Ta junctions. The best mixer noise is only 1.3 times the quantum limit. Both the mixer gain and the noise are in quantitative agreement with the quantum theory. DOE

N91-28993# California Univ., Berkeley. Lawrence Berkeley Lab.
FERROMAGNETIC MATERIAL IN THE SUPERCONDUCTOR AND ITS EFFECT ON THE MAGNETIZATION SEXTUPOLE AND DECAPOLE IN THE SSC DIPOLES AT INJECTION
M. A. Green, E. W. Collings, K. R. Marken, and M. D. Sumption (Battelle Memorial Inst., Columbus, OH.) Mar. 1991 10 p Presented at the 3rd Annual International Industrial Symposium on the Super Collider (IISSC), Atlanta, 13-15 Mar. 1991
(Contract DE-AC03-76SF-00098)
(DE91-011886; LBL-30403; CONF-910340-10) Avail: NTIS HC/MF A02

It has been shown that the magnetization of a multifilamentary superconductor can be altered by adding nickel to the composite strand. This report presents the results of calculations of the magnetization sextupole and higher multipoles in a five centimeter SSC dipole with and without nickel as part of the strand composite. The relative distribution of the nickel in the inner and outer coil conductors can be used to effectively eliminate sextupole and decapole at the SSC dipole injection field. Calculations of magnetization sextupole in the dipole are presented for strand with substituted nickel filaments and strand with electroplated nickel. The effect of nickel in the strand on the SSC dipole field quality at fields above the injection field is described. The effect of nickel in the strand on magnetization sextupole flux creep decay and the magnetization sextupole temperature dependence is also discussed. DOE

N91-28994# Brookhaven National Lab., Upton, NY.
MAGNETIZATION AND CRITICAL CURRENTS OF TIN-CORE MULTIFILAMENTARY Nb3Sn CONDUCTORS
A. K. Ghosh and M. Suenaga 1990 5 p Presented at the Applied Superconductivity Conference, Aspen, 24-28 Sep. 1990

(Contract DE-AC02-76CH-00016)
(DE91-012241; BNL-44556; CONF-900944-45) Avail: NTIS HC/MF A01

This paper presents critical current and magnetization data for some multifilamentary Nb3 Sn wires that have been produced by the internal-tin method. A comparison of magnetization and transport critical current measurements show that filament bridging during heat treatment is a common occurrence leading to effective filament diameters that are sometimes an order of magnitude larger than the geometrical filament size. At present, J(sub c)'s (in the non-copper region) greater than 1300 A/sq mm at 10T have been achieved in some conductors, which also exhibit high losses. Low losses have only been seen in conductors with a high local ratio of niobium to copper. Also the use of (Nb-1 percent Ti) alloy instead of pure Nb helps to reduce low field loss and increase high field J(sub c). Measurements of the temperature dependence of hysteretic loss to 5T indicate that loss decreases linearly with increasing temperature. DOE

N91-28995# Cornell Univ., Ithaca, NY. Dept. of Materials Science and Engineering.

SURFACE PHASES AND THEIR INFLUENCE ON METAL-OXIDE INTERFACES

J. Blakely Mar. 1991 6 p
(Contract DE-FG02-87ER-45328)
(DE91-012277; DOE/ER-45328/5) Avail: NTIS HC/MF A02

During the first part of the current grant period we have carried out an extensive series of experiments on the characteristics of S and O coadsorption on single crystal Ni surfaces, and the effect of S submonolayers on the growth of oxide films. At the submonolayers regime coadsorbed S and O form either a p(2 x 2) or a sq root of 3 x sq root of 3 R30(deg) ordered phase on Ni(111) depending on the conditions of exposure of the S2 molecular beam and the coverage of coadsorbed oxygen. The disordering temperatures of the phases of coadsorbed S and O have been measured by monitoring the intensity of LEED beams at selected electron energies. Preliminary phase diagrams for this 2-D binary, S + O, alloy system have been constructed from the variation of transition temperature with S fractional coverage. The dependence of the kinetics of the O adsorption and initial oxidation process on S coverage was studied in some detail. O adsorption is strongly retarded by the presence of adsorbed S probably due to inhibition of the dissociation step. The onset of oxide nucleation is also delayed by S coverage. XPS studies of the O(1S) and Ni(2p) levels as a function of S coverage show no major dependence on S coverage. Related studies of the atomic step structure of Ni surfaces vicinal to (111) was carried out with LEED using a position sensitive detector. LEED beam profiles measured as a function of temperature are being used to obtain details of the atomic step clustering transition. At a later stage of the work the coadsorption and oxidation studies will be extended to such surfaces with controlled defect (..step) arrays. DOE

N91-28996# Stanford Linear Accelerator Center, CA.

STRAIN ENHANCED ELECTRON SPIN POLARIZATION OBSERVED IN PHOTOEMISION FROM InGaAs

T. Maruyama, E. L. Garwin, R. Prepost, G. H. Zapalac, J. S. Smith, and J. D. Walker (California Univ., Berkeley.) May 1991 3 p Presented at the 1991 Institute of Electrical and Electronics Engineers (IEEE) Particle Accelerator Conference (PAC), San Francisco, 6-9 May 1991
(Contracts DE-AC03-76SF-00515; DE-AC02-76ER-00881)
(DE91-012319; SU-SLAC-PUB-5546; CONF-910505-84; WISC-EX-91-317) Avail: NTIS HC/MF A01

Electron spin polarization in excess of 70 percent has been observed in photoemission from a 0.1 micron thick epitaxial layer of In(x)Ga(1-x)As with x (approx) 0.13 grown on a GaAs substrate. Under these conditions, the epitaxial layer is expected to be highly strained by the 0.9 percent lattice mismatch, as confirmed by X-ray diffractometer measurements of the lattice parameter. The electron polarization and the quantum efficiency have been measured as a function of the excitation photon energy from 1.25 to 2.0 eV. A significant enhancement of the electron polarization occurs in the vicinity of 1.33 eV where the expected strain-induced level splitting permits optical excitation of a single band transition. Measurements made on a control sample of 1.14 micron thickness, significantly larger than the critical thickness for pseudomorphic strain, show no polarization enhancement. These measurements represent the first observation of strain-enhanced electron spin polarization for photoemitted electrons. DOE

N91-28997# California Univ., Berkeley. Lawrence Berkeley Lab.

HIGH-T(SUB c) THIN-FILM MICROELECTRONICS

J. Clarke, Du Quan, M. J. Ferrari, A. H. Miklich, J. J. Kingston, F. C. Wellstood, and M. S. Colclough (Conductus, Inc., Sunnyvale, CA.) Nov. 1990 10 p Presented at the 3rd International Symposium on Superconductivity, Sendai (Japan), 6-9 Nov. 1990
(Contract DE-AC03-76SF-00098)
(DE91-012340; LBL-29794; CONF-901169-7) Avail: NTIS HC/MF A02

A complete microelectronics technology based on high-transition temperature superconducting thin films requires two key components: a reproducible Josephson weak link and multilayer process for interconnects. Although many kinds of weak link have been studied, none is yet satisfactory for circuits involving more than a few elements. On the other hand, a viable, interconnect technology has been developed in which two YBa2Cu3O(7-x) films may be either electrically isolated or connected via a superconducting contact. The junctions and interconnect technology have been used to produce magnetometers involving a flux transformer with a multiturn input coil coupled to a direct current superconducting quantum interference device. DOE

N91-28998# California Univ., Berkeley. Lawrence Berkeley Lab.

PHOTOLITHOGRAPHICALLY PATTERENED THIN-FILM MULTILAYER DEVICES OF YBa2Cu3O(7-x)

J. J. Kingston, F. C. Wellstood, Du Quan, and J. Clarke Sep. 1990 5 p Presented at the Applied Superconductivity Conference, Aspen, 24-28 Sep. 1990
(Contract DE-AC03-76SF-00098)
(DE91-012350; LBL-28889; CONF-900944-47) Avail: NTIS HC/MF A01

We have fabricated thin-film YBa2Cu3O(7-x) SrTiO3YBa-2Cu3O(7-x) multilayer interconnect structures in which each in situ laser-deposited film is independently patterned by photolithography. In particular, we have constructed the two key components necessary for a superconducting multilayer interconnect technology, crossovers and window contacts. As a further demonstration of the technology, we have fabricated a thin-film flux transformer, suitable for use with a Superconducting Quantum Interference Device (SQUID), that includes a ten-turn input coil with 6 micrometer linewidth. Transport measurements showed that the critical temperature was 87K and the critical current was 135 microns A at 82K. DOE

N91-28999# Pacific Northwest Lab., Richland, WA.

BIOMIMETIC THIN FILM DEPOSITION

P. C. Rieke, A. A. Campbell, B. J. Tarasevich, G. E. Fryxell, and S. B. Bentjen Apr. 1991 22 p Presented at the 201st American Chemical Society (ACS) National Meeting, Atlanta, 14-19 Apr. 1991
(Contract DE-AC06-76RL-01830)
(DE91-012485; PNL-SA-19277; CONF-910402-16) Avail: NTIS HC/MF A03

Surfaces derivatized with organic functional groups were used to promote the deposition of thin films of inorganic minerals. These derivatized surfaces were designed to mimic the nucleation proteins that control mineral deposition during formation of bone, shell, and other hard tissues in living organisms. By the use of derivatized substrates control was obtained over the phase of mineral deposited, the orientation of the crystal lattice and the location of deposition. These features are of considerable importance in many technically important thin films, coatings, and composite materials.

Methods of derivatizing surfaces are considered and examples of controlled mineral deposition are presented. DOE

N91-29000# Oak Ridge National Lab., TN.

THERMODYNAMIC AND TRANSPORT PROPERTIES OF SUPERCONDUCTORS IN VERY HIGH MAGNETIC FIELDS

M. Rasolt May 1991 28 p Presented at the Physical Phenomena At High Magnetic Fields, Tallahassee, 15-18 May 1991
(Contract DE-AC05-84OR-21400)
(DE91-012530; CONF-9105151-1) Avail: NTIS HC/MF A03

The progress made in the last few years in understanding the properties of superconductors in very high magnetic fields is discussed. A key point emphasized is that the usual frustration of a superconductor, reflected in diamagnetic pair breaking, is completely obviated when all electrons reside in only a few Landau levels. A new relation between the superconducting order parameter and the magnetic field now exists which permits a strong enhancement of the critical temperature with increasing magnetic field. The issue of Pauli pair breaking and the effect of impurities in this new state are also discussed along with the important observation that the attractive component of the effective electron-electron interaction is enhanced with increasing magnetic field. DOE

N91-29001# Ames Lab., IA.

SYNTHESIS AND CHARACTERIZATION OF REDUCED TERNARY MOLYBDENUM OXIDES AND SOLUBLE COPPER (III) ALKOXIDE COMPLEXES Ph.D. Thesis

Sheng-Chang Chen 14 May 1991 217 p
(Contract W-7405-eng-82)
(DE91-012679; IS-T-1510) Avail: NTIS HC/MF A10

This research work involves both solid state and solution chemistry. In the area of solid state chemistry, a number of exciting reduced ternary molybdenum oxides containing both discrete oligomeric cluster units (K3Mo14O22 (1) and BaMo5O8 (2)) and infinite metal-metal bonded chains (KMo4O6 (3) and Sr(0.62)Mo4O6 (4)) were discovered. Compound 1 contains discrete oligomeric units of three trans-edge-shared Mo6 octahedra interconnected by Mo-O-Mo bonding to form chains along the monoclinic c-axis. The discrete oligomeric cluster units contained in compound 2 (Ba2Mo10O16) are trans-edge-shared Mo10 bioctahedral clusters interconnected along the a-axis of the monoclinic cell. In the area of copper(II) alkoxide chemistry, several interesting complexes with the anion of 2-(2-hydroxyethyl)pyridine (hep) as ligands were synthesized and structurally characterized. Compounds (CuCl(hep)2), (CuCl(hep)(Hhep)2)(center dot)2CH2Cl2, and (CuCl(hep)(py)2)(center dot)CH2Cl2 are doubly bridged copper(II) dimers involving a Cu2O2 moiety. The partially characterized compounds K(0.5)M(1.9)Mo14O22 (M = Ca, Sr, Ba, Pb, and Sn), Ca(3-x)Mo14O22, Sn(3.6Mo16O24, PbMo6O10, and a novel copper(II) alkoxide complex are also reported in this work. DOE

N91-29002# California Univ., Berkeley. Lawrence Berkeley Lab.

CHARACTERIZATION OF CRYSTALLINE INTERFACES BY ADVANCED ELECTRON MICROSCOPY

U. Dahmen, ed. Aug. 1990 53 p Presented at the Characterization of Crystalline Interfaces By Advanced Electron Microscopy, Berkeley, 20-24 Aug. 1990
(Contract DE-AC03-76SF-00098)
(DE91-011883; LBL-30365; CONF-9008187-Summ) Avail: NTIS HC/MF A04

The program was divided into three parts: one dealing with generic interface phenomena, another with materials related aspects of interfaces and the last concentrating on TEM technique. Naturally, there was some overlap between the different parts, but this only served to illuminate some problems from different angles. Although a good part of the discussion focused on high resolution imaging, it became clear that this is by no means the only electron microscopy technique capable of significant contributions to the field. Diffraction contrast techniques become increasingly important, especially in the area of irrational interfaces where HREM is severely handicapped by lack of crystal alignment. For the quantitative characterization of some interface features such as roughness, displacement and strain, convergent beam techniques are very powerful and probably underutilized. DOE

N91-29003# Sandia National Labs., Albuquerque, NM.

THE SPATIAL RESOLUTION OF X RAY MICROANALYSIS IN THIN FOILS

D. B. Williams, J. I. Goldstein, J. R. Michael, and A. D. Romig, Jr. (Lehigh Univ., Bethlehem, PA.) 1991 7 p Presented at the 49th Electron Microscopy Society of America (EMSA) Annual Meeting, San Jose, 4-9 Aug. 1991
(Contract DE-AC04-76DP-00789)
(DE91-011949; SAND-91-0855C; CONF-910870-12) Avail: NTIS HC/MF A02

The spatial resolution of x ray microanalysis is examined in thin foils. The theory of the scattering of an electron beam with a thin foil is discussed. DOE

N91-29004# Sandia National Labs., Albuquerque, NM.

DONOR FORMATION UNDER HYDROGEN PLASMA EXPOSURE AND ION IMPLANTATION

H. J. Stein and S. Hahn (Stanford Univ., CA.) 1991 8 p Presented at the 179th Meeting of the Electrochemical Society, Washington, 5-10 May 1991
(Contract DE-AC04-76DP-00789)
(DE91-011958; SAND-91-0898C; CONF-910552-10) Avail: NTIS HC/MF A02

Results were obtained on hydrogen dose, dose rate and substrate temperature dependence for hydrogen assisted thermal donor formation in Czochralski Si. The study combined ion implantation and hydrogen plasma exposure to inject hydrogen, and infrared absorption and spreading resistance probe measurements to detect the donors. Near surface donor concentrations increase with dose and temperature between 350 and 400 C. The penetration depth for thermal donor formation exhibits a (radical)t dependence, and a thermal activation energy of 1.5 (plus or minus) 0.2 eV. DOE

N91-29005# Oak Ridge National Lab., TN

INTERLAYER PAIRING AND c-AXIS VERSUS ab-PLANE GAP ANISOTROPY IN HIGH Tc SUPERCONDUCTOR

R. A. Klemm (Argonne National Lab., IL.) and S. H. Liu 1991 13 p Presented at the Workshop on Electronic Structures and Mechanisms for High Temperature Superconductivity, Miami, 3-9 Jan. 1991 Prepared in cooperation with Argonne National Lab., IL
(Contracts DE-AC05-84OR-21400; W-31-109-eng-38)
(DE91-012218; ANL/CP-73103; CONF-910190-4) Avail: NTIS HC/MF A03

Interlayer BCS-like (Bardeen-Cooper-Schrieffer Theory) pairing in nearly two-dimensional superconductors with N = 1,2,3 conducting layers per unit cell is investigated. For N = 1, the singlet delta(sub s) and triplet delta(sub t), order parameters have identical T(sub c)'s (T(sub cs) = T(sub ct)) and magnitudes, and the gap is isotropic. For N = 2, T(sub cs) is greater than or equal to T(sub ct) and the absolute value of delta(sub s) is greater than or equal to delta(sub t). In region 1 of the parameters, the gap is anisotropic and nodeless for T less than T(sub cs). In region 2, the gap has nodes near to T(sub cs), but is nodeless at low T. For N = 3, T(sub cs) is much greater than T(sub ct), and the gap is anisotropic but nodeless on two bands, but has a node on the third band. For N = 2,3, the k(sub z)-dependence of the gap and the quasiparticle density of states are found. For N = 1(2,3), intralayer and interlayer pairing are completely (essentially) incompatible. DOE

N91-29006# California Univ., Berkeley. Lawrence Berkeley Lab.

TEM ANALYSIS OF ENCLOSED CRYSTAL MICROSTRUCTURES AND INTERFACES

U. Dahmen Aug. 1990 2 p

(Contract DE-AC03-76SF-00098)
(DE91-012344; LBL-29592) Avail: NTIS HC/MF A01

The study of enclosed crystal shapes in relation to their interface structure is an area of phase transformations rich in new and interesting phenomena. It is shown that transmission electron microscopy (TEM) can make an important contribution to the understanding and control of materials properties through the experimental study of these phenomena by conventional, analytical, high resolution, diffraction and dynamic in-situ techniques. There is a close connection between the morphology, interface structure, defect substructure, and formation mechanism of precipitates in a solid matrix. Complementary to static observations, dynamic in-situ experiments by high voltage electron microscopy show that germanium precipitates in an aluminum matrix can be transformed between a strongly faceted, anisotropic shape and a rounded, isotropic shape. DOE

N91-29007# California Univ., Berkeley. Lawrence Berkeley Lab.
THIN-FILM FLUX TRANSFORMERS OF YBa2Cu3O(7-x)
F. C. Wellstood, J. J. Kingston, M. J. Ferrari, and J. Clarke Sep. 1990 5 p Presented at the Applied Superconductivity Conference, Aspen, 24-28 Sep. 1990
(Contract DE-AC03-76SF-00098)
(DE91-012363; LBL-28890; CONF-900944-48) Avail: NTIS HC/MF A01

Using a three layer in situ laser deposition process, superconducting thin film flux transformers were constructed of YBa2Cu3O(7-x) (YBCO). The transformers are designed for efficient coupling to a planar thin film dc SQUID, have 0.7 sq cm magnetic field pickup areas, and 10-turn input coils. When coupled to a low transition temperature (Tc) SQUID, the resulting hybrid magnetometer exhibits excess low frequency flux noise which arises in the transformer. This noise depends on the geometry of the flux transformer, and the observed behavior agrees with model calculations of the expected contribution from flux motion in the YBCO. The hybrid magnetometer attains a magnetic field sensitivity of about 0.9 pTHz(exp -1/2) at 1Hz with the transformer at 60K; the rms noise decreases as 1/f(exp 1/2) up to a frequency of (approx) 1kHz. It is believed that the sensitivity is high enough for use, for example, in magnetocardiography. DOE

N91-29008# Argonne National Lab., IL.
EFFECT OF SIZE AND GEOMETRY ON LEVITATION FORCE MEASUREMENTS BETWEEN PERMANENT MAGNETS AND HIGH-TEMPERATURE SUPERCONDUCTORS
Y. S. Cha, J. R. Hull, T. M. Mulcahy, and T. D. Rossing 1991 16 p Presented at the 5th Joint Magnetism and Magnetic Materials (MMM/INTERMAG) Conference, Pittsburgh, 18-21 Jun. 1991 Prepared in cooperation with University of Northern Illinois, De Kalb
(Contract W-31-109-eng-38)
(DE91-012472; ANL/CP-72199; CONF-910608-3) Avail: NTIS HC/MF A03

A series of experiments measuring the levitation force between a permanent magnet (PM) and a high temperature superconductor (HTS) and between pairs of PMs, coupled with finite element analysis of the experiments, has identified factors that influence the levitation force. The self demagnetizing factor within the HTS and, to some extent, within the PM has a profound effect on magnetic pressure. For large HTSs with strong flux pinning, the demagnetizing effect of the diamagnetic image of the PM is substantial. For short distances between the HTS and PM, compression of magnetic flux produces a dependence on PM diameter. DOE

N91-29009# Sandia National Labs., Albuquerque, NM.
MEASUREMENT ACCURACY OF MACROSCOPIC QUANTUM CIRCUITS WITH RF-BIASED JOSEPHSON JUNCTION ARRAYS
D. H. Dunlap and R. V. Duncan 1991 4 p Presented at the International Superconductive Electronics Conference (ISEC '91), Glasgow, Scotland, 25-27 Jun. 1991
(Contract DE-AC04-76DP-00789)
(DE91-012651; SAND-91-0954C; CONF-910623-1) Avail: NTIS HC/MF A01

The dc voltage output from an hysteretic Josephson junction which is locked to an ac frequency source differs from the ideal Josephson relation if the junction drives a current about a closed superconducting circuit. The difference in voltage Delta V from two hysteretic Josephson junctions driven in series opposition is proportional to the difference in their driving frequencies Delta(omega) if the junctions are each biased to the nth voltage step. It is shown here, however, that Delta V is systematically smaller than the voltage difference Delta V(sub 0) predicted by the ideal Josephson relation Delta V(sub 0) = (n(Plank constant)/2e) Delta(omega). If the loop inductance approaches zero, the smallest detectable voltage difference Delta V(sub 0) between two junctions is limited by the intrinsic Josephson inductance. For arrays of more than one junction, however, Delta V(sub 0) remains proportional to the loop inductance. DOE

N91-29010# Superconducting Super Collider Lab., Dallas, TX.
A SYSTEM APPROACH TO THE DESIGN OF SUPERCONDUCTING MAGNETS
A. Pennington Mar. 1991 11 p Presented at the 3rd Annual International Industrial Symposium on the Super Collider (IISSC), Atlanta, 13-15 Mar. 1991
(Contract DE-AC02-89ER-40486)
(DE91-012707; SSCL-377; CONF-910340-31) Avail: NTIS HC/MF A03

The design of superconducting magnets poses numerous technical, engineering and physics challenges to ensure that the magnets, when installed in the operational environment will satisfy performance requirements of the accelerator. The discussion presented in this paper will address the systematic, methodical process, as applied by the magnet system design engineer, that defines magnet performance requirements, the allocation of requirements to magnet components, and the development of design solutions which will satisfy the requirements. The approach presented will show how the system engineer parses top-level performance requirements as established by the system specification ('shall' statements), develops design solutions, performs design trades to ensure selection of the best solution in terms of life-cycle cost and performance, verifies the design through analysis and computer modelling, and then validates the design by build-and-test. The process shows the methods for achieving traceability of design and correlation of design solutions to performance parameters. DOE

N91-29011# Cornell Univ., Ithaca, NY.
DEFECT STUDIES IN III-V THIN FILM SEMICONDUCTORS
D. Ast 1991 26 p
(Contract DE-FG02-86ER-45278)
(DE91-012746; DOE/ER-45278/T1) Avail: NTIS HC/MF A03

GaAs based electronic devices usually consist of several different layers selected for their appropriate electronic properties (e.g., the emitter material in a heterojunction bipolar transistor must have a larger bandgap than the base material). These layers must be grown on top of each other on the available substrate materials (GaAs, InP) without introducing crystalline defects at the interface. The growth of defect free interfaces is generally accomplished by working with lattice matched alloys. However, the requirement of lattice match very greatly reduces the number of the materials systems that can be used. A much wider range of materials, permitting a much closer implementation of optimum bandgap engineering, could be used if the constraint of lattice match could be relaxed. DOE

N91-29012# Pacific Northwest Lab., Richland, WA.
RAMAN STUDIES OF STRESS-INDUCED PHASE TRANSFORMATION IN TITANIA FILMS
G. J. Exarhos and N. J. Hess May 1991 7 p Presented at the Spring Meeting of the Materials Research Society (MRS), Anaheim, 29 Apr. - 3 May 1991

(Contract DE-AC06-76RL-01830)
(DE91-012871; PNL-SA-19094; CONF-910406-11) Avail: NTIS HC/MF A02

Time-resolved micro-Raman spectroscopy is used to follow the amorphous to crystalline phase transformation in sol-gel deposited titania films induced thermally or through the action of applied hydrostatic pressure in a diamond anvil cell. Time-dependent phonon intensities intrinsic to the growing phase are related to the volume fraction of crystallite present at any time. The sigmoidally generated curves can be modeled in terms of modified Avrami ingrowth kinetics in which diffusion of the amorphous phase to the nucleation center is restricted by the morphology of the evolving phase. Phonon frequency and linewidth measurements during the course of the transformation probe changes in films stress and particle size which are used to understand the mechanistics of the transformation. Raman measurements also are used to derive a phase stability diagram for titania films. DOE

N91-29013# Cornell Univ., Ithaca, NY. Dept. of Chemistry.

SYNTHESIS AND PROPERTIES OF NOVEL CLUSTER PHASES

Francis DiSalvo 16 Apr. 1991 8 p
(Contract DE-FG02-87ER-45298)
(DE91-013006; DOE/ER-45298/7) Avail: NTIS HC/MF A02

Our approach to studying the solution chemistry of clusters has been to first synthesize cluster phases by solid state reactions, then to put the cluster into solution, and in some cases to reassemble a new cluster - containing solid phase from that solution. Two aspects of this work have been: (1) the study of the condensed cluster phase, LiMo3Se3, in which the condensed clusters form linear metallic chains; and (2) the solution chemistry of Nb6I11 and the solution synthesis of Mo6S8 like clusters. We have discovered several new families of compounds that are characterized by condensed sheets of metal atoms. The first class of materials has the general formula MM'Te2 where we have found so far that M = Fe, Co, or Ni and M' = Ta or Nb. While one might have expected to find an ordered NiAs structure type, or equivalently an M intercalated layered M'Te2 compound, both the M and M' are found to form a metal-metal bonded sheet that is bounded on the top and bottom by Te layers. The second class of materials also form sheet like structures with metal atoms sandwiched between two buckled layers of Te atoms. In these compounds, the metal atoms are bonded together to produce ribbons running in one direction. DOE

N91-29014# Oak Ridge National Lab., TN.

KOSTERLITZ-THOULESS-LIKE BEHAVIOR OVER EXTENDED RANGES OF TEMPERATURE AND LAYER THICKNESS IN CRYSTALLINE YBa2Cu3O(7-x) / PrBa2Cu3O(7-x) SUPERLATTICES

D. H. Lowndes and D. P. Norton Apr. 1991 13 p Presented at the Electronic Structure and Mechanisms for High Temperature Superconductivity, Coral Gables, 3-9 Jan. 1991
(Contract DE-AC05-84OR-21400)
(DE91-013237; CONF-910145-4) Avail: NTIS HC/MF A03

High-temperature superconductivity is associated with layered, quasi-two-dimensional (2D) crystal structures and with carriers moving in CuO2 planes. Because the c-axis superconducting coherence length is very short (e.g., zeta sub c) approximately 3 to 6 angstrom, vs. a lattice constant c approximately 11.7 angstroms in YBa2Cu3O(7-x), questions arise whether isolated single-cell-thick layers of these materials are superconducting and, if so, how their superconductivity is affected, first, by their extreme anisotropy (including possible reduced dimensionality) and, second, by residual interlayer coupling or other interactions. We and several other groups recently fabricated epitaxial M x N 123-family superlattices in which c-axis perpendicular (c sub perpendicular YBa2Cu3O(7-x)YBCO layers M unit cells in thickness are separated by N unit-cell-thick layers of semiconducting PrBa2Cu3O(7-x) (PBCO). The superlattice T(sub co)(R = 0) was found to decrease rapidly with increasing PBCO layer thickness, but then to saturate at T(sub co) (approximately) 19 K, 54 K, 71 K, or 80 K, for structures containing 1-, 2-, 3-, or 4-cell-thick YBCO layers, respectively. In contrast, recent measurements for Bi2Sr2Ca(1-x)Y(x)1Cu2O8 based superlattices, in which superconducting (x = 0.15) and semiconducting (x = 0.5) layers also alternate, show almost no change in Tc approximately 65 K with decreasing superlattice period. These results imply that high-(Tc) is an intrinsic property of CuO2 bilayers, but that 3-dimensional interactions are present, at least for the 123-family materials. DOE

N91-29015# Los Alamos National Lab., NM.

EPITAXIAL GROWTH OF SILICON ON CoSi2(001)/Si(001)

Q. F. Xiao, J. R. Jimenez, and L. J. Schowalter (Rensselaer Polytechnic Inst., Troy, NY.) 1991 7 p Presented at the Spring Meeting of the Materials Research Society (MRS), Anaheim, 29 Apr. - 3 May 1991
(Contract W-7405-eng-36)
(DE91-013387; LA-UR-91-1734; CONF-910406-12) Avail: NTIS HC/MF A02

Epitaxial Si layers have been grown under a variety of growth conditions on CoSi2(001) by molecular beam epitaxy (MBE). The structural properties of the Si overgrowth were studied by in-situ Reflection High Energy Electron Diffraction (RHEED), as well as ex-situ MeV He-4(+) ion channeling and High Resolution Transmission Electron Microscopy (HRTEM). Strong influences of the CoSi2 surface reconstruction on the Si overgrowth have been observed. RHEED studies show islanding growth Si on the CoSi2(001)(3 square root of 2 x square root of 2)R45 reconstructed surface, but smooth growth of Si on the CoSi2(001) (square root of 2 x square root of 2)R45 reconstructed surface, under the same growth conditions. The growth of Si on thin layers of CoSi2 (2nm-6nm) with (square root of 2 x square root of 2)R45 reconstructed surface at 160 C results in high crystalline quality for the Si top layer, as indicated by good channeling minimum yield (chi(sub min) less than 6 percent), but cross-sectional TEM shows that the CoSi2 layers are discontinuous. We also report preliminary results on Si grown on a 2 x 2 reconstructed CoSi2(001) surface. DOE

N91-29016# Oak Ridge National Lab., TN.

EXCESS HEAT PRODUCTION IN COMPOSITE SUPERCONDUCTORS DURING CURRENT REDISTRIBUTION

L. Dresner May 1991 17 p
(Contract DE-AC05-84OR-21400)
(DE91-013547; ORNL/TM-11827) Avail: NTIS HC/MF A03

Immediately after a large conductor with segregated matrix and superconductor is driven normal, the transport current is confined to the vicinity of the superconductor; thus, the Joule power is initially much larger than it would be if the current density were uniform. Subsequently, the current diffuses throughout the matrix and eventually fills it uniformly, so that the excess Joule power gradually falls to zero. This paper presents simple formulas for the time-integrated excess Joule power (the excess Joule heat) produced in conductors of various shapes with various dispositions of matrix and superconductor. DOE

N91-29017# International Centre for Theoretical Physics, Trieste (Italy).

THE DETERMINATION OF THE MOMENTUM MATRIX ELEMENTS INVOLVED IN CALCULATING THE DIELECTRIC CONSTANTS OF SUPERLATTICES USING THE TIGHT-BINDING METHOD

Zhizhong Xu Aug. 1990 14 p
(DE91-617789; IC-90/231) Avail: NTIS HC/MF A03

Using the Wigner-Eckart theorem, we have deduced formulae for momentum matrix elements in the tight-binding approach in terms of some parameters. For III-V compound semiconductors, some explicit expressions have been obtained with four parameters. These parameters can be determined by comparing the calculated values of electrical or optical constants with their corresponding experimental values. The formulae have been applied to calculation of the imaginary part of the dielectric constant for a monolayer superlattice Ga(0.47)In(0.53)As/InP(110). DOE

N91-29018# International Centre for Theoretical Physics, Trieste (Italy).

TRANSIT TIME FOR RESONANT TUNNELING

G. GarciaCalderon and A. Rubio Sep. 1990 12 p
(DE91-617799; IC-90/261) Avail: NTIS HC/MF A03

This work considers properties of the partial widths in one dimensional elastic resonant tunneling in order to propose a transit-time tau(sub tr) = (h/2(pi))/(gamma(sub n)T(sup res)) where gamma(sub n) is the elastic width and T(sup res) the transmission coefficient at resonance energy. This time is interpreted as an average over the resonance energy width. It is shown that the tunneling current density integrated across a sharp resonance is inversely proportional to tau(sub tr). This transit time may be much larger than the values predicted by other definitions. DOE

N91-29019# International Centre for Theoretical Physics, Trieste (Italy).

COHERENT CHARGE FLUCTUATIONS IN JOSEPHSON JUNCTIONS AND THE OSCILLATIONS OF THE EFFECTIVE CAPACITANCE

I. V. Krive and A. S. Rozhavsky Jul. 1990 5 p
(DE91-618098; IC-90/147) Avail: NTIS HC/MF A01

We predict novel voltage oscillations of the effective capacitance of small Josephson junctions. This macroscopic effect involves coherent charge fluctuations with charge 2e, leading to a period of oscillations, V(sub c) = 2e/C, where C is the junction capacitance. The amplitude of the effect decreases with temperature as exp(-pi(exp 2)T/epsilon(sub c)), where epsilon(sub c) = 2e(exp 2)/C. DOE

N91-29020# Pennsylvania Univ., Philadelphia. Dept. of Materials Science and Engineering.

STRUCTURE AND DYNAMICS IN LOW-DIMENSIONAL GUEST HOST SOLIDS

J. Fischer Apr. 1991 6 p
(Contract DE-FG02-86ER-45254)
(DE91-012169; DOE/ER-45254/5) Avail: NTIS HC/MF A02

This progress report presents results from work during the period of June 1, 1990 through May 31st, 1991. Topics discussed include instrumentation, publications, and personnel. Work areas discussed include: pressure-induced transitions in Li- and Ag-TiS2, hyper-dense superconducting GIC's, temperature-dependent x-ray structure of (CH)(x) and (CH)2(x): analogies to rotator phases in short-chain alkanes, trans-(CH)(x) at high pressure, broken symmetries in polymer intercalation channel lattices, high-resolution study of conductivity and cell potential vs. concentration in K-doped (CH)(x), new doped (CH)(x) phases: ternary compounds and amorphous intercalation compounds, and vibrational density states from inelastic neutron scattering. DOE

N91-29021# California Univ., Berkeley. Lawrence Berkeley Lab.

THE EFFECT OF THE QUANTUM SUSCEPTANCE ON THE GAIN OF SUPERCONDUCTING QUASIPARTICLE MIXERS

C. A. Mears, Qing Hu, and P. L. Richards Sep. 1990 6 p Presented at the Applied Superconductivity Conference, Aspen, 24-28 Sep. 1990
(Contract DE-AC03-76SF-00098)
(DE91-012352; LBL-29588; CONF-900944-46) Avail: NTIS HC/MF A02

A detailed analysis of the effects of the quantum susceptance on the performance of superconductor insulator superconductor (SIS) mixers is performed. It was found that the principal effects of the quantum susceptance is to change the dc bias at which optimum coupling of the signal to the mixer occurs, and to change the output admittance at the IF frequency, thus changing the available gain. DOE

N91-29022# EG and G Energy Measurements, Inc., Goleta, CA.

ELECTRICAL AND PHOTOMECHANICAL EFFECTS OF PLASTIC DEFORMATION OF MERCURIC IODIDE

J. Marschall, F. Milstein, G. Georgeson (Boeing Co., Seattle, WA.), and V. Gerrish 1991 19 p
(Contract DE-AC08-88NV-10617)
(DE91-013108; EGG-10617-2097) Avail: NTIS HC/MF A03

The effects of bulk plastic deformation of mercuric iodide (HgI2), upon some of the electronic properties relevant to the performance of HgI2 as a radiation detector were examined experimentally. Hole lifetimes, as well as hole and electron mobilities, were measured at various stages of sample deformation. Hole lifetimes were found to decrease by a factor of 2 under strains of several percent; carrier mobilities varied within experimental error, except during creep loading where electron and hole mobilities decreased by about 65 percent and 25 percent, respectively. Additionally, dark current measurements were made on specimens with varying degrees of accumulated plastic damage caused by c plane shear. Dark current values did not strongly reflect the extent of bulk plastic damage in deformed specimens. DOE

N91-29023# Los Alamos National Lab., NM.

SHOCK INITIATION OF PENTAERYTHRITOL TETRANITRATE CRYSTALS: OPTICAL ABSORPTION AND EMISSION STUDIES

R. N. Mulford, J. J. Dick, and D. R. Pettit 1991 5 p Presented at the 1991 American Physical Society (APS) Conference on Shock Compression of Condensed Matter, Williamsburg, 17-20 Jul. 1991
(Contract W-7405-eng-36)
(DE91-013381; LA-UR-91-1758; CONF-9107105-11) Avail: NTIS HC/MF A01

Absorption and emission spectra of initiating crystals are obtained at two times during initiation, and a time-resolved record of integrated light is obtained during plane-wave shock initiation of single crystals of PETN at 4 GPa. Time-resolved photodiode records clearly show an induction time during which the crystal becomes absorbing, a region of increasing emission with increasing shock travel time, and termination of emission by the returning rarefaction. Evidence exists for emergence of a superdetonation wave at least 1.5-mm behind the shock front. Resolved spectroscopic records identify the absorbing region as shocked PETN, and suggest evolution of NO2 and NO as part of the early chemistry in the initiation. DOE

N91-29024# Argonne National Lab., IL.

EVOLUTION OF DEFECT CLUSTER DISTRIBUTIONS DURING IRRADIATION

H. Wiedersich May 1991 20 p Presented at the International Conference on Physics of Irradiation Effects in Metals, Siofok (Hungary), 20-24 May 1991
(Contract W-31-109-eng-38)
(DE91-013405; ANL/CP-72655; CONF-9105130-3) Avail: NTIS HC/MF A03

Defects produced by irradiation are often strongly spatially correlated. Energetic primary recoil atoms produce cascades with vacant lattice sites predominantly in the central regions, and interstitial atoms at the periphery. A fraction of the defects produced form clusters during cascade events. Because of their spatial distribution more mobile interstitial atoms than vacancies are released into the matrix following the cascade events. Populations of vacancy and interstitial clusters evolve towards quasi-steady-state distributions. As long as vacancy clusters are thermally moderately stable, i.e., at temperatures below rapid self diffusion, an excess interstitial flux persists in the matrix; as a consequence, vacancy clusters formed in cascades shrink, and interstitial clusters grow. We examine the evolution of these cluster distributions, and their effects on sink strength and radiation-enhanced diffusion, as function of dose for irradiations at moderate temperatures. At temperatures at which thermal evaporation from vacancy clusters, can be neglected, the evolution of the cluster densities is characteristic of the primary recoil spectrum, but is independent of temperature or dose rate. The sink strength, radiation-enhanced diffusion, as well as other consequences of the evolving distributions such as the imbalance of the interstitial and vacancy fluxes in the matrix, approach slowly-changing quasi-steady-state values in a fraction of one displacement per atom, although certain details of the cluster distributions, e.g., the development of large interstitial loops, require several dpa's to approach steady state values. DOE

N91-29025# Los Alamos National Lab., NM.

AB INITIO CLUSTER STUDIES OF La2CuO4

R. L. Martin 1991 21 p Presented at the North Atlantic Treaty Organization (NATO) Advanced Research Workshop on Cluster Models for Surface and Bulk Phenomena, Sicily (Italy), 19-26 Apr. 1991
(Contract W-7405-eng-36)
(DE91-013520; LA-UR-91-1517; CONF-9104262-1) Avail: NTIS HC/MF A03

In this paper we examine the properties of small cluster models of La2CuO4. In Section 2, the Madelung/Pauli background potential used to imbed the primary cluster and the basis sets used to expand the cluster wavefunction are discussed. Section 3 presents the results of calculations on CuO6 in which the optical absorption and the photoemission spectrum are examined. The calculation on CuO6 and our earlier work on larger clusters suggest that a single-band Pariser-Parr-Pople (PPP) model be developed. Therefore, in Section 4 the PPP model and extensions which relax the zero-differential-overlap (ZDO) approximation upon which it is based are reviewed. Calculations on the states of Cu2O7 necessary to parameterize the PPP model are presented in Section 5 and compared with analogous calculations for Cu2O11. Section 6 discusses the problems associated with the direct ab initio determination of the anti-ferromagnetic exchange interaction, examines the magnitudes of the occupation-dependent hopping and direct exchange interactions which arise when the ZDO approximation is relaxed, and provides estimates of the uncertainties in the parameters due to electron correlation and polarization effects not recoverable with the present basis sets and finite clusters. A comparison of the parameters with those extracted from constrained LDF theory concludes Section 6. Finally, Section 7 summarizes the conclusions of this research. DOE

N91-29026# Colorado Univ., Boulder.

PARALLEL NANOMETER SCALE FABRICATION

K. Douglas May 1991 13 p
(Contract DE-FG02-89ER-14077)
(DE91-013016; DOE/ER-14077/2) Avail: NTIS HC/MF A03

Nanometer molecular lithography has been employed as a parallel (as opposed to serial) fabrication process for structures with features defined by single molecules. Structures on the 10 nm length scale (nanostructures) have been fabricated employing 2-D monolayer protein crystals as patterning elements. During this budget period substantial improvements in the uniformity of a nanostructured surfaces was achieved by minimizing the plastic deformation produced by surface tension forces during drying of the protein crystal patterning templates prior to metallization and ion milling. In addition, using atomic force microscopy (AFM) nanostructures fabricated on thick (bulk) substrates were imaged. Also, titanium oxides and nitrides were found to be the most promising materials for nanostructure fabrication. Moreover, in case of at least one oxide, preferential absorption of anionic absorbates onto nanostructures is accomplished without any further processing steps and thus one of the two essential criteria for nanoheterostructure fabrication is satisfied. DOE

N91-29027# Argonne National Lab., IL.

THE INTERACTION OF HVEM-GENERATED POINT-DEFECTS WITH DISSOCIATED DISLOCATIONS

S. L. King, M. L. Jenkins, M. A. Kirk, and C. A. English (United Kingdom Atomic Energy Authority, Harwell, England) May 1991 11 p Presented at the International Conference on Physics of Irradiation Effects in Metals, Siofok (Hungary), 20-24 May 1991
(Contract W-31-109-eng-38)
(DE91-013353; ANL/CP-72210; CONF-9105130-2) Avail: NTIS HC/MF A03

This paper describes experiments we have performed to investigate the mechanisms of interaction of HVEM-generated point-defects with dissociated dislocations in a series of austenitic Fe-Ni-Cr alloys and review earlier work in Cu-Al alloys and in Ag. In the Fe-Ni-Cr alloys interstitial climb was observed only at favorable sites such as pre-existing jogs, while vacancies clustered near dislocations to form stacking-fault tetrahedra. These observations are similar to those in Ag; the complex climb mechanisms seen in Cu-Al alloys were not found. The differences between materials is believed to be due to differences in the case of interstitial pipe diffusion. DOE

N91-29028# Los Alamos National Lab., NM.

KINETICS OF SOLID-STATE REACTIONS IN Ni-Zr THIN FILMS

R. B. Schwarz and J. B. Rubin 1991 17 p Presented at the Spring Meeting of the Materials Research Society (MRS), Anaheim, 29 Apr. - 3 May 1991
(Contract W-7405-eng-36)
(DE91-013652; LA-UR-91-1488; CONF-910406-16) Avail: NTIS HC/MF A03

We have studied the kinetics of the solid-state amorphizing reaction in thin film multilayers of Ni and Zr. Crystalline Ni and Zr films were deposited in ultra-high vacuum onto platinum resistance thermometer embedded in alumina. An electronic feedback circuit controls the temperature of the substrata by adjusting the power dissipated by the platinum resistors. We find that structural relaxation in the as-deposited Ni and Zr films affects the initial stages of the reaction. For long reaction times there is a discontinuous change in the reaction rate. The time to reach this transition increases with film thickness and depends exponentially on 1/T, with an apparent activation energy of 3 eV/atom. DOE

N91-29029# Los Alamos National Lab., NM.

METASTABLE PHASE EQUILIBRIA IN CO-DEPOSITED Ni(1-x)Zr(x) THIN FILMS

J. B. Rubin and R. B. Schwarz 1991 13 p Presented at the Spring Meeting of the Materials Research Society (MRS), Anaheim, 29 Apr. - 3 May 1991
(Contract W-7405-eng-36)
(DE91-013653; LA-UR-91-1487; CONF-910406-15) Avail: NTIS HC/MF A03

We determine the glass forming range (GFR) of co-deposited Ni(1-x)Zr(x) (0 less than x less than 1) thin films by measuring their electrical resistance during in situ constant-heating-rate anneals. The measured GFR is continuous for 0.10 less than x less than 0.87. We calculate the GFR of Ni-Zr melts as a function of composition and cooling rate using homogeneous nucleation theory and a published CALPHAD-type thermodynamic modeling of the equilibrium phase diagram. Assuming that the main competition to the retention of the amorphous structure during the cooling of the liquid comes from the partitionless crystallization of the terminal solid solutions, we calculate that for dT/dt = 10(exp 12) K/s, the GFR extends to x = 0.05 and x = 0.96. Better agreement with the measured values is obtained assuming a lower effective cooling rate during the condensation of the films. DOE

N91-29030# California Univ., Berkeley. Lawrence Berkeley Lab.

ELECTRON CORRELATIONS IN SOLID STATE PHYSICS Ph.D. Thesis

J. K. Freericks Apr. 1991 205 p
(Contract DE-AC03-76SF-00098)
(DE91-013752; LBL-30641) Avail: NTIS HC/MF A10

Exactly solvable models of electron correlations in solid state physics are presented. These models include the spinless Falicov-Kimball model, the t-t'-J model, and the Hubbard model. The spinless Falicov-Kimball model is analyzed in one-dimension. Perturbation theory and numerical techniques are employed to determine the phase diagram at zero temperature. A fractal structure is found where the ground-state changes (discontinuously) at each rational electron filling. The t-t'-J model (strongly interacting limit of a Hubbard model) is studied on eight-site small clusters in the simple-cubic, body-centered-cubic, face-centered-cubic, and square lattices. Symmetry is used to simplify the problem and determine the exact many-body wavefunctions. Ground states are found that exhibit magnetic order or heavy-fermionic character.

Attempts to extrapolate to the thermodynamic limit are also made. The Hubbard model is examined on an eight-site square-lattice cluster in the presence of and in the absence of a magnetic field that couples only to orbital motion. A new magnetic phase is discovered for the ordinary Hubbard model at half-filling. In the magnetic field case, it is found that the strongly frustrated Heisenberg model may be studied from adiabatic continuation of a tight-binding model (from weak to strong coupling) at one point. The full symmetries of the Hamiltonian are utilized to make the exact diagonalization feasibile. Finally, the presence of hidden extra symmetry for finite size clusters with periodic boundary conditions is analyzed for a variety of clusters. Moderately sized systems allow nonrigid transformations that map a lattice onto itself preserving its neighbor structure; similar operations are not present in smaller or larger systems. The additional symmetry requires particular representations of the space group to stick together explaining many puzzling degeneracies found in exact diagonalization studies. DOE

N91-29031# Brookhaven National Lab., Upton, NY.
NEUTRON SCATTERING STUDIES OF SPIN CORRELATIONS IN METALLIC YBa2Cu3O(6+x)
J. M. Tranquada 1991 12 p Presented at the Electronic Structure and Mechanisms for High Temperature Superconductivity, Coral Gables, 3-9 Jan. 1991
(Contract DE-AC02-76CH-00016)
(DE91-013794; BNL-46161; CONF-910145-5) Avail: NTIS HC/MF A03

Electron-electron correlations appear to play an important role in determining many properties of the copper oxide superconductors. One significant consequence of the electronic Coulomb interactions are spin correlations. In the insulating phases of the layered cuprates, where the antibonding band due to Cu 3d(sub x)2 - (sub y)2-O 2p(sub sigma) hybridization in the CuO2 planes is half filled, long-range antiferromagnetic order is observed. As the layers are doped with holes, the Neel order is rapidly destroyed, but dynamical antiferromagnetic correlations survive. In this paper, I will review some inelastic neutron scattering studies of the spin fluctuations in metallic YBa2Cu3O(6+x). The paper is organized as follows. In the first section I briefly discuss some background information concerning the phase diagram and spin waves in the insulating phase. Experimental results on metallic YBa2Cu3O(6+x) samples are presented in the second section. The interpretation of these results and their relationship to nuclear magnetic resonance (NMR) studies and to theory are discussed in the final section. DOE

N91-29032 Ohio State Univ., Columbus.
TOPICS ON FRUSTRATED SPIN SYSTEMS AND HIGH-TEMPERATURE SUPERCONDUCTORS Ph.D. Thesis
Yong Lu 1990 200 p
Avail: Univ. Microfilms Order No. DA9111752

The numerical study of frustrated spin systems using the Monte Carlo simulation method and the analytic study of fluctuation phenomenon of the thermoelectric power near the superconducting transition using Green's function techniques are presented. The first frustrated system considered was the B-site antiferromagnetic (AF) spinel. Based on an Ising model, various thermodynamic and magnetic properties for both the fully frustrated structure and partially frustrated cases of a small tetragonal distortion were studied. When fully frustrated, an interesting short range order and some unusual scaling behavior were obtained. In the two tetragonally distorted cases, contracting and expanding in the crystallographic c-direction, AF long range orders and some hysteresis behavior were found. A general phase diagram was constructed as a function of the degree of the distortion. The other frustrated spin system that was studied is the magnetic phase of YBa2Cu3O(6+x). A classical spin model, was constructed, and various properties in its Ising, Heisenberg, and x-y versions were studied. The susceptibility was calculated as a function of temperature for various values of x. In the study on the thermopower fluctuation, the thermopower was determined by the linear response of the electric and heat currents to an electric field, and the linear responses were in turn calculated from correlation functions of the current. Dissert. Abstr.

N91-29033# Los Alamos National Lab., NM.
DOPING AND PRESSURE STUDY OF U3Sb4Pt3
P. C. Canfield, A. Lacerda, J. D. Thompson, G. Sparn, W. P. Beyermann, M. F. Hundley, and Z. Fisk 1991 12 p Presented at the 19th Rare Earth Research Conference (RERC-19), Lexington, 14-19 Jul. 1991
(Contract W-7405-eng-36)
(DE91-013669; LA-UR-91-1545; CONF-910706-3) Avail: NTIS HC/MF A03

The effects of doping and pressure on the U3Sb4Pt3 system were studied. Substitution of either trivalent Y or Lu for U causes significant changes in temperature dependence of the electrical resistance and magnitude of the linear coefficient of the specific heat, gamma. However, doping with tetravalent Th causes little change in gamma, even though it affects the electrical resistance in a manner similar to that seen in the cases of Lu and Y. Finally, the application of hydrostatic pressures up to 16.5 kbar causes no significant change in the electrical resistance. DOE

N91-29034# Los Alamos National Lab., NM.
APPLICATION OF MUON SPIN RELAXATION EXPERIMENT TO THE MIXED STATE SUPERCONDUCTORS
M. Inui and D. R. Harshman (Bell Telephone Labs., Inc., Murray Hill, NJ.) May 1991 9 p Presented at the Physical Phenomena At High Magnetic Fields, Tallahassee, 15-18 May 1991
(Contract W-7405-eng-36)
(DE91-013689; LA-UR-91-1685; CONF-9105151-4) Avail: NTIS HC/MF A02

The use is discussed of muon spin relaxation (mu exp + SR) technique to study the mixed state of superconductors. Besides the application for static vortex configurations, it is argued that large vortex motion can manifest itself as a narrowed time-averaged field distribution, which in turn results in a smaller relaxation rate. A static but disordered vortex configuration can also reduce the relaxation. These arguments are summarized. DOE

N91-29035# Los Alamos National Lab., NM.
THE DERIVATION OF EFFECTIVE SPIN HAMILTONIANS AND THE ORIGIN OF THE MAGNETIC FIELD INDUCED TRANSITION IN ORTHORMBIC La2CuO4
D. Coffey 1991 20 p Presented at the Physical Phenomena At High Magnetic Fields, Tallahassee, 15-18 May 1991
(Contract W-7405-eng-36)
(DE91-013743; LA-UR-91-1680; CONF-9105151-5) Avail: NTIS HC/MF A03

La2CuO4 undergoes a magnetic field induced transition in a field of approx. 5.7 Tesla at low temperatures. The origin of this transition is the Dzyaloshinskii-Moriya interaction which is present in effective spin Hamiltonians for systems of sufficiently low symmetry, and, which leads to weak ferromagnetism in the CuO planes in La2CuO4. It is shown here how this interaction depends on symmetry and how its form changes with structural phase transitions which occur in compounds closely related to La2CuO4. These different forms of the interaction lead to different properties in magnetic fields. I also discuss how the approach presented here of determining an effective spin Hamiltonian from symmetry is related to the determination of terms in the free expansion close to a second order phase transition. It is pointed out that the present approach may be extended to itinerant systems and 1 take UPt sub 3 as an example. DOE

N91-29036# Argonne National Lab., IL.
FLUX DYNAMICS IN A SINGLE CRYSTAL OF Bi2Sr2CaCu2O(x)
Donglu Shi, X. S. Ling, and J. I. Budnick (Connecticut Univ., Storrs.) Apr. 1991 12 p Presented at the Physical Phenomena At High Magnetic Fields, Tallahassee, 15-18 May 1991
(Contract W-31-109-eng-38)

(DE91-013763; ANL/CP-73203; CONF-9105151-3) Avail: NTIS HC/MF A03

We report on a systemmatic study of the long-time decay of the irreversible magnetization of a Bi2Sr2CaCu2O(x) single crystal. The decay of magnetization cannot be well described by the Anderson-Kim flux creep model. We interpret the magnetic relaxation data with the self-organized criticality (SOC) theory. In contrast to the flux creep models in which only uncorrelated, individual flux hoppings occur, SOC theory describes a spatially and temporally correlated dynamics. The time dependence of magnetization can best be characterized by a stretched exponential, exp((minus)(t/t(sub 0))(sup n)) (0 less than n less than 1), or Kohlrausch's law. We argue that the dynamics of flux creep in Bean's critical state is governed by an avalanche-like dynamics of SOC theory. DOE

N91-29037# Argonne National Lab., IL.

X RAY DIFFRACTION STUDY OF HETEROEPITAXY OF MOCVD GROWN TIO2 AND VO2 FILMS ON SAPPHIRE SINGLE CRYSTALS

Hoydoo You, M. L. M. Chang, R. P. Chiarello, and D. J. Lam 1991 7 p Presented at the Spring Meeting of the Materials Research Society (MRS), Anaheim, 29 Apr. - 3 May 1991
(Contract W-31-109-eng-38)
(DE91-013764; ANL/CP-73159; CONF-910406-18) Avail: NTIS HC/MF A02

A four-circle diffractometry technique is used to determine the heteroepitaxial relations of VO2 and TiO2 thin films grown by an MOCVD technique on sapphire (0001) and (112'0) surfaces. The use of a reflective geometry eliminates special sample preparation of the sample for the x-ray diffraction measurements. The distribution of epitaxial domains is found to depend strongly on the symmetry of the underlying substrate. DOE

N91-29038# California Univ., Berkeley. Lawrence Berkeley Lab.

LONG-WAVELENGTH GERMANIUM PHOTODETECTORS BY ION IMPLANTATION

I. C. Wu, J. W. Beeman, P. N. Luke, W. L. Hansen, and E. E. Haller Nov. 1990 9 p Presented at the Fall Meeting of the Materials Research Society (MRS), Boston, 24 Nov. - 1 Dec. 1990
(Contract DE-AC03-76SF-00098)
(DE91-013848; LBL-29272; CONF-901105-127) Avail: NTIS HC/MF A02

Extrinsic far-infrared photoconductivity in thin high-purity germanium wafers implanted with multiple-energy boron ions has been investigated. Initial results from Fourier transform spectrometer (FTS) measurements have demonstrated that photodetectors fabricated from this material have an extended long-wavelength threshold near 192 microns. Due to the high-purity substrate, the ability to block the hopping conduction in the implanted IR-active layer yields dark currents of less than 100 electrons/sec at temperatures below 1.3 K under an operating bias of up to 70 mV. Optimum peak responsivity and noise equivalent power (NEP) for these sensitive detectors are 0.9 A/W and 5 times 10(exp -16) W/Hz(sup 1/2) at 99 microns respectively. The dependence of the performance of devices on the residual donor concentration in the implanted layer will be discussed. DOE

N91-29039# Brookhaven National Lab., Upton, NY.

THE DARPA COMPACT SUPERCONDUCTING X-RAY LITHOGRAPHY SOURCE FEATURES

R. Heese, S. Kalsi, and E. Leung (General Dynamics Corp., San Diego, CA.) 1991 4 p Presented at the 1991 Institute of Electrical and Electronics Engineers (IEEE) Particle Accelerator Conference (PAC), San Francisco, 6-9 May 1991
(Contract DE-AC02-76CH-00016)
(DE91-013864; BNL-46178; CONF-910505-233) Avail: NTIS HC/MF A01

Under DARPA sponsorship, a compact Superconducting X-ray Lithography Source (SXLS) is being designed and built by the Brookhaven National Laboratory (BNL) with industry participation from Grumman Corporation and General Dynamics. This source is optimized for lithography work for sub-micron high density computer chips, and is about the size of a billiard table (1.5 m x 4.0 m). The machine has a racetrack configuration with two 180 degree bending magnets being designed and built by General Dynamics under a subcontract with Grumman Corporation. The machine will have 18 photon ports which would deliver light peaked at a wave length of 10 Angstroms. Grumman is commercializing the SXLS device and plans to book orders for delivery of industrialized SXLS (ISXLS) versions in 1995. This paper will describe the major features of this device. The commercial machine will be equipped with a fully automated user-friendly control systems, major features of which are already working on a compact warm dipole ring at BNL. This ring has normal dipole magnets with dimensions identical to the SXLS device, and has been successfully commissioned. DOE

N91-29040# Superconducting Super Collider Lab., Dallas, TX.

NON SIMILARITY SOLUTION APPROXIMATION TO THE THERMAL HYDRAULIC QUENCHBACK IN SUPERCONDUCTORS

G. Lopez May 1991 5 p Presented at the 1991 Institute of Electrical and Electronics Engineers (IEEE) Particle Accelerator Conference (PAC), San Francisco, 6-9 May 1991
(Contract DE-AC02-89ER-40486)
(DE91-013964; SSCL-423; CONF-910505-256) Avail: NTIS HC/MF A01

Using an approximation to the conduction fluid equations, a solution is given using the direct method of integration of a differential equation. This solution establishes a possible increasing relation between the quench velocity and length of the conductor. DOE

N91-29041# Missouri Univ., Columbia. Dept. of Physics and Astronomy.

HIGH PRESSURE OPTICAL STUDIES OF SEMICONDUCTORS AND HETEROSTRUCTURES

H. R. Chandrasekhar Apr. 1991 6 p
(Contract DE-FG02-89ER-45402)
(DE91-014382; DOE/ER-45402/2) Avail: NTIS HC/MF A02

The following topics are discussed: strained layer heterostructures; the diluted magnetic semiconductors; pressure-induced fano resonance of excitons in semiconductors; and a new pressure activated deep trap in III-V semiconductors. DOE

N91-29042# Argonne National Lab., IL.

FLUX PINNING AND DISSIPATION IN HIGH-TEMPERATURE SUPERCONDUCTORS

K. E. Gray and D. H. Kim Apr. 1991 10 p Presented at the International Workshop on High Tc Superconductor Thin Films: Properties and Applications, Rome (Italy), 15-19 Apr. 1991
(Contract W-31-109-eng-38)
(DE91-014466; ANL/CP-73158; CONF-910410-1) Avail: NTIS HC/MF A02

The effect of anisotropy on the field-induced broadening of resistive transitions in the highly-anisotropic high-temperature superconductors (HTS) is considered. For the applied field, H, parallel to the superconducting Cu-O layers the absence of a Lorentz-force, together with intrinsic pinning of the insulating region between layers, leads to an explanation other than flux motion. However, for H parallel to the c-axis, the lack of intrinsic pinning implies that the much greater broadening is due to thermally-activated flux motion. We show experimental evidence that the associated flux motion occurs as a result of a crossover from three dimensional (3D) vortex lines to 2D independent pancake-like vortices, residing in the Cu-O layers. This 3D to 2D crossover occurs when k(sub B)T exceeds the Josephson coupling energy. For YBa2Cu3O7, this dimensional crossover does not occur below H(sub c2), presumably because the conducting Cu-O chains short circuit the Josephson interlayer coupling. DOE

N91-29043# Polytechnic Univ., Brooklyn, NY. Dept. of Physics.
SCANNING TUNNELING MICROSPECTROSCOPY OF SOLIDS AND SURFACES
E. L. Wolf 24 Nov. 1990 17 p
(Contract DE-FG02-87ER-45301)
(DE91-014515; DOE/ER-45301/4) Avail: NTIS HC/MF A03

Major progress has been made this year in our work on single crystals of Bi2Sr2CaCu2O(8+y) (BSCCO) grown in our laboratory in a transverse temperature gradient. We have obtained large crystals of improved quality and tunneling data which are superior to any we have seen elsewhere. In our first publication on this, we have identified a pair breaking process which appears near (Tc) and apparently is related to the absence of the Hebel-Slichter peak in 1/T(sub 1) vs T in this material. In more recent work much improved data reveal features in the tunnel conductance dI/dV which appear to agree with the proximity effect-superlattice model of the tunneling conductance of BSCCO described by Tachiki and coworkers. We devote a major portion of this report to this and other research topics, on which work is continuing, and briefly describe advances in instrumentation that have occurred this year. DOE

N91-29044# Oak Ridge National Lab., TN.
DIRECT IMAGING OF ORDERING IN Si-Ge ALLOYS, ULTRATHIN SUPERLATTICES, AND BURIED Ge LAYERS
D. E. Jesson, S. J. Pennycook, and J. M. Baribeau (National Research Council of Canada, Ottawa, Ontario) 1991 7 p Presented at the Spring Meeting of the Materials Research Society (MRS), Anaheim, 29 Apr. - 3 May 1991
(Contract DE-AC05-84OR-21400)
(DE91-014580; CONF-910406-23) Avail: NTIS HC/MF A02

We review recent Z-contrast imaging studies of Si--Ge ultrathin superlattices, alloys, and buried Ge layers. It is found that whenever Si is deposited onto a Ge 2 x 1 surface, Ge is pumped into the growing Si layer, and this is accompanied by interfacial ordering. This is explained by a novel Ge atom pump mechanism which occurs during molecular beam epitaxy (MBE) growth. Codeposition and alloy growth results in long range (111) ordering as a consequence of lateral segregation during nonequilibrium growth. DOE

N91-29045# Los Alamos National Lab., NM.
OVERVIEW OF THE STATUS OF AND PROSPECTS FOR HIGH-T(SUB c) WIRE AND TAPE DEVELOPMENT
M. P. Maley 1991 24 p Presented at the 5th Joint Magnetism and Magnetic Materials (MMM/INTERMAG) Conference, Pittsburgh, 18-21 Jun. 1991
(Contract W-7405-eng-36)
(DE91-014609; LA-UR-91-2030; CONF-910608-6) Avail: NTIS HC/MF A03

Recent world-wide progress in the effort to develop long continuous lengths of conductor based on high-(Tc) materials with high critical currents in substantial magnetic fields offers promise for a variety of applications. Two major problems, weak links and weak flux pinning have plagued conductor development efforts from the beginning. Recent advances in mechanical processing of tape conductors based on BSCCO show great promise in overcoming weak lines, with low-temperature J(sub c) values greater than 10(exp 5)A/sq cm extending to magnetic fields greater than 25T. Unfortunately, these materials continue to exhibit weak flux pinning at moderate temperatures for magnetic fields aligned along the crystalline c-axis. This manifests itself in a J(sub c) that declines precipitously with magnetic field for T greater than 30 K. By contrast conductors based on YBCO exhibit much stronger pinning at high temperature with smaller sensitivity to magnetic field orientation, but remain severely limited by weak links. The poor performance of BSCCO- and TBCCO-based materials appears to be strongly correlated with the high degree of intrinsic anisotropy. Phenomenological models describing this behavior and prospects for further progress are examined. DOE

N91-29046# Los Alamos National Lab., NM.
PRESSURE DEPENDENCE OF THE CURIE-TEMPERATURE IN THE KONDO-LATTICE-COMPOUND YbNiSn
G. Sparn, J. D. Thompson, and A. Hamzic (Zagreb Univ., Yugoslavia) 1991 16 p Presented at the 19th Rare Earth Research Conference (RERC-19), Lexington, 14-19 Jul. 1991
(Contract W-7405-eng-36)
(DE91-013672; LA-UR-91-1536; CONF-910706-5) Avail: NTIS HC/MF A03

The magnetic suceptibility (T between 2 and 300 K) and the electrical resistivity under pressure (T between 1.2 and 300 K; p less than 20 kbar) was measured of the Kondo-lattice compound YbNiSn, which may be considered as the hole analogue of the isostructural compound CeNiSn. In contrast to CeNiSn, YbNiSn does not show an energy gap at low temperatures, but instead undergoes a magnetic phase transition at T sub M = 5.5 K. The magnetic state might be either a weakly ferromagnetic or a complex antiferromagnetic state. By applying pressure the room temperature resistance (rho sub RT) decreases, while T sub M increases. This behavior can be interpreted with respect to Doniach's Kondo-necklace model as a decrease of the local exchange coupling constant J with increasing pressure, which reduces Kondo-spin compensation and favors long range magnetic order. These results show that the idea of YbNiSn being the hole counterpart to CeNiSn holds well for the properties such as dT sub M/dP and d rho sub RT/dP but that it fails in more detailed aspects like the origin of the gap formation. DOE

N91-29047# Sandia National Labs., Albuquerque, NM.
THE SURFACE CHEMISTRY OF GaAs ATOMIC LAYER EPITAXY
J. R. Creighton and B. A. Banse 1991 10 p Presented at the Spring Meeting of the Materials Research Society (MRS), Anaheim, 29 Apr. - 3 May 1991
(Contract DE-AC04-76DP-00789)
(DE91-014112; SAND-90-3130C; CONF-910406-20) Avail: NTIS HC/MF A02

In this paper we review three proposed mechanisms for GaAs ALE and review or present data support or contradiction of these mechanisms. Surface chemistry results clearly demonstrated that TMGa irreversibly chemisorbs on the Ga-rich GaAs(100) surface. The reactive sticking coefficient (RSC) of TMGa on the adsorbate-free Ga-rich GaAs(100) surface was measured to be approximately 0.5, conclusively demonstrating that the selective adsorption mechanism of ALE is not valid. We describe kinetic evidence for methyl radical desorption in support of the adsorbate inhibition mechanism. The methyl radical desorption rates determined by temperature programmed desorption (TPD) demonstrate that desorption is at least a factor of approximately 10 faster from the As-rich c(2 x 8)/(2 x 4) surface than from the Ga-rich surface. It is disparity in CH3 desorption rates between the As-rich and Ga-rich surfaces that is largely responsible for GaAs ALE behavior. A gallium alkyl radical (e.g., MMGa) is also observed during TPD and molecular beam experiments, in partial support of the flux balance mechanism. Stoichiometry issues of ALE are also discussed. We have discovered that arsine exposures typical of atmospheric pressure and reduced pressure ALE lead to As coverages greater than or equal to 1 ML, which provides the likely solution to the stoichiometry question regarding the arsine cycle. DOE

N91-29048# EG and G Energy Measurements, Inc., Goleta, CA.
CRYSTAL SURFACE ANALYSIS USING MATRIX TEXTURAL FEATURES CLASSIFIED BY A PROBABILISTIC NEURAL NETWORK
C. R. Sawyer, V. T. Quach, D. Nason, and L. vandenBerg (EG and G Energy Measurements, Inc., Goleta, CA.) 1991 11 p Presented at the Society of Photo-Optical Instrumentation Engineers (SPIE) Meeting, San Diego, 21-26 Jul. 1991
(Contract DE-AC08-88NV-10617)
(DE91-014120; EGG-10617-3004; CONF-9107115-3) Avail: NTIS HC/MF A03

A system is under development in which surface quality of a growing bulk mercuric iodide crystal is monitored by video camera at regular intervals for early detection of growth irregularities. Mercuric iodide single crystals are employed in radiation detectors. A microcomputer system is used for image capture and processing. The digitized image is divided into multiple overlappings subimage and features are extracted from each subimage based on statistical measures of the gray tone distribution, according to the method of Haralick. Twenty parameters are derived from each subimage and presented to a Probabilistic Neural Network (PNN) for classification. This number of parameters was found to be optimal for the system. The PNN is a hierarchical, feed-forward network that can be rapidly reconfigured as additional training data become available. Training data is gathered by reviewing digital images of many crystals during their growth cycle and compiling two sets of images, those with and without irregularities. DOE

N91-29049# Cornell Univ., Ithaca, NY. Dept. of Materials Science and Engineering.
DEFECTS AND TRANSPORT IN MIXED OXIDES
R. Dieckmann 26 Sep. 1990 20 p
(Contract DE-FG02-88ER-45357)
(DE91-014443; DOE/ER-45357/4) Avail: NTIS HC/MF A03

This report contains a brief review of work during the last period, personnel matters, laboratory installation and publications. Some topics of performed research are: non-stoichiometry of mixed oxides; Monte Carlo simulation of cation diffusion; thermodynamics of the system Fe-Mn-O at 1000 C; stabilities of oxides in the system Co-Fe-Mn-O at 1200 C; electrical conduction in mixed oxides; influence of grain size on point defects in oxides; influence of platinum present during non-stoichiometry measurements on their results; and tracer diffusion tests. DOE

N91-29050# Los Alamos National Lab., NM.
APPLICATION OF MUON SPIN RELAXATION EXPERIMENT TO THE VORTEX DYNAMICS OF HIGH TEMPERATURE SUPERCONDUCTORS
M. Inui and D. R. Harshman 1991 3 p Presented at the International Conference on Materials and Mechanisms of Superconductivity, Kanazawa, Japan, 22-26 Jul. 1991
(Contract W-7405-eng-36)
(DE91-014607; LA-UR-91-2034; CONF-910736-1) Avail: NTIS HC/MF A01

We discuss the potential use of the muon spin relaxation technique to investigate the dynamics of the magnetic flux lines (vortices) in the mixed state superconductors. We agree that with the high critical temperature and large anisotropy found in some high temperature superconductors, one can use muon spin relaxation to observe both static and dynamic behaviors of vortices. Recent experiments on Bi2Sr2CaCu2O8 are interpreted in this context. DOE

N91-29051# Sandia National Labs., Albuquerque, NM.
THE ECR-PLASMA DEPOSITION OF SILICON NITRIDE ON A TUNNEL OXIDE
J. C. Barbour, H. J. Stein, and C. A. Outten (Michigan Univ., Ann Arbor.) 1991 7 p Presented at the Spring Meeting of the Materials Research Society (MRS), Anaheim, 29 Apr. - 3 May 1991
(Contract DE-AC04-76DP-00789)
(DE91-014665; SAND-90-3100C; CONF-910406-25) Avail: NTIS HC/MF A02

Gate dielectric-quality silicon nitride films were deposited on a tunnel oxide from an SiH4/N2 gas mixture using an electron cyclotron resonance (ECR) plasma. Electrical characteristics depend not only upon the quality of the nitride film but also upon the state of the interfacial oxide. Quasi-static and 1 MHz capacitance-voltage measurements show that a nitride film deposited at 200 C on 2 nm thick thermally-grown oxide (tunnel oxide) on an unbiased Si substrate has an interface state density of 1.5 times 10(exp 11) sq cm-eV. Time-of-flight elastic recoil detection (TOF-ERD) was used to examine the level of mixing between the tunnel oxide and the deposited silicon nitride as a function of bias voltage. TOF-ERD showed that for an applied bias of -350 V (ion energy approx. 380 eV), the deposition of a 10 nm thick film was completely mixed to form an oxynitride whereas the tunnel oxide remained intact for an unbiased sample. Interdiffusion resulting from energetic-beam heating was ruled-out as a possibility for the mixing. DOE

N91-29052# Sandia National Labs., Albuquerque, NM.
ANNEALING AND STRUCTURE STUDIES ON Tl-2223 AND Tl-1223 CRYSTALS
B. Morosin, E. L. Venturini, and D. S. Ginley 1991 2 p Presented at the International Conference on Materials and Mechanisms of Superconductivity, Kanazawa, Japan, 22-26 Jul. 1991
(Contract DE-AC04-76DP-00789)
(DE91-014903; SAND-91-0771C; CONF-910736-4) Avail: NTIS HC/MF A01

Single crystals with nominal stoichiometry Tl2Ca2Ba2Cu3O10 (Tl-2223) and TlCa2Ba2Cu3O9 (Tl-1223) have been annealed in flowing oxygen or nitrogen and the complete crystal structure determined by least-squares refinement of Mo K(alpha) x-ray diffraction data. Small atomic displacements are found after the anneals that are consistent with a model in which small amounts of Tl(1+) present in the Tl-O layer are subsequently reversibly oxidized/reduced during mild oxygen/nitrogen anneals to Tl(3+). Despite substantial changes in oxygen content in the Tl-O layers with annealing, Meissner data show very modest shifts in the superconducting transition temperature, suggesting little change in the carrier concentration in the Cu-O2 planes. DOE

77 THERMODYNAMICS AND STATISTICAL PHYSICS

Includes quantum mechanics; theoretical physics; and Bose and Fermi statistics.

For related information see also *25 Inorganic and Physical Chemistry* and *34 Fluid Mechanics and Heat Transfer.*

N91-29053# Lawrence Livermore National Lab., CA.
TOPAZ2D BENCHMARK PROBLEMS NONLINEAR MATERIALS
A. B. Shapiro Jan. 1991 14 p Presented at the ASME/AIChE/ANS National Heat Transfer Conference, Minneapolis, 26-31 Jul. 1991
(Contract W-7405-eng-48)
(DE91-009753; UCRL-JC-104854; CONF-910739-11) Avail: NTIS HC/MF A03

The problems presented in this paper investigate potential error sources in numerical modeling of nonlinear material thermal properties in heat transfer computer codes. The problem is one dimensional heat conduction in a homogeneous isotropic slab with constant heat flux on one face and adiabatic conditions on the other face. The thermal properties vary with temperature in a linear, quadratic, and exponential manner such that the thermal diffusivity remains constant. The analytical answers are tabulated and compared graphically with numerical results calculated using the TOPAZ2D heat transfer code with various options (e.g., lumped mass matrix, consistent mass matrix). DOE

N91-29054# California Univ., Berkeley. Lawrence Berkeley Lab.
PHYSICS AT THE PLANCK SCALE
M. K. Gaillard Dec. 1990 11 p Presented at the International Conference on Trends in Astroparticle Physics, Santa Monica, 26 Nov. - 1 Dec. 1990
(Contract DE-AC03-76SF-00098)
(DE91-012346; LBL-29990; CONF-901141-5; UCB-PTH-90/49)
Avail: NTIS HC/MF A03

Effective supergravity theories suggested by superstrings can be explored to determine their potential for successfully describing both observed physics at zero temperature and an inflationary cosmology. An important ingredient in this study is the dynamics of gaugino condensation, which has been the subject of recent activity. DOE

N91-29055# Los Alamos National Lab., NM.
NONLINEAR MODELING OF CHAOTIC TIME SERIES: THEORY AND APPLICATIONS
M. Casdagli, S. Eubank, J. D. Farmer, J. Gibson, D. DesJardins, N. Hunter, and J. Theiler 1990 49 p Presented at the Electric Power Research Institute (EPRI) Workshop on Applications of Chaos, San Francisco, Dec. 1990
(Contract W-7405-eng-36)
(DE91-013076; LA-UR-91-1637; CONF-901246-4) Avail: NTIS HC/MF A03

We review recent developments in the modeling and prediction of nonlinear time series. In some cases, apparent randomness in time series may be due to chaotic behavior of a nonlinear but deterministic system. In such cases, it is possible to exploit the determinism to make short term forecasts that are much more accurate than one could make from a linear stochastic model. This is done by first reconstructing a state space, and then using nonlinear function approximation methods to create a dynamical model. Nonlinear models are valuable not only as short term forecasters, but also as diagnostic tools for identifying and quantifying low-dimensional chaotic behavior. During the past few years, methods for nonlinear modeling have developed rapidly, and have already led to several applications where nonlinear models motivated by chaotic dynamics provide superior predictions to linear models. These applications include prediction of fluid flows, sunspots, mechanical vibrations, ice ages, measles epidemics, and human speech. DOE

N91-29056# International Centre for Theoretical Physics, Trieste (Italy).
PATH-INTEGRAL MEASURE FOR CHERN-SIMONS THEORY WITHIN THE STOCHASTIC QUANTIZATION APPROACH
L. F. Cugliandolo, G. Lozano, and F. A. Schaposnik Aug. 1990 13 p
(DE91-617610; IC-90/234) Avail: NTIS HC/MF A03

We discuss how the dependence of the path-integral measure on the metric affects the generating functional for the $d = 3$ Chern-Simons theory. Using the stochastic quantization, we show that the choice of an invariant measure preserves the topological character of the theory. DOE

N91-29057# International Centre for Theoretical Physics, Trieste (Italy).
THE (2,0) SUPER BELTRAMI PARAMETRIZATION AND SUPERCONFORMAL STRUCTURES
M. Kachkachi and T. Lhallabi (Mohammed V Univ., Rabat, Morocco) Aug. 1990 21 p
(DE91-617611; IC-90/245) Avail: NTIS HC/MF A03

The superconformal structure of the (2,0) supergeometry of two dimensional superspace is characterized by the Beltrami differentials. The superdiffeomorphism transformations of the Beltrami variables are given and the superfields with arbitrary conformal weights are studied. DOE

N91-29058# Los Alamos National Lab., NM.
COMPLEX DYNAMICS OF THE INTEGER QUANTUM HALL EFFECT
S. A. Trugman and V. N. Nicopoulos (Florida Univ., Gainesville.) 1991 29 p Presented at the Physical Phenomena At High Magnetic Fields, Tallahassee, 15-18 May 1991
(Contract W-7405-eng-36)
(DE91-013383; LA-UR-91-1895; CONF-9105151-2) Avail: NTIS HC/MF A03

We investigate both classical and quantum potential scattering in two dimensions in a magnetic field, with applications to the integer quantum Hall effect. Classical scattering is complex, due in one case to the approach of scattering states to an infinite number of bound states. We show that bound states are generic, and occur for all but extremely smooth scattering potentials. Quantum scattering follows the classical behavior rather closely, exhibiting sharp resonances rather than classical bound states. Extended scatterers provide an explanation for the breakdown of the QHE at a comparatively small Hall voltage. DOE

N91-29059 Texas Univ., Austin.
THE 2+1 GRAVITY: A NEW APPROACH Ph.D. Thesis
Henri Waelbroeck 1990 150 p
Avail: Univ. Microfilms Order No. DA9117000

A new formulation is proposed of 2+1 gravity with a finite number of variables which described directly the observable properties of space-time. A surface is described as a nonplanar polygon embedded in Minkowski space, with an even number of edges that are identified two by two. As this polygon evolves in time, it carves a tube out of Minkowski space, with pairs of walls that are to be glued together. The theory is presented in the constrained Hamiltonian formulation. The initial value problem and the dynamical equations are solved for a sphere with g handles and N point particles, and for a plane with g wormholes and N particles. The total mass, which in the static case is just 2 pi times the Euler number, is computed for various time dependent solutions. A sphere with N moving particles has a total mass less than 4 pi; conversely for particles on a plane the total mass increases with velocity. A sphere with one or more handles can accommodate a particle with a deficit angle up to 2 pi, not included. Properties are discussed of the center of mass motion and relative motion. Dissert. Abstr.

N91-29060 Portland State Univ., OR.
OPTIMIZATION AND THERMODYNAMIC PERFORMANCE MEASURES FOR A CLASS OF FINITE TIME THERMODYNAMIC CYCLES Ph.D. Thesis
Joseph Douglass Walters 1990 137 p
Avail: Univ. Microfilms Order No. DA9115732

Modifications to the quasistatic Carnot cycle are developed in order to formulate improved theoretical bounds on the thermal efficiency of certain refrigeration cycles that produce finite cooling power. The modified refrigeration cycle is based on the idealized endoreversible finite time cycle. Two of the four cycle branches are reversible adiabats, and the other two are the high and low temperature branches along which finite heat fluxes couple the refrigeration cycle with external heat reservoirs. This finite time model was used to obtain the following results: (1) The performance of a finite time Carnot refrigeration cycle (FTCRC) is examined; (2) A finite time refrigeration cycle (FTRC) is optimized to obtain four distinct optimal cycling modes that maximize efficiency and cooling power, and minimize power consumption and irreversible entropy production; and (3) The problem of imperfect heat switches linking the working fluid of an FTRC to external heat reservoirs is studied. The maximum efficiency cycling mode is obtained by numerically optimizing the FTRC. Two distinct optimum cycling conditions exist: operation at the global maximum in efficiency; and operation at the frequency of maximum cooling power. Dissert. Abstr.

N91-29061# Wisconsin Univ., Madison. Center for Plasma Theory and Computation.
GENERALIZED GYROVISCOUS FORCE AND ITS EFFECT ON THE MOMENTUM BALANCE EQUATION
Zuoyang Chang and J. D. Callen May 1991 14 p
(Contract DE-FG02-86ER-53218)
(DE91-013344; UW-CPTC-91-3) Avail: NTIS HC/MF A03

The perturbed nonlinear gyroviscous force is calculated by solving the stress tensor evolution equation. The result shows that del x the gyroviscous stress tensor mostly cancels the diamagnetic convective term. This formula generalizes the usual, widely used gyroviscous cancellation in which the del x the gyroviscous stress tensor cancels mostly the total time derivative of the diamagnetic flow to include temperature variations and a perturbed stress tensor drift. It is proved that when temperature variations are neglected, the new formula reduces to the conventional form. When the temperature variations are considered, the new formula is much simpler and more rigorous than the conventional one. A new polarization drift formula deduced from the new gyroviscous force is also derived. DOE

N91-29062# California Univ., Berkeley. Lawrence Berkeley Lab.
TOPICS IN LOW-DIMENSIONAL FIELD THEORY Ph.D. Thesis
M. J. Crescimanno 30 Apr. 1991 175 p
(Contract DE-AC03-76SF-00098)
(DE91-013784; LBL-30676; UCB-PTH-91/9) Avail: NTIS HC/MF A08

Conformal field theory is a natural tool for understanding 2-D critical systems. Results are presented in the lagrangian approach to conformal field theory. The first sections are chiefly about a particular class of field theories called coset constructions and the last part is an exposition of the connection between 2-D conformal theory and a 3-D gauge theory whose lagrangian is the Chern-Simons density. DOE

N91-29063# Lawrence Livermore National Lab., CA.
TRANSPORT WITH FEYNMAN PROPAGATORS
R. H. White Nov. 1990 11 p Presented at the 1990 Nuclear Explosives Code Developers' Conference, Monterey, 6-9 Nov. 1990
(Contract W-7405-eng-48)
(DE91-013566; UCRL-JC-105692; CONF-9011149-16) Avail: NTIS HC/MF A03

Richard Feynman's formulation of quantum electrodynamics suggests a Monte Carlo algorithm for calculating wave propagation. We call this the Sum Over All Paths (SOAP) method. The method is applied to calculate diffraction by double slits of finite width and by a reflection grating. Calculations of reflection by plane and parabolic mirrors of finite aperture and from several figured surfaces are shown. An application to a one-dimensional scattering problem is discussed. A variation of SOAP can be applied to the diffusion equation. DOE

N91-29064# Washington Univ., Seattle. Dept. of Applied Mathematics.
CHAOS AND MICROBIAL SYSTEMS
M. Kot Jan. 1991 81 p
(Contract DE-FG06-90ER-61034)
(DE91-014908; DOE/ER-61034/1) Avail: NTIS HC/MF A05

Much of the recent work in nonlinear dynamics has centered on new techniques for identifying order in seemingly chaotic systems. To determine the robustness of these techniques, chaos must, to some extent, be brought into the laboratory. Preliminary investigations of the forded double-Monod equations, a model for a predator and a prey in a chemostat with periodic variation of inflowing substrate, suggested that simple microbial systems might provide the perfect framework for determining the efficacy and relevance of the new nonlinear dynamics in dealing with complex population dynamics. Progress in two areas of research, mathematical analysis and computer simulation of the periodically forced double-Monod equations and of related models; and experimental (chemostat) population studies that evaluate the accuracy and generality of the models, (and also judge the usefulness of various new techniques of nonlinear dynamics to the study of populations) is reported. DOE

80 SOCIAL SCIENCES (GENERAL)

Includes educational matters.

N91-29065# Sandia National Labs., Albuquerque, NM.
SANDAC V COMPUTER ELECTROMAGNETIC INTERFACE CHARACTERISTICS: PROBLEMS AND SOLUTIONS
G. A. Russell Jun. 1991 24 p
(Contract DE-AC04-76DP-00789)
(DE91-014334; SAND-91-0618) Avail: NTIS HC/MF A03

Electromagnetic Interference (EMI) problems have resulted in the redesign of the SANDAC V computer case and shielding of its connecting cables. In this report are detailed discussions on the use of computer models and of the tests performed to solve the EMI problems. Included is documentation on the specific changes made to the SANDAC V computer case and the shielding done on the connecting cables. Also documented are the current EMI capabilities relative to MIL Std. 461. DOE

81 ADMINISTRATION AND MANAGEMENT

Includes management planning and research.

N91-29066# Virginia Polytechnic Inst. and State Univ., Blacksburg. Management Systems Labs.
A SELECTION TOOL FOR CHOOSING THE BEST PARTICIPATIVE PROBLEM-SOLVING TECHNIQUE
J. F. Keeling, III, H. A. Kurstedt, Jr., and J. E. Hughes 1990 3 p
(Contract DE-FG02-88DP-48058)
(DE91-012421; DOE/DP-48058/T11) Avail: NTIS HC/MF A01

The primary purpose is to provide managers and group facilitators with a tool for selecting the best technique(s) to help a group solve a problem. The selection tool was created by matching available techniques to problem component examples using a contour map. The secondary purpose is to: (1) describe (by example) three components of a problem that requires a group to solve, and (2) describe available techniques for group problem solving. DOE

N91-29067# Virginia Polytechnic Inst. and State Univ., Blacksburg.
EXPERIENCE IN DESIGNING AND USING A FLAT STRUCTURE IN A MULTI-PROJECT RESEARCH ORGANIZATION
H. A. Kurstedt, Jr., E. J. Gardner, and T. B. Hindman, Jr. 1990 5 p
(Contract DE-FG02-88DP-48058)
(DE91-012427; DOE/DP-48058/T6) Avail: NTIS HC/MF A01

In early 1986, the organization of the Management Systems Laboratories (MSL) was changed from a standard matrix to a flat organization. The flat organization contributed more negative influences on the organization and its goals than positive ones. One year later, the flat organization was changed to a standard hierarchy and most negative influences were overcome. Before, during, and after the flat organization, MSL saw significant growth in funding and in its resource needs. This paper is an account of an experience with a type of flat organization, why the change to that organization, what worked and what didn't, why a change away from that organization, what was learned from the experience, and what would be recommended for research organizations considering flat organizations. DOE

N91-29068# Edgerton, Germeshausen and Grier, Inc., Idaho Falls, ID.
THE HUMAN SIDE OF VALUE ENGINEERING
J. Wixson and H. J. Heydt 1991 11 p Presented at the SAVE International Conference, Kansas City, May 1991
(Contract DE-AC07-76ID-01570)
(DE91-012817; EGG-M-90540; CONF-9105167-2) Avail: NTIS HC/MF A03

This paper addresses people, pride and performance and their interrelationship with the Value Engineering (VE) technique. It explores the importance of people for the successful application of the technique. It discusses leadership skills, verbal and non-verbal communication, team member recognition and participation, knowledge of right and left brain characteristics and the part each play in the job plan leading to the successful integration of philosophy and techniques to creat change and improve performance. DOE

N91-29069# Virginia Polytechnic Inst. and State Univ., Blacksburg. Management Systems Labs.
STRUCTURED MEETING TECHNIQUES IDENTIFY EMERGENCY MANAGEMENT ISSUES PRACTITIONERS REALLY WANT TO SEE ADDRESSED

G. E. Ruberg and J. F. Keeling, III Feb. 1991 10 p
(Contracts DE-FG02-88DP-48058; DE-FC06-87CH-10343)
(DE91-012414; DOE/DP-48058/T9) Avail: NTIS HC/MF A02

Emergency Management (EM) researchers need a proactive and systematic approach for obtaining research topics practitioners really want to see addressed. Because of the inter-disciplinary nature of EM, traditional research hasn't provided practitioners with the information and management tools they can readily use. Furthermore, because historically EM practitioners haven't been academically oriented, they haven't been inclined to make use of the research provided. It is felt that this is changing as evidenced by such activities as an increased emphasis on professional standards and training: one example is the National Coordinating Council on Emergency Management's project to develop professional standards for emergency managers. The method adds another link to the connection between research and practice to better meet the needs of emergency managers. Three structured meeting techniques are introduced that can be used to determine EM issues practitioners really want to see addressed. The benefits of using these techniques are listed and recommendations are provided for research based on three applications of the techniques. DOE

N91-29070# Virginia Polytechnic Inst. and State Univ., Blacksburg. Management Systems Labs.
HOW TO INCREASE MEETING EFFECTIVENESS AND EFFICIENCY
M. Grunau and H. A. Kurstedt, Jr. 1991 3 p
(Contract DE-FG02-88DP-48058)
(DE91-012420; DOE/DP-48058/T13) Avail: NTIS HC/MF A01

A model is presented which was adapted from control theory to gain insight into the dynamics of meetings. The system controller and feedback sensor in the model are related to the role of the facilitator in meetings. By drawing parallels between the control theory model and the adapted model for meetings, I came up with an operational definition of a group facilitator and derived the following hypothesis: Providing facilitators with information about group members prior to the meeting will improve their effectiveness and efficiency in facilitating the meeting. Such information, for example, could include the group members' personality types measured with the Myers-Briggs Type Indicator or their conflict modes measured through the Thomas-Kilmann Conflict Mode Instrument. DOE

N91-29071# Virginia Polytechnic Inst. and State Univ., Blacksburg.
WHY ENGINEERS MUST KNOW AND MANAGE ORGANIZATIONAL CULTURE
H. A. Kurstedt, Jr., L. A. Mallak, E. M. Howard, and P. S. Kurstedt 1990 5 p
(Contract DE-FG02-88DP-48058)
(DE91-012425; DOE/DP-48058/T4) Avail: NTIS HC/MF A01

The engineering manager's success is being judged more and more on qualitative measures concerning the human elements of their work. These new measures require engineers to become as skilled and at ease with the tools, methods, and techniques for qualitative issues as they are with more traditional quantitative tools, methods, and techniques. To achieve success toward these qualitative measures demands nothing short of a new way of thinking, indeed a new culture embodying new values and traditions. Engineering managers must use culture change mechanisms along with their other management tools so they can better understand and manage culture. They must view concepts such as just-in-time, total quality management, and continuous performance improvement as integral to culture change efforts; these concepts and corresponding programs require an underlying culture to create an environment for change. Engineers who want to manage and change culture and communicate these changes must become comfortable with hoopla and symbolism to add drama and life to their words and plans. Engineers must understand the elements of culture, become effective communicators, and master the tools, methods, and techniques of culture change. DOE

N91-28268*# National Aeronautics and Space Administration, Washington, DC.
MAJOR SYSTEM ACQUISITIONS PROCESS (A-109)
C. Saric *In its* Space Transportation Propulsion Technology Symposium. Volume 3: Panel Session Summaries and Presentations May 1991 p 1313-1323 (For primary document see N91-28235 20-20)
Avail: NTIS HC/MF A99 CSCL 05A

N91-28269*# National Aeronautics and Space Administration. Marshall Space Flight Center, Huntsville, AL.
THE CASE FOR TEAMING ON THE ALS-STME PROGRAM
S. F. Morea *In* NASA, Washington, Space Transportation Propulsion Technology Symposium. Volume 3: Panel Session Summaries and Presentations May 1991 p 1325-1335 (For primary document see N91-28235 20-20)
Avail: NTIS HC/MF A99 CSCL 05A

82 DOCUMENTATION AND INFORMATION SCIENCE

Includes information management; information storage and retrieval technology; technical writing; graphic arts; and micrography.

For computer documentation see *61 Computer Programming and Software.*

N91-29072# Defense Technical Information Center, Alexandria, VA.
DIRECTORY OF ORGANIZATIONAL TECHNICAL REPORT ACRONYM CODES (DOTRAC) Annual Report
Virginia Becks Jun. 1991 912 p Supersedes DTIC/TR-90/1
(AD-A237000; DTIC/TR-91/2; DTIC/TR-90/1) Avail: NTIS HC/MF A99 CSCL 05/2

This compilation is a guide to acronyms as assigned by the Defense Technical Information Center (DTIC). The listing contains entries from the Department of Defense, Federal Government, foreign military and non-government organizations. The acronyms reflect reports processed into the DTIC collections. In all instances the acronyms are those actually used by the organization itself. The listing is arranged in three parts, as follows: alphabetically by acronym, alphabetically by full name of organization, numerically by Corporate Author (Source Header) code as used in DTIC. The appendix contains cross-references which link the various report number acronyms used by organizations who have changed names and definitions of terms frequently used within DTIC. GRA

N91-29073# California Univ., Berkeley. Lawrence Berkeley Lab. Nuclear Science Div.
THE EOS TPC ANALYSIS SHELL
D. L. Olson Mar. 1991 10 p Presented at the Conference on Computing in High Energy Physics, Tsukuba (Japan), 11-15 Mar. 1991
(Contract DE-AC03-76SF-00098)
(DE91-011873; LBL-30425; CONF-910373-7) Avail: NTIS HC/MF A02

Key features of the general purpose event-based-data analysis shell (TAS) for the EOS TPC at LBL are described including the code development/code management procedures used. The architecture is designed with a view towards a distributed and multi-processing environment. TAS is interfaced seamlessly with the CERN PAW program and provides a consistent environment for both on-line and off-line analysis. The data model used is relational tables and the data structure definitions are maintained in a commercial database (INFORMIX). The interface for analysis modules is specified and enhances group participation in the development process. The use of commercial database as a data dictionary for both the table definitions and parameters used in the TAS kernel is extremely useful and productive. DOE

N91-29074# Pacific Northwest Lab., Richland, WA.
THREATENED AREA DATABASE SYSTEM (TADS) COMPUTER PROGRAM
M. Yurconic and D. H. Denham Apr. 1991 9 p Presented at the 3rd Topical Meeting on Emergency Preparedness and Response, Chicago, 16-19 Apr. 1991
(Contract DE-AC06-76RL-01830)
(DE91-012491; PNL-SA-18690; CONF-910434-4) Avail: NTIS HC/MF A02

The Threatened Area Database System (TADS) was developed to provide rapid identification of threatened areas (population areas, site boundaries, and facilities) from a potential hazardous material release. As part of the Emergency Management Support System at the U.S. Department of Energy's Hanford Site, TADS is part of a computer-based assessment system that provides information to personnel who would respond to a Hanford emergency. DOE

N91-29075# Virginia Polytechnic Inst. and State Univ., Blacksburg.
A FRAMEWORK FOR DATA AND INFORMATION
D. S. Berube, H. A. Kurstedt, Jr., and R. M. Jones 1991 3 p
(Contract DE-FG02-88DP-48058)
(DE91-012416; DOE/DP-48058/T12) Avail: NTIS HC/MF A01

The design information systems is still very much an art. Information systems are designed by looking at the characteristics of information, decisions, and the manager. For information system design to move from an art to a science, a detailed understanding of data, information, and the process by which data become information is needed. Information systems are failing because system designers and operators don't have enough detailed understanding of data, information, and the data-to-information process to satisfy managers' information needs. There currently are no comprehensive frameworks that define data and information in enough detail to describe the data-to-information process. Worse, there's generally confusion about the terms data and information, and the two terms are often used interchangeably. Upon close examination of the literature, definitions and relationships are found that each serve to describe a portion of the data-to-information process. By assembling these definitions and relationships, a framework is developed to describe the data, information, and the relationships between data and information. DOE

N91-29076# Virginia Polytechnic Inst. and State Univ., Blacksburg. Management Systems Labs.
THE EFFECTS OF INFORMATION AVAILABILITY ON THE GROUP CONSENSUS PROCESS
R. G. Fulmer, C. P. Koelling, A. R. Doss, and H. A. Kurstedt, Jr. 1990 4 p
(Contract DE-FG02-88DP-48058)
(DE91-012428; DOE/DP-48058/T7) Avail: NTIS HC/MF A01

Can a group reach consensus without the right information. To support group interaction, groupware must provide the correct amount and kind of information. This study tests the relationship between information availability and consensus. Availability includes amount of information, as well as the usefulness of information. Does the group have enough information. Does the group have and use the right information. Discovering the information availability/consensus relationship may help decide whether or not consensus is desired under certain information circumstances. DOE

N91-29077# Edgerton, Germeshausen and Grier, Inc., Idaho Falls, ID.
DISTRIBUTED RELATIONAL DATABASE DESIGN AND IMPLEMENTATION FOR A LARGE, DISTRIBUTED COMPUTER SYSTEM
L. A. Dean and B. J. Groeneveld Apr. 1991 22 p Presented at the Database Colloquium '91, San Diego, 24-26 Jun. 1991
(Contract DE-AC07-76ID-01570)
(DE91-012812; EGG-M-91022; CONF-9106191-1) Avail: NTIS HC/MF A03

This paper discusses the design and implementation of a distributed relational database developed for the U.S. Air Force Tactical Air Command at the Idaho National Engineering Laboratory (INEL). Key items discussed are the data analysis and database design issues encountered throughout development. Emphasis is placed on analysis and design issues surrounding the data and resultant database rather than any particular applications. The resultant database has been implemented using Oracle Corporation's ORACLE Relational Database Management System. Specific issues pertaining to a distributed implementation using ORACLE are also covered. DOE

N91-29078# Pacific Northwest Lab., Richland, WA.
DEVELOPING A GIS TO FACILITATE DATA ANALYSIS FOR ENVIRONMENTAL RESTORATION OF A LARGE WASTE SITE
S. Tzemos, B. J. Evans, and M. E. White May 1991 10 p Presented at the 11th Annual Environmental Systems Research Institution User's Conference, Palm Springs, 20-24 May 1991
(Contract DE-AC06-76RL-01830)
(DE91-013222; PNL-SA-19158; CONF-9105199-1) Avail: NTIS HC/MF A02

The Hanford Site area in southeastern Washington State is a U.S. Department of Energy Superfund cleanup site. The site contains a complex mixture of chemical and radioactive pollutants, which makes environmental monitoring, analysis, and restoration a complicated task. The Hanford Environmental Information System (HEIS) has been developed to manage the data generated from the characterization and environmental monitoring of the Hanford Site. The Geographic Information Systems (GIS) component of HEIS, known as HEISGIS, is being developed to help scientists spatially analyze the environmental data stored in the HEIS database and provide an integrated system for environmental restoration. HEISGIS is in its second stage of development. The first stage produced a working prototype. The second stage focuses on improvements in data accuracy, data standardization, analytical modeling capabilities, interfaces between the various software packages, and the graphical user interface. This paper describes the development of the HEISGIS and summarizes the considerations and difficulties encountered in the integration of the GIS with a large relational database. DOE

N91-29079# Superconducting Super Collider Lab., Dallas, TX.
DOCUMENT FORMAT CONSIDERATIONS FOR A DOCUMENT TRACKING AND STORAGE SYSTEM
N. E. Wells, I. Chow, and L. D. Johnson Mar. 1991 11 p Presented at the 3rd Annual International Industrial Symposium on the Super Collider (IISSC), Atlanta, 13-15 Mar. 1991
(Contracts DE-AC02-89ER-40486; W-31-109-eng-38)
(DE91-013402; SSCL-390; CONF-910340-36) Avail: NTIS HC/MF A03

The design and development of the detectors for the Superconducting Super Collider Laboratory (SSCL) will be facilitated by a central system to track and store the design documents and drawings. Collaborators and SSCL personnel need a single system that they can access from a terminal on their desks and use to locate and view the latest version of a document. The SSCL Physics Research Division has developed a prototype system to track documents and drawings and to make them accessible via local and wide-area networks. The prototype is being used to refine the requirements and to develop the procedures for a larger system that will be acquired later. The format for storing documents is a major challenge because there is no interoperable standard. This paper discusses the system requirements and architecture, and present results of research on standards for storing documents. DOE

N91-29080# Virginia Univ., Charlottesville. School of Engineering and Applied Science.
THE ADAMS INTERACTIVE INTERPRETER Ph.D. Thesis
E. R. Rietscha 17 Dec. 1990 45 p
(Contract DE-FG05-88ER-25063)
(DE91-014345; DOE/ER-25063/T9) Avail: NTIS HC/MF A03

The ADAMS (Advanced DAta Management System) project is exploring next generation database technology. Database management does not follow the usual programming paradigm.

Instead, the database dictionary provides an additional name space environment that should be interactively created and tested before writing application code. The implementation and operation is described of the ADAMS Interpreter, an interactive interface to the ADAMS data dictionary and runtime system. The Interpreter executes individual statements of the ADAMS Interface Language, providing a fast, interactive mechanism to define and access persistent databases. DOE

N91-29081 Sheffield Univ. (England).

THE COMPUTER STORAGE, RETRIEVAL, AND SEARCHING OF GENERIC STRUCTURES IN CHEMICAL PATENTS: THE MACHINE-READABLE REPRESENTATION OF GENERIC STRUCTURES Ph.D. Thesis

John Mordaunt Barnard 1982 400 p

Avail: Univ. Microfilms Order No. BRDX92394

The nature of the generic chemical structures found in patents is described with a discussion of the types of statements commonly found in them. The available representations for such structures are reviewed with particular emphasis on the suitability of the representation for searching files of such structures. Requirements for the unambiguous representation of generic structures in an ideal storage and retrieval system are discussed. The basic principles of the theory of formal languages are reviewed with particular consideration being given to parsing methods for context-free languages. The grammar and parsing of computer programming languages, as an example of artificial formal languages, are discussed. Applications of formal language theory to chemistry and information work are briefly reviewed. A formal language for the unambiguous description of generic structures from patents, GENSAL, is presented. It is designed to be intelligible to a chemist or patent agent, yet sufficiently formalized to be amenable to computer analysis. Detailed description is given of the facilities it provides for generic structure representation, and there is a discussion of its limitations and the principles behind its design. A connection table-based internal representation for generic structures, called an extended connection table representation (ECTR), is presented. It is designed to represent generic structures unambiguously and to be generated automatically from structures encoded in GENSAL. It is compared to other proposed representations, and its implementation using data types of the programming language Pascal is described. An interpreter program which generates an ECTR from structures encoded in a subset of the GENSAL language is presented. The principles of its operation are described. Possible applications of GENSAL outside the area of patent documentation are discussed, and suggestions are made for further work on the development of a generic structure storage and retrieval system based on GENSAL and ECTR's. Dissert. Abstr.

N91-29082# Energy Information Administration, Washington, DC.

EIA PUBLICATIONS DIRECTORY, 1990

10 Jun. 1991 52 p

(DE91-014350; DOE/EIA-0149(90)) Avail: NTIS HC/MF A04

Enacted in 1977, the Department of Energy (DOE) Organization Act established the Energy Information Administration (EIA) as the Department's independent statistical and analytical agency, with a mandate to collect and publish data and prepare analyses on energy production, consumption, prices, and resources, and projections of energy supply and demand. This edition of the EIA Publications Directory contains titles and abstracts of periodicals and one-time reports produced by the EIA from January through December 1990. This edition supplements EIA Publications Directory 1977 to 1989. The body of the Directory contains citations and abstracts arranged by broad subject categories, such as coal, petroleum, and natural gas and subcategories such as reserves, products and byproducts, and marketing and economics. All reports are indexed alphabetically by subject and title and numerically by report number. DOE

N91-29083 Cleveland State Univ., OH.

THE DESIGN OF A CLINICAL LABORATORY INFORMATION SYSTEM Ph.D. Thesis

Joseph Chungwan Su 1990 354 p

Avail: Univ. Microfilms Order No. DA9113974

The design of a truly distributed clinical laboratory information management system based on the use of personal computers in a bus-type local area network is presented. The system-wide file management system will allow the efficient access of data stored in one computer by any other computer on the network. Functions of this system such as test requests, accession number generation, instrument loading list generation and drawlist generation will be very versatile. Dissert. Abstr.

N91-29084 Glasgow Univ. (Scotland).

INFORMATION MANAGEMENT: A UNIFORM CONCEPTUAL MODEL AND ITS USER INTERFACE Ph.D. Thesis

Sunday Olusegun Ojo 1985 272 p

Avail: Univ. Microfilms Order No. BRDX91907

Some existing approaches to conceptual data modeling are reviewed. A conceptual modeling framework is developed which is based on the idea of conceptual semantics in linguistics theory. This consists of a Conceptual Schema model, the syntactic embodiment of which is a Conceptual Schema specification language. This approach adopts the principle of Scheme unification which enables the orthogonal treatment of various aspects of information management. This principle was used as a means to achieving the goal of Schema reliability, evolvability, usability, and reliability. Dissert. Abstr.

N91-29085 Ohio State Univ., Columbus.

DESIGN AND PERFORMANCE EVALUATION OF SIGNATURE FILES FOR TEXT RETRIEVAL SYSTEMS Ph.D. Thesis

Chun-Wu Roger Leng 1990 144 p

Avail: Univ. Microfilms Order No. DA9111746

Signature files can be used to support information retrieval in library systems, artificial intelligence, and office automation systems. However, signature file techniques require exhaustively searching the signature files themselves. In addition, data may be required by mistake because of the information loss during signature extraction. The objective was to construct an efficient structure of signature file, called partitioned signature file, so that a large number of unqualified signatures were eliminated from searching. Also, an optimal weighting strategy was proposed to hash each term to its corresponding signature with a specific weight to minimize the false drop probability. The partitioned signature file was able to reduce the number of signatures searched by 10 to 80 percent which highly depended on parameter values. The false drop rate of the new weighting strategy was only 30 to 50 percent of the uniform weighting strategy. All these new designs can be used together to enhance the performance. Dissert. Abstr.

N91-29086 Pennsylvania Univ., Philadelphia.

GENERALIZED HYPERTEXT IN A KNOWLEDGE-BASED DECISION SUPPORT SHELL ENVIRONMENT Ph.D. Thesis

Michael Paul Bieber 1990 183 p

Avail: Univ. Microfilms Order No. DA9112535

A decision support system (DSS) shell was developed serving DSS applications in a broad range of fields, such as finance, engineering and manufacturing. The shell uses a hypertext-style, direct manipulation interface for structuring and presenting information. To overcome the manual, static nature traditionally associated with hypertext, generalized hypertext was developed (an extension of standard hypertext to a dynamic, knowledge-based environment). Hypertext was viewed as system-level functionality, and available to all shell applications. In developing generalized hypertext, three of the outstanding hypertext research issues had to be solved: managing virtual hypertext entities, performing computation over a hypertext network during link traversal, and tailoring the hypertext network. Dissert. Abstr.

N91-29087 Minnesota Univ., Minneapolis.
A SIMULATED USER FOR LABORATORY INVESTIGATION OF INFORMATION SYSTEMS REQUIREMENTS DETERMINATION Ph.D. Thesis
Macedonio Alanis 1990 264 p
Avail: Univ. Microfilms Order No. DA9112654

The Knowledgeable Interview Subject System (KISS) is a computer program that simulates user answers to analyst questions. KISS is a frame-based knowledge structure with a natural language interface. The primary objective is to validate KISS as an acceptable simulation of user responses to analyst questions in laboratory experiments on information requirements determination. Volunteer subjects who were practicing systems analysts were given a realistic information requirements determination task. Their experimental assignment was to ask questions of the system to complete the task. The system's capability to answer those questions and the effect of those answers on the subjects' behavior were analyzed to assess the content and construct validity of the tool. Dissert. Abstr.

N91-29088* National Aeronautics and Space Administration, Washington, DC.
NASA PATENT ABSTRACTS BIBLIOGRAPHY: A CONTINUING BIBLIOGRAPHY. SECTION 2: INDEXES (SUPPLEMENT 39)
Jul. 1991 553 p
(NASA-SP-7039(39)-Sect-2; NAS 1.21:7039(39)-Sect-2) Avail: NTIS HC A24; NTIS standing order as PB89-911100, $53.00 domestic, $106.00 foreign CSCL 05B

A subject index is provided for over 5000 patents and patent applications for the period May 1969 through June 1991. Additional indexes list personal authors, corporate authors, contract numbers, NASA case numbers, U.S. patent class numbers, U.S. patent numbers, and NASA accession numbers. Author

N91-29089# Virginia Univ., Charlottesville. School of Engineering and Applied Science.
IMPLEMENTATION OF A HYPERCUBE DATABASE SYSTEM
J. L. Pfaltz, S. H. Son, and J. C. French May 1991 41 p
(Contract DE-FG05-88ER-25063)
(DE91-014285; DOE/ER-25063/3; UVA-527387/CS91/103)
Avail: NTIS HC/MF A03

This three year grant was an ambitious project to implement a hypercube database system; it was somewhat more ambitious than we had realized. For this final report we begin with an overview that reviews the original proposal; discusses its magnitude; explains our research approach; and outlines our results in terms of what we consider to be its major achievements and resulting publications. Then in sections 2 through 6 we will elaborate on: ADAMS interface language; system implementation; synchronization and reliability and system performance. DOE

N91-29090# Virginia Univ., Charlottesville. Dept. of Computer Science.
PERFORMANCE EVALUATION OF MULTIVERSION DATABASE SYSTEMS
S. H. Son and N. Haghighi 1990 9 p Presented at the 6th International Conference on Data Engineering, Los Angeles, 5-9 Feb. 1990
(Contract DE-FG05-88ER-25063)
(DE91-014340; CONF-900214-4) Avail: NTIS HC/MF A02

This paper describes a detailed simulation study of the performance of multiversion database systems, investigating the characteristics and the extent to which they provide performance benefits over their single-version counterparts. First, the paper presents the structure of a software prototyping environment for the evaluation of distributed database systems. Using this environment, it is shown that for specific workload, multiversion database systems offer performance improvements despite of additional CPU and I/O costs involved in accessing old versions of data. It is also shown that transaction size is one of the most critical parameters that affect the system performance. DOE

N91-29091# California Univ., Berkeley. Lawrence Berkeley Lab.
SAFE REFERENTIAL INTEGRITY STRUCTURES IN RELATIONAL DATABASES
V. M. Markowitz May 1991 12 p Presented at the 17th International Conference on Very Large Data Bases, Barcelona, Spain, 3-6 Sep. 1991
(Contract DE-AC03-76SF-00098)
(DE91-014586; LBL-28363; CONF-9109190-1) Avail: NTIS HC/MF A03

Referential integrity constraints express in relational databases existence dependencies between tuples. Although it is known that certain referential integrity structures may cause data manipulation problems, the nature of these problems has not been explored and the conditions for avoiding them have not been formally developed. In this paper we examine these data manipulation problems and formally develop safeness conditions for avoiding them. Next, we discuss the problem of specifying safe referential integrity constraints in three representative relational database management systems, IBM's DB2, SYBASE, and INGRES. DOE

83 ECONOMICS AND COST ANALYSIS

Includes cost effectiveness studies.

N91-28272*# Thiokol Corp., Brigham City, UT. Space Operations.
POSSIBLE FUNDING STRATEGIES
T. F. Davidson *In* NASA, Washington, Space Transportation Propulsion Technology Symposium. Volume 3: Panel Session Summaries and Presentations May 1991 p 1359-1362 (For primary document see N91-28235 20-20)
Avail: NTIS HC/MF A99 CSCL 05C

84 LAW, POLITICAL SCIENCE AND SPACE POLICY

Includes NASA appropriation hearings; aviation law; space law and policy; international law; international cooperation; and patent policy.

No abstracts in this category.

85 URBAN TECHNOLOGY AND TRANSPORTATION

Includes applications of space technology to urban problems; technology transfer; technology assessment; and surface and mass transportation.

For related information see also *03 Air Transportation and Safety, 16 Space Transportation,* and *44 Energy Production and Conversion.*

N91-29092# Pacific Northwest Lab., Richland, WA.
COMMUNICATING SUCCESS: WRITING ABOUT TECHNOLOGY TRANSFER
S. F. Liebetrau May 1991 18 p Presented at the Technology Transfer and Management of Federal Research and Development (R&D), Denver, 4-14 Jun. 1991
(Contract DE-AC06-76RL-01830)
(DE91-013994; PNL-SA-19310; CONF-9106211-1) Avail: NTIS HC/MF A03

A writer of technology transfer communications is on the exciting leading edge of research and development. However, this form of technical communication utilizes a special and demanding style. To be a technology transfer writer is to attract but not confuse, to be exciting but accurate, to reveal enough but not too much.

Some valuable guidelines are provided for those who practice the growing and important art of communication in technology transfer. DOE

N91-28239*# National Aeronautics and Space Administration. Lyndon B. Johnson Space Center, Houston, TX.
TECHNOLOGY TRANSFER METHODOLOGY
Rich Labotz, Don Connell, and Ken Kroll (Pratt and Whitney Aircraft, West Palm Beach, FL.) *In* NASA, Washington, Space Transportation Propulsion Technology Symposium. Volume 3: Panel Session Summaries and Presentations May 1991 p 915-921 (For primary document see N91-28235 20-20)
Avail: NTIS HC/MF A99 CSCL 05A

N91-28240*# Aerojet-General Corp., Sacramento, CA. Propulsion Div.
TECHNOLOGY TRANSFER METHODOLOGY
Rich LaBotz *In* NASA, Washington, Space Transportation Propulsion Technology Symposium. Volume 3: Panel Session Summaries and Presentations May 1991 p 923-929 (For primary document see N91-28235 20-20)
Avail: NTIS HC/MF A99 CSCL 05A

88 SPACE SCIENCES (GENERAL)

No abstracts in this category.

89 ASTRONOMY

Includes radio, gamma-ray, and infrared astronomy, and astrometry.

N91-29093 Southampton Univ. (England).
CODED APERTURE IMAGING WITH A HURA CODED APERTURE AND A DISCRETE PIXEL DETECTOR Ph.D. Thesis
Kevin Byard 1989 211 p
Avail: Univ. Microfilms Order No. BRDX92258

An investigation into the gamma ray imaging properties of a hexagonal uniformly redundant array (HURA) coded aperture and a detector consisting of discrete pixels constituted the major research effort. Such a system offers distinct advantages for the development of advanced gamma ray astronomical telescopes in terms of the provision of high quality sky images in conjunction with an imager plane which has the capacity to reject background noise efficiently. Much of the research was performed as part of the European Space Agency (ESA) sponsored study into a prospective space astronomy mission, GRASP. The effort involved both computer simulations and a series of laboratory test images. A detailed analysis of the system point spread function (SPSF) of imaging planes which incorporate discrete pixel arrays is presented and the imaging quality quantified in terms of the signal to noise ratio (SNR). Computer simulations of weak point sources in the presence of detector background noise were also investigated. Theories developed during the study were evaluated by a series of experimental measurements with a Co-57 gamma ray point source, an Anger camera detector, and a rotating HURA mask. These tests were complemented by computer simulations designed to reproduce, as close as possible, the experimental conditions. The 60 degree antisymmetry property of HURA's was also employed to remove noise due to detector systematic effects present in the experimental images, and rendered a more realistic comparison of the laboratory tests with the computer simulations. Plateau removal and weighted deconvolution techniques were also investigated as methods for the reduction of the coding error noise associated with the gamma ray images. Dissert. Abstr.

N91-29094 Florida Univ., Gainesville.
VISUAL, RED AND INFRARED PHOTOGRAPHIC SURFACE PHOTOMETRY OF NGC 55 AND NGC 253 Ph.D. Thesis
Gregory Lynn Fitzgibbons 1990 201 p
Avail: Univ. Microfilms Order No. DA9115981

Detailed photographic surface photometry is presented for the Sculptor Group Galaxies NGC 55 and NGC 253. Observations in visual, red, and infrared light from long and short exposure plates are used to produce isophote maps as well as major and minor axis profiles. The standard photometric parameters are derived and V-R, R-I, and V-I colors are presented for the major and minor axes. The integrated magnitude of NGC is V(sub t) = 8.17, R(sub t) = 7.49, and I(sub t) = 7.30. A thickening of the disk is detected that increases with increasing wavelength, indicating the presence of a faint, red halo. At the detection limits of V = 27.6 magnitude per square arc second, R = 27.8 magnitude per square arc second, and I = 27.0 magnitude per square arc second, the size of NGC 55 is given at the assumed distance of 1.78 Mpc. The asymmetry of the galaxy is discussed. The integrated magnitude of NGC 253 is: V(sub t) = 7.35, R(sub t) = 6.41, and I(sub t) = 5.75. The disk appears to thicken with increasing wavelength, again indicating the presence of a red halo. At limits of V = 26.9 magnitude per square arc second, R = 25.9 magnitude per square arc second, and I = 26.4 magnitude per square arc second, the size of NGC is given at the assumed distance of 2.85 Mpc. A large spur is detected to the south that is most obvious in the infrared image, and it increases the size. A three component model of the visual and infrared luminosity of NGC 253 is discussed. The relative contributions of a r(exp 0.25) spheroid, an exponential disk, and a spiral arm component are determined. Dissert. Abstr.

N91-29095 Michigan Univ., Ann Arbor.
EMISSION LINE REGIONS IN ACTIVE GALACTIC NUCLEI: STRUCTURE, KINEMATICS, PHYSICAL CONDITIONS, AND CHEMICAL ABUNDANCES Ph.D. Thesis
Anuradha Purushottam Koratkar 1990 198 p
Avail: Univ. Microfilms Order No. DA9116224

IUE archival data are used to study the structure and kinematics of the broad line region (BLR) in 11 active galactic nuclei (AGNs). The cross correlation technique advocated by Gaskell and Sparke was applied to spectra taken between 1978 and 1988. An extensive study of the errors was carried out. Three of the objects fail to satisfy the Gaskell and Peterson sampling criterion and only yield upper limits to the sizes of the emitting region. For 8 AGNs, the luminosity weighted radii and the inner radii of the line emitting regions were estimated and upper limits to their extents were obtained. It is confirmed that the high ionization lines are emitted from regions significantly smaller than had been predicted by the standard photoionization model and the lower ionization lines come from further away from the central source, especially in low luminosity sources. BLR sizes derived are used to estimate directly the masses of the central objects. Intensities and variability in the emission lines along with results of the cross correlation analysis are used to constrain a self-consistent numerical photoionization model for the BLR in NGC 3783. Dissert. Abstr.

N91-29096 Pennsylvania State Univ., University Park.
COORDINATED OPTICAL AND ULTRAVIOLET OBSERVATIONS OF SHORT PERIOD RS CVn AND W UMa TYPE STARS Ph.D. Thesis
Jeffrey Scott Newmark 1990 168 p
Avail: Univ. Microfilms Order No. DA9117728

Data from the Fiber Optic Echelle Charge Coupled Device (CCD) Spectrograph at KPNO as well as IUE data were analyzed in this study of short period RS CVn and W UMa type binaries. Optical data were analyzed using a spectral subtraction technique to find excess emission (or absorption) in the component spectra. Analysis of data for the W UMa type contact binary VW Cep strongly suggests the existence of extended material near the contact region but clearly outside the Roche lobes. This material is presumably confined in magnetic loops bridging the two components. Making simple assumptions, the density can be estimated at 4 to 5 times

10 (exp 12) cm (sup -3). A possible prominence was also detected on the secondary component of the detached short period RS CVn system DH Leo. Dissert. Abstr.

N91-29097 Cornell Univ., Ithaca, NY.
OBSERVATIONAL CONSTRAINTS ON PULSARS: LOCATION OF THE EMISSION REGION AND PULSE SHAPE STABILITY ON DECADE TIME SCALES Ph.D. Thesis
Michael Mathew Blaskiewicz 1991 243 p
Avail: Univ. Microfilms Order No. DA9113381

Twenty years after their discovery, many basic problems in pulsar physics remain unsolved. Plasma flow patterns along with the associated radio emission and energy loss mechanisms remain a mystery. The dynamical behavior of the neutron star spin rate has been explored via timing analyses but the presence of precession or wandering of the spin axis remain largely unconstrained. The possibility of surface activity such as plate tectonics or volcanism remains open. Observational limits are placed on these phenomena. An introduction is given to pulsars, with an emphasis on the aspects relevant to the remainder of the thesis. The implications of polar cap models are explored within the context of special relativity. Under fairly general conditions, it is found that the suppositions of polar cap models imply a time delay between the centroids of the intensity waveform and the polarization profile with the polarization profile lagging the intensity waveform. Dissert. Abstr.

N91-29098 California Inst. of Tech., Pasadena.
PROPERTIES OF INFRARED-LUMINOUS GALAXIES, OR, HOW I SPENT SEVEN SUMMER VACATIONS Ph.D. Thesis
David Paul Carico 1991 206 p
Avail: Univ. Microfilms Order No. DA9113595

Galaxies selected from the IRAS data base having unusually high 60 to 100 micron luminosities are studied at wavelengths ranging from approx. 1 to 1000 microns. It is found that these galaxies differ significantly from normal, optically selected galaxies, not only in their far infrared luminosities, but in their near infrared wavelengths as well. A substantial excess emission at near infrared wavelengths is attributed to emission from hot dust, with temperatures approx. 500 to 1000 K. Furthermore, this hot dust emission is confined to the central nuclear regions, within characteristic scale sizes approx. 1 to 3 kpc. This suggests that the bulk of the infrared luminosity, and hence the processes responsible for the extreme activity in infrared luminous galaxies, is highly localized about galaxy nuclei. High resolution images of a number of these nuclei reveals a high percentage of double nucleus sources amongst the most luminous galaxies, giving evidence that galaxy-galaxy interactions play a significant role in the generation of high infrared luminosities. The distribution of the mass of, and luminosity from, dust in infrared luminous galaxies is analyzed as a function of dust temperature. Dissert. Abstr.

N91-29099 Arizona Univ., Tucson.
THE OPTICAL POLARIZATION OF BL LACERTAE OBJECTS Ph.D. Thesis
Buell Tomasson Jannuzi 1990 365 p
Avail: Univ. Microfilms Order No. DA9111942

Researchers used the optical polarization properties of BL Lacertae objects to gain insights into the range and physical causes of their extreme and spectacular observed properties. Provided here is an introduction to BL Lacs and other active galactic nuclei, results of an extensive monitoring program of the optical polarization of x-ray selected BL Lacs (XSBLs), and the results of the most extensive optical polarization study so far undertaken. Dissert. Abstr.

90 ASTROPHYSICS

Includes cosmology; celestial mechanics; space plasmas; and interstellar and interplanetary gases and dust.
For related information see also *75 Plasma Physics.*

N91-29100 Durham Univ. (England).
A FAINT GALAXY REDSHIFT SURVEY AND IMPLICATIONS FOR COSMOLOGY Ph.D. Thesis
Thomas James Broadhurst 1990 244 p
Avail: Univ. Microfilms Order No. BRD-91814

A new faint galaxy redshift survey was constructed using the fiber optic coupler. Intermediate dispersion spectra with resolution approximately 4 A were gathered for over 200 field galaxies. Redshift completeness is 85 percent and the mean redshift agrees well from field to field. Models for the prediction of faint galaxy distributions are constructed from a bright galaxy redshift survey. Dissert. Abstr.

N91-29101 North Carolina Univ., Chapel Hill.
NUMERICAL MODELS OF EQUILIBRIUM BETWEEN MATTER AND BLACK HOLES Ph.D. Thesis
Darrel James Conway 1990 105 p
Avail: Univ. Microfilms Order No. DA9115606

Considerable progress was made in the study of black hole thermodynamics at the level of systems in which the effects of the surrounding matter are neglected. Research into the equilibrium between the black hole and the matter fields has recently given some interesting thermodynamic results. However, these new studies were limited to calculations which involved perturbed metrics around some already well understood background with a stress tensor for the matter calculated on the unperturbed background metric. In order to study the full system (black hole plus surrounding matter), Einstein's equations must be solved for the metric given appropriate components of the stress tensor for the matter. Then, the remaining stress tensor components may be calculated, resulting in a consistent description of the system under study. Because of the difficulty of these nonlinear equations, spherical symmetry is imposed from the outset, and the metric is computed numerically. One proposal for an equilibrium system consists of a black hole surrounded by a perfect liquid. It is demonstrated that this proposal is untenable. Instead, in this work the stress tensors in the calculation are those calculated by Page, Howard, and Candelas for a scalar field on a Schwarzschild background. Only two components of the tensor are used to derive the final configuration of the system, and the remaining components are calculated using the new metric. This results in an equilibrium configuration of a static scalar field surrounding a black hole. Dissert. Abstr.

N91-29102 Colorado Univ., Boulder.
EXPLOSION OF A SUPERBUBBLE IN A UNIFORM MAGNETIC FIELD Ph.D. Thesis
Katia Marcelle Ferriere 1990 120 p
Avail: Univ. Microfilms Order No. DA9117044

The effects of interstellar magnetic fields and cosmic rays on the evolution and structure of superbubbles. These giant cavities of hot gas surrounded by an expanding shell of cold material result from the combined action of stellar winds and supernova explosions in OB associations. They have an important impact on the structure of the interstellar medium, influence the interactions with the galactic halo, and are likely to play a role in the cycle of star formation. In the first part, concentration is on magnetic effects. The governing equations are derived and solved analytically in the limit of high expansion velocity. A numerical code capable of solving the governing equations in the general case is developed. In the second part, the cosmic ray pressure is calculated throughout the system and incorporated into the governing equations. The numerical code is adapted in order to include the effects of cosmic rays. It is found that magnetic fields and cosmic rays do not significantly modify the overall shape and dimensions of a superbubble. The shell elongates slightly in the direction of the external field. Magnetic and cosmic ray pressures dominate over gas pressure in most of the shell and forces it to thicken

substantially. Finally, because of the transverse mass motions which take place from the magnetic poles to the equator, the column density at the poles is considerably reduced.
Dissert. Abstr.

N91-29103 Oxford Univ. (England).
NON-HAUSDORFF TWISTOR SPACES AND THE GLOBAL STRUCTURE OF SPACE-TIME Ph.D. Thesis
James Fletcher 1990 147 p
Avail: Univ. Microfilms Order No. BRD-92330

In a space-time with two commuting Killing vectors, the metric can be constructed, by using twistor methods, from a holomorphic vector bundle over a non-Hausdorff reduced space. This procedure is reviewed, and it is shown that, by interpreting the space of the orbits of the Killing vectors as the set of quadratic maps from the Riemann sphere to the reduced space, the analytic extensions of such a space-time can also be obtained from its bundle. This is considered in detail for the Kerr Solution and the C-metric. Conditions are derived on the geometry of the bundle which ensure that the metric is regular at axes, horizons, and their intersections; this leads to a proof of the Black Hole Uniqueness Theorem.
Dissert. Abstr.

N91-29104 Florida Univ., Gainesville.
A SEARCH FOR COSMIC AXIONS Ph.D. Thesis
Christian Alexaner Hagmann 1990 132 p
Avail: Univ. Microfilms Order No. DA9115991

A search experiment was carried out to look for relic cosmic axions trapped in the halo of the Galaxy and limits on their abundance are presented for several axion mass ranges. The detector consisted of a high Q microwave cavity immersed in liquid helium and permeated by a strong magnetic field. A low noise microwave receiver with a cryogenic HEMT amplifier as its first stage was coupled to the cavity. The noise power within a cavity bandwidth was spectrum analyzed and searched for narrow peaks resulting from axion to photon conversions via the Primakoff effect. The resonance frequency was changed by displacing a dielectric rod inside the cavity.
Dissert. Abstr.

N91-29105 Michigan Univ., Ann Arbor.
STUDY OF GRAVITATIONAL COLLAPSE AND COSMIC RAY ABUNDANCES Ph.D. Thesis
Anup Majumder 1990 89 p
Avail: Univ. Microfilms Order No. DA9116248

All the existing neutrino data at the time of SN87A cannot be explained by conventional models of gravitational collapse. This has movitated the pursuit of an alternate scenario for gravitational collapse. The suggestion is examined that quantum mechanics changes the nature of gravitational forces and gravitational collapse yields an oscillating black hole. In this respect, the gravitational collapse of massive objects is studied by hydrodynamic equations. In particular, a dynamical reason is sought for bounce back behavior in gravitational collapse. This was done by following the evolution of hydrodynamic equations in time using thermodynamic relations to find pressure and energy instead of using an particular equation of state. Initial configurations are constructed using both standard polytropes and a power law density distribution. For both cases the collapse, triggered by perturbing the initial stable configuration, halts; and a stable state is reached by the inner zones while the outer zones expand. It is emphasized that such behavior is dynamical as well as thermodynamical in nature.
Dissert. Abstr.

N91-29106 California Inst. of Tech., Pasadena.
RADIATIVE TRANSFER IN VERY STRONG MAGNETIC FIELDS Ph.D. Thesis
Michael Coleman Miller 1990 165 p
Avail: Univ. Microfilms Order No. DA9113610

The study of the cooling of neutron stars is discussed. Young neutron stars are believed to have extremely strong magnetic fields, on the order of 10 (exp 12) G. These fields dominate the physics of the atmosphere. In particular, atoms in the atmospheres of neutron stars have much greater binding energies than in the zero field case, and they are constrained to move along the field lines. Researchers used a multi-configurational Hartree-Fock code, modified for very strong magnetic fields, to calculate wave functions, energies and oscillator strengths for several atoms in representative values of the magnetic field. Researchers then used these representations to construct model atmospheres for neutron stars. Researchers also used high-field energies to investigate soft x-ray lines in gamma-ray bursts. Highly ionized elements could create absorption lines in the 1 to 15 keV range, and the identification of such lines in conjunction with cyclotron lines would determine the magnetic field and gravitational redshift on the surface of the star, which would provide clues to the equation of state of the interior. The prospect of identifying these lines with future satellites is discussed.
Dissert. Abstr.

N91-29107*# Delaware Univ., Newark.
CORONA: COORDINATED RESEARCH ON NON-THERMAL PROCESSES IN ASTROPHYSICS Final Report, 1 May 1988 - 30 Apr. 1991
Dermott J. Mullan 23 Aug. 1991 9 p
(Grant NAGw-1295)
(NASA-CR-188692; NAS 1.26:188692) Avail: NTIS HC/MF A02 CSCL 03B

Several problems in astrophysics are examined where departures from purely thermal behavior are expected to produce effects which are detectable by a variety of NASA satellites. The problems identified as worthy of study include coronal heating in stars, deposition of non-thermal particle energy in stars from external sources, and turbulence in atmospheres and winds of stars. The progress in solving these problems is summarized.
Author

N91-29108*# Chicago Univ., IL.
ASPECTS OF REHEATING IN FIRST-ORDER INFLATION
Richard Watkins and Lawrence M. Widrow (Toronto Univ., Ontario) Jun. 1991 25 p Prepared in cooperation with Fermi National Accelerator Lab., Batavia, IL Sponsored in part by DOE
(Grant NAGw-1340)
(NASA-CR-188705; NAS 1.26:188705; FERMILAB-Pub-91/164-A)
Avail: NTIS HC/MF A03 CSCL 03B

Studied here is reheating in theories where inflation is completed by a first-order phase transition. In the scenarios, the Universe decays from its false vacuum state by bubble nucleation. In the first stage of reheating, vacuum energy is converted into kinetic energy for the bubble walls. To help understand this phase, researchers derive a simple expression for the equation of state of a universe filled with expanding bubbles. Eventually, the bubble walls collide. Researchers present numerical simulations of two-bubble collisions clarifying and extending previous work by Hawking, Moss, and Stewart. The researchers' results indicate that wall energy is efficiently converted into coherent scalar waves. Also discussed is particle production due to quantum effects. These effects lead to the decay of the coherent scalar waves. They also lead to direct particle production during bubble-wall collisions. Researchers calculate particle production for colliding walls in both sine-Gordon and theta (4) theories and show that it is far more efficient in the theta (4) case. The relevance of this work for recently proposed models of first order inflation is discussed.
Author

N91-29109*# Fermi National Accelerator Lab., Batavia, IL.
DIBARYONS IN NEUTRON STARS
Angela V. Olinto, Pawel Haensel (Polish Academy of Sciences, Warsaw.), and Joshua A. Frieman Jun. 1991 14 p
(Contract NAGw-1340; DE-FG02-90ER-40606; NSF AST-88-22595)
(NASA-CR-188704; NAS 1.26:188704; FERMILAB-Pub-91/176-A)
Avail: NTIS HC/MF A03 CSCL 03B

The effects are studied of H-dibaryons on the structure of neutron stars. It was found that H particles could be present in neutron stars for a wide range of dibaryon masses. The appearance of dibaryons softens the equations of state, lowers the maximum neutron star mass, and affects the transport properties of dense matter. The parameter space is constrained for dibaryons by requiring that a 1.44 solar mass neutron star be gravitationally stable. Author

N91-29110*# Minnesota Univ., Minneapolis.

NEUTRINO DEGENERACY AND COSMOLOGICAL NUCLEOSYNTHESIS, REVISITED

K. A. Olive, David N. Schramm, D. Thomas, and T. P. Walker (Ohio State Univ., Columbus.) Jul. 1991 16 p Submitted for publication
(Grant NAGw-1340)
(NASA-CR-188703; NAS 1.26:188703; FERMILAB-Pub-91/192-A)
Avail: NTIS HC/MF A03 CSCL 03B

A reexamination of the effects of non-zero degeneracies on Big Bang Nucleosynthesis is made. As previously noted, non-trivial alterations of the standard model conclusions can be induced only if excess lepton numbers L sub i, comparable to photon number densities eta sub tau, are assumed (where eta sub tau is approx. 3 times 10(exp 9) eta sub b). Furthermore, the required lepton number densities (L sub i eta sub tau) must be different for upsilon sub e than for upsilon sub mu and epsilon sub tau. It is shown that this loophole in the standard model of nucleosynthesis is robust and will not vanish as abundance and reaction rate determinations improve. However, it is also argued that theoretically (L sub e) approx. (L sub mu) approx. (L sub tau) approx. eta sub b is much less than eta sub tau which would preclude this loophole in standard unified models. Author

N91-29111*# Fermi National Accelerator Lab., Batavia, IL.

TESTING THE BIG BANG: LIGHT ELEMENTS, NEUTRINOS, DARK MATTER AND LARGE-SCALE STRUCTURE

David N. Schramm Jun. 1991 40 p Prepared for presentation at the 2nd Winter School of Physics, Puerto Rico, PR, 1991 Prepared in cooperation with Chicago Univ., IL
(NASA-CR-188701; NAS 1.26:188701; FERMILAB-Conf-91/179-A)
Avail: NTIS HC/MF A03 CSCL 03B

Several experimental and observational tests of the standard cosmological model are examined. In particular, a detailed discussion is presented regarding: (1) nucleosynthesis, the light element abundances, and neutrino counting; (2) the dark matter problems; and (3) the formation of galaxies and large-scale structure. Comments are made on the possible implications of the recent solar neutrino experimental results for cosmology. An appendix briefly discusses the 17 keV thing and the cosmological and astrophysical constraints on it. Author

N91-29112*# Fermi National Accelerator Lab., Batavia, IL.

PHASE TRANSITIONS TRIGGERED BY QUANTUM FLUCTUATIONS IN THE INFLATIONARY UNIVERSE

Michiyasu Nagasawa (Tokyo Univ., Japan) and Junichi Yokoyama Jul. 1991 23 p Sponsored in part by Ministry of Education, Science and Culture and DOE
(Grant NAGw-1340)
(NASA-CR-188698; NAS 1.26:188698; FERMILAB-Pub-91/186-A; UTAP-128/91) Avail: NTIS HC/MF A03 CSCL 03B

The dynamics of a second-order phase transition during inflation, which is induced by time-variation of spacetime curvature, is studied as a natural mechanism to produce topological defects of typical grand unification scales such as cosmic strings or global textures. It is shown that their distribution is almost scale-invariant with small- and large-scale cutoffs. Also discussed is how these cutoffs are given. Author

N91-29113*# Fermi National Accelerator Lab., Batavia, IL.

VOID PROBABILITY AS A FUNCTION OF THE VOID'S SHAPE AND SCALE-INVARIANT MODELS

E. Elizalde (Barcelona Univ., Spain) and E. Gaztanaga Jun. 1991 22 p Sponsored in part by DOE and Fulbright/MEC
(Contract NAGw-1340; AEN-90-0033)
(NASA-CR-188696; NAS 1.26:188696; FERMILAB-Pub-91/175-A)
Avail: NTIS HC/MF A03 CSCL 03B

The dependence of counts in cells on the shape of the cell for the large scale galaxy distribution is studied. A very concrete prediction can be done concerning the void distribution for scale invariant models. The prediction is tested on a sample of the CfA catalog, and good agreement is found. It is observed that the probability of a cell to be occupied is bigger for some elongated cells. A phenomenological scale invariant model for the observed distribution of the counts in cells, an extension of the negative binomial distribution, is presented in order to illustrate how this dependence can be quantitatively determined. An original, intuitive derivation of this model is presented. Author

N91-29114 Washington Univ., Seattle.

ISOTOPIC MEASUREMENTS OF SOLAR NOBLE GASES IN INDIVIDUAL MICROMETEORITES FROM GREENLAND AND ANTARCTICA Ph.D. Thesis

Chad Tracy Olinger 1990 236 p
Avail: Univ. Microfilms Order No. DA9114698

Noble gases are studied in individual 100 micron-size particles selected from Greenland and Antarctic glacial sediments. Noble gas isotopic and elemental patterns confirm the extraterrestrial origin of 81 out of 302 particles studied. Micrometeorites in this size range are particularly interesting because they correspond to the peak of the meteoritic mass flux distribution. Many particles studied are compositionally and morphologically similar to known meteoritic materials. Dissert. Abstr.

N91-29115 South Carolina Univ., Columbia.

THE LINE OF GRAVITATION: ON THE QUANTIZATION CONDITIONS IN CURVED SPACETIME AND UNCERTAINTY-DRIVEN INFLATION Ph.D. Thesis

Paul J. Camp 1990 184 p
Avail: Univ. Microfilms Order No. DA9113786

It is argued that the standard commutator relations for a quantum field in a classical background gravitational field are incomplete and that a nonlocal curvature dependent factor should be inserted. This is logically equivalent to making Planck's constant a function of curvature. Consideration of a scalar field propagating in a closed, radiation dominated Robertson-Walker spacetime reveals that the cosmological constant becomes a function of time, providing a vast amount of inflation no matter what the mass of the field or the effective potential. Furthermore, it is seen that this inflation arises solely out of the availability of equations of motion for the scalar field. The field modes are initially zero for all k and come into being as the universe evolves. In this sense, the universe creates its contents out of its own expansion. Dissert. Abstr.

N91-29116 Illinois Univ., Urbana-Champaign.

STAR FORMATION IN THE PRESENCE OF MAGNETIC FIELDS: MOLECULAR CLOUD CORE FORMATION AND DYNAMICAL CONTRACTION DUE TO AMBIPOLAR DIFFUSION:; A SIMULATION WITH AXIAL SYMMETRY Ph.D. Thesis

Robert Anthony Fiedler 1990 210 p
Avail: Univ. Microfilms Order No. DA9114234

Interstellar molecular clouds are generally believed to be the sites of active star formation in our galaxy. Observed densities, temperatures, and magnetic field strengths imply that well ordered magnetic fields dominate the thermal pressure in supporting these objects against self-gravity. The magnetic force is transferred to the neutrals through collisions with ions. Because the degree of ionization drops as the density increases, redistribution of the mass to flux ratio in a cloud's central flux tubes (ambipolar diffusion) takes place at an ever increasing rate, leading to the formation of high density cores, typically after 8 million years of quasi-static contraction. Eventually, the central mass to flux ratio exceeds the critical value for collapse, and the core begins to contract rapidly. The full nonlinear, non-ideal magnetohydrodynamic equations are solved by using a new, nonorthogonal, fully adaptive grid describing the evolution of a set of non-rotating, axially symmetric model clouds. Dissert. Abstr.

N91-29117 Harvard Univ., Cambridge, MA.
OBSERVATIONS OF EXTRAGALACTIC WATER VAPOR MASERS Ph.D. Thesis
Lincoln Jared Greenhill 1990 208 p
Avail: Univ. Microfilms Order No. DA9113164

High resolution (VLBI) studies of interstellar H2O masers can provide information about the dynamics, physical conditions, and distances of host star forming regions. Extragalactic H2O maser fall into two categories, normal masers and megamasers. There have been dozens of studies of masers in the Galaxy but only two of masers outside. Examination of these sources has implications for the extragalactic distance scale and the understanding of galactic nuclei. The first VLBI synthesis map of an extragalactic H2O maser (associated with the IC 133 H II complex in the galaxy M33) is presented. The characteristics of both the maser and the H II complex are very similar to those associated with the most powerful H2O maser in our Galaxy. Next, a second epoch map of the IC 133 maser is introduced. From the two maps of IC 133, the right ascension component was measured of proper motion for four maser features. A VLBI study is detailed of the H2O megamaser and nonthermal continuum source seen toward the nucleus of the galaxy NGC 3079; the maser has a phenomenal isotropic luminosity of approx. 500 solar luminosity. Dissert. Abstr.

N91-29118 Washington Univ., Seattle.
HIGH-OVERTONE BLACK-HOLE NORMAL MODES: A WKB CONTOUR-INTEGRAL APPROACH Ph.D. Thesis
James Williams Guinn 1990 120 p
Avail: Univ. Microfilms Order No. DA9114680

When black holes are perturbed by external sources, they oscillate, or ring, at discrete frequencies corresponding to a set of quasi-normal modes. Gravitational perturbations of the surrounding space-time, as well as 'test' perturbations of electromagnetic and scalar fields in a black hole background space-time, lead to normal modes. In all three cases, the perturbation equations can be reduced to a single Schroedinger-like equation in 1-D, which treats the three types of responses as mathematically equivalent to tunneling of quantum mechanical waves through a potential barrier. Normal modes correspond to tunneling transmission resonances. A high order Wentzel-Kramers-Brillouin (WKB) contour integral technique is shown to apply to the problem of black hole normal modes, first by studying tunneling and normal modes of a model potential barrier, the Poeschl-Teller potential, and then by comparing the contour integral technique with a method derived by Iyer and Will for tunneling near the peak of general potential barriers, which accurately describe low overtone black hole normal modes. The contour WKB technique is then applied to the high overtone normal modes. Results are compared to other techniques. Dissert. Abstr.

N91-29119 Harvard Univ., Cambridge, MA.
MULTIPLE NUCLEI, CLUSTER CORE DYNAMICS, AND THE VELOCITY DISTRIBUTIONS OF GRAVITATING SYSTEMS Ph.D. Thesis
Michael Ralph Merrifield 1990 157 p
Avail: Univ. Microfilms Order No. DA9113197

The dynamics of galaxies in the cores of clusters are investigated. Their spatial distribution within 250h(-1) kpc of a central dominant galaxy is shown to follow an exponential distribution, characteristic of the effects of dynamical friction. The shape of this density distribution means that the majority of the secondary condensations, or multiple nuclei, observed within the envelopes of central dominant galaxies can be explained as the line-of-sight projection of normal cluster members. However, the high central density associated with such a cusped distribution also raises the possibility that some multiple nuclei may be currently colliding with the underlying dominant galaxy. Kinematic observations are found to be in accord with the distribution of orbits in the cluster core being isotropic. These observations also imply that the fraction of multiple nuclei now merging with the central galaxies is too small for the central galaxy to have acquired its current stature by this process alone. Investigation of individual well sampled clusters does, however, suggest that a large central dominant galaxy can detectably affect the dynamics of the cluster core. Dissert. Abstr.

N91-29120 Queens Univ., Belfast (Northern Ireland).
INTERSTELLAR MAGNESIUM STUDIES Ph.D. Thesis
Mary Josephine Murray 1986 253 p
Avail: Univ. Microfilms Order No. BRDX91944

Magnesium in the interstellar medium is studied. A summary is given of the relevant background material; the nature of the interstellar medium and current theories on the physical processes which govern the formation and destruction of interstellar grains are outlined. The acquisition and reduction of observational data from two space telescopes (Copernicus and the International Ultraviolet Explorer) are described, and the problems associated with the data are discussed. Analysis of astronomical spectra requires accurate atomic data, and in particular the determination of elemental abundances from interstellar absorption lines requires the oscillator strengths of the transitions involved. The calculation of the oscillator strength for the Mg II are described, and results are discussed in terms of current theories on the formation and destruction processes of interstellar grains. The possibilities for extending the current work concomitant with the commencement of Hubble Space Telescope operation are discussed. Dissert. Abstr.

N91-29121 Princeton Univ., NJ.
GRAVITATIONAL EVOLUTION OF LARGE-SCALE STRUCTURE IN THE UNIVERSE Ph.D. Thesis
Changbom Park 1991 253 p
Avail: Univ. Microfilms Order No. DA9112300

Large scale properties of the Universe are studied under a popular hypothesis that the large scale structure has evolved from primordial Gaussian random fluctuations by gravitational instability. Researchers developed a highly efficient Particle-Mesh N-body code. Large simulations with a reasonable prescription for galaxy formation has shown that the biased Cold Dark Matter (CDM) model is quite successful in describing the observed large scale distribution and motions of galaxies. Researchers found that nonlinear gravitational evolution increases the zero crossing scale of the correlation function. The cluster correlation function from 5 large CDM simulations shows on average a lower amplitude than some observational claims. Since the observational correlation function is controversial, a deep 3D cluster survey with an objective cluster selection criterion is required. The supercluster correlation function calculated from these CDM simulations is consistent with observations. Researchers present a new technique of N-body simulation in a box with non-equal sides. A long rod simulation is made to simulate a recent pencil beam survey and a detailed statistical hypothesis test is made. Dissert. Abstr.

N91-29122 Washington Univ., Seattle.
A NEW MODEL OF PeV GAMMA RAY SOURCES AND MHD TURBULENCE IN NEUTRON STAR ACCRETION COLUMNS Ph.D. Thesis
Ian Andrew Smith 1990 142 p
Avail: Univ. Microfilms Order No. DA9114702

In recent years, several accreting X ray binary sources have been found to emit gamma rays. This requires the acceleration of protons to energies of 10(exp 16) to 10(exp 17) eV. It was proposed that protons could be accelerated to these energies in the outer regions of a neutron star's closed magnetosphere. However, the main source of energy is near the surface of the star, where matter falling down an accretion column releases its gravitational potential energy. Herein, it is postulated that at certain times for these sources, a hot, dense, optically thick plasma pool forms in the column. Using a magnetohydrodynamic (MHD) model, a linear instability analysis shows that the top portion of this pool can become unstable to convective motions in spite of the strong magnetic field. Assuming that fully developed turbulence results, a Lighthill-like analysis was performed, and it was found that perturbations to the strength of the background magnetic field travel from the turbulent region up the column carrying energy out to the region of the energetic protons. Using simple Mixing Length Theory arguments, it was found that there may be sufficient energy transfer to explain the observed high energy gamma ray luminosities. Dissert. Abstr.

N91-29123 Illinois Univ., Urbana-Champaign.
NUMERICAL SIMULATIONS OF MASS OUTFLOWS FROM STAR-FORMING REGIONS Ph.D. Thesis
James McLellan Stone 1990 257 p
Avail: Univ. Microfilms Order No. DA9114425

The development, testing, and application of a 2-D radiation magnetohydrodynamics (RMHD) code is described. Well developed Eulerian hydrodynamic algorithms are used, but are implemented in a new covariant formalism which facilitates simulations in any orthogonal coordinate system. The developed constrained transport (CT) algorithm is implemented for the numerical evolution of the components of a magnetic field for MHD simulations. It is found that in its original form, the CT algorithm is unable to propagate all modes of the MHD wave families (especially shear Alfven waves) stably. Thus, an extension to the CT algorithm is developed using the method of characteristics (MOC), and it is shown that the resulting hybrid CT/MOC method does provide for the stable evolution of all modes of MHD wave families. A 2-D full transport algorithm to evolve the radiation moment equations is developed and tested for RHD simulations. The code is then applied to two important problems regarding mass outflows from star forming regions. These problems are detailed. Dissert. Abstr.

N91-29124 Princeton Univ., NJ.
POPULATION SYNTHESIS MODELS FOR CLUSTER GALAXIES AT REDSHIFTS OF 0.4 TO 0.55 Ph.D. Thesis
Duncan Eliot Peter Walsh 1991 172 p
Avail: Univ. Microfilms Order No. DA9112303

Stellar population synthesis models were built for use with optical spectra with approx. 10A resolution. These make use of metal rich evolutionary tracks and the results compare very well with Galactic bulge giant data. It is suggested that most V band light in old populations comes from main sequence turnoff stars, not giants. Attention is drawn to important differences between two popular libraries of stellar spectra. Good fits are found for local giant elliptical galaxy spectra with metallicities Z approx. = 0.03 and ages approx. = 13 Gyr. There is no need to provide supplementary blue stars to produce the flux between 3160 and 4000A. The red cluster galaxies with z between 0.38 to 0.55 are redder than expected, but there are some considerable discrepancies between photometric and spectral data which make this uncertain. If the redness is real, either extinction or a metallicity higher than anticipated is required. The bluer cluster galaxies have undergone bursts of star formation with up to 20 pct of their stellar mass residing in stars younger than approx. 1 Gyr. These bursts may be the origin for the observed dispersion in the color magnitude relationship for early type galaxies. Dissert. Abstr.

N91-29125# California Univ., Berkeley. Lawrence Berkeley Lab.
IMPACT OF THE NUCLEAR EQUATION OF STATE ON MODELS OF ROTATING NEUTRON STARS
F. Weber and N. K. Glendenning 3 Jun. 1991 18 p Presented at the International Workshop on Unstable Nuclei in Astrophysics, Tokyo (Japan), 7-8 Jun. 1991
(Contract DE-AC03-76SF-00098)
(DE91-014615; LBL-30726; CONF-9106226-1) Avail: NTIS HC/MF A03

The impact of the nuclear equation of state on the properties of rotating neutron stars from two different sources, stable rotation at the general relativistic Kepler period and rotation at the gravitational radiation-reaction driven instability mode, is analyzed. For this purpose models of rotating neutron stars are constructed in the framework of Einstein's theory of general relativity by applying a refined version of Hartle's perturbative stellar structure equations. The investigation is based on a representative collection of a total of seventeen nuclear equations of state, covering both non-relativistic as well as relativistic ones. DOE

N91-29126# Wisconsin Univ., Madison.
SAWTEETH IN THE MST REVERSED FIELD PINCH Ph.D. Thesis
J. A. Beckstead Sep. 1990 76 p
(Contract DE-FG02-85ER-53198)
(DE91-014288; DOE/ER-53198/167) Avail: NTIS HC/MF A05

A dynamo mechanism has been used in astrophysics to explain the self-generation of the magnetic fields observed throughout the universe. This same type of phenomenon is believed to occur in the reversed field pinch (RFP) plasmas. The RFP dynamo has been a major theoretical and experimental investigation since the first observations of the self-reversal process in early pinch research. A discrete dynamo event has been observed in the experimental RFP plasmas; this event is termed the RFP sawtooth. This phenomenon is similar to the sawtooth phenomenon observed in tokamak plasmas, but the two events differ in many respects. Both events are a result of the inward diffusion of the plasma current density. This causes the plasma to become unstable to the $m = 1$ tearing modes. It has been shown theoretically that the nonlinear interaction of these modes can generate the reversed toroidal field in the RFP. This thesis is a study of the RFP sawtooth phenomenon on the MST RFP. This includes experimental observations as well as 1-D numerical simulations of the sawtooth rise-time. During the rise-time of the sawtooth, the plasma is undergoing a purely diffusive process - no dynamo is occurring during this phase. The dynamo only occurs during the sawtooth crash. During the rise-time, the $m = 1$ modes are observed to grow, and nonlinear interactions are observed prior to the sawtooth crash. At the time of the crash, many of the plasma profiles are flattened; these include the current density, the plasma temperature and the plasma density. The period of the sawteeth is observed to increase with the plasma current, as well as the magnetic Reynolds number, S. DOE

N91-28903# Tokyo Univ. (Japan). Faculty of Science.
MAGNETOHYDRODYNAMICAL FORMATION OF ASTROPHYSICAL JETS FROM GRAVITATIONALLY COLLAPSING OBJECTS Abstract Only
Yutaka Uchida *In* National Inst. for Fusion Science, Proceedings of the Second International Toki Conference on Plasma Physics and Controlled Nuclear Fusion. Nonlinear Phenomena in Fusion Plasmas: Theory and Computer Simulation Apr. 1991 p 78
Prepared in cooperation with National Inst. for Fusion Science, Nagoya, Japan (For primary document see N91-28881 20-75)
Avail: NTIS HC/MF A11

91 LUNAR AND PLANETARY EXPLORATION

Includes planetology; and manned and unmanned flights. For spacecraft design or space stations see *18 Spacecraft Design, Testing and Performance.*

N91-29127 New Mexico State Univ., Las Cruces.
SEARCH FOR REGULARITIES IN THE ATMOSPHERE OF JUPITER Ph.D. Thesis
Tom Harvey Little 1990 153 p
Avail: Univ. Microfilms Order No. DA9111288

Exploratory studies were made of phenomena occurring in Jupiter's atmosphere in two distinct phenomenal regimes. The first study deals with variations in the planets visible albedo over long periods of time. Photographic observations spanning the period 1967 to 1988 were reduced, calibrated relative to the disk average reflectivity of the planet, and arranged in a time series. The time series was then analyzed using periodograms and phase plots. A sharply defined periodicity is found in the North Temperate Belt (23 degrees N), having a period of 4.9 years. This period is not commensurate with any known periodicity bearing on the dynamics of Jupiter's atmosphere. The Equatorial Zone and South Equatorial Belt, although they exhibit small oscillations with similar periods, are dominated by aperiodic transitions between distinct states. The second study uses infrared observations from the Voyager 1 spacecraft to investigate the thermal structure of Jupiter's stratosphere. Data from the 3 mb and 9 mb pressure levels are separately averaged, guided by latitude, and analyzed for evidence of longitudinal structure. Fourier transform methods are used to search for spatial periodicities, such as might result from planetary waves. Although some such periodicities are found, they are not considered strong evidence for planetary waves; none of them show the vertical extent or temporal persistence expected of such waves. Dissert. Abstr.

92 SOLAR PHYSICS

Includes solar activity, solar flares, solar radiation and sunspots.

For related information see *93 Space Radiation.*

N91-29128# National Geophysical Data Center, Boulder, CO.
SOLAR-GEOPHYSICAL DATA NUMBER 558, AUGUST 1990. PART 2: (COMPREHENSIVE REPORTS). DATA FOR AUGUST 1990 AND MISCELLANEOUS
Helen E. Coffey Aug. 1990 107 p
(PB91-172262; SGD-558-Pt-2) Avail: NTIS HC/MF A06 CSCL 03B

In addition to a detailed index for 1990 to 1991, data are provided for May 1990 on: solar flares; solar radio bursts at fixed frequencies; interplanetary solar particles and plasma; solar x ray radiation from GOES Satellite; mass ejection from the Sun; and active prominences and filaments. GRA

N91-29129# National Geophysical Data Center, Boulder, CO.
SOLAR-GEOPHYSICAL DATA NUMBER 558, FEBRUARY 1991. PART 1: (PROMPT REPORTS). DATA FOR JANUARY 1991, DECEMBER 1990, AND LATE DATA
Helen E. Coffey Feb. 1991 168 p
(PB91-172270; SGD-558-Pt-1) Avail: NTIS HC/MF A08 CSCL 03B

In addition to a detailed index for 1990 to 1991, data are provided for Jan. 1991 on: the solar terrestrial environment; IUWDS alert periods (advanced and worldwide); solar activity indices; solar flares, solar radio emission; and Stanford mean solar magnetic field. Data are also provided for Dec. 1990 on: solar active regions; sudden ionospheric disturbances; solar radio spectral observations; cosmic ray measurements by neutron monitor; and geomagnetic indices. Geomagnetic activity indices for November 1990 and Pioneer Venus solar wind daily values for Jan. to Oct. 1990 are also presented. GRA

N91-29130# National Geophysical Data Center, Boulder, CO.
SOLAR-GEOPHYSICAL DATA NUMBER 557, JANUARY 1991. PART 1: (PROMPT REPORTS). DATA FOR DECEMBER, NOVEMBER 1990 AN LATE DATA
Helen E. Coffey, ed. Jan. 1991 175 p
(PB91-169102; SGD-557-Pt-1) Avail: NTIS HC/MF A08 CSCL 03B

A detailed index for 1990 is presented, and the data presented for Dec. 1990 covers: solar terrestrial environment; IUWDS alert periods (advanced and worldwide), solar activity indices; solar flares; solar radio emission; and Stanford mean solar magnetic field. Data presented for Nov. 1990 includes: solar active regions; sudden ionospheric disturbances; solar radio spectral observations; cosmic ray measurements by neutron monitor; and geomagnetic indices. Cosmic ray indices at Huancayo for Sep. 1990 and at Thule for Jul. to Oct. 1990, and provisional values of hourly equatorial Dst for Sep. 1989 to May 1990 are also presented. GRA

N91-29131# National Geophysical Data Center, Boulder, CO.
SOLAR-GEOPHYSICAL DATA NUMBER 557, JANUARY 1991. PART 2: (COMPREHENSIVE REPORTS). DATA FOR JULY 1990 AND MISCELLANEOUS
Helen E. Coffey, ed. Jan. 1991 86 p
(PB91-169110; SGD-557-Pt-2) Avail: NTIS HC/MF A05 CSCL 03B

A detailed index for 1990 is presented, and data is presented for July 1990 on: solar flares; solar radio bursts at fixed frequencies; interplanetary solar particles and plasma; solar x ray radiation form GOES satellite; mass ejections from the sun; and active prominences and filaments. GRA

N91-29132 Colorado Univ., Boulder.
ELECTRON ACCELERATION BY MAGNETOSONIC WAVES IN A SOLAR CORONAL LOOP Ph.D. Thesis
Jean-Francois deLaBeaujardiere 1990 151 p
Avail: Univ. Microfilms Order No. DA9117039

Particle acceleration is an important problem in astrophysics. During solar flares, intense electromagnetic emission and escaping high energy particles are observed. A means of accelerating these particles is required to explain the observations. The possible mechanisms are direct electric fields in magnetic reconnection regions, shocks, and stochastic acceleration by plasma turbulence. The latter mechanism is considered. The compressive magnetosonic oscillations of a solar coronal loop and their effect on electrons are investigated. The loop is modeled as a magnetized cylinder embedded in an infinite medium. A dispersion relation for the waves is derived and is solved both analytically and numerically. Characteristics of the normal modes of the system are discussed. the response of an electron to such a wave is described. The equation of motion is presented, and a Hamiltonian formulation is introduced. A physical explanation of the acceleration mechanism is provided. The behavior of test particles in an oscillating coronal loop by numerically integrating the equation of motion using the guiding center approximation. Individual particle trajectories are chaotic, and examples of this phenomenon are shown. The evolution of large samples of test electrons is computed. The waves can resonate with near-thermal electrons, and whether or not such particles can be accelerated out of the thermal pool by this mechanism is investigated. The dependence of the acceleration on wave strength and wave spectral shape, and the effect of pitch angle scattering and Coulomb collisions, are considered. Comparisons are made with analytic treatments of similar problems. Reasonable agreement with analytical solutions was found. Quantitative differences arise from the simplified nature of the diffusion coefficient used in the analytic work. The energy gains of thermal electrons via this mechanism are modest. It is concluded that stochastic acceleration by magnetosonic waves cannot be responsible for producing the observed energetic phenomena in flares. Dissert. Abstr.

N91-28904# National Inst. for Fusion Science, Nagoya (Japan).
COMPUTER SIMULATION OF SOLAR WIND-MAGNETOSPHERE INTERACTION
K. Watanabe, Tetsuya Sato, A. Kageyama, and A. Usadi (Hiroshima Univ., Japan) *In its* Proceedings of the Second International Toki Conference on Plasma Physics and Controlled Nuclear Fusion. Nonlinear Phenomena in Fusion Plasmas: Theory and Computer Simulation Apr. 1991 p 79-82 (For primary document see N91-28881 20-75)
Avail: NTIS HC/MF A11

N91-28912# Nagoya Univ., Toyokawa (Japan). Solar-Terrestrial Environment Lab.
HELICAL FIELD EFFECT IN SOLAR/STELLAR WIND
Haruichi Washimi *In* National Inst. for Fusion Science, Proceedings of the Second International Toki Conference on Plasma Physics and Controlled Nuclear Fusion. Nonlinear Phenomena in Fusion Plasmas: Theory and Computer Simulation Apr. 1991 p 107-110 (For primary document see N91-28881 20-75)
Avail: NTIS HC/MF A11

93 SPACE RADIATION

Includes cosmic radiation; and inner and outer earth's radiation belts.

For biological effects of radiation see *52 Aerospace Medicine*. For theory see *73 Nuclear and High-Energy Physics*.

N91-29133# California Univ., Berkeley. Lawrence Berkeley Lab.
GROUND-BASED MEASUREMENTS OF GALACTIC COSMIC RAY FRAGMENTATION IN SHIELDING
W. Schimmerling Nov. 1990 15 p Presented at the COSPAR Plenary Conference, The Hague, Netherlands, 25 Jun. - 6 Jul. 1990
(Contract DE-AC03-76SF-00098)
(DE91-012336; LBL-30022; CONF-9006220-8) Avail: NTIS HC/MF A03

The mean free path for nuclear interactions of galactic cosmic rays is comparable to shielding and tissue thicknesses present in human interplanetary exploration, resulting in a significant fraction of nuclear reaction products at depth. In order to characterize the radiation field, the energy spectrum, the angular distribution, and the multiplicity of each type of secondary particles must also be known as a function of depth. Reactions can take place anywhere in a thick absorber; therefore, it is necessary to know these quantities as a function of particle energy for all particles produced. HZE transport methods are used to predict the radiation field; they are dependent on models of the interaction of man-made systems with the space environment to an even greater extent than methods used for other types of radiation. Hence, there is a major need to validate these transport codes by comparison with experimental data. The most cost-effective method of validation is a comparison with ground-based experimental measurements. A research program to provide such validation measurements using neon, iron and other accelerated heavy ion beams will be discussed and illustrated using results from ongoing experiments and their comparison with current transport codes. The extent to which physical measurements yield radiobiological predictions will be discussed. DOE

N91-29134 Purdue Univ., West Lafayette, IN.
UPPER LIMITS FOR THE FLUX OF VERY HIGH-ENERGY GAMMA RADIATION FROM CYGNUS X-3 AND FOR THE EXPLOSION RATE OF PRIMORDIAL BLACK HOLES OBTAINED BY THE HALEAKALA GAMMA RAY OBSERVATORY Ph.D. Thesis
Robert Andreas Austin 1990 217 p
Avail: Univ. Microfilms Order No. DA9116349

Two possible sources of gamma radiation are considered: the X ray (binary) source, Cygnus X-3, and primordial black holes. In the case of Cygnus X-3, high multiplicity events are selected and an upper limit for the flux of very high energy gamma radiation from this source is obtained. An unsuccessful attempt to verify an earlier observation by the author of modulation of the cosmic ray rate at a period near Cygnus X-3' 4.8 hour X ray period is discussed. In the search for gamma radiation from primordial black holes, two models of their decay are considered: the quark model and the Hagedorn model. No primordial black hole explosions were detected and upper limits for the explosion rate are presented. Dissert. Abstr.

N91-29135 Michigan Univ., Ann Arbor.
THE GAMMA RAY CONTENT OF ULTRAHIGH ENERGY COSMIC RADIATION Ph.D. Thesis
Jeffrey Jay Kolodziejczak 1990 192 p
Avail: Univ. Microfilms Order No. DA9116222

Data from the Utah-Michigan (UM) extensive air shower (EAS) array at Dugway, Utah are examined for evidence of a gamma ray component in the UHE cosmic rays. The UM array consist of a 3 x 10(exp 4) sq m surface array with 40 sq m of charged particle detectors, and a 1200 sq m buried array for detecting muons. Data from the large muon array are used to search for a gamma ray signature, since gamma rays are expected to produce far fewer muons in EAS than hadronic cosmic ray primaries. When no evidence for gamma rays is found, limits are set based on expected gamma ray behavior. For a photon energy threshold of 200 TeV, results include: a limit on the omnidirectional gamma ray fraction of cosmic rays at 0.2 pct; a limit on the galactic gamma ray fraction of cosmic rays at 7 x 10(exp -5); no strong evidence for enduring gamma ray point sources at fluxes approx. = 4 x 10(exp -14)/sq cm/s; and no strong evidence for bursts on a one day time scale at a flux sensitivity approx. 2 x 10(exp -12)/sq cm/s. These limits and measurements are based on muon poor data. While no strong signal of UHE gamma rays is found, future application to the large Chicago Air Shower Array-Michigan Array (CASA-MIA) is possible. Dissert. Abstr.

N91-29136 Princeton Univ., NJ.
INTERACTION OF RADIATION WITH OUTFLOWS IN LATE-TYPE STARS Ph.D. Thesis
Nathan Netzer 1990 123 p
Avail: Univ. Microfilms Order No. DA9110400

The properties of molecular circumstellar envelopes formed by mass loss from evolved stars are investigated by studying their interaction with radiation. The equations of photodissociation and radiative transfer are solved for the photochemical chain H2O yields OH plus H yields O plus H plus H in the circumstellar envelopes produced by steady mass loss from cool evolved stars. The solution is performed for a large range of mass loss rates, outflow velocities and interstellar UV radiation field densities. Comparison with observations shows that, over a wide range of mass loss rates, the radius at which the OH density peaks is coincident with the radius defined by maser emission in the 1612-MHz line. This allows the use of these models, together with observations of OH maser shell radii and wind outflow velocities, to measure mass loss rates. A simple power law function relating mass loss rate to OH shell radius and wind outflow velocity is developed from these models and applied to the existing measurements of OH shell radii to derive mass loss rates for 42 stars. Dissert. Abstr.

N91-29137 California Inst. of Tech., Pasadena.
RADIATIVE PROCESSES IN ACTIVE GALACTIC NUCLEI Ph.D. Thesis
Paolo Severo Coppi 1991 228 p
Avail: Univ. Microfilms Order No. DA9113596

Processes relevant to the electron-positron pair plasmas thought to exist in Active Galactic Nuclei are studied. The processess considered include: Compton scattering, pair annihilation, two photon pair production, synchrotron emission, e-e bremsstrahlung, and Coulomb scattering. Approximations used in the past to treat these processes in the context of a kinetic code are examined, and improvements are presented. A two moment scattering formalism is presented to allow for important energy dispersion effects in scattering. This improved treatment of microphysical processes is implemented in a time dependent, kinetic code incorporating Klein-Nishina effects on both the pair and photon distributions, relativistic thermal Comptonization, and synchrotron reabsorption. The effects of pair plasma reprocessing on the emergent radiation spectrum are examined. Dissert. Abstr.

99 GENERAL

N91-29138*# National Aeronautics and Space Administration. Lewis Research Center, Cleveland, OH.
HISTORICAL PERSPECTIVES: THE ROLE OF THE NASA LEWIS RESEARCH CENTER IN THE NATIONAL SPACE NUCLEAR POWER PROGRAMS
H. S. Bloomfield and R. J. Sovie 1991 8 p Presented at the Conference on Advanced Space Exploration Initiative Technologies, Cleveland, OH, 4-6 Sep. 1991; cosponsored by AIAA and OAI
(NASA-TM-105196; E-6498; NAS 1.15:105196; AIAA-91-3462)
Avail: NTIS HC/MF A02 CSCL 05D

The history of the NASA Lewis Research Center's role in space nuclear power programs is reviewed. Lewis has provided leadership in research, development, and the advancement of space power and propulsion systems. Lewis' pioneering efforts in nuclear reactor technology, shielding, high temperature materials, fluid dynamics, heat transfer, mechanical and direct energy conversion, high-energy propellants, electric propulsion and high performance rocket fuels and nozzles have led to significant technical and management roles in many national space nuclear power and propulsion programs. Author

SUBJECT INDEX

SCIENTIFIC AND TECHNICAL AEROSPACE REPORTS VOLUME 29 NUMBER 20

Typical Subject Index Listing

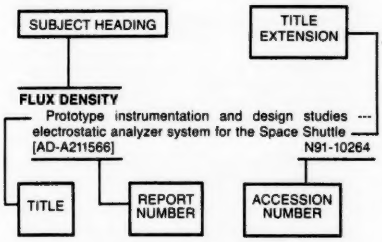
SUBJECT HEADING
TITLE EXTENSION
FLUX DENSITY
Prototype instrumentation and design studies --- electrostatic analyzer system for the Space Shuttle
[AD-A211566]
N91-10264
TITLE
REPORT NUMBER
ACCESSION NUMBER

The subject heading is a key to the subject content of the document. Titles, report numbers, and accession numbers of pertinent documents are provided under each subject heading. When the title is insufficiently descriptive of the document content, a title extension has been added, separated from the title by three hyphens. The report number helps to indicate the type of document cited (e.g., NASA report, NASA translation, NASA contractor report). The accession number is the number by which the document abstracts are arranged in this journal and by which the document is sold or requested. The titles, with title extensions if present, are arranged under each subject heading in ascending accession number order. The subject headings have been selected from the latest revision of the *NASA Thesaurus* (NASA SP-7064).

A

ABLATION
Chemical characterization of microparticles by laser ablation in an ion trap mass spectrometer
[DE91-012513] N91-28309
Evaporation as a diagnostic test for hydrodynamic cooling of laser-ablated clusters
[DE91-013416] N91-28555
ABLATIVE MATERIALS
Studies of the two-phase plume jet and wall erosion in a vertical launching system N91-28145
ABSORPTANCE
Subgap absorption in conjugated polymers
[DE91-012655] N91-28402
ABSORPTION
The effect of stress on hydrogen uptake and desorption by A-286
[NASA-TM-103537] N91-28341
Laser surface modification to impede hydrogen ingress into steel N91-28375
ABSORPTION SPECTRA
Subgap absorption in conjugated polymers
[DE91-012655] N91-28402
Shock initiation of pentaerythritol tetranitrate crystals: Optical absorption and emission studies
[DE91-013381] N91-29023
Coordinated optical and ultraviolet observations of short period RS CVn and W UMa type stars N91-29096
ABSORPTION SPECTROSCOPY
Radio absorption in the Antarctic ionosphere: Some observations in the region of the midlatitude trough
N91-28694
Development of nanovolt-resolution x ray diffraction using resonant nuclear scattering
[DE91-012217] N91-28847
Spectroscopic and ion probe characterization of laser produced plasmas used for thin film growth
[DE91-013425] N91-28959
Synthesis and characterization of reduced ternary molybdenum oxides and soluble copper (III) alkoxide complexes
[DE91-012679] N91-29001
ABSORPTIVITY
Acoustophoresis method and apparatus
[NASA-CASE-LAR-13388-1] N91-28321
High-throughput liquid-absorption air and aerosol sampler
[DE91-013762] N91-28670
ABSTRACTS
Large space structures and systems in the space station era: A bibliography with indexes
[NASA-SP-7085(02)] N91-28191
ABUNDANCE
Emission line regions in active galactic nuclei: Structure, kinematics, physical conditions, and chemical abundances N91-29095
Study of gravitational collapse and cosmic ray abundances N91-29105
AC GENERATORS
System and component design and test of a 10 hp, 18,000 rpm AC dynamometer utilizing a high frequency AC voltage link, part 1
[NASA-CR-188442] N91-28539
ACCELERATED LIFE TESTS
APFIM characterization of the spinodal decomposition in duplex stainless steels
[DE91-014256] N91-28371
Durability of polymeric materials used in zinc/bromine flow batteries
[DE91-012864] N91-28487
ACCELERATION (PHYSICS)
Sandia's new hypervelocity launcher (HVL)
[DE91-014335] N91-28178
Hypervelocity plate acceleration
[DE91-014738] N91-28179
Shock and reshock of an unstable fluid interface
[DE91-014737] N91-28528
Studies of laser-driven flyer acceleration using optical fiber coupling
[DE91-013503] N91-28562
ACCELERATION PROTECTION
Human body protection in a dynamic environment. Cushioning mechanics
[ITN-91-85149] N91-28733
ACCESS CONTROL
Providing common access mechanisms for dissimilar network interconnection nodes
[AD-A236630] N91-28770
ACCIDENTS
Using HSYS in the analysis of human-system interactions: Examples from the offshore petroleum industry
[DE91-013218] N91-28732
ACCURACY
Measurement accuracy of macroscopic quantum circuits with RF-biased Josephson junction arrays
[DE91-012651] N91-29009
ACID BASE EQUILIBRIUM
Analysis of southeastern Canada lake-water chemistry data in relation to acidic deposition
[DE91-014957] N91-28674
ACID RAIN
TREE: A model of the effects of acid precipitation and air pollutants on the growth of trees
[DE91-014131] N91-28672
Analysis of southeastern Canada lake-water chemistry data in relation to acidic deposition
[DE91-014957] N91-28674
Development and application of new modeling techniques for mesoscale atmospheric chemistry
N91-28692
ACIDITY
Thermodynamic and kinetic aspects of surface acidity
[DE91-014039] N91-28331
ACOUSTIC EMISSION
Changes with material properties of acoustic emission produced during single point machining
[DE91-011913] N91-28452
Origin of acoustic emission produced during single point machining
[DE91-011915] N91-28453
ACOUSTIC INSTABILITY
Measurements of the ion acoustic decay instability and the resultant enhanced laser absorption and enhanced bremsstrahlung in laser-plasma interaction experiments
[DE91-014250] N91-28956
ACOUSTIC MEASUREMENT
Origin of acoustic emission produced during single point machining
[DE91-011915] N91-28453
Signature analysis technique for diagnosing failures in mechanical systems N91-28604
ACOUSTIC PROPERTIES
Signature analysis technique for diagnosing failures in mechanical systems N91-28604
ACOUSTIC VELOCITY
Shock and soliton structures induced by poloidal flow in tokamaks N91-28929
ACOUSTICS
Phonon-mediated detection of elementary particles using silicon crystal acoustic detectors N91-28547
JPRS report: Science and technology. USSR: Physics and mathematics
[JPRS-UPM-90-006] N91-28811
ACTIVATION
Studies relevant to the catalytic activation of carbon monoxide
[DE91-012661] N91-28323
ACTIVATION ENERGY
Reactive characterization as a probe of the nature of catalytic sites
[DE91-014536] N91-28333
Creep and diffusion in nonstoichiometric oxides
[DE91-013766] N91-28435
ACTIVE CONTROL
F-106B airplane active control landing gear drop test performance N91-28164
Actively damped landing gear system N91-28165
Active control of panel vibrations induced by boundary-layer flow
[NASA-CR-188733] N91-28643
A reconfigurable strategy for distributed digital process control
[DE91-013740] N91-28786
Real-time adaptive active control of sound fields
N91-28819
ACTIVE GALACTIC NUCLEI
Magnetohydrodynamical formation of astrophysical jets from gravitationally collapsing objects N91-28903
Emission line regions in active galactic nuclei: Structure, kinematics, physical conditions, and chemical abundances N91-29095
The optical polarization of BL Lacertae objects
N91-29099
Radiative processes in active galactic nuclei
N91-29137
ACTIVITY (BIOLOGY)
Spontaneous emergence of a metabolism
[DE91-013684] N91-28714
Biomimetic thin film deposition
[DE91-012485] N91-28999
ACTUATORS
Robust and real-time control of magnetic bearings for space engines N91-28230
ADA (PROGRAMMING LANGUAGE)
Description of real-time Ada software implementation of a power system monitor for the Space Station Freedom PMAD DC testbed
[NASA-TM-105157] N91-28776
ADAPTIVE CONTROL
Real-time adaptive active control of sound fields
N91-28819
ADDITIVES
Relationships between polymer-additive molecular structure and intumescent flame retardant behavior
N91-28426
ADHESION
Perspective on plating for precision finishing
[DE91-011927] N91-28394

Adhesion between CVD diamond films and tungsten [DE91-013757] N91-28434

ADHESIVE BONDING
Chemistry and materials science research report [DE91-011507] N91-28305
Flush mounting of thin film sensors [NASA-CASE-LAR-14446-1] N91-28454

ADHESIVES
Process for bonding elastomers to metal [NASA-CASE-LAR-13645-1] N91-28424

ADIABATIC FLOW
Solution to quasi-axisymmetric internal compressible flows using the stream tube approach N91-28526

ADSORPTION
Analysis of the surface heterogeneity of different samples of aluminum oxide ceramic powders [DE91-013527] N91-28421
Validity of the model used to relate the energy distribution and the adsorption isotherm [DE91-013528] N91-28428
Surface phases and their influence on metal-oxide interfaces [DE91-012277] N91-28995
The surface chemistry of GaAs atomic layer epitaxy [DE91-014112] N91-29047

ADSORPTIVITY
Surface phases and their influence on metal-oxide interfaces [DE91-012277] N91-28995

ADVANCED LAUNCH SYSTEM (STS)
NASA's advanced space transportation system launch vehicles N91-28195
A white paper: Operational efficiency. New approaches to future propulsion systems N91-28197
Next generation solid boosters N91-28207
Advanced launch system N91-28208
Propulsion studies for advanced manned launch systems N91-28213
Life cycle cost based program decisions N91-28248
The propulsion system is the key to airline-like operation of ETO vehicles N91-28256
Propulsion technologies for near term N91-28262
The case for teaming on the ALS-STME program N91-28269

AERIAL PHOTOGRAPHY
A new approach to analyzing high-resolution aerial photographs of urban areas N91-28647

AEROBRAKING
Applications of low lift to drag ratio aerobrakes using angle of attack variation for control [NASA-TM-103544] N91-28189

AEROCAPTURE
Applications of low lift to drag ratio aerobrakes using angle of attack variation for control [NASA-TM-103544] N91-28189

AERODYNAMIC BRAKES
Applications of low lift to drag ratio aerobrakes using angle of attack variation for control [NASA-TM-103544] N91-28189

AERODYNAMIC CHARACTERISTICS
An experimental investigation of the effect of vortex generators on the aerodynamic characteristics of a NACA 0021 airfoil undergoing large amplitude pitch oscillations [DE91-012102] N91-28133

AERODYNAMIC DRAG
An active delay of separation on two-dimensional airfoils [ITN-91-85142] N91-28139
Effect of guideway discontinuities on magnetic levitation and drag forces [DE91-014011] N91-28815

AERODYNAMIC LOADS
Rotor and control system loads analysis of the XV-15 with the advanced technology blades [NASA-TM-102876] N91-28134

AERODYNAMIC STABILITY
Robust bifurcation behavior in the presence of external random excitation N91-28171
ASTROP2 users manual: A program for aeroelastic stability analysis of propfans [NASA-TM-4304] N91-28627

AERODYNAMIC STALLING
An active delay of separation on two-dimensional airfoils [ITN-91-85142] N91-28139

AERODYNAMICS
An experimental investigation of the effect of vortex generators on the aerodynamic characteristics of a NACA 0021 airfoil undergoing large amplitude pitch oscillations [DE91-012102] N91-28133
Calculation of interactions between air and ground of landing N91-28161
Technology needs for high speed rotorcraft (2) [NASA-CR-177590] N91-28168

AEROELASTICITY
A methodology for using nonlinear aerodynamics in aeroservoelastic analysis and design [NASA-TM-104087] N91-28131
Experimental flutter boundaries with unsteady pressure distributions for the NACA 0012 Benchmark Model [NASA-TM-104072] N91-28137
Longitudinal aerodynamic characteristics of a subsonic, energy-efficient transport configuration in the National Transonic Facility [NASA-TP-2922] N91-28143
Algorithm and code development for unsteady three-dimensional Navier-Stokes equations [NASA-CR-188039] 'N91-28503
ASTROP2 users manual: A program for aeroelastic stability analysis of propfans [NASA-TM-4304] N91-28627
Active control of panel vibrations induced by boundary-layer flow [NASA-CR-188733] N91-28643

AEROGELS
Equation-of-state from SiO2 aerogel Hugoniot data [DE91-011480] N91-28313
Aerogel composites for radioluminescent light/power sources [DE91-012012] N91-28395
Melamine-formaldehyde aerogels [DE91-012084] N91-28408
Shock compression of low-density microcellular materials [DE91-013586] N91-28628
Equation of state and crushing dynamics of low-density silica aerogels [DE91-014766] N91-28637

AEROSOLS
Inorganic components of atmospheric aerosols N91-28668
High-throughput liquid-absorption air and aerosol sampler [DE91-013762] N91-28670
Radiative transfer model for a spherical atmosphere N91-28689

AEROSPACE ENGINEERING
Infusion of instrumentation technology (engine plume diagnostics) into operational test programs N91-28249
NASA patent abstracts bibliography: A continuing bibliography. Section 2: Indexes (supplement 39) [NASA-SP-7039(39)-SECT-2] N91-29088

AEROSPACE ENVIRONMENTS
Perturbed environment assessments for space vehicles [DE91-012630] N91-28188

AEROSPACE INDUSTRY
Expendable launch vehicle propulsion N91-28199

AEROSPACE MEDICINE
Aerospace medicine and biology: A continuing bibliography with indexes (supplement 352) [NASA-SP-7011(352)] N91-28729

AEROSPACE PLANES
Life cycle cost based program decisions N91-28248

AEROSPACE SAFETY
Space transportation main engine reliability and safety N91-28271

AEROSPACE SYSTEMS
Space systems requirements: The Navy approach [AD-A236490] N91-28181
Cultural changes in aerospace N91-28265
Nondestructive evaluation tools and experimental studies for monitoring the health of space propulsion systems [NASA-TM-105164] N91-28605

AEROSPACE VEHICLES
WFOV star tracker camera [DE91-012776] N91-28148
Perturbed environment assessments for space vehicles [DE91-012630] N91-28188
Modeling two-point spatial turbulence spectra for analysis of gust variations over aerospace vehicles N91-28685

AGING (MATERIALS)
Effect of Li level, artificial aging, and TiB2 reinforcement on the modulus of Weldalite (tm) 049 N91-28340
Evaluation of aging of cast stainless steel components [DE91-014013] N91-28361
APFIM characterization of the spinodal decomposition in duplex stainless steels [DE91-014256] N91-28371
Effects of various parameters on the fatigue life of alloy 718 [DE91-014100] N91-28380
Durability of polymeric materials used in zinc/bromine flow batteries [DE91-012864] N91-28487

AGING (METALLURGY)
Effect of Li level, artificial aging, and TiB2 reinforcement on the fracture toughness of Weldalite (tm) 049-type alloys N91-28339

AGRICULTURE
Results of agriclimatological studies using multiple satellite sensors like NOAA AVHRR; GMS IR; and LANDSAT MSS and TM [DE91-618773] N91-28698

AIR
High-throughput liquid-absorption air and aerosol sampler [DE91-013762] N91-28670

AIR FLOW
Experimental investigation of pressure drop and heat transfer for air flow through enhanced tubes [DE91-012151] N91-28508
Pressure drop and heat transfer for spirally fluted tubes including validation of the role of transition [DE91-012242] N91-28509
Experimental study of growth rate enhancement and structure of compressible turbulent free shear layers N91-28517
An experimental study of the effect of small particles on the fluid turbulence in fully developed flow of air in a horizontal pipe N91-28525
A mathematical model for two-phase water, air, and heat flow around a linear heat source emplaced in a permeable medium [DE91-014614] N91-28527

AIR JETS
Quadrupole phenomena of noise from a subsonic jet impinging on a large, rigid, and flate plate N91-28818

AIR POLLUTION
The use of science in the management of hazardous air pollutants N91-28667
High-throughput liquid-absorption air and aerosol sampler [DE91-013762] N91-28670
TREE: A model of the effects of acid precipitation and air pollutants on the growth of trees [DE91-014131] N91-28672
Development and application of new modeling techniques for mesoscale atmospheric chemistry N91-28692
Data users guide to the mountain cloud chemistry project [PB91-168484] N91-28697
ARAC: A computer-based emergency-response dose-assessment service with global application potential [DE91-013248] N91-28700
Threatened Area Database System (TADS) computer program [DE91-012491] N91-29074

AIR SAMPLING
High-throughput liquid-absorption air and aerosol sampler [DE91-013762] N91-28670

AIR TRAFFIC CONTROL
Runway Visual Range (RVR) Operational Test and Evaluation (OT and E)/integration test plan [DOT/FAA/CT-TN91/4] N91-28176

AIR TRANSPORTATION
Assessing the risk of transporting hazardous materals by aircraft: A case study [DE91-014016] N91-28147

AIR WATER INTERACTIONS
An upper ocean model for the climatic aspects of air-sea interaction N91-28691
A study of El Nino/Southern Oscillation: Numerical experiments and data analysis N91-28710

AIRBORNE EQUIPMENT
Analytical calibration of the airborne photogrammetric system using a priori knowledge of the exposure station obtained from kinematic Global Positioning System techniques N91-28646

AIRBORNE/SPACEBORNE COMPUTERS
Description of real-time Ada software implementation of a power system monitor for the Space Station Freedom PMAD DC testbed [NASA-TM-105157] N91-28776

AIRCRAFT ACCIDENTS
Computer simulation of an aircraft seat and occupant(s) in a crash environment: Program SOM-LA/SOM-TA user manual [CR-R-90026] N91-28146

AIRCRAFT CONSTRUCTION MATERIALS
Materials sub-panel N91-28245

AIRCRAFT DESIGN
Landing Gear Design Loads [AGARD-CP-484] N91-28150
Application of the Air Force guide specification 87221A to ground loads N91-28152
Development of undercarriage design loads N91-28153

Considerations on optimality of landing gear arrangement and design N91-28156
Calculation of interactions between air and ground of landing N91-28161
Design landing loads evaluation by dynamic simulation of flexible aircraft N91-28163

AIRCRAFT LANDING
Application of the Air Force guide specification 87221A to ground loads N91-28152
Design landing loads evaluation by dynamic simulation of flexible aircraft N91-28163
Actively damped landing gear system N91-28165

AIRCRAFT PERFORMANCE
Recent developments in the area of aircraft rough field performance N91-28154

AIRCRAFT RELIABILITY
Operational loads on landing gear N91-28158

AIRFOIL OSCILLATIONS
Transonic shock-induced dynamics of a flexible wing with a thick circular-arc airfoil [NASA-TM-104088] N91-28132
An experimental investigation of the effect of vortex generators on the aerodynamic characteristics of a NACA 0021 airfoil undergoing large amplitude pitch oscillations [DE91-012102] N91-28133

AIRFOIL PROFILES
Experimental flutter boundaries with unsteady pressure distributions for the NACA 0012 Benchmark Model [NASA-TM-104072] N91-28137
A study of residual interference effects in adaptive wall testing of a 7-inch chord CAST-10-2/DOA 2 airfoil model [NASA-CR-4390] N91-28138

AIRFOILS
An experimental investigation of the effect of vortex generators on the aerodynamic characteristics of a NACA 0021 airfoil undergoing large amplitude pitch oscillations [DE91-012102] N91-28133
An active delay of separation on two-dimensional airfoils [ITN-91-85142] N91-28139
An abbreviated Reynolds stress turbulence model for airfoil flows N91-28140
A comparison of the potential and the Euler formulations of the equations of motion for transonic flow [DE91-014731] N91-28142

AIRFRAMES
F-106B airplane active control landing gear drop test performance N91-28164

ALASKA
Alaska wave data index [AD-A236635] N91-28707

ALBEDO
Search for regularities in the atmosphere of Jupiter N91-29127

ALCOHOLS
Development of biomass as an alternative fuel for gas turbines [DE91-012129] N91-28441
High resolution infrared spectroscopy of 2-fluorethanol in a molecular beam [AD-A236149] N91-28822

ALGAE
Photobiotechnology: Algal hydrogen production and photoconductivity of metalized chloroplasts [DE91-013232] N91-28718

ALGEBRA
Choosing processor array configuration by performance modeling for a highly parallel linear algebra algorithm [DE91-012486] N91-28749
Using trees to compute approximate solutions to ordinary differential equations exactly [LAC90-R24] N91-28788
Bialgebra deformations and algebras of trees N91-28790
Quantized planes and multiparameter deformations of Heisenberg and GL(N) algebras [DE91-012481] N91-28793
Spin 4 and 7/2 extended conformal algebra [DE91-617609] N91-28803

ALGORITHMS
Transmission/reflection and short-circuit line permittivity measurements [PB91-171959] N91-28482
Algorithm and code development for unsteady three-dimensional Navier-Stokes equations [NASA-CR-188039] N91-28503
Boussinesq algorithm for enclosed bouyant convection in two dimensions [PB91-178848] N91-28507
Numerical analyses of aero-optical flows: An application of parallel algorithm on high-performance Personal Computer (PC) base multitransputer system N91-28519
Development and application of new modeling techniques for mesoscale atmospheric chemistry N91-28692
Predicting thunderstorm evolution using ground-based lightning detection networks N91-28702
The apGA: An Adaptive Parallel Genetic Algorithm [DE91-009559] N91-28741
Bayesian design and analysis of computer experiments: Use of derivatives in surface prediction [DE91-013147] N91-28751
Searching for consensus patterns on a hypercube [DE91-013233] N91-28753
An iterative substructuring algorithm for problems in three dimensions [DE91-014388] N91-28758
Efficient soft decision decoding of Reed-Muller codes and related non-linear generalizations [ITN-91-85146] N91-28760
A multilingual parallelization of the icosahedral-hexagonal grid system for integration on the sphere [DE91-013615] N91-28762
General implementation of thin-slot algorithms into the finite-difference time-domain code, TSAR, based on a slot data file [DE91-014336] N91-28767
Elastic tracking versus neural network tracking for very high multiplicity problems [DE91-011825] N91-28768
Order reduction and synthesis of transfer function models N91-28769
Taxonomy and algorithms for volume rendering on multicomputers [AD-A236632] N91-28771
Toward a better parallel performance metric [DE91-012627] N91-28773
The PCP/PFP programming models on the BBN TC2000 [DE91-011537] N91-28781
The symbolic computation and automatic analysis of trajectories [NASA-CR-188159] N91-28787
Using trees to compute approximate solutions to ordinary differential equations exactly [LAC90-R24] N91-28788
Computations involving differential operators and their actions on functions N91-28789
A parallel algorithm for solving linear equations arising from one-dimensional network problems [DE91-012815] N91-28795
Parallelizing across time when solving time-dependent partial differential equations [DE91-012948] N91-28797
Transport with Feynman propagators [DE91-013566] N91-29063
Numerical simulations of mass outflows from star-forming regions N91-29123

ALKALI METALS
Analytical electron microscopy of catalyst preparations [DE91-014126] N91-28328

ALKANES
Structure and dynamics in low-dimensional guest host solids [DE91-012169] N91-29020

ALKYL COMPOUNDS
The solubility and dissociation kinetics of hydroxymethyl hydroperoxide in aqueous solution [DE91-013336] N91-28318

ALLOYING
Synthesis of metastable aluminum-based intermetallics by mechanical alloying [DE91-013651] N91-28376

ALLOYS
Magnetic studies of iron-rare-earth-metalloid alloys [DE91-013856] N91-28368

ALPHA PARTICLES
Implications of TAE modes for the design of ITER [DE91-013128] N91-28952

ALTERNATING CURRENT
System and component design and test of a 10 hp, 18,000 rpm AC dynamometer utilizing a high frequency AC voltage link, part 1 [NASA-CR-188442] N91-28539

ALTERNATIVES
Development of biomass as an alternative fuel for gas turbines [DE91-012129] N91-28441

ALUMINIDES
Aqueous corrosion characteristics and corrosion-related cracking susceptibilities of Fe3Al-type iron aluminides [DE91-013028] N91-28358
Erosion studies on a Fe3Al-based iron aluminide and 1100 Al [DE91-012529] N91-28360
Weldability of iron aluminides [DE91-013730] N91-28367

ALUMINUM
Ignition and combustion of metallized propellants N91-28224
Tribology of aluminum-based metal matrix composites: Fundamental study of wear behavior as influenced by microstructure N91-28297
Test of superplastically formed corrugated aluminum compression specimens with beaded webs [NASA-TM-104119] N91-28373
Desorption of Al, Au, Ag using surface plasmon excitation [DE91-013726] N91-28493
X ray generation by high irradiance exawatt/sq cm subpicosecond lasers [DE91-013497] N91-28556
Non-steady wave profiles and the fourth-power law [DE91-013576] N91-28631
Quantum mechanical effects on the shock Hugoniot [DE91-014750] N91-28636

ALUMINUM ALLOYS
Failure analysis case histories of Canadian forces aircraft landing gear components N91-28151
Sandia's new hypervelocity launcher (HVL) [DE91-014335] N91-28178
Joining of aluminum-based particulate-reinforced metal-matrix composites N91-28298
Identification of strengthening phases in Al-Cu-Li alloy Weldalite (tm) 049 N91-28335
The influence of Ag+Mg additions on the nucleation of strengthening precipitates in a non-cold-worked Al-Cu-Li alloy N91-28336
The effect of TiB2 reinforcement on the mechanical properties of an Al-Cu-Li alloy-based metal-matrix composite N91-28337
Rapid solidification processing of Al3Ti and Al3Ti plus copper [AD-A236600] N91-28343
Tensile deformation of Al-Cu-Li-Zr alloy 2090-T8E41 at 298 and 77 K [DE91-011885] N91-28345
The effect of fluoride gases on cylinder valve corrosion [DE91-012745] N91-28355
Properties of large heats of Fe3Al-based alloys [DE91-013268] N91-28359
Erosion studies on a Fe3Al-based iron aluminide and 1100 Al [DE91-012529] N91-28360
Atomistic studies of grain boundaries in alloys and compounds [DE91-014516] N91-28372
Synthesis of metastable aluminum-based intermetallics by mechanical alloying [DE91-013651] N91-28376
Alloy development of Fe3Al for improved creep rupture properties [DE91-014541] N91-28381
Processing and fabrication of Fe3Al-based alloys [DE91-014546] N91-28382
Changes with material properties of acoustic emission produced during single point machining [DE91-011913] N91-28452
The SNL, Livermore, Hopkinson bar apparatus for compressive materials testing at high strain-rates [DE91-013132] N91-28612

ALUMINUM OXIDES
Alumina-silicon carbide composites from coated powders [DE91-012357] N91-28281
Processing, compatibility and oxidation of diboride-reinforced oxide matrix composites for ultrahigh-temperature applications N91-28294
Mechanism of hydrodenitrogenation. Part 5: X ray diffraction of molybdenum catalysts [DE91-013853] N91-28327
Shock-induced optical emission in Al2O3 at 200 GPa: Implications for shock temperature measurements in metals [DE91-013584] N91-28365
Model catalytic oxidation studies using supported monometallic and heterobimetallic oxides [DE91-012144] N91-28409
Drying of gelcast ceramics [DE91-012955] N91-28413
Analysis of the surface heterogeneity of different samples of aluminum oxide ceramic powders [DE91-013527] N91-28421
Validity of the model used to relate the energy distribution and the adsorption isotherm [DE91-013528] N91-28428
Some high voltage DC breakdown properties of thick film circuits on alumina [DE91-014675] N91-28500

AMBIPOLAR DIFFUSION
Star formation in the presence of magnetic fields: Molecular cloud core formation and dynamical contraction due to ambipolar diffusion:; a simulation with axial symmetry N91-29116

AMIDES
Polyimides prepared from 3,5-diamino benzo trifluoride
[NASA-CASE-LAR-14206-1] N91-28425

AMMONIA
Plant growth is influenced by glutamine synthetase-catalyzed nitrogen metabolism
[DE91-014592] N91-28725

AMMONIUM CHLORIDES
Experimental studies of the volatility of ammonium chloride
[DE91-012526] N91-28311

AMORPHOUS MATERIALS
Ultra-low temperature properties of amorphous solids
[DE91-012782] N91-28312
Raman studies of stress-induced phase transformation in titania films
[DE91-012871] N91-29012

AMORPHOUS SILICON
Research on stable, high-efficiency amorphous silicon multijunction modules
[DE91-002138] N91-28480

AMPLIFIERS
Design of a multivariable RF control system using gain-shaping in the frequency domain
[DE91-013859] N91-28474
Modeling of a 1700-MHz cluster cavity of planar triodes
[DE91-013049] N91-28488
The superconducting flux flow transistor: Models and applications
[DE91-014702] N91-28501

ANALOG TO DIGITAL CONVERTERS
Direction discriminating hearing aid
[NASA-CASE-GSC-13027-1] N91-28726
High-speed and high-resolution analog-to-digital and digital-to-analog converters
[ETN-90-97265] N91-28735

ANALYZERS
Linked gas chromatograph-thermal energy analyzer/ion trap mass spectrometer
[DE91-013585] N91-28326

ANGLE OF ATTACK
Robust bifurcation behavior in the presence of external random excitation N91-28171
Applications of low lift to drag ratio aerobrakes using angle of attack variation for control
[NASA-TM-103544] N91-28189

ANGULAR DISTRIBUTION
Measurements of angular distributions of absolute cross sections and analyzing powers of the reaction bar-p p yields d(pi+) between 1.3 and 2.4 GeV
[DE91-012638] N91-28842

ANGULAR MOMENTUM
Steady-state dynamo and current drive in a nonuniform bounded plasma
[DE91-014865] N91-28974

ANIMALS
Chromosomal changes in cultured human epithelial cells transformed by low- and high-LET radiation
[DE91-013772] N91-28720

ANISOTROPY
A critical analysis of anisotropic k-epsilon modeling and its application to turbulence-driven secondary flows
N91-28533
Interlayer pairing and c-axis versus ab-plane gap anisotropy in high Tc superconductor
[DE91-012218] N91-29005
Flux pinning and dissipation in high-temperature superconductors
[DE91-014466] N91-29042
Overview of the status of and prospects for high-T(sub c) wire and tape development
[DE91-014609] N91-29045

ANNEALING
High-temperature solution annealing as an IASCC mitigation technique
[DE91-012220] N91-28352
Annealing and structure studies on Tl-2223 and Tl-1223 crystals
[DE91-014903] N91-29052

ANNIHILATION REACTIONS
Theoretical research in intermediate-energy nuclear physics
[DE91-012720] N91-28838

ANNUAL VARIATIONS
A study of El Nino/Southern Oscillation: Numerical experiments and data analysis N91-28710

ANTARCTIC REGIONS
Magnetospheric VLF line radiation N91-28693
Radio absorption in the Antarctic ionosphere: Some observations in the region of the midlatitude trough
N91-28694
Isotopic measurements of solar noble gases in individual micrometeorites from Greenland and Antarctica
N91-29114

ANTENNA ARRAYS
Proceedings of the 1990 Antenna Applications Symposium, volume 1
[AD-A237056] N91-28460
Proceedings of the 1990 Antenna Applications Symposium, volume 2
[AD-A237057] N91-28461
Borehole Radar Evaluation Program: Antenna designs for optimal directionality
[DE91-014322] N91-28475

ANTENNA DESIGN
Proceedings of the 1990 Antenna Applications Symposium, volume 1
[AD-A237056] N91-28460
Proceedings of the 1990 Antenna Applications Symposium, volume 2
[AD-A237057] N91-28461
Borehole Radar Evaluation Program: Antenna designs for optimal directionality
[DE91-014322] N91-28475

ANTENNA RADIATION PATTERNS
Borehole Radar Evaluation Program: Antenna designs for optimal directionality
[DE91-014322] N91-28475

ANTENNAS
Proceedings of the 1990 Antenna Applications Symposium, volume 1
[AD-A237056] N91-28460
Proceedings of the 1990 Antenna Applications Symposium, volume 2
[AD-A237057] N91-28461

ANTHROPOMETRY
Robotic mannequin technology for enhanced product testing
[DE91-013787] N91-28591

ANTIFERROMAGNETISM
The pressure-induced Mott transition in transition-metal iodides
[DE91-013671] N91-28366
Topics on frustrated spin systems and high-temperature superconductors N91-29032

ANTIMISSILE DEFENSE
Defending the defenders: Brilliant pebble defense against pop-up neutral particle beam suppression attacks
[DE91-012521] N91-28809
Interceptor combinations for theater defense
[DE91-012990] N91-28810

ANTIMONY COMPOUNDS
Doping and pressure study of U3Sb4Pt3
[DE91-013669] N91-29033

ANTIPROTONS
Antiproton-induced elastic and inelastic scattering at intermediate energies
[DE91-013068] N91-28849

ANTIREFLECTION COATINGS
Color effects in optical systems
[ITN-91-85150] N91-28878

ANVILS
High temperature solder device for flat cables
[NASA-CASE-GSC-13344-1] N91-28363

APERTURES
General implementation of thin-slot algorithms into the finite-difference time-domain code, TSAR, based on a slot data file
[DE91-014336] N91-28767
Coded aperture imaging with a HURA coded aperture and a discrete pixel detector N91-29093

APPLICATIONS PROGRAMS (COMPUTERS)
Network based concurrent computing on the PVM system
[DE91-014961] N91-28780
The symbolic computation and automatic analysis of trajectories
[NASA-CR-188159] N91-28787
TOPAZ2D benchmark problems nonlinear materials
[DE91-009753] N91-29053

APPROXIMATION
Using trees to compute approximate solutions to ordinary differential equations exactly
[LAC90-R24] N91-28788
A cluster approximation for the transfer-matrix method
[DE91-617790] N91-28804
Point vortex description of a modon solution
N91-28931

AQUEOUS SOLUTIONS
The solubility and dissociation kinetics of hydroxymethyl hydroperoxide in aqueous solution
[DE91-013336] N91-28318

AQUIFERS
Applications and challenges for thermal energy storage
[DE91-012873] N91-28654

ARC SPRAYING
Plasma transport in a new cathodic arc ion source, theory and experiment
[DE91-011511] N91-28944

ARCHITECTURE (COMPUTERS)
A geometry based method of integrated engineering design, analysis, and optimization
[DE91-008588] N91-28457
Building microelectronic systems in a university environment
[AD-A236629] N91-28477
The role of the UNIX(tm) central computing facility in a multi-purpose national laboratory
[DE91-012361] N91-28737
Parallel input/output architectures for multiprocessors
N91-28740
Prototyping parallel and distributed programs in proteus
[AD-A236597] N91-28746
A design space and design rules for user interface software architecture
[AD-A237049] N91-28748
Software development experiences with a distributed database in a large, distributed computer system
[DE91-012818] N91-28750
Visualization using a data flow-based paradigm
[DE91-013851] N91-28763
The cache group scheme for hardware-controlled cache coherence and the general need for hardware coherence control in large-scale multiprocessors
[DE91-012106] N91-28772
Network based concurrent computing on the PVM system
[DE91-014961] N91-28780
The PCP/PFP programming models on the BBN TC2000
[DE91-011537] N91-28781
Concurrent access to O-trees
[DE91-014348] N91-28782
ZLIB: A numerical library for differential algebra (A user's guide for version 1.0)
[DE91-012552] N91-28794
A parallel algorithm for solving linear equations arising from one-dimensional network problems
[DE91-012815] N91-28795
Mapping implicit spectral methods to distributed memory architectures
[NASA-CR-187592] N91-28806
SANDAC V computer electromagnetic interface characteristics: Problems and solutions
[DE91-014334] N91-29065
The EOS TPC analysis shell
[DE91-011873] N91-29073
Document format considerations for a document tracking and storage system
[DE91-013402] N91-29079
The ADAMS interactive interpreter
[DE91-014345] N91-29080
Safe referential integrity structures in relational databases
[DE91-014586] N91-29091

ARGON ISOTOPES
SDI: Statistical Dynamic Interactions
[DE91-012034] N91-28827

ARIANE LAUNCH VEHICLE
Overview of European and other non-US/USSR/Japan launch vehicle and propulsion technology programs
N91-28221

ARITHMETIC AND LOGIC UNITS
Toward a formal verification of a floating-point coprocessor and its composition with a central processing unit
[NASA-CR-187547] N91-28777

ARMOR
Experiments and calculations of jet penetration in glass
[DE91-013567] N91-28422

ARTIFICIAL INTELLIGENCE
Automated reasoning contributes to mathematics and logic
[DE91-014005] N91-28765
Proposal for continued basic research in intelligent machines at the Center for Engineering Systems Advanced Research: Fiscal years 1992-1996
[DE91-012997] N91-28784

ASSEMBLING
Method of preforming and assembling superconducting circuit elements
[NASA-CASE-LAR-14395-1-CU] N91-28490

ASTRONOMICAL MODELS
Testing the Big Bang: Light elements, neutrinos, dark matter and large-scale structure
[NASA-CR-188701] N91-29111
Gravitational evolution of large-scale structure in the universe N91-29121

ASTRONOMICAL PHOTOMETRY
Visual, red and infrared photographic surface photometry of NGC 55 and NGC 253 N91-29094
ASTRONOMY
Interstellar magnesium studies N91-29120
ASTROPHYSICS
Phonon-mediated detection of elementary particles using silicon crystal acoustic detectors N91-28547
Corona: Coordinated research on non-thermal processes in astrophysics
[NASA-CR-188692] N91-29107
ASYMPTOTIC SERIES
Phase-conjugated fluorescence
[AD-A231114] N91-28820
ATMOSPHERIC CHEMISTRY
Development and application of new modeling techniques for mesoscale atmospheric chemistry
N91-28692
ATMOSPHERIC CIRCULATION
Regional-scale flow in complex terrain: An observational and numerical investigation N91-28680
Atmospheric responses to lower tropospheric forcing in a multilayer isentropic model N91-28688
Development and application of new modeling techniques for mesoscale atmospheric chemistry
N91-28692
ATMOSPHERIC COMPOSITION
Regional oxidant model user's guide. Part 1: The ROM preprocessors
[PB91-171926] N91-28665
Inorganic components of atmospheric aerosols
N91-28668
Data users guide to the mountain cloud chemistry project
[PB91-168484] N91-28697
ATMOSPHERIC DENSITY
Lidar studies of sporadic sodium layers, gravity waves and density spectra in the mesopause and stratopause regions at Urbana and Arecibo N91-28690
ATMOSPHERIC ELECTRICITY
Effectivity of atmospheric electricity on launch availability N91-28260
ATMOSPHERIC GENERAL CIRCULATION MODELS
Observations and theoretical studies of tides and normal modes in the lower thermosphere N91-28681
An upper ocean model for the climatic aspects of air-sea interaction N91-28691
ATMOSPHERIC MODELS
Tropospheric scatter propagation at 5 and 16 GHz: Results for a 161 km path
[AD-A237012] N91-28458
Regional oxidant model user's guide. Part 1: The ROM preprocessors
[PB91-171926] N91-28665
Regional oxidant model user's guide. Part 2: The ROM processor network
[PB91-171934] N91-28666
Inorganic components of atmospheric aerosols
N91-28668
Natural and anthropogenic climate change
[DE91-014734] N91-28673
Regional-scale flow in complex terrain: An observational and numerical investigation N91-28680
Atmospheric responses to lower tropospheric forcing in a multilayer isentropic model N91-28688
Development and application of new modeling techniques for mesoscale atmospheric chemistry
N91-28692
ARAC: A computer-based emergency-response dose-assessment service with global application potential
[DE91-013248] N91-28700
Initialization of cloud and radiation in the Florida State University global spectral model N91-28703
On the initiation of surface cyclones by upper tropospheric disturbances N91-28704
A numerical simulation of a tornado-scale vortex in a three-dimensional cloud model N91-28705
A cloud fraction and radiative transfer model
N91-28706
ATMOSPHERIC MOISTURE
Measurement of the microwave propagation delay induced by atmospheric water vapor N91-28466
ATMOSPHERIC OPTICS
The in-flight calibration of a helicopter-mounted Daedalus multispectral scanner
[DE91-013054] N91-28170
ATMOSPHERIC REFRACTION
Measurement of the microwave propagation delay induced by atmospheric water vapor N91-28466
ATMOSPHERIC SCATTERING
Tropospheric scatter propagation at 5 and 16 GHz: Results for a 161 km path
[AD-A237012] N91-28458
ATMOSPHERIC SOUNDING
Radio absorption in the Antarctic ionosphere: Some observations in the region of the midlatitude trough
N91-28694
ATMOSPHERIC STRATIFICATION
Radiative transfer model for a spherical atmosphere
N91-28689
ATMOSPHERIC TEMPERATURE
Regional-scale flow in complex terrain: An observational and numerical investigation N91-28680
ATMOSPHERIC TURBULENCE
Robust bifurcation behavior in the presence of external random excitation N91-28171
Studies in cloud physics: Electrification, glaciation, and turbulence N91-28684
Modelling and analysis of geophysical turbulence: Use of optimal transforms and basis sets N91-28686
Corona: Coordinated research on non-thermal processes in astrophysics
[NASA-CR-188692] N91-29107
ATOMIC COLLISIONS
Mode selectivity in cluster-molecule interactions: Ni13 + D2
[DE91-013352] N91-28859
ATOMIC MOBILITIES
Nuclear magnetic resonance studies of atomic motion in lithium chloroborate and lithium thiosilicate glassy fast ionic conductors
[DE91-012677] N91-28843
ATOMIC PHYSICS
The Advanced Light Source: A new tool for research in atomic and molecular physics
[DE91-012860] N91-28844
ATOMIC STRUCTURE
Theoretical studies of zirconia and related materials
[DE91-013906] N91-28369
Atomistic studies of grain boundaries in alloys and compounds
[DE91-014516] N91-28372
Strongly interacting fermion systems
[DE91-012284] N91-28848
Ab initio cluster studies of La2CuO4
[DE91-013520] N91-29025
ATOMIZING
Liquid jet breakup and atomization in rocket chambers under dense spray conditions N91-28227
ATOMS
Phase-conjugated fluorescence
[AD-A231114] N91-28820
Reflection-asymmetric shapes in atomic nuclei
[DE91-013414] N91-28851
Optical analogs of model atoms in fields
[DE91-013392] N91-28855
ATTITUDE CONTROL
CFD applications in chemical propulsion engines
N91-28234
Impact of ion propulsion on performance, design, testing, and operation of a geosynchronous spacecraft
[AD-A237028] N91-28273
Attitude control of a spinning rocket via thrust vectoring
[DE91-006267] N91-28274
AUGMENTATION
Development program enhancement suggestions (propulsion related) N91-28252
AUTONOMOUS NAVIGATION
Control of autonomous mobile robots using custom-designed qualitative reasoning VLSI chips and boards
[DE91-012527] N91-28783
AUXILIARY POWER SOURCES
SEI power source alternatives for rovers and other multi-kWe distributed surface applications
[NASA-TM-104360] N91-28277
AVIONICS
Considerations for NATO satellite communications in the post 2000 era
[AGARD-AG-330] N91-28465
AXISYMMETRIC FLOW
Solution to quasi-axisymmetric internal compressible flows using the stream tube approach N91-28526

B

BACKSCATTERING
Fluctuations in near-surface backscattering to a descending CW radar
[ITN-91-85140] N91-28469
Performance of a polarization isolation enhancement method in the presence of errors
[DE91-013571] N91-28473
BACKWARD FACING STEPS
The computation of complex, two-dimensional turbulent flows using Reynolds stress closure N91-28535
BACKWARD WAVES
Nonlinear computer analysis of backward wave oscillator N91-28923
BACTERIA
Mechanisms of bacterial metals removal from solids
[DE91-012808] N91-28356
Regulation of photosynthetic membrane components in cyanobacteria
[DE91-012713] N91-28713
Antenna organization in green photosynthetic bacteria
[DE91-014814] N91-28723
Plant growth is influenced by glutamine synthetase-catalyzed nitrogen metabolism
[DE91-014592] N91-28725
BALANCE
Generalized gyroviscous force and its effect on the momentum balance equation
[DE91-013344] N91-29061
BALLOONING MODES
Self-similar evolution of nonlinear magnetic buoyancy instability N91-28913
Plasma properties
[DE91-013933] N91-28978
BARIUM COMPOUNDS
Neutron scattering studies of spin correlations in metallic YBa2Cu3O(6+x)
[DE91-013794] N91-29031
BARIUM OXIDES
Growth of high T(sub c) superconducting thin films for microwave applications
[DE91-011436] N91-28991
Superconducting bolometers: High-T(sub c) and low-T(sub c)
[DE91-011830] N91-28992
BAROCLINIC WAVES
On the initiation of surface cyclones by upper tropospheric disturbances N91-28704
BAROCLINITY
On the initiation of surface cyclones by upper tropospheric disturbances N91-28704
BARYONS
Dibaryons in neutron stars
[NASA-CR-188704] N91-29109
BATTERY CHARGERS
Laboratory testing of the dual traction battery GC12V100
[DE91-012743] N91-28491
BAUSCHINGER EFFECT
Bauschinger effect during shock loading
[DE91-014606] N91-28634
BAYES THEOREM
Bayesian design and analysis of computer experiments: Use of derivatives in surface prediction
[DE91-013147] N91-28751
BCS THEORY
Interlayer pairing and c-axis versus ab-plane gap anisotropy in high Tc superconductor
[DE91-012218] N91-29005
BEAM CURRENTS
Beam current monitoring in the AGS booster and its transfer lines
[DE91-013328] N91-28870
Space charge and wake field analysis for a high brightness electron source
[DE91-014788] N91-28874
Stability of annular equilibrium of energetic large orbit ion beam
[DE91-014365] N91-28963
BEAM INJECTION
Time-resolved emittance measurements of an excimer-laser-driven metal photocathode
[DE91-013066] N91-28558
Performance of the photoinjector accelerator for the Los Alamos free-electron laser
[DE91-013682] N91-28565
Ferromagnetic material in the superconductor and its effect on the magnetization sextupole and decapole in the SSC dipoles at injection
[DE91-011886] N91-28993
BEAM INTERACTIONS
Simulations on pair creation from beam-beam interaction in linear colliders
[DE91-012315] N91-28834
BEAM SPLITTERS
Color effects in optical systems
[ITN-91-85150] N91-28878
BEAMS (RADIATION)
Perturbation treatment of the longitudinal coupling impedance of a toroidal beam tube
[DE91-013884] N91-28495
A new wake-potential calculation method using orthogonal polynomials
[DE91-013045] N91-28799
Simulations on pair creation from beam-beam interaction in linear colliders
[DE91-012315] N91-28834

The Advanced Light Source: A new tool for research in atomic and molecular physics
[DE91-012860] N91-28844
Microwave instability at transition: Stability diagram approach
[DE91-013202] N91-28867
BEAT FREQUENCIES
Continuing studies of the plasma beat wave accelerator
[DE91-013641] N91-28976
BEND TESTS
Elevated-temperature fracture resistances (K(sub IC), R-curves, gamma sub (omega OF)) of monolithic and composite ceramics using chevron-notched, bend tests
[NASA-TM-105090] N91-28418
Interlaminar fracture characterization: A current review
[NASA-CR-187573] N91-28626
BESSEL FUNCTIONS
Effect of pressure on mode transition point of partially relaxed states with peripheral loss N91-28906
BETA FACTOR
Effect of pressure on mode transition point of partially relaxed states with peripheral loss N91-28906
BIBLIOGRAPHIES
Large space structures and systems in the space station era: A bibliography with indexes
[NASA-SP-7085(02)] N91-28191
Aerospace medicine and biology: A continuing bibliography with indexes (supplement 352)
[NASA-SP-7011(352)] N91-28729
NASA patent abstracts bibliography: A continuing bibliography. Section 2: Indexes (supplement 39)
[NASA-SP-7039(39)-SECT-2] N91-29088
BIG BANG COSMOLOGY
Neutrino degeneracy and cosmological nucleosynthesis, revisited
[NASA-CR-188703] N91-29110
Testing the Big Bang: Light elements, neutrinos, dark matter and large-scale structure
[NASA-CR-188701] N91-29111
BINARY ALLOYS
EXAFS studies of elastic strain in dilute binary alloys
[DE91-012678] N91-28353
Atomistic studies of grain boundaries in alloys and compounds
[DE91-014516] N91-28372
Alloy development of Fe3Al for improved creep rupture properties
[DE91-014541] N91-28381
Critical issues in de-alloying and transcrystalline stress-corrosion cracking
[DE91-010190] N91-28608
BINARY FLUIDS
Dynamics of interfaces with internal structures
N91-28926
BINARY STARS
Coordinated optical and ultraviolet observations of short period RS CVn and W UMa type stars N91-29096
BINAURAL HEARING
Direction discriminating hearing aid
[NASA-CASE-GSC-13027-1] N91-28726
BIOASSAY
Biomarker-based biomonitoring for evaluating health and ecological effects on environmental contamination
[DE91-013729] N91-28719
BIOASTRONAUTICS
Aerospace medicine and biology: A continuing bibliography with indexes (supplement 352)
[NASA-SP-7011(352)] N91-28729
BIOCHEMISTRY
Radiation physics, biophysics, and radiation biology
[DE91-012883] N91-28716
Antenna organization in green photosynthetic bacteria
[DE91-014814] N91-28723
The 1992 - 1997 renewal proposal interactive graphics for molecular studies
[AD-A236598] N91-28823
BIOCONVERSION
Photobiotechnology: Algal hydrogen production and photoconductivity of metalized chloroplasts
[DE91-013232] N91-28718
BIOLOGICAL EFFECTS
Microbeam studies of the sensitivity of structures within living cells
[DE91-012927] N91-28715
Radiation physics, biophysics, and radiation biology
[DE91-012883] N91-28716
Genetic changes in Mammalian cells transformed by helium cells
[DE91-013778] N91-28721
Protein-directed modulation of high-LET hyperthermic radiosensitization
[DE91-013783] N91-28722
Aerospace medicine and biology: A continuing bibliography with indexes (supplement 352)
[NASA-SP-7011(352)] N91-28729
BIOLOGICAL EVOLUTION
Spontaneous emergence of a metabolism
[DE91-013684] N91-28714
BIOMASS
Development of biomass as an alternative fuel for gas turbines
[DE91-012129] N91-28441
Plant growth is influenced by glutamine synthetase-catalyzed nitrogen metabolism
[DE91-014592] N91-28725
BIONICS
Chaos and microbial systems
[DE91-014908] N91-29064
BIOPHYSICS
Radiation physics, biophysics, and radiation biology
[DE91-012883] N91-28716
BIOSPHERE
Modeling molecular processes in the environment
[DE91-013790] N91-28671
BIOSYNTHESIS
Regulation of photosynthetic membrane components in cyanobacteria
[DE91-012713] N91-28713
BL LACERTAE OBJECTS
The optical polarization of BL Lacertae objects
N91-29099
BLACK HOLES (ASTRONOMY)
Numerical models of equilibrium between matter and black holes N91-29101
Non-Hausdorff twistor spaces and the global structure of space-time N91-29103
Study of gravitational collapse and cosmic ray abundances N91-29105
High-overtone black-hole normal modes: A WKB contour-integral approach N91-29118
Upper limits for the flux of very high-energy gamma radiation from Cygnus X-3 and for the explosion rate of primordial black holes obtained by the Haleakala Gamma Ray Observatory N91-29134
BLANKETS (FUSION REACTORS)
The Cascade inertial confinement fusion reactor concept
[DE91-013852] N91-28966
BLOCK COPOLYMERS
Polymers at surfaces
[DE91-013642] N91-28430
Cocrystallization in blends of poly(butylene terephthalate) and poly(ester-ether) segmented block copolymers
[DE91-012224] N91-28438
BODY KINEMATICS
Recursive linearization of multibody dynamics and application to control design N91-28588
BOILING WATER REACTORS
High-temperature solution annealing as an IASCC mitigation technique
[DE91-012220] N91-28352
BOLOMETERS
Superconducting bolometers: High-T(sub c) and low-T(sub c)
[DE91-011830] N91-28992
BOLTZMANN-VLASOV EQUATION
Microwave instability at transition: Stability diagram approach
[DE91-013202] N91-28867
BOMBS (ORDNANCE)
Fluctuations in near-surface backscattering to a descending CW radar
[ITN-91-85140] N91-28469
BONDING
Investigation of interlayer materials for the microwave joining of SiC
[DE91-013311] N91-28414
BONES
Ion beam sputtered coatings of bioglass N91-28384
BOOSTER ROCKET ENGINES
Space shuttle with common fuel tank for liquid rocket booster and main engines (supertanker space shuttle)
N91-28257
Determining criteria for single stage to orbit
N91-28258
BOOSTER ROCKETS
Advanced launch system N91-28208
BORANES
Nitrogen and boron-containing polymers as precursors of ceramic materials
[DE91-008890] N91-28390
BOREHOLES
Borehole Radar Evaluation Program: Antenna designs for optimal directionality
[DE91-014322] N91-28475
BORON COMPOUNDS
Nuclear magnetic resonance studies of atomic motion in lithium chloroborate and lithium thiosilicate glassy fast ionic conductors
[DE91-012677] N91-28843
BORON-EPOXY COMPOSITES
On the finite-strain-invariant failure criterion for composites
[DE91-011924] N91-28286
BOROSILICATE GLASS
Behavior of RuO2 in a glass melt
[DE91-013717] N91-28432
Pressure transducer and system for cryogenic environments
[NASA-CASE-LAR-14579-1] N91-28546
BOSONS
Statistical mechanics of soft-boson phase transitions
[NASA-CR-188697] N91-28858
BOUNDARIES
Radiative transfer model for a spherical atmosphere
N91-28689
BOUNDARY CONDITIONS
Suspension device for low-frequency structures
[NASA-CASE-LAR-14272-1-CU] N91-28184
The numerical solution of confined laminar flow past a moving boundary N91-28532
Computing minimal surfaces via level set curvature flow
[DE91-014709] N91-28759
Nonlinear reversed field pinch dynamics with nonideal boundaries
[DE91-013638] N91-28961
BOUNDARY ELEMENT METHOD
A numerical approach for modelling cavitating flows
[DE91-009178] N91-28505
BOUNDARY LAYER EQUATIONS
Receptivity of a laminar boundary layer to the interaction of a three-dimensional roughness element with time-harmonic free-stream disturbances N91-28518
BOUNDARY LAYER FLOW
Transonic shock-induced dynamics of a flexible wing with a thick circular-arc airfoil
[NASA-TM-104088] N91-28132
Numerical simulation of particle-wave interaction in boundary layers
[NASA-CR-187312] N91-28502
Active control of panel vibrations induced by boundary-layer flow
[NASA-CR-188733] N91-28643
BOUNDARY LAYER SEPARATION
An active delay of separation on two-dimensional airfoils
[ITN-91-85142] N91-28139
BOUNDARY LAYER TRANSITION
Longitudinal aerodynamic characteristics of a subsonic, energy-efficient transport configuration in the National Transonic Facility
[NASA-TP-2922] N91-28143
A study of methods to investigate nozzle boundary layer transition N91-28232
BOUNDARY LAYERS
Evaluation of a technique to generate artificially thickened boundary layers in supersonic and hypersonic flows
[NASA-TP-3142] N91-28136
Numerical simulation of particle-wave interaction in boundary layers
[NASA-CR-187312] N91-28502
Study of interfacial behavior in cocurrent gas-liquid flows
[DE91-013008] N91-28511
Regional-scale flow in complex terrain: An observational and numerical investigation N91-28680
Fluidlike studies of the presheath and sheath regions of a plasma
[DE91-013345] N91-28953
BOUNDARY LUBRICATION
Boundary lubrication of ceramic materials by soft metallic coating and synthetic oil
[DE91-014017] N91-28577
BOUNDARY VALUE PROBLEMS
The 2+1 gravity: A new approach N91-29059
BOUSSINESQ APPROXIMATION
Boussinesq algorithm for enclosed bouyant convection in two dimensions
[PB91-178848] N91-28507
BRAIN
New techniques for positron emission tomography in the study of human neurological disorders
[DE91-013855] N91-28728
BRAKING
Roller locking brake
[NASA-CASE-GSC-13376-1] N91-28579
BRANCHING (MATHEMATICS)
Stability theory of critical cases and the bifurcation points of the stationary solutions of the Lorenz model
[DE91-617575] N91-28802
BRAYTON CYCLE
Comparison of dynamic isotope power systems for distributed planet surface applications
[NASA-TM-4303] N91-28278

BRAZING
JPRS report: Science and technology. USSR: Materials science
[JPRS-UMS-91-003] N91-28342
Microstructural characterization of solders and brazes for advanced packaging technology
[DE91-011503] N91-28379
BREEDER REACTORS
A reconfigurable strategy for distributed digital process control
[DE91-013740] N91-28786
BREMSSTRAHLUNG
Measurements of the ion acoustic decay instability and the resultant enhanced laser absorption and enhanced bremsstrahlung in laser-plasma interaction experiments
[DE91-014250] N91-28956
BRITTLE MATERIALS
Advancements in ultrathinning section techniques for the characterization of brittle materials
[DE91-012930] N91-28364
BRITTLENESS
Effects of sample size and loading rate on the transition behavior of a DCI alloy
[DE91-012015] N91-28346
Brittle behavior of SSC yokes
[DE91-014031] N91-28370
Welding of ductile intermetallic alloys
[DE91-009553] N91-28594
Analysis of brittle intergranular crack propagation during stress corrosion cracking
[DE91-013666] N91-28630
BROADCASTING
Precise orbit determination for GPS satellites
N91-28183
BROKEN SYMMETRY
Physics at the Planck scale
[DE91-012346] N91-29054
Phase transitions triggered by quantum fluctuations in the inflationary universe
[NASA-CR-188698] N91-29112
BROMINATION
Inertial confinement fusion
[DE91-013479] N91-28960
BROMINE
Durability of polymeric materials used in zinc/bromine flow batteries
[DE91-012864] N91-28487
BRONZES
The effect of fluoride gases on cylinder valve corrosion
[DE91-012745] N91-28355
Bauschinger effect during shock loading
[DE91-014606] N91-28634
BRUSHES
Polymers at surfaces
[DE91-011000] N91-28392
BRUSHES (ELECTRICAL CONTACTS)
Development of a current collection loss management system for SDI homopolar power supplies
[DE91-012779] N91-28652
BUBBLES
Explosion of a superbubble in a uniform magnetic field
N91-29102
Aspects of reheating in first-order inflation
[NASA-CR-188705] N91-29108
BUCKLING
Overdriven shocks in solids and liquids
[DE91-013370] N91-28618
Stability of cylindrical laminates by higher orde r shear deformable theories N91-28638
A study of the buckling and vibration behavior of an initially stressed thick plate by Galerkin's method
N91-28641
BUDGETING
Possible funding strategies N91-28272
BUFFETING
Transonic shock-induced dynamics of a flexible wing with a thick circular-arc airfoil
[NASA-TM-104088] N91-28132
BUOYANCY
Boussinesq algorithm for enclosed bouyant convection in two dimensions
[PB91-178848] N91-28507
Self-similar evolution of nonlinear magnetic buoyancy instability N91-28913
BURGER EQUATION
Modelling and analysis of geophysical turbulence: Use of optimal transforms and basis sets N91-28686
Shock and soliton structures induced by poloidal flow in tokamaks N91-28929
BUTENES
Cocrystallization in blends of poly(butylene terephthalate) and poly(ester-ether) segmented block copolymers
[DE91-012224] N91-28438

C

C-130 AIRCRAFT
Landing gear improvements for transport aircraft
N91-28159
CABLES
Development of elements of a high T(sub c) superconducting cable
[AD-A236151] N91-28986
CADMIUM COMPOUNDS
Pretreatment of lubricated surfaces with sputtered cadmium oxide
[NASA-CASE-LEW-14474-1] N91-28423
CALCIFICATION
The avian eggshell as a model of biomineralization
[DE91-012608] N91-28400
CALCULUS OF VARIATIONS
Relaxed state and entropy production N91-28907
CALIBRATING
The in-flight calibration of a helicopter-mounted Daedalus multispectral scanner
[DE91-013054] N91-28170
Laser range camera calibration
[DE91-014939] N91-28570
Analytical calibration of the airborne photogrammetric system using a priori knowledge of the exposure station obtained from kinematic Global Positioning System techniques N91-28646
CALORIMETERS
Monolithic front end electronics for silicon calorimeters
[DE91-012063] N91-28484
The Soudan 2 honeycomb calorimeter
[DE91-013404] N91-28860
CAMERAS
WFOV star tracker camera
[DE91-012776] N91-28148
Liquid jet breakup and atomization in rocket chambers under dense spray conditions N91-28227
Laser range camera calibration
[DE91-014939] N91-28570
CANADA
Analysis of southeastern Canada lake-water chemistry data in relation to acidic deposition
[DE91-014957] N91-28674
CANONICAL FORMS
Refinement of the Hamilton-Jacobi solution using a second canonical transformation
[DE91-012965] N91-28798
CANTILEVER BEAMS
Interlaminar fracture characterization: A current review
[NASA-CR-187573] N91-28626
Explicit models for proportional damping in Timoshenko beams N91-28642
CAPACITANCE
Driven shielding capacitive proximity sensor
[NASA-CASE-GSC-13377-1] N91-28785
Coherent charge fluctuations in Josephson junctions and the oscillations of the effective capacitance
[DE91-618098] N91-29019
CAPACITORS
A 10,000 A 1000 Vdc solid state dump switch
[DE91-014141] N91-28497
CAPILLARY FLOW
On accurate determination of contact angle
[DE91-013849] N91-28450
CARBON
Mechanical properties of diamond and diamond-like films
[DE91-011373] N91-28406
Adhesion between CVD diamond films and tungsten
[DE91-013757] N91-28434
CARBON DIOXIDE LASERS
Laser surface modification to impede hydrogen ingress into steel N91-28375
CARBON FIBERS
Apparatus for intercalating large quantities of fibrous structures
[NASA-CASE-LEW-15077-2] N91-28289
CARBON MONOXIDE
Studies relevant to the catalytic activation of carbon monoxide
[DE91-012661] N91-28323
Vibrational spectroscopy of shock-compressed liquid CO
[DE91-013204] N91-28325
CARBON 14
The use of AMS to the biomedical sciences
[DE91-012037] N91-28712
CARCINOGENS
The use of AMS to the biomedical sciences
[DE91-012037] N91-28712
CARNOT CYCLE
Thermodynamics and efficiency in combustion and engines
[DE91-012781] N91-28320
Optimization and thermodynamic performance measures for a class of finite time thermodynamic cycles
N91-29060
CARRIER LIFETIME
Electrical and photomechanical effects of plastic deformation of mercuric iodide
[DE91-013108] N91-29022
CARRIER MOBILITY
Electrical and photomechanical effects of plastic deformation of mercuric iodide
[DE91-013108] N91-29022
CARTESIAN COORDINATES
Recursive linearization of multibody dynamics and application to control design N91-28588
CASCADE FLOW
The application of Particle Image Velocimetry (PIV) in a short duration transonic annular turbine cascade
[AD-A236639] N91-28504
CASE HISTORIES
Failure analysis case histories of Canadian forces aircraft landing gear components N91-28151
CAST ALLOYS
Effects of sample size and loading rate on the transition behavior of a DCI alloy
[DE91-012015] N91-28346
Evaluation of aging of cast stainless steel components
[DE91-014013] N91-28361
CASTING
Drying of gelcast ceramics
[DE91-012955] N91-28413
CASTINGS
Business not as usual N91-28266
CATALYSIS
Reactive characterization as a probe of the nature of catalytic sites
[DE91-014536] N91-28333
EXAFS studies of elastic strain in dilute binary alloys
[DE91-012678] N91-28353
Model catalytic oxidation studies using supported monometallic and heterobimetallic oxides
[DE91-012144] N91-28409
Spontaneous emergence of a metabolism
[DE91-013684] N91-28714
CATALYSTS
Mechanism of hydrodenitrogenation. Part 5: X ray diffraction of molybdenum catalysts
[DE91-013853] N91-28327
Analytical electron microscopy of catalyst preparations
[DE91-014126] N91-28328
Thermodynamic and kinetic aspects of surface acidity
[DE91-014039] N91-28331
Model catalytic oxidation studies using supported monometallic and heterobimetallic oxides
[DE91-012144] N91-28409
CATHODES
Recovery of saturated video signals from vidicons by dynamic cathode biasing
[DE91-012402] N91-28464
Plasma transport in a new cathodic arc ion source, theory and experiment
[DE91-011511] N91-28944
CAVITATION FLOW
A numerical approach for modelling cavitating flows
[DE91-009178] N91-28505
CAVITIES
Space charge and wake field analysis for a high brightness electron source
[DE91-014788] N91-28874
Explosion of a superbubble in a uniform magnetic field
N91-29102
CAVITY RESONATORS
Modeling of a 1700-MHz cluster cavity of planar triodes
[DE91-013049] N91-28488
E-beam accelerator cavity development for the ground-based free electron laser
[DE91-013760] N91-28563
CELLS (BIOLOGY)
Microbeam studies of the sensitivity of structures within living cells
[DE91-012927] N91-28715
Chromosomal changes in cultured human epithelial cells transformed by low- and high-LET radiation
[DE91-013772] N91-28720
Genetic changes in Mammalian cells transformed by helium cells
[DE91-013778] N91-28721
Antenna organization in green photosynthetic bacteria
[DE91-014814] N91-28723
CELLULOSE NITRATE
Shock compression of DuPont detasheet at low stress
[DE91-013229] N91-28443

CENTRAL PROCESSING UNITS
Toward a formal verification of a floating-point coprocessor and its composition with a central processing unit [NASA-CR-187547] N91-28777

CENTRIFUGAL FORCE
Recursive linearization of multibody dynamics and application to control design N91-28588

CERAMIC FIBERS
Processing, compatibility and oxidation of diboride-reinforced oxide matrix composites for ultrahigh-temperature applications N91-28294
Investigation of thermomechanical behavior of metal matrix composites N91-28296
Tribology of aluminum-based metal matrix composites: Fundamental study of wear behavior as influenced by microstructure N91-28297

CERAMIC MATRIX COMPOSITES
Fracture micromechanics of intermetallic and ceramic matrix continuous fiber composites [AD-A236638] N91-28280
The application of x ray tomographic microscopy to chemical vapor infiltration processing of ceramic matrix composites [DE91-011871] N91-28284
Processing, compatibility and oxidation of diboride-reinforced oxide matrix composites for ultrahigh-temperature applications N91-28294
Development of nondestructive evaluation methods and prediction of effects of flaws on the fracture behavior of structural ceramics [DE91-012471] N91-28410

CERAMICS
A review of silicon carbide/metal interactions with relevance to silicon carbide joining [DE91-012768] N91-28282
Sol-gel kinetics by NMR [DE91-011500] N91-28314
The effect of TiB2 reinforcement on the mechanical properties of an Al-Cu-Li alloy-based metal-matrix composite N91-28337
JPRS report: Science and technology. USSR: Materials science [JPRS-UMS-91-003] N91-28342
Microstructural characterization of solders and brazes for advanced packaging technology [DE91-011503] N91-28379
Ion beam sputtered coatings of bioglass N91-28384
Nitrogen and boron-containing polymers as precursors of ceramic materials [DE91-008890] N91-28390
Radiation disorder and aperiodicity in irradiated ceramics [DE91-010257] N91-28391
Radiation damage of ceramics by electron microscopy [DE91-012186] N91-28396
Characterization of silicon nitride synthesized by microwave heating [DE91-012219] N91-28397
Ordered ceramic membranes [DE91-012248] N91-28398
A study of the influence of temperature gradients on densification of glass powder compacts [DE91-012337] N91-28399
The avian eggshell as a model of biomineralization [DE91-012608] N91-28400
Chemistry of electronic ceramic materials. Proceedings of the International Conference on the Chemistry of Electronic Ceramic Materials [NASA-CR-188688] N91-28403
In-situ REM imaging of surface processes on ceramic bulk crystals from 300 to 1670 K in a conventional TEM [DE91-009923] N91-28405
Drying of gelcast ceramics [DE91-012955] N91-28413
Investigation of interlayer materials for the microwave joining of SiC [DE91-013311] N91-28414
Microwave enhanced diffusion? [DE91-013312] N91-28415
Ferroelectric fatigue in modified bulk lead zirconate titanate ceramics [DE91-012647] N91-28417
Elevated-temperature fracture resistances (K(sub IC), R-curves, gamma sub (omega OF)) of monolithic and composite ceramics using chevron-notched, bend tests [NASA-TM-105090] N91-28418
Analysis of the surface heterogeneity of different samples of aluminum oxide ceramic powders [DE91-013527] N91-28421
Validity of the model used to relate the energy distribution and the adsorption isotherm [DE91-013528] N91-28426
Computer modeling of ceramic melters to assess impacts of process and design variables on performance [DE91-013668] N91-28431
Semi-empirical calculations on model systems for organosilyldiamine preceramic polymers [DE91-013721] N91-28433
Shock-wave properties of high-strength ceramics [DE91-014105] N91-28439
Method of preforming and assembling superconducting circuit elements [NASA-CASE-LAR-14395-1-CU] N91-28490
Models for heat transport through assemblies of uniform-diameter hollow spheres [DE91-012998] N91-28512
Boundary lubrication of ceramic materials by soft metallic coating and synthetic oil [DE91-014017] N91-28577
Stress fields generated by kinetic energy projectile interaction with ceramic targets [DE91-013687] N91-28625
Quantitative modeling of the point defect structures of Fe-doped MgO and MgSiO3 perovskite [DE91-011405] N91-28990

CERTIFICATION
Infusion of instrumentation technology (engine plume diagnostics) into operational test programs N91-28249
Liquid rocket engine flight certification N91-28250
Space shuttle main engine: Certification for manned space flight N91-28270

CHANNEL FLOW
A critical analysis of anisotropic k-epsilon modeling and its application to turbulence-driven secondary flows N91-28533
Near-wall modelling of complex turbulent flows N91-28534

CHAOS
Chaos in the lowest Landau level [DE91-014800] N91-28866
Solitons and chaos in laser-plasma interaction N91-28898
Structures of magnetic field lines in the helical torus N91-28932
Regular motion and symmetry in the relativistic standard map N91-28933
Diffusion and relaxation in Hamiltonian chaos N91-28934
Statistical mechanics using symbolic dynamics N91-28940
Formation and dynamics of solitary waves and vortices in driven and damped systems N91-28942
Solitons and chaos in plasma N91-28943
Nonlinear modeling of chaotic time series: Theory and applications [DE91-013076] N91-29055
Chaos and microbial systems [DE91-014908] N91-29064

CHAPMAN-ENSKOG THEORY
Hybrid fluid/kinetic descriptions of tokamak plasmas N91-28888
Fluid/kinetic hybrid moment description of plasmas via a Chapman-Enskog-like approach [DE91-013346] N91-28949

CHARGE COUPLED DEVICES
WFOV star tracker camera [DE91-012776] N91-28148
Liquid jet breakup and atomization in rocket chambers under dense spray conditions N91-28227
Measuring neutron fluences and gamma/x ray fluxes with CCD cameras [DE91-014119] N91-28549

CHARGE TRANSFER
Dynamics of charge-transfer excited states relevant to photochemical energy conversion [DE91-012669] N91-28649
Studies in cloud physics: Electrification, glaciation, and turbulence N91-28684
Correlated charge-changing ion-atom collisions [DE91-013640] N91-28863
Photoinduced charge and energy transfer processes in molecular aggregates [DE91-014383] N91-28864

CHARGED PARTICLES
Nonadiabatic behavior of the magnetic moment of a charged particle in a dipole magnetic field N91-28920
Regular motion and symmetry in the relativistic standard map N91-28933
Evaluation of charged-particle reactions for fusion applications [DE91-014135] N91-28962
Nonlinear dynamics of the relativistic standard map [DE91-014368] N91-28972

CHARM (PARTICLE PHYSICS)
Heavy-quark physics in quantum chromodynamics [DE91-012113] N91-28828

CHARPY IMPACT TEST
Comparisons of irradiation-induced shifts in fracture toughness, crack arrest toughness, and Charpy impact energy in high-copper welds [DE91-008881] N91-28349

CHEMICAL ANALYSIS
Transition metal activation and functionalization of carbon-hydrogen bonds [DE91-014261] N91-28332
Model catalytic oxidation studies using supported monometallic and heterobimetallic oxides [DE91-012144] N91-28409
Photoinduced electron transfer in ordered polymers [DE91-014512] N91-28440
Analysis of southeastern Canada lake-water chemistry data in relation to acidic deposition [DE91-014957] N91-28674
Synthesis and characterization of reduced ternary molybdenum oxides and soluble copper (III) alkoxide complexes [DE91-012679] N91-29001

CHEMICAL ATTACK
The chemical resistance of protective handwear available through the Navy's supply system [AD-A235874] N91-28731

CHEMICAL BONDS
Transition metal activation and functionalization of carbon-hydrogen bonds [DE91-014261] N91-28332
Synthesis and characterization of reduced ternary molybdenum oxides and soluble copper (III) alkoxide complexes [DE91-012679] N91-29001

CHEMICAL COMPOSITION
Direct Monte Carlo simulation of chemical equilibrium composition of molecular fluid mixtures under shock conditions [DE91-013075] N91-28324
Effect of Li level, artificial aging, and TiB2 reinforcement on the fracture toughness of Weldalite (tm) 049-type alloys N91-28339
Evaluation of aging of cast stainless steel components [DE91-014013] N91-28361
Welding of ductile intermetallic alloys [DE91-009553] N91-28594
X ray microimaging of elemental composition and microstructure for materials science [DE91-012052] N91-28601
X ray microimaging of elemental composition and microstructure for materials science [DE91-012221] N91-28832
The computer storage, retrieval, and searching of generic structures in chemical patents: The machine-readable representation of generic structures N91-29081

CHEMICAL ENGINEERING
Technologies available from Martin Marietta Energy Systems, Inc. [DE91-013027] N91-28283

CHEMICAL EQUILIBRIUM
The solubility and dissociation kinetics of hydroxymethyl hydroperoxide in aqueous solution [DE91-013336] N91-28318
Direct Monte Carlo simulation of chemical equilibrium composition of molecular fluid mixtures under shock conditions [DE91-013075] N91-28324
Thin film hydrogen sensor [DE91-014197] N91-28550

CHEMICAL EXPLOSIONS
Experiments and calculations of jet penetration in glass [DE91-013567] N91-28422
Investigation of the Deflagration-to-Detonation (DDT) process: The role of ignition and explosive properties in DDT [DE91-011956] N91-28442
Mechanisms of EBW HE initiation [DE91-013565] N91-28447
The deflagration-to-detonation transition in granular HMX [DE91-014591] N91-28448
A study of the impact of reaction rates on equation of state [DE91-013375] N91-28621

CHEMICAL LASERS
Chemical characterization of microparticles by laser ablation in an ion trap mass spectrometer [DE91-012513] N91-28309

CHEMICAL PROPERTIES
Materials sub-panel N91-28245
Chemical characterization of microparticles by laser ablation in an ion trap mass spectrometer [DE91-012513] N91-28309

CHEMICAL PROPULSION
CFD applications in chemical propulsion engines N91-28234

CHEMICAL REACTIONS
CFD applications in chemical propulsion engines N91-28234

Energy dissipation in chemical reactions on ultrafast timescales
[DE91-012342] N91-28315
Combustion research program: Flame studies, laser diagnostics, and chemical kinetics
[DE91-014824] N91-28329
Transition metal activation and functionalization of carbon-hydrogen bonds
[DE91-014261] N91-28332
Reactive characterization as a probe of the nature of catalytic sites
[DE91-014536] N91-28333
Spontaneous cluster decomposition in a quadrupole ion trap
[DE91-012519] N91-28836
Biomimetic thin film deposition
[DE91-012485] N91-28999
The surface chemistry of GaAs atomic layer epitaxy
[DE91-014112] N91-29047

CHEMICAL WARFARE
Robotic mannequin technology for enhanced product testing
[DE91-013787] N91-28591

CHEMISORPTION
Pacific Northwest hydrogen feasibility study
[DE91-013427] N91-28445

CHEMISTRY
Chemistry and materials science research report
[DE91-011507] N91-28305

CHIPS (ELECTRONICS)
Microstructural characterization of solders and brazes for advanced packaging technology
[DE91-011503] N91-28379
Control of autonomous mobile robots using custom-designed qualitative reasoning VLSI chips and boards
[DE91-012527] N91-28783

CHLOROPHYLLS
Antenna organization in green photosynthetic bacteria
[DE91-014814] N91-28723

CHLOROPLASTS
Photobiotechnology: Algal hydrogen production and photoconductivity of metalized chloroplasts
[DE91-013232] N91-28718

CHLOROSILANES
Semi-empirical calculations on model systems for organosilyldiamine preceramic polymers
[DE91-013721] N91-28433

CHROMIUM
Analytical electron microscopy of catalyst preparations
[DE91-014126] N91-28328

CHROMIUM OXIDES
Alternative materials for solid oxide fuel cells: Chromite interconnections
[DE91-014447] N91-28664

CHROMIUM STEELS
The rate (time)-dependence mechanical behavior of modified 9Cr-1Mo. Part 2: Isothermal modeling at 538 C
[DE91-011100] N91-28350
The rate (time)-dependent mechanical behavior of modified 9Cr-1Mo steel. Part 1: Experiments at 538 C
[DE91-011097] N91-28615

CHROMOSOMES
Novel methods for physical mapping of the human genome applied to the long arm of chromosome 5
[DE91-012894] N91-28717
Chromosomal changes in cultured human epithelial cells transformed by low- and high-LET radiation
[DE91-013772] N91-28720
Genetic changes in Mammalian cells transformed by helium cells
[DE91-013778] N91-28721

CIRCUIT BOARDS
Control of autonomous mobile robots using custom-designed qualitative reasoning VLSI chips and boards
[DE91-012527] N91-28783

CIRCUITS
Method of preforming and assembling superconducting circuit elements
[NASA-CASE-LAR-14395-1-CU] N91-28490
A parallel algorithm for solving linear equations arising from one-dimensional network problems
[DE91-012815] N91-28795

CIRCULAR CYLINDERS
A new model of rate dependent elastic-plastic flow
[DE91-014600] N91-28633

CITIES
A new approach to analyzing high-resolution aerial photographs of urban areas N91-28647

CLASSICAL MECHANICS
Diffusion and relaxation in Hamiltonian chaos
N91-28934

CLAYS
Ordered ceramic membranes
[DE91-012248] N91-28398

CLEANING
Supercritical fluids cleaning
[DE91-013374] N91-28456

CLEARANCES
Assessment of the application of the working group 22 standard bump concept to a current military aircraft
N91-28166

CLIMATE
Natural and anthropogenic climate change
[DE91-014734] N91-28673

CLIMATE CHANGE
Natural and anthropogenic climate change
[DE91-014734] N91-28673

CLIMATOLOGY
An upper ocean model for the climatic aspects of air-sea interaction N91-28691
Report of Meeting of CLICOM Experts
[WCDP-9] N91-28695
Results of agriclimatological studies using multiple satellite sensors like NOAA AVHRR; GMS IR; and LANDSAT MSS and TM
[DE91-618773] N91-28698
Prediction of forecast skill with a quasi-geostrophic model N91-28699

CLOUD COVER
Initialization of cloud and radiation in the Florida State University global spectral model N91-28703
A cloud fraction and radiative transfer model
N91-28706

CLOUD GLACIATION
Studies in cloud physics: Electrification, glaciation, and turbulence N91-28684

CLOUD PHYSICS
Studies in cloud physics: Electrification, glaciation, and turbulence N91-28684

CLOUDS (METEOROLOGY)
Data users guide to the mountain cloud chemistry project
[PB91-168484] N91-28697
A numerical simulation of a tornado-scale vortex in a three-dimensional cloud model N91-28705
A cloud fraction and radiative transfer model
N91-28706

CLUMPS
Ab initio cluster studies of La2CuO4
[DE91-013520] N91-29025

CLUSTERS
Spontaneous cluster decomposition in a quadrupole ion trap
[DE91-012519] N91-28836

COAL
Formation and sustainment of a very low aspect ration tokamak using coaxial helicity injection (the Helicity Injected Torus (HIT) experiment)
[DE91-013948] N91-28967

COASTS
Alaska wave data index
[AD-A236635] N91-28707

COATING
Composite material systems for hydrogen management N91-28229
Perspective on plating for precision finishing
[DE91-011927] N91-28394

COATINGS
Alumina-silicon carbide composites from coated powders
[DE91-012357] N91-28281
Processing, compatibility and oxidation of diboride-reinforced oxide matrix composites for ultrahigh-temperature applications N91-28294
Process for bonding elastomers to metal
[NASA-CASE-LAR-13645-1] N91-28424
Adhesion between CVD diamond films and tungsten
[DE91-013757] N91-28434
Recent ASME Code Section 11 developments for surface examination through coatings
[DE91-014069] N91-28437

COBALT COMPOUNDS
Epitaxial growth of silicon on CoSi2(001)/Si(001)
[DE91-013387] N91-29015

COBALT ISOTOPES
Multilevel resonance analysis of Co-59 neutron transmission measurements
[DE91-012135] N91-28829

COBALT OXIDES
Creep and diffusion in nonstoichiometric oxides
[DE91-013766] N91-28435

CODERS
Direction discriminating hearing aid
[NASA-CASE-GSC-13027-1] N91-28726

CODES
Directory of Organizational Technical Report Acronym Codes (DOTRAC)
[AD-A237000] N91-29072

CODING
Multiple frequency atmospheric radar techniques
N91-28683
Directory of Organizational Technical Report Acronym Codes (DOTRAC)
[AD-A237000] N91-29072
Coded aperture imaging with a HURA coded aperture and a discrete pixel detector N91-29093

COERCIVITY
Fundamental magnetic studies of iron-rare-earth-metalloid alloys
[DE91-014816] N91-28383

COHERENT RADIATION
Modal study of refractive effects on x ray laser coherence
[DE91-012083] N91-28551

COLD FRONTS
Gravity wave propagation in a frontal environment
N91-28687

COLD PRESSING
Development of elements of a high T(sub c) superconducting cable
[AD-A236151] N91-28986

COLD WORKING
The influence of Ag+Mg additions on the nucleation of strengthening precipitates in a non-cold-worked Al-Cu-Li alloy N91-28336

COLLISION PARAMETERS
Selected topics in mechanisms and robotics: Singularities, inverse kinematics, and collision detection
N91-28598
Photodisintegration of the deuteron at medium and high energies
[DE91-014458] N91-28865
Evaluation of charged-particle reactions for fusion applications
[DE91-014135] N91-28962

COLLISIONAL PLASMAS
Fluidlike studies of the presheath and sheath regions of a plasma
[DE91-013345] N91-28953

COLLISIONLESS PLASMAS
Nonlinear phenomena and processes in high energy plasmas N91-28882
Hybrid fluid/kinetic descriptions of tokamak plasmas
N91-28888

COLOR
Color effects in optical systems
[ITN-91-85150] N91-28878

COMBAT
Effectiveness of tiltrotor support to ground combat
[DE91-013603] N91-28167
Air combat environment test and evaluation facility and the development of the offensive sensors laboratory
[DE91-011398] N91-28173

COMBUSTION
Spray combustion under oscillatory pressure conditions N91-28226
Historical problem areas lessons learned N91-28242
Thermodynamics and efficiency in combustion and engines
[DE91-012781] N91-28320
Combustion research program: Flame studies, laser diagnostics, and chemical kinetics
[DE91-014824] N91-28329
Ultra-fine powders using glycine-nitrate combustion synthesis
[DE91-012926] N91-28412

COMBUSTION CHAMBERS
Spray combustion under oscillatory pressure conditions N91-28226
Business not as usual N91-28266
Simulation of combustion processes in an MHD second stage combustor
[DE91-014014] N91-28968

COMBUSTION CHEMISTRY
Liquid-propellant droplet vaporization and combustion in high pressure environments N91-28225

COMBUSTION PHYSICS
Liquid-propellant droplet vaporization and combustion in high pressure environments N91-28225
Droplet-turbulence interactions in subcritical and supercritical evaporating sprays N91-28228
Simulation of combustion processes in an MHD second stage combustor
[DE91-014014] N91-28968

COMBUSTION PRODUCTS
Combustion research program: Flame studies, laser diagnostics, and chemical kinetics
[DE91-014824] N91-28329

COMBUSTION STABILITY
Spray combustion under oscillatory pressure conditions N91-28226

COMMUNICATION NETWORKS
Seeking solutions: High-performance computing for science
[PB91-169763] N91-28752
COMMUNICATION SATELLITES
Impact of ion propulsion on performance, design, testing, and operation of a geosynchronous spacecraft
[AD-A237028] N91-28273
COMMUTER AIRCRAFT
Long time measurements of landing gear loads on SAAB SF-340 commuter aircraft N91-28157
COMPACTING
A study of the influence of temperature gradients on densification of glass powder compacts
[DE91-012337] N91-28399
COMPARATORS
Direction discriminating hearing aid
[NASA-CASE-GSC-13027-1] N91-28726
COMPATIBILITY
Historical problem areas lessons learned N91-28242
Processing, compatibility and oxidation of diboride-reinforced oxide matrix composites for ultrahigh-temperature applications N91-28294
COMPLEX COMPOUNDS
Photoinduced charge and energy transfer processes in molecular aggregates
[DE91-014383] N91-28864
Synthesis and characterization of reduced ternary molybdenum oxides and soluble copper (III) alkoxide complexes
[DE91-012679] N91-29001
COMPLEX SYSTEMS
A methodology to determine the dynamic configuration of a reconfigurable manipulator
[DE91-010732] N91-28576
COMPOSITE MATERIALS
Heat resistant materials and their feasibility issues for a space nuclear transportation system
[DE91-014071] N91-28187
Composite material systems for hydrogen management N91-28229
Multiaxial failure characterization of composites
[DE91-011925] N91-28285
Process for application of powder particles to filamentary materials
[NASA-CASE-LAR-14231-1-CU] N91-28290
Finite element modeling of 2-D delamination growth in laminated composites N91-28302
The avian eggshell as a model of biomineralization
[DE91-012608] N91-28400
Elevated-temperature fracture resistances (K(sub IC), R-curves, gamma sub (omega OF)) of monolithic and composite ceramics using chevron-notched, bend tests
[NASA-TM-105090] N91-28418
Models for heat transport through assemblies of uniform-diameter hollow spheres
[DE91-012998] N91-28512
Excess heat production in composite superconductors during current redistribution
[DE91-013547] N91-29016
COMPOSITE STRUCTURES
Flutter of laminated rectangular plates including finite deflection and shear deformation N91-28639
COMPRESSED GAS
Vibrational spectroscopy of shock-compressed liquid CO
[DE91-013204] N91-28325
COMPRESSIBILITY
Damage development under compression-compression fatigue loading in a stitched uniwoven graphite/epoxy composite material
[NASA-CR-188693] N91-28292
The SNL, Livermore, Hopkinson bar apparatus for compressive materials testing at high strain-rates
[DE91-013132] N91-28612
COMPRESSIBLE FLOW
Evaluation of a technique to generate artificially thickened boundary layers in supersonic and hypersonic flows
[NASA-TP-3142] N91-28136
COMPRESSING
Shock compression of DuPont detasheet at low stress
[DE91-013229] N91-28443
COMPRESSION LOADS
Multiaxial failure characterization of composites
[DE91-011925] N91-28285
An analysis of interlaminar stresses in unsymmetrically laminated plates N91-28299
Vibrational spectroscopy of shock-compressed liquid CO
[DE91-013204] N91-28325
Test of superplastically formed corrugated aluminum compression specimens with beaded webs
[NASA-TM-104119] N91-28373
Response of the polymers KEL-F, polysulfone, high density polyethylene and polymethylmethacrylate to shock loading and release from 0.3 to 2.4 GPa
[DE91-012867] N91-28411
Dynamic plasticity in transition from thermal activation to viscous drag
[DE91-013031] N91-28617
Overdriven shocks in solids and liquids
[DE91-013370] N91-28618
Shock compression of low-density microcellular materials
[DE91-013586] N91-28628
Equation of state and crushing dynamics of low-density silica aerogels
[DE91-014766] N91-28637
Stability of cylindrical laminates by higher orde r shear deformable theories N91-28638
A study of the buckling and vibration behavior of an initially stressed thick plate by Galerkin's method
N91-28641
COMPRESSION WAVES
Seismic traveltime inversion in three-dimensional heterogeneous media N91-28678
COMPRESSIVE STRENGTH
Damage development under compression-compression fatigue loading in a stitched uniwoven graphite/epoxy composite material
[NASA-CR-188693] N91-28292
COMPUTATION
Searching for consensus patterns on a hypercube
[DE91-013233] N91-28753
Sound propagation in the atmosphere: Analysis of signal amplitude and phase temporal and spatial variations
[AD-A237034] N91-28816
Photodisintegration of the deuteron at medium and high energies
[DE91-014458] N91-28865
COMPUTATIONAL ASTROPHYSICS
Phase transitions triggered by quantum fluctuations in the inflationary universe
[NASA-CR-188698] N91-29112
COMPUTATIONAL FLUID DYNAMICS
A study of methods to investigate nozzle boundary layer transition N91-28232
Moving finite elements: A continuously adaptive method for computational fluid dynamics
[DE91-013391] N91-28513
Receptivity of a laminar boundary layer to the interaction of a three-dimensional roughness element with time-harmonic free-stream disturbances N91-28518
Numerical analyses of aero-optical flows: An application of parallel algorithm on high-performance Personal Computer (PC) base multitransputer system N91-28519
Use of a rotated Riemann solver for the two-dimensional Euler equations N91-28530
Near-wall modelling of complex turbulent flows
N91-28534
JPRS report: Science and technology. USSR: Physics and mathematics
[JPRS-UPM-90-006] N91-28811
COMPUTATIONAL GRIDS
Applications of a 2-D moving finite element formulation to elastic/viscoplastic dynamic fracture analysis
[DE91-009930] N91-28607
Load-balancing and performance of a gridless particle simulation on MIMD, SIMD, and vector supercomputers
[DE91-013758] N91-28756
Computing minimal surfaces via level set curvature flow
[DE91-014709] N91-28759
A multilingual parallelization of the icosahedral-hexagonal grid system for integration on the sphere
[DE91-013615] N91-28762
A 2D field solver for periodic structures with special corner elements
[DE91-012323] N91-28792
COMPUTER AIDED DESIGN
Calculation of interactions between air and ground of landing N91-28161
Building microelectronic systems in a university environment
[AD-A236629] N91-28477
Simulation of combustion processes in an MHD second stage combustor
[DE91-014014] N91-28968
COMPUTER AIDED MAPPING
Symplectic full-turn maps in a Fourier representation
[DE91-012912] N91-28796
COMPUTER AIDED TOMOGRAPHY
X ray Tomographic Microscopy (XTM)
[DE91-011930] N91-28599
Model-based computed tomography for nondestructive evaluation
[DE91-013462] N91-28602
New techniques for positron emission tomography in the study of human neurological disorders
[DE91-013855] N91-28728
COMPUTER GRAPHICS
Radiation disorder and aperiodicity in irradiated ceramics
[DE91-010257] N91-28391
ARAC: A computer-based emergency-response dose-assessment service with global application potential
[DE91-013248] N91-28700
Visualization using a data flow-based paradigm
[DE91-013851] N91-28763
Scientific data visualization
[DE91-014216] N91-28766
The 1992 - 1997 renewal proposal interactive graphics for molecular studies
[AD-A236598] N91-28823
COMPUTER INFORMATION SECURITY
Requirements for a network storage service
[DE91-014106] N91-28778
Design and performance evaluation of signature files for text retrieval systems N91-29085
COMPUTER NETWORKS
The role of the UNIX(tm) central computing facility in a multi-purpose national laboratory
[DE91-012361] N91-28737
Solving computational grand challenges using a network of heterogeneous supercomputers
[DE91-013725] N91-28755
The cache group scheme for hardware-controlled cache coherence and the general need for hardware coherence control in large-scale multiprocessors
[DE91-012106] N91-28772
Requirements for a network storage service
[DE91-014106] N91-28778
Network based concurrent computing on the PVM system
[DE91-014961] N91-28780
A parallel algorithm for solving linear equations arising from one-dimensional network problems
[DE91-012815] N91-28795
COMPUTER PROGRAM INTEGRITY
The software technical review process
[AD-A236139] N91-28743
COMPUTER PROGRAMMING
Design of an interactive satellite communications system analysis program
[AD-A237030] N91-28459
A multilingual parallelization of the icosahedral-hexagonal grid system for integration on the sphere
[DE91-013615] N91-28762
Toward a better parallel performance metric
[DE91-012627] N91-28773
The PCP/PFP programming models on the BBN TC2000
[DE91-011537] N91-28781
COMPUTER PROGRAMS
Numerical simulation of the dynamic behavior of landing gears N91-28160
Perturbed environment assessments for space vehicles
[DE91-012630] N91-28188
Design of an interactive satellite communications system analysis program
[AD-A237030] N91-28459
Fields and trajectories in the magnicon
[DE91-013070] N91-28492
Algorithm and code development for unsteady three-dimensional Navier-Stokes equations
[NASA-CR-188039] N91-28503
Atmospheric propagation of high-explosive blast waves
[DE91-012550] N91-28506
ZEPHYR3D: A finite difference computer program for three-dimensional, transient incompressible flow problems
[DE91-014331] N91-28515
Numerical analyses of aero-optical flows: An application of parallel algorithm on high-performance Personal Computer (PC) base multitransputer system N91-28519
Solution to quasi-axisymmetric internal compressible flows using the stream tube approach N91-28526
Applications of a 2-D moving finite element formulation to elastic/viscoplastic dynamic fracture analysis
[DE91-009930] N91-28607
MESA: A 3-D Eulerian hydrocode for penetration mechanics studies
[DE91-013308] N91-28613
Stress fields generated by kinetic energy projectile interaction with ceramic targets
[DE91-013687] N91-28625
ASTROP2 users manual: A program for aeroelastic stability analysis of propfans
[NASA-TM-4304] N91-28627

Calculation of pressure distribution in vacuum systems using a commercial finite element program
[DE91-013611] N91-28629
TREE: A model of the effects of acid precipitation and air pollutants on the growth of trees
[DE91-014131] N91-28672
Support materials for formal specification of software
[AD-A236121] N91-28742
The software technical review process
[AD-A236139] N91-28743
Software metrics
[AD-A236140] N91-28744
Prototyping parallel and distributed programs in proteus
[AD-A236597] N91-28746
A design space and design rules for user interface software architecture
[AD-A237049] N91-28748
Embedding ADAMS in FORTRAN
[DE91-014346] N91-28754
Guidelines for acquisition, installation, and testing of performance assessment software
[DE91-013910] N91-28764
Automated reasoning contributes to mathematics and logic
[DE91-014005] N91-28765
Scientific data visualization
[DE91-014216] N91-28766
General implementation of thin-slot algorithms into the finite-difference time-domain code, TSAR, based on a slot data file
[DE91-014336] N91-28767
Scintillation detector efficiencies for neutrons in the energy region above 20 MeV
[DE91-012544] N91-28837
Simulation of planar integrated photonics devices with the LLNL time-domain finite-difference code suite
[DE91-011929] N91-28876
Pulse propagation in inhomogeneous optical fibers
[DE91-014356] N91-28879
Nonlinear evolution of 2D and 3D Rayleigh-Taylor instability at stagnation phase in laser implosion
N91-28899
Turbulent mixing due to Rayleigh-Taylor instability in laser driven implosion N91-28914
The 3-D electromagnetic macroscale particle simulation of inhomogeneous, magnetized plasmas N91-28918
Threatened Area Database System (TADS) computer program
[DE91-012491] N91-29074
The ADAMS interactive interpreter
[DE91-014345] N91-29080
The computer storage, retrieval, and searching of generic structures in chemical patents: The machine-readable representation of generic structures
N91-29081
Numerical simulations of mass outflows from star-forming regions N91-29123

COMPUTER STORAGE DEVICES
Requirements for a network storage service
[DE91-014106] N91-28778
The computer storage, retrieval, and searching of generic structures in chemical patents: The machine-readable representation of generic structures
N91-29081

COMPUTER SYSTEMS DESIGN
Measuring and modelling disk I/O subsystems
[ISBN-90-6275-567-4] N91-28736
The PCP/PFP programming models on the BBN TC2000
[DE91-011537] N91-28781

COMPUTER SYSTEMS PERFORMANCE
Building microelectronic systems in a university environment
[AD-A236629] N91-28477
Toward a better parallel performance metric
[DE91-012627] N91-28773
Implementation of a hypercube database system
[DE91-014285] N91-29089
Performance evaluation of multiversion database systems
[DE91-014340] N91-29090

COMPUTER SYSTEMS PROGRAMS
The role of the UNIX(tm) central computing facility in a multi-purpose national laboratory
[DE91-012361] N91-28737
A design space and design rules for user interface software architecture
[AD-A237049] N91-28748

COMPUTER TECHNIQUES
Microcomputers: An exploratory study of their availability and use in the research process and their contribution to researcher productivity N91-28739
Nonlinear computer analysis of backward wave oscillator N91-28923
The computer storage, retrieval, and searching of generic structures in chemical patents: The machine-readable representation of generic structures
N91-29081

COMPUTER VISION
Laser range camera calibration
[DE91-014939] N91-28570
Analysis and modeling of early vision tasks for robot stereo vision N91-28585

COMPUTERIZED SIMULATION
Computer simulation of an aircraft seat and occupant(s) in a crash environment: Program SOM-LA/SOM-TA user manual
[CR-R-90026] N91-28146
Design landing loads evaluation by dynamic simulation of flexible aircraft N91-28163
Effectiveness of tiltrotor support to ground combat
[DE91-013603] N91-28167
A theoretical and experimental study of the interior ballistic processes of an electrothermal gun N91-28185
Perturbed environment assessments for space vehicles
[DE91-012630] N91-28188
Test vs. simulation N91-28251
Investigation of thermomechanical behavior of metal matrix composites N91-28296
Finite element modeling of 2-D delamination growth in laminated composites N91-28302
Direct Monte Carlo simulation of chemical equilibrium composition of molecular fluid mixtures under shock conditions
[DE91-013075] N91-28324
Atomistic studies of grain boundaries in alloys and compounds
[DE91-014516] N91-28372
Computer modeling of ceramic melters to assess impacts of process and design variables on performance
[DE91-013668] N91-28431
Electrostatic discharge effects on EBW detonators
[DE91-013250] N91-28467
Numerical simulation of particle-wave interaction in boundary layers
[NASA-CR-187312] N91-28502
Moving finite elements: A continuously adaptive method for computational fluid dynamics
[DE91-013391] N91-28513
Study of spherical couette flow via 3-D spectral simulations: Large and narrow-gap flows and their transitions N91-28520
Simulation of a storage ring free electron laser with a mapping algorithm for distribution functions
[DE91-012387] N91-28552
Modeling molecular processes in the environment
[DE91-013790] N91-28671
Observations and theoretical studies of tides and normal modes in the lower thermosphere N91-28681
ARAC: A computer-based emergency-response dose-assessment service with global application potential
[DE91-013248] N91-28700
Bayesian design and analysis of computer experiments: Use of derivatives in surface prediction
[DE91-013147] N91-28751
Load-balancing and performance of a gridless particle simulation on MIMD, SIMD, and vector supercomputers
[DE91-013758] N91-28756
Computing minimal surfaces via level set curvature flow
[DE91-014709] N91-28759
Multidimensional spectral estimation using iterative methods
[AD-A237025] N91-28791
Simulations on pair creation from beam-beam interaction in linear colliders
[DE91-012315] N91-28834
X ray spatial resolution at intermediate voltages: An assessment by massively parallel Monte Carlo electron trajectory simulation
[DE91-012018] N91-28841
Molecular dynamics simulations of bulk displacement threshold energies in Si
[DE91-011957] N91-28846
Simulation of planar integrated photonics devices with the LLNL time-domain finite-difference code suite
[DE91-011929] N91-28876
Computer simulation of solar wind-magnetosphere interaction N91-28904
Application of mathematica to energy principle
N91-28910
Helical field effect in solar/stellar wind N91-28912
Self-similar evolution of nonlinear magnetic buoyancy instability N91-28913
Turbulent mixing due to Rayleigh-Taylor instability in laser driven implosion N91-28914
Electrostatic particle simulations of density and temperature driven modes in a toroidal plasma
N91-28915
Internal kink mode simulation by 3-D gyrokinetic code
N91-28916
Particle simulation on the tilt stabilization of the FRC plasma N91-28917
The 3-D electromagnetic macroscale particle simulation of inhomogeneous, magnetized plasmas N91-28918
Study of kink instability and current relaxation by three dimensional macroscale particle simulation N91-28919
Numerical simulation of potential-driven ion cyclotron oscillation N91-28925
Dynamics of interfaces with internal structures
N91-28926
Evidences of trapping in tungsten and implications for plasma-facing components
[DE91-012734] N91-28951
Chamber propagation
[DE91-012797] N91-28954
Simulation of combustion processes in an MHD second stage combustor
[DE91-014014] N91-28968
Chaos and microbial systems
[DE91-014908] N91-29064
A simulated user for laboratory investigation of information systems requirements determination
N91-29087
Numerical simulations of mass outflows from star-forming regions N91-29123

COMPUTERS
Cultural changes in aerospace N91-28265
Automated verification of system configuration
[DE91-012520] N91-28481

CONCENTRATION (COMPOSITION)
Regional oxidant model user's guide. Part 1: The ROM preprocessors
[PB91-171926] N91-28665

CONCURRENT PROCESSING
Prototyping parallel and distributed programs in proteus
[AD-A236597] N91-28746

CONDUCTING POLYMERS
Polymers at surfaces
[DE91-013642] N91-28430
Preparation of ionic membranes for zinc/bromine storage batteries
[DE91-012008] N91-28483
Recent achievements in polymer electrolyte fuel cell (PEFC) research at Los Alamos National Laboratory
[DE91-013683] N91-28661

CONDUCTIVE HEAT TRANSFER
Boussinesq algorithm for enclosed bouyant convection in two dimensions
[PB91-178848] N91-28507
Numerical solution of a moving boundary problem as a model solution for a solar pipe
[ITN-91-85143] N91-28516
Coupling device with improved thermal interface
[NASA-CASE-GSC-13251-1] N91-28582
Model for marfe-detached plasma transition in tokamaks N91-28938
TOPAZ2D benchmark problems nonlinear materials
[DE91-009753] N91-29053

CONFERENCES
Landing Gear Design Loads
[AGARD-CP-484] N91-28150
Space Transportation Propulsion Technology Symposium. Volume 3: Panel Session Summaries and Presentations
[NASA-CP-3112-VOL-3] N91-28235
Chemistry of electronic ceramic materials. Proceedings of the International Conference on the Chemistry of Electronic Ceramic Materials
[NASA-CR-188688] N91-28403
Proceedings of the 1990 Antenna Applications Symposium, volume 1
[AD-A237056] N91-28460
Proceedings of the 1990 Antenna Applications Symposium, volume 2
[AD-A237057] N91-28461
Proceedings of the Second International Toki Conference on Plasma Physics and Controlled Nuclear Fusion. Nonlinear Phenomena in Fusion Plasmas: Theory and Computer Simulation
[NIFS-PROC-6] N91-28881

CONFINEMENT
The numerical solution of confined laminar flow past a moving boundary N91-28532
Numerical study of ion temperature gradient modes in a tokamak N91-28921
Large growth Rayleigh-Taylor experiments on Nova
[DE91-012885] N91-28955

CONFORMAL MAPPING
The (2,0) super Beltrami parametrization and superconformal structures
[DE91-617611] N91-29057
Topics in low-dimensional field theory
[DE91-013784] N91-29062
CONICAL BODIES
Prediction of the flow and heat transfer between a rotating and a stationary cone N91-28536
CONSERVATION EQUATIONS
Fluid/kinetic hybrid moment description of plasmas via a Chapman-Enskog-like approach
[DE91-013346] N91-28949
CONSERVATION LAWS
Simulation of combustion processes in an MHD second stage combustor
[DE91-014014] N91-28968
CONTACT LOADS
Thermal and non-Newtonian effects in elastohydrodynamic lubrication of rolling-sliding contacts N91-28590
Human body protection in a dynamic environment. Cushioning mechanics
[ITN-91-85149] N91-28733
CONTAMINANTS
Biomarker-based biomonitoring for evaluating health and ecological effects on environmental contamination
[DE91-013729] N91-28719
CONTINENTS
Heat flow data and thermal state of the continental lithosphere N91-28682
CONTINUITY EQUATION
Non similarity solution approximation to the thermal hydraulic quenchback in superconductors
[DE91-013964] N91-29040
CONTINUOUS WAVE RADAR
Fluctuations in near-surface backscattering to a descending CW radar
[ITN-91-85140] N91-28469
CONTINUUMS
Continuum x ray gauging of multiple-element materials
[DE91-011923] N91-28307
CONTROL EQUIPMENT
Design of a multivariable RF control system using gain-shaping in the frequency domain
[DE91-013859] N91-28474
Automated verification of system configuration
[DE91-012520] N91-28481
The DARPA compact superconducting x-ray lithography source features
[DE91-013864] N91-29039
CONTROL ROCKETS
Attitude control of a spinning rocket via thrust vectoring
[DE91-006267] N91-28274
CONTROL STABILITY
Stochastic robustness of linear multivariable control systems: Towards comprehensive robustness analysis N91-28172
CONTROL SYSTEMS DESIGN
Rotor and control system loads analysis of the XV-15 with the advanced technology blades
[NASA-TM-102876] N91-28134
Stochastic robustness of linear multivariable control systems: Towards comprehensive robustness analysis N91-28172
Apparatus for intercalating large quantities of fibrous structures
[NASA-CASE-LEW-15077-2] N91-28289
Design of a multivariable RF control system using gain-shaping in the frequency domain
[DE91-013859] N91-28474
Dynamic coupling effects in modeling and control of hard contact motion of a manipulator
[DE91-010393] N91-28574
Robust low-order control of flexible joint manipulators N91-28584
Recursive linearization of multibody dynamics and application to control design N91-28588
The symbolic computation and automatic analysis of trajectories
[NASA-CR-188159] N91-28787
Real-time adaptive active control of sound fields N91-28819
CONTROL THEORY
Robust and real-time control of magnetic bearings for space engines N91-28230
Real-time adaptive active control of sound fields N91-28819
How to increase meeting effectiveness and efficiency
[DE91-012420] N91-29070
CONTROL UNITS (COMPUTERS)
Measuring and modelling disk I/O subsystems
[ISBN-90-6275-567-4] N91-28736
CONTROLLABILITY
Design landing loads evaluation by dynamic simulation of flexible aircraft N91-28163
CONTROLLED FUSION
Proceedings of the Second International Toki Conference on Plasma Physics and Controlled Nuclear Fusion. Nonlinear Phenomena in Fusion Plasmas: Theory and Computer Simulation
[NIFS-PROC-6] N91-28881
Nonlinear phenomena and processes in high energy plasmas N91-28882
Implications of TAE modes for the design of ITER
[DE91-013128] N91-28952
Maryland controlled fusion research program
[DE91-014358] N91-28980
Performance of the 10-kV, 5-MA pulsed-power system for the FRX-C compression experiment
[DE91-014745] N91-28983
On the use of particle-in-cell methods for the study of magnetically-confined fusion plasmas
[DE91-015093] N91-28984
CONTROLLERS
Robust and real-time control of magnetic bearings for space engines N91-28230
Robust low-order control of flexible joint manipulators N91-28584
CONVECTION
Boussinesq algorithm for enclosed bouyant convection in two dimensions
[PB91-178848] N91-28507
Joint proposal for US/USSR on nonlinear dynamics and plasma transport
[DE91-014360] N91-28981
CONVERGENT-DIVERGENT NOZZLES
Generating strong shock waves with a supersonic peristaltic pump
[DE91-013228] N91-28174
COOL STARS
Interaction of radiation with outflows in late-type stars N91-29136
COOLING
Optimization and thermodynamic performance measures for a class of finite time thermodynamic cycles N91-29060
Radiative transfer in very strong magnetic fields N91-29106
COOLING SYSTEMS
Advanced cryo propulsion systems N91-28212
Prediction of high level vibration test results by use of available inelastic analysis techniques
[DE91-009437] N91-28606
COORDINATES
Kinematic GPS surveying N91-28149
COPOLYMERIZATION
Melamine-formaldehyde aerogels
[DE91-012084] N91-28408
COPOLYMERS
Polymers at surfaces
[DE91-011000] N91-28392
COPPER
High-resolution measurements of the thermal conductivity and boundary resistance of helium-4 near the lambda point N91-28322
Rapid solidification processing of Al3Ti and Al3Ti plus copper
[AD-A236600] N91-28343
Comparisons of irradiation-induced shifts in fracture toughness, crack arrest toughness, and Charpy impact energy in high-copper welds
[DE91-008881] N91-28349
Temperature dependence of the elastic behavior of structurally disordered metallic superlattices
[DE91-014007] N91-28377
A comparative second harmonic study of Cu(111) in UHV and in solution
[AD-A237023] N91-28479
Bauschinger effect during shock loading
[DE91-014606] N91-28634
Shear stress prediction in shock loaded copper
[DE91-014740] N91-28635
COPPER ALLOYS
Strength and electrical conductivity of deformation processed Cu-15 v/o Fe metal composites produced by powder metallurgy/techniques
[DE91-013658] N91-28291
Identification of strengthening phases in Al-Cu-Li alloy Weldalite (tm) 049 N91-28335
Tensile deformation of Al-Cu-Li-Zr alloy 2090-T8E41 at 298 and 77 K
[DE91-011885] N91-28345
COPPER COMPOUNDS
Synthesis and characterization of reduced ternary molybdenum oxides and soluble copper (III) alkoxide complexes
[DE91-012679] N91-29001
COPPER OXIDES
The effect of strong Coulomb correlations on electron-phonon interactions in the copper oxides: Implications for transport
[DE91-013333] N91-28854
Growth of high T(sub c) superconducting thin films for microwave applications
[DE91-011436] N91-28991
Superconducting bolometers: High-T(sub c) and low-T(sub c)
[DE91-011830] N91-28992
Ab initio cluster studies of La2CuO4
[DE91-013520] N91-29025
Neutron scattering studies of spin correlations in metallic YBa2Cu3O(6+x)
[DE91-013794] N91-29031
CORNERS
A 2D field solver for periodic structures with special corner elements
[DE91-012323] N91-28792
CORONAL LOOPS
Electron acceleration by magnetosonic waves in a solar coronal loop N91-29132
CORRELATION
Electron correlations in solid state physics
[DE91-013752] N91-29030
CORROSION
Failure analysis case histories of Canadian forces aircraft landing gear components N91-28151
JPRS report: Science and technology. USSR: Materials science
[JPRS-UMS-91-003] N91-28342
The effect of fluoride gases on cylinder valve corrosion
[DE91-012745] N91-28355
CORROSION RESISTANCE
Aqueous corrosion characteristics and corrosion-related cracking susceptibilities of Fe3Al-type iron aluminides
[DE91-013028] N91-28358
Corrosion of refractory metals in liquid metal and gaseous environments
[DE91-009555] N91-28378
Processing and fabrication of Fe3Al-based alloys
[DE91-014546] N91-28382
Biomimetic thin film deposition
[DE91-012485] N91-28999
CORROSION TESTS
High-temperature solution annealing as an IASCC mitigation technique
[DE91-012220] N91-28352
CORRUGATING
Test of superplastically formed corrugated aluminum compression specimens with beaded webs
[NASA-TM-104119] N91-28373
COSMIC DUST
Scanning Transmission Ion Microscopy (STIM): A new technique for density mapping of microstructures
[DE91-011917] N91-28825
Properties of infrared-luminous galaxies, or, how I spent seven summer vacations N91-29098
Interstellar magnesium studies N91-29120
COSMIC RAY SHOWERS
The gamma ray content of ultrahigh energy cosmic radiation N91-29135
COSMIC RAYS
Explosion of a superbubble in a uniform magnetic field N91-29102
Study of gravitational collapse and cosmic ray abundances N91-29105
The gamma ray content of ultrahigh energy cosmic radiation N91-29135
COSMOLOGY
Aspects of reheating in first-order inflation
[NASA-CR-188705] N91-29108
Phase transitions triggered by quantum fluctuations in the inflationary universe
[NASA-CR-188698] N91-29112
The line of gravitation: On the quantization conditions in curved spacetime and uncertainty-driven inflation N91-29115
COST ANALYSIS
Next generation: Unmanned launch vehicles and upper stages: The needs N91-28210
Life cycle cost based program decisions N91-28248
The propulsion system is the key to airline-like operation of ETO vehicles N91-28256
Space shuttle requirements/configuration evolution N91-28264
Major system acquisitions process (A-109) N91-28268
Possible funding strategies N91-28272
COST EFFECTIVENESS
Propulsion technologies for near term N91-28262

COST ESTIMATES
Performance evaluation of multiversion database systems
[DE91-014340] N91-29090

COST REDUCTION
A white paper: Operational efficiency. New approaches to future propulsion systems N91-28197
Business not as usual N91-28266

COSTS
Advanced launch system N91-28208
Manufacturing processes N91-28244
An evaluation of monochrome solid-state video cameras
[DE91-012368] N91-28543

COUETTE FLOW
Study of spherical couette flow via 3-D spectral simulations: Large and narrow-gap flows and their transitions N91-28520

COULOMB POTENTIAL
The effect of strong Coulomb correlations on electron-phonon interactions in the copper oxides: Implications for transport
[DE91-013333] N91-28854

COUPLED MODES
Evidence of vibrational mode-coupling in 2-fluorethanol via high resolution infrared spectroscopy in a molecular beam
[AD-A236132] N91-28821

COUPLERS
A faint galaxy redshift survey and implications for cosmology N91-29100

COUPLING
Dynamic coupling effects in modeling and control of hard contact motion of a manipulator
[DE91-010393] N91-28574

COVARIANCE
Multidimensional spectral estimation using iterative methods
[AD-A237025] N91-28791

CRACK ARREST
Comparisons of irradiation-induced shifts in fracture toughness, crack arrest toughness, and Charpy impact energy in high-copper welds
[DE91-008881] N91-28349

CRACK INITIATION
Damage development under compression-compression fatigue loading in a stitched uniwoven graphite/epoxy composite material
[NASA-CR-188693] N91-28292
Damage progression during static and fatigue loading in metal matrix composites, volumes 1-3 N91-28301
Crack initiation under generalized plane strain conditions
[DE91-013410] N91-28623

CRACK PROPAGATION
Fracture micromechanics of intermetallic and ceramic matrix continuous fiber composites
[AD-A236638] N91-28280
Damage development under compression-compression fatigue loading in a stitched uniwoven graphite/epoxy composite material
[NASA-CR-188693] N91-28292
Local delamination in laminates with angle ply matrix cracks. Part 1: Tension tests and stress analysis
[NASA-TM-104055] N91-28293
Damage progression during static and fatigue loading in metal matrix composites, volumes 1-3 N91-28301
Elevated-temperature fracture resistances (K(sub IC), R-curves, gamma sub (omega OF)) of monolithic and composite ceramics using chevron-notched, bend tests
[NASA-TM-105090] N91-28418
Improving fatigue life in near-eutectic Sn Pb solders
[DE91-013844] N91-28603
Applications of a 2-D moving finite element formulation to elastic/viscoplastic dynamic fracture analysis
[DE91-009930] N91-28607
Influence of crack depth on the fracture toughness of reactor pressure vessel steel
[DE91-012537] N91-28611
Crack initiation under generalized plane strain conditions
[DE91-013410] N91-28623
Analysis of brittle intergranular crack propagation during stress corrosion cracking
[DE91-013666] N91-28630

CRACK TIPS
Near crack tip transverse strain effects estimated with a large strain hollow cylinder analogy
[DE91-012072] N91-28619

CRACKS
Critical issues in de-alloying and transcrystalline stress-corrosion cracking
[DE91-010190] N91-28608
Influence of crack depth on the fracture toughness of reactor pressure vessel steel
[DE91-012537] N91-28611

CRASHWORTHINESS
Computer simulation of an aircraft seat and occupant(s) in a crash environment: Program SOM-LA/SOM-TA user manual
[CR-R-90026] N91-28146

CRAY COMPUTERS
Solving computational grand challenges using a network of heterogeneous supercomputers
[DE91-013725] N91-28755
Load-balancing and performance of a gridless particle simulation on MIMD, SIMD, and vector supercomputers
[DE91-013758] N91-28756

CREEP ANALYSIS
Irradiation creep by climb-enabled glide driven by transient point defect processes
[DE91-012950] N91-28348

CREEP PROPERTIES
Irradiation creep by climb-enabled glide driven by transient point defect processes
[DE91-012950] N91-28348
Alloy development of Fe3Al for improved creep rupture properties
[DE91-014541] N91-28381
Creep and diffusion in nonstoichiometric oxides
[DE91-013766] N91-28435

CRITICAL LOADING
Stability of cylindrical laminates by higher orde r shear deformable theories N91-28638

CROSS CORRELATION
Quadrupole phenomena of noise from a subsonic jet impinging on a large, rigid, and flate plate N91-28818

CROSS FLOW
Research and development entitled smart structures for fossil energy applications
[DE91-002064] N91-28875

CROSSLINKING
Photocross-linked second order nonlinear optical polymers
[AD-A235855] N91-28385
New photocrosslinkable polymers for second order nonlinear optical processes
[AD-A235856] N91-28386

CRUISE MISSILES
Interceptor combinations for theater defense
[DE91-012990] N91-28810

CRYOGENIC COOLING
Advanced cryo propulsion systems N91-28212

CRYOGENIC FLUID STORAGE
Slush hydrogen propellant production, transfer, and expulsion studies at the NASA K-Site Facility
[NASA-TM-105191] N91-28449

CRYOGENIC FLUIDS
Analysis of foil bearings for high speed operation in cryogenic applications N91-28231
Transient two-phase flow of cryogenic fluid in a vertical transfer line during the cooldown process N91-28522

CRYOGENIC ROCKET PROPELLANTS
Advanced cryo propulsion systems N91-28212
Cryogenic combustion laboratory N91-28223
Cryogenic transfer options for exploration missions
[NASA-TM-105197] N91-28538

CRYOGENIC STORAGE
Cryogenic transfer options for exploration missions
[NASA-TM-105197] N91-28538

CRYOGENIC TEMPERATURE
Ultra-low temperature properties of amorphous solids
[DE91-012782] N91-28312
Thermal conductivity of solid hydrogen at low temperature N91-28330

CRYOGENIC WIND TUNNELS
A study of residual interference effects in adaptive wall testing of a 7-inch chord CAST-10-2/DOA 2 airfoil model
[NASA-CR-4390] N91-28138

CRYOGENICS
Cryogenic upper stage propulsion: RL10 and derivative engines N91-28202
Cryogenic combustion laboratory N91-28223
Analysis of foil bearings for high speed operation in cryogenic applications N91-28231
Cryogenic transfer options for exploration missions
[NASA-TM-105197] N91-28538
Pressure transducer and system for cryogenic environments
[NASA-CASE-LAR-14579-1] N91-28546
Development of a current collection loss management system for SDI homopolar power supplies
[DE91-012779] N91-28652

CRYOSTATS
Ultra-low temperature properties of amorphous solids
[DE91-012782] N91-28312

CRYSTAL DEFECTS
Substructure and electrical resistivity analyses of pure tungsten sheet
[DE91-014098] N91-28362
Alloy development of Fe3Al for improved creep rupture properties
[DE91-014541] N91-28381
The SNL, Livermore, Hopkinson bar apparatus for compressive materials testing at high strain-rates
[DE91-013132] N91-28612
Dynamic plasticity in transition from thermal activation to viscous drag
[DE91-013031] N91-28617
TEM analysis of enclosed crystal microstructures and interfaces
[DE91-012344] N91-29006
Defect studies in III-V thin film semiconductors
[DE91-012746] N91-29011
Evolution of defect cluster distributions during irradiation
[DE91-013405] N91-29024
The interaction of HVEM-generated point-defects with dissociated dislocations
[DE91-013353] N91-29027

CRYSTAL GROWTH
Novel ways of depositing ZnTe films by a solution growth technique
[DE91-002189] N91-28429
Adhesion between CVD diamond films and tungsten
[DE91-013757] N91-28434
Defect studies in III-V thin film semiconductors
[DE91-012746] N91-29011
Epitaxial growth of silicon on CoSi2(001)/Si(001)
[DE91-013387] N91-29015
Flux dynamics in a single crystal of Bi2Sr2CaCu2O(x)
[DE91-013763] N91-29036
Scanning tunneling microspectroscopy of solids and surfaces
[DE91-014515] N91-29043
Direct imaging of ordering in Si-Ge alloys, ultrathin superlattices, and buried Ge layers
[DE91-014580] N91-29044
Crystal surface analysis using matrix textural features classified by a probabilistic neural network
[DE91-014120] N91-29048
Defects and transport in mixed oxides
[DE91-014443] N91-29049

CRYSTAL LATTICES
Microwave enhanced diffusion?
[DE91-013312] N91-28415
A cluster approximation for the transfer-matrix method
[DE91-617790] N91-28804
Enhancing atom densities in solid hydrogen by isotopic substitution
[DE91-011189] N91-28824
Fundamental theory of crystal decomposition
[AD-A236637] N91-28988
Biomimetic thin film deposition
[DE91-012485] N91-28999

CRYSTAL STRUCTURE
Substructure and electrical resistivity analyses of pure tungsten sheet
[DE91-014098] N91-28362
Temperature dependence of the elastic behavior of structurally disordered metallic superlattices
[DE91-014007] N91-28377
Shock initiation of pentaerythritol tetranitrate crystals: Steric effects due to plastic flow
[DE91-013389] N91-28420
Investigation of the Deflagration-to-Detonation (DDT) process: The role of ignition and explosive properties in DDT
[DE91-011956] N91-28442
Welding of ductile intermetallic alloys
[DE91-009553] N91-28594
Molecular dynamics simulations of bulk displacement threshold energies in Si
[DE91-011957] N91-28846
A spectroscopic differential reflectometry study of (100), (110), (111), (311), and (511) silicon surfaces
[AD-A231022] N91-28985
The structure of Ta3N5 at 16K by time-of-flight neutron diffraction
[AD-A236596] N91-28987
Indium compounds which contain two different organic substituents. Crystal structure of (In(CH2CMe3)(CH2SiMe3)Cl)2, an interesting case of partial Ligand disorder in the solid state
[AD-A236730] N91-28989
Characterization of crystalline interfaces by advanced electron microscopy
[DE91-011883] N91-29002
TEM analysis of enclosed crystal microstructures and interfaces
[DE91-012344] N91-29006
Structure and dynamics in low-dimensional guest host solids
[DE91-012169] N91-29020
Parallel nanometer scale fabrication
[DE91-013016] N91-29026

Annealing and structure studies on Tl-2223 and Tl-1223 crystals
[DE91-014903] N91-29052

CRYSTAL SURFACES
In-situ REM imaging of surface processes on ceramic bulk crystals from 300 to 1670 K in a conventional TEM
[DE91-009923] N91-28405
A spectroscopic differential reflectometry study of (100), (110), (111), (311), and (511) silicon surfaces
[AD-A231022] N91-28985
Crystal surface analysis using matrix textural features classified by a probabilistic neural network
[DE91-014120] N91-29048

CRYSTALLINITY
Critical issues in de-alloying and transcrystalline stress-corrosion cracking
[DE91-010190] N91-28608
Characterization of crystalline interfaces by advanced electron microscopy
[DE91-011883] N91-29002
Kosterlitz-Thouless-like behavior over extended ranges of temperature and layer thickness in crystalline YBa2Cu3O(7-x) / PrBa2Cu3O(7-x) superlattices
[DE91-013237] N91-29014

CRYSTALLIZATION
An extension of a kinetic theory of polymer crystallization through the exclusion of negative barriers
[AD-A236999] N91-28387
Cocrystallization in blends of poly(butylene terephthalate) and poly(ester-ether) segmented block copolymers
[DE91-012224] N91-28438
Raman studies of stress-induced phase transformation in titania films
[DE91-012871] N91-29012

CRYSTALS
Measurements of ionization cross-section for electron energy-loss microanalysis under well defined scattering conditions
[DE91-013745] N91-28862
Fundamental theory of crystal decomposition
[AD-A236637] N91-28988
Shock initiation of pentaerythritol tetranitrate crystals: Optical absorption and emission studies
[DE91-013381] N91-29023

CULTURE (SOCIAL SCIENCES)
Lessons learned and their application to program development and cultural issues N91-28263
Cultural changes in aerospace N91-28265
Why engineers must know and manage organizational culture
[DE91-012425] N91-29071

CURIE TEMPERATURE
Pressure dependence of the Curie-temperature in the Kondo-lattice-compound YbNiSn
[DE91-013672] N91-29046

CURING
Process for bonding elastomers to metal
[NASA-CASE-LAR-13645-1] N91-28424
Flush mounting of thin film sensors
[NASA-CASE-LAR-14446-1] N91-28454

CURRENT DENSITY
Excess heat production in composite superconductors during current redistribution
[DE91-013547] N91-29016
Overview of the status of and prospects for high-T(sub c) wire and tape development
[DE91-014609] N91-29045

CURRENT SHEETS
Current sheet formation and rapid reconnection in the solar corona N91-28884

CURVATURE
Computing minimal surfaces via level set curvature flow
[DE91-014709] N91-28759
Phase transitions triggered by quantum fluctuations in the inflationary universe
[NASA-CR-188698] N91-29112

CUSHIONS
Human body protection in a dynamic environment. Cushioning mechanics
[ITN-91-85149] N91-28733

CYCLOGENESIS
On the initiation of surface cyclones by upper tropospheric disturbances N91-28704
A numerical simulation of a tornado-scale vortex in a three-dimensional cloud model N91-28705

CYCLONES
On the initiation of surface cyclones by upper tropospheric disturbances N91-28704

CYCLOTRON FREQUENCY
An assessment of the lifetime of Faraday shield elements
[DE91-012228] N91-28463
Mode conversion of Alfven waves induced by quadrupole magnetic field modulation N91-28924

CYCLOTRON RADIATION
Rapid acceleration of protons in a nonlinear magnetosonic wave and their energy spectrum
N91-28905

CYCLOTRON RESONANCE
Mode conversion of Alfven waves induced by quadrupole magnetic field modulation N91-28924
Microwave-generated plasma thruster
[DE91-013131] N91-28948
The ECR-plasma deposition of silicon nitride on a tunnel oxide
[DE91-014665] N91-29051

CYGNUS CONSTELLATION
Upper limits for the flux of very high-energy gamma radiation from Cygnus X-3 and for the explosion rate of primordial black holes obtained by the Haleakala Gamma Ray Observatory N91-29134

CYLINDRICAL BODIES
Mechanical modeling of stress generation during cure of encapsulating resins
[DE91-011496] N91-28393
Near crack tip transverse strain effects estimated with a large strain hollow cylinder analogy
[DE91-012072] N91-28619
Stability of cylindrical laminates by higher orde r shear deformable theories N91-28638

CYLINDRICAL CHAMBERS
Viscoplastic analysis of an experimental cylindrical thrust chamber liner
[NASA-TM-103287] N91-28622

CZOCHRALSKI METHOD
Donor formation under hydrogen plasma exposure and ion implantation
[DE91-011958] N91-29004

D

DAMAGE
Damage development under compression-compression fatigue loading in a stitched uniwoven graphite/epoxy composite material
[NASA-CR-188693] N91-28292

DAMPING
Actively damped landing gear system N91-28165
Formation and dynamics of solitary waves and vortices in driven and damped systems N91-28942

DARK MATTER
Testing the Big Bang: Light elements, neutrinos, dark matter and large-scale structure
[NASA-CR-188701] N91-29111
Gravitational evolution of large-scale structure in the universe N91-29121

DATA ACQUISITION
X ray Tomographic Microscopy (XTM)
[DE91-011930] N91-28599
Work plan for the preliminary site investigation for McMurdo Station, Ross Island, Antarctica
[DE91-015100] N91-28675
Alaska wave data index
[AD-A236635] N91-28707

DATA BASE MANAGEMENT SYSTEMS
The DataShoP: A database of weak-shock constitutive data
[DE91-013349] N91-28620
ARAC: A computer-based emergency-response dose-assessment service with global application potential
[DE91-013248] N91-28700
Software development experiences with a distributed database in a large, distributed computer system
[DE91-012818] N91-28750
Embedding ADAMS in FORTRAN
[DE91-014346] N91-28754
Concurrent access to O-trees
[DE91-014348] N91-28782
The EOS TPC analysis shell
[DE91-011873] N91-29073
Threatened Area Database System (TADS) computer program
[DE91-012491] N91-29074
A framework for data and information
[DE91-012416] N91-29075
Distributed relational database design and implementation for a large, distributed computer system
[DE91-012812] N91-29077
Developing a GIS to facilitate data analysis for environmental restoration of a large waste site
[DE91-013222] N91-29078
Document format considerations for a document tracking and storage system
[DE91-013402] N91-29079
The ADAMS interactive interpreter
[DE91-014345] N91-29080
Implementation of a hypercube database system
[DE91-014285] N91-29089
Performance evaluation of multiversion database systems
[DE91-014340] N91-29090
Safe referential integrity structures in relational databases
[DE91-014586] N91-29091

DATA BASES
Solid rocket propulsion N91-28206
The DataShoP: A database of weak-shock constitutive data
[DE91-013349] N91-28620
Software development experiences with a distributed database in a large, distributed computer system
[DE91-012818] N91-28750
An introduction to the ADAMS interface language, part 1
[DE91-014344] N91-28757
The symbolic computation and automatic analysis of trajectories
[NASA-CR-188159] N91-28787
A portable and independent edge fluctuation diagnostic
[DE91-014357] N91-28971
Distributed relational database design and implementation for a large, distributed computer system
[DE91-012812] N91-29077
Safe referential integrity structures in relational databases
[DE91-014586] N91-29091

DATA FLOW ANALYSIS
Common reflection point stacking: A macro model driven approach to dip moveout
[ISBN-90-9003020-4] N91-28676

DATA LINKS
Runway Visual Range (RVR) Operational Test and Evaluation (OT and E)/integration test plan
[DOT/FAA/CT-TN91/4] N91-28176
Design of an interactive satellite communications system analysis program
[AD-A237030] N91-28459

DATA MANAGEMENT
Work plan for the preliminary site investigation for McMurdo Station, Ross Island, Antarctica
[DE91-015100] N91-28675
Performance evaluation of multiversion database systems
[DE91-014340] N91-29090

DATA PROCESSING
Common reflection point stacking: A macro model driven approach to dip moveout
[ISBN-90-9003020-4] N91-28676
Software development experiences with a distributed database in a large, distributed computer system
[DE91-012818] N91-28750
Visualization using a data flow-based paradigm
[DE91-013851] N91-28763
Distributed relational database design and implementation for a large, distributed computer system
[DE91-012812] N91-29077
Developing a GIS to facilitate data analysis for environmental restoration of a large waste site
[DE91-013222] N91-29078

DATA RECORDERS
Laser speckle velocimetry with photorefractive recording and anamorphic optical processing N91-28880

DATA REDUCTION
Performance of the Intel iPSC/860 and Ncube 6400 hypercubes
[DE91-012370] N91-28738

DATA STORAGE
Recovery of saturated video signals from vidicons by dynamic cathode biasing
[DE91-012402] N91-28464
The role of the UNIX(tm) central computing facility in a multi-purpose national laboratory
[DE91-012361] N91-28737

DATA STRUCTURES
A geometry based method of integrated engineering design, analysis, and optimization
[DE91-008588] N91-28457

DATA SYSTEMS
A PC based frequency domain LV processor
[DE91-009056] N91-28541

DATA TRANSMISSION
Wideband adaptive HF modem
[ITN-91-85147] N91-28471
Seeking solutions: High-performance computing for science
[PB91-169763] N91-28752

DECELERATION
Scanning Transmission Ion Microscopy (STIM): A new technique for density mapping of microstructures
[DE91-011917] N91-28825

DECISION MAKING
Space systems requirements: The Navy approach
[AD-A236490] N91-28181

A selection tool for choosing the best participative problem-solving technique
[DE91-012421] N91-29066
The human side of value engineering
[DE91-012817] N91-29068
How to increase meeting effectiveness and efficiency
[DE91-012420] N91-29070
Why engineers must know and manage organizational culture
[DE91-012425] N91-29071
The effects of information availability on the group consensus process
[DE91-012428] N91-29076
Generalized hypertext in a knowledge-based decision support shell environment N91-29086

DECISION THEORY
Efficient soft decision decoding of Reed-Muller codes and related non-linear generalizations
[ITN-91-85146] N91-28760
A framework for data and information
[DE91-012416] N91-29075
The effects of information availability on the group consensus process
[DE91-012428] N91-29076

DECODERS
Efficient soft decision decoding of Reed-Muller codes and related non-linear generalizations
[ITN-91-85146] N91-28760

DECODING
Direction discriminating hearing aid
[NASA-CASE-GSC-13027-1] N91-28726
Efficient soft decision decoding of Reed-Muller codes and related non-linear generalizations
[ITN-91-85146] N91-28760

DECOMPOSITION
Composite material systems for hydrogen management N91-28229
Spontaneous cluster decomposition in a quadrupole ion trap
[DE91-012519] N91-28836
Fundamental theory of crystal decomposition
[AD-A236637] N91-28988

DEFECTS
Failure analysis case histories of Canadian forces aircraft landing gear components N91-28151
Damage development under compression-compression fatigue loading in a stitched uniwoven graphite/epoxy composite material
[NASA-CR-188693] N91-28292
The influence of defects on the mechanical properties of short fibre reinfornced thermoplastics N91-28300
Development of nondestructive evaluation methods and prediction of effects of flaws on the fracture behavior of structural ceramics
[DE91-012471] N91-28410
Influence of crack depth on the fracture toughness of reactor pressure vessel steel
[DE91-012537] N91-28611
Stability of cylindrical laminates by higher orde r shear deformable theories N91-28638
Defects and transport in mixed oxides
[DE91-014443] N91-29049

DEFENSE PROGRAM
Interceptor combinations for theater defense
[DE91-012990] N91-28810

DEFLAGRATION
Investigation of the Deflagration-to-Detonation (DDT) process: The role of ignition and explosive properties in DDT
[DE91-011956] N91-28442
The deflagration-to-detonation transition in granular HMX
[DE91-014591] N91-28448

DEFLECTION
Flutter of laminated rectangular plates including finite deflection and shear deformation N91-28639

DEFORMATION
Strength and electrical conductivity of deformation processed Cu-15 v/o Fe metal composites produced by powder metallurgy/techniques
[DE91-013658] N91-28291
Joining of aluminum-based particulate-reinforced metal-matrix composites N91-28298
The DataShoP: A database of weak-shock constitutive data
[DE91-013349] N91-28620
Bauschinger effect during shock loading
[DE91-014606] N91-28634
Stability of cylindrical laminates by higher orde r shear deformable theories N91-28638
Quantized planes and multiparameter deformations of Heisenberg and GL(N) algebras
[DE91-012481] N91-28793

DEGRADATION
Joining of aluminum-based particulate-reinforced metal-matrix composites N91-28298
Modification and evaluation of Elastomer Test Machine (ETM)
[AD-A236143] N91-28540

DELAMINATING
Local delamination in laminates with angle ply matrix cracks. Part 1: Tension tests and stress analysis
[NASA-TM-104055] N91-28293
Finite element modeling of 2-D delamination growth in laminated composites N91-28302
Interlaminar fracture characterization: A current review
[NASA-CR-187573] N91-28626

DEMAGNETIZATION
Effect of size and geometry on levitation force measurements between permanent magnets and high-temperature superconductors
[DE91-012472] N91-29008

DEMAND (ECONOMICS)
EIA publications directory, 1990
[DE91-014350] N91-29082

DENDRITIC CRYSTALS
Interpreting solidification phenomena and microstructural evolution in metals through the use of transparent model alloy systems
[DE91-012629] N91-28347

DENSE PLASMAS
Hydrodynamic instabilities in laser driven implosion
N91-28897

DENSIFICATION
A study of the influence of temperature gradients on densification of glass powder compacts
[DE91-012337] N91-28399

DENSITY DISTRIBUTION
Lidar studies of sporadic sodium layers, gravity waves and density spectra in the mesopause and stratopause regions at Urbana and Arecibo N91-28690
Scanning Transmission Ion Microscopy (STIM): A new technique for density mapping of microstructures
[DE91-011917] N91-28825
Multiple nuclei, cluster core dynamics, and the velocity distributions of gravitating systems N91-29119

DENSITY MEASUREMENT
Optical diagnostic investigation of low Reynolds number nozzle flows N91-28233
Scanning Transmission Ion Microscopy (STIM): A new technique for density mapping of microstructures
[DE91-011917] N91-28825

DEOXYRIBONUCLEIC ACID
The use of AMS to the biomedical sciences
[DE91-012037] N91-28712
Novel methods for physical mapping of the human genome applied to the long arm of chromosome 5
[DE91-012894] N91-28717
Searching for consensus patterns on a hypercube
[DE91-013233] N91-28753

DEPOSITION
Novel ways of depositing ZnTe films by a solution growth technique
[DE91-002189] N91-28429
Data users guide to the mountain cloud chemistry project
[PB91-168484] N91-28697
Spectroscopic and ion probe characterization of laser produced plasmas used for thin film growth
[DE91-013425] N91-28959
Biomimetic thin film deposition
[DE91-012485] N91-28999
The ECR-plasma deposition of silicon nitride on a tunnel oxide
[DE91-014665] N91-29051

DERIVATION
Cryogenic upper stage propulsion: RL10 and derivative engines N91-28202

DESIGN ANALYSIS
Landing Gear Design Loads
[AGARD-CP-484] N91-28150
Failure analysis case histories of Canadian forces aircraft landing gear components N91-28151
Application of the Air Force guide specification 87221A to ground loads N91-28152
Considerations on optimality of landing gear arrangement and design N91-28156
Questions: Assessing the structure of knowledge and the use of information in design problem-solving
N91-28169
Discrete posynomial programming with applications to spacecraft protective structures design optimization
N91-28190
Space shuttle propulsion systems N91-28200
Liquid rocket engine flight certification N91-28250
Comparison of dynamic isotope power systems for distributed planet surface applications
[NASA-TM-4303] N91-28278
Advancing electric vehicle technology
[DE91-013004] N91-28575
Mechanical design optimization of robot manipulator performance N91-28589
Design and analysis of the 50 mm collider dipole vacuum vessel
[DE91-012490] N91-28610
A system approach to the design of superconducting magnets
[DE91-012707] N91-29010

DESORPTION
The effect of stress on hydrogen uptake and desorption by A-286
[NASA-TM-103537] N91-28341
Desorption of Al, Au, Ag using surface plasmon excitation
[DE91-013726] N91-28493
Desorption of large organic molecules by laser-induced plasmon excitation
[DE91-013415] N91-28852

DETECTION
ARAC: A computer-based emergency-response dose-assessment service with global application potential
[DE91-013248] N91-28700
High intensity neutrino beams at KAON
[DE91-012147] N91-28830

DETONATION
Semiconductor Bridge (SCB) research and development
[DE91-011493] N91-28319
Investigation of the Deflagration-to-Detonation (DDT) process: The role of ignition and explosive properties in DDT
[DE91-011956] N91-28442
Improving the performance of blasting caps
[NASA-CASE-LAR-13832-1] N91-28444
Mechanisms of EBW HE initiation
[DE91-013565] N91-28447
The deflagration-to-detonation transition in granular HMX
[DE91-014591] N91-28448
A study of the impact of reaction rates on equation of state
[DE91-013375] N91-28621

DETONATION WAVES
Comparisons between fast shock tube calculations and tests
[DE91-013496] N91-28177

DETONATORS
Improving the performance of blasting caps
[NASA-CASE-LAR-13832-1] N91-28444
Mechanisms of EBW HE initiation
[DE91-013565] N91-28447
Electrostatic discharge effects on EBW detonators
[DE91-013250] N91-28467

DEUTERIUM
Space fusion energy conversion using a field reversed configuration reactor: A new technical approach for space propulsion and power N91-28217
Reactive characterization as a probe of the nature of catalytic sites
[DE91-014536] N91-28333
Enhancing atom densities in solid hydrogen by isotopic substitution
[DE91-011189] N91-28824
Mode selectivity in cluster-molecule interactions: Ni13 + D2
[DE91-013352] N91-28859

DEUTERONS
Photodisintegration of the deuteron at medium and high energies
[DE91-014458] N91-28865

DIAMAGNETISM
Strongly interacting fermion systems
[DE91-012284] N91-28848

DIAMINES
Polyimides prepared from 3,5-diamino benzo trifluoride
[NASA-CASE-LAR-14206-1] N91-28425

DIAMONDS
US assessment of the new diamond technology in Japan
[PB91-167395] N91-28404
Mechanical properties of diamond and diamond-like films
[DE91-011373] N91-28406
Adhesion between CVD diamond films and tungsten
[DE91-013757] N91-28434

DIELECTRICS
Radiation damage of ceramics by electron microscopy
[DE91-012186] N91-28396
Chemistry of electronic ceramic materials. Proceedings of the International Conference on the Chemistry of Electronic Ceramic Materials
[NASA-CR-188688] N91-28403

DIFFERENTIAL CALCULUS
ZLIB: A numerical library for differential algebra (A user's guide for version 1.0)
[DE91-012552] N91-28794

DIFFERENTIAL EQUATIONS
Analysis of passive and active discrete-distributed linear dynamical systems using Green's function methods N91-28141
A comparison of the potential and the Euler formulations of the equations of motion for transonic flow
[DE91-014731] N91-28142
Using trees to compute approximate solutions to ordinary differential equations exactly
[LAC90-R24] N91-28788
Computations involving differential operators and their actions on functions N91-28789
JPRS report: Science and technology. USSR: Physics and mathematics
[JPRS-UPM-90-006] N91-28811
Equilibria and dynamics of temperature in a fusion reactor plasma N91-28937
Non similarity solution approximation to the thermal hydraulic quenchback in superconductors
[DE91-013964] N91-29040

DIFFRACTION PATTERNS
Diffraction patterns produced by periodic and turbulent flowing gases including applications of photorefractive temporal filtering
[DE91-012636] N91-28553
Characterization of crystalline interfaces by advanced electron microscopy
[DE91-011883] N91-29002

DIFFUSION
Microwave enhanced diffusion?
[DE91-013312] N91-28415
Creep and diffusion in nonstoichiometric oxides
[DE91-013766] N91-28435
Gas evolution from spheres
[DE91-012807] N91-28510
Diffusion and relaxation in Hamiltonian chaos N91-28934
Equilibria and dynamics of temperature in a fusion reactor plasma N91-28937
Diffusion through stochastic webs in two and more dimensions N91-28941
Defects and transport in mixed oxides
[DE91-014443] N91-29049

DIFFUSION COEFFICIENT
The effect of stress on hydrogen uptake and desorption by A-286
[NASA-TM-103537] N91-28341
Models of collisional transport across a magnetic field with destroyed surfaces N91-28900

DIGITAL COMPUTERS
SANDAC V computer electromagnetic interface characteristics: Problems and solutions
[DE91-014334] N91-29065

DIGITAL SYSTEMS
A reconfigurable strategy for distributed digital process control
[DE91-013740] N91-28786

DIGITAL TO ANALOG CONVERTERS
High-speed and high-resolution analog-to-digital and digital-to-analog converters
[ETN-90-97265] N91-28735

DIGITAL TRANSDUCERS
High-speed and high-resolution analog-to-digital and digital-to-analog converters
[ETN-90-97265] N91-28735

DIMPLING
Cross-sectional TEM specimen preparation of free-standing metal multi-layered films
[DE91-011117] N91-28351

DIRECTIVITY
Direction discriminating hearing aid
[NASA-CASE-GSC-13027-1] N91-28726
Quadrupole phenomena of noise from a subsonic jet impinging on a large, rigid, and flate plate N91-28818

DIRECTORIES
Directory of Organizational Technical Report Acronym Codes (DOTRAC)
[AD-A237000] N91-29072
EIA publications directory, 1990
[DE91-014350] N91-29082

DIRICHLET PROBLEM
An iterative substructuring algorithm for problems in three dimensions
[DE91-014388] N91-28758

DISCONTINUITY
Effect of guideway discontinuities on magnetic levitation and drag forces
[DE91-014011] N91-28815

DISCRIMINATION
Direction discriminating hearing aid
[NASA-CASE-GSC-13027-1] N91-28726

DISEASES
New techniques for positron emission tomography in the study of human neurological disorders
[DE91-013855] N91-28728

DISK OPERATING SYSTEM (DOS)
Measuring and modelling disk I/O subsystems
[ISBN-90-6275-567-4] N91-28736

DISLOCATIONS (MATERIALS)
The interaction of HVEM-generated point-defects with dissociated dislocations
[DE91-013353] N91-29027

DISPERSING
Energy dispersive x ray diffraction study of glassy Bi2Sr2CaCu2O(x) filaments produced by gas-jet fiberization
[DE91-012021] N91-28407
Direct contact heat transfer to a dispersal droplet with change of phase N91-28521
A study on particle dispersion in two-dimensional mixing layer flows N91-28537

DISPLACEMENT
An experimental investigation of a compliant surface beneath a turbulent boundary layer N91-28523
Modification and evaluation of Elastomer Test Machine (ETM)
[AD-A236143] N91-28540

DISPLAY DEVICES
Runway Visual Range (RVR) Operational Test and Evaluation (OT and E)/integration test plan
[DOT/FAA/CT-TN91/4] N91-28176
Using HSYS in the analysis of human-system interactions: Examples from the offshore petroleum industry
[DE91-013218] N91-28732
Visualization using a data flow-based paradigm
[DE91-013851] N91-28763

DISSIPATION
Flux pinning and dissipation in high-temperature superconductors
[DE91-014466] N91-29042

DISSOCIATION
The solubility and dissociation kinetics of hydroxymethyl hydroperoxide in aqueous solution
[DE91-013336] N91-28318
Mode selectivity in cluster-molecule interactions: Ni13 + D2
[DE91-013352] N91-28859

DISSOLVED GASES
Gas evolution from spheres
[DE91-012807] N91-28510

DISSOLVING
Mechanisms of bacterial metals removal from solids
[DE91-012808] N91-28356
Synthesis and properties of novel cluster phases
[DE91-013006] N91-29013

DISTRIBUTED PARAMETER SYSTEMS
Analysis of passive and active discrete-distributed linear dynamical systems using Green's function methods N91-28141
A reconfigurable strategy for distributed digital process control
[DE91-013740] N91-28786

DISTRIBUTED PROCESSING
The role of the UNIX(tm) central computing facility in a multi-purpose national laboratory
[DE91-012361] N91-28737
Prototyping parallel and distributed programs in proteus
[AD-A236597] N91-28746
Software development experiences with a distributed database in a large, distributed computer system
[DE91-012818] N91-28750
Taxonomy and algorithms for volume rendering on multicomputers
[AD-A236632] N91-28771
Mapping implicit spectral methods to distributed memory architectures
[NASA-CR-187592] N91-28806
The EOS TPC analysis shell
[DE91-011873] N91-29073
Distributed relational database design and implementation for a large, distributed computer system
[DE91-012812] N91-29077

DISTRIBUTION FUNCTIONS
Simulation of a storage ring free electron laser with a mapping algorithm for distribution functions
[DE91-012387] N91-28552

DOCUMENT STORAGE
Document format considerations for a document tracking and storage system
[DE91-013402] N91-29079

DOPED CRYSTALS
Chemistry and materials science research report
[DE91-011507] N91-28305
Photocross-linked second order nonlinear optical polymers
[AD-A235855] N91-28385
Effect of TCP doping on the remnant polarization in uniaxially oriented poly(vinylidene fluoride) films
[AD-A237001] N91-28388
Donor formation under hydrogen plasma exposure and ion implantation
[DE91-011958] N91-29004
Structure and dynamics in low-dimensional guest host solids
[DE91-012169] N91-29020

DOPPLER EFFECT
Edge technique for measurement of laser frequency shifts including the Doppler shift
[NASA-CASE-GSC-13343-1] N91-28557

DOPPLER RADAR
Multiple frequency atmospheric radar techniques N91-28683
Low-level curvature shear and supercell thunderstorm behavior N91-28701

DRAG
CFD applications in chemical propulsion engines N91-28234

DRILLING
Geothermal materials development
[DE91-013972] N91-28660

DROP SIZE
Liquid jet breakup and atomization in rocket chambers under dense spray conditions N91-28227

DROP TESTS
F-106B airplane active control landing gear drop test performance N91-28164

DROPS (LIQUIDS)
Liquid-propellant droplet vaporization and combustion in high pressure environments N91-28225
Spray combustion under oscillatory pressure conditions N91-28226
Liquid jet breakup and atomization in rocket chambers under dense spray conditions N91-28227
Droplet-turbulence interactions in subcritical and supercritical evaporating sprays N91-28228
Gas evolution from spheres
[DE91-012807] N91-28510
Direct contact heat transfer to a dispersal droplet with change of phase N91-28521

DRYING
Drying of gelcast ceramics
[DE91-012955] N91-28413

DUCTED FLOW
Experimental and theoretical investigation of unsteady forced convection in ducts N91-28524
A critical analysis of anisotropic k-epsilon modeling and its application to turbulence-driven secondary flows N91-28533

DUCTILITY
The effect of ductile innerlayers on the mechanical performance of fiber-reinforced composite materials N91-28295
The effect of TiB2 reinforcement on the mechanical properties of an Al-Cu-Li alloy-based metal-matrix composite N91-28337
Rapid solidification processing of Al3Ti and Al3Ti plus copper
[AD-A236600] N91-28343
Effects of sample size and loading rate on the transition behavior of a DCI alloy
[DE91-012015] N91-28346
Properties of large heats of Fe3Al-based alloys
[DE91-013268] N91-28359
Erosion studies on a Fe3Al-based iron aluminide and 1100 Al
[DE91-012529] N91-28360
Welding of ductile intermetallic alloys
[DE91-009553] N91-28594
Assessment of ductile fracture methodology based on applications to large-scale experiments
[DE91-009920] N91-28614

DUCTS
Solution to quasi-axisymmetric internal compressible flows using the stream tube approach N91-28526

DUPLEX OPERATION
APFIM characterization of the spinodal decomposition in duplex stainless steels
[DE91-014256] N91-28371

DURABILITY
Composite material systems for hydrogen management N91-28229
Durability of polymeric materials used in zinc/bromine flow batteries
[DE91-012864] N91-28487

DYE LASERS
Hydrodynamic evolution of picosecond laser-plasmas
[DE91-013245] N91-28958

DYNAMIC CHARACTERISTICS
Numerical simulation of the dynamic behavior of landing gears N91-28160
Modeling molecular processes in the environment
[DE91-013790] N91-28671

Nuclear magnetic resonance studies of atomic motion in lithium chloroborate and lithium thiosilicate glassy fast ionic conductors
[DE91-012677] N91-28843

DYNAMIC CONTROL
Dynamic coupling effects in modeling and control of hard contact motion of a manipulator
[DE91-010393] N91-28574
Recursive linearization of multibody dynamics and application to control design N91-28588

DYNAMIC LOADS
F-106B airplane active control landing gear drop test performance N91-28164

DYNAMIC MODELS
Kinematic analysis of legged system locomotion on smooth horizontal surfaces N91-28586
Invariant metrics for Hamiltonian systems
[DE91-014236] N91-28807

DYNAMIC RESPONSE
A methodology for using nonlinear aerodynamics in aeroservoelastic analysis and design
[NASA-TM-104087] N91-28131
Calculation of interactions between air and ground of landing N91-28161
Response of the polymers KEL-F, polysulfone, high density polyethylene and polymethylmethacrylate to shock loading and release from 0.3 to 2.4 GPa
[DE91-012867] N91-28411

DYNAMIC STABILITY
Microwave instability at transition: Stability diagram approach
[DE91-013202] N91-28867

DYNAMIC STRUCTURAL ANALYSIS
Experimental study of growth rate enhancement and structure of compressible turbulent free shear layers
N91-28517
Explicit models for proportional damping in Timoshenko beams N91-28642

DYNAMIC TESTS
Suspension device for low-frequency structures
[NASA-CASE-LAR-14272-1-CU] N91-28184

DYNAMICAL SYSTEMS
Analysis of passive and active discrete-distributed linear dynamical systems using Green's function methods
N91-28141
The symbolic computation and automatic analysis of trajectories
[NASA-CR-188159] N91-28787
Computations involving differential operators and their actions on functions N91-28789
Regular motion and symmetry in the relativistic standard map N91-28933

DYNAMO THEORY
Turbulent dynamo and subgrid-scale modeling of MHD turbulence N91-28887
Sawteeth in the MST reversed field pinch
[DE91-014288] N91-29126

DYNAMOMETERS
System and component design and test of a 10 hp, 18,000 rpm AC dynamometer utilizing a high frequency AC voltage link, part 1
[NASA-CR-188442] N91-28539

E

EARTH ATMOSPHERE
Natural and anthropogenic climate change
[DE91-014734] N91-28673
Radiative transfer model for a spherical atmosphere
N91-28689
ARAC: A computer-based emergency-response dose-assessment service with global application potential
[DE91-013248] N91-28700

EARTH CRUST
Heat flow data and thermal state of the continental lithosphere N91-28682

EARTH IONOSPHERE
Plasma properties
[DE91-013933] N91-28978

EARTH MAGNETOSPHERE
Magnetospheric VLF line radiation N91-28693
Plasma properties
[DE91-013933] N91-28978

EARTH MANTLE
High-temperature elasticity and Earth's upper mantle
N91-28679

EARTH ORBITS
A white paper: Operational efficiency. New approaches to future propulsion systems N91-28197
Heavy-lift launch vehicle propulsion considerations
N91-28236

EARTH SURFACE
Fluctuations in near-surface backscattering to a descending CW radar
[ITN-91-85140] N91-28469

ECONOMIC ANALYSIS
EIA publications directory, 1990
[DE91-014350] N91-29082

ECONOMIC FACTORS
Making energy efficiency happen
[DE91-013057] N91-28655

ECONOMIC IMPACT
Moving finite elements: A continuously adaptive method for computational fluid dynamics
[DE91-013391] N91-28513

ECONOMICS
Technology transfer methodology N91-28240

ECOSYSTEMS
Biomarker-based biomonitoring for evaluating health and ecological effects on environmental contamination
[DE91-013729] N91-28719

EDDY CURRENTS
Recent ASME Code Section 11 developments for surface examination through coatings
[DE91-014069] N91-28437
Nondestructive evaluation tools and experimental studies for monitoring the health of space propulsion systems
[NASA-TM-105164] N91-28605

EDGE DISLOCATIONS
Shock initiation of pentaerythritol tetranitrate crystals: Steric effects due to plastic flow
[DE91-013389] N91-28420

EIGENVALUES
A 2D field solver for periodic structures with special corner elements
[DE91-012323] N91-28792
Nonlinear equations for weakly unstable modes
N91-28927

EIGENVECTORS
Molecular eigenstate spectroscopy: Application to the intramolecular dynamics of some polyatomic molecules in the 3000 to 7000 cm(exp -1) region
[DE91-013154] N91-28839
Nonlinear equations for weakly unstable modes
N91-28927

EINSTEIN EQUATIONS
Numerical models of equilibrium between matter and black holes N91-29101

EKMAN LAYER
On the initiation of surface cyclones by upper tropospheric disturbances N91-28704

EL NINO
A study of El Nino/Southern Oscillation: Numerical experiments and data analysis N91-28710
Interactions between the north Pacific Ocean and the Northern Hemisphere atmosphere during El Nino
N91-28711

ELASTIC DEFORMATION
EXAFS studies of elastic strain in dilute binary alloys
[DE91-012678] N91-28353

ELASTIC PROPERTIES
An experimental investigation of a compliant surface beneath a turbulent boundary layer N91-28523
The DataShoP: A database of weak-shock constitutive data
[DE91-013349] N91-28620
High-temperature elasticity and Earth's upper mantle
N91-28679

ELASTIC SCATTERING
Antiproton-induced elastic and inelastic scattering at intermediate energies
[DE91-013068] N91-28849

ELASTOHYDRODYNAMICS
Thermal and non-Newtonian effects in elastohydrodynamic lubrication of rolling-sliding contacts
N91-28590

ELASTOMERS
Process for bonding elastomers to metal
[NASA-CASE-LAR-13645-1] N91-28424
Modification and evaluation of Elastomer Test Machine (ETM)
[AD-A236143] N91-28540

ELASTOPLASTICITY
Investigation of thermomechanical behavior of metal matrix composites N91-28296
Plastic analysis of a circular rod subjected to sinusoidal thermal cycling
[DE91-011845] N91-28609

ELECTRIC AUTOMOBILES
Pacific Northwest hydrogen feasibility study
[DE91-013427] N91-28445

ELECTRIC BATTERIES
Durability of polymeric materials used in zinc/bromine flow batteries
[DE91-012864] N91-28487
Electric and hybrid vehicles program
[DE91-013113] N91-28573
Advancing electric vehicle technology
[DE91-013004] N91-28575

ELECTRIC BRIDGES
Semiconductor Bridge (SCB) research and development
[DE91-011493] N91-28319
Electrostatic discharge effects on EBW detonators
[DE91-013250] N91-28467

ELECTRIC CHARGE
Recovery of saturated video signals from vidicons by dynamic cathode biasing
[DE91-012402] N91-28464

ELECTRIC CONNECTORS
Flush mounting of thin film sensors
[NASA-CASE-LAR-14446-1] N91-28454
Providing common access mechanisms for dissimilar network interconnection nodes
[AD-A236630] N91-28770

ELECTRIC CURRENT
Semiconductor Bridge (SCB) research and development
[DE91-011493] N91-28319
Magnetization and critical currents of tin-core multifilamentary Nb3Sn conductors
[DE91-012241] N91-28994
Overview of the status of and prospects for high-T(sub c) wire and tape development
[DE91-014609] N91-29045

ELECTRIC FIELDS
Ferroelectric fatigue in modified bulk lead zirconate titanate ceramics
[DE91-012647] N91-28417
Computer modeling of ceramic melters to assess impacts of process and design variables on performance
[DE91-013668] N91-28431
Desorption of Al, Au, Ag using surface plasmon excitation
[DE91-013726] N91-28493
The effect of strong Coulomb correlations on electron-phonon interactions in the copper oxides: Implications for transport
[DE91-013333] N91-28854

ELECTRIC GENERATORS
Development of biomass as an alternative fuel for gas turbines
[DE91-012129] N91-28441
Issues concerning centralized versus decentralized power deployment
[NASA-CR-187121] N91-28648

ELECTRIC HYBRID VEHICLES
Electric and hybrid vehicles program
[DE91-013113] N91-28573

ELECTRIC MOTOR VEHICLES
Laboratory testing of the dual traction battery GC12V100
[DE91-012743] N91-28491
Electric and hybrid vehicles program
[DE91-013113] N91-28573
Advancing electric vehicle technology
[DE91-013004] N91-28575

ELECTRIC POTENTIAL
Driven shielding capacitive proximity sensor
[NASA-CASE-GSC-13377-1] N91-28785
Coherent charge fluctuations in Josephson junctions and the oscillations of the effective capacitance
[DE91-618098] N91-29019

ELECTRIC POWER PLANTS
United States Department of Energy solar receiver technology development
[DE91-012653] N91-28651
Advanced water-cooled phosphoric acid fuel cell development
[DE91-012243] N91-28659

ELECTRIC POWER SUPPLIES
Issues concerning centralized versus decentralized power deployment
[NASA-CR-187121] N91-28648

ELECTRIC PROPULSION
Historical perspectives: The role of the NASA Lewis Research Center in the national space nuclear power programs
[NASA-TM-105196] N91-29138

ELECTRIC SPARKS
Electrostatic discharge effects on EBW detonators
[DE91-013250] N91-28467

ELECTRIC SWITCHES
Procyon experiments utilizing foil-fuse opening switches
[DE91-014605] N91-28499

ELECTRIC WIRE
Automated verification of system configuration
[DE91-012520] N91-28481

ELECTRICAL FAULTS
Some high voltage DC breakdown properties of thick film circuits on alumina
[DE91-014675] N91-28500
ELECTRICAL GROUNDING
Follow-on cable coupling lightning test, volume 1
[NASA-CR-184123] N91-28192
ELECTRICAL IMPEDANCE
Perturbation treatment of the longitudinal coupling impedance of a toroidal beam tube
[DE91-013884] N91-28495
Microwave instability at transition: Stability diagram approach
[DE91-013202] N91-28867
The effect of the quantum susceptance on the gain of superconducting quasiparticle mixers
[DE91-012352] N91-29021
ELECTRICAL MEASUREMENT
Transmission/reflection and short-circuit line permittivity measurements
[PB91-171959] N91-28482
ELECTRICAL PROPERTIES
Chemistry of electronic ceramic materials. Proceedings of the International Conference on the Chemistry of Electronic Ceramic Materials
[NASA-CR-188688] N91-28403
ELECTRICAL RESISTANCE
High-resolution measurements of the thermal conductivity and boundary resistance of helium-4 near the lambda point N91-28322
ELECTRICAL RESISTIVITY
Strength and electrical conductivity of deformation processed Cu-15 v/o Fe metal composites produced by powder metallurgy/techniques
[DE91-013658] N91-28291
Substructure and electrical resistivity analyses of pure tungsten sheet
[DE91-014098] N91-28362
Preparation of ionic membranes for zinc/bromine storage batteries
[DE91-012008] N91-28483
The effect of strong Coulomb correlations on electron-phonon interactions in the copper oxides: Implications for transport
[DE91-013333] N91-28854
Direct ion heating in MHD relaxation N91-28911
Doping and pressure study of U3Sb4Pt3
[DE91-013669] N91-29033
Flux pinning and dissipation in high-temperature superconductors
[DE91-014466] N91-29042
Pressure dependence of the Curie-temperature in the Kondo-lattice-compound YbNiSn
[DE91-013672] N91-29046
ELECTRIFICATION
Studies in cloud physics: Electrification, glaciation, and turbulence N91-28684
ELECTRO-OPTICS
New photocrosslinkable polymers for second order nonlinear optical processes
[AD-A235856] N91-28386
ELECTROCATALYSTS
Recent achievements in polymer electrolyte fuel cell (PEFC) research at Los Alamos National Laboratory
[DE91-013683] N91-28661
ELECTROCHEMICAL CELLS
Novel ways of depositing ZnTe films by a solution growth technique
[DE91-002189] N91-28429
ELECTROCHEMICAL CORROSION
Aqueous corrosion characteristics and corrosion-related cracking susceptibilities of Fe3Al-type iron aluminides
[DE91-013028] N91-28358
ELECTROCHEMICAL MACHINING
Effects of residual stresses on the fracture toughness of Zircaloy-2 tubes
[DE91-012736] N91-28354
ELECTROCHEMISTRY
Applications of scanning tunneling microscopy to electrochemistry
[AD-A237021] N91-28304
Analysis of metals in solution using electrospray ionization mass spectrometry
[DE91-012522] N91-28310
Electrochemical processes at solid electrode-electrolyte-gas interfaces
[DE91-012922] N91-28317
Exploratory battery technology development report for FY90
[DE91-012131] N91-28485
Alternative materials for solid oxide fuel cells: Chromite interconnections
[DE91-014447] N91-28664
Electron transfer reactions in microporous solids
[DE91-012299] N91-28833
ELECTRODEPOSITION
Perspective on plating for precision finishing
[DE91-011927] N91-28394
ELECTRODES
Electrochemical processes at solid electrode-electrolyte-gas interfaces
[DE91-012922] N91-28317
High temperature solder device for flat cables
[NASA-CASE-GSC-13344-1] N91-28363
High order calculation of the multipole content of three dimensional electrostatic geometries
[DE91-014707] N91-28476
Durability of polymeric materials used in zinc/bromine flow batteries
[DE91-012864] N91-28487
Some high voltage DC breakdown properties of thick film circuits on alumina
[DE91-014675] N91-28500
Advanced water-cooled phosphoric acid fuel cell development
[DE90-009700] N91-28657
Alternative materials for solid oxide fuel cells: Chromite interconnections
[DE91-014447] N91-28664
ELECTROLESS DEPOSITION
Perspective on plating for precision finishing
[DE91-011927] N91-28394
ELECTROLYSIS
Pacific Northwest hydrogen feasibility study
[DE91-013427] N91-28445
ELECTROLYTES
Polymers at surfaces
[DE91-013642] N91-28430
Exploratory battery technology development report for FY90
[DE91-012131] N91-28485
Durability of polymeric materials used in zinc/bromine flow batteries
[DE91-012864] N91-28487
Advanced water-cooled phosphoric acid fuel cell development
[DE90-009700] N91-28657
ELECTROLYTIC CELLS
Recent achievements in polymer electrolyte fuel cell (PEFC) research at Los Alamos National Laboratory
[DE91-013683] N91-28661
ELECTROMAGNETIC ABSORPTION
Radio absorption in the Antarctic ionosphere: Some observations in the region of the midlatitude trough
N91-28694
ELECTROMAGNETIC COUPLING
Follow-on cable coupling lightning test, volume 1
[NASA-CR-184123] N91-28192
ELECTROMAGNETIC FIELDS
High order calculation of the multipole content of three dimensional electrostatic geometries
[DE91-014707] N91-28476
Magnetospheric VLF line radiation N91-28693
ELECTROMAGNETIC INTERFERENCE
Impact of ion propulsion on performance, design, testing, and operation of a geosynchronous spacecraft
[AD-A237028] N91-28273
Mutual interference between many similar radars operating in physical proximity
[ITN-91-85139] N91-28468
Mind over matter: The intellectual content of experimental physics
[DE91-617571] N91-28813
SANDAC V computer electromagnetic interface characteristics: Problems and solutions
[DE91-014334] N91-29065
ELECTROMAGNETIC PULSES
Localized waves in complex environments
[DE91-011934] N91-28462
ELECTROMAGNETIC RADIATION
Gravitational influence of a static ring-like distribution of mass on electromagnetic waves N91-28472
Mind over matter: The intellectual content of experimental physics
[DE91-617571] N91-28813
The 3-D electromagnetic macroscale particle simulation of inhomogeneous, magnetized plasmas N91-28918
SANDAC V computer electromagnetic interface characteristics: Problems and solutions
[DE91-014334] N91-29065
ELECTROMAGNETIC SURFACE WAVES
Steady-state dynamo and current drive in a nonuniform bounded plasma
[DE91-014865] N91-28974
ELECTROMAGNETIC WAVE TRANSMISSION
Tropospheric scatter propagation at 5 and 16 GHz: Results for a 161 km path
[AD-A237012] N91-28458
ELECTRON ACCELERATION
Electron acceleration by magnetosonic waves in a solar coronal loop N91-29132
ELECTRON BEAM WELDING
Weldability of iron aluminides
[DE91-013730] N91-28367
ELECTRON BEAMS
Fields and trajectories in the magnicon
[DE91-013070] N91-28492
Simulation of a storage ring free electron laser with a mapping algorithm for distribution functions
[DE91-012387] N91-28552
Time-resolved emittance measurements of an excimer-laser-driven metal photocathode
[DE91-013066] N91-28558
E-beam accelerator cavity development for the ground-based free electron laser
[DE91-013760] N91-28563
Short wavelength FELS
[DE91-013759] N91-28566
Reduction of energy sweep of the ETA-2 beam
[DE91-013824] N91-28568
Beam emittance and the effects of the rf, space charge and wake fields: Application to the ATF photoelectron beam
[DE91-014789] N91-28569
X ray Tomographic Microscopy (XTM)
[DE91-011930] N91-28599
X ray spatial resolution at intermediate voltages: An assessment by massively parallel Monte Carlo electron trajectory simulation
[DE91-012018] N91-28841
Beam structure and transverse emittance studies of high-energy ion beams
[DE91-013499] N91-28871
Space charge and wake field analysis for a high brightness electron source
[DE91-014788] N91-28874
Direct ion heating in MHD relaxation N91-28911
Soliton phenomena in electron beam plasma
N91-28930
The spatial resolution of x ray microanalysis in thin foils
[DE91-011949] N91-29003
ELECTRON BUNCHING
Simulation of a storage ring free electron laser with a mapping algorithm for distribution functions
[DE91-012387] N91-28552
Space charge and wake field analysis for a high brightness electron source
[DE91-014788] N91-28874
ELECTRON CYCLOTRON HEATING
Mode conversion of Alfven waves induced by quadrupole magnetic field modulation N91-28924
Microwave-generated plasma thruster
[DE91-013131] N91-28948
ELECTRON DENSITY (CONCENTRATION)
Characteristics of edge plasma turbulence on the ATF torsatron
[DE91-012981] N91-28947
ELECTRON DIFFRACTION
Correcting channeling and diffraction effects in quantitative REELS surface microanalysis
[DE91-009924] N91-28840
ELECTRON GUNS
SLC polarized beam source electron optics design
[DE91-012911] N91-28869
Space charge and wake field analysis for a high brightness electron source
[DE91-014788] N91-28874
ELECTRON IRRADIATION
Radiation disorder and aperiodicity in irradiated ceramics
[DE91-010257] N91-28391
ELECTRON MICROSCOPES
Advancing conventional high-resolution electron microscopy
[DE91-013773] N91-28548
ELECTRON MICROSCOPY
Analytical electron microscopy of catalyst preparations
[DE91-014126] N91-28328
Characterization of silicon nitride synthesized by microwave heating
[DE91-012219] N91-28397
In-situ REM imaging of surface processes on ceramic bulk crystals from 300 to 1670 K in a conventional TEM
[DE91-009923] N91-28405
A controlled dispersion parallel wavelength x ray spectrometer for electron microscopy
[DE91-012011] N91-28544
Advancing conventional high-resolution electron microscopy
[DE91-013773] N91-28548
Correcting channeling and diffraction effects in quantitative REELS surface microanalysis
[DE91-009924] N91-28840
Characterization of crystalline interfaces by advanced electron microscopy
[DE91-011883] N91-29002

Parallel nanometer scale fabrication
[DE91-013016] N91-29026

ELECTRON OPTICS
SLC polarized beam source electron optics design
[DE91-012911] N91-28869

ELECTRON PHONON INTERACTIONS
The effect of strong Coulomb correlations on electron-phonon interactions in the copper oxides: Implications for transport
[DE91-013333] N91-28854

ELECTRON PLASMA
Rapid acceleration of protons in a nonlinear magnetosonic wave and their energy spectrum
N91-28905
Characteristics of edge plasma turbulence on the ATF torsatron
[DE91-012981] N91-28947
Microwave-generated plasma thruster
[DE91-013131] N91-28948

ELECTRON SCATTERING
Measurements of ionization cross-section for electron energy-loss microanalysis under well defined scattering conditions
[DE91-013745] N91-28862
Radiative processes in active galactic nuclei
N91-29137

ELECTRON SOURCES
SLC polarized beam source electron optics design
[DE91-012911] N91-28869
Strain enhanced electron spin polarization observed in photoemision from InGaAs
[DE91-012319] N91-28996

ELECTRON SPECTROSCOPY
Application of electron energy loss spectroscopy to microanalysis of irradiated stainless steels
[DE91-009913] N91-28344
Correcting channeling and diffraction effects in quantitative REELS surface microanalysis
[DE91-009924] N91-28840

ELECTRON SPIN
Strain enhanced electron spin polarization observed in photoemision from InGaAs
[DE91-012319] N91-28996
Topics on frustrated spin systems and high-temperature superconductors N91-29032

ELECTRON STATES
Chaos in the lowest Landau level
[DE91-014800] N91-28866
Electron correlations in solid state physics
[DE91-013752] N91-29030

ELECTRON TRAJECTORIES
Fields and trajectories in the magnicon
[DE91-013070] N91-28492
X ray spatial resolution at intermediate voltages: An assessment by massively parallel Monte Carlo electron trajectory simulation
[DE91-012018] N91-28841

ELECTRON TRANSFER
Photoinduced electron transfer in ordered polymers
[DE91-014512] N91-28440
Dynamics of charge-transfer excited states relevant to photochemical energy conversion
[DE91-012669] N91-28649
Fifteenth DOE Solar Photochemistry Research Conference
[DE91-002165] N91-28663
Magnetic resonance and optical spectroscopic studies of carotenoids
[DE91-014361] N91-28724
Electron transfer reactions in microporous solids
[DE91-012299] N91-28833
Correlated charge-changing ion-atom collisions
[DE91-013640] N91-28863
Photoinduced charge and energy transfer processes in molecular aggregates
[DE91-014383] N91-28864
Anomalous transport due to the skin size electromagnetic drift mode in tokamaks N91-28902

ELECTRON TRANSITIONS
The pressure-induced Mott transition in transition-metal iodides
[DE91-013671] N91-28366

ELECTRON TUNNELING
Ultra-high frequency superconductive devices
[AD-A236795] N91-28478

ELECTRON-POSITRON PAIRS
Radiative processes in active galactic nuclei
N91-29137

ELECTRON-POSITRON PLASMAS
Radiative processes in active galactic nuclei
N91-29137

ELECTRONIC PACKAGING
Microstructural characterization of solders and brazes for advanced packaging technology
[DE91-011503] N91-28379

ELECTRONS
Simulations on pair creation from beam-beam interaction in linear colliders
[DE91-012315] N91-28834
Chaos in the lowest Landau level
[DE91-014800] N91-28866
Three-dimensional particle simulation of trapped electron instabilities in tokamaks N91-28891

ELECTROPLATING
Cross-sectional TEM specimen preparation of free-standing metal multi-layered films
[DE91-011117] N91-28351

ELECTROSTATIC CHARGE
Electrostatic discharge effects on EBW detonators
[DE91-013250] N91-28467

ELECTROSTATIC PROBES
Photoinduced electron transfer in ordered polymers
[DE91-014512] N91-28440
A portable and independent edge fluctuation diagnostic
[DE91-014357] N91-28971

ELECTROSTATIC WAVES
Issues in direct numerical simulation of plasma turbulence and transport N91-28901
The 3-D electromagnetic macroscale particle simulation of inhomogeneous, magnetized plasmas N91-28918
Nonadiabatic behavior of the magnetic moment of a charged particle in a dipole magnetic field N91-28920

ELECTROSTATICS
Electrostatic discharge effects on EBW detonators
[DE91-013250] N91-28467
High order calculation of the multipole content of three dimensional electrostatic geometries
[DE91-014707] N91-28476
Electrostatic particle simulations of density and temperature driven modes in a toroidal plasma
N91-28915
Numerical simulation of potential-driven ion cyclotron oscillation N91-28925
Fluctuation spectrum of ion temperature gradient driven modes in sheared magnetic fields N91-28936
Exact solutions for a system of nonlinear plasma fluid equations
[DE91-014367] N91-28965
On the use of particle-in-cell methods for the study of magnetically-confined fusion plasmas
[DE91-015093] N91-28984

ELEMENTARY EXCITATIONS
Ring-laser solitons: A multipass approach
[DE91-013242] N91-28560
The effect of the quantum susceptance on the gain of superconducting quasiparticle mixers
[DE91-012352] N91-29021

ELEMENTARY PARTICLES
Ring-laser solitons: A multipass approach
[DE91-013242] N91-28560

ELLIPTICAL GALAXIES
Population synthesis models for cluster galaxies at redshifts of 0.4 to 0.55 N91-29124

EMBEDDING
A logic model for model management: An embedded languages approach N91-28761

EMBRITTLEMENT
Evaluation of aging of cast stainless steel components
[DE91-014013] N91-28361

EMERGENCIES
Structured meeting techniques identify emergency management issues practitioners really want to see addressed
[DE91-012414] N91-29069

EMISSION SPECTRA
Dynamics of charge-transfer excited states relevant to photochemical energy conversion
[DE91-012669] N91-28649
Spectroscopic and ion probe characterization of laser produced plasmas used for thin film growth
[DE91-013425] N91-28959
Shock initiation of pentaerythritol tetranitrate crystals: Optical absorption and emission studies
[DE91-013381] N91-29023
Emission line regions in active galactic nuclei: Structure, kinematics, physical conditions, and chemical abundances N91-29095
Population synthesis models for cluster galaxies at redshifts of 0.4 to 0.55 N91-29124
Radiative processes in active galactic nuclei
N91-29137

EMITTANCE
Time-resolved emittance measurements of an excimer-laser-driven metal photocathode
[DE91-013066] N91-28558
Beam emittance and the effects of the rf, space charge and wake fields: Application to the ATF photoelectron beam
[DE91-014789] N91-28569

ENCAPSULATING
Mechanical modeling of stress generation during cure of encapsulating resins
[DE91-011496] N91-28393
Method of preforming and assembling superconducting circuit elements
[NASA-CASE-LAR-14395-1-CU] N91-28490

ENCLOSURE
Boussinesq algorithm for enclosed bouyant convection in two dimensions
[PB91-178848] N91-28507

END EFFECTORS
Selected topics in mechanisms and robotics: Singularities, inverse kinematics, and collision detection
N91-28598

ENERGY CONSERVATION
Fixture efficiency program
[DE91-014470] N91-28498
Making energy efficiency happen
[DE91-013057] N91-28655
Environmental tradeoffs associated with various energy paths: A total energy cycle analysis approach
[DE91-013662] N91-28669
Internal kink mode simulation by 3-D gyrokinetic code
N91-28916
Simulation of combustion processes in an MHD second stage combustor
[DE91-014014] N91-28968

ENERGY CONSUMPTION
Fixture efficiency program
[DE91-014470] N91-28498
EIA publications directory, 1990
[DE91-014350] N91-29082

ENERGY CONVERSION
Dynamics of charge-transfer excited states relevant to photochemical energy conversion
[DE91-012669] N91-28649
SOLTECH 91: Proceedings, volume 2
[DE91-013767] N91-28656
Environmental tradeoffs associated with various energy paths: A total energy cycle analysis approach
[DE91-013662] N91-28669
The Cascade inertial confinement fusion reactor concept
[DE91-013852] N91-28966

ENERGY CONVERSION EFFICIENCY
Thermodynamics and efficiency in combustion and engines
[DE91-012781] N91-28320
A high power Klystrode with potential for space application
[DE91-013046] N91-28486
Fixture efficiency program
[DE91-014470] N91-28498
One-sun silicon solar cell research
[DE91-014329] N91-28662
Optimization and thermodynamic performance measures for a class of finite time thermodynamic cycles
N91-29060

ENERGY DISSIPATION
Proton Energy Loss (PEL) material characterization
[DE91-011545] N91-28306
Energy dissipation in chemical reactions on ultrafast timescales
[DE91-012342] N91-28315
Microwave enhanced diffusion?
[DE91-013312] N91-28415
Log-stable distribution of energy dissipation in turbulence N91-28885

ENERGY DISTRIBUTION
Laser ejection of Ag(sup +) ions from a roughened silver surface: Role of the surface plasmon
[DE91-012945] N91-28554
Environmental tradeoffs associated with various energy paths: A total energy cycle analysis approach
[DE91-013662] N91-28669
Description of real-time Ada software implementation of a power system monitor for the Space Station Freedom PMAD DC testbed
[NASA-TM-105157] N91-28776
Kinetic energy distributions of ions after surface collisions
[DE91-013412] N91-28850

ENERGY GAPS (SOLID STATE)
Interlayer pairing and c-axis versus ab-plane gap anisotropy in high Tc superconductor
[DE91-012218] N91-29005
Pressure dependence of the Curie-temperature in the Kondo-lattice-compound YbNiSn
[DE91-013672] N91-29046

ENERGY LEVELS
Scintillation detector efficiencies for neutrons in the energy region above 20 MeV
[DE91-012544] N91-28837

Molecular dynamics simulations of bulk displacement threshold energies in Si
[DE91-011957] N91-28846
Shell model calculations at superdeformed shapes
[DE91-012954] N91-28853
Light-cone quantization of quantum chromodynamics
[DE91-013991] N91-28856

ENERGY METHODS
Application of mathematica to energy principle
N91-28910

ENERGY POLICY
Making energy efficiency happen
[DE91-013057] N91-28655
Tiger Team assessment of the Princeton Plasma Physics Laboratory
[DE91-014395] N91-28957

ENERGY SOURCES
Advanced propulsion concepts N91-28218

ENERGY SPECTRA
Ground-based measurements of galactic cosmic ray fragmentation in shielding
[DE91-012336] N91-29133

ENERGY STORAGE
Pacific Northwest hydrogen feasibility study
[DE91-013427] N91-28445
Exploratory battery technology development report for FY90
[DE91-012131] N91-28485
Numerical solution of a moving boundary problem as a model solution for a solar pipe
[ITN-91-85143] N91-28516
Environmental tradeoffs associated with various energy paths: A total energy cycle analysis approach
[DE91-013662] N91-28669

ENERGY TECHNOLOGY
United States Department of Energy solar receiver technology development
[DE91-012653] N91-28651
SOLTECH 91: Proceedings, volume 2
[DE91-013767] N91-28656
Requirements for a network storage service
[DE91-014106] N91-28778
Evaluation of charged-particle reactions for fusion applications
[DE91-014135] N91-28962
EIA publications directory, 1990
[DE91-014350] N91-29082

ENERGY TRANSFER
Some new approaches to semiclassical and quantum transition state theory
[DE91-012345] N91-28308
Localized waves in complex environments
[DE91-011934] N91-28462
Interactions of molecules with surfaces
[DE91-014498] N91-28857
Photoinduced charge and energy transfer processes in molecular aggregates
[DE91-014383] N91-28864
Issues in direct numerical simulation of plasma turbulence and transport N91-28901
A new model of PeV gamma ray sources and MHD turbulence in neutron star accretion columns
N91-29122

ENGINE DESIGN
Follow-on cable coupling lightning test, volume 1
[NASA-CR-184123] N91-28192
A white paper: Operational efficiency. New approaches to future propulsion systems N91-28197
Operationally Efficient Propulsion System Study (OEPPS) N91-28198
Expendable launch vehicle propulsion N91-28199
Solid rocket propulsion N91-28206
Next generation solid boosters N91-28207
Advanced launch system N91-28208
Overview of European and other non-US/USSR/Japan launch vehicle and propulsion technology programs
N91-28221
CFD applications in chemical propulsion engines
N91-28234
Liquid rocket engine flight certification N91-28250
STV engine design considerations N91-28255
Space transportation main engine reliability and safety
N91-28271

ENGINE TESTS
Overview of European and other non-US/USSR/Japan launch vehicle and propulsion technology programs
N91-28221
Liquid rocket engine flight certification N91-28250
John C. Stennis Space Center roles and missions
N91-28259
Space shuttle main engine: Certification for manned space flight N91-28270

ENGINEERING DRAWINGS
Document format considerations for a document tracking and storage system
[DE91-013402] N91-29079

ENVIRONMENT EFFECTS
Assessing the risk of transporting hazardous materals by aircraft: A case study
[DE91-014016] N91-28147
Environmental tradeoffs associated with various energy paths: A total energy cycle analysis approach
[DE91-013662] N91-28669
Biomarker-based biomonitoring for evaluating health and ecological effects on environmental contamination
[DE91-013729] N91-28719

ENVIRONMENT POLLUTION
Environmental tradeoffs associated with various energy paths: A total energy cycle analysis approach
[DE91-013662] N91-28669
Work plan for the preliminary site investigation for McMurdo Station, Ross Island, Antarctica
[DE91-015100] N91-28675

ENVIRONMENT PROTECTION
The use of science in the management of hazardous air pollutants N91-28667
Data users guide to the mountain cloud chemistry project
[PB91-168484] N91-28697

ENZYMES
Photobiotechnology: Algal hydrogen production and photoconductivity of metalized chloroplasts
[DE91-013232] N91-28718

EPHEMERIDES
Precise orbit determination for GPS satellites
N91-28183

EPITAXY
X ray diffraction study of heteroepitaxy of MOCVD grown TiO2 and VO2 films on sapphire single crystals
[DE91-013764] N91-29037
The surface chemistry of GaAs atomic layer epitaxy
[DE91-014112] N91-29047

EPOXY COMPOUNDS
Multiaxial failure characterization of composites
[DE91-011925] N91-28285

EPOXY RESINS
Mechanical modeling of stress generation during cure of encapsulating resins
[DE91-011496] N91-28393

EQUALIZERS (CIRCUITS)
Performance evaluation of partial response continuous phase modulation: Discriminator detection
[ITN-91-85145] N91-28470

EQUATIONS OF MOTION
A comparison of the potential and the Euler formulations of the equations of motion for transonic flow
[DE91-014731] N91-28142
Numerical investigation of the thrust efficiency of a laser-propelled vehicle N91-28572
Recursive linearization of multibody dynamics and application to control design N91-28588
Regularization of the Lagrange planetary equations for numerical use N91-28808
Exact solution of a quantum forced time-dependent harmonic oscillator
[AD-A236633] N91-28812
Chaos in the lowest Landau level
[DE91-014800] N91-28866
Microwave instability at transition: Stability diagram approach
[DE91-013202] N91-28867

EQUATIONS OF STATE
Equation-of-state from SiO2 aerogel Hugoniot data
[DE91-011480] N91-28313
SESAME equation of state number 7740: Polycarbonate
[DE91-013970] N91-28436
A study of the impact of reaction rates on equation of state
[DE91-013375] N91-28621
Quantum mechanical effects on the shock Hugoniot
[DE91-014750] N91-28636
Equation of state and crushing dynamics of low-density silica aerogels
[DE91-014766] N91-28637
Radiative transfer in very strong magnetic fields
N91-29106
Impact of the nuclear equation of state on models of rotating neutron stars
[DE91-014615] N91-29125

ERGODIC PROCESS
Equilibrium beta limit of helical systems N91-28894
Diffusion through stochastic webs in two and more dimensions N91-28941

EROSION
Studies of the two-phase plume jet and wall erosion in a vertical launching system N91-28145
Erosion studies on a Fe3Al-based iron aluminide and 1100 Al
[DE91-012529] N91-28360

Investigation of laser diagnostics of PACVD processes for depositing hard face coatings
[DE91-012642] N91-28401
An assessment of the lifetime of Faraday shield elements
[DE91-012228] N91-28463

ERROR ANALYSIS
Performance of a polarization isolation enhancement method in the presence of errors
[DE91-013571] N91-28473
Transmission/reflection and short-circuit line permittivity measurements
[PB91-171959] N91-28482
The determination of mean sea level using GPS
N91-28708
TOPAZ2D benchmark problems nonlinear materials
[DE91-009753] N91-29053

ERRORS
Precise orbit determination for GPS satellites
N91-28183
Prediction of forecast skill with a quasi-geostrophic model N91-28699
Towards the exact nature of a certain error term
[DE91-617574] N91-28801

ETCHING
Cross-sectional TEM specimen preparation of free-standing metal multi-layered films
[DE91-011117] N91-28351

ETHYL COMPOUNDS
Evidence of vibrational mode-coupling in 2-fluorethanol via high resolution infrared spectroscopy in a molecular beam
[AD-A236132] N91-28821

ETHYLENE
Validity of the model used to relate the energy distribution and the adsorption isotherm
[DE91-013528] N91-28428

ETHYLENEDIAMINE
Semi-empirical calculations on model systems for organosilyldiamine preceramic polymers
[DE91-013721] N91-28433

EULER EQUATIONS OF MOTION
Use of a rotated Riemann solver for the two-dimensional Euler equations N91-28530

EUROPEAN SPACE AGENCY
Overview of European and other non-US/USSR/Japan launch vehicle and propulsion technology programs
N91-28221

EUTECTICS
Interpreting solidification phenomena and microstructural evolution in metals through the use of transparent model alloy systems
[DE91-012629] N91-28347

EVAPORATION
Droplet-turbulence interactions in subcritical and supercritical evaporating sprays N91-28228
Direct contact heat transfer to a dispersal droplet with change of phase N91-28521
Evaporation as a diagnostic test for hydrodynamic cooling of laser-ablated clusters
[DE91-013416] N91-28555

EVAPORATIVE COOLING
Evaporation as a diagnostic test for hydrodynamic cooling of laser-ablated clusters
[DE91-013416] N91-28555

EXCIMER LASERS
Time-resolved emittance measurements of an excimer-laser-driven metal photocathode
[DE91-013066] N91-28558
Magnetic resonance and optical spectroscopic studies of carotenoids
[DE91-014361] N91-28724

EXCITATION
Measurements of photo-induced changes in conjugated polymers
[DE91-013262] N91-28427
Desorption of Al, Au, Ag using surface plasmon excitation
[DE91-013726] N91-28493
Dynamics of charge-transfer excited states relevant to photochemical energy conversion
[DE91-012669] N91-28649
Phase-conjugated fluorescence
[AD-A231114] N91-28820
Ab initio cluster studies of La2CuO4
[DE91-013520] N91-29025

EXHAUST EMISSION
The use of science in the management of hazardous air pollutants N91-28667

EXHAUST GASES
Studies of the two-phase plume jet and wall erosion in a vertical launching system N91-28145
The use of science in the management of hazardous air pollutants N91-28667

EXOBIOLOGY
Aerospace medicine and biology: A continuing bibliography with indexes (supplement 352)
[NASA-SP-7011(352)] N91-28729
EXPERIMENT DESIGN
The use of AMS to the biomedical sciences
[DE91-012037] N91-28712
EXPERIMENTAL BREEDER REACTOR 2
A reconfigurable strategy for distributed digital process control
[DE91-013740] N91-28786
EXPERT SYSTEMS
Control of autonomous mobile robots using custom-designed qualitative reasoning VLSI chips and boards
[DE91-012527] N91-28783
Proposal for continued basic research in intelligent machines at the Center for Engineering Systems Advanced Research: Fiscal years 1992-1996
[DE91-012997] N91-28784
A reconfigurable strategy for distributed digital process control
[DE91-013740] N91-28786
Generalized hypertext in a knowledge-based decision support shell environment N91-29086
EXPLODING WIRES
Mechanisms of EBW HE initiation
[DE91-013565] N91-28447
EXPLOSIONS
Atmospheric propagation of high-explosive blast waves
[DE91-012550] N91-28506
Shock and reshock of an unstable fluid interface
[DE91-014737] N91-28528
Explosion of a superbubble in a uniform magnetic field N91-29102
Upper limits for the flux of very high-energy gamma radiation from Cygnus X-3 and for the explosion rate of primordial black holes obtained by the Haleakala Gamma Ray Observatory N91-29134
EXPLOSIVES
Semiconductor Bridge (SCB) research and development
[DE91-011493] N91-28319
Experiments and calculations of jet penetration in glass
[DE91-013567] N91-28422
Investigation of the Deflagration-to-Detonation (DDT) process: The role of ignition and explosive properties in DDT
[DE91-011956] N91-28442
Shock compression of DuPont detasheet at low stress
[DE91-013229] N91-28443
Mechanisms of EBW HE initiation
[DE91-013565] N91-28447
Electrostatic discharge effects on EBW detonators
[DE91-013250] N91-28467
Procyon experiments utilizing foil-fuse opening switches
[DE91-014605] N91-28499
Numerical and analytical analysis of thin laser-driven flyer plates
[DE91-013748] N91-28567
A study of the impact of reaction rates on equation of state
[DE91-013375] N91-28621
EXPONENTIAL FUNCTIONS
Operational interpolation of data in triangular array
[DE91-012987] N91-28800
EXTERNAL TANKS
Space shuttle with common fuel tank for liquid rocket booster and main engines (supertanker space shuttle) N91-28257
EXTRATERRESTRIAL MATTER
Numerical models of equilibrium between matter and black holes N91-29101
EXTREME ULTRAVIOLET RADIATION
Short wavelength FELS
[DE91-013759] N91-28566

F

F-15 AIRCRAFT
Recent developments in the area of aircraft rough field performance N91-28154
F-104 AIRCRAFT
Operational loads on landing gear N91-28158
F-106 AIRCRAFT
F-106B airplane active control landing gear drop test performance N91-28164
FABRICATION
Manufacturing processes N91-28244
ZrO2 reinforced-MoSi2 matrix composites
[DE91-013074] N91-28288
Processing and fabrication of Fe3Al-based alloys
[DE91-014546] N91-28382
Ordered ceramic membranes
[DE91-012248] N91-28398
Energy dispersive x ray diffraction study of glassy Bi2Sr2CaCu2O(x) filaments produced by gas-jet fiberization
[DE91-012021] N91-28407
FABRICS
The chemical resistance of protective handwear available through the Navy's supply system
[AD-A235874] N91-28731
FAILURE
Failure analysis case histories of Canadian forces aircraft landing gear components N91-28151
Operational loads on landing gear N91-28158
Historical problem areas lessons learned N91-28242
Nondestructive evaluation tools and experimental studies for monitoring the health of space propulsion systems
[NASA-TM-105164] N91-28605
FAILURE ANALYSIS
Failure analysis case histories of Canadian forces aircraft landing gear components N91-28151
Probabilistic structural analysis methods for space transportation propulsion systems N91-28238
Multiaxial failure characterization of composites
[DE91-011925] N91-28285
On the finite-strain-invariant failure criterion for composites
[DE91-011924] N91-28286
Investigation of thermomechanical behavior of metal matrix composites N91-28296
Damage progression during static and fatigue loading in metal matrix composites, volumes 1-3 N91-28301
Mechanical modeling of stress generation during cure of encapsulating resins
[DE91-011496] N91-28393
Signature analysis technique for diagnosing failures in mechanical systems N91-28604
Assessment of ductile fracture methodology based on applications to large-scale experiments
[DE91-009920] N91-28614
Interlaminar fracture characterization: A current review
[NASA-CR-187573] N91-28626
FAILURE MODES
Advanced launch system N91-28208
On the finite-strain-invariant failure criterion for composites
[DE91-011924] N91-28286
Damage development under compression-compression fatigue loading in a stitched uniwoven graphite/epoxy composite material
[NASA-CR-188693] N91-28292
FATIGUE (MATERIALS)
Damage progression during static and fatigue loading in metal matrix composites, volumes 1-3 N91-28301
FATIGUE LIFE
Effects of various parameters on the fatigue life of alloy 718
[DE91-014100] N91-28380
Improving fatigue life in near-eutectic Sn Pb solders
[DE91-013844] N91-28603
FATIGUE TESTS
Operational loads on landing gear N91-28158
Effects of various parameters on the fatigue life of alloy 718
[DE91-014100] N91-28380
FEASIBILITY ANALYSIS
Heat resistant materials and their feasibility issues for a space nuclear transportation system
[DE91-014071] N91-28187
Feasibility study of a 200 ampere battery
[DE91-014673] N91-28496
FEEDBACK
Design of a multivariable RF control system using gain-shaping in the frequency domain
[DE91-013859] N91-28474
FEEDBACK CONTROL
Stochastic robustness of linear multivariable control systems: Towards comprehensive robustness analysis N91-28172
Robust and real-time control of magnetic bearings for space engines N91-28230
Improved superconducting bearings
[NASA-CASE-GSC-13346-1] N91-28578
Robust low-order control of flexible joint manipulators N91-28584
Real-time adaptive active control of sound fields N91-28819
FERMIONS
Strongly interacting fermion systems
[DE91-012284] N91-28848
FERROELECTRICITY
Ferroelectric fatigue in modified bulk lead zirconate titanate ceramics
[DE91-012647] N91-28417
FERROMAGNETIC MATERIALS
Ferromagnetic material in the superconductor and its effect on the magnetization sextupole and decapole in the SSC dipoles at injection
[DE91-011886] N91-28993
FERROMAGNETISM
The derivation of effective spin Hamiltonians and the origin of the magnetic field induced transition in orthormbic La2CuO4
[DE91-013743] N91-29035
FEYNMAN DIAGRAMS
Transport with Feynman propagators
[DE91-013566] N91-29063
FIBER COMPOSITES
Fracture micromechanics of intermetallic and ceramic matrix continuous fiber composites
[AD-A236638] N91-28280
Multiaxial failure characterization of composites
[DE91-011925] N91-28285
Processing, compatibility and oxidation of diboride-reinforced oxide matrix composites for ultrahigh-temperature applications N91-28294
The effect of ductile innerlayers on the mechanical performance of fiber-reinforced composite materials N91-28295
Tribology of aluminum-based metal matrix composites: Fundamental study of wear behavior as influenced by microstructure N91-28297
The influence of defects on the mechanical properties of short fibre reinfornced thermoplastics N91-28300
High-resolution interferometric measurements of residual strains in composites N91-28303
FIBER OPTICS
Research and development entitled smart structures for fossil energy applications
[DE91-002064] N91-28875
Pulse propagation in inhomogeneous optical fibers
[DE91-014356] N91-28879
A faint galaxy redshift survey and implications for cosmology N91-29100
FIBER ORIENTATION
The effect of ductile innerlayers on the mechanical performance of fiber-reinforced composite materials N91-28295
The influence of defects on the mechanical properties of short fibre reinfornced thermoplastics N91-28300
FIBER STRENGTH
The effect of ductile innerlayers on the mechanical performance of fiber-reinforced composite materials N91-28295
FIELD EFFECT TRANSISTORS
Monolithic front end electronics for silicon calorimeters
[DE91-012063] N91-28484
FIELD THEORY (PHYSICS)
Spin 4 and 7/2 extended conformal algebra
[DE91-617609] N91-28803
Light-cone quantization of quantum chromodynamics
[DE91-013991] N91-28856
Path-integral measure for Chern-Simons theory within the stochastic quantization approach
[DE91-617610] N91-29056
The (2,0) super Beltrami parametrization and superconformal structures
[DE91-617611] N91-29057
Topics in low-dimensional field theory
[DE91-013784] N91-29062
FILAMENTS
Energy dispersive x ray diffraction study of glassy Bi2Sr2CaCu2O(x) filaments produced by gas-jet fiberization
[DE91-012021] N91-28407
FILE MAINTENANCE (COMPUTERS)
The software technical review process
[AD-A236139] N91-28743
FILLERS
Thermally activated retainer means
[NASA-CASE-MSC-21793-1] N91-28186
FILM BOILING
Direct contact heat transfer to a dispersal droplet with change of phase N91-28521
Transient two-phase flow of cryogenic fluid in a vertical transfer line during the cooldown process N91-28522
FINES
Ultra-fine powders using glycine-nitrate combustion synthesis
[DE91-012926] N91-28412
FINITE DIFFERENCE THEORY
Modeling of a 1700-MHz cluster cavity of planar triodes
[DE91-013049] N91-28488

ZEPHYR3D: A finite difference computer program for three-dimensional, transient incompressible flow problems
[DE91-014331] N91-28515
Thermal and non-Newtonian effects in elastohydrodynamic lubrication of rolling-sliding contacts N91-28590
MESA: A 3-D Eulerian hydrocode for penetration mechanics studies
[DE91-013308] N91-28613
General implementation of thin-slot algorithms into the finite-difference time-domain code, TSAR, based on a slot data file
[DE91-014336] N91-28767
Simulation of planar integrated photonics devices with the LLNL time-domain finite-difference code suite
[DE91-011929] N91-28876

FINITE ELEMENT METHOD
Numerical simulation of the dynamic behavior of landing gears N91-28160
Calculation of interactions between air and ground of landing N91-28161
On the finite-strain-invariant failure criterion for composites
[DE91-011924] N91-28286
Finite element modeling of 2-D delamination growth in laminated composites N91-28302
Mechanical modeling of stress generation during cure of encapsulating resins
[DE91-011496] N91-28393
Moving finite elements: A continuously adaptive method for computational fluid dynamics
[DE91-013391] N91-28513
Applications of a 2-D moving finite element formulation to elastic/viscoplastic dynamic fracture analysis
[DE91-009930] N91-28607
Plastic analysis of a circular rod subjected to sinusoidal thermal cycling
[DE91-011845] N91-28609
Design and analysis of the 50 mm collider dipole vacuum vessel
[DE91-012490] N91-28610
Calculation of pressure distribution in vacuum systems using a commercial finite element program
[DE91-013611] N91-28629
Flutter of laminated rectangular plates including finite deflection and shear deformation N91-28639
A 2D field solver for periodic structures with special corner elements
[DE91-012323] N91-28792

FINITE VOLUME METHOD
The computation of complex, two-dimensional turbulent flows using Reynolds stress closure N91-28535

FIRMWARE
Runway Visual Range (RVR) Operational Test and Evaluation (OT and E)/integration test plan
[DOT/FAA/CT-TN91/4] N91-28176

FIXTURES
Fixture efficiency program
[DE91-014470] N91-28498

FLAME RETARDANTS
Relationships between polymer-additive molecular structure and intumescent flame retardant behavior N91-28426

FLAMES
Combustion research program: Flame studies, laser diagnostics, and chemical kinetics
[DE91-014824] N91-28329

FLAPS (CONTROL SURFACES)
An active delay of separation on two-dimensional airfoils
[ITN-91-85142] N91-28139

FLAT SURFACES
Atomistic studies of grain boundaries in alloys and compounds
[DE91-014516] N91-28372
X ray Tomographic Microscopy (XTM)
[DE91-011930] N91-28599

FLEXIBLE BODIES
Design landing loads evaluation by dynamic simulation of flexible aircraft N91-28163
Robust low-order control of flexible joint manipulators N91-28584

FLEXIBLE WINGS
Transonic shock-induced dynamics of a flexible wing with a thick circular-arc airfoil
[NASA-TM-104088] N91-28132

FLIGHT CHARACTERISTICS
Considerations on optimality of landing gear arrangement and design N91-28156

FLIGHT CONTROL
Technology needs for high speed rotorcraft (2)
[NASA-CR-177590] N91-28168

FLIGHT CREWS
Questions: Assessing the structure of knowledge and the use of information in design problem-solving N91-28169

FLIGHT HAZARDS
Assessing the risk of transporting hazardous materals by aircraft: A case study
[DE91-014016] N91-28147

FLIGHT SIMULATION
Air combat environment test and evaluation facility and the development of the offensive sensors laboratory
[DE91-011398] N91-28173

FLIGHT TESTS
Rotor and control system loads analysis of the XV-15 with the advanced technology blades
[NASA-TM-102876] N91-28134
Long time measurements of landing gear loads on SAAB SF-340 commuter aircraft N91-28157
Air combat environment test and evaluation facility and the development of the offensive sensors laboratory
[DE91-011398] N91-28173

FLOATING POINT ARITHMETIC
Toward a formal verification of a floating-point coprocessor and its composition with a central processing unit
[NASA-CR-187547] N91-28777

FLOW CHARACTERISTICS
Vaporizing particle velocimeter
[NASA-CASE-LAR-14685-1] N91-28135
Slush hydrogen propellant production, transfer, and expulsion studies at the NASA K-Site Facility
[NASA-TM-105191] N91-28449
Solution to quasi-axisymmetric internal compressible flows using the stream tube approach N91-28526

FLOW DISTRIBUTION
Transonic shock-induced dynamics of a flexible wing with a thick circular-arc airfoil
[NASA-TM-104088] N91-28132
CFD applications in chemical propulsion engines N91-28234
Numerical simulation of particle-wave interaction in boundary layers
[NASA-CR-187312] N91-28502
The application of Particle Image Velocimetry (PIV) in a short duration transonic annular turbine cascade
[AD-A236639] N91-28504
A numerical approach for modelling cavitating flows
[DE91-009178] N91-28505
Experimental study of growth rate enhancement and structure of compressible turbulent free shear layers N91-28517
Transient two-phase flow of cryogenic fluid in a vertical transfer line during the cooldown process N91-28522
An experimental investigation of a compliant surface beneath a turbulent boundary layer N91-28523
Experimental and theoretical investigation of unsteady forced convection in ducts N91-28524
An experimental study of the effect of small particles on the fluid turbulence in fully developed flow of air in a horizontal pipe N91-28525
Use of a rotated Riemann solver for the two-dimensional Euler equations N91-28530
Experiments on the instabilities in swirling and non-swirling free jets N91-28531
Active control of panel vibrations induced by boundary-layer flow
[NASA-CR-188733] N91-28643
Modeling two-point spatial turbulence spectra for analysis of gust variations over aerospace vehicles N91-28685
Log-stable distribution of energy dissipation in turbulence N91-28885
Observational constraints on pulsars: Location of the emission region and pulse shape stability on decade time scales N91-29097

FLOW EQUATIONS
Analysis of shock propagation and shock-initiated reaction in granular energetic materials N91-28446
Application of mathematica to energy principle N91-28910
Exact solutions for a system of nonlinear plasma fluid equations
[DE91-014367] N91-28965

FLOW MEASUREMENT
A study on particle dispersion in two-dimensional mixing layer flows N91-28537

FLOW STABILITY
Experiments on the instabilities in swirling and non-swirling free jets N91-28531

FLOW VELOCITY
Vaporizing particle velocimeter
[NASA-CASE-LAR-14685-1] N91-28135
A study of methods to investigate nozzle boundary layer transition N91-28232
The application of Particle Image Velocimetry (PIV) in a short duration transonic annular turbine cascade
[AD-A236639] N91-28504
A review of theories for flowing granular materials with applications to fluidized beds and solids transport
[DE91-013111] N91-28514
An experimental study of the effect of small particles on the fluid turbulence in fully developed flow of air in a horizontal pipe N91-28525
Modelling and analysis of geophysical turbulence: Use of optimal transforms and basis sets N91-28686
Shock and soliton structures induced by poloidal flow in tokamaks N91-28929

FLOW VISUALIZATION
Experiments on the instabilities in swirling and non-swirling free jets N91-28531

FLUE GASES
Formation and sustainment of a very low aspect ration tokamak using coaxial helicity injection (the Helicity Injected Torus (HIT) experiment)
[DE91-013948] N91-28967

FLUID BOUNDARIES
A chemically reacting, turbulent stratified interface N91-28144

FLUID DYNAMICS
Solution to quasi-axisymmetric internal compressible flows using the stream tube approach N91-28526

FLUID FILMS
Analysis of foil bearings for high speed operation in cryogenic applications N91-28231
Transient two-phase flow of cryogenic fluid in a vertical transfer line during the cooldown process N91-28522

FLUID FILTERS
Research and development entitled smart structures for fossil energy applications
[DE91-002064] N91-28875

FLUID FLOW
An experimental investigation of the effect of vortex generators on the aerodynamic characteristics of a NACA 0021 airfoil undergoing large amplitude pitch oscillations
[DE91-012102] N91-28133
A mathematical model for two-phase water, air, and heat flow around a linear heat source emplaced in a permeable medium
[DE91-014614] N91-28527

FLUID MECHANICS
Integrated theoretical and experimental study of the thermophysical properties of fluid mixtures
[DE91-012660] N91-28316
On the use of particle-in-cell methods for the study of magnetically-confined fusion plasmas
[DE91-015093] N91-28984
Non similarity solution approximation to the thermal hydraulic quenchback in superconductors
[DE91-013964] N91-29040

FLUID PRESSURE
Monitoring structural response in pressurized environments. Part 1: Instrumentation techniques
[DE91-012654] N91-28616

FLUIDICS
Coupling device with improved thermal interface
[NASA-CASE-GSC-13251-1] N91-28582

FLUIDIZED BED PROCESSORS
A review of theories for flowing granular materials with applications to fluidized beds and solids transport
[DE91-013111] N91-28514

FLUIDS
Integrated theoretical and experimental study of the thermophysical properties of fluid mixtures
[DE91-012660] N91-28316

FLUORESCENCE
Fixture efficiency program
[DE91-014470] N91-28498
Phase-conjugated fluorescence
[AD-A231114] N91-28820

FLUORIDES
Effect of TCP doping on the remnant polarization in uniaxially oriented poly(vinylidene fluoride) films
[AD-A237001] N91-28388
Polyimides prepared from 3,5-diamino benzo trifluoride
[NASA-CASE-LAR-14206-1] N91-28425

FLUORINE COMPOUNDS
Evidence of vibrational mode-coupling in 2-fluorethanol via high resolution infrared spectroscopy in a molecular beam
[AD-A236132] N91-28821

FLUORINE ORGANIC COMPOUNDS
High resolution infrared spectroscopy of 2-fluorethanol in a molecular beam
[AD-A236149] N91-28822

FLUOROPOLYMERS
Effect of TCP doping on the remnant polarization in uniaxially oriented poly(vinylidene fluoride) films
[AD-A237001] N91-28388

FLUTTER
Algorithm and code development for unsteady three-dimensional Navier-Stokes equations
[NASA-CR-188039] N91-28503
FLUTTER ANALYSIS
Experimental flutter boundaries with unsteady pressure distributions for the NACA 0012 Benchmark Model
[NASA-TM-104072] N91-28137
FLUX PINNING
Flux pinning and dissipation in high-temperature superconductors
[DE91-014466] N91-29042
FM/PM (MODULATION)
Performance evaluation of partial response continuous phase modulation: Discriminator detection
[ITN-91-85145] N91-28470
FOAMS
Comparisons between fast shock tube calculations and tests
[DE91-013496] N91-28177
Melamine-formaldehyde aerogels
[DE91-012084] N91-28408
Human body protection in a dynamic environment. Cushioning mechanics
[ITN-91-85149] N91-28733
FOIL BEARINGS
Analysis of foil bearings for high speed operation in cryogenic applications N91-28231
FOILS
Large growth Rayleigh-Taylor experiments on Nova
[DE91-012885] N91-28955
FOILS (MATERIALS)
Continuum x ray gauging of multiple-element materials
[DE91-011923] N91-28307
X ray fiducial foils
[DE91-011193] N91-28542
Studies of laser-driven flyer acceleration using optical fiber coupling
[DE91-013503] N91-28562
The spatial resolution of x ray microanalysis in thin foils
[DE91-011949] N91-29003
FOKKER-PLANCK EQUATION
Fluid/kinetic hybrid moment description of plasmas via a Chapman-Enskog-like approach
[DE91-013346] N91-28949
FORCE DISTRIBUTION
Generalized gyroviscous force and its effect on the momentum balance equation
[DE91-013344] N91-29061
FORCED CONVECTION
Experimental and theoretical investigation of unsteady forced convection in ducts N91-28524
FORESTS
Data users guide to the mountain cloud chemistry project
[PB91-168484] N91-28697
FORGING
Business not as usual N91-28266
FORMAT
Sound propagation in the atmosphere: Analysis of signal amplitude and phase temporal and spatial variations
[AD-A237034] N91-28816
FORMING TECHNIQUES
Test of superplastically formed corrugated aluminum compression specimens with beaded webs
[NASA-TM-104119] N91-28373
FORTRAN
Embedding ADAMS in FORTRAN
[DE91-014346] N91-28754
FOUR BODY PROBLEM
Chaos in the lowest Landau level
[DE91-014800] N91-28866
FOURIER SERIES
Symplectic full-turn maps in a Fourier representation
[DE91-012912] N91-28796
FOURIER TRANSFORMATION
A PC based frequency domain LV processor
[DE91-009056] N91-28541
FRACTURE MECHANICS
Fracture micromechanics of intermetallic and ceramic matrix continuous fiber composites
[AD-A236638] N91-28280
Development of nondestructive evaluation methods and prediction of effects of flaws on the fracture behavior of structural ceramics
[DE91-012471] N91-28410
Applications of a 2-D moving finite element formulation to elastic/viscoplastic dynamic fracture analysis
[DE91-009930] N91-28607
Influence of crack depth on the fracture toughness of reactor pressure vessel steel
[DE91-012537] N91-28611
Assessment of ductile fracture methodology based on applications to large-scale experiments
[DE91-009920] N91-28614
Near crack tip transverse strain effects estimated with a large strain hollow cylinder analogy
[DE91-012072] N91-28619
FRACTURE STRENGTH
Fracture micromechanics of intermetallic and ceramic matrix continuous fiber composites
[AD-A236638] N91-28280
ZrO2 reinforced-MoSi2 matrix composites
[DE91-013074] N91-28288
Microstructure-property relationships in Al-Cu-Li-Ag-Mg Weldalite (tm) alloys, part 2
[NASA-CR-4364] N91-28334
Effect of Li level, artificial aging, and TiB2 reinforcement on the fracture toughness of Weldalite (tm) 049-type alloys N91-28339
Effects of sample size and loading rate on the transition behavior of a DCI alloy
[DE91-012015] N91-28346
Comparisons of irradiation-induced shifts in fracture toughness, crack arrest toughness, and Charpy impact energy in high-copper welds
[DE91-008881] N91-28349
Effects of residual stresses on the fracture toughness of Zircaloy-2 tubes
[DE91-012736] N91-28354
Elevated-temperature fracture resistances (K(sub IC), R-curves, gamma sub (omega OF)) of monolithic and composite ceramics using chevron-notched, bend tests
[NASA-TM-105090] N91-28418
Influence of crack depth on the fracture toughness of reactor pressure vessel steel
[DE91-012537] N91-28611
Near crack tip transverse strain effects estimated with a large strain hollow cylinder analogy
[DE91-012072] N91-28619
Interlaminar fracture characterization: A current review
[NASA-CR-187573] N91-28626
FRACTURES (MATERIALS)
Assessment of ductile fracture methodology based on applications to large-scale experiments
[DE91-009920] N91-28614
FRAGMENTATION
Ground-based measurements of galactic cosmic ray fragmentation in shielding
[DE91-012336] N91-29133
FREE BOUNDARIES
Numerical solution of a free-boundary viscous flow
N91-28529
FREE ELECTRON LASERS
Simulation of a storage ring free electron laser with a mapping algorithm for distribution functions
[DE91-012387] N91-28552
E-beam accelerator cavity development for the ground-based free electron laser
[DE91-013760] N91-28563
Performance of the photoinjector accelerator for the Los Alamos free-electron laser
[DE91-013682] N91-28565
Short wavelength FELS
[DE91-013759] N91-28566
Reduction of energy sweep of the ETA-2 beam
[DE91-013824] N91-28568
Beam emittance and the effects of the rf, space charge and wake fields: Application to the ATF photoelectron beam
[DE91-014789] N91-28569
FREE FLOW
Receptivity of a laminar boundary layer to the interaction of a three-dimensional roughness element with time-harmonic free-stream disturbances N91-28518
FREE JETS
Experiments on the instabilities in swirling and non-swirling free jets N91-28531
FREQUENCY DISCRIMINATORS
Performance evaluation of partial response continuous phase modulation: Discriminator detection
[ITN-91-85145] N91-28470
FREQUENCY HOPPING
Performance evaluation of partial response continuous phase modulation: Discriminator detection
[ITN-91-85145] N91-28470
FREQUENCY MEASUREMENT
Edge technique for measurement of laser frequency shifts including the Doppler shift
[NASA-CASE-GSC-13343-1] N91-28557
FREQUENCY RESPONSE
Order reduction and synthesis of transfer function models N91-28769
FREQUENCY SHIFT
Edge technique for measurement of laser frequency shifts including the Doppler shift
[NASA-CASE-GSC-13343-1] N91-28557
FRICTION
Thermal and non-Newtonian effects' in elastohydrodynamic lubrication of rolling-sliding contacts
N91-28590
FRICTION FACTOR
Pressure drop and heat transfer for spirally fluted tubes including validation of the role of transition
[DE91-012242] N91-28509
FRONTS (METEOROLOGY)
Modelling and analysis of geophysical turbulence: Use of optimal transforms and basis sets N91-28686
FUEL CELLS
Electrochemical processes at solid electrode-electrolyte-gas interfaces
[DE91-012922] N91-28317
Electric and hybrid vehicles program
[DE91-013113] N91-28573
Sealant research for SOFC
[DE91-014012] N91-28592
Recent achievements in polymer electrolyte fuel cell (PEFC) research at Los Alamos National Laboratory
[DE91-013683] N91-28661
Alternative materials for solid oxide fuel cells: Chromite interconnections
[DE91-014447] N91-28664
FUEL COMBUSTION
Space fusion energy conversion using a field reversed configuration reactor: A new technical approach for space propulsion and power N91-28217
Cryogenic combustion laboratory N91-28223
Numerical simulation of the air and fuel mixing process in fuel-injected engines using discrete vortex dynamics
N91-28587
FUEL INJECTION
Spray combustion under oscillatory pressure conditions N91-28226
Numerical simulation of the air and fuel mixing process in fuel-injected engines using discrete vortex dynamics
N91-28587
FUEL SPRAYS
Liquid-propellant droplet vaporization and combustion in high pressure environments N91-28225
Cryogenic transfer options for exploration missions
[NASA-TM-105197] N91-28538
FUEL TANKS
Cryogenic transfer options for exploration missions
[NASA-TM-105197] N91-28538
FUELS
Development of biomass as an alternative fuel for gas turbines
[DE91-012129] N91-28441
FUNCTIONAL ANALYSIS
Applications of a 2-D moving finite element formulation to elastic/viscoplastic dynamic fracture analysis
[DE91-009930] N91-28607
FUNCTIONS (MATHEMATICS)
Towards the exact nature of a certain error term
[DE91-617574] N91-28801
FUSELAGES
Test of superplastically formed corrugated aluminum compression specimens with beaded webs
[NASA-TM-104119] N91-28373
A reciprocity technique for the characterisation of sound transmission into aircraft fuselages N91-28817
FUSES (ORDNANCE)
Fluctuations in near-surface backscattering to a descending CW radar
[ITN-91-85140] N91-28469
Procyon experiments utilizing foil-fuse opening switches
[DE91-014605] N91-28499
FUSION REACTORS
Space propulsion by fusion in a magnetic dipole
[DE91-012033] N91-28275
Numerical study of ion temperature gradient modes in a tokamak N91-28921
Equilibria and dynamics of temperature in a fusion reactor plasma N91-28937
Implications of TAE modes for the design of ITER
[DE91-013128] N91-28952

G

GALACTIC CLUSTERS
Void probability as a function of the void's shape and scale-invariant models
[NASA-CR-188696] N91-29113
Gravitational evolution of large-scale structure in the universe N91-29121
GALACTIC COSMIC RAYS
A search for cosmic axions N91-29104
Ground-based measurements of galactic cosmic ray fragmentation in shielding
[DE91-012336] N91-29133
GALACTIC EVOLUTION
A faint galaxy redshift survey and implications for cosmology N91-29100

Testing the Big Bang: Light elements, neutrinos, dark matter and large-scale structure
[NASA-CR-188701] N91-29111
The line of gravitation: On the quantization conditions in curved spacetime and uncertainty-driven inflation N91-29115
Star formation in the presence of magnetic fields: Molecular cloud core formation and dynamical contraction due to ambipolar diffusion:; a simulation with axial symmetry N91-29116
Observations of extragalactic water vapor masers N91-29117
Gravitational evolution of large-scale structure in the universe N91-29121

GALACTIC NUCLEI
Properties of infrared-luminous galaxies, or, how I spent seven summer vacations N91-29098
Observations of extragalactic water vapor masers N91-29117

GALACTIC STRUCTURE
Visual, red and infrared photographic surface photometry of NGC 55 and NGC 253 N91-29094
Testing the Big Bang: Light elements, neutrinos, dark matter and large-scale structure
[NASA-CR-188701] N91-29111

GALAXIES
A faint galaxy redshift survey and implications for cosmology N91-29100
Multiple nuclei, cluster core dynamics, and the velocity distributions of gravitating systems N91-29119
Gravitational evolution of large-scale structure in the universe N91-29121

GALERKIN METHOD
A study of the buckling and vibration behavior of an initially stressed thick plate by Galerkin's method N91-28641

GALLIUM ARSENIDES
The surface chemistry of GaAs atomic layer epitaxy
[DE91-014112] N91-29047

GAMMA RAY TELESCOPES
Coded aperture imaging with a HURA coded aperture and a discrete pixel detector N91-29093

GAMMA RAYS
Measuring neutron fluences and gamma/x ray fluxes with CCD cameras
[DE91-014119] N91-28549
A new model of PeV gamma ray sources and MHD turbulence in neutron star accretion columns N91-29122
Upper limits for the flux of very high-energy gamma radiation from Cygnus X-3 and for the explosion rate of primordial black holes obtained by the Haleakala Gamma Ray Observatory N91-29134
The gamma ray content of ultrahigh energy cosmic radiation N91-29135

GAPS
Thermally activated retainer means
[NASA-CASE-MSC-21793-1] N91-28186

GAS ANALYSIS
Isotopic measurements of solar noble gases in individual micrometeorites from Greenland and Antarctica N91-29114

GAS CHROMATOGRAPHY
Linked gas chromatograph-thermal energy analyzer/ion trap mass spectrometer
[DE91-013585] N91-28326
Validity of the model used to relate the energy distribution and the adsorption isotherm
[DE91-013528] N91-28428

GAS DETECTORS
Thin film hydrogen sensor
[DE91-014197] N91-28550

GAS EVOLUTION
Gas evolution from spheres
[DE91-012807] N91-28510

GAS EXPANSION
Numerical investigation of the thrust efficiency of a laser-propelled vehicle N91-28572

GAS FLOW
Droplet-turbulence interactions in subcritical and supercritical evaporating sprays N91-28228
Gas evolution from spheres
[DE91-012807] N91-28510
Moving finite elements: A continuously adaptive method for computational fluid dynamics
[DE91-013391] N91-28513
Diffraction patterns produced by periodic and turbulent flowing gases including applications of photorefractive temporal filtering
[DE91-012636] N91-28553

GAS JETS
Energy dispersive x ray diffraction study of glassy Bi2Sr2CaCu2O(x) filaments produced by gas-jet fiberization
[DE91-012021] N91-28407

GAS SPECTROSCOPY
Linked gas chromatograph-thermal energy analyzer/ion trap mass spectrometer
[DE91-013585] N91-28326

GAS TUNGSTEN ARC WELDING
Weldability of Weldalite (tm) 049 with and without TiB2 reinforcement N91-28338
Weldability of iron aluminides
[DE91-013730] N91-28367

GAS TURBINES
Development of biomass as an alternative fuel for gas turbines
[DE91-012129] N91-28441
A laser based technique for particle sizing to study two phase expansion in turbines
[DE91-014172] N91-28595

GASES
Shock and reshock of an unstable fluid interface
[DE91-014737] N91-28528

GAUGE INVARIANCE
Light-cone quantization of quantum chromodynamics
[DE91-013991] N91-28856

GAUGE THEORY
Path-integral measure for Chern-Simons theory within the stochastic quantization approach
[DE91-617610] N91-29056
Topics in low-dimensional field theory
[DE91-013784] N91-29062

GEARS
Landing gear improvements for transport aircraft N91-28159

GELS
Ignition and combustion of metallized propellants N91-28224

GENE EXPRESSION
Regulation of photosynthetic membrane components in cyanobacteria
[DE91-012713] N91-28713

GENETIC CODE
Novel methods for physical mapping of the human genome applied to the long arm of chromosome 5
[DE91-012894] N91-28717

GENETIC ENGINEERING
Novel methods for physical mapping of the human genome applied to the long arm of chromosome 5
[DE91-012894] N91-28717

GENETICS
The use of AMS to the biomedical sciences
[DE91-012037] N91-28712
Genetic changes in Mammalian cells transformed by helium cells
[DE91-013778] N91-28721
The apGA: An Adaptive Parallel Genetic Algorithm
[DE91-009559] N91-28741

GEOLOGICAL FAULTS
Borehole Radar Evaluation Program: Antenna designs for optimal directionality
[DE91-014322] N91-28475
Close-range geophotogrammetric mapping of trench walls using multi-model stereo restitution software
[DE91-013105] N91-28645

GEOLOGICAL SURVEYS
Close-range geophotogrammetric mapping of trench walls using multi-model stereo restitution software
[DE91-013105] N91-28645
Work plan for the preliminary site investigation for McMurdo Station, Ross Island, Antarctica
[DE91-015100] N91-28675
A gravity model for the Coso geothermal area, California
[DE91-011874] N91-28677

GEOMAGNETISM
Turbulent dynamo and subgrid-scale modeling of MHD turbulence N91-28887

GEOMETRICAL OPTICS
Optical analogs of model atoms in fields
[DE91-013392] N91-28855

GEOMETRY
A geometry based method of integrated engineering design, analysis, and optimization
[DE91-008588] N91-28457

GEOPHYSICS
Solar-geophysical data number 558, August 1990. Part 2: (Comprehensive reports). Data for August 1990 and miscellaneous
[PB91-172262] N91-29128
Solar-geophysical data number 558, February 1991. Part 1: (Prompt reports). Data for January 1991, December 1990, and late data
[PB91-172270] N91-29129
Solar-geophysical data number 557, January 1991. Part 1: (Prompt reports). Data for December, November 1990 an late data
[PB91-169102] N91-29130
Solar-geophysical data number 557, January 1991. Part 2: (Comprehensive reports). Data for July 1990 and miscellaneous
[PB91-169110] N91-29131

GEOSTROPHIC WIND
Normal mode decomposition of small-scale oceanic motions N91-28709

GEOTHERMAL ENERGY UTILIZATION
Applications and challenges for thermal energy storage
[DE91-012873] N91-28654
Geothermal materials development
[DE91-013972] N91-28660

GEOTHERMAL RESOURCES
A gravity model for the Coso geothermal area, California
[DE91-011874] N91-28677

GERMANIUM
Long-wavelength germanium photodetectors by ion implantation
[DE91-013848] N91-29038

GLASS
Ultra-low temperature properties of amorphous solids
[DE91-012782] N91-28312
Sol-gel kinetics by NMR
[DE91-011500] N91-28314
Ion beam sputtered coatings of bioglass N91-28384
A study of the influence of temperature gradients on densification of glass powder compacts
[DE91-012337] N91-28399
Experiments and calculations of jet penetration in glass
[DE91-013567] N91-28422
Platinum solubility in phosphate laser glass
[DE91-015123] N91-28571
Sealant research for SOFC
[DE91-014012] N91-28592
Nuclear magnetic resonance studies of atomic motion in lithium chloroborate and lithium thiosilicate glassy fast ionic conductors
[DE91-012677] N91-28843
Metastable phase equilibria in co-deposited Ni(1-x)Zr(x) thin films
[DE91-013653] N91-29029

GLASS LASERS
High-peak power-Nd:Glass laser facilities for end users
[DE91-013246] N91-28561

GLASS TRANSITION TEMPERATURE
Resonant method for the measurement of the glass transition temperature at high frequencies
[DE91-618684] N91-28416

GLAUBER THEORY
Antiproton-induced elastic and inelastic scattering at intermediate energies
[DE91-013068] N91-28849

GLOBAL POSITIONING SYSTEM
Kinematic GPS surveying N91-28149
Precise orbit determination for GPS satellites N91-28183
Analytical calibration of the airborne photogrammetric system using a priori knowledge of the exposure station obtained from kinematic Global Positioning System techniques N91-28646
The determination of mean sea level using GPS N91-28708

GLOVES
The chemical resistance of protective handwear available through the Navy's supply system
[AD-A235874] N91-28731

GLOW DISCHARGES
Theoretical studies of nonlinear sheath dynamics N91-28896

GLUONS
Heavy-quark physics in quantum chromodynamics
[DE91-012113] N91-28828
Light-cone quantization of quantum chromodynamics
[DE91-013991] N91-28856

GLUTAMINE
Plant growth is influenced by glutamine synthetase-catalyzed nitrogen metabolism
[DE91-014592] N91-28725

GLYCINE
Ultra-fine powders using glycine-nitrate combustion synthesis
[DE91-012926] N91-28412

GOLD
Laser surface modification to impede hydrogen ingress into steel N91-28375
Desorption of Al, Au, Ag using surface plasmon excitation
[DE91-013726] N91-28493

GOVERNMENT/INDUSTRY RELATIONS
Maintaining technical excellence requires a national plan N91-28196
Possible funding strategies N91-28272

US assessment of the new diamond technology in Japan
[PB91-167395] N91-28404
GRAIN BOUNDARIES
Atomistic studies of grain boundaries in alloys and compounds
[DE91-014516] N91-28372
Temperature dependence of the elastic behavior of structurally disordered metallic superlattices
[DE91-014007] N91-28377
Alloy development of Fe3Al for improved creep rupture properties
[DE91-014541] N91-28381
Creep and diffusion in nonstoichiometric oxides
[DE91-013766] N91-28435
Defects and transport in mixed oxides
[DE91-014443] N91-29049
GRAIN SIZE
Effect of Li level, artificial aging, and TiB2 reinforcement on the fracture toughness of Weldalite (tm) 049-type alloys N91-28339
GRANULAR MATERIALS
Analysis of shock propagation and shock-initiated reaction in granular energetic materials N91-28446
The deflagration-to-detonation transition in granular HMX
[DE91-014591] N91-28448
A review of theories for flowing granular materials with applications to fluidized beds and solids transport
[DE91-013111] N91-28514
GRAPH THEORY
Ezekiel graphs
[DE91-012656] N91-28805
GRAPHITE
Multiaxial failure characterization of composites
[DE91-011925] N91-28285
Apparatus for intercalating large quantities of fibrous structures
[NASA-CASE-LEW-15077-2] N91-28289
GRAPHITE-EPOXY COMPOSITES
Damage development under compression-compression fatigue loading in a stitched uniwoven graphite/epoxy composite material
[NASA-CR-188693] N91-28292
Local delamination in laminates with angle ply matrix cracks. Part 1: Tension tests and stress analysis
[NASA-TM-104055] N91-28293
GRAPHS (CHARTS)
Solar-geophysical data number 558, February 1991. Part 1: (Prompt reports). Data for January 1991, December 1990, and late data
[PB91-172270] N91-29129
Solar-geophysical data number 557, January 1991. Part 1: (Prompt reports). Data for December, November 1990 an late data
[PB91-169102] N91-29130
GRAVITATION
A gravity model for the Coso geothermal area, California
[DE91-011874] N91-28677
Normal mode decomposition of small-scale oceanic motions N91-28709
The 2+1 gravity: A new approach N91-29059
Gravitational evolution of large-scale structure in the universe N91-29121
GRAVITATIONAL COLLAPSE
Study of gravitational collapse and cosmic ray abundances N91-29105
Star formation in the presence of magnetic fields: Molecular cloud core formation and dynamical contraction due to ambipolar diffusion:; a simulation with axial symmetry N91-29116
GRAVITATIONAL EFFECTS
On accurate determination of contact angle
[DE91-013849] N91-28450
Gravitational influence of a static ring-like distribution of mass on electromagnetic waves N91-28472
GRAVITATIONAL FIELDS
Gravitational influence of a static ring-like distribution of mass on electromagnetic waves N91-28472
The line of gravitation: On the quantization conditions in curved spacetime and uncertainty-driven inflation N91-29115
Impact of the nuclear equation of state on models of rotating neutron stars
[DE91-014615] N91-29125
GRAVITY ANOMALIES
A gravity model for the Coso geothermal area, California
[DE91-011874] N91-28677
GRAVITY WAVES
Gravity wave propagation in a frontal environment N91-28687
Lidar studies of sporadic sodium layers, gravity waves and density spectra in the mesopause and stratopause regions at Urbana and Arecibo N91-28690
Normal mode decomposition of small-scale oceanic motions N91-28709
GRAY SCALE
Recovery of saturated video signals from vidicons by dynamic cathode biasing
[DE91-012402] N91-28464
GREAT LAKES (NORTH AMERICA)
Mechanisms of bacterial metals removal from solids
[DE91-012808] N91-28356
GREEN'S FUNCTIONS
Analysis of passive and active discrete-distributed linear dynamical systems using Green's function methods N91-28141
A new wake-potential calculation method using orthogonal polynomials
[DE91-013045] N91-28799
Topics on frustrated spin systems and high-temperature superconductors N91-29032
GROUND STATE
Dynamics of charge-transfer excited states relevant to photochemical energy conversion
[DE91-012669] N91-28649
Phase-conjugated fluorescence
[AD-A231114] N91-28820
Electron correlations in solid state physics
[DE91-013752] N91-29030
GROUND TESTS
Propulsion system ground testing N91-28261
GROUP DYNAMICS
How to increase meeting effectiveness and efficiency
[DE91-012420] N91-29070
The effects of information availability on the group consensus process
[DE91-012428] N91-29076
GROUP THEORY
Bialgebra deformations and algebras of trees N91-28790
GUSTS
Modeling two-point spatial turbulence spectra for analysis of gust variations over aerospace vehicles N91-28685

H

HADRONS
Dynamical behavior of excited hadronic matter
[DE91-013024] N91-28845
Light-cone quantization of quantum chromodynamics
[DE91-013991] N91-28856
HAFNIUM ALLOYS
Synthesis of metastable aluminum-based intermetallics by mechanical alloying
[DE91-013651] N91-28376
HALL EFFECT
Complex dynamics of the integer quantum Hall effect
[DE91-013383] N91-29058
HALOS
A search for cosmic axions N91-29104
HAMILTON-JACOBI EQUATION
Refinement of the Hamilton-Jacobi solution using a second canonical transformation
[DE91-012965] N91-28798
HAMILTONIAN FUNCTIONS
Theoretical studies of zirconia and related materials
[DE91-013906] N91-28369
Quantized planes and multiparameter deformations of Heisenberg and GL(N) algebras
[DE91-012481] N91-28793
Refinement of the Hamilton-Jacobi solution using a second canonical transformation
[DE91-012965] N91-28798
Invariant metrics for Hamiltonian systems
[DE91-014236] N91-28807
Structures of magnetic field lines in the helical torus N91-28932
Regular motion and symmetry in the relativistic standard map N91-28933
Diffusion and relaxation in Hamiltonian chaos N91-28934
Diffusion through stochastic webs in two and more dimensions N91-28941
Solitons and chaos in plasma N91-28943
Thermodynamic and transport properties of superconductors in very high magnetic fields
[DE91-012530] N91-29000
The derivation of effective spin Hamiltonians and the origin of the magnetic field induced transition in orthormbic La2CuO4
[DE91-013743] N91-29035
HANDBOOKS
Lessons learned and their application to program development and cultural issues N91-28263
HANFORD REACTORS
Threatened Area Database System (TADS) computer program
[DE91-012491] N91-29074
HARDENING (MATERIALS)
Shear stress prediction in shock loaded copper
[DE91-014740] N91-28635
HARMONIC GENERATORS
Exact solution of a quantum forced time-dependent harmonic oscillator
[AD-A236633] N91-28812
HARMONIC OSCILLATORS
Exact solution of a quantum forced time-dependent harmonic oscillator
[AD-A236633] N91-28812
HARMONICS
A comparative second harmonic study of Cu(111) in UHV and in solution
[AD-A237023] N91-28479
HARRIER AIRCRAFT
The special requirements of a VSTOL aircraft N91-28155
HEAT EXCHANGERS
Direct contact heat transfer to a dispersal droplet with change of phase N91-28521
HEAT FLUX
Numerical study of ion temperature gradient modes in a tokamak N91-28921
HEAT MEASUREMENT
Thermal conductivity of solid hydrogen at low temperature N91-28330
HEAT PIPES
Small Ex-core Heat Pipe Thermionic Reactor concept (SEHPTR)
[DE91-014073] N91-28279
HEAT RESISTANT ALLOYS
Microstructure-property relationships in Al-Cu-Li-Ag-Mg Weldalite (tm) alloys, part 2
[NASA-CR-4364] N91-28334
Hydrogen embrittlement of selected nickel and iron base superalloys N91-28374
Effects of various parameters on the fatigue life of alloy 718
[DE91-014100] N91-28380
HEAT SOURCES
Comparison of dynamic isotope power systems for distributed planet surface applications
[NASA-TM-4303] N91-28278
A mathematical model for two-phase water, air, and heat flow around a linear heat source emplaced in a permeable medium
[DE91-014614] N91-28527
A gravity model for the Coso geothermal area, California
[DE91-011874] N91-28677
HEAT STORAGE
Applications and challenges for thermal energy storage
[DE91-012873] N91-28654
HEAT TRANSFER
Computer modeling of ceramic melters to assess impacts of process and design variables on performance
[DE91-013668] N91-28431
Experimental investigation of pressure drop and heat transfer for air flow through enhanced tubes
[DE91-012151] N91-28508
Pressure drop and heat transfer for spirally fluted tubes including validation of the role of transition
[DE91-012242] N91-28509
Models for heat transport through assemblies of uniform-diameter hollow spheres
[DE91-012998] N91-28512
Direct contact heat transfer to a dispersal droplet with change of phase N91-28521
Near-wall modelling of complex turbulent flows N91-28534
Prediction of the flow and heat transfer between a rotating and a stationary cone N91-28536
Calculation of pressure distribution in vacuum systems using a commercial finite element program
[DE91-013611] N91-28629
Atmospheric responses to lower tropospheric forcing in a multilayer isentropic model N91-28688
Models of collisional transport across a magnetic field with destroyed surfaces N91-28900
HEAT TRANSMISSION
A mathematical model for two-phase water, air, and heat flow around a linear heat source emplaced in a permeable medium
[DE91-014614] N91-28527
Heat flow data and thermal state of the continental lithosphere N91-28682
HEAT TREATMENT
Properties of large heats of Fe3Al-based alloys
[DE91-013268] N91-28359

Origin of acoustic emission produced during single point machining [DE91-011915] N91-28453

HEATING

Applications and challenges for thermal energy storage [DE91-012873] N91-28654

Aspects of reheating in first-order inflation [NASA-CR-188705] N91-29108

HEAVY IONS

SDI: Statistical Dynamic Interactions [DE91-012034] N91-28827

Chamber propagation [DE91-012797] N91-28954

Inertial confinement fusion [DE91-013479] N91-28960

HEAVY LIFT LAUNCH VEHICLES

NASA's advanced space transportation system launch vehicles N91-28195

Next generation solid boosters N91-28207

Next generation: Unmanned launch vehicles and upper stages: The needs N91-28210

Space transportation propulsion USSR launcher technology, 1990 N91-28220

Heavy-lift launch vehicle propulsion considerations N91-28236

Humans to Mars in 1999 N91-28237

HEISENBERG THEORY

Quantized planes and multiparameter deformations of Heisenberg and GL(N) algebras [DE91-012481] N91-28793

HELICAL FLOW

Equilibrium beta limit of helical systems N91-28894

Helical field effect in solar/stellar wind N91-28912

HELICAL WINDINGS

Reversed field pinch experiments [DE91-013643] N91-28977

HELICOPTER DESIGN

Technology needs for high speed rotorcraft (2) [NASA-CR-177590] N91-28168

HELICOPTERS

Effectiveness of tiltrotor support to ground combat [DE91-013603] N91-28167

HELIOSTATS

Second-generation central receiver technology comparison [DE91-012865] N91-28653

HELIOTRONS

Edge anomalous transport in heliotron/torsatron N91-28892

HELIUM IONS

Genetic changes in Mammalian cells transformed by helium cells [DE91-013778] N91-28721

HELIUM ISOTOPES

Space fusion energy conversion using a field reversed configuration reactor: A new technical approach for space propulsion and power N91-28217

High-resolution measurements of the thermal conductivity and boundary resistance of helium-4 near the lambda point N91-28322

HETEROGENEITY

Analysis of the surface heterogeneity of different samples of aluminum oxide ceramic powders [DE91-013527] N91-28421

Seismic traveltime inversion in three-dimensional heterogeneous media N91-28678

Solving computational grand challenges using a network of heterogeneous supercomputers [DE91-013725] N91-28755

HETEROJUNCTIONS

High pressure optical studies of semiconductors and heterostructures [DE91-014382] N91-29041

HEURISTIC METHODS

The SNL, Livermore, Hopkinson bar apparatus for compressive materials testing at high strain-rates [DE91-013132] N91-28612

HIGH ENERGY INTERACTIONS

Measurements of angular distributions of absolute cross sections and analyzing powers of the reaction bar-p p yields d(pi+) between 1.3 and 2.4 GeV [DE91-012638] N91-28842

New techniques in neutron data measurements above 30 MeV [DE91-013690] N91-28861

High Energy Physics Division semiannual report of research activities, July 1, 1990--December 31, 1990 [DE91-012339] N91-28868

HIGH FIELD MAGNETS

Light weight, high field, stable, superconducting magnets for advanced transportation systems [DE91-013667] N91-28814

HIGH FREQUENCIES

Resonant method for the measurement of the glass transition temperature at high frequencies [DE91-618684] N91-28416

HIGH POLYMERS

Subgap absorption in conjugated polymers [DE91-012655] N91-28402

HIGH POWER LASERS

Numerical and analytical analysis of thin laser-driven flyer plates [DE91-013748] N91-28567

HIGH PRESSURE

Liquid-propellant droplet vaporization and combustion in high pressure environments N91-28225

High pressure optical studies of semiconductors and heterostructures [DE91-014382] N91-29041

HIGH RESOLUTION

High-resolution interferometric measurements of residual strains in composites N91-28303

Advancing conventional high-resolution electron microscopy [DE91-013773] N91-28548

A new approach to analyzing high-resolution aerial photographs of urban areas N91-28647

Evidence of vibrational mode-coupling in 2-fluorethanol via high resolution infrared spectroscopy in a molecular beam [AD-A236132] N91-28821

High resolution infrared spectroscopy of 2-fluorethanol in a molecular beam [AD-A236149] N91-28822

HIGH SPEED

Technology needs for high speed rotorcraft (2) [NASA-CR-177590] N91-28168

Analysis of foil bearings for high speed operation in cryogenic applications N91-28231

HIGH STRENGTH ALLOYS

Microstructure-property relationships in Al-Cu-Li-Ag-Mg Weldalite (tm) alloys, part 2 [NASA-CR-4364] N91-28334

Neutron diffraction determination of the residual stress redistribution in cracked autofrettaged tubing [DE91-013688] N91-28632

HIGH STRENGTH STEELS

Laser surface modification to impede hydrogen ingress into steel N91-28375

HIGH TEMPERATURE

In-situ REM imaging of surface processes on ceramic bulk crystals from 300 to 1670 K in a conventional TEM [DE91-009923] N91-28405

Creep and diffusion in nonstoichiometric oxides [DE91-013766] N91-28435

HIGH TEMPERATURE ENVIRONMENTS

Weldability of Weldalite (tm) 049 with and without TiB2 reinforcement N91-28338

High-temperature elasticity and Earth's upper mantle N91-28679

HIGH TEMPERATURE PLASMAS

Hydrodynamic instabilities in laser driven implosion N91-28897

On the use of particle-in-cell methods for the study of magnetically-confined fusion plasmas [DE91-015093] N91-28984

HIGH TEMPERATURE SUPERCONDUCTORS

Improved superconducting bearings [NASA-CASE-GSC-13346-1] N91-28578

Light weight, high field, stable, superconducting magnets for advanced transportation systems [DE91-013667] N91-28814

Development of elements of a high T(sub c) superconducting cable [AD-A236151] N91-28986

Growth of high T(sub c) superconducting thin films for microwave applications [DE91-011436] N91-28991

Superconducting bolometers: High-T(sub c) and low-T(sub c) [DE91-011830] N91-28992

High-T(sub c) thin-film microelectronics [DE91-012340] N91-28997

Interlayer pairing and c-axis versus ab-plane gap anisotropy in high Tc superconductor [DE91-012218] N91-29005

Effect of size and geometry on levitation force measurements between permanent magnets and high-temperature superconductors [DE91-012472] N91-29008

Topics on frustrated spin systems and high-temperature superconductors N91-29032

Flux pinning and dissipation in high-temperature superconductors [DE91-014466] N91-29042

Application of muon spin relaxation experiment to the vortex dynamics of high temperature superconductors [DE91-014607] N91-29050

Annealing and structure studies on Tl-2223 and Tl-1223 crystals [DE91-014903] N91-29052

HIGH VOLTAGES

Some high voltage DC breakdown properties of thick film circuits on alumina [DE91-014675] N91-28500

HISTORIES

Historical perspectives: The role of the NASA Lewis Research Center in the national space nuclear power programs [NASA-TM-105196] N91-29138

HMX

The deflagration-to-detonation transition in granular HMX [DE91-014591] N91-28448

HOLE MOBILITY

Electrical and photomechanical effects of plastic deformation of mercuric iodide [DE91-013108] N91-29022

HOLES (MECHANICS)

Fracture micromechanics of intermetallic and ceramic matrix continuous fiber composites [AD-A236638] N91-28280

HOMOPOLAR GENERATORS

Development of a current collection loss management system for SDI homopolar power supplies [DE91-012779] N91-28652

HOMOTOPY THEORY

The solution of variable-geometry truss problems using new homotopy continuation methods N91-28640

HONEYCOMB STRUCTURES

Evaluation of a technique to generate artificially thickened boundary layers in supersonic and hypersonic flows [NASA-TP-3142] N91-28136

The Soudan 2 honeycomb calorimeter [DE91-013404] N91-28860

HOT PRESSING

Synthesis of metastable aluminum-based intermetallics by mechanical alloying [DE91-013651] N91-28376

HOUSINGS

Roller locking brake [NASA-CASE-GSC-13376-1] N91-28579

Device for removing foreign objects from anatomic organs [NASA-CASE-GSC-13306-1] N91-28727

HUBBLE SPACE TELESCOPE

Interstellar magnesium studies N91-29120

HUGONIOT EQUATION OF STATE

Equation-of-state from SiO2 aerogel Hugoniot data [DE91-011480] N91-28313

SESAME equation of state number 7740: Polycarbonate [DE91-013970] N91-28436

Quantum mechanical effects on the shock Hugoniot [DE91-014750] N91-28636

HUMAN BEHAVIOR

The human side of value engineering [DE91-012817] N91-29068

HUMAN BEINGS

New techniques for positron emission tomography in the study of human neurological disorders [DE91-013855] N91-28728

HUMAN FACTORS ENGINEERING

Robotic mannequin technology for enhanced product testing [DE91-013787] N91-28591

Using HSYS in the analysis of human-system interactions: Examples from the offshore petroleum industry [DE91-013218] N91-28732

A selection tool for choosing the best participative problem-solving technique [DE91-012421] N91-29066

The human side of value engineering [DE91-012817] N91-29068

Why engineers must know and manage organizational culture [DE91-012425] N91-29071

HUMAN RESOURCES

Launch operations manpower yesterday, today and tomorrow N91-28267

HYDROBORATION

Nitrogen and boron-containing polymers as precursors of ceramic materials [DE91-008890] N91-28390

HYDROCARBONS

A laser based technique for particle sizing to study two phase expansion in turbines [DE91-014172] N91-28595

Magnetic resonance and optical spectroscopic studies of carotenoids [DE91-014361] N91-28724

HYDRODYNAMICS
Energy dissipation in chemical reactions on ultrafast timescales [DE91-012342] N91-28315
A numerical approach for modelling cavitating flows [DE91-009178] N91-28505
Boussinesq algorithm for enclosed bouyant convection in two dimensions [PB91-178848] N91-28507
Evaporation as a diagnostic test for hydrodynamic cooling of laser-ablated clusters [DE91-013416] N91-28555
MESA: A 3-D Eulerian hydrocode for penetration mechanics studies [DE91-013308] N91-28613
Hydrodynamic evolution of picosecond laser-plasmas [DE91-013245] N91-28958

HYDROFLUORIC ACID
The effect of fluoride gases on cylinder valve corrosion [DE91-012745] N91-28355

HYDROGEN
Thermal conductivity of solid hydrogen at low temperature N91-28330
Reactive characterization as a probe of the nature of catalytic sites [DE91-014536] N91-28333
The effect of stress on hydrogen uptake and desorption by A-286 [NASA-TM-103537] N91-28341
Pacific Northwest hydrogen feasibility study [DE91-013427] N91-28445
Thin film hydrogen sensor [DE91-014197] N91-28550

HYDROGEN ATOMS
Enhancing atom densities in solid hydrogen by isotopic substitution [DE91-011189] N91-28824
Evidences of trapping in tungsten and implications for plasma-facing components [DE91-012734] N91-28951

HYDROGEN EMBRITTLEMENT
Composite material systems for hydrogen management N91-28229
Hydrogen embrittlement of selected nickel and iron base superalloys N91-28374
Laser surface modification to impede hydrogen ingress into steel N91-28375

HYDROGEN FUELS
Pacific Northwest hydrogen feasibility study [DE91-013427] N91-28445
Enhancing atom densities in solid hydrogen by isotopic substitution [DE91-011189] N91-28824

HYDROGEN IONS
H(-) beam characterization using laser-induced neutralization [DE91-013501] N91-28564

HYDROGEN ISOTOPES
Evidences of trapping in tungsten and implications for plasma-facing components [DE91-012734] N91-28951

HYDROGEN OXYGEN ENGINES
Advanced cryo propulsion systems N91-28212
STV engine design considerations N91-28255

HYDROGEN PLASMA
Donor formation under hydrogen plasma exposure and ion implantation [DE91-011958] N91-29004

HYDROGEN PRODUCTION
Slush hydrogen propellant production, transfer, and expulsion studies at the NASA K-Site Facility [NASA-TM-105191] N91-28449
Photobiotechnology: Algal hydrogen production and photoconductivity of metalized chloroplasts [DE91-013232] N91-28718

HYDROGENATION
Mechanism of hydrodenitrogenation. Part 5: X ray diffraction of molybdenum catalysts [DE91-013853] N91-28327

HYDROXYL EMISSION
Interaction of radiation with outflows in late-type stars N91-29136

HYPERBOLIC DIFFERENTIAL EQUATIONS
Parallelizing across time when solving time-dependent partial differential equations [DE91-012948] N91-28797

HYPERCUBE MULTIPROCESSORS
Performance of the Intel iPSC/860 and Ncube 6400 hypercubes [DE91-012370] N91-28738
Choosing processor array configuration by performance modeling for a highly parallel linear algebra algorithm [DE91-012486] N91-28749
Bayesian design and analysis of computer experiments: Use of derivatives in surface prediction [DE91-013147] N91-28751
Searching for consensus patterns on a hypercube [DE91-013233] N91-28753
Performance measurement of a parallel input/output system for the Intel iPSC/2 hypercube [DE91-014219] N91-28779
Mapping implicit spectral methods to distributed memory architectures [NASA-CR-187592] N91-28806
Implementation of a hypercube database system [DE91-014285] N91-29089

HYPERPLANES
Robust and real-time control of magnetic bearings for space engines N91-28230

HYPERSONIC FLOW
Evaluation of a technique to generate artificially thickened boundary layers in supersonic and hypersonic flows [NASA-TP-3142] N91-28136

HYPERSONIC SPEED
Experimental study of growth rate enhancement and structure of compressible turbulent free shear layers N91-28517

HYPERVELOCITY GUNS
Hypervelocity plate acceleration [DE91-014738] N91-28179
A theoretical and experimental study of the interior ballistic processes of an electrothermal gun N91-28185

HYPERVELOCITY LAUNCHERS
Sandia's new hypervelocity launcher (HVL) [DE91-014335] N91-28178

HYPOTHESES
Formation and dynamics of solitary waves and vortices in driven and damped systems N91-28942

HYSTERESIS
Measurement accuracy of macroscopic quantum circuits with RF-biased Josephson junction arrays [DE91-012651] N91-29009

I

IGNITERS
Semiconductor Bridge (SCB) research and development [DE91-011493] N91-28319

IGNITION
Ignition and combustion of metallized propellants N91-28224
Semiconductor Bridge (SCB) research and development [DE91-011493] N91-28319
Investigation of the Deflagration-to-Detonation (DDT) process: The role of ignition and explosive properties in DDT [DE91-011956] N91-28442
The deflagration-to-detonation transition in granular HMX [DE91-014591] N91-28448

IMAGE CONTRAST
Correcting channeling and diffraction effects in quantitative REELS surface microanalysis [DE91-009924] N91-28840

IMAGE ENHANCEMENT
Correcting channeling and diffraction effects in quantitative REELS surface microanalysis [DE91-009924] N91-28840

IMAGE INTENSIFIERS
WFOV star tracker camera [DE91-012776] N91-28148

IMAGE PROCESSING
Model-based computed tomography for nondestructive evaluation [DE91-013462] N91-28602
Close-range geophotogrammetric mapping of trench walls using multi-model stereo restitution software [DE91-013105] N91-28645
A new approach to analyzing high-resolution aerial photographs of urban areas N91-28647

IMAGE RESOLUTION
Applications of scanning tunneling microscopy to electrochemistry [AD-A237021] N91-28304

IMAGE TUBES
An evaluation of monochrome solid-state video cameras [DE91-012368] N91-28543

IMAGES
SDI: Statistical Dynamic Interactions [DE91-012034] N91-28827

IMAGING TECHNIQUES
The application of x ray tomographic microscopy to chemical vapor infiltration processing of ceramic matrix composites [DE91-011871] N91-28284
Proton Energy Loss (PEL) material characterization [DE91-011545] N91-28306
In-situ REM imaging of surface processes on ceramic bulk crystals from 300 to 1670 K in a conventional TEM [DE91-009923] N91-28405
Measuring neutron fluences and gamma/x ray fluxes with CCD cameras [DE91-014119] N91-28549
Laser range camera calibration [DE91-014939] N91-28570
X ray microimaging of elemental composition and microstructure for materials science [DE91-012052] N91-28601
Analytical calibration of the airborne photogrammetric system using a priori knowledge of the exposure station obtained from kinematic Global Positioning System techniques N91-28646
A new approach to analyzing high-resolution aerial photographs of urban areas N91-28647
Scanning Transmission Ion Microscopy (STIM): A new technique for density mapping of microstructures [DE91-011917] N91-28825
X ray microimaging of elemental composition and microstructure for materials science [DE91-012221] N91-28832
Correcting channeling and diffraction effects in quantitative REELS surface microanalysis [DE91-009924] N91-28840
Laser speckle velocimetry with photorefractive recording and anamorphic optical processing N91-28880
Characterization of crystalline interfaces by advanced electron microscopy [DE91-011883] N91-29002
Direct imaging of ordering in Si-Ge alloys, ultrathin superlattices, and buried Ge layers [DE91-014580] N91-29044
Coded aperture imaging with a HURA coded aperture and a discrete pixel detector N91-29093

IMPACT
A study of the impact of reaction rates on equation of state [DE91-013375] N91-28621

IMPACT LOADS
Operational loads on landing gear N91-28158
F-106B airplane active control landing gear drop test performance N91-28164
Shock-wave properties of high-strength ceramics [DE91-014105] N91-28439
Modification and evaluation of Elastomer Test Machine (ETM) [AD-A236143] N91-28540

IMPACT TESTS
Response of the polymers KEL-F, polysulfone, high density polyethylene and polymethylmethacrylate to shock loading and release from 0.3 to 2.4 GPa [DE91-012867] N91-28411
Shock-wave properties of high-strength ceramics [DE91-014105] N91-28439
MESA: A 3-D Eulerian hydrocode for penetration mechanics studies [DE91-013308] N91-28613
A new model of rate dependent elastic-plastic flow [DE91-014600] N91-28633

IMPEDANCE
Electrochemical processes at solid electrode-electrolyte-gas interfaces [DE91-012922] N91-28317
Perturbation treatment of the longitudinal coupling impedance of a toroidal beam tube [DE91-013884] N91-28495

IMPLOSIONS
Generating strong shock waves with a supersonic peristaltic pump [DE91-013228] N91-28174
Hydrodynamic instabilities in laser driven implosion N91-28897
Nonlinear evolution of 2D and 3D Rayleigh-Taylor instability at stagnation phase in laser implosion N91-28899
Turbulent mixing due to Rayleigh-Taylor instability in laser driven implosion N91-28914

IN-FLIGHT MONITORING
The in-flight calibration of a helicopter-mounted Daedalus multispectral scanner [DE91-013054] N91-28170

INCENTIVES
Technology transfer methodology N91-28239

INCOMPRESSIBLE FLOW
ZEPHYR3D: A finite difference computer program for three-dimensional, transient incompressible flow problems
[DE91-014331] N91-28515
The numerical solution of confined laminar flow past a moving boundary N91-28532
A critical analysis of anisotropic k-epsilon modeling and its application to turbulence-driven secondary flows
N91-28533
Steady-state dynamo and current drive in a nonuniform bounded plasma
[DE91-014865] N91-28974

INCONEL (TRADEMARK)
Composite material systems for hydrogen management N91-28229

INDEXES (DOCUMENTATION)
Large space structures and systems in the space station era: A bibliography with indexes
[NASA-SP-7085(02)] N91-28191
Aerospace medicine and biology: A continuing bibliography with indexes (supplement 352)
[NASA-SP-7011(352)] N91-28729
NASA patent abstracts bibliography: A continuing bibliography. Section 2: Indexes (supplement 39)
[NASA-SP-7039(39)-SECT-2] N91-29088

INDIUM COMPOUNDS
Indium compounds which contain two different organic substituents. Crystal structure of (In(CH2CMe3)(CH2SiMe3)Cl)2, an interesting case of partial Ligand disorder in the solid state
[AD-A236730] N91-28989

INDUSTRIAL PLANTS
Guidelines for acquisition, installation, and testing of performance assessment software
[DE91-013910] N91-28764

INDUSTRIES
Model-based computed tomography for nondestructive evaluation
[DE91-013462] N91-28602

INELASTIC SCATTERING
Antiproton-induced elastic and inelastic scattering at intermediate energies
[DE91-013068] N91-28849
Neutron scattering studies of spin correlations in metallic YBa2Cu3O(6+x)
[DE91-013794] N91-29031

INERTIAL CONFINEMENT FUSION
High-peak power-Nd:Glass laser facilities for end users
[DE91-013246] N91-28561
Nonlinear evolution of 2D and 3D Rayleigh-Taylor instability at stagnation phase in laser implosion
N91-28899
Turbulent mixing due to Rayleigh-Taylor instability in laser driven implosion N91-28914
Inertial confinement fusion
[DE91-013479] N91-28960
The Cascade inertial confinement fusion reactor concept
[DE91-013852] N91-28966

INERTIAL UPPER STAGE
Current systems: Upper stages N91-28201

INFORMATION DISSEMINATION
Large space structures and systems in the space station era: A bibliography with indexes
[NASA-SP-7085(02)] N91-28191

INFORMATION MANAGEMENT
The design of a clinical laboratory information system
N91-29083
Information management: A uniform conceptual model and its user interface N91-29084
Generalized hypertext in a knowledge-based decision support shell environment N91-29086

INFORMATION RETRIEVAL
The computer storage, retrieval, and searching of generic structures in chemical patents: The machine-readable representation of generic structures
N91-29081
Design and performance evaluation of signature files for text retrieval systems N91-29085
Generalized hypertext in a knowledge-based decision support shell environment N91-29086

INFORMATION SYSTEMS
Questions: Assessing the structure of knowledge and the use of information in design problem-solving
N91-28169
Seeking solutions: High-performance computing for science
[PB91-169763] N91-28752
Developing a GIS to facilitate data analysis for environmental restoration of a large waste site
[DE91-013222] N91-29078
The computer storage, retrieval, and searching of generic structures in chemical patents: The machine-readable representation of generic structures
N91-29081
The design of a clinical laboratory information system
N91-29083
A simulated user for laboratory investigation of information systems requirements determination
N91-29087

INFORMATION THEORY
A framework for data and information
[DE91-012416] N91-29075
The effects of information availability on the group consensus process
[DE91-012428] N91-29076

INFRARED ASTRONOMY
Visual, red and infrared photographic surface photometry of NGC 55 and NGC 253 N91-29094
Search for regularities in the atmosphere of Jupiter
N91-29127

INFRARED PHOTOGRAPHY
Visual, red and infrared photographic surface photometry of NGC 55 and NGC 253 N91-29094

INFRARED PHOTOMETRY
Visual, red and infrared photographic surface photometry of NGC 55 and NGC 253 N91-29094

INFRARED RADIATION
Superconducting bolometers: High-T(sub c) and low-T(sub c)
[DE91-011830] N91-28992
Properties of infrared-luminous galaxies, or, how I spent seven summer vacations N91-29098

INFRARED SPECTRA
Measurements of photo-induced changes in conjugated polymers
[DE91-013262] N91-28427
Research on stable, high-efficiency amorphous silicon multijunction modules
[DE91-002138] N91-28480

INFRARED SPECTROSCOPY
Evidence of vibrational mode-coupling in 2-fluorethanol via high resolution infrared spectroscopy in a molecular beam
[AD-A236132] N91-28821
High resolution infrared spectroscopy of 2-fluorethanol in a molecular beam
[AD-A236149] N91-28822
Molecular eigenstate spectroscopy: Application to the intramolecular dynamics of some polyatomic molecules in the 3000 to 7000 cm(exp -1) region
[DE91-013154] N91-28839

INHOMOGENEITY
Steady-state dynamo and current drive in a nonuniform bounded plasma
[DE91-014865] N91-28974

INJECTION
Cryogenic transfer options for exploration missions
[NASA-TM-105197] N91-28538

INJECTION MOLDING
The influence of defects on the mechanical properties of short fibre reinforced thermoplastics N91-28300

INLET FLOW
A study of methods to investigate nozzle boundary layer transition N91-28232

INLET TEMPERATURE
Experimental and theoretical investigation of unsteady forced convection in ducts N91-28524

INORGANIC COMPOUNDS
Chemistry of electronic ceramic materials. Proceedings of the International Conference on the Chemistry of Electronic Ceramic Materials
[NASA-CR-188688] N91-28403

INPUT/OUTPUT ROUTINES
Measuring and modelling disk I/O subsystems
[ISBN-90-6275-567-4] N91-28736
Parallel input/output architectures for multiprocessors
N91-28740
Performance measurement of a parallel input/output system for the Intel iPSC/2 hypercube
[DE91-014219] N91-28779

INSERTS
Improved method and apparatus for Mach number change in wind tunnel
[NASA-CASE-LAR-13548-1] N91-28175

INSPECTION
Nondestructive testing standards and the ASME code
[DE91-012643] N91-28600

INSTRUMENT COMPENSATION
Irradiance compensation control for high-energy laser propagation. Part 1: Theory and Fourier control model propagation results
[DE91-013130] N91-28559

INSULATION
A reciprocity technique for the characterisation of sound transmission into aircraft fuselages N91-28817

INTEGRATED CIRCUITS
Reflection mask technology for soft x ray projection lithography
[DE91-012561] N91-28877

INTEGRATED OPTICS
Simulation of planar integrated photonics devices with the LLNL time-domain finite-difference code suite
[DE91-011929] N91-28876

INTERACTIONAL AERODYNAMICS
Receptivity of a laminar boundary layer to the interaction of a three-dimensional roughness element with time-harmonic free-stream disturbances N91-28518

INTERCALATION
Apparatus for intercalating large quantities of fibrous structures
[NASA-CASE-LEW-15077-2] N91-28289

INTERCEPTION
Defending the defenders: Brilliant pebble defense against pop-up neutral particle beam suppression attacks
[DE91-012521] N91-28809

INTERFACE STABILITY
Study of interfacial behavior in cocurrent gas-liquid flows
[DE91-013008] N91-28511

INTERFACES
Electrochemical processes at solid electrode-electrolyte-gas interfaces
[DE91-012922] N91-28317
Shock and reshock of an unstable fluid interface
[DE91-014737] N91-28528
Dynamics of interfaces with internal structures
N91-28926
Characterization of crystalline interfaces by advanced electron microscopy
[DE91-011883] N91-29002
Direct imaging of ordering in Si-Ge alloys, ultrathin superlattices, and buried Ge layers
[DE91-014580] N91-29044

INTERFACIAL TENSION
An analysis of interlaminar stresses in unsymmetrically laminated plates N91-28299
Parallel nanometer scale fabrication
[DE91-013016] N91-29026

INTERFERENCE IMMUNITY
Mutual interference between many similar radars operating in physical proximity
[ITN-91-85139] N91-28468

INTERFEROMETERS
Studies of laser-driven flyer acceleration using optical fiber coupling
[DE91-013503] N91-28562

INTERFEROMETRY
A microwave interferometer to measure particle and shock velocities simultaneously
[DE91-013077] N91-28545

INTERGRANULAR CORROSION
Analysis of brittle intergranular crack propagation during stress corrosion cracking
[DE91-013666] N91-28630

INTERIOR BALLISTICS
A theoretical and experimental study of the interior ballistic processes of an electrothermal gun N91-28185

INTERLAYERS
The effect of ductile innerlayers on the mechanical performance of fiber-reinforced composite materials
N91-28295
Investigation of interlayer materials for the microwave joining of SiC
[DE91-013311] N91-28414
Interlayer pairing and c-axis versus ab-plane gap anisotropy in high Tc superconductor
[DE91-012218] N91-29005

INTERMETALLICS
Fracture micromechanics of intermetallic and ceramic matrix continuous fiber composites
[AD-A236638] N91-28280
Atomistic studies of grain boundaries in alloys and compounds
[DE91-014516] N91-28372
Welding of ductile intermetallic alloys
[DE91-009553] N91-28594

INTERNATIONAL COOPERATION
Overview of European and other non-US/USSR/Japan launch vehicle and propulsion technology programs
N91-28221

INTERPLANETARY FLIGHT
Space propulsion by fusion in a magnetic dipole
[DE91-012033] N91-28275

INTERPLANETARY SPACECRAFT
Space transfer vehicles and space basing
N91-28254
STV engine design considerations N91-28255

INTERPOLATION
Radiative transfer model for a spherical atmosphere
N91-28689

Operational interpolation of data in triangular array [DE91-012987] N91-28800

INTERPROCESSOR COMMUNICATION
Seeking solutions: High-performance computing for science [PB91-169763] N91-28752

INTERSTELLAR EXTINCTION
Population synthesis models for cluster galaxies at redshifts of 0.4 to 0.55 N91-29124

INTERSTELLAR GAS
Explosion of a superbubble in a uniform magnetic field N91-29102

INTERSTELLAR MAGNETIC FIELDS
Explosion of a superbubble in a uniform magnetic field N91-29102

INTERSTELLAR MASERS
Observations of extragalactic water vapor masers N91-29117

INTERSTELLAR MATTER
Star formation in the presence of magnetic fields: Molecular cloud core formation and dynamical contraction due to ambipolar diffusion:; a simulation with axial symmetry N91-29116
Interstellar magnesium studies N91-29120

INTERSTELLAR RADIATION
Interaction of radiation with outflows in late-type stars N91-29136

INTERSTITIALS
The interaction of HVEM-generated point-defects with dissociated dislocations [DE91-013353] N91-29027

INVARIANCE
Invariant metrics for Hamiltonian systems [DE91-014236] N91-28807

INVENTIONS
Process for application of powder particles to filamentary materials [NASA-CASE-LAR-14231-1-CU] N91-28290
Improving the performance of blasting caps [NASA-CASE-LAR-13832-1] N91-28444
Noncircular rolling joints for vibrational reduction in slewing maneuvers [NASA-CASE-LAR-14515-1-CU] N91-28580
Coupling device with improved thermal interface [NASA-CASE-GSC-13251-1] N91-28582
Direction discriminating hearing aid [NASA-CASE-GSC-13027-1] N91-28726

INVERSE KINEMATICS
Kinematic analysis of legged system locomotion on smooth horizontal surfaces N91-28586
Selected topics in mechanisms and robotics: Singularities, inverse kinematics, and collision detection N91-28598

INVERSIONS
Seismic traveltime inversion in three-dimensional heterogeneous media N91-28678
Multidimensional spectral estimation using iterative methods [AD-A237025] N91-28791

INVISCID FLOW
CFD applications in chemical propulsion engines N91-28234
Numerical investigation of the thrust efficiency of a laser-propelled vehicle N91-28572

IODIDES
The pressure-induced Mott transition in transition-metal iodides [DE91-013671] N91-28366
Electrical and photomechanical effects of plastic deformation of mercuric iodide [DE91-013108] N91-29022
Crystal surface analysis using matrix textural features classified by a probabilistic neural network [DE91-014120] N91-29048

IODINE ISOTOPES
The pressure-induced Mott transition in transition-metal iodides [DE91-013671] N91-28366

ION ACOUSTIC WAVES
Measurements of the ion acoustic decay instability and the resultant enhanced laser absorption and enhanced bremsstrahlung in laser-plasma interaction experiments [DE91-014250] N91-28956

ION ATOM INTERACTIONS
Correlated charge-changing ion-atom collisions [DE91-013640] N91-28863

ION BEAMS
Ion beam sputtered coatings of bioglass N91-28384
H(-) beam characterization using laser-induced neutralization [DE91-013501] N91-28564
Genetic changes in Mammalian cells transformed by helium cells [DE91-013778] N91-28721
Progress in light ion fusion [DE91-012019] N91-28826
Beam structure and transverse emittance studies of high-energy ion beams [DE91-013499] N91-28871
Suppression and control of magnetic islands in toroidal plasmas N91-28895
Direct ion heating in MHD relaxation N91-28911
Chamber propagation [DE91-012797] N91-28954
Stability of annular equilibrium of energetic large orbit ion beam [DE91-014365] N91-28963
Plasma immersion surface modification with metal ion plasma [DE91-014233] N91-28979
Parallel nanometer scale fabrication [DE91-013016] N91-29026

ION CURRENTS
Particle simulation on the tilt stabilization of the FRC plasma N91-28917

ION CYCLOTRON RADIATION
An assessment of the lifetime of Faraday shield elements [DE91-012228] N91-28463
Mode conversion of Alfven waves induced by quadrupole magnetic field modulation N91-28924
Numerical simulation of potential-driven ion cyclotron oscillation N91-28925

ION EMISSION
Beam structure and transverse emittance studies of high-energy ion beams [DE91-013499] N91-28871

ION ENGINES
Small Ex-core Heat Pipe Thermionic Reactor concept (SEHPTR) [DE91-014073] N91-28279

ION IMPACT
Impact of ion propulsion on performance, design, testing, and operation of a geosynchronous spacecraft [AD-A237028] N91-28273

ION IMPLANTATION
Radiation disorder and aperiodicity in irradiated ceramics [DE91-010257] N91-28391
Theoretical studies of nonlinear sheath dynamics N91-28896
Donor formation under hydrogen plasma exposure and ion implantation [DE91-011958] N91-29004
Long-wavelength germanium photodetectors by ion implantation [DE91-013848] N91-29038

ION MICROSCOPES
APFIM characterization of the spinodal decomposition in duplex stainless steels [DE91-014256] N91-28371
Scanning Transmission Ion Microscopy (STIM): A new technique for density mapping of microstructures [DE91-011917] N91-28825

ION PROBES
Kinetic energy distributions of ions after surface collisions [DE91-013412] N91-28850
Spectroscopic and ion probe characterization of laser produced plasmas used for thin film growth [DE91-013425] N91-28959

ION PROPULSION
Impact of ion propulsion on performance, design, testing, and operation of a geosynchronous spacecraft [AD-A237028] N91-28273

ION SOURCES
Plasma transport in a new cathodic arc ion source, theory and experiment [DE91-011511] N91-28944

ION TEMPERATURE
Ion temperature gradient turbulence and coherent structures N91-28890
Numerical study of ion temperature gradient modes in a tokamak N91-28921
Fluctuation spectrum of ion temperature gradient driven modes in sheared magnetic fields N91-28936

ION TRAPS (INSTRUMENTATION)
Chemical characterization of microparticles by laser ablation in an ion trap mass spectrometer [DE91-012513] N91-28309
Linked gas chromatograph-thermal energy analyzer/ion trap mass spectrometer [DE91-013585] N91-28326
Fixed-wavelength R2PI/tandem mass spectrometry for mixture analysis in the quadrupole ion trap [DE91-012506] N91-28835
Spontaneous cluster decomposition in a quadrupole ion trap [DE91-012519] N91-28836

IONIC COLLISIONS
Correlated charge-changing ion-atom collisions [DE91-013640] N91-28863

IONIZATION
Analysis of metals in solution using electrospray ionization mass spectrometry [DE91-012522] N91-28310
Interactions of molecules with surfaces [DE91-014498] N91-28857
Measurements of ionization cross-section for electron energy-loss microanalysis under well defined scattering conditions [DE91-013745] N91-28862

IONIZATION CROSS SECTIONS
Measurements of ionization cross-section for electron energy-loss microanalysis under well defined scattering conditions [DE91-013745] N91-28862

IONIZING RADIATION
Measuring neutron fluences and gamma/x ray fluxes with CCD cameras [DE91-014119] N91-28549
Chromosomal changes in cultured human epithelial cells transformed by low- and high-LET radiation [DE91-013772] N91-28720

IONOSPHERIC ELECTRON DENSITY
Radio absorption in the Antarctic ionosphere: Some observations in the region of the midlatitude trough N91-28694

IONOSPHERIC PROPAGATION
Radio absorption in the Antarctic ionosphere: Some observations in the region of the midlatitude trough N91-28694

IONS
Kinetic energy distributions of ions after surface collisions [DE91-013412] N91-28850
Particle simulation on the tilt stabilization of the FRC plasma N91-28917

IRON
Aqueous corrosion characteristics and corrosion-related cracking susceptibilities of Fe3Al-type iron aluminides [DE91-013028] N91-28358

IRON ALLOYS
Effects of sample size and loading rate on the transition behavior of a DCI alloy [DE91-012015] N91-28346
Aqueous corrosion characteristics and corrosion-related cracking susceptibilities of Fe3Al-type iron aluminides [DE91-013028] N91-28358
Properties of large heats of Fe3Al-based alloys [DE91-013268] N91-28359
Erosion studies on a Fe3Al-based iron aluminide and 1100 Al [DE91-012529] N91-28360
Weldability of iron aluminides [DE91-013730] N91-28367
Hydrogen embrittlement of selected nickel and iron base superalloys N91-28374
Alloy development of Fe3Al for improved creep rupture properties [DE91-014541] N91-28381
Processing and fabrication of Fe3Al-based alloys [DE91-014546] N91-28382
Fundamental magnetic studies of iron-rare-earth-metalloid alloys [DE91-014816] N91-28383

IRON COMPOUNDS
Weldability of iron aluminides [DE91-013730] N91-28367
Magnetic studies of iron-rare-earth-metalloid alloys [DE91-013856] N91-28368

IRRADIANCE
X ray generation by high irradiance exawatt/sq cm subpicosecond lasers [DE91-013497] N91-28556
Irradiance compensation control for high-energy laser propagation. Part 1: Theory and Fourier control model propagation results [DE91-013130] N91-28559

IRRADIATION
Irradiation creep by climb-enabled glide driven by transient point defect processes [DE91-012950] N91-28348
High-temperature solution annealing as an IASCC mitigation technique [DE91-012220] N91-28352
Photocross-linked second order nonlinear optical polymers [AD-A235855] N91-28385
Microbeam studies of the sensitivity of structures within living cells [DE91-012927] N91-28715
Enhancing atom densities in solid hydrogen by isotopic substitution [DE91-011189] N91-28824
Evolution of defect cluster distributions during irradiation [DE91-013405] N91-29024

The interaction of HVEM-generated point-defects with dissociated dislocations
[DE91-013353] N91-29027

IRREGULAR GALAXIES
Properties of infrared-luminous galaxies, or, how I spent seven summer vacations N91-29098

IRREVERSIBLE PROCESSES
Relaxed state and entropy production N91-28907

ISOMERIZATION
High resolution infrared spectroscopy of 2-fluorethanol in a molecular beam
[AD-A236149] N91-28822

ISOTHERMAL PROCESSES
The rate (time)-dependence mechanical behavior of modified 9Cr-1Mo. Part 2: Isothermal modeling at 538 C
[DE91-011100] N91-28350

ISOTHERMS
Thermodynamic and kinetic aspects of surface acidity
[DE91-014039] N91-28331
Validity of the model used to relate the energy distribution and the adsorption isotherm
[DE91-013528] N91-28428

ISOTOPES
Isotopic measurements of solar noble gases in individual micrometeorites from Greenland and Antarctica
N91-29114

ISOTOPIC LABELING
New techniques for positron emission tomography in the study of human neurological disorders
[DE91-013855] N91-28728

ISOTROPY
TOPAZ2D benchmark problems nonlinear materials
[DE91-009753] N91-29053

ITERATIVE SOLUTION
Numerical solution of a free-boundary viscous flow
N91-28529
The solution of variable-geometry truss problems using new homotopy continuation methods N91-28640
Choosing processor array configuration by performance modeling for a highly parallel linear algebra algorithm
[DE91-012486] N91-28749
Searching for consensus patterns on a hypercube
[DE91-013233] N91-28753
An iterative substructuring algorithm for problems in three dimensions
[DE91-014388] N91-28758
Order reduction and synthesis of transfer function models N91-28769
Multidimensional spectral estimation using iterative methods
[AD-A237025] N91-28791
Symplectic full-turn maps in a Fourier representation
[DE91-012912] N91-28796

J

J-2 ENGINE
Determining criteria for single stage to orbit
N91-28258

JAPAN
A review of liquid rocket propulsion programs in Japan
N91-28219
US assessment of the new diamond technology in Japan
[PB91-167395] N91-28404
Prediction of high level vibration test results by use of available inelastic analysis techniques
[DE91-009437] N91-28606

JET IMPINGEMENT
Quadrupole phenomena of noise from a subsonic jet impinging on a large, rigid, and flate plate N91-28818

JOINING
Investigation of interlayer materials for the microwave joining of SiC
[DE91-013311] N91-28414

JOINTS (JUNCTIONS)
Fluxless soldering of Ni-Au plated Kovar with a laser
[DE91-013261] N91-28451
A methodology to determine the dynamic configuration of a reconfigurable manipulator
[DE91-010732] N91-28576
Noncircular rolling joints for vibrational reduction in slewing maneuvers
[NASA-CASE-LAR-14515-1-CU] N91-28580
Robust low-order control of flexible joint manipulators
N91-28584

JOSEPHSON JUNCTIONS
Ultra-high frequency superconductive devices
[AD-A236795] N91-28478
Strongly interacting fermion systems
[DE91-012284] N91-28848
High-T(sub c) thin-film microelectronics
[DE91-012340] N91-28997
Measurement accuracy of macroscopic quantum circuits with RF-biased Josephson junction arrays
[DE91-012651] N91-29009
Coherent charge fluctuations in Josephson junctions and the oscillations of the effective capacitance
[DE91-618098] N91-29019

JOURNAL BEARINGS
Analysis of foil bearings for high speed operation in cryogenic applications N91-28231

JUPITER ATMOSPHERE
Search for regularities in the atmosphere of Jupiter
N91-29127

K

K-EPSILON TURBULENCE MODEL
A critical analysis of anisotropic k-epsilon modeling and its application to turbulence-driven secondary flows
N91-28533

KAPITZA RESISTANCE
High-resolution measurements of the thermal conductivity and boundary resistance of helium-4 near the lambda point N91-28322

KEL-F
Response of the polymers KEL-F, polysulfone, high density polyethylene and polymethylmethacrylate to shock loading and release from 0.3 to 2.4 GPa
[DE91-012867] N91-28411

KELVIN-HELMHOLTZ INSTABILITY
Experiments on the instabilities in swirling and non-swirling free jets N91-28531

KINEMATIC EQUATIONS
Kinematic analysis of legged system locomotion on smooth horizontal surfaces N91-28586
The solution of variable-geometry truss problems using new homotopy continuation methods N91-28640

KINEMATICS
Kinematic GPS surveying N91-28149
Viscoplastic analysis of an experimental cylindrical thrust chamber liner
[NASA-TM-103287] N91-28622
Emission line regions in active galactic nuclei: Structure, kinematics, physical conditions, and chemical abundances N91-29095
Multiple nuclei, cluster core dynamics, and the velocity distributions of gravitating systems N91-29119

KINETIC ENERGY
Laser ejection of Ag(sup +) ions from a roughened silver surface: Role of the surface plasmon
[DE91-012945] N91-28554
Stress fields generated by kinetic energy projectile interaction with ceramic targets
[DE91-013687] N91-28625
Kinetic energy distributions of ions after surface collisions
[DE91-013412] N91-28850
Aspects of reheating in first-order inflation
[NASA-CR-188705] N91-29108

KINETIC EQUATIONS
Internal kink mode simulation by 3-D gyrokinetic code
N91-28916
Statistical mechanics using symbolic dynamics
N91-28940
Fluid/kinetic hybrid moment description of plasmas via a Chapman-Enskog-like approach
[DE91-013346] N91-28949
Generalized gyroviscous force and its effect on the momentum balance equation
[DE91-013344] N91-29061

KINETIC THEORY
An extension of a kinetic theory of polymer crystallization through the exclusion of negative barriers
[AD-A236999] N91-28387
Numerical study of ion temperature gradient modes in a tokamak N91-28921
Fluidlike studies of the presheath and sheath regions of a plasma
[DE91-013345] N91-28953

KINETICS
Surface phases and their influence on metal-oxide interfaces
[DE91-012277] N91-28995

KLYSTRONS
A high power Klystrode with potential for space application
[DE91-013046] N91-28486

KNOWLEDGE BASES (ARTIFICIAL INTELLIGENCE)
Generalized hypertext in a knowledge-based decision support shell environment N91-29086
A simulated user for laboratory investigation of information systems requirements determination
N91-29087

KNOWLEDGE REPRESENTATION
Generalized hypertext in a knowledge-based decision support shell environment N91-29086

KONDO EFFECT
Pressure dependence of the Curie-temperature in the Kondo-lattice-compound YbNiSn
[DE91-013672] N91-29046

KRYPTON FLUORIDE LASERS
Spectroscopic and ion probe characterization of laser produced plasmas used for thin film growth
[DE91-013425] N91-28959

L

LABORATORIES
Cryogenic combustion laboratory N91-28223
Technologies available from Martin Marietta Energy Systems, Inc.
[DE91-013027] N91-28283
Building microelectronic systems in a university environment
[AD-A236629] N91-28477
Scientific data visualization
[DE91-014216] N91-28766
Experience in designing and using a flat structure in a multi-project research organization
[DE91-012427] N91-29067
The design of a clinical laboratory information system
N91-29083

LAGRANGE COORDINATES
Regularization of the Lagrange planetary equations for numerical use N91-28808

LAKES
Analysis of southeastern Canada lake-water chemistry data in relation to acidic deposition
[DE91-014957] N91-28674

LAMINAR BOUNDARY LAYER
A study of methods to investigate nozzle boundary layer transition N91-28232
Receptivity of a laminar boundary layer to the interaction of a three-dimensional roughness element with time-harmonic free-stream disturbances N91-28518

LAMINAR FLOW
Experimental investigation of pressure drop and heat transfer for air flow through enhanced tubes
[DE91-012151] N91-28508
Experimental and theoretical investigation of unsteady forced convection in ducts N91-28524
The numerical solution of confined laminar flow past a moving boundary N91-28532

LAMINATES
Composite material systems for hydrogen management N91-28229
Damage development under compression-compression fatigue loading in a stitched uniwoven graphite/epoxy composite material
[NASA-CR-188693] N91-28292
Local delamination in laminates with angle ply matrix cracks. Part 1: Tension tests and stress analysis
[NASA-TM-104055] N91-28293
An analysis of interlaminar stresses in unsymmetrically laminated plates N91-28299
Damage progression during static and fatigue loading in metal matrix composites, volumes 1-3 N91-28301
Finite element modeling of 2-D delamination growth in laminated composites N91-28302
Interlaminar fracture characterization: A current review
[NASA-CR-187573] N91-28626
Stability of cylindrical laminates by higher orde r shear deformable theories N91-28638
Flutter of laminated rectangular plates including finite deflection and shear deformation N91-28639

LANDAU FACTOR
Chaos in the lowest Landau level
[DE91-014800] N91-28866

LANDFORMS
Close-range geophotogrammetric mapping of trench walls using multi-model stereo restitution software
[DE91-013105] N91-28645

LANDING GEAR
Landing Gear Design Loads
[AGARD-CP-484] N91-28150
Failure analysis case histories of Canadian forces aircraft landing gear components N91-28151
Development of undercarriage design loads
N91-28153
Recent developments in the area of aircraft rough field performance N91-28154
The special requirements of a VSTOL aircraft
N91-28155
Considerations on optimality of landing gear arrangement and design N91-28156
Long time measurements of landing gear loads on SAAB SF-340 commuter aircraft N91-28157
Operational loads on landing gear N91-28158
Landing gear improvements for transport aircraft
N91-28159

Numerical simulation of the dynamic behavior of landing gears N91-28160
Calculation of interactions between air and ground of landing N91-28161
The use of Monte Carlo simulation in determining landing gear loads during landing N91-28162
Design landing loads evaluation by dynamic simulation of flexible aircraft N91-28163
F-106B airplane active control landing gear drop test performance N91-28164
Actively damped landing gear system N91-28165

LANDING LOADS
Operational loads on landing gear N91-28158
Design landing loads evaluation by dynamic simulation of flexible aircraft N91-28163
F-106B airplane active control landing gear drop test performance N91-28164

LANDING SIMULATION
Numerical simulation of the dynamic behavior of landing gears N91-28160

LANTHANUM COMPOUNDS
Ab initio cluster studies of La2CuO4
[DE91-013520] N91-29025

LARGE SPACE STRUCTURES
Large space structures and systems in the space station era: A bibliography with indexes
[NASA-SP-7085(02)] N91-28191
The solution of variable-geometry truss problems using new homotopy continuation methods N91-28640

LASER APPLICATIONS
Cryogenic combustion laboratory N91-28223
Combustion research program: Flame studies, laser diagnostics, and chemical kinetics
[DE91-014824] N91-28329
Laser surface modification to impede hydrogen ingress into steel N91-28375
Evaporation as a diagnostic test for hydrodynamic cooling of laser-ablated clusters
[DE91-013416] N91-28555
H(-) beam characterization using laser-induced neutralization
[DE91-013501] N91-28564
Laser range camera calibration
[DE91-014939] N91-28570
Numerical investigation of the thrust efficiency of a laser-propelled vehicle N91-28572
Desorption of large organic molecules by laser-induced plasmon excitation
[DE91-013415] N91-28852
Laser speckle velocimetry with photorefractive recording and anamorphic optical processing N91-28880
Inertial confinement fusion
[DE91-013479] N91-28960

LASER BEAMS
Diffraction patterns produced by periodic and turbulent flowing gases including applications of photorefractive temporal filtering
[DE91-012636] N91-28553
Irradiance compensation control for high-energy laser propagation. Part 1: Theory and Fourier control model propagation results
[DE91-013130] N91-28559

LASER DOPPLER VELOCIMETERS
A study on particle dispersion in two-dimensional mixing layer flows N91-28537
A PC based frequency domain LV processor
[DE91-009056] N91-28541

LASER FUSION
X ray fiducial foils
[DE91-011193] N91-28542
Turbulent mixing due to Rayleigh-Taylor instability in laser driven implosion N91-28914
Measurements of the ion acoustic decay instability and the resultant enhanced laser absorption and enhanced bremsstrahlung in laser-plasma interaction experiments
[DE91-014250] N91-28956

LASER INDUCED FLUORESCENCE
Combustion research program: Flame studies, laser diagnostics, and chemical kinetics
[DE91-014824] N91-28329

LASER MATERIALS
Platinum solubility in phosphate laser glass
[DE91-015123] N91-28571

LASER OUTPUTS
Edge technique for measurement of laser frequency shifts including the Doppler shift
[NASA-CASE-GSC-13343-1] N91-28557
Nonlinear evolution of 2D and 3D Rayleigh-Taylor instability at stagnation phase in laser implosion N91-28899

LASER PLASMA INTERACTIONS
Solitons and chaos in laser-plasma interaction N91-28898
Measurements of the ion acoustic decay instability and the resultant enhanced laser absorption and enhanced bremsstrahlung in laser-plasma interaction experiments
[DE91-014250] N91-28956

LASER PLASMAS
Laser ejection of Ag(sup +) ions from a roughened silver surface: Role of the surface plasmon
[DE91-012945] N91-28554
Numerical and analytical analysis of thin laser-driven flyer plates
[DE91-013748] N91-28567
Solitons and chaos in laser-plasma interaction N91-28898
Large growth Rayleigh-Taylor experiments on Nova
[DE91-012885] N91-28955
Hydrodynamic evolution of picosecond laser-plasmas
[DE91-013245] N91-28958
Spectroscopic and ion probe characterization of laser produced plasmas used for thin film growth
[DE91-013425] N91-28959

LASER TARGETS
X ray generation by high irradiance exawatt/sq cm subpicosecond lasers
[DE91-013497] N91-28556
Studies of laser-driven flyer acceleration using optical fiber coupling
[DE91-013503] N91-28562

LASER WEAPONS
Defending the defenders: Brilliant pebble defense against pop-up neutral particle beam suppression attacks
[DE91-012521] N91-28809

LASERS
Investigation of laser diagnostics of PACVD processes for depositing hard face coatings
[DE91-012642] N91-28401
JPRS report: Science and technology. USSR: Physics and mathematics
[JPRS-UPM-90-006] N91-28811

LATE STARS
Interaction of radiation with outflows in late-type stars N91-29136

LATENT HEAT
Numerical solution of a moving boundary problem as a model solution for a solar pipe
[ITN-91-85143] N91-28516
Direct contact heat transfer to a dispersal droplet with change of phase N91-28521

LATTICE VIBRATIONS
Microwave enhanced diffusion?
[DE91-013312] N91-28415

LAUNCH VEHICLE CONFIGURATIONS
NASA's advanced space transportation system launch vehicles N91-28195
Operationally Efficient Propulsion System Study (OEPPS) N91-28198
Expendable launch vehicle propulsion N91-28199

LAUNCH VEHICLES
Next generation earth-to-orbit space transportation systems: Unmanned vehicles and liquid/hybrid boosters N91-28205
Next generation solid boosters N91-28207
Space systems propulsion technology N91-28209
Next generation: Unmanned launch vehicles and upper stages: The needs N91-28210
Propulsion studies for advanced manned launch systems N91-28213
Heavy-lift launch vehicle propulsion considerations N91-28236
Historical problem areas: Lessons learned for expendable and reusable vehicle propulsion systems N91-28243

LEACHING
Mechanisms of bacterial metals removal from solids
[DE91-012808] N91-28356

LEAD (METAL)
Laser surface modification to impede hydrogen ingress into steel N91-28375

LEAD ACID BATTERIES
Exploratory battery technology development report for FY90
[DE91-012131] N91-28485
Laboratory testing of the dual traction battery GC12V100
[DE91-012743] N91-28491

LEAD ALLOYS
Improving fatigue life in near-eutectic Sn Pb solders
[DE91-013844] N91-28603

LEAD ZIRCONATE TITANATES
Ferroelectric fatigue in modified bulk lead zirconate titanate ceramics
[DE91-012647] N91-28417

LEGUMINOUS PLANTS
Plant growth is influenced by glutamine synthetase-catalyzed nitrogen metabolism
[DE91-014592] N91-28725

LEPTONS
Neutrino degeneracy and cosmological nucleosynthesis, revisited
[NASA-CR-188703] N91-29110

LEVELING
The determination of mean sea level using GPS N91-28708

LEVITATION
Chemical characterization of microparticles by laser ablation in an ion trap mass spectrometer
[DE91-012513] N91-28309
Improved superconducting bearings
[NASA-CASE-GSC-13346-1] N91-28578
Effect of guideway discontinuities on magnetic levitation and drag forces
[DE91-014011] N91-28815
Effect of size and geometry on levitation force measurements between permanent magnets and high-temperature superconductors
[DE91-012472] N91-29008

LIAPUNOV FUNCTIONS
Stability theory of critical cases and the bifurcation points of the stationary solutions of the Lorenz model
[DE91-617575] N91-28802

LIBRARIES
Support materials for formal specification of software
[AD-A236121] N91-28742

LIFE (DURABILITY)
Impact of ion propulsion on performance, design, testing, and operation of a geosynchronous spacecraft
[AD-A237028] N91-28273

LIFE CYCLE COSTS
Life cycle cost based program decisions N91-28248

LIFT
An active delay of separation on two-dimensional airfoils
[ITN-91-85142] N91-28139
Effect of guideway discontinuities on magnetic levitation and drag forces
[DE91-014011] N91-28815

LIFT DRAG RATIO
Applications of low lift to drag ratio aerobrakes using angle of attack variation for control
[NASA-TM-103544] N91-28189

LIGANDS
Resonance Raman and photophysical studies of transition metal complexes in solution and entrapped in zeolites
[DE91-013010] N91-28357
Indium compounds which contain two different organic substituents. Crystal structure of (In(CH2CMe3)(CH2SiMe3)Cl)2, an interesting case of partial Ligand disorder in the solid state
[AD-A236730] N91-28989

LIGHT BEAMS
Liquid jet breakup and atomization in rocket chambers under dense spray conditions N91-28227
Invariant metrics for Hamiltonian systems
[DE91-014236] N91-28807
SLC polarized beam source electron optics design
[DE91-012911] N91-28869

LIGHT ELEMENTS
Testing the Big Bang: Light elements, neutrinos, dark matter and large-scale structure
[NASA-CR-188701] N91-29111

LIGHT IONS
Progress in light ion fusion
[DE91-012019] N91-28826

LIGHT SCATTERING
A laser based technique for particle sizing to study two phase expansion in turbines
[DE91-014172] N91-28595
Solitons and chaos in laser-plasma interaction N91-28898

LIGHT SOURCES
The Advanced Light Source: A new tool for research in atomic and molecular physics
[DE91-012860] N91-28844

LIGHT TRANSMISSION
Measurements of photo-induced changes in conjugated polymers
[DE91-013262] N91-28427

LIGHTING EQUIPMENT
Device for removing foreign objects from anatomic organs
[NASA-CASE-GSC-13306-1] N91-28727

LIGHTNING
Follow-on cable coupling lightning test, volume 1
[NASA-CR-184123] N91-28192
Effectivity of atmospheric electricity on launch availability N91-28260
Predicting thunderstorm evolution using ground-based lightning detection networks N91-28702

LINE OF SIGHT
A cloud fraction and radiative transfer model N91-28706

LINE SPECTRA
Magnetospheric VLF line radiation N91-28693
Emission line regions in active galactic nuclei: Structure, kinematics, physical conditions, and chemical abundances N91-29095
LINEAR ACCELERATORS
Time-resolved emittance measurements of an excimer-laser-driven metal photocathode
[DE91-013066] N91-28558
H(-) beam characterization using laser-induced neutralization
[DE91-013501] N91-28564
Performance of the photoinjector accelerator for the Los Alamos free-electron laser
[DE91-013682] N91-28565
Short wavelength FELS
[DE91-013759] N91-28566
Reduction of energy sweep of the ETA-2 beam
[DE91-013824] N91-28568
Simulations on pair creation from beam-beam interaction in linear colliders
[DE91-012315] N91-28834
Beam current monitoring in the AGS booster and its transfer lines
[DE91-013328] N91-28870
Continuing studies of the plasma beat wave accelerator
[DE91-013641] N91-28976
Strain enhanced electron spin polarization observed in photoemision from InGaAs
[DE91-012319] N91-28996
LINEAR ENERGY TRANSFER (LET)
Protein-directed modulation of high-LET hyperthermic radiosensitization
[DE91-013783] N91-28722
LINEAR EQUATIONS
A parallel algorithm for solving linear equations arising from one-dimensional network problems
[DE91-012815] N91-28795
LINEAR QUADRATIC REGULATOR
Attitude control of a spinning rocket via thrust vectoring
[DE91-006267] N91-28274
Active control of panel vibrations induced by boundary-layer flow
[NASA-CR-188733] N91-28643
LINEAR SYSTEMS
Analysis of passive and active discrete-distributed linear dynamical systems using Green's function methods N91-28141
Stochastic robustness of linear multivariable control systems: Towards comprehensive robustness analysis N91-28172
LINEARIZATION
Recursive linearization of multibody dynamics and application to control design N91-28588
LINES OF FORCE
Effect of size and geometry on levitation force measurements between permanent magnets and high-temperature superconductors
[DE91-012472] N91-29008
LINGUISTICS
Information management: A uniform conceptual model and its user interface N91-29084
LIQUEFIED GASES
Vibrational spectroscopy of shock-compressed liquid CO
[DE91-013204] N91-28325
LIQUID COOLING
Advanced water-cooled phosphoric acid fuel cell development
[DE90-009700] N91-28657
LIQUID FLOW
Moving finite elements: A continuously adaptive method for computational fluid dynamics
[DE91-013391] N91-28513
Numerical solution of a free-boundary viscous flow N91-28529
LIQUID FUELS
Mechanism of hydrodenitrogenation. Part 5: X ray diffraction of molybdenum catalysts
[DE91-013853] N91-28327
LIQUID HELIUM
Brittle behavior of SSC yokes
[DE91-014031] N91-28370
LIQUID HYDROGEN
Cryogenic upper stage propulsion: RL10 and derivative engines N91-28202
LIQUID METALS
A review of silicon carbide/metal interactions with relevance to silicon carbide joining
[DE91-012768] N91-28282
Corrosion of refractory metals in liquid metal and gaseous environments
[DE91-009555] N91-28378
LIQUID PHASES
Apparatus for intercalating large quantities of fibrous structures
[NASA-CASE-LEW-15077-2] N91-28289
LIQUID PROPELLANT ROCKET ENGINES
A review of liquid rocket propulsion programs in Japan N91-28219
Cryogenic combustion laboratory N91-28223
Spray combustion under oscillatory pressure conditions N91-28226
Droplet-turbulence interactions in subcritical and supercritical evaporating sprays N91-28228
Analysis of foil bearings for high speed operation in cryogenic applications N91-28231
Liquid rocket engine flight certification N91-28250
Space shuttle with common fuel tank for liquid rocket booster and main engines (supertanker space shuttle) N91-28257
The case for teaming on the ALS-STME program N91-28269
LIQUID ROCKET PROPELLANTS
Liquid-propellant droplet vaporization and combustion in high pressure environments N91-28225
Spray combustion under oscillatory pressure conditions N91-28226
Droplet-turbulence interactions in subcritical and supercritical evaporating sprays N91-28228
The case for teaming on the ALS-STME program N91-28269
LIQUID-GAS MIXTURES
Study of interfacial behavior in cocurrent gas-liquid flows
[DE91-013008] N91-28511
LIQUID-SOLID INTERFACES
Polymers at surfaces
[DE91-013642] N91-28430
LIQUID-VAPOR EQUILIBRIUM
Inorganic components of atmospheric aerosols N91-28668
LIQUIDS
Overdriven shocks in solids and liquids
[DE91-013370] N91-28618
LITHIUM ALLOYS
Identification of strengthening phases in Al-Cu-Li alloy Weldalite (tm) 049 N91-28335
The influence of Ag+Mg additions on the nucleation of strengthening precipitates in a non-cold-worked Al-Cu-Li alloy N91-28336
The effect of TiB2 reinforcement on the mechanical properties of an Al-Cu-Li alloy-based metal-matrix composite N91-28337
Weldability of Weldalite (tm) 049 with and without TiB2 reinforcement N91-28338
Effect of Li level, artificial aging, and TiB2 reinforcement on the fracture toughness of Weldalite (tm) 049-type alloys N91-28339
Effect of Li level, artificial aging, and TiB2 reinforcement on the modulus of Weldalite (tm) 049 N91-28340
Tensile deformation of Al-Cu-Li-Zr alloy 2090-T8E41 at 298 and 77 K
[DE91-011885] N91-28345
LITHIUM COMPOUNDS
Nuclear magnetic resonance studies of atomic motion in lithium chloroborate and lithium thiosilicate glassy fast ionic conductors
[DE91-012677] N91-28843
Structure and dynamics in low-dimensional guest host solids
[DE91-012169] N91-29020
LITHOGRAPHY
Reflection mask technology for soft x ray projection lithography
[DE91-012561] N91-28877
The DARPA compact superconducting x-ray lithography source features
[DE91-013864] N91-29039
LITHOLOGY
A gravity model for the Coso geothermal area, California
[DE91-011874] N91-28677
LITHOSPHERE
Heat flow data and thermal state of the continental lithosphere N91-28682
LOAD TESTS
Interlaminar fracture characterization: A current review
[NASA-CR-187573] N91-28626
LOADING RATE
Effects of sample size and loading rate on the transition behavior of a DCI alloy
[DE91-012015] N91-28346
LOADS (FORCES)
Landing Gear Design Loads
[AGARD-CP-484] N91-28150
Application of the Air Force guide specification 87221A to ground loads N91-28152
Development of undercarriage design loads N91-28153
Considerations on optimality of landing gear arrangement and design N91-28156
Long time measurements of landing gear loads on SAAB SF-340 commuter aircraft N91-28157
The use of Monte Carlo simulation in determining landing gear loads during landing N91-28162
LOCAL AREA NETWORKS
Providing common access mechanisms for dissimilar network interconnection nodes
[AD-A236630] N91-28770
Description of real-time Ada software implementation of a power system monitor for the Space Station Freedom PMAD DC testbed
[NASA-TM-105157] N91-28776
Requirements for a network storage service
[DE91-014106] N91-28778
The design of a clinical laboratory information system N91-29083
LOCKING
Roller locking brake
[NASA-CASE-GSC-13376-1] N91-28579
LOCKS (FASTENERS)
Spline-locking payload fastener
[NASA-CASE-GSC-13378-1] N91-28581
LOCOMOTION
Kinematic analysis of legged system locomotion on smooth horizontal surfaces N91-28586
LOGARITHMS
Log-stable distribution of energy dissipation in turbulence N91-28885
LOGIC CIRCUITS
Direction discriminating hearing aid
[NASA-CASE-GSC-13027-1] N91-28726
LOGIC PROGRAMMING
A logic model for model management: An embedded languages approach N91-28761
LONG WAVE RADIATION
Natural and anthropogenic climate change
[DE91-014734] N91-28673
Initialization of cloud and radiation in the Florida State University global spectral model N91-28703
LONGITUDINAL STABILITY
Longitudinal aerodynamic characteristics of a subsonic, energy-efficient transport configuration in the National Transonic Facility
[NASA-TP-2922] N91-28143
LORENTZ TRANSFORMATIONS
Stability theory of critical cases and the bifurcation points of the stationary solutions of the Lorenz model
[DE91-617575] N91-28802
LOSSES
Interaction of radiation with outflows in late-type stars N91-29136
LOW DENSITY MATERIALS
Shock compression of low-density microcellular materials
[DE91-013586] N91-28628
Equation of state and crushing dynamics of low-density silica aerogels
[DE91-014766] N91-28637
LOW FREQUENCIES
Suspension device for low-frequency structures
[NASA-CASE-LAR-14272-1-CU] N91-28184
LOW REYNOLDS NUMBER
Optical diagnostic investigation of low Reynolds number nozzle flows N91-28233
CFD applications in chemical propulsion engines N91-28234
LOW SPEED
Technology needs for high speed rotorcraft (2)
[NASA-CR-177590] N91-28168
LUBRICANTS
JPRS report: Science and technology. USSR: Materials science
[JPRS-UMS-91-003] N91-28342
Thermal and non-Newtonian effects in elastohydrodynamic lubrication of rolling-sliding contacts N91-28590
LUBRICATING OILS
Boundary lubrication of ceramic materials by soft metallic coating and synthetic oil
[DE91-014017] N91-28577
LUBRICATION
Polymers at surfaces
[DE91-011000] N91-28392
Pretreatment of lubricated surfaces with sputtered cadmium oxide
[NASA-CASE-LEW-14474-1] N91-28423
Thermal and non-Newtonian effects in elastohydrodynamic lubrication of rolling-sliding contacts N91-28590
LUMINAIRES
Fixture efficiency program
[DE91-014470] N91-28498

LUMINESCENCE
Aerogel composites for radioluminescent light/power sources
[DE91-012012] N91-28395
LUMINOUS INTENSITY
Shock-induced optical emission in Al2O3 at 200 GPa: Implications for shock temperature measurements in metals
[DE91-013584] N91-28365
LUNAR BASED EQUIPMENT
Issues concerning centralized versus decentralized power deployment
[NASA-CR-187121] N91-28648
LUNAR BASES
SEI power source alternatives for rovers and other multi-kWe distributed surface applications
[NASA-TM-104360] N91-28277
Issues concerning centralized versus decentralized power deployment
[NASA-CR-187121] N91-28648
LUNAR ROVING VEHICLES
SEI power source alternatives for rovers and other multi-kWe distributed surface applications
[NASA-TM-104360] N91-28277
LUNAR SPACECRAFT
Next generation: In-space transportation system(s) N91-28211
Space transfer vehicles and space basing N91-28254
STV engine design considerations N91-28255

M

MACH NUMBER
Improved method and apparatus for Mach number change in wind tunnel
[NASA-CASE-LAR-13548-1] N91-28175
MACHINE LEARNING
An accelerated training method for back propagation networks
[NASA-CASE-MSC-21625-1] N91-28730
MACHINING
Perspective on plating for precision finishing
[DE91-011927] N91-28394
Changes with material properties of acoustic emission produced during single point machining
[DE91-011913] N91-28452
Origin of acoustic emission produced during single point machining
[DE91-011915] N91-28453
MACROMOLECULES
The 1992 - 1997 renewal proposal interactive graphics for molecular studies
[AD-A236598] N91-28823
MAGNESIUM
The influence of Ag+Mg additions on the nucleation of strengthening precipitates in a non-cold-worked Al-Cu-Li alloy N91-28336
Interstellar magnesium studies N91-29120
MAGNESIUM COMPOUNDS
Quantitative modeling of the point defect structures of Fe-doped MgO and MgSiO3 perovskite
[DE91-011405] N91-28990
MAGNESIUM OXIDES
Model catalytic oxidation studies using supported monometallic and heterobimetallic oxides
[DE91-012144] N91-28409
Quantitative modeling of the point defect structures of Fe-doped MgO and MgSiO3 perovskite
[DE91-011405] N91-28990
MAGNETIC BEARINGS
Robust and real-time control of magnetic bearings for space engines N91-28230
Improved superconducting bearings
[NASA-CASE-GSC-13346-1] N91-28578
MAGNETIC COMPRESSION
Procyon experiments utilizing foil-fuse opening switches
[DE91-014605] N91-28499
Performance of the 10-kV, 5-MA pulsed-power system for the FRX-C compression experiment
[DE91-014745] N91-28983
MAGNETIC DIPOLES
Space propulsion by fusion in a magnetic dipole
[DE91-012033] N91-28275
Design and analysis of the 50 mm collider dipole vacuum vessel
[DE91-012490] N91-28610
Ferromagnetic material in the superconductor and its effect on the magnetization sextupole and decapole in the SSC dipoles at injection
[DE91-011886] N91-28993
MAGNETIC EFFECTS
Ion temperature gradient turbulence and coherent structures N91-28890
Complex dynamics of the integer quantum Hall effect
[DE91-013383] N91-29058
Explosion of a superbubble in a uniform magnetic field N91-29102
MAGNETIC FIELD CONFIGURATIONS
Study of kink instability and current relaxation by three dimensional macroscale particle simulation N91-28919
Mode conversion of Alfven waves induced by quadrupole magnetic field modulation N91-28924
Particle confinement and fueling effects on the Maryland spheromak
[DE91-012396] N91-28945
Transport profiles induced by radially localized modes in tokamak
[DE91-014366] N91-28964
Steady-state dynamo and current drive in a nonuniform bounded plasma
[DE91-014865] N91-28974
Reversed field pinch experiments
[DE91-013643] N91-28977
MAGNETIC FIELD RECONNECTION
Current sheet formation and rapid reconnection in the solar corona N91-28884
Simulation study of MHD relaxation and reconnection processes N91-28908
MAGNETIC FIELDS
Effect of guideway discontinuities on magnetic levitation and drag forces
[DE91-014011] N91-28815
Optimization, non-local MHD-mode, and alpha-particle confinement behavior of Helias equilibria N91-28893
Models of collisional transport across a magnetic field with destroyed surfaces N91-28900
Magnetohydrodynamical formation of astrophysical jets from gravitationally collapsing objects N91-28903
Computer simulation of solar wind-magnetosphere interaction N91-28904
Rapid acceleration of protons in a nonlinear magnetosonic wave and their energy spectrum N91-28905
Effect of pressure on mode transition point of partially relaxed states with peripheral loss N91-28906
Helical field effect in solar/stellar wind N91-28912
Nonadiabatic behavior of the magnetic moment of a charged particle in a dipole magnetic field N91-28920
Structures of magnetic field lines in the helical torus N91-28932
Fluctuation spectrum of ion temperature gradient driven modes in sheared magnetic fields N91-28936
Stability of annular equilibrium of energetic large orbit ion beam
[DE91-014365] N91-28963
Reversed-Field Pinch dynamics and transport studies
[DE91-014317] N91-28970
Steady-state dynamo and current drive in a nonuniform bounded plasma
[DE91-014865] N91-28974
Progress in the development of a numerical tokamak
[DE91-013386] N91-28975
Joint proposal for US/USSR on nonlinear dynamics and plasma transport
[DE91-014360] N91-28981
Ferromagnetic material in the superconductor and its effect on the magnetization sextupole and decapole in the SSC dipoles at injection
[DE91-011886] N91-28993
Thermodynamic and transport properties of superconductors in very high magnetic fields
[DE91-012530] N91-29000
Thin-film flux transformers of YBa2Cu3O(7-x)
[DE91-012363] N91-29007
The derivation of effective spin Hamiltonians and the origin of the magnetic field induced transition in orthormbic La2CuO4
[DE91-013743] N91-29035
Flux pinning and dissipation in high-temperature superconductors
[DE91-014466] N91-29042
Complex dynamics of the integer quantum Hall effect
[DE91-013383] N91-29058
Radiative transfer in very strong magnetic fields N91-29106
Sawteeth in the MST reversed field pinch
[DE91-014288] N91-29126
MAGNETIC LEVITATION VEHICLES
Light weight, high field, stable, superconducting magnets for advanced transportation systems
[DE91-013667] N91-28814
Effect of guideway discontinuities on magnetic levitation and drag forces
[DE91-014011] N91-28815
MAGNETIC MATERIALS
Magnetic studies of iron-rare-earth-metalloid alloys
[DE91-013856] N91-28368
Fundamental magnetic studies of iron-rare-earth-metalloid alloys
[DE91-014816] N91-28383
MAGNETIC MIRRORS
Performance of the 10-kV, 5-MA pulsed-power system for the FRX-C compression experiment
[DE91-014745] N91-28983
MAGNETIC MOMENTS
Nonadiabatic behavior of the magnetic moment of a charged particle in a dipole magnetic field N91-28920
MAGNETIC PERMEABILITY
The effect of the quantum susceptance on the gain of superconducting quasiparticle mixers
[DE91-012352] N91-29021
Pressure dependence of the Curie-temperature in the Kondo-lattice-compound YbNiSn
[DE91-013672] N91-29046
MAGNETIC PROBES
Time-resolved emittance measurements of an excimer-laser-driven metal photocathode
[DE91-013066] N91-28558
MAGNETIC PROPERTIES
Chemistry and materials science research report
[DE91-011507] N91-28305
The pressure-induced Mott transition in transition-metal iodides
[DE91-013671] N91-28366
Magnetic studies of iron-rare-earth-metalloid alloys
[DE91-013856] N91-28368
Measurement of magnetic properties of confined compact toroid plasma (spheromak)
[DE91-012397] N91-28950
MAGNETIC RELAXATION
Application of muon spin relaxation experiment to the mixed state superconductors
[DE91-013689] N91-29034
Flux dynamics in a single crystal of Bi2Sr2CaCu2O(x)
[DE91-013763] N91-29036
Application of muon spin relaxation experiment to the vortex dynamics of high temperature superconductors
[DE91-014607] N91-29050
MAGNETIC SUSPENSION
Light weight, high field, stable, superconducting magnets for advanced transportation systems
[DE91-013667] N91-28814
Effect of guideway discontinuities on magnetic levitation and drag forces
[DE91-014011] N91-28815
Effect of size and geometry on levitation force measurements between permanent magnets and high-temperature superconductors
[DE91-012472] N91-29008
MAGNETIZATION
Ferromagnetic material in the superconductor and its effect on the magnetization sextupole and decapole in the SSC dipoles at injection
[DE91-011886] N91-28993
Magnetization and critical currents of tin-core multifilamentary Nb3Sn conductors
[DE91-012241] N91-28994
Flux dynamics in a single crystal of Bi2Sr2CaCu2O(x)
[DE91-013763] N91-29036
MAGNETOACOUSTIC WAVES
Rapid acceleration of protons in a nonlinear magnetosonic wave and their energy spectrum N91-28905
Electron acceleration by magnetosonic waves in a solar coronal loop N91-29132
MAGNETOHYDRODYNAMIC FLOW
Nonlinear phenomena and processes in high energy plasmas N91-28882
Transport profiles induced by radially localized modes in tokamak
[DE91-014366] N91-28964
Observational constraints on pulsars: Location of the emission region and pulse shape stability on decade time scales N91-29097
MAGNETOHYDRODYNAMIC GENERATORS
Simulation of combustion processes in an MHD second stage combustor
[DE91-014014] N91-28968
MAGNETOHYDRODYNAMIC STABILITY
Hybrid fluid/kinetic descriptions of tokamak plasmas N91-28888
Three-dimensional particle simulation of trapped electron instabilities in tokamaks N91-28891
Edge anomalous transport in heliotron/torsatron N91-28892
Optimization, non-local MHD-mode, and alpha-particle confinement behavior of Helias equilibria N91-28893
Equilibrium beta limit of helical systems N91-28894
Suppression and control of magnetic islands in toroidal plasmas N91-28895
Hydrodynamic instabilities in laser driven implosion N91-28897

Simulation study of MHD relaxation and reconnection processes N91-28908
Finite beta equilibrium for a pressure configuration N91-28909
Application of mathematica to energy principle N91-28910
Self-similar evolution of nonlinear magnetic buoyancy instability N91-28913
Electrostatic particle simulations of density and temperature driven modes in a toroidal plasma N91-28915
Internal kink mode simulation by 3-D gyrokinetic code N91-28916
Particle simulation on the tilt stabilization of the FRC plasma N91-28917
The 3-D electromagnetic macroscale particle simulation of inhomogeneous, magnetized plasmas N91-28918
Study of kink instability and current relaxation by three dimensional macroscale particle simulation N91-28919
Nonlinear behavior and transport property of multiple-helicity resistive interchange modes near marginally stable states N91-28922
Non-linear behaviour in tokamaks N91-28935
Propagation of drift waves in toroidal plasma systems N91-28939
Measurements of the ion acoustic decay instability and the resultant enhanced laser absorption and enhanced bremsstrahlung in laser-plasma interaction experiments
[DE91-014250] N91-28956
Nonlinear reversed field pinch dynamics with nonideal boundaries
[DE91-013638] N91-28961
Stability of annular equilibrium of energetic large orbit ion beam
[DE91-014365] N91-28963
Transport profiles induced by radially localized modes in tokamak
[DE91-014366] N91-28964
Exact solutions for a system of nonlinear plasma fluid equations
[DE91-014367] N91-28965
Progress in the development of a numerical tokamak
[DE91-013386] N91-28975
Plasma properties
[DE91-013933] N91-28978
Stability of drift-wave modons in the presence of temperature gradients
[DE91-014364] N91-28982
A new model of PeV gamma ray sources and MHD turbulence in neutron star accretion columns N91-29122

MAGNETOHYDRODYNAMIC TURBULENCE
Statistical properties of two-dimensional magnetohydrodynamic turbulence N91-28886
Turbulent dynamo and subgrid-scale modeling of MHD turbulence N91-28887
A new model of PeV gamma ray sources and MHD turbulence in neutron star accretion columns N91-29122

MAGNETOHYDRODYNAMIC WAVES
Direct ion heating in MHD relaxation N91-28911
Mode conversion of Alfven waves induced by quadrupole magnetic field modulation N91-28924
Steady-state dynamo and current drive in a nonuniform bounded plasma
[DE91-014865] N91-28974
Numerical simulations of mass outflows from star-forming regions N91-29123

MAGNETOHYDRODYNAMICS
Anomalous transport due to the skin size electromagnetic drift mode in tokamaks N91-28902
Magnetohydrodynamical formation of astrophysical jets from gravitationally collapsing objects N91-28903
Computer simulation of solar wind-magnetosphere interaction N91-28904
Helical field effect in solar/stellar wind N91-28912
Study of kink instability and current relaxation by three dimensional macroscale particle simulation N91-28919

MAGNETOMETERS
High-T(sub c) thin-film microelectronics
[DE91-012340] N91-28997

MAGNETOPLASMADYNAMICS
Nondestructive evaluation tools and experimental studies for monitoring the health of space propulsion systems
[NASA-TM-105164] N91-28605

MAGNETS
Fundamental magnetic studies of iron-rare-earth-metalloid alloys
[DE91-014816] N91-28383

MAGNONS
Neutron scattering studies of spin correlations in metallic YBa2Cu3O(6+x)
[DE91-013794] N91-29031

MAINTAINABILITY
A survey of reliability, maintainability, supportability, and testability software tools
[AD-A236148] N91-28745

MAINTENANCE
Failure analysis case histories of Canadian forces aircraft landing gear components N91-28151
Assessment of the application of the working group 22 standard bump concept to a current military aircraft N91-28166
Composite material systems for hydrogen management N91-28229

MALFUNCTIONS
Signature analysis technique for diagnosing failures in mechanical systems N91-28604

MAMMALS
Genetic changes in Mammalian cells transformed by helium cells
[DE91-013778] N91-28721

MAMMARY GLANDS
Chromosomal changes in cultured human epithelial cells transformed by low- and high-LET radiation
[DE91-013772] N91-28720

MAN ENVIRONMENT INTERACTIONS
Natural and anthropogenic climate change
[DE91-014734] N91-28673

MAN MACHINE SYSTEMS
Using HSYS in the analysis of human-system interactions: Examples from the offshore petroleum industry
[DE91-013218] N91-28732

MAN-COMPUTER INTERFACE
A design space and design rules for user interface software architecture
[AD-A237049] N91-28748
A simulated user for laboratory investigation of information systems requirements determination N91-29087

MANAGEMENT INFORMATION SYSTEMS
A logic model for model management: An embedded languages approach N91-28761
A framework for data and information
[DE91-012416] N91-29075

MANAGEMENT METHODS
Propulsion system ground testing N91-28261
Lessons learned and their application to program development and cultural issues N91-28263
Cultural changes in aerospace N91-28265
The use of science in the management of hazardous air pollutants N91-28667
Work plan for the preliminary site investigation for McMurdo Station, Ross Island, Antarctica
[DE91-015100] N91-28675
Experience in designing and using a flat structure in a multi-project research organization
[DE91-012427] N91-29067
Structured meeting techniques identify emergency management issues practitioners really want to see addressed
[DE91-012414] N91-29069

MANAGEMENT PLANNING
Major system acquisitions process (A-109) N91-28268
Research in mathematics and computer science at Argonne, September 1989-February 1991
[DE91-012989] N91-28734

MANAGEMENT SYSTEMS
Development of a current collection loss management system for SDI homopolar power supplies
[DE91-012779] N91-28652
Structured meeting techniques identify emergency management issues practitioners really want to see addressed
[DE91-012414] N91-29069

MANIPULATORS
Dynamic coupling effects in modeling and control of hard contact motion of a manipulator
[DE91-010393] N91-28574
A methodology to determine the dynamic configuration of a reconfigurable manipulator
[DE91-010732] N91-28576
Robust low-order control of flexible joint manipulators N91-28584
Mechanical design optimization of robot manipulator performance N91-28589
The creation of multi-degree-of-freedom mechanisms for robotic applications
[DE91-014359] N91-28596
Selected topics in mechanisms and robotics: Singularities, inverse kinematics, and collision detection N91-28598

MANNED MARS MISSIONS
Humans to Mars in 1999 N91-28237

MANNED SPACECRAFT
Propulsion studies for advanced manned launch systems N91-28213
Space transfer vehicles and space basing N91-28254

MANPOWER
Launch operations manpower yesterday, today and tomorrow N91-28267

MANUFACTURING
Technology transfer methodology N91-28239
Technology transfer methodology N91-28240
Manufacturing processes N91-28244
Sphere lapping
[DE91-014287] N91-28593
Model-based computed tomography for nondestructive evaluation
[DE91-013462] N91-28602

MANY BODY PROBLEM
Research in theoretical nuclear physics
[DE91-013644] N91-28872
Fundamental theory of crystal decomposition
[AD-A236637] N91-28988
Gravitational evolution of large-scale structure in the universe N91-29121

MAPPING
Threatened Area Database System (TADS) computer program
[DE91-012491] N91-29074

MAPS
Applications of scanning tunneling microscopy to electrochemistry
[AD-A237021] N91-28304
Close-range geophotogrammetric mapping of trench walls using multi-model stereo restitution software
[DE91-013105] N91-28645
A gravity model for the Coso geothermal area, California
[DE91-011874] N91-28677
Symplectic full-turn maps in a Fourier representation
[DE91-012912] N91-28796
Nonlinear dynamics of the relativistic standard map
[DE91-014368] N91-28972

MARINE TECHNOLOGY
Monitoring structural response in pressurized environments. Part 1: Instrumentation techniques
[DE91-012654] N91-28616

MARKETING
EIA publications directory, 1990
[DE91-014350] N91-29082

MARKOV PROCESSES
The theory of turbulence and anomalous transport in plasmas: Past, present, and future N91-28889

MARS LANDING
Humans to Mars in 1999 N91-28237

MASERS
Interaction of radiation with outflows in late-type stars N91-29136

MASKS
Reflection mask technology for soft x ray projection lithography
[DE91-012561] N91-28877

MASS DISTRIBUTION
Gravitational influence of a static ring-like distribution of mass on electromagnetic waves N91-28472

MASS SPECTROMETERS
Linked gas chromatograph-thermal energy analyzer/ion trap mass spectrometer
[DE91-013585] N91-28326

MASS SPECTROSCOPY
Analysis of metals in solution using electrospray ionization mass spectrometry
[DE91-012522] N91-28310
The use of AMS to the biomedical sciences
[DE91-012037] N91-28712
Fixed-wavelength R2PI/tandem mass spectrometry for mixture analysis in the quadrupole ion trap
[DE91-012506] N91-28835
Kinetic energy distributions of ions after surface collisions
[DE91-013412] N91-28850

MASS TRANSFER
Validity of the model used to relate the energy distribution and the adsorption isotherm
[DE91-013528] N91-28428
Dibaryons in neutron stars
[NASA-CR-188704] N91-29109

MASSIVELY PARALLEL PROCESSORS
Load-balancing and performance of a gridless particle simulation on MIMD, SIMD, and vector supercomputers
[DE91-013758] N91-28756
An interdisciplinary approach to massively parallel computation
[DE91-012652] N91-28775

MATERIALS SCIENCE
Technologies available from Martin Marietta Energy Systems, Inc.
[DE91-013027] N91-28283
Chemistry and materials science research report
[DE91-011507] N91-28305

MATHEMATICAL LOGIC

Automated reasoning contributes to mathematics and logic
[DE91-014005] N91-28765

MATHEMATICAL MODELS

Studies of the two-phase plume jet and wall erosion in a vertical launching system N91-28145

Landing gear improvements for transport aircraft N91-28159

A theoretical and experimental study of the interior ballistic processes of an electrothermal gun N91-28185

Discrete posynomial programming with applications to spacecraft protective structures design optimization N91-28190

Ignition and combustion of metallized propellants N91-28224

Experimental studies of the volatility of ammonium chloride
[DE91-012526] N91-28311

Equation-of-state from SiO2 aerogel Hugoniot data
[DE91-011480] N91-28313

Thermodynamics and efficiency in combustion and engines
[DE91-012781] N91-28320

Direct Monte Carlo simulation of chemical equilibrium composition of molecular fluid mixtures under shock conditions
[DE91-013075] N91-28324

The rate (time)-dependence mechanical behavior of modified 9Cr-1Mo. Part 2: Isothermal modeling at 538 C
[DE91-011100] N91-28350

EXAFS studies of elastic strain in dilute binary alloys
[DE91-012678] N91-28353

An extension of a kinetic theory of polymer crystallization through the exclusion of negative barriers
[AD-A236999] N91-28387

Mechanical modeling of stress generation during cure of encapsulating resins
[DE91-011496] N91-28393

The avian eggshell as a model of biomineralization
[DE91-012608] N91-28400

Reliable modeling of complex behavior
[DE91-013385] N91-28419

Validity of the model used to relate the energy distribution and the adsorption isotherm
[DE91-013528] N91-28428

Computer modeling of ceramic melters to assess impacts of process and design variables on performance
[DE91-013668] N91-28431

Creep and diffusion in nonstoichiometric oxides
[DE91-013766] N91-28435

Analysis of shock propagation and shock-initiated reaction in granular energetic materials N91-28446

A geometry based method of integrated engineering design, analysis, and optimization
[DE91-008588] N91-28457

Fields and trajectories in the magnicon
[DE91-013070] N91-28492

A numerical approach for modelling cavitating flows
[DE91-009178] N91-28505

Moving finite elements: A continuously adaptive method for computational fluid dynamics
[DE91-013391] N91-28513

Experimental study of growth rate enhancement and structure of compressible turbulent free shear layers N91-28517

Receptivity of a laminar boundary layer to the interaction of a three-dimensional roughness element with time-harmonic free-stream disturbances N91-28519

Transient two-phase flow of cryogenic fluid in a vertical transfer line during the cooldown process N91-28522

The numerical solution of confined laminar flow past a moving boundary N91-28532

Near-wall modelling of complex turbulent flows N91-28534

Numerical investigation of the thrust efficiency of a laser-propelled vehicle N91-28572

Dynamic coupling effects in modeling and control of hard contact motion of a manipulator
[DE91-010393] N91-28574

Applications of a 2-D moving finite element formulation to elastic/viscoplastic dynamic fracture analysis
[DE91-009930] N91-28607

Critical issues in de-alloying and transcrystalline stress-corrosion cracking
[DE91-010190] N91-28608

MESA: A 3-D Eulerian hydrocode for penetration mechanics studies
[DE91-013308] N91-28613

Viscoplastic analysis of an experimental cylindrical thrust chamber liner
[NASA-TM-103287] N91-28622

A new model of rate dependent elastic-plastic flow
[DE91-014600] N91-28633

Shear stress prediction in shock loaded copper
[DE91-014740] N91-28635

The solution of variable-geometry truss problems using new homotopy continuation methods N91-28640

United States Department of Energy solar receiver technology development
[DE91-012653] N91-28651

Modeling molecular processes in the environment
[DE91-013790] N91-28671

TREE: A model of the effects of acid precipitation and air pollutants on the growth of trees
[DE91-014131] N91-28672

Common reflection point stacking: A macro model driven approach to dip moveout
[ISBN-90-9003020-4] N91-28676

A gravity model for the Coso geothermal area, California
[DE91-011874] N91-28677

High-temperature elasticity and Earth's upper mantle N91-28679

Modeling two-point spatial turbulence spectra for analysis of gust variations over aerospace vehicles N91-28685

Modelling and analysis of geophysical turbulence: Use of optimal transforms and basis sets N91-28686

Gravity wave propagation in a frontal environment N91-28687

Prediction of forecast skill with a quasi-geostrophic model N91-28699

Low-level curvature shear and supercell thunderstorm behavior N91-28701

Predicting thunderstorm evolution using ground-based lightning detection networks N91-28702

A cloud fraction and radiative transfer model N91-28706

Spontaneous emergence of a metabolism
[DE91-013684] N91-28714

Radiation physics, biophysics, and radiation biology
[DE91-012883] N91-28716

New techniques for positron emission tomography in the study of human neurological disorders
[DE91-013855] N91-28728

Software metrics
[AD-A236140] N91-28744

Choosing processor array configuration by performance modeling for a highly parallel linear algebra algorithm
[DE91-012486] N91-28749

A logic model for model management: An embedded languages approach N91-28761

Order reduction and synthesis of transfer function models N91-28769

Split-join and message passing programming models on the BBN TC2000
[DE91-008067] N91-28774

Proceedings of the Second International Toki Conference on Plasma Physics and Controlled Nuclear Fusion. Nonlinear Phenomena in Fusion Plasmas: Theory and Computer Simulation
[NIFS-PROC-6] N91-28881

Turbulent dynamo and subgrid-scale modeling of MHD turbulence N91-28887

Hybrid fluid/kinetic descriptions of tokamak plasmas N91-28888

Edge anomalous transport in heliotron/torsatron N91-28892

Models of collisional transport across a magnetic field with destroyed surfaces N91-28900

Simulation study of MHD relaxation and reconnection processes N91-28908

Dynamics of interfaces with internal structures N91-28926

Structures of magnetic field lines in the helical torus N91-28932

Model for marfe-detached plasma transition in tokamaks N91-28938

Particle confinement and fueling effects on the Maryland spheromak
[DE91-012396] N91-28945

Simulation of combustion processes in an MHD second stage combustor
[DE91-014014] N91-28968

Plasma properties
[DE91-013933] N91-28978

Quantitative modeling of the point defect structures of Fe-doped MgO and MgSiO3 perovskite
[DE91-011405] N91-28990

Measurement accuracy of macroscopic quantum circuits with RF-biased Josephson junction arrays
[DE91-012651] N91-29009

Metastable phase equilibria in co-deposited Ni(1-x)Zr(x) thin films
[DE91-013653] N91-29029

Electron correlations in solid state physics
[DE91-013752] N91-29030

TOPAZ2D benchmark problems nonlinear materials
[DE91-009753] N91-29053

Chaos and microbial systems
[DE91-014908] N91-29064

Emission line regions in active galactic nuclei: Structure, kinematics, physical conditions, and chemical abundances N91-29095

Numerical models of equilibrium between matter and black holes N91-29101

MATRICES (MATHEMATICS)

An accelerated training method for back propagation networks
[NASA-CASE-MSC-21625-1] N91-28730

Multidimensional spectral estimation using iterative methods
[AD-A237025] N91-28791

ZLIB: A numerical library for differential algebra (A user's guide for version 1.0)
[DE91-012552] N91-28794

MATRIX MATERIALS

ZrO2 reinforced-MoSi2 matrix composites
[DE91-013074] N91-28288

The effect of ductile innerlayers on the mechanical performance of fiber-reinforced composite materials N91-28295

MATRIX METHODS

A cluster approximation for the transfer-matrix method
[DE91-617790] N91-28804

The determination of the momentum matrix elements involved in calculating the dielectric constants of superlattices using the tight-binding method
[DE91-617789] N91-29017

MATRIX THEORY

The determination of the momentum matrix elements involved in calculating the dielectric constants of superlattices using the tight-binding method
[DE91-617789] N91-29017

MAXIMUM LIKELIHOOD ESTIMATES

Seismic traveltime inversion in three-dimensional heterogeneous media N91-28678

MAXWELL EQUATION

General implementation of thin-slot algorithms into the finite-difference time-domain code, TSAR, based on a slot data file
[DE91-014336] N91-28767

MCMURDO SOUND

Work plan for the preliminary site investigation for McMurdo Station, Ross Island, Antarctica
[DE91-015100] N91-28675

MEAN FREE PATH

Fluidlike studies of the presheath and sheath regions of a plasma
[DE91-013345] N91-28953

Ground-based measurements of galactic cosmic ray fragmentation in shielding
[DE91-012336] N91-29133

MEASURE AND INTEGRATION

Path-integral measure for Chern-Simons theory within the stochastic quantization approach
[DE91-617610] N91-29056

MEASURING INSTRUMENTS

Technologies available from Martin Marietta Energy Systems, Inc.
[DE91-013027] N91-28283

Response of the polymers KEL-F, polysulfone, high density polyethylene and polymethylmethacrylate to shock loading and release from 0.3 to 2.4 GPa
[DE91-012867] N91-28411

Monitoring structural response in pressurized environments. Part 1: Instrumentation techniques
[DE91-012654] N91-28616

MECHANICAL PROPERTIES

Alumina-silicon carbide composites from coated powders
[DE91-012357] N91-28281

Investigation of thermomechanical behavior of metal matrix composites N91-28296

The influence of defects on the mechanical properties of short fibre reinfornced thermoplastics N91-28300

The rate (time)-dependence mechanical behavior of modified 9Cr-1Mo. Part 2: Isothermal modeling at 538 C
[DE91-011100] N91-28350

Mechanical properties of diamond and diamond-like films
[DE91-011373] N91-28406

Origin of acoustic emission produced during single point machining
[DE91-011915] N91-28453

Critical issues in de-alloying and transcrystalline stress-corrosion cracking
[DE91-010190] N91-28608

The rate (time)-dependent mechanical behavior of modified 9Cr-1Mo steel. Part 1: Experiments at 538 C
[DE91-011097] N91-28615

MELAMINE

Melamine-formaldehyde aerogels
[DE91-012084] N91-28408

MELTING

Properties of large heats of Fe3Al-based alloys
[DE91-013268] N91-28359

Behavior of RuO2 in a glass melt
[DE91-013717] N91-28432
MEMBRANES
Polymers at surfaces
[DE91-011000] N91-28392
Ordered ceramic membranes
[DE91-012248] N91-28398
The avian eggshell as a model of biomineralization
[DE91-012608] N91-28400
Preparation of ionic membranes for zinc/bromine storage batteries
[DE91-012008] N91-28483
Regulation of photosynthetic membrane components in cyanobacteria
[DE91-012713] N91-28713
MEMORY (COMPUTERS)
Taxonomy and algorithms for volume rendering on multicomputers
[AD-A236632] N91-28771
Split-join and message passing programming models on the BBN TC2000
[DE91-008067] N91-28774
Mapping implicit spectral methods to distributed memory architectures
[NASA-CR-187592] N91-28806
MERCURY COMPOUNDS
Electrical and photomechanical effects of plastic deformation of mercuric iodide
[DE91-013108] N91-29022
MESOPAUSE
Lidar studies of sporadic sodium layers, gravity waves and density spectra in the mesopause and stratopause regions at Urbana and Arecibo N91-28690
MESOSCALE PHENOMENA
Development and application of new modeling techniques for mesoscale atmospheric chemistry
N91-28692
MESOSPHERE
Observations and theoretical studies of tides and normal modes in the lower thermosphere N91-28681
METABOLISM
Spontaneous emergence of a metabolism
[DE91-013684] N91-28714
Plant growth is influenced by glutamine synthetase-catalyzed nitrogen metabolism
[DE91-014592] N91-28725
METABOLITES
New techniques for positron emission tomography in the study of human neurological disorders
[DE91-013855] N91-28728
METAL BONDING
Process for bonding elastomers to metal
[NASA-CASE-LAR-13645-1] N91-28424
METAL COATINGS
Boundary lubrication of ceramic materials by soft metallic coating and synthetic oil
[DE91-014017] N91-28577
METAL FATIGUE
Softening mechanisms and microstructural instabilities during high temperature, low cycle fatigue of Ni, Ni3Al, and their metal matrix composites
[DE91-012714] N91-28287
Damage progression during static and fatigue loading in metal matrix composites, volumes 1-3 N91-28301
Ferroelectric fatigue in modified bulk lead zirconate titanate ceramics
[DE91-012647] N91-28417
METAL FILMS
Cross-sectional TEM specimen preparation of free-standing metal multi-layered films
[DE91-011117] N91-28351
Kinetics of solid-state reactions in Ni-Zr thin films
[DE91-013652] N91-29028
METAL FOILS
Improving the performance of blasting caps
[NASA-CASE-LAR-13832-1] N91-28444
METAL IONS
Analysis of metals in solution using electrospray ionization mass spectrometry
[DE91-012522] N91-28310
Laser ejection of Ag(sup +) ions from a roughened silver surface: Role of the surface plasmon
[DE91-012945] N91-28554
Analysis of southeastern Canada lake-water chemistry data in relation to acidic deposition
[DE91-014957] N91-28674
Progress in light ion fusion
[DE91-012019] N91-28826
Plasma transport in a new cathodic arc ion source, theory and experiment
[DE91-011511] N91-28944
Plasma immersion surface modification with metal ion plasma
[DE91-014233] N91-28979
METAL MATRIX COMPOSITES
Softening mechanisms and microstructural instabilities during high temperature, low cycle fatigue of Ni, Ni3Al, and their metal matrix composites
[DE91-012714] N91-28287
ZrO2 reinforced-MoSi2 matrix composites
[DE91-013074] N91-28288
Strength and electrical conductivity of deformation processed Cu-15 v/o Fe metal composites produced by powder metallurgy/techniques
[DE91-013658] N91-28291
Investigation of thermomechanical behavior of metal matrix composites N91-28296
Tribology of aluminum-based metal matrix composites: Fundamental study of wear behavior as influenced by microstructure N91-28297
Joining of aluminum-based particulate-reinforced metal-matrix composites N91-28298
Damage progression during static and fatigue loading in metal matrix composites, volumes 1-3 N91-28301
The effect of TiB2 reinforcement on the mechanical properties of an Al-Cu-Li alloy-based metal-matrix composite N91-28337
METAL OXIDE SEMICONDUCTORS
Monolithic front end electronics for silicon calorimeters
[DE91-012063] N91-28484
METAL OXIDES
Behavior of RuO2 in a glass melt
[DE91-013717] N91-28432
Annealing and structure studies on Tl-2223 and Tl-1223 crystals
[DE91-014903] N91-29052
METAL PLATES
Hypervelocity plate acceleration
[DE91-014738] N91-28179
A study of the impact of reaction rates on equation of state
[DE91-013375] N91-28621
METAL PROPELLANTS
Ignition and combustion of metallized propellants
N91-28224
METAL SHEETS
Substructure and electrical resistivity analyses of pure tungsten sheet
[DE91-014098] N91-28362
Test of superplastically formed corrugated aluminum compression specimens with beaded webs
[NASA-TM-104119] N91-28373
METAL STRIPS
High temperature solder device for flat cables
[NASA-CASE-GSC-13344-1] N91-28363
METAL SURFACES
Cross-sectional TEM specimen preparation of free-standing metal multi-layered films
[DE91-011117] N91-28351
Analysis of the surface heterogeneity of different samples of aluminum oxide ceramic powders
[DE91-013527] N91-28421
Process for bonding elastomers to metal
[NASA-CASE-LAR-13645-1] N91-28424
Laser ejection of Ag(sup +) ions from a roughened silver surface: Role of the surface plasmon
[DE91-012945] N91-28554
METALLOIDS
Fundamental magnetic studies of iron-rare-earth-metalloid alloys
[DE91-014816] N91-28383
METALS
Interpreting solidification phenomena and microstructural evolution in metals through the use of transparent model alloy systems
[DE91-012629] N91-28347
Mechanisms of bacterial metals removal from solids
[DE91-012808] N91-28356
Supercritical fluids cleaning
[DE91-013374] N91-28456
METASTABLE STATE
Synthesis of metastable aluminum-based intermetallics by mechanical alloying
[DE91-013651] N91-28376
Metastable phase equilibria in co-deposited Ni(1-x)Zr(x) thin films
[DE91-013653] N91-29029
METEORITIC COMPOSITION
Isotopic measurements of solar noble gases in individual micrometeorites from Greenland and Antarctica
N91-29114
METEOROLOGICAL INSTRUMENTS
Meteorological instrumentation support for an adverse weather test facility
[AD-A236605] N91-28696
METEOROLOGICAL PARAMETERS
Meteorological instrumentation support for an adverse weather test facility
[AD-A236605] N91-28696
Data users guide to the mountain cloud chemistry project
[PB91-168484] N91-28697
METEOROLOGY
Effectivity of atmospheric electricity on launch availability N91-28260
Regional oxidant model user's guide. Part 1: The ROM preprocessors
[PB91-171926] N91-28665
Report of Meeting of CLICOM Experts
[WCDP-9] N91-28695
Results of agriclimatological studies using multiple satellite sensors like NOAA AVHRR; GMS IR; and LANDSAT MSS and TM
[DE91-618773] N91-28698
ARAC: A computer-based emergency-response dose-assessment service with global application potential
[DE91-013248] N91-28700
METHOD OF CHARACTERISTICS
Numerical simulations of mass outflows from star-forming regions N91-29123
METRIC SPACE
Invariant metrics for Hamiltonian systems
[DE91-014236] N91-28807
MICROANALYSIS
Application of electron energy loss spectroscopy to microanalysis of irradiated stainless steels
[DE91-009913] N91-28344
Correcting channeling and diffraction effects in quantitative REELS surface microanalysis
[DE91-009924] N91-28840
Measurements of ionization cross-section for electron energy-loss microanalysis under well defined scattering conditions
[DE91-013745] N91-28862
The spatial resolution of x ray microanalysis in thin foils
[DE91-011949] N91-29003
Scanning tunneling microspectroscopy of solids and surfaces
[DE91-014515] N91-29043
MICROCOMPUTERS
Microcomputers: An exploratory study of their availability and use in the research process and their contribution to researcher productivity N91-28739
MICROELECTRONICS
Building microelectronic systems in a university environment
[AD-A236629] N91-28477
Monolithic front end electronics for silicon calorimeters
[DE91-012063] N91-28484
Some high voltage DC breakdown properties of thick film circuits on alumina
[DE91-014675] N91-28500
High-T(sub c) thin-film microelectronics
[DE91-012340] N91-28997
MICROMECHANICS
Fracture micromechanics of intermetallic and ceramic matrix continuous fiber composites
[AD-A236638] N91-28280
MICROPARTICLES
Chemical characterization of microparticles by laser ablation in an ion trap mass spectrometer
[DE91-012513] N91-28309
Isotopic measurements of solar noble gases in individual micrometeorites from Greenland and Antarctica
N91-29114
MICROPOROSITY
Electron transfer reactions in microporous solids
[DE91-012299] N91-28833
MICROSCOPY
The application of x ray tomographic microscopy to chemical vapor infiltration processing of ceramic matrix composites
[DE91-011871] N91-28284
Advancements in ultrathinning section techniques for the characterization of brittle materials
[DE91-012930] N91-28364
X ray Tomographic Microscopy (XTM)
[DE91-011930] N91-28599
MICROSTRUCTURE
Softening mechanisms and microstructural instabilities during high temperature, low cycle fatigue of Ni, Ni3Al, and their metal matrix composites
[DE91-012714] N91-28287
The influence of defects on the mechanical properties of short fibre reinfornced thermoplastics N91-28300
Microstructure-property relationships in Al-Cu-Li-Ag-Mg Weldalite (tm) alloys, part 2
[NASA-CR-4364] N91-28334
Identification of strengthening phases in Al-Cu-Li alloy Weldalite (tm) 049 N91-28335
The influence of Ag+Mg additions on the nucleation of strengthening precipitates in a non-cold-worked Al-Cu-Li alloy N91-28336

Effect of Li level, artificial aging, and TiB2 reinforcement on the modulus of Weldalite (tm) 049 N91-28340

Rapid solidification processing of Al3Ti and Al3Ti plus copper
[AD-A236600] N91-28343

Tensile deformation of Al-Cu-Li-Zr alloy 2090-T8E41 at 298 and 77 K
[DE91-011885] N91-28345

Interpreting solidification phenomena and microstructural evolution in metals through the use of transparent model alloy systems
[DE91-012629] N91-28347

Properties of large heats of Fe3Al-based alloys
[DE91-013268] N91-28359

Advancements in ultrathinning section techniques for the characterization of brittle materials
[DE91-012930] N91-28364

Weldability of iron aluminides
[DE91-013730] N91-28367

Microstructural characterization of solders and brazes for advanced packaging technology
[DE91-011503] N91-28379

Fundamental magnetic studies of iron-rare-earth-metalloid alloys
[DE91-014816] N91-28383

X ray fiducial foils
[DE91-011193] N91-28542

X ray Tomographic Microscopy (XTM)
[DE91-011930] N91-28599

X ray microimaging of elemental composition and microstructure for materials science
[DE91-012052] N91-28601

Shock compression of low-density microcellular materials
[DE91-013586] N91-28628

Scanning Transmission Ion Microscopy (STIM): A new technique for density mapping of microstructures
[DE91-011917] N91-28825

X ray microimaging of elemental composition and microstructure for materials science
[DE91-012221] N91-28832

TEM analysis of enclosed crystal microstructures and interfaces
[DE91-012344] N91-29006

MICROWAVE AMPLIFIERS

Fields and trajectories in the magnicon
[DE91-013070] N91-28492

MICROWAVE CIRCUITS

Simulation of planar integrated photonics devices with the LLNL time-domain finite-difference code suite
[DE91-011929] N91-28876

MICROWAVE EQUIPMENT

Growth of high T(sub c) superconducting thin films for microwave applications
[DE91-011436] N91-28991

MICROWAVE FREQUENCIES

Fields and trajectories in the magnicon
[DE91-013070] N91-28492

Reduction of energy sweep of the ETA-2 beam
[DE91-013824] N91-28568

MICROWAVE INTERFEROMETERS

A microwave interferometer to measure particle and shock velocities simultaneously
[DE91-013077] N91-28545

MICROWAVE OSCILLATORS

Nonlinear computer analysis of backward wave oscillator N91-28923

MICROWAVE PLASMA PROBES

Microwave-generated plasma thruster
[DE91-013131] N91-28948

MICROWAVE SCATTERING

Influence of fast waves on the collective scattering of microwaves in fusion plasmas
[DE91-014759] N91-28973

MICROWAVES

Characterization of silicon nitride synthesized by microwave heating
[DE91-012219] N91-28397

Investigation of interlayer materials for the microwave joining of SiC
[DE91-013311] N91-28414

Microwave enhanced diffusion?
[DE91-013312] N91-28415

Measurement of the microwave propagation delay induced by atmospheric water vapor N91-28466

Microwave instability at transition: Stability diagram approach
[DE91-013202] N91-28867

Influence of fast waves on the collective scattering of microwaves in fusion plasmas
[DE91-014759] N91-28973

MILITARY OPERATIONS

Interceptor combinations for theater defense
[DE91-012990] N91-28810

MILITARY TECHNOLOGY

Space systems requirements: The Navy approach
[AD-A236490] N91-28181

MILLIMETER WAVES

Superconducting bolometers: High-T(sub c) and low-T(sub c)
[DE91-011830] N91-28992

MILLING (MACHINING)

Cross-sectional TEM specimen preparation of free-standing metal multi-layered films
[DE91-011117] N91-28351

MIMD (COMPUTERS)

Load-balancing and performance of a gridless particle simulation on MIMD, SIMD, and vector supercomputers
[DE91-013758] N91-28756

MIMO (CONTROL SYSTEMS)

Attitude control of a spinning rocket via thrust vectoring
[DE91-006267] N91-28274

MINERALS

Biomimetic thin film deposition
[DE91-012485] N91-28999

MINIMAL SURFACES

Computing minimal surfaces via level set curvature flow
[DE91-014709] N91-28759

MINKOWSKI SPACE

The 2+1 gravity: A new approach N91-29059

MIRROR FUSION

Performance of the 10-kV, 5-MA pulsed-power system for the FRX-C compression experiment
[DE91-014745] N91-28983

MIRRORS

Reflection mask technology for soft x ray projection lithography
[DE91-012561] N91-28877

Color effects in optical systems
[ITN-91-85150] N91-28878

MISSILE LAUNCHERS

Studies of the two-phase plume jet and wall erosion in a vertical launching system N91-28145

MISSION PLANNING

Next generation: Unmanned launch vehicles and upper stages: The needs N91-28210

The space exploration initiative. Operational efficiency panel space-basing technology requirements
N91-28253

Space shuttle requirements/configuration evolution
N91-28264

Major system acquisitions process (A-109)
N91-28268

MIXED OXIDES

Defects and transport in mixed oxides
[DE91-014443] N91-29049

Annealing and structure studies on Tl-2223 and Tl-1223 crystals
[DE91-014903] N91-29052

MIXING

Droplet-turbulence interactions in subcritical and supercritical evaporating sprays N91-28228

Numerical simulation of the air and fuel mixing process in fuel-injected engines using discrete vortex dynamics
N91-28587

MIXING LAYERS (FLUIDS)

A study on particle dispersion in two-dimensional mixing layer flows N91-28537

MIXING LENGTH FLOW THEORY

Implications of TAE modes for the design of ITER
[DE91-013128] N91-28952

MIXTURES

Integrated theoretical and experimental study of the thermophysical properties of fluid mixtures
[DE91-012660] N91-28316

MODELS

An extension of a kinetic theory of polymer crystallization through the exclusion of negative barriers
[AD-A236999] N91-28387

Experience in designing and using a flat structure in a multi-project research organization
[DE91-012427] N91-29067

MODEMS

Wideband adaptive HF modem
[ITN-91-85147] N91-28471

MODULATION

Wideband adaptive HF modem
[ITN-91-85147] N91-28471

Mode conversion of Alfven waves induced by quadrupole magnetic field modulation N91-28924

MODULES

Research on stable, high-efficiency amorphous silicon multijunction modules
[DE91-002138] N91-28480

MODULUS OF ELASTICITY

Microstructure-property relationships in Al-Cu-Li-Ag-Mg Weldalite (tm) alloys, part 2
[NASA-CR-4364] N91-28334

The effect of TiB2 reinforcement on the mechanical properties of an Al-Cu-Li alloy-based metal-matrix composite N91-28337

Effect of Li level, artificial aging, and TiB2 reinforcement on the modulus of Weldalite (tm) 049 N91-28340

Mechanical properties of diamond and diamond-like films
[DE91-011373] N91-28406

MOIRE INTERFEROMETRY

High-resolution interferometric measurements of residual strains in composites N91-28303

MOISTURE CONTENT

Effect of water content on the piezoelectric properties of nylon 11 and nylon 7
[AD-A237013] N91-28389

MOLECULAR BEAM EPITAXY

Epitaxial growth of silicon on CoSi2(001)/Si(001)
[DE91-013387] N91-29015

MOLECULAR BEAMS

Evidence of vibrational mode-coupling in 2-fluorethanol via high resolution infrared spectroscopy in a molecular beam
[AD-A236132] N91-28821

High resolution infrared spectroscopy of 2-fluorethanol in a molecular beam
[AD-A236149] N91-28822

MOLECULAR BIOLOGY

The use of AMS to the biomedical sciences
[DE91-012037] N91-28712

Searching for consensus patterns on a hypercube
[DE91-013233] N91-28753

MOLECULAR CHAINS

Synthesis and properties of novel cluster phases
[DE91-013006] N91-29013

MOLECULAR CLOUDS

Star formation in the presence of magnetic fields: Molecular cloud core formation and dynamical contraction due to ambipolar diffusion:; a simulation with axial symmetry N91-29116

MOLECULAR COLLISIONS

Energy dissipation in chemical reactions on ultrafast timescales
[DE91-012342] N91-28315

Mode selectivity in cluster-molecule interactions: Ni13 + D2
[DE91-013352] N91-28859

MOLECULAR DIFFUSION

The effect of stress on hydrogen uptake and desorption by A-286
[NASA-TM-103537] N91-28341

MOLECULAR ENERGY LEVELS

Some new approaches to semiclassical and quantum transition state theory
[DE91-012345] N91-28308

Energy dissipation in chemical reactions on ultrafast timescales
[DE91-012342] N91-28315

Molecular eigenstate spectroscopy: Application to the intramolecular dynamics of some polyatomic molecules in the 3000 to 7000 cm(exp -1) region
[DE91-013154] N91-28839

MOLECULAR EXCITATION

Desorption of large organic molecules by laser-induced plasmon excitation
[DE91-013415] N91-28852

MOLECULAR FLOW

Direct Monte Carlo simulation of chemical equilibrium composition of molecular fluid mixtures under shock conditions
[DE91-013075] N91-28324

MOLECULAR ORBITALS

Magnetic resonance and optical spectroscopic studies of carotenoids
[DE91-014361] N91-28724

MOLECULAR OSCILLATIONS

Molecular eigenstate spectroscopy: Application to the intramolecular dynamics of some polyatomic molecules in the 3000 to 7000 cm(exp -1) region
[DE91-013154] N91-28839

MOLECULAR RELAXATION

Energy dissipation in chemical reactions on ultrafast timescales
[DE91-012342] N91-28315

MOLECULAR SPECTROSCOPY

Molecular eigenstate spectroscopy: Application to the intramolecular dynamics of some polyatomic molecules in the 3000 to 7000 cm(exp -1) region
[DE91-013154] N91-28839

MOLECULAR STRUCTURE

Studies relevant to the catalytic activation of carbon monoxide
[DE91-012661] N91-28323

Transition metal activation and functionalization of carbon-hydrogen bonds
[DE91-014261] N91-28332

Relationships between polymer-additive molecular structure and intumescent flame retardant behavior
N91-28426
X ray microimaging of elemental composition and microstructure for materials science
[DE91-012052] N91-28601
Modeling molecular processes in the environment
[DE91-013790] N91-28671
Molecular dynamics simulations of bulk displacement threshold energies in Si
[DE91-011957] N91-28846
Mode selectivity in cluster-molecule interactions: Ni13 + D2
[DE91-013352] N91-28859
Photoinduced charge and energy transfer processes in molecular aggregates
[DE91-014383] N91-28864
Synthesis and characterization of reduced ternary molybdenum oxides and soluble copper (III) alkoxide complexes
[DE91-012679] N91-29001
Synthesis and properties of novel cluster phases
[DE91-013006] N91-29013
Parallel nanometer scale fabrication
[DE91-013016] N91-29026
The computer storage, retrieval, and searching of generic structures in chemical patents: The machine-readable representation of generic structures
N91-29081

MOLECULES
Desorption of large organic molecules by laser-induced plasmon excitation
[DE91-013415] N91-28852
Interactions of molecules with surfaces
[DE91-014498] N91-28857

MOLTEN SALTS
United States Department of Energy solar receiver technology development
[DE91-012653] N91-28651

MOLYBDENUM
Mechanism of hydrodenitrogenation. Part 5: X ray diffraction of molybdenum catalysts
[DE91-013853] N91-28327

MOLYBDENUM ALLOYS
The rate (time)-dependence mechanical behavior of modified 9Cr-1Mo. Part 2: Isothermal modeling at 538 C
[DE91-011100] N91-28350
Aqueous corrosion characteristics and corrosion-related cracking susceptibilities of Fe3Al-type iron aluminides
[DE91-013028] N91-28358
The rate (time)-dependent mechanical behavior of modified 9Cr-1Mo steel. Part 1: Experiments at 538 C
[DE91-011097] N91-28615

MOLYBDENUM OXIDES
Model catalytic oxidation studies using supported monometallic and heterobimetallic oxides
[DE91-012144] N91-28409
Synthesis and characterization of reduced ternary molybdenum oxides and soluble copper (III) alkoxide complexes
[DE91-012679] N91-29001

MOMENTUM
The determination of the momentum matrix elements involved in calculating the dielectric constants of superlattices using the tight-binding method
[DE91-617789] N91-29017
Generalized gyroviscous force and its effect on the momentum balance equation
[DE91-013344] N91-29061

MOMENTUM TRANSFER
Light-cone quantization of quantum chromodynamics
[DE91-013991] N91-28856

MONITORS
Nondestructive evaluation tools and experimental studies for monitoring the health of space propulsion systems
[NASA-TM-105164] N91-28605
ARAC: A computer-based emergency-response dose-assessment service with global application potential
[DE91-013248] N91-28700
Description of real-time Ada software implementation of a power system monitor for the Space Station Freedom PMAD DC testbed
[NASA-TM-105157] N91-28776

MONOMERS
Semi-empirical calculations on model systems for organosilyldiamine preceramic polymers
[DE91-013721] N91-28433

MONOTECTIC ALLOYS
Interpreting solidification phenomena and microstructural evolution in metals through the use of transparent model alloy systems
[DE91-012629] N91-28347

MONTE CARLO METHOD
The use of Monte Carlo simulation in determining landing gear loads during landing N91-28162
Direct Monte Carlo simulation of chemical equilibrium composition of molecular fluid mixtures under shock conditions
[DE91-013075] N91-28324
Probabilistic structural mechanics research for parallel processing computers
[NASA-CR-187162] N91-28644
X ray spatial resolution at intermediate voltages: An assessment by massively parallel Monte Carlo electron trajectory simulation
[DE91-012018] N91-28841
Topics on frustrated spin systems and high-temperature superconductors N91-29032
Transport with Feynman propagators
[DE91-013566] N91-29063

MORPHOLOGY
TEM analysis of enclosed crystal microstructures and interfaces
[DE91-012344] N91-29006

MOSSBAUER EFFECT
The pressure-induced Mott transition in transition-metal iodides
[DE91-013671] N91-28366

MOUNTAINS
Data users guide to the mountain cloud chemistry project
[PB91-168484] N91-28697

MOUNTING
Flush mounting of thin film sensors
[NASA-CASE-LAR-14446-1] N91-28454

MULTIGRID METHODS
Parallelizing across time when solving time-dependent partial differential equations
[DE91-012948] N91-28797

MULTIPOLES
High order calculation of the multipole content of three dimensional electrostatic geometries
[DE91-014707] N91-28476

MULTIPROCESSING (COMPUTERS)
Numerical analyses of aero-optical flows: An application of parallel algorithm on high-performance Personal Computer (PC) base multitransputer system N91-28519
Parallel input/output architectures for multiprocessors
N91-28740
Compile-time estimation of communication costs in multicomputers
[NASA-CR-188675] N91-28747
Choosing processor array configuration by performance modeling for a highly parallel linear algebra algorithm
[DE91-012486] N91-28749
A multilingual parallelization of the icosahedral-hexagonal grid system for integration on the sphere
[DE91-013615] N91-28762
Taxonomy and algorithms for volume rendering on multicomputers
[AD-A236632] N91-28771
The cache group scheme for hardware-controlled cache coherence and the general need for hardware coherence control in large-scale multiprocessors
[DE91-012106] N91-28772
Toward a better parallel performance metric
[DE91-012627] N91-28773
An interdisciplinary approach to massively parallel computation
[DE91-012652] N91-28775

MULTISPECTRAL BAND SCANNERS
The in-flight calibration of a helicopter-mounted Daedalus multispectral scanner
[DE91-013054] N91-28170

MULTISPECTRAL RADAR
Multiple frequency atmospheric radar techniques
N91-28683

MUON SPIN ROTATION
Application of muon spin relaxation experiment to the mixed state superconductors
[DE91-013689] N91-29034
Application of muon spin relaxation experiment to the vortex dynamics of high temperature superconductors
[DE91-014607] N91-29050

MUONS
Mind over matter: The intellectual content of experimental physics
[DE91-617571] N91-28813

MUTATIONS
The use of AMS to the biomedical sciences
[DE91-012037] N91-28712
Regulation of photosynthetic membrane components in cyanobacteria
[DE91-012713] N91-28713

MYLAR (TRADEMARK)
X ray fiducial foils
[DE91-011193] N91-28542

N

NASA PROGRAMS
Report of the Advisory Committee on the future of the US space program
[NASA-TM-105030] N91-28180
Shuttle derived manned transportation systems
N91-28204
Solid rocket propulsion N91-28206
Historical perspectives: The role of the NASA Lewis Research Center in the national space nuclear power programs
[NASA-TM-105196] N91-29138

NASA SPACE PROGRAMS
Report of the Advisory Committee on the future of the US space program
[NASA-TM-105030] N91-28180

NATIONAL AEROSPACE PLANE PROGRAM
National Aero-Space Plane (NASP) program
N91-28214

NATURAL SATELLITES
The 1990 update to strategy for exploration of the inner planets
[NASA-CR-188728] N91-28182

NAVIER-STOKES EQUATION
Numerical simulation of particle-wave interaction in boundary layers
[NASA-CR-187312] N91-28502
Algorithm and code development for unsteady three-dimensional Navier-Stokes equations
[NASA-CR-188039] N91-28503
Prediction of the flow and heat transfer between a rotating and a stationary cone N91-28536

NAVIGATION
WFOV star tracker camera
[DE91-012776] N91-28148

NAVSTAR SATELLITES
Precise orbit determination for GPS satellites
N91-28183

NAVY
Space systems requirements: The Navy approach
[AD-A236490] N91-28181

NEAR FIELDS
An assessment of the lifetime of Faraday shield elements
[DE91-012228] N91-28463

NEODYMIUM LASERS
Chemical characterization of microparticles by laser ablation in an ion trap mass spectrometer
[DE91-012513] N91-28309
Fluxless soldering of Ni-Au plated Kovar with a laser
[DE91-013261] N91-28451
High-peak power-Nd:Glass laser facilities for end users
[DE91-013246] N91-28561
Studies of laser-driven flyer acceleration using optical fiber coupling
[DE91-013503] N91-28562

NEURAL NETS
An accelerated training method for back propagation networks
[NASA-CASE-MSC-21625-1] N91-28730
Elastic tracking versus neural network tracking for very high multiplicity problems
[DE91-011825] N91-28768
Crystal surface analysis using matrix textural features classified by a probabilistic neural network
[DE91-014120] N91-29048

NEUTRAL ATMOSPHERES
Observations and theoretical studies of tides and normal modes in the lower thermosphere N91-28681

NEUTRALIZERS
H(-) beam characterization using laser-induced neutralization
[DE91-013501] N91-28564

NEUTRINOS
Phonon-mediated detection of elementary particles using silicon crystal acoustic detectors N91-28547
Mind over matter: The intellectual content of experimental physics
[DE91-617571] N91-28813
High intensity neutrino beams at KAON
[DE91-012147] N91-28830
Study of gravitational collapse and cosmic ray abundances N91-29105
Neutrino degeneracy and cosmological nucleosynthesis, revisited
[NASA-CR-188703] N91-29110
Testing the Big Bang: Light elements, neutrinos, dark matter and large-scale structure
[NASA-CR-188701] N91-29111

NEUTRON CROSS SECTIONS
New techniques in neutron data measurements above 30 MeV
[DE91-013690] N91-28861

NEUTRON DIFFRACTION

Residual stress measurement using the pulsed neutron source at LANSCE
[DE91-013494] N91-28624

Neutron diffraction determination of the residual stress redistribution in cracked autofrettaged tubing
[DE91-013688] N91-28632

Neutron scattering studies of spin correlations in metallic YBa2Cu3O(6+x)
[DE91-013794] N91-29031

NEUTRON FLUX DENSITY

Measuring neutron fluences and gamma/x ray fluxes with CCD cameras
[DE91-014119] N91-28549

NEUTRON IRRADIATION

Application of electron energy loss spectroscopy to microanalysis of irradiated stainless steels
[DE91-009913] N91-28344

NEUTRON SCATTERING

Neutron scattering studies of spin correlations in metallic YBa2Cu3O(6+x)
[DE91-013794] N91-29031

NEUTRON SOURCES

Residual stress measurement using the pulsed neutron source at LANSCE
[DE91-013494] N91-28624

Scintillation detector efficiencies for neutrons in the energy region above 20 MeV
[DE91-012544] N91-28837

New techniques in neutron data measurements above 30 MeV
[DE91-013690] N91-28861

NEUTRON STARS

Radiative transfer in very strong magnetic fields
N91-29106

Dibaryons in neutron stars
[NASA-CR-188704] N91-29109

A new model of PeV gamma ray sources and MHD turbulence in neutron star accretion columns
N91-29122

Impact of the nuclear equation of state on models of rotating neutron stars
[DE91-014615] N91-29125

NEUTRONS

Multilevel resonance analysis of Co-59 neutron transmission measurements
[DE91-012135] N91-28829

Nuclear structure studies via neutron interactions
[DE91-012165] N91-28831

Scintillation detector efficiencies for neutrons in the energy region above 20 MeV
[DE91-012544] N91-28837

Photodisintegration of the deuteron at medium and high energies
[DE91-014458] N91-28865

NEWTON-RAPHSON METHOD

A numerical approach for modelling cavitating flows
[DE91-009178] N91-28505

NICKEL

Mode selectivity in cluster-molecule interactions: Ni13 + D2
[DE91-013352] N91-28859

Surface phases and their influence on metal-oxide interfaces
[DE91-012277] N91-28995

Kinetics of solid-state reactions in Ni-Zr thin films
[DE91-013652] N91-29028

NICKEL ALLOYS

Aqueous corrosion characteristics and corrosion-related cracking susceptibilities of Fe3Al-type iron aluminides
[DE91-013028] N91-28358

Atomistic studies of grain boundaries in alloys and compounds
[DE91-014516] N91-28372

Hydrogen embrittlement of selected nickel and iron base superalloys N91-28374

Metastable phase equilibria in co-deposited Ni(1-x)Zr(x) thin films
[DE91-013653] N91-29029

NICKEL HYDROGEN BATTERIES

Exploratory battery technology development report for FY90
[DE91-012131] N91-28485

NICKEL OXIDES

Creep and diffusion in nonstoichiometric oxides
[DE91-013766] N91-28435

NIOBIUM ALLOYS

Strength and electrical conductivity of deformation processed Cu-15 v/o Fe metal composites produced by powder metallurgy/techniques
[DE91-013658] N91-28291

NIOBIUM COMPOUNDS

Magnetization and critical currents of tin-core multifilamentary Nb3Sn conductors
[DE91-012241] N91-28994

NITINOL ALLOYS

Coupling device with improved thermal interface
[NASA-CASE-GSC-13251-1] N91-28582

Device for removing foreign objects from anatomic organs
[NASA-CASE-GSC-13306-1] N91-28727

NITRATES

Ultra-fine powders using glycine-nitrate combustion synthesis
[DE91-012926] N91-28412

NITRIC OXIDE

Shock initiation of pentaerythritol tetranitrate crystals: Optical absorption and emission studies
[DE91-013381] N91-29023

NITRIDING

Characterization of silicon nitride synthesized by microwave heating
[DE91-012219] N91-28397

NITROGEN COMPOUNDS

Linked gas chromatograph-thermal energy analyzer/ion trap mass spectrometer
[DE91-013585] N91-28326

NITROGEN METABOLISM

Plant growth is influenced by glutamine synthetase-catalyzed nitrogen metabolism
[DE91-014592] N91-28725

NITROGEN POLYMERS

Nitrogen and boron-containing polymers as precursors of ceramic materials
[DE91-008890] N91-28390

NOISE PREDICTION (AIRCRAFT)

A reciprocity technique for the characterisation of sound transmission into aircraft fuselages N91-28817

NOISE REDUCTION

Real-time adaptive active control of sound fields
N91-28819

NONADIABATIC CONDITIONS

Longitudinal aerodynamic characteristics of a subsonic, energy-efficient transport configuration in the National Transonic Facility
[NASA-TP-2922] N91-28143

Nonadiabatic behavior of the magnetic moment of a charged particle in a dipole magnetic field N91-28920

NONDESTRUCTIVE TESTS

Overall goals N91-28246

The application of x ray tomographic microscopy to chemical vapor infiltration processing of ceramic matrix composites
[DE91-011871] N91-28284

Recent ASME Code Section 11 developments for surface examination through coatings
[DE91-014069] N91-28437

Nondestructive testing standards and the ASME code
[DE91-012643] N91-28600

Model-based computed tomography for nondestructive evaluation
[DE91-013462] N91-28602

Nondestructive evaluation tools and experimental studies for monitoring the health of space propulsion systems
[NASA-TM-105164] N91-28605

Residual stress measurement using the pulsed neutron source at LANSCE
[DE91-013494] N91-28624

Inertial confinement fusion
[DE91-013479] N91-28960

NONFERROUS METALS

JPRS report: Science and technology. USSR: Materials science
[JPRS-UMS-91-003] N91-28342

NONLINEAR EQUATIONS

Recursive linearization of multibody dynamics and application to control design N91-28588

Internal kink mode simulation by 3-D gyrokinetic code
N91-28916

Nonlinear equations for weakly unstable modes
N91-28927

Equilibria and dynamics of temperature in a fusion reactor plasma N91-28937

Model for marfe-detached plasma transition in tokamaks N91-28938

Exact solutions for a system of nonlinear plasma fluid equations
[DE91-014367] N91-28965

NONLINEAR PROGRAMMING

Discrete posynomial programming with applications to spacecraft protective structures design optimization
N91-28190

Design of an interactive satellite communications system analysis program
[AD-A237030] N91-28459

NONLINEAR SYSTEMS

A methodology for using nonlinear aerodynamics in aeroservoelastic analysis and design
[NASA-TM-104087] N91-28131

New photocrosslinkable polymers for second order nonlinear optical processes
[AD-A235856] N91-28386

The symbolic computation and automatic analysis of trajectories
[NASA-CR-188159] N91-28787

Rapid acceleration of protons in a nonlinear magnetosonic wave and their energy spectrum
N91-28905

Simulation study of MHD relaxation and reconnection processes N91-28908

Application of mathematica to energy principle
N91-28910

Self-similar evolution of nonlinear magnetic buoyancy instability N91-28913

Nonlinear behavior and transport property of multiple-helicity resistive interchange modes near marginally stable states N91-28922

Dynamics of interfaces with internal structures
N91-28926

Nonlinear equations for weakly unstable modes
N91-28927

Regular motion and symmetry in the relativistic standard map N91-28933

Nonlinear reversed field pinch dynamics with nonideal boundaries
[DE91-013638] N91-28961

Nonlinear dynamics of the relativistic standard map
[DE91-014368] N91-28972

TOPAZ2D benchmark problems nonlinear materials
[DE91-009753] N91-29053

Nonlinear modeling of chaotic time series: Theory and applications
[DE91-013076] N91-29055

Chaos and microbial systems
[DE91-014908] N91-29064

NONLINEARITY

Photocross-linked second order nonlinear optical polymers
[AD-A235855] N91-28385

New photocrosslinkable polymers for second order nonlinear optical processes
[AD-A235856] N91-28386

Recursive linearization of multibody dynamics and application to control design N91-28588

Numerical study of ion temperature gradient modes in a tokamak N91-28921

Nonlinear computer analysis of backward wave oscillator N91-28923

Non-linear behaviour in tokamaks N91-28935

Model for marfe-detached plasma transition in tokamaks N91-28938

Formation and dynamics of solitary waves and vortices in driven and damped systems N91-28942

Solitons and chaos in plasma N91-28943

NONUNIFORM PLASMAS

Steady-state dynamo and current drive in a nonuniform bounded plasma
[DE91-014865] N91-28974

NORTHERN HEMISPHERE

Interactions between the north Pacific Ocean and the Northern Hemisphere atmosphere during El Nino
N91-28711

NOTCH TESTS

Interlaminar fracture characterization: A current review
[NASA-CR-187573] N91-28626

NOTCHES

Near crack tip transverse strain effects estimated with a large strain hollow cylinder analogy
[DE91-012072] N91-28619

NOZZLE DESIGN

A study of methods to investigate nozzle boundary layer transition N91-28232

NOZZLE FLOW

Generating strong shock waves with a supersonic peristaltic pump
[DE91-013228] N91-28174

A study of methods to investigate nozzle boundary layer transition N91-28232

Optical diagnostic investigation of low Reynolds number nozzle flows N91-28233

NUCLEAR BINDING ENERGY

Radiative transfer in very strong magnetic fields
N91-29106

NUCLEAR CAPTURE

Multilevel resonance analysis of Co-59 neutron transmission measurements
[DE91-012135] N91-28829

NUCLEAR DEFORMATION

Reflection-asymmetric shapes in atomic nuclei
[DE91-013414] N91-28851

Shell model calculations at superdeformed shapes
[DE91-012954] N91-28853

NUCLEAR ELECTRIC PROPULSION

Futuristic systems: Solar and nuclear electric propulsion N91-28215

NUCLEAR ENGINE FOR ROCKET VEHICLES
Nuclear thermal propulsion N91-28216
NUCLEAR FISSION
Nuclear thermal propulsion N91-28216
NUCLEAR FUELS
Nonlinear evolution of 2D and 3D Rayleigh-Taylor instability at stagnation phase in laser implosion
N91-28899
NUCLEAR FUSION
Space fusion energy conversion using a field reversed configuration reactor: A new technical approach for space propulsion and power N91-28217
Space propulsion by fusion in a magnetic dipole
[DE91-012033] N91-28275
Evaluation of charged-particle reactions for fusion applications
[DE91-014135] N91-28962
Nonlinear dynamics of the relativistic standard map
[DE91-014368] N91-28972
Plasma properties
[DE91-013933] N91-28978
Neutrino degeneracy and cosmological nucleosynthesis, revisited
[NASA-CR-188703] N91-29110
NUCLEAR MAGNETIC RESONANCE
Chemistry and materials science research report
[DE91-011507] N91-28305
Thermodynamic and kinetic aspects of surface acidity
[DE91-014039] N91-28331
Nuclear magnetic resonance studies of atomic motion in lithium chloroborate and lithium thiosilicate glassy fast ionic conductors
[DE91-012677] N91-28843
Neutron scattering studies of spin correlations in metallic YBa2Cu3O(6+x)
[DE91-013794] N91-29031
NUCLEAR MODELS
Reflection-asymmetric shapes in atomic nuclei
[DE91-013414] N91-28851
Shell model calculations at superdeformed shapes
[DE91-012954] N91-28853
Optical analogs of model atoms in fields
[DE91-013392] N91-28855
Impact of the nuclear equation of state on models of rotating neutron stars
[DE91-014615] N91-29125
NUCLEAR PHYSICS
JPRS report: Science and technology. USSR: Physics and mathematics
[JPRS-UPM-90-006] N91-28811
Multilevel resonance analysis of Co-59 neutron transmission measurements
[DE91-012135] N91-28829
High intensity neutrino beams at KAON
[DE91-012147] N91-28830
Theoretical research in intermediate-energy nuclear physics
[DE91-012720] N91-28838
Research in theoretical nuclear physics
[DE91-013644] N91-28872
Theoretical studies in nuclear physics
[DE91-013909] N91-28873
Generalized gyroviscous force and its effect on the momentum balance equation
[DE91-013344] N91-29061
NUCLEAR POWER PLANTS
Nondestructive testing standards and the ASME code
[DE91-012643] N91-28600
Prediction of high level vibration test results by use of available inelastic analysis techniques
[DE91-009437] N91-28606
Influence of crack depth on the fracture toughness of reactor pressure vessel steel
[DE91-012537] N91-28611
A reconfigurable strategy for distributed digital process control
[DE91-013740] N91-28786
NUCLEAR PROPULSION
Heat resistant materials and their feasibility issues for a space nuclear transportation system
[DE91-014071] N91-28187
Nuclear thermal propulsion N91-28216
Space propulsion by fusion in a magnetic dipole
[DE91-012033] N91-28275
NUCLEAR REACTIONS
SDI: Statistical Dynamic Interactions
[DE91-012034] N91-28827
Multilevel resonance analysis of Co-59 neutron transmission measurements
[DE91-012135] N91-28829
Nuclear structure studies via neutron interactions
[DE91-012165] N91-28831
Measurements of angular distributions of absolute cross sections and analyzing powers of the reaction bar-p p yields d(pi+) between 1.3 and 2.4 GeV
[DE91-012638] N91-28842
Antiproton-induced elastic and inelastic scattering at intermediate energies
[DE91-013068] N91-28849
New techniques in neutron data measurements above 30 MeV
[DE91-013690] N91-28861
Theoretical studies in nuclear physics
[DE91-013909] N91-28873
The Cascade inertial confinement fusion reactor concept
[DE91-013852] N91-28966
The derivation of effective spin Hamiltonians and the origin of the magnetic field induced transition in orthormbic La2CuO4
[DE91-013743] N91-29035
Ground-based measurements of galactic cosmic ray fragmentation in shielding
[DE91-012336] N91-29133
NUCLEAR REACTOR CONTROL
A reconfigurable strategy for distributed digital process control
[DE91-013740] N91-28786
NUCLEAR REACTORS
Gas evolution from spheres
[DE91-012807] N91-28510
Progress in light ion fusion
[DE91-012019] N91-28826
Historical perspectives: The role of the NASA Lewis Research Center in the national space nuclear power programs
[NASA-TM-105196] N91-29138
NUCLEAR RESEARCH
Tiger Team assessment of the Princeton Plasma Physics Laboratory
[DE91-014395] N91-28957
NUCLEAR ROCKET ENGINES
Small Ex-core Heat Pipe Thermionic Reactor concept (SEHPTR)
[DE91-014073] N91-28279
NUCLEAR SCATTERING
Development of nanovolt-resolution x ray diffraction using resonant nuclear scattering
[DE91-012217] N91-28847
Theoretical studies in nuclear physics
[DE91-013909] N91-28873
NUCLEAR SPIN
Nuclear magnetic resonance studies of atomic motion in lithium chloroborate and lithium thiosilicate glassy fast ionic conductors
[DE91-012677] N91-28843
NUCLEAR STRUCTURE
Nuclear structure studies via neutron interactions
[DE91-012165] N91-28831
Reflection-asymmetric shapes in atomic nuclei
[DE91-013414] N91-28851
Shell model calculations at superdeformed shapes
[DE91-012954] N91-28853
NUCLEAR WEAPONS
Requirements for a network storage service
[DE91-014106] N91-28778
NUCLEATE BOILING
Direct contact heat transfer to a dispersal droplet with change of phase N91-28521
NUCLEATION
The influence of Ag+Mg additions on the nucleation of strengthening precipitates in a non-cold-worked Al-Cu-Li alloy N91-28336
The avian eggshell as a model of biomineralization
[DE91-012608] N91-28400
Biomimetic thin film deposition
[DE91-012485] N91-28999
NUCLEI (NUCLEAR PHYSICS)
Reflection-asymmetric shapes in atomic nuclei
[DE91-013414] N91-28851
NUCLEIC ACIDS
The 1992 - 1997 renewal proposal interactive graphics for molecular studies
[AD-A236598] N91-28823
NUCLEONS
The Soudan 2 honeycomb calorimeter
[DE91-013404] N91-28860
NUMERICAL ANALYSIS
A study of methods to investigate nozzle boundary layer transition N91-28232
Applications of scanning tunneling microscopy to electrochemistry
[AD-A237021] N91-28304
Numerical and analytical analysis of thin laser-driven flyer plates
[DE91-013748] N91-28567
Regional-scale flow in complex terrain: An observational and numerical investigation N91-28680
Computing minimal surfaces via level set curvature flow
[DE91-014709] N91-28759
NUMERICAL CONTROL
Automated verification of system configuration
[DE91-012520] N91-28481
A reconfigurable strategy for distributed digital process control
[DE91-013740] N91-28786
NUMERICAL INTEGRATION
Regularization of the Lagrange planetary equations for numerical use N91-28808
NUMERICAL STABILITY
Stability theory of critical cases and the bifurcation points of the stationary solutions of the Lorenz model
[DE91-617575] N91-28802
NUMERICAL WEATHER FORECASTING
Prediction of forecast skill with a quasi-geostrophic model N91-28699
Initialization of cloud and radiation in the Florida State University global spectral model N91-28703
NUTS (FASTENERS)
Spline-locking payload fastener
[NASA-CASE-GSC-13378-1] N91-28581
NYLON (TRADEMARK)
Effect of water content on the piezoelectric properties of nylon 11 and nylon 7
[AD-A237013] N91-28389

O

OBLATE SPHEROIDS
Gravitational influence of a static ring-like distribution of mass on electromagnetic waves N91-28472
OCCUPATION
Cultural changes in aerospace N91-28265
OCEAN CURRENTS
An upper ocean model for the climatic aspects of air-sea interaction N91-28691
Normal mode decomposition of small-scale oceanic motions N91-28709
OCEAN DYNAMICS
An upper ocean model for the climatic aspects of air-sea interaction N91-28691
Alaska wave data index
[AD-A236635] N91-28707
OCEAN MODELS
An upper ocean model for the climatic aspects of air-sea interaction N91-28691
Interactions between the north Pacific Ocean and the Northern Hemisphere atmosphere during El Nino
N91-28711
OCEAN SURFACE
The determination of mean sea level using GPS
N91-28708
OLIGOMERS
Semi-empirical calculations on model systems for organosilyldiamine preceramic polymers
[DE91-013721] N91-28433
OLIVINE
High-temperature elasticity and Earth's upper mantle
N91-28679
ON-LINE SYSTEMS
Long time measurements of landing gear loads on SAAB SF-340 commuter aircraft N91-28157
Robust and real-time control of magnetic bearings for space engines N91-28230
The EOS TPC analysis shell
[DE91-011873] N91-29073
ONE DIMENSIONAL FLOW
A parallel algorithm for solving linear equations arising from one-dimensional network problems
[DE91-012815] N91-28795
OPENINGS
Considerations on optimality of landing gear arrangement and design N91-28156
OPERATING COSTS
Compile-time estimation of communication costs in multicomputers
[NASA-CR-188675] N91-28747
OPERATORS (MATHEMATICS)
Explicit models for proportional damping in Timoshenko beams N91-28642
Using trees to compute approximate solutions to ordinary differential equations exactly
[LAC90-R24] N91-28788
Computations involving differential operators and their actions on functions N91-28789
OPTICAL COMMUNICATION
Pulse propagation in inhomogeneous optical fibers
[DE91-014356] N91-28879
OPTICAL DATA PROCESSING
Laser speckle velocimetry with photorefractive recording and anamorphic optical processing N91-28880
OPTICAL FIBERS
Studies of laser-driven flyer acceleration using optical fiber coupling
[DE91-013503] N91-28562

Numerical and analytical analysis of thin laser-driven flyer plates
[DE91-013748] N91-28567
Pulse propagation in inhomogeneous optical fibers
[DE91-014356] N91-28879

OPTICAL FILTERS
Color effects in optical systems
[ITN-91-85150] N91-28878

OPTICAL MATERIALS
Platinum solubility in phosphate laser glass
[DE91-015123] N91-28571
Laser speckle velocimetry with photorefractive recording and anamorphic optical processing N91-28880

OPTICAL MEASUREMENT
Cryogenic combustion laboratory N91-28223

OPTICAL MEASURING INSTRUMENTS
Research and development entitled smart structures for fossil energy applications
[DE91-002064] N91-28875

OPTICAL POLARIZATION
The optical polarization of BL Lacertae objects
N91-29099

OPTICAL PROPERTIES
Shock-induced optical emission in Al2O3 at 200 GPa: Implications for shock temperature measurements in metals
[DE91-013584] N91-28365
Photocross-linked second order nonlinear optical polymers
[AD-A235855] N91-28385
New photocrosslinkable polymers for second order nonlinear optical processes
[AD-A235856] N91-28386
High pressure optical studies of semiconductors and heterostructures
[DE91-014382] N91-29041

OPTICAL RADAR
Lidar studies of sporadic sodium layers, gravity waves and density spectra in the mesopause and stratopause regions at Urbana and Arecibo N91-28690

OPTICAL REFLECTION
Correcting channeling and diffraction effects in quantitative REELS surface microanalysis
[DE91-009924] N91-28840
Color effects in optical systems
[ITN-91-85150] N91-28878

OPTICAL THICKNESS
Radiative transfer model for a spherical atmosphere
N91-28689

OPTIMAL CONTROL
Robust low-order control of flexible joint manipulators
N91-28584

OPTIMIZATION
Considerations on optimality of landing gear arrangement and design N91-28156
Discrete posynomial programming with applications to spacecraft protective structures design optimization
N91-28190
A geometry based method of integrated engineering design, analysis, and optimization
[DE91-008588] N91-28457
Mechanical design optimization of robot manipulator performance N91-28589
Order reduction and synthesis of transfer function models N91-28769
Optimization, non-local MHD-mode, and alpha-particle confinement behavior of Helias equilibria N91-28893

ORBIT CALCULATION
Precise orbit determination for GPS satellites
N91-28183

ORBIT TRANSFER VEHICLES
Current systems: Upper stages N91-28201
Historical problem areas: Lessons learned for expendable and reusable vehicle propulsion systems
N91-28243
The space exploration initiative. Operational efficiency panel space-basing technology requirements
N91-28253

ORDER-DISORDER TRANSFORMATIONS
Thermal conductivity of solid hydrogen at low temperature N91-28330
Atomistic studies of grain boundaries in alloys and compounds
[DE91-014516] N91-28372
Temperature dependence of the elastic behavior of structurally disordered metallic superlattices
[DE91-014007] N91-28377
Self-organizing processes in magnetically confined plasma N91-28883
Indium compounds which contain two different organic substituents. Crystal structure of (In(CH2CMe3)(CH2SiMe3)Cl)2, an interesting case of partial Ligand disorder in the solid state
[AD-A236730] N91-28989

ORGANIC COMPOUNDS
Mechanisms of bacterial metals removal from solids
[DE91-012808] N91-28356
Photoinduced electron transfer in ordered polymers
[DE91-014512] N91-28440
Desorption of large organic molecules by laser-induced plasmon excitation
[DE91-013415] N91-28852

ORGANIC PHOSPHORUS COMPOUNDS
Relationships between polymer-additive molecular structure and intumescent flame retardant behavior
N91-28426

ORGANIZATIONS
Experience in designing and using a flat structure in a multi-project research organization
[DE91-012427] N91-29067
The human side of value engineering
[DE91-012817] N91-29068

ORGANOMETALLIC COMPOUNDS
Studies relevant to the catalytic activation of carbon monoxide
[DE91-012661] N91-28323
The surface chemistry of GaAs atomic layer epitaxy
[DE91-014112] N91-29047

ORGANS
Device for removing foreign objects from anatomic organs
[NASA-CASE-GSC-13306-1] N91-28727

ORTHOGONAL FUNCTIONS
A new wake-potential calculation method using orthogonal polynomials
[DE91-013045] N91-28799

OSCILLATIONS
Numerical simulation of potential-driven ion cyclotron oscillation N91-28925
Coherent charge fluctuations in Josephson junctions and the oscillations of the effective capacitance
[DE91-618098] N91-29019
Search for regularities in the atmosphere of Jupiter
N91-29127

OSCILLATORS
Ultra-high frequency superconductive devices
[AD-A236795] N91-28478
Quantized planes and multiparameter deformations of Heisenberg and GL(N) algebras
[DE91-012481] N91-28793

OXIDATION
Processing, compatibility and oxidation of diboride-reinforced oxide matrix composites for ultrahigh-temperature applications N91-28294
Model catalytic oxidation studies using supported monometallic and heterobimetallic oxides
[DE91-012144] N91-28409
Surface phases and their influence on metal-oxide interfaces
[DE91-012277] N91-28995

OXIDATION-REDUCTION REACTIONS
Mechanisms of bacterial metals removal from solids
[DE91-012808] N91-28356

OXIDES
Pretreatment of lubricated surfaces with sputtered cadmium oxide
[NASA-CASE-LEW-14474-1] N91-28423
The ECR-plasma deposition of silicon nitride on a tunnel oxide
[DE91-014665] N91-29051

OXIDIZERS
Regional oxidant model user's guide. Part 1: The ROM preprocessors
[PB91-171926] N91-28665
Regional oxidant model user's guide. Part 2: The ROM processor network
[PB91-171934] N91-28666

OXYGEN
Corrosion of refractory metals in liquid metal and gaseous environments
[DE91-009555] N91-28378
Surface phases and their influence on metal-oxide interfaces
[DE91-012277] N91-28995

OZONE
Regional oxidant model user's guide. Part 1: The ROM preprocessors
[PB91-171926] N91-28665
Regional oxidant model user's guide. Part 2: The ROM processor network
[PB91-171934] N91-28666
Radiative transfer model for a spherical atmosphere
N91-28689
Data users guide to the mountain cloud chemistry project
[PB91-168484] N91-28697

P

P-TYPE SEMICONDUCTORS
Novel ways of depositing ZnTe films by a solution growth technique
[DE91-002189] N91-28429

PACIFIC OCEAN
A study of El Nino/Southern Oscillation: Numerical experiments and data analysis N91-28710
Interactions between the north Pacific Ocean and the Northern Hemisphere atmosphere during El Nino
N91-28711

PACKING DENSITY
Development of nondestructive evaluation methods and prediction of effects of flaws on the fracture behavior of structural ceramics
[DE91-012471] N91-28410
The structure of Ta3N5 at 16K by time-of-flight neutron diffraction
[AD-A236596] N91-28987

PAIR PRODUCTION
Simulations on pair creation from beam-beam interaction in linear colliders
[DE91-012315] N91-28834

PALLADIUM
Thin film hydrogen sensor
[DE91-014197] N91-28550

PANEL FLUTTER
Flutter of laminated rectangular plates including finite deflection and shear deformation N91-28639
Active control of panel vibrations induced by boundary-layer flow
[NASA-CR-188733] N91-28643

PARABOLIC DIFFERENTIAL EQUATIONS
Parallelizing across time when solving time-dependent partial differential equations
[DE91-012948] N91-28797

PARALLEL COMPUTERS
Network based concurrent computing on the PVM system
[DE91-014961] N91-28780

PARALLEL PROCESSING (COMPUTERS)
Numerical analyses of aero-optical flows: An application of parallel algorithm on high-performance Personal Computer (PC) base multitransputer system N91-28519
Probabilistic structural mechanics research for parallel processing computers
[NASA-CR-187162] N91-28644
Parallel input/output architectures for multiprocessors
N91-28740
The apGA: An Adaptive Parallel Genetic Algorithm
[DE91-009559] N91-28741
Compile-time estimation of communication costs in multicomputers
[NASA-CR-188675] N91-28747
Choosing processor array configuration by performance modeling for a highly parallel linear algebra algorithm
[DE91-012486] N91-28749
Searching for consensus patterns on a hypercube
[DE91-013233] N91-28753
A multilingual parallelization of the icosahedral-hexagonal grid system for integration on the sphere
[DE91-013615] N91-28762
Toward a better parallel performance metric
[DE91-012627] N91-28773
An interdisciplinary approach to massively parallel computation
[DE91-012652] N91-28775
Performance measurement of a parallel input/output system for the Intel iPSC/2 hypercube
[DE91-014219] N91-28779
Network based concurrent computing on the PVM system
[DE91-014961] N91-28780
The PCP/PFP programming models on the BBN TC2000
[DE91-011537] N91-28781
Concurrent access to O-trees
[DE91-014348] N91-28782
ZLIB: A numerical library for differential algebra (A user's guide for version 1.0)
[DE91-012552] N91-28794
A parallel algorithm for solving linear equations arising from one-dimensional network problems
[DE91-012815] N91-28795
Parallelizing across time when solving time-dependent partial differential equations
[DE91-012948] N91-28797
X ray spatial resolution at intermediate voltages: An assessment by massively parallel Monte Carlo electron trajectory simulation
[DE91-012018] N91-28841
The EOS TPC analysis shell
[DE91-011873] N91-29073

Implementation of a hypercube database system
[DE91-014285] N91-29089
PARALLEL PROGRAMMING
Numerical analyses of aero-optical flows: An application of parallel algorithm on high-performance Personal Computer (PC) base multitransputer system N91-28519
Prototyping parallel and distributed programs in proteus
[AD-A236597] N91-28746
Split-join and message passing programming models on the BBN TC2000
[DE91-008067] N91-28774
PARAMETERIZATION
New photocrosslinkable polymers for second order nonlinear optical processes
[AD-A235856] N91-28386
PARTIAL DIFFERENTIAL EQUATIONS
Prediction of the flow and heat transfer between a rotating and a stationary cone N91-28536
Parallelizing across time when solving time-dependent partial differential equations
[DE91-012948] N91-28797
Mapping implicit spectral methods to distributed memory architectures
[NASA-CR-187592] N91-28806
Nonlinear computer analysis of backward wave oscillator N91-28923
Propagation of drift waves in toroidal plasma systems N91-28939
PARTICLE ACCELERATION
A chopper driven 11.4-GHz traveling-wave RF generator
[DE91-013568] N91-28489
Rapid acceleration of protons in a nonlinear magnetosonic wave and their energy spectrum N91-28905
PARTICLE ACCELERATOR TARGETS
Nuclear structure studies via neutron interactions
[DE91-012165] N91-28831
Antiproton-induced elastic and inelastic scattering at intermediate energies
[DE91-013068] N91-28849
Chamber propagation
[DE91-012797] N91-28954
PARTICLE ACCELERATORS
E-beam accelerator cavity development for the ground-based free electron laser
[DE91-013760] N91-28563
The use of AMS to the biomedical sciences
[DE91-012037] N91-28712
ZLIB: A numerical library for differential algebra (A user's guide for version 1.0)
[DE91-012552] N91-28794
Progress in light ion fusion
[DE91-012019] N91-28826
High intensity neutrino beams at KAON
[DE91-012147] N91-28830
PARTICLE BEAMS
Defending the defenders: Brilliant pebble defense against pop-up neutral particle beam suppression attacks
[DE91-012521] N91-28809
PARTICLE COLLISIONS
Dynamical behavior of excited hadronic matter
[DE91-013024] N91-28845
Kinetic energy distributions of ions after surface collisions
[DE91-013412] N91-28850
Interactions of molecules with surfaces
[DE91-014498] N91-28857
Correlated charge-changing ion-atom collisions
[DE91-013640] N91-28863
Fluidlike studies of the presheath and sheath regions of a plasma
[DE91-013345] N91-28953
PARTICLE DIFFUSION
Three-dimensional particle simulation of trapped electron instabilities in tokamaks N91-28891
Implications of TAE modes for the design of ITER
[DE91-013128] N91-28952
PARTICLE ENERGY
Corona: Coordinated research on non-thermal processes in astrophysics
[NASA-CR-188692] N91-29107
PARTICLE IN CELL TECHNIQUE
On the use of particle-in-cell methods for the study of magnetically-confined fusion plasmas
[DE91-015093] N91-28984
PARTICLE INTERACTIONS
High intensity neutrino beams at KAON
[DE91-012147] N91-28830
Theoretical research in intermediate-energy nuclear physics
[DE91-012720] N91-28838
Photodisintegration of the deuteron at medium and high energies
[DE91-014458] N91-28865
Evaluation of charged-particle reactions for fusion applications
[DE91-014135] N91-28962
PARTICLE MOTION
Vaporizing particle velocimeter
[NASA-CASE-LAR-14685-1] N91-28135
A study on particle dispersion in two-dimensional mixing layer flows N91-28537
Refinement of the Hamilton-Jacobi solution using a second canonical transformation
[DE91-012965] N91-28798
Direct ion heating in MHD relaxation N91-28911
The 3-D electromagnetic macroscale particle simulation of inhomogeneous, magnetized plasmas N91-28918
Reversed-Field Pinch dynamics and transport studies
[DE91-014317] N91-28970
Nonlinear dynamics of the relativistic standard map
[DE91-014368] N91-28972
Joint proposal for US/USSR on nonlinear dynamics and plasma transport
[DE91-014360] N91-28981
Strain enhanced electron spin polarization observed in photoemision from InGaAs
[DE91-012319] N91-28996
The derivation of effective spin Hamiltonians and the origin of the magnetic field induced transition in orthormbic La2CuO4
[DE91-013743] N91-29035
PARTICLE PRODUCTION
Heavy-quark physics in quantum chromodynamics
[DE91-012113] N91-28828
Dynamical behavior of excited hadronic matter
[DE91-013024] N91-28845
PARTICLE SIZE DISTRIBUTION
A laser based technique for particle sizing to study two phase expansion in turbines
[DE91-014172] N91-28595
PARTICLE THEORY
Heavy-quark physics in quantum chromodynamics
[DE91-012113] N91-28828
Light-cone quantization of quantum chromodynamics
[DE91-013991] N91-28856
Physics at the Planck scale
[DE91-012346] N91-29054
PATENT APPLICATIONS
NASA patent abstracts bibliography: A continuing bibliography. Section 2: Indexes (supplement 39)
[NASA-SP-7039(39)-SECT-2] N91-29088
PATENTS
NASA patent abstracts bibliography: A continuing bibliography. Section 2: Indexes (supplement 39)
[NASA-SP-7039(39)-SECT-2] N91-29088
PATHOGENESIS
Chromosomal changes in cultured human epithelial cells transformed by low- and high-LET radiation
[DE91-013772] N91-28720
PATTERN RECOGNITION
Mutual interference between many similar radars operating in physical proximity
[ITN-91-85139] N91-28468
Searching for consensus patterns on a hypercube
[DE91-013233] N91-28753
Elastic tracking versus neural network tracking for very high multiplicity problems
[DE91-011825] N91-28768
Crystal surface analysis using matrix textural features classified by a probabilistic neural network
[DE91-014120] N91-29048
PAYLOAD ASSIST MODULE
Current systems: Upper stages N91-28201
PAYLOAD INTEGRATION
Spline-locking payload fastener
[NASA-CASE-GSC-13378-1] N91-28581
PELLETS
Gas evolution from spheres
[DE91-012807] N91-28510
PENALTY FUNCTION
Discrete posynomial programming with applications to spacecraft protective structures design optimization N91-28190
PENETRATION
Experiments and calculations of jet penetration in glass
[DE91-013567] N91-28422
MESA: A 3-D Eulerian hydrocode for penetration mechanics studies
[DE91-013308] N91-28613
PEPTIDES
Photoinduced electron transfer in ordered polymers
[DE91-014512] N91-28440
PERFORMANCE PREDICTION
CFD applications in chemical propulsion engines N91-28234
Choosing processor array configuration by performance modeling for a highly parallel linear algebra algorithm
[DE91-012486] N91-28749
PERFORMANCE TESTS
Studies of the two-phase plume jet and wall erosion in a vertical launching system N91-28145
Materials sub-panel N91-28245
Test vs. simulation N91-28251
Impact of ion propulsion on performance, design, testing, and operation of a geosynchronous spacecraft
[AD-A237028] N91-28273
Fixture efficiency program
[DE91-014470] N91-28498
Modification and evaluation of Elastomer Test Machine (ETM)
[AD-A236143] N91-28540
Advancing electric vehicle technology
[DE91-013004] N91-28575
Robotic mannequin technology for enhanced product testing
[DE91-013787] N91-28591
Performance of the Intel iPSC/860 and Ncube 6400 hypercubes
[DE91-012370] N91-28738
The Soudan 2 honeycomb calorimeter
[DE91-013404] N91-28860
Design and performance evaluation of signature files for text retrieval systems N91-29085
Performance evaluation of multiversion database systems
[DE91-014340] N91-29090
PERIODIC VARIATIONS
Search for regularities in the atmosphere of Jupiter N91-29127
PERMANENT MAGNETS
Effect of guideway discontinuities on magnetic levitation and drag forces
[DE91-014011] N91-28815
Effect of size and geometry on levitation force measurements between permanent magnets and high-temperature superconductors
[DE91-012472] N91-29008
PERMEABILITY
The effect of stress on hydrogen uptake and desorption by A-286
[NASA-TM-103537] N91-28341
A mathematical model for two-phase water, air, and heat flow around a linear heat source emplaced in a permeable medium
[DE91-014614] N91-28527
PERMEATING
Composite material systems for hydrogen management N91-28229
Evidences of trapping in tungsten and implications for plasma-facing components
[DE91-012734] N91-28951
PERMITTIVITY
Transmission/reflection and short-circuit line permittivity measurements
[PB91-171959] N91-28482
The determination of the momentum matrix elements involved in calculating the dielectric constants of superlattices using the tight-binding method
[DE91-617789] N91-29017
PEROVSKITES
Quantitative modeling of the point defect structures of Fe-doped MgO and MgSiO3 perovskite
[DE91-011405] N91-28990
PEROXIDES
The solubility and dissociation kinetics of hydroxymethyl hydroperoxide in aqueous solution
[DE91-013336] N91-28318
PERSONAL COMPUTERS
Numerical analyses of aero-optical flows: An application of parallel algorithm on high-performance Personal Computer (PC) base multitransputer system N91-28519
A PC based frequency domain LV processor
[DE91-009056] N91-28541
PERSONALITY
How to increase meeting effectiveness and efficiency
[DE91-012420] N91-29070
PERSONNEL MANAGEMENT
A selection tool for choosing the best participative problem-solving technique
[DE91-012421] N91-29066
The human side of value engineering
[DE91-012817] N91-29068
How to increase meeting effectiveness and efficiency
[DE91-012420] N91-29070
Why engineers must know and manage organizational culture
[DE91-012425] N91-29071
PERTURBATION
Perturbation treatment of the longitudinal coupling impedance of a toroidal beam tube
[DE91-013884] N91-28495

Normal mode decomposition of small-scale oceanic motions N91-28709
Non-linear behaviour in tokamaks N91-28935
PERTURBATION THEORY
A chemically reacting, turbulent stratified interface N91-28144
Perturbation treatment of the longitudinal coupling impedance of a toroidal beam tube
[DE91-013884] N91-28495
Light-cone quantization of quantum chromodynamics
[DE91-013991] N91-28856
Nonlinear equations for weakly unstable modes N91-28927
Electron correlations in solid state physics
[DE91-013752] N91-29030
High-overtone black-hole normal modes: A WKB contour-integral approach N91-29118
PETN
Shock initiation of pentaerythritol tetranitrate crystals: Steric effects due to plastic flow
[DE91-013389] N91-28420
Shock compression of DuPont detasheet at low stress
[DE91-013229] N91-28443
Mechanisms of EBW HE initiation
[DE91-013565] N91-28447
Shock initiation of pentaerythritol tetranitrate crystals: Optical absorption and emission studies
[DE91-013381] N91-29023
PH FACTOR
Experimental studies of the volatility of ammonium chloride
[DE91-012526] N91-28311
PHASE CHANGE MATERIALS
Numerical solution of a moving boundary problem as a model solution for a solar pipe
[ITN-91-85143] N91-28516
PHASE CONTRAST
Advancing conventional high-resolution electron microscopy
[DE91-013773] N91-28548
PHASE DIAGRAMS
A review of silicon carbide/metal interactions with relevance to silicon carbide joining
[DE91-012768] N91-28282
Strength and electrical conductivity of deformation processed Cu-15 v/o Fe metal composites produced by powder metallurgy/techniques
[DE91-013658] N91-28291
Identification of strengthening phases in Al-Cu-Li alloy Weldalite (tm) 049 N91-28335
The structure of Ta3N5 at 16K by time-of-flight neutron diffraction
[AD-A236596] N91-28987
Metastable phase equilibria in co-deposited Ni(1-x)Zr(x) thin films
[DE91-013653] N91-29029
Electron correlations in solid state physics
[DE91-013752] N91-29030
PHASE TRANSFORMATIONS
Thermal conductivity of solid hydrogen at low temperature N91-28330
Theoretical studies of zirconia and related materials
[DE91-013906] N91-28369
Shock-wave properties of high-strength ceramics
[DE91-014105] N91-28439
Direct contact heat transfer to a dispersal droplet with change of phase N91-28521
Welding of ductile intermetallic alloys
[DE91-009553] N91-28594
High-temperature elasticity and Earth's upper mantle N91-28679
Statistical mechanics of soft-boson phase transitions
[NASA-CR-188697] N91-28858
Solitons and chaos in laser-plasma interaction N91-28898
Surface phases and their influence on metal-oxide interfaces
[DE91-012277] N91-28995
TEM analysis of enclosed crystal microstructures and interfaces
[DE91-012344] N91-29006
Raman studies of stress-induced phase transformation in titania films
[DE91-012871] N91-29012
Structure and dynamics in low-dimensional guest host solids
[DE91-012169] N91-29020
Phase transitions triggered by quantum fluctuations in the inflationary universe
[NASA-CR-188698] N91-29112
PHASED ARRAYS
Proceedings of the 1990 Antenna Applications Symposium, volume 1
[AD-A237056] N91-28460
PHONONS
Phonon-mediated detection of elementary particles using silicon crystal acoustic detectors N91-28547
PHOSPHATES
Relationships between polymer-additive molecular structure and intumescent flame retardant behavior N91-28426
Platinum solubility in phosphate laser glass
[DE91-015123] N91-28571
PHOSPHORIC ACID
Advanced water-cooled phosphoric acid fuel cell development
[DE91-012243] N91-28659
PHOSPHORIC ACID FUEL CELLS
Advanced water-cooled phosphoric acid fuel cell development
[DE90-009700] N91-28657
Advanced water-cooled phosphoric acid fuel cell development
[DE91-012243] N91-28659
PHOSPHORS
Aerogel composites for radioluminescent light/power sources
[DE91-012012] N91-28395
PHOTOCATHODES
Time-resolved emittance measurements of an excimer-laser-driven metal photocathode
[DE91-013066] N91-28558
Performance of the photoinjector accelerator for the Los Alamos free-electron laser
[DE91-013682] N91-28565
Beam emittance and the effects of the rf, space charge and wake fields: Application to the ATF photoelectron beam
[DE91-014789] N91-28569
SLC polarized beam source electron optics design
[DE91-012911] N91-28869
Space charge and wake field analysis for a high brightness electron source
[DE91-014788] N91-28874
Strain enhanced electron spin polarization observed in photoemision from InGaAs
[DE91-012319] N91-28996
PHOTOCHEMICAL REACTIONS
Photoinduced electron transfer in ordered polymers
[DE91-014512] N91-28440
Dynamics of charge-transfer excited states relevant to photochemical energy conversion
[DE91-012669] N91-28649
Fifteenth DOE Solar Photochemistry Research Conference
[DE91-002165] N91-28663
Regional oxidant model user's guide. Part 1: The ROM preprocessors
[PB91-171926] N91-28665
High resolution infrared spectroscopy of 2-fluorethanol in a molecular beam
[AD-A236149] N91-28822
Electron transfer reactions in microporous solids
[DE91-012299] N91-28833
Photoinduced charge and energy transfer processes in molecular aggregates
[DE91-014383] N91-28864
Interaction of radiation with outflows in late-type stars N91-29136
PHOTOCONDUCTIVITY
Research on stable, high-efficiency amorphous silicon multijunction modules
[DE91-002138] N91-28480
Photobiotechnology: Algal hydrogen production and photoconductivity of metalized chloroplasts
[DE91-013232] N91-28718
Long-wavelength germanium photodetectors by ion implantation
[DE91-013848] N91-29038
PHOTODISSOCIATION
Interaction of radiation with outflows in late-type stars N91-29136
PHOTOELECTRIC EMISSION
Strain enhanced electron spin polarization observed in photoemision from InGaAs
[DE91-012319] N91-28996
Ab initio cluster studies of La2CuO4
[DE91-013520] N91-29025
PHOTOELECTRONS
Beam emittance and the effects of the rf, space charge and wake fields: Application to the ATF photoelectron beam
[DE91-014789] N91-28569
PHOTOGRAMMETRY
Analytical calibration of the airborne photogrammetric system using a priori knowledge of the exposure station obtained from kinematic Global Positioning System techniques N91-28646
PHOTOGRAPHIC FILM
X ray fiducial foils
[DE91-011193] N91-28542
PHOTOGRAPHIC RECORDING
Search for regularities in the atmosphere of Jupiter N91-29127
PHOTOGRAPHY
Close-range geophotogrammetric mapping of trench walls using multi-model stereo restitution software
[DE91-013105] N91-28645
PHOTOLYSIS
Studies relevant to the catalytic activation of carbon monoxide
[DE91-012661] N91-28323
Transition metal activation and functionalization of carbon-hydrogen bonds
[DE91-014261] N91-28332
Photobiotechnology: Algal hydrogen production and photoconductivity of metalized chloroplasts
[DE91-013232] N91-28718
Magnetic resonance and optical spectroscopic studies of carotenoids
[DE91-014361] N91-28724
PHOTOMECHANICAL EFFECT
Electrical and photomechanical effects of plastic deformation of mercuric iodide
[DE91-013108] N91-29022
PHOTOMETERS
Long-wavelength germanium photodetectors by ion implantation
[DE91-013848] N91-29038
PHOTONICS
Simulation of planar integrated photonics devices with the LLNL time-domain finite-difference code suite
[DE91-011929] N91-28876
Pulse propagation in inhomogeneous optical fibers
[DE91-014356] N91-28879
PHOTONS
Continuum x ray gauging of multiple-element materials
[DE91-011923] N91-28307
X ray microimaging of elemental composition and microstructure for materials science
[DE91-012052] N91-28601
Phase-conjugated fluorescence
[AD-A231114] N91-28820
Transport with Feynman propagators
[DE91-013566] N91-29063
A search for cosmic axions N91-29104
PHOTONUCLEAR REACTIONS
Dynamical behavior of excited hadronic matter
[DE91-013024] N91-28845
Photodisintegration of the deuteron at medium and high energies
[DE91-014458] N91-28865
PHOTOSYNTHESIS
Fifteenth DOE Solar Photochemistry Research Conference
[DE91-002165] N91-28663
Regulation of photosynthetic membrane components in cyanobacteria
[DE91-012713] N91-28713
Photobiotechnology: Algal hydrogen production and photoconductivity of metalized chloroplasts
[DE91-013232] N91-28718
Antenna organization in green photosynthetic bacteria
[DE91-014814] N91-28723
Magnetic resonance and optical spectroscopic studies of carotenoids
[DE91-014361] N91-28724
PHOTOVOLTAIC CONVERSION
Polycrystalline thin film photovoltaic technology
[DE91-002136] N91-28650
One-sun silicon solar cell research
[DE91-014329] N91-28662
PHYSICAL OPTICS
SLC polarized beam source electron optics design
[DE91-012911] N91-28869
PHYSICAL PROPERTIES
Materials sub-panel N91-28245
Chemistry of electronic ceramic materials. Proceedings of the International Conference on the Chemistry of Electronic Ceramic Materials
[NASA-CR-188688] N91-28403
PIEZOELECTRICITY
Effect of water content on the piezoelectric properties of nylon 11 and nylon 7
[AD-A237013] N91-28389
Response of the polymers KEL-F, polysulfone, high density polyethylene and polymethylmethacrylate to shock loading and release from 0.3 to 2.4 GPa
[DE91-012867] N91-28411
PIGMENTS
Antenna organization in green photosynthetic bacteria
[DE91-014814] N91-28723

Magnetic resonance and optical spectroscopic studies of carotenoids [DE91-014361] N91-28724

PINHOLE CAMERAS
Laser range camera calibration [DE91-014939] N91-28570

PINS
Coupling device with improved thermal interface [NASA-CASE-GSC-13251-1] N91-28582

PIPE FLOW
Experimental investigation of pressure drop and heat transfer for air flow through enhanced tubes [DE91-012151] N91-28508
An experimental study of the effect of small particles on the fluid turbulence in fully developed flow of air in a horizontal pipe N91-28525
Near-wall modelling of complex turbulent flows N91-28534

PIPES (TUBES)
Solution to quasi-axisymmetric internal compressible flows using the stream tube approach N91-28526
Prediction of high level vibration test results by use of available inelastic analysis techniques [DE91-009437] N91-28606
Neutron diffraction determination of the residual stress redistribution in cracked autofrettaged tubing [DE91-013688] N91-28632
Geothermal materials development [DE91-013972] N91-28660

PISTON ENGINES
Numerical simulation of the air and fuel mixing process in fuel-injected engines using discrete vortex dynamics N91-28587

PIXELS
Coded aperture imaging with a HURA coded aperture and a discrete pixel detector N91-29093

PLANE STRAIN
Effect of Li level, artificial aging, and TiB2 reinforcement on the fracture toughness of Weldalite (tm) 049-type alloys N91-28339
Crack initiation under generalized plane strain conditions [DE91-013410] N91-28623

PLANETARY EVOLUTION
The 1990 update to strategy for exploration of the inner planets [NASA-CR-188728] N91-28182

PLANETARY ORBITS
Regularization of the Lagrange planetary equations for numerical use N91-28808

PLANETARY SURFACES
Comparison of dynamic isotope power systems for distributed planet surface applications [NASA-TM-4303] N91-28278

PLANETARY WAVES
Atmospheric responses to lower tropospheric forcing in a multilayer isentropic model N91-28688

PLANETS
The 1990 update to strategy for exploration of the inner planets [NASA-CR-188728] N91-28182
Search for regularities in the atmosphere of Jupiter N91-29127

PLANNING
Stochastic plans for robotic manipulation N91-28597

PLANTS (BOTANY)
Antenna organization in green photosynthetic bacteria [DE91-014814] N91-28723

PLASMA ACCELERATORS
Theoretical studies of nonlinear sheath dynamics N91-28896
Continuing studies of the plasma beat wave accelerator [DE91-013641] N91-28976

PLASMA ARC WELDING
Weldability of Weldalite (tm) 049 with and without TiB2 reinforcement N91-28338

PLASMA COMPOSITION
Particle confinement and fueling effects on the Maryland spheromak [DE91-012396] N91-28945

PLASMA CONTROL
Proceedings of the Second International Toki Conference on Plasma Physics and Controlled Nuclear Fusion. Nonlinear Phenomena in Fusion Plasmas: Theory and Computer Simulation [NIFS-PROC-6] N91-28881
Nonlinear phenomena and processes in high energy plasmas N91-28882
Self-organizing processes in magnetically confined plasma N91-28883
Current sheet formation and rapid reconnection in the solar corona N91-28884
Optimization, non-local MHD-mode, and alpha-particle confinement behavior of Helias equilibria N91-28893
Equilibrium beta limit of helical systems N91-28894
Suppression and control of magnetic islands in toroidal plasmas N91-28895
Hydrodynamic instabilities in laser driven implosion N91-28897
Models of collisional transport across a magnetic field with destroyed surfaces N91-28900
Issues in direct numerical simulation of plasma turbulence and transport N91-28901
Nonlinear behavior and transport property of multiple-helicity resistive interchange modes near marginally stable states N91-28922
Particle confinement and fueling effects on the Maryland spheromak [DE91-012396] N91-28945
Confinement projections for the Burning Plasma Experiment (BPX) [DE91-012516] N91-28946
Fluid/kinetic hybrid moment description of plasmas via a Chapman-Enskog-like approach [DE91-013346] N91-28949
Measurement of magnetic properties of confined compact toroid plasma (spheromak) [DE91-012397] N91-28950
Formation and sustainment of a very low aspect ration tokamak using coaxial helicity injection (the Helicity Injected Torus (HIT) experiment) [DE91-013948] N91-28967
Plasma turbulence calculations on supercomputers [DE91-014210] N91-28969
Plasma properties [DE91-013933] N91-28978
Maryland controlled fusion research program [DE91-014358] N91-28980
Performance of the 10-kV, 5-MA pulsed-power system for the FRX-C compression experiment [DE91-014745] N91-28983
On the use of particle-in-cell methods for the study of magnetically-confined fusion plasmas [DE91-015093] N91-28984

PLASMA CURRENTS
Effect of pressure on mode transition point of partially relaxed states with peripheral loss N91-28906
Sawteeth in the MST reversed field pinch [DE91-014288] N91-29126

PLASMA DENSITY
Measurements of the ion acoustic decay instability and the resultant enhanced laser absorption and enhanced bremsstrahlung in laser-plasma interaction experiments [DE91-014250] N91-28956
Hydrodynamic evolution of picosecond laser-plasmas [DE91-013245] N91-28958

PLASMA DIAGNOSTICS
Evaporation as a diagnostic test for hydrodynamic cooling of laser-ablated clusters [DE91-013416] N91-28555
Particle confinement and fueling effects on the Maryland spheromak [DE91-012396] N91-28945
Measurement of magnetic properties of confined compact toroid plasma (spheromak) [DE91-012397] N91-28950
Measurements of the ion acoustic decay instability and the resultant enhanced laser absorption and enhanced bremsstrahlung in laser-plasma interaction experiments [DE91-014250] N91-28956
Hydrodynamic evolution of picosecond laser-plasmas [DE91-013245] N91-28958
Formation and sustainment of a very low aspect ration tokamak using coaxial helicity injection (the Helicity Injected Torus (HIT) experiment) [DE91-013948] N91-28967
A portable and independent edge fluctuation diagnostic [DE91-014357] N91-28971
Influence of fast waves on the collective scattering of microwaves in fusion plasmas [DE91-014759] N91-28973
Sawteeth in the MST reversed field pinch [DE91-014288] N91-29126

PLASMA DYNAMICS
Proceedings of the Second International Toki Conference on Plasma Physics and Controlled Nuclear Fusion. Nonlinear Phenomena in Fusion Plasmas: Theory and Computer Simulation [NIFS-PROC-6] N91-28881
Nonlinear phenomena and processes in high energy plasmas N91-28882
Hybrid fluid/kinetic descriptions of tokamak plasmas N91-28888
The theory of turbulence and anomalous transport in plasmas: Past, present, and future N91-28889
Finite beta equilibrium for a pressure configuration N91-28909
Hole dynamics of one-dimensional plasma N91-28928
Plasma transport in a new cathodic arc ion source, theory and experiment [DE91-011511] N91-28944
Nonlinear reversed field pinch dynamics with nonideal boundaries [DE91-013638] N91-28961
Exact solutions for a system of nonlinear plasma fluid equations [DE91-014367] N91-28965

PLASMA EQUILIBRIUM
Optimization, non-local MHD-mode, and alpha-particle confinement behavior of Helias equilibria N91-28893
Equilibrium beta limit of helical systems N91-28894
Finite beta equilibrium for a pressure configuration N91-28909
Application of mathematica to energy principle N91-28910
Progress in the development of a numerical tokamak [DE91-013386] N91-28975

PLASMA GENERATORS
Microwave-generated plasma thruster [DE91-013131] N91-28948

PLASMA GUNS
Plasma immersion surface modification with metal ion plasma [DE91-014233] N91-28979

PLASMA HEATING
An assessment of the lifetime of Faraday shield elements [DE91-012228] N91-28463
Reduction of energy sweep of the ETA-2 beam [DE91-013824] N91-28568
Direct ion heating in MHD relaxation N91-28911
Mode conversion of Alfven waves induced by quadrupole magnetic field modulation N91-28924
Confinement projections for the Burning Plasma Experiment (BPX) [DE91-012516] N91-28946
Characteristics of edge plasma turbulence on the ATF torsatron [DE91-012981] N91-28947
Implications of TAE modes for the design of ITER [DE91-013128] N91-28952
Performance of the 10-kV, 5-MA pulsed-power system for the FRX-C compression experiment [DE91-014745] N91-28983
Corona: Coordinated research on non-thermal processes in astrophysics [NASA-CR-188692] N91-29107

PLASMA LAYERS
Computer simulation of solar wind-magnetosphere interaction N91-28904

PLASMA PHYSICS
JPRS report: Science and technology. USSR: Physics and mathematics [JPRS-UPM-90-006] N91-28811
Proceedings of the Second International Toki Conference on Plasma Physics and Controlled Nuclear Fusion. Nonlinear Phenomena in Fusion Plasmas: Theory and Computer Simulation [NIFS-PROC-6] N91-28881
Solitons and chaos in plasma N91-28943
Plasma immersion surface modification with metal ion plasma [DE91-014233] N91-28979
Maryland controlled fusion research program [DE91-014358] N91-28980

PLASMA SHEATHS
An assessment of the lifetime of Faraday shield elements [DE91-012228] N91-28463
Theoretical studies of nonlinear sheath dynamics N91-28896
Fluidlike studies of the presheath and sheath regions of a plasma [DE91-013345] N91-28953

PLASMA TURBULENCE
The theory of turbulence and anomalous transport in plasmas: Past, present, and future N91-28889
Ion temperature gradient turbulence and coherent structures N91-28890
Edge anomalous transport in heliotron/torsatron N91-28892
Issues in direct numerical simulation of plasma turbulence and transport N91-28901
Anomalous transport due to the skin size electromagnetic drift mode in tokamaks N91-28902
Characteristics of edge plasma turbulence on the ATF torsatron [DE91-012981] N91-28947
Plasma turbulence calculations on supercomputers [DE91-014210] N91-28969
A portable and independent edge fluctuation diagnostic [DE91-014357] N91-28971

Electron acceleration by magnetosonic waves in a solar coronal loop N91-29132

PLASMA WAVES

Continuing studies of the plasma beat wave accelerator
[DE91-013641] N91-28976

PLASMAS (PHYSICS)

Chemistry and materials science research report
[DE91-011507] N91-28305

Moving finite elements: A continuously adaptive method for computational fluid dynamics
[DE91-013391] N91-28513

Helical field effect in solar/stellar wind N91-28912

Numerical study of ion temperature gradient modes in a tokamak N91-28921

Mode conversion of Alfven waves induced by quadrupole magnetic field modulation N91-28924

Numerical simulation of potential-driven ion cyclotron oscillation N91-28925

Hole dynamics of one-dimensional plasma N91-28928

Soliton phenomena in electron beam plasma N91-28930

Point vortex description of a modon solution N91-28931

Equilibria and dynamics of temperature in a fusion reactor plasma N91-28937

Model for marfe-detached plasma transition in tokamaks N91-28938

Solitons and chaos in plasma N91-28943

Confinement projections for the Burning Plasma Experiment (BPX)
[DE91-012516] N91-28946

Large growth Rayleigh-Taylor experiments on Nova
[DE91-012885] N91-28955

Stability of annular equilibrium of energetic large orbit ion beam
[DE91-014365] N91-28963

The Cascade inertial confinement fusion reactor concept
[DE91-013852] N91-28966

Influence of fast waves on the collective scattering of microwaves in fusion plasmas
[DE91-014759] N91-28973

Steady-state dynamo and current drive in a nonuniform bounded plasma
[DE91-014865] N91-28974

Stability of drift-wave modons in the presence of temperature gradients
[DE91-014364] N91-28982

The ECR-plasma deposition of silicon nitride on a tunnel oxide
[DE91-014665] N91-29051

Generalized gyroviscous force and its effect on the momentum balance equation
[DE91-013344] N91-29061

PLASMONS

Desorption of Al, Au, Ag using surface plasmon excitation
[DE91-013726] N91-28493

Laser ejection of Ag(sup +) ions from a roughened silver surface: Role of the surface plasmon
[DE91-012945] N91-28554

PLASTIC DEFORMATION

Reliable modeling of complex behavior
[DE91-013385] N91-28419

Dynamic plasticity in transition from thermal activation to viscous drag
[DE91-013031] N91-28617

Electrical and photomechanical effects of plastic deformation of mercuric iodide
[DE91-013108] N91-29022

Parallel nanometer scale fabrication
[DE91-013016] N91-29026

PLASTIC FLOW

Shock initiation of pentaerythritol tetranitrate crystals: Steric effects due to plastic flow
[DE91-013389] N91-28420

PLASTIC PROPERTIES

Reliable modeling of complex behavior
[DE91-013385] N91-28419

Prediction of high level vibration test results by use of available inelastic analysis techniques
[DE91-009437] N91-28606

Overdriven shocks in solids and liquids
[DE91-013370] N91-28618

The DataShoP: A database of weak-shock constitutive data
[DE91-013349] N91-28620

A new model of rate dependent elastic-plastic flow
[DE91-014600] N91-28633

Electrical and photomechanical effects of plastic deformation of mercuric iodide
[DE91-013108] N91-29022

PLATELETS

Alumina-silicon carbide composites from coated powders
[DE91-012357] N91-28281

PLATES (STRUCTURAL MEMBERS)

Sandia's new hypervelocity launcher (HVL)
[DE91-014335] N91-28178

Finite element modeling of 2-D delamination growth in laminated composites N91-28302

PLATES (TECTONICS)

Observational constraints on pulsars: Location of the emission region and pulse shape stability on decade time scales N91-29097

PLATING

Perspective on plating for precision finishing
[DE91-011927] N91-28394

PLATINUM

Laser surface modification to impede hydrogen ingress into steel N91-28375

Platinum solubility in phosphate laser glass
[DE91-015123] N91-28571

PLUMES

Studies of the two-phase plume jet and wall erosion in a vertical launching system N91-28145

Impact of ion propulsion on performance, design, testing, and operation of a geosynchronous spacecraft
[AD-A237028] N91-28273

PLY ORIENTATION

An analysis of interlaminar stresses in unsymmetrically laminated plates N91-28299

POINT DEFECTS

Irradiation creep by climb-enabled glide driven by transient point defect processes
[DE91-012950] N91-28348

Fundamental theory of crystal decomposition
[AD-A236637] N91-28988

Quantitative modeling of the point defect structures of Fe-doped MgO and MgSiO3 perovskite
[DE91-011405] N91-28990

Evolution of defect cluster distributions during irradiation
[DE91-013405] N91-29024

The interaction of HVEM-generated point-defects with dissociated dislocations
[DE91-013353] N91-29027

Defects and transport in mixed oxides
[DE91-014443] N91-29049

POINT SOURCES

The gamma ray content of ultrahigh energy cosmic radiation N91-29135

POISSON EQUATION

Model for marfe-detached plasma transition in tokamaks N91-28938

POLARIZATION (CHARGE SEPARATION)

Effect of TCP doping on the remnant polarization in uniaxially oriented poly(vinylidene fluoride) films
[AD-A237001] N91-28388

Strongly interacting fermion systems
[DE91-012284] N91-28848

POLARIZATION (SPIN ALIGNMENT)

Strain enhanced electron spin polarization observed in photoemision from InGaAs
[DE91-012319] N91-28996

Neutron scattering studies of spin correlations in metallic YBa2Cu3O(6+x)
[DE91-013794] N91-29031

The derivation of effective spin Hamiltonians and the origin of the magnetic field induced transition in orthormbic La2CuO4
[DE91-013743] N91-29035

POLARIZATION (WAVES)

Performance of a polarization isolation enhancement method in the presence of errors
[DE91-013571] N91-28473

Simulation of planar integrated photonics devices with the LLNL time-domain finite-difference code suite
[DE91-011929] N91-28876

POLICIES

Space systems requirements: The Navy approach
[AD-A236490] N91-28181

POLISHING

Perspective on plating for precision finishing
[DE91-011927] N91-28394

Sphere lapping
[DE91-014287] N91-28593

POLLUTION CONTROL

Mechanisms of bacterial metals removal from solids
[DE91-012808] N91-28356

Fluxless soldering of Ni-Au plated Kovar with a laser
[DE91-013261] N91-28451

The use of science in the management of hazardous air pollutants N91-28667

Work plan for the preliminary site investigation for McMurdo Station, Ross Island, Antarctica
[DE91-015100] N91-28675

POLLUTION MONITORING

High-throughput liquid-absorption air and aerosol sampler
[DE91-013762] N91-28670

Threatened Area Database System (TADS) computer program
[DE91-012491] N91-29074

POLLUTION TRANSPORT

Development and application of new modeling techniques for mesoscale atmospheric chemistry N91-28692

POLOIDAL FLUX

Shock and soliton structures induced by poloidal flow in tokamaks N91-28929

POLYACETYLENE

Measurements of photo-induced changes in conjugated polymers
[DE91-013262] N91-28427

POLYATOMIC MOLECULES

Molecular eigenstate spectroscopy: Application to the intramolecular dynamics of some polyatomic molecules in the 3000 to 7000 cm(exp -1) region
[DE91-013154] N91-28839

POLYCARBONATES

SESAME equation of state number 7740: Polycarbonate
[DE91-013970] N91-28436

POLYCHLORINATED BIPHENYLS

Assessing the risk of transporting hazardous materals by aircraft: A case study
[DE91-014016] N91-28147

POLYCRYSTALS

Polycrystalline thin film photovoltaic technology
[DE91-002136] N91-28650

POLYESTERS

Cocrystallization in blends of poly(butylene terephthalate) and poly(ester-ether) segmented block copolymers
[DE91-012224] N91-28438

POLYETHER RESINS

Cocrystallization in blends of poly(butylene terephthalate) and poly(ester-ether) segmented block copolymers
[DE91-012224] N91-28438

POLYETHYLENES

Response of the polymers KEL-F, polysulfone, high density polyethylene and polymethylmethacrylate to shock loading and release from 0.3 to 2.4 GPa
[DE91-012867] N91-28411

Strongly interacting fermion systems
[DE91-012284] N91-28848

POLYIMIDES

Polyimides prepared from 3,5-diamino benzo trifluoride
[NASA-CASE-LAR-14206-1] N91-28425

POLYMER BLENDS

Cocrystallization in blends of poly(butylene terephthalate) and poly(ester-ether) segmented block copolymers
[DE91-012224] N91-28438

Photoinduced electron transfer in ordered polymers
[DE91-014512] N91-28440

POLYMER CHEMISTRY

Subgap absorption in conjugated polymers
[DE91-012655] N91-28402

Photoinduced electron transfer in ordered polymers
[DE91-014512] N91-28440

Spontaneous emergence of a metabolism
[DE91-013684] N91-28714

POLYMER PHYSICS

Resonant method for the measurement of the glass transition temperature at high frequencies
[DE91-618684] N91-28416

POLYMERIC FILMS

Photocross-linked second order nonlinear optical polymers
[AD-A235855] N91-28385

Polymers at surfaces
[DE91-011000] N91-28392

Subgap absorption in conjugated polymers
[DE91-012655] N91-28402

POLYMERIZATION

An extension of a kinetic theory of polymer crystallization through the exclusion of negative barriers
[AD-A236999] N91-28387

Polyimides prepared from 3,5-diamino benzo trifluoride
[NASA-CASE-LAR-14206-1] N91-28425

Relationships between polymer-additive molecular structure and intumescent flame retardant behavior N91-28426

Semi-empirical calculations on model systems for organosilyldiamine preceramic polymers
[DE91-013721] N91-28433

POLYMERS

Ion beam sputtered coatings of bioglass N91-28384

Relationships between polymer-additive molecular structure and intumescent flame retardant behavior N91-28426

POLYMETHYL METHACRYLATE

Response of the polymers KEL-F, polysulfone, high density polyethylene and polymethylmethacrylate to shock loading and release from 0.3 to 2.4 GPa [DE91-012867] N91-28411

POLYNOMIALS

Order reduction and synthesis of transfer function models N91-28769

A new wake-potential calculation method using orthogonal polynomials [DE91-013045] N91-28799

POROUS MATERIALS

Ordered ceramic membranes [DE91-012248] N91-28398

A mathematical model for two-phase water, air, and heat flow around a linear heat source emplaced in a permeable medium [DE91-014614] N91-28527

POSITIONING

Precise orbit determination for GPS satellites N91-28183

POSITRONS

Simulations on pair creation from beam-beam interaction in linear colliders [DE91-012315] N91-28834

POTENTIAL FLOW

A comparison of the potential and the Euler formulations of the equations of motion for transonic flow [DE91-014731] N91-28142

POWDER (PARTICLES)

Alumina-silicon carbide composites from coated powders [DE91-012357] N91-28281

Process for application of powder particles to filamentary materials [NASA-CASE-LAR-14231-1-CU] N91-28290

Strength and electrical conductivity of deformation processed Cu-15 v/o Fe metal composites produced by powder metallurgy/techniques [DE91-013658] N91-28291

Processing, compatibility and oxidation of diboride-reinforced oxide matrix composites for ultrahigh-temperature applications N91-28294

A study of the influence of temperature gradients on densification of glass powder compacts [DE91-012337] N91-28399

Analysis of the surface heterogeneity of different samples of aluminum oxide ceramic powders [DE91-013527] N91-28421

POWDER METALLURGY

Development of elements of a high T(sub c) superconducting cable [AD-A236151] N91-28986

POWER BEAMING

SPGD: A central power system for space [DE91-012610] N91-28276

POWER CONDITIONING

Issues concerning centralized versus decentralized power deployment [NASA-CR-187121] N91-28648

POWER CONVERTERS

System and component design and test of a 10 hp, 18,000 rpm AC dynamometer utilizing a high frequency AC voltage link, part 1 [NASA-CR-188442] N91-28539

POWER LINES

Follow-on cable coupling lightning test, volume 1 [NASA-CR-184123] N91-28192

Automated verification of system configuration [DE91-012520] N91-28481

Issues concerning centralized versus decentralized power deployment [NASA-CR-187121] N91-28648

Magnetospheric VLF line radiation N91-28693

POWER SUPPLIES

SEI power source alternatives for rovers and other multi-kWe distributed surface applications [NASA-TM-104360] N91-28277

Aerogel composites for radioluminescent light/power sources [DE91-012012] N91-28395

PREAMPLIFIERS

Monolithic front end electronics for silicon calorimeters [DE91-012063] N91-28484

PRECESSION

Observational constraints on pulsars: Location of the emission region and pulse shape stability on decade time scales N91-29097

PRECIPITATES

The influence of Ag+Mg additions on the nucleation of strengthening precipitates in a non-cold-worked Al-Cu-Li alloy N91-28336

PREDICTION ANALYSIS TECHNIQUES

Transient two-phase flow of cryogenic fluid in a vertical transfer line during the cooldown process N91-28522

Shear stress prediction in shock loaded copper [DE91-014740] N91-28635

Inorganic components of atmospheric aerosols N91-28668

Nonlinear modeling of chaotic time series: Theory and applications [DE91-013076] N91-29055

PREDICTIONS

Prediction of forecast skill with a quasi-geostrophic model N91-28699

Bayesian design and analysis of computer experiments: Use of derivatives in surface prediction [DE91-013147] N91-28751

PREPREGS

Process for application of powder particles to filamentary materials [NASA-CASE-LAR-14231-1-CU] N91-28290

PRESSURE DEPENDENCE

Pressure dependence of the Curie-temperature in the Kondo-lattice-compound YbNiSn [DE91-013672] N91-29046

PRESSURE DISTRIBUTION

Experimental flutter boundaries with unsteady pressure distributions for the NACA 0012 Benchmark Model [NASA-TM-104072] N91-28137

Spray combustion under oscillatory pressure conditions N91-28226

Solution to quasi-axisymmetric internal compressible flows using the stream tube approach N91-28526

Calculation of pressure distribution in vacuum systems using a commercial finite element program [DE91-013611] N91-28629

A reciprocity technique for the characterisation of sound transmission into aircraft fuselages N91-28817

PRESSURE DROP

Pressure drop and heat transfer for spirally fluted tubes including validation of the role of transition [DE91-012242] N91-28509

PRESSURE EFFECTS

Spray combustion under oscillatory pressure conditions N91-28226

Joining of aluminum-based particulate-reinforced metal-matrix composites N91-28298

Shock-induced optical emission in Al2O3 at 200 GPa: Implications for shock temperature measurements in metals [DE91-013584] N91-28365

Calculation of pressure distribution in vacuum systems using a commercial finite element program [DE91-013611] N91-28629

Effect of pressure on mode transition point of partially relaxed states with peripheral loss N91-28906

Doping and pressure study of U3Sb4Pt3 [DE91-013669] N91-29033

High pressure optical studies of semiconductors and heterostructures [DE91-014382] N91-29041

PRESSURE GAGES

Monitoring structural response in pressurized environments. Part 1: Instrumentation techniques [DE91-012654] N91-28616

PRESSURE GRADIENTS

Hydrodynamic instabilities in laser driven implosion N91-28897

PRESSURE SENSORS

Pressure transducer and system for cryogenic environments [NASA-CASE-LAR-14579-1] N91-28546

PRESSURE VESSELS

Design and analysis of the 50 mm collider dipole vacuum vessel [DE91-012490] N91-28610

Influence of crack depth on the fracture toughness of reactor pressure vessel steel [DE91-012537] N91-28611

Monitoring structural response in pressurized environments. Part 1: Instrumentation techniques [DE91-012654] N91-28616

Crack initiation under generalized plane strain conditions [DE91-013410] N91-28623

PRESSURIZED WATER REACTORS

Crack initiation under generalized plane strain conditions [DE91-013410] N91-28623

PRINTED CIRCUITS

Microstructural characterization of solders and brazes for advanced packaging technology [DE91-011503] N91-28379

PROBABILITY THEORY

The use of Monte Carlo simulation in determining landing gear loads during landing N91-28162

Probabilistic structural analysis methods for space transportation propulsion systems N91-28238

Probabilistic structural mechanics research for parallel processing computers [NASA-CR-187162] N91-28644

A cloud fraction and radiative transfer model N91-28706

Statistical properties of two-dimensional magnetohydrodynamic turbulence N91-28886

Void probability as a function of the void's shape and scale-invariant models [NASA-CR-188696] N91-29113

PROBLEM SOLVING

Using HSYS in the analysis of human-system interactions: Examples from the offshore petroleum industry [DE91-013218] N91-28732

A selection tool for choosing the best participative problem-solving technique [DE91-012421] N91-29066

PROCEDURES

Sphere lapping [DE91-014287] N91-28593

PROCESS CONTROL (INDUSTRY)

Space transportation main engine reliability and safety N91-28271

PROCESSING

Strength and electrical conductivity of deformation processed Cu-15 v/o Fe metal composites produced by powder metallurgy/techniques [DE91-013658] N91-28291

PROCUREMENT

Major system acquisitions process (A-109) N91-28268

PRODUCTIVITY

Microcomputers: An exploratory study of their availability and use in the research process and their contribution to researcher productivity N91-28739

PROGRAM VERIFICATION (COMPUTERS)

Automated verification of system configuration [DE91-012520] N91-28481

Toward a formal verification of a floating-point coprocessor and its composition with a central processing unit [NASA-CR-187547] N91-28777

A simulated user for laboratory investigation of information systems requirements determination N91-29087

PROGRAMMING LANGUAGES

An introduction to the ADAMS interface language, part 1 [DE91-014344] N91-28757

A logic model for model management: An embedded languages approach N91-28761

A multilingual parallelization of the icosahedral-hexagonal grid system for integration on the sphere [DE91-013615] N91-28762

The computer storage, retrieval, and searching of generic structures in chemical patents: The machine-readable representation of generic structures N91-29081

Implementation of a hypercube database system [DE91-014285] N91-29089

PROJECT MANAGEMENT

An overview of the Penn State Propulsion Engineering Research Center N91-28222

Concurrent engineering N91-28247

Lessons learned and their application to program development and cultural issues N91-28263

Report of Meeting of CLICOM Experts [WCDP-9] N91-28695

Research in mathematics and computer science at Argonne, September 1989-February 1991 [DE91-012989] N91-28734

Tiger Team assessment of the Princeton Plasma Physics Laboratory [DE91-014395] N91-28957

Structured meeting techniques identify emergency management issues practitioners really want to see addressed [DE91-012414] N91-29069

PROJECT PLANNING

Air combat environment test and evaluation facility and the development of the offensive sensors laboratory [DE91-011398] N91-28173

An overview of the Penn State Propulsion Engineering Research Center N91-28222

Work plan for the preliminary site investigation for McMurdo Station, Ross Island, Antarctica [DE91-015100] N91-28675

PROJECTILES

Sandia's new hypervelocity launcher (HVL) [DE91-014335] N91-28178

A theoretical and experimental study of the interior ballistic processes of an electrothermal gun N91-28185

Stress fields generated by kinetic energy projectile interaction with ceramic targets [DE91-013687] N91-28625

PROP-FAN TECHNOLOGY
ASTROP2 users manual: A program for aeroelastic stability analysis of propfans [NASA-TM-4304] N91-28627

PROPAGATION MODES
Chamber propagation [DE91-012797] N91-28954

PROPAGATION VELOCITY
Seismic traveltime inversion in three-dimensional heterogeneous media N91-28678

PROPELLANT ADDITIVES
Ignition and combustion of metallized propellants N91-28224

PROPELLANT COMBUSTION
A theoretical and experimental study of the interior ballistic processes of an electrothermal gun N91-28185
Ignition and combustion of metallized propellants N91-28224
Liquid-propellant droplet vaporization and combustion in high pressure environments N91-28225

PROPELLANT TANKS
Space shuttle with common fuel tank for liquid rocket booster and main engines (supertanker space shuttle) N91-28257

PROPELLANT TRANSFER
Slush hydrogen propellant production, transfer, and expulsion studies at the NASA K-Site Facility [NASA-TM-105191] N91-28449

PROPELLER FANS
ASTROP2 users manual: A program for aeroelastic stability analysis of propfans [NASA-TM-4304] N91-28627

PROPELLER NOISE
A reciprocity technique for the characterisation of sound transmission into aircraft fuselages N91-28817

PROPULSION
Cryogenic upper stage propulsion: RL10 and derivative engines N91-28202
Composite material systems for hydrogen management N91-28229
National test bed concept N91-28241

PROPULSION SYSTEM CONFIGURATIONS
Heat resistant materials and their feasibility issues for a space nuclear transportation system [DE91-014071] N91-28187
Space Transportation Propulsion Technology Symposium. Volume 2: Symposium proceedings [NASA-CP-3112-VOL-2] N91-28193
The space exploration initiative N91-28194
Maintaining technical excellence requires a national plan N91-28196
A white paper: Operational efficiency. New approaches to future propulsion systems N91-28197
Operationally Efficient Propulsion System Study (OEPPS) N91-28198
Space shuttle propulsion systems N91-28200
Satellite/spacecraft propulsion N91-28203
Shuttle derived manned transportation systems N91-28204
Advanced cryo propulsion systems N91-28212
Advanced propulsion concepts N91-28218
A review of liquid rocket propulsion programs in Japan N91-28219
Space Transportation Propulsion Technology Symposium. Volume 3: Panel Session Summaries and Presentations [NASA-CP-3112-VOL-3] N91-28235
Probabilistic structural analysis methods for space transportation propulsion systems N91-28238
National test bed concept N91-28241
Historical problem areas lessons learned N91-28242
Overall goals N91-28246
Concurrent engineering N91-28247
John C. Stennis Space Center roles and missions N91-28259
Possible funding strategies N91-28272
Space propulsion by fusion in a magnetic dipole [DE91-012033] N91-28275
Nondestructive evaluation tools and experimental studies for monitoring the health of space propulsion systems [NASA-TM-105164] N91-28605
Historical perspectives: The role of the NASA Lewis Research Center in the national space nuclear power programs [NASA-TM-105196] N91-29138

PROPULSION SYSTEM PERFORMANCE
Space Transportation Propulsion Technology Symposium. Volume 2: Symposium proceedings [NASA-CP-3112-VOL-2] N91-28193
The space exploration initiative N91-28194
Maintaining technical excellence requires a national plan N91-28196
A white paper: Operational efficiency. New approaches to future propulsion systems N91-28197
Operationally Efficient Propulsion System Study (OEPPS) N91-28198
Expendable launch vehicle propulsion N91-28199
Space shuttle propulsion systems N91-28200
Satellite/spacecraft propulsion N91-28203
Shuttle derived manned transportation systems N91-28204
Advanced propulsion concepts N91-28218
A review of liquid rocket propulsion programs in Japan N91-28219
Probabilistic structural analysis methods for space transportation propulsion systems N91-28238
National test bed concept N91-28241
Overall goals N91-28246
Concurrent engineering N91-28247
Test vs. simulation N91-28251
Propulsion system ground testing N91-28261
Space transportation main engine reliability and safety N91-28271
Nondestructive evaluation tools and experimental studies for monitoring the health of space propulsion systems [NASA-TM-105164] N91-28605
Historical perspectives: The role of the NASA Lewis Research Center in the national space nuclear power programs [NASA-TM-105196] N91-29138

PROTECTIVE CLOTHING
The chemical resistance of protective handwear available through the Navy's supply system [AD-A235874] N91-28731

PROTECTIVE COATINGS
Composite material systems for hydrogen management N91-28229
Investigation of laser diagnostics of PACVD processes for depositing hard face coatings [DE91-012642] N91-28401

PROTEIN SYNTHESIS
Protein-directed modulation of high-LET hyperthermic radiosensitization [DE91-013783] N91-28722

PROTEINS
The 1992 - 1997 renewal proposal interactive graphics for molecular studies [AD-A236598] N91-28823
Parallel nanometer scale fabrication [DE91-013016] N91-29026

PROTON BEAMS
Progress in light ion fusion [DE91-012019] N91-28826

PROTON ENERGY
Proton Energy Loss (PEL) material characterization [DE91-011545] N91-28306
Measurements of angular distributions of absolute cross sections and analyzing powers of the reaction bar-p p yields d(pi+) between 1.3 and 2.4 GeV [DE91-012638] N91-28842
Rapid acceleration of protons in a nonlinear magnetosonic wave and their energy spectrum N91-28905

PROTONS
Photodisintegration of the deuteron at medium and high energies [DE91-014458] N91-28865
Rapid acceleration of protons in a nonlinear magnetosonic wave and their energy spectrum N91-28905

PSYCHOLOGY
A selection tool for choosing the best participative problem-solving technique [DE91-012421] N91-29066
The human side of value engineering [DE91-012817] N91-29068

PUBLIC HEALTH
Biomarker-based biomonitoring for evaluating health and ecological effects on environmental contamination [DE91-013729] N91-28719

PULSARS
Observational constraints on pulsars: Location of the emission region and pulse shape stability on decade time scales N91-29097
Impact of the nuclear equation of state on models of rotating neutron stars [DE91-014615] N91-29125

PULSE COMMUNICATION
Pulse propagation in inhomogeneous optical fibers [DE91-014356] N91-28879

PULSE GENERATORS
A chopper driven 11.4-GHz traveling-wave RF generator [DE91-013568] N91-28489
Procyon experiments utilizing foil-fuse opening switches [DE91-014605] N91-28499
High-peak power-Nd:Glass laser facilities for end users [DE91-013246] N91-28561
Performance of the 10-kV, 5-MA pulsed-power system for the FRX-C compression experiment [DE91-014745] N91-28983

PULSE RADAR
Multiple frequency atmospheric radar techniques N91-28683

PULSED LASERS
Numerical and analytical analysis of thin laser-driven flyer plates [DE91-013748] N91-28567
Numerical investigation of the thrust efficiency of a laser-propelled vehicle N91-28572

PULSES
Procyon experiments utilizing foil-fuse opening switches [DE91-014605] N91-28499

PUMPS
Generating strong shock waves with a supersonic peristaltic pump [DE91-013228] N91-28174

PYRAZINES
Resonance Raman and photophysical studies of transition metal complexes in solution and entrapped in zeolites [DE91-013010] N91-28357

PYRIDINES
Resonance Raman and photophysical studies of transition metal complexes in solution and entrapped in zeolites [DE91-013010] N91-28357

PYROELECTRICITY
Effect of TCP doping on the remnant polarization in uniaxially oriented poly(vinylidene fluoride) films [AD-A237001] N91-28388
Effect of water content on the piezoelectric properties of nylon 11 and nylon 7 [AD-A237013] N91-28389

PYROTECHNICS
Semiconductor Bridge (SCB) research and development [DE91-011493] N91-28319

Q

QUADRUPOLES
H(-) beam characterization using laser-induced neutralization [DE91-013501] N91-28564
Quadrupole phenomena of noise from a subsonic jet impinging on a large, rigid, and flate plate N91-28818
Fixed-wavelength R2PI/tandem mass spectrometry for mixture analysis in the quadrupole ion trap [DE91-012506] N91-28835
Spontaneous cluster decomposition in a quadrupole ion trap [DE91-012519] N91-28836
Mode conversion of Alfven waves induced by quadrupole magnetic field modulation N91-28924

QUALITATIVE ANALYSIS
Parallel nanometer scale fabrication [DE91-013016] N91-29026

QUALITY CONTROL
Software metrics [AD-A236140] N91-28744
Guidelines for acquisition, installation, and testing of performance assessment software [DE91-013910] N91-28764

QUANTITATIVE ANALYSIS
Continuum x ray gauging of multiple-element materials [DE91-011923] N91-28307
Studies relevant to the catalytic activation of carbon monoxide [DE91-012661] N91-28323

QUANTUM CHROMODYNAMICS
Heavy-quark physics in quantum chromodynamics [DE91-012113] N91-28828
Light-cone quantization of quantum chromodynamics [DE91-013991] N91-28856
Research in theoretical nuclear physics [DE91-013644] N91-28872

QUANTUM ELECTRODYNAMICS
Transport with Feynman propagators [DE91-013566] N91-29063

QUANTUM MECHANICS
Some new approaches to semiclassical and quantum transition state theory [DE91-012345] N91-28308
Quantum mechanical effects on the shock Hugoniot [DE91-014750] N91-28636
Quantized planes and multiparameter deformations of Heisenberg and GL(N) algebras [DE91-012481] N91-28793

Optical analogs of model atoms in fields
[DE91-013392] N91-28855
Complex dynamics of the integer quantum Hall effect
[DE91-013383] N91-29058
Topics in low-dimensional field theory
[DE91-013784] N91-29062

QUANTUM THEORY
Some new approaches to semiclassical and quantum transition state theory
[DE91-012345] N91-28308
Light-cone quantization of quantum chromodynamics
[DE91-013991] N91-28856
The effect of the quantum susceptance on the gain of superconducting quasiparticle mixers
[DE91-012352] N91-29021
Path-integral measure for Chern-Simons theory within the stochastic quantization approach
[DE91-617610] N91-29056
The line of gravitation: On the quantization conditions in curved spacetime and uncertainty-driven inflation
N91-29115

QUARKS
Heavy-quark physics in quantum chromodynamics
[DE91-012113] N91-28828
Light-cone quantization of quantum chromodynamics
[DE91-013991] N91-28856

QUARTZ
Equation-of-state from SiO2 aerogel Hugoniot data
[DE91-011480] N91-28313

QUASARS
Magnetohydrodynamical formation of astrophysical jets from gravitationally collapsing objects N91-28903

QUERY LANGUAGES
An introduction to the ADAMS interface language, part 1
[DE91-014344] N91-28757

R

RADAR ANTENNAS
Performance of a polarization isolation enhancement method in the presence of errors
[DE91-013571] N91-28473

RADAR ECHOES
Mutual interference between many similar radars operating in physical proximity
[ITN-91-85139] N91-28468
Fluctuations in near-surface backscattering to a descending CW radar
[ITN-91-85140] N91-28469

RADAR FILTERS
Mutual interference between many similar radars operating in physical proximity
[ITN-91-85139] N91-28468

RADAR MEASUREMENT
Performance of a polarization isolation enhancement method in the presence of errors
[DE91-013571] N91-28473

RADIANT HEATING
Investigation of interlayer materials for the microwave joining of SiC
[DE91-013311] N91-28414

RADIATION DAMAGE
Application of electron energy loss spectroscopy to microanalysis of irradiated stainless steels
[DE91-009913] N91-28344
Radiation disorder and aperiodicity in irradiated ceramics
[DE91-010257] N91-28391
Radiation damage of ceramics by electron microscopy
[DE91-012186] N91-28396
The interaction of HVEM-generated point-defects with dissociated dislocations
[DE91-013353] N91-29027

RADIATION DETECTORS
A controlled dispersion parallel wavelength x ray spectrometer for electron microscopy
[DE91-012011] N91-28544
Phonon-mediated detection of elementary particles using silicon crystal acoustic detectors N91-28547
Measuring neutron fluences and gamma/x ray fluxes with CCD cameras
[DE91-014119] N91-28549
The Soudan 2 honeycomb calorimeter
[DE91-013404] N91-28860
Electrical and photomechanical effects of plastic deformation of mercuric iodide
[DE91-013108] N91-29022

RADIATION DISTRIBUTION
Interaction of radiation with outflows in late-type stars
N91-29136

RADIATION DOSAGE
Microbeam studies of the sensitivity of structures within living cells
[DE91-012927] N91-28715
Protein-directed modulation of high-LET hyperthermic radiosensitization
[DE91-013783] N91-28722
Evolution of defect cluster distributions during irradiation
[DE91-013405] N91-29024

RADIATION EFFECTS
Perturbed environment assessments for space vehicles
[DE91-012630] N91-28188
Irradiation creep by climb-enabled glide driven by transient point defect processes
[DE91-012950] N91-28348
Comparisons of irradiation-induced shifts in fracture toughness, crack arrest toughness, and Charpy impact energy in high-copper welds
[DE91-008881] N91-28349
Monolithic front end electronics for silicon calorimeters
[DE91-012063] N91-28484
Microbeam studies of the sensitivity of structures within living cells
[DE91-012927] N91-28715
Radiation physics, biophysics, and radiation biology
[DE91-012883] N91-28716
Chromosomal changes in cultured human epithelial cells transformed by low- and high-LET radiation
[DE91-013772] N91-28720
Genetic changes in Mammalian cells transformed by helium cells
[DE91-013778] N91-28721
Protein-directed modulation of high-LET hyperthermic radiosensitization
[DE91-013783] N91-28722
Evolution of defect cluster distributions during irradiation
[DE91-013405] N91-29024

RADIATION MEASUREMENT
High intensity neutrino beams at KAON
[DE91-012147] N91-28830

RADIATION SHIELDING
SANDAC V computer electromagnetic interface characteristics: Problems and solutions
[DE91-014334] N91-29065
Ground-based measurements of galactic cosmic ray fragmentation in shielding
[DE91-012336] N91-29133

RADIATION SOURCES
Short wavelength FELS
[DE91-013759] N91-28566
The DARPA compact superconducting x-ray lithography source features
[DE91-013864] N91-29039

RADIATION TOLERANCE
Protein-directed modulation of high-LET hyperthermic radiosensitization
[DE91-013783] N91-28722

RADIATION TRANSPORT
Perturbed environment assessments for space vehicles
[DE91-012630] N91-28188
Multilevel resonance analysis of Co-59 neutron transmission measurements
[DE91-012135] N91-28829
Transport with Feynman propagators
[DE91-013566] N91-29063

RADIATIVE TRANSFER
Radiative transfer model for a spherical atmosphere
N91-28689
A cloud fraction and radiative transfer model
N91-28706
Radiative transfer in very strong magnetic fields
N91-29106
Interaction of radiation with outflows in late-type stars
N91-29136

RADII
Structures of magnetic field lines in the helical torus
N91-28932
Interaction of radiation with outflows in late-type stars
N91-29136

RADIO DIRECTION FINDERS
Predicting thunderstorm evolution using ground-based lightning detection networks N91-28702

RADIO EMISSION
Magnetospheric VLF line radiation N91-28693
Observational constraints on pulsars: Location of the emission region and pulse shape stability on decade time scales N91-29097

RADIO FILTERS
Performance evaluation of partial response continuous phase modulation: Discriminator detection
[ITN-91-85145] N91-28470

RADIO FREQUENCIES
Acoustophoresis method and apparatus
[NASA-CASE-LAR-13388-1] N91-28321
An assessment of the lifetime of Faraday shield elements
[DE91-012228] N91-28463
Wideband adaptive HF modem
[ITN-91-85147] N91-28471
Design of a multivariable RF control system using gain-shaping in the frequency domain
[DE91-013859] N91-28474
A chopper driven 11.4-GHz traveling-wave RF generator
[DE91-013568] N91-28489
H(-) beam characterization using laser-induced neutralization
[DE91-013501] N91-28564
Beam emittance and the effects of the rf, space charge and wake fields: Application to the ATF photoelectron beam
[DE91-014789] N91-28569
Theoretical studies of nonlinear sheath dynamics
N91-28896
Measurement accuracy of macroscopic quantum circuits with RF-biased Josephson junction arrays
[DE91-012651] N91-29009

RADIO FREQUENCY HEATING
Characterization of silicon nitride synthesized by microwave heating
[DE91-012219] N91-28397
Nonlinear dynamics of the relativistic standard map
[DE91-014368] N91-28972

RADIO FREQUENCY INTERFERENCE
Wideband adaptive HF modem
[ITN-91-85147] N91-28471

RADIO INTERFEROMETERS
Multiple frequency atmospheric radar techniques
N91-28683

RADIO JETS (ASTRONOMY)
Magnetohydrodynamical formation of astrophysical jets from gravitationally collapsing objects N91-28903

RADIO RECEIVERS
Performance evaluation of partial response continuous phase modulation: Discriminator detection
[ITN-91-85145] N91-28470

RADIO SIGNALS
Measurement of the microwave propagation delay induced by atmospheric water vapor N91-28466

RADIO SPECTRA
Radio absorption in the Antarctic ionosphere: Some observations in the region of the midlatitude trough
N91-28694

RADIO TRANSMISSION
Precise orbit determination for GPS satellites
N91-28183

RADIOACTIVE DECAY
Application of electron energy loss spectroscopy to microanalysis of irradiated stainless steels
[DE91-009913] N91-28344
Heavy-quark physics in quantum chromodynamics
[DE91-012113] N91-28828
The Soudan 2 honeycomb calorimeter
[DE91-013404] N91-28860

RADIOACTIVE MATERIALS
Application of electron energy loss spectroscopy to microanalysis of irradiated stainless steels
[DE91-009913] N91-28344

RADIOACTIVE WASTES
Behavior of RuO2 in a glass melt
[DE91-013717] N91-28432
Guidelines for acquisition, installation, and testing of performance assessment software
[DE91-013910] N91-28764
Developing a GIS to facilitate data analysis for environmental restoration of a large waste site
[DE91-013222] N91-29078

RADIOBIOLOGY
Radiation physics, biophysics, and radiation biology
[DE91-012883] N91-28716
Protein-directed modulation of high-LET hyperthermic radiosensitization
[DE91-013783] N91-28722

RADIOCHEMISTRY
New techniques for positron emission tomography in the study of human neurological disorders
[DE91-013855] N91-28728

RADIOGRAPHY
Liquid jet breakup and atomization in rocket chambers under dense spray conditions N91-28227

RADIOLYSIS
Magnetic resonance and optical spectroscopic studies of carotenoids
[DE91-014361] N91-28724

RAIL TRANSPORTATION
Light weight, high field, stable, superconducting magnets for advanced transportation systems
[DE91-013667] N91-28814

RAILGUN ACCELERATORS
A theoretical and experimental study of the interior ballistic processes of an electrothermal gun N91-28185

RAMAN SPECTRA
Vibrational spectroscopy of shock-compressed liquid CO
[DE91-013204] N91-28325
Resonance Raman and photophysical studies of transition metal complexes in solution and entrapped in zeolites
[DE91-013010] N91-28357
Inertial confinement fusion
[DE91-013479] N91-28960

RAMAN SPECTROSCOPY
Vibrational spectroscopy of shock-compressed liquid CO
[DE91-013204] N91-28325
Raman studies of stress-induced phase transformation in titania films
[DE91-012871] N91-29012

RANDOM PROCESSES
Ezekiel graphs
[DE91-012656] N91-28805

RANDOM VIBRATION
Robust bifurcation behavior in the presence of external random excitation N91-28171

RAPID QUENCHING (METALLURGY)
Rapid solidification processing of Al3Ti and Al3Ti plus copper
[AD-A236600] N91-28343

RAPID TRANSIT SYSTEMS
Light weight, high field, stable, superconducting magnets for advanced transportation systems
[DE91-013667] N91-28814

RARE EARTH ALLOYS
Magnetic studies of iron-rare-earth-metalloid alloys
[DE91-013856] N91-28368
Fundamental magnetic studies of iron-rare-earth-metalloid alloys
[DE91-014816] N91-28383

RARE GASES
Isotopic measurements of solar noble gases in individual micrometeorites from Greenland and Antarctica N91-29114

RAY TRACING
Common reflection point stacking: A macro model driven approach to dip moveout
[ISBN-90-9003020-4] N91-28676
Gravity wave propagation in a frontal environment N91-28687
Sound propagation in the atmosphere: Analysis of signal amplitude and phase temporal and spatial variations
[AD-A237034] N91-28816

RAYLEIGH SCATTERING
A laser based technique for particle sizing to study two phase expansion in turbines
[DE91-014172] N91-28595

RAYLEIGH WAVES
Overdriven shocks in solids and liquids
[DE91-013370] N91-28618

REACTION KINETICS
Some new approaches to semiclassical and quantum transition state theory
[DE91-012345] N91-28308
Sol-gel kinetics by NMR
[DE91-011500] N91-28314
Electrochemical processes at solid electrode-electrolyte-gas interfaces
[DE91-012922] N91-28317
The solubility and dissociation kinetics of hydroxymethyl hydroperoxide in aqueous solution
[DE91-013336] N91-28318
Thermodynamics and efficiency in combustion and engines
[DE91-012781] N91-28320
Studies relevant to the catalytic activation of carbon monoxide
[DE91-012661] N91-28323
Combustion research program: Flame studies, laser diagnostics, and chemical kinetics
[DE91-014824] N91-28329
Thermodynamic and kinetic aspects of surface acidity
[DE91-014039] N91-28331
A study of the impact of reaction rates on equation of state
[DE91-013375] N91-28621
Antenna organization in green photosynthetic bacteria
[DE91-014814] N91-28723
SDI: Statistical Dynamic Interactions
[DE91-012034] N91-28827
Spontaneous cluster decomposition in a quadrupole ion trap
[DE91-012519] N91-28836
Evaluation of charged-particle reactions for fusion applications
[DE91-014135] N91-28962
Kinetics of solid-state reactions in Ni-Zr thin films
[DE91-013652] N91-29028
The derivation of effective spin Hamiltonians and the origin of the magnetic field induced transition in orthormbic La2CuO4
[DE91-013743] N91-29035
The surface chemistry of GaAs atomic layer epitaxy
[DE91-014112] N91-29047

REACTION PRODUCTS
Evaluation of charged-particle reactions for fusion applications
[DE91-014135] N91-28962
Ground-based measurements of galactic cosmic ray fragmentation in shielding
[DE91-012336] N91-29133

REACTIVITY
A chemically reacting, turbulent stratified interface N91-28144
Reactive characterization as a probe of the nature of catalytic sites
[DE91-014536] N91-28333
Analysis of shock propagation and shock-initiated reaction in granular energetic materials N91-28446
Sealant research for SOFC
[DE91-014012] N91-28592

REACTOR CORES
Small Ex-core Heat Pipe Thermionic Reactor concept (SEHPTR)
[DE91-014073] N91-28279

REACTOR MATERIALS
High-temperature solution annealing as an IASCC mitigation technique
[DE91-012220] N91-28352
The effect of fluoride gases on cylinder valve corrosion
[DE91-012745] N91-28355
Evaluation of aging of cast stainless steel components
[DE91-014013] N91-28361
Evidences of trapping in tungsten and implications for plasma-facing components
[DE91-012734] N91-28951

REACTOR SAFETY
Prediction of high level vibration test results by use of available inelastic analysis techniques
[DE91-009437] N91-28606

REACTOR TECHNOLOGY
Particle confinement and fueling effects on the Maryland spheromak
[DE91-012396] N91-28945

REAL TIME OPERATION
Robust and real-time control of magnetic bearings for space engines N91-28230
Description of real-time Ada software implementation of a power system monitor for the Space Station Freedom PMAD DC testbed
[NASA-TM-105157] N91-28776
Real-time adaptive active control of sound fields N91-28819
The ADAMS interactive interpreter
[DE91-014345] N91-29080

RECEIVERS
Kinematic GPS surveying N91-28149
Superconducting bolometers: High-T(sub c) and low-T(sub c)
[DE91-011830] N91-28992

RECOIL IONS
Plasma immersion surface modification with metal ion plasma
[DE91-014233] N91-28979

RECOMBINATION REACTIONS
Correlated charge-changing ion-atom collisions
[DE91-013640] N91-28863

RECOMMENDATIONS
Guidelines for acquisition, installation, and testing of performance assessment software
[DE91-013910] N91-28764

RECRYSTALLIZATION
Softening mechanisms and microstructural instabilities during high temperature, low cycle fatigue of Ni, Ni3Al, and their metal matrix composites
[DE91-012714] N91-28287

RECTANGULAR PLATES
Flutter of laminated rectangular plates including finite deflection and shear deformation N91-28639
A study of the buckling and vibration behavior of an initially stressed thick plate by Galerkin's method N91-28641

RED SHIFT
Statistical mechanics of soft-boson phase transitions
[NASA-CR-188697] N91-28858
A faint galaxy redshift survey and implications for cosmology N91-29100
Population synthesis models for cluster galaxies at redshifts of 0.4 to 0.55 N91-29124

REDUCED GRAVITY
On accurate determination of contact angle
[DE91-013849] N91-28450
Cryogenic transfer options for exploration missions
[NASA-TM-105197] N91-28538

REDUCTION (CHEMISTRY)
Mechanism of hydrodenitrogenation. Part 5: X ray diffraction of molybdenum catalysts
[DE91-013853] N91-28327

REFLECTANCE
Reflection mask technology for soft x ray projection lithography
[DE91-012561] N91-28877
Search for regularities in the atmosphere of Jupiter N91-29127

REFLECTOMETERS
A spectroscopic differential reflectometry study of (100), (110), (111), (311), and (511) silicon surfaces
[AD-A231022] N91-28985

REFRACTION
Modal study of refractive effects on x ray laser coherence
[DE91-012083] N91-28551
Radiative transfer model for a spherical atmosphere N91-28689

REFRACTIVITY
Modal study of refractive effects on x ray laser coherence
[DE91-012083] N91-28551
Diffraction patterns produced by periodic and turbulent flowing gases including applications of photorefractive temporal filtering
[DE91-012636] N91-28553
Laser speckle velocimetry with photorefractive recording and anamorphic optical processing N91-28880

REFRACTORY MATERIALS
Heat resistant materials and their feasibility issues for a space nuclear transportation system
[DE91-014071] N91-28187

REFRACTORY METALS
Corrosion of refractory metals in liquid metal and gaseous environments
[DE91-009555] N91-28378

REFRIGERATING
Optimization and thermodynamic performance measures for a class of finite time thermodynamic cycles N91-29060

REFUELING
Particle confinement and fueling effects on the Maryland spheromak
[DE91-012396] N91-28945

REGULATORS
Coupling device with improved thermal interface
[NASA-CASE-GSC-13251-1] N91-28582

REINFORCEMENT (STRUCTURES)
Thermally activated retainer means
[NASA-CASE-MSC-21793-1] N91-28186

REINFORCING FIBERS
The effect of ductile innerlayers on the mechanical performance of fiber-reinforced composite materials N91-28295
The effect of TiB2 reinforcement on the mechanical properties of an Al-Cu-Li alloy-based metal-matrix composite N91-28337
Effect of Li level, artificial aging, and TiB2 reinforcement on the modulus of Weldalite (tm) 049 N91-28340

RELATIVISTIC EFFECTS
Regular motion and symmetry in the relativistic standard map N91-28933
Nonlinear dynamics of the relativistic standard map
[DE91-014368] N91-28972

RELATIVISTIC ELECTRON BEAMS
Nonlinear computer analysis of backward wave oscillator N91-28923

RELATIVITY
Light-cone quantization of quantum chromodynamics
[DE91-013991] N91-28856

RELAXATION METHOD (MATHEMATICS)
Parallelizing across time when solving time-dependent partial differential equations
[DE91-012948] N91-28797
Diffusion and relaxation in Hamiltonian chaos N91-28934

RELIABILITY
A survey of reliability, maintainability, supportability, and testability software tools
[AD-A236148] N91-28745

RELIABILITY ENGINEERING
Operationally Efficient Propulsion System Study (OEPPS) N91-28198
Space transportation main engine reliability and safety N91-28271
Probabilistic structural mechanics research for parallel processing computers
[NASA-CR-187162] N91-28644

RELIC RADIATION
A search for cosmic axions N91-29104
REMOTE SENSING
Localized waves in complex environments
[DE91-011934] N91-28462
Results of agriclimatological studies using multiple satellite sensors like NOAA AVHRR; GMS IR; and LANDSAT MSS and TM
[DE91-618773] N91-28698
REMOVAL
Device for removing foreign objects from anatomic organs
[NASA-CASE-GSC-13306-1] N91-28727
RENORMALIZATION GROUP METHODS
High-resolution measurements of the thermal conductivity and boundary resistance of helium-4 near the lambda point N91-28322
REQUIREMENTS
The special requirements of a VSTOL aircraft
N91-28155
Impact of ion propulsion on performance, design, testing, and operation of a geosynchronous spacecraft
[AD-A237028] N91-28273
RESEARCH
Microcomputers: An exploratory study of their availability and use in the research process and their contribution to researcher productivity N91-28739
RESEARCH AND DEVELOPMENT
An overview of the Penn State Propulsion Engineering Research Center N91-28222
Materials sub-panel N91-28245
Concurrent engineering N91-28247
Lessons learned and their application to program development and cultural issues N91-28263
Chemistry and materials science research report
[DE91-011507] N91-28305
Semiconductor Bridge (SCB) research and development
[DE91-011493] N91-28319
United States Department of Energy solar receiver technology development
[DE91-012653] N91-28651
An interdisciplinary approach to massively parallel computation
[DE91-012652] N91-28775
Theoretical studies in nuclear physics
[DE91-013909] N91-28873
RESEARCH FACILITIES
An overview of the Penn State Propulsion Engineering Research Center N91-28222
John C. Stennis Space Center roles and missions
N91-28259
Technologies available from Martin Marietta Energy Systems, Inc.
[DE91-013027] N91-28283
Tiger Team assessment of the Princeton Plasma Physics Laboratory
[DE91-014395] N91-28957
A portable and independent edge fluctuation diagnostic
[DE91-014357] N91-28971
RESEARCH MANAGEMENT
Exploratory battery technology development report for FY90
[DE91-012131] N91-28485
Advancing electric vehicle technology
[DE91-013004] N91-28575
Geothermal materials development
[DE91-013972] N91-28660
Microcomputers: An exploratory study of their availability and use in the research process and their contribution to researcher productivity N91-28739
Proposal for continued basic research in intelligent machines at the Center for Engineering Systems Advanced Research: Fiscal years 1992-1996
[DE91-012997] N91-28784
Progress in light ion fusion
[DE91-012019] N91-28826
Theoretical research in intermediate-energy nuclear physics
[DE91-012720] N91-28838
High Energy Physics Division semiannual report of research activities, July 1, 1990--December 31, 1990
[DE91-012339] N91-28868
Theoretical studies in nuclear physics
[DE91-013909] N91-28873
RESEARCH PROJECTS
Radiation disorder and aperiodicity in irradiated ceramics
[DE91-010257] N91-28391
Proposal for continued basic research in intelligent machines at the Center for Engineering Systems Advanced Research: Fiscal years 1992-1996
[DE91-012997] N91-28784
RESIDUAL STRENGTH
Damage development under compression-compression fatigue loading in a stitched uniwoven graphite/epoxy composite material
[NASA-CR-188693] N91-28292
RESIDUAL STRESS
High-resolution interferometric measurements of residual strains in composites N91-28303
Effects of residual stresses on the fracture toughness of Zircaloy-2 tubes
[DE91-012736] N91-28354
Elevated-temperature fracture resistances (K(sub IC), R-curves, gamma sub (omega OF)) of monolithic and composite ceramics using chevron-notched, bend tests
[NASA-TM-105090] N91-28418
Residual stress measurement using the pulsed neutron source at LANSCE
[DE91-013494] N91-28624
Neutron diffraction determination of the residual stress redistribution in cracked autofrettaged tubing
[DE91-013688] N91-28632
RESINS
Preparation of ionic membranes for zinc/bromine storage batteries
[DE91-012008] N91-28483
RESISTORS
A 10,000 A 1000 Vdc solid state dump switch
[DE91-014141] N91-28497
RESONANCE
Multilevel resonance analysis of Co-59 neutron transmission measurements
[DE91-012135] N91-28829
Diffusion through stochastic webs in two and more dimensions N91-28941
RESONANT FREQUENCIES
Resonant method for the measurement of the glass transition temperature at high frequencies
[DE91-618684] N91-28416
RESONANT TUNNELING
Transit time for resonant tunneling
[DE91-617799] N91-29018
RESONANT VIBRATION
Acoustophoresis method and apparatus
[NASA-CASE-LAR-13388-1] N91-28321
RESTORATION
Developing a GIS to facilitate data analysis for environmental restoration of a large waste site
[DE91-013222] N91-29078
REUSABLE HEAT SHIELDING
Thermally activated retainer means
[NASA-CASE-MSC-21793-1] N91-28186
REUSABLE ROCKET ENGINES
Historical problem areas: Lessons learned for expendable and reusable vehicle propulsion systems
N91-28243
REUSABLE SPACECRAFT
Next generation earth-to-orbit space transportation systems: Unmanned vehicles and liquid/hybrid boosters
N91-28205
Propulsion studies for advanced manned launch systems N91-28213
Space transfer vehicles and space basing
N91-28254
REVERSE FIELD PINCH
Space fusion energy conversion using a field reversed configuration reactor: A new technical approach for space propulsion and power N91-28217
Turbulent dynamo and subgrid-scale modeling of MHD turbulence N91-28887
Relaxed state and entropy production N91-28907
Simulation study of MHD relaxation and reconnection processes N91-28908
Nonlinear reversed field pinch dynamics with nonideal boundaries
[DE91-013638] N91-28961
Reversed-Field Pinch dynamics and transport studies
[DE91-014317] N91-28970
Reversed field pinch experiments
[DE91-013643] N91-28977
Sawteeth in the MST reversed field pinch
[DE91-014288] N91-29126
REYNOLDS STRESS
An abbreviated Reynolds stress turbulence model for airfoil flows N91-28140
The computation of complex, two-dimensional turbulent flows using Reynolds stress closure N91-28535
RIEMANN MANIFOLD
Use of a rotated Riemann solver for the two-dimensional Euler equations N91-28530
The (2,0) super Beltrami parametrization and superconformal structures
[DE91-617611] N91-29057
RIGID STRUCTURES
Suspension device for low-frequency structures
[NASA-CASE-LAR-14272-1-CU] N91-28184
RING LASERS
Ring-laser solitons: A multipass approach
[DE91-013242] N91-28560
ROBOT ARMS
Planning of minimum-time trajectories for robotic arms
[ITN-91-85141] N91-28583
Mechanical design optimization of robot manipulator performance N91-28589
The creation of multi-degree-of-freedom mechanisms for robotic applications
[DE91-014359] N91-28596
Driven shielding capacitive proximity sensor
[NASA-CASE-GSC-13377-1] N91-28785
ROBOT CONTROL
Dynamic coupling effects in modeling and control of hard contact motion of a manipulator
[DE91-010393] N91-28574
A methodology to determine the dynamic configuration of a reconfigurable manipulator
[DE91-010732] N91-28576
Kinematic analysis of legged system locomotion on smooth horizontal surfaces N91-28586
Control of autonomous mobile robots using custom-designed qualitative reasoning VLSI chips and boards
[DE91-012527] N91-28783
ROBOT DYNAMICS
Dynamic coupling effects in modeling and control of hard contact motion of a manipulator
[DE91-010393] N91-28574
A methodology to determine the dynamic configuration of a reconfigurable manipulator
[DE91-010732] N91-28576
Planning of minimum-time trajectories for robotic arms
[ITN-91-85141] N91-28583
Kinematic analysis of legged system locomotion on smooth horizontal surfaces N91-28586
The creation of multi-degree-of-freedom mechanisms for robotic applications
[DE91-014359] N91-28596
Selected topics in mechanisms and robotics: Singularities, inverse kinematics, and collision detection
N91-28598
Control of autonomous mobile robots using custom-designed qualitative reasoning VLSI chips and boards
[DE91-012527] N91-28783
ROBOT SENSORS
Analysis and modeling of early vision tasks for robot stereo vision N91-28585
ROBOTICS
Mechanical design optimization of robot manipulator performance N91-28589
Robotic mannequin technology for enhanced product testing
[DE91-013787] N91-28591
The creation of multi-degree-of-freedom mechanisms for robotic applications
[DE91-014359] N91-28596
Stochastic plans for robotic manipulation N91-28597
Selected topics in mechanisms and robotics: Singularities, inverse kinematics, and collision detection
N91-28598
Proposal for continued basic research in intelligent machines at the Center for Engineering Systems Advanced Research: Fiscal years 1992-1996
[DE91-012997] N91-28784
ROBOTS
Analysis and modeling of early vision tasks for robot stereo vision N91-28585
Mechanical design optimization of robot manipulator performance N91-28589
Stochastic plans for robotic manipulation N91-28597
ROBUSTNESS (MATHEMATICS)
Robust bifurcation behavior in the presence of external random excitation N91-28171
Stochastic robustness of linear multivariable control systems: Towards comprehensive robustness analysis
N91-28172
Robust low-order control of flexible joint manipulators
N91-28584
Chaos and microbial systems
[DE91-014908] N91-29064
ROCKET ENGINES
Maintaining technical excellence requires a national plan N91-28196
Expendable launch vehicle propulsion N91-28199
Cryogenic upper stage propulsion: RL10 and derivative engines N91-28202
Overview of European and other non-US/USSR/Japan launch vehicle and propulsion technology programs
N91-28221
Historical problem areas lessons learned N91-28242
ROCKET EXHAUST
Studies of the two-phase plume jet and wall erosion in a vertical launching system N91-28145

ROCKET PROPELLANTS
Overview of European and other non-US/USSR/Japan launch vehicle and propulsion technology programs
N91-28221
Enhancing atom densities in solid hydrogen by isotopic substitution
[DE91-011189] N91-28824
Historical perspectives: The role of the NASA Lewis Research Center in the national space nuclear power programs
[NASA-TM-105196] N91-29138

ROCKET THRUST
Attitude control of a spinning rocket via thrust vectoring
[DE91-006267] N91-28274

ROCKS
Geothermal materials development
[DE91-013972] N91-28660

RODS
Plastic analysis of a circular rod subjected to sinusoidal thermal cycling
[DE91-011845] N91-28609

ROLLERS
Roller locking brake
[NASA-CASE-GSC-13376-1] N91-28579
Thermal and non-Newtonian effects in elastohydrodynamic lubrication of rolling-sliding contacts
N91-28590

ROLLING
Thermal and non-Newtonian effects in elastohydrodynamic lubrication of rolling-sliding contacts
N91-28590

ROTARY WING AIRCRAFT
Technology needs for high speed rotorcraft (2)
[NASA-CR-177590] N91-28168

ROTATION
Suspension device for low-frequency structures
[NASA-CASE-LAR-14272-1-CU] N91-28184
Apparatus for intercalating large quantities of fibrous structures
[NASA-CASE-LEW-15077-2] N91-28289
Prediction of the flow and heat transfer between a rotating and a stationary cone N91-28536

ROTOR BLADES
Rotor and control system loads analysis of the XV-15 with the advanced technology blades
[NASA-TM-102876] N91-28134

ROTORS
Improved superconducting bearings
[NASA-CASE-GSC-13346-1] N91-28578

RUBBER
Resonant method for the measurement of the glass transition temperature at high frequencies
[DE91-618684] N91-28416
Method and apparatus for cleaning rubber deposits from airport runways and roadways
[NASA-CASE-LAR-14483-1] N91-28455

RUN TIME (COMPUTERS)
Compile-time estimation of communication costs in multicomputers
[NASA-CR-188675] N91-28747

RUNGE-KUTTA METHOD
Solution to quasi-axisymmetric internal compressible flows using the stream tube approach N91-28526

RUNWAY CONDITIONS
Runway Visual Range (RVR) Operational Test and Evaluation (OT and E)/integration test plan
[DOT/FAA/CT-TN91/4] N91-28176

RUNWAYS
Recent developments in the area of aircraft rough field performance N91-28154
F-106B airplane active control landing gear drop test performance N91-28164
Assessment of the application of the working group 22 standard bump concept to a current military aircraft
N91-28166
Runway Visual Range (RVR) Operational Test and Evaluation (OT and E)/integration test plan
[DOT/FAA/CT-TN91/4] N91-28176

RUPTURING
Alloy development of Fe3Al for improved creep rupture properties
[DE91-014541] N91-28381

RUTHENIUM COMPOUNDS
Resonance Raman and photophysical studies of transition metal complexes in solution and entrapped in zeolites
[DE91-013010] N91-28357
Behavior of RuO2 in a glass melt
[DE91-013717] N91-28432

S

SAMPLERS
High-throughput liquid-absorption air and aerosol sampler
[DE91-013762] N91-28670

SAPPHIRE
X ray diffraction study of heteroepitaxy of MOCVD grown TiO2 and VO2 films on sapphire single crystals
[DE91-013764] N91-29037

SATELLITE ANTENNAS
Proceedings of the 1990 Antenna Applications Symposium, volume 1
[AD-A237056] N91-28460
Proceedings of the 1990 Antenna Applications Symposium, volume 2
[AD-A237057] N91-28461

SATELLITE COMMUNICATION
Design of an interactive satellite communications system analysis program
[AD-A237030] N91-28459
Considerations for NATO satellite communications in the post 2000 era
[AGARD-AG-330] N91-28465

SATELLITE DESIGN
Considerations for NATO satellite communications in the post 2000 era
[AGARD-AG-330] N91-28465

SATELLITE INSTRUMENTS
Results of agriclimatological studies using multiple satellite sensors like NOAA AVHRR; GMS IR; and LANDSAT MSS and TM
[DE91-618773] N91-28698

SATELLITE OBSERVATION
Results of agriclimatological studies using multiple satellite sensors like NOAA AVHRR; GMS IR; and LANDSAT MSS and TM
[DE91-618773] N91-28698
Initialization of cloud and radiation in the Florida State University global spectral model N91-28703

SATELLITE ORBITS
Precise orbit determination for GPS satellites
N91-28183

SATURN 1B LAUNCH VEHICLES
Test vs. simulation N91-28251

SATURN 5 LAUNCH VEHICLES
Test vs. simulation N91-28251
Determining criteria for single stage to orbit
N91-28258

SAWTOOTH WAVEFORMS
Sawteeth in the MST reversed field pinch
[DE91-014288] N91-29126

SCALE MODELS
Prediction of high level vibration test results by use of available inelastic analysis techniques
[DE91-009437] N91-28606

SCANNERS
Scanning Transmission Ion Microscopy (STIM): A new technique for density mapping of microstructures
[DE91-011917] N91-28825

SCANNING TUNNELING MICROSCOPY
Applications of scanning tunneling microscopy to electrochemistry
[AD-A237021] N91-28304
Scanning tunneling microspectroscopy of solids and surfaces
[DE91-014515] N91-29043

SCATTER PROPAGATION
Tropospheric scatter propagation at 5 and 16 GHz: Results for a 161 km path
[AD-A237012] N91-28458

SCATTERING
Nuclear structure studies via neutron interactions
[DE91-012165] N91-28831
Measurements of ionization cross-section for electron energy-loss microanalysis under well defined scattering conditions
[DE91-013745] N91-28862

SCATTERING AMPLITUDE
Antiproton-induced elastic and inelastic scattering at intermediate energies
[DE91-013068] N91-28849
Influence of fast waves on the collective scattering of microwaves in fusion plasmas
[DE91-014759] N91-28973

SCATTERING CROSS SECTIONS
Measurements of angular distributions of absolute cross sections and analyzing powers of the reaction bar-p p yields d(pi+) between 1.3 and 2.4 GeV
[DE91-012638] N91-28842

SCHROEDINGER EQUATION
Optical analogs of model atoms in fields
[DE91-013392] N91-28855

SCINTILLATION COUNTERS
High intensity neutrino beams at KAON
[DE91-012147] N91-28830
Scintillation detector efficiencies for neutrons in the energy region above 20 MeV
[DE91-012544] N91-28837

SEA LEVEL
The determination of mean sea level using GPS
N91-28708

SEA SURFACE TEMPERATURE
Interactions between the north Pacific Ocean and the Northern Hemisphere atmosphere during El Nino
N91-28711

SEALERS
Sealant research for SOFC
[DE91-014012] N91-28592

SEALS (STOPPERS)
Sealant research for SOFC
[DE91-014012] N91-28592

SEATS
Computer simulation of an aircraft seat and occupant(s) in a crash environment: Program SOM-LA/SOM-TA user manual
[CR-R-90026] N91-28146
Human body protection in a dynamic environment. Cushioning mechanics
[ITN-91-85149] N91-28733

SECONDARY FLOW
A critical analysis of anisotropic k-epsilon modeling and its application to turbulence-driven secondary flows
N91-28533

SEDIMENTS
Mechanisms of bacterial metals removal from solids
[DE91-012808] N91-28356

SEISMIC WAVES
Common reflection point stacking: A macro model driven approach to dip moveout
[ISBN-90-9003020-4] N91-28676
Seismic traveltime inversion in three-dimensional heterogeneous media N91-28678
High-temperature elasticity and Earth's upper mantle
N91-28679

SELF CONSISTENT FIELDS
Models of collisional transport across a magnetic field with destroyed surfaces N91-28900

SEMANTICS
Information management: A uniform conceptual model and its user interface N91-29084

SEMICONDUCTING FILMS
Novel ways of depositing ZnTe films by a solution growth technique
[DE91-002189] N91-28429

SEMICONDUCTOR DEVICES
Semiconductor Bridge (SCB) research and development
[DE91-011493] N91-28319
A 10,000 A 1000 Vdc solid state dump switch
[DE91-014141] N91-28497

SEMICONDUCTOR JUNCTIONS
Research on stable, high-efficiency amorphous silicon multijunction modules
[DE91-002138] N91-28480

SEMICONDUCTORS (MATERIALS)
Radiation damage of ceramics by electron microscopy
[DE91-012186] N91-28396
Research on stable, high-efficiency amorphous silicon multijunction modules
[DE91-002138] N91-28480
Chaos in the lowest Landau level
[DE91-014800] N91-28866
The determination of the momentum matrix elements involved in calculating the dielectric constants of superlattices using the tight-binding method
[DE91-617789] N91-29017
Doping and pressure study of U3Sb4Pt3
[DE91-013669] N91-29033
High pressure optical studies of semiconductors and heterostructures
[DE91-014382] N91-29041
The ECR-plasma deposition of silicon nitride on a tunnel oxide
[DE91-014665] N91-29051

SENSITIVITY
Microbeam studies of the sensitivity of structures within living cells
[DE91-012927] N91-28715

SEPARATION
Acoustophoresis method and apparatus
[NASA-CASE-LAR-13388-1] N91-28321

SEQUENCING
Ezekiel graphs
[DE91-012656] N91-28805
Statistical mechanics using symbolic dynamics
N91-28940

SERVICE LIFE
An assessment of the lifetime of Faraday shield elements
[DE91-012228] N91-28463
Laboratory testing of the dual traction battery GC12V100
[DE91-012743] N91-28491

SERVOCONTROL
A methodology for using nonlinear aerodynamics in aeroservoelastic analysis and design
[NASA-TM-104087] N91-28131

SET THEORY
Topics in low-dimensional field theory
[DE91-013784] N91-29062

SHAFTS (MACHINE ELEMENTS)
Suspension device for low-frequency structures
[NASA-CASE-LAR-14272-1-CU] N91-28184
Robust and real-time control of magnetic bearings for space engines N91-28230
Analysis of foil bearings for high speed operation in cryogenic applications N91-28231
Noncircular rolling joints for vibrational reduction in slewing maneuvers
[NASA-CASE-LAR-14515-1-CU] N91-28580

SHAPE MEMORY ALLOYS
Device for removing foreign objects from anatomic organs
[NASA-CASE-GSC-13306-1] N91-28727

SHAPED CHARGES
Experiments and calculations of jet penetration in glass
[DE91-013567] N91-28422

SHEAR FLOW
Modelling and analysis of geophysical turbulence: Use of optimal transforms and basis sets N91-28686
Low-level curvature shear and supercell thunderstorm behavior N91-28701

SHEAR LAYERS
Experimental study of growth rate enhancement and structure of compressible turbulent free shear layers
N91-28517

SHEAR PROPERTIES
Mechanical modeling of stress generation during cure of encapsulating resins
[DE91-011496] N91-28393
Overdriven shocks in solids and liquids
[DE91-013370] N91-28618
Stability of cylindrical laminates by higher orde r shear deformable theories N91-28638
Ion temperature gradient turbulence and coherent structures N91-28890

SHEAR STRESS
Near crack tip transverse strain effects estimated with a large strain hollow cylinder analogy
[DE91-012072] N91-28619
Shear stress prediction in shock loaded copper
[DE91-014740] N91-28635
Flutter of laminated rectangular plates including finite deflection and shear deformation N91-28639

SHELL THEORY
Shell model calculations at superdeformed shapes
[DE91-012954] N91-28853

SHIELDING
Driven shielding capacitive proximity sensor
[NASA-CASE-GSC-13377-1] N91-28785

SHOCK LAYERS
Transonic shock-induced dynamics of a flexible wing with a thick circular-arc airfoil
[NASA-TM-104088] N91-28132

SHOCK LOADS
Vibrational spectroscopy of shock-compressed liquid CO
[DE91-013204] N91-28325
Shock compression of DuPont detasheet at low stress
[DE91-013229] N91-28443
Shock compression of low-density microcellular materials
[DE91-013586] N91-28628
Shear stress prediction in shock loaded copper
[DE91-014740] N91-28635
Equation of state and crushing dynamics of low-density silica aerogels
[DE91-014766] N91-28637

SHOCK TESTS
Bauschinger effect during shock loading
[DE91-014606] N91-28634

SHOCK TUBES
Generating strong shock waves with a supersonic peristaltic pump
[DE91-013228] N91-28174
Comparisons between fast shock tube calculations and tests
[DE91-013496] N91-28177
Hypervelocity plate acceleration
[DE91-014738] N91-28179
Shock and reshock of an unstable fluid interface
[DE91-014737] N91-28528

SHOCK WAVE GENERATORS
Generating strong shock waves with a supersonic peristaltic pump
[DE91-013228] N91-28174

SHOCK WAVE PROPAGATION
Analysis of shock propagation and shock-initiated reaction in granular energetic materials N91-28446
Atmospheric propagation of high-explosive blast waves
[DE91-012550] N91-28506

SHOCK WAVES
Generating strong shock waves with a supersonic peristaltic pump
[DE91-013228] N91-28174
Shock-induced optical emission in Al2O3 at 200 GPa: Implications for shock temperature measurements in metals
[DE91-013584] N91-28365
Shock initiation of pentaerythritol tetranitrate crystals: Steric effects due to plastic flow
[DE91-013389] N91-28420
Shock-wave properties of high-strength ceramics
[DE91-014105] N91-28439
Analysis of shock propagation and shock-initiated reaction in granular energetic materials N91-28446
Shock and reshock of an unstable fluid interface
[DE91-014737] N91-28528
Dynamic plasticity in transition from thermal activation to viscous drag
[DE91-013031] N91-28617
Overdriven shocks in solids and liquids
[DE91-013370] N91-28618
The DataShoP: A database of weak-shock constitutive data
[DE91-013349] N91-28620
Non-steady wave profiles and the fourth-power law
[DE91-013576] N91-28631
Bauschinger effect during shock loading
[DE91-014606] N91-28634
Quantum mechanical effects on the shock Hugoniot
[DE91-014750] N91-28636
Shock and soliton structures induced by poloidal flow in tokamaks N91-28929
Shock initiation of pentaerythritol tetranitrate crystals: Optical absorption and emission studies
[DE91-013381] N91-29023

SHORT CIRCUITS
Transmission/reflection and short-circuit line permittivity measurements
[PB91-171959] N91-28482

SHRINKAGE
Drying of gelcast ceramics
[DE91-012955] N91-28413

SHUTTLE DERIVED VEHICLES
Next generation solid boosters N91-28207
Determining criteria for single stage to orbit
N91-28258

SIALON
Drying of gelcast ceramics
[DE91-012955] N91-28413

SIDESLIP
Robust bifurcation behavior in the presence of external random excitation N91-28171

SIGNAL DETECTION
Mutual interferencc between many similar radars operating in physical proximity
[ITN-91-85139] N91-28468

SIGNAL DETECTORS
Performance evaluation of partial response continuous phase modulation: Discriminator detection
[ITN-91-85145] N91-28470
Phonon-mediated detection of elementary particles using silicon crystal acoustic detectors N91-28547

SIGNAL PROCESSING
Fluctuations in near-surface backscattering to a descending CW radar
[ITN-91-85140] N91-28469
A PC based frequency domain LV processor
[DE91-009056] N91-28541
A portable and independent edge fluctuation diagnostic
[DE91-014357] N91-28971

SIGNAL REFLECTION
Common reflection point stacking: A macro model driven approach to dip moveout
[ISBN-90-9003020-4] N91-28676

SIGNAL TO NOISE RATIOS
Mutual interference between many similar radars operating in physical proximity
[ITN-91-85139] N91-28468
Elastic tracking versus neural network tracking for very high multiplicity problems
[DE91-011825] N91-28768

SIGNAL TRANSMISSION
Performance evaluation of partial response continuous phase modulation: Discriminator detection
[ITN-91-85145] N91-28470
Multiple frequency atmospheric radar techniques
N91-28683

SIGNATURE ANALYSIS
Signature analysis technique for diagnosing failures in mechanical systems N91-28604
Initialization of cloud and radiation in the Florida State University global spectral model N91-28703

SILICATES
Quantitative modeling of the point defect structures of Fe-doped MgO and MgSiO3 perovskite
[DE91-011405] N91-28990

SILICIDES
Epitaxial growth of silicon on CoSi2(001)/Si(001)
[DE91-013387] N91-29015

SILICON
Monolithic front end electronics for silicon calorimeters
[DE91-012063] N91-28484
Pressure transducer and system for cryogenic environments
[NASA-CASE-LAR-14579-1] N91-28546
Phonon-mediated detection of elementary particles using silicon crystal acoustic detectors N91-28547
Bauschinger effect during shock loading
[DE91-014606] N91-28634
Molecular dynamics simulations of bulk displacement threshold energies in Si
[DE91-011957] N91-28846
A spectroscopic differential reflectometry study of (100), (110), (111), (311), and (511) silicon surfaces
[AD-A231022] N91-28985
Epitaxial growth of silicon on CoSi2(001)/Si(001)
[DE91-013387] N91-29015

SILICON CARBIDES
Alumina-silicon carbide composites from coated powders
[DE91-012357] N91-28281
A review of silicon carbide/metal interactions with relevance to silicon carbide joining
[DE91-012768] N91-28282
Investigation of interlayer materials for the microwave joining of SiC
[DE91-013311] N91-28414

SILICON DIOXIDE
Equation-of-state from SiO2 aerogel Hugoniot data
[DE91-011480] N91-28313
Model catalytic oxidation studies using supported monometallic and heterobimetallic oxides
[DE91-012144] N91-28409
Shock compression of low-density microcellular materials
[DE91-013586] N91-28628
Equation of state and crushing dynamics of low-density silica aerogels
[DE91-014766] N91-28637

SILICON NITRIDES
Characterization of silicon nitride synthesized by microwave heating
[DE91-012219] N91-28397
Development of nondestructive evaluation methods and prediction of effects of flaws on the fracture behavior of structural ceramics
[DE91-012471] N91-28410
Drying of gelcast ceramics
[DE91-012955] N91-28413
Semi-empirical calculations on model systems for organosilyldiamine preceramic polymers
[DE91-013721] N91-28433
The ECR-plasma deposition of silicon nitride on a tunnel oxide
[DE91-014665] N91-29051

SILICON OXIDES
Characterization of silicon nitride synthesized by microwave heating
[DE91-012219] N91-28397
Ordered ceramic membranes
[DE91-012248] N91-28398

SILVER
The influence of Ag+Mg additions on the nucleation of strengthening precipitates in a non-cold-worked Al-Cu-Li alloy N91-28336
Desorption of Al, Au, Ag using surface plasmon excitation
[DE91-013726] N91-28493
Laser ejection of Ag(sup +) ions from a roughened silver surface: Role of the surface plasmon
[DE91-012945] N91-28554
Development of elements of a high T(sub c) superconducting cable
[AD-A236151] N91-28986

SILVER COMPOUNDS
Structure and dynamics in low-dimensional guest host solids
[DE91-012169] N91-29020

SIMD (COMPUTERS)
Load-balancing and performance of a gridless particle simulation on MIMD, SIMD, and vector supercomputers
[DE91-013758] N91-28756

SIMPLIFICATION
Business not as usual N91-28266

SIMULATION
Actively damped landing gear system N91-28165
Suspension device for low-frequency structures
[NASA-CASE-LAR-14272-1-CU] N91-28184
Thyristor converter simulation and analysis
[DE91-013802] N91-28494
Numerical simulation of the air and fuel mixing process in fuel-injected engines using discrete vortex dynamics
N91-28587
A new model of rate dependent elastic-plastic flow
[DE91-014600] N91-28633
Interactions between the north Pacific Ocean and the Northern Hemisphere atmosphere during El Nino
N91-28711
Numerical study of ion temperature gradient modes in a tokamak N91-28921
Hole dynamics of one-dimensional plasma
N91-28928
Gravitational evolution of large-scale structure in the universe N91-29121

SINE WAVES
Plastic analysis of a circular rod subjected to sinusoidal thermal cycling
[DE91-011845] N91-28609

SINGLE CRYSTALS
Shock initiation of pentaerythritol tetranitrate crystals: Steric effects due to plastic flow
[DE91-013389] N91-28420
A comparative second harmonic study of Cu(111) in UHV and in solution
[AD-A237023] N91-28479
Flux dynamics in a single crystal of Bi2Sr2CaCu2O(x)
[DE91-013763] N91-29036
X ray diffraction study of heteroepitaxy of MOCVD grown TiO2 and VO2 films on sapphire single crystals
[DE91-013764] N91-29037
Scanning tunneling microspectroscopy of solids and surfaces
[DE91-014515] N91-29043
Crystal surface analysis using matrix textural features classified by a probabilistic neural network
[DE91-014120] N91-29048
Annealing and structure studies on Tl-2223 and Tl-1223 crystals
[DE91-014903] N91-29052

SINGLE STAGE TO ORBIT VEHICLES
The propulsion system is the key to airline-like operation of ETO vehicles N91-28256
Determining criteria for single stage to orbit
N91-28258

SINGULARITY (MATHEMATICS)
Selected topics in mechanisms and robotics: Singularities, inverse kinematics, and collision detection
N91-28598

SINTERING
A study of the influence of temperature gradients on densification of glass powder compacts
[DE91-012337] N91-28399
Microwave enhanced diffusion?
[DE91-013312] N91-28415

SIS (SUPERCONDUCTORS)
The effect of the quantum susceptance on the gain of superconducting quasiparticle mixers
[DE91-012352] N91-29021

SISO (CONTROL SYSTEMS)
A methodology for using nonlinear aerodynamics in aeroservoelastic analysis and design
[NASA-TM-104087] N91-28131
Attitude control of a spinning rocket via thrust vectoring
[DE91-006267] N91-28274

SIZE DISTRIBUTION
Liquid jet breakup and atomization in rocket chambers under dense spray conditions N91-28227

SLABS
TOPAZ2D benchmark problems nonlinear materials
[DE91-009753] N91-29053

SLEWING
Noncircular rolling joints for vibrational reduction in slewing maneuvers
[NASA-CASE-LAR-14515-1-CU] N91-28580

SLIDING
Robust and real-time control of magnetic bearings for space engines N91-28230

SLIDING CONTACT
Thermal and non-Newtonian effects in elastohydrodynamic lubrication of rolling-sliding contacts
N91-28590

SLIDING FRICTION
Tribology of aluminum-based metal matrix composites: Fundamental study of wear behavior as influenced by microstructure N91-28297
Polymers at surfaces
[DE91-013642] N91-28430
Boundary lubrication of ceramic materials by soft metallic coating and synthetic oil
[DE91-014017] N91-28577

SLURRY PROPELLANTS
Ignition and combustion of metallized propellants
N91-28224

SLUSH HYDROGEN
Slush hydrogen propellant production, transfer, and expulsion studies at the NASA K-Site Facility
[NASA-TM-105191] N91-28449

SMALL PERTURBATION FLOW
Irradiance compensation control for high-energy laser propagation. Part 1: Theory and Fourier control model propagation results
[DE91-013130] N91-28559

SMART STRUCTURES
Research and development entitled smart structures for fossil energy applications
[DE91-002064] N91-28875

SOCIOLOGY
A selection tool for choosing the best participative problem-solving technique
[DE91-012421] N91-29066

SODIUM
Lidar studies of sporadic sodium layers, gravity waves and density spectra in the mesopause and stratopause regions at Urbana and Arecibo N91-28690

SODIUM SULFUR BATTERIES
Exploratory battery technology development report for FY90
[DE91-012131] N91-28485

SOFTENING
Softening mechanisms and microstructural instabilities during high temperature, low cycle fatigue of Ni, Ni3Al, and their metal matrix composites
[DE91-012714] N91-28287

SOFTWARE ENGINEERING
Support materials for formal specification of software
[AD-A236121] N91-28742
Software development experiences with a distributed database in a large, distributed computer system
[DE91-012818] N91-28750
Visualization using a data flow-based paradigm
[DE91-013851] N91-28763

SOFTWARE TOOLS
A survey of reliability, maintainability, supportability, and testability software tools
[AD-A236148] N91-28745
The 1992 - 1997 renewal proposal interactive graphics for molecular studies
[AD-A236598] N91-28823
Design and performance evaluation of signature files for text retrieval systems N91-29085
A simulated user for laboratory investigation of information systems requirements determination
N91-29087

SOL-GEL PROCESSES
Sol-gel kinetics by NMR
[DE91-011500] N91-28314
Melamine-formaldehyde aerogels
[DE91-012084] N91-28408
Raman studies of stress-induced phase transformation in titania films
[DE91-012871] N91-29012

SOLAR ACTIVITY
Solar-geophysical data number 558, February 1991. Part 1: (Prompt reports). Data for January 1991, December 1990, and late data
[PB91-172270] N91-29129
Solar-geophysical data number 557, January 1991. Part 1: (Prompt reports). Data for December, November 1990 an late data
[PB91-169102] N91-29130
Solar-geophysical data number 557, January 1991. Part 2: (Comprehensive reports). Data for July 1990 and miscellaneous
[PB91-169110] N91-29131

SOLAR CELLS
SPGD: A central power system for space
[DE91-012610] N91-28276
Novel ways of depositing ZnTe films by a solution growth technique
[DE91-002189] N91-28429
Research on stable, high-efficiency amorphous silicon multijunction modules
[DE91-002138] N91-28480
Polycrystalline thin film photovoltaic technology
[DE91-002136] N91-28650
One-sun silicon solar cell research
[DE91-014329] N91-28662

SOLAR COLLECTORS
Numerical solution of a moving boundary problem as a model solution for a solar pipe
[ITN-91-85143] N91-28516
United States Department of Energy solar receiver technology development
[DE91-012653] N91-28651
Second-generation central receiver technology comparison
[DE91-012865] N91-28653
SOLTECH 91: Proceedings, volume 2
[DE91-013767] N91-28656
SOLTECH 91: Proceedings, volume 1
[DE91-002163] N91-28658

SOLAR COOLING
SOLTECH 91: Proceedings, volume 1
[DE91-002163] N91-28658

SOLAR CORONA
Current sheet formation and rapid reconnection in the solar corona N91-28884
Electron acceleration by magnetosonic waves in a solar coronal loop N91-29132

SOLAR ELECTRIC PROPULSION
Futuristic systems: Solar and nuclear electric propulsion N91-28215

SOLAR ENERGY
Applications and challenges for thermal energy storage
[DE91-012873] N91-28654
SOLTECH 91: Proceedings, volume 2
[DE91-013767] N91-28656
SOLTECH 91: Proceedings, volume 1
[DE91-002163] N91-28658

SOLAR ENERGY CONVERSION
Numerical solution of a moving boundary problem as a model solution for a solar pipe
[ITN-91-85143] N91-28516
United States Department of Energy solar receiver technology development
[DE91-012653] N91-28651
Second-generation central receiver technology comparison
[DE91-012865] N91-28653
Applications and challenges for thermal energy storage
[DE91-012873] N91-28654
SOLTECH 91: Proceedings, volume 1
[DE91-002163] N91-28658
Fifteenth DOE Solar Photochemistry Research Conference
[DE91-002165] N91-28663

SOLAR FLARES
Solar-geophysical data number 558, August 1990. Part 2: (Comprehensive reports). Data for August 1990 and miscellaneous
[PB91-172262] N91-29128
Solar-geophysical data number 558, February 1991. Part 1: (Prompt reports). Data for January 1991, December 1990, and late data
[PB91-172270] N91-29129
Electron acceleration by magnetosonic waves in a solar coronal loop N91-29132

SOLAR GENERATORS
Second-generation central receiver technology comparison
[DE91-012865] N91-28653

SOLAR HEATING
SOLTECH 91: Proceedings, volume 1
[DE91-002163] N91-28658

SOLAR MAGNETIC FIELD
Current sheet formation and rapid reconnection in the solar corona N91-28884
Solar-geophysical data number 558, February 1991. Part 1: (Prompt reports). Data for January 1991, December 1990, and late data
[PB91-172270] N91-29129

SOLAR PHYSICS
Solar-geophysical data number 558, August 1990. Part 2: (Comprehensive reports). Data for August 1990 and miscellaneous
[PB91-172262] N91-29128
Solar-geophysical data number 558, February 1991. Part 1: (Prompt reports). Data for January 1991, December 1990, and late data
[PB91-172270] N91-29129
Solar-geophysical data number 557, January 1991. Part 1: (Prompt reports). Data for December, November 1990 an late data
[PB91-169102] N91-29130

Solar-geophysical data number 557, January 1991. Part 2: (Comprehensive reports). Data for July 1990 and miscellaneous
[PB91-169110] N91-29131

SOLAR PROMINENCES
Solar-geophysical data number 558, August 1990. Part 2: (Comprehensive reports). Data for August 1990 and miscellaneous
[PB91-172262] N91-29128

SOLAR RADIATION
Natural and anthropogenic climate change
[DE91-014734] N91-28673

SOLAR RADIO BURSTS
Solar-geophysical data number 558, August 1990. Part 2: (Comprehensive reports). Data for August 1990 and miscellaneous
[PB91-172262] N91-29128

SOLAR SYSTEM
The 1990 update to strategy for exploration of the inner planets
[NASA-CR-188728] N91-28182

SOLAR WIND
Computer simulation of solar wind-magnetosphere interaction N91-28904
Helical field effect in solar/stellar wind N91-28912

SOLDERED JOINTS
Microstructural characterization of solders and brazes for advanced packaging technology
[DE91-011503] N91-28379
Improving fatigue life in near-eutectic Sn Pb solders
[DE91-013844] N91-28603

SOLDERING
High temperature solder device for flat cables
[NASA-CASE-GSC-13344-1] N91-28363
Microstructural characterization of solders and brazes for advanced packaging technology
[DE91-011503] N91-28379
Fluxless soldering of Ni-Au plated Kovar with a laser
[DE91-013261] N91-28451

SOLDERS
JPRS report: Science and technology. USSR: Materials science
[JPRS-UMS-91-003] N91-28342
Improving fatigue life in near-eutectic Sn Pb solders
[DE91-013844] N91-28603

SOLID CRYOGENS
Thermal conductivity of solid hydrogen at low temperature N91-28330
Enhancing atom densities in solid hydrogen by isotopic substitution
[DE91-011189] N91-28824

SOLID ELECTROLYTES
Electrochemical processes at solid electrode-electrolyte-gas interfaces
[DE91-012922] N91-28317
Polymers at surfaces
[DE91-011000] N91-28392
Sealant research for SOFC
[DE91-014012] N91-28592
Alternative materials for solid oxide fuel cells: Chromite interconnections
[DE91-014447] N91-28664

SOLID LUBRICANTS
Tribology of aluminum-based metal matrix composites: Fundamental study of wear behavior as influenced by microstructure N91-28297
Pretreatment of lubricated surfaces with sputtered cadmium oxide
[NASA-CASE-LEW-14474-1] N91-28423

SOLID PHASES
Synthesis and properties of novel cluster phases
[DE91-013006] N91-29013

SOLID PROPELLANT ROCKET ENGINES
Follow-on cable coupling lightning test, volume 1
[NASA-CR-184123] N91-28192
Solid rocket propulsion N91-28206
Next generation solid boosters N91-28207
A review of liquid rocket propulsion programs in Japan N91-28219

SOLID STATE
Fundamental theory of crystal decomposition
[AD-A236637] N91-28988
Indium compounds which contain two different organic substituents. Crystal structure of (In(CH2CMe3)(CH2SiMe3)Cl)2, an interesting case of partial Ligand disorder in the solid state
[AD-A236730] N91-28989
Kinetics of solid-state reactions in Ni-Zr thin films
[DE91-013652] N91-29028
Electron correlations in solid state physics
[DE91-013752] N91-29030

SOLID STATE DEVICES
An evaluation of monochrome solid-state video cameras
[DE91-012368] N91-28543
Pulse propagation in inhomogeneous optical fibers
[DE91-014356] N91-28879

SOLID STATE LASERS
Platinum solubility in phosphate laser glass
[DE91-015123] N91-28571

SOLID-SOLID INTERFACES
A review of silicon carbide/metal interactions with relevance to silicon carbide joining
[DE91-012768] N91-28282

SOLIDIFICATION
Rapid solidification processing of Al3Ti and Al3Ti plus copper
[AD-A236600] N91-28343
Interpreting solidification phenomena and microstructural evolution in metals through the use of transparent model alloy systems
[DE91-012629] N91-28347
Metastable phase equilibria in co-deposited Ni(1-x)Zr(x) thin films
[DE91-013653] N91-29029

SOLIDS
Mechanisms of bacterial metals removal from solids
[DE91-012808] N91-28356
Chemistry of electronic ceramic materials. Proceedings of the International Conference on the Chemistry of Electronic Ceramic Materials
[NASA-CR-188688] N91-28403
Overdriven shocks in solids and liquids
[DE91-013370] N91-28618
Electron transfer reactions in microporous solids
[DE91-012299] N91-28833
Structure and dynamics in low-dimensional guest host solids
[DE91-012169] N91-29020
Ab initio cluster studies of La2CuO4
[DE91-013520] N91-29025
Scanning tunneling microspectroscopy of solids and surfaces
[DE91-014515] N91-29043

SOLIDS FLOW
A review of theories for flowing granular materials with applications to fluidized beds and solids transport
[DE91-013111] N91-28514

SOLITARY WAVES
Ring-laser solitons: A multipass approach
[DE91-013242] N91-28560
Solitons and chaos in laser-plasma interaction N91-28898
Shock and soliton structures induced by poloidal flow in tokamaks N91-28929
Soliton phenomena in electron beam plasma N91-28930
Point vortex description of a modon solution N91-28931
Formation and dynamics of solitary waves and vortices in driven and damped systems N91-28942
Solitons and chaos in plasma N91-28943
Stability of drift-wave modons in the presence of temperature gradients
[DE91-014364] N91-28982

SOLUBILITY
The solubility and dissociation kinetics of hydroxymethyl hydroperoxide in aqueous solution
[DE91-013336] N91-28318
Platinum solubility in phosphate laser glass
[DE91-015123] N91-28571

SOLVATION
Analysis of metals in solution using electrospray ionization mass spectrometry
[DE91-012522] N91-28310

SOUND FIELDS
A reciprocity technique for the characterisation of sound transmission into aircraft fuselages N91-28817
Quadrupole phenomena of noise from a subsonic jet impinging on a large, rigid, and flate plate N91-28818

SOUND PRESSURE
A reciprocity technique for the characterisation of sound transmission into aircraft fuselages N91-28817

SOUND PROPAGATION
Sound propagation in the atmosphere: Analysis of signal amplitude and phase temporal and spatial variations
[AD-A237034] N91-28816

SOUND TRANSMISSION
Sound propagation in the atmosphere: Analysis of signal amplitude and phase temporal and spatial variations
[AD-A237034] N91-28816
A reciprocity technique for the characterisation of sound transmission into aircraft fuselages N91-28817

SOUND WAVES
Acoustophoresis method and apparatus
[NASA-CASE-LAR-13388-1] N91-28321
Localized waves in complex environments
[DE91-011934] N91-28462

SPACE BASES
The space exploration initiative. Operational efficiency panel space-basing technology requirements N91-28253

SPACE CHARGE
Beam emittance and the effects of the rf, space charge and wake fields: Application to the ATF photoelectron beam
[DE91-014789] N91-28569
Space charge and wake field analysis for a high brightness electron source
[DE91-014788] N91-28874

SPACE COLONIES
Humans to Mars in 1999 N91-28237

SPACE EXPLORATION
The 1990 update to strategy for exploration of the inner planets
[NASA-CR-188728] N91-28182
Heat resistant materials and their feasibility issues for a space nuclear transportation system
[DE91-014071] N91-28187
The space exploration initiative N91-28194
Next generation earth-to-orbit space transportation systems: Unmanned vehicles and liquid/hybrid boosters N91-28205
Next generation: In-space transportation system(s) N91-28211
Advanced propulsion concepts N91-28218
Life cycle cost based program decisions N91-28248
The space exploration initiative. Operational efficiency panel space-basing technology requirements N91-28253

SPACE LAW
Next generation earth-to-orbit space transportation systems: Unmanned vehicles and liquid/hybrid boosters N91-28205

SPACE LOGISTICS
Space shuttle requirements/configuration evolution N91-28264

SPACE MISSIONS
The space exploration initiative. Operational efficiency panel space-basing technology requirements N91-28253

SPACE PLASMAS
Current sheet formation and rapid reconnection in the solar corona N91-28884

SPACE POWER REACTORS
Heat resistant materials and their feasibility issues for a space nuclear transportation system
[DE91-014071] N91-28187
SPGD: A central power system for space
[DE91-012610] N91-28276
A high power Klystrode with potential for space application
[DE91-013046] N91-28486

SPACE PROBES
NASA's advanced space transportation system launch vehicles N91-28195

SPACE PROGRAMS
Space systems requirements: The Navy approach
[AD-A236490] N91-28181

SPACE SHUTTLE MAIN ENGINE
Robust and real-time control of magnetic bearings for space engines N91-28230
Probabilistic structural analysis methods for space transportation propulsion systems N91-28238
Space shuttle with common fuel tank for liquid rocket booster and main engines (supertanker space shuttle) N91-28257
Determining criteria for single stage to orbit N91-28258
The case for teaming on the ALS-STME program N91-28269
Space shuttle main engine: Certification for manned space flight N91-28270
Viscoplastic analysis of an experimental cylindrical thrust chamber liner
[NASA-TM-103287] N91-28622

SPACE SHUTTLES
The space exploration initiative N91-28194
Space shuttle propulsion systems N91-28200
Historical problem areas lessons learned N91-28242
Historical problem areas: Lessons learned for expendable and reusable vehicle propulsion systems N91-28243
Test vs. simulation N91-28251
Space shuttle with common fuel tank for liquid rocket booster and main engines (supertanker space shuttle) N91-28257
Determining criteria for single stage to orbit N91-28258
Space shuttle requirements/configuration evolution N91-28264

SPACE STATION POWER SUPPLIES
Description of real-time Ada software implementation of a power system monitor for the Space Station Freedom PMAD DC testbed
[NASA-TM-105157] N91-28776

SPACE STATIONS
Large space structures and systems in the space station era: A bibliography with indexes
[NASA-SP-7085(02)] N91-28191
NASA's advanced space transportation system launch vehicles N91-28195
Shuttle derived manned transportation systems N91-28204
Heavy-lift launch vehicle propulsion considerations N91-28236

SPACE TRANSPORTATION
Space Transportation Propulsion Technology Symposium. Volume 2: Symposium proceedings
[NASA-CP-3112-VOL-2] N91-28193
Next generation solid boosters N91-28207
Space transportation propulsion USSR launcher technology, 1990 N91-28220
Space Transportation Propulsion Technology Symposium. Volume 3: Panel Session Summaries and Presentations
[NASA-CP-3112-VOL-3] N91-28235
Humans to Mars in 1999 N91-28237
Historical problem areas: Lessons learned for expendable and reusable vehicle propulsion systems N91-28243

SPACE TRANSPORTATION SYSTEM
Space Transportation Propulsion Technology Symposium. Volume 2: Symposium proceedings
[NASA-CP-3112-VOL-2] N91-28193
Next generation earth-to-orbit space transportation systems: Unmanned vehicles and liquid/hybrid boosters N91-28205
Next generation: Unmanned launch vehicles and upper stages: The needs N91-28210
Next generation: In-space transportation system(s) N91-28211
Propulsion studies for advanced manned launch systems N91-28213
Space Transportation Propulsion Technology Symposium. Volume 3: Panel Session Summaries and Presentations
[NASA-CP-3112-VOL-3] N91-28235
Heavy-lift launch vehicle propulsion considerations N91-28236
Probabilistic structural analysis methods for space transportation propulsion systems N91-28238
Historical problem areas lessons learned N91-28242
Overall goals N91-28246
John C. Stennis Space Center roles and missions N91-28259

SPACE WEAPONS
Development of a current collection loss management system for SDI homopolar power supplies
[DE91-012779] N91-28652
Defending the defenders: Brilliant pebble defense against pop-up neutral particle beam suppression attacks
[DE91-012521] N91-28809

SPACE-TIME FUNCTIONS
Light-cone quantization of quantum chromodynamics
[DE91-013991] N91-28856
The 2+1 gravity: A new approach N91-29059
Non-Hausdorff twistor spaces and the global structure of space-time N91-29103
Phase transitions triggered by quantum fluctuations in the inflationary universe
[NASA-CR-188698] N91-29112
The line of gravitation: On the quantization conditions in curved spacetime and uncertainty-driven inflation N91-29115

SPACECRAFT CONFIGURATIONS
Space transfer vehicles and space basing N91-28254
Space shuttle with common fuel tank for liquid rocket booster and main engines (supertanker space shuttle) N91-28257

SPACECRAFT CONSTRUCTION MATERIALS
Materials sub-panel N91-28245
Overall goals N91-28246

SPACECRAFT CONTROL
Applications of low lift to drag ratio aerobrakes using angle of attack variation for control
[NASA-TM-103544] N91-28189
Satellite/spacecraft propulsion N91-28203
CFD applications in chemical propulsion engines N91-28234
Description of real-time Ada software implementation of a power system monitor for the Space Station Freedom PMAD DC testbed
[NASA-TM-105157] N91-28776

SPACECRAFT DESIGN
NASA's advanced space transportation system launch vehicles N91-28195
STV engine design considerations N91-28255
Space shuttle requirements/configuration evolution N91-28264

SPACECRAFT LAUNCHING
Shuttle derived manned transportation systems N91-28204
Next generation earth-to-orbit space transportation systems: Unmanned vehicles and liquid/hybrid boosters N91-28205
Effectivity of atmospheric electricity on launch availability N91-28260
Launch operations manpower yesterday, today and tomorrow N91-28267

SPACECRAFT POWER SUPPLIES
Space Transportation Propulsion Technology Symposium. Volume 2: Symposium proceedings
[NASA-CP-3112-VOL-2] N91-28193
Space fusion energy conversion using a field reversed configuration reactor: A new technical approach for space propulsion and power N91-28217
SPGD: A central power system for space
[DE91-012610] N91-28276
Comparison of dynamic isotope power systems for distributed planet surface applications
[NASA-TM-4303] N91-28278
Historical perspectives: The role of the NASA Lewis Research Center in the national space nuclear power programs
[NASA-TM-105196] N91-29138

SPACECRAFT PROPULSION
The space exploration initiative N91-28194
Maintaining technical excellence requires a national plan N91-28196
Satellite/spacecraft propulsion N91-28203
Shuttle derived manned transportation systems N91-28204
Next generation earth-to-orbit space transportation systems: Unmanned vehicles and liquid/hybrid boosters N91-28205
Solid rocket propulsion N91-28206
Space systems propulsion technology N91-28209
Next generation: In-space transportation system(s) N91-28211
Advanced cryo propulsion systems N91-28212
Propulsion studies for advanced manned launch systems N91-28213
Futuristic systems: Solar and nuclear electric propulsion N91-28215
Nuclear thermal propulsion N91-28216
Space fusion energy conversion using a field reversed configuration reactor: A new technical approach for space propulsion and power N91-28217
Advanced propulsion concepts N91-28218
A review of liquid rocket propulsion programs in Japan N91-28219
Space transportation propulsion USSR launcher technology, 1990 N91-28220
Overview of European and other non-US/USSR/Japan launch vehicle and propulsion technology programs N91-28221
An overview of the Penn State Propulsion Engineering Research Center N91-28222
Space Transportation Propulsion Technology Symposium. Volume 3: Panel Session Summaries and Presentations
[NASA-CP-3112-VOL-3] N91-28235
Heavy-lift launch vehicle propulsion considerations N91-28236
Historical problem areas lessons learned N91-28242
Concurrent engineering N91-28247
Life cycle cost based program decisions N91-28248
Infusion of instrumentation technology (engine plume diagnostics) into operational test programs N91-28249
Test vs. simulation N91-28251
Development program enhancement suggestions (propulsion related) N91-28252
STV engine design considerations N91-28255
The propulsion system is the key to airline-like operation of ETO vehicles N91-28256
Propulsion system ground testing N91-28261
Propulsion technologies for near term N91-28262
Space propulsion by fusion in a magnetic dipole
[DE91-012033] N91-28275
Nondestructive evaluation tools and experimental studies for monitoring the health of space propulsion systems
[NASA-TM-105164] N91-28605

SPACECRAFT SHIELDING
Thermally activated retainer means
[NASA-CASE-MSC-21793-1] N91-28186

SPACECRAFT STRUCTURES
Discrete posynomial programming with applications to spacecraft protective structures design optimization N91-28190
The solution of variable-geometry truss problems using new homotopy continuation methods N91-28640

SPATIAL DISTRIBUTION
Sound propagation in the atmosphere: Analysis of signal amplitude and phase temporal and spatial variations
[AD-A237034] N91-28816
Multiple nuclei, cluster core dynamics, and the velocity distributions of gravitating systems N91-29119

SPATIAL RESOLUTION
X ray spatial resolution at intermediate voltages: An assessment by massively parallel Monte Carlo electron trajectory simulation
[DE91-012018] N91-28841
The spatial resolution of x ray microanalysis in thin foils
[DE91-011949] N91-29003

SPECIFIC HEAT
Thermal conductivity of solid hydrogen at low temperature N91-28330
Doping and pressure study of U3Sb4Pt3
[DE91-013669] N91-29033

SPECIFICATIONS
Application of the Air Force guide specification 87221A to ground loads N91-28152
Nondestructive testing standards and the ASME code
[DE91-012643] N91-28600
Design and analysis of the 50 mm collider dipole vacuum vessel
[DE91-012490] N91-28610
Support materials for formal specification of software
[AD-A236121] N91-28742

SPECKLE PATTERNS
Laser speckle velocimetry with photorefractive recording and anamorphic optical processing N91-28880

SPECTRAL METHODS
Initialization of cloud and radiation in the Florida State University global spectral model N91-28703
Multidimensional spectral estimation using iterative methods
[AD-A237025] N91-28791
Mapping implicit spectral methods to distributed memory architectures
[NASA-CR-187592] N91-28806

SPECTRAL REFLECTANCE
The in-flight calibration of a helicopter-mounted Daedalus multispectral scanner
[DE91-013054] N91-28170
Model catalytic oxidation studies using supported monometallic and heterobimetallic oxides
[DE91-012144] N91-28409
A spectroscopic differential reflectometry study of (100), (110), (111), (311), and (511) silicon surfaces
[AD-A231022] N91-28985

SPECTROMETERS
Monolithic front end electronics for silicon calorimeters
[DE91-012063] N91-28484

SPECTRORADIOMETERS
The in-flight calibration of a helicopter-mounted Daedalus multispectral scanner
[DE91-013054] N91-28170

SPECTROSCOPY
Measurements of photo-induced changes in conjugated polymers
[DE91-013262] N91-28427
X ray microimaging of elemental composition and microstructure for materials science
[DE91-012221] N91-28832
A spectroscopic differential reflectometry study of (100), (110), (111), (311), and (511) silicon surfaces
[AD-A231022] N91-28985
Scanning tunneling microspectroscopy of solids and surfaces
[DE91-014515] N91-29043

SPECTRUM ANALYSIS
Study of spherical couette flow via 3-D spectral simulations: Large and narrow-gap flows and their transitions N91-28520
Modeling two-point spatial turbulence spectra for analysis of gust variations over aerospace vehicles N91-28685
Magnetospheric VLF line radiation N91-28693
Radio absorption in the Antarctic ionosphere: Some observations in the region of the midlatitude trough N91-28694
A search for cosmic axions N91-29104
Interstellar magnesium studies N91-29120

SPECULAR REFLECTION
Seismic traveltime inversion in three-dimensional heterogeneous media N91-28678
Phase-conjugated fluorescence
[AD-A231114] N91-28820

SPHERES
Gas evolution from spheres
[DE91-012807] N91-28510
Models for heat transport through assemblies of uniform-diameter hollow spheres
[DE91-012998] N91-28512
Sphere lapping
[DE91-014287] N91-28593

SPHEROMAKS
Particle confinement and fueling effects on the Maryland spheromak
[DE91-012396] N91-28945
Measurement of magnetic properties of confined compact toroid plasma (spheromak)
[DE91-012397] N91-28950

SPIN DYNAMICS
Application of muon spin relaxation experiment to the vortex dynamics of high temperature superconductors
[DE91-014607] N91-29050

SPINDLES
Noncircular rolling joints for vibrational reduction in slewing maneuvers
[NASA-CASE-LAR-14515-1-CU] N91-28580

SPIRAL GALAXIES
Visual, red and infrared photographic surface photometry of NGC 55 and NGC 253 N91-29094

SPIRALS
Pressure drop and heat transfer for spirally fluted tubes including validation of the role of transition
[DE91-012242] N91-28509

SPLINE FUNCTIONS
Symplectic full-turn maps in a Fourier representation
[DE91-012912] N91-28796

SPLINES
Spline-locking payload fastener
[NASA-CASE-GSC-13378-1] N91-28581

SPORADIC E LAYER
Lidar studies of sporadic sodium layers, gravity waves and density spectra in the mesopause and stratopause regions at Urbana and Arecibo N91-28690

SPRAYERS
Spray combustion under oscillatory pressure conditions N91-28226
Liquid jet breakup and atomization in rocket chambers under dense spray conditions N91-28227
Droplet-turbulence interactions in subcritical and supercritical evaporating sprays N91-28228
Cryogenic transfer options for exploration missions
[NASA-TM-105197] N91-28538

SPRAYING
Analysis of metals in solution using electrospray ionization mass spectrometry
[DE91-012522] N91-28310

SPUTTERING
Ion beam sputtered coatings of bioglass N91-28384

SQUID (DETECTORS)
High-T(sub c) thin-film microelectronics
[DE91-012340] N91-28997
Photolithographically patterened thin-film multilayer devices of YBa2Cu3O(7-x)
[DE91-012350] N91-28998
Thin-film flux transformers of YBa2Cu3O(7-x)
[DE91-012363] N91-29007

STABLE OSCILLATIONS
New photocrosslinkable polymers for second order nonlinear optical processes
[AD-A235856] N91-28386

STAINLESS STEELS
Hypervelocity plate acceleration
[DE91-014738] N91-28179
The effect of stress on hydrogen uptake and desorption by A-286
[NASA-TM-103537] N91-28341
Application of electron energy loss spectroscopy to microanalysis of irradiated stainless steels
[DE91-009913] N91-28344
High-temperature solution annealing as an IASCC mitigation technique
[DE91-012220] N91-28352
Evaluation of aging of cast stainless steel components
[DE91-014013] N91-28361
APFIM characterization of the spinodal decomposition in duplex stainless steels
[DE91-014256] N91-28371
Changes with material properties of acoustic emission produced during single point machining
[DE91-011913] N91-28452
Origin of acoustic emission produced during single point machining
[DE91-011915] N91-28453
Residual stress measurement using the pulsed neutron source at LANSCE
[DE91-013494] N91-28624

STANDARD DEVIATION
An accelerated training method for back propagation networks
[NASA-CASE-MSC-21625-1] N91-28730

STANDARDIZATION
Assessment of the application of the working group 22 standard bump concept to a current military aircraft N91-28166

STANDARDS
Nondestructive testing standards and the ASME code
[DE91-012643] N91-28600
The use of science in the management of hazardous air pollutants N91-28667
Performance of the Intel iPSC/860 and Ncube 6400 hypercubes
[DE91-012370] N91-28738

STAR DISTRIBUTION
Void probability as a function of the void's shape and scale-invariant models
[NASA-CR-188696] N91-29113

STAR FORMATION
Magnetohydrodynamical formation of astrophysical jets from gravitationally collapsing objects N91-28903
Star formation in the presence of magnetic fields: Molecular cloud core formation and dynamical contraction due to ambipolar diffusion:; a simulation with axial symmetry N91-29116
Observations of extragalactic water vapor masers N91-29117
Numerical simulations of mass outflows from star-forming regions N91-29123
Population synthesis models for cluster galaxies at redshifts of 0.4 to 0.55 N91-29124

STAR TRACKERS
WFOV star tracker camera
[DE91-012776] N91-28148

STATIC LOADS
Damage progression during static and fatigue loading in metal matrix composites, volumes 1-3 N91-28301

STATIONS
Design of an interactive satellite communications system analysis program
[AD-A237030] N91-28459

STATISTICAL ANALYSIS
The use of Monte Carlo simulation in determining landing gear loads during landing N91-28162
SDI: Statistical Dynamic Interactions
[DE91-012034] N91-28827
The theory of turbulence and anomalous transport in plasmas: Past, present, and future N91-28889

STATISTICAL DISTRIBUTIONS
Log-stable distribution of energy dissipation in turbulence N91-28885
Statistical properties of two-dimensional magnetohydrodynamic turbulence N91-28886

STATISTICAL MECHANICS
Statistical mechanics of soft-boson phase transitions
[NASA-CR-188697] N91-28858
Diffusion and relaxation in Hamiltonian chaos N91-28934
Statistical mechanics using symbolic dynamics N91-28940
Reversed-Field Pinch dynamics and transport studies
[DE91-014317] N91-28970

STEADY FLOW
Numerical solution of a free-boundary viscous flow N91-28529

STEADY STATE
Study of interfacial behavior in cocurrent gas-liquid flows
[DE91-013008] N91-28511

STEELS
Failure analysis case histories of Canadian forces aircraft landing gear components N91-28151
Sandia's new hypervelocity launcher (HVL)
[DE91-014335] N91-28178
Comparisons of irradiation-induced shifts in fracture toughness, crack arrest toughness, and Charpy impact energy in high-copper welds
[DE91-008881] N91-28349

STELLAR ATMOSPHERES
Radiative transfer in very strong magnetic fields N91-29106

STELLAR CORONAS
Corona: Coordinated research on non-thermal processes in astrophysics
[NASA-CR-188692] N91-29107

STELLAR ENVELOPES
Interaction of radiation with outflows in late-type stars N91-29136

STELLAR GRAVITATION
High-overtone black-hole normal modes: A WKB contour-integral approach N91-29118

STELLAR LUMINOSITY
Properties of infrared-luminous galaxies, or, how I spent seven summer vacations N91-29098

STELLAR MAGNETIC FIELDS
Star formation in the presence of magnetic fields: Molecular cloud core formation and dynamical contraction due to ambipolar diffusion:; a simulation with axial symmetry N91-29116

STELLAR MASS
Statistical mechanics of soft-boson phase transitions
[NASA-CR-188697] N91-28858
Dibaryons in neutron stars
[NASA-CR-188704] N91-29109
Numerical simulations of mass outflows from star-forming regions N91-29123

STELLAR MASS EJECTION
Interaction of radiation with outflows in late-type stars N91-29136

STELLAR MODELS
Radiative transfer in very strong magnetic fields N91-29106
Population synthesis models for cluster galaxies at redshifts of 0.4 to 0.55 N91-29124
Impact of the nuclear equation of state on models of rotating neutron stars
[DE91-014615] N91-29125

STELLAR OSCILLATIONS
High-overtone black-hole normal modes: A WKB contour-integral approach N91-29118

STELLAR ROTATION
Impact of the nuclear equation of state on models of rotating neutron stars
[DE91-014615] N91-29125

STELLAR SPECTRA
Coordinated optical and ultraviolet observations of short period RS CVn and W UMa type stars N91-29096
A faint galaxy redshift survey and implications for cosmology N91-29100
Population synthesis models for cluster galaxies at redshifts of 0.4 to 0.55 N91-29124

STELLAR STRUCTURE
Statistical mechanics of soft-boson phase transitions
[NASA-CR-188697] N91-28858
Dibaryons in neutron stars
[NASA-CR-188704] N91-29109

STELLAR WINDS
Corona: Coordinated research on non-thermal processes in astrophysics
[NASA-CR-188692] N91-29107

STELLARATORS
Edge anomalous transport in heliotron/torsatron N91-28892
Optimization, non-local MHD-mode, and alpha-particle confinement behavior of Helias equilibria N91-28893
Characteristics of edge plasma turbulence on the ATF torsatron
[DE91-012981] N91-28947

STEREOSCOPIC VISION
Analysis and modeling of early vision tasks for robot stereo vision N91-28585

STIRLING CYCLE
Comparison of dynamic isotope power systems for distributed planet surface applications
[NASA-TM-4303] N91-28278

STOCHASTIC PROCESSES
Stochastic robustness of linear multivariable control systems: Towards comprehensive robustness analysis N91-28172
Stochastic plans for robotic manipulation N91-28597
Diffusion through stochastic webs in two and more dimensions N91-28941
Nonlinear dynamics of the relativistic standard map
[DE91-014368] N91-28972
Path-integral measure for Chern-Simons theory within the stochastic quantization approach
[DE91-617610] N91-29056
Electron acceleration by magnetosonic waves in a solar coronal loop N91-29132

STOICHIOMETRY
Defects and transport in mixed oxides
[DE91-014443] N91-29049

STORAGE RINGS (PARTICLE ACCELERATORS)
Simulation of a storage ring free electron laser with a mapping algorithm for distribution functions
[DE91-012387] N91-28552
Short wavelength FELS
[DE91-013759] N91-28566
Refinement of the Hamilton-Jacobi solution using a second canonical transformation
[DE91-012965] N91-28798
Microwave instability at transition: Stability diagram approach
[DE91-013202] N91-28867
The DARPA compact superconducting x-ray lithography source features
[DE91-013864] N91-29039

STORM ENHANCEMENT
Predicting thunderstorm evolution using ground-based lightning detection networks N91-28702

STRAIN GAGES
Long time measurements of landing gear loads on SAAB SF-340 commuter aircraft N91-28157
Effects of residual stresses on the fracture toughness of Zircaloy-2 tubes [DE91-012736] N91-28354
Monitoring structural response in pressurized environments. Part 1: Instrumentation techniques [DE91-012654] N91-28616

STRAIN HARDENING
Erosion studies on a Fe3Al-based iron aluminide and 1100 Al [DE91-012529] N91-28360
Dynamic plasticity in transition from thermal activation to viscous drag [DE91-013031] N91-28617
Crack initiation under generalized plane strain conditions [DE91-013410] N91-28623

STRAIN MEASUREMENT
High-resolution interferometric measurements of residual strains in composites N91-28303

STRAIN RATE
The rate (time)-dependent mechanical behavior of modified 9Cr-1Mo steel. Part 1: Experiments at 538 C [DE91-011097] N91-28615
The DataShoP: A database of weak-shock constitutive data [DE91-013349] N91-28620
Non-steady wave profiles and the fourth-power law [DE91-013576] N91-28631

STRATOCUMULUS CLOUDS
A chemically reacting, turbulent stratified interface N91-28144

STRATOPAUSE
Lidar studies of sporadic sodium layers, gravity waves and density spectra in the mesopause and stratopause regions at Urbana and Arecibo N91-28690

STRATOSPHERE
Regional oxidant model user's guide. Part 1: The ROM preprocessors [PB91-171926] N91-28665
Regional oxidant model user's guide. Part 2: The ROM processor network [PB91-171934] N91-28666
Atmospheric responses to lower tropospheric forcing in a multilayer isentropic model N91-28688
Search for regularities in the atmosphere of Jupiter N91-29127

STRESS ANALYSIS
An abbreviated Reynolds stress turbulence model for airfoil flows N91-28140
F-106B airplane active control landing gear drop test performance N91-28164
On the finite-strain-invariant failure criterion for composites [DE91-011924] N91-28286
Local delamination in laminates with angle ply matrix cracks. Part 1: Tension tests and stress analysis [NASA-TM-104055] N91-28293
Finite element modeling of 2-D delamination growth in laminated composites N91-28302
EXAFS studies of elastic strain in dilute binary alloys [DE91-012678] N91-28353
Effects of residual stresses on the fracture toughness of Zircaloy-2 tubes [DE91-012736] N91-28354
Response of the polymers KEL-F, polysulfone, high density polyethylene and polymethylmethacrylate to shock loading and release from 0.3 to 2.4 GPa [DE91-012867] N91-28411
Design and analysis of the 50 mm collider dipole vacuum vessel [DE91-012490] N91-28610
Analysis of brittle intergranular crack propagation during stress corrosion cracking [DE91-013666] N91-28630
Neutron diffraction determination of the residual stress redistribution in cracked autofrettaged tubing [DE91-013688] N91-28632
Flutter of laminated rectangular plates including finite deflection and shear deformation N91-28639
A study of the buckling and vibration behavior of an initially stressed thick plate by Galerkin's method N91-28641

STRESS CORROSION CRACKING
High-temperature solution annealing as an IASCC mitigation technique [DE91-012220] N91-28352
Critical issues in de-alloying and transcrystalline stress-corrosion cracking [DE91-010190] N91-28608
Analysis of brittle intergranular crack propagation during stress corrosion cracking [DE91-013666] N91-28630

STRESS DISTRIBUTION
Stress fields generated by kinetic energy projectile interaction with ceramic targets [DE91-013687] N91-28625
Neutron diffraction determination of the residual stress redistribution in cracked autofrettaged tubing [DE91-013688] N91-28632

STRESS INTENSITY FACTORS
Critical issues in de-alloying and transcrystalline stress-corrosion cracking [DE91-010190] N91-28608

STRESS MEASUREMENT
Monitoring structural response in pressurized environments. Part 1: Instrumentation techniques [DE91-012654] N91-28616
Residual stress measurement using the pulsed neutron source at LANSCE [DE91-013494] N91-28624

STRESS TENSORS
Numerical models of equilibrium between matter and black holes N91-29101

STRESS WAVES
The SNL, Livermore, Hopkinson bar apparatus for compressive materials testing at high strain-rates [DE91-013132] N91-28612

STRESS-STRAIN RELATIONSHIPS
The rate (time)-dependent mechanical behavior of modified 9Cr-1Mo steel. Part 1: Experiments at 538 C [DE91-011097] N91-28615
Viscoplastic analysis of an experimental cylindrical thrust chamber liner [NASA-TM-103287] N91-28622
Shear stress prediction in shock loaded copper [DE91-014740] N91-28635

STRESSES
Bauschinger effect during shock loading [DE91-014606] N91-28634
Raman studies of stress-induced phase transformation in titania films [DE91-012871] N91-29012

STRING THEORY
Spin 4 and 7/2 extended conformal algebra [DE91-617609] N91-28803
Physics at the Planck scale [DE91-012346] N91-29054

STRONG INTERACTIONS (FIELD THEORY)
Research in theoretical nuclear physics [DE91-013644] N91-28872

STRUCTURAL ANALYSIS
Calculation of interactions between air and ground of landing N91-28161
Probabilistic structural analysis methods for space transportation propulsion systems N91-28238
Viscoplastic analysis of an experimental cylindrical thrust chamber liner [NASA-TM-103287] N91-28622
Stress fields generated by kinetic energy projectile interaction with ceramic targets [DE91-013687] N91-28625
Stability of cylindrical laminates by higher orde r shear deformable theories N91-28638
Probabilistic structural mechanics research for parallel processing computers [NASA-CR-187162] N91-28644

STRUCTURAL DESIGN
Application of the Air Force guide specification 87221A to ground loads N91-28152
Probabilistic structural mechanics research for parallel processing computers [NASA-CR-187162] N91-28644

STRUCTURAL ENGINEERING
A design space and design rules for user interface software architecture [AD-A237049] N91-28748

STRUCTURAL RELIABILITY
Probabilistic structural mechanics research for parallel processing computers [NASA-CR-187162] N91-28644

STRUCTURAL STABILITY
Stability of cylindrical laminates by higher orde r shear deformable theories N91-28638

STRUCTURAL VIBRATION
A study of the buckling and vibration behavior of an initially stressed thick plate by Galerkin's method N91-28641

STRUTS
Recent developments in the area of aircraft rough field performance N91-28154
Landing gear improvements for transport aircraft N91-28159

SUBMERGING
Apparatus for intercalating large quantities of fibrous structures [NASA-CASE-LEW-15077-2] N91-28289

SUBSONIC FLOW
Solution to quasi-axisymmetric internal compressible flows using the stream tube approach N91-28526
Quadrupole phenomena of noise from a subsonic jet impinging on a large, rigid, and flate plate N91-28818

SUBSONIC SPEED
Longitudinal aerodynamic characteristics of a subsonic, energy-efficient transport configuration in the National Transonic Facility [NASA-TP-2922] N91-28143

SUBSTRATES
Pressure transducer and system for cryogenic environments [NASA-CASE-LAR-14579-1] N91-28546
Defect studies in III-V thin film semiconductors [DE91-012746] N91-29011

SULFIDES
Structure and dynamics in low-dimensional guest host solids [DE91-012169] N91-29020

SULFONATES
Preparation of ionic membranes for zinc/bromine storage batteries [DE91-012008] N91-28483

SULFUR
Surface phases and their influence on metal-oxide interfaces [DE91-012277] N91-28995

SUPERCOMPUTERS
Solving computational grand challenges using a network of heterogeneous supercomputers [DE91-013725] N91-28755
Load-balancing and performance of a gridless particle simulation on MIMD, SIMD, and vector supercomputers [DE91-013758] N91-28756
ZLIB: A numerical library for differential algebra (A user's guide for version 1.0) [DE91-012552] N91-28794
Plasma turbulence calculations on supercomputers [DE91-014210] N91-28969

SUPERCONDUCTING FILMS
The superconducting flux flow transistor: Models and applications [DE91-014702] N91-28501
Spectroscopic and ion probe characterization of laser produced plasmas used for thin film growth [DE91-013425] N91-28959
Growth of high T(sub c) superconducting thin films for microwave applications [DE91-011436] N91-28991
High-T(sub c) thin-film microelectronics [DE91-012340] N91-28997
Photolithographically patterened thin-film multilayer devices of YBa2Cu3O(7-x) [DE91-012350] N91-28998
Thin-film flux transformers of YBa2Cu3O(7-x) [DE91-012363] N91-29007
Defect studies in III-V thin film semiconductors [DE91-012746] N91-29011
Kosterlitz-Thouless-like behavior over extended ranges of temperature and layer thickness in crystalline YBa2Cu3O(7-x) / PrBa2Cu3O(7-x) superlattices [DE91-013237] N91-29014

SUPERCONDUCTING MAGNETS
Brittle behavior of SSC yokes [DE91-014031] N91-28370
A 10,000 A 1000 Vdc solid state dump switch [DE91-014141] N91-28497
Improved superconducting bearings [NASA-CASE-GSC-13346-1] N91-28578
Refinement of the Hamilton-Jacobi solution using a second canonical transformation [DE91-012965] N91-28798
Light weight, high field, stable, superconducting magnets for advanced transportation systems [DE91-013667] N91-28814
Ferromagnetic material in the superconductor and its effect on the magnetization sextupole and decapole in the SSC dipoles at injection [DE91-011886] N91-28993
A system approach to the design of superconducting magnets [DE91-012707] N91-29010
The DARPA compact superconducting x-ray lithography source features [DE91-013864] N91-29039
Non similarity solution approximation to the thermal hydraulic quenchback in superconductors [DE91-013964] N91-29040

SUPERCONDUCTING SUPER COLLIDER
Brittle behavior of SSC yokes [DE91-014031] N91-28370
Monolithic front end electronics for silicon calorimeters [DE91-012063] N91-28484
Symplectic full-turn maps in a Fourier representation [DE91-012912] N91-28796

A system approach to the design of superconducting magnets
[DE91-012707] N91-29010
Non similarity solution approximation to the thermal hydraulic quenchback in superconductors
[DE91-013964] N91-29040
Document format considerations for a document tracking and storage system
[DE91-013402] N91-29079

SUPERCONDUCTIVITY
Chemistry and materials science research report
[DE91-011507] N91-28305
Method of preforming and assembling superconducting circuit elements
[NASA-CASE-LAR-14395-1-CU] N91-28490
The superconducting flux flow transistor: Models and applications
[DE91-014702] N91-28501
Phonon-mediated detection of elementary particles using silicon crystal acoustic detectors N91-28547
Improved superconducting bearings
[NASA-CASE-GSC-13346-1] N91-28578
JPRS report: Science and technology. USSR: Physics and mathematics
[JPRS-UPM-90-006] N91-28811
Strongly interacting fermion systems
[DE91-012284] N91-28848
Kosterlitz-Thouless-like behavior over extended ranges of temperature and layer thickness in crystalline YBa2Cu3O(7-x) / PrBa2Cu3O(7-x) superlattices
[DE91-013237] N91-29014
Structure and dynamics in low-dimensional guest host solids
[DE91-012169] N91-29020
The effect of the quantum susceptance on the gain of superconducting quasiparticle mixers
[DE91-012352] N91-29021
Topics on frustrated spin systems and high-temperature superconductors N91-29032
The DARPA compact superconducting x-ray lithography source features
[DE91-013864] N91-29039

SUPERCONDUCTORS
Energy dispersive x ray diffraction study of glassy Bi2Sr2CaCu2O(x) filaments produced by gas-jet fiberization
[DE91-012021] N91-28407
Ultra-high frequency superconductive devices
[AD-A236795] N91-28478
Method of preforming and assembling superconducting circuit elements
[NASA-CASE-LAR-14395-1-CU] N91-28490
Ferromagnetic material in the superconductor and its effect on the magnetization sextupole and decapole in the SSC dipoles at injection
[DE91-011886] N91-28993
Magnetization and critical currents of tin-core multifilamentary Nb3Sn conductors
[DE91-012241] N91-28994
Thermodynamic and transport properties of superconductors in very high magnetic fields
[DE91-012530] N91-29000
Measurement accuracy of macroscopic quantum circuits with RF-biased Josephson junction arrays
[DE91-012651] N91-29009
Excess heat production in composite superconductors during current redistribution
[DE91-013547] N91-29016
Application of muon spin relaxation experiment to the mixed state superconductors
[DE91-013689] N91-29034
Non similarity solution approximation to the thermal hydraulic quenchback in superconductors
[DE91-013964] N91-29040
Overview of the status of and prospects for high-T(sub c) wire and tape development
[DE91-014609] N91-29045

SUPERCOOLING
An extension of a kinetic theory of polymer crystallization through the exclusion of negative barriers
[AD-A236999] N91-28387

SUPERCRITICAL FLUIDS
Supercritical fluids cleaning
[DE91-013374] N91-28456

SUPERCRITICAL WINGS
Longitudinal aerodynamic characteristics of a subsonic, energy-efficient transport configuration in the National Transonic Facility
[NASA-TP-2922] N91-28143

SUPERGRAVITY
Physics at the Planck scale
[DE91-012346] N91-29054
The (2,0) super Beltrami parametrization and superconformal structures
[DE91-617611] N91-29057

SUPERHIGH FREQUENCIES
A microwave interferometer to measure particle and shock velocities simultaneously
[DE91-013077] N91-28545

SUPERLATTICES
Temperature dependence of the elastic behavior of structurally disordered metallic superlattices
[DE91-014007] N91-28377
Kosterlitz-Thouless-like behavior over extended ranges of temperature and layer thickness in crystalline YBa2Cu3O(7-x) / PrBa2Cu3O(7-x) superlattices
[DE91-013237] N91-29014
The determination of the momentum matrix elements involved in calculating the dielectric constants of superlattices using the tight-binding method
[DE91-617789] N91-29017
Direct imaging of ordering in Si-Ge alloys, ultrathin superlattices, and buried Ge layers
[DE91-014580] N91-29044

SUPERNOVAE
Study of gravitational collapse and cosmic ray abundances N91-29105

SUPERPLASTICITY
Test of superplastically formed corrugated aluminum compression specimens with beaded webs
[NASA-TM-104119] N91-28373

SUPERSONIC FLOW
Evaluation of a technique to generate artificially thickened boundary layers in supersonic and hypersonic flows
[NASA-TP-3142] N91-28136
Solution to quasi-axisymmetric internal compressible flows using the stream tube approach N91-28526

SUPERSONIC TURBINES
The application of Particle Image Velocimetry (PIV) in a short duration transonic annular turbine cascade
[AD-A236639] N91-28504

SUPERSYMMETRY
Physics at the Planck scale
[DE91-012346] N91-29054
The (2,0) super Beltrami parametrization and superconformal structures
[DE91-617611] N91-29057

SUPPORT SYSTEMS
Questions: Assessing the structure of knowledge and the use of information in design problem-solving N91-28169

SURFACE DEFECTS
Molecular dynamics simulations of bulk displacement threshold energies in Si
[DE91-011957] N91-28846

SURFACE FINISHING
Cross-sectional TEM specimen preparation of free-standing metal multi-layered films
[DE91-011117] N91-28351
Perspective on plating for precision finishing
[DE91-011927] N91-28394

SURFACE LAYERS
Pretreatment of lubricated surfaces with sputtered cadmium oxide
[NASA-CASE-LEW-14474-1] N91-28423
An experimental investigation of a compliant surface beneath a turbulent boundary layer N91-28523
The surface chemistry of GaAs atomic layer epitaxy
[DE91-014112] N91-29047

SURFACE PROPERTIES
EXAFS studies of elastic strain in dilute binary alloys
[DE91-012678] N91-28353
Polymers at surfaces
[DE91-011000] N91-28392
In-situ REM imaging of surface processes on ceramic bulk crystals from 300 to 1670 K in a conventional TEM
[DE91-009923] N91-28405
Analysis of the surface heterogeneity of different samples of aluminum oxide ceramic powders
[DE91-013527] N91-28421
Polymers at surfaces
[DE91-013642] N91-28430
A comparative second harmonic study of Cu(111) in UHV and in solution
[AD-A237023] N91-28479
An experimental investigation of a compliant surface beneath a turbulent boundary layer N91-28523
Sphere lapping
[DE91-014287] N91-28593
Interactions of molecules with surfaces
[DE91-014498] N91-28857
Surface phases and their influence on metal-oxide interfaces
[DE91-012277] N91-28995

SURFACE REACTIONS
Plasma immersion surface modification with metal ion plasma
[DE91-014233] N91-28979
The surface chemistry of GaAs atomic layer epitaxy
[DE91-014112] N91-29047

SURFACE ROUGHNESS
Recent developments in the area of aircraft rough field performance N91-28154
Receptivity of a laminar boundary layer to the interaction of a three-dimensional roughness element with time-harmonic free-stream disturbances N91-28518

SURFACE TEMPERATURE
Interactions of molecules with surfaces
[DE91-014498] N91-28857

SURFACES
Bayesian design and analysis of computer experiments: Use of derivatives in surface prediction
[DE91-013147] N91-28751

SURFACTANTS
Dynamics of interfaces with internal structures N91-28926

SURVEILLANCE
An evaluation of monochrome solid-state video cameras
[DE91-012368] N91-28543

SURVEYS
Kinematic GPS surveying N91-28149

SWITCHES
A 10,000 A 1000 Vdc solid state dump switch
[DE91-014141] N91-28497

SYMBOLS
Statistical mechanics using symbolic dynamics N91-28940

SYMMETRY
Regular motion and symmetry in the relativistic standard map N91-28933
Electron correlations in solid state physics
[DE91-013752] N91-29030

SYNCHRONOUS SATELLITES
Impact of ion propulsion on performance, design, testing, and operation of a geosynchronous spacecraft
[AD-A237028] N91-28273
Design of an interactive satellite communications system analysis program
[AD-A237030] N91-28459

SYNCHROTRON RADIATION
X ray microimaging of elemental composition and microstructure for materials science
[DE91-012052] N91-28601
The Advanced Light Source: A new tool for research in atomic and molecular physics
[DE91-012860] N91-28844
The DARPA compact superconducting x-ray lithography source features
[DE91-013864] N91-29039

SYNCHROTRONS
Thyristor converter simulation and analysis
[DE91-013802] N91-28494
Development of nanovolt-resolution x ray diffraction using resonant nuclear scattering
[DE91-012217] N91-28847
Beam current monitoring in the AGS booster and its transfer lines
[DE91-013328] N91-28870

SYNTHESIS (CHEMISTRY)
Sol-gel kinetics by NMR
[DE91-011500] N91-28314
Nitrogen and boron-containing polymers as precursors of ceramic materials
[DE91-008890] N91-28390
Ultra-fine powders using glycine-nitrate combustion synthesis
[DE91-012926] N91-28412
Polyimides prepared from 3,5-diamino benzo trifluoride
[NASA-CASE-LAR-14206-1] N91-28425
Synthesis and characterization of reduced ternary molybdenum oxides and soluble copper (III) alkoxide complexes
[DE91-012679] N91-29001
Synthesis and properties of novel cluster phases
[DE91-013006] N91-29013

SYSTEMS ANALYSIS
Design of an interactive satellite communications system analysis program
[AD-A237030] N91-28459
Using HSYS in the analysis of human-system interactions: Examples from the offshore petroleum industry
[DE91-013218] N91-28732

SYSTEMS ENGINEERING
Technology transfer methodology N91-28239
National test bed concept N91-28241
Propulsion system ground testing N91-28261
Considerations for NATO satellite communications in the post 2000 era
[AGARD-AG-330] N91-28465
Automated verification of system configuration
[DE91-012520] N91-28481
Issues concerning centralized versus decentralized power deployment
[NASA-CR-187121] N91-28648

Development of a current collection loss management system for SDI homopolar power supplies
[DE91-012779] N91-28652

SYSTEMS INTEGRATION
A geometry based method of integrated engineering design, analysis, and optimization
[DE91-008588] N91-28457

SYSTEMS MANAGEMENT
The role of the UNIX(tm) central computing facility in a multi-purpose national laboratory
[DE91-012361] N91-28737

T

TABLES (DATA)
Solar-geophysical data number 558, August 1990. Part 2: (Comprehensive reports). Data for August 1990 and miscellaneous
[PB91-172262] N91-29128
Solar-geophysical data number 558, February 1991. Part 1: (Prompt reports). Data for January 1991, December 1990, and late data
[PB91-172270] N91-29129
Solar-geophysical data number 557, January 1991. Part 1: (Prompt reports). Data for December, November 1990 an late data
[PB91-169102] N91-29130
Solar-geophysical data number 557, January 1991. Part 2: (Comprehensive reports). Data for July 1990 and miscellaneous
[PB91-169110] N91-29131

TACTICS
Effectiveness of tiltrotor support to ground combat
[DE91-013603] N91-28167

TAKEOFF
The special requirements of a VSTOL aircraft
N91-28155
Long time measurements of landing gear loads on SAAB SF-340 commuter aircraft N91-28157

TANTALUM NITRIDES
The structure of Ta3N5 at 16K by time-of-flight neutron diffraction
[AD-A236596] N91-28987

TARGETS
Stress fields generated by kinetic energy projectile interaction with ceramic targets
[DE91-013687] N91-28625
Progress in light ion fusion
[DE91-012019] N91-28826

TASK PLANNING (ROBOTICS)
Planning of minimum-time trajectories for robotic arms
[ITN-91-85141] N91-28583

TASKS
Cultural changes in aerospace N91-28265

TAXIING
Long time measurements of landing gear loads on SAAB SF-340 commuter aircraft N91-28157
Operational loads on landing gear N91-28158
Actively damped landing gear system N91-28165

TAXONOMY
Taxonomy and algorithms for volume rendering on multicomputers
[AD-A236632] N91-28771

TAYLOR INSTABILITY
Nonlinear evolution of 2D and 3D Rayleigh-Taylor instability at stagnation phase in laser implosion
N91-28899
Turbulent mixing due to Rayleigh-Taylor instability in laser driven implosion N91-28914
Large growth Rayleigh-Taylor experiments on Nova
[DE91-012885] N91-28955

TEARING MODES (PLASMAS)
Suppression and control of magnetic islands in toroidal plasmas N91-28895

TECHNICAL WRITING
Communicating success: Writing about technology transfer
[DE91-013994] N91-29092

TECHNOLOGIES
Technology transfer methodology N91-28239
Technology transfer methodology N91-28240
Technologies available from Martin Marietta Energy Systems, Inc.
[DE91-013027] N91-28283

TECHNOLOGY ASSESSMENT
Space transportation propulsion USSR launcher technology, 1990 N91-28220
Infusion of instrumentation technology (engine plume diagnostics) into operational test programs N91-28249
The space exploration initiative. Operational efficiency panel space-basing technology requirements
N91-28253
US assessment of the new diamond technology in Japan
[PB91-167395] N91-28404
Proceedings of the 1990 Antenna Applications Symposium, volume 1
[AD-A237056] N91-28460
Proceedings of the 1990 Antenna Applications Symposium, volume 2
[AD-A237057] N91-28461
Electric and hybrid vehicles program
[DE91-013113] N91-28573

TECHNOLOGY TRANSFER
Technology transfer methodology N91-28239
Advancing electric vehicle technology
[DE91-013004] N91-28575
Geothermal materials development
[DE91-013972] N91-28660
Communicating success: Writing about technology transfer
[DE91-013994] N91-29092

TECHNOLOGY UTILIZATION
Advanced propulsion concepts N91-28218
Technology transfer methodology N91-28240
Infusion of instrumentation technology (engine plume diagnostics) into operational test programs N91-28249
Propulsion technologies for near term N91-28262
Space propulsion by fusion in a magnetic dipole
[DE91-012033] N91-28275

TECTONICS
Close-range geophotogrammetric mapping of trench walls using multi-model stereo restitution software
[DE91-013105] N91-28645

TELECOMMUNICATION
Compile-time estimation of communication costs in multicomputers
[NASA-CR-188675] N91-28747

TELEVISION CAMERAS
An evaluation of monochrome solid-state video cameras
[DE91-012368] N91-28543

TEMPERATURE DEPENDENCE
Experimental studies of the volatility of ammonium chloride
[DE91-012526] N91-28311
Temperature dependence of the elastic behavior of structurally disordered metallic superlattices
[DE91-014007] N91-28377
A study of the influence of temperature gradients on densification of glass powder compacts
[DE91-012337] N91-28399
The effect of strong Coulomb correlations on electron-phonon interactions in the copper oxides: Implications for transport
[DE91-013333] N91-28854
Photolithographically patterened thin-film multilayer devices of YBa2Cu3O(7-x)
[DE91-012350] N91-28998
Doping and pressure study of U3Sb4Pt3
[DE91-013669] N91-29033
Scanning tunneling microspectroscopy of solids and surfaces
[DE91-014515] N91-29043

TEMPERATURE DISTRIBUTION
Computer modeling of ceramic melters to assess impacts of process and design variables on performance
[DE91-013668] N91-28431
Numerical solution of a moving boundary problem as a model solution for a solar pipe
[ITN-91-85143] N91-28516
Regional-scale flow in complex terrain: An observational and numerical investigation N91-28680
Search for regularities in the atmosphere of Jupiter
N91-29127

TEMPERATURE EFFECTS
Joining of aluminum-based particulate-reinforced metal-matrix composites N91-28298
The effect of TiB2 reinforcement on the mechanical properties of an Al-Cu-Li alloy-based metal-matrix composite N91-28337
Substructure and electrical resistivity analyses of pure tungsten sheet
[DE91-014098] N91-28362
Effects of various parameters on the fatigue life of alloy 718
[DE91-014100] N91-28380
A study of the influence of temperature gradients on densification of glass powder compacts
[DE91-012337] N91-28399
In-situ REM imaging of surface processes on ceramic bulk crystals from 300 to 1670 K in a conventional TEM
[DE91-009923] N91-28405
Elevated-temperature fracture resistances (K(sub IC), R-curves, gamma sub (omega OF)) of monolithic and composite ceramics using chevron-notched, bend tests
[NASA-TM-105090] N91-28418
Thermal and non-Newtonian effects in elastohydrodynamic lubrication of rolling-sliding contacts
N91-28590
Donor formation under hydrogen plasma exposure and ion implantation
[DE91-011958] N91-29004

TEMPERATURE GRADIENTS
A study of the influence of temperature gradients on densification of glass powder compacts
[DE91-012337] N91-28399
Ion temperature gradient turbulence and coherent structures N91-28890
Numerical study of ion temperature gradient modes in a tokamak N91-28921
Fluctuation spectrum of ion temperature gradient driven modes in sheared magnetic fields N91-28936
Stability of drift-wave modons in the presence of temperature gradients
[DE91-014364] N91-28982
Scanning tunneling microspectroscopy of solids and surfaces
[DE91-014515] N91-29043

TEMPERATURE MEASUREMENT
Resonant method for the measurement of the glass transition temperature at high frequencies
[DE91-618684] N91-28416

TEMPERATURE PROFILES
Optical diagnostic investigation of low Reynolds number nozzle flows N91-28233
Scanning Transmission Ion Microscopy (STIM): A new technique for density mapping of microstructures
[DE91-011917] N91-28825
Hydrodynamic instabilities in laser driven implosion
N91-28897

TEMPORAL DISTRIBUTION
Sound propagation in the atmosphere: Analysis of signal amplitude and phase temporal and spatial variations
[AD-A237034] N91-28816

TENSILE DEFORMATION
Tensile deformation of Al-Cu-Li-Zr alloy 2090-T8E41 at 298 and 77 K
[DE91-011885] N91-28345
Origin of acoustic emission produced during single point machining
[DE91-011915] N91-28453

TENSILE PROPERTIES
Brittle behavior of SSC yokes
[DE91-014031] N91-28370
Effects of various parameters on the fatigue life of alloy 718
[DE91-014100] N91-28380
Shock-wave properties of high-strength ceramics
[DE91-014105] N91-28439

TENSILE STRENGTH
Microstructure-property relationships in Al-Cu-Li-Ag-Mg Weldalite (tm) alloys, part 2
[NASA-CR-4364] N91-28334
The influence of Ag+Mg additions on the nucleation of strengthening precipitates in a non-cold-worked Al-Cu-Li alloy N91-28336
Weldability of Weldalite (tm) 049 with and without TiB2 reinforcement N91-28338
Effect of Li level, artificial aging, and TiB2 reinforcement on the modulus of Weldalite (tm) 049 N91-28340

TENSILE STRESS
The effect of stress on hydrogen uptake and desorption by A-286
[NASA-TM-103537] N91-28341

TENSILE TESTS
Local delamination in laminates with angle ply matrix cracks. Part 1: Tension tests and stress analysis
[NASA-TM-104055] N91-28293
High-temperature solution annealing as an IASCC mitigation technique
[DE91-012220] N91-28352

TENSOR ANALYSIS
Numerical models of equilibrium between matter and black holes N91-29101

TEREPHTHALATE
Cocrystallization in blends of poly(butylene terephthalate) and poly(ester-ether) segmented block copolymers
[DE91-012224] N91-28438

TERMINAL BALLISTICS
Fluctuations in near-surface backscattering to a descending CW radar
[ITN-91-85140] N91-28469
MESA: A 3-D Eulerian hydrocode for penetration mechanics studies
[DE91-013308] N91-28613

TERRAIN
Regional-scale flow in complex terrain: An observational and numerical investigation N91-28680

TEST EQUIPMENT
Modification and evaluation of Elastomer Test Machine (ETM)
[AD-A236143] N91-28540

TEST FACILITIES
Air combat environment test and evaluation facility and the development of the offensive sensors laboratory
[DE91-011398] N91-28173
National test bed concept N91-28241
Analytical electron microscopy of catalyst preparations
[DE91-014126] N91-28328
Meteorological instrumentation support for an adverse weather test facility
[AD-A236605] N91-28696
TETRAHEDRONS
Radiation disorder and aperiodicity in irradiated ceramics
[DE91-010257] N91-28391
TEXTILES
Damage development under compression-compression fatigue loading in a stitched uniwoven graphite/epoxy composite material
[NASA-CR-188693] N91-28292
TEXTURES
Crystal surface analysis using matrix textural features classified by a probabilistic neural network
[DE91-014120] N91-29048
THALLIUM COMPOUNDS
Annealing and structure studies on Tl-2223 and Tl-1223 crystals
[DE91-014903] N91-29052
THEMATIC MAPPERS (LANDSAT)
Results of agriclimatological studies using multiple satellite sensors like NOAA AVHRR; GMS IR; and LANDSAT MSS and TM
[DE91-618773] N91-28698
THEOREM PROVING
Automated reasoning contributes to mathematics and logic
[DE91-014005] N91-28765
THEORETICAL PHYSICS
Spin 4 and 7/2 extended conformal algebra
[DE91-617609] N91-28803
Theoretical research in intermediate-energy nuclear physics
[DE91-012720] N91-28838
Theoretical studies in nuclear physics
[DE91-013909] N91-28873
THERMAL ANALYSIS
Linked gas chromatograph-thermal energy analyzer/ion trap mass spectrometer
[DE91-013585] N91-28326
THERMAL BATTERIES
Feasibility study of a 200 ampere battery
[DE91-014673] N91-28496
THERMAL CONDUCTIVITY
High-resolution measurements of the thermal conductivity and boundary resistance of helium-4 near the lambda point N91-28322
Thermal conductivity of solid hydrogen at low temperature N91-28330
Models for heat transport through assemblies of uniform-diameter hollow spheres
[DE91-012998] N91-28512
Coupling device with improved thermal interface
[NASA-CASE-GSC-13251-1] N91-28582
Geothermal materials development
[DE91-013972] N91-28660
THERMAL CYCLING TESTS
Composite material systems for hydrogen management N91-28229
Plastic analysis of a circular rod subjected to sinusoidal thermal cycling
[DE91-011845] N91-28609
THERMAL DIFFUSIVITY
Anomalous transport due to the skin size electromagnetic drift mode in tokamaks N91-28902
THERMAL ENERGY
Linked gas chromatograph-thermal energy analyzer/ion trap mass spectrometer
[DE91-013585] N91-28326
THERMAL EXPANSION
Flush mounting of thin film sensors
[NASA-CASE-LAR-14446-1] N91-28454
THERMAL FATIGUE
Softening mechanisms and microstructural instabilities during high temperature, low cycle fatigue of Ni, Ni3Al, and their metal matrix composites
[DE91-012714] N91-28287
Microstructural characterization of solders and brazes for advanced packaging technology
[DE91-011503] N91-28379
THERMAL INSULATION
Models for heat transport through assemblies of uniform-diameter hollow spheres
[DE91-012998] N91-28512
THERMAL SHOCK
Assessment of ductile fracture methodology based on applications to large-scale experiments
[DE91-009920] N91-28614
THERMAL STABILITY
Relationships between polymer-additive molecular structure and intumescent flame retardant behavior N91-28426
Sealant research for SOFC
[DE91-014012] N91-28592
Evolution of defect cluster distributions during irradiation
[DE91-013405] N91-29024
THERMAL STRESSES
An analysis of interlaminar stresses in unsymmetrically laminated plates N91-28299
THERMIONIC POWER GENERATION
Small Ex-core Heat Pipe Thermionic Reactor concept (SEHPTR)
[DE91-014073] N91-28279
THERMODYNAMIC EFFICIENCY
Optimization and thermodynamic performance measures for a class of finite time thermodynamic cycles N91-29060
THERMODYNAMIC EQUILIBRIUM
Inorganic components of atmospheric aerosols N91-28668
Numerical models of equilibrium between matter and black holes N91-29101
THERMODYNAMIC PROPERTIES
Investigation of thermomechanical behavior of metal matrix composites N91-28296
Thermodynamic and transport properties of superconductors in very high magnetic fields
[DE91-012530] N91-29000
TOPAZ2D benchmark problems nonlinear materials
[DE91-009753] N91-29053
THERMODYNAMICS
Experimental studies of the volatility of ammonium chloride
[DE91-012526] N91-28311
Thermodynamics and efficiency in combustion and engines
[DE91-012781] N91-28320
Thermodynamic and kinetic aspects of surface acidity
[DE91-014039] N91-28331
Relaxed state and entropy production N91-28907
Equilibria and dynamics of temperature in a fusion reactor plasma N91-28937
Defects and transport in mixed oxides
[DE91-014443] N91-29049
THERMOELASTICITY
An analysis of interlaminar stresses in unsymmetrically laminated plates N91-28299
THERMOELECTRIC GENERATORS
Comparison of dynamic isotope power systems for distributed planet surface applications
[NASA-TM-4303] N91-28278
THERMOELECTRIC POWER GENERATION
Topics on frustrated spin systems and high-temperature superconductors N91-29032
THERMOELECTRICITY
Topics on frustrated spin systems and high-temperature superconductors N91-29032
THERMOGRAVIMETRY
Thermodynamic and kinetic aspects of surface acidity
[DE91-014039] N91-28331
THERMOPHYSICAL PROPERTIES
Integrated theoretical and experimental study of the thermophysical properties of fluid mixtures
[DE91-012660] N91-28316
THERMOPLASTIC RESINS
The influence of defects on the mechanical properties of short fibre reinfornced thermoplastics N91-28300
Durability of polymeric materials used in zinc/bromine flow batteries
[DE91-012864] N91-28487
THERMOSPHERE
Observations and theoretical studies of tides and normal modes in the lower thermosphere N91-28681
THICK FILMS
Some high voltage DC breakdown properties of thick film circuits on alumina
[DE91-014675] N91-28500
X ray fiducial foils
[DE91-011193] N91-28542
THICK PLATES
A study of the buckling and vibration behavior of an initially stressed thick plate by Galerkin's method N91-28641
THICKNESS
Advancements in ultrathinning section techniques for the characterization of brittle materials
[DE91-012930] N91-28364
THIN FILMS
Photocross-linked second order nonlinear optical polymers
[AD-A235855] N91-28385
Radiation damage of ceramics by electron microscopy
[DE91-012186] N91-28396
Mechanical properties of diamond and diamond-like films
[DE91-011373] N91-28406
Flush mounting of thin film sensors
[NASA-CASE-LAR-14446-1] N91-28454
Ultra-high frequency superconductive devices
[AD-A236795] N91-28478
Phonon-mediated detection of elementary particles using silicon crystal acoustic detectors N91-28547
Thin film hydrogen sensor
[DE91-014197] N91-28550
Critical issues in de-alloying and transcrystalline stress-corrosion cracking
[DE91-010190] N91-28608
Polycrystalline thin film photovoltaic technology
[DE91-002136] N91-28650
Spectroscopic and ion probe characterization of laser produced plasmas used for thin film growth
[DE91-013425] N91-28959
The structure of Ta3N5 at 16K by time-of-flight neutron diffraction
[AD-A236596] N91-28987
High-T(sub c) thin-film microelectronics
[DE91-012340] N91-28997
Photolithographically patterened thin-film multilayer devices of YBa2Cu3O(7-x)
[DE91-012350] N91-28998
Biomimetic thin film deposition
[DE91-012485] N91-28999
Thin-film flux transformers of YBa2Cu3O(7-x)
[DE91-012363] N91-29007
Defect studies in III-V thin film semiconductors
[DE91-012746] N91-29011
Raman studies of stress-induced phase transformation in titania films
[DE91-012871] N91-29012
Kinetics of solid-state reactions in Ni-Zr thin films
[DE91-013652] N91-29028
Metastable phase equilibria in co-deposited Ni(1-x)Zr(x) thin films
[DE91-013653] N91-29029
THIN PLATES
An analysis of interlaminar stresses in unsymmetrically laminated plates N91-28299
Numerical and analytical analysis of thin laser-driven flyer plates
[DE91-013748] N91-28567
THREE BODY PROBLEM
Chaos in the lowest Landau level
[DE91-014800] N91-28866
THREE DIMENSIONAL FLOW
Numerical simulation of particle-wave interaction in boundary layers
[NASA-CR-187312] N91-28502
Algorithm and code development for unsteady three-dimensional Navier-Stokes equations
[NASA-CR-188039] N91-28503
ZEPHYR3D: A finite difference computer program for three-dimensional, transient incompressible flow problems
[DE91-014331] N91-28515
Receptivity of a laminar boundary layer to the interaction of a three-dimensional roughness element with time-harmonic free-stream disturbances N91-28518
THREE DIMENSIONAL MODELS
Computer simulation of an aircraft seat and occupant(s) in a crash environment: Program SOM-LA/SOM-TA user manual
[CR-R-90026] N91-28146
A gravity model for the Coso geothermal area, California
[DE91-011874] N91-28677
Seismic traveltime inversion in three-dimensional heterogeneous media N91-28678
A numerical simulation of a tornado-scale vortex in a three-dimensional cloud model N91-28705
Three-dimensional particle simulation of trapped electron instabilities in tokamaks N91-28891
THREE DIMENSIONAL MOTION
High order calculation of the multipole content of three dimensional electrostatic geometries
[DE91-014707] N91-28476
THRUST
Numerical investigation of the thrust efficiency of a laser-propelled vehicle N91-28572
THRUST CHAMBERS
Liquid jet breakup and atomization in rocket chambers under dense spray conditions N91-28227
Viscoplastic analysis of an experimental cylindrical thrust chamber liner
[NASA-TM-103287] N91-28622
THRUST VECTOR CONTROL
Attitude control of a spinning rocket via thrust vectoring
[DE91-006267] N91-28274

THUNDERSTORMS
Low-level curvature shear and supercell thunderstorm behavior N91-28701
Predicting thunderstorm evolution using ground-based lightning detection networks N91-28702
THYRISTORS
Thyristor converter simulation and analysis [DE91-013802] N91-28494
TIDES
Observations and theoretical studies of tides and normal modes in the lower thermosphere N91-28681
TILES
Thermally activated retainer means [NASA-CASE-MSC-21793-1] N91-28186
TIME DEPENDENCE
The rate (time)-dependence mechanical behavior of modified 9Cr-1Mo. Part 2: Isothermal modeling at 538 C [DE91-011100] N91-28350
The numerical solution of confined laminar flow past a moving boundary N91-28532
The rate (time)-dependent mechanical behavior of modified 9Cr-1Mo steel. Part 1: Experiments at 538 C [DE91-011097] N91-28615
Parallelizing across time when solving time-dependent partial differential equations [DE91-012948] N91-28797
Exact solution of a quantum forced time-dependent harmonic oscillator [AD-A236633] N91-28812
Optical analogs of model atoms in fields [DE91-013392] N91-28855
Equilibria and dynamics of temperature in a fusion reactor plasma N91-28937
The 2+1 gravity: A new approach N91-29059
TIME LAG
Measurement of the microwave propagation delay induced by atmospheric water vapor N91-28466
TIME SERIES ANALYSIS
Nonlinear modeling of chaotic time series: Theory and applications [DE91-013076] N91-29055
Search for regularities in the atmosphere of Jupiter N91-29127
TIMOSHENKO BEAMS
Explicit models for proportional damping in Timoshenko beams N91-28642
TIN ALLOYS
Improving fatigue life in near-eutectic Sn Pb solders [DE91-013844] N91-28603
TIN COMPOUNDS
Magnetization and critical currents of tin-core multifilamentary Nb3Sn conductors [DE91-012241] N91-28994
TIRES
Method and apparatus for cleaning rubber deposits from airport runways and roadways [NASA-CASE-LAR-14483-1] N91-28455
TISSUES (BIOLOGY)
Ion beam sputtered coatings of bioglass N91-28384
TITANIA
Raman studies of stress-induced phase transformation in titania films [DE91-012871] N91-29012
TITANIUM
Phonon-mediated detection of elementary particles using silicon crystal acoustic detectors N91-28547
TITANIUM ALLOYS
JPRS report: Science and technology. USSR: Materials science [JPRS-UMS-91-003] N91-28342
Rapid solidification processing of Al3Ti and Al3Ti plus copper [AD-A236600] N91-28343
Synthesis of metastable aluminum-based intermetallics by mechanical alloying [DE91-013651] N91-28376
Changes with material properties of acoustic emission produced during single point machining [DE91-011913] N91-28452
TITANIUM OXIDES
Ordered ceramic membranes [DE91-012248] N91-28398
X ray diffraction study of heteroepitaxy of MOCVD grown TiO2 and VO2 films on sapphire single crystals [DE91-013764] N91-29037
TOKAMAK DEVICES
An assessment of the lifetime of Faraday shield elements [DE91-012228] N91-28463
Self-organizing processes in magnetically confined plasma N91-28883
Three-dimensional particle simulation of trapped electron instabilities in tokamaks N91-28891
Suppression and control of magnetic islands in toroidal plasmas N91-28895
Issues in direct numerical simulation of plasma turbulence and transport N91-28901
Anomalous transport due to the skin size electromagnetic drift mode in tokamaks N91-28902
Internal kink mode simulation by 3-D gyrokinetic code N91-28916
Study of kink instability and current relaxation by three dimensional macroscale particle simulation N91-28919
Numerical study of ion temperature gradient modes in a tokamak N91-28921
Shock and soliton structures induced by poloidal flow in tokamaks N91-28929
Non-linear behaviour in tokamaks N91-28935
Fluctuation spectrum of ion temperature gradient driven modes in sheared magnetic fields N91-28936
Model for marfe-detached plasma transition in tokamaks N91-28938
Confinement projections for the Burning Plasma Experiment (BPX) [DE91-012516] N91-28946
Measurement of magnetic properties of confined compact toroid plasma (spheromak) [DE91-012397] N91-28950
Evidences of trapping in tungsten and implications for plasma-facing components [DE91-012734] N91-28951
Implications of TAE modes for the design of ITER [DE91-013128] N91-28952
Transport profiles induced by radially localized modes in tokamak [DE91-014366] N91-28964
Formation and sustainment of a very low aspect ration tokamak using coaxial helicity injection (the Helicity Injected Torus (HIT) experiment) [DE91-013948] N91-28967
A portable and independent edge fluctuation diagnostic [DE91-014357] N91-28971
Progress in the development of a numerical tokamak [DE91-013386] N91-28975
Plasma properties [DE91-013933] N91-28978
Maryland controlled fusion research program [DE91-014358] N91-28980
Joint proposal for US/USSR on nonlinear dynamics and plasma transport [DE91-014360] N91-28981
Sawteeth in the MST reversed field pinch [DE91-014288] N91-29126
TOLLMIEN-SCHLICHTING WAVES
Numerical simulation of particle-wave interaction in boundary layers [NASA-CR-187312] N91-28502
TOMOGRAPHY
The application of x ray tomographic microscopy to chemical vapor infiltration processing of ceramic matrix composites [DE91-011871] N91-28284
Proton Energy Loss (PEL) material characterization [DE91-011545] N91-28306
Scanning Transmission Ion Microscopy (STIM): A new technique for density mapping of microstructures [DE91-011917] N91-28825
TOPOGRAPHY
Close-range geophotogrammetric mapping of trench walls using multi-model stereo restitution software [DE91-013105] N91-28645
TOPOLOGY
Computing minimal surfaces via level set curvature flow [DE91-014709] N91-28759
Diffusion through stochastic webs in two and more dimensions N91-28941
TORNADOES
Low-level curvature shear and supercell thunderstorm behavior N91-28701
A numerical simulation of a tornado-scale vortex in a three-dimensional cloud model N91-28705
TOROIDAL PLASMAS
Perturbation treatment of the longitudinal coupling impedance of a toroidal beam tube [DE91-013884] N91-28495
Self-organizing processes in magnetically confined plasma N91-28883
Hybrid fluid/kinetic descriptions of tokamak plasmas N91-28888
Ion temperature gradient turbulence and coherent structures N91-28890
Three-dimensional particle simulation of trapped electron instabilities in tokamaks N91-28891
Equilibrium beta limit of helical systems N91-28894
Suppression and control of magnetic islands in toroidal plasmas N91-28895
Relaxed state and entropy production N91-28907
Simulation study of MHD relaxation and reconnection processes N91-28908
Finite beta equilibrium for a pressure configuration N91-28909
Electrostatic particle simulations of density and temperature driven modes in a toroidal plasma N91-28915
Particle simulation on the tilt stabilization of the FRC plasma N91-28917
Shock and soliton structures induced by poloidal flow in tokamaks N91-28929
Propagation of drift waves in toroidal plasma systems N91-28939
Characteristics of edge plasma turbulence on the ATF torsatron [DE91-012981] N91-28947
Measurement of magnetic properties of confined compact toroid plasma (spheromak) [DE91-012397] N91-28950
Implications of TAE modes for the design of ITER [DE91-013128] N91-28952
Maryland controlled fusion research program [DE91-014358] N91-28980
Performance of the 10-kV, 5-MA pulsed-power system for the FRX-C compression experiment [DE91-014745] N91-28983
Sawteeth in the MST reversed field pinch [DE91-014288] N91-29126
TORQUE
Roller locking brake [NASA-CASE-GSC-13376-1] N91-28579
TORSION
Suspension device for low-frequency structures [NASA-CASE-LAR-14272-1-CU] N91-28184
TORUSES
Structures of magnetic field lines in the helical torus N91-28932
Regular motion and symmetry in the relativistic standard map N91-28933
TOUCHDOWN
Development of undercarriage design loads N91-28153
TOWING
Long time measurements of landing gear loads on SAAB SF-340 commuter aircraft N91-28157
TOXIC HAZARDS
Assessing the risk of transporting hazardous materals by aircraft: A case study [DE91-014016] N91-28147
The use of science in the management of hazardous air pollutants N91-28667
TRACKING (POSITION)
Symplectic full-turn maps in a Fourier representation [DE91-012912] N91-28796
TRACTION
Thermal and non-Newtonian effects in elastohydrodynamic lubrication of rolling-sliding contacts N91-28590
TRAJECTORY ANALYSIS
Applications of low lift to drag ratio aerobrakes using angle of attack variation for control [NASA-TM-103544] N91-28189
The symbolic computation and automatic analysis of trajectories [NASA-CR-188159] N91-28787
TRAJECTORY OPTIMIZATION
Planning of minimum-time trajectories for robotic arms [ITN-91-85141] N91-28583
TRAJECTORY PLANNING
Planning of minimum-time trajectories for robotic arms [ITN-91-85141] N91-28583
TRANSATMOSPHERIC VEHICLES
National Aero-Space Plane (NASP) program N91-28214
TRANSDUCERS
Acoustophoresis method and apparatus [NASA-CASE-LAR-13388-1] N91-28321
TRANSFER FUNCTIONS
Order reduction and synthesis of transfer function models N91-28769
TRANSFER ORBITS
Current systems: Upper stages N91-28201
TRANSFORMATIONS (MATHEMATICS)
Refinement of the Hamilton-Jacobi solution using a second canonical transformation [DE91-012965] N91-28798
TRANSFORMERS
Thin-film flux transformers of YBa2Cu3O(7-x) [DE91-012363] N91-29007
TRANSIENT RESPONSE
Irradiation creep by climb-enabled glide driven by transient point defect processes [DE91-012950] N91-28348
TRANSISTORS
Microstructural characterization of solders and brazes for advanced packaging technology [DE91-011503] N91-28379

The superconducting flux flow transistor: Models and applications
[DE91-014702] N91-28501

TRANSIT TIME
Transit time for resonant tunneling
[DE91-617799] N91-29018

TRANSITION FLOW
Experimental investigation of pressure drop and heat transfer for air flow through enhanced tubes
[DE91-012151] N91-28508
Study of spherical couette flow via 3-D spectral simulations: Large and narrow-gap flows and their transitions N91-28520

TRANSITION METALS
Transition metal activation and functionalization of carbon-hydrogen bonds
[DE91-014261] N91-28332
The pressure-induced Mott transition in transition-metal iodides
[DE91-013671] N91-28366
Magnetic studies of iron-rare-earth-metalloid alloys
[DE91-013856] N91-28368
Photoinduced charge and energy transfer processes in molecular aggregates
[DE91-014383] N91-28864

TRANSITION POINTS
High-resolution measurements of the thermal conductivity and boundary resistance of helium-4 near the lambda point N91-28322
Effect of pressure on mode transition point of partially relaxed states with peripheral loss N91-28906

TRANSITION TEMPERATURE
Resonant method for the measurement of the glass transition temperature at high frequencies
[DE91-618684] N91-28416

TRANSMISSION
Transmission/reflection and short-circuit line permittivity measurements
[PB91-171959] N91-28482
Color effects in optical systems
[ITN-91-85150] N91-28878

TRANSMISSION LOSS
Tropospheric scatter propagation at 5 and 16 GHz: Results for a 161 km path
[AD-A237012] N91-28458

TRANSMITTANCE
The in-flight calibration of a helicopter-mounted Daedalus multispectral scanner
[DE91-013054] N91-28170

TRANSONIC FLOW
A comparison of the potential and the Euler formulations of the equations of motion for transonic flow
[DE91-014731] N91-28142
The application of Particle Image Velocimetry (PIV) in a short duration transonic annular turbine cascade
[AD-A236639] N91-28504

TRANSONIC WIND TUNNELS
A study of residual interference effects in adaptive wall testing of a 7-inch chord CAST-10-2/DOA 2 airfoil model
[NASA-CR-4390] N91-28138

TRANSPARENCE
Interpreting solidification phenomena and microstructural evolution in metals through the use of transparent model alloy systems
[DE91-012629] N91-28347
Cross-sectional TEM specimen preparation of free-standing metal multi-layered films
[DE91-011117] N91-28351

TRANSPORT PROPERTIES
Inorganic components of atmospheric aerosols
N91-28668
Beam structure and transverse emittance studies of high-energy ion beams
[DE91-013499] N91-28871
Proceedings of the Second International Toki Conference on Plasma Physics and Controlled Nuclear Fusion. Nonlinear Phenomena in Fusion Plasmas: Theory and Computer Simulation
[NIFS-PROC-6] N91-28881
Nonlinear phenomena and processes in high energy plasmas N91-28882
The theory of turbulence and anomalous transport in plasmas: Past, present, and future N91-28889
Three-dimensional particle simulation of trapped electron instabilities in tokamaks N91-28891
Edge anomalous transport in heliotron/torsatron
N91-28892
Anomalous transport due to the skin size electromagnetic drift mode in tokamaks N91-28902
Nonlinear behavior and transport property of multiple-helicity resistive interchange modes near marginally stable states N91-28922
Plasma transport in a new cathodic arc ion source, theory and experiment
[DE91-011511] N91-28944
Characteristics of edge plasma turbulence on the ATF torsatron
[DE91-012981] N91-28947
Transport profiles induced by radially localized modes in tokamak
[DE91-014366] N91-28964
A portable and independent edge fluctuation diagnostic
[DE91-014357] N91-28971
Thermodynamic and transport properties of superconductors in very high magnetic fields
[DE91-012530] N91-29000

TRANSPORT THEORY
New techniques in neutron data measurements above 30 MeV
[DE91-013690] N91-28861

TRANSPORTATION
Shuttle derived manned transportation systems
N91-28204
Electric and hybrid vehicles program
[DE91-013113] N91-28573

TRANSPUTERS
Numerical analyses of aero-optical flows: An application of parallel algorithm on high-performance Personal Computer (PC) base multitransputer system N91-28519

TRANSVERSE OSCILLATION
Spray combustion under oscillatory pressure conditions N91-28226

TRAPPED PARTICLES
Three-dimensional particle simulation of trapped electron instabilities in tokamaks N91-28891

TRAPPING
Evidences of trapping in tungsten and implications for plasma-facing components
[DE91-012734] N91-28951

TRAVELING WAVES
Localized waves in complex environments
[DE91-011934] N91-28462
A chopper driven 11.4-GHz traveling-wave RF generator
[DE91-013568] N91-28489
A 2D field solver for periodic structures with special corner elements
[DE91-012323] N91-28792

TREES (MATHEMATICS)
Concurrent access to O-trees
[DE91-014348] N91-28782
Using trees to compute approximate solutions to ordinary differential equations exactly
[LAC90-R24] N91-28788
Computations involving differential operators and their actions on functions N91-28789
Bialgebra deformations and algebras of trees
N91-28790

TREES (PLANTS)
TREE: A model of the effects of acid precipitation and air pollutants on the growth of trees
[DE91-014131] N91-28672

TRIBOLOGY
Tribology of aluminum-based metal matrix composites: Fundamental study of wear behavior as influenced by microstructure N91-28297

TRIODES
Modeling of a 1700-MHz cluster cavity of planar triodes
[DE91-013049] N91-28488

TRITIUM
Aerogel composites for radioluminescent light/power sources
[DE91-012012] N91-28395
Gas evolution from spheres
[DE91-012807] N91-28510
Enhancing atom densities in solid hydrogen by isotopic substitution
[DE91-011189] N91-28824

TROPICAL METEOROLOGY
A study of El Nino/Southern Oscillation: Numerical experiments and data analysis N91-28710

TROPICAL REGIONS
A study of El Nino/Southern Oscillation: Numerical experiments and data analysis N91-28710
Interactions between the north Pacific Ocean and the Northern Hemisphere atmosphere during El Nino
N91-28711

TROPOSPHERE
Atmospheric responses to lower tropospheric forcing in a multilayer isentropic model N91-28688
On the initiation of surface cyclones by upper tropospheric disturbances N91-28704

TROPOSPHERIC SCATTERING
Tropospheric scatter propagation at 5 and 16 GHz: Results for a 161 km path
[AD-A237012] N91-28458

TROPOSPHERIC WAVES
On the initiation of surface cyclones by upper tropospheric disturbances N91-28704

TROUGHS
Numerical solution of a free-boundary viscous flow
N91-28529

TRUSSES
The solution of variable-geometry truss problems using new homotopy continuation methods N91-28640

TUBES
Effects of residual stresses on the fracture toughness of Zircaloy-2 tubes
[DE91-012736] N91-28354
Pressure drop and heat transfer for spirally fluted tubes including validation of the role of transition
[DE91-012242] N91-28509

TUNGSTEN
Substructure and electrical resistivity analyses of pure tungsten sheet
[DE91-014098] N91-28362
Adhesion between CVD diamond films and tungsten
[DE91-013757] N91-28434
Evidences of trapping in tungsten and implications for plasma-facing components
[DE91-012734] N91-28951

TUNGSTEN OXIDES
Model catalytic oxidation studies using supported monometallic and heterobimetallic oxides
[DE91-012144] N91-28409

TURBINE BLADES
An experimental investigation of the effect of vortex generators on the aerodynamic characteristics of a NACA 0021 airfoil undergoing large amplitude pitch oscillations
[DE91-012102] N91-28133
Development of biomass as an alternative fuel for gas turbines
[DE91-012129] N91-28441

TURBINE PUMPS
Robust and real-time control of magnetic bearings for space engines N91-28230
Analysis of foil bearings for high speed operation in cryogenic applications N91-28231

TURBOMACHINERY
Composite material systems for hydrogen management N91-28229

TURBULENCE
Droplet-turbulence interactions in subcritical and supercritical evaporating sprays N91-28228
A critical analysis of anisotropic k-epsilon modeling and its application to turbulence-driven secondary flows
N91-28533
Numerical simulation of the air and fuel mixing process in fuel-injected engines using discrete vortex dynamics
N91-28587
Reversed-Field Pinch dynamics and transport studies
[DE91-014317] N91-28970
Joint proposal for US/USSR on nonlinear dynamics and plasma transport
[DE91-014360] N91-28981

TURBULENCE EFFECTS
A review of theories for flowing granular materials with applications to fluidized beds and solids transport
[DE91-013111] N91-28514
Experiments on the instabilities in swirling and non-swirling free jets N91-28531
Characteristics of edge plasma turbulence on the ATF torsatron
[DE91-012981] N91-28947

TURBULENCE MODELS
An abbreviated Reynolds stress turbulence model for airfoil flows N91-28140

TURBULENT BOUNDARY LAYER
Evaluation of a technique to generate artificially thickened boundary layers in supersonic and hypersonic flows
[NASA-TP-3142] N91-28136
A study of methods to investigate nozzle boundary layer transition N91-28232
An experimental investigation of a compliant surface beneath a turbulent boundary layer N91-28523

TURBULENT FLOW
An abbreviated Reynolds stress turbulence model for airfoil flows N91-28140
Experimental investigation of pressure drop and heat transfer for air flow through enhanced tubes
[DE91-012151] N91-28508
ZEPHYR3D: A finite difference computer program for three-dimensional, transient incompressible flow problems
[DE91-014331] N91-28515
Experimental study of growth rate enhancement and structure of compressible turbulent free shear layers
N91-28517
Experimental and theoretical investigation of unsteady forced convection in ducts N91-28524
An experimental study of the effect of small particles on the fluid turbulence in fully developed flow of air in a horizontal pipe N91-28525

A critical analysis of anisotropic k-epsilon modeling and its application to turbulence-driven secondary flows N91-28533

Near-wall modelling of complex turbulent flows N91-28534

The computation of complex, two-dimensional turbulent flows using Reynolds stress closure N91-28535

Prediction of the flow and heat transfer between a rotating and a stationary cone N91-28536

Diffraction patterns produced by periodic and turbulent flowing gases including applications of photorefractive temporal filtering [DE91-012636] N91-28553

Modelling and analysis of geophysical turbulence: Use of optimal transforms and basis sets N91-28686

Quadrupole phenomena of noise from a subsonic jet impinging on a large, rigid, and flate plate N91-28818

Log-stable distribution of energy dissipation in turbulence N91-28885

Issues in direct numerical simulation of plasma turbulence and transport N91-28901

TURBULENT MIXING

A chemically reacting, turbulent stratified interface N91-28144

Studies in cloud physics: Electrification, glaciation, and turbulence N91-28684

Turbulent mixing due to Rayleigh-Taylor instability in laser driven implosion N91-28914

TWO DIMENSIONAL FLOW

Numerical simulation of particle-wave interaction in boundary layers [NASA-CR-187312] N91-28502

Numerical solution of a free-boundary viscous flow N91-28529

Use of a rotated Riemann solver for the two-dimensional Euler equations N91-28530

The numerical solution of confined laminar flow past a moving boundary N91-28532

The computation of complex, two-dimensional turbulent flows using Reynolds stress closure N91-28535

A study on particle dispersion in two-dimensional mixing layer flows N91-28537

TWO DIMENSIONAL MODELS

Finite element modeling of 2-D delamination growth in laminated composites N91-28302

Applications of a 2-D moving finite element formulation to elastic/viscoplastic dynamic fracture analysis [DE91-009930] N91-28607

A gravity model for the Coso geothermal area, California [DE91-011874] N91-28677

TWO FLUID MODELS

Transient two-phase flow of cryogenic fluid in a vertical transfer line during the cooldown process N91-28522

TWO PHASE FLOW

Analysis of shock propagation and shock-initiated reaction in granular energetic materials N91-28446

Study of interfacial behavior in cocurrent gas-liquid flows [DE91-013008] N91-28511

A review of theories for flowing granular materials with applications to fluidized beds and solids transport [DE91-013111] N91-28514

Transient two-phase flow of cryogenic fluid in a vertical transfer line during the cooldown process N91-28522

An experimental study of the effect of small particles on the fluid turbulence in fully developed flow of air in a horizontal pipe N91-28525

A mathematical model for two-phase water, air, and heat flow around a linear heat source emplaced in a permeable medium [DE91-014614] N91-28527

A laser based technique for particle sizing to study two phase expansion in turbines [DE91-014172] N91-28595

U

U.S.S.R. SPACE PROGRAM

Space transportation propulsion USSR launcher technology, 1990 N91-28220

ULTRAHIGH FREQUENCIES

Impact of ion propulsion on performance, design, testing, and operation of a geosynchronous spacecraft [AD-A237028] N91-28273

ULTRAHIGH VACUUM

A comparative second harmonic study of Cu(111) in UHV and in solution [AD-A237023] N91-28479

ULTRAVIOLET ASTRONOMY

Coordinated optical and ultraviolet observations of short period RS CVn and W UMa type stars N91-29096

ULTRAVIOLET RADIATION

Interaction of radiation with outflows in late-type stars N91-29136

UNDERCARRIAGES

Development of undercarriage design loads N91-28153

Actively damped landing gear system N91-28165

UNIFIED FIELD THEORY

Phase transitions triggered by quantum fluctuations in the inflationary universe [NASA-CR-188698] N91-29112

UNIQUENESS THEOREM

Non-Hausdorff twistor spaces and the global structure of space-time N91-29103

UNITED STATES

Current systems: Upper stages N91-28201

Prediction of high level vibration test results by use of available inelastic analysis techniques [DE91-009437] N91-28606

UNIVERSE

Aspects of reheating in first-order inflation [NASA-CR-188705] N91-29108

Phase transitions triggered by quantum fluctuations in the inflationary universe [NASA-CR-188698] N91-29112

Void probability as a function of the void's shape and scale-invariant models [NASA-CR-188696] N91-29113

The line of gravitation: On the quantization conditions in curved spacetime and uncertainty-driven inflation N91-29115

Gravitational evolution of large-scale structure in the universe N91-29121

UNIX (OPERATING SYSTEM)

The role of the UNIX(tm) central computing facility in a multi-purpose national laboratory [DE91-012361] N91-28737

UNMANNED SPACECRAFT

Next generation: Unmanned launch vehicles and upper stages: The needs N91-28210

UNSTEADY AERODYNAMICS

A methodology for using nonlinear aerodynamics in aeroservoelastic analysis and design [NASA-TM-104087] N91-28131

UNSTEADY FLOW

Experimental flutter boundaries with unsteady pressure distributions for the NACA 0012 Benchmark Model [NASA-TM-104072] N91-28137

Algorithm and code development for unsteady three-dimensional Navier-Stokes equations [NASA-CR-188039] N91-28503

ZEPHYR3D: A finite difference computer program for three-dimensional, transient incompressible flow problems [DE91-014331] N91-28515

UPPER STAGE ROCKET ENGINES

Next generation: Unmanned launch vehicles and upper stages: The needs N91-28210

URANIUM

The effect of fluoride gases on cylinder valve corrosion [DE91-012745] N91-28355

URANIUM COMPOUNDS

Doping and pressure study of U3Sb4Pt3 [DE91-013669] N91-29033

URANIUM 238

SDI: Statistical Dynamic Interactions [DE91-012034] N91-28827

USER MANUALS (COMPUTER PROGRAMS)

Computer simulation of an aircraft seat and occupant(s) in a crash environment: Program SOM-LA/SOM-TA user manual [CR-R-90026] N91-28146

ZEPHYR3D: A finite difference computer program for three-dimensional, transient incompressible flow problems [DE91-014331] N91-28515

ASTROP2 users manual: A program for aeroelastic stability analysis of propfans [NASA-TM-4304] N91-28627

Regional oxidant model user's guide. Part 1: The ROM preprocessors [PB91-171926] N91-28665

Regional oxidant model user's guide. Part 2: The ROM processor network [PB91-171934] N91-28666

USER REQUIREMENTS

Requirements for a network storage service [DE91-014106] N91-28778

V

V/STOL AIRCRAFT

The special requirements of a VSTOL aircraft N91-28155

VACUUM

Design and analysis of the 50 mm collider dipole vacuum vessel [DE91-012490] N91-28610

Aspects of reheating in first-order inflation [NASA-CR-188705] N91-29108

VACUUM SYSTEMS

Calculation of pressure distribution in vacuum systems using a commercial finite element program [DE91-013611] N91-28629

VALUE ENGINEERING

The human side of value engineering [DE91-012817] N91-29068

VALVES

The effect of fluoride gases on cylinder valve corrosion [DE91-012745] N91-28355

VANADIUM ALLOYS

Changes with material properties of acoustic emission produced during single point machining [DE91-011913] N91-28452

VANADIUM OXIDES

X ray diffraction study of heteroepitaxy of MOCVD grown TiO2 and VO2 films on sapphire single crystals [DE91-013764] N91-29037

VAPOR DEPOSITION

Investigation of laser diagnostics of PACVD processes for depositing hard face coatings [DE91-012642] N91-28401

US assessment of the new diamond technology in Japan [PB91-167395] N91-28404

Adhesion between CVD diamond films and tungsten [DE91-013757] N91-28434

X ray diffraction study of heteroepitaxy of MOCVD grown TiO2 and VO2 films on sapphire single crystals [DE91-013764] N91-29037

VAPORIZING

Vaporizing particle velocimeter [NASA-CASE-LAR-14685-1] N91-28135

Liquid-propellant droplet vaporization and combustion in high pressure environments N91-28225

Spray combustion under oscillatory pressure conditions N91-28226

Droplet-turbulence interactions in subcritical and supercritical evaporating sprays N91-28228

A study of El Nino/Southern Oscillation: Numerical experiments and data analysis N91-28710

VECTOR ANALYSIS

Kinematic GPS surveying N91-28149

VECTOR PROCESSING (COMPUTERS)

ZLIB: A numerical library for differential algebra (A user's guide for version 1.0) [DE91-012552] N91-28794

VECTOR SPACES

Using trees to compute approximate solutions to ordinary differential equations exactly [LAC90-R24] N91-28788

VEGETATION GROWTH

TREE: A model of the effects of acid precipitation and air pollutants on the growth of trees [DE91-014131] N91-28672

Plant growth is influenced by glutamine synthetase-catalyzed nitrogen metabolism [DE91-014592] N91-28725

VELOCITY DISTRIBUTION

An active delay of separation on two-dimensional airfoils [ITN-91-85142] N91-28139

A study of methods to investigate nozzle boundary layer transition N91-28232

Optical diagnostic investigation of low Reynolds number nozzle flows N91-28233

Solution to quasi-axisymmetric internal compressible flows using the stream tube approach N91-28526

Planning of minimum-time trajectories for robotic arms [ITN-91-85141] N91-28583

Numerical simulation of the air and fuel mixing process in fuel-injected engines using discrete vortex dynamics N91-28587

Log-stable distribution of energy dissipation in turbulence N91-28885

Multiple nuclei, cluster core dynamics, and the velocity distributions of gravitating systems N91-29119

VELOCITY MEASUREMENT

Vaporizing particle velocimeter [NASA-CASE-LAR-14685-1] N91-28135

The application of Particle Image Velocimetry (PIV) in a short duration transonic annular turbine cascade [AD-A236639] N91-28504

A microwave interferometer to measure particle and shock velocities simultaneously [DE91-013077] N91-28545

Shock compression of low-density microcellular materials [DE91-013586] N91-28628

Laser speckle velocimetry with photorefractive recording and anamorphic optical processing N91-28880

VERTICAL LANDING
The special requirements of a VSTOL aircraft N91-28155

VERY HIGH FREQUENCIES
Multiple frequency atmospheric radar techniques N91-28683

VERY LARGE SCALE INTEGRATION
Control of autonomous mobile robots using custom-designed qualitative reasoning VLSI chips and boards [DE91-012527] N91-28783

VERY LOW FREQUENCIES
Magnetospheric VLF line radiation N91-28693

VIBRATION
F-106B airplane active control landing gear drop test performance N91-28164
Robust and real-time control of magnetic bearings for space engines N91-28230
Noncircular rolling joints for vibrational reduction in slewing maneuvers [NASA-CASE-LAR-14515-1-CU] N91-28580
Evidence of vibrational mode-coupling in 2-fluorethanol via high resolution infrared spectroscopy in a molecular beam [AD-A236132] N91-28821

VIBRATION DAMPING
Explicit models for proportional damping in Timoshenko beams N91-28642
Active control of panel vibrations induced by boundary-layer flow [NASA-CR-188733] N91-28643
Human body protection in a dynamic environment. Cushioning mechanics [ITN-91-85149] N91-28733

VIBRATION ISOLATORS
Human body protection in a dynamic environment. Cushioning mechanics [ITN-91-85149] N91-28733

VIBRATION TESTS
Prediction of high level vibration test results by use of available inelastic analysis techniques [DE91-009437] N91-28606

VIBRATIONAL SPECTRA
Vibrational spectroscopy of shock-compressed liquid CO [DE91-013204] N91-28325

VIDEO SIGNALS
Recovery of saturated video signals from vidicons by dynamic cathode biasing [DE91-012402] N91-28464

VIDICONS
Recovery of saturated video signals from vidicons by dynamic cathode biasing [DE91-012402] N91-28464

VINYLIDENE
Effect of TCP doping on the remnant polarization in uniaxially oriented poly(vinylidene fluoride) films [AD-A237001] N91-28388

VIRTUAL MEMORY SYSTEMS
Regional oxidant model user's guide. Part 2: The ROM processor network [PB91-171934] N91-28666

VISCOELASTICITY
Viscoplastic analysis of an experimental cylindrical thrust chamber liner [NASA-TM-103287] N91-28622

VISCOPLASTICITY
The rate (time)-dependence mechanical behavior of modified 9Cr-1Mo. Part 2: Isothermal modeling at 538 C [DE91-011100] N91-28350
The rate (time)-dependent mechanical behavior of modified 9Cr-1Mo steel. Part 1: Experiments at 538 C [DE91-011097] N91-28615
Viscoplastic analysis of an experimental cylindrical thrust chamber liner [NASA-TM-103287] N91-28622

VISCOSITY
Generalized gyroviscous force and its effect on the momentum balance equation [DE91-013344] N91-29061

VISCOUS DRAG
Dynamic plasticity in transition from thermal activation to viscous drag [DE91-013031] N91-28617

VISCOUS FLOW
Algorithm and code development for unsteady three-dimensional Navier-Stokes equations [NASA-CR-188039] N91-28503
Study of spherical couette flow via 3-D spectral simulations: Large and narrow-gap flows and their transitions N91-28520
Numerical solution of a free-boundary viscous flow N91-28529
The numerical solution of confined laminar flow past a moving boundary N91-28532

VISIBILITY
Runway Visual Range (RVR) Operational Test and Evaluation (OT and E)/integration test plan [DOT/FAA/CT-TN91/4] N91-28176

VISUAL OBSERVATION
Coordinated optical and ultraviolet observations of short period RS CVn and W UMa type stars N91-29096

VISUAL TASKS
Analysis and modeling of early vision tasks for robot stereo vision N91-28585

VITRIFICATION
Computer modeling of ceramic melters to assess impacts of process and design variables on performance [DE91-013668] N91-28431

VLASOV EQUATIONS
Hole dynamics of one-dimensional plasma N91-28928

VOIDS
Void probability as a function of the void's shape and scale-invariant models [NASA-CR-188696] N91-29113

VOLATILITY
Experimental studies of the volatility of ammonium chloride [DE91-012526] N91-28311

VOLCANOLOGY
Observational constraints on pulsars: Location of the emission region and pulse shape stability on decade time scales N91-29097

VOLTAGE CONVERTERS (AC TO AC)
System and component design and test of a 10 hp, 18,000 rpm AC dynamometer utilizing a high frequency AC voltage link, part 1 [NASA-CR-188442] N91-28539

VOLTAGE CONVERTERS (DC TO DC)
Thyristor converter simulation and analysis [DE91-013802] N91-28494

VOLTERRA EQUATIONS
A methodology for using nonlinear aerodynamics in aeroservoelastic analysis and design [NASA-TM-104087] N91-28131

VON KARMAN EQUATION
Flutter of laminated rectangular plates including finite deflection and shear deformation N91-28639

VORTEX GENERATORS
An experimental investigation of the effect of vortex generators on the aerodynamic characteristics of a NACA 0021 airfoil undergoing large amplitude pitch oscillations [DE91-012102] N91-28133

VORTICES
An experimental investigation of the effect of vortex generators on the aerodynamic characteristics of a NACA 0021 airfoil undergoing large amplitude pitch oscillations [DE91-012102] N91-28133
Atmospheric responses to lower tropospheric forcing in a multilayer isentropic model N91-28688
A numerical simulation of a tornado-scale vortex in a three-dimensional cloud model N91-28705
Normal mode decomposition of small-scale oceanic motions N91-28709
Ion temperature gradient turbulence and coherent structures N91-28890
Point vortex description of a modon solution N91-28931
Formation and dynamics of solitary waves and vortices in driven and damped systems N91-28942
Stability of drift-wave modons in the presence of temperature gradients [DE91-014364] N91-28982
Application of muon spin relaxation experiment to the vortex dynamics of high temperature superconductors [DE91-014607] N91-29050

VORTICITY
Numerical simulation of the air and fuel mixing process in fuel-injected engines using discrete vortex dynamics N91-28587
Atmospheric responses to lower tropospheric forcing in a multilayer isentropic model N91-28688

VORTICITY EQUATIONS
The numerical solution of confined laminar flow past a moving boundary N91-28532

VOYAGER 1 SPACECRAFT
Search for regularities in the atmosphere of Jupiter N91-29127

W

WAFERS
Phonon-mediated detection of elementary particles using silicon crystal acoustic detectors N91-28547

WAKES
Beam emittance and the effects of the rf, space charge and wake fields: Application to the ATF photoelectron beam [DE91-014789] N91-28569
A new wake-potential calculation method using orthogonal polynomials [DE91-013045] N91-28799
Space charge and wake field analysis for a high brightness electron source [DE91-014788] N91-28874

WALKING MACHINES
Kinematic analysis of legged system locomotion on smooth horizontal surfaces N91-28586

WALL FLOW
Near-wall modelling of complex turbulent flows N91-28534

WALL TEMPERATURE
Longitudinal aerodynamic characteristics of a subsonic, energy-efficient transport configuration in the National Transonic Facility [NASA-TP-2922] N91-28143

WALLS
Test of superplastically formed corrugated aluminum compression specimens with beaded webs [NASA-TM-104119] N91-28373
Stability of annular equilibrium of energetic large orbit ion beam [DE91-014365] N91-28963

WASHING
Method and apparatus for cleaning rubber deposits from airport runways and roadways [NASA-CASE-LAR-14483-1] N91-28455

WASTE DISPOSAL
Biomarker-based biomonitoring for evaluating health and ecological effects on environmental contamination [DE91-013729] N91-28719
Guidelines for acquisition, installation, and testing of performance assessment software [DE91-013910] N91-28764

WASTE TREATMENT
Guidelines for acquisition, installation, and testing of performance assessment software [DE91-013910] N91-28764

WATER
Mechanisms of bacterial metals removal from solids [DE91-012808] N91-28356
Pacific Northwest hydrogen feasibility study [DE91-013427] N91-28445
Method and apparatus for cleaning rubber deposits from airport runways and roadways [NASA-CASE-LAR-14483-1] N91-28455
Interaction of radiation with outflows in late-type stars N91-29136

WATER COOLED REACTORS
Evaluation of aging of cast stainless steel components [DE91-014013] N91-28361
Advanced water-cooled phosphoric acid fuel cell development [DE90-009700] N91-28657

WATER FLOW
A mathematical model for two-phase water, air, and heat flow around a linear heat source emplaced in a permeable medium [DE91-014614] N91-28527

WATER MASERS
Observations of extragalactic water vapor masers N91-29117

WATER VAPOR
Measurement of the microwave propagation delay induced by atmospheric water vapor N91-28466
Natural and anthropogenic climate change [DE91-014734] N91-28673
Observations of extragalactic water vapor masers N91-29117

WATER WAVES
Alaska wave data index [AD-A236635] N91-28707

WAVE DIFFRACTION
Transport with Feynman propagators [DE91-013566] N91-29063

WAVE DISPERSION
Propagation of drift waves in toroidal plasma systems N91-28939

WAVE EQUATIONS
Localized waves in complex environments [DE91-011934] N91-28462
Optical analogs of model atoms in fields [DE91-013392] N91-28855
Mode conversion of Alfven waves induced by quadrupole magnetic field modulation N91-28924
Stability of drift-wave modons in the presence of temperature gradients [DE91-014364] N91-28982

WAVE FUNCTIONS
- Light-cone quantization of quantum chromodynamics [DE91-013991] N91-28856
- Ab initio cluster studies of La2CuO4 [DE91-013520] N91-29025
- Radiative transfer in very strong magnetic fields N91-29106

WAVE PROPAGATION
- Comparisons between fast shock tube calculations and tests [DE91-013496] N91-28177
- Localized waves in complex environments [DE91-011934] N91-28462
- Gravitational influence of a static ring-like distribution of mass on electromagnetic waves N91-28472
- Irradiance compensation control for high-energy laser propagation. Part 1: Theory and Fourier control model propagation results [DE91-013130] N91-28559
- Ring-laser solitons: A multipass approach [DE91-013242] N91-28560
- The SNL, Livermore, Hopkinson bar apparatus for compressive materials testing at high strain-rates [DE91-013132] N91-28612
- Non-steady wave profiles and the fourth-power law [DE91-013576] N91-28631
- Bauschinger effect during shock loading [DE91-014606] N91-28634
- Seismic traveltime inversion in three-dimensional heterogeneous media N91-28678
- Gravity wave propagation in a frontal environment N91-28687
- Atmospheric responses to lower tropospheric forcing in a multilayer isentropic model N91-28688
- Pulse propagation in inhomogeneous optical fibers [DE91-014356] N91-28879
- Propagation of drift waves in toroidal plasma systems N91-28939
- Joint proposal for US/USSR on nonlinear dynamics and plasma transport [DE91-014360] N91-28981
- Transport with Feynman propagators [DE91-013566] N91-29063

WAVE REFLECTION
- Transmission/reflection and short-circuit line permittivity measurements [PB91-171959] N91-28482

WAVEGUIDES
- A 2D field solver for periodic structures with special corner elements [DE91-012323] N91-28792

WEAPONS
- Feasibility study of a 200 ampere battery [DE91-014673] N91-28496

WEAR
- Analysis of foil bearings for high speed operation in cryogenic applications N91-28231
- Boundary lubrication of ceramic materials by soft metallic coating and synthetic oil [DE91-014017] N91-28577

WEAR RESISTANCE
- Erosion studies on a Fe3Al-based iron aluminide and 1100 Al [DE91-012529] N91-28360
- Pretreatment of lubricated surfaces with sputtered cadmium oxide [NASA-CASE-LEW-14474-1] N91-28423

WEAR TESTS
- Tribology of aluminum-based metal matrix composites: Fundamental study of wear behavior as influenced by microstructure N91-28297

WEATHER
- Effectivity of atmospheric electricity on launch availability N91-28260
- Tropospheric scatter propagation at 5 and 16 GHz: Results for a 161 km path [AD-A237012] N91-28458
- Atmospheric propagation of high-explosive blast waves [DE91-012550] N91-28506
- Report of Meeting of CLICOM Experts [WCDP-9] N91-28695
- Meteorological instrumentation support for an adverse weather test facility [AD-A236605] N91-28696

WEAVING
- Damage development under compression-compression fatigue loading in a stitched uniwoven graphite/epoxy composite material [NASA-CR-188693] N91-28292

WELDABILITY
- Microstructure-property relationships in Al-Cu-Li-Ag-Mg Weldalite (tm) alloys, part 2 [NASA-CR-4364] N91-28334
- Identification of strengthening phases in Al-Cu-Li alloy Weldalite (tm) 049 N91-28335
- Weldability of Weldalite (tm) 049 with and without TiB2 reinforcement N91-28338
- Weldability of iron aluminides [DE91-013730] N91-28367
- Welding of ductile intermetallic alloys [DE91-009553] N91-28594

WELDED JOINTS
- Comparisons of irradiation-induced shifts in fracture toughness, crack arrest toughness, and Charpy impact energy in high-copper welds [DE91-008881] N91-28349
- Weldability of iron aluminides [DE91-013730] N91-28367

WELDING
- JPRS report: Science and technology. USSR: Materials science [JPRS-UMS-91-003] N91-28342
- Welding of ductile intermetallic alloys [DE91-009553] N91-28594

WELDING MACHINES
- High temperature solder device for flat cables [NASA-CASE-GSC-13344-1] N91-28363

WELLS
- Geothermal materials development [DE91-013972] N91-28660

WENTZEL-KRAMER-BRILLOUIN METHOD
- High-overtone black-hole normal modes: A WKB contour-integral approach N91-29118

WHEATSTONE BRIDGES
- Pressure transducer and system for cryogenic environments [NASA-CASE-LAR-14579-1] N91-28546

WHEELS
- Failure analysis case histories of Canadian forces aircraft landing gear components N91-28151

WHISKER COMPOSITES
- Development of nondestructive evaluation methods and prediction of effects of flaws on the fracture behavior of structural ceramics [DE91-012471] N91-28410

WHISKERS (CRYSTALS)
- Development of nondestructive evaluation methods and prediction of effects of flaws on the fracture behavior of structural ceramics [DE91-012471] N91-28410

WIDEBAND COMMUNICATION
- Wideband adaptive HF modem [ITN-91-85147] N91-28471

WIGGLER MAGNETS
- The Advanced Light Source: A new tool for research in atomic and molecular physics [DE91-012860] N91-28844
- Development of nanovolt-resolution x ray diffraction using resonant nuclear scattering [DE91-012217] N91-28847

WIND PROFILES
- Low-level curvature shear and supercell thunderstorm behavior N91-28701

WIND TUNNEL MODELS
- Evaluation of a technique to generate artificially thickened boundary layers in supersonic and hypersonic flows [NASA-TP-3142] N91-28136
- A study of residual interference effects in adaptive wall testing of a 7-inch chord CAST-10-2/DOA 2 airfoil model [NASA-CR-4390] N91-28138

WIND TUNNEL NOZZLES
- Improved method and apparatus for Mach number change in wind tunnel [NASA-CASE-LAR-13548-1] N91-28175

WIND TUNNEL TESTS
- Transonic shock-induced dynamics of a flexible wing with a thick circular-arc airfoil [NASA-TM-104088] N91-28132
- A study of residual interference effects in adaptive wall testing of a 7-inch chord CAST-10-2/DOA 2 airfoil model [NASA-CR-4390] N91-28138

WIND TUNNEL WALLS
- A study of residual interference effects in adaptive wall testing of a 7-inch chord CAST-10-2/DOA 2 airfoil model [NASA-CR-4390] N91-28138

WIND TUNNELS
- An experimental investigation of the effect of vortex generators on the aerodynamic characteristics of a NACA 0021 airfoil undergoing large amplitude pitch oscillations [DE91-012102] N91-28133
- Improved method and apparatus for Mach number change in wind tunnel [NASA-CASE-LAR-13548-1] N91-28175

WIND TURBINES
- An experimental investigation of the effect of vortex generators on the aerodynamic characteristics of a NACA 0021 airfoil undergoing large amplitude pitch oscillations [DE91-012102] N91-28133

WINDOWS (APERTURES)
- Shock-induced optical emission in Al2O3 at 200 GPa: Implications for shock temperature measurements in metals [DE91-013584] N91-28365

WINDS ALOFT
- Observations and theoretical studies of tides and normal modes in the lower thermosphere N91-28681

WIRE
- Coupling device with improved thermal interface [NASA-CASE-GSC-13251-1] N91-28582
- Device for removing foreign objects from anatomic organs [NASA-CASE-GSC-13306-1] N91-28727
- Magnetization and critical currents of tin-core multifilamentary Nb3Sn conductors [DE91-012241] N91-28994
- Overview of the status of and prospects for high-T(sub c) wire and tape development [DE91-014609] N91-29045

WORK HARDENING
- Investigation of thermomechanical behavior of metal matrix composites N91-28296
- Tensile deformation of Al-Cu-Li-Zr alloy 2090-T8E41 at 298 and 77 K [DE91-011885] N91-28345

X

X RAY ANALYSIS
- The spatial resolution of x ray microanalysis in thin foils [DE91-011949] N91-29003

X RAY DIFFRACTION
- Mechanism of hydrodenitrogenation. Part 5: X ray diffraction of molybdenum catalysts [DE91-013853] N91-28327
- Characterization of silicon nitride synthesized by microwave heating [DE91-012219] N91-28397
- Energy dispersive x ray diffraction study of glassy Bi2Sr2CaCu2O(x) filaments produced by gas-jet fiberization [DE91-012021] N91-28407
- Development of nanovolt-resolution x ray diffraction using resonant nuclear scattering [DE91-012217] N91-28847
- X ray diffraction study of heteroepitaxy of MOCVD grown TiO2 and VO2 films on sapphire single crystals [DE91-013764] N91-29037

X RAY IMAGERY
- X ray microimaging of elemental composition and microstructure for materials science [DE91-012052] N91-28601

X RAY INSPECTION
- The application of x ray tomographic microscopy to chemical vapor infiltration processing of ceramic matrix composites [DE91-011871] N91-28284
- Local delamination in laminates with angle ply matrix cracks. Part 1: Tension tests and stress analysis [NASA-TM-104055] N91-28293

X RAY LASERS
- X ray fiducial foils [DE91-011193] N91-28542
- Modal study of refractive effects on x ray laser coherence [DE91-012083] N91-28551
- X ray generation by high irradiance exawatt/sq cm subpicosecond lasers [DE91-013497] N91-28556

X RAY SOURCES
- The DARPA compact superconducting x-ray lithography source features [DE91-013864] N91-29039
- A new model of PeV gamma ray sources and MHD turbulence in neutron star accretion columns N91-29122
- Upper limits for the flux of very high-energy gamma radiation from Cygnus X-3 and for the explosion rate of primordial black holes obtained by the Haleakala Gamma Ray Observatory N91-29134

X RAY SPECTRA
- X ray generation by high irradiance exawatt/sq cm subpicosecond lasers [DE91-013497] N91-28556

X RAY SPECTROSCOPY
- A controlled dispersion parallel wavelength x ray spectrometer for electron microscopy [DE91-012011] N91-28544
- X ray generation by high irradiance exawatt/sq cm subpicosecond lasers [DE91-013497] N91-28556

X RAY TUBES
Continuum x ray gauging of multiple-element materials
[DE91-011923] N91-28307

X RAYS
Liquid jet breakup and atomization in rocket chambers under dense spray conditions N91-28227
Continuum x ray gauging of multiple-element materials
[DE91-011923] N91-28307
X ray fiducial foils
[DE91-011193] N91-28542
Measuring neutron fluences and gamma/x ray fluxes with CCD cameras
[DE91-014119] N91-28549
X ray generation by high irradiance exawatt/sq cm subpicosecond lasers
[DE91-013497] N91-28556
X ray Tomographic Microscopy (XTM)
[DE91-011930] N91-28599
Nondestructive evaluation tools and experimental studies for monitoring the health of space propulsion systems
[NASA-TM-105164] N91-28605
X ray microimaging of elemental composition and microstructure for materials science
[DE91-012221] N91-28832
Reflection mask technology for soft x ray projection lithography
[DE91-012561] N91-28877

XV-15 AIRCRAFT
Rotor and control system loads analysis of the XV-15 with the advanced technology blades
[NASA-TM-102876] N91-28134

Y

YIELD
Plant growth is influenced by glutamine synthetase-catalyzed nitrogen metabolism
[DE91-014592] N91-28725

YOKES
Brittle behavior of SSC yokes
[DE91-014031] N91-28370

YTTRIUM COMPOUNDS
Neutron scattering studies of spin correlations in metallic YBa2Cu3O(6+x)
[DE91-013794] N91-29031
Doping and pressure study of U3Sb4Pt3
[DE91-013669] N91-29033

YTTRIUM OXIDES
Growth of high T(sub c) superconducting thin films for microwave applications
[DE91-011436] N91-28991
Superconducting bolometers: High-T(sub c) and low-T(sub c)
[DE91-011830] N91-28992

Z

ZEOLITES
Resonance Raman and photophysical studies of transition metal complexes in solution and entrapped in zeolites
[DE91-013010] N91-28357

ZINC
Durability of polymeric materials used in zinc/bromine flow batteries
[DE91-012864] N91-28487

ZINC TELLURIDES
Novel ways of depositing ZnTe films by a solution growth technique
[DE91-002189] N91-28429

ZINC-BROMIDE BATTERIES
Preparation of ionic membranes for zinc/bromine storage batteries
[DE91-012008] N91-28483

ZIRCALOY 2 (TRADEMARK)
Effects of residual stresses on the fracture toughness of Zircaloy-2 tubes
[DE91-012736] N91-28354

ZIRCONIUM
Kinetics of solid-state reactions in Ni-Zr thin films
[DE91-013652] N91-29028

ZIRCONIUM ALLOYS
Tensile deformation of Al-Cu-Li-Zr alloy 2090-T8E41 at 298 and 77 K
[DE91-011885] N91-28345
Synthesis of metastable aluminum-based intermetallics by mechanical alloying
[DE91-013651] N91-28376
Metastable phase equilibria in co-deposited Ni(1-x)Zr(x) thin films
[DE91-013653] N91-29029

ZIRCONIUM OXIDES
Theoretical studies of zirconia and related materials
[DE91-013906] N91-28369
Ordered ceramic membranes
[DE91-012248] N91-28398

PERSONAL AUTHOR INDEX

SCIENTIFIC AND TECHNICAL AEROSPACE REPORTS VOLUME 29 NUMBER 20

Typical Personal Author Index Listing

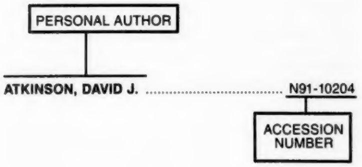

Listings in this index are arranged alphabetically by personal author. The accession number denotes the number by which the citation is identified.

A

ABADA, AHMED N91-28294
ABDULNOUR, BASHAR SULAIMAN N91-28532
ABEGG, R. N91-28842
ABRAHAMS, P. N91-28433
ADHIKARI, S. D. N91-28801
AHN, JOONG BAE N91-28710
AJAYI, O. O. N91-28577
AKHIL, A. A. N91-28485
ALAM, M. N91-28434
ALAN, IRFAN N91-28539
ALANIS, MACEDONIO N91-29087
ALCARAZ, A. N91-28326
ALCARAZ, J. N91-28670
ALEXANDER, MICHAEL ADAM N91-28711
ALFORD, C. N91-28542
ALI, M. M. N91-28923
ALLEN, S. L. N91-28568
ALLEY, G. T. N91-28484
ALLEY, W. E. N91-28958
ALVISO, C. T. N91-28408
AMENDT, P. N91-28551
ANASTASIADIS, JOHN S. N91-28638
ANDERL, R. A. N91-28362
N91-28951
ANDERSON, M. A. N91-28398
ANDERSON, M. U. N91-28411
N91-28443
ANDERSON, P. N91-28672
ANDERTON, EDWYN CHRISTOPHER MORGAN
N91-28426
ANDRESEN, B. D. N91-28326
ANDREWS, E. P. N91-28264
ANDREWS, W. H., JR. N91-28481
ANGULO, EARL D. N91-28727
ANIS, C. N91-28238
ANNAPAREDDY, NARASIMHA REDDY LAKSHMI
N91-28740
ANTOLAK, A. J. N91-28306
ANTONSEN, T. M., JR. N91-28980
N91-28981
ARAKAWA, E. T. N91-28493
N91-28852
ARAN, SHMUEL N91-28760
ARIAS, J. L. N91-28400
ARMENTROUT, D. L. N91-28452
N91-28453
ARNOLD, C., JR. N91-28483
N91-28487
ARNOLD, D. N91-28610
ARNOLD, STEVEN M. N91-28622
ARNOLDUS, HENK F. N91-28820
ARTER, W. N91-28901
ARUN, VEERARAGHAVAN N91-28640
ARYA, R. N91-28480
ARYA, VINOD K. N91-28622
ASANO, K. G. N91-28836
ASAY, B. N91-28448
ASAY, B. W. N91-28443
ASAY, J. R. N91-28178
ASKLEY, C. S. N91-28395
ASSINK, R. A. N91-28314
N91-28483
AST, D. N91-29011
ASTORGA, JOAQUIN N91-28584
AUERBACH, A. N91-28854
AULD, A. B. K. N91-28155
AUSTIN, ROBERT ANDREAS N91-29134
AVINASH, K. N91-28938
AXELROD, T. S. N91-28148
AZEVEDO, S. G. N91-28602
AZUMI, MASAFUMI N91-28921
N91-28936

B

BAAKLINI, GEORGE N91-28246
BAEK, YOON SU N91-28586
BAGLEY, R. J. N91-28714
BAKASOV, A. A. N91-28802
BAKER-JARVIS, J. N91-28482
BAKER, BRADLEY AARON N91-28684
BAKER, DAVID N91-28237
BAKER, G. L. N91-28402
N91-28427
BAKER, S. P. N91-28481
BAKUCKAS, JOHN G., JR. N91-28301
BALDWIN, A. R. N91-28496
BALDWIN, R. H. N91-28359
BALES, THOMAS T. N91-28373
BALICK, L. K. N91-28170
BALUJA, S. N91-28741
BANERJEE, PRITHVIRAJ N91-28747
BANSE, B. A. N91-29047
BARBOUR, J. C. N91-29051
BARDOS, RUSSELL N91-28200
BARIBEAU, J. M. N91-29044
BARKER, L. M. N91-28178
BARKER, TIMOTHY WAYNE N91-28699
BARNARD, JOHN MORDAUNT N91-29081
BARTMESS, J. E. N91-28836
BASKER, GUY ASHBOURNE N91-28708
BASS, B. R. N91-28607
N91-28614
BATEMAN, G. N91-28946
BATES, J. L. N91-28317
N91-28412
N91-28664
BATTA, GEORGE RICHARD N91-28819
BAUCOM, ROBERT M. N91-28290
BAUER, M. L. N91-28484
BAUM, H. R. N91-28507
BEACHELY, O. T., JR. N91-28989
BEATTY, TIMOTHY JON N91-28690
BEAUCHAMP, J. J. N91-28674
BEAUDET, P. N91-28151
BEBRICH, C. A. N91-28675
BECKER, M. N91-28653
BECKERMAN, M. N91-28784
BECKS, VIRGINIA N91-29072
BECKSTEAD, J. A. N91-29126
BEEMAN, J. W. N91-29038
BEGUELIN, A. N91-28755
BEKLEMISHEV, A. D. N91-28964
BELL, G. E. C. N91-28352
BELL, J. D. N91-28947
BEMENT, LAURENCE J. N91-28444
BENCH, G. N91-28825
BENCI, JOHN N91-28343
BENDER, L. N91-28665
N91-28666
BENDER, S. C. N91-28565
BENJAMIN, R. F. N91-28528
BENNET, JAY N91-28244
BENNETT, B. I. N91-28636
BENNETT, D. W. N91-28591
BENNETT, GARY L. N91-28216
BENNETT, M. N91-28480
BENNETT, R. G. N91-28279
BENNETT, ROBERT M. N91-28132
N91-28137
BENTJEN, S. B. N91-28999
BENTLEY, J. N91-28344
N91-28405
N91-28840
BENTS, DAVID J. N91-28277
N91-28278
BERG, J. S. N91-28796
BERGER, E. N91-28868
BERK, H. L. N91-28963
BERKE, L. N91-28247
BERNAT, T. P. N91-28960
BERNHARD, R. J. N91-28457
BERNHARDT, JOHN CHARLES N91-28739
BERNSTEIN, E. M. N91-28863
BERO, C. N91-28393
BERUBE, D. S. N91-29075
BERZ, M. N91-28476
BERZTISS, ALFS N91-28742
BESIERIS, I. M. N91-28462
BETHEL, W. N91-28763
BEYERMANN, W. P. N91-29033
BHARGAVA, HEMANT KUMAR N91-28761
BHAT, BIL N91-28245
BHATTACHARJEE, A. N91-28884
N91-28895
BICKES, R. W., JR. N91-28319
BIEBER, MICHAEL PAUL N91-29086
BIGGAR, S. F. N91-28170
BIRINGEN, S. N91-28502
BIRKMIRE, R. W. N91-28429
BISHNOI, PEEUSH KUMAR N91-28533
BISKAMP, D. N91-28886
BLACK, W. M. N91-28414
BLAIR, A. B., JR. N91-28136
BLAKE, R. D. N91-28414
N91-28415
BLAKELY, J. N91-28995
BLAKERS, A. W. N91-28662
BLALOCK, A. V. N91-28481
BLANKENSHIP, R. E. N91-28723
BLANN, M. N91-28827
BLASKIEWICZ, MICHAEL MATHEW N91-29097
BLOM, A. F. N91-28157
BLOOM, I. N91-28592
BLOOMFIELD, H. S. N91-29138
BOEHM, T. N91-28665
N91-28666
BOERCHER, D. B. N91-28944
BOETTGER, J. C. N91-28436
BOGACZ, S. A. N91-28867
BOIVIN, M. N91-28842
BOSCHETTO, M. N91-28163
BOSSERT, JAMES E. N91-28680
BOUDARD, A. N91-28842
BOURKE, M. A. M. N91-28624
N91-28632
BOURQUE, R. F. N91-28966
BOYD, J. N91-28489
BOYLE, E. J. N91-28514
BRABY, L. A. N91-28715
BRACKBILL, J. U. N91-28975
BRADLEY, R. N91-28479
BRAITHWAITE, J. W. N91-28485
BRANSCOME, DARRELL R. N91-28195
BRENNER, A. N91-28333
BRESE, NATHANIEL N91-28987
BRICE, D. K. N91-28846
BRINKER, C. J. N91-28395
BRITTON, C. L., JR. N91-28484
BRNDON, S. L. N91-28612
BROADHURST, THOMAS JAMES N91-29100
BROCK, B. C. N91-28473
BRODSKY, S. J. N91-28828
N91-28856
BROOKER, M. J. N91-28155
BROOKS, E. D., III N91-28774
N91-28781
BROOKS, FREDERICK P., JR. N91-28823
BROOKS, HAROLD EDWARD N91-28701
BROWER, DAVID N91-28244
BROWN, D. W. N91-28652
BROWN, I. G. N91-28979
BROWN, J. E. N91-28371
BROWN, JAMES R. N91-28202
BROWNELL, J. H. N91-28499

BROWNING, R. N91-28877
BRUGE, G. N91-28842
BRUMMEL, CHRISTOPHER L. N91-28821
N91-28822
BRYANSTON-CROSS, P. J. N91-28504
BRYSON, J. W. N91-28611
BUCHANAN, R. A. N91-28358
BUCKLEY, JOHN D. N91-28490
BUDNICK, J. I. N91-29036
BUHRMAN, ROBERT A. N91-28478
BULLOCK, O. N91-28665
N91-28666
BULTMAN, N. K. N91-28563
BURKE, MICHAEL J. N91-28696
BURKETT, M. W. N91-28625
BUTLER, P. C. N91-28485
BUTLER, R. N91-28765
BUTNER, S. N91-28456
BYARD, KEVIN N91-29093
BYERS, DAVE N91-28215
BYRD, R. J. N91-28198

C

CALLCOTT, T. A. N91-28493
N91-28852
CALLEN, J. D. N91-28888
N91-28949
N91-28953
N91-29061
CAMP, PAUL J. N91-29115
CAMP, W. J. N91-28775
CAMPBELL, A. A. N91-28999
CAMPBELL, A. W. N91-28448
CAMPBELL, J. H. N91-28571
CANAVAN, G. H. N91-28809
N91-28810
CANFIELD, P. C. N91-29033
CAPLAN, A. I. N91-28400
CARICO, DAVID PAUL N91-29098
CARLSON, N. N91-28513
CARLSON, R. N91-28558
CARLSTEN, B. E. N91-28565
CARLTON, R. F. N91-28831
CAROLI, JOSEPH A. N91-28745
CARPENTER, S. H. N91-28452
N91-28453
CARPINO, MARC N91-28231
CARRERAS, B. A. N91-28969
CARRUTHERS, P. N91-28845
CASDAGLI, M. N91-29055
CASPERSON, D. E. N91-28556
CASTAING, J. N91-28435
CASTILLO, V. N91-28870
CASTLE, J. G. N91-28475
CATALANO, A. N91-28480
CAUGHMAN, J. B. O., II N91-28463
CEGLIO, N. M. N91-28877
CELESTE, J. N91-28599
CHA, Y. S. N91-29008
CHAMBERS, F. W. N91-28568
CHAMBERS, R. S. N91-28393
CHAMIS, C. C. N91-28238
N91-28247
CHAN, STEPHEN C. N91-28519
CHANDRASEKHAR, H. R. N91-29041
CHANG, L. K. N91-28609
CHANG, M. L. M. N91-29037
CHANG, P. N91-28722
CHANG, S. L. N91-28968
CHANG, SHOU REI N91-28641
CHANG, Z. N91-28888
CHANG, ZUOYANG N91-29061
CHAPMAN, JOHN J. N91-28546
CHARLTON, L. A. N91-28969
CHATO, DAVID J. N91-28538
CHAVEZ, J. M. N91-28651
CHEN, H. H. N91-28898
CHEN, HEH-CHYUN N91-28644
CHEN, JUN-LON N91-28185
CHEN, LONG-JENG N91-28446
CHEN, P. N91-28834
CHEN, SHENG-CHANG N91-29001
CHEN, Y. M. N91-28385
CHENEVERT, DON J. N91-28259
CHENG, ANDREW F. N91-28182
CHENG, C. Z. N91-28891
N91-28939
CHENG, JUNG-WEI N91-28642
CHENG, S. N91-28615
CHEUNG, FAN-BILL N91-28227
CHEW, MENG-SANG N91-28184
N91-28580
CHHABILDAS, L. C. N91-28178
CHIARELLO, R. P. N91-29037
CHICK, L. A. N91-28412
N91-28664
CHIU, S. C. N91-28973
CHOI, D. I. N91-28890
CHOLEWA, M. N91-28825
CHONG, C. M. N91-28662
CHONGSAWANGVIROD, S. N91-28985
CHOPP, D. L. N91-28759
CHOUDHURY, A. M. N91-28698
CHOW, I. N91-29079
CHOW, PAO-LIU N91-28643
CHU, C. Y. N91-28410
CHU, D. N91-28345
CHUNG, H. M. N91-28361
CHURCHILL, MELVYN R. N91-28989
CLARK, M. AMANDA N91-28681
CLARKE, J. N91-28997
N91-28998
N91-29007
CLAUS, R. O. N91-28875
CLINQUE, R. B. N91-28399
CLINTON, C. N91-28206
CLIPPARD, R. L. N91-28541
CLOUGH, S. A. N91-28673
COBB, W. T. N91-28432
COBBLE, J. A. N91-28556
COE, J. A. N91-28645
COFFEY, D. N91-29035
COFFEY, HELEN E. N91-29128
N91-29129
N91-29130
N91-29131
COHEN, GERALD C. N91-28777
COLCLOUGH, M. S. N91-28997
COLDWELL, CHARLES E., JR. N91-28585
COLLICOTT, STEVEN H. N91-28880
COLLINGS, E. W. N91-28993
COLLINS, G. W. N91-28824
COLLOFELLO, JAMES S. N91-28743
COLOZZA, A. N91-28277
COMPTON, R. N. N91-28554
CONCUS, P. N91-28450
CONNELL, DON N91-28239
CONWAY, DARREL JAMES N91-29101
COOK, D. L. N91-28826
COOK, J. F. N91-28437
COOK, R. B. N91-28674
COOKE, D. W. N91-28991
COPPI, B. N91-28882
COPPI, PAOLO SEVERO N91-29137
CORLEY, D. M. N91-28507
CORVO, A. N91-28553
CORWIN, W. R. N91-28349
COSTELLO, J. F. N91-28606
COUVERT, P. N91-28842
COWLES, BRAD N91-28245
COWLES, S. N91-28672
COY, EDWARD N91-28228
CRAISE, L. M N91-28720
CRANE, ROBERT K. N91-28458
CREIGHTON, J. R. N91-29047
CRENSHAW, B. M. N91-28159
CRENSHAW, T. B. N91-28346
CRESCIMANNO, M. J. N91-29062
CROUCH, PETER E. N91-28789
CUGLIANDOLO, L. F. N91-29056
CUNNINGHAM, M. E. N91-28354

D

DAHMEN, U. N91-29002
N91-29006
DAI, X. N91-28662
DALE, J. M. N91-28309
DANABASOGLU, G. N91-28502
DANFORD, MERLIN D. N91-28341
DANFORTH, RICHARD N91-28192
DANSBERRY, BRYAN E. N91-28132
N91-28137
DAS-GUPTA, D. K. N91-28540
DAS, M. N91-28779
DAUGHERTY, ROBERT H. N91-28164
DAVID, S. A. N91-28367
N91-28594
DAVIDSON, D. L. N91-28280
DAVIDSON, T. F. N91-28196
N91-28272
DAVIES, P. K. N91-28403
DAVIS, D. O. N91-28136
DAVIS, M. J. N91-28147
DAVIS, RANDALL C. N91-28373
DEAN, L. A. N91-28750
N91-29077
DEGROOT, J. S. N91-28956
DELABEAUJARDIERE, JEAN-FRANCOIS N91-29132
DENHAM, D. H. N91-29074
DESAUSSURE, G. N91-28829
DESCH, P. B. N91-28376
DESHPANDE, S. N91-28938
DESJARDINS, D. N91-29055
DICK, J. J. N91-28420
N91-28637
N91-29023
DICK, JAMES S. N91-28248
DICKENS, J. K. N91-28837
DICKERSON, GEORGE E. N91-28424
DIECKMAN, S. L. N91-28410
DIECKMANN, R. N91-29049
DINI, J. W. N91-28394
DISALVO, FRANCIS N91-28987
N91-29013
DISTEFANO, J. R. N91-28378
DIVER, R. B. N91-28651
DOBACZEWSKI, J. N91-28853
DOLIN, R. M. N91-28457
DOMINGUEZ, N. N91-28969
DOMINIQUES-RODRIGUEZ, A. N91-28435
DONGARRA, J. N91-28755
DORRELL, L. R. N91-28616
DOSANJH, S. S. N91-28775
DOSS, A. R. N91-29076
DOUGHTY, C. N91-28527
DOUGLAS, K. N91-29026
DOWDY, MACK W. N91-28203
DRAGT, A. J. N91-28807
DRAKE, J. B. N91-28969
DRAKE, J. F. N91-28980
N91-28981
DRESHFIELD, BOB N91-28245
DRESNER, L. N91-28814
N91-29016
DREXLER, R. L. N91-28279
DUDMAN, A. E. N91-28166
DUMAS, GUY N91-28520
DUMESIC, J. A. N91-28331
DUNCAN, R. V. N91-29009
DUNIGAN, T. H. N91-28738
DUNLAP, D. H. N91-29009
DUNLAP, J. L. N91-28947
DUNNING, T. H. N91-28671
DURANTE, M. N91-28721
DURHAM, JOSEPH ELBERT, JR. N91-28685
DYBWAD, G. L. N91-28500
DYE, R. C. N91-28991

E

EADES, C. A. N91-28737
EARLY, J. W. N91-28565
EARLY, R. A. N91-28869
EBIANA, ASUQUO BASSEY N91-28587
ECHER, C. J. N91-28862
ECKSTROM, CLINTON V. N91-28132
N91-28137
EDWARDS, R. N91-28991
EDWARDS, ROBERT M. N91-28786
EKERDT, J. G. N91-28409
ELIZALDE, E. N91-29113
ELLEFSON, R. E. N91-28395
ELLINGSON, W. A. N91-28410
ELLIOTT, M. L. N91-28431
ELSHAIK, NAGWA MAHMOUD N91-28521
ELY, J. F. N91-28316
EMERY, V. J. N91-28866
ENDICOTT, J. F. N91-28864
ENGERAND, JEAN LUC N91-28160
ENGLISH, C. A. N91-29027
EPPLEY, K. R. N91-28869
ERCK, R. A. N91-28577
ERDEMIR, A. N91-28577
ERNST, JOHN A. N91-28260
ESEN, E. B. N91-28508
N91-28509
ESPOSITO, LARRY W. N91-28182
EUBANK, S. N91-29055
EVANS, B. J. N91-29078
EVANS, N. D. N91-28344
EXARHOS, G. J. N91-29012
EYLER, L. L. N91-28431
EZE, MOSES O. J. N91-28604

F

FAIRLIE, D. B. N91-28793
FALABELLA, S. N91-28944
FARMER, J. D. N91-28714
N91-29055
FARMER, MOSES G. N91-28132
N91-28137

FARNSWORTH, A. V., JR. N91-28567
FAWLEY, W. M. N91-28476
FECHT, B. A. N91-28591
FEIGHNER, M. A. N91-28677
FELDMAN, A. N91-28404
FELDMAN, D. W. N91-28565
FELDMAN, E. E. N91-28609
FELDMAN, R. B. N91-28565
FELLER, D. F. N91-28671
FENG, K. N91-28433
FENG, W. W. N91-28285
N91-28286
FERBER, M. K. N91-28418
FERNANDEZ, M. S. N91-28400
FERRAINOLO, JOHN J. N91-28191
FERRARI, M. J. N91-28997
N91-29007
FERRIERE, KATIA MARCELLE N91-29102
FESTER, DALE A. N91-28242
N91-28243
FIEDLER, ROBERT ANTHONY N91-29116
FIESELMANN, B. N91-28480
FILUK, A. B. N91-28945
FINKENTHAL, D. N91-28952
FINN, CHRISTOPHER JUDE N91-28678
FINN, J. M. N91-28980
N91-28981
FINN, R. N91-28450
FIORI, C. E. N91-28544
FISCHER, J. N91-29020
FISK, Z. N91-29033
FITZGIBBONS, GREGORY LYNN N91-29094
FLETCHER, JAMES N91-29103
FLOM, YURY N91-28578
FLYNN, G. J. N91-28825
FOLLANSBEE, P. S. N91-28635
FOLTYN, S. R. N91-28991
FORD, P. C. N91-28323
FOWLER, T. K. N91-28275
N91-28952
FRANK, A. M. N91-28447
FRAZIER, WILLIAM F. N91-28343
FREAR, D. R. N91-28379
FREEMAN, D. N91-28213
FREERICKS, J. K. N91-29030
FREESE, J. M. N91-28485
FREKERS, D. N91-28830
FRENCH, J. C. N91-28757
N91-28779
N91-29089
FREYMANN, RAYMOND N91-28165
FRIEDRICH, A. N91-28479
FRIEDRICHS, C., JR. N91-28488
FRIEMAN, JOSHUA A. N91-29109
FRISBEE, ROBERT H. N91-28218
FRONABARGER, J. W. N91-28442
FRYXELL, G. E. N91-28999
FUJIMURA, K. N91-28784
FUKUMASA, O. N91-28916
FULLER, PAUL N. N91-28199
FULMER, R. G. N91-29076
FULTON, R. D. N91-28556
FURNISH, G. N91-28915
FURUSAWA, T. N91-28907
FUSARO, ROBERT L. N91-28423

G

GABEL, M. R. N91-28307
GABELLA, W. E. N91-28796
GAFFNEY, RICHARD LEE, JR. N91-28140
GAIER, JAMES R. N91-28289
GAILLARD, M. K. N91-29054
GAINES, D. P. N91-28877
GALLAGHER, K. P. N91-28438
GAMAGE, NIMAL KUMAR KETAGODA N91-28686
GARCIA-GARCIA, C. N91-28860
GARCIA, A. R. N91-28991
GARCIA, E. N91-28420
GARCIA, H. E. N91-28786
GARCIA, L. N91-28969
GARCIA, R. N91-28564
GARCIACALDERON, G. N91-29018
GARCON, M. N91-28842
GARDNER, E. J. N91-29067
GARNER, KENNETH N. N91-28227
GARRETT, S. E. N91-28500
GARWIN, E. L. N91-28996
GAVEL, D. N91-28559
GAZTANAGA, E. N91-29113
GEIST, A. N91-28755
GEIST, G. A. N91-28780
GENERAZIO, EDWARD R. N91-28605
GEOHEGAN, D. B. N91-28959
GEORGE, THOMAS F. N91-28812
N91-28820
GEORGESON, G. N91-29022
GERAMI, ROBERT N91-28152
GERARDI, TONY N91-28154
GERBER, MARGARET K. N91-28425
GERRISH, V. N91-29022
GHIRINGHELLI, G. L. N91-28163
GHOSH, A. K. N91-28994
GHOSH, ASISH N91-28418
GIBSON, J. N91-29055
GIEL, T. V., JR. N91-28541
GILL, J. T. N91-28395
GIM, CHUNG KEUN N91-28302
GINLEY, D. S. N91-28501
N91-29052
GLASS, A. J. N91-28275
GLASSER, A. H. N91-28513
GLENDENNING, N. K. N91-29125
GLENDINNING, S. G. N91-28955
GLENN, L. A. N91-28422
GLISH, G. L. N91-28310
N91-28835
N91-28836
GLOSS, BLAIR B. N91-28143
GODECHOT, X. N91-28979
GOERINGER, D. E. N91-28835
GOETSCH, J. A. N91-28750
GOFORTH, J. H. N91-28499
GOLANICS, C. J. N91-28170
GOLDBERG, KENNETH YIGAEL N91-28597
GOLDSTEIN, J. I. N91-28841
N91-29003
GOLDSTEIN, N. E. N91-28677
GOLDSTON, R. J. N91-28946
GOLDSTONE, J. A. N91-28624
GOODMAN, STEVEN JAY N91-28702
GOPALSAMI, N. N91-28410
GORDA, B. C. N91-28774
N91-28781
GORETTA, K. C. N91-28435
GOSLIN, JOSEPH N91-28176
GOSWAMI, D. Y. N91-28595
GOTTESFELD, S. N91-28661
GOTTSTEIN, G. N91-28287
GOVORKOV, B. B., JR. N91-28802
GOYANES, S. N. N91-28416
GRADY, D. N91-28439
GRAHAM, R. A. N91-28443
GRAY, G. T., III N91-28634
GRAY, K. E. N91-29042
GREEN, M. A. N91-28662
N91-28993
GREENBAUM, E. N91-28718
GREENE, A. E. N91-28499
GREENE, E. F. N91-28857
GREENFIELD, STUART N91-28228
GREENHILL, LINCOLN JARED N91-29117
GREENWOLL, D. A. N91-28543
GREGOREK, G. M. N91-28133
GREINER, W. N91-28827
GRIMALDI, MARGARET E. N91-28186
GRIMLEY, A. J. N91-28442
GRIMM, C. C. N91-28850
GRIMSHAW, A. N91-28757
GROENEVELD, B. J. N91-28750
N91-29077
GRONSKY, R. N91-28548
GROSSI, G. N91-28721
GROSSMAN, ROBERT N91-28787
N91-28788
N91-28789
N91-28790
GROVER, R. N91-28313
GROVES, S. E. N91-28285
N91-28286
GRUGEL, R. N. N91-28347
GRUMMON, D. S. N91-28287
GRUNAU, M. N91-29070
GUAN, X. N91-28753
GUESS, T. R. N91-28393
GUEVENC, Z. B. N91-28859
GUINN, JAMES WILLIAMS N91-29118
GUIOCHON, G. N91-28421
N91-28428
GUNN, CHARLES R. N91-28201
N91-28210
GUPTA, ARUN K. N91-28858
GUPTA, MANISH N91-28747
GUSTAFSON, J. L. N91-28773
GUSTAVSSON, A. I. N91-28157
GUTOWSKI, W. J. N91-28673
GUZDAR, P. N. N91-28898
N91-28980
N91-28981
GYULASSY, M. N91-28768

H

HAALAND, C. M. N91-28188
HAAN, S. W. N91-28955
HAAS, F. A. N91-28901
HADJIPANAYIS, G. C. N91-28383
HAEHNER, CARL L. N91-28363
HAENSEL, PAWEL N91-29109
HAERTLING, GENE H. N91-28490
HAGEN, GARY D. N91-28181
HAGHIGHI, N. N91-29090
HAGMANN, CHRISTIAN ALEXANER N91-29104
HAHN, H. N91-28495
HAHN, K. N91-28476
HAHN, S. N91-29004
HAHN, SANG JUNE N91-28896
HAIGHT, R. C. N91-28861
HAILEY, C. E. N91-28505
HAIMSON, J. N91-28489
HAINES, G. H. N91-28153
HALL, E. J. N91-28716
HALLER, E. E. N91-29038
HAMMERBERG, J. E. N91-28633
HAMMETT, C. P. N91-28355
HAMMOND, S. J. N91-28762
HAMMONDS, J. P. N91-28407
HAMRICK, J. T. N91-28441
HAMZIC, A. N91-29046
HAN, UK N91-28682
HANLON, JAMES C. N91-28277
N91-28278
HANNAH, P. R. N91-28593
HANNON, K. N91-28173
HANSEN, W. L. N91-29038
HARASGAMA, S. P. N91-28504
HARBOUR, J. L. N91-28732
HARDIN, J. E. N91-28491
HARDY, TERRY L. N91-28449
HARLAN, J. G. N91-28442
HARLANDER, M. N91-28768
HAROUN, L. A. N91-28147
HARRIS, C. B. N91-28315
HARRIS, J. H. N91-28947
HARSHMAN, D. R. N91-29034
N91-29050
HARTY, RICHARD B. N91-28648
HARVEY, J. A N91-28829
HASEGAWA, A. N91-28275
N91-28920
HASSAM, A. B. N91-28980
N91-28981
HATORI, T. N91-28932
HAWKINS, R. J. N91-28560
N91-28876
HAWRYLUK, A. M. N91-28877
HAYASHI, T. N91-28883
N91-28894
HAYDEN, Y. T. N91-28571
HAYNES, R. A. N91-28778
HAZELTINE, R. D. N91-28965
HEDAYATPOUR, ALI N91-28522
HEEGER, A. J. N91-28402
N91-28427
HEESE, R. N91-29039
HEGER, T. N91-28610
HEGNA, C. C. N91-28895
HEIERMANN, P. N91-28942
HEIPLE, C. R. N91-28452
N91-28453
HELMERSSON, L. N91-28157
HENCH, LARRY L. N91-28384
HENNINGER, R. N91-28613
HERRMANNSFELDT, W. B. N91-28869
HERTZ, LESLIE S. N91-28186
HESS, A. C. N91-28671
HESS, DAVID EARL N91-28523
HESS, N. J. N91-29012
HEUER, A. H. N91-28400
HEWETT, R. N91-28656
N91-28658
HEYDT, H. J. N91-29068
HEYMAN, JOSEPH S. N91-28246
N91-28321
HICKS, PETER DAVID N91-28374
HIDALGO, C. N91-28947
HIETALA, V. M. N91-28501
HILL, C. G., JR. N91-28398
HILL, CHRISTOPHER T. N91-28858
HILL, N. W. N91-28829
HILL, S. G. N91-28732
HILLS, R. F. N91-28148
HINDMAN, T. B., JR. N91-29067
HINGORANI, S. N91-28595
HINGST, W. R. N91-28136
HIROSE, AKIRA N91-28902

HIRSCH, L. M. N91-28990
HIRST, E. N91-28655
HITE, DALE N91-28209
HIXSON, R. S. N91-28634
HJERESEN, D. N91-28456
HLAVA, P. F. N91-28379
HO, Y. L. N91-28961
HOAG, J. E. N91-28772
HOBBS, L. W. N91-28391
HOFFHEINS, B. S. N91-28550
HOFFMAN, D. J. N91-28463
HOFMAYER, C. H. N91-28606
HOGAN, W. J. N91-28966
HOJO, H. N91-28924
HOLCOMBE, C. E. N91-28397
HOLDEN, T. M. N91-28624
HOLIAN, K. S. N91-28613
HOLLAND, D. F. N91-28951
HOLLENBERG, J. B. N91-28888
HOLMAN, RICHARD N91-28858
HOLMES, H. N91-28763
HOLMES, N. C. N91-28313
N91-28365
N91-28628
HONG, B. G. N91-28890
HONNELL, R. E. N91-28288
HOOPER, E. B. N91-28948
HOOPER, S. J. N91-28293
HOPWOOD, S. T. N91-28504
HORIUCHI, R. N91-28883
HORIUCHI, RITOKU N91-28917
HORTON, W. N91-28933
N91-28964
N91-28972
N91-28982
HOSKING, F. M. N91-28379
N91-28451
HOUCK, T. N91-28489
HOULBERG, W. A. N91-28946
HOUTEKAMER, GILLES ELIZA N91-28736
HOWARD, CHARLES C. N91-28459
HOWARD, E. M. N91-29071
HOWARTH, WILLIAM GUY N91-28694
HOWELL, C. R. N91-28359
HOWELL, J. N91-28629
HOWELL, WILLIAM E. N91-28164
HOWITT, D. G. N91-28396
HRMA, P. R. N91-28432
HSIEH, J.-H. N91-28577
HSU, MENG-BOR N91-28295
HU, QING N91-29021
HUANG, CHAO-SHANG N91-28803
HUBBARD, C. R. N91-28397
HUETER, UWE N91-28205
HUFFAKER, FREDRICK N91-28211
HUGHES, J. E. N91-29066
HULL, J. R. N91-28815
N91-29008
HUMPHREYS, K. K. N91-28669
HUNDLEY, M. F. N91-29033
HUNT, J. T. N91-28561
HUNTER, D. N91-28247
HUNTER, N. N91-29055
HUYNH-BA, GIA N91-28438
HWANG, FU-KWUN N91-28950

I

IACONO, M. N91-28673
ICE, G. E. N91-28601
N91-28832
N91-28847
ICHIKAWA, YOSHI H. N91-28933
N91-28943
N91-28972
ICHIMURA, M. N91-28924
INCE, A. NEJAT N91-28465
INGBER, M. S. N91-28505
INUI, M. N91-29034
N91-29050
INUTAKE, M. N91-28924
IRENE, E. A. N91-28985
ISAAK, DONALD GEORGE N91-28679
ISHIBASHI, N, ... N91-28928
ISHIGURO, S. N91-28925
ISHII, Y. N91-28929
ISKANDER, S. K. N91-28349
ITAKURA, M. N91-28923

J

JACHIM, S. P. N91-28474
JACOBS, A. J. N91-28352
JACOBS, H. R. N91-28226
JACOBS, PETER F. N91-28143
JACOX, M. G. N91-28279
JAKOSKY, BRUCE M. N91-28182
JAMES, WILLIAM F. N91-28373
JANICKI, J. N91-28400
JANKOWSKI, A. N91-28542
JANNUZI, BUELL TOMASSON N91-29099
JANSEN, H. J. F. N91-28369
JARBOE, T. R. N91-28967
JASZCZAK, J. A. N91-28377
JEANLOZ, R. N91-28366
JELLINEK, J. N91-28859
JENG, R. J. N91-28386
JENKINS, M. G. N91-28418
JENKINS, M. L. N91-29027
JERMAN, G. A. N91-28291
JESSON, D. E. N91-29044
JEWETT, BOB N91-28245
JHABVALA, M. N91-28726
JIMENEZ, B. D. N91-28719
JIMENEZ, J. R. N91-29015
JOHNSON, J. N91-28155
JOHNSON, J. D. N91-28325
JOHNSON, J. N. N91-28617
JOHNSON, K. F. N91-28564
N91-28871
JOHNSON, L. D. N91-29079
JOHNSON, W. J. D. N91-28565
JOHNSTON, N. N91-28763
JONES, C. N91-28247
JONES, G., II N91-28440
JONES, J. P. N91-28784
JONES, L. A. N91-28556
JONES, R. H. N91-28630
JONES, R. M. N91-29075
JONES, W. D. N91-28332
JONG, R. A. N91-28568
JORTNER, J. N91-28756
JOSHI, C. N91-28976
JOSTLEIN, H. N91-28629
JOVANOVIC, D. N91-28982
JUANG, JER-NAN N91-28184
N91-28580

K

KACHKACHI, M. N91-29057
KAGEYAMA, A. N91-28904
KAJITA, SHINSAKU N91-28909
KALLMAN, J. S. N91-28876
KALSI, S. N91-29039
KANG, S. W. N91-28506
KANNBERG, L. D. N91-28654
KARACA, MEHMET N91-28691
KARALEKAS, DIMITRIOS N91-28296
KARR, T. J. N91-28559
KATO, S. N91-28897
KATO, T. N91-28907
KATZ, J. D. N91-28414
N91-28415
KAUPPILA, T. N91-28558
KAW, P. K. N91-28938
KAWAHARA, W. A. N91-28612
KAWAKATSU, TOSHIHIRO N91-28926
KAWASAKI, KYOZI N91-28926
KAY, B. D. N91-28314
KAYE, S. M. N91-28946
KAZA, K. R. V. N91-28627
KEELING, J. F., III N91-29066
N91-29069
KEENEY-WALKER, J. N91-28614
KEICHER, D. M. N91-28451
KEISER, J. N91-28360
KEIZMAN, YAACOV N91-28516
KELLEY, DAVID L. N91-28211
KELLEY, HENRY L. N91-28424
KELLEY, JOE N91-28254
KELLY, S. M. N91-28778
KEMPF, G. N91-28153
KENDALL, R. A. N91-28671
KENIK, E. A. N91-28344
KENKRE, V. M. N91-28415
KENNEDY, E. J. N91-28484
KENNEY, W. J. N91-28814
KERBOUL, C. N91-28842
KERCHER, J. R. N91-28672
KERLEY, G. I. N91-28178
KERRISK, J. F. N91-28177
KHOSLA, P. K. N91-28576
KIDA, SHIGEO N91-28885
KIEFFER, JONATHAN CHARLES N91-28598
KIGGANS, J. O. N91-28397
KILKENNY, J. D. N91-28955
KIM, D. H. N91-29042
KIM, J. G. N91-28358
KIM, J. H. N91-28854
KIM, K. G. N91-28389
KIMREY, H. D. N91-28397
KINCAID, J. R. N91-28357
KING, S. L. N91-29027
KINGSTON, J. J. N91-28997
N91-28998
N91-29007
KINNEY, J. H. N91-28284
KIRK, M. A. N91-29027
KIRSTEINS, ANDRA N91-28731
KISPERT, L. D. N91-28724
KITAHARA, K. N91-28928
KLEIBER, J. C., JR. N91-28506
KLEMM, R. A. N91-29005
KLEVA, R. N91-28980
KLIBANSKY, BEN-TSIYON N91-28469
KLIMAS, P. C. N91-28651
N91-28653
KLOTS, C. E. N91-28555
KNUDSON, D. A. N91-28675
KOCKS, U. F. N91-28419
KOELLING, C. P. N91-29076
KOHOUT, L. L. N91-28277
KOLB, EDWARD W. N91-28858
KOLLI, SUDHAKAR N91-28298
KOLODZIEJCZAK, JEFFREY JAY N91-29135
KONDOH, YOSHIOMI N91-28906
KONISHI, TETSURO N91-28934
KORATKAR, ANURADHA PURUSHOTTAM . N91-29095
KORB, LARRY N91-28557
KORDAS, J. F. N91-28148
KORTE, R. N91-28815
KORTH, G. E. N91-28380
KOSTELNIK, K. M. N91-28764
KOT, M. N91-29064
KRAUSS, A. J. N91-28156
KREMPL, E. N91-28350
N91-28615
KRISHNAN, A. N91-28576
KRISHNAN, K. M. N91-28862
KRIVE, I. V. N91-29019
KROLL, KEN N91-28239
KROMMES, JOHN A. N91-28889
KRUMPELT, M. N91-28592
KRUSE, H. W. N91-28499
KUHL, D. E. N91-28728
KUKACKA, L. E. N91-28660
KUMANO, MAMI N91-28908
KUMAR, J. N91-28385
N91-28386
KUNIMOTO, KAITO N91-28908
KUNZ, A. B. N91-28988
KUO, KENNETH K. N91-28223
N91-28227
KURSTEDT, H. A., JR. N91-29066
N91-29067
N91-29070
N91-29071
N91-29075
N91-29076
KURSTEDT, P. S. N91-29071
KUSANO, K. N91-28883
KUSANO, KANYA N91-28908
KUSUBOV, A. N91-28422
KYRALA, G. A. N91-28556

L

LAANANEN, DAVID H. N91-28146
LABOTZ, RICH N91-28239
N91-28240
LACERDA, A. N91-29033
LACKNER, K. S. N91-28174
LADDA, V. N91-28158
LAEDKE, E. W. N91-28942
LAGASSE, R. R. N91-28393
LAI, YONG-GEN N91-28534
LAKE, CHARLES H. N91-28989
LAM, D. J. N91-29037
LANDAU, R. H. N91-28873
LANDEN, O. L. N91-28958
LANE, THOMAS G. N91-28748
LANGAN, T. J. N91-28334
LANGDON, B. N91-28954
LANGLEY, R. A. N91-28463
LANGSTON-UNKEFER, P. J. N91-28725
LAPINE, LEWIS A. N91-28646
LARAIA, V. J. N91-28400
LARSON, B. C. N91-28847
LARSON, N. M. N91-28829
LARSON, RICHARD N91-28789
LASHER, WILLIAM CHARLES N91-28535
LAUF, R. J. N91-28550
LAVAL, G. N91-28900

LAVINE, T. L. N91-28869
LAWRENCE, GEORGE F. N91-28191
LAWRENCE, R. J. N91-28567
LAWSON, D. N91-28670
LAY, KENNETH W. N91-28986
LAYNE, T. C. N91-28541
LEBOEUF, J. N. N91-28969
LEBRUN, M. J. N91-28915
LEDEBUHR, A. G. N91-28148
LEE, B. J. N91-28953
LEE, D. K. N91-28969
LEE, I. N91-28493
N91-28852
LEE, J. Y. N91-28385
LEE, JAE KOO N91-28896
LEE, JOOSIK N91-28303
LEE, K. N91-28173
LEE, M. J. N91-28609
LEE, R. E. N91-28467
LEE, R. S. N91-28467
LEE, T. S. H. N91-28865
LEE, W. W. N91-28916
LEE, Y. C. N91-28898
LEE, YIN-NAN N91-28318
LEGER, L. N91-28247
LEGGE, G. J. F. N91-28825
LENG, CHUN-WU ROGER N91-29085
LENG, GERARD SIEW BING N91-28171
LESLIE, LYNN D. N91-28707
LESSOR, D. L. N91-28431
LEUNG, E. N91-29039
LEVIN, K. N91-28854
LEVIN, MOSHE N91-28468
LEVINE, STAN N91-28244
LEVITT, KARL N. N91-28777
LEVY, DAVID WILLIAM N91-28530
LEWIS, D. L. N91-28307
LEWIS, I. T. N91-28148
LEWIS, M. B. N91-28463
LEWIS, NATHAN S. N91-28304
LEWIS, S. N91-28230
LHALLABI, T. N91-29057
LI, QIANG N91-28322
LI, WEIGONG N91-28524
LI, XIAOYU N91-28330
LI, Y. N91-28480
LIBERMAN, D. A. N91-28636
LICHTENBERG, ALLAN J. N91-28941
LIEBETRAU, S. F. N91-29092
LIEN, REN-CHIEH N91-28709
LIEPINS, G. E. N91-28741
LILJEGREN, LUCIA M. N91-28525
LIM, E. C. N91-28649
LIN, H. C. N91-28726
LIN, J. S. N91-28438
LIN, TSUNG-CHIEH N91-28588
LINDEMUTH, I. R. N91-28499
LING, X. S. N91-29036
LIPO, THOMAS A. N91-28539
LISOWSKI, P. W. N91-28861
LITTLE, TOM HARVEY N91-29127
LITTLEFIELD, R. J. N91-28749
LIU, C. S. N91-28898
N91-28980
LIU, S. H. N91-29005
LOGAN, C. M. N91-28306
N91-28307
LONDON, R. A. N91-28551
LONGHURST, G. R. N91-28510
N91-28951
LOPEZ, G. N91-29040
LOTT, S. E. N91-28485
LOTTES, S. A. N91-28968
LOTZ, W. N91-28893
LOVELACE, R. V. N91-28963
LOWERY, P. S. N91-28431
LOWNDES, D. H. N91-29014
LOYD, L. D. N91-28782
LOZANO, G. N91-29056
LU, YONG N91-29032
LUBELL, M. S. N91-28814
LUDWIG, KIMBERLY N91-28776
LUE, J. W. N91-28814
LUETHI, T. N91-28410
LUGTU, SPOTRIZANO D. N91-28273
LUKE, P. N. N91-29038
LUMPKIN, A. H. N91-28565
LUND, R. K. N91-28207
LUNDBERG, L. B. N91-28279
LUNDGREN, C. A. N91-28284
LUNINE, JONATHAN I. N91-28182
LUO, GANG N91-28706
LUSK, E. N91-28765
LUTHER, G. G. N91-28545
LUTON, J. N. N91-28814
LYMAN, C. E. N91-28328
LYNCH, V. E. N91-28969

M

MA, W. H. N91-28849
MACKIN, MICHAEL N91-28776
MACKUSE, FRANCES A. N91-28176
MACONE, D. N91-28173
MADARAS, ERIC N91-28246
MADDEN, JOHN F., III N91-28134
MADSEN, V. A. N91-28873
MAGNANI, N. J. N91-28485
MAGNOTTA, F. N91-28824
MAJORS, P. S. N91-28350
MAJUMDER, ANUP N91-29105
MAKOWIECKI, D. N91-28542
MALEY, M. P. N91-29045
MALLAK, L. A. N91-29071
MALLOUK, T. E. N91-28833
MALONEY, JOHN D. N91-28989
MANCHEK, R. N91-28755
MANDAL, B. K. N91-28385
N91-28386
MANDELL, D. A. N91-28613
MANN, R. C. N91-28753
N91-28784
MANOHAR, MURALI N91-28375
MANSUR, L. K. N91-28348
MAPOLES, E. R. N91-28824
MARCHELLO, JOSEPH M. N91-28290
MARIAM, Y. H. N91-28433
MARKEN, K. R. N91-28993
MARKOWITZ, V. M. N91-29091
MARSCHALL, J. N91-29022
MARSH, S. P. N91-28179
MARTENS, J. S. N91-28501
MARTIN-SIEGFRIED, YVES N91-28161
MARTIN, KAREN MARIE N91-28667
MARTIN, R. L. N91-29025
MARTIN, RODERICK H. N91-28626
MARTIN, W. H. N91-28326
MARTIN, WILLIAM R. N91-28644
MARUYAMA, T. N91-28996
MARZOCCA, A. J. N91-28416
MASCHHOFF, K. J. N91-28749
MASON, JAMES MEREDITH N91-28817
MASSOUDI, M. N91-28514
MASTERS, JOHN E. N91-28292
MATSUMOTO, R. N91-28913
MATSUOKA, CHIHIRO N91-28931
MATTHEWS, S. D. N91-28764
MAUPIN, G. D. N91-28412
MAY, E. N91-28868
MAY, NICHOLAS EDWARD N91-28536
MAYA, L. N91-28390
MAYER, B. N91-28842
MAYES, PAUL N91-28460
N91-28461
MAZIASZ, P. J. N91-28381
MCAFEE, J. M. N91-28448
MCBRANCH, D. N91-28402
N91-28427
MCCAMPBELL, C. B. N91-28319
MCCARTHY, J. F. N91-28719
MCCEHEE, JOHN R. N91-28164
MCCLAIN, J. GREER N91-28159
MCCLELLAN, K. J. N91-28288
MCCLELLAND, M. N91-28717
MCCONNELL, ROBERT L. N91-28785
MCCRACKEN, JAMES RICHARD N91-28169
MCCREADY, M. J. N91-28511
MCCUNE, W. N91-28765
MCELROY, D. L. N91-28512
MCFADDEN, LUCY-ANN N91-28182
MCFARLAND, DONALD MICHAEL N91-28141
MCGEHEE, DAVID D. N91-28707
MCGILLIVRAY, H. J. N91-28632
MCGINNIS, L. D. N91-28675
MCGRATTAN, K. N91-28142
MCHARGUE, C. J. N91-28406
MCILWAIN, MELVIN N91-28241
MCKAMEY, C. G. N91-28359
N91-28381
MCKAY, CHRISTOPHER P. N91-28182
MCKINNON, WILLIAM B. N91-28182
MCKISSOCK, BARBARA I. N91-28277
N91-28278
MCLEOD, R. N91-28876
MCLUCKEY, S. A. N91-28310
N91-28835
N91-28836
MCNERNEY, K. N91-28421
MEARS, C. A. N91-29021
MEASE, K. N91-28230
MECKLENBURG, B. N91-28489
MEHTA, GOPAL N91-28262
MEIER, J. K. N91-28177
MEIER, W. R. N91-28966
MENGES, JOHN N91-28770
MENICUCCI, D. N91-28656
N91-28658
MENIKOFF, R. N91-28174
MENYUK, C. R. N91-28879
MERKLE, CHARLES L. N91-28219
N91-28222
N91-28234
MERKLE, J. G. N91-28619
N91-28623
MERRIFIELD, MICHAEL RALPH N91-29119
MESINA, G. L. N91-28795
METCALF, KENNETH J. N91-28648
METT, R. R. N91-28974
MEYER, ROGER N91-28241
MICCI, MICHAEL M. N91-28233
MICHAEL, J. R. N91-28841
N91-29003
MIKLICH, A. H. N91-28997
MILAM, M. BRUCE N91-28582
MILEY, GEORGE H. N91-28217
MILICH, L. N91-28665
N91-28666
MILLER, B. G. N91-28279
MILLER, K. N91-28513
MILLER, L. A. N91-28846
MILLER, M. K. N91-28371
MILLER, MICHAEL COLEMAN N91-29106
MILLER, P. N91-28385
MILLER, R. H. N91-28869
MILLER, W. H. N91-28308
MILLS, EVERALD E. N91-28744
MILLS, PETER H. N91-28746
MILNE, A. M. N91-28662
MILONNI, P. W. N91-28855
MILSTEIN, F. N91-29022
MIMA, K. N91-28897
MINAMI, K. N91-28923
MINES, G. N91-28595
MIRANDA, R. N91-28327
MIRSHAMS, A. R. N91-28354
MITCHELL, R. L. N91-28650
MITCHELL, T. D., JR. N91-28281
MITCHELL, T. E. N91-28288
MITCHELL, T. J. N91-28751
MIYOSHI, S. N91-28924
MIZUNO, K. N91-28956
MOG, ROBERT ALAN N91-28190
MOHAMADIAN, H. P. N91-28354
MOHNEN, V. A. N91-28697
MOIR, D. N91-28558
MOLNAR, G. N91-28673
MONK, JAN C. N91-28208
N91-28271
MOONIER, P. N91-28868
MOORE, D. S. N91-28325
MOORE, N. N91-28238
MOORE, THOMAS C., SR. N91-28454
MORAN, B. N91-28422
MOREA, S. F. N91-28269
MORK, STEVEN W. N91-28821
N91-28822
MOROSIN, B. N91-29052
MORRIS, B. R. N91-28166
MORRIS, C. E. N91-28634
MORRIS, DAVID N91-28154
MORRIS, DON H. N91-28292
MORRIS, H. E. N91-28475
MORRIS, J. N91-28480
MORRIS, J. R. N91-28559
MORRIS, J. W., JR. N91-28345
MORRIS, M. D. N91-28751
MORRISON, P. J. N91-28965
MORSE, D. H. N91-28306
MUENCHAUSEN, R. E. N91-28991
MUHLEMAN, DUANE O. N91-28182
MULCAHY, T. M. N91-29008
MULFORD, R. N. N91-29023
MULLAN, DERMOTT J. N91-29107
MULQUEEN, J. A. N91-28189
MULROY, JAMES RANDOLPH N91-28572
MUNRO, D. H. N91-28955
MURAKAMI, S. N91-28920
MURAL, R. N91-28753
MURRAY, MARY JOSEPHINE N91-29120
MURTHY, A. V. N91-28138
MUSTAFA, M. G. N91-28827

N

NAGASAWA, MICHIYASU N91-29112
NAGPAL, V. N91-28238

NAITOU, H. N91-28916
NAKAGAWA, K. N91-28925
NAKAJIMA, N. N91-28927
NAKAMURA, Y. N91-28895
NANSTAD, R. K. N91-28349
NARAYANAN, G. V. N91-28627
NASON, D. N91-29048
NATTER, E. F. N91-28474
NAULIN, V. N91-28942
NAZAREWICZ, W. N91-28851
N91-28853
NEILSON, G. H. N91-28946
NELSON, B. A. N91-28967
NELSON, E. N91-28792
NERI, F. N91-28807
NETZER, NATHAN N91-29136
NETZER, VLADIMIR N91-28583
NEUBURGER, DORON N91-28139
NEUMANN, ULRICH N91-28771
NEWELL, J. N91-28238
N91-28247
NEWMAN, BRIAN A. N91-28387
N91-28388
N91-28389
NEWMAN, H. T. N91-28155
NEWMARK, JEFFREY SCOTT N91-29096
NEWTON, J. N91-28480
NEXSEN, W. E. N91-28568
NICHOLS, F. A. N91-28577
NICHOLS, M. C. N91-28284
NICHOLS, RONALD L. N91-28206
NICHOLSON, PHILIP N91-28182
NICOL, T. N91-28610
NICOPOULOS, V. N. N91-29058
NISHIGUCHI, A. N91-28897
NISHIHARA, KATSUNOBU N91-28899
NOGAR, N. S. N91-28991
NOMURA, Y. N91-28933
N91-28972
NOREM, J. N91-28868
NORTON, D. P. N91-29014
NORWOOD, DONALD SCOTT N91-28299
NOUFI, R. N91-28650
NOVAK, J. N91-28665
N91-28666
NOZAKI, KAZUHIRO N91-28931
NUEHRENBERG, JURGEN N91-28893
NYLAND, LARS S. N91-28746

O

OBAYASHI, SHIGERU N91-28503
OBLOW, E. M. N91-28784
OBOT, N. T. N91-28508
N91-28509
OBRIEN, CHARLES J. N91-28256
OBRIEN, T. KEVIN N91-28293
OGURA, K. N91-28923
OHSAWA, Y. N91-28905
OHYABU, N. N91-28894
OJALEHTO, GEORGE N91-28267
OJO, SUNDAY OLUSEGUN N91-29084
OKEEFFE, MICHAEL N91-28987
OKUDA, H. N91-28891
OLINGER, CHAD TRACY N91-29114
OLINTO, ANGELA V. N91-29109
OLIVE, K. A. N91-29110
OLNESS, D. U. N91-28167
OLSEN, C. S. N91-28187
OLSON, D. L. N91-29073
OLSON, R. J. N91-28674
OMATETE, O. O. N91-28413
OONA, H. N91-28499
ORDWAY, WAYNE L. N91-28204
N91-28236
ORNSTEIN, R. L. N91-28671
OSHEA, P. G. N91-28565
OTT, E. N91-28980
OTTAVIANI, M. N91-28890
OTU, JOSEPH OBI N91-28472
OUTTEN, C. A. N91-29051
OVERBEEK, R. N91-28765
OVERMAN, ANDREA L. N91-28806

P

PACKER, M. N91-28498
PAIGE, M. E. N91-28315
PALAITH, D. N91-28414
PALMER, D. A. N91-28311
PAN, JING N91-28777
PAN, W. Y. N91-28417
PAN, YI-MING N91-28297
PANDA, JAYANTA N91-28531
PANGBORN, R. N. N91-28229
PARAKKA, A. N91-28353
PARK, CHANGBOM N91-29121
PARK, Y. J. N91-28606
PARKER, J. V. N91-28499
PARROTT, J. S. N91-28607
PARSA, Z. N91-28569
N91-28874
PASTERNAK, M. P. N91-28366
PATTAY, R. S. N91-28783
PATTON, T. L. N91-28675
PAUL, A. C. N91-28568
PAULEY, LAURA L. N91-28232
PAULI, H. C. N91-28856
PAYNE, S. A. N91-28571
PEASE, R. N91-28877
PEDERSON, L. R. N91-28412
PEEBLES, D. E. N91-28434
PEILERT, G. N91-28827
PEKALA, R. W. N91-28408
PENA, LUIS R. N91-28253
PENNINGTON, A. N91-29010
PENNYCOOK, S. J. N91-29044
PEPIN, ROBERT O. N91-28182
PERETZ, MOSHE N91-28878
PERKINS, F. W. N91-28946
PERRY, D. S. N91-28839
PERRY, RONNIE B. N91-28444
PETRONE, LOUIS N91-28387
PETROVIC, J. J. N91-28288
PETTIT, D. R. N91-29023
PEUSSA, J. N91-28418
PFALTZ, J. L. N91-28757
N91-29089
PHILIPS, LAURA A. N91-28821
N91-28822
PHILLIPS, TIMOTHY DWAYNE N91-28647
PICEL, K. C. N91-28670
N91-28675
PICKENS, J. R. N91-28334
PICRAUX, S. T. N91-28846
PIEPER, G. W. N91-28734
PIETSCH, H. N91-28942
PILLION, D. W. N91-28877
PIMPER, J. E. N91-28167
PIN, F. G. N91-28783
N91-28784
PINCUS, P. N91-28392
N91-28430
PIQUE, A. N91-28991
PITTS, J. H. N91-28966
PLACET, M. N91-28669
PLAZEK, D. J. N91-28393
PLEIM, JONATHAN EDWARD N91-28692
PLIMPTON, S. N91-28756
PODLESNY, R. N91-28480
POMPHREY, N. N91-28946
PONTAU, A. E. N91-28306
PORKOLAB, M. N91-28946
PORRO, A. R. N91-28136
POULTON, JOHN N91-28477
POVOLO, F. N91-28416
PRAGER, S. C. N91-28961
PRAHOVIC, M. G. N91-28965
PRATT, J. RICHARD N91-28425
PRATT, T. W. N91-28779
PREIST, D. H. N91-28486
PREPOST, R. N91-28996
PRESTON, D. L. N91-28633
PRESTON, J. F. N91-28355
PRIEST, PETE N91-28194
PRINJA, A. K. N91-28846
PRINS, JAN F. N91-28746
PRIOLEAU, J. C. N91-28720
PROCASSINI, R. J. N91-28984
PRUESS, K. N91-28527
PRYFOGLE, P. A. N91-28356
PUGH, C. E. N91-28614
PUMPHREY, P. H. N91-28371
PUSTER, RICHARD L. N91-28175

Q

QUACH, V. T. N91-29048
QUAN, DU N91-28997
N91-28998
QUEENEY, R. A. N91-28229

R

RABAS, T. J. N91-28509
RABERN, D. A. N91-28625
RABIE, R. N91-28637
RABIN, B. H. N91-28282
RADFORD, DAVID N91-28790
RAINISH, DORON N91-28471
RAMSAY, J. B. N91-28443
N91-28448
RAMSEY, J. M. N91-28309
RANDAZZO, ALANNA N91-28176
RANGARAJAN, G. N91-28807
RAO, M. N91-28360
RASOLT, M. N91-29000
RATH, S. N91-28938
RAUCH, PAUL N91-28987
RAY, A. N91-28786
RAY, LAURA RYAN N91-28172
RECHESTER, ALEXANDER B. N91-28940
REDUS, JERRY N91-28211
REE, F. N91-28313
REED, S. T. N91-28395
REES, D. E. N91-28488
N91-28492
REHAK, M. L. N91-28370
REHM, R. G. N91-28507
REID, D. W. N91-28486
REIF, JOHN H. N91-28746
REINOVSKY, R. E. N91-28499
REJ, D. J. N91-28983
REMINGTON, B. A. N91-28955
RESLER, D. A. N91-28962
RHIM, J. S. N91-28720
RHODES, RUSSEL N91-28197
RHODES, T. L. N91-28947
RICE, ERIC E. N91-28221
RICHARDS, P. L. N91-28992
N91-29021
RICHARDS, STEVE N91-28250
RICHMOND, G. L. N91-28479
RICKEL, D. G. N91-28499
RIDLON, R. N91-28558
RIEKE, P. C. N91-28999
RIETSCHA, E. R. N91-29080
RILEY, D. J. N91-28767
RITZ, C. P. N91-28947
N91-28971
RIVERA, JOSE A., JR. N91-28132
N91-28137
ROACH, D. P. N91-28616
ROBERSTON, S. N91-28977
ROBIN, JAMES F. N91-28648
ROBINSON, A. N91-28844
RODRIGUEZ, C. D. N91-28277
RODRIGUEZ, CARLOS D. N91-28278
ROGERS, D. N91-28489
ROGERS, J. H. N91-28956
ROLES, J. N91-28421
N91-28428
ROLLETT, A. D. N91-28991
ROMAN, W. C. N91-28401
ROMANELLI, F. N91-28890
ROMIG, A. D., JR. N91-28379
N91-28544
N91-28841
N91-29003
ROOTS, R. N91-28721
ROSS-TODD, B. M. N91-28674
ROSS, J. N91-28320
ROSSING, T. D. N91-28815
N91-29008
ROSTOKER, N. N91-28963
ROTH, GILBERT L. N91-28263
ROTH, M. N91-28151
ROTH, R. S. N91-28403
ROUTBORT, J. L. N91-28435
ROYSTER, DICK M. N91-28373
ROYSTON, JAMES D. N91-28578
ROZHAVSKY, A. S. N91-29019
RUBERG, G. E. N91-29069
RUBIN, J. B. N91-29028
N91-29029
RUBINSTEIN, F. M. N91-28498
RUBIO, A. N91-29018
RUEGER, M. L. N91-28133
RUGGLES, M. B. N91-28350
N91-28615
RUNT, J. P. N91-28438
RUSSELL, D. J. N91-28315
RUSSELL, G. A. N91-29065
RUTH, R. D. N91-28798
RUZAKOWSKI, PATRICIA HENRIETTA ANNE
N91-28384
RUZIC, D. N. N91-28463
RYAN, P. M. N91-28463
RYNE, R. N91-28489

S

SAADALDIN, H. S. N91-28414

SAADATMAND, K. N91-28564
N91-28871
SACKHEIM, BOB N91-28242
SAENZ, N. T. N91-28364
SAGDEEV, R. Z. N91-28981
SAINT, A. N91-28825
SAKAGAMI, HITOSHI N91-28899
SALEM, JONATHAN A. N91-28418
SALKOWSKI, CHARLES N91-28246
SALTZEN, E. N91-28570
SALZBRENNER, R. N91-28346
SAMPAYAN, S. E. N91-28568
SANCHEZ, R. J. N91-28285
SANDER, O. R. N91-28564
SANDERS, D. M. N91-28944
SANDOVAL, D. N91-28564
SANTARIUS, JOHN F. N91-28217
N91-28275
SANTAVICCA, DOMENIC A. N91-28228
SANTORO, R. J. N91-28223
N91-28226
SARCEVIC, I. N91-28845
SARIC, C. N91-28268
SATO, N. N91-28925
SATO, TETSUYA N91-28883
N91-28894
N91-28904
N91-28908
N91-28917
N91-28919
N91-28920
SAWYER, C. R. N91-29048
SCHAPOSNIK, F. A. N91-29056
SCHAPPERT, G. T. N91-28556
SCHEINBEIM, JERRY I. N91-28387
N91-28388
N91-28389
SCHILLING, S. P. N91-28645
SCHIMMEL, MORRY L. N91-28444
SCHIMMERLING, W. N91-29133
SCHLACHTER, F. N91-28844
SCHMIDT, S. C. N91-28325
SCHMITZ, PAUL C. N91-28277
N91-28278
SCHNACK, D. D. N91-28970
SCHNEIDER, J. D. N91-28871
SCHOWALTER, L. J. N91-29015
SCHRAMM, DAVID N. N91-29110
N91-29111
SCHULTZ, D. C. N91-28869
SCHULZ, H. N91-28614
SCHULZE, NORMAN R. N91-28217
SCHUTT, J. A. N91-28515
SCHWAB, C. N91-28893
SCHWARTZ, L. H. N91-28404
SCHWARZ, R. B. N91-28376
N91-29028
N91-29029
SCHWENTERLY, S. W. N91-28814
SCOTT, MARK W. N91-28168
SEAGER, C. H. N91-28402
N91-28427
SEE, E. F. N91-28365
N91-28628
SEIDEL, DAVID A. N91-28132
N91-28137
SEITZ, R. R. N91-28764
SEKI, R. N91-28838
SELLERS, C. H. N91-28362
SERDUKE, F. N91-28542
SHAARAWI, A. M. N91-28462
SHANKLAND, T. J. N91-28990
SHAPIRO, A. B. N91-29053
SHAU, YIOWHA RICHARD N91-28517
SHAW, D. C. N91-28420
SHAW, M. S. N91-28324
N91-28325
SHEA, M. J. N91-28554
SHEETS, DAN N91-28152
SHEFFIELD, R. L. N91-28565
N91-28566
SHELTON, ROBERT O. N91-28730
SHEN, JIANPING N91-28818
SHEPHERD, C. M. N91-28352
SHERMAN, L. A. N91-28713
SHI, DONGLU N91-29036
SHIBATA, K. N91-28913
SHINAS, M. N91-28564
SHINES, J. E. N91-28170
SHINN, JOSEPH M., JR. N91-28373
SHOKAIR, I. N91-28756
SHOLA, PETER BAMIDELE N91-28529
SHORT, R. T. N91-28850
SHRADER, M. B. N91-28486
SHUGART, L. R. N91-28719
SHUM, D. K. M. N91-28623
SHY, SHENQYANG STEVEN N91-28144
SHYU, W. N91-28898
SIDIKMAN, K. N91-28969
SIERADZKI, K. N91-28608
SIEVERS, J. N91-28614
SIKKA, V. K. N91-28359
N91-28382
SILBERGLITT, R. N91-28414
SILVA, L. N91-28456
SILVA, WALTER A. N91-28131
SILVER, G. L. N91-28800
SIMINOVITCH, M. J. N91-28498
SIMMONS, G. J. N91-28805
SIMONSON, J. M. N91-28311
SIMS, J. S. N91-28507
SINCLAIR, M. N91-28402
SINCLAIR, M. B. N91-28427
SINGH, J. P. N91-28410
SINGHAL, S. N91-28238
N91-28247
SINHA, ALOK N91-28230
SLATER, P. N. N91-28170
SMITH, B. F. N91-28758
SMITH, G. D. W. N91-28371
SMITH, G. W. N91-28549
SMITH, IAN ANDREW N91-29122
SMITH, J. S. N91-28996
SNELL, K. H. N91-28509
SNOHA, JOHN J. N91-28290
SNOW, DANIEL EDWARD N91-28808
SOLOMON, S. R. N91-28816
SON, S. H. N91-29089
N91-29090
SONG, YOUNG-HOON N91-28228
SOUERS, P. C. N91-28824
SOVIE, R. J. N91-29138
SPALEK, G. N91-28563
SPALL, D. N91-28456
SPANNER, J. C. N91-28600
SPANOS, JOHN T. N91-28769
SPARKS, C. J. N91-28601
N91-28832
SPARN, G. N91-29033
N91-29046
SPATSCHEK, K. H. N91-28942
SPENCER, C. M. N91-28869
SPONG, D. A. N91-28969
SPRAGUE, R. N91-28247
SPRINGER, R. W. N91-28565
SPRINGER, T. E. N91-28661
SRINIVASAN, S. N91-28376
ST. CLAIR, ANNE K. N91-28425
ST. CLAIR, TERRY L. N91-28425
STAMPFER, M. R. N91-28720
STARR, T. L. N91-28284
STEARNS, D. G. N91-28958
STEELE, R. R. N91-28397
STEFANO, J. E. N91-28675
STEFFENS, JERRY LEE N91-28687
STEIN, H. J. N91-29004
N91-29051
STEPHENS, J. J. N91-28379
STEPHENSON, R. N91-28456
STEVENS, R. N91-28765
STEWART, D. D. N91-28593
STITT, GARY RICHARD N91-28683
STOCK, S. R. N91-28284
STOECKER, H. N91-28827
STONE, JAMES MCLELLAN N91-29123
STORJOHANN, K. N91-28570
STOTLER, D. P. N91-28946
STRAUSS, M. N91-28551
STREHLOW, R. A. N91-28413
STROBL, BILL N91-28265
STROTTMAN, D. D. N91-28849
STRUCK, H. N91-28158
STUBBS, SANDY M. N91-28455
SU, JOSEPH CHUNGWAN N91-29083
SUENAGA, M. N91-28994
SUES, ROBERT H. N91-28644
SUGAMA, H. N91-28892
N91-28922
SULLIVAN, T. J. N91-28700
SUMMERFIELD, PHILIP JOHN N91-28149
SUMMERS, T. S. E. N91-28603
SUMPTION, M. D. N91-28993
SUN, XIAN-HE N91-28773
SUNDERAM, V. N91-28755
SUNDERAM, V. S. N91-28780
SURDA, A. N91-28804
SUTTON, S. R. N91-28825
SWEGLE, J. N91-28631
SYDORA, R. D. N91-28916

T

TABATA, WILLIAM K. N91-28212
TADJFAR, MEHRAN N91-28518
TAJIMA, T. N91-28913
N91-28915
TAKABE, H. N91-28897
N91-28914
TAKAMARU, H. N91-28919
TAKASE, Y. N91-28388
TAKEI, A. N91-28894
TALLANT, D. R. N91-28434
TALLERICO, P. J. N91-28492
TAMANO, TERUO N91-28908
TAN, T. H. N91-28179
TANAKA, MOTOHIKO N91-28918
N91-28919
TANG, H. C. N91-28507
TANG, P. K. N91-28621
TANIS, J. A. N91-28863
TANIUTI, T. N91-28929
TANK, MING H. N91-28214
TANNO, K. N91-28928
TAO, XIN N91-28688
TARASEVICH, B. J. N91-28999
TAUCHI, T. N91-28834
TAYLOR, A. J. N91-28556
TAYLOR, E. M. N91-28645
TAYLOR, J. B. N91-28974
TAYLOR, R. D. N91-28366
TELEGDI, V. L. N91-28813
TELLER, E. N91-28275
TEPIKIAN, S. N91-28495
TERASHIMA, Y. N91-28905
THEILER, J. N91-29055
THEISS, T. J. N91-28611
THESKEN, J. C. N91-28607
THOMAS, D. N91-29110
THOMAS, M. C. N91-28549
THOME, KURTIS JOHN N91-28689
THOMPSON, J. D. N91-29033
N91-29046
THOMSON, D. W. N91-28816
THORBY, D. C. N91-28155
THORPE, DOUGLAS G. N91-28257
N91-28258
THYAGARAJA, A. N91-28901
TIEGS, T. N. N91-28397
TIGGES, C. P. N91-28501
TISCHLER, J. Z. N91-28847
TOBIN, M. T. N91-28966
TODD, P. J. N91-28850
TODD, R. A. N91-28484
TOEDTE, R. J. N91-28766
TOMLINSON, J. T. N91-28654
TONKS, D. L. N91-28617
N91-28620
TORMA, A. E. N91-28356
TOTAH, JOSEPH J. N91-28134
TOTTEN, J. J. N91-28612
TOWERS, C. E. N91-28504
TRACHTMAN, EYAL N91-28470
TRANQUADA, J. M. N91-29031
TRAUGOTT, W. N91-28656
N91-28658
TRIPATHY, S. N91-28386
TRIVEDI, R. N91-28347
TROTT, W. M. N91-28562
TRUCANO, T. G. N91-28178
TRUGMAN, S. A. N91-29058
TRUNNELL, M. N91-28843
TRYBUS, C. L. N91-28362
TSAI, LUNG-WEN N91-28596
TSUI, H. Y. W. N91-28971
TUDA, TAKASHI N91-28936
TURCHI, P. J. N91-28499
TURNER, C. D. N91-28767
TURNER, J. R. N91-28370
TURNER, W. C. N91-28568
TURNS, STEPHEN R. N91-28224
TUTTLE, B. A. N91-28417
TWISDALE, LAWRENCE A. N91-28644
TYNDALL, HARRY N91-28343
TZEMOS, S. N91-29078

U

UBERBACHER, E. N91-28753
UCHIDA, YUTAKA N91-28903
UCKAN, T. N91-28947
ULLAL, H. S. N91-28650
ULRICH, NATHAN THATCHER N91-28589
UM, CHUNG I. N91-28812
UNSEREN, M. A. N91-28574
N91-28784

USADI, A. N91-28904
UZELAC, M. J. N91-28167

V

VANBERKEL, G. J. N91-28310
VANDENBERG, L. N91-29048
VANDEPLASSCHE, RUDY JOHAN N91-28735
VANDERMEY, NANCY E. N91-28292
VANDERSCHOOT, ADRIAAN N91-28676
VANDERVALK, R. N91-28162
VANISACKER, P. N91-28853
VANROSENDALE, JOHN N91-28806
VENTURINI, E. L. N91-29052
VESSER, L. N91-28545
VIANCO, P. T. N91-28379
VISSER, A. N91-28497
VITEK, V. N91-28372
VOGEL, J. S. N91-28712
VOGLER, WILLIAM A. N91-28164
VRANISH, JOHN M. N91-28579
N91-28581
N91-28785
VU, B. T. N91-28958

W

WADE, R. K. N91-28288
WAELBROECK, F. N91-28980
WAELBROECK, HENRI N91-29059
WAGANAAR, W. J. N91-28983
WAGH, A. S. N91-28410
WAGNER, J. N91-28756
WAGNER, J. W. N91-28608
WAGNER, ROBERT A. N91-28746
WAHLIN, E. K. N91-28556
WAKATANI, M. N91-28892
N91-28895
N91-28929
WALDROP, G. S. N91-28198
WALKER, J. D. N91-28996
WALKER, RAY N91-28244
WALKER, T. P. N91-29110
WALKO, R. J. N91-28395
WALL, M. N91-28351
N91-28542
WALLACE, B. S. N91-28766
WALLACE, D. C. N91-28618
N91-28633
WALLACE, R. J. N91-28955
WALLS, C. A. N91-28413
WALSH, DUNCAN ELIOT PETER N91-29124
WALTER, STEVEN JAY N91-28466
WALTERS, JOSEPH DOUGLASS N91-29060
WANG, A. N91-28662
WANG, J. P. N91-28888
N91-28949
WANG, KON-WELL N91-28230
WANG, TAI-SEN F. N91-28799
WANG, W. C. N91-28673
WANG, XIAOGANG N91-28884
WANG, Z. L. N91-28405
N91-28840
WARE, BRUCE E. N91-28176
WARNOCK, R. L. N91-28796
N91-28798
WARREN, K. H. N91-28774
N91-28781
WARSHAW, S. I. N91-28962
WARSHAWSKY, A. S. N91-28167
WARTHEN, B. N91-28545
WASHIMI, HARUICHI N91-28912
WATANABE, K. N91-28883
N91-28892
N91-28904
N91-28929
WATANABE, T. N91-28923
N91-28932
WATKINS, RICHARD N91-29108
WATSON, G. C. N91-28754
WEAVER, F. J. N91-28512
WEBER, F. N91-29125
WEBER, W. J N91-28317
WEBSTER, G. A. N91-28632
WEBSTER, P. J. N91-28632
WEESNER, RONALD G. N91-28270
WEHRLE, B. N91-28629
WEINER, ALLAN MEREDITH N91-28703
WEINSTEIN, LEONARD M. N91-28135
WEIRUP, D. N91-28825
WEIRUP, D. L. N91-28306
WEITZNER, H. N91-28978
WELCOME, T. S. N91-28774
WELLS, N. E. N91-29079
WELLSTOOD, F. C. N91-28997
N91-28998
N91-29007
WELTER, H. N91-28886
WEN, FENG N91-28537
WENHAM, S. R. N91-28662
WENTZCOVITCH, R. N91-28854
WESSON, J. A. N91-28935
WESTENSKOW, G. N91-28489
WESTER, RODERICK C. N91-28791
WESTON, BERT N91-28246
WEXLER, ANTHONY STEIN N91-28668
WHALEN, MARGARET V. N91-28449
WHALLEY, STEPHEN N91-28183
WHITAKER, JEFFREY STUART N91-28704
WHITE, J. E. N91-28274
WHITE, M. E. N91-29078
WHITE, R. H. N91-29063
WHITE, R. M. N91-28962
WHITE, ROSCOE B. N91-28940
WHITTEN, W. B. N91-28309
WICKER, LOUIS JOHN N91-28705
WIDRIG, R. D. N91-28276
WIDROW, LAWRENCE M. N91-29108
WIEDEMAN, S. N91-28480
WIEDERSICH, H. N91-29024
WIGHT, S. A. N91-28544
WILD, E. F. N91-28166
WILGEN, J. B. N91-28947
WILHELMSSON, HANS N91-28937
WILKE, G. D. N91-28571
WILKINS, J. W. N91-28848
WILLIAMS, D. B. N91-29003
WILSON, J. N91-28167
N91-28384
WILSON, M. S. N91-28661
WINKER, S. N91-28765
WINTENBERG, A. L. N91-28484
WITHROW, C. A. N91-28277
WITHROW, COLLEEN A. N91-28278
WITKOVER, R. L. N91-28870
WIXSON, J. N91-29068
WOLF, D. N91-28377
WOLF, E. L. N91-29043
WONG, E. L. N91-28479
WONG, G. S. N91-28198
WONG, GEORGE N91-28197
WONG, H. V. N91-28963
WOO, C. S. N91-28670
WOO, JONGSIK N91-28639
WOOD, CHARLES C. N91-28251
N91-28261
WOODIS, KEN N91-28246
WOODS, E. G. N91-28249
WOODWARD, ROGER D. N91-28227
WOOTEN, JOHN N91-28244
WOOTTON, A. J. N91-28947
N91-28971
WORLEY, P. H. N91-28797
WOS, L. N91-28765
WOZADLO, G. P. N91-28352
WRIGHT, THEODORE N91-28776
WRIGHT, WILLIAM V. N91-28823
WU, I. C. N91-29038
WU, X. D. N91-28991

X

XANTHEAS, S. S. N91-28671
XIAO, Q. F. N91-29015
XU, ZHIZHONG N91-29017

Y

YAGI, MASATOSHI N91-28892
N91-28921
N91-28936
YAJIMA, TETSU N91-28930
YAMAGISHI, T. N91-28910
YAMAMOTO, A. N91-28914
YAMAMOTO, Y. N91-28560
YAN, CHIUNG-YING N91-28794
YAN, YITON N91-28794
YANG, L. N91-28480
YANG, LI-FARN N91-28184
N91-28580
YANG, T. C. N91-28721
YANG, TRACY CHUI-HSU N91-28720
YANG, VIGOR N91-28225
YAO, D. N91-28345
YARBROUGH, D. W. N91-28512
YATES, G. J. N91-28464
N91-28549
YEARBY, KEITH HOWARD N91-28693
YEH, YEU-PIN N91-28145
YEON, KYU H. N91-28812
YEREMIAN, A. D. N91-28869
YLVISAKER, D. N91-28751
YOKOYA, K. N91-28834
YOKOYAMA, JUNICHI N91-29112
YONNET, J. N91-28842
YOO, C. S. N91-28365
YOSHIDA, Z. N91-28911
YOSHIKAWA, S. N91-28939
YOSHIZAWA, AKIRA N91-28887
YOU, HOYDOO N91-29037
YOUNG, BETTY AILEEN N91-28547
YOUNGBLOOD, G. E. N91-28317
YU, K. M. N91-28979
YUAN, V. W. N91-28564
YUE, C. F. N91-28417
YUN, F. N91-28662
YURCONIC, M. N91-29074

Z

ZABDAWI, MARWAN N91-28526
ZACHARIA, T. N91-28367
N91-28594
ZACHOS, C. N91-28793
ZADHOUSH, ALI N91-28300
ZAGARINO, P. N91-28549
ZAIDER, M. N91-28716
ZAND, MOOSA N91-28590
ZANGER, ISRAEL N91-28733
ZANTER, JOSEPH N91-28343
ZAPALAC, G. H. N91-28996
ZARNSTORFF, M. C. N91-28946
ZAROMB, S. N91-28670
ZAWODZINSKI, T. A. N91-28661
ZELTNER, W. A. N91-28398
ZHANG, DE-HAI N91-28803
ZHANG, F. N91-28662
ZHANG, S. Y. N91-28494
ZHANG, XUIFANG N91-28438
ZHAO, J. N91-28662
ZHOU, XIANLIANG N91-28318
ZIEMANN, V. N91-28552
ZIESE, J. M. N91-28198
ZIOLKOWSKI, R. W. N91-28462
ZIOMEK, C. D. N91-28474
ZIPPERIAN, T. E. N91-28501
ZITVOGEL, E. N91-28870
ZOTTER, B. N91-28799
ZSCHACK, P. N91-28847
ZUBRIN, ROBERT N91-28237
ZWEIBEL, K. N91-28650

CORPORATE SOURCE INDEX

Typical Corporate Source Index Listing

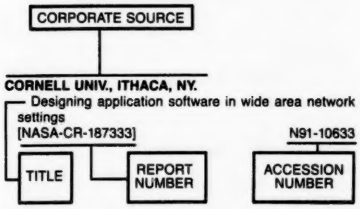
CORPORATE SOURCE
CORNELL UNIV., ITHACA, NY.
Designing application software in wide area network settings
[NASA-CR-187333]
N91-10633
TITLE
REPORT NUMBER
ACCESSION NUMBER

Listings in this index are arranged alphabetically by corporate source. The title of the document provides the user with a brief description of the subject matter. The report number helps to indicate the type of document cited (e.g., NASA report, translation, NASA contractor report). The accession number denotes the number by which the citation is identified. The titles are arranged under each corporate source in ascending accession number order.

A

ADVISORY GROUP FOR AEROSPACE RESEARCH AND DEVELOPMENT, NEUILLY-SUR-SEINE (FRANCE).

Landing Gear Design Loads
[AGARD-CP-484] N91-28150

Considerations for NATO satellite communications in the post 2000 era
[AGARD-AG-330] N91-28465

AEROJET-GENERAL CORP., SACRAMENTO, CA.

Technology transfer methodology N91-28240

The propulsion system is the key to airline-like operation of ETO vehicles N91-28256

Business not as usual N91-28266

AERONAUTICAL RESEARCH INST. OF SWEDEN, BROMMA.

Long time measurements of landing gear loads on SAAB SF-340 commuter aircraft N91-28157

AERONAUTICAL SYSTEMS DIV., WRIGHT-PATTERSON AFB, OH.

Application of the Air Force guide specification 87221A to ground loads N91-28152

AEROSPACE INDUSTRIES ASSOCIATION OF AMERICA, INC., WASHINGTON, DC.

Maintaining technical excellence requires a national plan N91-28196

AICHI UNIV. OF EDUCATION (JAPAN).

Self-similar evolution of nonlinear magnetic buoyancy instability N91-28913

AIR FORCE AVIONICS LAB., WRIGHT-PATTERSON AFB, OH.

Space systems propulsion technology N91-28209

AKRON UNIV., OH.

Dynamics of charge-transfer excited states relevant to photochemical energy conversion
[DE91-012669] N91-28649

Molecular eigenstate spectroscopy: Application to the intramolecular dynamics of some polyatomic molecules in the 3000 to 7000 cm(exp -1) region
[DE91-013154] N91-28839

ALABAMA UNIV., BIRMINGHAM.

Gravitational influence of a static ring-like distribution of mass on electromagnetic waves N91-28472

ALABAMA UNIV., HUNTSVILLE.

Discrete posynomial programming with applications to spacecraft protective structures design optimization
N91-28190

Numerical analyses of aero-optical flows: An application of parallel algorithm on high-performance Personal Computer (PC) base multitransputer system N91-28519

Predicting thunderstorm evolution using ground-based lightning detection networks N91-28702

ALABAMA UNIV., UNIVERSITY.

Magnetic resonance and optical spectroscopic studies of carotenoids
[DE91-014361] N91-28724

AMES LAB., IA.

Strength and electrical conductivity of deformation processed Cu-15 v/o Fe metal composites produced by powder metallurgy/techniques
[DE91-013658] N91-28291

Interpreting solidification phenomena and microstructural evolution in metals through the use of transparent model alloy systems
[DE91-012629] N91-28347

EXAFS studies of elastic strain in dilute binary alloys
[DE91-012678] N91-28353

Energy dispersive x ray diffraction study of glassy Bi2Sr2CaCu2O(x) filaments produced by gas-jet fiberization
[DE91-012021] N91-28407

Toward a better parallel performance metric
[DE91-012627] N91-28773

Nuclear magnetic resonance studies of atomic motion in lithium chloroborate and lithium thiosilicate glassy fast ionic conductors
[DE91-012677] N91-28843

Synthesis and characterization of reduced ternary molybdenum oxides and soluble copper (III) alkoxide complexes
[DE91-012679] N91-29001

ANALYTICAL SERVICES AND MATERIALS, INC., HAMPTON, VA.

Interlaminar fracture characterization: A current review
[NASA-CR-187573] N91-28626

APPLIED RESEARCH ASSOCIATES, INC., RALEIGH, NC.

Probabilistic structural mechanics research for parallel processing computers
[NASA-CR-187162] N91-28644

ARGONNE NATIONAL LAB., IL.

Assessing the risk of transporting hazardous materals by aircraft: A case study
[DE91-014016] N91-28147

Evaluation of aging of cast stainless steel components
[DE91-014013] N91-28361

Temperature dependence of the elastic behavior of structurally disordered metallic superlattices
[DE91-014007] N91-28377

Development of nondestructive evaluation methods and prediction of effects of flaws on the fracture behavior of structural ceramics
[DE91-012471] N91-28410

Creep and diffusion in nonstoichiometric oxides
[DE91-013766] N91-28435

Boundary lubrication of ceramic materials by soft metallic coating and synthetic oil
[DE91-014017] N91-28577

Sealant research for SOFC
[DE91-014012] N91-28592

Plastic analysis of a circular rod subjected to sinusoidal thermal cycling
[DE91-011845] N91-28609

Calculation of pressure distribution in vacuum systems using a commercial finite element program
[DE91-013611] N91-28629

High-throughput liquid-absorption air and aerosol sampler
[DE91-013762] N91-28670

Work plan for the preliminary site investigation for McMurdo Station, Ross Island, Antarctica
[DE91-015100] N91-28675

Research in mathematics and computer science at Argonne, September 1989-February 1991
[DE91-012989] N91-28734

An iterative substructuring algorithm for problems in three dimensions
[DE91-014388] N91-28758

A multilingual parallelization of the icosahedral-hexagonal grid system for integration on the sphere
[DE91-013615] N91-28762

Automated reasoning contributes to mathematics and logic
[DE91-014005] N91-28765

Quantized planes and multiparameter deformations of Heisenberg and GL(N) algebras
[DE91-012481] N91-28793

Effect of guideway discontinuities on magnetic levitation and drag forces
[DE91-014011] N91-28815

Mode selectivity in cluster-molecule interactions: Ni13 + D2
[DE91-013352] N91-28859

The Soudan 2 honeycomb calorimeter
[DE91-013404] N91-28860

Photodisintegration of the deuteron at medium and high energies
[DE91-014458] N91-28865

High Energy Physics Division semiannual report of research activities, July 1, 1990--December 31, 1990
[DE91-012339] N91-28868

Simulation of combustion processes in an MHD second stage combustor
[DE91-014014] N91-28968

Interlayer pairing and c-axis versus ab-plane gap anisotropy in high Tc superconductor
[DE91-012218] N91-29005

Effect of size and geometry on levitation force measurements between permanent magnets and high-temperature superconductors
[DE91-012472] N91-29008

Evolution of defect cluster distributions during irradiation
[DE91-013405] N91-29024

The interaction of HVEM-generated point-defects with dissociated dislocations
[DE91-013353] N91-29027

Flux dynamics in a single crystal of Bi2Sr2CaCu2O(x)
[DE91-013763] N91-29036

X ray diffraction study of heteroepitaxy of MOCVD grown TiO2 and VO2 films on sapphire single crystals
[DE91-013764] N91-29037

Flux pinning and dissipation in high-temperature superconductors
[DE91-014466] N91-29042

ARIZONA STATE UNIV., TEMPE.

Computer simulation of an aircraft seat and occupant(s) in a crash environment: Program SOM-LA/SOM-TA user manual
[CR-R-90026] N91-28146

Near-wall modelling of complex turbulent flows
N91-28534

Antenna organization in green photosynthetic bacteria
[DE91-014814] N91-28723

The software technical review process
[AD-A236139] N91-28743

Computations involving differential operators and their actions on functions N91-28789

ARIZONA UNIV., TUCSON.

Gravity wave propagation in a frontal environment
N91-28687

Radiative transfer model for a spherical atmosphere
N91-28689

Dynamical behavior of excited hadronic matter
[DE91-013024] N91-28845

The optical polarization of BL Lacertae objects
N91-29099

ARMY ARMAMENT RESEARCH, DEVELOPMENT AND ENGINEERING CENTER, PICATINNY ARSENAL, NJ.

Meteorological instrumentation support for an adverse weather test facility
[AD-A236605] N91-28696

ARMY AVIATION SYSTEMS COMMAND, HAMPTON, VA.

Local delamination in laminates with angle ply matrix cracks. Part 1: Tension tests and stress analysis
[NASA-TM-104055] N91-28293

ARMY WAR COLL., CARLISLE BARRACKS, PA.

Space systems requirements: The Navy approach
[AD-A236490] N91-28181

SOURCE

ATMOSPHERIC AND ENVIRONMENTAL RESEARCH, INC., CAMBRIDGE, MA.
Natural and anthropogenic climate change [DE91-014734] N91-28673

B

BMW-A.G., MUNICH (GERMANY, F. R.).
Actively damped landing gear system N91-28165
BOEING AEROSPACE CO., SEATTLE, WA.
STV engine design considerations N91-28255
BOEING MILITARY AIRPLANE DEVELOPMENT, SEATTLE, WA.
Toward a formal verification of a floating-point coprocessor and its composition with a central processing unit [NASA-CR-187547] N91-28777
BOSTON UNIV., MA.
Photoinduced electron transfer in ordered polymers [DE91-014512] N91-28440
BRITISH AEROSPACE PUBLIC LTD. CO., KINGSTON-UPON-THAMES (ENGLAND).
The special requirements of a VSTOL aircraft N91-28155
BRITISH COLUMBIA UNIV., VANCOUVER.
Measurements of angular distributions of absolute cross sections and analyzing powers of the reaction bar-p p yields d(pi+) between 1.3 and 2.4 GeV [DE91-012638] N91-28842
BROOKHAVEN NATIONAL LAB., UPTON, NY.
The solubility and dissociation kinetics of hydroxymethyl hydroperoxide in aqueous solution [DE91-013336] N91-28318
Brittle behavior of SSC yokes [DE91-014031] N91-28370
Thyristor converter simulation and analysis [DE91-013802] N91-28494
Perturbation treatment of the longitudinal coupling impedance of a toroidal beam tube [DE91-013884] N91-28495
Beam emittance and the effects of the rf, space charge and wake fields: Application to the ATF photoelectron beam [DE91-014789] N91-28569
Prediction of high level vibration test results by use of available inelastic analysis techniques [DE91-009437] N91-28606
Geothermal materials development [DE91-013972] N91-28660
The effect of strong Coulomb correlations on electron-phonon interactions in the copper oxides: Implications for transport [DE91-013333] N91-28854
Chaos in the lowest Landau level [DE91-014800] N91-28866
Beam current monitoring in the AGS booster and its transfer lines [DE91-013328] N91-28870
Space charge and wake field analysis for a high brightness electron source [DE91-014788] N91-28874
Magnetization and critical currents of tin-core multifilamentary Nb3Sn conductors [DE91-012241] N91-28994
Neutron scattering studies of spin correlations in metallic YBa2Cu3O(6+x) [DE91-013794] N91-29031
The DARPA compact superconducting x-ray lithography source features [DE91-013864] N91-29039
BROWN UNIV., PROVIDENCE, RI.
Interactions of molecules with surfaces [DE91-014498] N91-28857
BRUNEL UNIV., UXBRIDGE (ENGLAND).
The influence of defects on the mechanical properties of short fibre reinforced thermoplastics N91-28300

C

CALIFORNIA INST. OF BIOLOGICAL RESEARCH, LA JOLLA.
Novel methods for physical mapping of the human genome applied to the long arm of chromosome 5 [DE91-012894] N91-28717
CALIFORNIA INST. OF TECH., PASADENA.
Applications of scanning tunneling microscopy to electrochemistry [AD-A237021] N91-28304
Study of spherical couette flow via 3-D spectral simulations: Large and narrow-gap flows and their transitions N91-28520
Inorganic components of atmospheric aerosols N91-28668
Properties of infrared-luminous galaxies, or, how I spent seven summer vacations N91-29098
Radiative transfer in very strong magnetic fields N91-29106
Radiative processes in active galactic nuclei N91-29137
CALIFORNIA STATE UNIV., NORTHRIDGE.
Theoretical research in intermediate-energy nuclear physics [DE91-012720] N91-28838
CALIFORNIA UNIV., BERKELEY.
Diffusion through stochastic webs in two and more dimensions N91-28941
On the use of particle-in-cell methods for the study of magnetically-confined fusion plasmas [DE91-015093] N91-28984
CALIFORNIA UNIV., BERKELEY. LAWRENCE BERKELEY LAB.
Alumina-silicon carbide composites from coated powders [DE91-012357] N91-28281
Some new approaches to semiclassical and quantum transition state theory [DE91-012345] N91-28308
Energy dissipation in chemical reactions on ultrafast timescales [DE91-012342] N91-28315
Tensile deformation of Al-Cu-Li-Zr alloy 2090-T8E41 at 298 and 77 K [DE91-011885] N91-28345
A study of the influence of temperature gradients on densification of glass powder compacts [DE91-012337] N91-28399
On accurate determination of contact angle [DE91-013849] N91-28450
High order calculation of the multipole content of three dimensional electrostatic geometries [DE91-014707] N91-28476
Fixture efficiency program [DE91-014470] N91-28498
A mathematical model for two-phase water, air, and heat flow around a linear heat source emplaced in a permeable medium [DE91-014614] N91-28527
Advancing conventional high-resolution electron microscopy [DE91-013773] N91-28548
Improving fatigue life in near-eutectic Sn Pb solders [DE91-013844] N91-28603
A gravity model for the Coso geothermal area, California [DE91-011874] N91-28677
Chromosomal changes in cultured human epithelial cells transformed by low- and high-LET radiation [DE91-013772] N91-28720
Genetic changes in Mammalian cells transformed by helium cells [DE91-013778] N91-28721
Protein-directed modulation of high-LET hyperthermic radiosensitization [DE91-013783] N91-28722
The role of the UNIX(tm) central computing facility in a multi-purpose national laboratory [DE91-012361] N91-28737
Computing minimal surfaces via level set curvature flow [DE91-014709] N91-28759
Visualization using a data flow-based paradigm [DE91-013851] N91-28763
Elastic tracking versus neural network tracking for very high multiplicity problems [DE91-011825] N91-28768
Invariant metrics for Hamiltonian systems [DE91-014236] N91-28807
The Advanced Light Source: A new tool for research in atomic and molecular physics [DE91-012860] N91-28844
Measurements of ionization cross-section for electron energy-loss microanalysis under well defined scattering conditions [DE91-013745] N91-28862
Plasma immersion surface modification with metal ion plasma [DE91-014233] N91-28979
Superconducting bolometers: High-T(sub c) and low-T(sub c) [DE91-011830] N91-28992
Ferromagnetic material in the superconductor and its effect on the magnetization sextupole and decapole in the SSC dipoles at injection [DE91-011886] N91-28993
High-T(sub c) thin-film microelectronics [DE91-012340] N91-28997
Photolithographically patterened thin-film multilayer devices of YBa2Cu3O(7-x) [DE91-012350] N91-28998
Characterization of crystalline interfaces by advanced electron microscopy [DE91-011883] N91-29002
TEM analysis of enclosed crystal microstructures and interfaces [DE91-012344] N91-29006
Thin-film flux transformers of YBa2Cu3O(7-x) [DE91-012363] N91-29007
The effect of the quantum susceptance on the gain of superconducting quasiparticle mixers [DE91-012352] N91-29021
Electron correlations in solid state physics [DE91-013752] N91-29030
Long-wavelength germanium photodetectors by ion implantation [DE91-013848] N91-29038
Physics at the Planck scale [DE91-012346] N91-29054
Topics in low-dimensional field theory [DE91-013784] N91-29062
The EOS TPC analysis shell [DE91-011873] N91-29073
Safe referential integrity structures in relational databases [DE91-014586] N91-29091
Impact of the nuclear equation of state on models of rotating neutron stars [DE91-014615] N91-29125
Ground-based measurements of galactic cosmic ray fragmentation in shielding [DE91-012336] N91-29133
CALIFORNIA UNIV., DAVIS.
Studies relevant to the catalytic activation of carbon monoxide [DE91-012661] N91-28323
Radiation damage of ceramics by electron microscopy [DE91-012186] N91-28396
Measurements of the ion acoustic decay instability and the resultant enhanced laser absorption and enhanced bremsstrahlung in laser-plasma interaction experiments [DE91-014250] N91-28956
CALIFORNIA UNIV., LOS ANGELES.
Explicit models for proportional damping in Timoshenko beams N91-28642
High-temperature elasticity and Earth's upper mantle N91-28679
An upper ocean model for the climatic aspects of air-sea interaction N91-28691
Order reduction and synthesis of transfer function models N91-28769
Quadrupole phenomena of noise from a subsonic jet impinging on a large, rigid, and flate plate N91-28818
Continuing studies of the plasma beat wave accelerator [DE91-013641] N91-28976
CALIFORNIA UNIV., SANTA BARBARA.
Polymers at surfaces [DE91-011000] N91-28392
Polymers at surfaces [DE91-013642] N91-28430
CARNEGIE-MELLON UNIV., PITTSBURGH, PA.
A methodology to determine the dynamic configuration of a reconfigurable manipulator [DE91-010732] N91-28576
Stochastic plans for robotic manipulation N91-28597
Support materials for formal specification of software [AD-A236121] N91-28742
The software technical review process [AD-A236139] N91-28743
Software metrics [AD-A236140] N91-28744
A design space and design rules for user interface software architecture [AD-A237049] N91-28748
CASE WESTERN RESERVE UNIV., CLEVELAND, OH.
Processing, compatibility and oxidation of diboride-reinforced oxide matrix composites for ultrahigh-temperature applications N91-28294
CHALMERS UNIV. OF TECHNOLOGY, GOETEBORG (SWEDEN).
Equilibria and dynamics of temperature in a fusion reactor plasma N91-28937
CHICAGO UNIV., IL.
Aspects of reheating in first-order inflation [NASA-CR-188705] N91-29108
Testing the Big Bang: Light elements, neutrinos, dark matter and large-scale structure [NASA-CR-188701] N91-29111
CHUBU UNIV., KASUGAI (JAPAN).
Shock and soliton structures induced by poloidal flow in tokamaks N91-28929
CINCINNATI UNIV., OH.
A critical analysis of anisotropic k-epsilon modeling and its application to turbulence-driven secondary flows N91-28533

CLARK-ATLANTA UNIV., GA.

Semi-empirical calculations on model systems for organosilyldiamine preceramic polymers [DE91-013721] N91-28433

CLARKSON UNIV., POTSDAM, NY.

Experimental investigation of pressure drop and heat transfer for air flow through enhanced tubes [DE91-012151] N91-28508

Pressure drop and heat transfer for spirally fluted tubes including validation of the role of transition [DE91-012242] N91-28509

CLEMSON UNIV., SC.

Observations and theoretical studies of tides and normal modes in the lower thermosphere N91-28681

CLEVELAND STATE UNIV., OH.

The design of a clinical laboratory information system N91-29083

COASTAL ENGINEERING RESEARCH CENTER, VICKSBURG, MS.

Alaska wave data index [AD-A236635] N91-28707

COLORADO STATE UNIV., FORT COLLINS.

Signature analysis technique for diagnosing failures in mechanical systems N91-28604

Regional-scale flow in complex terrain: An observational and numerical investigation N91-28680

COLORADO UNIV., BOULDER.

Measurement of the microwave propagation delay induced by atmospheric water vapor N91-28466

Numerical simulation of particle-wave interaction in boundary layers [NASA-CR-187312] N91-28502

Reversed field pinch experiments [DE91-013643] N91-28977

Parallel nanometer scale fabrication [DE91-013016] N91-29026

Explosion of a superbubble in a uniform magnetic field N91-29102

Electron acceleration by magnetosonic waves in a solar coronal loop N91-29132

COLUMBIA UNIV., NEW YORK, NY.

Radiation physics, biophysics, and radiation biology [DE91-012883] N91-28716

Current sheet formation and rapid reconnection in the solar corona N91-28884

Suppression and control of magnetic islands in toroidal plasmas N91-28895

COMPUTER SCIENCES CORP., RESEARCH TRIANGLE PARK, NC.

Regional oxidant model user's guide. Part 1: The ROM preprocessors [PB91-171926] N91-28665

Regional oxidant model user's guide. Part 2: The ROM processor network [PB91-171934] N91-28666

CORNELL UNIV., ITHACA, NY.

Ultra-high frequency superconductive devices [AD-A236795] N91-28478

Evidence of vibrational mode-coupling in 2-fluorethanol via high resolution infrared spectroscopy in a molecular beam [AD-A236132] N91-28821

High resolution infrared spectroscopy of 2-fluorethanol in a molecular beam [AD-A236149] N91-28822

The structure of Ta3N5 at 16K by time-of-flight neutron diffraction [AD-A236596] N91-28987

Surface phases and their influence on metal-oxide interfaces [DE91-012277] N91-28995

Defect studies in III-V thin film semiconductors [DE91-012746] N91-29011

Synthesis and properties of novel cluster phases [DE91-013006] N91-29013

Defects and transport in mixed oxides [DE91-014443] N91-29049

Observational constraints on pulsars: Location of the emission region and pulse shape stability on decade time scales N91-29097

COUNCIL FOR NATIONAL ACADEMIC AWARDS (ENGLAND).

Relationships between polymer-additive molecular structure and intumescent flame retardant behavior N91-28426

Prediction of the flow and heat transfer between a rotating and a stationary cone N91-28536

D

DARTMOUTH COLL., HANOVER, NH.

Tropospheric scatter propagation at 5 and 16 GHz: Results for a 161 km path [AD-A237012] N91-28458

DASSAULT (E. M.) CO., SAINT CLOUD (FRANCE).

Calculation of interactions between air and ground of landing N91-28161

DEFENSE TECHNICAL INFORMATION CENTER, ALEXANDRIA, VA.

Directory of Organizational Technical Report Acronym Codes (DOTRAC) [AD-A237000] N91-29072

DELAWARE UNIV., NEWARK.

Fundamental magnetic studies of iron-rare-earth-metalloid alloys [DE91-014816] N91-28383

Corona: Coordinated research on non-thermal processes in astrophysics [NASA-CR-188692] N91-29107

DEPARTMENT OF ENERGY, WASHINGTON, DC.

Electric and hybrid vehicles program [DE91-013113] N91-28573

Tiger Team assessment of the Princeton Plasma Physics Laboratory [DE91-014395] N91-28957

DEUTSCHE AIRBUS G.M.B.H., BREMEN (GERMANY, F.R.).

Operational loads on landing gear N91-28158

DREXEL UNIV., PHILADELPHIA, PA.

Damage progression during static and fatigue loading in metal matrix composites, volumes 1-3 N91-28301

Finite element modeling of 2-D delamination growth in laminated composites N91-28302

DUESSELDORF UNIV. (GERMANY, F.R.).

Formation and dynamics of solitary waves and vortices in driven and damped systems N91-28942

DUKE UNIV., DURHAM, NC.

Thermal conductivity of solid hydrogen at low temperature N91-28330

DURHAM UNIV. (ENGLAND).

A faint galaxy redshift survey and implications for cosmology N91-29100

E

ECOLE POLYTECHNIQUE, PALAISEAU (FRANCE).

Models of collisional transport across a magnetic field with destroyed surfaces N91-28900

EDGERTON, GERMESHAUSEN AND GRIER, INC., IDAHO FALLS, ID.

Heat resistant materials and their feasibility issues for a space nuclear transportation system [DE91-014071] N91-28187

Small Ex-core Heat Pipe Thermionic Reactor concept (SEHPTR) [DE91-014073] N91-28279

A review of silicon carbide/metal interactions with relevance to silicon carbide joining [DE91-012768] N91-28282

Mechanisms of bacterial metals removal from solids [DE91-012808] N91-28356

Substructure and electrical resistivity analyses of pure tungsten sheet [DE91-014098] N91-28362

Effects of various parameters on the fatigue life of alloy 718 [DE91-014100] N91-28380

Recent ASME Code Section 11 developments for surface examination through coatings [DE91-014069] N91-28437

Laboratory testing of the dual traction battery GC12V100 [DE91-012743] N91-28491

Gas evolution from spheres [DE91-012807] N91-28510

A laser based technique for particle sizing to study two phase expansion in turbines [DE91-014172] N91-28595

Using HSYS in the analysis of human-system interactions: Examples from the offshore petroleum industry [DE91-013218] N91-28732

Software development experiences with a distributed database in a large, distributed computer system [DE91-012818] N91-28750

Guidelines for acquisition, installation, and testing of performance assessment software [DE91-013910] N91-28764

A parallel algorithm for solving linear equations arising from one-dimensional network problems [DE91-012815] N91-28795

Evidences of trapping in tungsten and implications for plasma-facing components [DE91-012734] N91-28951

The human side of value engineering [DE91-012817] N91-29068

Distributed relational database design and implementation for a large, distributed computer system [DE91-012812] N91-29077

EG AND G ENERGY MEASUREMENTS, INC., GOLETA, CA.

Electrical and photomechanical effects of plastic deformation of mercuric iodide [DE91-013108] N91-29022

Crystal surface analysis using matrix textural features classified by a probabilistic neural network [DE91-014120] N91-29048

EG AND G ENERGY MEASUREMENTS, INC., LAS VEGAS, NV.

The in-flight calibration of a helicopter-mounted Daedalus multispectral scanner [DE91-013054] N91-28170

Measuring neutron fluences and gamma/x ray fluxes with CCD cameras [DE91-014119] N91-28549

EG AND G MOUND APPLIED TECHNOLOGIES, MIAMISBURG, OH.

Operational interpolation of data in triangular array [DE91-012987] N91-28800

EG AND G ROCKY FLATS, INC., GOLDEN, CO.

Changes with material properties of acoustic emission produced during single point machining [DE91-011913] N91-28452

Origin of acoustic emission produced during single point machining [DE91-011915] N91-28453

ENERGY INFORMATION ADMINISTRATION, WASHINGTON, DC.

EIA publications directory, 1990 [DE91-014350] N91-29082

ESSEX UNIV., COLCHESTER (ENGLAND).

Numerical solution of a free-boundary viscous flow N91-28529

EUROPEAN ORGANIZATION FOR NUCLEAR RESEARCH, GENEVA (SWITZERLAND).

Mind over matter: The intellectual content of experimental physics [DE91-617571] N91-28813

F

FEDERAL AVIATION ADMINISTRATION, ATLANTIC CITY, NJ.

Runway Visual Range (RVR) Operational Test and Evaluation (OT and E)/integration test plan [DOT/FAA/CT-TN91/4] N91-28176

FERMI NATIONAL ACCELERATOR LAB., BATAVIA, IL.

A 10,000 A 1000 Vdc solid state dump switch [DE91-014141] N91-28497

Design and analysis of the 50 mm collider dipole vacuum vessel [DE91-012490] N91-28610

Statistical mechanics of soft-boson phase transitions [NASA-CR-188697] N91-28858

Microwave instability at transition: Stability diagram approach [DE91-013202] N91-28867

Aspects of reheating in first-order inflation [NASA-CR-188705] N91-29108

Dibaryons in neutron stars [NASA-CR-188704] N91-29109

Testing the Big Bang: Light elements, neutrinos, dark matter and large-scale structure [NASA-CR-188701] N91-29111

Phase transitions triggered by quantum fluctuations in the inflationary universe [NASA-CR-188698] N91-29112

Void probability as a function of the void's shape and scale-invariant models [NASA-CR-188696] N91-29113

FLORIDA STATE UNIV., TALLAHASSEE.

Initialization of cloud and radiation in the Florida State University global spectral model N91-28703

On the initiation of surface cyclones by upper tropospheric disturbances N91-28704

FLORIDA UNIV., GAINESVILLE.

Ion beam sputtered coatings of bioglass N91-28384

Visual, red and infrared photographic surface photometry of NGC 55 and NGC 253 N91-29094

A search for cosmic axions N91-29104

FLUOR DANIEL, INC., IRVINE, CA.

Pacific Northwest hydrogen feasibility study [DE91-013427] N91-28445

FOKKER B.V., SCHIPOL-OOST (NETHERLANDS).

The use of Monte Carlo simulation in determining landing gear loads during landing N91-28162

FUKUI UNIV. (JAPAN).

Application of mathematica to energy principle N91-28910

G

GENERAL ATOMIC CO., SAN DIEGO, CA.
Influence of fast waves on the collective scattering of microwaves in fusion plasmas
[DE91-014759] N91-28973

GENERAL DYNAMICS CORP., SAN DIEGO, CA.
The space exploration initiative. Operational efficiency panel space-basing technology requirements
N91-28253
Propulsion technologies for near term N91-28262
Cultural changes in aerospace N91-28265

GENERAL ELECTRIC CO., SCHENECTADY, NY.
Development of elements of a high T(sub c) superconducting cable
[AD-A236151] N91-28986

GEOLOGICAL SURVEY, DENVER, CO.
Close-range geophotogrammetric mapping of trench walls using multi-model stereo restitution software
[DE91-013105] N91-28645

GEORGIA INST. OF TECH., ATLANTA.
Stability of cylindrical laminates by higher orde r shear deformable theories N91-28638
A cloud fraction and radiative transfer model
N91-28706

GIFU UNIV. (JAPAN).
Finite beta equilibrium for a pressure configuration
N91-28909

GLASGOW UNIV. (SCOTLAND).
Information management: A uniform conceptual model and its user interface N91-29084

GUNMA UNIV., MAEBASHI (JAPAN).
Effect of pressure on mode transition point of partially relaxed states with peripheral loss N91-28906

H

HARVARD UNIV., CAMBRIDGE, MA.
Observations of extragalactic water vapor masers
N91-29117
Multiple nuclei, cluster core dynamics, and the velocity distributions of gravitating systems N91-29119

HAWAII UNIV., HONOLULU.
Normal mode decomposition of small-scale oceanic motions N91-28709

HIROSHIMA UNIV. (JAPAN).
Simulation study of MHD relaxation and reconnection processes N91-28908
Study of kink instability and current relaxation by three dimensional macroscale particle simulation N91-28919
Nonadiabatic behavior of the magnetic moment of a charged particle in a dipole magnetic field N91-28920

I

IDAHO NATIONAL ENGINEERING LAB., IDAHO FALLS.
Advancing electric vehicle technology
[DE91-013004] N91-28575

ILLINOIS INST. OF TECH., CHICAGO.
Flutter of laminated rectangular plates including finite deflection and shear deformation N91-28639

ILLINOIS UNIV., CHICAGO.
Selected topics in mechanisms and robotics: Singularities, inverse kinematics, and collision detection
N91-28598
The symbolic computation and automatic analysis of trajectories
[NASA-CR-188159] N91-28787
Using trees to compute approximate solutions to ordinary differential equations exactly
[LAC90-R24] N91-28788
Bialgebra deformations and algebras of trees
N91-28790

ILLINOIS UNIV., URBANA.
Compile-time estimation of communication costs in multicomputers
[NASA-CR-188675] N91-28747

ILLINOIS UNIV., URBANA-CHAMPAIGN.
Analysis of passive and active discrete-distributed linear dynamical systems using Green's function methods
N91-28141
Robust bifurcation behavior in the presence of external random excitation N91-28171
Hydrogen embrittlement of selected nickel and iron base superalloys N91-28374
An experimental study of the effect of small particles on the fluid turbulence in fully developed flow of air in a horizontal pipe N91-28525
Robust low-order control of flexible joint manipulators
N91-28584
Multiple frequency atmospheric radar techniques
N91-28683
Lidar studies of sporadic sodium layers, gravity waves and density spectra in the mesopause and stratopause regions at Urbana and Arecibo N91-28690
Low-level curvature shear and supercell thunderstorm behavior N91-28701
A numerical simulation of a tornado-scale vortex in a three-dimensional cloud model N91-28705
Parallel input/output architectures for multiprocessors
N91-28740
Star formation in the presence of magnetic fields: Molecular cloud core formation and dynamical contraction due to ambipolar diffusion:; a simulation with axial symmetry N91-29116
Numerical simulations of mass outflows from star-forming regions N91-29123

INSTITUTE FOR COMPUTER APPLICATIONS IN SCIENCE AND ENGINEERING, HAMPTON, VA.
Mapping implicit spectral methods to distributed memory architectures
[NASA-CR-187592] N91-28806

INSTITUTE FOR PLASMA RESEARCH, GANDHINGAR (INDIA).
Model for marfe-detached plasma transition in tokamaks N91-28938

INTERNATIONAL CENTRE FOR THEORETICAL PHYSICS, TRIESTE (ITALY).
Resonant method for the measurement of the glass transition temperature at high frequencies
[DE91-618684] N91-28416
Results of agriclimatological studies using multiple satellite sensors like NOAA AVHRR; GMS IR; and LANDSAT MSS and TM
[DE91-618773] N91-28698
Towards the exact nature of a certain error term
[DE91-617574] N91-28801
Stability theory of critical cases and the bifurcation points of the stationary solutions of the Lorenz model
[DE91-617575] N91-28802
Spin 4 and 7/2 extended conformal algebra
[DE91-617609] N91-28803
A cluster approximation for the transfer-matrix method
[DE91-617790] N91-28804
The determination of the momentum matrix elements involved in calculating the dielectric constants of superlattices using the tight-binding method
[DE91-617789] N91-29017
Transit time for resonant tunneling
[DE91-617799] N91-29018
Coherent charge fluctuations in Josephson junctions and the oscillations of the effective capacitance
[DE91-618098] N91-29019
Path-integral measure for Chern-Simons theory within the stochastic quantization approach
[DE91-617610] N91-29056
The (2,0) super Beltrami parametrization and superconformal structures
[DE91-617611] N91-29057

INTERNATIONAL FUEL CELLS CORP., SOUTH WINDSOR, CT.
Advanced water-cooled phosphoric acid fuel cell development
[DE90-009700] N91-28657
Advanced water-cooled phosphoric acid fuel cell development
[DE91-012243] N91-28659

IOWA UNIV., IOWA CITY.
Analysis of shock propagation and shock-initiated reaction in granular energetic materials N91-28446
Recursive linearization of multibody dynamics and application to control design N91-28588

J

JAPAN ATOMIC ENERGY RESEARCH INST., IBARAKI.
Numerical study of ion temperature gradient modes in a tokamak N91-28921
Fluctuation spectrum of ion temperature gradient driven modes in sheared magnetic fields N91-28936

JAPAN ATOMIC ENERGY RESEARCH INST., TOKYO.
Electrostatic particle simulations of density and temperature driven modes in a toroidal plasma
N91-28915

JET PROPULSION LAB., CALIFORNIA INST. OF TECH., PASADENA.
Satellite/spacecraft propulsion N91-28203
Advanced propulsion concepts N91-28218

JOHNS HOPKINS UNIV., BALTIMORE, MD.
An experimental investigation of a compliant surface beneath a turbulent boundary layer N91-28523
Critical issues in de-alloying and transcrystalline stress-corrosion cracking
[DE91-010190] N91-28608

JOINT EUROPEAN TORUS PROJECT, ABINGDON (ENGLAND).
Non-linear behaviour in tokamaks N91-28935

JOINT PUBLICATIONS RESEARCH SERVICE, ARLINGTON, VA.
JPRS report: Science and technology. USSR: Materials science
[JPRS-UMS-91-003] N91-28342
JPRS report: Science and technology. USSR: Physics and mathematics
[JPRS-UPM-90-006] N91-28811

K

KOREA ADVANCED INST. OF SCIENCE AND TECHNOLOGY, CHONGRYANG (REPUBLIC OF KOREA).
Ion temperature gradient turbulence and coherent structures N91-28890

KYOTO UNIV. (JAPAN).
Log-stable distribution of energy dissipation in turbulence N91-28885
Edge anomalous transport in heliotron/torsatron
N91-28892

KYUSHU UNIV., FUKUOKA (JAPAN).
Dynamics of interfaces with internal structures
N91-28926

L

LANCASTER UNIV. (ENGLAND).
Radio absorption in the Antarctic ionosphere: Some observations in the region of the midlatitude trough
N91-28694

LAWRENCE LIVERMORE NATIONAL LAB., CA.
WFOV star tracker camera
[DE91-012776] N91-28148
Effectiveness of tiltrotor support to ground combat
[DE91-013603] N91-28167
Space propulsion by fusion in a magnetic dipole
[DE91-012033] N91-28275
The application of x ray tomographic microscopy to chemical vapor infiltration processing of ceramic matrix composites
[DE91-011871] N91-28284
Multiaxial failure characterization of composites
[DE91-011925] N91-28285
On the finite-strain-invariant failure criterion for composites
[DE91-011924] N91-28286
Chemistry and materials science research report
[DE91-011507] N91-28305
Proton Energy Loss (PEL) material characterization
[DE91-011545] N91-28306
Continuum x ray gauging of multiple-element materials
[DE91-011923] N91-28307
Equation-of-state from SiO2 aerogel Hugoniot data
[DE91-011480] N91-28313
Linked gas chromatograph-thermal energy analyzer/ion trap mass spectrometer
[DE91-013585] N91-28326
Cross-sectional TEM specimen preparation of free-standing metal multi-layered films
[DE91-011117] N91-28351
Shock-induced optical emission in Al2O3 at 200 GPa: Implications for shock temperature measurements in metals
[DE91-013584] N91-28365
Perspective on plating for precision finishing
[DE91-011927] N91-28394
Melamine-formaldehyde aerogels
[DE91-012084] N91-28408
Experiments and calculations of jet penetration in glass
[DE91-013567] N91-28422
Mechanisms of EBW HE initiation
[DE91-013565] N91-28447
Localized waves in complex environments
[DE91-011934] N91-28462
Electrostatic discharge effects on EBW detonators
[DE91-013250] N91-28467
A chopper driven 11.4-GHz traveling-wave RF generator
[DE91-013568] N91-28489
Atmospheric propagation of high-explosive blast waves
[DE91-012550] N91-28506
X ray fiducial foils
[DE91-011193] N91-28542
Modal study of refractive effects on x ray laser coherence
[DE91-012083] N91-28551
Irradiance compensation control for high-energy laser propagation. Part 1: Theory and Fourier control model propagation results
[DE91-013130] N91-28559

Ring-laser solitons: A multipass approach
[DE91-013242] N91-28560
High-peak power-Nd:Glass laser facilities for end users
[DE91-013246] N91-28561
Reduction of energy sweep of the ETA-2 beam
[DE91-013824] N91-28568
Platinum solubility in phosphate laser glass
[DE91-015123] N91-28571
X ray Tomographic Microscopy (XTM)
[DE91-011930] N91-28599
Model-based computed tomography for nondestructive evaluation
[DE91-013462] N91-28602
Shock compression of low-density microcellular materials
[DE91-013586] N91-28628
TREE: A model of the effects of acid precipitation and air pollutants on the growth of trees
[DE91-014131] N91-28672
ARAC: A computer-based emergency-response dose-assessment service with global application potential
[DE91-013248] N91-28700
The use of AMS to the biomedical sciences
[DE91-012037] N91-28712
The cache group scheme for hardware-controlled cache coherence and the general need for hardware coherence control in large-scale multiprocessors
[DE91-012106] N91-28772
Split-join and message passing programming models on the BBN TC2000
[DE91-008067] N91-28774
The PCP/PFP programming models on the BBN TC2000
[DE91-011537] N91-28781
Enhancing atom densities in solid hydrogen by isotopic substitution
[DE91-011189] N91-28824
Scanning Transmission Ion Microscopy (STIM): A new technique for density mapping of microstructures
[DE91-011917] N91-28825
SDI: Statistical Dynamic Interactions
[DE91-012034] N91-28827
Simulation of planar integrated photonics devices with the LLNL time-domain finite-difference code suite
[DE91-011929] N91-28876
Reflection mask technology for soft x ray projection lithography
[DE91-012561] N91-28877
Plasma transport in a new cathodic arc ion source, theory and experiment
[DE91-011511] N91-28944
Microwave-generated plasma thruster
[DE91-013131] N91-28948
Implications of TAE modes for the design of ITER
[DE91-013128] N91-28952
Chamber propagation
[DE91-012797] N91-28954
Large growth Rayleigh-Taylor experiments on Nova
[DE91-012885] N91-28955
Hydrodynamic evolution of picosecond laser-plasmas
[DE91-013245] N91-28958
Inertial confinement fusion
[DE91-013479] N91-28960
Evaluation of charged-particle reactions for fusion applications
[DE91-014135] N91-28962
The Cascade inertial confinement fusion reactor concept
[DE91-013852] N91-28966
On the use of particle-in-cell methods for the study of magnetically-confined fusion plasmas
[DE91-015093] N91-28984
TOPAZ2D benchmark problems nonlinear materials
[DE91-009753] N91-29053
Transport with Feynman propagators
[DE91-013566] N91-29063

LEHIGH UNIV., BETHLEHEM, PA.
Analytical electron microscopy of catalyst preparations
[DE91-014126] N91-28328

LOCKHEED ENGINEERING AND SCIENCES CO., LAS CRUCES, NM.
National test bed concept N91-28241

LOCKHEED SPACE OPERATIONS CO., WASHINGTON, DC.
Space shuttle requirements/configuration evolution
N91-28264

LOS ALAMOS NATIONAL LAB., NM.
Air combat environment test and evaluation facility and the development of the offensive sensors laboratory
[DE91-011398] N91-28173
Generating strong shock waves with a supersonic peristaltic pump
[DE91-013228] N91-28174
Comparisons between fast shock tube calculations and tests
[DE91-013496] N91-28177
Hypervelocity plate acceleration
[DE91-014738] N91-28179
ZrO2 reinforced-MoSi2 matrix composites
[DE91-013074] N91-28288
Direct Monte Carlo simulation of chemical equilibrium composition of molecular fluid mixtures under shock conditions
[DE91-013075] N91-28324
Vibrational spectroscopy of shock-compressed liquid CO
[DE91-013204] N91-28325
The pressure-induced Mott transition in transition-metal iodides
[DE91-013671] N91-28366
Synthesis of metastable aluminum-based intermetallics by mechanical alloying
[DE91-013651] N91-28376
Investigation of interlayer materials for the microwave joining of SiC
[DE91-013311] N91-28414
Microwave enhanced diffusion?
[DE91-013312] N91-28415
Reliable modeling of complex behavior
[DE91-013385] N91-28419
Shock initiation of pentaerythritol tetranitrate crystals: Steric effects due to plastic flow
[DE91-013389] N91-28420
SESAME equation of state number 7740: Polycarbonate
[DE91-013970] N91-28436
Shock compression of DuPont detasheet at low stress
[DE91-013229] N91-28443
The deflagration-to-detonation transition in granular HMX
[DE91-014591] N91-28448
Supercritical fluids cleaning
[DE91-013374] N91-28456
A geometry based method of integrated engineering design, analysis, and optimization
[DE91-008588] N91-28457
Recovery of saturated video signals from vidicons by dynamic cathode biasing
[DE91-012402] N91-28464
Design of a multivariable RF control system using gain-shaping in the frequency domain
[DE91-013859] N91-28474
A high power Klystrode with potential for space application
[DE91-013046] N91-28486
Modeling of a 1700-MHz cluster cavity of planar triodes
[DE91-013049] N91-28488
Fields and trajectories in the magnicon
[DE91-013070] N91-28492
Procyon experiments utilizing foil-fuse opening switches
[DE91-014605] N91-28499
Moving finite elements: A continuously adaptive method for computational fluid dynamics
[DE91-013391] N91-28513
Shock and reshock of an unstable fluid interface
[DE91-014737] N91-28528
A microwave interferometer to measure particle and shock velocities simultaneously
[DE91-013077] N91-28545
X ray generation by high irradiance exawatt/sq cm subpicosecond lasers
[DE91-013497] N91-28556
Time-resolved emittance measurements of an excimer-laser-driven metal photocathode
[DE91-013066] N91-28558
E-beam accelerator cavity development for the ground-based free electron laser
[DE91-013760] N91-28563
H(-) beam characterization using laser-induced neutralization
[DE91-013501] N91-28564
Performance of the photoinjector accelerator for the Los Alamos free-electron laser
[DE91-013682] N91-28565
Short wavelength FELS
[DE91-013759] N91-28566
Sphere lapping
[DE91-014287] N91-28593
MESA: A 3-D Eulerian hydrocode for penetration mechanics studies
[DE91-013308] N91-28613
Dynamic plasticity in transition from thermal activation to viscous drag
[DE91-013031] N91-28617
Overdriven shocks in solids and liquids
[DE91-013370] N91-28618
The DataShoP: A database of weak-shock constitutive data
[DE91-013349] N91-28620
A study of the impact of reaction rates on equation of state
[DE91-013375] N91-28621
Residual stress measurement using the pulsed neutron source at LANSCE
[DE91-013494] N91-28624
Stress fields generated by kinetic energy projectile interaction with ceramic targets
[DE91-013687] N91-28625
Neutron diffraction determination of the residual stress redistribution in cracked autofrettaged tubing
[DE91-013688] N91-28632
A new model of rate dependent elastic-plastic flow
[DE91-014600] N91-28633
Bauschinger effect during shock loading
[DE91-014606] N91-28634
Shear stress prediction in shock loaded copper
[DE91-014740] N91-28635
Quantum mechanical effects on the shock Hugoniot
[DE91-014750] N91-28636
Equation of state and crushing dynamics of low-density silica aerogels
[DE91-014766] N91-28637
Recent achievements in polymer electrolyte fuel cell (PEFC) research at Los Alamos National Laboratory
[DE91-013683] N91-28661
Spontaneous emergence of a metabolism
[DE91-013684] N91-28714
Plant growth is influenced by glutamine synthetase-catalyzed nitrogen metabolism
[DE91-014592] N91-28725
A new wake-potential calculation method using orthogonal polynomials
[DE91-013045] N91-28799
Defending the defenders: Brilliant pebble defense against pop-up neutral particle beam suppression attacks
[DE91-012521] N91-28809
Interceptor combinations for theater defense
[DE91-012990] N91-28810
Antiproton-induced elastic and inelastic scattering at intermediate energies
[DE91-013068] N91-28849
Optical analogs of model atoms in fields
[DE91-013392] N91-28855
New techniques in neutron data measurements above 30 MeV
[DE91-013690] N91-28861
Beam structure and transverse emittance studies of high-energy ion beams
[DE91-013499] N91-28871
Progress in the development of a numerical tokamak
[DE91-013386] N91-28975
Performance of the 10-kV, 5-MA pulsed-power system for the FRX-C compression experiment
[DE91-014745] N91-28983
Quantitative modeling of the point defect structures of Fe-doped MgO and MgSiO3 perovskite
[DE91-011405] N91-28990
Growth of high T(sub c) superconducting thin films for microwave applications
[DE91-011436] N91-28991
Epitaxial growth of silicon on CoSi2(001)/Si(001)
[DE91-013387] N91-29015
Shock initiation of pentaerythritol tetranitrate crystals: Optical absorption and emission studies
[DE91-013381] N91-29023
Ab initio cluster studies of La2CuO4
[DE91-013520] N91-29025
Kinetics of solid-state reactions in Ni-Zr thin films
[DE91-013652] N91-29028
Metastable phase equilibria in co-deposited Ni(1-x)Zr(x) thin films
[DE91-013653] N91-29029
Doping and pressure study of U3Sb4Pt3
[DE91-013669] N91-29033
Application of muon spin relaxation experiment to the mixed state superconductors
[DE91-013689] N91-29034
The derivation of effective spin Hamiltonians and the origin of the magnetic field induced transition in orthorhombic La2CuO4
[DE91-013743] N91-29035
Overview of the status of and prospects for high-T(sub c) wire and tape development
[DE91-014609] N91-29045
Pressure dependence of the Curie-temperature in the Kondo-lattice-compound YbNiSn
[DE91-013672] N91-29046
Application of muon spin relaxation experiment to the vortex dynamics of high temperature superconductors
[DE91-014607] N91-29050

Nonlinear modeling of chaotic time series: Theory and applications
[DE91-013076] N91-29055
Complex dynamics of the integer quantum Hall effect
[DE91-013383] N91-29058

LOUISIANA STATE UNIV., BATON ROUGE.
A new approach to analyzing high-resolution aerial photographs of urban areas N91-28647

LOUISVILLE UNIV., KY.
Mechanism of hydrodenitrogenation. Part 5: X ray diffraction of molybdenum catalysts
[DE91-013853] N91-28327

LOWELL UNIV., MA.
Photocross-linked second order nonlinear optical polymers
[AD-A235855] N91-28385
New photocrosslinkable polymers for second order nonlinear optical processes
[AD-A235856] N91-28386
A study of the buckling and vibration behavior of an initially stressed thick plate by Galerkin's method
N91-28641

M

MARQUETTE UNIV., MILWAUKEE, WI.
Resonance Raman and photophysical studies of transition metal complexes in solution and entrapped in zeolites
[DE91-013010] N91-28357

MARTIN MARIETTA AEROSPACE, DENVER, CO.
Humans to Mars in 1999 N91-28237
Historical problem areas: Lessons learned for expendable and reusable vehicle propulsion systems
N91-28243
Space transfer vehicles and space basing
N91-28254

MARTIN MARIETTA LABS., BALTIMORE, MD.
Microstructure-property relationships in Al-Cu-Li-Ag-Mg Weldalite (tm) alloys, part 2
[NASA-CR-4364] N91-28334
Identification of strengthening phases in Al-Cu-Li alloy Weldalite (tm) 049 N91-28335
The influence of Ag+Mg additions on the nucleation of strengthening precipitates in a non-cold-worked Al-Cu-Li alloy N91-28336
The effect of TiB2 reinforcement on the mechanical properties of an Al-Cu-Li alloy-based metal-matrix composite N91-28337
Weldability of Weldalite (tm) 049 with and without TiB2 reinforcement N91-28338
Effect of Li level, artificial aging, and TiB2 reinforcement on the fracture toughness of Weldalite (tm) 049-type alloys N91-28339
Effect of Li level, artificial aging, and TiB2 reinforcement on the modulus of Weldalite (tm) 049 N91-28340

MARYLAND UNIV., BALTIMORE.
Pulse propagation in inhomogeneous optical fibers
[DE91-014356] N91-28879

MARYLAND UNIV., COLLEGE PARK.
The creation of multi-degree-of-freedom mechanisms for robotic applications
[DE91-014359] N91-28596
Solitons and chaos in laser-plasma interaction
N91-28898
Particle confinement and fueling effects on the Maryland spheromak
[DE91-012396] N91-28945
Measurement of magnetic properties of confined compact toroid plasma (spheromak)
[DE91-012397] N91-28950
Maryland controlled fusion research program
[DE91-014358] N91-28980
Joint proposal for US/USSR on nonlinear dynamics and plasma transport
[DE91-014360] N91-28981

MASSACHUSETTS INST. OF TECH., CAMBRIDGE.
Radiation disorder and aperiodicity in irradiated ceramics
[DE91-010257] N91-28391
Nonlinear phenomena and processes in high energy plasmas N91-28882

MAX-PLANCK-INST. FUER PLASMAPHYSIK, GARCHING (GERMANY, F.R.).
Statistical properties of two-dimensional magnetohydrodynamic turbulence N91-28886
Optimization, non-local MHD-mode, and alpha-particle confinement behavior of Helias equilibria N91-28893

MCAT INST., SAN JOSE, CA.
Algorithm and code development for unsteady three-dimensional Navier-Stokes equations
[NASA-CR-188039] N91-28503

MCDONNELL-DOUGLAS CORP., SAINT LOUIS, MO.
Space transfer vehicles and space basing
N91-28254

MESSERSCHMITT-BOELKOW-BLOHM G.M.B.H., MUNICH (GERMANY, F.R.).
Development of undercarriage design loads
N91-28153
Considerations on optimality of landing gear arrangement and design N91-28156

MESSIER-HISPANO-BUGATTI S.A., MONTROUGE (FRANCE).
Numerical simulation of the dynamic behavior of landing gears N91-28160

MIAMI UNIV., CORAL GABLES, FL.
Experimental and theoretical investigation of unsteady forced convection in ducts N91-28524

MICHIGAN STATE UNIV., EAST LANSING.
Softening mechanisms and microstructural instabilities during high temperature, low cycle fatigue of Ni, Ni3Al, and their metal matrix composites
[DE91-012714] N91-28287
The numerical solution of confined laminar flow past a moving boundary N91-28532
Numerical simulation of the air and fuel mixing process in fuel-injected engines using discrete vortex dynamics
N91-28587

MICHIGAN TECHNOLOGICAL UNIV., HOUGHTON.
Fundamental theory of crystal decomposition
[AD-A236637] N91-28988

MICHIGAN UNIV., ANN ARBOR.
Use of a rotated Riemann solver for the two-dimensional Euler equations N91-28530
New techniques for positron emission tomography in the study of human neurological disorders
[DE91-013855] N91-28728
Emission line regions in active galactic nuclei: Structure, kinematics, physical conditions, and chemical abundances N91-29095
Study of gravitational collapse and cosmic ray abundances N91-29105
The gamma ray content of ultrahigh energy cosmic radiation N91-29135

MIDDLE TENNESSEE STATE UNIV., MURFREESBORO.
Nuclear structure studies via neutron interactions
[DE91-012165] N91-28831

MIDWEST RESEARCH INST., GOLDEN, CO.
Novel ways of depositing ZnTe films by a solution growth technique
[DE91-002189] N91-28429
Research on stable, high-efficiency amorphous silicon multijunction modules
[DE91-002138] N91-28480
Polycrystalline thin film photovoltaic technology
[DE91-002136] N91-28650
SOLTECH 91: Proceedings, volume 2
[DE91-013767] N91-28656
SOLTECH 91: Proceedings, volume 1
[DE91-002163] N91-28658
Fifteenth DOE Solar Photochemistry Research Conference
[DE91-002165] N91-28663

MINNESOTA UNIV., MINNEAPOLIS.
A simulated user for laboratory investigation of information systems requirements determination
N91-29087
Neutrino degeneracy and cosmological nucleosynthesis, revisited
[NASA-CR-188703] N91-29110

MISSOURI UNIV., COLUMBIA.
High pressure optical studies of semiconductors and heterostructures
[DE91-014382] N91-29041

N

NAGOYA UNIV. (JAPAN).
Rapid acceleration of protons in a nonlinear magnetosonic wave and their energy spectrum
N91-28905
Point vortex description of a modon solution
N91-28931
Diffusion and relaxation in Hamiltonian chaos
N91-28934

NAGOYA UNIV., TOYOKAWA (JAPAN).
Helical field effect in solar/stellar wind N91-28912

NATIONAL ACADEMY OF SCIENCES - NATIONAL RESEARCH COUNCIL, WASHINGTON, DC.
The 1990 update to strategy for exploration of the inner planets
[NASA-CR-188728] N91-28182

NATIONAL AERONAUTICS AND SPACE ADMINISTRATION, WASHINGTON, DC.
Report of the Advisory Committee on the future of the US space program
[NASA-TM-105030] N91-28180
Large space structures and systems in the space station era: A bibliography with indexes
[NASA-SP-7085(02)] N91-28191
Space Transportation Propulsion Technology Symposium. Volume 2: Symposium proceedings
[NASA-CP-3112-VOL-2] N91-28193
NASA's advanced space transportation system launch vehicles N91-28195
Space shuttle propulsion systems N91-28200
Current systems: Upper stages N91-28201
Next generation: Unmanned launch vehicles and upper stages: The needs N91-28210
National Aero-Space Plane (NASP) program
N91-28214
Nuclear thermal propulsion N91-28216
Space fusion energy conversion using a field reversed configuration reactor: A new technical approach for space propulsion and power N91-28217
Space Transportation Propulsion Technology Symposium. Volume 3: Panel Session Summaries and Presentations
[NASA-CP-3112-VOL-3] N91-28235
Development program enhancement suggestions (propulsion related) N91-28252
Effectivity of atmospheric electricity on launch availability N91-28260
Lessons learned and their application to program development and cultural issues N91-28263
Major system acquisitions process (A-109)
N91-28268
Space shuttle main engine: Certification for manned space flight N91-28270
Aerospace medicine and biology: A continuing bibliography with indexes (supplement 352)
[NASA-SP-7011(352)] N91-28729
NASA patent abstracts bibliography: A continuing bibliography. Section 2: Indexes (supplement 39)
[NASA-SP-7039(39)-SECT-2] N91-29088

NATIONAL AERONAUTICS AND SPACE ADMINISTRATION. AMES RESEARCH CENTER, MOFFETT FIELD, CA.
Rotor and control system loads analysis of the XV-15 with the advanced technology blades
[NASA-TM-102876] N91-28134

NATIONAL AERONAUTICS AND SPACE ADMINISTRATION. GODDARD SPACE FLIGHT CENTER, GREENBELT, MD.
High temperature solder device for flat cables
[NASA-CASE-GSC-13344-1] N91-28363
Edge technique for measurement of laser frequency shifts including the Doppler shift
[NASA-CASE-GSC-13343-1] N91-28557
Improved superconducting bearings
[NASA-CASE-GSC-13346-1] N91-28578
Roller locking brake
[NASA-CASE-GSC-13376-1] N91-28579
Spline-locking payload fastener
[NASA-CASE-GSC-13378-1] N91-28581
Coupling device with improved thermal interface
[NASA-CASE-GSC-13251-1] N91-28582
Direction discriminating hearing aid
[NASA-CASE-GSC-13027-1] N91-28726
Device for removing foreign objects from anatomic organs
[NASA-CASE-GSC-13306-1] N91-28727
Driven shielding capacitive proximity sensor
[NASA-CASE-GSC-13377-1] N91-28785

NATIONAL AERONAUTICS AND SPACE ADMINISTRATION. JOHN C. STENNIS SPACE CENTER, BAY SAINT LOUIS, MS.
Life cycle cost based program decisions N91-28248
Infusion of instrumentation technology (engine plume diagnostics) into operational test programs N91-28249
John C. Stennis Space Center roles and missions
N91-28259

NATIONAL AERONAUTICS AND SPACE ADMINISTRATION. JOHN F. KENNEDY SPACE CENTER, COCOA BEACH, FL.
A white paper: Operational efficiency. New approaches to future propulsion systems N91-28197

NATIONAL AERONAUTICS AND SPACE ADMINISTRATION. LYNDON B. JOHNSON SPACE CENTER, HOUSTON, TX.
Thermally activated retainer means
[NASA-CASE-MSC-21793-1] N91-28186
Shuttle derived manned transportation systems
N91-28204
Heavy-lift launch vehicle propulsion considerations
N91-28236
Technology transfer methodology N91-28239
Manufacturing processes N91-28244
An accelerated training method for back propagation networks
[NASA-CASE-MSC-21625-1] N91-28730

NATIONAL AERONAUTICS AND SPACE ADMINISTRATION. LANGLEY RESEARCH CENTER, HAMPTON, VA.

A methodology for using nonlinear aerodynamics in aeroservoelastic analysis and design
[NASA-TM-104087] N91-28131

Transonic shock-induced dynamics of a flexible wing with a thick circular-arc airfoil
[NASA-TM-104088] N91-28132

Vaporizing particle velocimeter
[NASA-CASE-LAR-14685-1] N91-28135

Experimental flutter boundaries with unsteady pressure distributions for the NACA 0012 Benchmark Model
[NASA-TM-104072] N91-28137

Longitudinal aerodynamic characteristics of a subsonic, energy-efficient transport configuration in the National Transonic Facility
[NASA-TP-2922] N91-28143

F-106B airplane active control landing gear drop test performance N91-28164

Improved method and apparatus for Mach number change in wind tunnel
[NASA-CASE-LAR-13548-1] N91-28175

Suspension device for low-frequency structures
[NASA-CASE-LAR-14272-1-CU] N91-28184

Propulsion studies for advanced manned launch systems N91-28213

Process for application of powder particles to filamentary materials
[NASA-CASE-LAR-14231-1-CU] N91-28290

Local delamination in laminates with angle ply matrix cracks. Part 1: Tension tests and stress analysis
[NASA-TM-104055] N91-28293

Acoustophoresis method and apparatus
[NASA-CASE-LAR-13388-1] N91-28321

Test of superplastically formed corrugated aluminum compression specimens with beaded webs
[NASA-TM-104119] N91-28373

Process for bonding elastomers to metal
[NASA-CASE-LAR-13645-1] N91-28424

Polyimides prepared from 3,5-diamino benzo trifluoride
[NASA-CASE-LAR-14206-1] N91-28425

Improving the performance of blasting caps
[NASA-CASE-LAR-13832-1] N91-28444

Flush mounting of thin film sensors
[NASA-CASE-LAR-14446-1] N91-28454

Method and apparatus for cleaning rubber deposits from airport runways and roadways
[NASA-CASE-LAR-14483-1] N91-28455

Method of preforming and assembling superconducting circuit elements
[NASA-CASE-LAR-14395-1-CU] N91-28490

Pressure transducer and system for cryogenic environments
[NASA-CASE-LAR-14579-1] N91-28546

Noncircular rolling joints for vibrational reduction in slewing maneuvers
[NASA-CASE-LAR-14515-1-CU] N91-28580

NATIONAL AERONAUTICS AND SPACE ADMINISTRATION. LEWIS RESEARCH CENTER, CLEVELAND, OH.

Evaluation of a technique to generate artificially thickened boundary layers in supersonic and hypersonic flows
[NASA-TP-3142] N91-28136

Advanced cryo propulsion systems N91-28212

Futuristic systems: Solar and nuclear electric propulsion N91-28215

Probabilistic structural analysis methods for space transportation propulsion systems N91-28238

Overall goals N91-28246

Concurrent engineering N91-28247

SEI power source alternatives for rovers and other multi-kWe distributed surface applications
[NASA-TM-104360] N91-28277

Comparison of dynamic isotope power systems for distributed planet surface applications
[NASA-TM-4303] N91-28278

Apparatus for intercalating large quantities of fibrous structures
[NASA-CASE-LEW-15077-2] N91-28289

Elevated-temperature fracture resistances (K(sub IC), R-curves, gamma sub (omega OF)) of monolithic and composite ceramics using chevron-notched, bend tests
[NASA-TM-105090] N91-28418

Pretreatment of lubricated surfaces with sputtered cadmium oxide
[NASA-CASE-LEW-14474-1] N91-28423

Slush hydrogen propellant production, transfer, and expulsion studies at the NASA K-Site Facility
[NASA-TM-105191] N91-28449

Cryogenic transfer options for exploration missions
[NASA-TM-105197] N91-28538

Nondestructive evaluation tools and experimental studies for monitoring the health of space propulsion systems
[NASA-TM-105164] N91-28605

Viscoplastic analysis of an experimental cylindrical thrust chamber liner
[NASA-TM-103287] N91-28622

ASTROP2 users manual: A program for aeroelastic stability analysis of propfans
[NASA-TM-4304] N91-28627

Description of real-time Ada software implementation of a power system monitor for the Space Station Freedom PMAD DC testbed
[NASA-TM-105157] N91-28776

Historical perspectives: The role of the NASA Lewis Research Center in the national space nuclear power programs
[NASA-TM-105196] N91-29138

NATIONAL AERONAUTICS AND SPACE ADMINISTRATION. MARSHALL SPACE FLIGHT CENTER, HUNTSVILLE, AL.

Applications of low lift to drag ratio aerobrakes using angle of attack variation for control
[NASA-TM-103544] N91-28189

The space exploration initiative N91-28194

Next generation earth-to-orbit space transportation systems: Unmanned vehicles and liquid/hybrid boosters N91-28205

Solid rocket propulsion N91-28206

Advanced launch system N91-28208

Next generation In-space transportation system(s) N91-28211

Materials sub-panel N91-28245

Liquid rocket engine flight certification N91-28250

The case for teaming on the ALS-STME program N91-28269

Space transportation main engine reliability and safety N91-28271

The effect of stress on hydrogen uptake and desorption by A-286
[NASA-TM-103537] N91-28341

NATIONAL DEFENCE HEADQUARTERS, OTTAWA (ONTARIO).

Failure analysis case histories of Canadian forces aircraft landing gear components N91-28151

NATIONAL GEOPHYSICAL DATA CENTER, BOULDER, CO.

Solar-geophysical data number 558, August 1990. Part 2: (Comprehensive reports). Data for August 1990 and miscellaneous
[PB91-172262] N91-29128

Solar-geophysical data number 558, February 1991. Part 1: (Prompt reports). Data for January 1991, December 1990, and late data
[PB91-172270] N91-29129

Solar-geophysical data number 557, January 1991. Part 1: (Prompt reports). Data for December, November 1990 an late data
[PB91-169102] N91-29130

Solar-geophysical data number 557, January 1991. Part 2: (Comprehensive reports). Data for July 1990 and miscellaneous
[PB91-169110] N91-29131

NATIONAL INST. FOR FUSION SCIENCE, NAGOYA (JAPAN).

Proceedings of the Second International Toki Conference on Plasma Physics and Controlled Nuclear Fusion. Nonlinear Phenomena in Fusion Plasmas: Theory and Computer Simulation
[NIFS-PROC-6] N91-28881

Self-organizing processes in magnetically confined plasma N91-28883

Equilibrium beta limit of helical systems N91-28894

Magnetohydrodynamical formation of astrophysical jets from gravitationally collapsing objects N91-28903

Computer simulation of solar wind-magnetosphere interaction N91-28904

Particle simulation on the tilt stabilization of the FRC plasma N91-28917

The 3-D electromagnetic macroscale particle simulation of inhomogeneous, magnetized plasmas N91-28918

Nonlinear behavior and transport property of multiple-helicity resistive interchange modes near marginally stable states N91-28922

Nonlinear computer analysis of backward wave oscillator N91-28923

Nonlinear equations for weakly unstable modes N91-28927

Structures of magnetic field lines in the helical torus N91-28932

Regular motion and symmetry in the relativistic standard map N91-28933

Solitons and chaos in plasma N91-28943

NATIONAL INST. OF STANDARDS AND TECHNOLOGY, BOULDER, CO.

Integrated theoretical and experimental study of the thermophysical properties of fluid mixtures
[DE91-012660] N91-28316

Transmission/reflection and short-circuit line permittivity measurements
[PB91-171959] N91-28482

NATIONAL INST. OF STANDARDS AND TECHNOLOGY, GAITHERSBURG, MD.

Chemistry of electronic ceramic materials. Proceedings of the International Conference on the Chemistry of Electronic Ceramic Materials
[NASA-CR-188688] N91-28403

US assessment of the new diamond technology in Japan
[PB91-167395] N91-28404

Boussinesq algorithm for enclosed bouyant convection in two dimensions
[PB91-178848] N91-28507

NAVAL AIR DEVELOPMENT CENTER, WARMINSTER, PA.

Rapid solidification processing of Al3Ti and Al3Ti plus copper
[AD-A236600] N91-28343

NAVAL POSTGRADUATE SCHOOL, MONTEREY, CA.

Impact of ion propulsion on performance, design, testing, and operation of a geosynchronous spacecraft
[AD-A237028] N91-28273

Design of an interactive satellite communications system analysis program
[AD-A237030] N91-28459

Multidimensional spectral estimation using iterative methods
[AD-A237025] N91-28791

NAVY CLOTHING AND TEXTILE RESEARCH FACILITY, NATICK, MA.

The chemical resistance of protective handwear available through the Navy's supply system
[AD-A235874] N91-28731

NEBRASKA UNIV., LINCOLN.

Magnetic studies of iron-rare-earth-metalloid alloys
[DE91-013856] N91-28368

NEW MEXICO STATE UNIV., LAS CRUCES.

Search for regularities in the atmosphere of Jupiter N91-29127

NEW SOUTH WALES UNIV., KENSINGTON (AUSTRALIA).

One-sun silicon solar cell research
[DE91-014329] N91-28662

NEW YORK UNIV., NEW YORK.

A comparison of the potential and the Euler formulations of the equations of motion for transonic flow
[DE91-014731] N91-28142

Plasma properties
[DE91-013933] N91-28978

NORTH CAROLINA STATE UNIV., RALEIGH.

An abbreviated Reynolds stress turbulence model for airfoil flows N91-28140

Direct contact heat transfer to a dispersal droplet with change of phase N91-28521

Thermal and non-Newtonian effects in elastohydrodynamic lubrication of rolling-sliding contacts N91-28590

NORTH CAROLINA UNIV., CHAPEL HILL.

Building microelectronic systems in a university environment
[AD-A236629] N91-28477

The use of science in the management of hazardous air pollutants N91-28667

Prototyping parallel and distributed programs in proteus
[AD-A236597] N91-28746

Providing common access mechanisms for dissimilar network interconnection nodes
[AD-A236630] N91-28770

Taxonomy and algorithms for volume rendering on multicomputers
[AD-A236632] N91-28771

The 1992 - 1997 renewal proposal interactive graphics for molecular studies
[AD-A236598] N91-28823

A spectroscopic differential reflectometry study of (100), (110), (111), (311), and (511) silicon surfaces
[AD-A231022] N91-28985

Numerical models of equilibrium between matter and black holes N91-29101

NORTHWESTERN UNIV., EVANSTON, IL.

Investigation of thermomechanical behavior of metal matrix composites N91-28296

Tribology of aluminum-based metal matrix composites: Fundamental study of wear behavior as influenced by microstructure N91-28297

NOTRE DAME UNIV., IN.
Study of interfacial behavior in cocurrent gas-liquid flows
[DE91-013008] N91-28511
NOTTINGHAM UNIV. (ENGLAND).
Kinematic GPS surveying N91-28149
Precise orbit determination for GPS satellites N91-28183
The determination of mean sea level using GPS N91-28708

O

OAK RIDGE K-25 SITE, TN.
The effect of fluoride gases on cylinder valve corrosion
[DE91-012745] N91-28355
OAK RIDGE NATIONAL LAB., TN.
Perturbed environment assessments for space vehicles
[DE91-012630] N91-28188
Technologies available from Martin Marietta Energy Systems, Inc.
[DE91-013027] N91-28283
Chemical characterization of microparticles by laser ablation in an ion trap mass spectrometer
[DE91-012513] N91-28309
Analysis of metals in solution using electrospray ionization mass spectrometry
[DE91-012522] N91-28310
Experimental studies of the volatility of ammonium chloride
[DE91-012526] N91-28311
Application of electron energy loss spectroscopy to microanalysis of irradiated stainless steels
[DE91-009913] N91-28344
Irradiation creep by climb-enabled glide driven by transient point defect processes
[DE91-012950] N91-28348
Comparisons of irradiation-induced shifts in fracture toughness, crack arrest toughness, and Charpy impact energy in high-copper welds
[DE91-008881] N91-28349
The rate (time)-dependence mechanical behavior of modified 9Cr-1Mo. Part 2: Isothermal modeling at 538 C
[DE91-011100] N91-28350
High-temperature solution annealing as an IASCC mitigation technique
[DE91-012220] N91-28352
Aqueous corrosion characteristics and corrosion-related cracking susceptibilities of Fe3Al-type iron aluminides
[DE91-013028] N91-28358
Properties of large heats of Fe3Al-based alloys
[DE91-013268] N91-28359
Erosion studies on a Fe3Al-based iron aluminide and 1100 Al
[DE91-012529] N91-28360
Weldability of iron aluminides
[DE91-013730] N91-28367
APFIM characterization of the spinodal decomposition in duplex stainless steels
[DE91-014256] N91-28371
Corrosion of refractory metals in liquid metal and gaseous environments
[DE91-009555] N91-28378
Alloy development of Fe3Al for improved creep rupture properties
[DE91-014541] N91-28381
Processing and fabrication of Fe3Al-based alloys
[DE91-014546] N91-28382
Nitrogen and boron-containing polymers as precursors of ceramic materials
[DE91-008890] N91-28390
Characterization of silicon nitride synthesized by microwave heating
[DE91-012219] N91-28397
In-situ REM imaging of surface processes on ceramic bulk crystals from 300 to 1670 K in a conventional TEM
[DE91-009923] N91-28405
Drying of gelcast ceramics
[DE91-012955] N91-28413
Cocrystallization in blends of poly(butylene terephthalate) and poly(ester-ether) segmented block copolymers
[DE91-012224] N91-28438
An assessment of the lifetime of Faraday shield elements
[DE91-012228] N91-28463
Automated verification of system configuration
[DE91-012520] N91-28481
Monolithic front end electronics for silicon calorimeters
[DE91-012063] N91-28484
Desorption of Al, Au, Ag using surface plasmon excitation
[DE91-013726] N91-28493
Models for heat transport through assemblies of uniform-diameter hollow spheres
[DE91-012998] N91-28512
Thin film hydrogen sensor
[DE91-014197] N91-28550
Laser ejection of Ag(sup +) ions from a roughened silver surface: Role of the surface plasmon
[DE91-012945] N91-28554
Evaporation as a diagnostic test for hydrodynamic cooling of laser-ablated clusters
[DE91-013416] N91-28555
Laser range camera calibration
[DE91-014939] N91-28570
Dynamic coupling effects in modeling and control of hard contact motion of a manipulator
[DE91-010393] N91-28574
Welding of ductile intermetallic alloys
[DE91-009553] N91-28594
X ray microimaging of elemental composition and microstructure for materials science
[DE91-012052] N91-28601
Applications of a 2-D moving finite element formulation to elastic/viscoplastic dynamic fracture analysis
[DE91-009930] N91-28607
Influence of crack depth on the fracture toughness of reactor pressure vessel steel
[DE91-012537] N91-28611
Assessment of ductile fracture methodology based on applications to large-scale experiments
[DE91-009920] N91-28614
The rate (time)-dependent mechanical behavior of modified 9Cr-1Mo steel. Part 1: Experiments at 538 C
[DE91-011097] N91-28615
Near crack tip transverse strain effects estimated with a large strain hollow cylinder analogy
[DE91-012072] N91-28619
Crack initiation under generalized plane strain conditions
[DE91-013410] N91-28623
Making energy efficiency happen
[DE91-013057] N91-28655
Analysis of southeastern Canada lake-water chemistry data in relation to acidic deposition
[DE91-014957] N91-28674
Photobiotechnology: Algal hydrogen production and photoconductivity of metalized chloroplasts
[DE91-013232] N91-28718
Biomarker-based biomonitoring for evaluating health and ecological effects on environmental contamination
[DE91-013729] N91-28719
Performance of the Intel iPSC/860 and Ncube 6400 hypercubes
[DE91-012370] N91-28738
The apGA: An Adaptive Parallel Genetic Algorithm
[DE91-009559] N91-28741
Bayesian design and analysis of computer experiments: Use of derivatives in surface prediction
[DE91-013147] N91-28751
Searching for consensus patterns on a hypercube
[DE91-013233] N91-28753
Solving computational grand challenges using a network of heterogeneous supercomputers
[DE91-013725] N91-28755
Scientific data visualization
[DE91-014216] N91-28766
Network based concurrent computing on the PVM system
[DE91-014961] N91-28780
Control of autonomous mobile robots using custom-designed qualitative reasoning VLSI chips and boards
[DE91-012527] N91-28783
Proposal for continued basic research in intelligent machines at the Center for Engineering Systems Advanced Research: Fiscal years 1992-1996
[DE91-012997] N91-28784
Parallelizing across time when solving time-dependent partial differential equations
[DE91-012948] N91-28797
Light weight, high field, stable, superconducting magnets for advanced transportation systems
[DE91-013667] N91-28814
Multilevel resonance analysis of Co-59 neutron transmission measurements
[DE91-012135] N91-28829
X ray microimaging of elemental composition and microstructure for materials science
[DE91-012221] N91-28832
Fixed-wavelength R2PI/tandem mass spectrometry for mixture analysis in the quadrupole ion trap
[DE91-012506] N91-28835
Spontaneous cluster decomposition in a quadrupole ion trap
[DE91-012519] N91-28836
Scintillation detector efficiencies for neutrons in the energy region above 20 MeV
[DE91-012544] N91-28837
Correcting channeling and diffraction effects in quantitative REELS surface microanalysis
[DE91-009924] N91-28840
Development of nanovolt-resolution x ray diffraction using resonant nuclear scattering
[DE91-012217] N91-28847
Kinetic energy distributions of ions after surface collisions
[DE91-013412] N91-28850
Reflection-asymmetric shapes in atomic nuclei
[DE91-013414] N91-28851
Desorption of large organic molecules by laser-induced plasmon excitation
[DE91-013415] N91-28852
Shell model calculations at superdeformed shapes
[DE91-012954] N91-28853
Confinement projections for the Burning Plasma Experiment (BPX)
[DE91-012516] N91-28946
Characteristics of edge plasma turbulence on the ATF torsatron
[DE91-012981] N91-28947
Spectroscopic and ion probe characterization of laser produced plasmas used for thin film growth
[DE91-013425] N91-28959
Plasma turbulence calculations on supercomputers
[DE91-014210] N91-28969
Thermodynamic and transport properties of superconductors in very high magnetic fields
[DE91-012530] N91-29000
Interlayer pairing and c-axis versus ab-plane gap anisotropy in high Tc superconductor
[DE91-012218] N91-29005
Kosterlitz-Thouless-like behavior over extended ranges of temperature and layer thickness in crystalline YBa2Cu3O(7-x) / PrBa2Cu3O(7-x) superlattices
[DE91-013237] N91-29014
Excess heat production in composite superconductors during current redistribution
[DE91-013547] N91-29016
Direct imaging of ordering in Si-Ge alloys, ultrathin superlattices, and buried Ge layers
[DE91-014580] N91-29044
OFFICE OF TECHNOLOGY ASSESSMENT, WASHINGTON, DC.
Seeking solutions: High-performance computing for science
[PB91-169763] N91-28752
OHIO STATE UNIV., COLUMBUS.
Questions: Assessing the structure of knowledge and the use of information in design problem-solving N91-28169
Joining of aluminum-based particulate-reinforced metal-matrix composites N91-28298
Laser surface modification to impede hydrogen ingress into steel N91-28375
Receptivity of a laminar boundary layer to the interaction of a three-dimensional roughness element with time-harmonic free-stream disturbances N91-28518
Analytical calibration of the airborne photogrammetric system using a priori knowledge of the exposure station obtained from kinematic Global Positioning System techniques N91-28646
Strongly interacting fermion systems
[DE91-012284] N91-28848
Topics on frustrated spin systems and high-temperature superconductors N91-29032
Design and performance evaluation of signature files for text retrieval systems N91-29085
ORBITAL TECHNOLOGIES CORP., MADISON, WI.
Overview of European and other non-US/USSR/Japan launch vehicle and propulsion technology programs N91-28221
OREGON STATE UNIV., CORVALLIS.
Theoretical studies of zirconia and related materials
[DE91-013906] N91-28369
Kinematic analysis of legged system locomotion on smooth horizontal surfaces N91-28586
Modelling and analysis of geophysical turbulence: Use of optimal transforms and basis sets N91-28686
A study of El Nino/Southern Oscillation: Numerical experiments and data analysis N91-28710
Theoretical studies in nuclear physics
[DE91-013909] N91-28873
OREGON UNIV., EUGENE.
A comparative second harmonic study of Cu(111) in UHV and in solution
[AD-A237023] N91-28479
OSAKA UNIV., SUITA (JAPAN).
Hydrodynamic instabilities in laser driven implosion N91-28897

Nonlinear evolution of 2D and 3D Rayleigh-Taylor instability at stagnation phase in laser implosion N91-28899
Turbulent mixing due to Rayleigh-Taylor instability in laser driven implosion N91-28914

OXFORD UNIV. (ENGLAND).
Non-Hausdorff twistor spaces and the global structure of space-time N91-29103

P

PACIFIC NORTHWEST LAB., RICHLAND, WA.
SPGD: A central power system for space [DE91-012610] N91-28276
Electrochemical processes at solid electrode-electrolyte-gas interfaces [DE91-012922] N91-28317
Effects of residual stresses on the fracture toughness of Zircaloy-2 tubes [DE91-012736] N91-28354
Advancements in ultrathinning section techniques for the characterization of brittle materials [DE91-012930] N91-28364
The avian eggshell as a model of biomineralization [DE91-012608] N91-28400
Ultra-fine powders using glycine-nitrate combustion synthesis [DE91-012926] N91-28412
Computer modeling of ceramic melters to assess impacts of process and design variables on performance [DE91-013668] N91-28431
Behavior of RuO2 in a glass melt [DE91-013717] N91-28432
Development of biomass as an alternative fuel for gas turbines [DE91-012129] N91-28441
Robotic mannequin technology for enhanced product testing [DE91-013787] N91-28591
Nondestructive testing standards and the ASME code [DE91-012643] N91-28600
Analysis of brittle intergranular crack propagation during stress corrosion cracking [DE91-013666] N91-28630
Applications and challenges for thermal energy storage [DE91-012873] N91-28654
Alternative materials for solid oxide fuel cells: Chromite interconnections [DE91-014447] N91-28664
Environmental tradeoffs associated with various energy paths: A total energy cycle analysis approach [DE91-013662] N91-28669
Modeling molecular processes in the environment [DE91-013790] N91-28671
Microbeam studies of the sensitivity of structures within living cells [DE91-012927] N91-28715
Choosing processor array configuration by performance modeling for a highly parallel linear algebra algorithm [DE91-012486] N91-28749
Biomimetic thin film deposition [DE91-012485] N91-28999
Raman studies of stress-induced phase transformation in titania films [DE91-012871] N91-29012
Threatened Area Database System (TADS) computer program [DE91-012491] N91-29074
Developing a GIS to facilitate data analysis for environmental restoration of a large waste site [DE91-013222] N91-29078
Communicating success: Writing about technology transfer [DE91-013994] N91-29092

PENNSYLVANIA STATE UNIV., UNIVERSITY PARK.
Studies of the two-phase plume jet and wall erosion in a vertical launching system N91-28145
A theoretical and experimental study of the interior ballistic processes of an electrothermal gun N91-28185
A review of liquid rocket propulsion programs in Japan N91-28219
An overview of the Penn State Propulsion Engineering Research Center N91-28222
Cryogenic combustion laboratory N91-28223
Ignition and combustion of metallized propellants N91-28224
Liquid-propellant droplet vaporization and combustion in high pressure environments N91-28225
Spray combustion under oscillatory pressure conditions N91-28226
Liquid jet breakup and atomization in rocket chambers under dense spray conditions N91-28227
Droplet-turbulence interactions in subcritical and supercritical evaporating sprays N91-28228
Composite material systems for hydrogen management N91-28229
Robust and real-time control of magnetic bearings for space engines N91-28230
Analysis of foil bearings for high speed operation in cryogenic applications N91-28231
A study of methods to investigate nozzle boundary layer transition N91-28232
Optical diagnostic investigation of low Reynolds number nozzle flows N91-28233
CFD applications in chemical propulsion engines N91-28234
Experiments on the instabilities in swirling and non-swirling free jets N91-28531
A reconfigurable strategy for distributed digital process control [DE91-013740] N91-28786
Sound propagation in the atmosphere: Analysis of signal amplitude and phase temporal and spatial variations [AD-A237034] N91-28816
Coordinated optical and ultraviolet observations of short period RS CVn and W UMa type stars N91-29096

PENNSYLVANIA UNIV., PHILADELPHIA.
Atomistic studies of grain boundaries in alloys and compounds [DE91-014516] N91-28372
Chemistry of electronic ceramic materials. Proceedings of the International Conference on the Chemistry of Electronic Ceramic Materials [NASA-CR-188688] N91-28403
Mechanical design optimization of robot manipulator performance N91-28589
A logic model for model management: An embedded languages approach N91-28761
Structure and dynamics in low-dimensional guest host solids [DE91-012169] N91-29020
Generalized hypertext in a knowledge-based decision support shell environment N91-29086

PITTSBURGH ENERGY TECHNOLOGY CENTER, PA.
A review of theories for flowing granular materials with applications to fluidized beds and solids transport [DE91-013111] N91-28514

PITTSBURGH UNIV., PA.
Support materials for formal specification of software [AD-A236121] N91-28742

POHANG INST. OF SCIENCE AND TECHNOLOGY (REPUBLIC OF KOREA).
Theoretical studies of nonlinear sheath dynamics N91-28896

POLITECNICO DI MILANO (ITALY).
Design landing loads evaluation by dynamic simulation of flexible aircraft N91-28163

POLYTECHNIC UNIV., BROOKLYN, NY.
Scanning tunneling microspectroscopy of solids and surfaces [DE91-014515] N91-29043

PORTLAND STATE UNIV., OR.
Optimization and thermodynamic performance measures for a class of finite time thermodynamic cycles N91-29060

PRATT AND WHITNEY AIRCRAFT, WEST PALM BEACH, FL.
Cryogenic upper stage propulsion: RL10 and derivative engines N91-28202
Business not as usual N91-28266

PRINCETON UNIV., NJ.
Stochastic robustness of linear multivariable control systems: Towards comprehensive robustness analysis N91-28172
Atmospheric responses to lower tropospheric forcing in a multilayer isentropic model N91-28688
The theory of turbulence and anomalous transport in plasmas: Past, present, and future N91-28889
Three-dimensional particle simulation of trapped electron instabilities in tokamaks N91-28891
Propagation of drift waves in toroidal plasma systems N91-28939
Statistical mechanics using symbolic dynamics N91-28940
Gravitational evolution of large-scale structure in the universe N91-29121
Population synthesis models for cluster galaxies at redshifts of 0.4 to 0.55 N91-29124
Interaction of radiation with outflows in late-type stars N91-29136

PURDUE UNIV., WEST LAFAYETTE, IN.
Regulation of photosynthetic membrane components in cyanobacteria [DE91-012713] N91-28713
Real-time adaptive active control of sound fields N91-28819
Upper limits for the flux of very high-energy gamma radiation from Cygnus X-3 and for the explosion rate of primordial black holes obtained by the Haleakala Gamma Ray Observatory N91-29134

Q

QUEENS UNIV., BELFAST (NORTHERN IRELAND).
Interstellar magnesium studies N91-29120

R

ROCHESTER UNIV., NY.
Transition metal activation and functionalization of carbon-hydrogen bonds [DE91-014261] N91-28332

ROCKWELL INTERNATIONAL CORP., CANOGA PARK, CA.
Operationally Efficient Propulsion System Study (OEPPS) N91-28198
Expendable launch vehicle propulsion N91-28199
Space transportation propulsion USSR launcher technology, 1990 N91-28220
Business not as usual N91-28266
Issues concerning centralized versus decentralized power deployment [NASA-CR-187121] N91-28648

ROCKWELL INTERNATIONAL CORP., HUNTSVILLE, AL.
Test vs. simulation N91-28251
Propulsion system ground testing N91-28261

ROME AIR DEVELOPMENT CENTER, GRIFFISS AFB, NY.
Proceedings of the 1990 Antenna Applications Symposium, volume 1 [AD-A237056] N91-28460
Proceedings of the 1990 Antenna Applications Symposium, volume 2 [AD-A237057] N91-28461
A survey of reliability, maintainability, supportability, and testability software tools [AD-A236148] N91-28745

ROYAL AEROSPACE ESTABLISHMENT, FARNBOROUGH (ENGLAND).
The application of Particle Image Velocimetry (PIV) in a short duration transonic annular turbine cascade [AD-A236639] N91-28504

RUTGERS - THE STATE UNIV., PISCATAWAY, NJ.
An extension of a kinetic theory of polymer crystallization through the exclusion of negative barriers [AD-A236999] N91-28387
Effect of TCP doping on the remnant polarization in uniaxially oriented poly(vinylidene fluoride) films [AD-A237001] N91-28388
Effect of water content on the piezoelectric properties of nylon 11 and nylon 7 [AD-A237013] N91-28389

S

SAC TECHNOLOGY LTD., WALTON-ON-THAMES (ENGLAND).
Assessment of the application of the working group 22 standard bump concept to a current military aircraft N91-28166

SANDIA NATIONAL LABS., ALBUQUERQUE, NM.
An experimental investigation of the effect of vortex generators on the aerodynamic characteristics of a NACA 0021 airfoil undergoing large amplitude pitch oscillations [DE91-012102] N91-28133
Sandia's new hypervelocity launcher (HVL) [DE91-014335] N91-28178
Attitude control of a spinning rocket via thrust vectoring [DE91-006267] N91-28274
Sol-gel kinetics by NMR [DE91-011500] N91-28314
Semiconductor Bridge (SCB) research and development [DE91-011493] N91-28319
Effects of sample size and loading rate on the transition behavior of a DCI alloy [DE91-012015] N91-28346
Microstructural characterization of solders and brazes for advanced packaging technology [DE91-011503] N91-28379
Mechanical modeling of stress generation during cure of encapsulating resins [DE91-011496] N91-28393
Aerogel composites for radioluminescent light/power sources [DE91-012012] N91-28395
Subgap absorption in conjugated polymers [DE91-012655] N91-28402
Response of the polymers KEL-F, polysulfone, high density polyethylene and polymethylmethacrylate to shock loading and release from 0.3 to 2.4 GPa [DE91-012867] N91-28411

Ferroelectric fatigue in modified bulk lead zirconate titanate ceramics
[DE91-012647] N91-28417

Measurements of photo-induced changes in conjugated polymers
[DE91-013262] N91-28427

Adhesion between CVD diamond films and tungsten
[DE91-013757] N91-28434

Shock-wave properties of high-strength ceramics
[DE91-014105] N91-28439

Investigation of the Deflagration-to-Detonation (DDT) process: The role of ignition and explosive properties in DDT
[DE91-011956] N91-28442

Fluxless soldering of Ni-Au plated Kovar with a laser
[DE91-013261] N91-28451

Performance of a polarization isolation enhancement method in the presence of errors
[DE91-013571] N91-28473

Borehole Radar Evaluation Program: Antenna designs for optimal directionality
[DE91-014322] N91-28475

Preparation of ionic membranes for zinc/bromine storage batteries
[DE91-012008] N91-28483

Exploratory battery technology development report for FY90
[DE91-012131] N91-28485

Durability of polymeric materials used in zinc/bromine flow batteries
[DE91-012864] N91-28487

Feasibility study of a 200 ampere battery
[DE91-014673] N91-28496

Some high voltage DC breakdown properties of thick film circuits on alumina
[DE91-014675] N91-28500

The superconducting flux flow transistor: Models and applications
[DE91-014702] N91-28501

A numerical approach for modelling cavitating flows
[DE91-009178] N91-28505

ZEPHYR3D: A finite difference computer program for three-dimensional, transient incompressible flow problems
[DE91-014331] N91-28515

An evaluation of monochrome solid-state video cameras
[DE91-012368] N91-28543

A controlled dispersion parallel wavelength x ray spectrometer for electron microscopy
[DE91-012011] N91-28544

Diffraction patterns produced by periodic and turbulent flowing gases including applications of photorefractive temporal filtering
[DE91-012636] N91-28553

Studies of laser-driven flyer acceleration using optical fiber coupling
[DE91-013503] N91-28562

Numerical and analytical analysis of thin laser-driven flyer plates
[DE91-013748] N91-28567

Monitoring structural response in pressurized environments. Part 1: Instrumentation techniques
[DE91-012654] N91-28616

Non-steady wave profiles and the fourth-power law
[DE91-013576] N91-28631

United States Department of Energy solar receiver technology development
[DE91-012653] N91-28651

Second-generation central receiver technology comparison
[DE91-012865] N91-28653

SOLTECH 91: Proceedings, volume 2
[DE91-013767] N91-28656

SOLTECH 91: Proceedings, volume 1
[DE91-002163] N91-28658

One-sun silicon solar cell research
[DE91-014329] N91-28662

Load-balancing and performance of a gridless particle simulation on MIMD, SIMD, and vector supercomputers
[DE91-013758] N91-28756

General implementation of thin-slot algorithms into the finite-difference time-domain code, TSAR, based on a slot data file
[DE91-014336] N91-28767

An interdisciplinary approach to massively parallel computation
[DE91-012652] N91-28775

Requirements for a network storage service
[DE91-014106] N91-28778

Ezekiel graphs
[DE91-012656] N91-28805

Progress in light ion fusion
[DE91-012019] N91-28826

X ray spatial resolution at intermediate voltages: An assessment by massively parallel Monte Carlo electron trajectory simulation
[DE91-012018] N91-28841

Molecular dynamics simulations of bulk displacement threshold energies in Si
[DE91-011957] N91-28846

The spatial resolution of x ray microanalysis in thin foils
[DE91-011949] N91-29003

Donor formation under hydrogen plasma exposure and ion implantation
[DE91-011958] N91-29004

Measurement accuracy of macroscopic quantum circuits with RF-biased Josephson junction arrays
[DE91-012651] N91-29009

The surface chemistry of GaAs atomic layer epitaxy
[DE91-014112] N91-29047

The ECR-plasma deposition of silicon nitride on a tunnel oxide
[DE91-014665] N91-29051

Annealing and structure studies on Tl-2223 and Tl-1223 crystals
[DE91-014903] N91-29052

SANDAC V computer electromagnetic interface characteristics: Problems and solutions
[DE91-014334] N91-29065

SANDIA NATIONAL LABS., LIVERMORE, CA.

The SNL, Livermore, Hopkinson bar apparatus for compressive materials testing at high strain-rates
[DE91-013132] N91-28612

SASKATCHEWAN UNIV., SASKATOON.

Anomalous transport due to the skin size electromagnetic drift mode in tokamaks N91-28902

SCIENCE APPLICATIONS INTERNATIONAL CORP., SAN DIEGO, CA.

Reversed-Field Pinch dynamics and transport studies
[DE91-014317] N91-28970

SEATTLE UNIV., WA.

Software metrics
[AD-A236140] N91-28744

SHEFFIELD UNIV. (ENGLAND).

Magnetospheric VLF line radiation N91-28693

The computer storage, retrieval, and searching of generic structures in chemical patents: The machine-readable representation of generic structures N91-29081

SIKORSKY AIRCRAFT, STRATFORD, CT.

Technology needs for high speed rotorcraft (2)
[NASA-CR-177590] N91-28168

SOCIETE ANONYME D'ETUDES ET REALISATIONS NUCLEAIRES, LIMEIL-BREVANNES (FRANCE).

Plasma immersion surface modification with metal ion plasma
[DE91-014233] N91-28979

SOUTH CAROLINA UNIV., COLUMBIA.

The line of gravitation: On the quantization conditions in curved spacetime and uncertainty-driven inflation N91-29115

SOUTHAMPTON UNIV. (ENGLAND).

A reciprocity technique for the characterisation of sound transmission into aircraft fuselages N91-28817

Coded aperture imaging with a HURA coded aperture and a discrete pixel detector N91-29093

SOUTHWEST RESEARCH INST., SAN ANTONIO, TX.

Fracture micromechanics of intermetallic and ceramic matrix continuous fiber composites
[AD-A236638] N91-28280

SRI INTERNATIONAL CORP., MENLO PARK, CA.

Combustion research program: Flame studies, laser diagnostics, and chemical kinetics
[DE91-014824] N91-28329

STANFORD LINEAR ACCELERATOR CENTER, CA.

Simulation of a storage ring free electron laser with a mapping algorithm for distribution functions
[DE91-012387] N91-28552

A 2D field solver for periodic structures with special corner elements
[DE91-012323] N91-28792

Symplectic full-turn maps in a Fourier representation
[DE91-012912] N91-28796

Refinement of the Hamilton-Jacobi solution using a second canonical transformation
[DE91-012965] N91-28798

Heavy-quark physics in quantum chromodynamics
[DE91-012113] N91-28828

Simulations on pair creation from beam-beam interaction in linear colliders
[DE91-012315] N91-28834

Light-cone quantization of quantum chromodynamics
[DE91-013991] N91-28856

SLC polarized beam source electron optics design
[DE91-012911] N91-28869

Strain enhanced electron spin polarization observed in photoemision from InGaAs
[DE91-012319] N91-28996

STANFORD UNIV., CA.

Ultra-low temperature properties of amorphous solids
[DE91-012782] N91-28312

Thermodynamics and efficiency in combustion and engines
[DE91-012781] N91-28320

High-resolution measurements of the thermal conductivity and boundary resistance of helium-4 near the lambda point N91-28322

Phonon-mediated detection of elementary particles using silicon crystal acoustic detectors N91-28547

Numerical investigation of the thrust efficiency of a laser-propelled vehicle N91-28572

Laser speckle velocimetry with photorefractive recording and anamorphic optical processing N91-28880

STATE UNIV. OF NEW YORK, ALBANY.

Development and application of new modeling techniques for mesoscale atmospheric chemistry N91-28692

Data users guide to the mountain cloud chemistry project
[PB91-168484] N91-28697

STATE UNIV. OF NEW YORK, BUFFALO.

Exact solution of a quantum forced time-dependent harmonic oscillator
[AD-A236633] N91-28812

Phase-conjugated fluorescence
[AD-A231114] N91-28820

Indium compounds which contain two different organic substituents. Crystal structure of (In(CH2CMe3)(CH2SiMe3)Cl)2, an interesting case of partial Ligand disorder in the solid state
[AD-A236730] N91-28989

STATE UNIV. OF NEW YORK, STONY BROOK.

Research in theoretical nuclear physics
[DE91-013644] N91-28872

STATE UNIV. OF NEW YORK AT BUFFALO, AMHERST.

The computation of complex, two-dimensional turbulent flows using Reynolds stress closure N91-28535

SUPERCONDUCTING SUPER COLLIDER LAB., DALLAS, TX.

ZLIB: A numerical library for differential algebra (A user's guide for version 1.0)
[DE91-012552] N91-28794

A system approach to the design of superconducting magnets
[DE91-012707] N91-29010

Non similarity solution approximation to the thermal hydraulic quenchback in superconductors
[DE91-013964] N91-29040

Document format considerations for a document tracking and storage system
[DE91-013402] N91-29079

T

TECHNISCHE UNIV., DELFT (NETHERLANDS).

Common reflection point stacking: A macro model driven approach to dip moveout
[ISBN-90-9003020-4] N91-28676

High-speed and high-resolution analog-to-digital and digital-to-analog converters
[ETN-90-97265] N91-28735

Measuring and modelling disk I/O subsystems
[ISBN-90-6275-567-4] N91-28736

TEL-AVIV UNIV. (ISRAEL).

An active delay of separation on two-dimensional airfoils
[ITN-91-85142] N91-28139

Mutual interference between many similar radars operating in physical proximity
[ITN-91-85139] N91-28468

Fluctuations in near-surface backscattering to a descending CW radar
[ITN-91-85140] N91-28469

Performance evaluation of partial response continuous phase modulation: Discriminator detection
[ITN-91-85145] N91-28470

Wideband adaptive HF modem
[ITN-91-85147] N91-28471

Numerical solution of a moving boundary problem as a model solution for a solar pipe
[ITN-91-85143] N91-28516

Planning of minimum-time trajectories for robotic arms
[ITN-91-85141] N91-28583

Human body protection in a dynamic environment. Cushioning mechanics
[ITN-91-85149] N91-28733

Efficient soft decision decoding of Reed-Muller codes and related non-linear generalizations
[ITN-91-85146] N91-28760

Color effects in optical systems
[ITN-91-85150] N91-28878

TENNESSEE UNIV., KNOXVILLE.
Mechanical properties of diamond and diamond-like films
[DE91-011373] N91-28406
Analysis of the surface heterogeneity of different samples of aluminum oxide ceramic powders
[DE91-013527] N91-28421
Validity of the model used to relate the energy distribution and the adsorption isotherm
[DE91-013528] N91-28428
Transient two-phase flow of cryogenic fluid in a vertical transfer line during the cooldown process N91-28522
Modeling two-point spatial turbulence spectra for analysis of gust variations over aerospace vehicles N91-28685

TENNESSEE UNIV., TULLAHOMA.
A PC based frequency domain LV processor
[DE91-009056] N91-28541

TEXAS UNIV., ARLINGTON.
Analysis and modeling of early vision tasks for robot stereo vision N91-28585

TEXAS UNIV., AUSTIN.
Model catalytic oxidation studies using supported monometallic and heterobimetallic oxides
[DE91-012144] N91-28409
Experimental study of growth rate enhancement and structure of compressible turbulent free shear layers N91-28517
Seismic traveltime inversion in three-dimensional heterogeneous media N91-28678
Regularization of the Lagrange planetary equations for numerical use N91-28808
Electron transfer reactions in microporous solids
[DE91-012299] N91-28833
Stability of annular equilibrium of energetic large orbit ion beam
[DE91-014365] N91-28963
Transport profiles induced by radially localized modes in tokamak
[DE91-014366] N91-28964
Exact solutions for a system of nonlinear plasma fluid equations
[DE91-014367] N91-28965
A portable and independent edge fluctuation diagnostic
[DE91-014357] N91-28971
Nonlinear dynamics of the relativistic standard map
[DE91-014368] N91-28972
Steady-state dynamo and current drive in a nonuniform bounded plasma
[DE91-014865] N91-28974
Stability of drift-wave modons in the presence of temperature gradients
[DE91-014364] N91-28982
The 2+1 gravity: A new approach N91-29059

THIOKOL CORP., BRIGHAM CITY, UT.
Follow-on cable coupling lightning test, volume 1
[NASA-CR-184123] N91-28192
Next generation solid boosters N91-28207
Possible funding strategies N91-28272

TOHOKU UNIV., SENDAI (JAPAN).
Numerical simulation of potential-driven ion cyclotron oscillation N91-28925

TOKYO INST. OF TECH. (JAPAN).
Hole dynamics of one-dimensional plasma N91-28928

TOKYO UNIV. (JAPAN).
Turbulent dynamo and subgrid-scale modeling of MHD turbulence N91-28887
Magnetohydrodynamical formation of astrophysical jets from gravitationally collapsing objects N91-28903
Direct ion heating in MHD relaxation N91-28911
Soliton phenomena in electron beam plasma N91-28930

TOLEDO UNIV., OH.
Solution to quasi-axisymmetric internal compressible flows using the stream tube approach N91-28526

TRI-UNIV. MESON FACILITY, VANCOUVER (BRITISH COLUMBIA).
High intensity neutrino beams at KAON
[DE91-012147] N91-28830

TRW SPACE TECHNOLOGY LABS., REDONDO BEACH, CA.
Historical problem areas lessons learned N91-28242

TSUKUBA UNIV. (JAPAN).
Mode conversion of Alfven waves induced by quadrupole magnetic field modulation N91-28924

U

UNITED KINGDOM ATOMIC ENERGY AUTHORITY, CULHAM (ENGLAND).
Issues in direct numerical simulation of plasma turbulence and transport N91-28901

UNITED TECHNOLOGIES CORP., EAST HARTFORD, CT.
Investigation of laser diagnostics of PACVD processes for depositing hard face coatings
[DE91-012642] N91-28401

UNIVERSITY COLL. OF NORTH WALES, BANGOR.
Modification and evaluation of Elastomer Test Machine (ETM)
[AD-A236143] N91-28540

UNIVERSITY OF CENTRAL FLORIDA, ORLANDO.
Space shuttle with common fuel tank for liquid rocket booster and main engines (supertanker space shuttle) N91-28257
Determining criteria for single stage to orbit N91-28258

UNIVERSITY OF NORTHERN ILLINOIS, DE KALB.
Effect of size and geometry on levitation force measurements between permanent magnets and high-temperature superconductors
[DE91-012472] N91-29008

UNIVERSITY OF WESTERN MICHIGAN, KALAMAZOO.
Correlated charge-changing ion-atom collisions
[DE91-013640] N91-28863

UTAH UNIV., SALT LAKE CITY.
Heat flow data and thermal state of the continental lithosphere N91-28682
Prediction of forecast skill with a quasi-geostrophic model N91-28699
Microcomputers: An exploratory study of their availability and use in the research process and their contribution to researcher productivity N91-28739

V

VIGYAN RESEARCH ASSOCIATES, INC., HAMPTON, VA.
A study of residual interference effects in adaptive wall testing of a 7-inch chord CAST-10-2/DOA 2 airfoil model
[NASA-CR-4390] N91-28138

VIRGINIA POLYTECHNIC INST. AND STATE UNIV., BLACKSBURG.
Damage development under compression-compression fatigue loading in a stitched uniwoven graphite/epoxy composite material
[NASA-CR-188693] N91-28292
An analysis of interlaminar stresses in unsymmetrically laminated plates N91-28299
High-resolution interferometric measurements of residual strains in composites N91-28303
The solution of variable-geometry truss problems using new homotopy continuation methods N91-28640
Research and development entitled smart structures for fossil energy applications
[DE91-002064] N91-28875
A selection tool for choosing the best participative problem-solving technique
[DE91-012421] N91-29066
Experience in designing and using a flat structure in a multi-project research organization
[DE91-012427] N91-29067
Structured meeting techniques identify emergency management issues practitioners really want to see addressed
[DE91-012414] N91-29069
How to increase meeting effectiveness and efficiency
[DE91-012420] N91-29070
Why engineers must know and manage organizational culture
[DE91-012425] N91-29071
A framework for data and information
[DE91-012416] N91-29075
The effects of information availability on the group consensus process
[DE91-012428] N91-29076

VIRGINIA UNIV., CHARLOTTESVILLE.
Embedding ADAMS in FORTRAN
[DE91-014346] N91-28754
An introduction to the ADAMS interface language, part 1
[DE91-014344] N91-28757
Performance measurement of a parallel input/output system for the Intel iPSC/2 hypercube
[DE91-014219] N91-28779
Concurrent access to O-trees
[DE91-014348] N91-28782
The ADAMS interactive interpreter
[DE91-014345] N91-29080
Implementation of a hypercube database system
[DE91-014285] N91-29089
Performance evaluation of multiversion database systems
[DE91-014340] N91-29090

VITRO CORP., WASHINGTON, DC.
Launch operations manpower yesterday, today and tomorrow N91-28267

W

WASEDA UNIV., TOKYO (JAPAN).
Relaxed state and entropy production N91-28907

WASHINGTON STATE UNIV., PULLMAN.
A study on particle dispersion in two-dimensional mixing layer flows N91-28537

WASHINGTON UNIV., SAINT LOUIS, MO.
A chemically reacting, turbulent stratified interface N91-28144

WASHINGTON UNIV., SEATTLE.
The effect of ductile innerlayers on the mechanical performance of fiber-reinforced composite materials N91-28295
Studies in cloud physics: Electrification, glaciation, and turbulence N91-28684
Formation and sustainment of a very low aspect ration tokamak using coaxial helicity injection (the Helicity Injected Torus (HIT) experiment)
[DE91-013948] N91-28967
Chaos and microbial systems
[DE91-014908] N91-29064
Isotopic measurements of solar noble gases in individual micrometeorites from Greenland and Antarctica N91-29114
High-overtone black-hole normal modes: A WKB contour-integral approach N91-29118
A new model of PeV gamma ray sources and MHD turbulence in neutron star accretion columns N91-29122

WAYNE STATE UNIV., DETROIT, MI.
Reactive characterization as a probe of the nature of catalytic sites
[DE91-014536] N91-28333
Active control of panel vibrations induced by boundary-layer flow
[NASA-CR-188733] N91-28643
Photoinduced charge and energy transfer processes in molecular aggregates
[DE91-014383] N91-28864

WESTINGHOUSE ELECTRIC CORP., PITTSBURGH, PA.
Development of a current collection loss management system for SDI homopolar power supplies
[DE91-012779] N91-28652

WISCONSIN UNIV., MADISON.
Thermodynamic and kinetic aspects of surface acidity
[DE91-014039] N91-28331
Ordered ceramic membranes
[DE91-012248] N91-28398
System and component design and test of a 10 hp, 18,000 rpm AC dynamometer utilizing a high frequency AC voltage link, part 1
[NASA-CR-188442] N91-28539
Interactions between the north Pacific Ocean and the Northern Hemisphere atmosphere during El Nino N91-28711
Hybrid fluid/kinetic descriptions of tokamak plasmas N91-28888
Fluid/kinetic hybrid moment description of plasmas via a Chapman-Enskog-like approach
[DE91-013346] N91-28949
Fluidlike studies of the presheath and sheath regions of a plasma
[DE91-013345] N91-28953
Nonlinear reversed field pinch dynamics with nonideal boundaries
[DE91-013638] N91-28961
Generalized gyroviscous force and its effect on the momentum balance equation
[DE91-013344] N91-29061
Sawteeth in the MST reversed field pinch
[DE91-014288] N91-29126

WORLD METEOROLOGICAL ORGANIZATION, GENEVA (SWITZERLAND).
Report of Meeting of CLICOM Experts
[WCDP-9] N91-28695

WRIGHT RESEARCH DEVELOPMENT CENTER, WRIGHT-PATTERSON AFB, OH.
Recent developments in the area of aircraft rough field performance N91-28154
Landing gear improvements for transport aircraft N91-28159

Y

YAMAGUCHI UNIV. (JAPAN).
Internal kink mode simulation by 3-D gyrokinetic code N91-28916

CONTRACT NUMBER INDEX

Typical Contract Number Index Listing

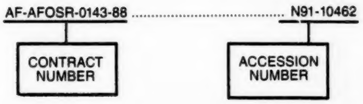

Listings in this index are arranged alphanumerically by contract number. Under each contract number the accession numbers denoting documents that have been produced as a result of research done under that contract are arranged in ascending order. The accession number denotes the number by which the citation is identified.

AEN-90-0033 ..... N91-29113
DAJA45-88-C-0038 ..... N91-28540
DE-AC02-76CH-00016 ..... N91-28318
N91-28370
N91-28494
N91-28495
N91-28569
N91-28606
N91-28660
N91-28854
N91-28866
N91-28870
N91-28874
N91-28994
N91-29031
N91-29039
DE-AC02-76CH-03000 ..... N91-28497
N91-28610
N91-28867
DE-AC02-76CH-03073 ..... N91-28889
N91-28940
DE-AC02-76ER-00881 ..... N91-28996
DE-AC02-76ER-03066 ..... N91-28858
DE-AC02-79ET-10815 ..... N91-28541
DE-AC02-83CH-10093 ..... N91-28429
N91-28480
N91-28650
N91-28656
N91-28658
N91-28663
DE-AC02-89ER-40486 ..... N91-28794
N91-29010
N91-29040
N91-29079
DE-AC03-76SF-00098 ..... N91-28281
N91-28308
N91-28315
N91-28345
N91-28399
N91-28450
N91-28476
N91-28498
N91-28527
N91-28548
N91-28603
N91-28677
N91-28720
N91-28721
N91-28722
N91-28737
N91-28759
N91-28763
N91-28768
N91-28807
N91-28844
N91-28862
N91-28979
N91-28992
N91-28993
N91-28997
N91-28998
N91-29002
N91-29006
N91-29007
N91-29021
N91-29030
N91-29038
N91-29054
N91-29062
N91-29073
N91-29091
N91-29125
N91-29133
DE-AC03-76SF-00515 ..... N91-28552
N91-28792
N91-28796
N91-28798
N91-28828
N91-28834
N91-28856
N91-28869
N91-28996
DE-AC03-83ER-53150 ..... N91-28970
DE-AC03-86SF-16518 ..... N91-28652
DE-AC03-89ER-53277 ..... N91-28973
DE-AC04-76DP-00789 ..... N91-28133
N91-28178
N91-28274
N91-28306
N91-28314
N91-28319
N91-28346
N91-28379
N91-28393
N91-28395
N91-28402
N91-28411
N91-28417
N91-28427
N91-28434
N91-28439
N91-28442
N91-28443
N91-28451
N91-28473
N91-28475
N91-28483
N91-28485
N91-28487
N91-28496
N91-28500
N91-28501
N91-28505
N91-28515
N91-28543
N91-28544
N91-28553
N91-28562
N91-28567
N91-28616
N91-28631
N91-28651
N91-28653
N91-28662
N91-28756
N91-28767
N91-28775
N91-28778
N91-28805
N91-28826
N91-28841
N91-28846
N91-29003
N91-29004
N91-29009
N91-29047
N91-29051
N91-29052
N91-29065
DE-AC04-76DR-00789 ..... N91-28612
DE-AC04-88DP-43495 ..... N91-28395
N91-28800
DE-AC05-76OR-00033 ..... N91-28344
DE-AC05-84OR-21400 ..... N91-28188
N91-28283
N91-28309
N91-28310
N91-28311
N91-28344
N91-28348
N91-28349
N91-28350
N91-28352
N91-28358
N91-28359
N91-28360
N91-28367
N91-28371
N91-28378
N91-28381
N91-28382
N91-28390
N91-28397
N91-28405
N91-28406
N91-28413
N91-28418
N91-28438
N91-28463
N91-28481
N91-28484
N91-28493
N91-28512
N91-28550
N91-28554
N91-28555
N91-28570
N91-28574
N91-28594
N91-28601
N91-28607
N91-28611
N91-28614
N91-28615
N91-28619
N91-28623
N91-28655
N91-28674
N91-28718
N91-28719
N91-28738
N91-28741
N91-28751
N91-28753
N91-28755
N91-28766
N91-28780
N91-28783
N91-28784
N91-28797
N91-28814
N91-28829
N91-28832
N91-28835
N91-28836
N91-28837
N91-28840
N91-28847
N91-28850
N91-28851
N91-28852
N91-28946
N91-28947
N91-28959
N91-28969
N91-29000
N91-29005
N91-29014
N91-29016
N91-29044
DE-AC05-84OT-21400 ..... N91-28355
DE-AC06-76RL-01830 ..... N91-28276
N91-28317
N91-28354
N91-28364
N91-28400
N91-28412

N91-28431
N91-28432
N91-28441
N91-28591
N91-28600
N91-28630
N91-28654
N91-28664
N91-28669
N91-28671
N91-28715
N91-28749
N91-28999
N91-29012
N91-29074
N91-29078
N91-29092
DE-AC07-76ID-01570 .... N91-28187
N91-28279
N91-28282
N91-28356
N91-28362
N91-28380
N91-28437
N91-28491
N91-28510
N91-28575
N91-28595
N91-28732
N91-28750
N91-28764
N91-28795
N91-28951
N91-29068
N91-29077
DE-AC08-88NV-10617 .... N91-28170
N91-28549
N91-29022
N91-29048
DE-AC21-88MC-24221 .... N91-28657
N91-28659
DE-AC21-89MC-25159 .... N91-28875
DE-AC34-90DP-62349 .... N91-28452
N91-28453
DE-AI05-89ER-13992 .... N91-28316
DE-AI08-78ET-44802 .... N91-28645
DE-AM79-86BP-63056 .... N91-28445
DE-AS03-83ER-40120 .... N91-28976
DE-AS07-86ID-12626 .... N91-28398
DE-FC06-87CH-10343 .... N91-29069
DE-FG02-84ER-13183 .... N91-28331
DE-FG02-85ER-13388 .... N91-28723
DE-FG02-85ER-13441 .... N91-28857
DE-FG02-85ER-45205 .... N91-28287
DE-FG02-85ER-53198 .... N91-29126
DE-FG02-85ER-53212 .... N91-28961
DE-FG02-86ER-13560 .... N91-28401
DE-FG02-86ER-13566 .... N91-28350
DE-FG02-86ER-13569 .... N91-28332
DE-FG02-86ER-13619 .... N91-28357
DE-FG02-86ER-40302 .... N91-28798
DE-FG02-86ER-45254 .... N91-29020
DE-FG02-86ER-45262 .... N91-28368
DE-FG02-86ER-45269 .... N91-28328
DE-FG02-86ER-45278 .... N91-29011
DE-FG02-86ER-53218 .... N91-28888
N91-28949
N91-28953
N91-29061
DE-FG02-86ER-53222 .... N91-28895
DE-FG02-86ER-53223 .... N91-28978
DE-FG02-86ER-60485 .... N91-28673
DE-FG02-87ER-13778 .... N91-28863
DE-FG02-87ER-45295 .... N91-28372
DE-FG02-87ER-45298 .... N91-29013
DE-FG02-87ER-45301 .... N91-29043
DE-FG02-87ER-45328 .... N91-28995
DE-FG02-87ER-53244 .... N91-28977
DE-FG02-87ER-60561 .... N91-28728
DE-FG02-88DP-48058 .... N91-29066
N91-29067
N91-29069
N91-29070
N91-29071
N91-29075
N91-29076
DE-FG02-88ER-13879 .... N91-28333
DE-FG02-88ER-13905 .... N91-28440
DE-FG02-88ER-13913 .... N91-28511
DE-FG02-88ER-13944 .... N91-28864
DE-FG02-88ER-25053 .... N91-28142
DE-FG02-88ER-40388 .... N91-28872
DE-FG02-88ER-40456 .... N91-28845
DE-FG02-88ER-45347 .... N91-28848
DE-FG02-88ER-45357 .... N91-29049
DE-FG02-88ER-60631 .... N91-28716
DE-FG02-89CE-90029 .... N91-28508
N91-28509
DE-FG02-89ER-14024 .... N91-28649
DE-FG02-89ER-14028 .... N91-28713
DE-FG02-89ER-14042 .... N91-28576
DE-FG02-89ER-14077 .... N91-29026
DE-FG02-89ER-45396 .... N91-28391
DE-FG02-89ER-45402 .... N91-29041
DE-FG02-90ER-14151 .... N91-28839
DE-FG02-90ER-40606 .... N91-29109
DE-FG02-90ER-45413 .... N91-28383
DE-FG02-90ER-45421 .... N91-28608
DE-FG03-85ER-13317 .... N91-28323
DE-FG03-86ER-13479 .... N91-28320
DE-FG03-86ER-13571 .... N91-28329
DE-FG03-86ER-45279 .... N91-28396
DE-FG03-86ER-53220 .... N91-28984
DE-FG03-87ER-40347 .... N91-28838
DE-FG03-87ER-45288 .... N91-28392
N91-28430
DE-FG03-89ER-60913 .... N91-28717
DE-FG03-89SF-18014 .... N91-28956
DE-FG03-90ER-45435 .... N91-28312
DE-FG05-80ET-53088 .... N91-28963
N91-28964
N91-28965
N91-28972
N91-28974
N91-28982
DE-FG05-86ER-13465 .... N91-28724
DE-FG05-86ER-13487 .... N91-28421
DE-FG05-86ER-13604 .... N91-28409
DE-FG05-86ER-40293 .... N91-28831
DE-FG05-86ER-53221 .... N91-28980
DE-FG05-86ER-53241 .... N91-28945
N91-28950
DE-FG05-87ER-13789 .... N91-28833
DE-FG05-87ER-40361 .... N91-28853
DE-FG05-87ER-45306 .... N91-28433
DE-FG05-88ER-13859 .... N91-28421
N91-28428
DE-FG05-88ER-13977 .... N91-28596
DE-FG05-88ER-25063 .... N91-28754
N91-28757
N91-28779
N91-28782
N91-29080
N91-29089
N91-29090
DE-FG05-89ER-14090 .... N91-28879
DE-FG05-89ER-53295 .... N91-28971
DE-FG05-89ER-53301 .... N91-28981
DE-FG06-86ER-40283 .... N91-28873
DE-FG06-88ER-45352 .... N91-28369
DE-FG06-90ER-54095 .... N91-28967
DE-FG06-90ER-61034 .... N91-29064
DE-FG07-89ER-12889 .... N91-28786
DE-FG22-89PC-89771 .... N91-28327
DTFA03-89-A-00004 .... N91-28146
EPA-68-01-7365 .... N91-28665
N91-28666
F19628-86-K-0034 .... N91-28478
F19628-90-C-0003 .... N91-28742
N91-28743
N91-28744
N91-28748
F30602-88-D-0027 .... N91-28458
NADC PROJ. RS-3-4-A50 .... N91-28343
NAGW-1295 .... N91-29107
NAGW-1321 .... N91-28858
NAGW-1340 .... N91-28858
N91-29108
N91-29109
N91-29110
N91-29112
N91-29113
NAG1-343 .... N91-28292
NAG1-613 .... N91-28747
NAG1-798 .... N91-28502
NAG1-1175 .... N91-28643
NAG2-513 .... N91-28787
NAG3-940 .... N91-28539
NASW-4102 .... N91-28182
NAS1-18531 .... N91-28334
N91-28335
N91-28336
N91-28337
NAS1-18585 .... N91-28138
NAS1-18586 .... N91-28777
NAS1-18599 .... N91-28626
NAS1-18605 .... N91-28806
NAS2-13058 .... N91-28168
NAS3-25266 .... N91-28277
N91-28627
NAS3-25808 .... N91-28648
NAS3-25824 .... N91-28644
NAS8-30490 .... N91-28192
NAS10-11568 .... N91-28198
NCC2-605 .... N91-28503
NSF AST-88-22595 .... N91-28858
N91-29109
NSF CHE-90-16789 .... N91-28820
NSF DMS-89-04740 .... N91-28789
N91-28790
NSF ECS-85-17364 .... N91-28941
NSF INT-89-14643 .... N91-28789
NSF MIP-86-57563 .... N91-28747
NSG-3273 .... N91-28384
N00014-84-K-0367 .... N91-28941
N00014-85-C-0206 .... N91-28280
N00014-86-K-0680 .... N91-28477
N91-28770
N91-28771
N91-28823
N00014-86-K-0688 .... N91-28816
N00014-88-C-0681 .... N91-28986
N00014-88-K-0122 .... N91-28387
N91-28388
N91-28389
N00014-88-K-0482 .... N91-28304
N00014-89-J-1178 .... N91-28985
N00014-89-J-1261 .... N91-28479
N00014-89-J-1601 .... N91-28988
N00014-90-J-1148 .... N91-28385
N91-28386
N00014-90-J-1193 .... N91-28812
N91-28820
N00014-90-J-1530 .... N91-28989
N00014-90-J-1971 .... N91-28821
N91-28822
N00014-90-K-0004 .... N91-28746
N00014-91-J-1096 .... N91-28747
N00014-91-J-1269 .... N91-28987
W-31-109-ENG-38 .... N91-28147
N91-28361
N91-28377
N91-28410
N91-28435
N91-28577
N91-28592
N91-28609
N91-28629
N91-28670
N91-28675
N91-28734
N91-28758
N91-28762
N91-28765
N91-28793
N91-28815
N91-28859
N91-28860
N91-28865
N91-28868
N91-28968
N91-29005
N91-29008
N91-29024
N91-29027
N91-29036
N91-29037
N91-29042
N91-29079
W-7405-ENG-36 .... N91-28173
N91-28174
N91-28177
N91-28179
N91-28288
N91-28324
N91-28325
N91-28366
N91-28376
N91-28414
N91-28415
N91-28419
N91-28420
N91-28443
N91-28448
N91-28456
N91-28457
N91-28464
N91-28474
N91-28486
N91-28488
N91-28492
N91-28499
N91-28513
N91-28528
N91-28545
N91-28556
N91-28558
N91-28563

N91-28564
N91-28565
N91-28566
N91-28593
N91-28613
N91-28617
N91-28618
N91-28620
N91-28621
N91-28624
N91-28625
N91-28632
N91-28633
N91-28634
N91-28635
N91-28636
N91-28637
N91-28661
N91-28714
N91-28725
N91-28799
N91-28809
N91-28810
N91-28849
N91-28855
N91-28861
N91-28871
N91-28975
N91-28983
N91-28990
N91-28991
N91-29015
N91-29023
N91-29025
N91-29028
N91-29029
N91-29033
N91-29034
N91-29035
N91-29045
N91-29046
N91-29050
N91-29055
N91-29058
W-7405-ENG-48 .... N91-28148
N91-28167
N91-28275
N91-28284
N91-28285
N91-28286
N91-28305
N91-28306
N91-28307
N91-28313
N91-28326
N91-28351
N91-28365
N91-28394
N91-28408
N91-28422
N91-28436
N91-28447
N91-28462
N91-28467
N91-28489
N91-28506
N91-28542
N91-28551
N91-28559
N91-28560
N91-28561
N91-28568
N91-28571
N91-28599
N91-28602
N91-28628
N91-28672
N91-28700
N91-28712
N91-28772
N91-28774
N91-28781
N91-28824
N91-28825
N91-28827
N91-28876
N91-28877
N91-28944
N91-28948
N91-28952
N91-28954
N91-28955
N91-28958
N91-28960
N91-28962
N91-28966
N91-28984
N91-29053
N91-29063
W-7405-ENG-82 .... N91-28291
N91-28347
N91-28353
N91-28407
N91-28773
N91-28843
N91-29001
326-81-10 .... N91-28278
432-06-51 .... N91-28134
474-42-10 .... N91-28776
505-13-00 .... N91-28644
505-59-85-01 .... N91-28138
505-61-21-03 .... N91-28143
505-63-1B N91-28627
505-63-50-02 .... N91-28334
505-63-50-04 .... N91-28293
N91-28626
505-63-50-16 .... N91-28137
505-64-10-07 .... N91-28777
505-80-21 .... N91-28136
505-90-52-01 .... N91-28806
506-48-21 .... N91-28538
509-10-02-03 .... N91-28131
N91-28132
510-01-1A N91-28605
510-02-13-01 .... N91-28373
535-03-01 .... N91-28627
553-13-00 .... N91-28622
591-14-11 .... N91-28277
593-31-1A N91-29138
763-22-21 .... N91-28449

REPORT/ACCESSION NUMBER INDEX

Typical Report Number Index Listing

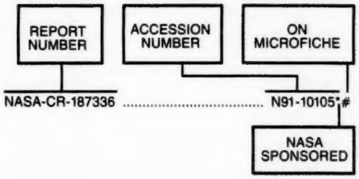
REPORT NUMBER
ACCESSION NUMBER
ON MICROFICHE
NASA-CR-187336 .... N91-10105*#
NASA SPONSORED

Listings in this index are arranged alphanumerically by report number. The accession number denotes the number by which the citation is identified. An asterisk (*) indicates that the item is a NASA report. A pound sign (#) indicates that the item is available on microfiche.

A-90316 N91-28134* #
A-91215 N91-28168* #

AD-A231022 N91-28985 #
AD-A231114 N91-28820 #
AD-A235855 N91-28385 #
AD-A235856 N91-28386 #
AD-A235874 N91-28731 #
AD-A236121 N91-28742 #
AD-A236132 N91-28821 #
AD-A236139 N91-28743 #
AD-A236140 N91-28744 #
AD-A236143 N91-28540 #
AD-A236148 N91-28745 #
AD-A236149 N91-28822 #
AD-A236151 N91-28986 #
AD-A236490 N91-28181 #
AD-A236596 N91-28987 #
AD-A236597 N91-28746 #
AD-A236598 N91-28823 #
AD-A236600 N91-28343 #
AD-A236601 N91-28747* #
AD-A236605 N91-28696 #
AD-A236629 N91-28477 #
AD-A236630 N91-28770 #
AD-A236632 N91-28771 #
AD-A236633 N91-28812 #
AD-A236635 N91-28707 #
AD-A236637 N91-28988 #
AD-A236638 N91-28280 #
AD-A236639 N91-28504 #
AD-A236730 N91-28989 #
AD-A236795 N91-28478 #
AD-A236999 N91-28387 #
AD-A237000 N91-29072 #
AD-A237001 N91-28388 #
AD-A237012 N91-28458 #
AD-A237013 N91-28389 #
AD-A237021 N91-28304 #
AD-A237023 N91-28479 #
AD-A237025 N91-28791 #
AD-A237028 N91-28273 #
AD-A237030 N91-28459 #
AD-A237034 N91-28816 #
AD-A237049 N91-28748 #
AD-A237056 N91-28460 #
AD-A237057 N91-28461 #

AGARD-AG-330 N91-28465 #

AGARD-CP-484 N91-28150 #

AIAA-PAPER-91-1107 N91-28132* #

AIAA-91-3433 N91-28605* #
AIAA-91-3462 N91-29138* #
AIAA-91-3541 N91-28538* #
AIAA-91-3550 N91-28449* #

ANL-HEP-CP-90-124 N91-28860 #
ANL-HEP-CP-91-28 N91-28793 #

ANL-HEP-TR-91-05 N91-28868 #

ANL-91/16 N91-28734 #

ANL/CP-70872 N91-28361 #
ANL/CP-71294 N91-28147 #
ANL/CP-71926 N91-28435 #
ANL/CP-71950 N91-28670 #
ANL/CP-71981 N91-28815 #
ANL/CP-72199 N91-29008 #
ANL/CP-72210 N91-29027 #
ANL/CP-72362 N91-28577 #
ANL/CP-72369 N91-28968 #
ANL/CP-72538 N91-28609 #
ANL/CP-72570 N91-28765 #
ANL/CP-72655 N91-29024 #
ANL/CP-73103 N91-29005 #
ANL/CP-73132 N91-28592 #
ANL/CP-73152 N91-28410 #
ANL/CP-73154 N91-28762 #
ANL/CP-73158 N91-29042 #
ANL/CP-73159 N91-29037 #
ANL/CP-73203 N91-29036 #
ANL/CP-73224 N91-28758 #
ANL/CP-73246 N91-28629 #
ANL/CP-73275 N91-28859 #
ANL/CP-73338 N91-28377 #
ANL/CP-73422 N91-28865 #

ANL/EAIS/TM-48 N91-28675 #

ARA-5589 N91-28644* #

ARFSD-TR-91006 N91-28696 #

AVSCOM-TR-91-B-010-PT-1 N91-28293* #

BNL-NUREG-45835 N91-28606 #

BNL-44556 N91-28994 #
BNL-45331 N91-28318 #
BNL-45387 N91-28870 #
BNL-45435 N91-28494 #
BNL-45513 N91-28495 #
BNL-45541 N91-28370 #
BNL-45998 N91-28660 #
BNL-46112 N91-28854 #
BNL-46161 N91-29031 #
BNL-46178 N91-29039 #
BNL-46191 N91-28569 #
BNL-46271 N91-28874 #
BNL-46293 N91-28866 #

BP-625 N91-28575 #

CCMS-91-16 N91-28292* #

CERC-91-1 N91-28707 #

CERN-90-09 N91-28813 #

CESAR-91/07 N91-28784 #

CMU-HEP91-08 N91-28858* #

CMU/SEI-SM-8-1-0 N91-28742 #

CMU/SEI-90-TR-22 N91-28748 #

CONF-900214-4 N91-29090 #
CONF-900402-14 N91-28433 #
CONF-900556-2 N91-28719 #
CONF-900726-6 N91-28842 #
CONF-900765-2 N91-28765 #
CONF-900823-13 N91-28677 #
CONF-900944-45 N91-28994 #
CONF-900944-46 N91-29021 #
CONF-900944-47 N91-28998 #
CONF-900944-48 N91-29007 #
CONF-901007-68 N91-28951 #
CONF-901105-124 N91-28400 #
CONF-901105-127 N91-29038 #
CONF-901141-5 N91-29054 #
CONF-901169-7 N91-28997 #
CONF-901219-16 N91-28954 #
CONF-901246-4 N91-29055 #
CONF-901291-2 N91-28854 #
CONF-910123-32 N91-28561 #
CONF-910123-33 N91-28958 #
CONF-910145-4 N91-29014 #
CONF-910145-5 N91-29031 #
CONF-910162-7 N91-28288 #
CONF-910190-4 N91-29005 #
CONF-910202-16 N91-28345 #
CONF-910202-17 N91-28419 #
CONF-910202-18 N91-28362 #
CONF-910229-3 N91-28828 #
CONF-910247-2 N91-28955 #
CONF-910291-3 N91-28395 #
CONF-910326-4 N91-28797 #
CONF-910326-5 N91-28755 #
CONF-910340-10 N91-28993 #
CONF-910340-13 N91-28610 #
CONF-910340-31 N91-29010 #
CONF-910340-36 N91-29079 #
CONF-910340-42 N91-28370 #
CONF-910373-7 N91-29073 #
CONF-910373-11 N91-28737 #
CONF-910373-13 N91-28763 #
CONF-910379-1 N91-28595 #
CONF-910399-3 N91-28307 #
CONF-910402-16 N91-28999 #
CONF-910406-4 N91-28393 #
CONF-910406-10 N91-28402 #
CONF-910406-11 N91-29012 #
CONF-910406-12 N91-29015 #
CONF-910406-13 N91-28451 #
CONF-910406-14 N91-28427 #
CONF-910406-15 N91-29029 #
CONF-910406-16 N91-29028 #
CONF-910406-18 N91-29037 #
CONF-910406-19 N91-28377 #
CONF-910406-20 N91-29047 #
CONF-910406-21 N91-28630 #
CONF-910406-22 N91-28979 #
CONF-910406-23 N91-29044 #
CONF-910406-25 N91-29051 #
CONF-910410-1 N91-29042 #
CONF-910414-36 N91-28795 #
CONF-910427-3 N91-28874 #
CONF-910430-3 N91-28397 #
CONF-910430-4 N91-28417 #
CONF-910430-9 N91-28413 #
CONF-910430-10 N91-28415 #
CONF-910430-11 N91-28414 #
CONF-910430-13 N91-28435 #
CONF-910430-15 N91-28571 #
CONF-910434-4 N91-29074 #
CONF-910450-11 N91-28148 #
CONF-910450-12 N91-28170 #
CONF-910456-1 N91-28276 #
CONF-910503-21 N91-28861 #
CONF-910503-24 N91-28962 #
CONF-910505-56 N91-28826 #
CONF-910505-71 N91-28552 #
CONF-910505-80 N91-28792 #
CONF-910505-84 N91-28996 #
CONF-910505-88 N91-28834 #
CONF-910505-94 N91-28796 #
CONF-910505-95 N91-28869 #
CONF-910505-104 N91-28798 #
CONF-910505-107 N91-28799 #
CONF-910505-122 N91-28867 #
CONF-910505-137 N91-28870 #
CONF-910505-149 N91-28488 #
CONF-910505-150 N91-28486 #
CONF-910505-154 N91-28558 #
CONF-910505-159 N91-28492 #
CONF-910505-172 N91-28564 #
CONF-910505-174 N91-28871 #
CONF-910505-178 N91-28489 #
CONF-910505-186 N91-28565 #
CONF-910505-191 N91-28629 #
CONF-910505-222 N91-28474 #
CONF-910505-227 N91-28563 #
CONF-910505-230 N91-28566 #

CONF-910505-233 .... N91-29039 #
CONF-910505-235 .... N91-28568 #
CONF-910505-238 .... N91-28495 #
CONF-910505-245 .... N91-28494 #
CONF-910505-256 .... N91-29040 #
CONF-910505-295 .... N91-28807 #
CONF-910505-323-REV .... N91-28476 #
CONF-910505-329 .... N91-28569 #
CONF-910552-10 .... N91-29004 #
CONF-910552-11 .... N91-28434 #
CONF-910555-1 .... N91-28670 #
CONF-910568-2 .... N91-28654 #
CONF-910591-2 .... N91-28354 #
CONF-910595-11 .... N91-28560 #
CONF-910602-34 .... N91-28609 #
CONF-910602-42 .... N91-28616 #
CONF-910602-45 .... N91-28361 #
CONF-910602-46 .... N91-28437 #
CONF-910608-3 .... N91-29008 #
CONF-910608-4 .... N91-28366 #
CONF-910608-5 .... N91-28815 #
CONF-910608-6 .... N91-29045 #
CONF-910614-4 .... N91-28380 #
CONF-910617-2 .... N91-28577 #
CONF-910623-1 .... N91-29009 #
CONF-910624-1 .... N91-28619 #
CONF-910624-2 .... N91-28346 #
CONF-910624-3 .... N91-28623 #
CONF-910640-16 .... N91-28983 #
CONF-910640-18 .... N91-28499 #
CONF-910654-2 .... N91-28411 #
CONF-910659 .... N91-28147 #
CONF-910706-3 .... N91-29033 #
CONF-910706-5 .... N91-29046 #
CONF-910731-2-REV-1 .... N91-28285 #
CONF-910731-3 .... N91-28286 #
CONF-910736-1 .... N91-29050 #
CONF-910736-4 .... N91-29052 #
CONF-910739-11 .... N91-29053 #
CONF-910739-14 .... N91-28509 #
CONF-910739-18 .... N91-28527 #
CONF-910751-9 .... N91-28549 #
CONF-910784-2 .... N91-28741 #
CONF-910801-1 .... N91-28483 #
CONF-910801-2 .... N91-28487 #
CONF-910801-5 .... N91-28661 #
CONF-910801-6 .... N91-28279 #
CONF-910802-1 .... N91-28650 #
CONF-910808-1 .... N91-28352 #
CONF-910808-3 .... N91-28371 #
CONF-910812-1 .... N91-28390 #
CONF-910812-3 .... N91-28408 #
CONF-910812-4 .... N91-28438 #
CONF-910817-3 .... N91-28349 #
CONF-910817-6 .... N91-28606 #
CONF-910817-10 .... N91-28607 #
CONF-910817-11 .... N91-28614 #
CONF-910817-12-PT-1 .... N91-28615 #
CONF-910817-13-PT-2 .... N91-28350 #
CONF-910847-1 .... N91-28274 #
CONF-910854-2 .... N91-28406 #
CONF-910858-1 .... N91-28774 #
CONF-910861-1 .... N91-28541 #
CONF-910863-1 .... N91-28505 #
CONF-910870-2 .... N91-28344 #
CONF-910870-3 .... N91-28840 #
CONF-910870-4 .... N91-28405 #
CONF-910870-12 .... N91-29003 #
CONF-910870-13 .... N91-28379 #
CONF-910870-14 .... N91-28841 #
CONF-910870-15 .... N91-28548 #
CONF-910870-16 .... N91-28862 #
CONF-910871-1 .... N91-28574 #
CONF-910872-2 .... N91-28351 #
CONF-910872-4 .... N91-28544 #
CONF-910872-5 .... N91-28379 #
CONF-910872-6 .... N91-28841 #
CONF-910888-1 .... N91-28314 #
CONF-910909-1-DRAFT .... N91-28378 #
CONF-910909-2 .... N91-28594 #
CONF-910909-5 .... N91-28187 #
CONF-910909-7 .... N91-28382 #
CONF-910936-1 .... N91-28497 #
CONF-910957-1 .... N91-28457 #
CONF-9002163-2 .... N91-28714 #
CONF-9006220-8 .... N91-29133 #
CONF-9006220-9 .... N91-28720 #
CONF-9006220-10 .... N91-28721 #
CONF-9006333-1 .... N91-28576 #
CONF-9007211-1 .... N91-28356 #
CONF-9008139-4 .... N91-28651 #
CONF-9008139-5 .... N91-28653 #
CONF-9008187-SUMM .... N91-29002 #
CONF-9008209-1 .... N91-28786 #
CONF-9009381-1 .... N91-28463 #
CONF-9009382-1 .... N91-28315 #
CONF-9009383-1 .... N91-28308 #
CONF-9010155-5 .... N91-28732 #
CONF-9010232-3 .... N91-28462 #
CONF-9010283-7 .... N91-28860 #
CONF-9010364-1 .... N91-28452 #
CONF-9011149-16 .... N91-29063 #
CONF-9101101-1 .... N91-28793 #
CONF-9101102-1 .... N91-28592 #
CONF-9102109-2 .... N91-28824 #
CONF-9102117-1 .... N91-28805 #
CONF-9103109-VOL-1 .... N91-28658 #
CONF-9103109-VOL-2 .... N91-28656 #
CONF-9103130-2 .... N91-28624 #
CONF-9103130-3 .... N91-28632 #
CONF-9103134-4 .... N91-28825 #
CONF-9103136-6 .... N91-28762 #
CONF-9103146-3 .... N91-28844 #
CONF-9103172-2 .... N91-28645 #
CONF-9103176-1 .... N91-28853 #
CONF-9103180-1 .... N91-28856 #
CONF-9104111-2 .... N91-28600 #
CONF-9104158-2 .... N91-28749 #
CONF-9104158-3 .... N91-28753 #
CONF-9104164-3 .... N91-28551 #
CONF-9104164-5 .... N91-28556 #
CONF-9104187-3 .... N91-28944 #
CONF-9104192-5 .... N91-28554 #
CONF-9104192-6 .... N91-28959 #
CONF-9104192-7 .... N91-28852 #
CONF-9104192-8 .... N91-28555 #
CONF-9104192-9 .... N91-28493 #
CONF-9104201-1 .... N91-28601 #
CONF-9104203-2 .... N91-28877 #
CONF-9104206-3 .... N91-28394 #
CONF-9104231-2 .... N91-28542 #
CONF-9104232-1 .... N91-28173 #
CONF-9104234-1 .... N91-28992 #
CONF-9104234-3 .... N91-28991 #
CONF-9104236-1 .... N91-28990 #
CONF-9104244-1 .... N91-28876 #
CONF-9104245-1 .... N91-28712 #
CONF-9104248-1 .... N91-28832 #
CONF-9104261-4 .... N91-28431 #
CONF-9104261-5 .... N91-28432 #
CONF-9104262-1 .... N91-29025 #
CONF-9104264-1 .... N91-28422 #
CONF-9104265-1 .... N91-28756 #
CONF-9104267-1 .... N91-28766 #
CONF-9104269-1-VUGRAPHS .... N91-28448 #
CONF-9104272-1 .... N91-28498 #
CONF-9105106-3 .... N91-28849 #
CONF-9105116-2 .... N91-28783 #
CONF-9105130-1 .... N91-28348 #
CONF-9105130-2 .... N91-29027 #
CONF-9105130-3 .... N91-29024 #
CONF-9105133-1 .... N91-28814 #
CONF-9105144-2 .... N91-28827 #
CONF-9105151-1 .... N91-29000 #
CONF-9105151-2 .... N91-29058 #
CONF-9105151-3 .... N91-29036 #
CONF-9105151-4 .... N91-29034 #
CONF-9105151-5 .... N91-29035 #
CONF-9105151-7 .... N91-28866 #
CONF-9105166-3 .... N91-28284 #
CONF-9105166-4 .... N91-28306 #
CONF-9105166-5 .... N91-28599 #
CONF-9105167-2 .... N91-29068 #
CONF-9105172-1 .... N91-28846 #
CONF-9105174-1 .... N91-28484 #
CONF-9105177-1 .... N91-28275 #
CONF-9105180-1 .... N91-28847 #
CONF-9105181-1 .... N91-28310 #
CONF-9105181-2 .... N91-28835 #
CONF-9105181-4-EXTD-ABST .... N91-28836 #
CONF-9105181-6 .... N91-28309 #
CONF-9105181-11-EXTD-ABST .... N91-28850 #
CONF-9105181-15 .... N91-28326 #
CONF-9105182-2 .... N91-28376 #
CONF-9105184-1 .... N91-28410 #
CONF-9105184-2 .... N91-28360 #
CONF-9105184-3 .... N91-28317 #
CONF-9105184-4 .... N91-28412 #
CONF-9105184-6 .... N91-28367 #
CONF-9105184-7 .... N91-28381 #
CONF-9105188-1 .... N91-28611 #
CONF-9105189-1 .... N91-28347 #
CONF-9105189-2 .... N91-28364 #
CONF-9105190-1 .... N91-28837 #
CONF-9105197-1 .... N91-28715 #
CONF-9105199-1 .... N91-29078 #
CONF-9105200-1 .... N91-28859 #
CONF-9105202-1 .... N91-28975 #
CONF-9105202-3 .... N91-28513 #
CONF-9105202-4 .... N91-28671 #
CONF-9105202-5 .... N91-28969 #
CONF-9105204-1 .... N91-28855 #
CONF-9105206-1 .... N91-28669 #
CONF-9105215-1 .... N91-28779 #
CONF-9105217-1 .... N91-28758 #
CONF-9105222-1 .... N91-28865 #
CONF-9105223-1 .... N91-28664 #
CONF-9106106-1 .... N91-28968 #
CONF-9106118-3 .... N91-28473 #
CONF-9106178-2 .... N91-28946 #
CONF-9106179-2 .... N91-28775 #
CONF-9106183-1 .... N91-28319 #
CONF-9106184-1 .... N91-28453 #
CONF-9106187-1 .... N91-28442 #
CONF-9106187-2 .... N91-28467 #
CONF-9106188-1 .... N91-28481 #
CONF-9106189-1 .... N91-28311 #
CONF-9106191-1 .... N91-29077 #
CONF-9106191-2 .... N91-28750 #
CONF-9106192-1 .... N91-28718 #
CONF-9106193-1 .... N91-28456 #
CONF-9106195-1 .... N91-28655 #
CONF-9106196-1 .... N91-28851 #
CONF-9106202-1 .... N91-28591 #
CONF-9106209-2 .... N91-28973 #
CONF-9106211-1 .... N91-29092 #
CONF-9106213-ABSTS .... N91-28663 #
CONF-9106214-1 .... N91-28550 #
CONF-9106222-2 .... N91-28528 #
CONF-9106224-1 .... N91-28501 #
CONF-9106225-1 .... N91-28725 #
CONF-9106226-1 .... N91-29125 #
CONF-9107104-4 .... N91-28318 #
CONF-9107105-3 .... N91-28313 #
CONF-9107105-6 .... N91-28617 #
CONF-9107105-7 .... N91-28324 #
CONF-9107105-8 .... N91-28174 #
CONF-9107105-9 .... N91-28325 #
CONF-9107105-10 .... N91-28613 #
CONF-9107105-11 .... N91-29023 #
CONF-9107105-12 .... N91-28618 #
CONF-9107105-13 .... N91-28420 #
CONF-9107105-14 .... N91-28443 #
CONF-9107105-15 .... N91-28545 #
CONF-9107105-16 .... N91-28621 #
CONF-9107105-19 .... N91-28562 #
CONF-9107105-20 .... N91-28177 #
CONF-9107105-22 .... N91-28447 #
CONF-9107105-23 .... N91-28625 #
CONF-9107105-24 .... N91-28365 #
CONF-9107105-25 .... N91-28628 #
CONF-9107105-27 .... N91-28631 #
CONF-9107105-28 .... N91-28567 #
CONF-9107105-30 .... N91-28439 #
CONF-9107105-32 .... N91-28634 #
CONF-9107105-34 .... N91-28635 #
CONF-9107105-37 .... N91-28633 #
CONF-9107105-40 .... N91-28636 #
CONF-9107105-43 .... N91-28179 #
CONF-9107105-46 .... N91-28637 #
CONF-9107113-1 .... N91-28418* #
CONF-9107114-1 .... N91-28700 #
CONF-9107115-3 .... N91-29048 #
CONF-9107131-1 .... N91-28778 #
CONF-9109135-1 .... N91-28768 #
CONF-9109137-1 .... N91-28781 #
CONF-9109167-1 .... N91-28450 #
CONF-9109190-1 .... N91-29091 #

COO-4974-13 .... N91-28857 #

CR-R-90026 .... N91-28146 #

CRHC-91-16 .... N91-28747* #

DE90-009700 .... N91-28657 #
DE91-002064 .... N91-28875 #
DE91-002136 .... N91-28650 #
DE91-002138 .... N91-28480 #
DE91-002163 .... N91-28658 #
DE91-002165 .... N91-28663 #
DE91-002189 .... N91-28429 #
DE91-006267 .... N91-28274 #
DE91-008067 .... N91-28774 #
DE91-008588 .... N91-28457 #
DE91-008881 .... N91-28349 #
DE91-008890 .... N91-28390 #
DE91-009056 .... N91-28541 #
DE91-009178 .... N91-28505 #
DE91-009437 .... N91-28606 #
DE91-009553 .... N91-28594 #
DE91-009555 .... N91-28378 #
DE91-009559 .... N91-28741 #
DE91-009753 .... N91-29053 #
DE91-009913 .... N91-28344 #
DE91-009920 .... N91-28614 #
DE91-009923 .... N91-28405 #
DE91-009924 .... N91-28840 #

DE91-009930 .... N91-28607 #
DE91-010190 .... N91-28608 #
DE91-010257 .... N91-28391 #
DE91-010393 .... N91-28574 #
DE91-010732 .... N91-28576 #
DE91-011000 .... N91-28392 #
DE91-011097 .... N91-28615 #
DE91-011100 .... N91-28350 #
DE91-011117 .... N91-28351 #
DE91-011189 .... N91-28824 #
DE91-011193 .... N91-28542 #
DE91-011373 .... N91-28406 #
DE91-011398 .... N91-28173 #
DE91-011405 .... N91-28990 #
DE91-011436 .... N91-28991 #
DE91-011480 .... N91-28313 #
DE91-011493 .... N91-28319 #
DE91-011496 .... N91-28393 #
DE91-011500 .... N91-28314 #
DE91-011503 .... N91-28379 #
DE91-011507 .... N91-28305 #
DE91-011511 .... N91-28944 #
DE91-011537 .... N91-28781 #
DE91-011545 .... N91-28306 #
DE91-011825 .... N91-28768 #
DE91-011830 .... N91-28992 #
DE91-011845 .... N91-28609 #
DE91-011871 .... N91-28284 #
DE91-011873 .... N91-29073 #
DE91-011874 .... N91-28677 #
DE91-011883 .... N91-29002 #
DE91-011885 .... N91-28345 #
DE91-011886 .... N91-28993 #
DE91-011913 .... N91-28452 #
DE91-011915 .... N91-28453 #
DE91-011917 .... N91-28825 #
DE91-011923 .... N91-28307 #
DE91-011924 .... N91-28286 #
DE91-011925 .... N91-28285 #
DE91-011927 .... N91-28394 #
DE91-011929 .... N91-28876 #
DE91-011930 .... N91-28599 #
DE91-011934 .... N91-28462 #
DE91-011949 .... N91-29003 #
DE91-011956 .... N91-28442 #
DE91-011957 .... N91-28846 #
DE91-011958 .... N91-29004 #
DE91-012008 .... N91-28483 #
DE91-012011 .... N91-28544 #
DE91-012012 .... N91-28395 #
DE91-012015 .... N91-28346 #
DE91-012018 .... N91-28841 #
DE91-012019 .... N91-28826 #
DE91-012021 .... N91-28407 #
DE91-012033 .... N91-28275 #
DE91-012034 .... N91-28827 #
DE91-012037 .... N91-28712 #
DE91-012052 .... N91-28601 #
DE91-012063 .... N91-28484 #
DE91-012072 .... N91-28619 #
DE91-012083 .... N91-28551 #
DE91-012084 .... N91-28408 #
DE91-012102 .... N91-28133 #
DE91-012106 .... N91-28772 #
DE91-012113 .... N91-28828 #
DE91-012129 .... N91-28441 #
DE91-012131 .... N91-28485 #
DE91-012135 .... N91-28829 #
DE91-012144 .... N91-28409 #
DE91-012147 .... N91-28830 #
DE91-012151 .... N91-28508 #
DE91-012165 .... N91-28831 #
DE91-012169 .... N91-29020 #
DE91-012186 .... N91-28396 #
DE91-012217 .... N91-28847 #
DE91-012218 .... N91-29005 #
DE91-012219 .... N91-28397 #
DE91-012220 .... N91-28352 #
DE91-012221 .... N91-28832 #
DE91-012224 .... N91-28438 #
DE91-012228 .... N91-28463 #
DE91-012241 .... N91-28994 #
DE91-012242 .... N91-28509 #
DE91-012243 .... N91-28659 #
DE91-012248 .... N91-28398 #
DE91-012277 .... N91-28995 #
DE91-012284 .... N91-28848 #
DE91-012299 .... N91-28833 #
DE91-012315 .... N91-28834 #
DE91-012319 .... N91-28996 #
DE91-012323 .... N91-28792 #
DE91-012336 .... N91-29133 #
DE91-012337 .... N91-28399 #
DE91-012339 .... N91-28868 #
DE91-012340 .... N91-28997 #
DE91-012342 .... N91-28315 #
DE91-012344 .... N91-29006 #
DE91-012345 .... N91-28308 #
DE91-012346 .... N91-29054 #
DE91-012350 .... N91-28998 #
DE91-012352 .... N91-29021 #
DE91-012357 .... N91-28281 #
DE91-012361 .... N91-28737 #
DE91-012363 .... N91-29007 #
DE91-012368 .... N91-28543 #
DE91-012370 .... N91-28738 #
DE91-012387 .... N91-28552 #
DE91-012396 .... N91-28945 #
DE91-012397 .... N91-28950 #
DE91-012402 .... N91-28464 #
DE91-012414 .... N91-29069 #
DE91-012416 .... N91-29075 #
DE91-012420 .... N91-29070 #
DE91-012421 .... N91-29066 #
DE91-012425 .... N91-29071 #
DE91-012427 .... N91-29067 #
DE91-012428 .... N91-29076 #
DE91-012471 .... N91-28410 #
DE91-012472 .... N91-29008 #
DE91-012481 .... N91-28793 #
DE91-012485 .... N91-28999 #
DE91-012486 .... N91-28749 #
DE91-012490 .... N91-28610 #
DE91-012491 .... N91-29074 #
DE91-012506 .... N91-28835 #
DE91-012513 .... N91-28309 #
DE91-012516 .... N91-28946 #
DE91-012519 .... N91-28836 #
DE91-012520 .... N91-28481 #
DE91-012521 .... N91-28809 #
DE91-012522 .... N91-28310 #
DE91-012526 .... N91-28311 #
DE91-012527 .... N91-28783 #
DE91-012529 .... N91-28360 #
DE91-012530 .... N91-29000 #
DE91-012537 .... N91-28611 #
DE91-012544 .... N91-28837 #
DE91-012550 .... N91-28506 #
DE91-012552 .... N91-28794 #
DE91-012561 .... N91-28877 #
DE91-012608 .... N91-28400 #
DE91-012610 .... N91-28276 #
DE91-012627 .... N91-28773 #
DE91-012629 .... N91-28347 #
DE91-012630 .... N91-28188 #
DE91-012636 .... N91-28553 #
DE91-012638 .... N91-28842 #
DE91-012642 .... N91-28401 #
DE91-012643 .... N91-28600 #
DE91-012647 .... N91-28417 #
DE91-012651 .... N91-29009 #
DE91-012652 .... N91-28775 #
DE91-012653 .... N91-28651 #
DE91-012654 .... N91-28616 #
DE91-012655 .... N91-28402 #
DE91-012656 .... N91-28805 #
DE91-012660 .... N91-28316 #
DE91-012661 .... N91-28323 #
DE91-012669 .... N91-28649 #
DE91-012677 .... N91-28843 #
DE91-012678 .... N91-28353 #
DE91-012679 .... N91-29001 #
DE91-012707 .... N91-29010 #
DE91-012713 .... N91-28713 #
DE91-012714 .... N91-28287 #
DE91-012720 .... N91-28838 #
DE91-012734 .... N91-28951 #
DE91-012736 .... N91-28354 #
DE91-012743 .... N91-28491 #
DE91-012745 .... N91-28355 #
DE91-012746 .... N91-29011 #
DE91-012768 .... N91-28282 #
DE91-012776 .... N91-28148 #
DE91-012779 .... N91-28652 #
DE91-012781 .... N91-28320 #
DE91-012782 .... N91-28312 #
DE91-012797 .... N91-28954 #
DE91-012807 .... N91-28510 #
DE91-012808 .... N91-28356 #
DE91-012812 .... N91-29077 #
DE91-012815 .... N91-28795 #
DE91-012817 .... N91-29068 #
DE91-012818 .... N91-28750 #
DE91-012860 .... N91-28844 #
DE91-012864 .... N91-28487 #
DE91-012865 .... N91-28653 #
DE91-012867 .... N91-28411 #
DE91-012871 .... N91-29012 #
DE91-012873 .... N91-28654 #
DE91-012883 .... N91-28716 #
DE91-012885 .... N91-28955 #
DE91-012894 .... N91-28717 #
DE91-012911 .... N91-28869 #
DE91-012912 .... N91-28796 #
DE91-012922 .... N91-28317 #
DE91-012926 .... N91-28412 #
DE91-012927 .... N91-28715 #
DE91-012930 .... N91-28364 #
DE91-012945 .... N91-28554 #
DE91-012948 .... N91-28797 #
DE91-012950 .... N91-28348 #
DE91-012954 .... N91-28853 #
DE91-012955 .... N91-28413 #
DE91-012961 .... N91-28418* #
DE91-012965 .... N91-28798 #
DE91-012981 .... N91-28947 #
DE91-012987 .... N91-28800 #
DE91-012989 .... N91-28734 #
DE91-012990 .... N91-28810 #
DE91-012997 .... N91-28784 #
DE91-012998 .... N91-28512 #
DE91-013004 .... N91-28575 #
DE91-013006 .... N91-29013 #
DE91-013008 .... N91-28511 #
DE91-013010 .... N91-28357 #
DE91-013016 .... N91-29026 #
DE91-013024 .... N91-28845 #
DE91-013027 .... N91-28283 #
DE91-013028 .... N91-28358 #
DE91-013031 .... N91-28617 #
DE91-013045 .... N91-28799 #
DE91-013046 .... N91-28486 #
DE91-013049 .... N91-28488 #
DE91-013054 .... N91-28170 #
DE91-013057 .... N91-28655 #
DE91-013066 .... N91-28558 #
DE91-013068 .... N91-28849 #
DE91-013070 .... N91-28492 #
DE91-013074 .... N91-28288 #
DE91-013075 .... N91-28324 #
DE91-013076 .... N91-29055 #
DE91-013077 .... N91-28545 #
DE91-013105 .... N91-28645 #
DE91-013108 .... N91-29022 #
DE91-013111 .... N91-28514 #
DE91-013113 .... N91-28573 #
DE91-013128 .... N91-28952 #
DE91-013130 .... N91-28559 #
DE91-013131 .... N91-28948 #
DE91-013132 .... N91-28612 #
DE91-013147 .... N91-28751 #
DE91-013154 .... N91-28839 #
DE91-013202 .... N91-28867 #
DE91-013204 .... N91-28325 #
DE91-013218 .... N91-28732 #
DE91-013222 .... N91-29078 #
DE91-013228 .... N91-28174 #
DE91-013229 .... N91-28443 #
DE91-013232 .... N91-28718 #
DE91-013233 .... N91-28753 #
DE91-013237 .... N91-29014 #
DE91-013242 .... N91-28560 #
DE91-013245 .... N91-28958 #
DE91-013246 .... N91-28561 #
DE91-013248 .... N91-28700 #
DE91-013250 .... N91-28467 #
DE91-013261 .... N91-28451 #
DE91-013262 .... N91-28427 #
DE91-013268 .... N91-28359 #
DE91-013308 .... N91-28613 #
DE91-013311 .... N91-28414 #
DE91-013312 .... N91-28415 #
DE91-013328 .... N91-28870 #
DE91-013333 .... N91-28854 #
DE91-013336 .... N91-28318 #
DE91-013344 .... N91-29061 #
DE91-013345 .... N91-28953 #
DE91-013346 .... N91-28949 #
DE91-013349 .... N91-28620 #
DE91-013352 .... N91-28859 #
DE91-013353 .... N91-29027 #
DE91-013370 .... N91-28618 #
DE91-013374 .... N91-28456 #
DE91-013375 .... N91-28621 #
DE91-013381 .... N91-29023 #
DE91-013383 .... N91-29058 #
DE91-013385 .... N91-28419 #
DE91-013386 .... N91-28975 #
DE91-013387 .... N91-29015 #
DE91-013389 .... N91-28420 #
DE91-013391 .... N91-28513 #
DE91-013392 .... N91-28855 #
DE91-013402 .... N91-29079 #
DE91-013404 .... N91-28860 #
DE91-013405 .... N91-29024 #
DE91-013410 .... N91-28623 #
DE91-013412 .... N91-28850 #
DE91-013414 .... N91-28851 #

DE91-013415 N91-28852 #
DE91-013416 N91-28555 #
DE91-013425 N91-28959 #
DE91-013427 N91-28445 #
DE91-013462 N91-28602 #
DE91-013479 N91-28960 #
DE91-013494 N91-28624 #
DE91-013496 N91-28177 #
DE91-013497 N91-28556 #
DE91-013499 N91-28871 #
DE91-013501 N91-28564 #
DE91-013503 N91-28562 #
DE91-013520 N91-29025 #
DE91-013527 N91-28421 #
DE91-013528 N91-28428 #
DE91-013547 N91-29016 #
DE91-013565 N91-28447 #
DE91-013566 N91-29063 #
DE91-013567 N91-28422 #
DE91-013568 N91-28489 #
DE91-013571 N91-28473 #
DE91-013576 N91-28631 #
DE91-013584 N91-28365 #
DE91-013585 N91-28326 #
DE91-013586 N91-28628 #
DE91-013603 N91-28167 #
DE91-013611 N91-28629 #
DE91-013615 N91-28762 #
DE91-013638 N91-28961 #
DE91-013640 N91-28863 #
DE91-013641 N91-28976 #
DE91-013642 N91-28430 #
DE91-013643 N91-28977 #
DE91-013644 N91-28872 #
DE91-013651 N91-28376 #
DE91-013652 N91-29028 #
DE91-013653 N91-29029 #
DE91-013658 N91-28291 #
DE91-013662 N91-28669 #
DE91-013666 N91-28630 #
DE91-013667 N91-28814 #
DE91-013668 N91-28431 #
DE91-013669 N91-29033 #
DE91-013671 N91-28366 #
DE91-013672 N91-29046 #
DE91-013682 N91-28565 #
DE91-013683 N91-28661 #
DE91-013684 N91-28714 #
DE91-013687 N91-28625 #
DE91-013688 N91-28632 #
DE91-013689 N91-29034 #
DE91-013690 N91-28861 #
DE91-013717 N91-28432 #
DE91-013721 N91-28433 #
DE91-013725 N91-28755 #
DE91-013726 N91-28493 #
DE91-013729 N91-28719 #
DE91-013730 N91-28367 #
DE91-013740 N91-28786 #
DE91-013743 N91-29035 #
DE91-013745 N91-28862 #
DE91-013748 N91-28567 #
DE91-013752 N91-29030 #
DE91-013757 N91-28434 #
DE91-013758 N91-28756 #
DE91-013759 N91-28566 #
DE91-013760 N91-28563 #
DE91-013762 N91-28670 #
DE91-013763 N91-29036 #
DE91-013764 N91-29037 #
DE91-013766 N91-28435 #
DE91-013767 N91-28656 #
DE91-013772 N91-28720 #
DE91-013773 N91-28548 #
DE91-013778 N91-28721 #
DE91-013783 N91-28722 #
DE91-013784 N91-29062 #
DE91-013787 N91-28591 #
DE91-013790 N91-28671 #
DE91-013794 N91-29031 #
DE91-013802 N91-28494 #
DE91-013824 N91-28568 #
DE91-013844 N91-28603 #
DE91-013848 N91-29038 #
DE91-013849 N91-28450 #
DE91-013851 N91-28763 #
DE91-013852 N91-28966 #
DE91-013853 N91-28327 #
DE91-013855 N91-28728 #
DE91-013856 N91-28368 #
DE91-013859 N91-28474 #
DE91-013864 N91-29039 #
DE91-013884 N91-28495 #
DE91-013906 N91-28369 #
DE91-013909 N91-28873 #
DE91-013910 N91-28764 #
DE91-013933 N91-28978 #
DE91-013948 N91-28967 #
DE91-013964 N91-29040 #
DE91-013970 N91-28436 #
DE91-013972 N91-28660 #
DE91-013991 N91-28856 #
DE91-013994 N91-29092 #
DE91-014005 N91-28765 #
DE91-014007 N91-28377 #
DE91-014011 N91-28815 #
DE91-014012 N91-28592 #
DE91-014013 N91-28361 #
DE91-014014 N91-28968 #
DE91-014016 N91-28147 #
DE91-014017 N91-28577 #
DE91-014031 N91-28370 #
DE91-014039 N91-28331 #
DE91-014069 N91-28437 #
DE91-014071 N91-28187 #
DE91-014073 N91-28279 #
DE91-014098 N91-28362 #
DE91-014100 N91-28380 #
DE91-014105 N91-28439 #
DE91-014106 N91-28778 #
DE91-014112 N91-29047 #
DE91-014119 N91-28549 #
DE91-014120 N91-29048 #
DE91-014126 N91-28328 #
DE91-014131 N91-28672 #
DE91-014135 N91-28962 #
DE91-014141 N91-28497 #
DE91-014172 N91-28595 #
DE91-014197 N91-28550 #
DE91-014210 N91-28969 #
DE91-014216 N91-28766 #
DE91-014219 N91-28779 #
DE91-014233 N91-28979 #
DE91-014236 N91-28807 #
DE91-014250 N91-28956 #
DE91-014256 N91-28371 #
DE91-014261 N91-28332 #
DE91-014285 N91-29089 #
DE91-014287 N91-28593 #
DE91-014288 N91-29126 #
DE91-014317 N91-28970 #
DE91-014322 N91-28475 #
DE91-014329 N91-28662 #
DE91-014331 N91-28515 #
DE91-014334 N91-29065 #
DE91-014335 N91-28178 #
DE91-014336 N91-28767 #
DE91-014340 N91-29090 #
DE91-014344 N91-28757 #
DE91-014345 N91-29080 #
DE91-014346 N91-28754 #
DE91-014348 N91-28782 #
DE91-014350 N91-29082 #
DE91-014356 N91-28879 #
DE91-014357 N91-28971 #
DE91-014358 N91-28980 #
DE91-014359 N91-28596 #
DE91-014360 N91-28981 #
DE91-014361 N91-28724 #
DE91-014364 N91-28982 #
DE91-014365 N91-28963 #
DE91-014366 N91-28964 #
DE91-014367 N91-28965 #
DE91-014368 N91-28972 #
DE91-014382 N91-29041 #
DE91-014383 N91-28864 #
DE91-014388 N91-28758 #
DE91-014395 N91-28957 #
DE91-014443 N91-29049 #
DE91-014447 N91-28664 #
DE91-014458 N91-28865 #
DE91-014466 N91-29042 #
DE91-014470 N91-28498 #
DE91-014498 N91-28857 #
DE91-014512 N91-28440 #
DE91-014515 N91-29043 #
DE91-014516 N91-28372 #
DE91-014536 N91-28333 #
DE91-014541 N91-28381 #
DE91-014546 N91-28382 #
DE91-014580 N91-29044 #
DE91-014586 N91-29091 #
DE91-014591 N91-28448 #
DE91-014592 N91-28725 #
DE91-014600 N91-28633 #
DE91-014605 N91-28499 #
DE91-014606 N91-28634 #
DE91-014607 N91-29050 #
DE91-014609 N91-29045 #
DE91-014614 N91-28527 #
DE91-014615 N91-29125 #
DE91-014665 N91-29051 #
DE91-014673 N91-28496 #
DE91-014675 N91-28500 #
DE91-014702 N91-28501 #
DE91-014707 N91-28476 #
DE91-014709 N91-28759 #
DE91-014731 N91-28142 #
DE91-014734 N91-28673 #
DE91-014737 N91-28528 #
DE91-014738 N91-28179 #
DE91-014740 N91-28635 #
DE91-014745 N91-28983 #
DE91-014750 N91-28636 #
DE91-014759 N91-28973 #
DE91-014766 N91-28637 #
DE91-014788 N91-28874 #
DE91-014789 N91-28569 #
DE91-014800 N91-28866 #
DE91-014814 N91-28723 #
DE91-014816 N91-28383 #
DE91-014824 N91-28329 #
DE91-014865 N91-28974 #
DE91-014903 N91-29052 #
DE91-014908 N91-29064 #
DE91-014939 N91-28570 #
DE91-014957 N91-28674 #
DE91-014961 N91-28780 #
DE91-015093 N91-28984 #
DE91-015100 N91-28675 #
DE91-015123 N91-28571 #
DE91-617571 N91-28813 #
DE91-617574 N91-28801 #
DE91-617575 N91-28802 #
DE91-617609 N91-28803 #
DE91-617610 N91-29056 #
DE91-617611 N91-29057 #
DE91-617789 N91-29017 #
DE91-617790 N91-28804 #
DE91-617799 N91-29018 #
DE91-618098 N91-29019 #
DE91-618684 N91-28416 #
DE91-618773 N91-28698 #

DOE/BP-63056/3 N91-28445 #

DOE/CE-0305P N91-28573 #
DOE/CE-90029/5 N91-28508 #

DOE/DP-48058/T4 N91-29071 #
DOE/DP-48058/T6 N91-29067 #
DOE/DP-48058/T7 N91-29076 #
DOE/DP-48058/T9 N91-29069 #
DOE/DP-48058/T11 N91-29066 #
DOE/DP-48058/T12 N91-29075 #
DOE/DP-48058/T13 N91-29070 #

DOE/EH-0165 N91-28957 #

DOE/EIA-0149(90) N91-29082 #

DOE/ER-13183/5 N91-28331 #
DOE/ER-13317/T1 N91-28323 #
DOE/ER-13388/5 N91-28723 #
DOE/ER-13441/T1 N91-28857 #
DOE/ER-13465/6 N91-28724 #
DOE/ER-13479/T1 N91-28320 #
DOE/ER-13560/5 N91-28401 #
DOE/ER-13569/6 N91-28332 #
DOE/ER-13571/1 N91-28329 #
DOE/ER-13604/16 N91-28409 #
DOE/ER-13619/5 N91-28357 #
DOE/ER-13778/4 N91-28863 #
DOE/ER-13789/4 N91-28833 #
DOE/ER-13859/11 N91-28421 #
DOE/ER-13859/12 N91-28428 #
DOE/ER-13879/3 N91-28333 #
DOE/ER-13905/2 N91-28440 #
DOE/ER-13913/3 N91-28511 #
DOE/ER-13944/4 N91-28864 #
DOE/ER-13977/4 N91-28596 #
DOE/ER-13992/T1 N91-28316 #
DOE/ER-14024/1 N91-28649 #
DOE/ER-14028/2 N91-28713 #
DOE/ER-14042/1 N91-28576 #
DOE/ER-14077/2 N91-29026 #
DOE/ER-14090/2 N91-28879 #
DOE/ER-14151/1 N91-28839 #
DOE/ER-25053/4 N91-28142 #
DOE/ER-25063/T8-PT-1 N91-28757 #
DOE/ER-25063/T9 N91-29080 #
DOE/ER-25063/T10 N91-28754 #
DOE/ER-25063/T12 N91-28782 #
DOE/ER-25063/3 N91-29089 #
DOE/ER-40120/T2 N91-28976 #
DOE/ER-40283/10 N91-28873 #
DOE/ER-40293/5 N91-28831 #
DOE/ER-40347/T1 N91-28838 #

DOE/ER-40388/71 .... N91-28872 #
DOE/ER-40456/8 .... N91-28845 #
DOE/ER-45205/6 .... N91-28287 #
DOE/ER-45254/5 .... N91-29020 #
DOE/ER-45262/4 .... N91-28368 #
DOE/ER-45269/2 .... N91-28328 #
DOE/ER-45278/T1 .... N91-29011 #
DOE/ER-45279/3 .... N91-28396 #
DOE/ER-45288/T1 .... N91-28392 #
DOE/ER-45288/T2 .... N91-28430 #
DOE/ER-45295/T1 .... N91-28372 #
DOE/ER-45298/7 .... N91-29013 #
DOE/ER-45301/4 .... N91-29043 #
DOE/ER-45306/4 .... N91-28433 #
DOE/ER-45328/5 .... N91-28995 #
DOE/ER-45347/31 .... N91-28848 #
DOE/ER-45352/3 .... N91-28369 #
DOE/ER-45357/4 .... N91-29049 #
DOE/ER-45396/2 .... N91-28391 #
DOE/ER-45402/2 .... N91-29041 #
DOE/ER-45413/1 .... N91-28383 #
DOE/ER-45421/1 .... N91-28608 #
DOE/ER-45435/T1 .... N91-28312 #
DOE/ER-53198/167 .... N91-29126 #
DOE/ER-53212/172 .... N91-28961 #
DOE/ER-53221/6 .... N91-28980 #
DOE/ER-53223/159 .... N91-28978 #
DOE/ER-53241/T1 .... N91-28945 #
DOE/ER-53241/T2 .... N91-28950 #
DOE/ER-53244/17 .... N91-28977 #
DOE/ER-53295/2 .... N91-28971 #
DOE/ER-53301/3 .... N91-28981 #
DOE/ER-54095/1 .... N91-28967 #
DOE/ER-60485/T2 .... N91-28673 #
DOE/ER-60561/5 .... N91-28728 #
DOE/ER-60631/7 .... N91-28716 #
DOE/ER-60913/T1 .... N91-28717 #
DOE/ER-61034/1 .... N91-29064 #

DOE/ET-10815/157 .... N91-28541 #
DOE/ET-53088/480-REV .... N91-28982 #
DOE/ET-53088/484 .... N91-28963 #
DOE/ET-53088/490 .... N91-28974 #
DOE/ET-53088/494 .... N91-28964 #
DOE/ET-53088/495 .... N91-28965 #
DOE/ET-53088/496 .... N91-28972 #

DOE/ID-12626/T2 .... N91-28398 #

DOE/LLW-102 .... N91-28764 #

DOE/MC-24221/T19 .... N91-28659 #
DOE/MC-24221/2881 .... N91-28657 #
DOE/MC-25159/2984 .... N91-28875 #

DOE/PC-89771/5-PT-5 .... N91-28327 #

DOE/PETC-TR/91/8 .... N91-28514 #

DOE/SF-16518/T1 .... N91-28652 #
DOE/SF-18014/T1 .... N91-28956 #

DOT/FAA/CT-TN91/4 .... N91-28176 #

DOT/FAA/CT-90/4 .... N91-28146 #

DRIC-BR-301039 .... N91-28504 #

DTIC/TR-90/1 .... N91-29072 #
DTIC/TR-91/2 .... N91-29072 #

DTP-91/19 .... N91-28793 #

E-5660 .... N91-28136* #
E-5746 .... N91-28622* #
E-5768 .... N91-28627* #
E-5905 .... N91-28278* #
E-6155 .... N91-28277* #
E-6444 .... N91-28776* #
E-6453 .... N91-28605* #
E-6493 .... N91-28449* #
E-6498 .... N91-29138* #
E-6499 .... N91-28538* #

EGG-EP-9296 .... N91-28491 #

EGG-FSP-9634 .... N91-28510 #

EGG-M-90238 .... N91-28951 #
EGG-M-90269 .... N91-28732 #
EGG-M-90290 .... N91-28356 #
EGG-M-90292 .... N91-28380 #
EGG-M-90383 .... N91-28795 #
EGG-M-90485 .... N91-28187 #
EGG-M-90504 .... N91-28362 #
EGG-M-90540 .... N91-29068 #
EGG-M-91022 .... N91-29077 #
EGG-M-91023 .... N91-28750 #
EGG-M-91085 .... N91-28437 #
EGG-M-91136 .... N91-28595 #
EGG-M-91251 .... N91-28279 #

EGG-MS-9633 .... N91-28282 #

EGG-10617-1127 .... N91-28170 #
EGG-10617-2095 .... N91-28549 #
EGG-10617-2097 .... N91-29022 #
EGG-10617-3004 .... N91-29048 #

EPA/600/8-90/083A .... N91-28665 #
EPA/600/8-90/083B .... N91-28666 #
EPA/600/8-91/009 .... N91-28697 #

ESD-PUBL-3509 .... N91-28674 #

ESD-TR-90-223 .... N91-28748 #

ETN-90-97221 .... N91-28676
ETN-90-97265 .... N91-28735
ETN-90-97266 .... N91-28736

FCR-11137 .... N91-28659 #

FERMILAB-CONF-91/179-A .... N91-29111* #

FERMILAB-PUB-91/164-A .... N91-29108* #
FERMILAB-PUB-91/175-A .... N91-29113* #
FERMILAB-PUB-91/176-A .... N91-29109* #
FERMILAB-PUB-91/186-A .... N91-29112* #
FERMILAB-PUB-91/192-A .... N91-29110* #

FNAL-PUB-91/167-T/A .... N91-28858* #

FNAL-TM-1727 .... N91-28610 #

FNAL/C-91/114 .... N91-28497 #
FNAL/C-91/119 .... N91-28867 #

GA-A-20539 .... N91-28973 #

HIFAN-499 .... N91-28476 #

IC-90/147 .... N91-29019 #
IC-90/211 .... N91-28803 #
IC-90/231 .... N91-29017 #
IC-90/233 .... N91-28416 #
IC-90/234 .... N91-29056 #
IC-90/238 .... N91-28698 #
IC-90/244 .... N91-28801 #
IC-90/245 .... N91-29057 #
IC-90/247 .... N91-28802 #
IC-90/253 .... N91-28804 #
IC-90/261 .... N91-29018 #

ICASE-91-52 .... N91-28806* #

IFSR-480-REV .... N91-28982 #
IFSR-484 .... N91-28963 #
IFSR-490 .... N91-28974 #
IFSR-494 .... N91-28964 #
IFSR-495 .... N91-28965 #
IFSR-496 .... N91-28972 #

INEL/MISC-91055 .... N91-28575 #

IPC-TR-91-06-PT-1 .... N91-28757 #
IPC-TR-91-002 .... N91-28779 #

IS-M-667 .... N91-28347 #

IS-T-1510 .... N91-29001 #
IS-T-1525 .... N91-28843 #
IS-T-1527 .... N91-28407 #
IS-T-1560 .... N91-28291 #
IS-T-1562 .... N91-28353 #

IS-5053 .... N91-28773 #

ISBN-90-6275-567-4 .... N91-28736
ISBN-90-9003020-4 .... N91-28676
ISBN-92-835-0611-1 .... N91-28150 #
ISBN-92-835-0622-7 .... N91-28465 #

ISSN-0915-6348 .... N91-28881 #

ITN-91-85139 .... N91-28468
ITN-91-85140 .... N91-28469
ITN-91-85141 .... N91-28583
ITN-91-85142 .... N91-28139
ITN-91-85143 .... N91-28516
ITN-91-85145 .... N91-28470
ITN-91-85146 .... N91-28760
ITN-91-85147 .... N91-28471
ITN-91-85149 .... N91-28733
ITN-91-85150 .... N91-28878

JPRS-UMS-91-003 .... N91-28342 #

JPRS-UPM-90-006 .... N91-28811 #

K/ETO-56 .... N91-28355 #

L-16569 .... N91-28143* #

LA-UR-91-533 .... N91-28457 #
LA-UR-91-1117 .... N91-28173 #
LA-UR-91-1286 .... N91-28990 #
LA-UR-91-1329 .... N91-28991 #
LA-UR-91-1444 .... N91-28492 #
LA-UR-91-1448 .... N91-28849 #
LA-UR-91-1451 .... N91-28558 #
LA-UR-91-1458 .... N91-28488 #
LA-UR-91-1461 .... N91-28486 #
LA-UR-91-1462 .... N91-28799 #
LA-UR-91-1483 .... N91-28474 #
LA-UR-91-1487 .... N91-29029 #
LA-UR-91-1488 .... N91-29028 #
LA-UR-91-1490 .... N91-28376 #
LA-UR-91-1495 .... N91-28563 #
LA-UR-91-1500 .... N91-28566 #
LA-UR-91-1517 .... N91-29025 #
LA-UR-91-1522 .... N91-28564 #
LA-UR-91-1524 .... N91-28871 #
LA-UR-91-1526 .... N91-28556 #
LA-UR-91-1527 .... N91-28177 #
LA-UR-91-1530 .... N91-28624 #
LA-UR-91-1535 .... N91-28565 #
LA-UR-91-1536 .... N91-29046 #
LA-UR-91-1538 .... N91-28366 #
LA-UR-91-1545 .... N91-29033 #
LA-UR-91-1559 .... N91-28415 #
LA-UR-91-1560 .... N91-28414 #
LA-UR-91-1587 .... N91-28613 #
LA-UR-91-1612 .... N91-28443 #
LA-UR-91-1614 .... N91-28174 #
LA-UR-91-1636 .... N91-28545 #
LA-UR-91-1637 .... N91-29055 #
LA-UR-91-1638 .... N91-28324 #
LA-UR-91-1642 .... N91-28288 #
LA-UR-91-1648 .... N91-28617 #
LA-UR-91-1666 .... N91-28325 #
LA-UR-91-1680 .... N91-29035 #
LA-UR-91-1684 .... N91-28861 #
LA-UR-91-1685 .... N91-29034 #
LA-UR-91-1687 .... N91-28632 #
LA-UR-91-1693 .... N91-28625 #
LA-UR-91-1707 .... N91-28714 #
LA-UR-91-1708 .... N91-28661 #
LA-UR-91-1714 .... N91-28855 #
LA-UR-91-1716 .... N91-28513 #
LA-UR-91-1730 .... N91-28420 #
LA-UR-91-1734 .... N91-29015 #
LA-UR-91-1758 .... N91-29023 #
LA-UR-91-1789 .... N91-28621 #
LA-UR-91-1801 .... N91-28456 #
LA-UR-91-1820 .... N91-28618 #
LA-UR-91-1840 .... N91-28975 #
LA-UR-91-1892 .... N91-28419 #
LA-UR-91-1895 .... N91-29058 #
LA-UR-91-1944 .... N91-28637 #
LA-UR-91-1964 .... N91-28636 #
LA-UR-91-1980 .... N91-28963 #
LA-UR-91-1994 .... N91-28635 #
LA-UR-91-2001 .... N91-28179 #
LA-UR-91-2003 .... N91-28528 #
LA-UR-91-2030 .... N91-29045 #
LA-UR-91-2034 .... N91-29050 #
LA-UR-91-2041 .... N91-28634 #
LA-UR-91-2049 .... N91-28499 #
LA-UR-91-2058 .... N91-28633 #
LA-UR-91-2100 .... N91-28725 #
LA-UR-91-2103 .... N91-28448 #

LA-11822-MS .... N91-28809 #
LA-12024-MS .... N91-28593 #
LA-12068-MS .... N91-28620 #
LA-12069-MS .... N91-28810 #
LA-12091-MS .... N91-28464 #
LA-12120-MS .... N91-28436 #

LAC90-R24 .... N91-28788* #

LBL-28363 .... N91-29091 #
LBL-28878 .... N91-28677 #
LBL-28889 .... N91-28998 #
LBL-28890 .... N91-29007 #
LBL-29272 .... N91-29038 #
LBL-29588 .... N91-29021 #

LBL-29592 N91-29006 #
LBL-29735 N91-28315 #
LBL-29794 N91-28997 #
LBL-29914 N91-28979 #
LBL-29938 N91-28308 #
LBL-29990 N91-29054 #
LBL-29994 N91-28399 #
LBL-30022 N91-29133 #
LBL-30024 N91-28720 #
LBL-30025 N91-28721 #
LBL-30050 N91-28527 #
LBL-30322-REV N91-28476 #
LBL-30365 N91-29002 #
LBL-30403 N91-28993 #
LBL-30411 N91-28737 #
LBL-30412 N91-28763 #
LBL-30421 N91-28345 #
LBL-30425 N91-29073 #
LBL-30474 N91-28281 #
LBL-30497 N91-28450 #
LBL-30512 N91-28768 #
LBL-30549 N91-28548 #
LBL-30573 N91-28992 #
LBL-30582 N91-28844 #
LBL-30605 N91-28603 #
LBL-30618 N91-28862 #
LBL-30641 N91-29030 #
LBL-30646 N91-28498 #
LBL-30676 N91-29062 #
LBL-30680 N91-28722 #
LBL-30685 N91-28759 #
LBL-30705 N91-28807 #
LBL-30726 N91-29125 #

LNS/PH-90-21 N91-28842 #

MCAT-91-005 N91-28503* #

MISC-90087 N91-28764 #

MLM-3689 N91-28800 #

MML-TR-90-27C-PT-2 N91-28334* #

NADC-91002-60 N91-28343 #

NAS 1.15:4303 N91-28278* #
NAS 1.15:4304 N91-28627* #
NAS 1.15:102876 N91-28134* #
NAS 1.15:103287 N91-28622* #
NAS 1.15:103537 N91-28341* #
NAS 1.15:103544 N91-28189* #
NAS 1.15:104055 N91-28293* #
NAS 1.15:104072 N91-28137* #
NAS 1.15:104087 N91-28131* #
NAS 1.15:104088 N91-28132* #
NAS 1.15:104119 N91-28373* #
NAS 1.15:104360 N91-28277* #
NAS 1.15:105030 N91-28180* #
NAS 1.15:105090 N91-28418* #
NAS 1.15:105157 N91-28776* #
NAS 1.15:105164 N91-28605* #
NAS 1.15:105191 N91-28449* #
NAS 1.15:105196 N91-29138* #
NAS 1.15:105197 N91-28538* #
NAS 1.21:7011(352) N91-28729*
NAS 1.21:7039(39)-SECT-2 N91-29088*
NAS 1.21:7085(02) N91-28191*
NAS 1.26:4364 N91-28334* #
NAS 1.26:4390 N91-28138* #
NAS 1.26:177590 N91-28168* #
NAS 1.26:184123 N91-28192* #
NAS 1.26:187121 N91-28648* #
NAS 1.26:187162 N91-28644* #
NAS 1.26:187312 N91-28502* #
NAS 1.26:187547 N91-28777* #
NAS 1.26:187573 N91-28626* #
NAS 1.26:187592 N91-28806* #
NAS 1.26:188039 N91-28503* #
NAS 1.26:188159 N91-28787* #
NAS 1.26:188442 N91-28539* #
NAS 1.26:188675 N91-28747* #
NAS 1.26:188688 N91-28403* #
NAS 1.26:188692 N91-29107* #
NAS 1.26:188693 N91-28292* #
NAS 1.26:188696 N91-29113* #
NAS 1.26:188697 N91-28858* #
NAS 1.26:188698 N91-29112* #
NAS 1.26:188701 N91-29111* #
NAS 1.26:188703 N91-29110* #
NAS 1.26:188704 N91-29109* #
NAS 1.26:188705 N91-29108* #
NAS 1.26:188728 N91-28182* #
NAS 1.26:188733 N91-28643* #
NAS 1.55:3112-VOL-2 N91-28193* #
NAS 1.55:3112-VOL-3 N91-28235* #
NAS 1.60:2922 N91-28143* #
NAS 1.60:3142 N91-28136* #
NAS 1.71:GSC-13027-1 N91-28726* #
NAS 1.71:GSC-13251-1 N91-28582* #
NAS 1.71:GSC-13306-1 N91-28727* #
NAS 1.71:GSC-13343-1 N91-28557* #
NAS 1.71:GSC-13344-1 N91-28363* #
NAS 1.71:GSC-13346-1 N91-28578* #
NAS 1.71:GSC-13376-1 N91-28579* #
NAS 1.71:GSC-13377-1 N91-28785* #
NAS 1.71:GSC-13378-1 N91-28581* #
NAS 1.71:LAR-13388-1 N91-28321* #
NAS 1.71:LAR-13548-1 N91-28175* #
NAS 1.71:LAR-13645-1 N91-28424* #
NAS 1.71:LAR-13832-1 N91-28444* #
NAS 1.71:LAR-14206-1 N91-28425* #
NAS 1.71:LAR-14231-1-CU N91-28290* #
NAS 1.71:LAR-14272-1-CU N91-28184* #
NAS 1.71:LAR-14395-1-CU N91-28490* #
NAS 1.71:LAR-14446-1 N91-28454* #
NAS 1.71:LAR-14483-1 N91-28455* #
NAS 1.71:LAR-14515-1-CU N91-28580* #
NAS 1.71:LAR-14579-1 N91-28546* #
NAS 1.71:LAR-14685-1 N91-28135* #
NAS 1.71:LEW-14474-1 N91-28423* #
NAS 1.71:LEW-15077-2 N91-28289* #
NAS 1.71:MSC-21625-1 N91-28730* #
NAS 1.71:MSC-21793-1 N91-28186* #

NASA-CASE-GSC-13027-1 N91-28726* #
NASA-CASE-GSC-13251-1 N91-28582* #
NASA-CASE-GSC-13306-1 N91-28727* #
NASA-CASE-GSC-13343-1 N91-28557* #
NASA-CASE-GSC-13344-1 N91-28363* #
NASA-CASE-GSC-13346-1 N91-28578* #
NASA-CASE-GSC-13376-1 N91-28579* #
NASA-CASE-GSC-13377-1 N91-28785* #
NASA-CASE-GSC-13378-1 N91-28581* #

NASA-CASE-LAR-13388-1 N91-28321* #
NASA-CASE-LAR-13548-1 N91-28175* #
NASA-CASE-LAR-13645-1 N91-28424* #
NASA-CASE-LAR-13832-1 N91-28444* #
NASA-CASE-LAR-14206-1 N91-28425* #
NASA-CASE-LAR-14231-1-CU N91-28290* #
NASA-CASE-LAR-14272-1-CU N91-28184* #
NASA-CASE-LAR-14395-1-CU N91-28490* #
NASA-CASE-LAR-14446-1 N91-28454* #
NASA-CASE-LAR-14483-1 N91-28455* #
NASA-CASE-LAR-14515-1-CU N91-28580* #
NASA-CASE-LAR-14579-1 N91-28546* #
NASA-CASE-LAR-14685-1 N91-28135* #

NASA-CASE-LEW-14474-1 N91-28423* #
NASA-CASE-LEW-15077-2 N91-28289* #

NASA-CASE-MSC-21625-1 N91-28730* #
NASA-CASE-MSC-21793-1 N91-28186* #

NASA-CP-3112-VOL-2 N91-28193* #
NASA-CP-3112-VOL-3 N91-28235* #

NASA-CR-4364 N91-28334* #
NASA-CR-4390 N91-28138* #
NASA-CR-177590 N91-28168* #
NASA-CR-184123 N91-28192* #
NASA-CR-187121 N91-28648* #
NASA-CR-187162 N91-28644* #
NASA-CR-187312 N91-28502* #
NASA-CR-187547 N91-28777* #
NASA-CR-187573 N91-28626* #
NASA-CR-187592 N91-28806* #
NASA-CR-188039 N91-28503* #
NASA-CR-188159 N91-28787* #
NASA-CR-188442 N91-28539* #
NASA-CR-188675 N91-28747* #
NASA-CR-188688 N91-28403* #
NASA-CR-188692 N91-29107* #
NASA-CR-188693 N91-28292* #
NASA-CR-188696 N91-29113* #
NASA-CR-188697 N91-28858* #
NASA-CR-188698 N91-29112* #
NASA-CR-188701 N91-29111* #
NASA-CR-188703 N91-29110* #
NASA-CR-188704 N91-29109* #
NASA-CR-188705 N91-29108* #
NASA-CR-188728 N91-28182* #
NASA-CR-188733 N91-28643* #

NASA-SP-7011(352) N91-28729*
NASA-SP-7039(39)-SECT-2 N91-29088*
NASA-SP-7085(02) N91-28191*

NASA-TM-4303 N91-28278* #
NASA-TM-4304 N91-28627* #
NASA-TM-102876 N91-28134* #
NASA-TM-103287 N91-28622* #
NASA-TM-103537 N91-28341* #
NASA-TM-103544 N91-28189* #
NASA-TM-104055 N91-28293* #
NASA-TM-104072 N91-28137* #
NASA-TM-104087 N91-28131* #
NASA-TM-104088 N91-28132* #
NASA-TM-104119 N91-28373* #
NASA-TM-104360 N91-28277* #
NASA-TM-105030 N91-28180* #
NASA-TM-105090 N91-28418* #
NASA-TM-105157 N91-28776* #
NASA-TM-105164 N91-28605* #
NASA-TM-105191 N91-28449* #
NASA-TM-105196 N91-29138* #
NASA-TM-105197 N91-28538* #

NASA-TP-2922 N91-28143* #
NASA-TP-3142 N91-28136* #

NCTRF-184 N91-28731 #

NIFS-PROC-6 N91-28881 #

NIST/SP-804 N91-28403* #
NIST/SP-807 N91-28404 #

NIST/TN-1341 N91-28482 #

NISTIR-4540 N91-28507 #

ORNL/M-1312 N91-28283 #

ORNL/SUB-88-07685/01 N91-28358 #

ORNL/TM-11397 N91-28512 #
ORNL/TM-11576 N91-28674 #
ORNL/TM-11623 N91-28947 #
ORNL/TM-11699 N91-28751 #
ORNL/TM-11722 N91-28188 #
ORNL/TM-11723 N91-28570 #
ORNL/TM-11760 N91-28780 #
ORNL/TM-11762 N91-28829 #
ORNL/TM-11790 N91-28738 #
ORNL/TM-11796 N91-28359 #
ORNL/TM-11810 N91-28784 #
ORNL/TM-11827 N91-29016 #

OTA-BP-TCT-77 N91-28752 #

PB91-167395 N91-28404 #
PB91-168484 N91-28697 #
PB91-169102 N91-29130 #
PB91-169110 N91-29131 #
PB91-169763 N91-28752 #
PB91-171918 N91-28665 #
PB91-171918 N91-28666 #
PB91-171926 N91-28665 #
PB91-171934 N91-28666 #
PB91-171959 N91-28482 #
PB91-172262 N91-29128 #
PB91-172270 N91-29129 #
PB91-178822 N91-28403* #
PB91-178848 N91-28507 #
PB91-181529 N91-28180* #

PNL-SA-18369 N91-28600 #
PNL-SA-18472 N91-28364 #
PNL-SA-18689 N91-28354 #
PNL-SA-18690 N91-29074 #
PNL-SA-18750 N91-28276 #
PNL-SA-18812 N91-28400 #
PNL-SA-18917 N91-28749 #
PNL-SA-18938 N91-28630 #
PNL-SA-19094 N91-29012 #
PNL-SA-19158 N91-29078 #
PNL-SA-19249 N91-28412 #
PNL-SA-19277 N91-28999 #
PNL-SA-19298 N91-28317 #
PNL-SA-19310 N91-29092 #
PNL-SA-19359 N91-28654 #
PNL-SA-19418 N91-28431 #
PNL-SA-19443 N91-28715 #
PNL-SA-19455 N91-28591 #
PNL-SA-19544 N91-28432 #
PNL-SA-19561 N91-28664 #
PNL-SA-19582 N91-28671 #
PNL-SA-19619 N91-28669 #

PNL-7673 N91-28441 #

PSU/ARL-TR-91-007 N91-28816 #

PUBL-91230 N91-28192* #

R/D-6101-MS-01 N91-28540 #

RADC-TR-90-259 .... N91-28458 #

RAE-TM-P-1203 .... N91-28504 #

REPT-1148-13 .... N91-28385 #

RFP-4413 .... N91-28452 #
RFP-4447 .... N91-28453 #

RL-TR-91-55 .... N91-28478 #
RL-TR-91-87 .... N91-28745 #
RL-TR-91-156-VOL-1 .... N91-28460 #
RL-TR-91-156-VOL-2 .... N91-28461 #

SAIC-91/1136/APPAT-143 .... N91-28970 #

SAND-90-0740C .... N91-28841 #
SAND-90-0934C .... N91-28651 #
SAND-90-0947C .... N91-28653 #
SAND-90-1050 .... N91-28475 #
SAND-90-2092 .... N91-28500 #
SAND-90-2112 .... N91-28496 #
SAND-90-2418C .... N91-28505 #
SAND-90-2533 .... N91-28543 #
SAND-90-2634C .... N91-28395 #
SAND-90-2671C .... N91-28756 #
SAND-90-2690C .... N91-28616 #
SAND-90-2961C .... N91-28434 #
SAND-90-3007C .... N91-28451 #
SAND-90-3023C .... N91-28402 #
SAND-90-3033C .... N91-28393 #
SAND-90-3100C .... N91-29051 #
SAND-90-3130C .... N91-29047 #
SAND-90-3172C .... N91-28473 #
SAND-90-3186C .... N91-28483 #
SAND-90-3230C .... N91-28274 #
SAND-90-7037 .... N91-28662 #
SAND-90-7111 .... N91-28133 #
SAND-91-0039C .... N91-28439 #
SAND-91-0054C .... N91-28411 #
SAND-91-0060C .... N91-28631 #
SAND-91-0067C .... N91-28442 #
SAND-91-0102C .... N91-28826 #
SAND-91-0121 .... N91-28553 #
SAND-91-0148C .... N91-28562 #
SAND-91-0197C .... N91-28567 #
SAND-91-0217C .... N91-28805 #
SAND-91-0310C .... N91-28319 #
SAND-91-0350 .... N91-28515 #
SAND-91-0618 .... N91-29065 #
SAND-91-0657 .... N91-28178 #
SAND-91-0672 .... N91-28485 #
SAND-91-0695C .... N91-28314 #
SAND-91-0698C .... N91-28379 #
SAND-91-0771C .... N91-29052 #
SAND-91-0855C .... N91-29003 #
SAND-91-0898C .... N91-29004 #
SAND-91-0951C .... N91-28417 #
SAND-91-0954C .... N91-29009 #
SAND-91-0999C .... N91-28846 #
SAND-91-1000C .... N91-28427 #
SAND-91-1020C .... N91-28346 #
SAND-91-1056C .... N91-28544 #
SAND-91-1061 .... N91-28767 #
SAND-91-1096C .... N91-28487 #
SAND-91-1143C .... N91-28775 #
SAND-91-1272C .... N91-28501 #
SAND-91-1290C .... N91-28778 #
SAND-91-8215 .... N91-28612 #

SEI-CM-3-1-5 .... N91-28743 #
SEI-CM-12-1-1 .... N91-28744 #

SERI/CP-236-4396 .... N91-28663 #
SERI/CP-250-4254-VOL-1 .... N91-28658 #
SERI/CP-250-4254-VOL-2 .... N91-28656 #

SERI/TP-210-4319 .... N91-28429 #
SERI/TP-211-4212 .... N91-28650 #
SERI/TP-214-4271 .... N91-28480 #

SGD-557-PT-1 .... N91-29130 #
SGD-557-PT-2 .... N91-29131 #
SGD-558-PT-1 .... N91-29129 #
SGD-558-PT-2 .... N91-29128 #

SSCL-300 .... N91-28794 #
SSCL-377 .... N91-29010 #
SSCL-390 .... N91-29079 #
SSCL-423 .... N91-29040 #

SU-SLAC-PUB-5453 .... N91-28869 #
SU-SLAC-PUB-5458 .... N91-28796 #
SU-SLAC-PUB-5478 .... N91-28552 #
SU-SLAC-PUB-5529 .... N91-28828 #
SU-SLAC-PUB-5532 .... N91-28792 #
SU-SLAC-PUB-5546 .... N91-28996 #
SU-SLAC-PUB-5557 .... N91-28834 #
SU-SLAC-PUB-5558 .... N91-28856 #
SU-SLAC-PUB-5565 .... N91-28798 #

SWRI-06-8602/6 .... N91-28280 #

TR-1 .... N91-28821 #
TR-2 .... N91-28822 #
TR-10 .... N91-28987 #
TR-16 .... N91-28388 #
TR-22 .... N91-28387 #
TR-29 .... N91-28989 #
TR-32 .... N91-28985 #

TRI-PP-90-88 .... N91-28842 #
TRI-PP-91-3 .... N91-28830 #

TR90-041 .... N91-28746 #
TR91-013 .... N91-28770 #
TR91-020 .... N91-28823 #

TWR-60187-VOL-1 .... N91-28192* #

UBUFFALO/DC/91/TR-40 .... N91-28820 #
UBUFFALO/DC/91/TR-51 .... N91-28812 #

UCB-PTH-90/49 .... N91-29054 #
UCB-PTH-91/9 .... N91-29062 #

UCID-20622-90-2 .... N91-28305 #

UCRL-ID-106416 .... N91-28167 #
UCRL-ID-107112-PT-1 .... N91-28559 #
UCRL-ID-107211 .... N91-28948 #
UCRL-ID-107220 .... N91-28984 #
UCRL-ID-107222 .... N91-28952 #

UCRL-JC-10639 .... N91-28313 #
UCRL-JC-104111 .... N91-28307 #
UCRL-JC-104112 .... N91-28306 #
UCRL-JC-104164 .... N91-28462 #
UCRL-JC-104674 .... N91-28408 #
UCRL-JC-104854 .... N91-29053 #
UCRL-JC-105138 .... N91-28599 #
UCRL-JC-105244-REV-1 .... N91-28285 #
UCRL-JC-105345 .... N91-28148 #
UCRL-JC-105475 .... N91-28571 #
UCRL-JC-105481 .... N91-28560 #
UCRL-JC-105557 .... N91-28568 #
UCRL-JC-105585 .... N91-28489 #
UCRL-JC-105644 .... N91-28467 #
UCRL-JC-105647 .... N91-28447 #
UCRL-JC-105692 .... N91-29063 #
UCRL-JC-105704 .... N91-28542 #
UCRL-JC-105736 .... N91-28551 #
UCRL-JC-105806 .... N91-28954 #
UCRL-JC-105997 .... N91-28958 #
UCRL-JC-105998 .... N91-28561 #
UCRL-JC-106181 .... N91-28774 #
UCRL-JC-106271 .... N91-28955 #
UCRL-JC-106338 .... N91-28628 #
UCRL-JC-106341 .... N91-28365 #
UCRL-JC-106508 .... N91-28824 #
UCRL-JC-106553 .... N91-28825 #
UCRL-JC-106555 .... N91-28286 #
UCRL-JC-106567 .... N91-28944 #
UCRL-JC-106766 .... N91-28351 #
UCRL-JC-106807 .... N91-28275 #
UCRL-JC-106852 .... N91-28394 #
UCRL-JC-106863 .... N91-28876 #
UCRL-JC-106927 .... N91-28827 #
UCRL-JC-107019 .... N91-28781 #
UCRL-JC-107069 .... N91-28284 #
UCRL-JC-107081 .... N91-28326 #
UCRL-JC-107116 .... N91-28712 #
UCRL-JC-107118 .... N91-28877 #
UCRL-JC-107158 .... N91-28962 #
UCRL-JC-107201 .... N91-28700 #
UCRL-JC-107276 .... N91-28422 #

UCRL-LR-104546 .... N91-28966 #
UCRL-LR-105821-91-1 .... N91-28960 #
UCRL-LR-106630 .... N91-28506 #
UCRL-LR-106884 .... N91-28602 #
UCRL-LR-106975 .... N91-28772 #

UCRL-21290 .... N91-28672 #

UILU-ENG-91-2226 .... N91-28747* #

US-PATENT-APPL-SN-363807 .... N91-28726* #
US-PATENT-APPL-SN-429574 .... N91-28425* #
US-PATENT-APPL-SN-524109 .... N91-28290* #
US-PATENT-APPL-SN-628062 .... N91-28321* #
US-PATENT-APPL-SN-666536 .... N91-28490* #
US-PATENT-APPL-SN-674828 .... N91-28727* #
US-PATENT-APPL-SN-677008 .... N91-28579* #
US-PATENT-APPL-SN-678551 .... N91-28580* #
US-PATENT-APPL-SN-678553 .... N91-28184* #
US-PATENT-APPL-SN-682151 .... N91-28444* #
US-PATENT-APPL-SN-682153 .... N91-28455* #
US-PATENT-APPL-SN-690198 .... N91-28546* #
US-PATENT-APPL-SN-691609 .... N91-28578* #
US-PATENT-APPL-SN-699288 .... N91-28454* #
US-PATENT-APPL-SN-702529 .... N91-28557* #
US-PATENT-APPL-SN-710633 .... N91-28581* #
US-PATENT-APPL-SN-710845 .... N91-28785* #
US-PATENT-APPL-SN-714814 .... N91-28582* #
US-PATENT-APPL-SN-716182 .... N91-28730* #
US-PATENT-APPL-SN-718046 .... N91-28363* #
US-PATENT-APPL-SN-718313 .... N91-28135* #
US-PATENT-APPL-SN-720133 .... N91-28423* #
US-PATENT-APPL-SN-721038 .... N91-28424* #
US-PATENT-APPL-SN-721039 .... N91-28175* #
US-PATENT-APPL-SN-731829 .... N91-28186* #
US-PATENT-APPL-SN-735548 .... N91-28289* #

UTAP-128/91 .... N91-29112* #

UVA-527387/CS91/103 .... N91-29089 #

UW-CPTC-90-8-REV .... N91-28949 #
UW-CPTC-91-3 .... N91-29061 #
UW-CPTC-91-5 .... N91-28953 #

UWAERP-28 .... N91-28967 #

VPI-E-91-14 .... N91-28292* #

WCDP-9 .... N91-28695 #

WISC-EX-91-317 .... N91-28996 #

WMO/TD-342 .... N91-28695 #

Appendix

NASA SCIENTIFIC AND TECHNICAL INFORMATION PROGRAM PRODUCTS AND SERVICES

The NASA Scientific and Technical Information (STI) Program provides for the collection and announcement of aerospace-related reports and literature obtained worldwide through agreements and exchanges. The result of the collection is the comprehensive NASA STI Database that covers aeronautics, space, and supporting disciplines.

The STI Database, documents generated or obtained by NASA, and products and services derived from or supporting the database are made available to the NASA research community and to the public. Descriptions and sources of these items are presented in the following pages.

Scientific and Technical Aerospace Reports (*STAR*) is an abstract journal, listing citations with abstracts for aerospace-related reports obtained from worldwide sources. *STAR* is issued on the 8th and 23rd of each month and announces current documents that have been entered into the NASA STI Database during the previous two weeks. The reports are of the following types:

- NASA, NASA contractor, and NASA grantee reports;
- Reports issued by other U.S. Government agencies, domestic and foreign institutions, universities, and private firms;
- Translations in report form;
- NASA-owned patents and patent applications;
- Other U.S. Government agency and foreign patents and patent applications;
- Domestic and foreign dissertations and theses.

Journal, book, and conference literature, journal translations, and certain foreign dissertations having the same subject scope as *STAR* are announced in a companion journal, *International Aerospace Abstracts* (*IAA*). *IAA* is issued on the 1st and 15th of each month and is available from the American Institute of Aeronautics and Astronautics, Technical Information Service, 555 West 57th Street, 12th Floor, New York, NY 10019.

ELIGIBILITY AND REGISTRATION FOR NASA STI PRODUCTS AND SERVICES

Organizations of the type listed below that have registered with NASA can receive products and services.

- NASA offices and installations, contractors, subcontractors, grantees, and consultants;
- Other U.S. Government agencies and their contractors;
- Libraries in the United States that have arrangements with NASA to maintain collections of NASA documents for public reference;
- Other organizations in the United States having a need for NASA documents in work related to aeronautics and space research;
- Organizations abroad that have established reciprocal documents exchange arrangements with NASA.

Only the central service points or central points of document acquisition and control within qualified organizations are eligible to register for NASA STI products and services. Domestic organizations that may be eligible to receive various classes of NASA publications and services should address their requests for registration or further information to:

NASA Center for AeroSpace Information
ATTN: Registration Services
P.O. Box 8757
BWI Airport, MD 21240
301-621-0153

Organizations abroad should direct requests to:

National Aeronautics and Space Administration
Director, Scientific and Technical Information Program
Code NTT
Washington, DC 20546
USA
703-271-5640

SUBJECT SCOPE

The subject scope of *STAR* and *IAA* includes all aspects of aeronautics and space research and development, supporting basic and applied research, and applications. Aerospace aspects of Earth resources, energy development, conservation, oceanography, environmental protection, urban transportation, and other topics of high national priority are also covered.

HOW TO USE *STAR* SUBJECT CATEGORIES

Abstracts in *STAR* are categorized by 10 major subject divisions that are divided further into 76 specific subject categories. The subject divisions and categories are listed in the Table of Contents together with a note for each that defines its scope and provides any cross-references. For example:

> **16 SPACE TRANSPORTATION**
> Includes passenger and cargo space transportation, e.g., shuttle operations; and space rescue techniques. For related information see also *03 Air Transportation and Safety* and *18 Spacecraft Design, Testing and Performance.* For space suits see *54 Man/System Technology and Life Support.*

CROSS-REFERENCES

Individual *STAR* abstracts are not ordinarily cross-referenced, except for certain conference reports or book translations that have had separate abstracts written for their component papers or chapters. Citations and abstracts of the components follow immediately after those of the parent document. When the subject content of a component differs sufficiently from the general content of the parent, a cross-reference citation also is printed at the end of the category to which it normally would have been assigned if it were independent.

DOCUMENTS ON MICROFICHE

Documents available on microfiche are designated by a pound sign (#) following the accession number.

LIMITED REPRODUCIBILITY

A note of limited reproducibility appears in the citation, if there are factors affecting the reproducibility of more than 20% of the document. These factors include faint or broken type, color photographs, black and white photographs, foldouts, dot matrix print, or some other factor that limits the reproducibility of the document. This notation also appears on the microfiche header with the specific factor checked off on a list visible in the second frame.

COLOR COPIES

An increasing number of NASA scientific and technical reports are being produced with color graphs, charts, illustrations, and photographs. An indication that a document has color pages follows the source and pricing (SAP) information in the *STAR* citation.

Registered users of the NASA Scientific and Technical Information Program will receive ordered documents with color at no additional cost, as long as stock copies of the document are available. Otherwise, an additional fee of $2.00 per color page will be charged. The NASA Center for AeroSpace Information staff will contact registered users to determine individual user's needs.

NASA PATENTS AND PATENT APPLICATIONS

Patents and patent applications owned by NASA are announced in *STAR* under appropriate subject categories and are referenced in the *STAR* indexes. In the Report/Accession Number Index, patents are indexed by the NASA Case Number, and the U.S. Patent Class. Patent applications are indexed by the NASA Case Number and the U.S. Patent Application Serial Number.

Printed copies of patents (which are not microfiched) are available for purchase from the U.S. Patent and Trademark Office.

NASA patent application specifications are sold in both paper copy and microfiche by the National Technical Information Service (NTIS). The US-Patent-Appl-SN-number should be used in ordering either paper copy or microfiche from NTIS.

When ordering patents, the U.S. Patent Number should be used, and payment must be remitted in advance, by money order or check payable to the Commissioner of Patents and Trademarks. Prepaid purchase coupons for ordering are also available from the U.S. Patent and Trademark Office.

The patents and patent applications announced in *STAR* are owned by NASA and are available for royalty-free licensing. Requests for licensing terms and further information should be addressed to:

National Aeronautics and Space Administration
Associate General Counsel for Intellectual Property
Code GP
Washington, DC 20546

SOURCES FOR DOCUMENTS

One or more sources from which a document announced in *STAR* is available to the public is given in each citation. The most commonly indicated sources and their acronyms or abbreviations are listed on page A-6. If the publication is available from a source other than those listed, the publisher and address will be displayed on the availability line or in combination with the corporate source line.

Avail: NTIS. Sold by the National Technical Information Service. Prices for hard copy (HC) and microfiche (MF) are indicated by a price code following the letters HC or MF in the *STAR* citation. Current values for the price codes are given in the tables on page A-7.

Initially distributed microfiche under the NTIS SRIM (Selected Research in Microfiche) is available at greatly reduced unit prices. For this service and for information concerning subscription to NASA printed reports, consult the NTIS Subscription Section, Springfield, VA 22161.

NOTE ON ORDERING DOCUMENTS: When ordering NASA publications (those followed by the * symbol), use the N accession number. NASA patent applications (only the specifications are offered) should be ordered by the US-Patent-Appl-SN number. Non-NASA publications (no asterisk) should be ordered by the AD, PB, or other *report number* shown on the last line of the citation, not by the N accession number. It is also advisable to cite the title and other bibliographic identification.

Avail: SOD (or GPO). Sold by the Superintendent of Documents, U.S. Government Printing Office, in hard copy. The current price and order number are given following the availability line. (NTIS will fill microfiche requests, as indicated above, for those documents identified by a # symbol.)

Avail: BLL (formerly NLL): British Library Lending Division, Boston Spa, Wetherby, Yorkshire, England. Photocopies available from this organization at the price shown. (If none is given, address inquiry to the BLL.)

Avail: DOE Depository Libraries. Organizations in U.S. cities and abroad that maintain collections of Department of Energy reports, usually in microfiche form, are listed in *Energy Research Abstracts.* Services available from the DOE and its depositories are described in a booklet, *DOE Technical Information Center - Its Functions and Services* (TID-4660), which may be obtained without charge from the DOE Technical Information Center.

Avail: ESDU. Pricing information on specific data, computer programs, and details on Engineering Sciences Data Unit (ESDU) topic categories can be obtained from ESDU International Ltd. Requesters in North America should use the Virginia address while all other requesters should use the London address, both of which are on page A-6.

Avail: Fachinformationszentrum, Karlsruhe. Sold by the Fachinformationszentrum Energie, Physik, Mathematik GMBH, Eggenstein Leopoldshafen, Federal Republic of Germany, at the price shown in deutschmarks (DM).

Avail: HMSO. Publications of Her Majesty's Stationery Office are sold in the U.S. by Pendragon House, Inc. (PHI), Redwood City, CA. The U.S. price (including a service and mailing charge) is given, or a conversion table may be obtained from PHI.

Avail: NASA Public Document Rooms. Documents so indicated may be examined at or purchased from the National Aeronautics and Space Administration, Public Documents Room (Room 126), 600 Independence Ave., S.W., Washington, DC 20546, or public document rooms located at NASA installations, and the NASA Pasadena Office at the Jet Propulsion Laboratory.

Avail: Univ. Microfilms. Documents so indicated are dissertations selected from *Dissertation Abstracts* and are sold by University Microfilms as xerographic copy (HC) and microfilm. All requests should cite the author and the Order Number as they appear in the citation.

Avail: US Patent and Trademark Office. Sold by Commissioner of Patents and Trademarks, U.S. Patent and Trademark Office, at the standard price of $1.50 each, postage free. (See discussion of NASA patents and patent applications below.)

Avail: (US Sales Only). These foreign documents are available to users within the United States from the National Technical Information Service (NTIS). They are available to users outside the United States through the International Nuclear Information Service (INIS) representative in their country, or by applying directly to the issuing organization.

Avail: USGS. Originals of many reports from the U.S. Geological Survey, which may contain color illustrations, or otherwise may not have the quality of illustrations preserved in the microfiche or facsimile reproduction, may be examined by the public at the libraries of the USGS field offices whose addresses are listed on page A-6. The libraries may be queried concerning the availability of specific documents and the possible utilization of local copying services, such as color reproduction.

Avail: Issuing Activity, or Corporate Author, or no indication of availability. Inquiries as to the availability of these documents should be addressed to the organization shown in the citation as the corporate author of the document.

FEDERAL DEPOSITORY LIBRARIES: To provide the general public with greater access to U.S. Government publications, Congress established the Federal Depository Library Program under the Government Printing Office (GPO), with 52 regional depositories responsible for permanent retention of material, inter-library loan, and reference services. (These libraries are not sales outlets.) At least one copy of nearly every NASA and NASA-sponsored publication, either in printed or microfiche format, is received and retained by the 52 regional depositories. A list of the regional GPO libraries, appears on page A-8. A local library can contact a regional depository library to help locate specific reports, or direct contact may be made by an individual.

PUBLIC COLLECTION OF NASA DOCUMENTS

An extensive collection of NASA and NASA-sponsored publications is maintianed by the British Library Lending Divison, Boston Spa, Wetherby, Yorkshire, England, for public access. The British Library Lending Division also has available many of the non-NASA publications cited in *STAR.*

European requesters may purchase facsimile copy or microfiche of NASA and NASA-sponsored documents, those identified by both the symbols # and * from ESA—Information Retrieval Service, European Space Agency, 8-10 rue Mario-Nikis, 75738 Paris CEDEX 15, France.

SUBMITTING DOCUMENTS

All users of this abstract service are urged to forward reports to be considered for announcement in *STAR*. This will aid NASA in its efforts to provide the fullest possible coverage of all scientific and technical publications that might support aeronautics and space research and development. If you have prepared relevant reports (other than those you will transmit to NASA, DOD, or DOE through the usual contract- or grant-reporting channels), please send them for consideration to the NASA Center for AeroSpace Information, P.O. Box 8757, BWI Airport, MD 21240.

Reprints of journal articles, book chapters, and conference papers are also welcome. These will be considered for announcement in *STAR*'s companion journal, *IAA*.

You may specify a particular source to be included in a report announcement if you wish; otherwise the report will be placed on a public sale at the National Technical Information Service. Copyrighted publications will be announced but not distributed or sold.

PURCHASE OF *STAR*

STAR is publicly available on annual subscription from the Superintendent of Documents, U.S. Government Printing Office, Washington, DC 20402.

STAR is available to registered users on annual subscription from the NASA Center for AeroSpace Information, ATTN: Registration Services, P.O. Box 8757, BWI Airport, MD 21240.

Microfiche of the abstract sections of *STAR* are available, on annual subscription only, from NTIS as PB91-911300, Attn: Subscriptions, 5285 Port Royal Road, Springfield, VA 22161. Annual subscription rates are $85.00 North America; $170.00 foreign. Abstract sections for previous years retroactive to 1964 are available at the current rates.

ADDRESSES OF ORGANIZATIONS

American Institute of Aeronautics and Astronautics
Technical Information Service
555 West 57th Street, 12th Floor
New York, New York 10019

British Library Lending Division,
Boston Spa, Wetherby, Yorkshire,
England

Commissioner of Patents and Trademarks
U.S. Patent and Trademark Office
Washington, DC 20231

Department of Energy
Technical Information Center
P.O. Box 62
Oak Ridge, Tennessee 37830

European Space Agency-Information Retrieval Service
ESRIN
Via Galileo Galilei
00044 Frascati (Rome) Italy

Engineering Sciences Data Unit International
P.O. Box 1633
Manassas, Virginia 22110

Engineering Sciences Data Unit International, Ltd.
251-259 Regent Street
London, W1R 7AD, England

Fachinformationszentrum Energie, Physik, Mathematik
GMBH
7514 Eggenstein Leopoldshafen
Federal Republic of Germany

Her Majesty's Stationery Office
P.O. Box 569, S.E. 1
London, England

NASA Center for AeroSpace Information
P.O. Box 8757
BWI Airport, Maryland 21240

National Aeronautics and Space Administration
Scientific and Technical Information Program (NTT)
Washington, DC 20546

National Technical Information Service
5285 Port Royal Road
Springfield, Virginia 22161

Pendragon House, Inc.
899 Broadway Avenue
Redwood City, California 94063

Superintendent of Documents
U.S. Government Printing Office
Washington, DC 20402

University Microfilms
A Xerox Company
300 North Zeeb Road
Ann Arbor, Michigan 48106

University Microfilms, Ltd.
Tylers Green
London, England

U.S. Geological Survey Library National Center
MS 950
12201 Sunrise Valley Drive
Reston, Virginia 22092

U.S. Geological Survey Library
2255 North Gemini Drive
Flagstaff, Arizona 86001

U.S. Geological Survey
345 Middlefield Road
Menlo Park, California 94025

U.S. Geological Survey Library
Box 25046
Denver Federal Center, MS914
Denver, Colorado 80225

NTIS PRICE SCHEDULES

(Effective October 1, 1991)

Schedule A
STANDARD PRICE DOCUMENTS AND MICROFICHE**

PRICE CODE	NORTH AMERICAN PRICE	FOREIGN PRICE
A01	$ 9.00	$ 18.00
A02	12.50	25.00
A03	17.00	34.00
A04-A05	19.00	38.00
A06-A09	26.00	52.00
A10-A13	35.00	70.00
A14-A17	43.00	86.00
A18-A21	50.00	100.00
A22-A25	59.00	118.00
A99	*	*
N01	60.00	120.00
N02	59.00	118.00
N03	20.00	40.00

Schedule E
EXCEPTION PRICE DOCUMENTS AND MICROFICHE**

PRICE CODE	NORTH AMERICAN PRICE	FOREIGN PRICE
E01	$11.00	$ 22.00
E02	14.00	28.00
E03	16.00	32.00
E04	19.00	38.00
E05	21.00	42.00
E06	24.00	48.00
E07	27.00	54.00
E08	30.00	60.00
E09	33.00	66.00
E10	36.00	72.00
E11	39.00	78.00
E12	43.00	86.00
E13	46.00	92.00
E14	50.00	100.00
E15	54.00	108.00
E16	59.00	118.00
E17	64.00	128.00
E18	69.00	138.00
E19	76.00	152.00
E20	88.00	176.00
E99	*	*

* Contact NTIS for price quote.

** Effective January 1, 1991, the microfiche copy of any new document entering the NTIS collection will be priced the same as the paper copy of the document.

IMPORTANT NOTICE

NTIS Shipping and Handling Charges

U.S., Canada, Mexico — ADD $3.00 per TOTAL ORDER

All Other Countries — ADD $4.00 per TOTAL ORDER

Exceptions — Does NOT apply to:

ORDERS REQUESTING NTIS RUSH HANDLING
ORDERS FOR SUBSCRIPTION OR STANDING ORDER PRODUCTS *ONLY*

NOTE: Each additional delivery address on an order requires a separate shipping and handling charge.

FEDERAL REGIONAL DEPOSITORY LIBRARIES

ALABAMA

AUBURN UNIV. AT MONTGOMERY LIBRARY
Documents Dept.
7300 University Drive
Montgomery, AL 36117-3596
(205) 244-3650 FAX: (205) 244-0678

UNIV. OF ALABAMA
Amelia Gayle Gorgas Library
Govt. Documents
Box 870266
Tuscaloosa, AL 35487-0266
(205) 348-6046 FAX: (205) 348-8833

ARIZONA

DEPT. OF LIBRARY, ARCHIVES, AND PUBLIC RECORDS
Federal Documents
Third Floor State Capitol
1700 West Washington
Phoenix, AZ 85007
(602) 542-4121 FAX: (602) 542-4400; 542-4500

ARKANSAS

ARKANSAS STATE LIBRARY
State Library Services
One Capitol Mall
Little Rock, AR 72201
(501) 682-2869

CALIFORNIA

CALIFORNIA STATE LIBRARY
Govt. Publications Section
914 Capitol Mall - P.O. Box 942837
Sacramento, CA 94237-0001
(916) 322-4572 FAX: (916) 324-8120

COLORADO

UNIV. OF COLORADO - BOULDER
Norlin Library
Govt. Publications
Campus Box 184
Boulder, CO 80309-0184
(303) 492-8834 FAX: (303) 492-2185

DENVER PUBLIC LIBRARY
Govt. Publications Dept. BS/GPD
1357 Broadway
Denver, CO 80203
(303) 571-2135

CONNECTICUT

CONNECTICUT STATE LIBRARY
231 Capitol Avenue
Hartford, CT 06106
(203) 566-4971 FAX: (203) 566-3322

FLORIDA

UNIV. OF FLORIDA LIBRARIES
Documents Dept.
Library West
Gainesville, FL 32611-2048
(904) 392-0366 FAX: (904) 392-7251

GEORGIA

UNIV. OF GEORGIA LIBRARIES
Govt. Documents Dept.
Jackson Street
Athens, GA 30602
(404) 542-8949 FAX: (404) 542-6522

HAWAII

UNIV. OF HAWAII
Hamilton Library
Govt. Documents Collection
2550 The Mall
Honolulu, HI 96822
(808) 948-8230 FAX: (808) 956-5968

IDAHO

UNIV. OF IDAHO LIBRARY
Documents Section
Moscow, ID 83843
(208) 885-6344 FAX: (208) 885-6817

ILLINOIS

ILLINOIS STATE LIBRARY
Reference Dept.
300 South Second
Springfield, IL 62701-1796
(217) 782-7596 FAX: (217) 524-0041

INDIANA

INDIANA STATE LIBRARY
Serials/Documents Section
140 North Senate Avenue
Indianapolis, IN 46204
(317) 232-3678 FAX: (317) 232-3728

IOWA

UNIV. OF IOWA LIBRARIES
Govt. Publications Dept.
Washington & Madison Streets
Iowa City, IA 52242
(319) 335-5926 FAX: (319) 335-5830

KANSAS

UNIV. OF KANSAS
Govt. Documents & Map Library
6001 Malatt Hall
Lawrence, KS 66045-2800
(913) 864-4660 FAX: (913) 864-5380

KENTUCKY

UNIV. OF KENTUCKY LIBRARIES
Govt. Publications/Maps Dept.
Lexington, KY 40506-0039
(606) 257-3139 FAX: (606) 257-1563; 257-8379

LOUISIANA

LOUISIANA STATE UNIV.
Middleton Library
Govt. Documents Dept.
Baton Rouge, LA 70803
(504) 388-2570 FAX: (504) 388-6992

LOUISIANA TECHNICAL UNIV.
Prescott Memorial Library
Govt. Documents Dept.
305 Wisteria Street
Ruston, LA 71270-9985
(318) 257-4962 FAX: (318) 257-2447

MAINE

TRI-STATE DOCUMENTS DEPOSITORY
Raymond H. Fogler Library
Govt. Documents & Microforms Dept.
Univ. of Maine
Orono, ME 04469
(207) 581-1680

MARYLAND

UNIV. OF MARYLAND
Hornbake Library
Govt. Documents/Maps Unit
College Park, MD 20742
(301) 454-3034 FAX: (301) 454-4985

MASSACHUSETTS

BOSTON PUBLIC LIBRARY
Govt. Documents Dept.
666 Boylston Street
Boston, MA 02117
(617) 536-5400 ext. 226
FAX: (617) 267-8273; 267-8248

MICHIGAN

DETROIT PUBLIC LIBRARY
5201 Woodward Avenue
Detroit, MI 48202-4093
(313) 833-1440; 833-1409
FAX: (313) 833-5039

LIBRARY OF MICHIGAN
Govt. Documents Unit
P.O. Box 30007
Lansing, MI 48909
(517) 373-0640 FAX: (517) 373-3381

MINNESOTA

UNIV. OF MINNESOTA
Wilson Library
Govt. Publications Library
309 19th Avenue South
Minneapolis, MN 55455
(612) 624-5073 FAX: (612) 626-9353

MISSISSIPPI

UNIV. OF MISSISSIPPI
J.D. Williams Library
Federal Documents Dept.
106 Old Gym Bldg.
University, MS 38677
(601) 232-5857 FAX: (601) 232-5453

MISSOURI

UNIV. OF MISSOURI - COLUMBIA
Ellis Library
Govt. Documents
Columbia, MO 65201
(314) 882-6733 FAX: (314) 882-8044

MONTANA

UNIV. OF MONTANA
Maureen & Mike Mansfield Library
Documents Div.
Missoula, MT 59812-1195
(406) 243-6700 FAX: (406) 243-2060

NEBRASKA

UNIV. OF NEBRASKA - LINCOLN
D.L. Love Memorial Library
Documents Dept.
Lincoln, NE 68588
(402) 472-2562

NEVADA

UNIV. OF NEVADA
Reno Library
Govt. Publications Dept.
Reno, NV 89557
(702) 784-6579 FAX: (702) 784-1751

NEW JERSEY

NEWARK PUBLIC LIBRARY
U.S. Documents Div.
5 Washington Street - P.O. Box 630
Newark, NJ 07101-0630
(201) 733-7812 FAX: (201) 733-5648

NEW MEXICO

UNIV. OF NEW MEXICO
General Library
Govt. Publications Dept.
Albuquerque, NM 87131-1466
(505) 277-5441 FAX: (505) 277-6019

NEW MEXICO STATE LIBRARY
325 Don Gaspar Avenue
Santa Fe, NM 87503
(505) 827-3826 FAX: (505) 827-3820

NEW YORK

NEW YORK STATE LIBRARY
Documents/Gift & Exchange Section
Federal Depository Program
Cultural Education Center
Albany, NY 12230
(518) 474-5563 FAX: (518) 474-5786

NORTH CAROLINA

UNIV. OF NORTH CAROLINA - CHAPEL HILL
CB#3912, Davis Library
BA/SS Dept.—Documents
Chapel Hill, NC 27599
(919) 962-1151 FAX: (919) 962-0484

NORTH DAKOTA

NORTH DAKOTA STATE UNIV. LIBRARY
Documents Office
Fargo, ND 58105
(701) 237-8886 FAX: (701) 237-7138
In cooperation with Univ. of North Dakota, Chester Fritz Library Grand Forks

OHIO

STATE LIBRARY OF OHIO
Documents Dept.
65 South Front Street
Columbus, OH 43266
(614) 644-7051 FAX: (614) 752-9178

OKLAHOMA

OKLAHOMA DEPT. OF LIBRARIES
U.S. Govt. Information Div.
200 NE 18th Street
Oklahoma City, OK 73105-3298
(405) 521-2502, ext. 252, 253
FAX: (405) 525-7804

OKLAHOMA STATE UNIV.
Edmon Low Library
Documents Dept.
Stillwater, OK 74078
(405) 744-6546 FAX: (405) 744-5183

OREGON

PORTLAND STATE UNIV.
Millar Library
934 SW Harrison - P.O. Box 1151
Portland, OR 97207
(503) 725-3673 FAX: (503) 725-4527

PENNSYLVANIA

STATE LIBRARY OF PENN.
Govt. Publications Section
Walnut St. & Commonwealth Ave. - P.O. Box 1601
Harrisburg, PA 17105
(717) 787-3752

SOUTH CAROLINA

CLEMSON UNIV.
Cooper Library
Public Documents Unit
Clemson, SC 29634-3001
(803) 656-5174 FAX: (803) 656-3025
In cooperation with Univ. of South Carolina, Thomas Cooper Library, Columbia

TENNESSEE

MEMPHIS STATE UNIV. LIBRARIES
Govt. Documents
Memphis, TN 38152
(901) 678-2586 FAX: (901) 678-2511

TEXAS

TEXAS STATE LIBRARY
United States Documents
P.O. Box 12927 - 1201 Brazos
Austin, TX 78711
(512) 463-5455 FAX: (512) 463-5436

TEXAS TECH. UNIV. LIBRARY
Documents Dept.
Lubbock, TX 79409
(806) 742-2268 FAX: (806) 742-1920

UTAH

UTAH STATE UNIV.
Merrill Library & Learning Resources Center, UMC-3000
Documents Dept.
Logan, UT 84322-3000
(801) 750-2684 FAX: (801) 750-2677

VIRGINIA

UNIV. OF VIRGINIA
Alderman Library
Govt. Documents
Charlottesville, VA 22903-2498
(804) 924-3133 FAX: (804) 924-4337

WASHINGTON

WASHINGTON STATE LIBRARY
Document Section
MS AJ-11
Olympia, WA 98504-0111
(206) 753-4027 FAX: (206) 753-3546

WEST VIRGINIA

WEST VIRGINIA UNIV. LIBRARY
Govt. Documents Section
P.O. Box 6069
Morgantown, WV 26506
(304) 293-3640

WISCONSIN

ST. HIST. SOC. OF WISCONSIN LIBRARY
Govt. Publications Section
816 State Street
Madison, WI 53706
(608) 262-2781 FAX: (608) 262-4711
In cooperation with Univ. of Wisconsin-Madison, Memorial Library

MILWAUKEE PUBLIC LIBRARY
Documents Div.
814 West Wisconsin Avenue
Milwaukee, WI 53233
(414) 278-2167 FAX: (414) 278-2137

WYOMING

WYOMING STATE LIBRARY
Supreme Court & Library Bldg.
Govt. Publications
Cheyenne, WY 82002
(307) 777-5920 FAX: (307) 777-6289

National Aeronautics and
Space Administration
Code NTT
Washington, D.C.
20546

Official Business
Penalty for Private Use, $300

SPECIAL FOURTH-CLASS RATE
POSTAGE & FEES PAID
NASA
PERMIT No. G27

NASA

POSTMASTER: If Undeliverable (Section 158
Postal Manual) Do Not Return